Tokyo Medical and Dental University
Global Center of Excellence (GCOE) Program
International Research Center forMolecular Science in Tooth and Bone Diseases

東京医科歯科大学　グローバルCOEプログラム

歯と骨の分子疾患科学 国際教育研究拠点

～デント・メドミクスのインテリジェンスハブ～

平成20年度 実績報告書

東京医科歯科大学

はじめに

グローバルCOEプログラムは我が国の文部科学省が平成14年から行った21世紀COEプログラムの評価、継承を行い、重点的な大学院を世界的レベルまで高めることを目標とする基本的な考え方を継承しつつ、大学院教育研究機能の一層の充実評価を図り、世界最高水準の研究基盤の下での世界をリードする総合的な人材育成を図るために、国際的に卓越した教育研究拠点の形成を支援するプログラムとして開始されている。特にその重点は国際的な競争力のある大学作りの推進である。「歯と骨の分子疾患科学の国際教育研究拠点−デント・メドミクスのインテリジェンスハブ−」をタイトルとする本拠点は20年度の医学の領域で採択された。

歯と骨の分子疾患科学の国際教育研究拠点を課題とするGCOEプログラムにおいても、選抜した若手研究者や大学院生を重点的に教育するプログラムを設定した。これは歯と骨の領域における新時代の大学院教育として特に博士課程大学院生に対する経済的支援を重点として、若手研究者が自立して活躍できる機会を設定しており、国際PIシャペロンやAISS（スーパースチューデント）として選抜した若手研究者がその能力を十分に発揮できる環境整備を行っている。

本プログラムについては国際競争力を評価するために審査・評価体制として外国人レフェリーによる審査が採用され歯と骨の領域の国際的な研究者による英文資料に基づく審査が実施された。

将来的には、歯と骨の医学においても学術の急速な発展による専門家や細分化に対応できる深い専門性と一方で新たな学問分野や急速な科学技術に対応できる幅広い応用力を持つ人材の養成を目標としてている。本、歯と骨の教育研究拠点は既にアジアの指導者、欧米の一流研究室での研究者を輩出し、今後も国際的な人材育成を推進する。

医学・歯学においてはその国際性や大学院教育の活性化がより強く求められている。歯と骨のグローバルCOE研究拠点は、21世紀COEにおける高い実績に基づき、新たな国際性の高い、実力のある若手研究者の育成と将来性の高い大学院生を育てることを主体に掲げている。大学の全体での取り組みでの一環としての歯と骨の伝統ある本学の先輩方の業績に基づき、新しい領域を開きつつ、未来の指導者を養成する場としてのグローバルCOEの今後の展開が望まれており、平成20年度もその目標に向かい事業推進担当者の多くの尽力により本報告書に記載されております本拠点の活動がなされました。今後とも皆様の一層のご支援をお願い致します。

野田　政樹
Masaki Noda

平成20年度
GCOEプログラム実績報告書

拠点のプログラム名称

歯と骨の分子疾患科学の国際教育研究拠点

専攻等名

医歯学総合研究科器官システム制御学系専攻・口腔機能再構築学系専攻・生体支持組織学系専攻
顎顔面頸部機能再建学系専攻・先端医療開発学系専攻・生体環境応答学系専攻・疾病生命科学研究部
生体材料工学研究所・難治疾患研究所

野 田　政 樹 Masaki Noda
拠点リーダー/医歯学総合研究科・器官システム制御学系専攻・教授
分子薬理学/医学博士・歯学博士

拠点形成統括および先端硬組織分子再建科学の研究

田 上　順 次 Junji Tagami
医歯学総合研究科・口腔機能再構築学系専攻・教授
齲蝕制御学/歯学博士

先端硬組織分子再建科学

高 柳　広 Hiroshi Takayanagi
東京医科歯科大学大学院医歯学総合研究科・教授
分子情報伝達学/医学博士

硬組織分子喪失病態学

森 田　育 男 Ikuo Morita
医歯学総合研究科・顎顔面頸部機能再建学系専攻・教授
分子細胞機能学/薬学博士

先端硬組織分子再建科学

小 村　健 Ken Omura
医歯学総合研究科・口腔機能再構築学系専攻・教授
口腔機能再建学/医学博士

硬組織疾患ゲノム科学

春 日 井　昇 平 Shohei Kasugai
医歯学総合研究科・口腔機能再構築学系専攻・教授
摂食機能制御学／歯学博士

先端硬組織分子再建科学

須 田　英 明 Hideaki Suda
医歯学総合研究科・口腔機能再構築学系専攻・教授
歯髄生物学／歯学博士

先端硬組織分子再建科学

和泉　雄一 Yuichi　Izumi
医歯学総合研究科・生体支持組織学系専攻・教授
歯周病学／歯学博士

硬組織分子喪失病態学

柳 下　正 樹 Masaki Yanagisita
医歯学総合研究科・生体支持組織学系専攻・教授
硬組織病態制御学 ／医学士

先端硬組織分子再建科学

山 口　朗 Akira Yamaguchi
医歯学総合研究科・口腔機能再構築学系専攻・教授
口腔病理学／医学博士

先端硬組織分子再建科学

森 山　啓 司 Keiji Moriyama
医歯学総合研究科・顎顔面頚部機能再構築学系専攻・教授
顎顔面矯正学／薬学博士

硬組織分子喪失病態学

四 宮　謙 一 Kenichi Shinomiya
医歯学総合研究科・先端医療開発学系専攻・教授
脊椎・脊髄神経外科学／医学博士

先端硬組織分子再建科学

宮 坂　信 之 Nobuyuki Miyasaka
医歯学総合研究科・生体環境応答学系専攻・教授
臨床免疫学／医学博士

硬組織分子喪失病態学

宗 田　大 Takeshi Muneta
医歯学総合研究科・生体支持組織学系専攻・教授
運動機能再建学／医学博士

先端硬組織分子再建科学

秋 吉　一 成 Kazunari Akiyoshi
生体材料工学研究所・素材研究部門・教授
有機材料学／工学博士

先端硬組織分子再建科学

稲 澤　譲 治 Johji Inazawa
難治疾患研究所・遺伝疾患研究部門・教授
分子細胞遺伝学／医学博士

硬組織疾患ゲノム科学

三 木　義 男 Yoshio Miki
難治疾患研究所・遺伝疾患研究部門・教授
遺伝子応用医学／医学博士

硬組織疾患ゲノム科学

石 野　史 敏 Fumitoshi Ishino
教授
分子生物学／理学博士

硬組織疾患ゲノム科学

澁 谷　浩 司 Hiroshi Shibuya
医歯学総合研究科・器官システム制御学系専攻・教授
細胞機能調節学／理学博士

硬組織基礎生命科学

小 川　佳 宏 Yoshihiro Ogawa
医歯学総合研究科・器官システム制御学系専攻・教授
内分泌学／医学博士

硬組織基礎生命科学

萩 原　正 敏 Masatoshi Hagiwara
疾患生命科学研究部・高次生命制御研究部門・教授
形質発現制御学／医学博士

硬組織基礎生命科学

平成20年度

GCOEプログラム
実績報告書

CONTENTS

野田　政樹（分子薬理学分野）…… 8
田上　順次（う蝕制御学分野）…… 26
高柳　広（分子情報伝達学分野）…… 46
森田　育男（分子細胞機能学）…… 74
小村　健（顎口腔外科学分野）…… 92
春日井 昇平（インプラント口腔再生学分野）…… 108
須田　英明（歯髄生物学分野）…… 114
和泉　雄一（歯周病学分野）…… 130
柳下　正樹（硬組織病態制御学）…… 146
山口　朗（口腔病理学分野）…… 156
森山　啓司（顎顔面矯正学分野）…… 170
四宮　謙一（整形外科学分野）…… 190
宮坂　信之（膠原病・リウマチ内科）…… 210
宗田　大（運動器外科分野）…… 236
秋吉　一成（有機材料分野）…… 262
稲澤　譲治（分子細胞遺伝学分野）…… 274
三木　義男（分子遺伝分野）…… 302
石野　史敏（分子生物学分野）…… 320
澁谷　浩司（分子細胞生物学分野）…… 334
小川　佳宏（分子代謝学分野）…… 338
荻原　正敏（形質発現分野）…… 354

分子薬理学

野田 政樹

医歯学総合研究科・器官システム制御学系専攻
分子薬理学・教授

1. 研究の課題名

主題1: 骨形成制御機構の研究

骨量増加を支える骨の形成に関わる全身性の因子と局所性の因子のそれぞれにおける相互作用のメカニズムはなお不明な点が多い。そのメカニズムの解析を行い、分子の機能を明らかにすることは今後の新たな治療を開発する上でも基盤となる。そこで骨形成の生体における制御についての検討を行い、副甲状腺ホルモンのシグナルならびに細胞外基質の蛋白の相互作用の存在することを明らかにした（Journal of Biological Chemistry 2008）。また、骨量の制御に関わるエストロゲンの作用の下流にある転写因子を解析した結果、AP1分子グループであるJunDが骨量の維持の上で機能する転写因子であることが明らかとなった。（Journal of Cellular Biochemistry 2008, Biochemical & Biophysical Research Communication 2008）。

主題2: 破骨細胞の機能制御に関わる研究

骨吸収する破骨細胞はその活性や分化の制御に関わる要因が最終的な骨量の決定に関わる。従って、その制御のメカニズムの解明が課題となる。特にメカニカルストレスに応答する骨量の減少においては、骨形成の低下ならびに骨吸収の亢進が関わるが、その入口であるチャンネルについては、なお十分には明らかではない。このメカニズムの解析として陽イオンチャンネルであるTRPV4が破骨細胞に関わる非荷重のシグナルの伝達の上で、その担い手の一つであることを明らかにした（Journal of Cellular Physiology 2008, Anatomical Record 2008, J Anat 2008）。

主題3: 骨形成と骨吸収の共役に関わるメカニズム

骨のリモデリングにおいては、その形成および吸収のバランスが制御されるが、この平衡を担う分子の機構はまだなお十分に明らかではない。骨量の制御メカニズムの中で歯の移動の際における形成と吸収のバランスは歯槽骨の維持と歯牙の安定的な支持の上で重要となる。外力に応答したこのような骨形成と骨吸収が並行して起こるメカニズムの中で、細胞外基質の役割を明らかにした（Journal of Cellular Physiology 2008）

2.

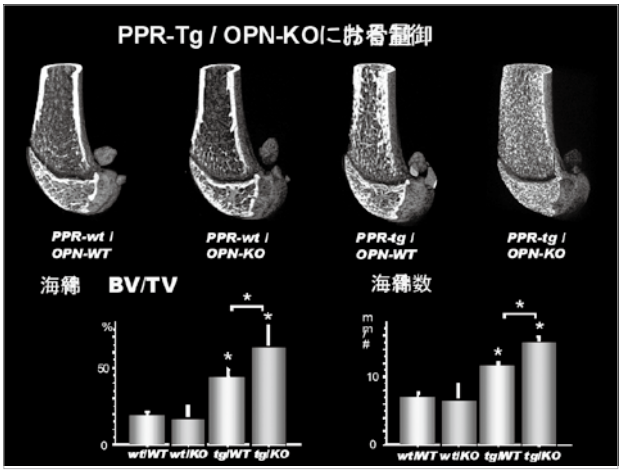

3. 2008年、2009年（平成21年3月までの）に発表した全ての研究内容についての英文要約

Bone mechanism is maintained by bone formation and bone resorption

With respect to bone resorption and bone formation, we have identified that another signaling by hydrohormone, with being enhanced by the access of osteopontin. Osteopontin is a ECM protein and cytokine and has been known for its role, in the maintenance of bone mass. However, we identified that osteopontin is present in bone to be an regulatory factor in the mass of bone with respect to bone formation. We have further identified transcription factors, Jun D, to be involved in the maintenance of bone mass as well. Furthermore, bone resorption analysis

identified TRPV 4 is a new cation channel which is mediating mechanical signals in these bone. These observations from bone formation and resorption as well as coupling phenomena were clarified in the year of during this research.

4. 本事業に関連して世界的な研究拠点形成に向けて、以下の点で改善・整備等されたこと

A（研究拠点体制）

研究拠点体制として若手教員ならびに選抜された大学院生による研究体制が整えられた。

B（研究教育環境）

複数の教員による研究教育環境と選抜された研究者ならびに事業推進担当者による総合プレゼンテーションによる教育環境が整えられた。

C（人材確保）

国際公募による若手研究者の選抜が行われ、優秀な人材が確保された。

D（人材育成）

大学院生の中で特に優れた者を選抜し、教育する体制が整えられた。

E（国際化）

大学院生の中で国際的な交流に基づく学生は約50%であり、また国際公募による若手研究者の選抜が行われた。

5. GCOE事業を推進するに当たって力を入れた点

世界最高水準の研究を推進する為に事業推進担当者同士の研究体制がInnovation研究費によって整えられると共に若手研究者を選抜し、選抜大学院生と共に研究を推進する体制が整えられた。

6. 英文原著論文

1. ○Miyai K, Yoneda M, Hasegawa U）, Toida S, Izu Y, Hiroaki H, Hayata T, Ezura Y, Mizutani S, Miyazono K, Akiyoshi K, Yamamoto T, Noda M. ANA deficiency enhances BMP-induced ectopic bone formation via transcriptional events. Journal of Biological Chemistry; 2009（in press）

2. ○Izu Y, Mizoguchi F, Kawamata A, Hayata T, Nakamoto T, Nakashima K, Inagami T, Ezura Y, Noda M. Angiotensin II type 2 receptor blockade increases bone mass. Journal of Biological Chemistry 284:4857-64; 2009

3. ○Ono N., Nakashima K., Rittling S.R., Schipani E., Hayata T., Ezura Y., Soma K., Denhardt D.T., Kronenberg H.M., Noda M. Osteopontin Negatively Regulates parathyroid hormone receptor signaling in osteoblasts Journal of Biological Chemistry 283:19400-19409, 2008

4. ○Kawamata A., Izu Y., Yokoyama H., Hayata T., Amagasa T., Wagner E.F., Nakashima K., Ezura Y., Noda M. JunD suppresses bone formation and contributes to low bone mass induced by estrogen depletion. Journal of Cellular Biochemistry. 103:1037-45, 2008

5. ○Mizoguchi F., Mizuno A., Hayata T., Nakashima K., Heller S., Ushida T., Sokabe M., Miyasaka N., Suzuki M., Ezura Y., Noda M. Transient Receptor Potential Vanilloid 4 Deficiency Suppresses Unloading-Induced Bone Loss. Journal of Cellular Physiology. 216:47-53, 2008

6. ○Hayashi C, Hasegawa U, Saita Y, Hemmi H, Hayata T, Nakashima K, Ezura Y, Amagasa T, Akiyoshi K, Noda M. Osteoblastic Bone Formation Is Induced by Using Nanogel-Crosslinking Hydrogel as Novel Scaffold for Bone Growth Factor. Journal of Cellular Physiology; 2009（in press）

7. ○Hayata T., Nakamoto T., Ezura Y., Noda M. Ciz, a transcription factor with a nucleocytoplasmic shuttling activity, interacts with C-propeptides of type I collagen Biochemical and Biophysical Research Communications. 368:205-10, 2008

8. ○Chung C.J., Soma K., Rittling S.R., Denhardt D.T., Hayata T., Nakashima K., Ezura Y., Noda M. OPN deficiency suppresses appearance of odontoclastic cells and resorption of the tooth root induced by experimental force application. Journal of Cellular Physiology 214:614-20, 2008

9. Suzuki H., Amizuka N., Oda K., Noda M., Ohshima H., Maeda T., Involvement of the klotho protein in dentin formation and mineralization. Anatomical Record 291:183-190, 2008

10. Suzuki H., Amizuka N., Oda K., Noda M., Ohshima H., Maeda T. Histological and elemental analyses of impaired bone mineralization in klotho-deficient mice. J Anat. 212:275-85, 2008

11. ○Nakamoto T., Seo S., Sakai R., Kato T., Kutsuna H., Kurokawa M., Noda M., Miyasaka N., Kitagawa S. Expression and tyrosine phosphorylation of Crk associated substrate lymphocyte type（Cas-L）protein in human neutrophils. Journal of Cellular Biochemistry;105:121-128, 2008

12. Ajima R., Akiyama T., Usui M., Yoneda M., Yoshida Y., Nakamura T., Minowa O., Noda M., Tanaka S., Noda T., Yamamoto T. Osteoporotic bone formation in mice lacking tob2; involvement of Tob2 in RANK ligand expression and osteoclasts differentiation. FEBS Lett.; 582:1313-8, 2008

13. Tazaki T, Miyazaki K, Hiyama E, Nakamoto T, Sakai R, Yamasaki N, Honda Z, Noda M, Miyasaka N, Sueda T, Honda H. Functional analysis of Src homology 3-encoding exon（exon 2）of p130Cas in primary fibroblasts derived from exon 2-specific knockout mice. Genes Cells;13:145-57, 2008

14. Hemmi H, Idoyaga J, Suda K, Suda N, Kennedy K, Noda M, Aderem A, Steinman RM, A new Trem family member, Treml4, binds to dead cells and is a DAP12 linked marker for subsets of mouse macrophages and dendritic cells. Journal of Immunology; 182:1278-86, 2008

15. ○Ezura Y, Koga H, Muneta T, Sekiya I, Noda M. Methylation status of CpG-islands in the promoter regions of signature genes during chondrogenesis of human synovium-derived mesenchymal stem cells. Arthritis & Rheumatism; 2009（in press）

7. 特許取得、特許申請

名称:抗オステオポンチン抗体及びその用途/ ANTI-OSTEOPONTIN AND USE THEREOF
国際出願番号:PCT/JP02/0338
（申請中）名称:骨形成促進物質とナノゲルを含有する骨形成用生体材料
国際出願番号:PCT/JP2007/50555
代表者:秋吉一成、野田政樹

8. 平成21年3月までの　自己評価

研究の上では新たな骨形成に関わる分子ならびに破骨細胞の機能制御に関わるチャンネルを見出し、またこれらの相互関係を維持する為のメカニズムが見出された。さらに人材ならびに教育体制、研究体制がグローバルCOEの拠点として整えられたことが評価される。

12）和文原著論文または総説:　2008年、2009年（平成21年3月までの）に発表した全てのもの（ただし平成21年3月まで）。著者名、タイトル、雑誌名、出版年は上の例に倣ってください。印刷中は　最後のところを（印刷中）、2009としてください。

1. 野田政樹 「難治疾患研究の将来について」 BIO Clinica　23（3）: 193, 2008.
2. 野田政樹, 宮井健太郎, 早田匡芳, 江面陽一.「骨における細胞研究のフロンティア」 内分泌・糖尿病科 27（3）: 209-212, 2008.
3. 野田政樹 「分子生物学と整形外科」 臨床雑誌「整形外科」59（7）: 691-697, 2008.

9. 学会発表（英文）

1. Miyai K., Yoneda M., Hayata T., Ezura Y., Nakashima K., Yamamoto T., Mizutani S., Noda M. A role of ANA in osteoblast and in bone formation Harverd School of Dental Medicine Sutudent Research Day 2008, Boston, April 22, 2008

2. Kawamata A., Izu Y., Yokoyama H., Hayata T., Amagasa T., Wagner E.F., Nakashima K., Ezura Y., Noda M. Ovariectomy induced bone loss was prevented by the deficiency of JunD which reduces basal levels of bone mass Harverd School of Dental Medicine Sutudent Research Day 2008, Boston, April 22, 2008

3. Mizoguchi F., Izu Y., Hayata T., Hemmi H., Nakashima K., Nakamura T.,Kohsaka H., Miyasaka N., Harfe B., Kato S., Ezura Y., Noda M., Osteoclast Specific Dicer Deficiency Suppress Osteoclast　Differentiation and Increase Bone Mass. 2nd International Conference of Osteoimmunology（Aegean Conferences）, Rhodes, Greece, June 8-13, 2008

4. Ono N., Nakashima K., Schipani E., Hayata T., Ezura Y., Soma K,　Kronenberg H.M., Noda M. Osteoblast-specific constitutive activation of PTH/PTHrP receptor enhances marrow-ablation-induced osteoprogenitor activities. International Association for Dental Rearch General Session, Toronto, Canda, July 2-5, 2008

5. Ezura Y., Nagata J., Hemmi H., Hayata T, Nakamoto T., Noda M. Increased Expression of Osteopontin in Peripheral Blood Mononuclear Cells is Associated with Alteration in the Fractions of Lymphocytes in Hindlimb-unloaded Mice The 30th Annual Meeting of American Society for Bone and Mineral Research, Montreal, Canada, September 12-16, 2008

6. Hayata T., Nakamoto T., Ezura Y., Noda M. Interaction of Ciz, a Nucleo-cytoplasmic Shuttling transcription factor with C-propeptides of type I collagen The 30th Annual Meeting of American Society for Bone and Mineral Research, Montreal, Canada, September 12-16, 2008

7. Nakamoto T., Mizoguchi F., Izu Y., Hayata T., Ezura Y., Mathis D., C.　Benoist, Miyasaka N., Noda M. Deficiency of the Nucleocytoplasmic Shuttling Protein CIZ

Suppresses K/BxN Serum-Induced Model of Rheumatoid Arthritis The 30th Annual Meeting of American Society for Bone and Mineral Research, Montreal, Canada, September 12-16, 2008

8. Izu Y., Hayata T., Mizoguchi F., Kawamata A., Nakamoto T., Ezura Y., Noda M., Angiotensin II type 2 receptor blockade increases bone mass The 30th Annual Meeting of American Society for Bone and Mineral Research, Montreal, Canada, September 12-16, 2008

9. Hanyu R., Saita Y., Nagata J. , Izu Y., Hayata T., Henmi H., Takeda S.,Ezura Y., Kurosawa H., Noda M. Aging dependent and independent effects of b2 adrenergic receptor signaling on bone formation induced by intermittent PTH treatment in female mice The 30th Annual Meeting of American Society for Bone and Mineral Research, Montreal, Canada, September 12-16, 2008

10. Kamolratanakul P., Kawamata A., Yamamoto Y., Ezura Y., Akiyoshi K., Amagasa T., Noda M. Nanotechnological Scaffold with Combination of Prostaglandin E2 Receptor EP4 Agonist and rhBMP2, Enhances Bone Repair in the Defect of Mouse Calvarium Bone. he 30th Annual Meeting of American Society for Bone and Mineral Research, Montreal, Canada, September 12-16, 2008

11. Hemmi H., Idoyaga J., Suda K., Suda N., Noda M., Steinman R.M. Identification and characterization of a Trem-like molecule expressed on mouse splenic DCs and macrophages The 10th International Symposium on Dendritic Cells. October 1-5, 2008

10. 学会発表（和文）

1. 江面陽一、永田純史、野田 政樹　尾部懸垂マウス大腿骨における網羅的遺伝子発現の部位別解析　第28回日本骨形態計測学会　7月25日-27日, 2008

2. 早田匡芳、中元哲也、江面陽一、野田政樹　核-細胞質シャトリングタンパク質Cizは、Ⅰ型コラーゲンのC-プロペプチドと相互作用する。 第28回日本骨形態計測学会　7月25日-27日, 2008

3. 伊豆弥生、早田匡芳、中元哲也、江面陽一、野田政樹　アンギオテンシンⅡtype2受容体阻害剤は骨量を増加させる　第28回日本骨形態計測学会　7月25日-27日, 2008

4. 宮井　健太郎、野田　政樹　ANAは骨芽細胞におけるBMP2シグナルのネガティヴフィードバックに関与し骨形成を抑制する　第28回日本骨形態計測学会　7月25日-27日, 2008

5. 川俣　綾、野田　政樹、天笠　光雄　AP-1構成因子であるJunDは骨量増加を抑制し、エストロゲン欠乏による骨量減少に関与する　第53回日本口腔外科学会学術大会　10月20日-21日, 2008

6. 長尾雅史、斎田良知、永田純史、伊豆弥生、早田匡芳、辺見弘明、江面陽一、黒澤尚、野田政樹　交感神経β刺激による骨吸収と骨形成にオステオポチンは必要である　第30回日本整形外科学会基礎学術集会　10月23日-24日, 2008

7. 羽生亮、斎田良知、伊豆弥生、竹田秀、江面陽一、黒澤尚、野田政樹　アドレナリンβ2受容体遺伝子欠損の高週令（1年）マウスにおけるPTHによる骨形態計測学的検討　第30回日本整形外科学会基礎学術集会　10月23日-24日, 2008

8. 江面陽一、関矢一郎、宗田大、野田政樹　ヒト滑膜由来間葉系幹細胞の軟骨細胞分化過程における主な遺伝子上流CpGアイランドのメチル化状態は定常的に維持される　第26回日本骨代謝学会学術集会　10月29日-31日, 2008

9. 早田匡芳、中元哲也、江面陽一、野田政樹　Ⅰ型コラーゲンC-プロペプチドは、骨形成抑制因子Cizと結合する　第26回日本骨代謝学会学術集会　10月29日-31日, 2008

10. 溝口史高、伊豆弥生、早田匡芳、辺見弘明、中島和久、中村貴、Brian Harfe、加藤茂明、宮坂信之、江面陽一、野田政樹　破骨細胞特異的Dicer欠損は破骨細胞分化を抑制し骨量を増加させる　10月17日-18日, 2008

11. 外部資金の獲得状況

（科学研究費補助金、受託研究費、外部財団の助成など）

グローバルCOEプログラム

研究題目:歯と骨の分子疾患科学の国際教育研究拠点-デント・メドミクスのインテリジェンスハブー

代表:野田政樹

期間:2008年-2012年
研究費　397,150万円（2008年度分）

文部科学省科学技術振興調整費
研究題目:メディカル・トップトラック制度の確立
代表:野田政樹
期間:2006年-2010年
研究費:90,000万円（2006-2008年度分）

先端研究拠点事業
研究題目:　骨・軟骨疾患の先端的分子病態生理学の国際的拠点形成
代表:野田政樹
期間:2004-2008年
研究費総額:26,100万円

特別教育研究経費
研究題目:硬組織疾患プロジェクト
代表:野田政樹
期間:2005-2009年
研究費:9,851万円（2005-2008年年度分）

日本学術振興会研究費補助金（基盤S）
研究題目:骨形成メカニズムとしてのニッチの分子的解明と治療への応用基盤の先端ナノサイエンス
代表:野田政樹
期間:2006-2010年
研究費:5,584万円（2006-2008年）

日本学術振興会研究費補助金（特定・がん）
研究題目:悪性黒色腫の骨の転移のメカニズムの解明
代表:野田政樹
期間:2008-2009年
研究費:430万円（2008年度分）

12. 特別講演、招待講演

2009年
・野田政樹:第61回関西カルシウム懇話会
2009年3月28日
・野田政樹:第12回超音波骨折治療研究会
2009年1月17日
演題:メカニカルストレスと骨代謝
・野田政樹:宇宙医学生物学ワークショップ「微小重力と骨代謝」（財団法人日本宇宙フォーラム）　2009年1月16日
演題:メカニカルストレスと骨

2008年
・野田政樹:米国細胞生物学会　2008年12月13日-17日
演題:Regulation of Bone
・野田政樹:BMB2008（第31回日本分子生物学会年会・第81回日本生化学会　合同大会）　2008年12月12日
演題:骨のメカニカル応答性と細胞制御機構
・野田政樹:岡山大学特別講義　2008年11月21日
演題:BMPとその抑止因子、メカニカルストレスと骨代謝
・野田政樹:岡山大学セミナー　2008年11月20日
演題:骨代謝制御の分子機構
・野田政樹:ÖGEKM Autumn Symposium 2008, October 25th, 2008
演題:Fracture risk assessment in Japan
・野田政樹:23回日本整形外科学会基礎学術集会
2008年10月24日
演題:骨の基礎研究から
・野田政樹:International Association for Dental Rearch Gerneral Session, July 4th, 2008
演題:Mechnobiology of osteoblasts and osteoclasts.
・野田政樹:第19回長崎骨粗鬆症研究会
2008年5月27日
演題:骨形成の基礎
・野田政樹:30th Asia Pacific Dental Congress, May 8th, 2008
演題:Anabolic agents for bone formation in osteopenic state
・野田政樹:1st Thailand International Conference in Oral Biology, May 7th, 2008
演題:Mechanical signaling in regulation of bone metabolism

13. 主催学会

ABJS国際シンポジウム・ワークショップ
平成20年12月2-5日
骨と関節の先端的疾患分子医科学
骨と軟骨の分子制御

第28回日本骨形態計測学会　平成20年7月25-28日
骨の形と機能に対する疾患分子的アプローチの最前線

14. GCOE総合講義のサマリー

骨の形成は現在の骨粗鬆症治療薬の中で吸収の抑止を図る薬剤がなお50%程度の骨折率抑止に留まることに対し、さらなる骨折率の改善に向けた必須の課題と考えられる。この点において、現在開発が進められている。欧米で使用されている薬剤としてはPTHが挙げられる。PTHの作用のメカニズムについて現時点での知見を概説し、またそのシグナルが細胞外基質分子と相互作用することを解説した。この相互作用は全身性のカルシウム制御の重要なフィードバックループの一翼を成しており、ターゲットは転写レベルでの相互作用と至る。

15. 講座の准教授、講師、助教、特別研究員、ポスドク、指導を受けた大学院生の名前（AISSには○印）のリスト

准 教 授　江面陽一
助　　教　早田匡芳
特任講師　辺見弘明
特任講師　納富拓也（国際PIシャペロン）
大学院生　宮井健太郎
　　羽生亮（共同研究者）
　　長尾雅史（共同研究者）
　　○中川朋美
　　○Paksinee Kamolratanakul
　　Smriti Ayral（専攻生）

In pressの論文抄録

Title
Osteoblastic Bone Formation Is Induced by Using Nanogel-Crosslinking Hydrogel as Novel Scaffold for Bone Growth Factor

Author
Chikako Hayashi, Urara Hasegawa, Yoshitomo Saita, Hiroaki Hemmi,
Tadayoshi Hayata, Kazuhisa Nakashima, Yoichi Ezura, Teruo Amagasa,
Kazunari Akiyoshi, Masaki Noda

Abstract
Bone regeneration for the defects in revision surgery of joint replacement is an
increasingly important issue. To repair bone defects, bone cell activation by growth factors using synthetic resorbable scaffold is a useful and safe option. We examine the efficiency of nanogel-crosslinking hydrogel as a novel synthetic scaffold for BMP to stimulate osteoblasts and to induce bone formation. Cholesterol-bearing pullulan nanogel-crosslinking hydrogel (CHPA Hydrogel) was used to deliver BMP. The CHPA hydrogel pellets were implanted in vivo. Single implantation of CHPA/Hydrogel containing low amounts of BMP induced osteoblastic activation and new bone formation in vivo. Furthermore, nanogel in a disc shape established recruitment of osteoblastic cells that vigorously formed bone to heal the calvarial defects which did not heal spontaneously without it. In conclusion, CHPA/Hydrogel serves as an efficient and versatile scaffold for the stimulation of osteoblasts to from bone and to repair defects via delivery of BMP.

Title
Methylation status of CpG-islands in the promoter regions of signature genes during chondrogenesis of human synovium-derived mesenchymal stem cells

Author
Yoichi Ezura, Ichiro Sekiya, Hideyuki Koga, Takeshi Muneta, and Masaki Noda

Abstract
[Objective]
Human synovium derived mesenchymal stem cells (SMSCs) can efficiently differentiate into mature chondrocytes. In human chondrogenesis, mechanism of methylation has been suggested, however the status of methylation in genes related to the chondrogenic differentiation is not known. To clarify it from a viewpoint aiming therapeutic use for osteoarthritis, we investigated status of CpG-methylation in human SMSCs during experimental chondrogenesis.

[Methods]
Human SMSCs were subjected to chondrogenic pellet-culture for three weeks. Methylation status of 12 regions in the promoters of 10 candidate genes (i.e., SOX9, RUNX2, CHM-1, FGFR3, CHAD, MATN4, SOX4, GREM1, GPR39, and SDF1) was analyzed by bisulfite sequencing before and after differentiation. Expression levels of these genes were analyzed by real-time RT-PCR. Methylation status was also examined in human articular cartilage.

[Results]
Bisulfite sequencing analysis indicated that 10 out of the analyzed 11 CpG-rich regions were hypo-methylated in the human progenitor cells before and after 3 weeks of pellet-culture, regardless of the expression levels of the genes; the methylation status was consistently low in SOX9, RUNX2 CHM-1, CHAD, and FGFR3 after the increased expression upon differentiation, and in GREM1 and

GPR39 after its reduction upon chondrogenesis. One exceptional instance of differentially methylated CpG-rich region was in 1-kb upstream sequence of SDF1 whose expression decreased upon differentiation; hyper-methylation status of this region was relaxed after 3 weeks of pellet culture, paradoxically.

[Conclusion]
DNA methylation levels of CpG-rich promoters of the genes related to chondrocyte phenotypes are largely kept low during chondrogenesis in human SMSCs.

Title
ANA deficiency enhances BMP-induced ectopic bone formation via transcriptional events

Author
Kentaro Miyai, Mitsuhiro Yoneda , Urara Hasegawa , Sayaka Toida , Yayoi Izu ,Hiroaki Hemmi, Tadayoshi Hayata, Yoichi Ezura, Shu-ki Mizutani, Kohei Miyazono, Kazunari Akiyoshi, Tadashi Yamamoto, Masaki Noda

Abstract
Ectopic bone formation after joint replacement or brain injury in humans is a serious complication that causes immobility of joints and severe pain. However, mechanisms underlying such ectopic bone formation are not fully understood. BMPs are defined as inducers of ectopic bone formation while they are regulated by several types of inhibitors. ANA is an antiproliferative molecule that belongs to Tob/BTG family, but its activity in bone metabolism has not been known. Here, we examined the role of ANA on ectopic bone formation activity of BMP. In ANA-deficient and wild type mice, BMP2 was implanted to induce ectopic bone formation in muscle. ANA deficiency increased mass of newly formed bone in vivo compared to wild type based on 3D-micro CT analyses. ANA mRNA was expressed in bone in vivo as well as in osteoblastic cells in vitro. Such ANA mRNA levels were increased by BMP2 treatment in MC3T3-E1 osteoblastic cells. Overexpression of ANA suppressed BMP-induced expression of luciferase reporter gene linked to BMP response elements (BRE) in these cells. Conversely, ANA mRNA knock-down by siRNA enhanced the BMP-dependent BRE reporter expression. It also enhanced BMP-induced osteoblastic differentiation in muscle derived C2C12 cells. Immunoprecipitation assay indicated that ANA interacts with Smad8. Thus, ANA is a suppressor of ectopic bone formation induced by BMP and this inhibitory ANA activity is a part of the negative feedback regulation of BMP function.

Supplemental Material can be found at:
http://www.jbc.org/cgi/content/full/M800005200/DC1

THE JOURNAL OF BIOLOGICAL CHEMISTRY VOL. 283, NO. 28, pp. 19400–19409, July 11, 2008
© 2008 by The American Society for Biochemistry and Molecular Biology, Inc. Printed in the U.S.A.

Osteopontin Negatively Regulates Parathyroid Hormone Receptor Signaling in Osteoblasts*[S]

Received for publication, January 2, 2008, and in revised form, April 16, 2008 Published, JBC Papers in Press, April 16, 2008, DOI 10.1074/jbc.M800005200

Noriaki Ono[‡§¶], Kazuhisa Nakashima[‡§1], Susan R. Rittling[‖], Ernestina Schipani[**], Tadayoshi Hayata[‡], Kunimichi Soma[¶], David T. Denhardt[‡‡], Henry M. Kronenberg[**], Yoichi Ezura[‡1], and Masaki Noda[‡§§§¶¶1]

From the [‡]Department of Molecular Pharmacology, Medical Research Institute and [§]21st Century Center of Excellence Program for the Frontier Research on Molecular Destruction and Reconstruction of Tooth and Bone, 2-3-10 Kanda-surugadai, Chiyoda-ku, 101-0062, Tokyo, Japan, [¶]Orthodontic Science, Graduate School, Tokyo Medical and Dental University, 1-5-45 Yushima, Bunkyo-ku, 113-8510, Tokyo, Japan, [‖]The Forsyth Institute, Boston, Massachusetts 02115, [**]Endocrine Unit, Massachusetts General Hospital and Harvard Medical School, Boston, Massachusetts 02114, [‡‡]Department of Cell Biology and Neuroscience, Rutgers University, Piscataway, New Jersey 08701, [§§]Advanced Bone and Joint Science (ABJS) Integrated Action Initiative in Japan Society for the Promotion of Science Core to Core Program and [¶¶]Hard Tissue Genome Research Center, Tokyo Medical and Dental University, Tokyo, Japan

Systemic hormonal control exerts its effect through the regulation of local target tissues, which in turn regulate upstream signals in a feedback loop. The parathyroid hormone (PTH) axis is a well defined hormonal signaling system that regulates calcium levels and bone metabolism. To understand the interplay between systemic and local signaling in bone, we examined the effects of deficiency of the bone matrix protein osteopontin (OPN) on the systemic effects of PTH specifically within osteoblastic cell lineages. Parathyroid hormone receptor (PPR) transgenic mice expressing a constitutively active form of the receptor (caPPR) specifically in cells of the osteoblast lineage have a high bone mass phenotype. In these mice, OPN deficiency further increased bone mass. This increase was associated with conversion of the major intertrabecular cell population from hematopoietic cells to stromal/osteoblastic cells and parallel elevations in histomorphometric and biochemical parameters of bone formation and resorption. Treatment with small interfering RNA (siRNA) for osteopontin enhanced H223R mutant caPPR-induced cAMP-response element (CRE) activity levels by about 10-fold. Thus, in addition to the well known calcemic feedback system for PTH, local feedback regulation by the bone matrix protein OPN also plays a significant role in the regulation of PTH actions.

Body homeostasis is maintained under a precise coordination of systemic hormones and local cytokines and an imbalance in this regulation leads to pathological situations and disorders. Hormones affect multiple organs, and tight feedback systems exist between upstream and downstream organs. In addition, target organs by themselves are horizontally linked with each other, making the whole system versatile but complex. This makes it difficult to identify points of malfunction of the system in pathological situations. It is, therefore, necessary to identify a well delineated system to unravel new layers of regulation in the hormonal control of homeostasis.

The parathyroid hormone (PTH)[2] axis is a well defined hormonal system that maintains the calcium level in body fluid. Proper calcium levels are critical for numerous cellular activities. Parathyroid hormone is secreted from the parathyroid gland, which senses small reductions in blood calcium levels (1). PTH acts systemically on targets such as kidney and bone to correct calcium levels in the blood. These target organs of PTH are themselves horizontally linked. For instance, PTH acts on the kidney to produce an active form of vitamin D, which in turn affects cellular activities in bone and increases calcium absorption from intestine (2–4). These direct and indirect (horizontal) actions of PTH eventually result in an increase in the blood calcium, which in turn reduces the release of PTH from the parathyroid gland to complete the cycle of these calcemic events. Furthermore, antagonists such as calcitonin counteract pro-calcemic actions of PTH and maintain the homeostasis of blood calcium levels (5).

In addition to this systemic role in maintenance of calcium levels in body fluids, PTH also modulates local events such as vasodilation (6) and accumulation of bone mass (7). In fact, PTH increases bone formation and is approved as a drug for severe osteoporosis, where there is solid evidence for its ability to reduce fracture risk (8–11). Understanding the mechanism of these anabolic actions of PTH in bone is valuable in the light

* This work was supported by grants-in-aid received from the Japanese Ministry of Education (21st Century Center of Excellence Program, Molecular Destruction and Reconstitution of Tooth and Bone, Grants 18109011, 18659438, 18123456, and 20013014) and grants from the Japan Space Forum, NASDA, and the Japan Society for Promotion of Science (JSPS Core to Core Program). The costs of publication of this article were defrayed in part by the payment of page charges. This article must therefore be hereby marked "*advertisement*" in accordance with 18 U.S.C. Section 1734 solely to indicate this fact.

[S] The on-line version of this article (available at http://www.jbc.org) contains supplemental supplemental Figs. 1 and 2.

[1] To whom correspondence should be addressed: Dept. of Molecular Pharmacology, Medical Research Institute, Tokyo Medical and Dental University, 2-3-10 Kanda-Surugadai, Chiyoda-ku, 101-0062, Tokyo, Japan. Tel.: 81-3-5280-8066; Fax: 81-3-5280-8066; E-mail: noda.mph@mri.tmd.ac.jp.

[2] The abbreviations used are: PTH, parathyroid hormone; PTHrP, parathyroid hormone related peptide; PPR, PTH/PTHrP receptor; caPPR, constitutively active PPR; OPN, osteopontin; CRE, cyclic AMP-response element; micro-CT, micro-computed tomography; TRAP, tartrate-resistant acid phosphatase; MS, mineralizing surface; HSC, hematopoietic stem cell; siRNA, small interfering RNA; BV/TV, bone volume/tissue volume; MTT, 3-[4,5-dimethylthiazol-2-yl]-2,5 diphenyltetrazolium bromide; MS, mineralizing surface; BS, bone surface; N.Oc, osteoclasts per area; WT, wild type; KO, knock out.

Downloaded from www.jbc.org at Tokyo Ikashika Daigaku on March 18, 2009

ASBMB The Journal of Biological Chemistry jbc

of two major aspects. First, administration of PTH to patients is restricted to only two years, in part resulting from concern for development of osteosarcoma, as found in preclinical studies (12). Currently, no rational counter-modalities are available for osteosarcoma. Second, fractures in patients treated with PTH still occurs, although the rate is significantly reduced (13). This fact indicates that PTH alone is not enough to fully prevent fractures associated with osteoporosis (14, 15).

Although antagonists for systemic calcemic actions of PTH are relatively well studied, local antagonists of PTH action in bone are poorly understood. We have recently observed that the anabolic action of PTH at an optimal dosage was enhanced in mice deficient in osteopontin (OPN) (16), suggesting that OPN plays a role as a local antagonist. OPN is a major non-collagenous protein expressed by osteoblasts and primarily localized on bone surfaces and in the cement lines in bone. OPN accumulates in mineralized bone matrix, supports attachment of bone cells to matrix surfaces, and inhibits hydroxyapatite crystal formation and growth. Furthermore, OPN functions as a cytokine acting on intracellular signaling pathways through its interaction with receptors. OPN is involved in a variety of cellular events such as proliferation, apoptosis, and chemotaxis (17, 18).

OPN-deficient mice are fertile, their litter size is normal, and they develop normally. Bones and teeth of OPN-null mice are morphologically normal. Furthermore, osteoblasts and osteoclasts *in vivo* do not show major abnormalities in OPN-null mice (19). OPN-null mice exhibit impaired type 1 immunity to viral and bacterial infection (20) and are resistant to ovariectomy-induced (21) or unloading-induced bone loss (22).

Col1a1-caPPR transgenic (PPR-tg) expresses a constitutively active form of the PTH receptor specifically in osteoblasts under the control of the collagen α1 promoter. These mice have increased trabecular bone volume and a decrease in cortical bone thickness (23). The transgenic mice show an increased number of osteoblast precursors and mature osteoblasts as well as osteoclasts. Histological examination revealed an intense staining for OPN in trabecular bone in these mice, suggesting a role for OPN in this system (24), but the nature of this role is not known.

Because injection of PTH has systemic effects and OPN is expressed by diverse cell types in the body, it is not clear at what level OPN may modulate PTH signaling. To address specifically the interaction of PTH and OPN in osteoblasts, we overexpressed the constitutively active PTH/PTHrP receptor mutant (H223R, caPPR) specifically in cells of the osteoblastic lineage *in vivo* in the absence of OPN.

EXPERIMENTAL PROCEDURES

Generation of OPN-deficient Col1a1-caPPR Transgenic Mice—$OPN^{-/-}$ mice in 129/(S1,S7) mixed background (19) and Col1a1-caPPR transgenic (PPR-tg) mice in FVB/N background were previously reported (23). For Col1a1-caPPR transgenic mice, a 2.3-kilobase fragment of the mouse Col1a1 promoter was ligated upstream to the entire coding region of human mutated Jansen type PTH/PTHrP receptor (HKrk-H223R, along with the cloning vector pcDNAI sequence that contains poly(A) signal. Generation of OPN-deficient Col1a1-caPPR transgenic mice was performed by crossing male hemizygous PPR-tg $OPN^{+/-}$ mice with female $OPN^{+/-}$ mice. Ten-week-old male littermates of four genotypes (PPR-wt/OPN-WT, PPR-wt/OPN-KO, PPR-tg/OPN-WT, PPR-tg/OPN-KO) were analyzed. All experiments were performed according to institutionally approved guidelines for animal welfare.

Three-dimensional Micro-CT Analysis of Bone—Imaging of distal metaphyses of the femora was performed using a micro-CT apparatus (Scan Xmate-E090, Comscan Techno Co. Kanagawa, Japan). Three-dimensional micro-CT images were analyzed and quantified using an automated image analyzer (TRI/3D-BON, Ratoc System Engineering Co. Tokyo, Japan). Trabecular bone mass was examined in an area with its closest and furthest edges at 0.25 and 2.00 mm, respectively, from the growth plate in the distal ends of the femora.

Histomorphometric Analysis of Bone—Calcein (1.6 mg/kg body weight) was injected intraperitoneally 9 and 2 days before sacrifice. Femora were embedded in methyl methacrylate, and 3-μm-thick sagittal sections of distal metaphyses and horizontal sections of midshaft regions were prepared. Calcein labeling was visualized using a confocal laser microscope (LSM510, Carl Zeiss) with an excitation wavelength of 488 nm and a 550-nm band-pass filter. The dynamic histomorphometry was conducted in the secondary spongiosa (1.0 × 1.0 mm); the cortical bone compartment was excluded from the analysis. von Kossa staining and Masson-Goldner staining were conducted as described elsewhere. Tibiae were decalcified in 10% EDTA and embedded in paraffin, and 7-μm-thick sagittal serial sections of proximal metaphyses were prepared. Tartrate-resistant acid phosphatase (TRAP) staining was used to quantify osteoclast number and osteoclast surface.

Serum Osteocalcin—Blood samples were collected at the time of sacrifice, and serum was separated. Serum osteocalcin levels were determined by using IRMA kit (Immutopics).

Urinary Deoxypyridinoline—Urine samples were individually collected in metabolic cages (Natsume) during the last 24 h before sacrifice. Urinary deoxypyridinoline levels were measured by enzyme-linked immunosorbent assay (DPD EIA kit, Metra Biosystems).

Transfection and Luciferase Assay—MC3T3-E1 osteoblastic cells were plated on 24-well plates at a density of 10^4 cells per well. Transfection of siRNA and plasmid DNA was performed on day 1 using Lipofectamine 2000 (Invitrogen). siRNA for OPN was manufactured by Ambion (Silencer Pre-designed siRNA, ID #150969 for mouse Spp1). Silencer Negative Control #1 siRNA was used as a control. Plasmid DNA containing human mutated PTH/PTHrP receptor (H223R) was previously described (25). pcDNA3.1 (Invitrogen) was used as a control. For reporter plasmids, pCRE-luc (PathDetect, Stratagene) reporter plasmid was used to measure cAMP-response element activity. Renilla luciferase reporter vector pGL4 (Promega) was used as an internal control. For transfection, each well received 0.2 μg of H223R plasmid DNA or control, 20 pmol of siRNA for OPN or control, 0.2 μg of pCRE-luc, and 40 ng of Renilla luciferase plasmid combined with 1.0 μl of Lipofectamine 2000. The luciferase assay was performed using the Dual Luciferase Reporter Assay System (Promega) 48 h after transfection (day

Downloaded from www.jbc.org at Tokyo Ikashika Daigaku on March 18, 2009

3). Luciferase activity was measured using a luminometer (Lumat LB 9507, Berthold Technologies).

Quantitative Real-time PCR Analysis—Transfected cells were lysed 3 days after transfection in TRIzol reagent (Invitrogen). One microgram of total RNA was treated with DNase I (Invitrogen) before reverse transcription. First-strand cDNA was synthesized using SuperScript II transcriptase and oligo(dT)$_{12-18}$ primers (Invitrogen). Quantitative real-time PCR analysis was carried out using an iCycler (Bio-Rad) and iQ5 data analyzing software. The reaction was performed in a 25-μl reaction mixture containing 2-μl cDNA samples, 1-μl sense and antisense primer mix (5 μM), and 12.5 μl of iQ SYBR Green Supermix. The primer sequences were designed based on a Beacon Designer (Bio-Rad) program. PCR conditions were 95 °C for 15 s, 55 °C for 30 s, and 72 °C for 30 s for 40–50 cycles.

Statistical Analysis—Results are expressed as the mean values ± S.D. Statistical evaluation was conducted based on analysis of variance followed by Fisher's protected least significant difference test after the Bartlett test. A p value of <0.05 was considered significant.

RESULTS

Osteopontin Deficiency Enhances the Increase in Trabecular Bone Mass Induced by Osteoblast-specific Transgenic Expression of caPPR—Osteopontin deficiency by itself did not appreciably increase fractional trabecular bone volume (BV/TV), although there was a slight extension of the spongiosa into the diaphyseal area as reported previously (19) (Fig. 1*a*, *PPR-wt/OPN-KO*, #). Transgenic mice harboring the constitutively active mutant type of PTH/PTHrP receptor in osteoblastic cells (PPR-tg/OPN-WT) showed an increase in the trabecular bone in the adult mice, consistent with previous results (23). This increase was seen on three-dimensional micro-CT images as the presence of dense trabeculation in the epiphyseal regions of the distal end of the femur (Fig. 1*a*, *PPR-tg/OPN-WT*). Three-dimensional micro-CT images also revealed that transgenic expression of caPPR resulted in an extension of trabecular bone toward the diaphyseal regions, where the meshwork pattern of the trabecular bone was maintained (Fig. 1*a*, PPR-tg/OPN-WT, *asterisk*). These observations were comparable to those in mice treated with intermittent administration of PTH (23).

It has been reported that PPR-tg mice exhibit intense staining for osteopontin in trabecular bones, suggesting a role of OPN in this system (24). As shown in Fig. 1*a* (PPR-tg/OPN-KO), OPN-deficiency increased trabecular bone dramatically and resulted in a denser and finer meshwork patterning of the trabecular bone than that in PPR-tg mice (PPR-tg/OPN-WT). A dense trabecular bone patterning was observed not only in the epiphyseal region but also far into the diaphyseal region (Fig. 1*a*, *PPR-tg/OPN-KO*, §). The increase in fractional bone volume (three-dimensional BV/TV) due to caPPR expression in osteoblasts was significantly enhanced by osteopontin-deficiency (Fig. 1*b*). It was also observed that the increase in trabecular number (three-dimensional *Tb.N*) induced by caPPR was further enhanced by OPN-deficiency (Fig. 1*c*). Changes in trabecular thickness (Fig. 1*d*) and trabecular separation in PPR-tg/OPN-WT mice (Fig. 1*e*) were not significantly altered by the absence of OPN.

We also observed a slight trabeculation of the cortical bone in PPR-tg mice (Fig. 1*a*, *open arrowhead*). This trabeculation of the cortical bone was increased and extended in the absence of OPN (Fig. 1*a*, *thin arrows*). In addition, the tapering of the metaphyseal region of the femur was reduced by the absence of OPN in transgenic mice expressing caPPR (Fig. 1*a*, *open arrow*).

These observations were consistently obtained in eight independent sets of littermates. These observations suggest that OPN prevents excessive trabecular bone formation caused by caPPR overexpression in cells of the osteoblastic lineage.

The bone mineral density of PPR-tg/OPN-KO femora was significantly higher than that of PPR-wt/OPN-WT and PPR-wt/OPN-KO mice (Fig. 1*f*), and the entire medullary cavity of the PPR-tg/OPN-KO femora was filled with cancellous bone as shown by two-dimensional micro-CT cross-sectional images made at the middle of the femur (Fig. 1*i*). Furthermore, the effects of PPR-tg/OPN-KO genotype were not exclusive to the appendicular skeleton. Craniofacial flat bones (calvariae) and axial bones (lumbar vertebrae) exhibit phenotypic characteristics consistent with those apparent in the appendicular skeleton (femur) as shown by three-dimensional micro-CT images of the fourth lumbar vertebrae and the calvariae (Fig. 1, *k* and *l*).

Other phenotypic differences between the four mouse groups such as mobility, gait pattern, pain sensation, or any other noticeable manifestations were not obvious except for the slightly reduced body weight and smaller size in PPR-tg/OPN-KO mice (Fig. 1*g* and data not shown). Accordingly, the bones tended to be slightly shorter in the double mutant mice (Fig. 1, *h* and *j*).

Osteopontin Deficiency Changes the Cellular Content of the Bone Marrow Space in the Presence of Osteoblast-specific Transgenic Expression of caPPR—Hematoxylin and eosin staining of the tibiae from wild-type and osteopontin-deficient mice-expressing caPPR transgene indicated that osteopontin deficiency induced an alteration in the cellular composition in bone marrow. An increase in the number of mesenchymal cells was observed in the bone marrow spaces of PPR-tg mice, and this change was strongly enhanced by the absence of OPN (Fig. 2*b*). Hematopoietic cells, which are recognized by their high nuclear-cytoplasmic ratio (Fig. 2*b*), were reduced in number in the bones of PPR-tg/OPN-KO mice (Fig. 2*b*, *right panel*), indicating that OPN deficiency changed the cellular content of the bone marrow space in these animals. It appeared that the bone marrow space in PPR-tg/OPN-KO mice was occupied by predominantly mesenchymal cells.

Higher magnification images of the cells adjacent to the trabecular bones showed thick lining cells on the trabecular bone surface in PPR-tg/OPN-WT mice (Fig. 2*b*, *open arrowhead*) compared with thin lining cells in PPR-wt/OPN-WT or PPR-wt/OPN-KO mice (Fig. 2*b*, *closed arrowheads*). This alteration was further enhanced by the absence of OPN in the transgenic mice. To examine the nature of these stromal cells, we stained the sections for alkaline phosphatase activity. Compared with PPR-wt/OPN-WT or PPR-wt/OPN-KO, overexpression of caPPR under the control of Col1a1 promoter (PPR-tg/OPN-WT) resulted in strong staining for alkaline phosphatase activity in cells on the trabecular bone surface (Fig. 2*c*, *red arrowheads*). In these sections most of the alkaline phospha-

Downloaded from www.jbc.org at Tokyo Ikashika Daigaku on March 18, 2009

The Journal of Biological Chemistry

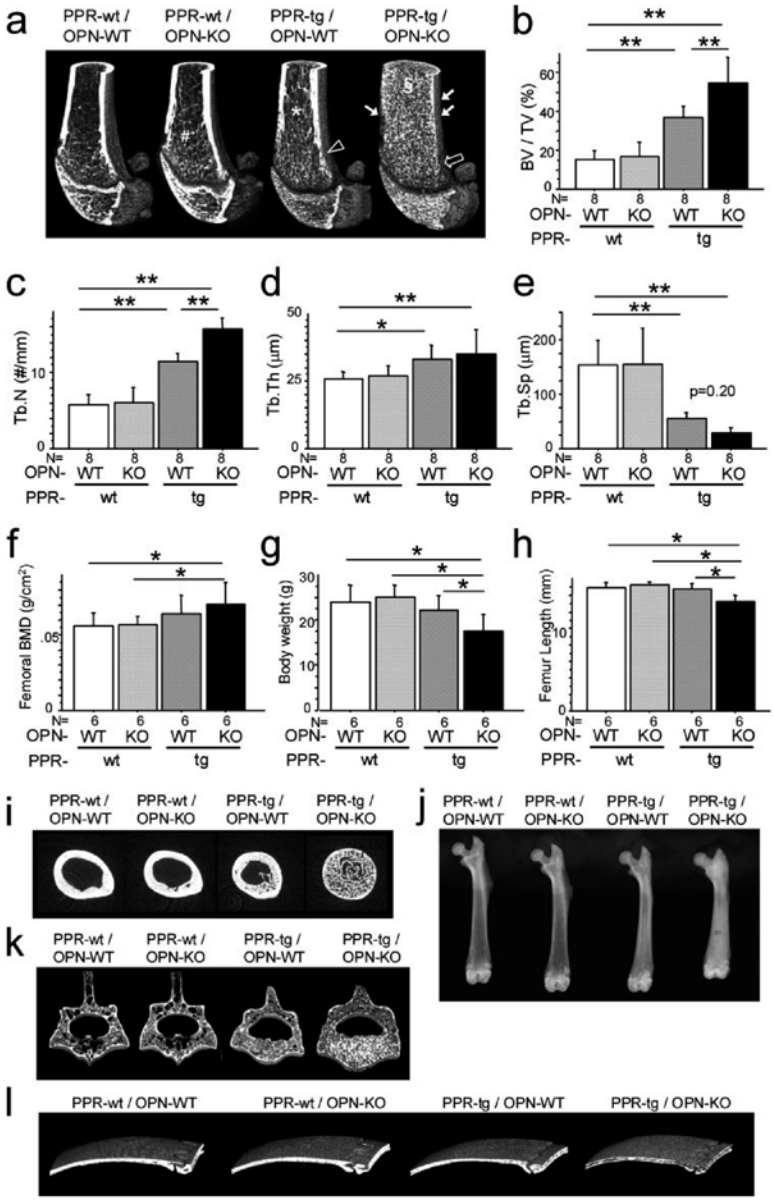

FIGURE 1. **OPN deficiency enhanced skeletal phenotypes of Col1a1-caPPR transgenic mice.** Three-dimensional micro-CT images of the distal metaphyses of the femora (*a*) and bone volume/tissue volume (*BV/TV*, %) (*b*), trabecular number (*#/mm*) (*c*), trabecular thickness (*μm*) (*d*), and trabecular separation (*e*) in the secondary trabeculae. OPN deficiency enhanced trabecular BV/TV and trabecular number of Col1a1-caPPR transgenic mice (*, $p < 0.05$; **, $p < 0.01$, $n = 8$ per group; *a*, #, *, §, extension of trabecular bone regions in each mutant mice; *open* and *thin arrow*, tapering of the metaphyses in each mutant mice). The bone mineral density of the whole femora determined by DEXA (*f*), body weight (*g*), and the length of the femora (*h*) ($n = 6$ per group). The bone mineral density of PPR-tg/OPN-KO femora was significantly higher than PPR-wt/OPN-WT and PPR-wt/OPN-KO mice because the entire diaphyseal medullary cavity was filled with cancellous bone. Body weights and femur lengths of PPR-tg/OPN-KO mice were significantly lower than all other mouse genotypes. Two-dimensional micro-CT cross-sectional images of the diaphysis at the middle of the femora (*i*), x-ray radiographs of the femora (*j*), three-dimensional micro-CT images of the fourth lumbar vertebrae (*k*), and the calvariae (*l*). Effects of PPR-tg/OPN-KO genotype were not exclusive to the appendicular skeleton. Craniofacial flat bones (calvariae) and axial bones (lumbar vertebrae) exhibit phenotypic characteristics consistent with those apparent in the appendicular skeleton (femur).

Downloaded from www.jbc.org at Tokyo Ikashika Daigaku on March 18, 2009

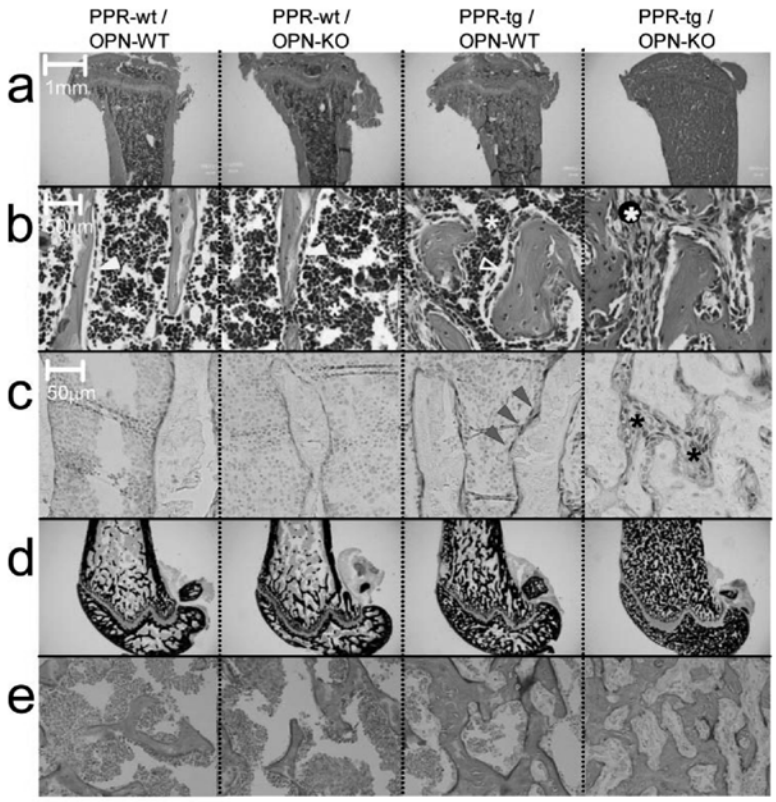

f Complete blood count (CBC)

	WBC	RBC	Hemoglobin	Hematocrit	Plt	MCV	MCH	MCHC
PPR-tg/OPN-WT (1)	2900	856	13.2	47	33.5	55	15.4	28.1
PPR-tg/OPN-WT (2)	2900	936	13.8	52.5	27.2	56	14.7	26.3
PPR-tg/OPN-KO	4100	947	14.7	52	95.4	55	15.5	28.3

FIGURE 2. **Histology of the metaphyses of the tibiae of the mutant mice.** Shown are hematoxylin and eosin ×20 (*a*) and ×400 (*b*), alkaline phosphatase ×400 (*c*), von Kossa (*d*), and Masson-Goldner (*e*) staining of wild-type (*PPR-wt/OPN-WT*), OPN-deficient (*PPR-wt/OPN-KO*), Col1a1-caPPR Tg (*PPR-tg/OPN-WT*), and OPN-deficient Col1a1-caPPR Tg (*PPR-tg/OPN-KO*) mice. PPR-tg/OPN-KO bone marrow was occupied with alkaline phosphatase-positive stromal cells, and their mineralization and osteoid volume were normal (*b*, *open* and *closed arrowhead*, lining cells on the bone surface; *closed asterisk*, cells in hematopoietic lineage; *open asterisk*, stromal/osteoblastic cells; *c*, *red arrowhead*, alkaline phosphatase-positive cells on the bone surface; *asterisks*, alkaline phosphatase-positive cells within the intertrabecular space in the bone marrow). *f*, complete blood cell (*CBC*) count of the mutant mice (*RBC*, red blood cells; *WBC*, white blood cells; *Plt*, platelet; *MCV*, mean corpuscular volume; *MCH*, mean corpuscular hemoglobin; *MCHC*, mean corpuscular hemoglobin concentration). Red blood cell counts, hemoglobin, and hematocrit were equivalent between PPR-tg/OPN-WT and PPR-tg/OPN-KO mice. White blood cell counts for PPR-tg/OPN-KO mice were ~30%higher than PPR-tg/OPN-WT mice, and platelet counts for PPR-tg/OPN-KO mice were 3-fold higher than PPR-tg/OPN-WT mice.

tase-positive cells were closely attached to the trabecular bone (Fig. 2*c*, *PPR-tg/OPN-WT*). In contrast to PPR transgenic mice, osteopontin deficiency in the presence of caPPR (PPR-tg/OPN-KO) resulted in numerous alkaline phosphatase-positive cells within the intertrabecular space in the bone marrow (Fig. 2*c*, *asterisks*). Some of these cells were attached to the trabecular bone surface, whereas others were found inside the intertrabecular space. These data indicated that osteopontin deficiency in the presence of osteoblast-specific caPPR expression increased the number of alkaline phosphatase-positive osteoblastic cells to a level that almost fully occupied the intertrabecular space.

The trabecular bone filling the bone marrow space of PPR-tg/OPN-KO mice was well mineralized, at least based on analysis using von Kossa staining (Fig. 2*d*). Osteoid, stained red in Masson-Goldner staining, was only marginally increased in PPR-tg/OPN-KO mice (Fig. 2*e*). Therefore, although osteopontin deficiency increased bone mass in the trabecular bone in the transgenic mice, the calcification state of the bone was similar to that of PPR-tg/OPN-WT mice.

Despite the reduced marrow cavity, hematopoiesis was sustained in PPR-tg/OPN-KO mice. Red blood cell counts, hemoglobin, and hematocrit in peripheral blood were equivalent between PPR-tg/OPN-WT and PPR-tg/OPN-KO mice, whereas white blood cell counts and platelet counts for PPR-tg/OPN-KO mice were higher than those of PPR-tg/OPN-WT mice (Fig. 2*f*).

Osteopontin Deficiency Further Enhances Bone Formation Activity Induced by Osteoblast-specific Transgenic Expression of caPPR—To address whether the absence of osteopontin affects bone formation *in vivo* in caPPR transgenic mice, we carried out histomorphometric analysis of the distal femora. Calcein injections yielded a consistent dual labeling in trabecular bone in PPR-wt/OPN-WT and PPR-wt/OPN-KO mice; this dual labeling was also observed in trabecular bone of PPR-tg/OPN-WT mice. However, in PPR-tg/OPN-KO mice, the calcein labeling was uneven, possibly reflecting the crowded nature of the trabecular bone in these mice (Fig. 3*a*). Such an uneven pattern of calcein labeling is a characteristic feature of rapid cancellous bone formation. In wild-type bone, osteoblasts are laterally connected by several molecules including connexin, and many osteoblasts work in concert to form bone in a planar fashion, resulting in the even pattern of calcein labeling seen in histological sections. Possibly, this lateral connectivity is impaired in the event of enhanced bone formation. This uneven pattern of labeling is also observed in the case of rapid cancellous bone formation after fracture.

Downloaded from www.jbc.org at Tokyo Ikashika Daigaku on March 18, 2009

ASBMB
The Journal of Biological Chemistry
jbc

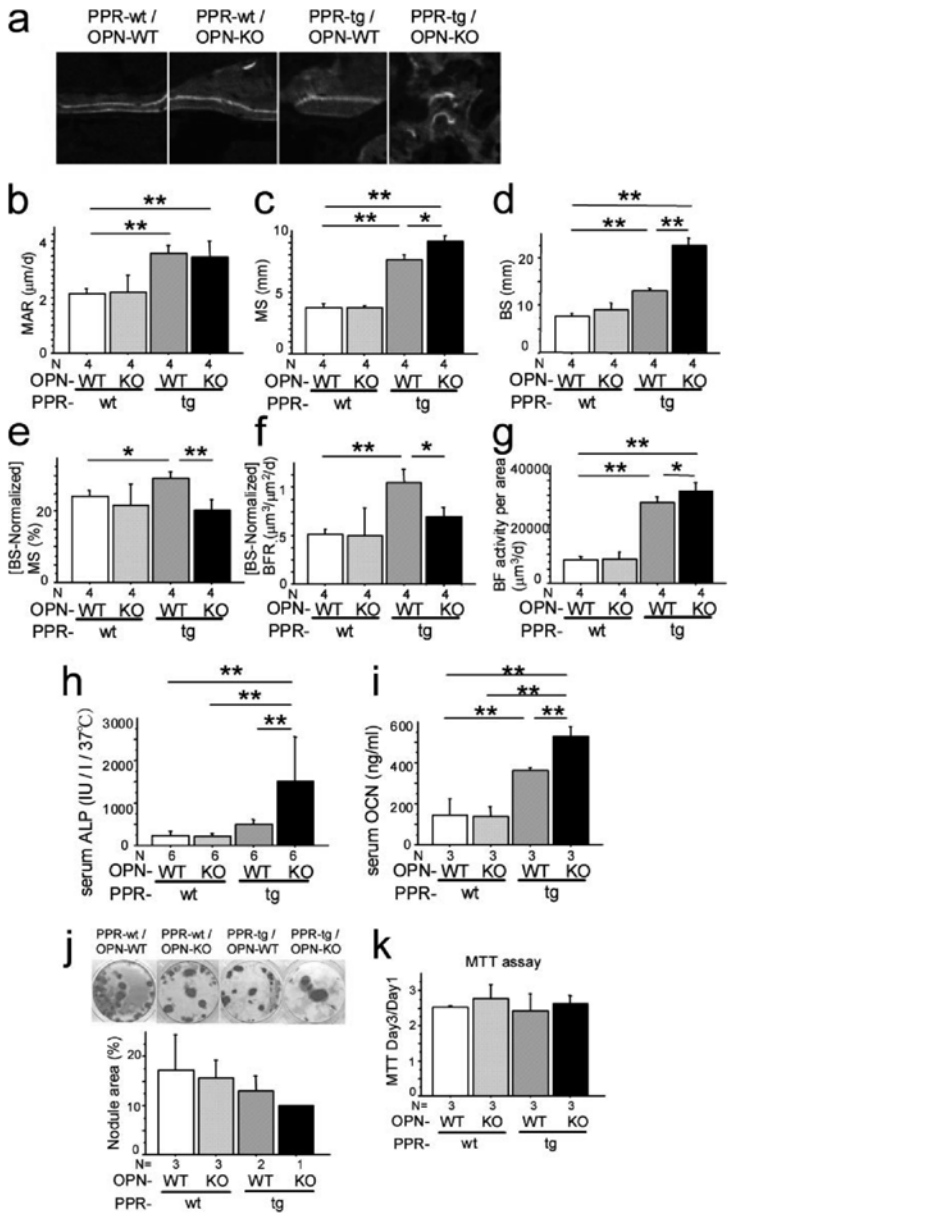

FIGURE 3. **Osteopontin deficiency enhanced bone formation activities of Col1a1-caPPR transgenic mice.** Dynamic histomorphometry of the trabecular bone in the distal metaphyses of the femora is shown. Calcein was injected at 7-day intervals, and undecalcified sections were scanned with confocal laser microscopy. PPR-tg/OPN-KO trabeculae exhibited an uneven pattern of calcein labeling (*a*). Mineral apposition rate (*MAR*) (*b*), mineralized surface per area (*MS*) (*c*), bone surface per area (*BS*) (*d*), mineralized surface per bone surface (*MS/BS*) (*e*), bone formation rate per bone surface (*BFR*) (*f*), and bone formation activity per area (BF activity per area) (*g*) ($n = 4$ per group) are shown. *i*, serum alkaline phosphatase (*ALP*, *h*) ($n = 6$ per group; *IU/l*, international unit per liter) and osteocalcin (*OCN*) levels ($n = 3$ per group). OPN deficiency enhanced systemic bone formation parameters of Col1a1-caPPR transgenic mice (*, $p < 0.05$; **, $p < 0.01$). *j*, mineralized nodule formation of bone marrow cells. Bone marrow cell cultures were set up from marrow tissues from all four mouse genotypes, cultured under osteogenic conditions, and assayed for nodule area per standard area well ($n = 3$ for PPR-wt/OPN-WT, PPR-wt/OPN-KO, $n = 2$ for PPR-tg/OPN-WT, $n = 1$ for PPR-tg/OPN-KO mice). All marrow sources yielded roughly similar nodule areas although there was a progressive negative trend in the data (not statistically significant). MTT assays of osteoblastic cells (*k*) ($n = 3$ per group) are shown. Osteoblastic cells were obtained from calvarial outgrowth cultures for all four mouse genotypes. These cells were cultured for 1 or 3 days and assayed for a metabolic activity via MTT, and these values were used as a surrogate measure for cell number. Calvarial outgrowth-derived osteoblastic cell cultures from all mouse genotypes exhibited similar MTT conversion ratios (day 3 over day1), indicating that similar numbers of cells proliferated during the culture.

Downloaded from www.jbc.org at Tokyo Ikashika Daigaku on March 18, 2009

As noted previously, PPR-tg mice exhibited an increase in mineral apposition rate (Fig. 3, *a* and *b*). Osteopontin deficiency in the presence of caPPR did not further enhance the mineral apposition rate (Fig. 3*b*). Analyses of mineralizing surface per area (MS) showed an increase in PPR-tg mice and osteopontin deficiency in the presence of caPPR, further enhanced mineralizing surface per area (Fig. 3*c*). Bone surface per unit area (BS) was significantly increased in PPR-tg mice, and OPN deficiency in these mice further increased the bone surface per area by about 80% (Fig. 3*d*). Because BS was significantly higher in the double mutant mice (PPR-tg/OPN-KO), calculated values (MS normalized against BS) for MS/BS indicated a decrease in these animals (Fig. 3*e*). Similarly, bone formation rate normalized against the BS was somewhat reduced due to the large increase of the BS in the double mutant mice (PPR-tg/OPN-KO) (Fig. 3*f*). Total bone formation activities per unit area (1 mm^2) of the bone were higher in the double mutant mice than in PPR-tg mice (Fig. 3*g*).

We further tested whether such elevated bone formation activities observed in histomorphometry (Fig. 3*g*) were reflected in biochemical parameters. Serum alkaline phosphatase activities were barely altered in PPR-tg mice. However, osteopontin deficiency in the presence of caPPR significantly (about 3-fold) increased serum alkaline phosphatase levels compared with PPR-tg mice, reflecting the presence of high numbers of osteoblastic cells expressing alkaline phosphatase in the skeleton of these animals (Fig. 3*h*). Osteocalcin levels were increased in PPR-tg mice. Similarly, osteopontin deficiency in the presence of caPPR significantly enhanced serum osteocalcin levels (Fig. 3*i*). These observations indicated that osteopontin deficiency further increased the number of cells producing these markers in caPPR transgenic mice, in which the levels of these markers were already higher than those of wild-type mice. Together, these results suggest that PTH signaling in bone-forming cells is under negative control of the bone matrix protein, osteopontin.

Additionally, mineralized nodule formation of bone marrow cells and MTT assays of osteoblastic cells obtained from calvarial outgrowth cultures were performed (Fig. 3, *j* and *k*). The results of these *in vitro* assays suggest that the contribution of cell-autonomous effects to the phenotype of PPR-tg/OPN-KO mice is relatively minor.

Osteopontin Deficiency Further Enhances Bone Resorption Activity Induced by Osteoblast-specific Transgenic Expression of caPPR—It was shown previously that PPR-tg mice exhibited an elevation in bone formation as well as bone resorption, with the balance favoring bone formation. This results in the net increase in bone mass (23). We further asked whether the absence of osteopontin in the local milieu alters osteoclastic activity in the transgenic mice.

The number of osteoclasts per area (N.Oc) based on histomorphometric analysis was increased in PPR-tg mice as noted before (Fig. 4, *a* and *b*) (23). Because of the increase in bone surface per area, osteoclast number normalized against bone surface (N.Oc/BS) of PPR-tg mice was not altered compared with wild-type mice (Fig. 4*c*). N.Oc was further enhanced by osteopontin deficiency in the transgenic mice (Fig. 4, *a* and *b*). Despite a further increase in the bone surface per area in PPR-tg/OPN-KO mice, osteoclast number normalized against bone surface (N.Oc/BS) was significantly increased in the double mutant mice (Fig. 4*c*), indicating that osteopontin deficiency enhanced osteoclast number per unit surface in the transgenic mice (Fig. 4*c*). Osteoclast surface per bone surface (*OcS/BS*) was

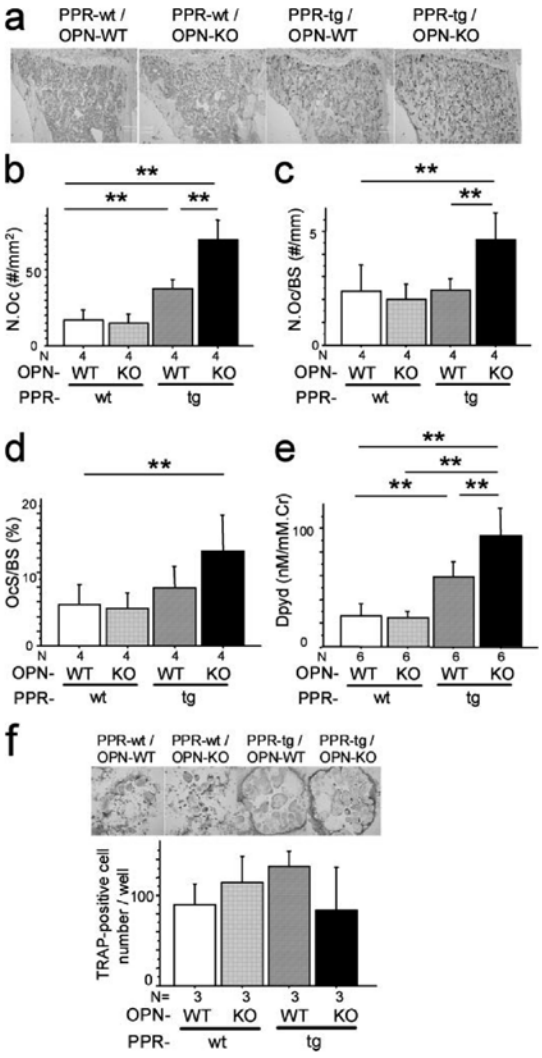

FIGURE 4. **Osteopontin deficiency enhanced bone resorption activities of Col1a1-caPPR transgenic mice.** *a*, TRAP staining of decalcified sections of the mesial metaphyses of the tibiae. Shown are osteoclast number per area (*N.Oc, #/mm²*) (*b*), osteoclast number per bone surface (*N.Oc/BS, #/mm*) (*c*), and osteoclast surface per bone surface (OcS/BS, %) (*d*) (*, $p < 0.05$; **, $p < 0.01$, $n = 4$ per group). *e*, urinary deoxypyridinoline (*Dpyd*) excretion levels ($n = 6$ per group). *Cr*, creatinine. OPN deficiency enhanced not only the number but also the activity of osteoclasts of Col1a1-caPPR transgenic mice. *f*, TRAP-positive multinucleated cell development of bone marrow cells. Osteoclastic cell cultures were set up from bone marrow tissues derived from all four mouse genotypes ($n = 3$ per group). Similar numbers of TRAP-positive multinucleated cells were generated in these cultures with no differences noted between genotypes.

Downloaded from www.jbc.org at Tokyo Ikashika Daigaku on March 18, 2009

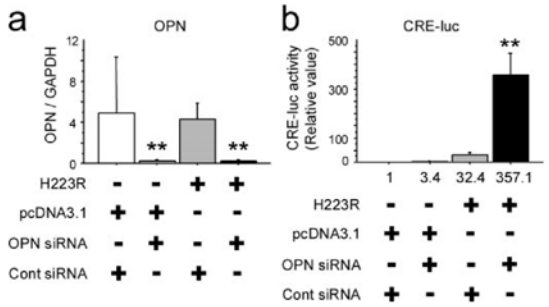

FIGURE 5. **Osteopontin mRNA knockdown and constitutively active PTH/PTHrP receptor (H223R) synergistically enhanced cAMP-response element activity in MC3T3-E1 osteoblastic cells.** MC3T3-E1 osteoblastic cells were plated on 24-well plates at a density of 10^4 cells per well, and small interference RNAs for OPN and H223R were cotransfected the following day. CRE activity was evaluated by the luciferase assay, and OPN mRNA expression was measured by quantitative real-time PCR after 48 h. OPN mRNA expression was efficiently knocked down by siRNA in this experiment (*a*). As a reference, control siRNA were used. *b*, cAMP-response element activity after cotransfection of OPN siRNA and H223R. H223R increased CRE activity by 32.4-fold. Cotransfection of OPN siRNA and H223R synergistically enhanced CRE activity by over 350-fold (*, $p < 0.05$; **, $p < 0.01$). Data represent three independent experiments.

not significantly increased in PPR-tg mice (Fig. 4*d*). Osteopontin deficiency tended to increase the levels of osteoclast surface per bone surface in the transgenic mice, although the difference was not statistically significant (Fig. 4*d*, $p = 0.056$).

Despite the presence of elevated bone resorption activity, high bone mass was observed in PPR-tg/OPN-KO mice. This is possibly due to an even higher bone formation activity in these mice (Fig. 3). In terms of PPR-tg single mutant mice, high bone mass, despite enhanced osteoclastic activity, has been attributed to even more enhanced osteoblastic activity (23).

To examine whether these morphological observation could be reflected in biochemical aspects, we measured urinary excretion levels of deoxypyridinoline. Transgenic mice expressing caPPR under Col1a1 promoter had increased levels of deoxypyridinoline excretion in the urine, as compared with control mice (Fig. 4*e*). Osteopontin deficiency in the presence of caPPR further increased urinary deoxypyridinoline excretion (Fig. 4*e*). These observations indicated that the presence of osteopontin suppressed the elevation of osteoclastic resorption activities caused by osteoblast-specific overexpression of constitutively active PTH/PTHrP receptor.

Additionally, bone marrow cells of the four genotypes were cultured, and TRAP-positive multinucleated cells were developed *ex vivo* to investigate osteoclast differentiation. TRAP-positive cell development was similar among the four genotypes (Fig. 4*f*), suggesting that the ability of osteoclast precursors to differentiate is similar in cells from both genotypes. Although we did not measure the actual resorptive activity levels of these osteoclast-like cell cultures, the presence of TRAP strongly suggests that these cells are osteoclasts.

Molecular Convergence of OPN Signaling and PPR Signaling on cAMP-response Element (CRE) Activities in Osteoblastic Cells—To address whether caPPR signaling inside the osteoblastic cell compartment is down-regulated by osteopontin, we utilized MC3T3-E1 osteoblastic cells that express high levels of OPN. OPN mRNA levels were significantly reduced in MC3T3-E1 cells treated with OPN siRNA compared with the cells treated with control siRNA (Fig. 5*a*). This suppression was observed regardless of the presence of caPPR (H223R) or control plasmid (Fig. 5*a*). In cotransfection experiments with a CRE-luciferase reporter, OPN siRNA did not affect luciferase activity significantly, whereas the forced expression of the H223R mutant form of PPR (caPPR) elevated luciferase activity about 30-fold. Suppression of OPN by siRNA further enhanced the luciferase activity up to 300-fold compared with control: *i.e.* 10-fold compared with the group where H223R plasmid and control siRNA were transfected (Fig. 5*b*). These observations indicated that at least one of the actions of OPN is to suppress the intracellular events triggered by the presence of constitutively active (H223R) PPR in osteoblastic cells.

DISCUSSION

Our discovery of OPN as a suppressor of the PTH signaling-induced increase in bone mass reveals more functional significance of this molecule. OPN shares some features with cytokines and has additional roles as an inhibitor of mineralization (19). In addition, OPN regulates signaling within osteoblastic cells, as caPPR-induced CRE-activities were enhanced by the reduction of OPN. Our data indicate that the effects of OPN-deficiency are, at least in part, due to the modulation of transcriptional events regulated by signaling downstream of PTH/PTHrP receptor.

It is intriguing that PTH has been shown to increase the niche activity for hematopoietic stem cells (HSCs) (26, 27) and that osteopontin has been reported as a suppressive component of HSC niche (24, 28). However, the mechanism of OPN action on HSCs and their niche has not been fully elucidated. Because osteoblastic cells are important components of the niche within the bone microenvironment, any reduction of osteoblastic function suppresses niche function (29). For instance, recent reports indicated that the sympathetic nervous system suppresses osteoblastic cells (30, 31), and this suppression of osteoblasts results in the down-regulation of the niche function for hematopoietic stem cells in the bone marrow microenvironment, releasing HSCs into the blood stream (29). The suppressive effects of OPN on bone formation discovered in our experiments could also be a part of the OPN functions that negatively regulate the hematopoietic stem cell niche. As noted before, the hematopoietic and bone systems share many components. OPN may be one of them, not only as a regulator of osteoblastic activities but also as a merging center for the signals from PTH and the HSC niche in the microenvironment.

For hematopoietic cells, OPN can either induce apoptosis or suppress proliferation (24, 28). The absence of OPN may increase HSC numbers in response to stimulation by the presence of PPR-tg/OPN-KO osteoblasts. For instance, administration of PTH to OPN-null mice induced an increase in HSCs as compared with wild-type mice (24). However, the PPR-tg/OPN-KO double mutant mice did not develop anemia. Rather, they showed a significant increase of white blood cells and platelets compared with PPR-tg/OPN-WT mice (Fig. 2*f*). Therefore, although the marrow cavity was reduced due to an increase in trabecular bone mass, hematopoiesis is sustained at

Downloaded from www.jbc.org at Tokyo Ikashika Daigaku on March 18, 2009

least under our experimental conditions. Although not appreciable in the histological sections, certain levels of HSCs may still exist in the marrow environment of the double mutant mice. In fact, we observed that the number of osteoclasts was increased in PPR-tg/OPN-KO mice (Fig. 4, *a*–c), suggesting that HSCs were not deficient in these mice.

We showed previously that signals generated by mechanical stress require OPN for bone formation (22). Because bone formation is affected by mechanical stress and mechanical stress promotes proper bone formation and coupling of bone remodeling, OPN may link the PTH axis and mechanical signaling in bone.

OPN is produced by several tissue sources in both insoluble (extracellular matrix-associated) and soluble forms. These forms of OPN are part of the microenvironment in bone. OPN binds to several types of receptors including integrins and variant forms of CD44 (32), and therefore, the absence of OPN may alter more than one signaling pathway. CD44 is a cell surface glycoprotein that serves as an adhesion molecule, and its isoforms exert diverse functions. OPN-CD44 signal facilitates cell motility (33) and survival (34). Additionally, OPN increases CD44 expression in RAW264.7 leukemia cells (35), and the absence of OPN decreases surface expression of CD44 (18). Reduced CD44 signaling may impair migration and survival of hematopoietic cells, and this may contribute in part to the bone phenotype in the double mutant mice.

OPN was also shown to suppress proliferation and differentiation in a certain type of osteoblastic cells (36). We observed that stromal cells occupied the narrowed bone marrow space in PPR-tg/OPN-KO double mutant mice (Fig. 2*b*). Therefore, it would be possible that the *in vivo* environment could allow an increase in stromal cells and/or osteogenic precursors in the absence of OPN in the transgenic mice. In fact, *in vitro* assays for nodule formation, MTT, and PCR analysis suggested that contribution of cell-autonomous effects in the cells taken from PPR-tg/OPN-KO mice were relatively minor (Fig. 3, *j* and *k*, and data not shown). Additionally, when bone marrow cells of the four genotypes were cultured and TRAP-positive multinucleated cells were developed *ex vivo*, TRAP-positive cell development was similar among the four genotypes (Fig. 4*f*). These *in vitro* results suggest that the changes seen in osteoblasts and osteoclasts in PPR-tg/OPN-KO bone might not be due to cell-autonomous mechanisms, and *in vivo* environmental cues may play a role in causing the phenomena observed in our experiments.

The appearance of the high levels of cancellous bone in the diaphysis of PPR-tg/OPN-KO mice is similar to the early osteogenic phase observed after marrow ablation. This similarity is only at the early phase; in the marrow ablation model, the high turnover state in osteoblastic and osteoclastic remodeling phase in cancellous bone is transient, whereas that in the PPR-tg/OPN-KO mice is sustained and is not followed by the osteoclastic remodeling phase of the injury model.

Abundant TRAP-positive osteoclasts in the double mutant mice resulted in an increase in remodeling in two distinct compartments. Osteoclastic resorption in the cortical bone leads to a trabeculation of cortex, whereas osteoclastic resorption in the cancellous bone leads to an increase in eroded surfaces on trabecular bone (Fig. 4*a*), suggesting that the osteoclasts are not ineffective at resorbing bone. In fact, osteoclasts are effective in both cancellous and cortical bone. The net increase in bone mass of PPR-tg/OPN-KO mice is not the reflection of osteoclast dysfunction but is due to the fact that high turnover state of the bone metabolism in PPR-tg/OPN-KO mice is sustained, and the balance between osteoblasts and osteoclasts is in favor of the former. The increase in the urinary deoxypyridinoline levels gives biochemical support for the notion mentioned above (osteoclasts are effective) and coincides with the morphological observations of increase in eroded surface. The increase in serum levels of alkaline phosphatase and osteocalcin also supports the idea that high turnover state (with high levels of osteoblastic activities) is the predominant feature of bone in PPR-tg/OPN-KO mice.

It was previously reported that Col1a1-caPPR delays the transition from bone to bone marrow during postnatal growth and the formation of marrow cavities (37). Considering that OPN knockdown enhanced transcriptional events downstream to PTH/PTHrP receptor (Fig. 5) in osteoblastic cells, it is possible that OPN deficiency further delayed the transition of bone to bone marrow in PPR-tg/OPN-KO mice.

Trabeculation of cortical bone was observed in micro-CT images in PPR-tg/OPN-KO mice. Patients exhibiting primary hyperparathyroidism show similar structural characteristics. Therefore, this observation is significant and relevant along with the enormous increase in cancellous bone. However, the PPR-tg/OPN-KO mice did not develop spontaneous stress fractures in their long bones. High levels of bone mass and/or bone mineral density may compensate for the reduction in the strength of the bone in these mice.

Calvarial bones and the lumbar vertebrae were also analyzed based on three-dimensional micro-CT images and DEXA (Fig. 1, *k* and *l*, and supplemental Fig. 1). Calvarial bones recapitulated the cortical bone phenotype of PPR-tg/OPN-KO mice in that they showed a higher porosity, whereas vertebral bones recapitulated the cancellous bone phenotype of PPR-tg/OPN-KO mice, showing a higher bone volume (supplemental Fig. 1). These observations suggest that appendicular, axial, and craniofacial bones were all affected in the double mutant mice.

Overall, we have shown that the action of the systemic hormone PTH is regulated by feedback systems locally in bone where the bone matrix protein osteopontin plays an important suppressive role. Our observation will give rise to a widened concept with respect to multiple layers of feedback regulation in the PTH axis. Such multiple layers of regulation would render the body system to be versatile to adapt various environmental conditions.

REFERENCES

1. Marx, S. J. (2000) *N. Engl. J. Med.* **343,** 1863–1875
2. Bell, N. H. (1985) *J. Clin. Investig.* **76,** 1–6
3. DeLuca, H. F. (1973) *N. Engl. J. Med.* **289,** 359–365
4. Avioli, L. V., and Haddad, J. G. (1984) *N. Engl. J. Med.* **311,** 47–49
5. Rosenblatt, M. (1986) *N. Engl. J. Med.* **315,** 1004–1013
6. Schluter, K. D., and Piper, H. M. (1998) *Cardiovasc. Res.* **37,** 34–41
7. Dempster, D. W., Cosman, F., Parisien, M., Shen, V., and Lindsay, R. (1993) *Endocr. Rev.* **14,** 690–709
8. Hodsman, A. B., Bauer, D. C., Dempster, D. W., Dian, L., Hanley, D. A.,

Downloaded from www.jbc.org at Tokyo Ikashika Daigaku on March 18, 2009

Harris, S. T., Kendler, D. L., McClung, M. R., Miller, P. D., Olszynski, W. P., Orwoll, E., and Yuen, C. K. (2005) *Endocr. Rev.* **26,** 688–703
9. Jiang, Y., Zhao, J. J., Mitlak, B. H., Wang, O., Genant, H. K., and Eriksen, E. F. (2003) *J. Bone Miner. Res.* **18,** 1932–1941
10. Neer, R. M., Arnaud, C. D., Zanchetta, J. R., Prince, R., Gaich, G. A., Reginster, J. Y., Hodsman, A. B., Eriksen, E. F., Ish-Shalom, S., Genant, H. K., Wang, O., and Mitlak, B. H. (2001) *N. Engl. J. Med.* **344,** 1434–1441
11. Rosen, C. J. (2004) *Trends Endocrinol. Metab.* **15,** 229–233
12. Cinamon, U., and Turcotte, R. E. (2006) *Bone* (*NY*) **39,** 420–423
13. Rosen, C. J., and Bilezikian, J. P. (2001) *J. Clin. Endocrinol. Metab.* **86,** 957–964
14. Black, D. M., Greenspan, S. L., Ensrud, K. E., Palermo, L., McGowan, J. A., Lang, T. F., Garnero, P., Bouxsein, M. L., Bilezikian, J. P., and Rosen, C. J. (2003) *N. Engl. J. Med.* **349,** 1207–1215
15. Vestergaard, P., Jorgensen, N. R., Mosekilde, L., and Schwarz, P. (2007) *Osteoporos. Int.* **18,** 45–57
16. Kitahara, K., Ishijima, M., Rittling, S. R., Tsuji, K., Kurosawa, H., Nifuji, A., Denhardt, D. T., and Noda, M. (2003) *Endocrinology* **144,** 2132–2140
17. Denhardt, D. T., and Noda, M. (1998) *J. Cell. Biochem. Suppl.* **30–31,** 92–102
18. Denhardt, D. T., Noda, M., O'Regan, A. W., Pavlin, D., and Berman, J. S. (2001) *J. Clin. Investig.* **107,** 1055–1061
19. Rittling, S. R., Matsumoto, H. N., McKee, M. D., Nanci, A., An, X. R., Novick, K. E., Kowalski, A. J., Noda, M., and Denhardt, D. T. (1998) *J. Bone Miner. Res.* **13,** 1101–1111
20. Ashkar, S., Weber, G. F., Panoutsakopoulou, V., Sanchirico, M. E., Jansson, M., Zawaideh, S., Rittling, S. R., Denhardt, D. T., Glimcher, M. J., and Cantor, H. (2000) *Science* **287,** 860–864
21. Yoshitake, H., Rittling, S. R., Denhardt, D. T., and Noda, M. (1999) *Proc. Natl. Acad. Sci. U. S. A.* **96,** 8156–8160
22. Ishijima, M., Rittling, S. R., Yamashita, T., Tsuji, K., Kurosawa, H., Nifuji, A., Denhardt, D. T., and Noda, M. (2001) *J. Exp. Med.* **193,** 399–404
23. Calvi, L. M., Sims, N. A., Hunzelman, J. L., Knight, M. C., Giovannetti, A., Saxton, J. M., Kronenberg, H. M., Baron, R., and Schipani, E. (2001) *J. Clin. Investig.* **107,** 277–286
24. Stier, S., Ko, Y., Forkert, R., Lutz, C., Neuhaus, T., Grunewald, E., Cheng, T., Dombkowski, D., Calvi, L. M., Rittling, S. R., and Scadden, D. T. (2005) *J. Exp. Med.* **201,** 1781–1791
25. Schipani, E., Langman, C. B., Parfitt, A. M., Jensen, G. S., Kikuchi, S., Kooh, S. W., Cole, W. G., and Juppner, H. (1996) *N. Engl. J. Med.* **335,** 708–714
26. Calvi, L. M., Adams, G. B., Weibrecht, K. W., Weber, J. M., Olson, D. P., Knight, M. C., Martin, R. P., Schipani, E., Divieti, P., Bringhurst, F. R., Milner, L. A., Kronenberg, H. M., and Scadden, D. T. (2003) *Nature* **425,** 841–846
27. Adams, G. B., Martin, R. P., Alley, I. R., Chabner, K. T., Cohen, K. S., Calvi, L. M., Kronenberg, H. M., and Scadden, D. T. (2007) *Nat. Biotechnol.* **25,** 238–243
28. Nilsson, S. K., Johnston, H. M., Whitty, G. A., Williams, B., Webb, R. J., Denhardt, D. T., Bertoncello, I., Bendall, L. J., Simmons, P. J., and Haylock, D. N. (2005) *Blood* **106,** 1232–1239
29. Katayama, Y., Battista, M., Kao, W. M., Hidalgo, A., Peired, A. J., Thomas, S. A., and Frenette, P. S. (2006) *Cell* **124,** 407–421
30. Kondo, H., Nifuji, A., Takeda, S., Ezura, Y., Rittling, S. R., Denhardt, D. T., Nakashima, K., Karsenty, G., and Noda, M. (2005) *J. Biol. Chem.* **280,** 30192–30200
31. Elefteriou, F., Ahn, J. D., Takeda, S., Starbuck, M., Yang, X., Liu, X., Kondo, H., Richards, W. G., Bannon, T. W., Noda, M., Clement, K., Vaisse, C., and Karsenty, G. (2005) *Nature* **434,** 514–520
32. Katagiri, Y. U., Sleeman, J., Fujii, H., Herrlich, P., Hotta, H., Tanaka, K., Chikuma, S., Yagita, H., Okumura, K., Murakami, M., Saiki, I., Chambers, A. F., and Uede, T. (1999) *Cancer Res.* **59,** 219–226
33. Zohar, R., Suzuki, N., Suzuki, K., Arora, P., Glogauer, M., McCulloch, C. A., and Sodek, J. (2000) *J. Cell Physiol.* **184,** 118–130
34. Lin, Y. H., and Yang-Yen, H. F. (2001) *J. Biol. Chem.* **276,** 46024–46030
35. Marroquin, C. E., Downey, L., Guo, H., and Kuo, P. C. (2004) *Immunol. Lett.* **95,** 109–112
36. Huang, W., Carlsen, B., Rudkin, G., Berry, M., Ishida, K., Yamaguchi, D. T., and Miller, T. A. (2004) *Bone* (*NY*) **34,** 799–808
37. Kuznetsov, S. A., Riminucci, M., Ziran, N., Tsutsui, T. W., Corsi, A., Calvi, L., Kronenberg, H. M., Schipani, E., Robey, P. G., and Bianco, P. (2004) *J. Cell Biol.* **167,** 1113–1122

Downloaded from www.jbc.org at Tokyo Ikashika Daigaku on March 18, 2009

MEMO

う蝕制御学分野

田上 順次

医歯学総合研究科・口腔機能再構築学系専攻
齲蝕制御学・教授

1. 研究の課題名

・光干渉断層画像診断法によるう蝕の診査

Caries detection using optical coherence tomography

光干渉断層画像法（Optical Coherence Tomography, OCT）は電離放射線による被曝を伴わない撮像技術であり、生体への侵襲が極めて少なく、チェアーサイドで得られるため、歯科への導入が期待されている。本研究ではう蝕のOCTによる断層画像診査を試みた。咬合面裂溝の初期う蝕ならびに歯根面う蝕に対し、OCTによる断層画像診査を行い、視診と比較した。またダイヤモンドブレードにて半切し、実際の病巣の拡がりを実体顕微鏡にて観察した。結果、OCTを用いた早期う蝕の検出は、散乱した光の輝度変換によって得られ、視診よりも精度の高いことが判明した。特に根面う蝕の場合、臨床的なう蝕病変の拡がりとOCTによって得られた輝度変換した部分とはほぼ一致していた。また咬合面う蝕では、従来の視診やX線写真では検知不可能な脱灰病変を検出することができ、早期の臨床介入に貢献するものと期待された。一方、比較的大きなう蝕では、病巣の深部への拡がりを画像化することは困難であり、他の診断法との併用が望まれた。

・う蝕象牙質におけるマトリックスメタロプロテアーゼ（MMP）の局在性

Localization of matrix metalloproteinases（MMPs）in carious dentin

象牙質う蝕の進行に、細菌感染による脱灰のみならずマトリックスメタロプロテアーゼ（MMP）の関与が指摘されている。しかしながらMMPは脱灰操作により流出しやすく、う蝕病巣における局在性を調査することは困難であり、その詳細な検討はなされていない。そこで本研究では象牙質う蝕の未脱灰切片を作成し、病巣におけるMMP2,,8,9,20の局在性を、金コロイド法による免疫電子顕微鏡により観察した。結果、う蝕病巣におけるMMPの局在は、それぞれ異なる様相を呈していた。MMP2は健全象牙質、う蝕病巣ともに同レベルで観察されたのに対し、MMP8,9は健全象牙質と細菌感染したう蝕象牙質第1層において多く観察され、非感染のう蝕象牙質第2層では有意に減少していた。またMMP20は健全象牙質からう蝕の外層に向かうにしたがい、減少していた。細菌感染し象牙質気質の崩壊したう蝕象牙質第1層には唾液のMMPが進入し、病巣拡大に関与している可能性が示唆された。

・レジンセメントにおけるナノサイズのリーケージ試験

Evaluation of nanoleakage on resin cements

間接法修復における微小漏洩は、知覚過敏や修復物の長期耐久性に影響を及ぼす因子として指摘されている。本研究では、レジンセメントによりレジンインレーを接着させた場合の、電子顕微鏡レベルのリーケージを比較し調査した。レジンセメントとして、セルフエッチングプライマーにより象牙質処理を行うパナビアフルオロセメントと、象牙質処理を特に行わないセルフアドヒーシブセメントであるユニセムとを使用した。ナノリーケージの調査は、硝酸銀水溶液を使用し、接着界面における銀粒子の浸入をEDSにより検出後、銀粒子の面積を画像処理により計算した。またそれぞれのセメントを用いてレジンインレーを象牙質に接着させ、その接着強さを微小剪断接着試験により調査した。結果、2つのセメントの接着強さに差は見られなかったが、ナノリーケージの発現はユニセムにおいて有意に少なかった。パナビアフルオロセメントにおけるナノリーケージの発生は、セルフエッチングプライマーの脱灰による影響と考えられた。

・う蝕により変成した象牙質の硬さが市販接着材の剪断接着強さに及ぼす影響

Effect of Hardness of Caries-affected Dentin on Shear Bond Strength of Current Adhesives

コンポジットレジンの象牙質に対する接着は、接着材の種類のみならず、象牙質の性状などによる影響を受けることが知られている。本研究は、開発コンセプトの異なる3種類の接着材（2ステップ接着材でリン酸エッチングを行うシングルボンド、同じく2ステップ接着材でセルフエッチングプライマーを用いるクリアフィルメガボンド、1ステップ接着材のクリアフィルトライエスボンド）の、う蝕により変化した象牙質と正常な象牙質における接着強さを比較し、それぞれの象牙質における硬さとの関連性を調査した。健全象牙質ならびにう蝕により変成した象牙質の硬さはナノインデンテーション試験法により、また接着試験は微小剪断接着試験により調査した。結果、う蝕の影響を受けた象牙質では、3種類の接着材すべてにおいて接着強さの低下が見られたが、3種類の間に差は見られなかった。脱灰や有機質の変性、また硬さの分散により、それぞれの性能が発揮されなかったためと考えられた。

・コンポジットレジン修復物の象牙質接着強さと窩壁適合性に及ぼす治療用放射線照射の影響

The effect of radiotherapy on resin-dentin bond strength and　resin composite adaptation to the cavity wall

口腔領域の悪性腫瘍に対して放射線治療を行うと"radiation caries"が生じる。唾液腺を含む口腔顔面組織や味蕾、歯は頚部や頭部の放射線治療により影響を受けると考えられる。しかしながら、象牙質に対する放射線照射の影響については明らかではない。そこで、放射線照射がレジンと象牙質の接着強さ、窩壁適合性ならびに象牙質の硬さと弾性に与える影響について評価検討した。ウシ下顎永久切歯の一方の群にコバルト60治療用装置を用いて60Gyのγ線を照射した。一方の群はコントロールとしてγ線の照射を行わなかった。

接着試験においては、唇側象牙質平坦面を作製し、その面をClearfil Mega Bondを用いて処理した後、Clearfil AP-Xを築盛し、出力600 mW/cm2で40秒間光照射を行い重合硬化させた。24時間水中保管後試片を切り出し、micro-tensile bond testに供し、引張り接着強さを測定した。次に、両群における象牙質の硬さと弾性をnano-indentation testerにより測定した。一方、窩壁適合性試験では、直径3 mm、深さ1.5 mm（C-factor=3）の円柱状の窩洞を象牙質平坦面に形成した後、Clearfil SE BondとワンステップボンディングシステムであるTokuyama Bond ForceかClearfil tri-S Bondの接着システムを使用して、Clearfil AP-Xを填塞し、重合硬化させた。コントロール群はサーマルストレスをかけず、一方の群は5000回のサーマルサイクルに供し、窩縁と半切面の窩壁に色素浸透試験を行った。色素浸入度は、色素浸入部位の長さの窩壁全周に対する百分率を算出して評価した。

γ線の照射は短期的なコンポジットレジンと象牙質の接着強さ、レジン修復物の窩壁適合性に直接的には影響を及ぼさなかったが、硬さと弾性率を低下させることが分かった。また、γ線を照射した象牙質は、窩壁適合性において、接着システム間で健全象牙質と異なった挙動を示した。これらのことより、60Gyのγ線の照射は、コラーゲン組織等に何らかの変性を引き起こし、より長期的には接着強さを低下させ、窩壁適合性に影響を及ぼす可能性が示唆された。

・微小pHセンサーを用いたう蝕活動性評価とう蝕原因細菌叢遺伝子分析

Intraoral pH measurement of caries and quantification of cariogenic bacteria

試作微小pHセンサーを用い、初期エナメル質う蝕（8症例）ならびに象牙質う蝕（32症例）表層pH値を測定し、pH値を指標とした口腔内う蝕活動性評価を試みた。象牙質う蝕では、臨床症状に基づき急性または慢性う蝕に分類した。pH測定は、被験歯のエナメル質健全部における値を健全pH値とし、続いて初期エナメル質う蝕では再石灰化療法前後におけるpH変化を、象牙質う蝕ではう蝕除去前後のpH値を測定した。また、初期エナメル質う蝕では唾液サンプル中の、象牙質う蝕ではう蝕サンプル中のう蝕原因細菌叢（S.mutans, S.sobrinus, mutns Streptococci）を、各々Real-Time PCR法を用いて定量的に遺伝子分析し、測定されたpH値環境を形成するう蝕細菌叢について検討を加えた。その結果、初期う蝕では、全症例において再石灰化療法前後における著名なpH変化を認めたものの、唾液サンプル中のう蝕原因細菌叢に変化を認めなかった。一方、象牙質う蝕表層pH値は、急性う蝕でpH 3.8から5.4を、慢性う蝕でpH5.8から6.3を、t検定において、急性症例と慢性症例との間に統計学的有意差を認めた。う蝕除去後の平均pH値は、各症例ともにウィットロカイトの臨界pH値

6.4に近接した値を示した。さらに、S. mutansならびにmutns Streptococciは、急性・亜急性症例と慢性症例との間にゲノムDNA比率の定量的な違いを認められず、S. sobrinusは、急性・亜急性症例にて未検出の割合が多く、慢性症例と比較して低い検出率を示した。以上より、本pHセンサーを用い、患者口腔内にて、各種う蝕表層pH値を直接測定することで、定量的なう蝕活動性診断が可能であることが示唆された。また、象牙質う蝕表層pH変化に伴い、同pH環境を形成するう蝕細菌叢にも変化が生じていることが確認された。

可視光応答型酸化チタン光触媒含有漂白材の評価

Evaluation of tooth bleaching materials containing visible-light activate

う蝕制御学分野　大槻 昌幸

近年、可視光応答型酸化チタン光触媒（以下、光触媒）を含有するオフィスブリーチング材が臨床応用されてきているものの、照射光源、照射時間などが、漂白効果に及ぼす影響については明らかではない。本研究では、in vitroにおいて、光触媒を含有するオフィスブリーチング材の漂白効果に及ぼす影響について評価を行った。

メチレンブルーを添加した過酸化水素に、オフィスブリーチング材（Pirenees、三菱ガス化学）に含有されている光触媒を加えて、各種光源を用いて光照射を行い、メチレンブルーの濃度変化を経時的に測定した。その結果、光触媒を添加することによって、メチレンブルーの濃度は経時的に減少し、漂白効果が認められた。青色LED光源よりもハロゲン光源の方が、また、同種の光源では、より大きな光量のほうが、より高い漂白効果が認められた。さらに、405nm青紫半導体レーザーを光源として用いたところ、その有用性が示唆された。

次いで、ウシ下顎切歯を紅茶で染色して、変色歯モデルを作成した。光触媒を含有するオフィスブリーチング材（TiON in-office、GC America）にて、各種光源を用いて漂白処置を行って、歯科用色彩計（ShadeEye NCC、松風）で測色した。その結果、漂白処置を繰り返すことによって、被漂白歯の明度は上昇した。また、ハロゲン照射器においては光量が大きいほうが、高い漂白効果を示し、LED照射器においてはピーク波長405nmの青紫色LEDが漂白に有効であることが示唆された。

以上より、本研究において確立した漂白材料評価のためのin vitroモデルは、スクリーニングテストとして有用であり、また、可視光応答酸化チタン光触媒を含むオフィスホワイトニング材は、照射光の種類、照射時間、照射光強度の影響を受けることが明らかになった。

2. 2008年、2009年（平成21年3月までの）に発表した全ての研究内容についての英文要約

The mechanism of the deconstruction of enamel and dentin was analyzed and the reconstruction of them with the adhesive materials and remineralizing therapies were evaluated. New information regarding to the super tooth was obtained. Especially, super dentin created adjacent to the adhesive materials were revealed to be variable among the adhesives used. The characteristics of the caries lesion was compared between the active lesion and inactive lesion from the view points of pH difference and bacteria.

3. 本事業に関連して世界的な研究拠点形成に向けて、以下の点で改善・整備等されたこと

A（研究拠点体制）

1. Super Tooth をテーマにしたシンポジウムを開催し、国際的にも評価の高い研究者とのネットワークを構築した。
2. OCT画像診断装置の実用化に向けての拠点となるべく、長寿医療センター、企業、当分野のネットワークを構築した。
3. 初期う蝕病巣の再石灰化研究の拠点となるべく他の研究機関との協力体制を構築した。
4. 人工口腔装置による研究推進のため他分野との共同研究を推進した。

B（研究教育環境）

1. X線マイクロCTの画像構築ソフトを充実させ、従来にない歯のう蝕病巣の解析を可能にした。
2. OCT画像診断装置を導入し、研究を推進する体制を構築した。

C（人材確保）

1. Super Tooth 計画に必要な人材として、適任者をシャペロンとして採用した。
2. 研究推進に必要な人材との共同研究体制を構築した。特に生体ガラス、材料の表面加工に必要な革新的技術を有する学外研究者との協力関係が確立された。

D（人材育成）

1. 大学院学生に対し論文作成、学会発表など多くの成果が得られた。
2. 留学生（大学院生）が母国中国の大学教員として採用された。
3. 留学生2名が日本の歯科材料メーカーに就職した。

E（国際化）

1. 国際シンポジウムを開催して、Super Tooth に関する研究の国際的なネットワークを形成した。
2. 国際的にも評価の高まりつつあるシャペロンを採用した。
3. 大学院を修了した留学生が母国中国で教員に採用され、今後の協力関係推進の人材となった。

4. GCOE事業を推進するに当たって力を入れた点

1. 初年度であることから、国際的な研究拠点となるべくシンポジウムを開催し、国際的なネットワークを形成した。
2. “Super Tooth”の概念を国際的に認知されるべく、国際学会でSupertooth に関する講演を行った。また、質の高い国際誌に投稿した論文でSuper Tooth についての考察を展開させて受理された。
3. 優秀なシャペロンの採用に努力した
4. OCT画像診断の研究推進のため、早期に試作装置を購入し、研究に着手した。
5. 多くの大学院生、留学生の確保に努めた。

5. 英文原著論文

Aiuchi H, Kitasako Y, Fukuda Y, Nkashima S, Burrow MF, Tagami J. Relationship between quantitative assessments of salivary buffering capacity and ion activity product for hydroxyapatite in relation to cariogenic potential. Australian Dental Journal 53（2）: 167-171, 2008.

Aksornmuang J, Nakajima M, Foxton RM, Panyayong W, Tagami J. Regional bond strength and failure analysis of fiber post bonded to root canal dentin. Oper Dent 33（6）: 636-643, 2008.

Anjum A, Matin K, Uchida R, Tagami J. Influence of Aging on Direct Resin Composite Repair Bond. International Chinese Journal of Dentistry 8: 53-61, 2008.

Ariyoshi M, Nikaido T, Foxton RM, Tagami J. Microtensile bond strengths of composite cores to pulpal floor dentin with resin coating Dent Mater J 27（3）:400-7. 2008.

Ariyoshi M, Nikaido T, Okada A, Foxton RM, Tagami J. Dentin bond strengths of three adhesive / composite core systems using different curing units. Dent Mater J. 27（2）:187-94. 2008.

Burrow MF, Kitasako Y, Thomas CD, Tagami J. Comparison of enamel and dentin microshear bond strengths of a two-step self-etchoing priming system with five all-in-one system. Operative Dentistry 33（4）: 456-460, 2008.

Daneshmehr L, Matin K, Nikaido T, Tagami J. Effects of root dentin surface coating with all-in-one adhesive materials on biofilm adherence. J Dent 36（1）: 33-41, 2008.

de Carvalho RC. de Freitas PM. Otsuki M. de Eduardo CP. Tagami J. Micro-shear bond strength of Er:YAG-laser-treated dentin. Lasers in Medical Science. 23（2）:117-24, 2008.

dos Santos Daroz CB, Oliveira MT, de Góes MF, Nikaido T, Tagami J, Giannini M. Bond strength of a resin cement to dentin using the resin coating technique. Braz Oral Res 22（3）: 198-204, 2008.

Gyo M, Nikaido T, Okada K, Yamauchi J, Tagami J, Matin K. Surface Response of Fluorine-polymer Incorporated Resin Composites to Cariogenic Biofilm Adherence. Appl Environ Microbiol 74（5）:1428-1435, 2008.

He Z, Shimada Y, Sadr A, Ikeda M, Tagami J. The effects of cavity size and filling method on the bonding to Class I cavities. The Journal of Adhesive Dentistry10（6）: 447-453, 2008.

Kitasako Y, Burrow MF, Stacey M, Huq L, Reynolds EC, Tagami J. Comparative analysis of three commercial saliva testing kits with a standard saliva buffering test. Australian Dental Journal 53（2）: 140-144, 2008.

Kitasako Y, Ikeda M, Tagami J. Pulpal responses to bacterial contamination following dentin bridging beneath hard-setting calciu, hydroxide and self-etching adhesive resin system. Dental Traumatology 24（2）: 201-206, 2008.

Kitasako Y, Ikeda M, Burrow MF, Tagami J. A technique using resin composite with orthodontic wire to replace a missing tooth rapidly. Dental Traumatology 24（1）: 127-130, 2008.

Jaberi Ansari Z, Sadr A, Moezizadeh M, Aminian R, Ghasemi A, Shimada Y, Tagami J, Jaberi Ansari S, Moayedi S. Effects of one-year storage in water on bond strength of self-etching adhesives to enamel and dentin. Dental Materials Journal 27（2）: 266-272, 2008.

◎Makishi P, Shimada Y, Sadr A, Wei S, Ichinose S, Tagami J. nanoleakage expression and micro-shear bond strength in the resin cement-dentin interface. The Journal of Adhesive Dentistry（in press）.

Nayif MM, Nakajima M, Foxton RM, Tagami J. Bond strength and ultimate tensile strength of resin composite bonded into dentine cavity; Effect of bulk and incremental technique. J Dent 36（3）: 228-234, 2008.

Nayif MM, Nakajima M, Aksornmuang J, Ikeda M, Tagami J. Effect of adhesion to the cavity walls on the mechanical properties of resin composites. Dent Mater 24（1）: 83-89, 2008.

Nikaido T, Kitasako Y, Burrow MF, Umino A, Maruoka R, Ikeda M, Tagami J. Effect of resin coating on dentin bond durability of a resin cement over 1 year. Am J Dent 21（1）: 64-68, 2008.

◎Nikaido T, Weerasinghe DDS, Waidyasekera K, Inoue G, Foxton RM, Tagami J. Assessment of nanostructure of acid-base resistant zone by application of all-in-one adhesive systems: Super dentin formation. Bio-Medical Materials and Engineering（in press）.

Nishimoto Y. Otsuki M. Yamauti M. Eguchi T. Sato Y. Foxton RM. Tagami J. Effect of pulse duration of Er: YAG laser on dentin ablation. Dental Materials Journal 27（3）:433-9, 2008.

Okada A, Nikaido T, Ikeda M, Okada K, Yamauchi J, Foxton RM, Sawada H, Tagami J, Matin K. Inhibition of biofilm formation using newly developed coating materials with self-cleaning properties. Dent Mater J 27（4）: 565-572, 2008.

Sadr A, Shimada Y, Lu H, Tagami J. The viscoelastic behavior of dental adhesives: A nanoindentation study. Dental Materials 25（1）: 13-19, 2009.

Senawongse P. Otsuki M. Tagami J. Mjor IA. Morphological characterization and permeability of attrited human dentine. Archives of Oral Biology 53（1）:14-9, 2008.

◎ Shida K, Kitasako Y, Burrow MF, Tagami J. Micro-shear bond strengths and surface pH change of self-etching adhesive systems to fluorosed and non-fluorosed enamel. European Journal of Dental Science（in press）.

Takagaki T, Nikaido T, Tsuchiya S, Ikeda M, Foxton RM, Tagami J. Effect of hybridization on bond strength and adhesive interface after acid-base challenge in 4-META/MMA-TBB resin. Dental Materials Journal（in press）.

Torkabadi S, Nakajima M, Ikeda M, Foxton RM, Tagami J. Bonding durability of HEMA-free and HEMA-containing one-step adhesives to dentine surrounded by bonded enamel. J Dent 36（1）: 80-86, 2008.

Takanashi E, Kishikawa R, Ikeda M, Inai N, Masayuki Otsuki M, Foxton RM, Tagami J. Influence of Abrasive Particle Size on Surface Properties of Flowable Composites. Dental Materials Journal 27（6）: 780-786, 2008.

Wei S, Sadr A, Shimada Y, Tagami J. Effects of caries-affected dentin hardness on the shear bond strength of current adhesives. The Journal of Adhesive Dentistry 10（6）: 431-440, 2008.

Yuan Y, Shimada Y, Ichinose S, Tagami J. Hybridization quality in cervical cementum and superficial dentin using current adhesives. Dental Materials 24（5）: 584-593, 2008.

6. 著書

田上順次、桃井保子、花田光弘　う蝕学、永末書店、東京、2008

二階堂徹、田上順次.う蝕治療（2）象牙質の保護（レジンコーティング法）について、別冊the Quintessence Year Book 2008、現代の治療指針 歯周治療と全治療分野編、クインテッセンス出版、東京、P236-237, 2008年1月10日発行.

島田康史,田上順次.接着ここが知りたい歯科衛生士編.歯髄保護　う蝕が深いときに裏層するか？ P64-66　日本接着歯学会編　財団法人口腔保健協会　東京　2008.

姜亭、二階堂徹、田上順次、他2名編、実用口腔粘接修復技術Practical Adhesive Dentistry、第一版、人民軍医出版社、北京、2008年9月発行（中国語）。

二階堂徹、田上順次.う蝕治療（1）象牙質の保護（レジンコーティング法）について、別冊the Quintessence Year Book 2009、現代の治療指針 欠損・審美補綴と全治療分野編、クインテッセンス出版、東京、160-161、2009年1月10日.

7. 自己評価

Super Tooth の概念を国際的に普及させるため、国際学会での講演、国際雑誌への投稿を行い、国際シンポジウムを開催し、関連の研究者との交流、ネットワーク形成を行った。国内でも同様の活動を行うとともに、研

究設備の充実に努め、研究推進の体制を構築することができた。

8. 和文原著論文

島田康史, 岡田　浩, 田上順次. セメント質に対する1ステップ接着材の微小剪断接着強さ. 接着歯学 26（1）: 36-40, 2008.

中島正俊、谷口玄、Sitthikorn Kunawarote、保坂啓一、高橋真広、岩本奈々子、岸川隆蔵、田上順次.う蝕象牙質に対する2ステップ・セルフエッチ接着システムの接着性能の改良. 日本歯科保存学雑誌51（4）: 396-402, 2008.

吉川孝子, WATTANAWONGPITAK Nipaporn, 高橋英和, 田上順次. コンポジットレジン修復物の象牙質接着強さに及ぼす治療用放射線照射の影響. 日本歯科保存学雑誌 51（5）: 508-512, 2008.

吉川孝子, 高橋英和, 田上順次. コンポジットレジン修復物の象牙質窩壁適合性に及ぼす治療用放射線照射の影響. 接着歯学 26（2）: 87-91, 2008.

9. 学会発表（英文）

Iwamoto.N, Uctasli.S, Ikeda.M, Nakajima.M, Tagami.J. Shear Bond Strength of New Self Adhesive Cement to Enamel and Dentin. Poster, International Symposium for Adhesive Dentistry 2008 in Kanazawa, Kanazawa, February 16-17, 2008.

Ikeda M, Nikaido T, Tagami J, Miura H. Bond strengths of a resin cement to zirconia using internal coating. Poster, International Symposium for Adhesive Dentistry 2008 in Kanazawa, Kanazawa, February 16-17, 2008.

Waidyasekera PGK, Nikaido T, Tagami J. Bonding efficacy and morphological analysis of adhesive systems to human fluorosed dentin. Poster, International Symposium for Adhesive Dentistry 2008 in Kanazawa, Kanazawa, February 16-17, 2008.

Yoshikawa T, Miura M, Tagami J. The effect of radiotherapy on resin composite adaptation using one step bonding system. Poster, International Symposium for Adhesive Dentistry 2008 in Kanazawa, Kanazawa, February 16-17, 2008.

Yamamoto T, Otsuki H, Nishimoto C, Iwasaki S, Nikaido T, Tagami J. Influence of adhesion on wear resistance of resin-coating materials. Poster, AADR 37th Annual Meeting and Exhibition, Oral, Dallas, April 3, 2008

Pashley DH, Nishitani Y, Yoshiyama M, Hosaka K, Agee K, Brackett WW, Tay FR. Durability of Resins Bonded to Water Vs. Ethanol-Saturated Acid-Etched Dentin. AADR 37th Annual Meeting and Exhibition, Oral, Dallas, April 3, 2008

Nikaido T, Weerasinghe DDS, Inoue G, Tagami J: Assessment of nanostructure of "Super Dentin" formation by application of all-in-one adhesive systems. Oral, ISNT 2008, Sapporo, June 16, 17, 2008.

Bakry AS, Matin K, Tanaka Y, Takahashi H, Otsuki M, Yamashita K, Tagami J、CO2 Laser Irradiation Enhances Interaction of 45S5 Bioglass with Dentin, IADR 86th General Session. Oral, IADR 86th General Session, Toronto, July2-5, 2008.

Hosaka K, Nakajima M, Takahashi M, Ito S, Ikeda M, Taniguchi G, Nishitani Y, Yoshiyama M, Pashley DH, Tay FR, Tagami J. Mechanical properties of one-step adhesive-polymers in dry vs. wet. Oral, IADR 86th General Session, Toronto, July2-5, 2008.

Kondo Y, Okuda M, Ikeda M, Kadoma Y, Okada K, Nojiri Y, Nikaido T, Tagami J. Effect of additional PMMA fillers in composites on compressive strength. Poster, IADR 86th General Session, Toronto, July2-5, 2008.

Makishi P, Shimada Y, Sadr A, Wei S, Ichinose S, Tagami J. Nanoleakage expression in the resin cement-dentin interface. Poster, IADR 86th General Session, Toronto, July2-5, 2008.

Matin K, Okada A, Gyo M and Tagami J. Oxidative Stress of Ozone Down-regulates Streptococcus mutans Extra-cellular Protein Expression. Oral,IADR 86th General Session, Toronto, July 2-5, 2008.

Okada A, Matin K, Hanada N, and Tagami J. Electrolyzed Waters with Different Hypochlorite Concentrations in Controlling Cariogenic Biofilms. Poster, IADR 86th General Session, Toronto, July2-5, 2008.IADR 86th General Session, Toronto, July 2-5, 2008.

Hayati F, Matin K, Okada A and Tagami J. Efficacy of ozone in Inhobiting Biofilm Induced Secondary Caries. Poster, IADR 86th General Session, Toronto, July 2-5, 2008.

Nakajima M, Taniguchi G, Kunawarote S, Hosaka K, Iwamoto N, Takahashi M, Tagami J. Effect of anti-oxidant/ NaOCl treatment on bonding to caries-affected dentin. Oral, IADR 86th General Session, Toronto, July2-5, 2008.

Nikaido T, Weerasinghe DDS, Inoue G, Tagami J. Ultrastructure of acid-base resistant zone in a fluoride-releasing adhesive system. Oral, IADR 86th General Session, Toronto, July2-5, 2008.

Nishitani Y, Yoshiyama M, Hoshika T, Takahashi K, Hosaka K, Tagami J, Tay FR and Pashley DH. Effects of incorporating chlorhexidine into all-in-one adhesives. Poster, IADR 86th General Session, Tronto, July 2-5, 2008.

Pashley DH, Agee K, Hosaka K, Nishitani Y, Carvalho RM, Tay FR. Macrohybrid Layer: Correlations Between Changes in Matrix Height and μ TBS. Oral, IADR 86th General Session, Toronto, July2-5, 2008.

Sadr A, Shimada Y, Tagami J. microleakage of Class V inlays using an experimental self-adhesive resin cement. Poster, IADR 86th General Session, Toronto, July2-5, 2008.

Shimada Y, Chow LC, Takagi S, Tagami J. Properties of injectable apatite forming premixed cements. Oral, IADR 86th General Session, Toronto, July2-5, 2008.

Tajima K, Inoue G, Nikaido T, Tagami J. Effect of a resin coating on prevention of root caries. Poster, IADR 86th General Session, Toronto, July2-5, 2008.

Uzzaman MA, Shimada Y, Tagami J, Junaidi MT. Micro-shear bond-strength of resin-inlays to different enamel regions. Poster, IADR 86th General Session, Toronto, July2-5, 2008.

Y. Iida, D. Weerasinghe, G. Inoue, T. Nikaido, J. Tagami. Structural analysis of acid-base resistant zone using self-etching primer systems. Poster, IADR 86th General Session, Toronto, July2-5, 2008.

Yoshikawa T, Miura M, Tagami J. Effect of Radiotherapy on Resin/Dentin Adaptation using One-Step Bonding System. Oral, IADR 86th General Session. Toronto. July 2-5. 2008.

Matin K, Hayati F, Uchida R, Oyanagi T, Tagami J. Prevention Potential of Ozone Gas and Functional Waters; Verification Using Biofilm Induce Secondary Caries. 2008年度バイオフィルムと複合系研究会, 東京, 2008年7月16, 17日

◎Anjum A, Matin K, Uchida R, Tagami J. Influence of Aging on Direct Resin Composite Repair Bond. Poster, The 3rd International Congress on Adhesive Dentistry, Xi'an, September 26-28, 2008.

◎Ariyoshi M, Nikaido T, Tagami J. Influence of Filling Technique and Curing Mode on Bond Strengths of Composite Core to Pulpal Floor Dentin. Oral, The 3rd International Congress on Adhesive Dentistry. The 3rd International Congress on Adhesive Dentistry, Xi'an, September 26-28, 2008.

◎Kunawarote S, Tanigichi G, Nakajima M, Tagami J. Effect of pretreatment with neutral hypochlorous acid and sodium hypochlorite aqueous solutions on bonding to dentin. Poster, The 3rd International Congress on Adhesive Dentistry. Xi'an, September 26-28, 2008.

◎Matin K, Okada A, Gyo M, Anjum A, Daneshmehr L, Hayati F, Shida K, Uchida R, Tanaka Y, Kitasako Y, Nikaido T, Otsuki M, Hanawa T and Tagami J. Multidimensional Inhibition Strategies Offered against Cariogenic Biofilm Challenge; Studies Performed Using an Oral Biofilm Reactor. The 3rd International Congress on Adhesive Dentistry, Xi'an, September 26-28, 2008.

Nayif M, Shimada Y, Ichinose S, Tagami J. Intrapulpal nanoleakage of current self-etch adhesives bonded to artificial carious dentin. Oral, The 3rd International Congress on Adhesive Dentistry, Xian, September 26-28, 2008.

Shimada Y, He Z, Tagami J. Composite resin restoration to deep cavity. Poster, The 4th Japanese-Sino Conference on Stomatology. Poster, The 3rd International Congress on Adhesive Dentistry, Xi'an, September 26-28, 2008.

◎Takahashi R, Ariyoshi M, Nikaido T, Tagami J. Microtensile bond strengths of a dual-cure resin cement to dentin resin-coated with an all-in-one adhesive system using two curing strategies. Oral, The 3rd International Congress on Adhesive Dentistry, Xi'an, September 26-28, 2008.

◎Takagaki T, Nikaido T, Inoue G, Tagami J. Effect of shortening the curing time on wear of a resin composite with RAP-technology. Oral, The 3rd International Congress on Adhesive Dentistry, Xi'an, September 26-28, 2008.

◎Weerasinghe D, Nikaido T, Waidyasekera K, Tagami J. Reinforcement of dentin in two-step self-etching adhesive systems. Oral, The 3rd International Congress on Adhesive Dentistry, Xi'an, September 26-28, 2008.

◎Wei S, Shimada Y, Sadr A, Tagami J. Effects of double-applicatuion of three all-in-one adhesives on dentin bonding

and mechanical properties of resin-dentin area. Oral, The 3rd International Congress on Adhesive Dentistry, Xi’an, September 26-28, 2008.

Zhu L, Kitayama S, Ikeda M, Nikaido T, Tagami J. Effect of surface treatments on bond strengths of resin cement to zirconia. Oral, The 3rd International Congress on Adhesive Dentistry, Xi’an, September 26-28, 2008.

◎Matin K, Okada A, Gyo M, Anjum A, Daneshmehr L, Hayati F, Shida K, Uchida R, Tanaka Y, Kitasako Y, Nikaido T, Otsuki M, Hanawa T and Tagami J. Multidimensional Inhibition Strategies Offered against Cariogenic Biofilm Challenge; Studies Performed Using an Oral Biofilm Reactor. The 3rd International Congress on Adhesive Dentistry, Xi’an, September 26-28, 2008.

◎Matin K, Gyo M, Okada A, Shida K, Nagayama M, Saihara Y and Tagami J. Influence of Alkai-ion Water on Removing Cariogenic Biofilm by Jet-washer. Poster, The 56th Annual meeting of JADR, Nagoya, November, 29, 30, 2008.

Nikaido T, Yahagi C, Tajima K, Tagami J. Effects of surface coating with adhesive materials on prevention of root surface caries. Poster, The 4th Sino-Japan Conference on Stomatology, September 28, 29, 2008.

◎Okada A, Matin K, Zaman S, Hanada N and Tagami J. Electrolyzed Water with Functional-chlorine Effectively Penetrates Deep into Cariogenic Biofilms. Poster, The 56th Annual meeting of JADR, Nagoya, November, 29, 30, 2008.

◎Nayif M, Otsuki M, Kishi A, Tagami J. Bleaching Efficiency Employing Various Light Units and Irradiation Time. Oral, The 56th Annual meeting of JADR, Nagoya, November, 29, 30, 2008.

◎Zaman S, Matin K, Okada A, Hanada N and Tagami J. Effects of HClO Incorporated Electrolyzed Water on Proliferation of KB-cells. Poster, The 56th Annual meeting of JADR, Nagoya, November, 29, 30, 2008.

◎Tgami J. Creating the “Super tooth” with innovative technologies, Oral, G-COE 1st International Symposium “Strategies to create the super tooth”, Tokyo, January 22, 2009.

◎Waidyasekera Kanchana, Nikaido Toru, Hamid Nurrohman, Tagami Junji. Bonding the root fragments with self-etch adhesives in complete vertical root fracture. Oral, 第27回日本接着歯学会学術大会, 仙台, 2009年2月21, 22日

Wei S, Shimada Y, Tagami J. Micro-shear bond strength of G Bond Plus to enamel and dentin. Oral, 第27回日本接着歯学会学術大会, 仙台, 2009年2月21,22日

10. 学会発表（和文）

田中勇太,暁万里子,岡田彩子,Khairul Matin,田上順次,塙隆夫. PEG 固定化によるチタン表面のバイオフィルム付着性防止. 日本金属学会2008年春期大会,東京,2008年3月26-28日

西村耕三、池田正臣、二階堂徹、田上順次. ボンディングレジンの変色, 第51回日本歯科理工学会学術講演会, 鶴見, 2008年4月26, 27日

田中勇太,堤祐介,土居壽,カイルール マティン,田上順次,塙隆夫:ポリエチレングリコール電着によるチタン表面のバイオフィルム形成防止,第51 回日本歯科理工学会学術講演会,鶴見,2008年4月26, 27日

市川千秋、井上剛、二階堂徹、田上順次. 長期水中保管後の Acid-base Resistant Zone の SEM 観察. 第128回日本歯科保存学会学術大会, 新潟, 2008年6月5, 6日

内田僚一郎,Khairul Matin,池田正臣,二階堂徹,田上順次.コンポジットレジン表面性状とバイオフィルム形成の関連性. 第128回日本歯科保存学会学術大会, 新潟, 2008年6月5, 6日

関奈央子、岸川隆蔵、荻巣慎一郎、陶山雄司、池田正臣、田上順次. 照射光量の減少が象牙質接着強さに及ぼす影響. 第128回日本歯科保存学会学術大会, 新潟, 2008年6月5, 6日

高橋真広、岩本奈々子、保坂啓一、青木香那子、池田正臣、中島正俊、田上順次. 新規MMA系レジンセメントPRC-01の歯質接着性能. 第128回日本歯科保存学会学術大会, 新潟, 2008年6月5, 6日

岸川隆蔵、趙 永哲、田上順次. 保存修復学実習後に行った学生アンケート調査についての報告. 第27回日本歯科医学教育学会学術大会, 東京, 2008年7月11, 12日

趙 永哲、南 一郎、吉岡隆、岸川隆蔵、川島伸之、和達礼子、木下淳博、須田英明、田上順次. 「歯科診療室―

講義室間のインターネット同時中継によるライブ講義システムの開発と評価」第27回日本歯科医学教育学会, 東京, 2008年7月11, 12日

岡田彩子, Khairul MATIN, Shawket ZAMAN, 暁万里子, 花田信弘, 田上順次. Effectiveness Electorolyzed Water with Different Functional-Chlorine Concentration in Inhibiting Cariogenesis. 2008年度バイオフィルムと複合系研究会, 東京, 2008年7月16, 17日

田野絵里、高岡丈博、陶山雄司、岸川隆蔵、大槻昌幸、田上順次　405nm半導体レーザーの可視光対応型二酸化チタン光触媒に及ぼす効果. 第20回日本レーザー歯学会学術大会, 大阪, 2008年9月20, 21日

大槻昌幸、岸綾香、田上順次、青紫LED（405nm）光源が可視光応答型酸化チタン光触媒含有の漂白材に及ぼす影響. 第52回日本歯科理工学会学術講演会, 豊中, 2008年9月21, 22日

田中勇太,Khairul Matin,田上順次,堤祐介,土居壽,野村直之,塙隆夫. Ti 表面のバイオフィルム初期形成に及ぼす電着固定PEG鎖の影響,日本金属学会2008年秋期大会,熊本,2008年9月23-25日

田中勇太,Khairul Matin,田上順次,野村直之,塙隆夫. 電着生体機能分子による金属表面でのバイオフィルム形成防止,日本鉄鋼協会討論会秋季大会,熊本,2008年9月23-25日

岸 綾香、大槻 昌幸、田上 順次、可視光応答型光触媒含有の漂白材（GC TiON in-office）に関する研究　— 各種光源が漂白効果に及ぼす影響 —. 第19回日本歯科審美学会学術大会, 新潟, 2008年10月12, 13日

藤田 由美子、指田 麻由子、吉増 秀實、大槻 昌幸、田上 順次、ホームケア用品による歯の着色除去効果に関する研究. 第19回日本歯科審美学会学術大会, 新潟, 2008年10月12, 13日

岩本奈々子、岸川隆蔵、中島正俊、井高沙織、杉森匡、田上順次.コンポジットレジンに対する加温がヌープ硬さ及びヒト象牙質への接着強さに与える影響. 第129回日本歯科保存学会学術大会, 富山, 2008年11月6、7日

大槻 昌幸、岸 綾香、田上 順次、可視光応答型酸化チタン光触媒含有の漂白材（GC TiON in office）の漂白効果に関する研究. 第129回日本歯科保存学会学術大会, 富山, 2008年11月6, 7日

大槻 昌幸、池田 正臣、田上 順次、新規ホームホワイトニング材（ティオン ホーム）の臨床評価. 第129回日本歯科保存学会学術大会, 富山, 2008年11月6, 7日

吉川孝子、三浦雅彦、田上順次. コンポジットレジン修復物の象牙質窩壁適合性に及ぼす治療用放射線照射の影響. 第129回日本歯科保存学会秋季学術大会, 富山, 2008年11月6, 7日

中島正俊、谷口玄、クナワロッテ シッティコーン、保坂啓一、高橋真広、岩本奈々子、田上順次. う蝕象牙質に対するレジンの接着性能の改良. 第21回日本歯科医学会総会 ポスターセッション, 横浜, 2008年11月14, 15日

田中勇太,Khairul Matin,堤祐介,土居壽,野村直之,田上順次,米山隆之,塙隆夫. 血小板粘着および細菌付着を抑制するPEG電着固定チタンの創製,日本バイオマテリアル学会シンポジウム2008,東京, 2008年11月17, 18日

暁万里子, マティン カイルール, 野尻大和, 岡田浩一, 今里聡, 二階堂徹, 田上順次　MDPB/フッ素オリゴマー含有レジンコーティング材のう蝕関連細菌に対する効果について, 日本バイオマテリアル学会シンポジウム2008, 東京, 2008年11月17, 18日

池田正臣、二階堂徹、安江透、兼井寛行、田上順次、三浦宏之. ジルコニアと陶材焼付け界面のSEM/EDS分析. 第30回日本歯科技工学会学術大会, 大阪, 2008年11月22日

佐野滋信、池田正臣、二階堂徹、田上順次、安江透、三浦宏之. ハイブリッド型硬質レジンと非貴金属に対するレジンセメントの接着強さ. 第30回日本歯科技工学会学術大会, 大阪, 2008年11月22日

二階堂徹、池田正臣、佐野滋信、田上順次、安江透、三浦宏之. ジルコニア、セラミックスおよび貴金属に対するレジンセメントの接着強さ. 第30回日本歯科技工学会学術大会, 大阪, 2008年11月22日

兼井寛行、池田正臣、二階堂徹、田上順次、渡辺昭彦、安江透、三浦宏之. サンドブラスト処理がジルコニア表面性状に及ぼす影響について. 第30回日本歯科技工学会学術大会, 大阪, 2008年11月22日

関奈央子、鶴田潤、森尾郁子、田上順次. 歯学部における英語教育の必要性について. 第73回口腔病学会, 東京, 2008年12月5, 6日

吉川孝子、三浦雅彦、田上順次. コンポジットレジン修復物の象牙質窩壁適合性に及ぼす治療用放射線照射の影響. 第73回口腔病学会, 東京, 2008年12月5, 6日

青木香那子、北迫勇一、有吉芽生、二階堂徹、田上順次、MMA系レジンセメントの象牙質に対する10年後の接着耐久性. 第27回日本接着歯学会, 仙台, 2009年2月21, 22日

斉藤季夫、島田康史、田上順次.直接法コンポジットレジン接着ブリッジの耐久度と効果. 第27回日本接着歯学会, 仙台, 2009年2月21, 22日

藤井美恵、北迫勇一、田上順次、各種飲み物に浸漬した牛歯エナメル質の表面性状. 第27回日本接着歯学会, 仙台, 2009年2月21, 22日

11. 受賞

2008年11月　英国King's College of London から Honorary Degree　授賞

12. 特別講演、招待講演

・基調講演　Adhesive dentistry for well being of the patient, International Symposium for adhesive dentistry, 2008年1月16日、金沢市
・基調講演　“Esthetic dentistry for Everyone”1st Congree of Phillipine Academy of Esthetid Dentistry　2008年1月20日　マニラ市
・特別講演　歯の硬組織の疾患予防と再構築における技術革新
日本学術会議シンポジウム、2008年1月25日　東京
・歯科医療ビジョン 2008年3月18日　医療ビジョン会議 厚生労働省
・特別講演　“Improvement of bonding technology and its clinical application”
日英シンポジウム　2008年　月　日、東京
・招待講演　Minimally invasive aesthetic restorations with innovative technologies. The Sino-Japanese Symposium of Conservative Dentistry, 2008年9月9日、成都市
・特別講演、”Reinforcement of teeth with adhesive technology”The 3rd International Congress of Adhesive Dentistry、2008年　9月　日　西安市
・会長講演　審美歯科もCure からCareへ
第21回日本歯科審美学会、2008年10月11日、新潟市
・招待講演、Innovations in restorative dentistry, Riyaddh International Dental and Pharmacy Meeting, 2008年10月18日　、リヤド市
・ランチョンセミナー　「口腔ケアプログラムとしての審美歯科」第21回日本歯科医学会総会　2008年11月16日　横浜
・特別講演　Direct aesthetic restorations supported by dental labo-technology
第5回　国際歯科技工学会、2008年11月22日、大阪
・特別講演（名誉学位授賞記念講演）
Innovations in Operative Dentistry,　2008年11月24日King's College of London,　ロンドン
・招待講演　Innovations supporting the minimal intervention in operative　dentistry　台湾歯科医学会、2008年11月29日　台北市
・特別講演　Super Tooth の創出に向けて、第27回日本接着歯学会学術大会、
2009年2月21日、仙台市

13. 主催学会

東京医科歯科大学第1回GCOE国際シンポジウム
“Creating the Super Tooth”　主催
平成21年1月22日　学士会館（東京）

14. 新聞、雑誌、TV報道

・読売新聞第6回「デンタルヘルスシリーズ」シンポジウム
大人世代こそ必要なオーラルケア　平成20年6月7日　読売新聞に掲載
・読売新聞夕刊　2月22日　ホワイトニング
・読売ウィークリー臨時増刊「歯科の実力」読売新聞医療情報部編　平成20年6月29日
・日本テレビ　「世界一受けたい授業」に出演（収録日平成20年4月26日）

・NHKテレビ「試してガッテン」に出演　平成20年11月5日

15. 講座の准教授、講師、助教、特別研究員、ポスドク、指導を受けた大学院生の名前（AISSには○印）のリスト

准教授　大槻昌幸

講　師　二階堂徹、中島正俊

助　教　島田康史、吉川孝子、北迫勇二、岸川隆蔵、岩本奈々子、趙永哲

大学院生

相内　紘子、飯田　康博、池田　一郎、
荻巣　慎一朗、來山　修三、暁　万里子、
陶山　雄司、田島　賢、谷口　玄、中田　景子、
Bakry Ahmed Samir Ibarahim、魏　聖華、
DANESMMEHR LEILA、ATIA ANJUM、
WAIDYASEKERA　GAYANI
PETHTHAHANDI　KANCHANA、
伊藤志麻、志田嘉奈子、近藤義子、大熊麻紗子、
篠木 毅、有本綾子、西村　美穂、朱　蕾、
Fahimeh Hayati、市川　千秋、内田　僚一郎、
荒牧　音、篠田　祐子、堀江　加奈子、関　奈央子、
高橋　礼奈、高橋　真広、岸　綾香、
青木　香那子、藤井　美恵、高井　智行、
森　文彦、丹野　恵造、Makishi Patricia、
田中　美由、矢作　智花、小柳　岳大、
夏目　悠子、坪根　真子、武田　絵里、半場　秀典、
神原　啓介、閔　元敬、Sitthikorn Kunawarote、
Prasansuttiporn Taweesan, Nuprohman Hamid,
Nazari Amir, Ilnaz Hariri

Dental Materials Journal 2008; 27(3): 400−407

Original Paper

Microtensile Bond Strengths of Composite Cores to Pulpal Floor Dentin with Resin Coating

Meu ARIYOSHI[1], Toru NIKAIDO[1], Richard M. FOXTON[2] and Junji TAGAMI[1,3]

[1]*Cariology and Operative Dentistry, Department of Restorative Sciences, Graduate School, Tokyo Medical and Dental University, 1-5-45 Yushima, Bunkyo-ku, Tokyo 113-8549, Japan*
[2]*Division of Conservative Dentistry, King's College London Dental Institute at Guy's, King's College and St. Thomas' Hospitals, King's College London, London SE1-9RT, UK*
[3]*Center of Excellence Program for Frontier Research on Molecular Destruction and Reconstruction of Tooth and Bone, Tokyo Medical and Dental University, 1-5-45, Yushima, Bunkyo-ku, Tokyo 113-8549, Japan*
Corresponding author, Meu ARIYOSHI; E-mail: ariyoshipirro@yahoo.co.jp

The purpose of this study was to evaluate the effect of resin coating on the microtensile bond strength (MTBS) of indirect composite cores to pulpal floor dentin. Thirty extracted human molars with root canal fillings were used. After post space preparation, dentin surface was coated with either Clearfil SE Bond (SE) or SE with Clearfil Flow FX (SE+FX) for the resin-coated groups, while dentin was treated with ED Primer II (ED) for the non-coated group. Indirect composite cores were cemented with either Panavia F2.0 (PA) or Clearfil DC Core Automix (DC). After 24-hour storage, MTBSs were measured at a crosshead speed of 1 mm/min. Two-way ANOVA indicated that the MTBSs of resin-coated groups were significantly higher than those of the non-coated groups. In particular, the SE+FX/DC group exhibited the highest MTBS. It was thus concluded that resin coating enhanced the dentin bond strength of indirect composite cores to pulpal floor dentin.

Key words: Microtensile bond strength, Composite core, Resin coating

Received Oct 4, 2007: Accepted Nov 29, 2007

INTRODUCTION

With a conventional post and core system, a post space is prepared to gain mechanical retention of the core, meaning further removal of sound tooth substance[1]. Besides, a great degree of stress is concentrated at the root[2]. These factors adversely affect the longevity of a non-adhesively restored tooth. If good retention can be obtained using a dentin bonding system, a post may not be necessary — thereby preserving sound tooth structure.

Recently, tooth-colored composite core materials have been used as core buildup materials to restore non-vital teeth, especially with rapidly escalating demand for esthetic restorations in dentistry. In terms of beneficial effects, composite core systems can prevent root fractures of non-vital teeth, since a good dentin bonding system has been shown to reinforce the remaining tooth structure[3,4]. Further, in comparison with a metal post, the elastic modulus of a composite core material is similar to that of dentin[5], which plays a role in preserving the remaining tooth structure against root fractures[6].

In clinical situations, direct composite core restorations are preferred over indirect composite core restorations because they require minimal intervention and cavity preparation[2]. However, when teeth require large restorations, or for patients who cannot keep their mouths open for a long time, indirect composite core restorations are recommended to avoid contamination by saliva[7]. For an indirect composite core restoration to be successful, resin cement selection is a key step to obtaining good dentin bonding. However, the bonding performance of resin cements to dentin is still lower than that of direct resin adhesives[8,9].

Recently, a resin coating technique has been used in indirect restorations. In this technique, a hybrid layer and a tight-sealing film are produced on the dentin surface by means of a dentin adhesive system and a low-viscosity microfilled resin[10,11]. The resin coating covers and protects the prepared dentin immediately after cavity preparation and enables good bonding of the resin cement[8,12] and adaptation of composite inlays[9,13] — if a proper combination of adhesive and low-viscosity microfilled resin were selected[14]. Therefore, this technique presents the potential to minimize pulp irritation and postoperative sensitivity[15,16]. In addition, this technique can also be applied in the restoration of non-vital teeth. It has been found that application of a resin coating to coronal openings reduces the incidence of coronal leakage[17].

For successful adhesive restorations of non-vital molars, it is important to obtain good dentin bonding to pulpal floor dentin as the latter always remains

in any non-vital molar which requires restoration. To date, several studies have reported on the bond strength of direct composite restorations to pulpal floor dentin[18-20]. Akagawa *et al.*[20] evaluated the shear bond strengths of resin bonding systems to coronal dentin and pulp chamber floor dentin using a single plane shear test assembly. They reported that a self-etching primer bonding system was able to provide high bond strength to pulp chamber floor dentin as well as to superficial and deep coronal dentin. As for Toba *et al.*[18], they measured the bond strengths of a self-etch bonding system and an acid-etch dentin bonding system to coronal dentin and pulp chamber floor dentin using a microshear bond test. It was found that the self-etching primer system showed more reliable bonding to both regions of the dentin.

However, there is very little published research on the bond strength of indirect composite cores to pulpal floor dentin. Given the paucity of information, there is a need to evaluate the effect of resin coating on the dentin bonding performance of indirect composite core restorations. The purpose of this study, therefore, was to evaluate the effect of resin coating on the MTBS of indirect composite cores to pulpal floor dentin.

MATERIALS AND METHODS

Specimen preparation

Figure 1 shows the specimen preparation procedure. Thirty extracted noncarious human molars were used in this study. Initially, the access cavity preparation of the molars was performed using a high-speed diamond bur (ISO #109, Shofu, Kyoto, Japan) under a water spray. Following this, pulpal tissue was carefully removed using endodontic files (K-files, GC, Tokyo, Japan) which were instrumented to size #35 and filled with gutta percha #35 (GC, Tokyo, Japan). Gutta percha in the pulp chamber was then completely removed with a steel bur (ISO #012, Shofu, Kyoto, Japan) to expose the pulpal floor dentin. The occlusal portion of their crowns were cut perpendicularly to the tooth axis using a high-speed diamond bur under a water spray to standardize the cavity walls to a height of 6 mm from the pulpal floor dentin.

Table 1 lists the materials used in this study. The prepared cavities were randomly divided into two groups. In one group, the cavities were left without any treatment (non-coated group). In the other group, the cavity surfaces were coated with either a two-step self-etching primer bonding system, Clearfil SE Bond (SE) (Kuraray Medical, Tokyo, Japan) or a

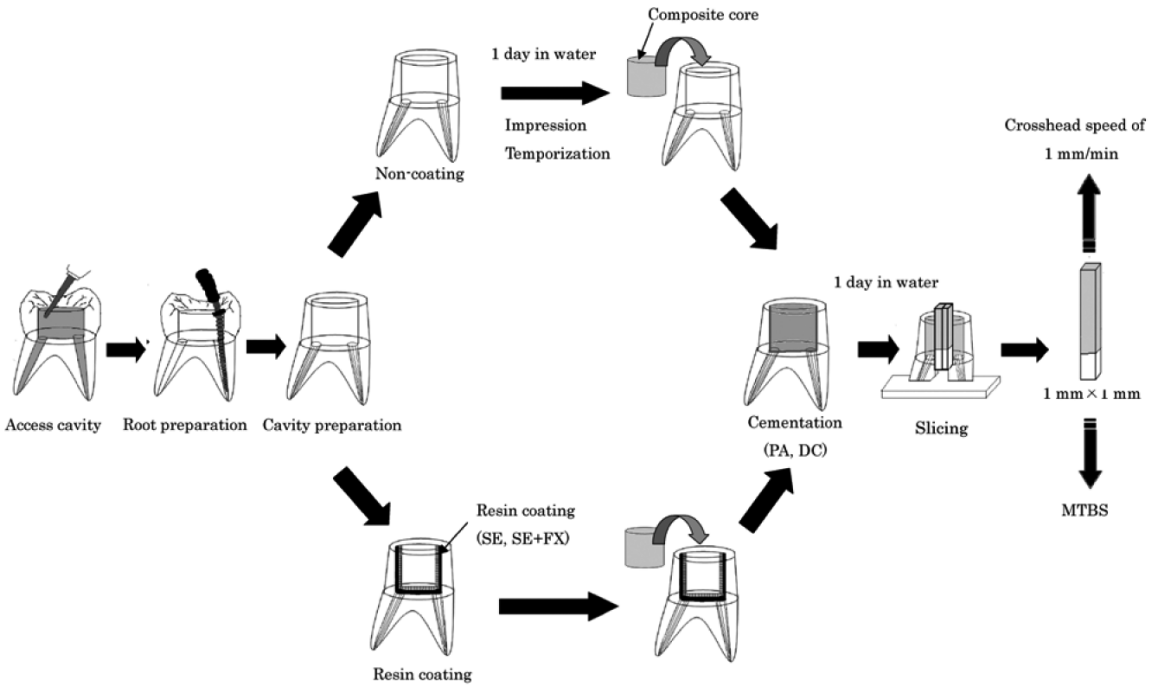

Fig. 1　Specimen preparation procedure.

combination of Clearfil SE Bond and a flowable resin composite, Clearfil Flow FX (Kuraray Medical, Tokyo, Japan). Thereafter, impressions of the cavities were taken for all the groups. Impressions of the dentin surface or resin-coated surface were taken using an agar alginate combined impression, and stone dies were made with a slurry composed of dental stone. After a cotton pellet was placed in the cavities, the cavity was temporized with a water-setting temporary filling material (Caviton, GC, Tokyo, Japan) to simulate the oral situation and then stored in water at 37℃ for 24 hours. The temporary filling material was then removed with a spoon excavator, and the cavity surface cleaned with a cotton pellet containing ethanol for 10 seconds.

To fabricate the indirect composite cores, a dual-cure composite resin core material, Clearfil DC Core Automix (Kuraray Medical, Tokyo, Japan), was built up and light-cured for 60 seconds on the working cast. Trial insertion of the indirect composite cores prior to cementation was performed to check their fit. Surfaces of the indirect composite cores to be cemented were treated with 37% phosphoric acid for 10 seconds, rinsed, dried, and then silanized with a mixture of one drop of SE primer and one drop of Clearfil Porcelain Bond Activator (Kuraray Medical, Tokyo, Japan).

For the non-coated groups, the prepared dentin surfaces were treated with ED Primer (Kuraray Medical, Tokyo, Japan) for 60 seconds. For the resin-coated groups, the coated surfaces were treated with 37% phosphoric acid for 10 seconds, rinsed, and dried to remove debris. After which, ED Primer was applied and gently air-blown.

The indirect composite cores were cemented in the cavity with either Panavia F2.0 (PA) or Clearfil DC Core Automix (DC), then light-cured for 60 seconds from an occlusal direction. All light curing procedures were performed using a halogen light curing unit (Optilux 500, Demetron, Danbury, CT, USA) with a standard irradiation mode of 650 mW/cm^2.

Microtensile bond strength test

All specimens were stored in water at 37℃ for 24 hours. Thereafter, each specimen was cross-sectioned longitudinally using a low-speed diamond saw (Isomet, Buehler, Lake Bluff, IL, USA) to obtain beam-shaped specimens measuring 1.0 mm×1.0 mm. The cross-sectional area of each beam was measured using digital calipers (Mitutoyo CD15, Mitutoyo, Kawasaki, Japan) prior to testing. The ends of the

Table 1　Materials used in this study

Material	Batch number	Composition	Procedure
ED Primer Ⅱ	00200A	Liquid A; HEMA, MDP, 5-NMSA, accelerator, water	Apply A+B 30s, dry
	00080A	Liquid B; 5-NMSA, chemical initiator, water	
Clearfil SE Bond	00562A	Primer; HEMA, MDP, hydrophilic dimethacrylates, photo-initiator, water	Apply 20s, gentle air-blow
	00792A	Bond; Bis-GMA, MDP, HEMA, photoinitiator	Apply 15s, mild air-blow, light-cure 20s
Clearfil Flow FX	0005AA	Bis-GMA, TEGDMA, UDMA, filler, photo initiator	Light-cure 20s
Paravia F 2.0	00077A	Paste A; Quartz glass, microfiller, MDP, methacrylates,	Mix A+B, light-cure 60s
	00048B	Paste B; photoinitiator, barium glass, NaF, methacrylates, chemical initiator	
Clearfil DC Core Automix	00009A	Catalyst; Bis-GMA, TEGDMA, silanized glass filler, silica microfillers, photo/chemical initiator Universal; TEGDMA, methacrylate monomers, silanized glass fillers, silica microfillers, photo/chemical initiator	Light-cure 60s

Manufacturer: Kuraray Medical, Tokyo, Japan
HEMA: 2-hydroxyethyl methacrylate; MDP: 10-methacryloyloxyl methacrylate; 5-NMSA: N-Methacryloyl 5 amino salicylic acid; Bis-GMA: bisphenol-A diglycidylmethacrylate; TEGDMA: triethylene glycol dimethacrylate; UDMA: urethane dimethacrylate; NaF: sodium fluoride

beam and the remaining interface were glued to a testing device in a table-top testing machine (EZ Test, Shimadzu, Kyoto, Japan) using cyanoacrylate glue (Zapit, DVA, Anaheim, CA, USA) and subjected to a tensile force at a crosshead speed of 1 mm/min. The number of specimens in each group was five. Since the area of pulpal floor dentin for bonding varied for each tooth, the average bond strength for each tooth calculated was designated as the bond strength of one tooth. The results were statistically analyzed with two-way ANOVA and Dunnett's test ($p<0.05$).

SEM observation

The fractured surfaces after debonding were visually inspected and then several representative examples were selected for ultrastructural examination by a SEM (JSM-5310LV, JEOL, Tokyo, Japan). Fracture modes were classified into four categories as follows — A: Complete fracture at the interface; B: Partial fracture at the interface; C: Less than 50% of cohesive failure in resin cement, including fracture at the interface between resin coating material and resin cement; D: More than 50% of cohesive failure in resin cement, including fracture at the interface between resin coating material and resin cement.

RESULTS

Microtensile bond strength

Table 2 presents the mean MTBSs to pulpal floor dentin with and without resin coating. MTBSs with resin coating were significantly higher than those without resin coating, except for the SE/DC group ($p<0.05$). With Panavia F 2.0, the mean original MTBS without resin coating (ED/PA) was 8.0 MPa, which was the lowest value among all the groups. Resin coating with Clearfil SE Bond (SE/PA) significantly improved the bond strength to pulpal floor dentin. However, no significant differences were observed in MTBS between the resin coating with SE only and that with the combination of SE and FX.

In the case of cementation with Clearfil DC Core Automix, the mean original MTBS (ED/DC) was 11.3 MPa, which was significantly higher than ED/PA. There were no differences in MTBS between non-coating (ED/DC) and coating with SE (SE/DC). However, resin coating with the combination of SE and FX (SE+FX/DC) provided a statistically higher bond strength to dentin than that with SE only ($p<0.05$), and which was the highest MTBS among all the groups.

Fracture pattern

Table 2 summarizes the fracture modes after MTBS test. The SEM photomicrographs of the typical fracture patterns are shown in Fig. 2. All the specimens of the non-coated groups showed fracture modes A (complete fracture at the interface) and B (partial fracture at the interface). In particular, fracture mode A was observed mainly in the non-coated groups. For resin coating with Clearfil SE Bond (SE/PA, SE/DC), fracture modes C (less than 50% of cohesive failure in resin cement, including

Table 2　MTBSs of composite cores to pulpal floor dentin with/without resin coasting and fracture modes

Experimental group		MTBS (MPa)	Fracture mode (%)			
			A	B	C	D
Non-coating	ED/PA	8.0 (1.4)[a]	92	8	0	0
	ED/DC	11.3 (0.9)[b]	91	9	0	0
Resin-coating	SE/PA	17.5 (4.4)[c]	0	0	57	43
	SE/DC	13.1 (2.3)[b]	0	0	47	53
	SE+FX/PA	22.1 (1.2)[c]	0	0	25	75
	SE+FX/DC	27.5 (3.8)[d]	0	0	56	44

mean (SD); n=5.

Same superscript letters represent no statistically significant difference ($p<0.05$).

Fracture modes: A-Complete fracture at the initerface; B-Partial fracture at the interface; C-Less than 50% of cohesive failure in resin cement, including fracture at the interface between resin coating material and resin cement; D-More than 50% of cohesive failure in resin cement, including fracture at the interface between resin coating material an resin cement.

ED: ED Primer Ⅱ, SE: Clearifil SE Bond, FX: Clearfil Flow FX, PA: Panavia F 2.0, DC: Clearfil DC Core Automix

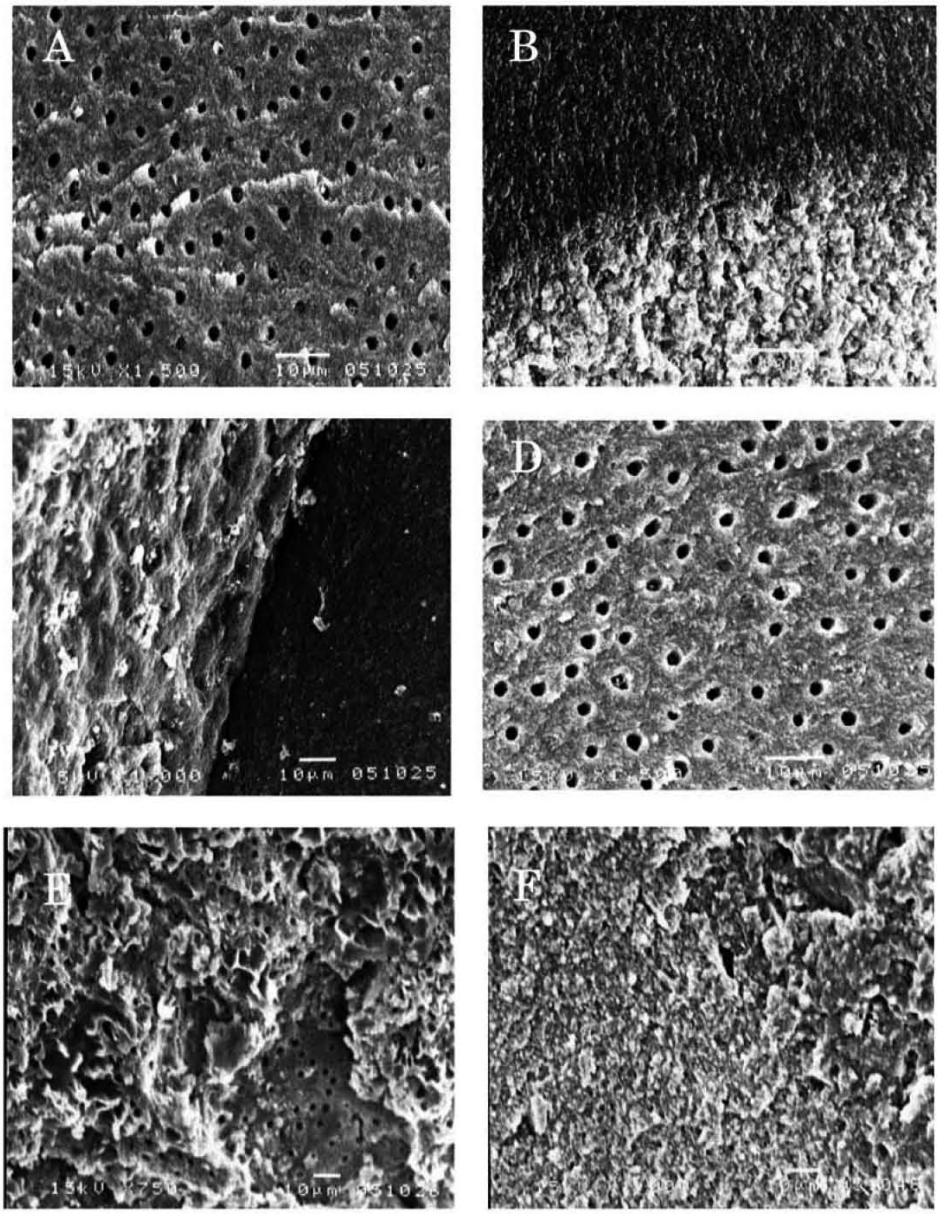

Fig. 2　SEM images of typical fracture patterns after MTBS testing. A: Adhesive fracture at the interface (mode A) observed in ED/PA; B: Failure at the interface between coating and cement (mode C) observed in SE/PA; C: Failure at the interface between coating and cement (mode D) observed in SE+FX/PA; D: Adhesive fracture at the interface (mode A) observed in ED/DC; E: Failure at the interface between coating and cement (mode C) observed in SE/DC; F: Failure at the interface between coating and cement (mode D) observed in SE+FX/DC.

fracture at the interface between resin coating material and resin cement) and D (more than 50% of cohesive failure in resin cement, including fracture at the interface between resin coating material and resin cement) were observed. For resin coating with the combination of SE and FX (SE+FX/PA, SE+FX/DC), fracture modes C and D were observed. In all the groups, there were no differences between the fracture modes of PA group and DC group. However, fracture mode D was observed mainly in the specimens of SE+FX/PA.

DISCUSSION

The dentin bonding performance of resin cements to root dentin has been evaluated by several methods, such as push-out test[21], pull-out test[22], and fracture toughness test[23]. However, these methods are not appropriate for elucidating the bonding ability of resin cements to root dentin, because these outputs are strongly influenced by the mechanical properties of the materials used.

Loading stress is theoretically concentrated around the interface in tensile bond testing. Koibuchi *et al.*[24] evaluated the efficacy of a miniaturized dumbbell test procedure designed to more easily identify defects in bonded dentin test specimens. They suggested that this protocol was capable of clearly elucidating defective resin infiltration of demineralized dentin in bonded interfaces. Separately, Sano *et al.*[25] introduced a MTBS test to measure the bond strength of small surface areas (*ca.* 1 mm^2), enabling some degree of correlation of bond strength to clinically relevant cavity preparations. Chen *et al.*[26] then reported that the non-trimming microtensile test potentially rendered a more realistic expectation of resin-dentin bonding than with conventional bulk specimens. Therefore, in this study, MTBS test with beam-shaped specimens was selected as the method to measure the bonding performance of composite core materials to pulpal floor dentin.

The resin coating technique has been shown to enhance the dentin bonding performance of resin cements[8,9,12-14], marginal sealing[8,13], and interfacial adaptation to the cavity. This technique also minimizes pulpal irritation of vital teeth[15,16]. Obtaining a hermetic seal is one key step to achieving a successful long-term root filling. Application of a resin coating to the coronal openings of endodontically treated teeth significantly reduced the incidence of coronal leakage[17]. Perfect sealing was achieved by coating with a combination of Clearfil SE Bond and Protect Liner F (Kuraray Medical, Tokyo, Japan)[17].

Clearfil SE Bond is a two-step self-etching primer adhesive system, which has been shown to provide reliable bonding to dentin and enamel[27,28]. The SE Primer contains an acidic monomer, MDP, which simultaneously conditions both enamel and dentin, before SE Bond is applied to the conditioned tooth surface[29]. Aksornmuang *et al.*[30] reported that the bond strength of Clearfil SE Bond was significantly improved at both coronal and apical regions when the photo-irradiation time was extended.

The ultrastructure of pulp chamber floor dentin appears similar to secondary and reparative dentin, containing irregular, fewer and narrower tubules compared to coronal dentin[31,32]. Toba *et al.*[18] reported that the bond strengths of dentin bonding systems to pulp chamber floor dentin were lower than those to coronal dentin; however, the self-etching primer systems provided a more reliable bond to the dentin of both regions. Akagawa *et al.*[19] evaluated the bond strength of Clearfil SE Bond to pulpal floor dentin in an access cavity. They demonstrated that the bond strength to pulpal floor dentin was influenced by cavity configuration, dentin depth, and curing behavior of resin composites[33,34].

In the present study, we sought to evaluate the bond strength of indirect composite cores to pulp chamber floor dentin. Results of this study demonstrated that resin coating enhanced the microtensile bond strengths of indirect composite cores to pulpal floor dentin. Highest bond strength was obtained when Clearfil DC Core Automix was applied with a resin coating of a combination of Clearfil SE Bond and Clearfil Flow FX.

Udo *et al.*[35] demonstrated that materials with higher ultimate tensile strength used in resin coating and cementation enhanced the bond strength between the resin coating material and resin cement. They measured the ultimate tensile strengths of some composite materials used for resin coating. The ultimate tensile strength of Clearfil Flow FX was significantly higher than that of a flowable composite, Protect Liner F. In addition, the ultimate tensile strength of Clearfil DC Core Automix was significantly higher than that of Panavia F.2.0. Clearfil DC Core Automix is used as a dual-cured resin composite for core buildup[36]. However, this can be also applied for cementation of indirect restorations in the clinic. Based on the results obtained by Udo *et al.*[35], the combination of Clearfil DC Core Automix and Clearfil Flow FX as a resin coating provided the highest microtensile bond strength. This result was in strong agreement with the present results.

Resin coating with the combination of SE and FX increased the bond strength to dentin, as compared with a mere application of SE[35]. Similar tendencies were reported by previous studies[8]. By coating the dentin bonding system with a flowable resin composite, an oxygen inhibition layer containing uncured resin of the dentin bonding system can be reduced. Moreover, uncured resin in the oxygen inhibition layer may subsequently polymerize with the free radicals diffused from the flowable resin composite. To add on to the list of benefits, the flowable resin composite can help compensate for polymerization stress due to its greater elasticity.

With regard to cementation of an indirect composite core in an access cavity, the light irradiated by a light curing unit probably did not reach the dual-cured composite material sufficiently through the indirect composite core[37]. Tashiro *et al.*[38] reported that the thicker the composite restoration, the greater was the reduction in light

intensity through the composite. In light of this report, it was chiefly chemical polymerization of the dual-cured resin cement that would have occurred at the cavity floor in this study. Tay *et al.*[39] demonstrated that there was an inverse relation between the acidity of adhesive and MTBS of resin composite to dentin when a chemical-cured resin composite was used with a photo-cured adhesive. A tertiary amine in the chemical-cured resin composite forms a charge transfer complex with an acidic monomer of the bonding agent, such as MDP of SE Bond, and which consequently affects the polymerization of the chemical-cured resin composite[40].

Based on the failure mode results, all specimens of the non-coated groups showed complete or partial fracture at the interface. As for the resin-coated groups, cohesive failure in resin cement including fracture at the interface between resin coating material and resin cement was observed. Since debonding of a bonded specimen theoretically takes place at the weakest point in the bonding interface[24], there might be some difficulty for the non-coated groups to sufficiently reinforce a smear layer to the same level as hybridized intact dentin. On the other hand, fracture failure shifted from adhesive failure (mode A) to cohesive failure within the cement and between the coating and cement (modes C and D), when a resin coating was applied. This suggested that the cement might be the weakest link in these complex bonded assemblies. From a clinical view point, the resin coating has beneficial effects because even if the restoration fractures, the resin coating material can still protect the prepared dentin from chemical, physical, and biological insults[41].

Dentin bond strength is influenced by many clinical factors[42,43]. The material selected for impression making[44] and the provisional restoration[45] after application of the resin coating play a pivotal role in the success of the final restoration. A water-setting material, Caviton, was used for temporization in this study because this material does not influence the bond strength to resin-coated cavities[44,45]. Conversely, chemical irrigants such as sodium hypochlorite and hydrogen peroxide, which are used in endodontic treatments, affect adhesion to dentin.

Built-up direct cores should be the first choice for non-vital teeth. This is because direct cores are less invasive than indirect cores. Besides, the bonding performance of resin cements to dentin is still lower than that of direct resin adhesives[8,9]. However, if an indirect core is chosen, a resin coating should be applied to enhance the dentin bond strength of the resin cement as pulpal floor dentin is an important substrate to be bonded to.

Kitasako *et al.*[12] has demonstrated the long-term durability of indirect restorations to coronal dentin. However, there is little information on long-term durability to root dentin. Therefore, further studies should be carried out to elucidate the clinical significance of resin coating technique in indirect restorations for non-vital teeth.

ACKNOWLEDGEMENTS

This work was supported by the Center of Excellence Program for Frontier Research on Molecular Destruction and Reconstruction of Tooth and Bone at Tokyo Medical and Dental University, and by a Grant-in-aid from the Japan Society for the Promotion of Science (JSPS No. 19209059).

REFERENCES

1) Wagnild GW, Mueller KI. Restoration of the endodontically treated tooth. In: Pathways of the pulp, 8th ed, St Louis, Mosby, 2000, pp.765-795.
2) Tyas MJ, Anusavice KJ, Frencken JE, Mount GJ. Minimal intervention dentistry: A review. FDI Commission Project 1-97. Int Dent J 2000; 50: 1-12.
3) Mannocci F, Innocenti M, Ferrari M, Watson TF. Confocal and scanning electron microscopic study of teeth restored with fiber posts, metal posts, and composite resins. J Endod 1999; 25: 789-794.
4) Ferrari M, Mannocci F, Vichi A, Cagidiaco MC, Mjor IA. Bonding to root canal: structural characteristics of the substrate. Am J Dent 2000; 13: 255-260.
5) Ukon S, Moroi H, Okimoto K, Fujita M, Ishikawa M, Terada Y, Satoh H. Influence of different elastic moduli of dowel and core on stress distribution in root. Dent Mater J 2000; 19: 50-64.
6) Morgano SM. Restoration of pulpless teeth: Application of traditional principles in present and future contexts. J Prosthet Dent 1996; 75: 375-380.
7) Yoo HM, Oh TS, Pereira PN. Effect of saliva contamination on the microshear bond strength of one-step self-etching adhesive systems to dentin. Oper Dent. 2006; 31: 127-134.
8) Jayasooriya PR, Pereira PN, Nikaido T, Tagami J. Efficacy of a resin coating on bond strengths of resin cement to dentin. J Esthet Restor Dent 2003; 15: 105-113.
9) Okuda M, Nikaido T, Maruoka R, Foxton RM, Tagami J. Microtensile bond strengths to cavity floor dentin in indirect composite restorations using resin coating. J Esthet Restor Dent 2007; 19: 38-46.
10) Nikaido T, Takada T, Burrow MF, Tagami J. The early bond strength of dual cured resin cement to enamel and dentin. J Jpn Dent Mater 1992; 11: 910-915.
11) Otsuki M, Yamada T, Inokoshi S, Hosada H. Establishment of a composite resin inlay technique. Part 7: Use of low viscous resin. J Jpn Conserv Dent 1993; 36: 1324-1330.
12) Kitasako Y, Burrow MF, Nikaido T, Tagami J. Effect of resin-coating technique on dentin tensile bond strengths over 3 years. J Esthet Restor Dent 2002; 14: 115-122.
13) Jayasooriya PR, Pereira PN, Nikaido T, Burrow MF, Tagami J. The effect of a "resin coating" on

the interfacial adaptation of composite inlays. Oper Dent 2003; 28: 28-35.
14) Nikaido T. A resin coating technique to achieve minimal intervention in indirect resin composites: A case report. Int Chin J Dent 2003; 3: 62-68.
15) Christensen GJ. Resin cements and postoperative sensitivity. JADA 2000; 131: 1197-1199.
16) Satoh M, Inai N, Nikaido T, Tagami J. How to use Liner Bond System as a dentin and pulp protector in indirect restorations. J Jpn Adhes Dent 1994; 12: 41-47.
17) Maruoka R, Nikaido T, Ikeda M, Ishizuka T, Foxton RM, Tagami J. Coronal leakage inhibition in endodontically treated teeth using resin-coating technique. Dent Mater J 2006; 25: 97-103.
18) Toba S, Veerapravati W, Shimada Y, Nikaido T, Tagami J. Micro-shear bond strengths of adhesive resins to coronal dentin *versus* the floor of the pulp chamber. Am J Dent 2003; 16: 51-56.
19) Akagawa H, Nikaido T, Burrow MF, Tagami J. Influence of cavity configuration on the adhesion of two resin-based composites to pulpal floor dentin. Am J Dent 2005; 18: 233-236.
20) Akagawa H, Nikaido T, Takada T, Burrow MF, Tagami J. Shear bond strengths to coronal and pulp chamber floor dentin. Am J Dent 2002; 15: 383-388.
21) Bitter K, Meyer-Lückel H, Priehn K, Martus P, Kielbassa AM. Bond strengths of resin cements to fiber-reinforced composite posts. Am J Dent 2006; 19: 138-142.
22) Di Felice R, Rappelli G, Camaioni E, Cattani M, Meyer JM, Belser UC. Cementable implant crowns composed of cast superstructure frameworks luted to electroformed primary copings: an *in vitro* retention study. Clin Oral Implants Res 2007; 18: 108-113.
23) Bapna MS, Mueller HJ. Fracture toughness, diametrical strength, and fractography of amalgam and of amalgam to amalgam bonds. Dent Mater 1993; 9: 51-56.
24) Koibuchi H, Yasuda N, Nakabayashi N. Bonding to dentin with a self-etching primer: the effect of smear layers. Dent Mater 2001; 17: 122-126.
25) Sano H, Yoshikawa T, Pereira PN, Kanemura N, Morigami M, Tagami J, Pashley DH. Long-term durability of dentin bonds made with a self-etching primer, *in vivo*. J Dent Res 1999; 78: 906-911.
26) Chen KK, Shono Y, Ogawa T, Kozono Y, Terashita M. Fracture aspects of resin-dentin bonding in non-trimming microtensile test. Dent Mater J 2001; 20: 315-324.
27) Aksornmuang J, Nakajima M, Foxton RM, Tagami J. Regional bond strength of four self-etching primer/adhesive systems to root canal dentin. Dent Mater J 2005; 24: 261-267.
28) Wattanawongpitak N, Yoshikawa T, Burrow MF, Tagami J. The effect of bonding system and composite type on adaptation of different C-factor restorations. Dent Mater J 2006; 25: 45-50.
29) Watanabe I, Nakabayashi N, Pashley DH. Bonding to ground dentin by a phenyl-P self-etching primer. J Dent Res 1994; 73: 1212-1220.
30) Aksornmuang J, Nakajima M, Foxton RM, Tagami J. Effect of prolonged photo-irradiation time of three self-etch systems on the bonding to root canal dentine. J Dent 2006; 34: 389-397.
31) Yoshiba K, Yoshiba N, Iwaku M. Histological observations of hard tissue barrier formation in amputated dental pulp capped with alpha-tricalcium phosphate containing calcium hydroxide. Endod Dent Traumatol 1994; 10: 113-120.
32) Morse DR. Age-related changes of the dental pulp complex and their relationship to systemic aging. Oral Surg Oral Med Oral Pathol 1991; 72: 721-745.
33) Yoshikawa T, Sano H, Burrow MF, Tagami J, Pashley DH. Effects of dentin depth and cavity configuration on bond strength. J Dent Res 1999; 78: 898-905.
34) Nikaido T, Kunzelmann KH, Ogata M, Harada N, Yamaguchi S, Cox CF, Hickel R, Tagami J. The *in vitro* dentin bond strengths of two adhesive systems in Class I cavities of human molars. J Adhes Dent 2002; 4: 31-39.
35) Udo T, Nikaido T, Ikeda M, Weerasinghe DS, Harada N, Foxton RM, Tagami J. Enhancement of adhesive between resin coating materials and resin cements. Dent Mater J 2007; 26: 519-525.
36) Ariyoshi M, Nikaido T, Foxton RM, Tagami J. Dentin bond strengths of three adhesive/composite core systems using different curing units. Dental Mater J (in press).
37) Price RB, Derand T, Loney RW, Andreou P. Effect of light source and specimen thickness on the surface hardness of resin composite. Am J Dent 2002; 15: 47-53.
38) Tashiro H, Inai N, Nikaido T, Tagami J. Effects of light intensity through resin inlays on the bond strength of dual-cured resin cement. J Adhes Dent 2004; 6: 233-238.
39) Tay FR, King NM, Suh BI, Pashley DH. Effect of delayed activation of light-cured resin composites on bonding of all-in-one adhesives. J Adhes Dent 2001; 3: 207-225.
40) Giannini M, De Goes MF, Nikaido T, Shimada Y, Tagami J. Influence of activation mode of dual-cured resin composite cores and low-viscosity composite liners on bond strength to dentin treated with self-etching adhesives. J Adhes Dent 2004; 6: 301-306.
41) Islam MR, Takada T, Weerasinghe DS, Uzzaman MA, Foxton RM, Nikaido T, Tagami J. Effect of resin coating on adhesion of composite crown restoration. Dent Mater J 2006; 25: 272-279.
42) Nikaido T, Takano Y, Sasafuchi Y, Burrow MF, Tagami J. Bond strengths to endodontically treated teeth. Am J Dent 1999; 12: 177-180.
43) Sasafuchi Y, Nikaido T, Tagami J. Effect of chemical irrigants and medicaments for endodontic treatment on dentin bonding. Int Chin J Dent 2003; 3: 7-12.
44) Nakano M, Takada T, Nikaido T, Tagami J. Effect of impression material on adhesion of resin cement to resin coated teeth. J Jpn Adhes Dent 1999; 17: 198-204.
45) Nikaido T, Koh Y, Satoh M, Takakura H, Inokoshi S, Takatsu T, Hosoda H. Effect of temporary filling materials on adhesion of dual cured resin cement to low viscosity resin. J Jpn Dent Mater 1993; 12: 655-661.

MEMO

分子情報伝達学分野

高柳　広

東京医科歯科大学大学院医歯学総合研究科
分子情報伝達学・教授

1. 研究の題目及び平成21年2月までの研究内容

研究の題目

骨代謝制御ネットワークの解明: Elucidation of novel regulatory mechanisms in bone metabolism

研究内容

骨代謝は、骨自身だけではなく他臓器や組織の恒常性維持にも重要である事が明らかにされている。しかしながら、骨による全身へのマクロな制御機構だけでなく、破骨細胞や骨芽細胞といった骨構成細胞間や細胞内シグナルのようなミクロな制御機構も依然として不明な点が多い。本研究は骨代謝制御ネットワークを、骨を構成する個々の細胞間から最終的に全身の組織、臓器レベルで解明する。この実現の為に、研究内容は3つの項目から構成され、段階的に遂行することになっている。A）骨構成細胞に発現する遺伝子・タンパク質の網羅解析;B）コンディショナル遺伝子改変マウスを用いた骨代謝制御遺伝子の機能解析; C）骨による全身性制御機構の解明である。本年度は、まず、この制御機構の全貌を明らかとするため、各細胞の網羅的なトランスクリプトーム解析とプロテオーム解析に着手した。現在までに、破骨細胞、骨芽細胞、骨細胞に発現する遺伝子のプロファイリングが終了し、その情報を基盤として、標的候補遺伝子群のshRNAライブラリーの作製の準備を進めている。shRNAの効果は、各細胞の分化や機能に与える影響を指標として評価を行なう予定である。プロテオーム解析に関しては、リン酸化タンパク質を当面の指標として、各細胞においてプロテオーム解析を進めている。以上の解析を基に、骨代謝の制御に関わる有力な候補遺伝子を同定次第、次段階の遺伝子改変マウスの作製に取りかかる。

2.

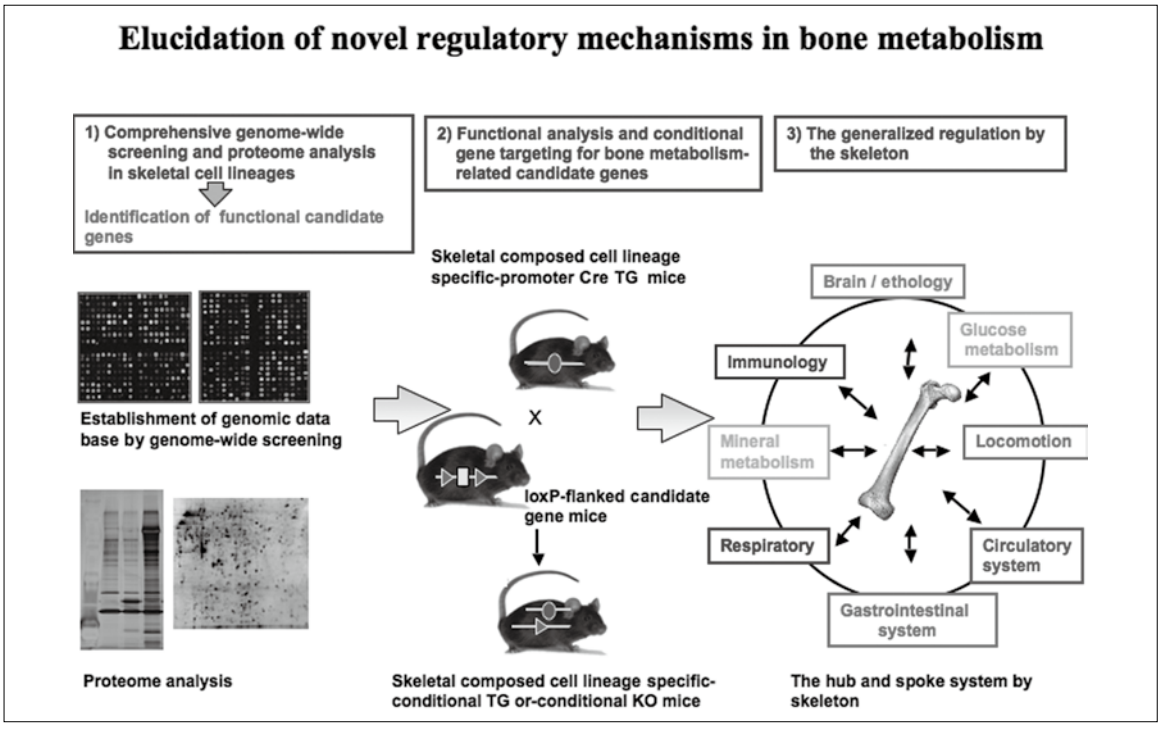

3. 2008年、2009年（平成21年3月までの）に発表した全ての研究内容についての英文要約

(1) Identification of the negative regulation of osteoclast formation by cell-surface: We identified that PIR-B/LILRB, inhibitory immunoglobulin-like receptors, negatively regulate the development of osteoclast. PIR-B/LILRB constitutively binds with MHC class I molecules on the same cell surface but also recruits SHP-1 in the presence of RANKL（ref 1）. (2) Identification of new roles of RANKL as an essential cytokine in the thymic architecture: We elucidated that RANKL, a crucial cytokine for oseteoclast differentiation, was one of the important cytokines for thymic medulla formation. RANK-RANKL signal is critical for establishing central tolerance（ref 2,3）. (3) Elucidation of the regulatory mechanism of osteoclast differentiation by Tec family kinases: We found that mice lacking Btk and Tec showed severe osteopetrosis caused by a defect of oseteoclast differentiation. We revealed that Btk（Tec）/BLNK（SLP-76）-containing complex connects RANK and ITAM signals to PLC γ -induced calcium influx（ref 4）. (4) Identification of Cathepsin K-dependent TLR9 signaling in autoimmune arthritis: We found that inhibition of cathepsin K suppressed inflammation of the joints as well as osteoclastic bone resorption in autoimmune arthritis. We revealed that cathepsin K is a critical regulator of TLR9 signaling in dendritic cells in response to unmethylated CpG DNA（ref 5）.

4. 本事業に関連して世界的な研究拠点形成に向けて、以下の点で改善・整備等されたこと

A（研究拠点体制）、B（研究教育環境）、C（人材確保）、D（人材育成）、E（国際化）

A, 骨研究に従事する拠点内研究者のみならず、他分野（特に免疫学）の学外研究者との共同研究を通じて、世界的な成果を発表できた。

B, 本年度は GCOE AISS学生の博士号取得に向けた確実な研究指導を行った。

C, D 他大学ならびに他分野からのGCOE拠点形成教員、国内外からのポスドク、大学院生、技術補佐員を増員し、学際的環境下での骨代謝研究を推進できる環境を整備した。

E, 多数の海外での講演、国際学会のorganizeを行った。また、海外からのポスドクが常時研究に参画しており、ラボ内セミナーでの公用語は英語としている。

5）GCOE事業を推進するに当たって力を入れた点

GCOEシンポジウムや国際学会を活用して、世界の優れた研究者と意見交換を行い、第一線の研究レベルを意識した研究推進を行った。さらに本年度は、GCOE拠点内にとどまらず東京医科歯科大学や他大学の研究者と広く密接な連携を行うことで、各分野の先端的な発想を自分の研究領域と融合させ、研究成果として結実させることを心がけた。

5. 英文原著論文

1. Mori Y, Tsuji S, Inui M, Sakamoto Y, Endo S, Ito Y, Fujimura S, Koga T, Nakamura A, Takayanagi H, Itoi E, Takai T.
Inhibitory immunoglobulin-like receptors LILRB and PIR-B negatively regulate osteoclast development. J Immunol 181:4742-4751、2008

2. Akiyama T, Shimo Yu, Yanai H, Qin J, Ohshima D, Maruyama Y, Asaumi Y, Kitazawa J, Takayanagi H, Penninger JM, Matsumoto M, Nitta T, Takahama Y, Inoue J.
The tumor necrosis factor family receptors RANK and CD40 cooperatively establish the thymic medullary microenvironment and self-tolerance. Immunity 29:423-437、2008

3. Hikosaka Y, Nitta T, Ohigashi I, Yano K, Ishimaru N, Hayashi Y, Matsumoto M, Matsuo K, Penninger JM, Takayanagi H, Yokota Y, Yamada H, Yoshikai Y, Inoue J, Akiyam, T, Takahama Y.
The cytokine RANKL produced by positively selected thymocytes fosters medullary thymic epithelial cells that express autoimmune regulator. Immunity 29:438-450、2008

◎ 4. Shinohara, M., Koga, T., Okamoto, K., Sakaguchi, S., Arai, K., Yasuda, H., Takai, T., Kodama, T., Morio, T., Geha, R. S., Kitamura, D., Kurosaki, T., Ellmeier, W., and Takayanagi, H. Tyrosine kinases Btk and Tec regulate osteoclast differentiation by linking RANK and ITAM signals. Cell 132, 794-806（2008）

◎ 5. Asagiri M, Hirai T, Kunigami T, Kamano S, Gober HJ, Okamoto K, Nishikawa K, Latz E, Golenbock DT, Aoki K, Ohya K, Imai Y, Morishita Y, Miyazono K, Kato S, Saftig P, Takayanagi H.
Cathepsin K-dependent toll-like receptor 9 signaling revealed in experimental arthritis. Science 319:624-627、2008

◎ 6. Nakashima T, Takayanagi H.
The dynamic interplay between osteoclasts and the immune system. Arch Biochem Biophys（Highlight Issue: Bone Remodeling）473（2）:166-171、2008--Review

6. 特許取得、特許申請

発明名称:カテプシン阻害剤を有効成分として含有するToll様受容体のシグナル伝達の調整剤（特願:2007-276937）（PCT/JP2008/069235）

①発明者:高柳広、朝霧成挙、平井利武

②出願日:2007年10月24日　PCT:2008年10月23日

③出願人:国立大学法人　東京医科歯科大学、
日本ケミファ株式会社

7. 自己評価

本年度は、破骨細胞特異的に機能すると考えられていたRANKLが、T細胞の分化に重要な胸腺髄質の形成に不可欠であることを発見したことに加え、カテプシンKが樹状細胞におけるTLR9シグナルに重要な役割を果たす事を明らかにした。さらに、抑制性免疫グロブリン様受容体であるPIR-B/LILRBが、破骨細胞の分化を負に制御していることを発見した。また、Tecファミリーキナーゼが ITAM受容体とRANKによるカルシウムシグナルの誘導に必須であることを明らかにした。以上、本年度は骨と免疫系が密接に関与している事を多数発見でき、6本の論文として発表した。また本年度は、骨構成細胞の各細胞における網羅的なトランスクリプトーム解析を行ない、骨代謝系と免疫系に関わる候補遺伝子群の選択を行なった。今後、さらに解析を進め骨と免疫の相互作用の解明に取り組む予定である。

8. 和文原著論文

1. 岡本一男、高柳広.自己免疫疾患にかかわるcathepsin Kの新たな役割. 実験医学　26（20）:182-187、2008
2. 高柳広.破骨細胞分化制御と骨免疫学.最新医学　63（11）:28（2176）-33（2181）、2008
3. 國上敏浩、高柳広.自己免疫性炎症におけるカテプシンKとToll-like receptor9の役割.内分泌・糖尿病科　27（3）:264-269、2008
4. 古賀貴子、高柳広.骨免疫学研究の歴史とup to date. リウマチ科　40（2）:105-111、2008
5. 高柳広.破骨細胞分化シグナルと骨免疫学（第18回婦人科骨粗鬆症研究会、特別講演I）. Osteoporosis Japan 16（3）74（446）-83（455）、2008
6. 岡本一男、高柳広.炎症性骨破壊におけるTh17細胞の役割—Th17細胞による破骨細胞制御のメカニズム. 医学のあゆみ　226（4）291-294、2008
7. 高柳広.関節破壊のメカニズム. 整形外科　59（8）850-854 2008
8. 中島友紀、高柳広.骨免疫学の最先端. Mebio 25（8）24-35 2008
9. 林幹人、中島友紀、高柳広.免疫と骨:骨免疫学Osteoimmunologyの幕開け. 臨床検査　52（5）556-560、2008
10. 高柳広.骨免疫学. The BONE 22（3）57-61,2008
11. 篠原正浩、高柳広.破骨細胞形成のメカニズム—新たな骨破壊疾患治療法の可能性. DENTAL DIAMOND 33（475）68-71、2008
12. 高柳広.Osteoimmunologyと破骨細胞. 医学部のあゆみ　別冊　骨粗鬆症—臨床と研究の最新動向 p37-45、2008
13. 高柳広.関節リウマチ骨破壊のメカニズムと骨免疫学（第8回日本リウマチ財団　中国・四国リウマチ外科セミナー記録集）. Pharma Medica 26（3）27-31、2008

9. 学会発表（英文）

T. Koga, M. Shinohara, K. Okamoto, K. Arai, H. Takayanagi.
Tec kinases form an osteoclastogenic signaling complex with SLP adaptor proteins.
The 13th Asia Pacific League of Associations for Rheumatology Congress. Oral. Yokohama, 2008.9.26

K. Okamoto, M. Asagiri, T. Hirai, T. Kunigami, H.J. Gober, K. Nishikawa, K. Aoki, K. Ohya, S. Kato, P. Saftig, H. Takayanagi.
A Novel Role of Cathepsin K In Autoimmunity: Regulation of Toll-Like Receptor 9 signaling in Dendritic Cells
The 13th Asia Pacific League of Associations for Rheumatology Congress. Oral. Yokohama, 2008.9.24.

Okamoto K, Asagiri M, Hirai T, Kunigami T, Gober HJ, Nishikawa K, Aoki K, Ohya K, Kato S, Saftig P, Takayanagi H. Osteoclast-Independent Function of Cathepsin K: Regulation of Toll-like Receptor 9 Signaling in Autoimmunity.
The 30th Annual Meeting of the American Society for Bone and Mineral Research. Oral. Montreal, Canada, 2008.9.12,13

10. 学会発表（和文）

古賀貴子、篠原正浩、高柳広.
Tecファミリーチロシンキナーゼによる破骨細胞分化制御.
第31回日本分子生物学会年会・第81回日本生化学会大会 合同大会、神戸、2008.12.11

西川恵三、高橋智、高柳広.
加齢に伴い発現変動する転写因子Mafの細胞分化に及ぼす影響.
第31回日本分子生物学会年会・第81回日本生化学会大会 合同大会、神戸、2008.12.11

西川恵三、竹田秀、山口朗、高柳広.
加齢に伴う骨量減少の原因となる転写メカニズムの探索.
第26回日本骨代謝学会学術集会、大阪、2008.10.29

篠原正浩、古賀貴子、岡本一男、高柳広.
免疫不全と骨代謝―Tecファミリーチロシンキナーゼによる破骨細胞分化制御―.
第29回日本炎症・再生医学会、東京、2008.7.10

篠原正浩、古賀貴子、岡本一男、高柳広.
Tecファミリーキナーゼによる破骨細胞分化制御機構.(The role of Tec family kinases in osteoclast differentiation)
第52回日本リウマチ学会総会・学術集会ワークショップ32「骨代謝と骨粗鬆症」、札幌、2008.4.23

◎朝霧成挙、平井利武、國上敏浩、GOBER Hans-Jeurgen、岡本一男、西川恵三、高柳広.
カテプシンKはToll様受容体9シグナルを介して自己免疫性炎症疾患の重症度を決定する.
第52回日本リウマチ学会総会・学術集会ワークショップ9「関節リウマチの病因・病態1」、札幌、2008.4.22

11. 受賞

高柳広,財団法人　持田記念医学薬学振興財団　持田記念学術賞　2008.10.17
高柳広,財団法人　井上科学振興財団　井上学術賞　2009.2.4

12. 外部資金の獲得状況

文部科学省科学研究費補助金　学術創成研究費
研究題目　骨免疫学の創成
代表:　高柳　広
期間:　平成17年度―平成21年度
研究費総額:54110万円

文部科学省科学研究費補助金　萌芽研究
研究題目　炎症性破骨細胞の同定とその特異的プロテアーゼに着目した骨破壊防御法の開発
代表:　高柳　広
期間:　平成19年度―平成21年度
研究費総額:　320万円

文部科学省ゲノムネットワークプロジェクト　代表研究者
研究題目　個別生命機能の解析「運動器の形成・維持・老化に関わる遺伝子制御ネットワークの解明」
代表:　高柳　広
期間:　平成17年度―平成21年度
研究費総額:12300万円

日本学術振興会科学研究費補助金特別研究員奨励費
研究題目　:性ホルモンを介した骨代謝制御における制御性T細胞の意義
代表:　高柳広
期間:　平成20年度―平成22年
研究費総額:　300万円

財団法人　武田科学振興財団生命科学研究助成
研究題目　骨の老化機構の解明とその制御法の確立
代表:　高柳　広
期間:　平成20年―平成21年度
研究費総額:1000万円

財団法人　金原一郎記念医学医療振興財団　研究助成金
研究題目　骨芽細胞を制御する新規遺伝子の同定と機能解析
代表:　高柳　広
期間:　平成20年―平成21年度
研究費総額:45万円

文部科学省科学研究費補助金　若手研究A
研究題目　骨リモデリングの開始と制御機構の解明
代表:　中島友紀
期間:　平成19年度―平成21年度
研究費総額:　2080万円

文部科学省科学研究費補助金　若手研究A
研究題目　骨破壊性疾患における非ヒストンタンパク質のメチル化修飾の意義
代表:　古賀貴子

期間:　平成20年度―平成22年度
研究費総額:　1960万円

文部科学省科学研究費補助金若手研究（スタートアップ）
研究題目　:加齢に伴う骨芽細胞・脂肪細胞分化スイッチにおける転写因子Mafの役割
代表:　西川恵三
期間:　平成20年度―平成21年度
研究費総額:　300万円

日本リウマチ財団リウマチ性疾患調査　研究助成費
破骨細胞を標的とした関節リウマチ骨破壊治療の分子基盤の確立
研究代表者:中島友紀
期間:　平成20年度
研究費総額:　100万円

病態代謝研究会平成20年度研究助成金
破骨細胞の表面抗原を標的とした新規抗体治療の分子基盤の確立
研究代表者:中島友紀
期間:　平成20年度
研究費総額:　100万円

13. 特別講演、招待講演

Takayanagi H. Osteoimmunology-Interactions and shared mechanisms between the immune system and bone.
The Annual Symposium of IFReC（Immunology Frontier Research Center）, Osaka University, Osaka, 2009.2.12

Takayanagi H. Molecular mechanism in osteoclastogenesis.
JSPS Core-to-Core Program International Workshop on Advanced Bone and Joint Science（ABJS）. Tokyo, 2008.12.4

Takayanagi H. Bone and Immune System.
Annual Meeting of Korean Endocrine Society. Jeju, Korea, 2008.11.8

Takayanagi H. Osteoimmunology -unexpected link between immune and bone cells. Seminar, New York University, New York, 2008.10.3

Takayanagi H. Bone destruction in inflammation and osteoimmunology
HSDM Basic & Clinical Science Forum, Boston, 2008.10.2

Takayanagi H. Th17 Cytokines and their Effects.
2008 ACR Basic Research conference. San Francisco, 2008.10.24

Takayanagi H. Osteoclasts in Arthritis and Osteoimmunology.
13th Congres of the Asia Pacific League of Associations for Rheumatology. Yokohama, 2008.9.23

Takayanagi H. Use of mouse genetics in bone biology and osteoimmunology.
EMBO Practice Course on "Anatomy and Embryology of the Mouse". Zagreb, Croatia, 2008.9.10

Takayanagi H. Unexpected link between osteoclast and the immune system.
2nd International Conference on Osteoimmunology:Interactions of the Immune and Skeletal Systems. Rhodos. Greece, 2008.6.11

Takayanagi H. Regulation of Osteoclastogenesis and Osteoimmunology.
International Bone & Mineral Society Davos Workshops. Davos, Switzerland, 2008.3.10

高柳広.関節リウマチ骨破壊と骨免疫学.
第37回九州リウマチ学会イブニングセミナー　長崎、2009.3.14

高柳広.関節リウマチ骨破壊と骨免疫学.
兵庫県リウマチ医の会　兵庫、2009.3.7

高柳広.炎症性骨破壊と骨免疫学.
第32回皮膚脈管膠原病研究会　京都、2009.1.23

高柳広.関節リウマチの骨破壊と骨免疫学.

山口県整形外科医会　山口、2009.1.17

高柳広.運動器疾患の分子ネットワークの解明と治療応用.
ゲノムネットワークプロジェクト公開シンポジウム「ゲノムネットワークが拓く新しい医学・生物学」 東京、2009.1.16

高柳広.関節リウマチ骨破壊と骨免疫学.
病態代謝血管医学セミナー、熊本、2008.11.13

高柳広.『骨免疫学の最前線』破骨細胞の新たな制御メカニズム.
第26回日本骨代謝学会学術集会ランチョンセミナー
大阪、2008.10.31

高柳広.RANKLと骨免疫学.
第26回日本骨代謝学会学術集会イブニングセミナー
大阪、2008.10.30

高　柳　広 .Molecular determinant in osteoclast differentiation.
第70回日本血液学会総会、京都、2008.10.10

高柳広.炎症性骨破壊と骨免疫学.
第3回大阪皮膚アンチエイジング研究会、大阪、2008.10.9

高柳広.新たな破骨細胞制御メカニズム.
第28回骨形態計測学会、東京、2008.7.26

高柳広.関節リウマチ骨破壊と骨免疫学.
東京骨関節フォーラム、東京、2008.7.12

高柳広.関節リウマチ骨破壊と骨免疫.
免疫シンフォニー、2008.6.28、大阪

高柳広.関節リウマチ骨破壊と骨免疫学.
城北関節炎・RA・OA・AS談話会、2008.6.26、東京

高柳広.破骨細胞の新たな制御メカニズム.
第4回ビタミンD3研究会、東京、2008.6.2

高柳広.関節リウマチ骨破壊と骨免疫学.
埼玉医大整形同門会、2008.5.31、東京

高柳広.関節リウマチの骨破壊と骨免疫学.
第81回日本整形外科学会教育研修講演、2008.5.22、札幌

高柳広.免疫と骨を壊す細胞のつながり.
免疫ふしぎ未来（日本免疫学会主催） 東京、2008.5.3-4、

高柳広.破骨細胞の新たな制御メカニズム.
第52回日本リウマチ学会総会・学術集会シンポジウム「関節リウマチ病態解明のトピックス」、札幌、2008.4.23

高柳広.サイトカインと骨破壊.
第52回日本リウマチ学会総会・学術集会イブニングセミナー　札幌、2008.4.22

高柳広.関節リウマチ骨破壊と骨免疫学　―生物学的製剤および抗リウマチ薬の骨破壊抑制機序の理解のために―
静岡リウマチ治療研究会、浜松、2008.3.29

高柳広.関節リウマチ骨破壊と抗TNF-α療法.
1st Psoriasis Workshop　東京、2008.3.15

高柳広.骨免疫学による運動器疾患の新たな治療戦略.
第3回産業医科大学大学院シンポジウム　平成19年度文部科学省「魅力ある大学院教育」イニシアティブ事業
『Trends in Medical Science～世界最先端の科学者たちから学ぶ～』 福岡、2008.3.8

高柳広.関節リウマチ骨破壊と骨免疫学.
盛岡臨床整形外科医会、盛岡、2008.1.30

高柳広.関節リウマチ骨破壊と骨免疫学.
リウマチ性疾患研究会、東京、2008.1.26

高柳広.関節リウマチ骨破壊と骨免疫学.
埼玉リウマチ研究会、大宮、2008.1.25

14. 主催学会

第5回Osteoimmunology Forum
　2008年2月16日　主婦会館
第2回国際骨免疫学会議
　2008年6月8日～13日　ギリシャ・ロドス島
第4回骨免疫学ワークショップ
　2008年11月28日　パークハイアット東京
第6回Osteoimmunology Forum

2009年2月21日　東京大学山上会館

15. 新聞、雑誌、TV報道

日経産業新聞　2008.4.10
2008年度技術トレンド調査（第1回）
東京新聞　2008.3.7　破骨細胞つくる酵素発見
産経新聞　2008.2.1　関節リウマチに新薬
日本経済新聞　2008.2.1
関節リウマチ薬候補　骨減少と免疫抑制に効果

16. 講座の准教授、講師、助教、特別研究員、ポスドク、指導を受けた大学院生の名前（AISSには○印）のリスト

准　教　授　本郷敏雄
特任准教授　大洞将嗣
助　　教　篠原正浩
　　中島友紀
　　春宮覚
特任助教　古賀貴子
特別研究員　Ling Wang
ポスドク　西川恵三
　　Hans-Juergen Gober
指導を受けた大学院生　○林幹人、○Erik Idrus、武智香織、Abdul Alim Al-Bari

Cell

Tyrosine Kinases Btk and Tec Regulate Osteoclast Differentiation by Linking RANK and ITAM Signals

Masahiro Shinohara,[1,2] Takako Koga,[1,2] Kazuo Okamoto,[1,2] Shinya Sakaguchi,[4] Kimiko Arai,[1,5] Hisataka Yasuda,[7] Toshiyuki Takai,[6] Tatsuhiko Kodama,[8] Tomohiro Morio,[3] Raif S. Geha,[9] Daisuke Kitamura,[10] Tomohiro Kurosaki,[11] Wilfried Ellmeier,[4] and Hiroshi Takayanagi[1,2,*]

[1]Department of Cell Signaling, Graduate School
[2]Center of Excellence Program for Frontier Research on Molecular Destruction and Reconstruction of Tooth and Bone
[3]Department of Pediatrics and Developmental Biology, Graduate School
Tokyo Medical and Dental University, Yushima 1-5-45, Bunkyo-ku, Tokyo 113-8549, Japan
[4]Institute of Immunology, Center for Physiology, Pathophysiology, and Immunology, Medical University of Vienna, Lazarettgasse 19, Vienna 1090, Austria
[5]Division of Orthodontics and Dentofacial Orthopedics, Graduate School of Dentistry
[6]Department of Experimental Immunology, Institute of Development, Aging, and Cancer
Tohoku University, Seiryo-machi 4-1, Aoba-ku, Sendai, Miyagi 980-8575, Japan
[7]Nagahama Institute for Biochemical Science, Oriental Yeast Co., Ltd., Kanoh-cho 50, Nagahama, Shiga 526-0804, Japan
[8]Department of Molecular Biology and Medicine, Research Center for Advanced Science and Technology, University of Tokyo, Komaba 4-6-1, Meguro-ku, Tokyo 153-8904, Japan
[9]Division of Immunology, Children's Hospital, One Blackfin Circle, Boston, MA 02115, USA
[10]Division of Molecular Biology, Research Institute for Biological Sciences, Tokyo University of Science, Yamazaki 2669, Noda, Chiba 278-0022, Japan
[11]Laboratory for Lymphocyte Differentiation, RIKEN Research Center for Allergy and Immunology, RIKEN Yokohama Institute, Suehiro-cho 1-7-22, Tsurumi-ku, Yokohama, Kanagawa 230-0045, Japan
*Correspondence: taka.csi@tmd.ac.jp
DOI 10.1016/j.cell.2007.12.037

SUMMARY

Certain autoimmune diseases result in abnormal bone homeostasis, but association of immunodeficiency with bone is poorly understood. Osteoclasts, which derive from bone marrow cells, are under the control of the immune system. Differentiation of osteoclasts is mainly regulated by signaling pathways activated by RANK and immune receptors linked to ITAM-harboring adaptors. However, it is unclear how the two signals merge to cooperate in osteoclast differentiation. Here we report that mice lacking the tyrosine kinases Btk and Tec show severe osteopetrosis caused by a defect in bone resorption. RANK and ITAM signaling results in formation of a Btk(Tec)/BLNK(SLP-76)-containing complex and PLCγ-mediated activation of an essential calcium signal. Furthermore, Tec kinase inhibition reduces osteoclastic bone resorption in models of osteoporosis and inflammation-induced bone destruction. Thus, this study reveals the importance of the osteoclastogenic signaling complex composed of tyrosine kinases, which may provide the molecular basis for a new therapeutic strategy.

INTRODUCTION

Bone homeostasis depends on balanced action of bone-resorbing osteoclasts and bone-forming osteoblasts (Karsenty and Wagner, 2002). Tipping the balance in favor of osteoclasts leads to diseases with a low bone mass, whereas impaired osteoclastic bone resorption results in diseases with a high bone mass, including osteopetrosis (Teitelbaum and Ross, 2003). Bone reserves calcium and responds to calcium-regulating hormones, but osteoclasts and osteoblasts are not only regulated by the endocrine system. The immune and bone systems share numerous regulatory factors, including cytokines, receptors, signaling molecules, and transcription factors (Theill et al., 2002; Walsh et al., 2006; Takayanagi, 2007). Therefore, the pathology of one system may very well affect the other: it is well documented that enhanced bone resorption is associated with activation of the immune system observed in autoimmune or inflammatory diseases such as rheumatoid arthritis and periodontitis (Theill et al., 2002; Takayanagi, 2007).

Diseases with impaired immune responses are also associated with bone abnormalities, but it is poorly understood how the immunodeficiencies are functionally related to bone disorders. Hyperimmunoglobulin E (IgE) syndrome is characterized by skeletal symptoms such as osteoporosis (Kirchner et al., 1985) and scoliosis (Grimbacher et al., 1999), which are partly explained by the abnormality of osteoblasts and osteoclasts

caused by the mutation in the *STAT3* gene. (Minegishi et al., 2007). X-linked hyper-IgM syndrome (caused by a mutation in the *CD40L* gene) has a skeletal complication, osteopenia, which is attributed to enhanced osteoclast formation due to the impaired production of interferon-γ by T cells (Lopez-Granados et al., 2007). Thus, exploring the mechanisms underlying skeletal complications in primary immunodeficiencies will be important for understanding the shared mechanisms and crosstalk between immune and bone systems.

The osteoclast was the first skeletal cell to be determined to be under the control of the immune system (Horton et al., 1972). Because osteoclasts originate from bone marrow-derived monocyte/macrophage precursor cells (BMMs) of hematopoietic lineage, many regulators of osteoclast differentiation are also utilized in the control of the innate and adaptive immune systems. The differentiation of osteoclasts is mainly regulated by three signaling pathways activated by receptor activator of nuclear factor-κB ligand (RANKL), macrophage colony-stimulating factor (M-CSF), and immunoreceptor tyrosine-based activation motif (ITAM) (Asagiri and Takayanagi, 2007). Whereas M-CSF promotes the proliferation and survival of BMMs (Ross and Teitelbaum, 2005), RANKL activates the differentiation process by inducing the master transcription factor for osteoclastogenesis, nuclear factor of activated T cells c1 (NFATc1), via the tumor necrosis factor receptor-associated factor 6 (TRAF6) and c-Fos pathways (Takayanagi et al., 2002). The induction of NFATc1 is also dependent on the calcium signal, which is mediated by the activation of ITAM in adaptor molecules such as DNAX-activating protein 12 (DAP12) and Fc receptor common γ subunit (FcRγ) (Koga et al., 2004; Mocsai et al., 2004) in association with costimulatory receptors of the immunoglobulin superfamily, including triggering receptor expressed in myeloid cells-2 (TREM-2), signal-regulatory protein β1 (SIRPβ1), paired immunoglobulin-like receptor-A (PIR-A), and osteoclast-associated receptor (OSCAR) (Koga et al., 2004). Phosphorylation of ITAM results in recruitment of the nonreceptor tyrosine kinase Syk, leading to the activation of phospholipase Cγ (PLCγ) and calcium mobilization (Faccio et al., 2003; Koga et al., 2004; Mocsai et al., 2004; Mao et al., 2006), but osteoclastogenesis cannot be induced by costimulatory signals alone and requires RANKL stimulation. However, it has been unclear how RANK and ITAM signals merge to cooperatively stimulate the downstream signaling pathway.

To identify the molecules activated by RANKL that stimulate the calcium signaling pathway by functioning as an integrator of the RANK and ITAM signals, we focused on nonreceptor tyrosine kinases because PLCγ initiates the calcium signal after tyrosine phosphorylation. Among the nonreceptor tyrosine kinases, genome-wide screening revealed Btk and Tec to be highly expressed in osteoclasts. The Tec kinase family, consisting of Bmx, Btk, Itk, Rlk, and Tec, is preferentially expressed in the hematopoietic system. T cell receptor (TCR) and B cell receptor (BCR) signaling complexes include Itk/Rlk and Tec/Btk, respectively (Schmidt et al., 2004). The role of Btk in antibody production is well recognized by the existence of immunodeficiencies, X-linked agammaglobulinemia (XLA) in humans (Tsukada et al., 1993) and X-linked immunodeficiency (Xid) in mice (Kerner et al., 1995), caused by a mutation in the *Btk* gene; in addition, mice with a combined deficiency of Tec family kinases display both unique and redundant functions in B cells (Btk and Tec) (Ellmeier et al., 2000) and T cells (Itk and Rlk) (Schaeffer et al., 1999). Here we report the crucial role of Btk and Tec in RANKL-induced osteoclastogenesis based on the genetic evidence obtained from $Tec^{-/-}Btk^{-/-}$ mice. In response to RANKL stimulation, Btk and Tec kinases form a signaling complex required for osteoclastogenesis with adaptor molecules such as BLNK, which also recruits Syk, thus linking the RANK and ITAM signals to phosphorylate PLCγ. This study provides a clear example of immunodeficiency association with abnormal bone homeostasis owing to defects in signaling molecules shared by B cells and osteoclasts. Moreover, therapeutic models suggest that suppression of Tec kinases can serve as a molecular basis for the development of future therapeutic strategies against bone diseases.

RESULTS

Osteoclasts Selectively Express Btk and Tec among Tec Kinases

RANK and ITAM signals cooperate to induce calcium signaling, but it has been unknown how these two signals are integrated. To gain insight into the molecules activated by RANKL that are potentially involved in the activation of tyrosine phosphorylation of the PLCγ pathway, we performed a genome-wide screening of mRNAs for nonreceptor tyrosine kinases expressed during osteoclast and osteoblast differentiation (Figure 1A). We identified high expression of *Src* and *Syk*, whose crucial functions in the osteoclast lineage have been well documented (Soriano et al., 1991; Faccio et al., 2003; Koga et al., 2004). Interestingly, osteoclasts, but not osteoblasts, express the mRNAs for *Btk* and *Tec* at a higher level than that for *Src* (Figure 1A). The selective expression of Btk and Tec in osteoclast precursor cells was also confirmed by RT-PCR (Figure 1B) and immunoblot analysis (Figure 1C).

Osteopetrotic Phenotype of Mice Doubly Deficient in Btk and Tec

The results led us to analyze the bone phenotype of mice deficient in Tec (Ellmeier et al., 2000), Btk (Kerner et al., 1995), or both (Ellmeier et al., 2000). Microradiological analysis revealed the trabecular bone volume to be normal in $Tec^{-/-}$ mice, minimally increased in $Btk^{-/-}$ mice, and markedly increased in $Tec^{-/-}Btk^{-/-}$ mice (Figure 1D). Microcomputed tomography clearly indicated that the bone volume was greatly enhanced in $Tec^{-/-}Btk^{-/-}$ mice (Figure 1E). Histological analysis revealed the osteoclast number was significantly reduced in the epiphyseal region, and the bone marrow was abnormally filled with trabecular bone in $Tec^{-/-}Btk^{-/-}$ mice (Figure 1F). We also observed cartilage remnants characteristic of osteopetrosis in $Tec^{-/-}Btk^{-/-}$ mice (Figure 1F). Bone morphometric analysis indicated an increase in bone volume associated with a reduced osteoclast number, a decrease in the indicators of osteoclastic bone resorption (Figure 1G), and a normal level of bone formation in $Tec^{-/-}Btk^{-/-}$ mice (Figure 1H). There was no significant difference in the resorption and formation parameters among the wild-type (WT), $Tec^{-/-}$, and $Btk^{-/-}$ mice (see Figure S1 available online). These results collectively suggest that the increase in bone mass in $Tec^{-/-}Btk^{-/-}$ mice is caused by impaired osteoclastic bone resorption owing to a defect in osteoclast differentiation.

Cell

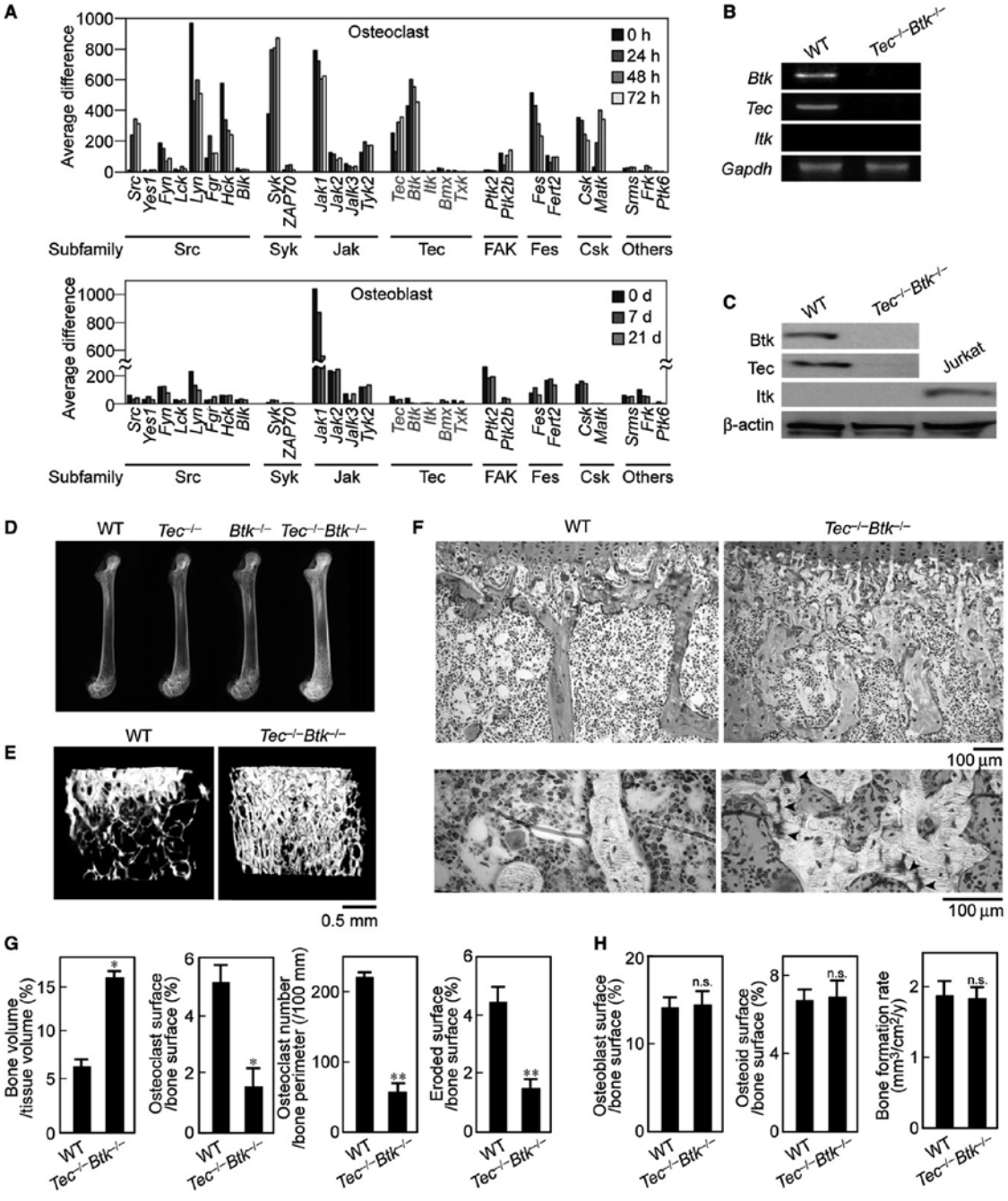

Figure 1. Osteopetrotic Phenotype of *Tec*$^{-/-}$*Btk*$^{-/-}$ Mice

(A) GeneChip analysis of mRNAs for nonreceptor tyrosine kinases during osteoclast and osteoblast differentiation. FAK, focal adhesion kinase; Fes, feline sarcoma oncogene; Csk, c-src tyrosine kinase.

(B) RT-PCR analysis of *Tec*, *Btk*, and *Itk* mRNAs in WT and *Tec*$^{-/-}$*Btk*$^{-/-}$ BMMs.

(C) Expression of Tec, Btk, and Itk proteins in WT and *Tec*$^{-/-}$*Btk*$^{-/-}$ BMMs.

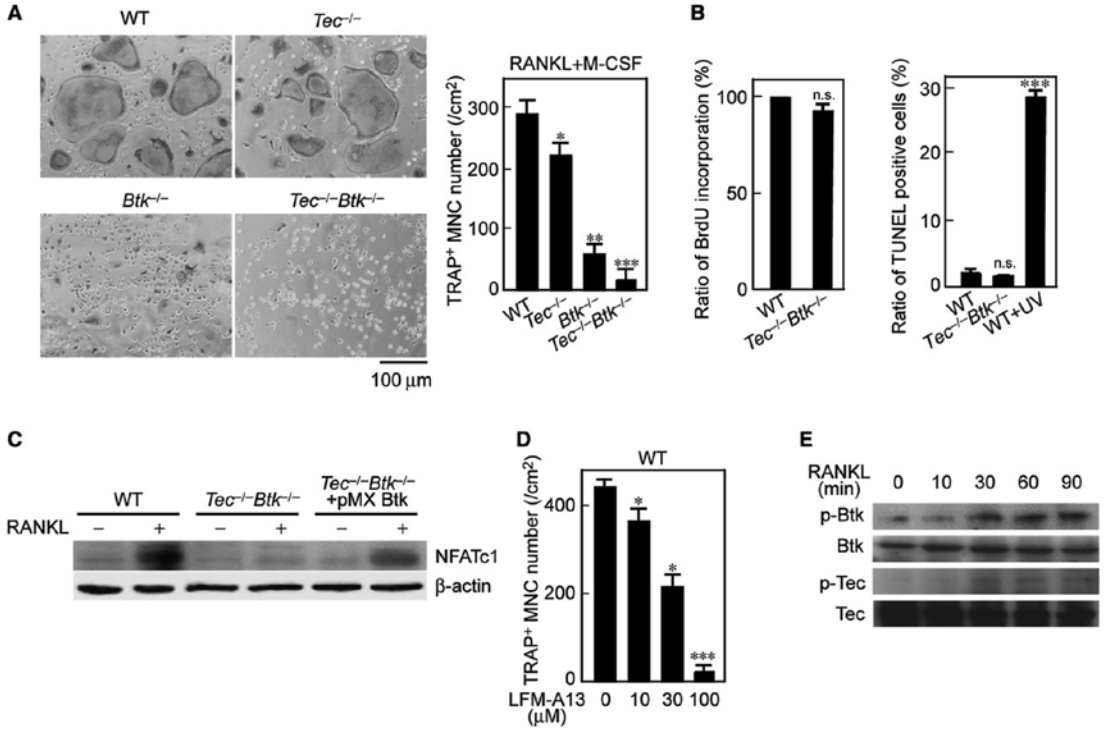

Figure 2. Crucial Role of Tec Family Kinases in RANKL-Induced Osteoclast Differentiation

(A) Osteoclast differentiation from WT, $Tec^{-/-}$, $Btk^{-/-}$, and $Tec^{-/-}Btk^{-/-}$ BMMs in response to RANKL and M-CSF.

(B) Cell proliferation rate (BrdU incorporation assay) and apoptosis (TUNEL assay) of WT and $Tec^{-/-}Btk^{-/-}$ BMMs stimulated with RANKL and M-CSF.

(C) NFATc1 induction in WT and $Tec^{-/-}Btk^{-/-}$ BMMs 72 hr after RANKL stimulation. Retroviral introduction of Btk into $Tec^{-/-}Btk^{-/-}$ BMMs recovers the NFATc1 induction.

(D) Effect of the Tec kinase inhibitor LFM-A13 on the osteoclast differentiation induced by RANKL and M-CSF.

(E) Phosphorylation of Btk and Tec in BMMs in response to RANKL.

Despite the severe defect in osteoclastic bone resorption, the $Tec^{-/-}Btk^{-/-}$ mice had normal tooth eruption, but the results nevertheless suggest that the two kinases play a critically important role in osteoclast differentiation.

Btk and Tec Are Activated by RANKL and Indispensable for Osteoclastogenesis

In vitro osteoclast differentiation was evaluated by counting the multinucleated cells (MNCs) positive for the osteoclast marker tartrate-resistant acid phosphatase (TRAP) after stimulation of BMMs with recombinant RANKL in the presence of M-CSF. Osteoclast differentiation was only minimally affected in $Tec^{-/-}$ cells but was severely impaired in $Btk^{-/-}$ cells and almost completely abrogated in $Tec^{-/-}Btk^{-/-}$ cells (Figure 2A). There was no significant difference in M-CSF-dependent proliferation of precursor cells or the rate of apoptosis between WT and $Tec^{-/-}Btk^{-/-}$ cells (Figure 2B) or in the number of $CD11b^{+}$ cells in the M-CSF-stimulated bone marrow cells (data not shown). Therefore, there is no defect in the generation of osteoclast precursor cells in $Tec^{-/-}Btk^{-/-}$ mice, although we observed that the survival of mature macrophages derived from $Tec^{-/-}Btk^{-/-}$ mice was partly impaired when cultured with a low concentration of M-CSF (W.E., unpublished data). RANKL-stimulated induction of NFATc1, the key transcription factor for osteoclastogenesis, was severely suppressed in $Tec^{-/-}Btk^{-/-}$ cells (Figure 2C) and $Btk^{-/-}$ cells (data not shown). We also analyzed the effect of the Tec kinase inhibitor LFM-A13 (Mahajan et al., 1999), which was designed to specifically bind the ATP-binding site of Btk,

(D) Microradiograph of the femur of WT, $Tec^{-/-}$, $Btk^{-/-}$, and $Tec^{-/-}Btk^{-/-}$ mice.

(E) Microcomputed tomography of the epiphyseal region of the femurs of WT and $Tec^{-/-}Btk^{-/-}$ mice.

(F) Histological analysis of the proximal tibiae of WT and $Tec^{-/-}Btk^{-/-}$ mice (upper, TRAP/hematoxylin; lower, toluidine blue stainings). Note that the number of TRAP-positive cells is markedly decreased in $Tec^{-/-}Btk^{-/-}$ mice. The bone marrow is filled with unresorbed bone, in which cartilage remnants (arrowheads) characteristic of osteopetrosis are observed.

(G and H) (G) Bone volume and parameters for osteoclastic bone resorption and (H) parameters for osteoblastic bone formation in the bone morphometric analysis of WT and $Tec^{-/-}Btk^{-/-}$ mice. *$p < 0.05$; **$p < 0.01$; ***$p < 0.005$; n.s., not significant (throughout the paper).

Cell

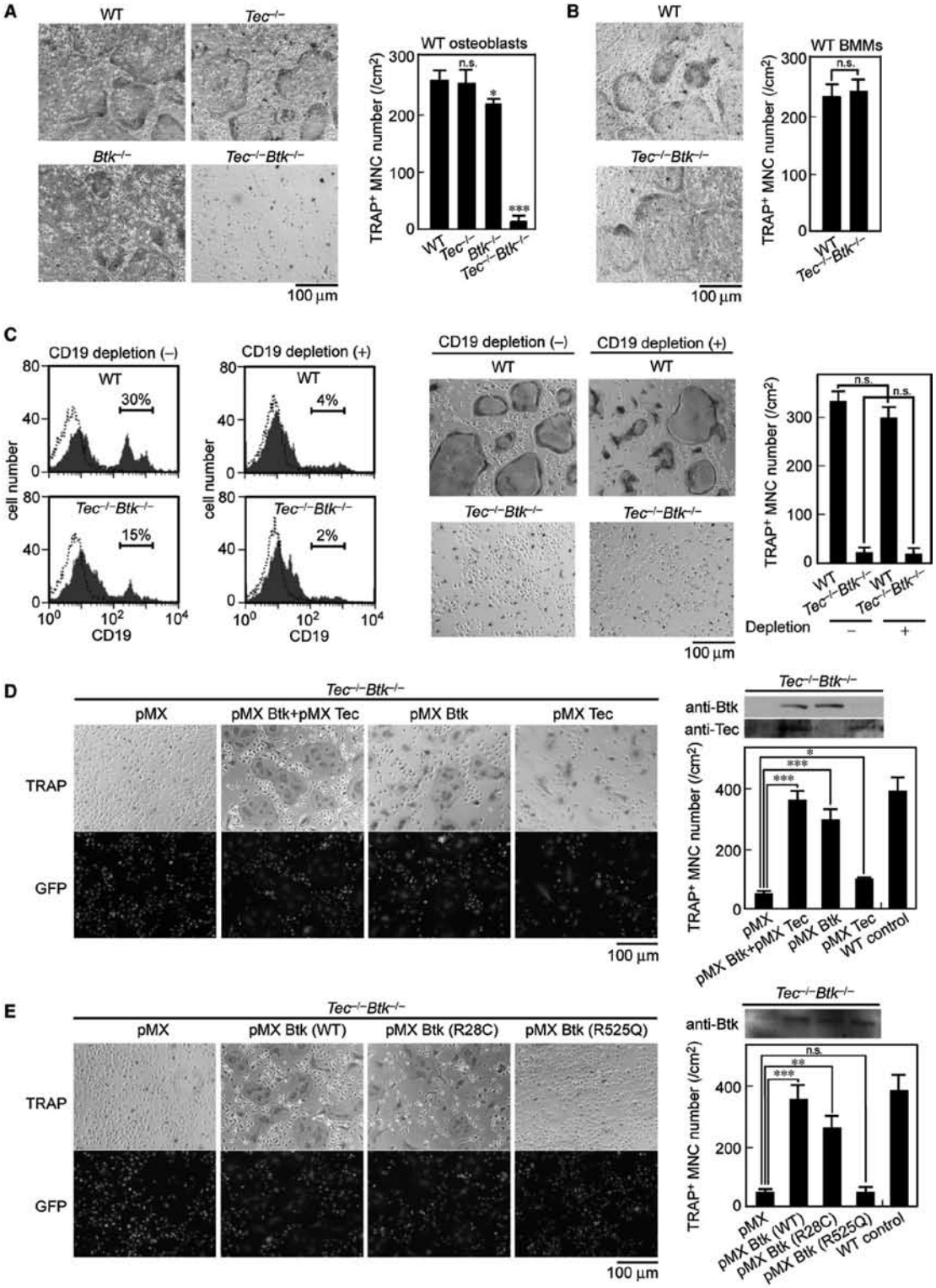
A
WT
Tec−/−
Btk−/−
Tec−/−Btk−/−
100 μm
WT osteoblasts
TRAP+ MNC number (/cm2)
n.s.
*
***
WT
Tec−/−
Btk−/−
Tec−/−Btk−/−
B
WT
Tec−/−Btk−/−
100 μm
WT BMMs
TRAP+ MNC number (/cm2)
n.s.
WT
Tec−/−Btk−/−
C
CD19 depletion (–)
CD19 depletion (+)
WT
30%
4%
Tec−/−Btk−/−
15%
2%
cell number
CD19
CD19 depletion (–)
CD19 depletion (+)
WT
WT
Tec−/−Btk−/−
Tec−/−Btk−/−
100 μm
TRAP+ MNC number (/cm2)
n.s.
n.s.
WT
Tec−/−Btk−/−
WT
Tec−/−Btk−/−
Depletion
–
+
D
Tec−/−Btk−/−
pMX
pMX Btk+pMX Tec
pMX Btk
pMX Tec
TRAP
GFP
100 μm
Tec−/−Btk−/−
anti-Btk
anti-Tec
TRAP+ MNC number (/cm2)
*
***
***
pMX
pMX Btk+pMX Tec
pMX Btk
pMX Tec
WT control
E
Tec−/−Btk−/−
pMX
pMX Btk (WT)
pMX Btk (R28C)
pMX Btk (R525Q)
TRAP
GFP
100 μm
Tec−/−Btk−/−
anti-Btk
TRAP+ MNC number (/cm2)
n.s.
**
***
pMX
pMX Btk (WT)
pMX Btk (R28C)
pMX Btk (R525Q)
WT control

and which was revealed subsequently to suppress other Tec kinases additionally (Fernandes et al., 2005), on osteoclast differentiation. LFM-A13 strongly inhibited RANKL-induced osteoclastogenesis (Figure 2D) and NFATc1 induction (data not shown). In contrast, this compound only slightly affected the bone resorption activity of osteoclasts (Figure S2). Importantly, phosphorylation of Btk and Tec was induced by RANKL stimulation in BMMs (Figure 2E). Thus, the tyrosine kinases Btk and Tec are activated by RANKL and play a crucial role in RANKL-induced signal transduction during osteoclastogenesis.

Impaired Osteoclastogenesis in *Tec*$^{-/-}$*Btk*$^{-/-}$ Mice Caused by a Cell-Autonomous Mechanism

To determine whether impaired osteoclastogenesis in *Tec*$^{-/-}$*Btk*$^{-/-}$ mice is caused by a cell-autonomous mechanism, we evaluated the osteoclastogenesis in the coculture system of bone marrow cells with osteoblasts. In the coculture of bone marrow cells derived from mutant mice with WT osteoblasts, osteoclast formation was not severely affected in *Tec*$^{-/-}$ or *Btk*$^{-/-}$ cells but was almost abrogated in *Tec*$^{-/-}$*Btk*$^{-/-}$ cells (Figure 3A). In contrast, *Tec*$^{-/-}$*Btk*$^{-/-}$ osteoblasts were normally able to support osteoclastogenesis of WT bone marrow cells (Figure 3B). These results suggest that the impaired osteoclastogenesis in *Tec*$^{-/-}$*Btk*$^{-/-}$ mice is caused by a defect in osteoclast precursor cells. Consistent with the observation that the *Btk*$^{-/-}$ mice have a normal number of osteoclasts in vivo (Figure S1), *Btk*$^{-/-}$ cells differentiate into osteoclasts in the coculture system essentially in a normal manner (Figure 3A), indicating that the larger contribution of Btk is observed only under limited in vitro conditions, including the RANKL/M-CSF-stimulated BMM culture system (Figure 2A). Since a similar observation has been made in *DAP12*$^{-/-}$ cells (Koga et al., 2004), we infer that Btk is more closely associated with the DAP12-dependent pathway.

Since *Tec*$^{-/-}$*Btk*$^{-/-}$ mice have almost no B cells and exhibit severe immunodeficiency (but their T cells are not affected) (Ellmeier et al., 2000), it is possible that the impaired osteoclastogenesis is influenced by differences in the B cell number in the bone marrow. Therefore, we examined whether depletion or addition of CD19$^+$ B cells had any effect on osteoclastogenesis from bone marrow cells containing B cells. Osteoclast differentiation was not influenced by the coexistence of B cells in either WT or *Tec*$^{-/-}$*Btk*$^{-/-}$ cells (Figure 3C). Taken together, these results indicate that the impaired osteoclastogenesis in *Tec*$^{-/-}$*Btk*$^{-/-}$ mice is not related to an abnormality of other cell types such as osteoblasts or B cells, supporting the notion that the impaired osteoclast differentiation is caused by a cell-autonomous mechanism.

Consistent with this notion, retrovirus-mediated expression of Btk and Tec almost completely recovered the osteoclast differentiation in *Tec*$^{-/-}$*Btk*$^{-/-}$ BMMs. The introduction of Btk into *Tec*$^{-/-}$*Btk*$^{-/-}$ BMMs by retroviral transfer markedly rescued the differentiation blockade, but that of Tec rescued it to a lesser extent (Figure 3D). This result is consistent with the dominant role of Btk in osteoclastogenesis in the BMM culture system (Figure 2A). Tec family kinases contain a pleckstrin-homology (PH) domain that binds to phosphatidylinositol-3,4,5-triphosphate (PtdIns[3,4,5]P_3), a lipid product of phosphoinositide 3-kinase, a Tec homology domain, and a carboxyl-terminal kinase domain (Schmidt et al., 2004). A kinase-inactive mutant of Btk (R525Q) that carries a mutation in the kinase domain (Takata and Kurosaki, 1996) did not rescue the osteoclast differentiation blockade, but another mutant (R28C) that harbors a mutation in the PH domain (Takata and Kurosaki, 1996), which causes a certain type of XLA in humans (Tsukada et al., 1993), exhibited a capacity for rescue comparable to the WT Btk (Figure 3E). The results suggest that the function of Btk in osteoclastogenesis requires its kinase activity but does not completely depend on the interaction with PtdIns(3,4,5)P_3 through the PH domain.

Tec Kinases Link the RANK Signal to the Phosphorylation of PLCγ

How does deficiency of Btk and Tec affect the osteoclastogenic signaling pathways? To address these issues by a systems biology approach, we utilized a systematic protein-protein interaction database created by the Genome Network Project (http://genomenetwork.nig.ac.jp/index.html), in which our laboratory has served as a working member. From this database, we extracted the protein-protein interaction network related to the two major signaling pathways regulating osteoclastogenesis, the RANK and ITAM pathways, with which we merged our original data on the increase in mRNA expression after RANKL stimulation (Figure 4A). The RANK-associated gene network included TRAF6, NF-κB, and mitogen-activated protein kinase (MAPK), whereas the ITAM (DAP12/FcRγ)-associated gene network included Syk, PLCγ, and Btk/Tec. As expected, the expression of many RANK-associated molecules was upregulated by RANKL stimulation. Interestingly, the expression of many of the genes in the ITAM-associated gene network was also upregulated by RANKL stimulation.

Based on these results, together with the observation that Btk and Tec were activated by RANKL (Figure 2E), we hypothesized that Btk and Tec are the molecules that bridge the RANK and ITAM pathways to activate calcium signaling. Notably, RANKL-induced tyrosine phosphorylation of PLCγ1 and PLCγ2 was markedly suppressed in *Tec*$^{-/-}$*Btk*$^{-/-}$ cells (Figure 4B). Furthermore, the RANKL-induced calcium oscillation required for *NFATc1* induction was barely observed in *Tec*$^{-/-}$*Btk*$^{-/-}$ cells (Figure 4C). In contrast, we observed a normal level of RANKL-induced activation of MAPKs (ERK, JNK, p38), IκB kinase α (IKKα),

Figure 3. Impaired Osteoclastogenesis in *Tec*$^{-/-}$*Btk*$^{-/-}$ Mice Caused by a Cell-Autonomous Mechanism

(A) Osteoclast differentiation from WT, *Tec*$^{-/-}$, *Btk*$^{-/-}$, and *Tec*$^{-/-}$*Btk*$^{-/-}$ bone marrow cells in the coculture system with WT osteoblasts.

(B) Osteoclast differentiation from WT bone marrow cells in the coculture system with WT or *Tec*$^{-/-}$*Btk*$^{-/-}$ osteoblasts.

(C) Effect of CD19$^+$ B cell depletion on osteoclast differentiation. The number of CD19$^+$ cells before and after depletion of CD19$^+$ B cells in bone marrow cells derived from WT or *Tec*$^{-/-}$*Btk*$^{-/-}$ mice (left). Osteoclast differentiation from WT and *Tec*$^{-/-}$*Btk*$^{-/-}$ BMMs after depletion of CD19$^+$ B cells in response to RANKL and M-CSF (right).

(D) Effects of retroviral expression of Tec (pMX Tec) and/or Btk (pMX Btk) on osteoclastogenesis from *Tec*$^{-/-}$*Btk*$^{-/-}$ BMMs stimulated with RANKL and M-CSF.

(E) Effects of retroviral expression of WT Btk or Btk mutants harboring a mutation in the PH domain (R28C) or the kinase domain (R525Q) on osteoclastogenesis from *Tec*$^{-/-}$*Btk*$^{-/-}$ BMMs stimulated with RANKL and M-CSF.

Cell

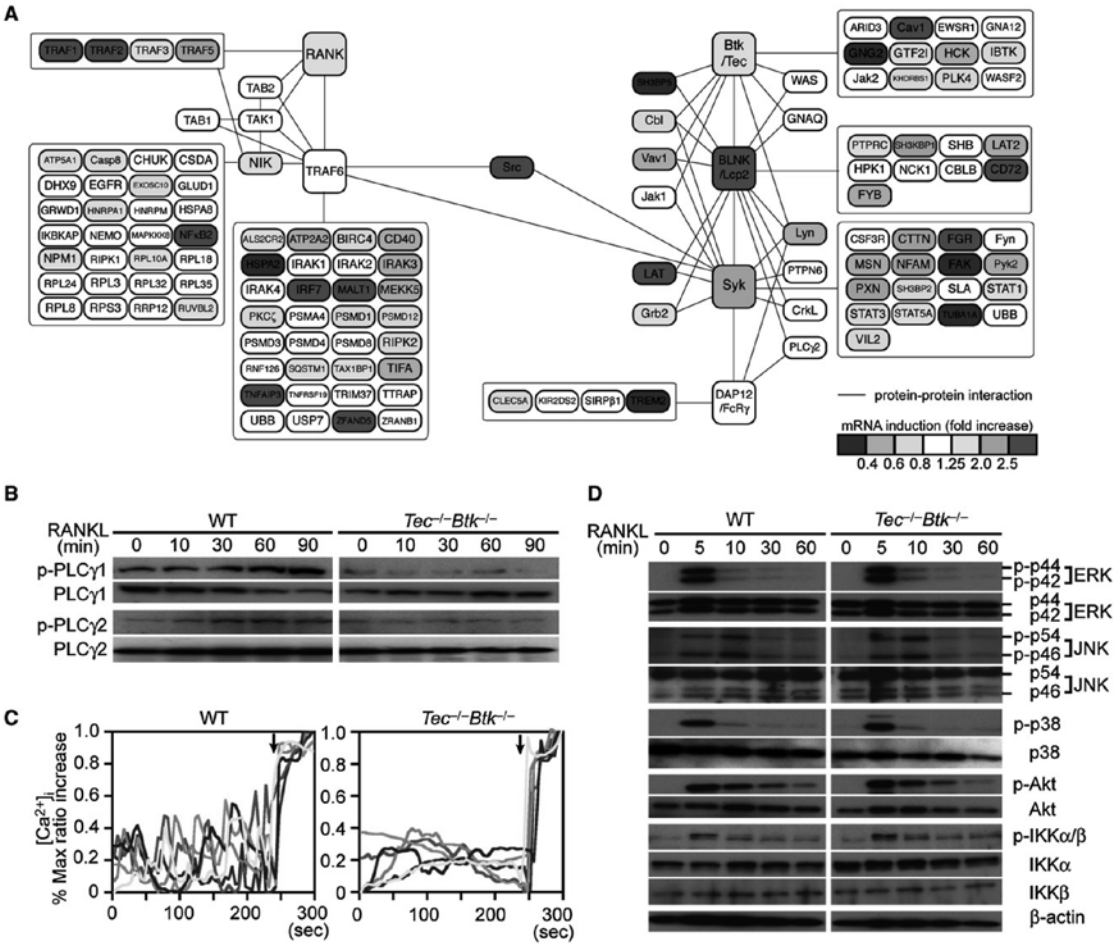

Figure 4. Tec Kinases Mediate Osteoclastogenic Signaling Pathway

(A) Dynamic protein-protein interaction network in osteoclast differentiation. Proteins connected with a black line are interacting partners, and the color indicates how many fold mRNA expression was increased 24 hr after RANKL stimulation.

(B) RANKL-induced PLCγ1 and PLCγ2 phosphorylation in WT and *Tec*$^{-/-}$*Btk*$^{-/-}$ BMMs.

(C) Oscillatory change in the intracellular Ca^{2+} concentration in WT and *Tec*$^{-/-}$*Btk*$^{-/-}$ BMMs after RANKL stimulation. The addition of 10 μM ionomycin at the end of each experiment is indicated by an arrow. Each color indicates a different cell in the same field.

(D) RANKL-induced ERK, JNK, p38, Akt, and IKK phosphorylation in WT and *Tec*$^{-/-}$*Btk*$^{-/-}$ BMMs.

IKKβ, and Akt, all of which are activated downstream of TRAF6 (Wong et al., 1999) (Figure 4D). These results indicate that RANKL-activated Btk and Tec are selectively involved in the phosphorylation of PLCγ, and a defect in calcium signaling causes the impaired *NFATc1* induction in *Tec*$^{-/-}$*Btk*$^{-/-}$ cells. Thus, Btk and Tec link the RANK signal to calcium signaling in the osteoclast lineage.

Tec Kinases Form an Osteoclastogenic Signaling Complex with Scaffold Proteins

Since PLCγ activation is known to be dependent on the ITAM signal, another question arises as to how PLCγ activation is regulated by both RANK and ITAM signals. The ITAM-associated gene network indicates that ITAM associates with Syk, which associates with and phosphorylates scaffold proteins such as BLNK (Ishiai et al., 1999). Because BLNK associates with Btk in a phosphorylation-dependent manner in B cells (Hashimoto et al., 1999), we examined whether RANKL-activated Btk is recruited to BLNK in BMMs. The colocalization of Btk and BLNK was increased, at what appeared to be the plasma membrane, after RANKL stimulation (Figure 5A and Figure S3). This translocation was not observed in *DAP12*$^{-/-}$*FcRγ*$^{-/-}$ cells (Figure 5A and Figure S3), suggesting that the ITAM signals are also required for the formation of the Btk-BLNK complex. Consistent with this, immunoblot analysis showed that Btk coimmunoprecipitated with BLNK in BMMs in the presence of RANKL, but

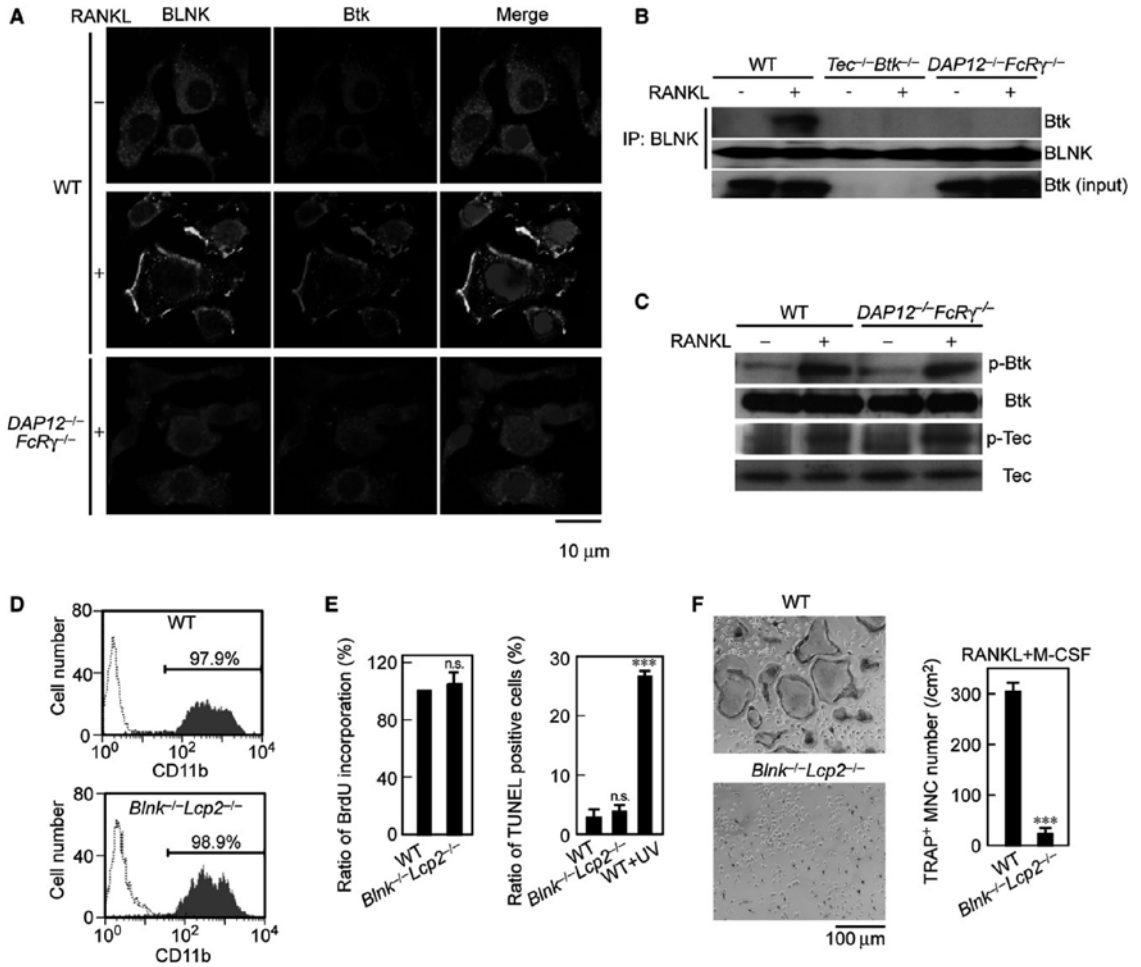

Figure 5. Tec Kinases Form an Osteoclastogenic Signaling Complex with Scaffold Proteins

(A) Immunofluorescence microscopic analysis of colocalization of Btk and BLNK in WT and *DAP12*$^{-/-}$*FcRγ*$^{-/-}$ cells 15 min after RANKL stimulation. The nuclei were stained with Hoechst 33342.

(B) Immunoprecipitation analysis of the interaction between Btk and BLNK in WT and *DAP12*$^{-/-}$*FcRγ*$^{-/-}$ cells 15 min after RANKL stimulation.

(C) Tyrosine phosphorylation of Tec kinases in WT and *DAP12*$^{-/-}$*FcRγ*$^{-/-}$ cells 15 min after RANKL stimulation.

(D) Expression of CD11b in the M-CSF-stimulated bone marrow cells from WT and *Blnk*$^{-/-}$*Lcp2*$^{-/-}$ mice (flow cytometry).

(E) Cell proliferation rate (BrdU incorporation assay) and apoptosis (TUNEL assay) of WT and *Blnk*$^{-/-}$*Lcp2*$^{-/-}$ BMMs stimulated with RANKL and M-CSF.

(F) Osteoclast differentiation from WT and *Blnk*$^{-/-}$*Lcp2*$^{-/-}$ BMMs in response to RANKL and M-CSF.

the association was abrogated in *DAP12*$^{-/-}$*FcRγ*$^{-/-}$ cells (Figure 5B). Furthermore, Tec kinases were phosphorylated in response to RANKL, even in *DAP12*$^{-/-}$*FcRγ*$^{-/-}$ cells (Figure 5C). Thus, the activation of Btk by RANK and the activation of BLNK by the ITAM signal are both required for the association of Btk with BLNK, which may function as the molecular switch that integrates RANK and ITAM signals.

To further investigate the role of BLNK in osteoclastogenesis, we analyzed osteoclast differentiation in BMMs derived from *Blnk*$^{-/-}$ mice (Hayashi et al., 2003). However, there was no significant difference in RANKL-induced osteoclastogenesis between the WT and *Blnk*$^{-/-}$ cells (data not shown), suggesting that another molecule(s) compensates for the loss of BLNK. SLP-76 (encoded by *Lcp2*) is an adaptor protein homologous to BLNK, functioning mainly in T cells (Pivniouk and Geha, 2000). Since there was no significant difference in RANKL-induced osteoclastogenesis between the WT and *Lcp2*$^{-/-}$ cells (data not shown), we analyzed mice doubly deficient in BLNK and SLP-76 (*Blnk*$^{-/-}$*Lcp2*$^{-/-}$ mice). Although *Blnk*$^{-/-}$ mice frequently develop acute leukemia (Jumaa et al., 2003), there was a normal number of CD11b^{+} osteoclast precursor cells in the M-CSF-stimulated bone marrow cells from *Blnk*$^{-/-}$*Lcp2*$^{-/-}$ mice (Figure 5D), and

Cell

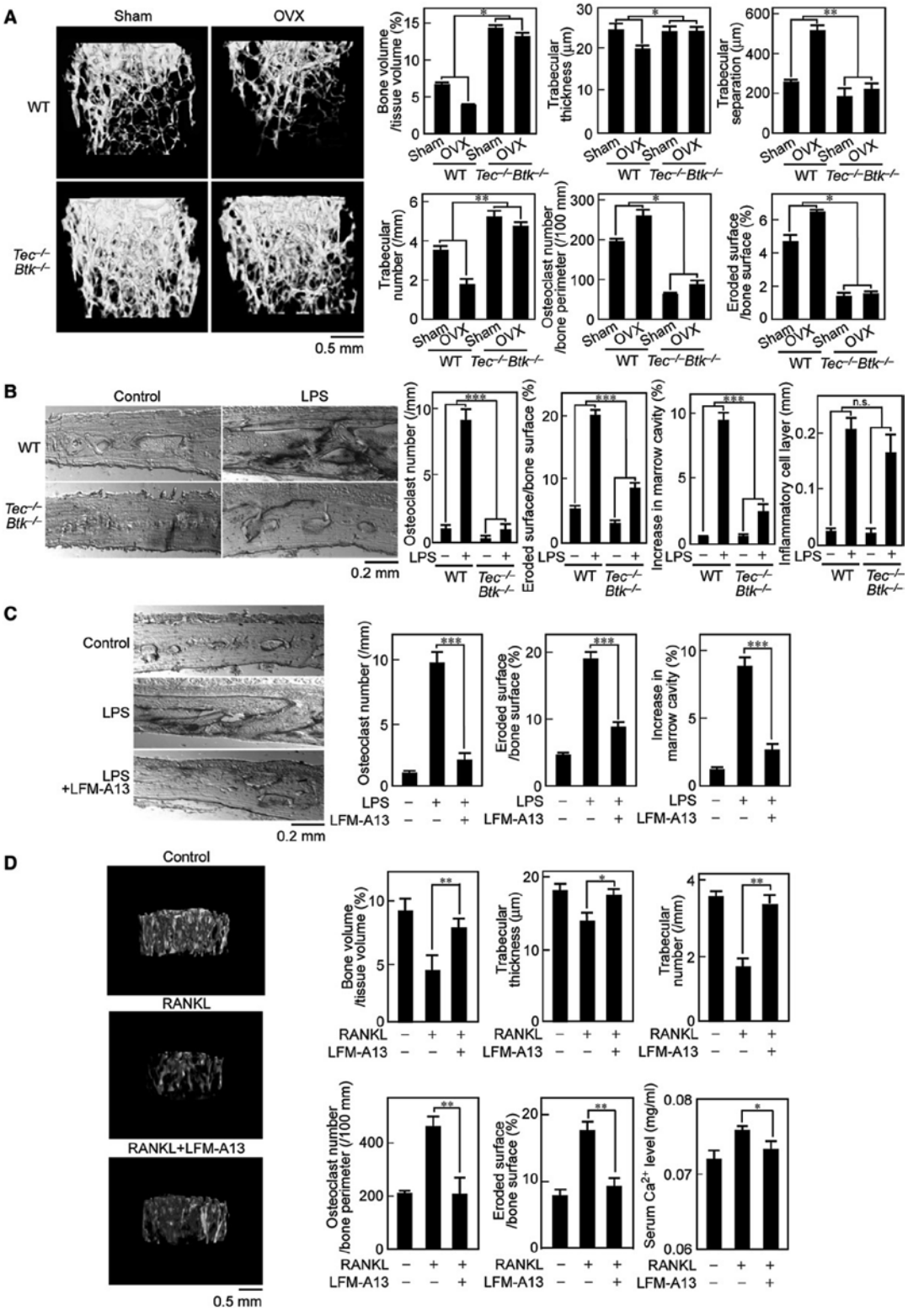
A
Sham
OVX
WT
Tec−/−Btk−/−
0.5 mm
Bone volume /tissue volume (%)
Trabecular thickness (μm)
Trabecular separation (μm)
Trabecular number (/mm)
Osteoclast number /bone perimeter (/100 mm)
Eroded surface /bone surface (%)
Sham OVX Sham OVX
WT Tec−/−Btk−/−
B
Control
LPS
WT
Tec−/−Btk−/−
0.2 mm
Osteoclast number (/mm)
Eroded surface/bone surface (%)
Increase in marrow cavity (%)
Inflammatory cell layer (mm)
n.s.
LPS − + − +
WT Tec−/−Btk−/−
C
Control
LPS
LPS +LFM-A13
0.2 mm
Osteoclast number (/mm)
Eroded surface /bone surface (%)
Increase in marrow cavity (%)
LPS − + +
LFM-A13 − − +
D
Control
RANKL
RANKL+LFM-A13
0.5 mm
Bone volume /tissue volume (%)
Trabecular thickness (μm)
Trabecular number (/mm)
Osteoclast number /bone perimeter (/100 mm)
Eroded surface /bone surface (%)
Serum Ca2+ level (mg/ml)
RANKL − + +
LFM-A13 − − +

the rate of proliferation or apoptosis in *Blnk*$^{-/-}$*Lcp2*$^{-/-}$ BMMs was not significantly different from that in WT BMMs (Figure 5E). We found that in vitro osteoclast differentiation was severely abrogated in *Blnk*$^{-/-}$*Lcp2*$^{-/-}$ BMMs (Figure 5F), suggesting an important role for BLNK and SLP-76 in osteoclast differentiation. Thus, the scaffold proteins, with which the Tec kinases form a complex, have emerged as critical mediators of osteoclastogenic signals. These results further lend support to the crucial role of the RANKL-stimulated formation of the osteoclastogenic complex: the interaction of Tec kinases and their scaffold proteins results in the efficient phosphorylation of PLCγ.

Tec Kinases as Potential Therapeutic Targets for Bone Diseases

To investigate the role of Btk and Tec in the pathological activation of osteoclastogenesis, *Tec*$^{-/-}$*Btk*$^{-/-}$ mice were subjected to an ovariectomy (OVX)-induced model of postmenopausal osteoporosis (Aoki et al., 2006). The bone volume and trabecular bone number/connectivity were significantly reduced by the estrogen withdrawal in WT mice, but such a reduction was observed to a much lesser extent in *Tec*$^{-/-}$*Btk*$^{-/-}$ mice (Figure 6A and Figure S4). An increase in osteoclast number induced by OVX was also much lower in *Tec*$^{-/-}$*Btk*$^{-/-}$ mice (Figure 6A and Figure S4), suggesting a key role of Btk and Tec in the pathological activation of osteoclastogenesis.

Furthermore, *Tec*$^{-/-}$*Btk*$^{-/-}$ mice were subjected to a lipopolysaccharide (LPS)-induced model of inflammatory bone destruction (Takayanagi et al., 2000). *Tec*$^{-/-}$*Btk*$^{-/-}$ mice were protected from the activation of osteoclastogenesis and bone loss (Figure 6B), whereas the formation of an inflammatory cell layer, the number of infiltrated inflammatory cells, IKK activation, and serum levels of TNF-α and IL-6 in *Tec*$^{-/-}$*Btk*$^{-/-}$ mice were not different from those in WT mice (Figure 6B and Figure S5). These results prompted us to examine the therapeutic effects of Tec kinase inhibitor in disease models. Local administration of the Tec kinase inhibitor LFM-A13 had a marked therapeutic effect on the excessive osteoclast formation and bone destruction induced by LPS (Figure 6C) without affecting IKK activation or inflammatory cytokine levels in the serum (Figure S5), although it has been reported that Tec kinases are involved in the activation of immune cells, including lymphocytes and macrophages (Horwood et al., 2003; Mangla et al., 2004). These results suggest that the therapeutic effects of Tec kinase inhibitor in an LPS-induced model are not due to attenuated immune responses but rather are mainly caused by direct inhibitory effects on osteoclast precursor cells. It has been consistently reported that Btk is not essential for LPS-induced inflammatory cytokine production in macrophages under certain conditions (Hata et al., 1998; Perez de Diego et al., 2006).

To determine whether the Tec kinase inhibitor has therapeutic efficacy in a model of osteoporosis, we treated mice that were intraperitoneally injected with GST-RANKL. GST-RANKL injection resulted in an increase in osteoclast number and serum calcium concentration and a decrease in trabecular bone volume, but LFM-A13 treatment significantly ameliorated RANKL-induced bone loss (Figure 6D). These results demonstrate the inactivation of Tec family kinases to be a novel strategy for suppressing osteoclastogenesis in vivo.

DISCUSSION

RANKL-Induced Formation of the Osteoclastogenic Signaling Complex

An osteopetrotic phenotype in *Tec*$^{-/-}$*Btk*$^{-/-}$ mice revealed these two kinases to play a crucial role in the regulation of osteoclast differentiation. Btk and Tec are known to play a key role in proximal BCR signaling (Ellmeier et al., 2000), but this study establishes their crucial role in the integration of the two essential osteoclastogenic signals, RANK and ITAM (Figure 7). Thus, although immune and bone cells share components of signaling cascades, they play distinct roles in each cell type. Furthermore, this study identified an osteoclastogenic signaling complex composed of Tec kinases and adaptor proteins that may provide a new paradigm for the signal transduction mechanism of osteoclast differentiation: ITAM phosphorylation results in the recruitment of Syk, which phosphorylates adaptor proteins such as BLNK and SLP-76, which in turn function as scaffolds to recruit the Tec kinases activated by RANK and PLCγ to the osteoclast signaling complex so as to induce maximal calcium influx.

Such complexes are similar to those formed in the immunological synapse in T cells, which are associated with membrane rafts (Cherukuri et al., 2001). It has been reported that RANK accumulates in membrane rafts, and these specialized domains may play an important role in the RANK signal transduction (Ha et al., 2003). We observed that DAP12, Btk, BLNK, and PLCγ, as well as RANK, were recruited to caveolin-rich membrane domains, which are the crucial signaling domains contained in lipid rafts, after RANKL stimulation (Figure S6). Thus, it is likely that the complex containing both the RANK and ITAM signaling pathways is generated by RANKL stimulation and contributes to the facilitation of the osteoclastogenic signal transduction.

Linkage between Primary Immunodeficiency and Bone Homeostasis

The mutation of *Btk* in humans causes XLA, which is characterized by an arrest in B cell development and immunodeficiency

Figure 6. Tec Kinases as Potential Therapeutic Targets in Bone Diseases

(A) OVX-induced bone loss in WT and *Tec*$^{-/-}$*Btk*$^{-/-}$ mice (evaluated in the femurs and tibiae 3 weeks after sham operation or OVX). The trabecular thickness, separation, and number were obtained from three-dimensional microstructural analysis by microcomputed tomography. Bone volume, osteoclast number, and eroded surface were based on the bone morphometric analysis.

(B) Inflammation-induced bone destruction in WT and *Tec*$^{-/-}$*Btk*$^{-/-}$ mice. Histology of the calvarial bone injected with saline (control) or LPS in WT and *Tec*$^{-/-}$*Btk*$^{-/-}$ mice (TRAP and hematoxylin staining).

(C) Effect of local administration of the Tec kinase inhibitor LFM-A13 (20 mg/kg) on LPS-induced osteoclast formation and bone destruction (TRAP and hematoxylin staining). This inhibitor at this dosage had marginal effects on B cells.

(D) Effect of local administration of LFM-A13 (20 mg/kg) on RANKL-induced osteoclast formation and bone loss. After mice were sacrificed 1.5 hr after the final injection, serum calcium level was measured, and three-dimensional microstructural analysis (femur) and the bone morphometric analysis (tibia) were performed.

Cell

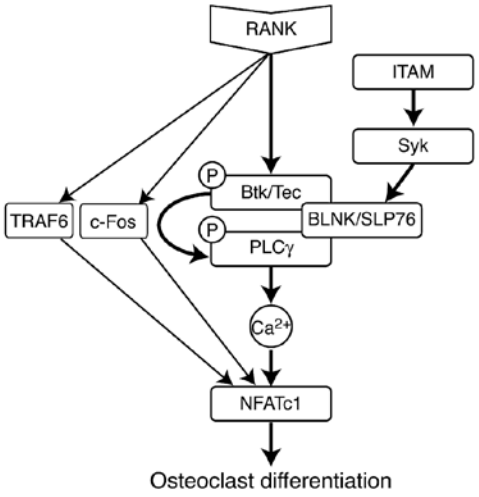

Figure 7. Integration of the RANK and ITAM Signals by Tec Kinases
RANKL binding to RANK results in activation of classical pathways involving TRAF6 and c-Fos. In addition, Tec kinases are phosphorylated by RANK. ITAM phosphorylation results in the recruitment of Syk, leading to activation of adaptor proteins such as BLNK and SLP-76, which function as scaffolds that recruit both Tec kinases and PLCγ to form the osteoclastogenic signaling complex. This complex is crucial for efficient activation of calcium signaling required for the induction and activation of NFATc1, the key transcription factor for osteoclast differentiation.

(Tsukada et al., 1993). Targeted disruption of *Btk* alone did not result in an obvious bone phenotype in mice, and B cell immunoglobulin production was also not severely affected in this strain (Kerner et al., 1995). Therefore, it is possible that the mouse and human utilization of Tec family kinases is not strictly the same. Because immunoglobulin production is completely abrogated in the combined deficiency of Btk and Tec (Ellmeier et al., 2000), $Tec^{-/-}Btk^{-/-}$ mice may serve as a better model of XLA. Currently there is no report on abnormalities of bone metabolism in the XLA patients, but it will be of great significance to analyze bone density and quality in patients with primary immunodeficiencies in the future. These studies, together with others, including recent data on hyper-IgM syndrome (Lopez-Granados et al., 2007), will surely shed light on unexpected aspects of the linkage between the immune and bone systems.

Upstream and Downstream of Tec Kinases in the Osteoclastogenic Signal Transduction

Although phosphorylation of Tec kinases is dependent on Src family kinases in immune cells (Schmidt et al., 2004), c-Src deficiency or inhibition of Src family kinases by PP2 has little effect on osteoclast differentiation (T.K. and H.T., unpublished data). Although it is possible that other Src family members may compensate, to date there has been no clear evidence demonstrating an essential role for Src kinases in osteoclast differentiation; therefore, the kinases that phosphorylate the Tec kinases in osteoclasts remain to be elucidated.

Based on the in vitro data (Figure 4B), the phosphorylation of PLCγ by RANKL is mostly dependent on Btk and Tec. However, osteopetrosis in $Tec^{-/-}Btk^{-/-}$ mice is less severe than that in $DAP12^{-/-}FcR\gamma^{-/-}$ mice, and pathological bone loss is not completely abrogated in the $Tec^{-/-}Btk^{-/-}$ mice or the Tec kinase inhibitor-treated mice. It is conceivable that the loss of Btk and Tec is partly compensated by other Tec kinases or that an alternative kinase(s) partially functions as a PLCγ kinase during osteoclastogenesis.

Despite the crucial role of BLNK and SLP-76 in osteoclast differentiation in vitro, bone mineral density was not markedly increased in $Blnk^{-/-}Lcp2^{-/-}$ mice (M.S., T.K., and H.T., unpublished data). One explanation for this discrepancy is that BLNK and SLP-76 do play a substantially important role, but another adaptor molecule, such as cytokine-dependent hematopoietic cell linker (Clnk), may compensate for the loss in vivo. Although further studies are necessary to elucidate the mechanism(s), it is likely that membrane-bound or soluble factors, which induce or activate Clnk, are compensatorily upregulated only in vivo. In addition, as $Blnk^{-/-}Lcp2^{-/-}$ mice develop acute leukemia at a very high frequency (more than 90%; D.K., unpublished data), the onset of acute leukemia may affect bone homeostasis by producing soluble factors that activate osteoclastogenesis or inhibit osteoblastic bone formation.

Tec Family Kinases as Therapeutic Targets for Bone Diseases

$Tec^{-/-}Btk^{-/-}$ mice are resistant to OVX-induced bone loss, but $DAP12^{-/-}FcR\gamma^{-/-}$ mice, which exhibit more severe osteopetrosis, do lose bone after OVX in certain bones (Wu et al., 2007). These results suggest that osteoclastogenesis under pathological conditions is dependent on a signaling mechanism distinct from that in physiological bone remodeling. Whatever the detailed mechanism, the results indicate that the Tec kinases offer some auspicious therapeutic targets in the treatment of metabolic and inflammatory bone diseases (see Figure 6).

Considering the severe immunodeficiency in XLA, careful attention would obviously have to be given to side effects on other cell types, including B cells, if Tec kinases were systemically inhibited in order to treat metabolic bone diseases. In the case of inflammatory bone diseases such as rheumatoid arthritis, certain immunosuppressants have already been successfully utilized in the clinic, so the inhibition of these kinases may prove to be a potentially effective strategy for preventing bone destruction associated with inflammation. Undoubtedly, the suppression of molecules shared by immune and bone cells will require a very careful evaluation in both systems prior to any clinical application, but these efforts will be rewarded by the provision of a molecular basis for novel drug design in the future.

EXPERIMENTAL PROCEDURES

Mice and Analysis of Bone Phenotype

We previously described the generation of $Tec^{-/-}$ $Btk^{-/-}$ (Ellmeier et al., 2000) and $DAP12^{-/-}$ $FcR\gamma^{-/-}$ (Koga et al., 2004) mice. $Blnk^{-/-}$ (Hayashi et al., 2003) and $Lcp2^{-/-}$ (Pivniouk et al., 1998) mice were described previously. Histomorphometric and microradiographic examinations were performed as described (Koga et al., 2004).

In Vitro Osteoclast Formation, Ca^{2+} Measurement, and GeneChip Analysis

Bone marrow cells were cultured with 10 ng/ml M-CSF (R & D Systems) for 2 days, and they were used as BMMs. BMMs were cultured with 50 ng/ml RANKL (Peprotech) and 10 ng/ml M-CSF for 3 days. RANKL and M-CSF were added at these concentrations unless otherwise indicated. In the coculture system, bone marrow cells were cultured with calvarial osteoblasts with 10^{-8} M 1,25-dihydroxyvitamin D_3 and 10^{-6} M prostaglandin E_2. TRAP-positive MNCs ($TRAP^+$ MNCs, more than three nuclei) were counted. Proliferation rate was determined 24 hr after RANKL stimulation using Cell Proliferation ELISA Kit (Roche). Apoptosis was assayed 24 hr after RANKL stimulation using In Situ Cell Death Detection Kit (Roche). In Figure 2D, LFM-A13 (Calbiochem) was added at the same time as RANKL. Concentration of intracellular calcium was measured and GeneChip analysis was performed as described (Takayanagi et al., 2002).

Retroviral Gene Transfer

Retroviral vectors, pMX-Tec-IRES-GFP, pMX-Btk-IRES-GFP, pMX-Btk (R28C)-IRES-GFP, and pMX-Btk (R525Q)-IRES-GFP, were constructed by inserting cDNA fragments of Tec, Btk, Btk (R28C), or Btk (R525Q) (Takata and Kurosaki, 1996) into pMX-IRES-EGFP. Retrovirus packaging was performed by transfecting Plat-E cells with the plasmids as described previously (Morita et al., 2000). After 6 hr inoculation, BMMs were stimulated with RANKL for 3 days.

Depletion of $CD19^+$ B Cells

Bone marrow cells contain $CD19^+$ cells at the ratio of about 30% in WT mice and about 15% in $Tec^{-/-}Btk^{-/-}$ mice. $CD19^+$ cells were depleted with a magnetic sorter and anti-CD19 microbeads (MACS; Miltenyi Biotec). The purity was confirmed by FACS, and the population of $CD19^+$ B cells was less than 5% in these preparations.

Immunoblot Analysis, Immunofluorescence Staining, and Flow Cytometry

After being stimulated with RANKL and M-CSF, BMMs were harvested and cell lysates were subjected to immunoblot or immunoprecipitation analyses with specific antibodies against Tec (Mano et al., 1995), Btk, NFATc1, PLCγ1, BLNK, DAP12, β-actin (Santa Cruz), phospho-PLCγ2, PLCγ2, phospho-ERK, ERK, phospho-p38, p38, phospho-JNK, JNK, phospho-Akt, Akt, phospho-IKKα/β, IKKα, IKKβ (Cell Signaling), phospho-PLCγ1 (Biosource International), Itk, 4G10 (Upstate), and phospho-Btk (BD Biosciences). For immunofluorescence staining, cells were fixed with 4% paraformaldehyde, permeabilized, and then treated with the indicated specific antibodies followed by staining with Alexa Fluor 488- or 546-labeled secondary antibody (Molecular Probes). For flow cytometry, bone marrow cells were incubated with the anti-CD11b antibody (BD Biosciences) or control rat IgG for 30 min followed by staining with PE-conjugated anti-rat IgG antibody.

Ovariectomy-Induced Bone Loss

Seven-week-old female mice were ovariectomized under anesthesia. Three or 8 weeks after surgery, all of the mice were sacrificed and subjected to histomorphometric and microradiographic examinations. Parameters for trabecular bone (thickness, separation, and number) were calculated on the basis of data obtained from microcomputed tomography analysis as described (Aoki et al., 2006).

LPS-Induced Bone Destruction

Seven-week-old female mice were administered with a local calvarial injection of LPS (Sigma) at 25 mg/kg body weight with a simultaneous injection of LFM-A13 (20 mg/kg body weight) or saline and were analyzed after 5 days as described (Takayanagi et al., 2000). For the detection of IKK phosphorylation, the calvarial tissues were homogenized 15 min after LPS injection, and lysates were subjected to immunoblot analysis. The serum levels of TNF-α and IL-6 (30 min after LPS injection) were measured by ELISA kits (R & D Systems).

RANKL-Induced Bone Loss

Seven-week-old C57BL/6 female mice were intraperitoneally injected with 20 μg of GST or GST-RANKL (Oriental Yeast Co., Ltd.) three times at intervals of 24 hr. LFM-A13 (20 mg/kg body weight) or saline was injected 1 hr prior to GST-RANKL treatment. One and a half hours after the final injection, all of the mice were sacrificed and subjected to histomorphometric and microradiographic examinations. The serum level of Ca^{2+} was measured by Calcium C (Wako).

Statistical Analysis

All data are expressed as the mean ± SEM (n = 5). Statistical analysis was performed by using Student's t test or ANOVA followed by Bonferroni test when applicable (*$p < 0.05$; **$p < 0.01$; ***$p < 0.005$; n.s., not significant). Results are representative examples of more than four independent experiments. In Figure 6, statistical analysis was performed between WT and $Tec^{-/-}Btk^{-/-}$ mice (n = 5 per group) on the fold increase of each parameter.

SUPPLEMENTAL DATA

Supplemental Data include six figures and can be found with this article online at http://www.cell.com/cgi/content/full/132/5/794/DC1/.

ACKNOWLEDGMENTS

We thank T. Kitamura, H. Mano, K. Mori, Y. Tomimori, H. Yanagawa, and E. Miyamoto for reagents and technical advice. We also thank M. Isobe-Ohba, T. Nakashima, M. Asagiri, K. Nishikawa, H.J. Gober, K. Kuroda, S. Ochi, Y. Suzuki, and H. Murayama for helpful discussion and assistance. This work was supported in part by a Grant-in-Aid for Creative Scientific Research from the Japan Society for the Promotion of Science (JSPS); grants for the Genome Network Project from the Ministry of Education, Culture, Sports, Science, and Technology of Japan (MEXT); Health Sciences Research grants from the Ministry of Health, Labor, and Welfare of Japan; the Austrian Science Fund and the START Program of the Austrian Ministry of Education, Science, and Culture; and grants from Kanae Foundation for Life and Socio-Medical Science, Tokyo Biochemical Research Foundation, Yokoyama Foundation for Clinical Pharmacology, and Hayashi Memorial Foundation for Female Natural Scientists. No authors have any financial interest related to this work.

Received: June 12, 2007
Revised: November 8, 2007
Accepted: December 27, 2007
Published: March 6, 2008

REFERENCES

Aoki, K., Saito, H., Itzstein, C., Ishiguro, M., Shibata, T., Blanque, R., Mian, A.H., Takahashi, M., Suzuki, Y., Yoshimatsu, M., et al. (2006). A TNF receptor loop peptide mimic blocks RANK ligand-induced signaling, bone resorption, and bone loss. J. Clin. Invest. *116*, 1525–1534.

Asagiri, M., and Takayanagi, H. (2007). The molecular understanding of osteoclast differentiation. Bone *40*, 251–264.

Cherukuri, A., Dykstra, M., and Pierce, S.K. (2001). Floating the raft hypothesis: lipid rafts play a role in immune cell activation. Immunity *14*, 657–660.

Ellmeier, W., Jung, S., Sunshine, M.J., Hatam, F., Xu, Y., Baltimore, D., Mano, H., and Littman, D.R. (2000). Severe B cell deficiency in mice lacking the tec kinase family members Tec and Btk. J. Exp. Med. *192*, 1611–1624.

Faccio, R., Zou, W., Colaianni, G., Teitelbaum, S.L., and Ross, F.P. (2003). High dose M-CSF partially rescues the Dap12−/− osteoclast phenotype. J. Cell. Biochem. *90*, 871–883.

Fernandes, M.J., Lachance, G., Pare, G., Rollet-Labelle, E., and Naccache, P.H. (2005). Signaling through CD16b in human neutrophils involves the Tec family of tyrosine kinases. J. Leukoc. Biol. *78*, 524–532.

Cell

Grimbacher, B., Holland, S.M., Gallin, J.I., Greenberg, F., Hill, S.C., Malech, H.L., Miller, J.A., O'Connell, A.C., and Puck, J.M. (1999). Hyper-IgE syndrome with recurrent infections—an autosomal dominant multisystem disorder. N. Engl. J. Med. *340*, 692–702.

Ha, H., Kwak, H.B., Lee, S.K., Na, D.S., Rudd, C.E., Lee, Z.H., and Kim, H.H. (2003). Membrane rafts play a crucial role in receptor activator of nuclear factor κB signaling and osteoclast function. J. Biol. Chem. *278*, 18573–18580.

Hashimoto, S., Iwamatsu, A., Ishiai, M., Okawa, K., Yamadori, T., Matsushita, M., Baba, Y., Kishimoto, T., Kurosaki, T., and Tsukada, S. (1999). Identification of the SH2 domain binding protein of Bruton's tyrosine kinase as BLNK—functional significance of Btk-SH2 domain in B-cell antigen receptor-coupled calcium signaling. Blood *94*, 2357–2364.

Hata, D., Kawakami, Y., Inagaki, N., Lantz, C.S., Kitamura, T., Khan, W.N., Maeda-Yamamoto, M., Miura, T., Han, W., Hartman, S.E., et al. (1998). Involvement of Bruton's tyrosine kinase in FcεRI-dependent mast cell degranulation and cytokine production. J. Exp. Med. *187*, 1235–1247.

Hayashi, K., Yamamoto, M., Nojima, T., Goitsuka, R., and Kitamura, D. (2003). Distinct signaling requirements for Dμ selection, IgH allelic exclusion, pre-B cell transition, and tumor suppression in B cell progenitors. Immunity *18*, 825–836.

Horton, J.E., Raisz, L.G., Simmons, H.A., Oppenheim, J.J., and Mergenhagen, S.E. (1972). Bone resorbing activity in supernatant fluid from cultured human peripheral blood leukocytes. Science *177*, 793–795.

Horwood, N.J., Mahon, T., McDaid, J.P., Campbell, J., Mano, H., Brennan, F.M., Webster, D., and Foxwell, B.M. (2003). Bruton's tyrosine kinase is required for lipopolysaccharide-induced tumor necrosis factor alpha production. J. Exp. Med. *197*, 1603–1611.

Ishiai, M., Kurosaki, M., Pappu, R., Okawa, K., Ronko, I., Fu, C., Shibata, M., Iwamatsu, A., Chan, A.C., and Kurosaki, T. (1999). BLNK required for coupling Syk to PLCγ2 and Rac1-JNK in B cells. Immunity *10*, 117–125.

Jumaa, H., Bossaller, L., Portugal, K., Storch, B., Lotz, M., Flemming, A., Schrappe, M., Postila, V., Riikonen, P., Pelkonen, J., et al. (2003). Deficiency of the adaptor SLP-65 in pre-B-cell acute lymphoblastic leukaemia. Nature *423*, 452–456.

Karsenty, G., and Wagner, E.F. (2002). Reaching a genetic and molecular understanding of skeletal development. Dev. Cell *2*, 389–406.

Kerner, J.D., Appleby, M.W., Mohr, R.N., Chien, S., Rawlings, D.J., Maliszewski, C.R., Witte, O.N., and Perlmutter, R.M. (1995). Impaired expansion of mouse B cell progenitors lacking Btk. Immunity *3*, 301–312.

Kirchner, S.G., Sivit, C.J., and Wright, P.F. (1985). Hyperimmunoglobulinemia E syndrome: association with osteoporosis and recurrent fractures. Radiology *156*, 362.

Koga, T., Inui, M., Inoue, K., Kim, S., Suematsu, A., Kobayashi, E., Iwata, T., Ohnishi, H., Matozaki, T., Kodama, T., et al. (2004). Costimulatory signals mediated by the ITAM motif cooperate with RANKL for bone homeostasis. Nature *428*, 758–763.

Lopez-Granados, E., Temmerman, S.T., Wu, L., Reynolds, J.C., Follmann, D., Liu, S., Nelson, D.L., Rauch, F., and Jain, A. (2007). Osteopenia in X-linked hyper-IgM syndrome reveals a regulatory role for CD40 ligand in osteoclastogenesis. Proc. Natl. Acad. Sci. USA *104*, 5056–5061.

Mahajan, S., Ghosh, S., Sudbeck, E.A., Zheng, Y., Downs, S., Hupke, M., and Uckun, F.M. (1999). Rational design and synthesis of a novel anti-leukemic agent targeting Bruton's tyrosine kinase (BTK), LFM-A13. J. Biol. Chem. *274*, 9587–9599.

Mangla, A., Khare, A., Vineeth, V., Panday, N.N., Mukhopadhyay, A., Ravindran, B., Bal, V., George, A., and Rath, S. (2004). Pleiotropic consequences of Bruton tyrosine kinase deficiency in myeloid lineages lead to poor inflammatory responses. Blood *104*, 1191–1197.

Mano, H., Yamashita, Y., Sato, K., Yazaki, Y., and Hirai, H. (1995). Tec protein-tyrosine kinase is involved in interleukin-3 signaling pathway. Blood *85*, 343–350.

Mao, D., Epple, H., Uthgenannt, B., Novack, D.V., and Faccio, R. (2006). PLCγ2 regulates osteoclastogenesis via its interaction with ITAM proteins and GAB2. J. Clin. Invest. *116*, 2869–2879.

Minegishi, Y., Saito, M., Tsuchiya, S., Tsuge, I., Takada, H., Hara, T., Kawamura, N., Ariga, T., Pasic, S., Stojkovic, O., et al. (2007). Dominant-negative mutations in the DNA-binding domain of STAT3 cause hyper-IgE syndrome. Nature *448*, 1058–1062.

Mocsai, A., Humphrey, M.B., Van Ziffle, J.A., Hu, Y., Burghardt, A., Spusta, S.C., Majumdar, S., Lanier, L.L., Lowell, C.A., and Nakamura, M.C. (2004). The immunomodulatory adapter proteins DAP12 and Fc receptor γ-chain (FcRγ) regulate development of functional osteoclasts through the Syk tyrosine kinase. Proc. Natl. Acad. Sci. USA *101*, 6158–6163.

Morita, S., Kojima, T., and Kitamura, T. (2000). Plat-E: an efficient and stable system for transient packaging of retroviruses. Gene Ther. *7*, 1063–1066.

Perez de Diego, R., Lopez-Granados, E., Pozo, M., Rodriguez, C., Sabina, P., Ferreira, A., Fontan, G., Garcia-Rodriguez, M.C., and Alemany, S. (2006). Bruton's tyrosine kinase is not essential for LPS-induced activation of human monocytes. J. Allergy Clin. Immunol. *117*, 1462–1469.

Pivniouk, V.I., and Geha, R.S. (2000). The role of SLP-76 and LAT in lymphocyte development. Curr. Opin. Immunol. *12*, 173–178.

Pivniouk, V., Tsitsikov, E., Swinton, P., Rathbun, G., Alt, F.W., and Geha, R.S. (1998). Impaired viability and profound block in thymocyte development in mice lacking the adaptor protein SLP-76. Cell *94*, 229–238.

Ross, F.P., and Teitelbaum, S.L. (2005). $\alpha_v\beta_3$ and macrophage colony-stimulating factor: partners in osteoclast biology. Immunol. Rev. *208*, 88–105.

Schaeffer, E.M., Debnath, J., Yap, G., McVicar, D., Liao, X.C., Littman, D.R., Sher, A., Varmus, H.E., Lenardo, M.J., and Schwartzberg, P.L. (1999). Requirement for Tec kinases Rlk and Itk in T cell receptor signaling and immunity. Science *284*, 638–641.

Schmidt, U., Boucheron, N., Unger, B., and Ellmeier, W. (2004). The role of Tec family kinases in myeloid cells. Int. Arch. Allergy Immunol. *134*, 65–78.

Soriano, P., Montgomery, C., Geske, R., and Bradley, A. (1991). Targeted disruption of the *c-src* proto-oncogene leads to osteopetrosis in mice. Cell *64*, 693–702.

Takata, M., and Kurosaki, T. (1996). A role for Bruton's tyrosine kinase in B cell antigen receptor-mediated activation of phospholipase C-γ2. J. Exp. Med. *184*, 31–40.

Takayanagi, H. (2007). Osteoimmunology: shared mechanisms and crosstalk between the immune and bone systems. Nat. Rev. Immunol. *7*, 292–304.

Takayanagi, H., Ogasawara, K., Hida, S., Chiba, T., Murata, S., Sato, K., Takaoka, A., Yokochi, T., Oda, H., Tanaka, K., et al. (2000). T-cell-mediated regulation of osteoclastogenesis by signalling cross-talk between RANKL and IFN-γ. Nature *408*, 600–605.

Takayanagi, H., Kim, S., Koga, T., Nishina, H., Isshiki, M., Yoshida, H., Saiura, A., Isobe, M., Yokochi, T., Inoue, J., et al. (2002). Induction and activation of the transcription factor NFATc1 (NFAT2) integrate RANKL signaling in terminal differentiation of osteoclasts. Dev. Cell *3*, 889–901.

Teitelbaum, S.L., and Ross, F.P. (2003). Genetic regulation of osteoclast development and function. Nat. Rev. Genet. *4*, 638–649.

Theill, L.E., Boyle, W.J., and Penninger, J.M. (2002). RANK-L and RANK: T cells, bone loss, and mammalian evolution. Annu. Rev. Immunol. *20*, 795–823.

Tsukada, S., Saffran, D.C., Rawlings, D.J., Parolini, O., Allen, R.C., Klisak, I., Sparkes, R.S., Kubagawa, H., Mohandas, T., Quan, S., et al. (1993). Deficient expression of a B cell cytoplasmic tyrosine kinase in human X-linked agammaglobulinemia. Cell *72*, 279–290.

Walsh, M.C., Kim, N., Kadono, Y., Rho, J., Lee, S.Y., Lorenzo, J., and Choi, Y. (2006). Osteoimmunology: interplay between the immune system and bone metabolism. Annu. Rev. Immunol. *24*, 33–63.

Wong, B.R., Besser, D., Kim, N., Arron, J.R., Vologodskaia, M., Hanafusa, H., and Choi, Y. (1999). TRANCE, a TNF family member, activates Akt/PKB through a signaling complex involving TRAF6 and c-Src. Mol. Cell *4*, 1041–1049.

Wu, Y., Torchia, J., Yao, W., Lane, N.E., Lanier, L.L., Nakamura, M.C., and Humphrey, M.B. (2007). Bone microenvironment specific roles of ITAM adapter signaling during bone remodeling induced by acute estrogen-deficiency. PLoS ONE *2*, e586. 10.1371/journal.pone.0000586.

EXTENDED PDF FORMAT
SPONSORED BY
usb
www.usbweb.com

Science
AAAS

Cathepsin K-Dependent Toll-Like Receptor 9 Signaling Revealed in Experimental Arthritis

Masataka Asagiri, *et al.*

Science **319**, 624 (2008);
DOI: 10.1126/science.1150110

The following resources related to this article are available online at www.sciencemag.org (this information is current as of February 2, 2008):

Updated information and services, including high-resolution figures, can be found in the online version of this article at:
http://www.sciencemag.org/cgi/content/full/319/5863/624

A list of selected additional articles on the Science Web sites **related to this article** can be found at:
http://www.sciencemag.org/cgi/content/full/319/5863/624#related-content

This article **cites 26 articles**, 7 of which can be accessed for free:
http://www.sciencemag.org/cgi/content/full/319/5863/624#otherarticles

This article appears in the following **subject collections**:
Immunology
http://www.sciencemag.org/cgi/collection/immunology

Information about obtaining **reprints** of this article or about obtaining **permission to reproduce this article** in whole or in part can be found at:
http://www.sciencemag.org/about/permissions.dtl

Downloaded from www.sciencemag.org on February 2, 2008

Science (print ISSN 0036-8075; online ISSN 1095-9203) is published weekly, except the last week in December, by the American Association for the Advancement of Science, 1200 New York Avenue NW, Washington, DC 20005. Copyright 2008 by the American Association for the Advancement of Science; all rights reserved. The title *Science* is a registered trademark of AAAS.

8. K. Berns *et al.*, *Nature* **428**, 431 (2004).
9. T. R. Brummelkamp *et al.*, *Nat. Chem. Biol.* **2**, 202 (2006).
10. T. Sjoblom *et al.*, *Science* **314**, 268 (2006).
11. L. D. Wood *et al.*, *Science* **318**, 1108 (2007).
12. R. A. Dickins *et al.*, *Nat. Genet.* **37**, 1289 (2005).
13. G. K. Smyth, T. Speed, *Methods* **31**, 265 (2003).
14. V. M. Draviam *et al.*, *Nat. Cell Biol.* **9**, 556 (2007).
15. M. Ito, T. Nakano, F. Erdodi, D. J. Hartshorne, *Mol. Cell. Biochem.* **259**, 197 (2004).
16. H. Jin, T. Sperka, P. Herrlich, H. Morrison, *Nature* **442**, 576 (2006).
17. L. T. Vassilev *et al.*, *Science* **303**, 844 (2004).
18. N. L. Solimini, J. Luo, S. J. Elledge, *Cell* **130**, 986 (2007).
19. J. M. Silva *et al.*, *Science* **319**, 617 (2008).

20. We thank A. L. Brass for the pMSCV-PM, pMSCV-PM-FF, and pMSCV-PM-mir30 vectors and for scientific advice; M. J. Solimini for help with data analysis; E. R. McDonald for scientific advice; T. Waldman and B. Vogelstein for the HCT116 and DLD-1 cell lines; and T. Moore from Open Biosystems for help with assembling library pools. G.H. is a fellow of the Helen Hay Whitney Foundation. X.L.A. is supported by a National Research Service Award fellowship, M.E.S. is supported by an American Cancer Society fellowship, and A.S. is supported by grant T32CA09216 to the MGH Pathology Department. T.F.W. is a fellow of the Susan G. Komen Foundation and is supported by grant PDF0403175. This work is supported by grants from NIH and the U.S. Department of Defense to G.J.H., J.W.H., and S.J.E. G.J.H. has a paid consulting relationship with Open Biosystems.

Supporting Online Material

www.sciencemag.org/cgi/content/full/319/5863/620/DC1
Materials and Methods
SOM Text
Figs. S1 to S3
Tables S1 to S6
References
Data Sets S1 to S9

14 August 2007; accepted 20 December 2007
10.1126/science.1149200

Cathepsin K–Dependent Toll-Like Receptor 9 Signaling Revealed in Experimental Arthritis

Masataka Asagiri,[1,2] Toshitake Hirai,[1,4] Toshihiro Kunigami,[1,4] Shunya Kamano,[1,5] Hans-Jürgen Gober,[1] Kazuo Okamoto,[1] Keizo Nishikawa,[1] Eicke Latz,[6] Douglas T. Golenbock,[6] Kazuhiro Aoki,[3] Keiichi Ohya,[3] Yuuki Imai,[7,9] Yasuyuki Morishita,[8] Kohei Miyazono,[8] Shigeaki Kato,[7,9] Paul Saftig,[10] Hiroshi Takayanagi[1,2]*

Cathepsin K was originally identified as an osteoclast-specific lysosomal protease, the inhibitor of which has been considered might have therapeutic potential. We show that inhibition of cathepsin K could potently suppress autoimmune inflammation of the joints as well as osteoclastic bone resorption in autoimmune arthritis. Furthermore, *cathepsin K*$^{-/-}$ mice were resistant to experimental autoimmune encephalomyelitis. Pharmacological inhibition or targeted disruption of cathepsin K resulted in defective Toll-like receptor 9 signaling in dendritic cells in response to unmethylated CpG DNA, which in turn led to attenuated induction of T helper 17 cells, without affecting the antigen-presenting ability of dendritic cells. These results suggest that cathepsin K plays an important role in the immune system and may serve as a valid therapeutic target in autoimmune diseases.

Both innate and adaptive immune systems contribute to the inflammation seen in autoimmune diseases, but the molecular mechanism underlying this process is not completely understood (*1*, *2*). The cathepsins constitute a family of lysosomal cysteine proteases that were initially recognized as nonspecific scavengers of cellular proteins and that were also found to display cell type–specific functions (*3*, *4*). Cathepsins L and S are fundamental in processing of major histocompatibility complex (MHC) class II antigens and MHC class II trafficking and maturation (*3*, *4*). In contrast, cathepsin K is highly expressed in osteoclasts and is involved in degradation of bone matrices such as type I collagen (*5*). The loss-of-function mutation in the *cathepsin K* gene in humans causes pycnodysostosis, a rare genetic disorder characterized by impaired osteoclastic bone resorption (*6*). In mice, the targeted disruption of *cathepsin K* similarly results in the pycnodysostotic phenotype (*4*, *5*, *7*). Among matrix-degrading enzymes expressed in osteoclasts, cathepsin K is the only one for which an essential role in bone resorption has been clearly demonstrated in both mice and humans (*8*). Thus, cathepsin K remains a potential therapeutic target for the treatment of bone diseases such as osteoporosis and autoimmune arthritis, in which osteoclast activity is increased (*9*, *10*).

Through screening, we obtained a potent orally active cathepsin K inhibitor named NC-2300 (Fig. 1A and figs. S1 to S3), which suppresses osteoclastic bone resorption both in vivo and in vitro (figs. S1 and S4). Computer-assisted simulation of the cathepsin K/NC-2300 complex indicated that NC-2300 blocks the active-site cleft where Cys^{25} and His^{162} of cathepsin K form the catalytic site (Fig. 1B and fig. S5). To test the effects of the inhibitor on disease models, we treated adjuvant-induced arthritis (AIA) in rats with oral administration of NC-2300 and compared the results with the effects of alendronate, which is one of the bisphosphonate compounds used clinically as an inhibitor of osteoclastic bone resorption. Bone loss in arthritis occurs mainly in two forms: bone erosion at the inflamed joints and periarticular osteoporosis (*11*). Radiological analysis revealed that NC-2300, but not alendronate, markedly suppressed bone erosion (Fig. 1C), although bone mineral density analysis showed that both compounds had a comparable inhibitory effect on periarticular osteoporosis (fig. S6A). NC-2300 also ameliorated paw swelling (Fig. 1D) and improved locomotive activity (fig. S6B) without affecting the onset rate of arthritis. NC-2300 reduced inflammation even when administered after the onset of disease (fig. S7). These results indicate that cathepsin K also functions in cells other than osteoclasts, allowing it to participate in autoimmune inflammation.

In AIA, local injection of adjuvant stimulates antigen presentation by dendritic cells (DCs), leading to T cell autoimmunity, the production of inflammatory cytokines by macrophages, and osteoclast-mediated bone destruction (*9*, *12*, *13*). The adjuvant effects are mainly dependent on the pathogen-associated molecular patterns (PAMPs)–induced activation of Toll-like receptor (TLR) signaling (*14*, *15*). Therefore, we next analyzed the expression and function of cathepsin K in T cells, macrophages, and DCs. Cathepsin K mRNA was barely detected in nonadherent bone marrow (BM) cells or splenic T cells (Fig. 2A), and NC-2300 showed no effects on T cell activation (fig. S8A). Although macrophages have been reported to express cathepsin K (*4*), NC-2300 had no effects on the activation of BM-derived macrophages stimulated by PAMPs (fig. S8B). BM-derived DCs (BM-DCs) did express a detectable level of cathepsin K mRNA, although this was much lower than expression in osteoclasts (Fig. 2A). Nevertheless, cathepsin K activity was confirmed in DCs and was inhibited by NC-2300 (Fig. 2B).

To investigate whether cathepsin K has a role in antigen presentation in DCs, DCs were cultured with fluorescein isothiocyanate (FITC)–labeled ovalbumin. The uptake of ovalbumin-FITC was observed by flow cytometry in NC-2300–treated DCs as well as in nontreated cells (Fig. 2C). In addition, NC-2300–treated DCs stimulated proliferation of splenic T cells from ovalbumin-specific DO11.10 TCR transgenic mice to an extent similar to that of nontreated DCs (Fig. 2D). These results suggest that cathepsin K activity is not required for the antigen uptake, processing, or presentation by

[1]Department of Cell Signaling, Graduate School, Tokyo Medical and Dental University, Tokyo 113-8549, Japan. [2]Center of Excellence Program for Frontier Research on Molecular Destruction and Reconstruction of Tooth and Bone, Tokyo Medical and Dental University, Tokyo 113-8549, Japan. [3]Department of Hard Tissue Engineering, Section of Pharmacology, Graduate School, Tokyo Medical and Dental University, Tokyo 113-8549, Japan. [4]Nippon Chemiphar Co., Ltd., Saitama 341-0005, Japan. [5]Department of Orthopaedic Surgery, Juntendo University School of Medicine, Tokyo 113-8421, Japan. [6]Division of Infectious Diseases and Immunology, University of Massachusetts Medical School, Worcester, MA 01605, USA. [7]Institute of Molecular and Cellular Biosciences, University of Tokyo, Tokyo 113-0032, Japan. [8]Department of Molecular Pathology, Graduate School of Medicine, University of Tokyo, Tokyo 113-0033, Japan. [9]Exploratory Research for Advanced Technology, Japan Science and Technology Agency, Saitama 332-0012, Japan. [10]Biochemical Institute, Christian-Albrechts-University Kiel, D-24098 Kiel, Germany.

*To whom correspondence should be addressed. E-mail: taka.csi@tmd.ac.jp

Downloaded from www.sciencemag.org on February 2, 2008

DCs. Considering the crucial role of cathepsins L and S in antigen presentation (*3*, *4*, *16*), these results also indicate that the effects of NC-2300 on these cathepsins are negligible.

Complete Freund's adjuvant (CFA) is composed of killed mycobacteria, which contain various PAMPs including TLR2, TLR4, and TLR9 agonists (*14*, *17*). Therefore, we tested the responses of DCs to these PAMPs with or without cathepsin K inactivation. Enzyme-linked immunosorbent assay revealed that the production of cytokines such as interleukin-12 (IL-12) and IL-23 by DCs was significantly inhibited by NC-2300 when stimulated with oligodeoxynucleotides containing unmethylated CpG motif (CpG: the TLR9 ligand), but not with Malp2 and peptidoglycan (PGN) (the TLR2 ligands) or lipopolysaccharide (LPS: the TLR4 ligand) (Fig. 2E). CpG-induced expression of IL-6, IL-12, and IL-23 in BM-DCs was down-regulated at the mRNA level (Fig. 2F), and IFN-β production by Flt3L-induced BM-DCs in response to CpG was suppressed by NC-2300 (Fig. 2F). These results suggest that cathepsin K plays an important role in the gene induction program regulated by TLR9 signaling.

Deoxyribonuclease treatment of the mycobacterial components in CFA greatly reduces the severity of AIA without affecting the induction efficiency, and this reduction is recovered by supplementation with CpG DNA (*18*, *19*), indicating that TLR9-mediated immune responses determine the severity of autoimmune inflammation. Because mycobacterial DNA can be detected weeks after CFA inoculation (*19*), CpG DNA may augment autoimmune inflammation throughout the course of arthritis. These observations lend support to the notion that cathepsin K–dependent TLR9 signaling contributes to autoimmune inflammation.

How does cathepsin K regulate TLR9 signaling? After being taken up into the cells, CpG DNA locates within the endosomal compartment, where CpG DNA binds to TLR9 (*14*, *18*). The binding of CpG with TLR9 results in the conformational change of TLR9 (*20*), leading to activation of MyD88 and downstream signaling such as the mitogen-activated protein kinase, interferon regulatory factor (IRF), and nuclear factor kappa B (NF-κB) pathways (*14*). Activation of these pathways leads to the production of inflammatory cytokines and up-regulation of cell-

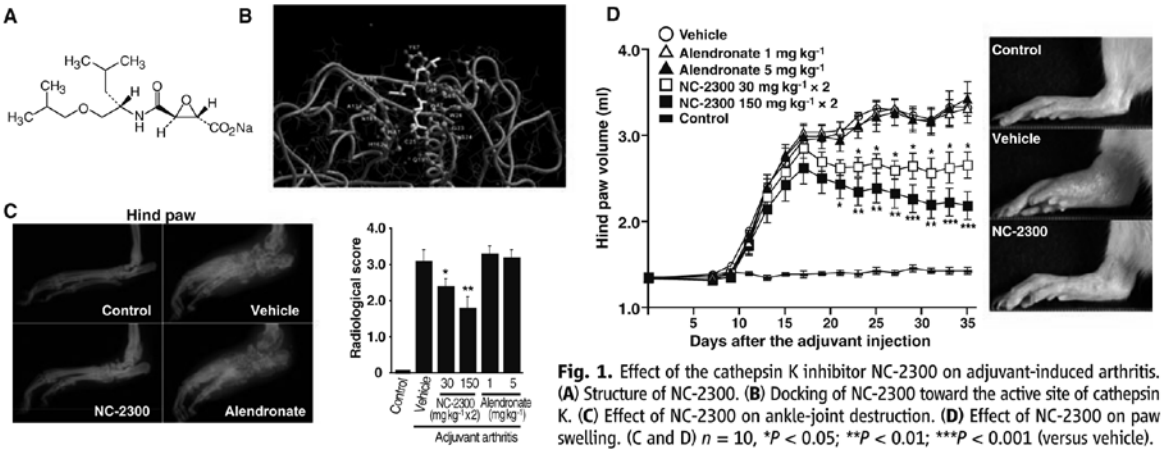

Fig. 1. Effect of the cathepsin K inhibitor NC-2300 on adjuvant-induced arthritis. **(A)** Structure of NC-2300. **(B)** Docking of NC-2300 toward the active site of cathepsin K. **(C)** Effect of NC-2300 on ankle-joint destruction. **(D)** Effect of NC-2300 on paw swelling. (C and D) $n = 10$, $^{*}P < 0.05$; $^{**}P < 0.01$; $^{***}P < 0.001$ (versus vehicle).

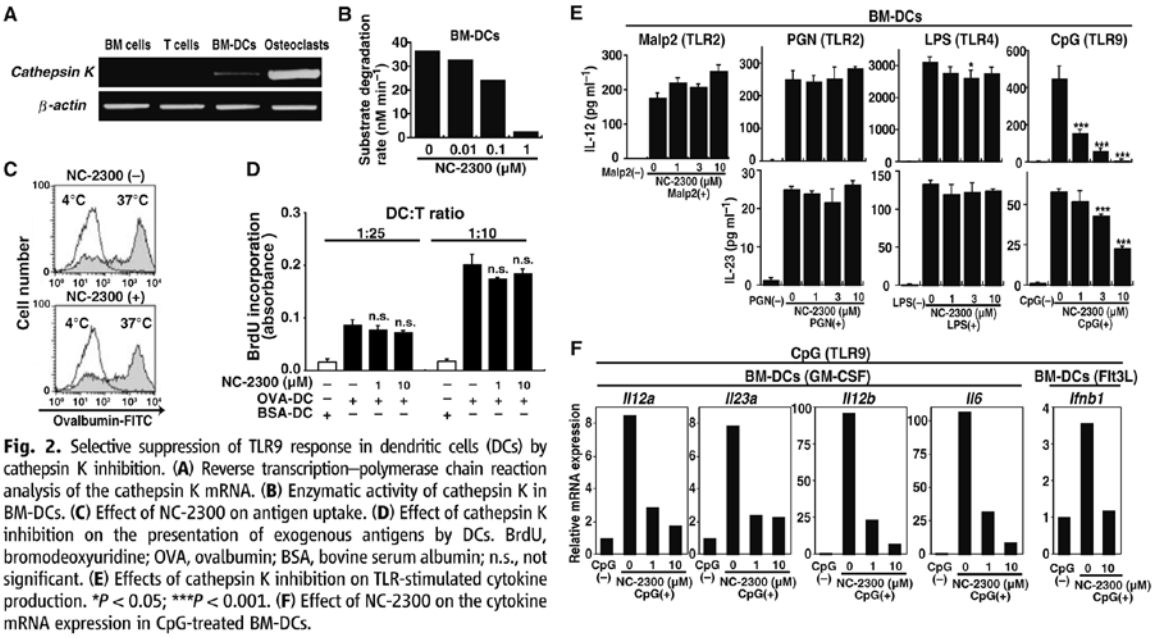

Fig. 2. Selective suppression of TLR9 response in dendritic cells (DCs) by cathepsin K inhibition. **(A)** Reverse transcription–polymerase chain reaction analysis of the cathepsin K mRNA. **(B)** Enzymatic activity of cathepsin K in BM-DCs. **(C)** Effect of NC-2300 on antigen uptake. **(D)** Effect of cathepsin K inhibition on the presentation of exogenous antigens by DCs. BrdU, bromodeoxyuridine; OVA, ovalbumin; BSA, bovine serum albumin; n.s., not significant. **(E)** Effects of cathepsin K inhibition on TLR-stimulated cytokine production. $^{*}P < 0.05$; $^{***}P < 0.001$. **(F)** Effect of NC-2300 on the cytokine mRNA expression in CpG-treated BM-DCs.

Downloaded from www.sciencemag.org on February 2, 2008

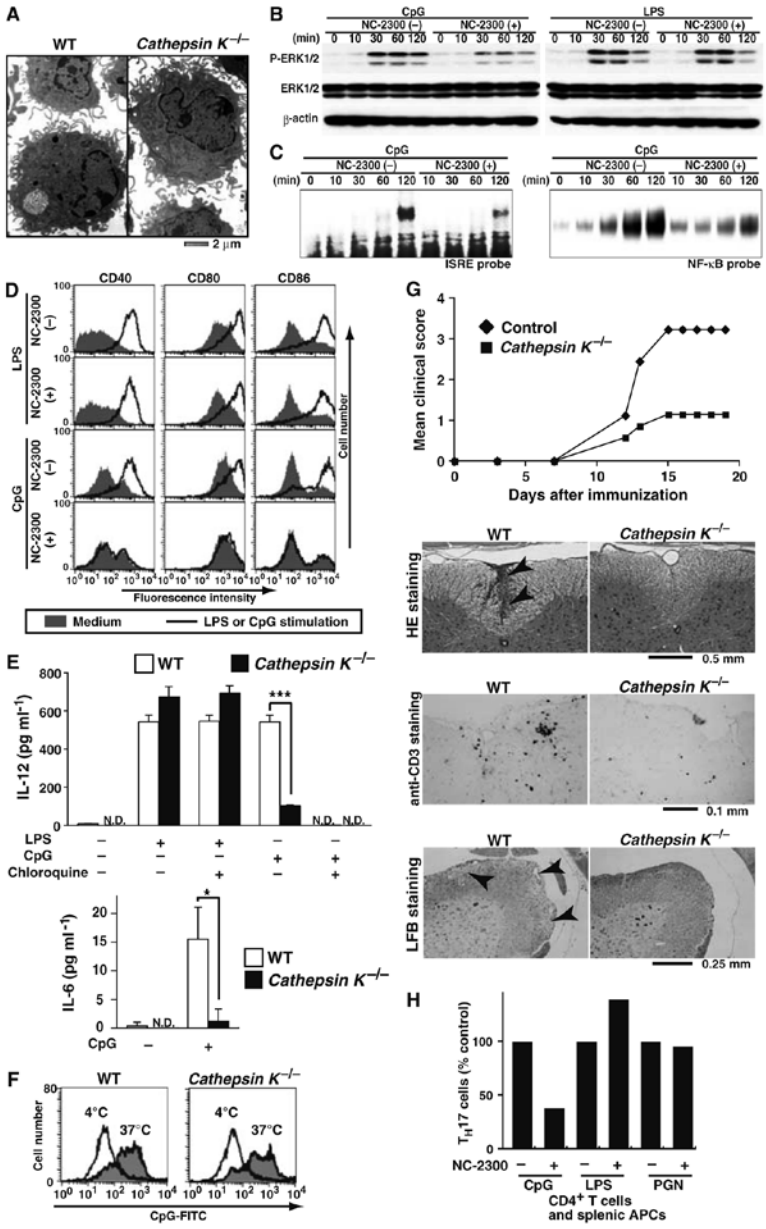

Fig. 3. Cathepsin K regulation of TLR9-mediated immune responses and autoimmune inflammation. (**A**) Electron micrographs of WT and *cathepsin* $K^{-/-}$ BM-DCs. (**B**) Suppression of ERK phosphorylation by NC-2300 in CpG-stimulated DCs. (**C**) Effect of NC-2300 on CpG-induced activation of transcription factors, IRF (left) and NF-κB (right) (electrophoretic mobility shift assay). ISRE, IFN-stimulated response element. (**D**) Impaired TLR9-mediated expression of cell-surface molecules in NC-2300–treated DCs. (**E**) Cytokine production in WT or *cathepsin* $K^{-/-}$ DCs in response to LPS or CpG. N.D., not detected. $*P < 0.05$; $***P < 0.001$. (**F**) Uptake of CpG in *cathepsin* $K^{-/-}$ DCs. (**G**) Severity of EAE in *cathepsin* $K^{-/-}$ mice. Clinical scores (top). Lumbar spinal cord sections stained with hematoxylin and eosin (HE), immunostained for CD3, and stained with luxol fast blue (LFB) (bottom). Arrowheads indicate inflammatory cellular infiltrates (HE) and demyelinated areas (LFB). (**H**) Cathepsin K inactivation results in defective T_H17 polarization in response to CpG, but not to LPS or PGN.

surface molecules such as CD40, CD80, and CD86 in DCs (*2*, *21*). Compounds that block endosomal acidification such as chloroquine inhibit CpG-driven signaling (*14*, *18*). A normal number of BM-DCs were generated in BM cells derived from *cathepsin* $K^{-/-}$ mice (*5*, *22*), and they exhibited a normal morphology (Fig. 3A), suggesting that cathepsin K is dispensable for the DC differentiation. CpG-induced, but not LPS-induced, phosphorylation of extracellular-signal regulated kinases 1 and 2 (ERK 1/2) in DCs was suppressed by cathepsin K inactivation (Fig. 3B). CpG-induced activation of IRF and NF-κB was also suppressed by cathepsin K inactivation in DCs (Fig. 3C). In addition, NC-2300 reduced expression of CD40, CD80, and CD86 in DCs (Fig. 3D). CpG-induced, but not LPS-induced, production of cytokines such as IL-12 and IL-6 in *cathepsin* $K^{-/-}$ DCs was significantly suppressed (Fig. 3E). Thus, cathepsin K inactivation leads to the blockade of essentially all the downstream pathways of TLR9 signaling in DCs, suggesting that cathepsin K plays a critical role in the signaling events proximal to TLR9. However, the endocytosis of CpG was not affected in *cathepsin* $K^{-/-}$ DCs (Fig. 3F) and the endosomal acidification was not inhibited by NC-2300 (fig. S9), whereas chloroquine suppressed the cathepsin K activity in DCs (fig. S10).

It remains to be elucidated how cathepsin K regulates CpG-TLR9 signaling in the endosome, but the results of pharmacological inhibition indicate that the proteolytic activity of this enzyme is crucial for the mechanism. It is conceivable that cathepsin K may be involved in the degradation of proteins that inhibit the interaction between CpG and TLR9, or cathepsin K–mediated proteolysis may result in the conformational change of TLR9 that augments its signal transduction (*20*). Because fluorescence resonance energy transfer analysis showed that the CpG-induced conformational change of TLR9 was not affected in human embryonic kidney (HEK) 293 cells by NC-2300 (fig. S11), we cannot rule out the possibility that cathepsin K degrades a cytoplasmic protein that modifies the proximal TLR9 signaling. The observation that *cathepsin* $K^{-/-}$ DCs responded normally to TLR3 or TLR7/8 stimulation suggests that the role of cathepsin K is TLR9-specific in DCs (fig. S12).

To clearly demonstrate that cathepsin K plays a critical role in autoimmune inflammation in an osteoclast-independent manner, we subjected *cathepsin* $K^{-/-}$ mice to experimental autoimmune encephalomyelitis (EAE), in which TLR9 signaling plays an important role (*23*, *24*). The frequency of the onset of EAE was not different between control and *cathepsin* $K^{-/-}$ mice, but the severity of the paralytic symptoms was much lower in the *cathepsin* $K^{-/-}$ mice than in control mice (Fig. 3G, top). Histological analysis of spinal cords demonstrated a marked decrease in inflammation (Fig. 3G, HE staining), T cell infiltration (Fig. 3G, anti-CD3 staining), and demyelination (Fig. 3G, LFB staining) in *cathepsin* $K^{-/-}$ mice. Because T helper 17 (T_H17) cells play an essential role in the autoimmune inflammation in EAE (*25*), we examined the effect of cathepsin K inactivation on the ability of DCs to induce

Downloaded from www.sciencemag.org on February 2, 2008

T_H17 cells. The ability of DCs to induce T_H17 cells was markedly inhibited by cathepsin K inactivation when stimulated with CpG, but not with LPS or PGN (Fig. 3H). Taken together with the results on the role of cathepsin K in CpG-induced cytokine expression in DCs, the impaired induction of T_H17 cells by cathepsin K inactivation was caused, at least in part, by the reduced DC expression of cytokines that are involved in the induction and expansion of T_H17 cells such as IL-6 and IL-23 (*25*, *26*).

Our results show that cathepsin K, which was thought to be an osteoclast-specific enzyme, plays a critical role in the immune system. Cathepsin K functions under the acidified conditions in the endosome, where engagement of CpG by TLR9 occurs, and plays an important role in the signaling events proximal to TLR9. Thus, careful attention should be paid to the side effects of cathepsin K inhibitors on the immune system in the treatment of osteoporosis, whereas they may have dual benefits in the treatment of autoimmune arthritis, the pathogenesis of which is dependent on both DCs and osteoclasts (*9*).

References and Notes

1. J. Banchereau, V. Pascual, A. K. Palucka, *Immunity* **20**, 539 (2004).
2. R. M. Steinman, D. Hawiger, M. C. Nussenzweig, *Annu. Rev. Immunol.* **21**, 685 (2003).
3. V. Turk, B. Turk, D. Turk, *EMBO J.* **20**, 4629 (2001).
4. K. Honey, A. Y. Rudensky, *Nat. Rev. Immunol.* **3**, 472 (2003).
5. P. Saftig *et al.*, *Proc. Natl. Acad. Sci. U.S.A.* **95**, 13453 (1998).
6. B. D. Gelb, G. P. Shi, H. A. Chapman, R. J. Desnick, *Science* **273**, 1236 (1996).
7. W. Chen *et al.*, *Hum. Mol. Genet.* **16**, 410 (2007).
8. M. Asagiri, H. Takayanagi, *Bone* **40**, 251 (2007).
9. H. Takayanagi, *Nat. Rev. Immunol.* **7**, 292 (2007).
10. Y. Yasuda, J. Kaleta, D. Brömme, *Adv. Drug Deliv. Rev.* **57**, 973 (2005).
11. S. Ochi *et al.*, *Proc. Natl. Acad. Sci. U.S.A.* **104**, 11394 (2007).
12. R. Holmdahl *et al.*, *Immunol. Rev.* **184**, 184 (2001).
13. A. Marshak-Rothstein, *Nat. Rev. Immunol.* **6**, 823 (2006).
14. S. Akira, S. Uematsu, O. Takeuchi, *Cell* **124**, 783 (2006).
15. A. Iwasaki, R. Medzhitov, *Nat. Immunol.* **5**, 987 (2004).
16. R. J. Riese *et al.*, *J. Clin. Invest.* **101**, 2351 (1998).
17. S. B. Su *et al.*, *J. Immunol.* **175**, 6303 (2005).
18. A. M. Krieg, *Annu. Rev. Immunol.* **20**, 709 (2002).
19. A. Ronaghy *et al.*, *J. Immunol.* **168**, 51 (2002).
20. E. Latz *et al.*, *Nat. Immunol.* **8**, 772 (2007).
21. I. Mellman, R. M. Steinman, *Cell* **106**, 255 (2001).
22. T. Nakamura *et al.*, *Cell* **130**, 811 (2007).
23. M. Prinz *et al.*, *J. Clin. Invest.* **116**, 456 (2006).
24. B. M. Segal, J. T. Chang, E. M. Shevach, *J. Immunol.* **164**, 5683 (2000).
25. H. Park *et al.*, *Nat. Immunol.* **6**, 1133 (2005).
26. E. Bettelli *et al.*, *Nature* **441**, 235 (2006).

27. We thank K. Takeda, M. Yamamoto, H. Oda, S. Imajoh-Ohmi, M. Matsuura, K. Nishioka, T. Kanda, K. Sato, S. Hida, Y. Iwai, H. Hemmi, H. Yanai, S. Kano, Y. Omatsu, T. Onodera, T. Honda, and A. Suematsu for discussion and assistance. This work was supported in part by a Grant-in-Aid for Creative Scientific Research from the Japan Society for the Promotion of Science (JSPS); grants for the Genome Network Project from the Ministry of Education, Culture, Sports, Science and Technology of Japan (MEXT); Grants-in-Aid for Scientific Research from JSPS and MEXT; Health Sciences Research Grants from the Ministry of Health, Labor and Welfare of Japan; and grants from the Deutsche Forschungsgemeinschaft and the NIH.

Supporting Online Material

www.sciencemag.org/cgi/content/full/319/5863/624/DC1
Materials and Methods
Figs. S1 to S12
References

5 September 2007; accepted 14 December 2007
10.1126/science.1150110

Systemic Leukocyte-Directed siRNA Delivery Revealing Cyclin D1 as an Anti-Inflammatory Target

Dan Peer,[1] Eun Jeong Park,[1] Yoshiyuki Morishita,[1] Christopher V. Carman,[2] Motomu Shimaoka[1]*

Cyclin D1 (CyD1) is a pivotal cell cycle–regulatory molecule and a well-studied therapeutic target for cancer. Although CyD1 is also strongly up-regulated at sites of inflammation, its exact roles in this context remain uncharacterized. To address this question, we developed a strategy for selectively silencing CyD1 in leukocytes in vivo. Targeted stabilized nanoparticles (tsNPs) were loaded with CyD1–small interfering RNA (siRNA). Antibodies to β_7 integrin (β_7 I) were then used to target specific leukocyte subsets involved in gut inflammation. Systemic application of β_7 I-tsNPs silenced CyD1 in leukocytes and reversed experimentally induced colitis in mice by suppressing leukocyte proliferation and T helper cell 1 cytokine expression. This study reveals CyD1 to be a potential anti-inflammatory target, and suggests that the application of similar modes of targeting by siRNA may be feasible in other therapeutic settings.

RNA interference (RNAi) has emerged as a powerful strategy for suppressing gene expression, offering the potential to dramatically accelerate in vivo drug target validation, as well as the promise to create novel therapeutic approaches if it can be effectively applied in vivo (*1*). Cyclin D1 (CyD1) is a key cell cycle–regulating molecule that governs the proliferation of normal and malignant cells (*2*, *3*). In inflammatory bowel diseases, colon-expressed CyD1 is aberrantly up-regulated in both epithelial and immune cells (*4*, *5*). Although CyD1 has also been implicated in promoting epithelial colorectal dysplasia and carcinogenesis, it is not clear whether leukocyte-expressed CyD1 contributes directly to the pathogenesis of inflammation and whether it might serve as a therapeutic target.

To address these questions, we used RNAi silencing of CyD1 in an experimental model of intestinal inflammation. A major limitation to the use of RNAi in vivo is the effective delivery of siRNAs to the target cells (*6*, *7*). RNAi in leukocytes, a prime target for anti-inflammatory therapeutics, has remained particularly challenging, as these cells are difficult to transduce by conventional transfection methods and are often disseminated throughout the body, thus requiring systemic delivery approaches (*8*). One possibility is to use integrins, which are an important family of cell-surface adhesion molecules, as targets for siRNA delivery (*8*). Specifically, we have shown that antibody-protamine fusion proteins directed to the lymphocyte function-associated antigen–1 (LFA-1) integrin selectively delivered siRNAs to leukocytes, both in vitro and in vivo (*8*). However, whether an integrin-directed siRNA delivery approach can induce

[1]Immune Disease Institute and Department of Anesthesia, Harvard Medical School, 200 Longwood Avenue, Boston, MA 02115, USA. [2]Department of Medicine, Beth Israel Deaconess Medical Center, and Harvard Medical School, 330 Brookline Avenue, Boston, MA 02215, USA.

*To whom correspondence should be addressed. E-mail: shimaoka@cbrinstitute.org

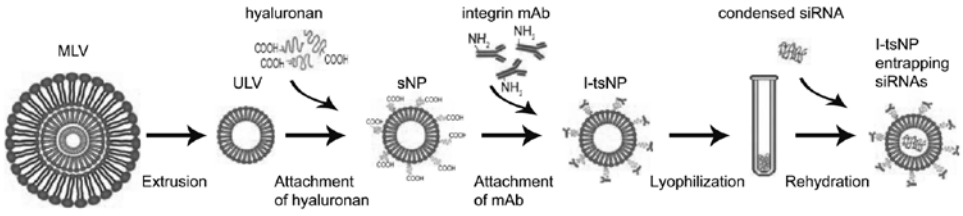

Fig. 1. The processes involved in generating I-tsNPs. Multilamellar vesicle (MLV) [prepared as described in (*9*)] is extruded to form a unilamellar vesicle (ULV) with a diameter of ~100 nm. Hyaluronan is covalently attached to DPPE in the ULV. A monoclonal antibody (mAb) to the integrin is covalently attached to hyaluronan, generating I-tsNP. siRNAs are entrapped by rehydrating lyophilized β_7 I-tsNP with water containing protamine-condensed siRNAs.

Downloaded from www.sciencemag.org on February 2, 2008

日経産業新聞　2008年(平成20年)4月10日(木曜日)
ハイテクmonthly

医療分野で重要成果目立つ

2008年度 技術トレンド調査（第1回）

日本経済新聞社は、二〇〇八年度第一・四半期（〇七年十二月—〇八年二月）の技術トレンド調査では、大学で誕生した生命科学分野の成果が総合評価の一—三位を占めた。高齢化などに伴って増える疾病の克服に向けて重点的に研究が進められ、着実に成果が登場している。エレクトロニクス分野では発光素子に関する技術開発がランキング上位に入り、この分野における日本の層の厚さを示した。（1面参照）

京大、皮膚以外からiPS細胞を作製

iPS細胞は、受精卵を分割して作製する胚（はい）性幹細胞（ES細胞）と同等の分化機能を備え、倫理的な制約なく再生医療に応用できると期待が膨らんでいる。京大の山中教授らは〇六年にマウスで、〇七年にヒトで初めて開発したが、いずれも皮膚細胞を使った。新しい成果は、マウスの胃と肝臓の細胞から作製した。手法は、皮膚細胞からiPS細胞を開発した時とほぼ同じ。皮膚以外の細胞からでも作製できることを示し、技術の普遍性を高めた。

同時に、より安全性の高いiPS細胞が作製できることも分かった。最初にマウスの皮膚細胞から作った際、がん化する割合が高い問題を抱えていたが、胃や肝臓の細胞を使うとほとんどがん化しなくなったという。ヒトの場合の確認はこれからだが、同じ結果が見込め臨床着手に向け好材料と受け止められている。

◎　◎

総合二位には、東京医科歯科大学などが開発した関節リウマチの候補薬が入った。同大学の高柳広教授らは、骨を分解する酵素「カテプシンK」が免疫を活性化することを発見し、この働きを止める化合物を日本ケミファと共同開発した。ネズミでの実験で骨の分解を阻害し、炎症も抑えられることを確認した。

関節リウマチは、免疫が異常に活性化して自分の骨を壊す病気。新化合物は骨の分解と免疫活性化の両方を抑制し、強い治療効果を見込める。メカニズムが似ている骨粗しょう症や多発性骨髄腫などにも効果が期待でき、高柳教授らは米ベンチャー企業と協力して臨床試験を計画している。

学術的な意義と実用性がうまくかみ合った成果で、国立大学のバイオ系教授は「たんぱく質分解酵素の働きを抑える薬の研究は進んでおり、実用化につながる可能性は高い」と評価した。

このほか、乳がんが悪性化して他の組織へ広がる際に働くたんぱく質を見つけた大阪バイオサイエンス研究所と、血小板を増やす人工抗体を開発したキリンファーマの成果がそれぞれ三位と九位になり、医療関連の新技術四件が上位十件に入った。

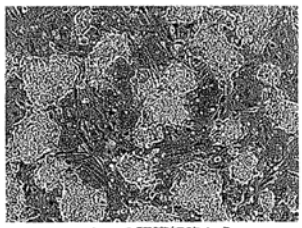

マウスの肝臓細胞から作製したiPS細胞

発光素子にも高い評価

電子・情報分野では、百ｷﾞｶﾞ(ｷﾞｶﾞは十億)ﾋﾞｯﾄ級と、記憶容量を現在の約六倍に高められるフラッシュメモリー用の新しい素子構造を開発した東芝の成果が五位になった。フラッシュメモリーは動作が高速で消費電力が少なく、磁気ディスクを脅かす小型の記録媒体として急成長している。「実用性」の評価では最も高い評価点を付けた。

東芝は、回路線幅十五ﾅﾉ(ﾅﾉは十億分の一)ﾒｰﾄﾙと四世代先の超微細加工技術を試し、実現できそうな手応えをつかんだ。長期使用時の耐久性が課題だが、解決手段も次々と登場しそう。同社は四—五年後をメドに商品化を検討している。

短距離の無線通信の速度を格段に高めたKDDI研究所の成果は、実用性と市場性の両方で高い評価を得て総合六位に付けた。携帯電話に搭載されている赤外線通信に代わり、〇九年にも実用化される見通しだ。

◎　◎

このほか発光素子に関する成果も、総合評価の上位で目立った。京大の川上養一教授らと日亜化学工業が共同で開発した発光ダイオード（LED）は、微細構造の変化だけで青色・黄色・赤色の多色発光を可能にした。蛍光体を使わずに白色光を出せ、将来の照明の有望株と目される。

京大の野田進教授らが開発した青紫色の面発光レーザーは、ビームを小さく絞り込むなどの調節ができ、光ディスクの容量を新世代DVDの五十倍に高める基礎技術になるという。いずれも独自の技術で「新規性」を中心に高い評価を得た。

今回のトレンド調査で、ロボット関連の成果は、「話題性」の上位を占めた。代表はトヨタ自動車の「パートナーロボット」と、複数台で協調作業ができるホンダの「ASIMO」。

トヨタは、左右の車輪が独立して上下し段差を移動する近距離の移動支援ロボットと、バイオリンを演奏する細かな指使いを実現した二足歩行ロボットを実演した。ホンダは、ASIMOに通信機能を加え、一台がワゴンを押し、もう一台がお茶を配る分担作業ができるようにした。人に道を譲ったり、電池の容量が少なくなったりすると自動で充電場所に移動する機能も付け加えた。

両社とも、家事や介護などを支援する需要を想定し、一〇年代初頭の実用化を目指している。ただ専門家の評価では「まだ夢の段階」との意見が多く、実用性や市場性の点数は伸びなかった。

（編集委員　永田好生）

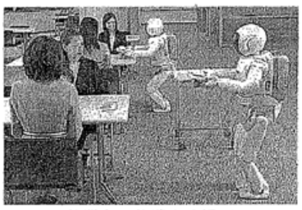

複数台で作業を分担できるホンダの人型ロボット「ASIMO」

総合順位（1—20位）

順位	研究開発者（発表日）	成果の概要	評価点
1	京都大学（2月15日）	新型万能細胞、がん化しにくく，マウスの胃・肝臓から作製	10.75
2	東京医科歯科大学など（2月1日）	関節リウマチ薬候補、骨減少と免疫抑制に効果	10
3	大阪バイオサイエンス研究所（12月16日）	乳がん、乳腺外への拡大「浸潤」、原因の酵素など発見	9.75
4	奈良先端科学技術大学院大学（12月21日）	イネの免疫指令、たんぱく質発見	9.67
5	東芝（12月12日）	フラッシュメモリー、容量6倍、100ギガビット、基本素子を試作	9.6
6	KDDI研究所（1月8日）	CDアルバム無線転送1秒、数センチの通信速度250倍、半導体レーザー利用	9.4
7	京大、日亜化学工業（1月17日）	LEDよりどりミドリ、照明多彩に	9.3
	日油、東京農業大学（2月22日）	スギ花粉飛散防ぐ薬剤、4—5年後に実用化	
9	京大、科学技術振興機構（12月21日）	青紫色レーザー、「面発光」で発振、光ディスク容量増へ	9
	キリンファーマ（12月23日）	血小板増やす抗体、治療薬応用めざす	
11	東京工業大学、科技振興機構（2月18日）	新タイプの超電導物質、不向きの鉄含む	8.86
12	東北大学、大阪大学など（12月9日）	感染症菌の増殖防ぐたんぱく質発見、予防薬に期待	8.83
	理化学研究所など（12月26日）	省電力で磁気記録、電流で磁石の向き反転	
14	日立製作所、オプネクスト（2月29日）	光通信向け半導体レーザー、毎秒25ギガ伝送、実験成功	8.8
15	NEC（2月7日）	ミリ波通信向け送受信チップ、シリコン半導体で試作、高出力でも壊れず、価格1／10で実用化へ	8.7
16	理研（1月2日）	ナノサイズ、配線の電流漏れ防ぐ、絶縁技術を開発	8.67
17	北海道大学、浜松ホトニクス、NTTなど（1月15日）	LED、超電導で光20倍強く、量子暗号通信に応用	8.6
	理研など（2月7日）	車用タイヤ、耐久性高める新技術、高温で合成促す触媒	
	東北大、科技振興機構（2月26日）	量子暗号の通信距離伸長	
20	三菱電機（12月12日）	高周波トランジスタ、耐電圧性8倍に向上、次々世代品を開発	8.57

話題性順位（1—5位）

順位	研究開発者（発表日）	成果の概要	評価点
1	国際電気通信基礎技術研究所、科技振興機構など（1月15日）	ロボット、サル脳信号で遠隔操作	2.67
	日油、東京農業大（2月22日）	スギ花粉飛散防ぐ薬剤、4—5年後に実用化	
3	京大（2月15日）	新型万能細胞、がん化しにくく，マウスの胃・肝臓から作製	2.5
4	トヨタ自動車（12月6日）	ロボットで生活支援、家事や高齢者手助け	2.29
	ホンダ（12月11日）	「アシモ」協調、お仕事分担、最適接客、自分で判断	

《調査の方法》大学や企業などの国内研究機関が二〇〇七年十二月から〇八年二月までに公表した研究開発成果を、日本経済新聞社が組織した外部の専門家に評価してもらった。対象とした成果は六十三件。評価の指標は①実用性②市場性③新規性④学術性⑤話題性——の五項目。評価の高い順に三点、二点、一点と採点して平均点を算出し、五項目の平均点を合計して総合順位を決めた。

技術経営を

社長兼研究所長　井上　雅博氏

体制

ース

ティティー

激しい。研究員には「特許はとってね」と、要

書情報の自動判別など、取り組みたいテーマは多い。現状は適任の研究者が見つ

企業が研究開発や技術活用を効率的に行うために「オープン・イノベー

ない研究開発案件の九二%が社内に留保されている。最近急増している大

技術の管理・運用はオープン・ビジネスモデルで行う必要がある。技術

関節リウマチに新薬

東京医科歯科大など開発

骨の破壊と炎症の両方を抑えることができる新たな関節リウマチの治療薬を、東京医科歯科大の高柳広教授と日本ケミファ（東京）などの共同研究チームが開発した。これまでにないメカニズムで、非常に強い効果が期待できるという。1日付の米科学誌「サイエンス」に掲載された。

関節リウマチは、過剰な免疫反応によって関節の骨が破壊され、腫れを伴う炎症が起きる病気。国内の推定患者数は約70万人。現在の治療薬は炎症を抑えるタイプが主流で、骨に対する効果はほとんどないという。

高柳教授らは、骨を分解するときに働く「カテプシンK」というタンパク質分解酵素に着目。この働きを阻害する物質を見つけ、関節リウマチの症状を示すラットに経口投与して効果を調べた。その結果、関節の骨の破壊が予想通りに抑えられただけでなく、周囲の炎症も大幅に軽減されることを確認。遺伝子操作したマウスでメカニズムを詳しく調べたところ、骨の破壊と免疫活性化による炎症の両方を同時に抑えることが分かった。

多発性硬化症などの自己免疫疾患や、骨粗鬆症などにも効果があるとみており、まず多発性骨髄腫を対象に年内に米国で臨床試験を開始する。

2008年2月1日　産経新聞

東京医科歯科大など 関節リウマチ薬候補

骨減少と免疫抑制に効果

東京医科歯科大学の高柳広教授と朝霧成挙講師、日本ケミファなどの研究チームは、関節リウマチや多発性硬化症などの新たな治療薬候補を開発した。骨の減少と免疫の過剰な働きによる炎症の両方を抑制する物質を見つけた。今年中に米企業と協力して米国で臨床試験を始める。二月一日付の米科学誌サイエンスに掲載される。

関節リウマチや多発性硬化症などの自己免疫疾患になると骨の量が減ったり、免疫が過剰に働き炎症を起こしたりする。研究チームは酵素「カテプシンK」が両方の症状を促していることを見つけた。

この酵素の働きを抑える新薬候補物質を試作。関節リウマチのネズミに投与したところ、骨の減少が止まっただけでなく、炎症も抑えられた。カテプシンKには免疫細胞を活性化する働きがあり、新薬候補物質が骨の吸収を抑えるとともに、炎症を抑制したという。

米ベンチャー企業と協力し、多発性骨髄腫の治療薬として臨床試験を計画中。がんが骨に転移する際に骨を壊す症状を抑制できるとみている。

2008年2月1日、日本経済新聞

〔3〕　総合・核心　12版　2008年（平成2

体内で過剰になると、骨粗しょう症や関節リウマチを起こす「破骨細胞」をつくる酵素を、高柳広・東京医科歯科大教授（骨免疫学）らのチームが発見、七日付の米医学誌セルに発表した。人でこの酵素の働きを抑える物質が開発できればこれらの病気の治療薬につながる可能性があるという。

破骨細胞は骨を吸収する役割をしており、骨をつくる骨芽細胞とバランスよく働くことで正常な骨を保っている。

研究チームは破骨細胞で働いている遺伝子を網羅的に解析。「Btk」と「Tec」という二つの酵素をつくる遺伝子の働きが高まっていることを見つけた。

遺伝子を欠いたマウスを作製したところ、破骨細胞がつくられず、骨がすき間なく埋まり強度が低下する「大理石骨病」を発症。研究チームは、二つの酵素が破骨細胞を形成する役割をしていると判断した。二つの酵素の働きを抑える薬剤を、関節リウマチや骨粗しょう症を発症させたマウスに投与したところ、症状が改善したという。

「破骨細胞」つくる酵素発見

骨粗しょう症治療に道

医科歯科大など

東京新聞　2008年3月7日（金）朝刊

MEMO

分子細胞機能学

森田 育男

医歯学総合研究科・顎顔面頸部機能再建学系専攻
分子細胞機能学・教授

1. 研究の課題名

1）血管新生の制御機構の解明及び再生医療への応用

Regulatory mechanism of angiogenesis and application to regenerative medicine

血管新生は、多くの疾患と関係しているが、褥瘡、心筋梗塞、創傷治癒、バージャー病、閉塞性動脈硬化症などは、血管新生を促進することにより治療が可能となる病気であり、一方、固形腫瘍、関節リウマチ、動脈硬化、加齢黄斑変性、糖尿病性網膜症、炎症などは、血管新生を抑制することにより治癒、もしくは改善効果が得られる疾患である。一方、組織移植においては、移植された組織への酸素、栄養の供給のための血管新生が必須とされている。しかし血管促進物質の全身投与によるガン増殖、転移の可能性や炎症の悪化の可能性、また組織移植への応用を考え、局所でのアプリケーションを行うため、印刷技術を応用した全く新しい概念のもとでの血管形成術を考案した。本方法により、自由なパターンの血管をin vitro で作成することが可能となり、この体外で作成した血管を生体内に移植し、血流改善効果が期待できるようになった。さらに、血管内皮細胞前駆細胞を臍帯血、抹消血から単離、増殖することが可能になった。

2）骨形成、骨吸収機構の解明

Bone remodeling and cell communication

骨代謝には骨形成と骨吸収のcouplingが必須であるが、これまでの研究は骨芽細胞による破骨細胞形成に焦点が当てられていた。しかし、骨のリモデリングを考えた場合、骨細胞―骨芽細胞のシグナルおよび、骨芽細胞―破骨細胞のシグナルが重要であることが考えられる。そこで、そのシグナルの解明を行っている。また、従来、当研究室では破骨細胞形成における接着分子の役割に関し多くの研究を行ってきたが、前破骨細胞同士の融合を阻止することにより破骨細胞形成を抑制するnegativeなシグナルに関しての研究は行ってこなかった。そこで、本年度はそれらに関しても研究を行い、接着分子の役割の重要性を報告した。

また、プロスタサイクリンの骨代謝への影響を調べるため、プロスタサイクリン合成酵素欠損マウスにおける骨への影響を調べ、プロスタサイクリンは骨の現象を引き起こすことを明らかにしている。

3）炎症ならびに組織再生のメカニズム

Inflammation under hypoxic conditions（epigenetic control of gene expression）

炎症局所や固形ガンの中心部における低酸素状態は、病態の進展に重要な各種サイトカイン・ケモカインの産生を調節している。しかし、これまでのサイトカインネットワークの構築に関する研究は通常の酸素分圧で行われており、炎症局所を反映していない。この低酸素下のケモカイン産生を担う転写因子はHIF-1だけでなく、NF-κBが重要な役割を果たしているが、我々はクロマチン構造そのものが低酸素における転写調節に重要であることをHDAC阻害剤を用いて明らかにしてきた。そこで、本研究では低酸素による種々のケモカイン産生の調節におけるケモカインのプロモータ領域へのNF-κB/HDACを含むタンパク複合体の結合の重要性を明らかにすることを目的としている。そこで、このタンパク複合体を同定するとともに、低酸素による変動を調べた。このことは、従来の概念とは異なる新しいタイプの抗炎症薬の開発に貢献できるものと期待している。

組織再生に関しては、血小板、網膜、歯根膜の再生を目指して、研究を行っており、ヒト臍帯血からのメガカリオサイトの産生系の確立、羊膜を用いた網膜の再生、および歯根膜組織からの多分化能をもった幹細胞の単離に成功している。

4）ギャップ結合の機序および応用

Life of gap junction

ギャップ結合に関与するコネキシン（Cx）タンパクの役割を解明するため、単にギャップ結合だけではなく、Cxタンパクそのものにも焦点を当て、Cx遺伝子の発現から、コネクソンの構築、細胞膜へのインテグレート、細胞膜での挙動、ヘミチャネル、ギャップ結合に至る過程のタンパクの構造変化、およびリン酸化に伴うギャップ結合の安定化、開閉、役割を終えたギャップ結合の細胞内への取り込み（annular gap形成）、プロテアソーム、リソソームでの分解、再利用など、すべての過程を網羅的に、しかも時間的要素を含めてCxタンパクの一生を明らかにすることにより、各種疾患におけるCxの関与を明らかにすることを目的としている。すなわち、本研究においては分子生物学的手法に加えて、タイムラプス付き共焦点位相差蛍光顕微鏡を用いた光学的手法、免疫電子顕微鏡による微細組織学的手法、およびCx43を膜にインテグレートさせたリポソームなどを用いて、Cx43の四次元解析を可能にし、口腔疾患、特に腫瘍増殖、骨代謝疾患に焦点をあて、Cx43-ギャップ結合の各過程における調節機序を解明し、Cx関与の病態の全貌を明らかにすることを目的としている。また、このようなギャップ結合を外因的に形成させる実験系を確立させるために、Cx43を膜に組み込ませたリポソームを作製した。この系を用いて、ギャップ結合に依存した生理作用と依存しない生理作用とを分けることができ、ギャップ結合やCx研究のさらなる発展のために重要である。また、構築した系を用いて、ギャップ結合の形成そのものがCx43の発現量やトラフィッキングを調節するという仮説の検証を行った。さらに、リポソーム-細胞間のギャップ結合を利用した薬剤導入は新しいDDSとしての大きな可能性を秘めており、是非とも確立したいと考えている。さらに、このCxを人為的に操作することにより、各種疾患の治療に展開していく。

2.

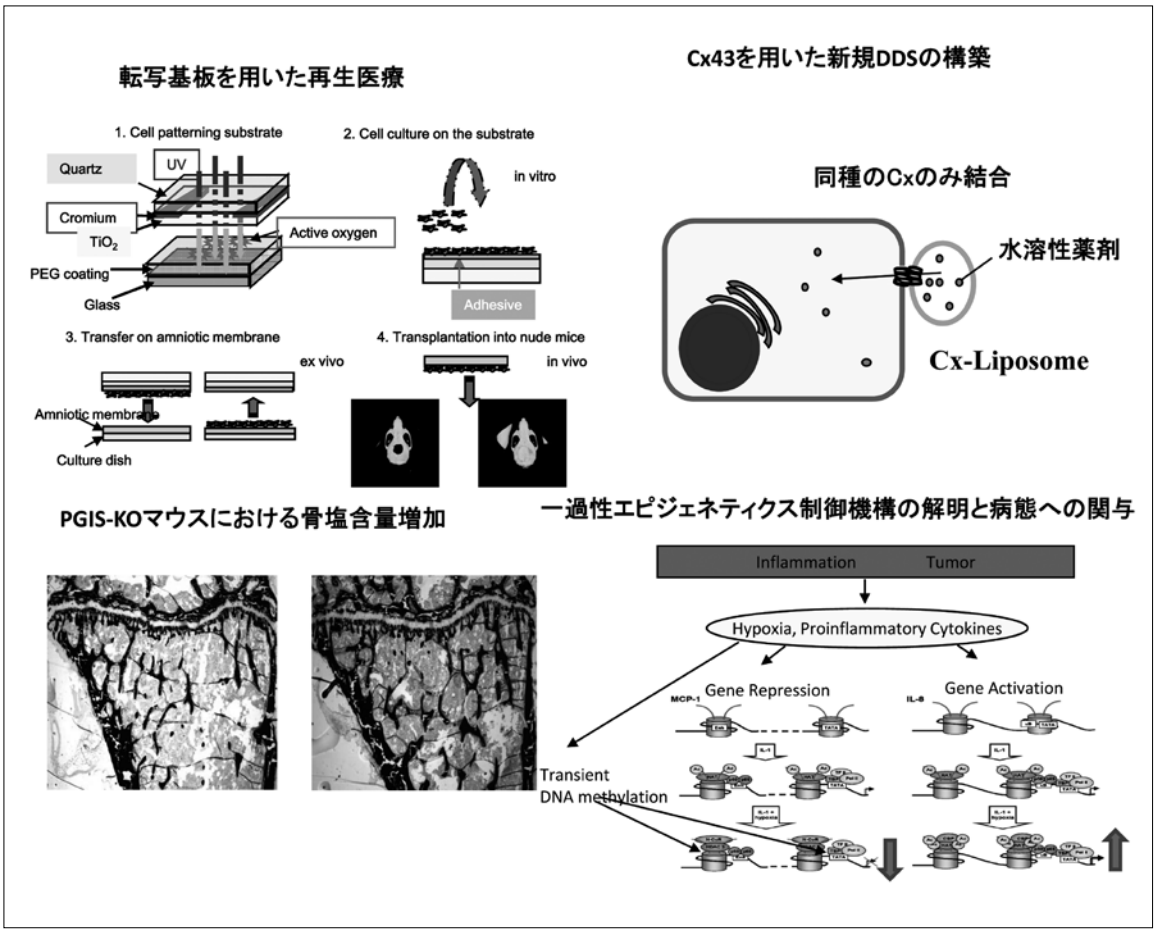

3. 研究内容についての英文要約

Regulatory mechanism of angiogenesis and application to regenerative medicine

The identification of circulating endothelial progenitor cells (EPCs) has revolutionized approaches to cell-based therapy for injured and ischemic tissues. However, the mechanisms by which EPCs promote the formation of new vessels remain unclear. In this study, we obtained early EPCs from human peripheral blood and late EPCs from umbilical cord blood. Human umbilical vascular endothelial cells (HUVECs) were also used. Cells were evaluated for their tube-forming potential using our novel in vitro assay system. Cells were seeded linearly along a 60 μ mwide path generated by photolithographic methods. After cells had established a linear pattern on the substrate, they were transferred onto Matrigel. Late EPCs formed tubular structures similar to those of HUVECs, whereas early EPCs randomlymigrated and failed to form tubular structures. Moreover, late EPCs participate in tubule formation with HUVECs. Interestingly, late EPCs in Matrigel migrated toward pre-existing tubular structures constructed by HUVECs, after which they were incorporated into the tubules. In contrast, early EPCs promote sprouting of HUVECs from tubular structures. The phenomena were also observed in the in vivo model. These observations suggest that early EPCs cause the disorganization of pre-existing vessels, whereas late EPCs constitute and orchestrate vascular tube formation.

Bone remodeling and cell communication

Apicularen A and the known vacuolar-type (H+) -ATPase (V-ATPase) inhibitor bafilomycin A1 induced apoptosis of RAW 264.7 cells, while apicularen B, an N-acetyl-glucosamine glycoside of apicularen A, was far less effective. Apicularen A inhibited vital staining with acridine orange of the intracellular organelles of RAW 264.7 cells, inhibited the ATP-dependent proton transport into inside-out microsome vesicles, and inhibited the bafilomycin A1-sensitive ATP hydrolysis. The IC50 values of the proton transport were 0.58 nM for apicularen A, 13 nM for apicularen B, and 0.95 nM for bafilomycin A1. Furthermore, apicularen A inhibited the bafilomycin A1-sensitive ATP hydrolysis more potently than apicularen B. F-ATPase and P-ATPase were not inhibited by apicularen A. We concluded that apicularen A inhibits V-ATPase, and thus induces apoptosis in RAW 264.7 cells.

Inflammation under hypoxic conditions (epigenetic control of gene expression)

Hypoxia is a microenvironmental pathophysiologic factor frequently associated with tumors and inflammation. This study addresses the question of how hypoxia modulates the basal and IL-1 β -induced production of cytokines and aims to identify the underlying mechanism of hypoxic transcriptional repression. We found that despite the similarities of the promoter structures of IL-8 and MCP-1, these chemokines were differently regulated by hypoxia (an increase in IL-8, but a decrease in MCP-1 mRNA and protein expression). Such differences were not observed in a reporter gene assay, in which both of the promoters were activated by hypoxia. The HDAC inhibitor abolished the inhibitory actions of hypoxia on IL1 β -induced MCP-1 gene expression. Furthermore, hypoxia induced HDAC activity in the nuclear extracts. Collectively, our findings suggest that transiently transfected promoters are not subject to the same NF- κ B regulatory mechanisms as their chromatinized counterparts. NF- κ B, activated by hypoxia, can act as a transcriptional repressor via a mechanism that involves deacetylase activity of HDAC.

4. 本事業に関連して世界的な研究拠点形成に向けて、以下の点で改善・整備等されたこと

A（研究拠点体制）

新たな枠組みにおいて、新しいタイプのDDSと再生医療技術のコラボレーションによる研究が展開されつつある。

C（人材確保）

シャペロンとして若手研究者を確保し、新たな研究を推進することが可能となった。

D（人材育成）

AI-SSとして多くの大学院生を採用し、彼らの育成のためのプログラムの構築を行っている。

5. GCOE事業を推進するに当たって力を入れた点

G-COE事業を円滑に推進するための組織づくり。リーダーにのみ負担がかからなくするため、ステアリング委員会を立ち上げるとともに、事務部門にはG-COE支援室を設置し、教員と事務方が協力してこの事業の推進のために努力しやすい環境づくりに努力した。

6. 英文原著論文

1. Wang J, Ohno-Matsui K, Yoshida T, Shimada N, Ichinose S, Sato T, Mochizuki M, Morita I. Amyloid- β up-regulates complement factor B in retinal pigment epithelial cells through cytokines released from recruited macrophages/microglia; Another mechanism of complement activation in age-related macular degeneration J Cell Phsiol in press
2. Tsuchiya T, Nakahama K, Asakawa Y, Maemura T, Tanaka M, Takeda S, Morita M, Morita The reduction in pigment epithelium-derived factor is a sign of malignancy

in ovarian cancer expressing low-level of vascular endothelial growth factor. Gyncol Endocrinol 25（2）104–109, 2009
3. Hayashi H, Nakahama K, Sato T, Tuchiya T, Asakawa Y, MaemuraT, Tanaka M, Morita I, The role of Mac-1（CD11b/CD18）in osteoclast differentiation induced by receptor activator of nuclear factor- κ B ligand., FEBS Letters, 582（21-22）:3243-3248, 2008
4. Fujimori H, Asahina K, Shimizu-Saito K, Ikeda R, Tanaka Y, Teramoto K, Morita I, Teraoka H. Vascular endothelial growth factor promotes proliferation and function of hepatocyte-like cells in embryoid bodies formed from mouse embryonic stem cells. J. Hepatol,. 48（6）:962-973, 2008
5. Wang J, Ohno-Matsui K, Yoshida T, Kojima A, Shimada N, Nakahama K, Safranova O, Iwata N, Saido TC, Mochizuki M, Morita I.Altered function of factor I caused by amyloid beta: implication for pathogenesis of age-related macular degeneration from Drusen. J Immunol. 181（1）:712-720、2008.
6. Kaneda M, Zhang D, Bhattacharjee R, Nakahama K, Arii S, Morita I. Vitamin K（2）suppresses malignancy of HuH7 hepatoma cells via inhibition of connexin 43. Cancer Lett, 263（1）: 53-60, 2008.
7. Mukai N, Akahori T, Komaki M, Li Q, Kanayasu-Toyoda T, Ishii-Watabe A, Kobayashi A, Yamaguchi T, Abe M, Amagasa T, Morita I. A comparison of the tube forming potentials of early and late endothelial progenitor cells. Exp Cell Res, 314（3）: 430-440, 2008.
8. Kojima A, Nakahama K, Ohno-Matsui K, Shimada N, Mori K, Iseki S, Sato T, Mochizuki M, Morita I. Connexin 43 contributes to differentiation of retinal pigment epithelial cells via cyclic AMP signaling. Biochem Biophys Res Commun, 366（2）: 532-538, 2008.
9. Huang, C, Wang J, Kikkawa U, Mukai H, Shen M, Morita I, Chen B, Chang WC, Calcineurin-mediated dephosphorylation of c-Jun Ser-243 is required for c-Jun protein stability and cell transformation. Oncogene, 27（17）:2422-2429, 2008
10. Pluemsampant S, Safronova O, Nakahama K, Morita I. Protein kinase CK2 is a key activator of histone deacetylase in hypoxia-associated tumors. Int J Cancer, 122（2）: 333-341, 2008

7. 著書

森田育男、小野寺光江.COX-2阻害薬の位置づけ.NSAIDsを知る・使いこなす/徹底分析シリーズ.LISA 15（7）:666-673, 2008

8. 特許取得、特許申請

国内出願

発明の名称:人工細胞組織の作成法、及びそのための基材
（特許第4247231）
発明者:森田育男、中村真人、服部秀志、三宅秀之、小林弘典、栗原正彰
出願人:森田育男、中村真人、大日本印刷株式会社
登録日:平成21年（2009）年1月16日

国際特許

オーストラリア
発明の名称:人工細胞組織の作成法、及びそのための基材
発明者:森田育男、中村真人、服部秀志、三宅秀之、小林弘典、栗原正彰
出願人:森田育男、中村真人、大日本印刷株式会社
特許登録:平成20年（2008）年1月24日（特許番号2004282462）

韓国
発明の名称:人工細胞組織の作成法、及びそのための基材
発明者:森田育男、中村真人、服部秀志、三宅秀之、小林弘典、栗原正彰
出願人:森田育男、中村真人、大日本印刷株式会社
特許登録:平成20年（2008）年5月20日（特許番号832286）

9. 自己評価

大学院教育改革など大学業務が忙しく、なかなか研究に時間を割くことができないが、本G-COEに関しては、その立案の段階から関与させていただき、それなりに努力はしてきた。しかし、依然として、問題点がないわけではなく力不足を感じている。

10. 学会発表（英文）

1. Makoto Keneda. Research Presentations. Connexin-interated Liposomes: A Novel Tool for Drug Delivery into Mammalian Cells. Officially approved by UK-Japan 2008, Anglo-Japanese Symposium: Network for International Education and Research in Advanced Dental Sciences, Tokyo, Japan, February 4, 2008. UK-Japan 2008公認イベント、先端国際教育研究ネットワーク「日・英シンポジウム」、東京、2008年2月4-5日

2. Yoshida T, Komaki M, Morita I, Abe M. Ex vivo formation of capillary structures by human adipose tissue-derived microvascular endothelial cells. 15th International Vascular Biology Meeting, Sydney, Australia, 1-5 June 2008.
3. Akahori T, Mukai N, Komaki M, Abe M, Morita I. Evolution of Engineered capillary network developed by innovative printing technique. 15th International Vascular Biology Meeting, Sydney, Australia, 1-5 June 2008
4. Nakahama K, Hayashi H, Sato T, Morita I. The role of Mac-1 (CD11/CD18) in osteoclast differentiation induced by receptor activator of nuclear factor-κB ligand (RANKLE). 48th The American Society for Cell Biology Annual Meeting, San Francisco, USA, December 13-17, 2008
5. ◎Bhattacharjee R, Kaneda M, Nakahama K, Morita I. Phosphatidylinositol 3-kinase akt regulates connexin43 expression through mRNA stability osteoblasts. 48th The American Society for Cell Biology Annual Meeting, San Francisco, USA, December 13-17, 2008

11. 学会発表（和文）

1. 吉田朋子、小牧基浩、森田育男、安部まゆみ.ヒト脂肪組織由来血管内皮細胞を用いたex vivoによる血管構築.第39回血管研究会.東京.2008年5月15日
2. 津川順一、小牧基浩、中浜健一、天笠光雄、森田育男.印刷技術を用いて羊膜に転写した骨芽細胞による骨再生療法.ポスター演題.第26回日本骨代謝学会学術集会.大阪.2008年10月29-31日
3. 林 秀隆、中浜健一、森田育男.破骨細胞形成におけるMac-1,（CD11b/CD18）の役割について.ポスター演題.第26回日本骨代謝学会学術集会.大阪.2008年10月29-31日
4. 小牧基浩、津川順一、中浜健一、森田育男.歯根膜細胞の骨芽細胞分化におけるCP23発現の検討.第26回日本骨代謝学会学術集会.大阪.2008年10月29-31日
5. 青井陽子.低酸素がサイトカイン産生に及ぼす影響とその機序.平成20年度先端歯学国際教育ネットワーク.三浦.2008年10月20-21日
6. 吉田朋子、小牧基浩、森田育男、安部まゆみ.Role of sphingosine 1-phosphate in engineering of capillary network constituted of human omental microvascular endothelial cells. 第16回日本血管生物医学会, 金沢、2008年12月3-5日
7. 滝 敦子、安部まゆみ、奥起久子、水谷修紀、森田育 男 . Expression of angiogenesis-related factors in placenta and umbilical vessels in complicated pregnancies. 第16回日本血管生物医学会, 金沢、2008年12月3-5日
8. Chalida N, Yokoyama C, Miura H, Alles NR, Aoki K, Ohya k, Morita I. Roles of prostacyclin on bone metabolism. 一般口頭発表・ポスター.第31回日本分子生物学会年会・第81回日本生化学会大会合同大会.神戸.2008年12月9-12日
9. Aoi Y, Safronova O, Nakahama K, Morita I. The involvement of DNA and histone methylation in the repression of IL-1beta-induced MCP-1 production by hypoxia. 一般口頭発表・ポスター.第31回日本分子生物学会年会・第81回日本生化学会大会合同大会.神戸.2008年12月9-12日
10. Kato K, Morita I. Analysis of accelerated osteoclast formation by metabolic acidosis. ポスター.第31回日本分子生物学会年会・第81回日本生化学会大会合同大会.神戸.2008年12月9-12日
11. 豊田淑江、石井明子、鈴木浩子、李 勤、田村悦臣、森田育男、山口照英.血管内皮前駆細胞（EPC）であるEarly EPCとOutgrowth Endothelial Cellの特性解析.ポスター.第31回日本分子生物学会年会・第81回日本生化学会大会合同大会.神戸.2008年12月9-12日

12. 受賞

青井陽子:G-COE　DC-1
平成20年度先端歯学国際教育ネットワークサマースクール最優秀賞.2008年10月20-21日

13. 外部資金の獲得状況

（科学研究費補助金、受託研究費、外部財団の助成など）

1）科学研究費補助金、基盤研究（B）
研究題目:コネキシン43を介した組織の高次機能恒常性機構の解明
代表:森田育男
期間:平成20年-平成22年
研究費総額:1460万円

2）科学研究費補助金、萌芽研究
研究題目:転写技術を応用した歯槽骨再生医療法の開発
代表:森田育男
期間:平成20年—平成21年
研究費総額:320万円

3）特別研究員奨励費（DC1）

研究課題　低酸素下におけるサイトカイン産生変動機序-メチル化の関与
代表:青井陽子
期間:平成20年-平成22年
研究費総額:180万円

4）共同研究費
研究課題:ナノテクノロジーを応用した再生医療および薬物導入技術の開発とその応用
代表:森田育男
期間:平成17年-平成22年
研究費総額:1500万円

5）共同研究費
研究課題:天然物由来生体機能性分子の探索および多成分系による多変量解析に基づく有効性・安全性の網羅的解析技術の開発とその応用
代表:森田育男
期間:平成17年-平成20年
研究費総額: 500万円

6）寄附講座
ナノメディスン（DNP）
代表:森田育男
期間:平成17年-平成22年
研究費総額:27500万円

14. 特別講演、招待講演

1. 森田育男.講演.東京医科歯科大学での幹細胞臨床研究・倫理審査の試み（1）.セッション1・演題1.第38回全国医学系大学委員会連絡会議　国際シンポジウム.第38回全国医学系大学委員会連絡会議事務局　東京医科歯科大学生命倫理研究センター.東京.2008年1月25日
2. 森田育男.特別講演.慶応大学.東京.2008年4月14日
3. 森田育男.特別講演.NHRI.（National Health Research Institute）. Taiwan, R.O.C. May 7-10, 2008
4. 森田育男.招待講演.広島大学.2008年9月10日
5. 森田育男.講演.日本血管生物医学会プレスセミナー.東京.2008年9月24日
6. 森田育男.公開模擬授業.血管新生の調節と再生医療への新展開.お茶の水祭.東京.2008年10月18日

15. 主催学会

6th Korea-Japan Joint Symposium on Vascular Biology、2008年12月4,5日　石川県立音楽堂、金沢

16. サマリー

再生医療において、血管再生は2つの意義を持っている。一つは、虚血部位への栄養・酸素補給で、直径6mm以上の大血管に関しては人工血管、直径1~3mm程度の血管に関してはバイパス手術を、それ以下の血管に関しては自己再生力に任せるという方法が取られてきた。具体的には骨髄や末梢血由来の単核細胞の局所移入、VEGF, HGF, b-FGF遺伝子・タンパクの局所注射が行なわれている。しかし、このような細胞などの移入は、その有効性のばらつき、効果が現れるまでの時間および移入された細胞が実際に血管を構築するかなどの問題を抱えている。もう一つは、移植した組織への栄養・酸素供給のための血管の新生である。そのためには血管網を生体外で作成し、直接体内に移植する方法が考えられる。我々はこの2つを同時にクリアーできる方法として、in vitroでパターニングした血管内皮細胞をマトリクスに転写することにより毛細血管を構築する系を考案した。すなわち、1）光触媒を用いた独自の親疎水パターン形成技術を応用し培養基板を作成する。2）血管内皮細胞をデザインされた基板上に培養後、高気圧で脱細胞化した羊膜に接触させることで毛細血管構造物を形成し、基盤の剥離により基質側に転写する。3）羊膜上に作成した管腔をマウスに移植し、血流回復、機能回復を調べる。次に用いるべき細胞の選択に移り、大網由来血管内皮細胞を用いるための方法論、臍帯血、自己血より血管内皮細胞を単離・培養する系を確立した。その結果、自己の末梢血を用いた血管再生が可能となり、今後の再生医療への応用が期待される。

17. 講座の准教授、講師、助教、特別研究員、ポスドク、指導を受けた大学院生の名前（AISSには○印）のリスト

准 教 授　中浜健一
助　　教　加藤幸太郎
特任教授　横山知永子
特任助教　Olga Safronova
特任助教　穐山雅子（11月以降）
大学院生
○Bhattacharjee Rajib、
○青井陽子
Praween Wayakanon（10月～）
○Wanida Techawattanawisal
○Nakalekha Chalida
○元 吉鐘

○津川順一
滝 敦子
大島乃里子
土屋雄彦
李 勤
李 香蘭
輿石太郎

寄付講座　ナノメディスン（DNP）
教　授　安部まゆみ
助　教　小牧基浩
助　教　吉田朋子
寄付講座　生体機能性分子探索学講座
准教授　佐藤孝浩
助　教　穐山雅子（11月まで）

EXPERIMENTAL CELL RESEARCH 314 (2008) 430–440

available at www.sciencedirect.com

ScienceDirect

www.elsevier.com/locate/yexcr

Research Article

A comparison of the tube forming potentials of early and late endothelial progenitor cells

Nana Mukai[a,b,c], *Taichi Akahori*[a], *Motohiro Komaki*[d], *Qin Li*[a], *Toshie Kanayasu-Toyoda*[e], *Akiko Ishii-Watabe*[e], *Akiko Kobayashi*[a], *Teruhide Yamaguchi*[e], *Mayumi Abe*[d], *Teruo Amagasa*[b], *Ikuo Morita*[a,c,*]

[a]*Department of Cellular Physiological Chemistry, Graduate School, Tokyo Medical and Dental University, Japan*
[b]*Department of Maxillofacial Surgery, Graduate School, Tokyo Medical and Dental University, Japan*
[c]*21st Century COE, Tokyo Medical and Dental University, Japan*
[d]*Department of Nanomedicine (DNP), Graduate School, Tokyo Medical and Dental University, Japan*
[e]*Division of Biological Chemistry and Biologicals, National Institute of Health Sciences, Japan*

ARTICLE INFORMATION

Article Chronology:
Received 1 February 2007
Revised version received
9 November 2007
Accepted 14 November 2007
Available online 20 December 2007

Keywords:
Early endothelial progenitor cells
Late endothelial progenitor cells
Tube-forming activity
Endothelial cells
Human umbilical endothelial cells
Mononuclear cells

ABSTRACT

The identification of circulating endothelial progenitor cells (EPCs) has revolutionized approaches to cell-based therapy for injured and ischemic tissues. However, the mechanisms by which EPCs promote the formation of new vessels remain unclear. In this study, we obtained early EPCs from human peripheral blood and late EPCs from umbilical cord blood. Human umbilical vascular endothelial cells (HUVECs) were also used. Cells were evaluated for their tube-forming potential using our novel *in vitro* assay system. Cells were seeded linearly along a 60 μm wide path generated by photolithographic methods. After cells had established a linear pattern on the substrate, they were transferred onto Matrigel. Late EPCs formed tubular structures similar to those of HUVECs, whereas early EPCs randomly migrated and failed to form tubular structures. Moreover, late EPCs participate in tubule formation with HUVECs. Interestingly, late EPCs in Matrigel migrated toward pre-existing tubular structures constructed by HUVECs, after which they were incorporated into the tubules. In contrast, early EPCs promote sprouting of HUVECs from tubular structures. The phenomena were also observed in the *in vivo* model. These observations suggest that early EPCs cause the disorganization of pre-existing vessels, whereas late EPCs constitute and orchestrate vascular tube formation.

© 2007 Elsevier Inc. All rights reserved.

Introduction

In healthy individuals, endothelial cells are rarely found in the blood. However, mature endothelial cells can be found in the circulation following detachment from injured vessels. For example, circulating endothelial cells substantially increase in a wide variety of pathological conditions associated with profound vascular insult. Therefore, circulating endothelial cells are a useful marker of vascular damage [1,2]. Endothelial progenitor cells (EPCs), derived from bone marrow, are also found in the circulation and are involved in tumor vasculogenesis and wound healing

* *Corresponding author*. Department of Cellular Physiological Chemistry, Graduate School, Tokyo Medical and Dental University, Japan, 1-5-45 Yushima, Bunkyo-ku, Tokyo, 113-8549, Japan. Fax: +81 3 5803 0212.
E-mail address: morita.cell@tmd.ac.jp (I. Morita).

0014-4827/$ – see front matter © 2007 Elsevier Inc. All rights reserved.
doi:10.1016/j.yexcr.2007.11.016

[3,4]. The discovery of EPCs in human blood has led to a new paradigm in which vasculogenesis and angiogenesis occur in adult tissues [5]. These results have suggested a potential new approach to the treatment of cardiovascular and ischemic diseases. Preclinical studies have shown that transplantation of human EPCs to nude mice with hind limb ischemia improved blood flow recovery and capillary density resulting in a significant reduction in the rate of limb loss [5–10]. Clinical trials using autologous EPC transplantation have already been performed and significant improvements have been observed in myocardial function and ischemic diseases [11–15]. The strict roles of EPCs in neovascularization are not well understood because various populations of cells with varying differentiation potentials were transplanted.

EPCs consist of two different subpopulations, termed early and late EPCs [16–18]. Although both EPCs are derived from mononuclear cells (MNC) and express endothelial cell markers, they have different morphologies and growth patterns [18,19]. Early EPCs exhibit a spindle-like morphology and the majority of them are derived from CD14(+) subpopulations [16,19–21]. Late EPCs, named after their late outgrowth potential, exhibit a cobblestone morphology and are derived from CD14(−) fractions [17,19]. These two populations have been characterized for production of vascular endothelial growth factor (VEGF), VEGF receptor expression, cytokine secretion, and tube forming activity *in vitro* and *in vivo* [19].

Using photo-catalytic lithography, we have developed a new cell culturing technology for capillary engineering [22]. In this approach, endothelial cells are patterned on a substrate and then transferred to Matrigel. The endothelial cells change their morphology and form tubular vessels as confirmed by electron microscopy and dye microinjection. In the present study, using this novel technology, we focused on the tube-forming activity of early and late EPCs. In addition, we asked whether EPCs were incorporated into preexisting tubular structures.

Materials and methods

Human samples

Human peripheral blood was provided by 7 healthy human volunteers. Human umbilical cords and cord bloods were obtained from 12 healthy newborns. Informed consent was obtained from all donors, and samples were handled according to the tenets of the Declaration of Helsinki, with the approval of university review boards.

Cell isolation

Blood was diluted 1:1 with PBS containing 2 mM EDTA, and overlayed on Lymphoprep (AXIS-SHIELD, Oslo, Norway). Cells were centrifuged at 1100×*g* for 10 min. The resulting mononuclear cells (MNC) were collected and washed three times in PBS. Human umbilical vein endothelial cells (HUVECs) were isolated enzymatically.

Cell culture

Isolated MNC were resuspended in endothelial basal medium-2 (EBM-2) (Clonetics, San Diego, CA) supplemented with the EGM-2 bullet kit (Clonetics), plated on culture dishes precoated with human fibronectin (Sigma, Saint Louis, MO), and maintained in the medium. To obtain early EPCs from peripheral blood MNC and cord blood MNC, medium was changed every 2 days, and after 5 to 7 days of culture, early EPCs were isolated. Late EPCs were obtained from cord blood as previously described by Gulati et al. [17]. Medium was then changed daily for 7 days and on alternate days thereafter. The characteristic colonies of late EPCs were observed under a phase-contrast microscopy (IMT-2; Olympus Optical, Tokyo, Japan) and these cells were cloned by colony isolation. HUVECs were used at passages 1–3.

Cell characterization

Early and late EPCs were seeded onto a chamber slide glass (Nalge Nunc, Naperville, IL) coated with fibronectin (Sigma) and fixed in 4% paraform aldehyde (PFA) next day. Immunocytochemistry was performed using PE-conjugated anti-human CD31 antibody (555446; BD Pharmingen, San Diego, CA; diluted 1:50) and primary antibodies against human VEGFR2, (sc-6251; Santa Cruz Biotechnology, Santa Cruz, CA; 2 μg/ml) or von Willebrand factor (vWF) (M0616; Dako, Glostrup, Denmark; 1.2 μg/ml), followed with Alexa 488-conjugated anti-mouse IgG (A-11029; Molecular Probe, Leiden, Netherlands; 2 μg/ml). Non-immune mouse IgG_1 (sc-3877; Santa Cruz; diluted 1:100) was used as a control. Cell nuclei were stained with 1 μg/ml of To-Pro3 (T3605; Molecular Probe). Samples were observed and photographed under a laser confocal microscope (LSM510META; Carl-Zeiss, Jena, Germany).

Flow cytometric analysis of CD14, CD31, CD45 and VEGFR2 expression in early EPCs and late EPCs

Cells were collected non-enzymatically using Cell Dissociation Buffer (Invitrogen Corp, San Diego, CA) and labeled with FITC-conjugated anti-CD45 monoclonal antibody (Beckman Coulter, Marseilles, France), FITC-conjugated anti-CD31 monoclonal antibody (Pharmingen) and anti-VEGFR2 monoclonal antibody (Santa Cruz Biotechnology) at 4 °C for 30 min. Cells incubated with anti-VEGFR2 monoclonal antibody were subsequently stained with PE-conjugated anti-mouse IgG antibody at 4 °C for 30 min. After washing with PBS containing 1% BSA, flow cytometric analysis was performed with a FACS Calibur (Becton-Dickenson, NJ).

Photo-mask preparation

STK-03 titanium dioxide (TiO_2) photo-catalyst aqueous dispersion (Ishihara Sangyo; Osaka, Japan) was diluted to 33 wt.% with isopropyl alcohol, stirred for 1 h and filtered using a 3.0 μm pore size polytetrafluoroethylene filter (Advantec, Tokyo, Japan). Cr-Quartz photo-masks with slit width 60 μm and slit interval 300 μm were cleaned using a VUM-3184 UV-ozone washing machine (Oak Manufacturing, Tokyo, Japan) to

decompose low molecular weight adsorbents on the mask surface. The mask was coated with the TiO_2 dispersion by spin-coating at ~700 rpm for 15 s and then baking at 150 °C for 10 min.

Substrate preparation

NA35 polished glass substrates (NH Techno Glass, Yokohama, Japan) were cleaned using the VUM-3184 for 420 s. Next, 1.5 g of heptadecafluorodecyltrimethoxysilane solution (TSL-8233; GE Toshiba Silicone, Tokyo, Japan), 5.0 g of tetramethoxysilane solution (TSL-8114; GE Toshiba Silicone), and 2.4 g of 0.005 N HCl were mixed and stirred for 24 h at room temperature to make fluoro-alkyl-silane (FAS) mixture solution. The mixture was diluted with 1 wt.% isopropyl alcohol, stirred for 15 min, filtered by Chromato-Disc (filter type 0.45 μm; Kurabo) and then coated onto the glass substrate by spin-coating at ~1000 rpm for 15 s. The FAS-coated substrate was then baked at 150 °C for 10 min.

Surface modification and patterning

Both TiO_2-coated photo-masks and FAS-coated substrates were immersed and sonicated in deionized water for more than 5 min, and then baked at 120 °C for 5 min. The TiO_2-coated side of the photo-mask was irradiated with UV for 15 min at irradiation energy of ~30 J/cm^2 to rejuvenate the photo-catalytic activity of TiO_2. The FAS-coated side of the glass substrate was placed facing and in contact with the TiO_2 layer of the photo-mask and UV-irradiated for several minutes through the mask to form hydrophilic regions on the FAS layer.

Cell patterning

Prior to cell seeding, glass substrates were placed on cell culture dishes. The cells were trypsinized and suspended, and labeled with PKH26 Red (Sigma) according to the manufacturer's instructions. Cells were counted, seeded on the substrates, and incubated for 18 h at 37 °C. A total of 2×10^5 cells were seeded per substrate. During incubation, cells in hydrophobic areas moved to hydrophilic areas.

Transplant to matrigel

The patterned cells on the substrate were turned over onto Matrigel (Becton Dickinson, Bedford, TX) and incubated with the culture medium containing 0.2% FBS for 24 h. When the substrate was removed, the cells were transferred from the substrate to the Matrigel.

Observation of the tube formation

Firstly, the pattern of cells on Matrigel was observed by a phase-contrast microscopy (IMT-2; Olympus Optical). Next, live cells which formed tubular structures were labeled with 500 ng/ml Calcein-AM (Molecular Probes) for 30 min in 37 °C, and three-dimensional structures of capillaries were analyzed by a laser confocal microscope. Furthermore, the engineered capillaries on Matrigel were fixed with 4% PFA and stained with 4 μg/ml of anti-human VE-cadherin rabbit polyclonal antibody (210-232-c100; ALEXIS, San Diego, CA), followed by 4 μg/ml of Alexa 488-conjugated anti-rabbit IgG (Molecular Probe). Capillaries were observed by a laser confocal microscope.

EPC incorporation into tube-like structure

Early and late EPCs were pre-labeled with PKH26 Red, mixed with unlabeled HUVECs, and seeded on the substrate. Twenty-four hours after transplant to Matrigel, the cells were labeled with Calcein-AM, the fluorescence of EPCs and HUVECs were analyzed by a laser confocal microscope.

To quantify EPC incorporation into tube-like structure, early and late EPCs were pre-labeled with PKH26 Green. These cells were mixed with HUVECs which were pre-labeled with PKH26 Red, and cultured on the substrate. The fluorescence of EPC and HUVECs was analyzed by a fluorescence microscopy (BZ-8000; Keyence, Osaka, Japan). The incorporation ratio of EPCs into the tube structure was calculated by the cellular area of EPC (μm^2)/mm of tube structure.

In vivo angiogenesis assay

We developed an ear vessel occlusion model for an *in vitro* angiogenesis assay. After occlusion of the murine auricular vessel, cells were introduced into the subcutaneous pocket below the occlusion point, and newly formed vessels were analyzed. Twelve hours before the cell injection, the mice were anesthetized with an intraperitoneal injection of pentobarbital (50 mg/kg) and auricular vessels were occluded. Collateral circulation was observed under a stereomicroscope (LEICA Mz9, Leica Microsystems, Wetzlar, Germany). Early or late EPCs were labeled with PKH26 and suspended in growth media, and 5×10^4 of each EPCs were subcutaneously injected into the occluded pinna within 12 h of vessel occlusion. Forty-eight hours after the cell injection, the mice were given 250 μg of *Banderiaea simplicifolia* lectin 1 (BS1-lectin) (Vector Laboratories, Burlingame, CA) intravenously and sacrificed 45 min later. Sections (4-μm thickness) of cell-transplanted pinna were made for histological observation. This experiment was performed using 7-week nude mice and all procedures were carried out with the full approval of the ethical committee of Tokyo Medical and Dental University.

Calculations and statistical analysis

The statistical significance of differences in the data was evaluated by use of analysis of Welch's *t*-test or Student *t*-test. A value of $P<0.05$ was accepted as statistically significant.

Results

Characterization of two types of EPCs

MNC were harvested from human peripheral blood of healthy individuals or from cord blood and seeded on fibronectin-coated dishes. Following 5 to 7 days of cultivation, adherent cells were observed in clusters. The cells exhibited a spindle-

like shape (Fig. 1A, left) and displayed several endothelial cell markers including CD31. vWF and VEGFR2 (Fig. 1B, left). When MNC were isolated from human cord blood, early EPCs were also observed after 3 days of cultivation. Their morphology and expression of endothelial markers used here were almost the same as those of early EPCs derived from peripheral blood (data not shown). They proliferated and thereafter gradually disappeared over the next 1 week.

After early EPCs had disappeared, colonies with different morphology emerged over 12–21 days of cultivation. They exhibited a cobblestone morphology, spindle-like shape (Fig. 1A, right) and displayed several endothelial cell markers such as CD31, vWF and VEGFR2. Also, eNOS expression was observed in both early and late EPCs (data not shown). Thus, these cells were late EPCs as reported by Hur et al. [18]. To characterize two types of EPCs, we carried out a flow

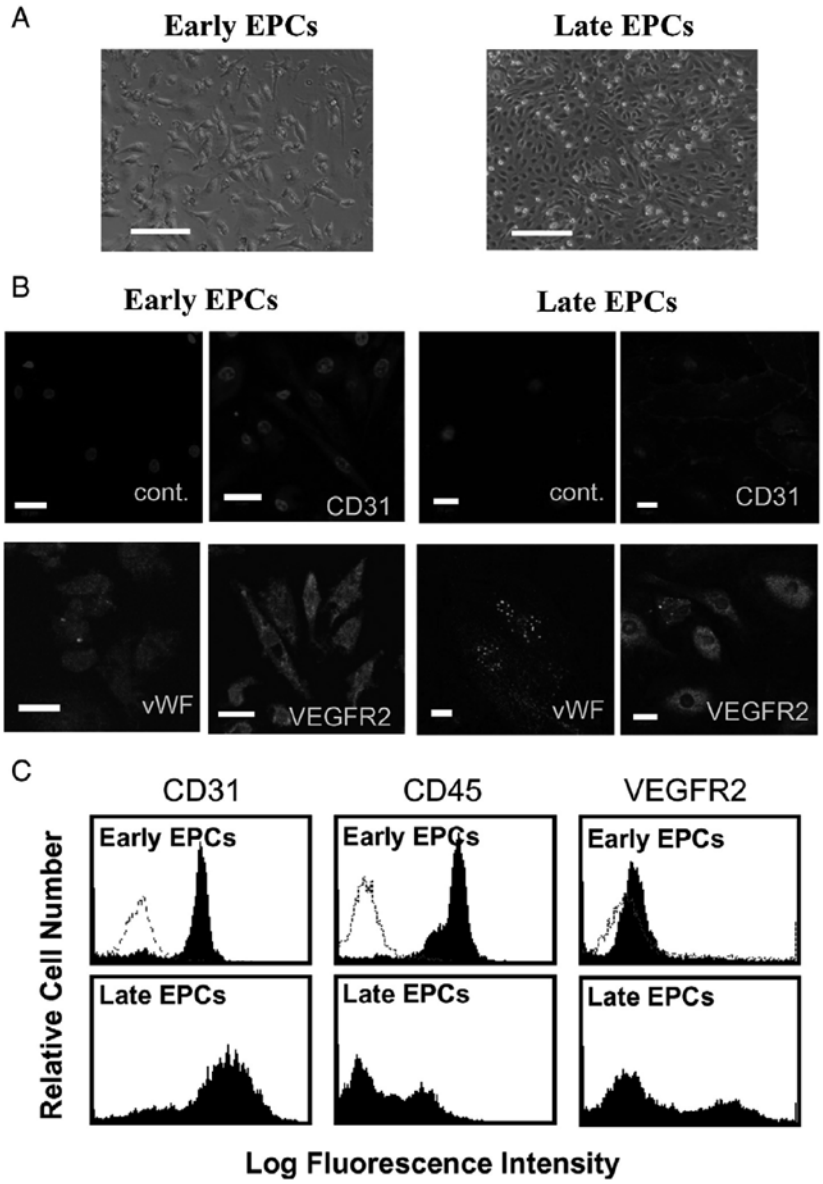

Fig. 1 – Morphological and immunophenotypical characterization of early and late EPCs. (A) Early EPCs cultured for 7 days and late EPCs cultured for 14 days. Scale bar=100 μm. (B) Immunocytochemistry of CD31, vWF and VEGFR-2 was demonstrated. Scale bar=20 μm. Shown are representative data from 7 independent experiments using early EPCs isolated from different peripheral blood and 7 independent experiments using late EPCs isolated from different cord blood with similar results. (C) Flow cytometric analysis of CD31, CD45 and VEGFR2 expression in early EPCs and late EPCs. Shown are representative data from 5 independent experiments using early EPCs and late EPCs isolated from different cord blood with similar results. Isotype controls are overlaid in a dot line on each histogram for each surface antigen tested.

cytometric analysis of CD31, CD45 and VEGFR2 expression in early EPCs and late EPCs derived from cord blood (Fig. 1C). Similar to the immunocytochemical staining, the expression of CD45 in late EPC was weaker than that in early EPCs, while VEGFR2 expression in late EPCs was stronger than that in early EPCs. CD14 expression was observed only in early EPCs (data not shown).

Tubular structures could be constructed by late EPC, but not by early EPC

To assess the tube-forming activities of early and late EPCs, both cell types were analyzed by a novel method which promoted capillary formation *in vitro*. Early EPCs, late EPCs and HUVECs were distributed linearly on a specific substrate

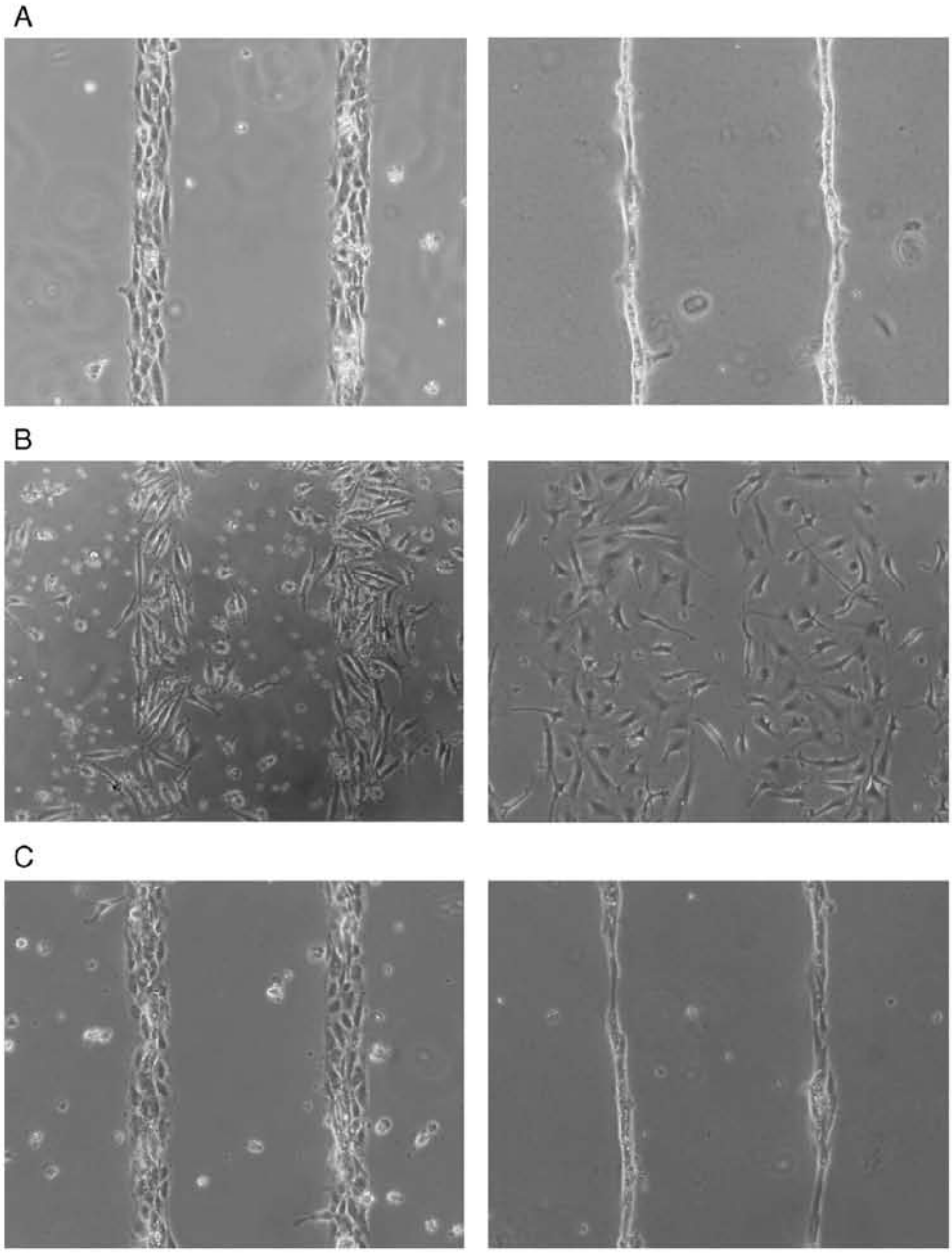

Fig. 2 – Tube forming activities in early and late EPCs compared with HUVECs. Cells (2×10^5) were seeded on the glass substrate and cultured for 18 h (A–C, left), then transplanted to Matrigel. Twenty-four hours after transplantation (right), HUVECs formed tubular structures (A). Early EPCs spread on Matrigel and did not form tubular structures (B). Late EPCs formed tubular structures (C).

(Fig. 2, left) and were subsequently transferred to Matrigel (Fig. 2, right). During the transfer of patterned cells to Matrigel, HUVECs changed cellular morphology to form capillary-like structures. Twenty-four hours after cell transfer, the substrate was removed and tubular structures were readily observed by a light microscopy (Fig. 2A). Electron microscopic observation revealed that the luminal structure consisted of four to five HUVECs [22]. In contrast, linearly arrayed early EPCs did not form tubular structures (Fig. 2B). The time course of tube formation in late EPCs was quite similar to that in HUVECs (Fig. 2C).

After HUVECs or late EPC were loaded with calcein-AM, the tubular structures were assessed with a laser confocal microscope. The luminal structure formed by late EPCs was observed as well as that by HUVECs (Figs. 3A, B). When tubes formed by HUVECs and late EPCs were stained for VE-

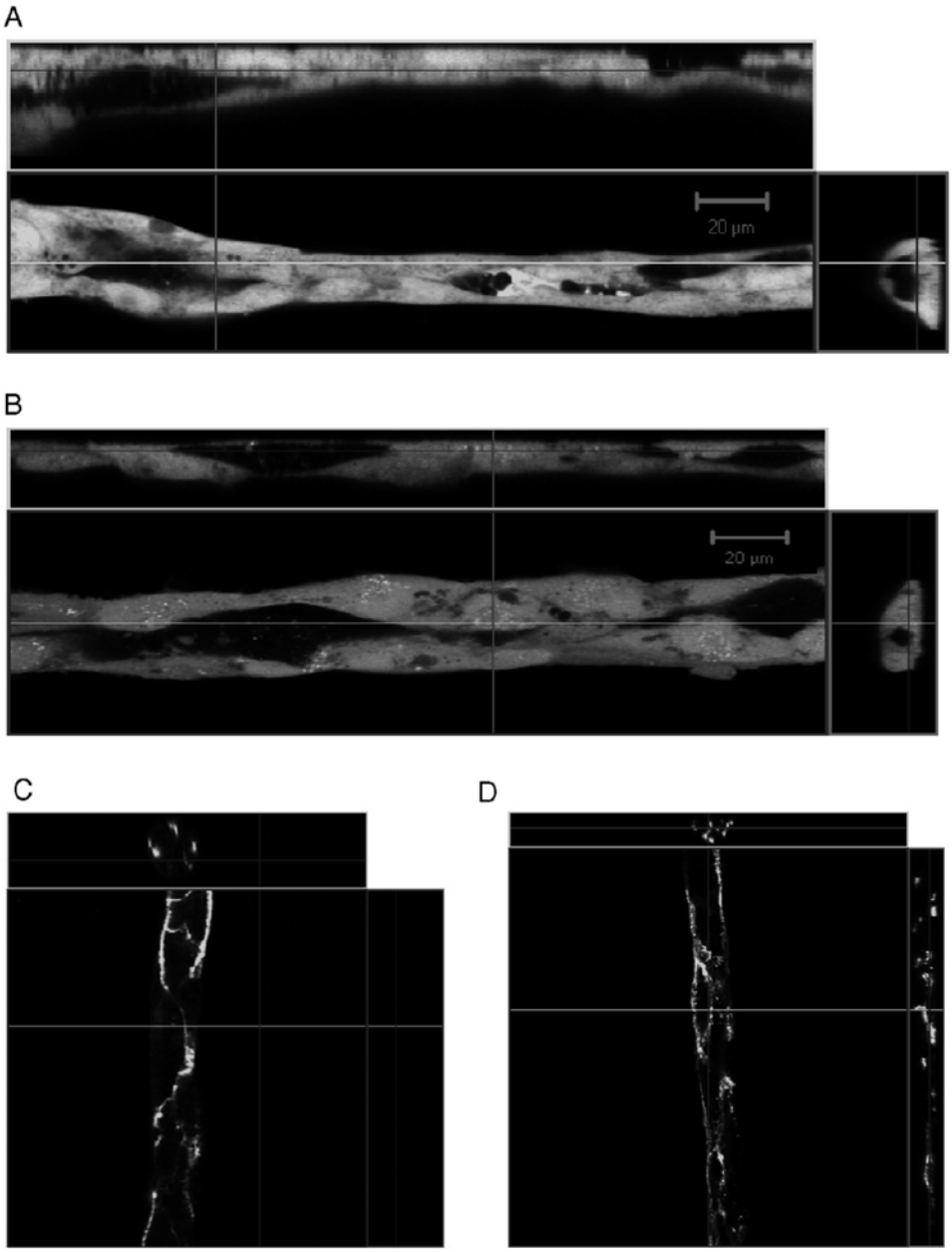

Fig. 3 – Three-dimensional images of tubular structures formed by HUVECs and late EPCs. Tubular structures formed by HUVECs (A) and late EPCs (B) were stained with calcein-AM. The luminal structure was observed with a laser confocal microscope. Scale bar=20 μm. Immunostaining of HUVEC (C) and late EPCs (D) tubular structures with anti-VE-cadherin. The localization of VE-cadherin was observed at cell–cell junctions.

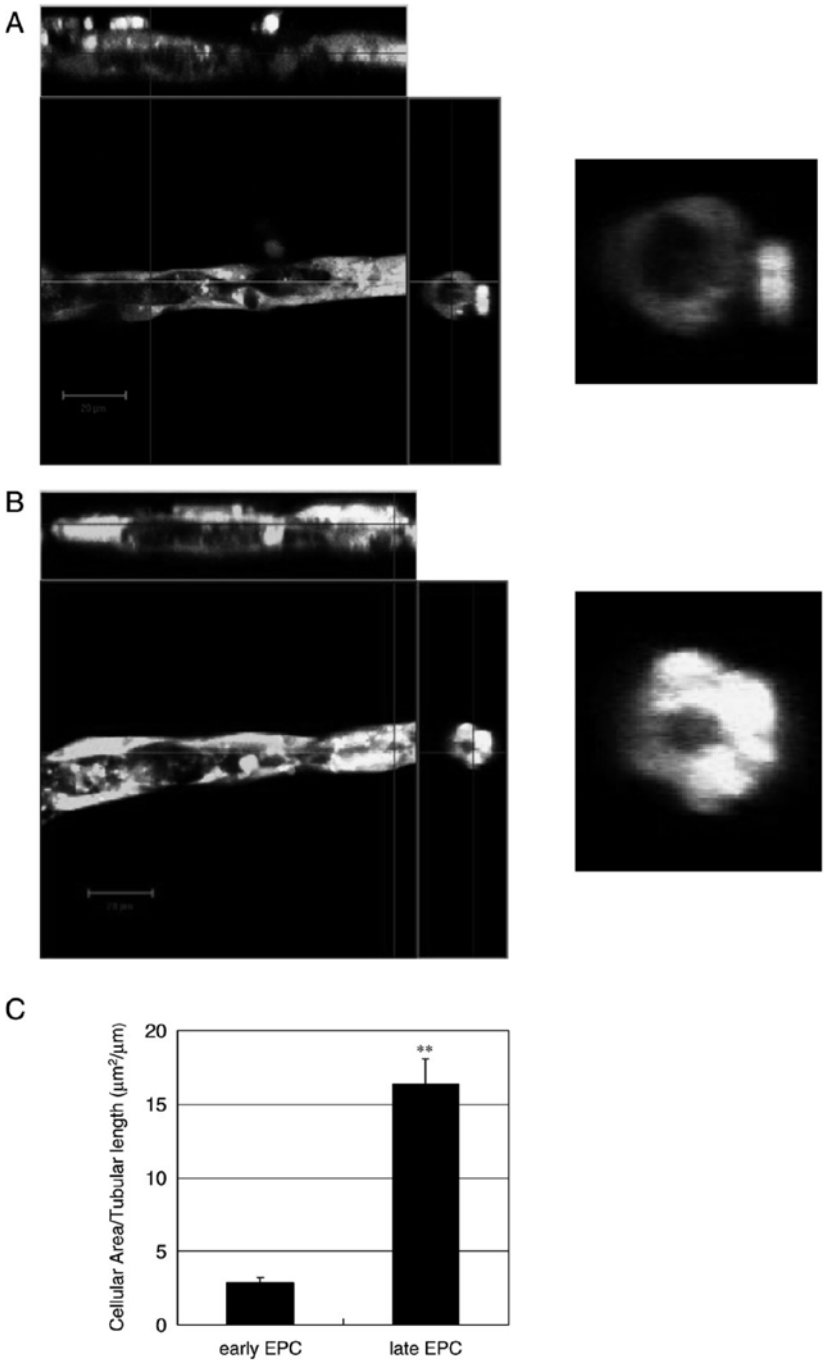

Fig. 4 – Cooperative tube-forming activity of EPCs and HUVECs. After early or late EPCs were stained with PKH26 Red, EPCs and HUVECs were mixed and co-cultured on the substrate, and then transplanted to Matrigel. The ratio of EPCs to HUVECs was 1:10. (A) Tubular structures formed by these EPCs and HUVECs were then labeled with Calcein-AM. Tubular structure constructed with both early EPCs (yellow) and HUVECs (green). Tubular structures were observed three dimensionally with a laser confocal microscopy. The early EPCs attached to the tube surface and were not incorporated into the tubular structure formed by HUVECs. Scale bar=20 μm. (B) Tubular structure constructed with both late EPCs (yellow) and HUVECs (green). The late EPCs participated in tube formation with HUVECs. Scale bar=20 μm. (C) The incorporation of EPCs into tube structure was calculated by the area of EPC in the indicated length of tubular structure. Value is the mean and SE (standard error) of 30. **P<0.01 vs. early EPCs.

cadherin, a specific endothelial cell–cell adhesion molecule, we observed VE-cadherin at cell–cell junctions (Figs. 3C, D).

Late EPCs, but not early EPCs, participated in tube formation with HUVECs

When EPCs are mixed with HUVECs and incubated on Matrigel, EPCs are incorporated into the tubular structure formed by HUVECs [5]. To confirm this, early EPCs or late EPCs were mixed with HUVECs and they were applied to the same tube formation systems. To distinguish the EPCs from HUVECs, the EPCs were labeled with PKH26 Red. Tubular structures formed by these EPCs and HUVECs were then labeled with Calcein-AM. The fluorescence of EPC and HUVECs was observed with a laser confocal microscopy. The early EPC as well as the late EPCs were observed in the tubular structure. However, by a three-dimensional imaging, we demonstrated that the early EPCs were only attached to the tube surface and were not incorporated into the tube structure formed by HUVECs (Fig. 4A). In contrast, the late EPCs participated in tube formation with HUVECs (Fig. 4B). To quantify the incorporation of EPCs into tube structure was calculated by the area of EPC per the indicated length of tubular structure. The incorporation of late EPCs into tubular structures was over 5-fold larger than that of early EPCs (Fig. 4C).

Late EPCs integrated into pre-existing tubular structures formed by HUVECs while early EPCs caused tubular sprouting

In order to investigate whether EPCs could substitute for HUVECs in preformed tubular structures, EPCs and HUVECs were independently cultured. HUVECs labeled with PKH26 Red were seeded onto the substrate and EPCs labeled with PKH26 Green were suspended in Matrigel. The patterned HUVECs on the substrate were transferred to the EPC-containing Matrigel. The late EPCs migrated toward the tubular structures and were observed adjacent after 6 h (Fig. 5A) and attached to the tubes 10 h later (Fig. 5B). Thereafter, they were incorporated into the tubular structure 24 h later (Fig. 5C). In contrast, early EPCs did not migrate toward the tubes and were not

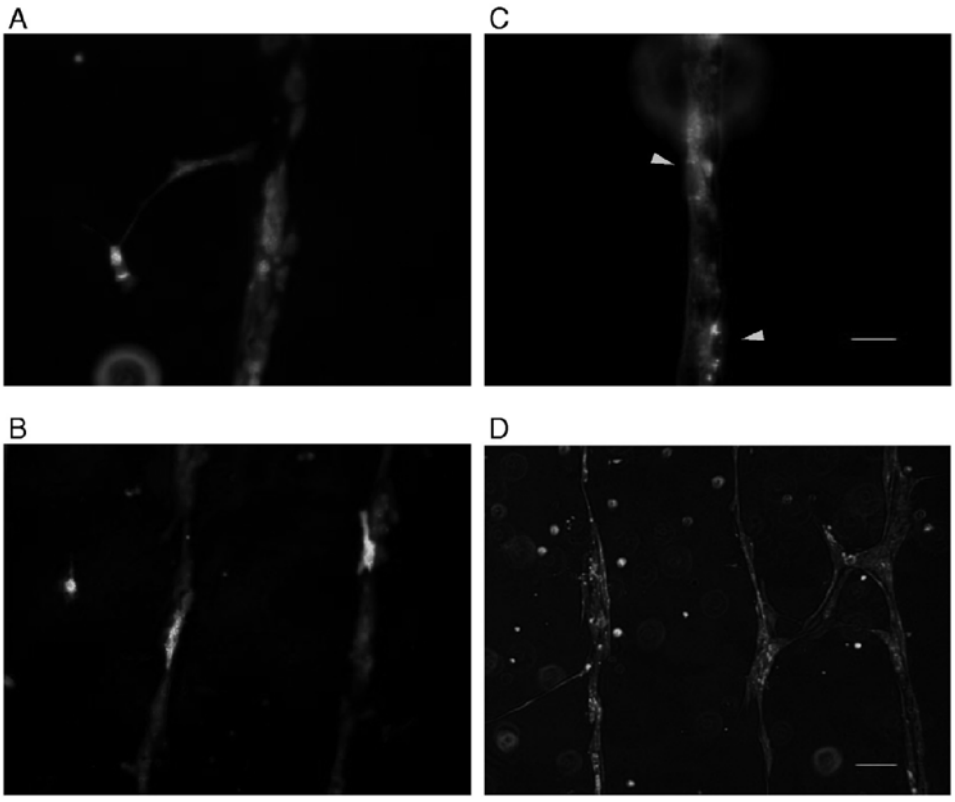

Fig. 5 – Incorporation of EPCs into preformed tubular structures. HUVECs labeled with PKH26 Red were seeded on the substrate and EPCs labeled with PKH26 Green were suspended in Matrigel. The patterned HUVECs on the substrate were transferred to the EPC-containing Matrigel. (A) Six hours after transplantation, late EPCs were migrating toward the tubular structure preformed by HUVECs. (B) Ten hours after transplantation, late EPCs were attached to the tube. (C) Twenty-four hours after transplantation, late EPCs were incorporated into the tubular structure preformed by HUVECs (yellow arrow heads). Scale bar=30 μm. (D) Twenty-four hours after transplantation, early EPCs had not been incorporated into the tubular structure preformed by HUVECs. The HUVECs in the tubular structure were sprouting and migrating. Scale bar=100 μm.

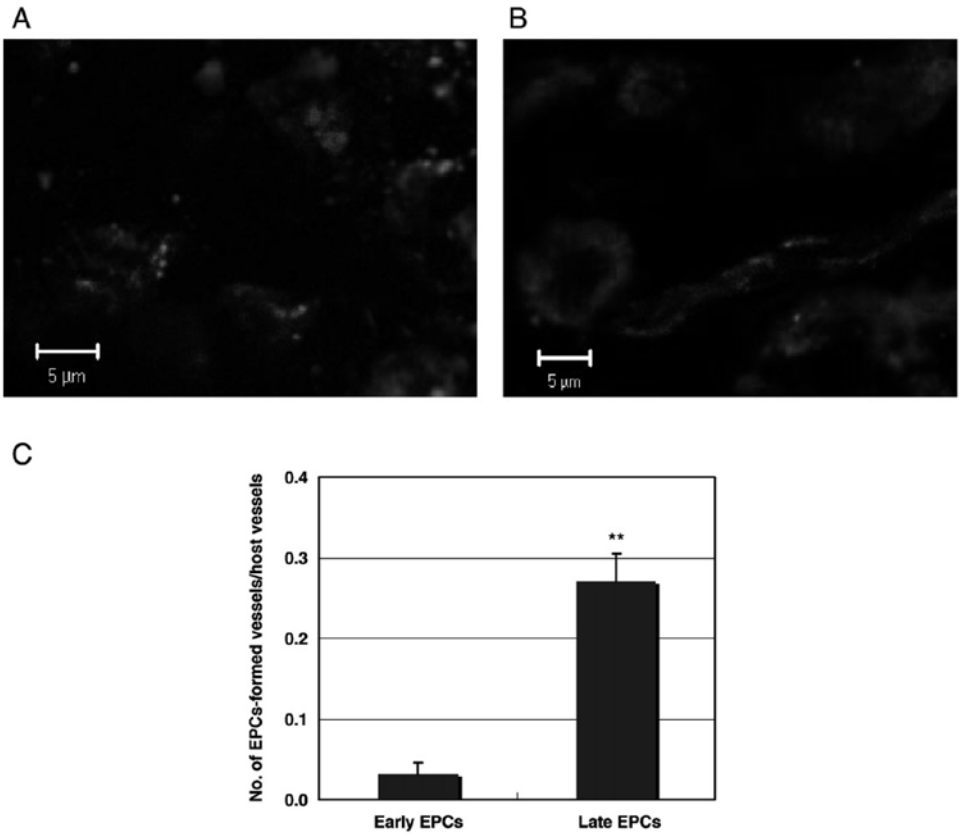

Fig. 6 – *In vivo* angiogenesis assay. After occlusion of murine auricular vessel, early (A) or late (B) EPCs labeled with PKH26 Red were subcutaneously injected into the occluded pinna. Forty-eight hours after the cell injection, the mice were given BS1-lectin (green) intravenously and sacrificed. Scale bar=5 μm. (C) The numbers of blood vessels derived from each EPCs observed in 5 sections were normalized to the number of recipient blood vessels. The data are shown as the mean and SE of three mice and data are mean of 5 fields/mouse.P<0.01 vs. early EPCs.**

incorporated during the observation period. However, after HUVECs were transferred to Matrigel containing early EPCs, the HUVECs in the tubular structures initiated sprouting and migrated toward early EPCs as evidenced by branching patterns between the tubular structures (Fig. 5D).

In vivo angiogenesis assay

To confirm the tube forming activity of each EPCs *in vivo*, the vessels derived from implanted EPCs were observed in the ear vessel occlusion model, early or late EPCs labeled with PKH26 Red were injected into the occluded pinna. Blood vessels derived from the late EPCs were observed in the pinna, but only a few blood vessels derived from early EPCs were observed (Fig. 6).

Discussion

We investigated the tube-forming capacity of early EPCs and late EPCs isolated from human peripheral blood and umbilical cord blood, respectively. In the previous report, it was demonstrated that late EPCs were enriched in umbilical cord blood compared with adult peripheral blood [23]. Therefore, we isolated late EPCs from human umbilical cord blood. We used our novel method for capillary engineering which makes use of photo-catalytic lithography. Traditional assays for assessing characteristics of tube formation *in vitro* have been carried out by cultivation of endothelial cells in type I collagen and Matrigel. However, these methods could not distinguish between tube formation and morphological changes in the cells. The luminal structure of the vascular tube made in our present method was confirmed by an electron microscopy, a confocal laser microscopy and dye microinjection [22]. This technique is unique because the method allows one to focus on the process of tube formation. In contrast, tube formation in collagen and Matrigel evaluates the total activity of endothelial cells including migration, invasion and tube formation [24]. Using this novel method, we demonstrated that late EPCs participated in the formation of tubular structures with mature endothelial cells, *i.e.*, HUVECs. It is interesting that late EPCs migrated toward and adjacent to pre-existing tubular structures and finally were incorporated

into the structure itself. In contrast, early EPCs could not form tubular structures, and they induced migration and sprouting of HUVECs present in the tubular structure. In a previous study using Matrigel, Hur et al. [18] demonstrated that early EPCs were incorporated into tubules when co-cultured with HUVECs, although the formation was weaker than that of late EPCs. However, that paper demonstrated the incorporation of EPCs into network structures of HUVECs on Matrigel, but could not show the incorporation of EPCs in tubular structures.

Our results showed that early EPCs were not capable of constructing tubular luminal structures even when they were co-cultured with mature endothelial cells. Instead, they stimulated the migration and sprouting of HUVECs from the tubular structure. These phenomena may be interpreted by the release of some growth factors from early EPCs. In our experiment, the amount of secreted interleukin-8 from early EPCs was significantly higher than that from late EPCs (0.81±0.07 vs. 0.44±0.02, ng/ml, $P<0.01$). It has been also reported that early EPCs secrete angiogenic factors such as VEGF [18,21], hepatocyte growth factor (HGF), and granulocyte-colony stimulating factor (G-CSF) [21]. These factors are known to stimulate endothelial cell migration and proliferation. In vivo experiments, implanted late EPCs in the occlusion tissues cause to construct new blood vessels by themselves, but early EPC could not. This result may be discussed with a hierarchy of EPCs [23]. It has been also reported that the different types of cells derived from peripheral blood have distinct actions in healing activity [25]. In this study, we demonstrated specific and distinct behaviors of early and late EPCs in tube formation and how they affected mature ECs in tube formation.

Although numerous reports have demonstrate that early EPCs have the potential to construct new blood vessels by themselves [5,6], some studies argued that early EPCs were not actually incorporated into newly formed vessels [26,27]. This discrepancy may be due to marked heterogeneity of EPCs used in their experiments. Numerous studies have fractioned EPC by phenotypic markers such as CD34, CD133, and VEGFR2 and various methods of EPCs isolation have been reported [5,6,28,29]. Among them CD34 has been often used for the marker of EPCs. However, Romagnani et al. showed that CD14 positive MNC-derived EPCs, which had been fractioned as CD34 negative, express very low level of CD34 using an antibody-conjugated magnetofluorescent liposomes (ACMFL) technique [30]. From these results, they suggested that $CD14^{+}$ $CD34^{low}$ cells are the major source of early EPCs obtained from human peripheral blood MNC. This subset exhibited clonogenicity and multipotency to differentiate not only into endothelial cells, but also into osteocytes, or neural cells [30]. This report suggests that it is difficult to sort EPCs into highly defined fractions by ordinary FACS technique. In fact, each EPC population in previous studies is supposed to have a different phenotype even from the same source. To avoid these complexities, we collected and isolated early and late EPCs by focusing on their characteristics such as morphologies and proliferation pattern, and compared their tube-forming activities in short duration *in vitro* assays.

While the regenerative potential of EPCs has been demonstrated in animal models of myocardial and limb ischemia, the number of EPC available for transplantation is very important for cell-based therapy. Because EPCs are derived from a limited endogenous pool, it is necessary to expand the number of EPCs *in vitro* or modulate phenotypes of EPCs. Iwaguro et al. reported that VEGF gene transfer in EPCs stimulated neovascularization in an *in vivo* model [31]. Murasawa et al. demonstrated that gene transfer of human telomerase reverse transcriptase into EPCs enhanced their angiogenic properties, mitogenic and migratory activities, and cell survival [32]. From the standpoint of cellular proliferation and phenotypic stability, late EPCs are superior to early EPCs. Therefore, the use of late EPCs for tissue engineering has been challenged [33–35]. With our method of generating transplantable capillary networks, the formation of tubular structures *in vitro* is a necessary precondition. The data presented here are thus important since the results demonstrate that late EPCs are a candidate for tissue engineering.

In conclusion, our data provide the first definitive evidence that early EPCs promote angiogenesis through migration and proliferation of mature endothelial cells, whereas late EPCs can form blood vessels. These results suggest that early EPCs and late EPCs have different roles in neovascularization *in vivo*. Finally, we expect that the novel culture system using a patterned substrate might be useful for future *in vitro* analyses of neovascularization.

Acknowledgments

This work was supported in part by research grants, 17209058, 1752342, the 21st Century COE Program from the Japan Society for the Promotion of Science, and KH31031 from Human Science Foundation, Tokyo, Japan. We thank Dai Nippon Printing Co. Ltd (Tokyo, Japan) for their kind preparation of substrate.

REFERENCES

[1] P.K.Y. Goon, C.J. Boos, G.Y.H. Lip, Circulating endothelial cells: markers of vascular dysfunction, Clin. Lab. 51 (2005) 531–538.
[2] N. Werner, S. Kosiol, T. Schiegl, P. Ahlers, K. Walenta, A. Link, M. Bohm, G. Nickenig, Circulating endothelial progenitor cells and cardiovascular outcomes, N. Engl. J. Med. 353 (2005) 999–1007.
[3] S. Rafii, D. Lyden, R. Benezra, K. Hattori, B. Heissig, Vascular and haematopoietic stem cells: novel targets for anti-angiogenesis therapy? Nat. Rev., Cancer 2 (2002) 826–835.
[4] W. Suh, K.L. Kim, J.M. Kim, I.S. Shin, Y.S. Lee, J.Y. Lee, H.S. Jang, J.S. Lee, J. Byun, J.H. Choi, E.S. Jeon, D.K. Kim, Transplantation of endothelial progenitor cells accelerates dermal wound healing with increased recruitment of monocytes/macrophages and neovascularization, Stem Cells 23 (2005) 1571–1588.
[5] T. Asahara, T. Murohara, A. Sullivan, M. Silver, R. van der Ze, T. Li, B. Witzenbichler, G. Schatteman, Isner, Isolation of putative progenitor endothelial cells for angiogenesis, Science 275 (1997) 964–967.
[6] T. Takahashi, C. Kalka, H. Masuda, D. Chen, M. Silver, M. Kearney, M. Magner, J.M. Isner, T. Asahara, Ischemia- and cytokine-induced mobilization of bone marrow derived endothelial progenitor cells for neovascularization, Nat. Med. 5 (1999) 434–438.
[7] T. Asahara, H. Masuda, T. Takahashi, C. Kalka, C. Pastore, M. Silver, M. Kearne, M. Magner, J.M. Isner, Bone marrow

origin of endothelial progenitor cells responsible for postnatal vasculogenesis in physiological and pathological neovascularization, Circ. Res. 85 (1999) 221–228.
[8] C. Kalk, H. Masuda, T. Takahashi, W.M. Kalka-Moll, M. Silver, M. Kearney, T. Li, JM. Isner, T. Asahara, Transplantation of ex vivo expanded endothelial progenitor cells for therapeutic neovascularization, Proc. Natl. Acad. Sci. U. S. A. 97 (2000) 3422–3427.
[9] T. Murohara, H. Ikeda, J. Duan, S. Shintani, K. Sasaki, H. Eguchi, I. Onitsuka, K. Matsui, T. Imaizumi, Transplanted cord blood-derived endothelial precursor cells augment postnatal neovascularization, J. Clin. Invest. 105 (2000) 1527–1536.
[10] M. Hristov, W. Erl, P.C. Weber, Endothelial progenitor cells: mobilization, differentiation, and homing, Arterioscler. Thromb. Vasc. Biol. 23 (2003) 1185–1189.
[11] E. Tateishi-Yuyama, H. Matsubara, T. Murohara, U. Ikeda, S. Shintani, H. Masaki, K. Amano, Y. Kishimoto, K. Yoshimoto, H. Akashi, K. Shimada, T. Iwasaka, T. Imaizumi, Therapeutic angiogenesis using cell transplantation (TACT) study investigators, therapeutic angiogenesis for patients with limb ischaemia by autologous transplantation of bone-marrow cells: a pilot study and a randomised controlled trial, Lancet 360 (2002) 427–435.
[12] F.A. Kudo, T. Nishibe, M. Nishibe, K. Yasuda, Autologous transplantation of peripheral blood endothelial progenitor cells (CD34+) for therapeutic angiogenesis in patients with critical limb ischemia, Int. Angiol. 4 (2003) 344–348.
[13] S. Shintani, T. Murohara, H. Ikeda, T. Ueno, T. Honma, A. Katoh, K. Sasaki, T. Shimada, Y. Oike, T. Imaizumi, Mobilization of endothelial progenitor cells in patients with acute myocardial infarction, Circulation 103 (2001) 2776–2779.
[14] B. Assmus, V. Schachinger, C. Teupe, M. Britten, R. Lehmann, N. Dobert, F. Grunwald, A. Aicher, C. Urbich, H. Martin, D. Hoelzer, S. Dimmeler, A.M. Zeiher, Transplantation of progenitor cells and regeneration enhancement in acute myocardial infarction (TOPCARE AMI), Circulation 106 (2002) 3009–3017.
[15] M.B. Britten, N.D. Abolmaali, B. Assmus, R. Lehmann, J. Honold, J. Schmitt, T.J. Vogl, H. Martin, V. Schachinger, S. Dimmeler, A.M. Zeiher, Infarct remodeling after intracoronary progenitor cell treatment in patients with acute myocardial infarction (TOPCARE-AMI): mechanistic insights from serial contrast-enhanced magnetic resonance imaging, Circulation 108 (2003) 2212–2218.
[16] Y. Lin, D.J. Weisdorf, A. Solovey, R.P. Hebbel, Origins of circulating endothelial cells and endothelial outgrowth from blood, J. Clin. Invest. 105 (2000) 71–77.
[17] R. Gulati, D. Jevremovic, T.E. Peterson, S. Chatterjee, V. Shah, R.G. Vile, R.D. Simari, Diverse origin and function of cells with endothelial phenotype obtained from adult human blood, Circ. Res. 93 (2003) 1023–1025.
[18] J. Hur, C.H. Yoon, H.S. Kim, J.H. Choi, H.J. Kang, K.K. Hwang, B.H. Oh, M.M. Lee, Y.B. Park, Characterization of two types of endothelial progenitor cells and their different contributions to neovasculogenesis, Arterioscler. Thromb. Vasc. Biol. 24 (2004) 288–293.
[19] C.H. Yoon, J. Hur, K.W. Park, J.H. Kim, C.S. Lee, I.Y. Oh, T.Y. Kim, H.J. Cho, H.J. Kang, I.H. Chae, H.K. Yang, B.H. Oh, Y.B. Park, H.S. Kim, Synergistic neovascularization by mixed transplantation of early endothelial progenitor cells and late outgrowth endothelial cells: the role of angiogenic cytokines and matrix metalloproteinases, Circulation 112 (2005) 1618–1627.
[20] C. Urbich, C. Heeschen, A. Aicher, E. Dernbach, A.M. Zeiher, S. Dimmeler, Relevance of monocytic features for neovascularization capacity of circulating endothelial progenitor cells, Circulation 108 (2003) 2511–2516.
[21] J. Rehman, J. Li, C.M. Orschell, K.L. March, Peripheral blood "endothelial progenitor cells" are derived from monocyte/macrophages and secrete angiogenic growth factors, Circulation 107 (2003) 1164–1169.
[22] A. Kobayashi, H. Miyake, H. Hattori, R. Kuwana, Y. Hiruma, KI. Nakahama, S. Ichinose, M. Ota, M. Nakamura, S. Takeda, I. Morita, In vitro formation of capillary networks using optical lithographic techniques, Biochem. Biophys. Res. Commun. 358 (2007) 692–697.
[23] D.A. Ingram, L.E. Mead, H. Tanaka, V. Meade, A. Fenoglio, K. Mortell, K. Pollok, M.J. Ferkowicz, D. Gilley, M.C. Yoder, Identification of a novel hierarchy of endothelial progenitor cells using human peripheral and umbilical cord blood, Blood 104 (2004) 2752–2760.
[24] T.J. Lawley, Y. Kubota, Induction to morphologic differentiation of endothelial cells in culture, J. Invest. Dermatol. 93 (1989) 59S–61S.
[25] O. Awad, E.L. Dedkov, C. Jiao, S. Bloomer, R.J. Tomanek, G.C Schatteman, Differential healing activities of CD34+ and CD14+ endothelial cell progenitors, Arterioscler. Thromb. Vasc. Biol. 26 (2006) 758–764.
[26] T. Ziegelhoeffer, B. Fernandez, S. Kostin, M. Heil, R. Voswinckel, A. Helisch, W. Schaper, Bone marrow-derived cells do not incorporate into the adult growing vasculature, Circ. Res. 94 (2004) 230–238.
[27] L. Zentilin, S. Tafuro, S. Zacchigna, N. Arsic, L. Pattarini, M. Sinigaglia, M. Giacca, Bone marrow mononuclear cells are recruited to the sites of VEGF-induced neovascularization but are not incorporated into the newly formed vessels, Blood 107 (2006) 3546–3554.
[28] U.M. Gehling, S. Ergun, U. Schumacher, C. Wagener, K. Pantel, M. Otte, G. Schuch, P. Schafhausen, T. Mende, N. Kilic, K. Kluge, B. Schafer, D.K. Hossfeld, W. Fiedler, In vitro differentiation of endothelial cells from AC133-positive progenitor cells, Blood 95 (2000) 3106–3112.
[29] J. Yamashita, H. Itoh, M. Hirashima, M. Ogawa, S. Nishikawa, T. Yurugi, M. Naito, K. Nakao, S. Nishikawa, Flk1-positive cells derived from embryonic stem cells serve as vascular progenitors, Nature 408 (2000) 92–96.
[30] P. Romagnani, F. Annunziato, F. Liotta, E. Lazzeri, B. Mazzinghi, F. Frosali, L. Cosmi, L. Maggi, L. Lasagni, A. Scheffold, M. Kruger, S. Dimmeler, F. Marra, G. Gensini, E. Maggi, S. Romagnani, CD14+CD34low cells with stem cell phenotypic and functional features are the major source of circulating endothelial progenitors, Circ. Res. 97 (2005) 314–322.
[31] H. Iwaguro, J. Yamaguchi, C. Kalka, S. Murasawa, H. Masuda, S. Hayashi, M. Silver, T. Li, J.M. Isner, T. Asahara, Endothelial progenitor cell vascular endothelial growth factor gene transfer for vascular regeneration, Circulation 105 (2002) 732–738.
[32] S. Murasawa, J. Llevadot, M. Silver, J.M. Isner, D.W. Losordo, T. Asahara, Constitutive human telomerase reverse transcriptase expression enhances regenerative properties of endothelial progenitor cells, Circulation 106 (2002) 1133–1139.
[33] S. Fuchs, A. Motta, C. Migliaresi, C.J. Kirkpatrick, Outgrowth endothelial cells isolated and expanded from human peripheral blood progenitor cells as a potential source of autologous cells for endothelialization of silk fibroin biomaterials, Biomaterials 31 (2006) 5399–5408.
[34] D. Schmidt, L.M. Asmis, B. Odermatt, J. Kelm, C. Breymann, M. Gossi, M. Genoni, G. Zund, S.P. Hoerstrup, Engineered living blood vessels: functional endothelia generated from human umbilical cord-derived progenitors, Ann. Thorac. Surg. 82 (2006) 1465–1471.
[35] T. Aper, A. Schmidt, M. Duchrow, H.P. Bruch, Autologous blood vessels engineered from peripheral blood sample, Eur. J. Vasc. Endovasc. Surg. 33 (2006) 33–39.

顎口腔外科分野

小村　健

医歯学総合研究科・口腔機能再構築学系専攻
口腔機能再建学／医学博士・教授

1. 研究の課題名

「口腔癌の分子基盤解析」

Molecular basis analysis of oral cancer.

われわれは、口腔癌治療においてさらなる治療成績の向上を目指し、エビデンスに基づいた診断・予測・治療を実現するための研究を行っている。診断については、含嗽液による口腔癌・前癌病変の早期診断に関する試みで、これは、癌が口腔に存在する特徴から、含嗽によって剥離する細胞をターゲットにSCCAをマーカーとしてPCR法により口腔癌・前癌病変を検出するもので、当科での検討では、口腔癌において94.1%の陽性率があり、大規模で簡便な検診が実現可能と考えている。また、前癌病変である口腔白板症の上皮性異型性程度を遺伝子発現パターンによって診断するシステムの構築を目指し、マイクロアレイ解析による診断マーカー候補が抽出された。これは将来的な癌化マーカーの開発につながる成果と考えられる。また、バイオマーカーを用いて口腔癌におけるセンチネルリンパ節概念の成立を検証し、正確な診断に基づいた手術療法におけるminimal invasive surgeryの実践をすすめている。一方、画像診断や病理組織学的診断などの臨床データから後発転移の有無や予後をある程度予測できるものの、オーダーメード治療につながるような正確な予後予測は難しく、これらを実現すべくバイオマーカーの探求をすすめた。その1つとして、舌扁平上皮癌組織標本の免疫組織染色によりcIAP-1の発現が頸部リンパ節転移を予測する新規バイオマーカーとして有用であることが示された。これら予防・診断・予測のシステム開発とともに、口腔癌の悪性化や浸潤・転移メカニズムを解明することにより新たな治療法が確立されることを目指し、われわれが独自に開発した骨浸潤モデルマウスを用いた浸潤メカニズムの解析をすすめ、骨膜の重要性について報告している。

2.

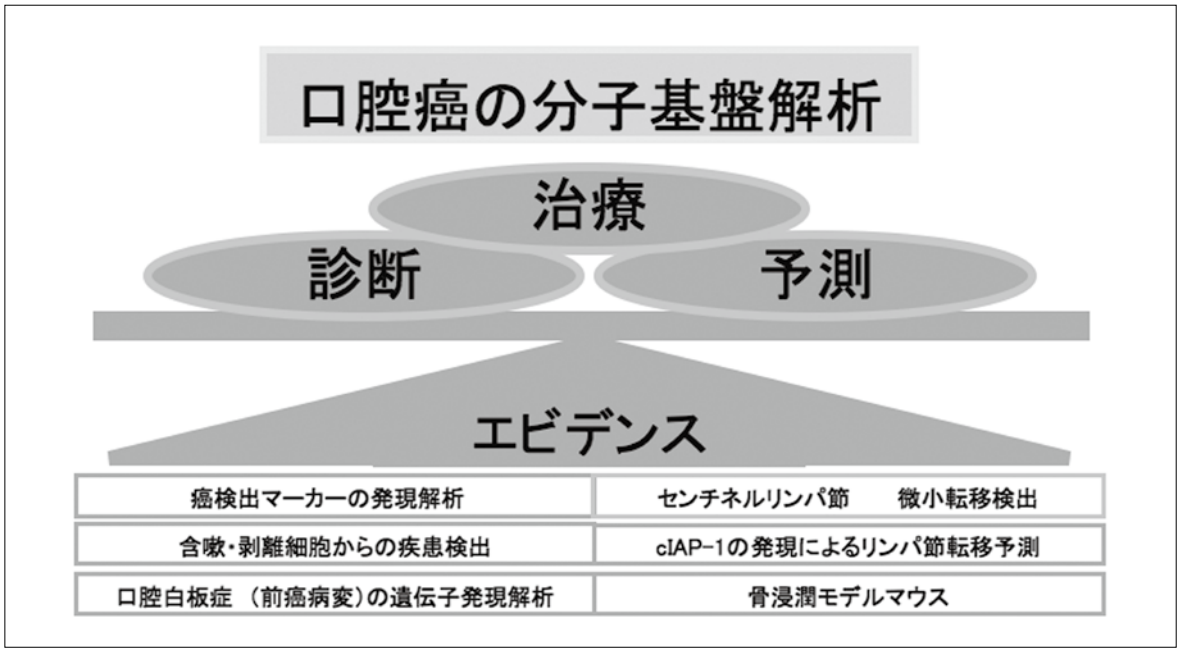

3. 研究内容についての英文要約

「Expression of cIAP-1 correlates with nodal metastasis in squamous cell carcinoma of the tongue」
Cellular inhibitor-of-apoptosis protein 1（cIAP-1）is a member of the inhibitor-of- apoptosis protein family, which predominantly regulates apoptosis. It has been suggested that expression of cIAP-1 correlates with certain clinicopathological features. The possible significance of cIAP-1 expression in cervical lymph node metastasis of tongue squamous cell carcinoma（SCC）is investigated. Seventy-five tongue SCCs were analyzed by immunohistochemistry. cIAP-1 immunoreactivity patterns were nuclear in 38（51%）, cytoplasmic in 47（63%）, and concurrent in 37（49%）cases. Nuclear, cytoplasmic and concurrent cIAP-1 immunoreactions were significantly correlated with lymph node metastasis in tongue SCCs. The cleaved caspase-3, which is a marker of tumor apoptosis, and Ki-67 index, which is a marker of tumor proliferation, were immunohistochemically examined in 21 tongue SCCs with concurrent nuclear and cytoplasmic cIAP-1 expression and with metastasis, and in 23 tongue SCCs without concurrent nuclear and cytoplasmic cIAP-1 expression and without metastasis. Concurrent cIAP-1 expression was inversely correlated with caspase-3, but was positively correlated with Ki-67 expression. These results suggest that both patterns of cIAP-1 are useful markers for predicting cervical lymph node metastasis in tongue SCC.

「 Gene expression analysis by oligonucleotide microarray in oral leukoplakia」
Oral leukoplakias（LP）are the most frequent types of oral precancerous lesions, but there is no accurate assessment of this malignant transformation or even genetic diagnosis of the oral epithelial dysplasia. We need to identify the new genetic diagnosis system of the epithelial dysplasia. Oligonucleotide microarray was used to analyze expression patterns of 29952 genes in 10 LP patients. We compared the different gene expressions between mild dysplasia cases and severe dysplasia cases. Ninety-six genes expressed differentially were selected as candidates for up-regulated in severe dysplasia. Subsequently, we further selected 16 genes with highest differentially expression. By hierarchical clustering analysis, the 10 cases were divided mild dysplasia from severe dysplasia. The 16 genes are suggested as biomarker gene sets of efficacy and quickly recognized in the development of oral epithelial dysplasia.

「Effect of irradiation on tumor invasion into bone」
In the process of direct bone invasion of malignant tumors, the periosteum is known to act as a protective barrier against the entry of the tumor cells. Injuries of the periosteum may cause an impairment of its barrier function. In this study, we examined the effect of irradiation on the tumor bone invasion using a mouse tumor transplantation model. Forty-four C57BL/6J mice were used to evaluate the irradiation effect. Calvarias of mice were scratched and/or irradiated at a dose of 10 Gy, and B16F10 melanoma cells were inoculated. Calvaria specimens were radiologically and histologically evaluated. The quantity of bone resorption were examined. Bone invasion was not evident in non-irradiated/non-scratched control mice even when the tumor size reached to 15-20 mm. On the other hand, cortical bone resorption and tumor cell entry was observed in irradiation-only（R）and scratch-only（S）mice. More aggressive invasion of B16F10 was found in irradiation+scratch（RS）calvarias. Mice of the R group were inoculated with B16F10 cells 1, 7, or 14 days after irradiation and the duration of the irradiation effects was evaluated. Injuries caused by irradiation make the periosteum more prone to malignant tumor invasion, and that the effect of irradiation might be long-standing.

「Minimally invasive surgical technique in oral cancer -sentinel node navigation surgery-」
The sentinel lymph node（SN）biopsy is landmark stability and may be a minimally invasive technique that samples firstechelon lymph node to predict the need for neck dissection. Therefore, SN navigation surgery may be administered. In this study, we investigate the possibility of identifying the SN combined with lymphoscintigraphy in oral cancer and the detection of metastases in SN by HE stain, IHC and RT-PCR. No metastases were identified using HE and cytokeratin IHC staining in non-SNs. The result strongly suggested approval of the SN concept in oral cancer as well as for better assessment of the status of the cervical lymph nodes. Based on the acknowledgment, we performed SN navigation surgery for 11cases and suggest that it is highly useful. SN navigation surgery in oral cancer is still at the stage of preliminary research, and is not enforced generally. To assume SN navigation surgery to be standard treatment in the future, we will avoid an excessive neck dissection. As a result, we would provide more benefits to the oral cancer patients.

4. 本事業に関連して世界的な研究拠点形成に向けて、以下の点で改善・整備等されたこと

A（研究拠点体制）

硬組織領域における教育、研究、臨床について優れた実績を上げるため、平成15年度より開始の21世紀COEプログラム「歯と骨の分子破壊と再構築のフロンティア」において形成した研究基盤をさらに発展させ、一方、特別教育研究経費による「硬組織疾患ゲノムセンター」との密なる連携を図りつつ、口腔扁平上皮癌などの口腔外

科学領域における悪性腫瘍を中心とした硬組織疾患のテーラーメイド医療の実現とともに、トランスレーショナル・リサーチへの発展を視野にいれた研究を展開している。

B（研究教育環境）

教育・研究基盤をさらに発展させ、基礎医・歯学分野から臨床分野までの融合型国際教育研究拠点の強化・拡大を図ることによって、博士課程学生に優れた教育環境・プログラムを提供し、国内外の研究機関とも連携して“国際的創造型科学者”の育成を目指す。

C（人材確保）

基礎医・歯学分野から臨床分野までの様々な情報・技術交流を目指し、学外研究所等との大学院生・教員の相互的な派遣・受け入れの体制を整備し、基礎研究、臨床研究の両分野について先端的かつ十分な知識と技術を持つ人材の確保に取り組んでいる。

D（人材育成）

顎顔面疾患におけるテーラーメイド医療の実現とQOLの向上をも目指したトランスレーショナル・リサーチを推進することによって、基礎医・歯学分野から臨床・応用医学分野までを両立させた“国際的創造型科学者”を養成する。

E（国際化）

国際的な情報交換と技術交流を目指し、アジア各国からの留学生を大学院生として受け入れて研究を遂行し、また基礎研究、臨床研究の両分野についてシンポジウムを開催するなどして、相互の発展に寄与している。

5. GCOE事業を推進するに当たって力を入れた点

臨床情報を具備した口腔扁平上皮癌症例の外科切除試料の系統的な収集と本学に既に設置済みのバイオリソースセンターにおける保存を進めつつ、これらの臨床検体を用いた網羅的発現解析によって口腔扁平上皮癌の頸部リンパ節転移診断モデルを構築するとともに、口腔扁平上皮癌細胞株での網羅的ゲノム・エピゲノム解析などにより新規口腔癌抑制遺伝子や口腔癌抑制microRNAを単離・同定し、口腔扁平上皮癌における遺伝子変異の同定などについても明らかにすべく研究を推進してきた。また、硬組織疾患ゲノムセンターとの密接な学内連携のもと、これらのバイオリソースを用いた分子・細胞・組織・個体すべてのレベルにおける分子メカニズムの解明、顎顔面疾患の新たな診断から外科的治療法の開発を目指した系統的研究基盤の整備をすすめている。

6. 英文原著論文

1. Ariyoshi Y, Shimahara M, Omura K, Yamamoto E, Mizuki H, Chiba H, Imai Y, Fujita S, Shinohara M, Seto K : Epidemiological study of malignant tumors in the oral and maxillofacial region: survey of member institutions of the Japanese Society of Oral and Maxillofacial Surgeons, 2002. Int J Clin Oncol 13（3）:220-228, 2008.
2. Harada H, Omura K: Metastasis of oral cancer to the parotid node. Eur J Surg Oncol, 2008, Nov 10（Epub ahead of print）.
3. Ida M, Yoshitake H, Okoch K, Tetsumura A, Ohbayashi N, Amagasa T, Omura K, Okada N, Kurabayashi T : An investigation of magnetic resonance imaging features in 14 patients with synovial chondromatosis of temporomandibular joint. Dentomaxillofac Radiol 37（3）:213-219, 2008.
4. Iino G, Nishimura K, Omura K, Kasugai S.: Effects of prostaglandin E1 application on rat incisal sockets. Int J Oral Maxillofac Implants. 23（5）:835-40, 2008.
5. Kabasawa Y, Nagumo K, Takeda Y, Kawasima N, Okada N, Omura K, Yamaguchi A, Katsube K: Amelogenin positive cells scattered in the interstitial odontogenic fibromas. J Clin Pathol 61（7）:851-855, 2008.
6. Koida N, Ozaki T, Yamamoto H, Ono S, Koda T, Ando K, Okoshi R, Kamijo T, Omura K, Nakagawara A : Inhibitory role of Plk1 in the regulation of p73-dependent apoptosis through physical interaction and phosphorylation. J Biol Chem 283（13）:8555-8563, 2008.
7. Kozaki K, Imoto I, Mogi S, Omura K, Inazawa J : Exploration of tumor-suppressive microRNAs silenced by DNA hypermethylation in oral cancer. Cancer Res 68（7）:2094-2105, 2008.
8. Kuprash DV, Qin Z, Ito D, Grivennikov SI, Abe K, Drutskaya LN, Blankenstein T, Nedospasov SA : Ablation of TNF or lymphotoxin signaling and the frequency of spontaneous tumors in p53-deficient mice. Cancer Lett 268（1）:70-75, 2008.
9. Momin MA, Okochi K, Watanabe H, Imaizumi A, Omura K, Amagasa T, Okada N, Ohbayashi N. Kurabayashi T : Diagnostic accuracy of cone-beam CT in the assessment of mandibular invasion of lower gingival carcinoma: Comparison with conventional panoramic radiography. Eur J Radiol. 2008 Jul 23（Epub ahead of print）.
10. Morita K, Iwasa T, Imaizumi F, Negishi A, Omura K: A case of maxillary duplication with a soft palate reconstruction using a forearm flap. Int J Oral Maxillofac Surg. 37（9）:862-5 2008.
11. Negishi A, Ono M, Handa Y, Kato H, Yamashita K, Honda K, Shitashige M, Satow R, Sakuma T, Kuwabara H, Omura K, Hirohashi S, Yamada T: Large-scale quantitative clinical proteomics by label-free liquid chromatography and mass spectrometry. Cancer Sci 2008, Dec 19（Epub ahead of print）.

12. Qi S, Mogi S, Tsuda H, Tanaka Y, Kozaki K, Imoto I, Inazawa J, Hasegawa S, Omura K : Expression of cIAP-1 correlates with nodal metastasis in squamous cell carcinoma of the tongue. Int J Oral Maxillofac Surg. 37: 1047-1053, 2008.
13. Satoh Y, Kabasawa Y, Omura K: Analysis of clinical usefulness of the heat flux technique: predictability of the recovery from neurosensory disturbances in the chin undergoing mandibular sagittal split ramus osteotomy. Oral Surg Oral Med Oral Pathol Oral Radiol Endod. 106:637-643, 2008.
14. Youngnak-Piboonratanakit P, Takahashi Y, Nakajima Y, Omura K : Acute angioedema and urticaria associated with herpes simplex infection?. Acta Stomatol Croat 42（1）:64-71, 2008.
15. Kaneoya A, Hasegawa S, Tanaka Y, Omura K: Quantitative analysis of invasive front in tongue cancer using ultrasonography. J Oral Maxillofac Surg. 67（1）:40-46, 2009.
16. ◎Kuribayashi Y, Morita K, Tomioka H, Uekusa M, Ito D, Omura K: Gene expression analysis by oligonucleotide microarray in oral leukoplakia. J Oral Pathol Med, 2009 Feb 7.（Epub ahead of print）.
17. Mochizuki Y, Matushima E, Omura K: Perioperative assessment of psychological states and quality of life of head and neck cancer patients undergoing surgery. Int J Oral Maxillofac Surg. in press.
18. Miyazaki H, Kato J, Watanabe H, Harada H, Kakizaki H, Tetsumura A, Sato A, Omura K: Intralesional laser treatment of voluminous vascular lesions in the oral cavity. Oral Surg Oral Med Oral Pathol Oral Radiol Endod 107（2）:164-72, 2009.
19. Tachasuttirut K, Hasegawa S, Yoshino N, Ito D, Omura K: Effect of irradiation on malignant tumor invasion into bone. Asian J Oral Maxillofac Surg, 2009, in press.
20. Yoshiba S, Ito D, Nagumo T, Shirota T, Hatori M, Shintani S: Hypoxia induces resistance to 5-fluorouracil in oral cancer cells via G1 phase cell cycle arrest. Oral Oncology 45（2）:109-15, 2009.

7. 平成21年3月までの自己評価

平成15年度より開始の21世紀COEプログラム「歯と骨の分子破壊と再構築のフロンティア」において形成した研究基盤をさらに発展させ、硬組織領域における教育、研究、臨床については世界的にトップレベルの優れた実績を上げ、一方、特別教育研究経費による「硬組織疾患ゲノムセンター」との密なる連携を図りつつ、口腔扁平上皮癌などの口腔外科学領域における悪性腫瘍を中心とした硬組織疾患のテーラーメイド医療の実現とともに、トランスレーショナル・リサーチへの発展を視野にいれた研究が展開できた。

8. 和文原著論文

1. 石井良昌、工藤雅範、濱崎　健、鈴木久美子、新井広幸、佐藤佑輔:下唇に発生した外傷性神経腫の1例. 日本口腔外科学会雑誌　54（3）:182-185, 2008.
2. 伊東大典、橋本有央、伊藤秀寿、代田達夫、羽鳥仁志、新谷　悟: 頬部脂肪体有茎弁移植による口蓋腫瘍切除後の再建:症例報告と文献的考察. Dental Med Res（昭和歯学会雑誌）28（1）: 26-29, 2008.
3. 佐藤百合子、小村 健、原田浩之、島本裕彰、澤井俊宏: 耳下腺に発生したリンパ上皮性嚢胞の3例. 口腔病学会雑誌　75（3）:162-167, 2008.
4. 高根　努、森田圭一、佐藤　昌、樺沢勇司、丸岡　豊、小村　健: Le Fort I型骨切り術後に生じたsurgical ciliated cystの1例. 日本口腔外科学会雑誌　54（11）:616-620, 2008.
5. 田中香衣、小村　健、原田浩之、伊原英世、岡田憲彦: 耳下腺深葉に発生した上皮筋上皮癌の1例. 日本口腔腫瘍学会誌　20（3）: 145-150, 2008.
6. 長谷川正午、小村　健、原田浩之、吉田文彦、植草　優、南雲清子、岡田憲彦、戸川貴史: 口腔癌における新しい低侵襲治療　-センチネルリンパ節ナビゲーション手術-. 日本歯科医学会雑誌 27:40-44, 2008.
7. 望月裕美、小村　健、平井秀明、澤井俊宏、栢森高、山口　朗: 術前診断に苦慮した顎下腺海綿状血管腫の1例. 日本口腔外科学会雑誌　54（10）:572-576, 2008.
8. 望月裕美、小村　健、松島英介: 口腔がん手術患者の心理特性とQOLの経時的変化. 口腔病学会雑誌（印刷中）、2009.

9. 学会発表（英文）

1. Shimamoto H, Omura K, Harada H, Ikuta M, Tomioka H.:Primary intraosseous squamous cell carcinoma of the mandible. 12th International Congress on Oral Cancer. May 22-25 2008, Shanghai, China　口頭
2. Qi S, Mogi S, Tsuda H, Tanaka Y, Kozaki K, Imoto I, Inazawa J, Hasegawa S, Omura K: Expression of cIAP-1 correlates with nodal metastasis in squamous cell carcinoma of the tongue. 12th International Congress on Oral Cancer. May, 22-25 2008. Shanghai, China　示説
3. Marukawa E, Omura K.: Bone regeneration with β-TCP（Osferion）. 16th Annual Meeting & Scientific Congress of the Korean College of Oral Implantology –INTRENATIONAL-. May 31, Seoul, Korea　口頭
4. Miyazaki H, Kato J, Watanabe H, Uetake H, Hashimoto K, Omura K.:Laser surgical treatment of oral lesions

assisted by glycerol submucosal injection. 11th Meeting of the World Federation for Laser Dentistry. July 28-30 2008. Hong Kong, China　示説
5. Kabasawa Y, Satoh Y, Jinno S, Omura K: Analysis of the clinical usefulness of heat flux technique. XIX Congress of the European Association for Cranio-Maxillo-Facial Surgery. Sep 9-12 2008. Bologna, Italy　口頭
6. Shimamoto H, Omura K, Harada H, Uekusa M: Primary intraosseous squamous cell carcinoma of the maxilla. XIX Congress of the European Association for Cranio-Maxillo-Facial Surgery. Sep 9-12 2008. Bologna, Italy　口頭
7. ◎Kuribayashi Y, Morita K, Tomioka H, Uekusa M, Ito D, Omura K: Gene expression analysis by oligonucleotide microarray in oral leukoplakias. The 8th Asian Congress on Oral and Maxillofacial Surgery. Nov 4-7 2008. Bangkok, Thailand　示説
8. Morita K, Imaizumi F, Negishi A, Omura K: Alveolar bone grafting with a segmental osteotomy in patients with cleft lip and palate. The 8th Asian Congress on Oral and Maxillofacial Surgery. Nov 4-7 2008. Bangkok, Thailand　示説
9. Negishi A, Ono M, Masuda M, Omura K, Yamada T: Quantitative proteomics using formalin-fixed paraffin-embedded tissue of squamous cell carcinoma of the tongue. The 8th Asian Congress on Oral and Maxillofacial Surgery. Nov 4-7 2008. Bangkok, Thailand 示説

10. 学会発表（和文）

1. 島本裕彰、小村　健、原田浩之、中島雄介、富岡寛文、植草　優、金親あや乃、平井秀明、栗林悠里:口底扁平上皮癌の治療成績．第26回日本口腔腫瘍学会総会 2008年1月24-25日　別府市
2. 原田浩之、小村　健、島本裕彰、富岡寛文、植草 優、金親あや乃、平井秀明:頬粘膜扁平上皮癌の治療成績．第26回日本口腔腫瘍学会総会 2008年1月24-25日　別府市
3. 樺沢勇司、小村　健: 当科における顎顔面骨骨折の臨床的検討. 第62回 日本口腔科学会総会　2008年4月17-18日　福岡市
4. 富岡寛文、小村　健、原田浩之: 口腔に発生した顆粒細胞腫9例の臨床病理学的検討. 第62回 日本口腔科学会総会　2008年4月17-18日　福岡市
5. 根岸綾子、尾野雅哉、小村　健、山田哲司: ホルマリン固定パラフィン包埋組織を用いた舌扁平上皮癌のバイオマーカーの探索. 第4回日本臨床プロテオーム研究会 2008年5月10日 大阪市
6. 森田圭一、今泉史子、根岸綾子、小村　健: Segmental osteotomyおよび上顎洞底挙上を併施した顎裂骨移植術. 第32回 日本口蓋裂学会総会　2008年5月28-29日　広島市
7. 今泉史子、森田圭一、根岸綾子、小村　健: 永久歯多数歯欠損を認めるEEC症候群の2例. 第32回日本口蓋裂学会総会 2008年5月28-29日　広島市
8. 田中香衣、小村　健、原田浩之、生田　稔、富岡寛文:顎骨に発生したランゲルハンス細胞組織球症の3例. 第32回 日本頭頸部癌学会総会　2008年6月12-13日　東京
9. 原田浩之、小村　健、中島雄介、島本裕彰、富岡寛文、田中香衣、金親あや乃、植草　優:口腔扁平上皮癌における拡大頸部郭清術施行例の治療成績．第32回日本頭頸部癌学会総会　2008年6月12-13日　東京
10. 島本裕彰、小村　健、原田浩之、富岡寛文、田中香衣、植草　優、金親あや乃、平井秀明:下顎骨中心性扁平上皮癌の検討. 第32回 日本頭頸部癌学会総会　2008年6月12-13日　東京
11. 望月裕美、小村 健、平井秀明、澤井俊宏、栢森　高、山口　朗: 術前診断に苦慮した顎下腺海綿状血管腫の1例. 第185回 日本口腔外科学会関東地方会 2008年6月14日　さいたま市
12. 金親あや乃、島本裕彰、原田浩之、小村　健: 転移リンパ節に石灰化を認めた舌扁平上皮癌の1例. 第185回 日本口腔外科学会関東地方会　2008年6月14日　さいたま市
13. 樺沢勇司、山口　朗、小村　健、勝部憲一: 角化嚢胞性歯原性腫瘍におけるNotchおよびGliシグナルの検討. 日仏生物学会　第169回例会　2008年6月14日　東京
14. 尾崎俊文、小井田奈美、山本英輝、上條岳彦、中川原章: Plk1によるp73のリン酸化を介した制癌剤による新たな細胞死誘導の阻害機構. 第12回がん分子標的治療研究会総会 2008年6月26-27日　東京
15. 近見明子、小村　健、今井英樹、島本裕彰: 小児の下顎骨骨折に対して観血的整復固定術を施行した1例. 第10回 日本口腔顎顔面外傷学会総会 2008年7月20日　東京
16. 生田　稔、樺沢勇司、津島文彦、石井良昌、桜井仁亨、向山　仁、小村　健: 下顎骨骨折の影響因子に関する検討. 第10回 日本口腔顎顔面外傷学会総会　2008年7月20日　東京
17. 菊池　剛、樺沢勇司、佐藤　昌、佐藤百合子、樋口

佑輔、小村　健:下顎後退術後の咽頭気道形態およびIA indexの変化についての検討. 第18回 日本顎変形症学会総会　2008年6月17-18日　名古屋市

18. 角倉可奈子、高　楠旻、今井英樹、須田里香、依田　泰、宮村壽一、塚原宏泰、森田　伸、小村　健: 術後MRIにて長期経過観察を行った顎関節滑膜軟骨腫症の2例. 第21回日本顎関節学会総会　2008年7月26-27日　大阪市
19. 栗林悠里、森田圭一、植草　優、富岡寛文、伊東大典、小村　健: 口腔白板症のoligonucleotide microarrayによる遺伝子解析. 第18回日本口腔粘膜学会総会　2008年9月19-20　東京
20. 伊東大典、櫻井仁亨、佐藤　昌、栗林悠里、プラピンチャムルーン・チャーンウィット、小村　健: 当科における口腔扁平苔癬の臨床的検討. 第18回日本口腔粘膜学会総会　2008年9月19-20　東京
21. 松本佳奈子、森田圭一、神野成治、小村　健: 巨舌症に対する舌縮小術前後における舌の知覚変化. 第42回日本口腔科学会関東地方部会 2008年10月4日 東京
22. 望月裕美、小村　健、小泉　文、松島英介:手術を受ける口腔がん患者の心理特性およびQOLの経時的変化の傾向. 第21回　日本サイコオンコロジー学会総会　2008年10月9 -10日　東京
23. 森田圭一、今泉史子、根岸綾子、小村　健: 口唇裂口蓋裂患者に対する顎矯正手術に関する臨床的検討. 第53回日本口腔外科学会総会　2008年10月20-21日　徳島市
24. 平井秀明、原田浩之、小村　健: 片側頸部郭清後の嚥下動態の経時的変化. 第53回日本口腔外科学会総会　2008年10月20-21日　徳島市
25. 原田浩之、小村　健: 口腔扁平上皮癌における術前TS-1・放射線同時併用療法の臨床第I相試験. 第53回日本口腔外科学会総会　2008年10月20-21日　徳島市
26. 島本裕彰、小村　健、原田浩之、富岡寛文、田中香衣、植草　優、金親あや乃、平井秀明: 上顎骨中心性扁平上皮癌の検討. 第53回日本口腔外科学会総会　2008年10月20-21日　徳島市
27. Negishi A, Ono M, Hirohashi S, Omura K, Yamada T: Quantitative proteomics using formalin-fixed paraffin-embedded（FFPE）tissue of squamous cell carcinoma of the tongue. 第67回日本癌学会学術総会 2008年10月28-30日 名古屋市
28. 原田浩之、小村　健、中島雄介、生田　稔、島本裕彰、富岡寛文、田中香衣、金親あや乃、植草　優: 口腔癌における耳下腺リンパ節転移例の検討. 第46回日本癌治療学会総会 2008年10月30-31日 名古屋市
29. 佐藤　潔、中島雄介、島本裕彰、原田浩之、小村　健: 11歳男児の軟口蓋に生じた粘表皮癌の1例. 第186回日本口腔外科学会関東地方会 2008年11月22日 東京
30. 小村　健: 口腔癌はここまで治る. 第2回硬組織疾患ゲノムセンター・シンポジウム 2008年11月25日 東京
31. 森田圭一: 口腔癌における予防・診断・予測・治療のための分子基盤解析. 第2回硬組織疾患ゲノムセンター・シンポジウム 2008年11月25日　東京
32. 樋口佑輔、樺沢勇司、菊池　剛、佐藤　昌、青木和広、大谷啓一、小村　健: β-TCPを応用したウサギ下顎骨延長における線維芽細胞増殖因子（FGF-2）の効果. 第73回口腔病学会学術大会　2008年12月5-6日　東京
33. 工藤雅範、原田浩之、小村　健: 舌癌手術症例における構音・咀嚼機能の経時的変化. 第73回口腔病学会学術大会　2008年12月5-6日　東京
34. 松本佳奈子、島本裕彰、栢森　高、小村　健: VELscopeを用いた口腔癌スクリーニングの検討. 第73回口腔病学会学術大会　2008年12月5-6日　東京

11. 受賞

平井秀明、原田浩之、小村　健: 第53回日本口腔外科学会総会　メダルティス賞　2008年10月20-21日　徳島市
「片側頸部郭清後の嚥下動態の経時的変化.」

12. 外部資金の獲得状況

（科学研究費補助金、受託研究費、外部財団の助成など）

1. 日本学術振興会科学研究費補助金・萌芽研究
   研究題目:「含嗽液による口腔癌検診システムの開発」
   代表:小村　健
   期間:平成19-21年度
   研究費総額:320万円
2. 日本学術振興会科学研究費補助金・若手研究B
   研究題目:「熱流束を用いたオトガイ部におけるアロディニアの客観的予測法についての検討」
   代表:樺沢勇司
   期間:平成19-20年度
   研究費総額:250万円

3. 日本学術振興会科学研究費補助金・若手研究B
研究題目:「ティッシュエンジニアリングによる培養粘膜・骨膜・骨複合型バイオ人工顎骨の開発」
代表:丸川恵理子
期間:平成18-20年度
研究費総額:330万円
4. 日本学術振興会科学研究費補助金・若手研究B
研究題目:「口腔癌幹細胞同定法の確立」
代表:島本裕彰
期間:平成19-21年度
研究費総額:330万円
5. 日本学術振興会科学研究費補助金・若手研究B
研究題目:「新規半導体レーザーの開発と軟組織への応用」
代表:宮崎英隆
期間:平成19-20年度
研究費総額:330万円
6. 日本学術振興会科学研究費補助金・若手研究B
研究題目:「ビスフォスフォネート長期投与による骨髄炎モデルの確立とその骨代謝機構に対する解明」
代表:今泉史子
期間:平成20-23年度
研究費総額:330万円
7. 日本学術振興会科学研究費補助金・若手研究B
研究題目:「口腔がん顎骨浸潤における骨破壊分子メカニズムの解明」
代表:森田圭一
期間:平成20-21年度
研究費総額:320万円
8. 日本学術振興会科学研究費補助金・基盤研究C
研究題目:「TGF阻害と新規癌抗原を組み合わせた強化型口腔癌樹状細胞療法開発のための研究」
代表:伊東大典
期間:平成20-22年度
研究費総額:350万円
9. 受託研究費オリンパス
研究題目:「有機酸誘導体と生体高分子から構成される2成分系接着剤の口腔粘膜間接着に関する研究」
代表:丸川恵理子
期間:平成19年10月1日から平成21年3月31日
研究費総額:1000万円

13. 特別講演、招待講演

1. 小村　健: ビスフォスフォネートに関連する顎骨壊死. 平成19年度第4回朝霞地区歯科医師会例会, 朝霞市, 2008年2月1日
2. 小村　健: 見逃さない口腔腫瘍. 北海道医療大学歯学部同窓会学術講演会, 北海道, 2008年4月12日
3. 小村　健: ビスフォスフォネート投与患者の歯科治療における注意事項　-顎骨壊死の予防と治療-. 平成20年度文京区歯科医師会学術講演会, 東京, 2008年5月13日
4. 小村　健: Sentinel node navigation surgery for oral cancer. 内蒙古医学院, 内蒙古, 2008年5月26日
5. 小村　健: 口腔癌におけるセンチネルリンパ節ナビゲーション手術. 第69回日本核医学会関東甲信越地方会, 東京, 2008年7月5日
6. 小 村　健 : Mandibulectomy in cancer surgery. AO Craniomaxillofacial Principles Course 2008, 横 浜 , 2008年7月26日
7. 小村　健: ビスフォスフォネート製剤に関連する顎骨壊死の予防と治療, 第1回豊島区三師会合同学術講演会, 東京, 2008年10月29日
8. 小村　健: ビスフォスフォネート製剤に関連する顎骨壊死の予防と治療, 鶴見区歯科医師会講演会, 横浜 , 2008年11月13日

14. 主催学会

1. 第3回 紹介医のための口腔外科セミナー（講師:中島、原田）2008年5月18日 参加者 200名
2. C.E.D. 日常診療に活かす口腔外科の知識と基本
2008年7月6日, 17日　　東京
3. 平成20年度東京都歯科医師会卒後研修会
「口腔外科小手術の基本とリスクマネージメント」
2008年7月27日　東京　参加者 100名

15. 新聞、雑誌、TV報道

1. 小村　健: 病を知る　口腔の健康・口腔がん
日本経済新聞　2008年8月19日夕刊

16. 講座の准教授、講師、助教、特別研究員、ポスドク、指導を受けた大学院生の名前（AISSには○印）のリスト

講　師　原田浩之, 中島雄介, 桜井仁亨（～3月）
助　教　生田　稔（4月～）, 森田圭一, 樺沢勇司,
島本裕彰, 丸川恵理子, 宮崎英隆,
佐藤　昌
硬組織疾患ゲノムセンター特任講師
茂木世紀（～3月）, 伊東大典（4月～）
大学院生
七十（～3月）, 植草　優（～3月）,
佐藤百合子（～3月）, 望月裕美（～3月）,
カタウット・タチャスティラート（～9月）, 根岸綾子,
小井田奈美, 平井秀明, 樋口佑輔, 栗林悠里,
プラピンチャムルーン・チャーンウィット, 花畑泰子,
上杉篤史, 猪俣謙次, 松本佳奈子,
釘本琢磨（4月～）, 佐藤　潔（4月～）,
高橋幸伸（4月～）, 吉本光洋（4月～）

doi: 10.1111/j.1600-0714.2008.00731.x

J Oral Pathol Med
© 2009 John Wiley & Sons A/S · All rights reserved
interscience.wiley.com/journal/jop

Gene expression analysis by oligonucleotide microarray in oral leukoplakia

Yuri Kuribayashi[1], Kei-ichi Morita[1], Hirofumi Tomioka[1], Masaru Uekusa[1], Daisuke Ito[1,2], Ken Omura[1,2,3]

[1]Oral and Maxillofacial Surgery, Department of Oral Restitution, Division of Oral Health Sciences, Graduate School; [2]Department of Advanced Molecular Diagnosis and Maxillofacial Surgery, Hard Tissue Genome Research Center; [3]Grobal Center of Excellence Program, International Research Center for Molecular Science in Tooth and Bone Diseases, Tokyo Medical and Dental University, Yushima, Bunkyo-ku, Tokyo, Japan

BACKGROUND: Oral leukoplakias (LP) are the most frequent types of oral pre-cancerous lesions, but there is no accurate assessment of this malignant transformation or even genetic diagnosis of the oral epithelial dysplasia. We need to identify the new genetic diagnosis system of the epithelial dysplasia.
METHODS: Oligonucleotide microarray was used to analyze expression patterns of 29 952 genes in 10 LP patients. We compared the different gene expressions between mild dysplasia cases and severe dysplasia cases.
RESULTS: Ninety-six genes expressed differentially were selected as candidates for up-regulated in severe dysplasia. Subsequently, we further selected 16 genes with highest differentially expression. By hierarchical clustering analysis, the 10 cases were divided mild dysplasia from severe dysplasia.
CONCLUSIONS: The 16 genes are suggested as biomarker gene sets of efficacy and quickly recognized in the development of oral epithelial dysplasia.
J Oral Pathol Med (2009)

Keywords: epithelial dysplasia; gene expression; leukoplakia; microarray; oral cancer

Introduction

Oral leukoplakias (LP) are the most frequent type of oral pre-cancerous lesions; they show a variable rate of malignant transformation to oral squamous cell carcinoma (OSCC). Previous studies have shown that the overall prevalence of malignant change is 3–33% over 10 years (1). At present, there are no means of predicting with certainty the risk of cancerous transformation. Malignancy risk of LP includes clinical type, site, presence and grade of epithelial dysplasia, and smoking (2–4).

Oral epithelial dysplasia is classified as either none, mild, moderate or severe, based on histopathological findings. In addition, the grade of epithelial dysplasia seems to be an indicator for malignant development. Nevertheless, it is recognized that occasionally non-dysplastic lesions may turn into cancer, while not all dysplastic lesions become malignant (5, 6). There are several reports on the application of molecular biological markers for the assessment of cancer risk, such as heterozygosity or microsatellite instability (7–9). However, no general agreement has been reached for the use of either of them in routine diagnosis. The diagnosis of LP was still, for the most part, dependent on traditional clinico- and histo-pathological observations (10). Therefore, we need to identify the reliable biomarkers that are potential for malignant transformation (11).

The final deciphering of the complete sequencing of the human genome, together with the improvement of high throughput technologies, is causing a fundamental transformation in cancer research. Microarray analysis allows the evaluation of a large number of potential candidate genes and pathways that may be related to carcinogenesis and cervical lymph node metastasis in head and neck squamous cell carcinoma. Several studies have already demonstrated the usefulness of this technique for identifying novel cancer-related genes and predictive genes of cervical lymph node metastasis (12, 13).

To identify the new biomarkers that predict their potential for malignant transformation of LP, we initially investigated the gene expression profiles of LP that differentiate between mild dysplasia cases and severe dysplasia cases. Our study suggests that gene expression profiling by oligonucleotide microarrays could prove to be the new genetic diagnosis of the oral epithelial dysplasia and could also provide important

Correspondence: Yuri Kuribayashi, DDS, Oral and Maxillofacial Surgery, Department of Oral Restitution, Division of Oral Health Sciences, Graduate School, Tokyo Medical and Dental University, 1-5-45, Yushima, Bunkyo-ku, Tokyo 113-8549, Japan. Tel: +81 3 5803 5506, Fax: +81 3 5803 0199, E-mail: kuriosur@tmd.ac.jp
Accepted for publication October 22, 2008

information concerning the molecular mechanisms for the oral carcinogenesis.

Materials and methods

Patients and cell lines

The study subjects included 20 patients with histopathologically defined LP.

These samples had been surgically resected in the Tokyo Medical and Dental University Hospital. The male:female ratio was 13:7 and the mean age was 65.2 years. The patient clinical and pathological data was summarized in Table 1.

The histopathological assessment scoring based on the architectural and cytological changes of grading epithelial dysplasia that was described in the WHO classification was made by evaluating (14): (i) the loss of the polarity of the basal cells; (ii) the presence of more than one layer having a basaloid appearance; (iii) the increased nuclear–cytoplasmic ratio; (iv) the drop-shaped rete-ridges; (v) the irregular epithelial stratification; (vi) the increased number of mitotic figures; (vii) the mitotic figures that are abnormal in form, (viii) the presence of mitotic figures in the superficial half of the epithelium, (ix) the cellular and nuclear pleomorphism; (x) the nuclear hyperchromatism; (xi) the enlarged nucleoli; (xii) the loss of intercellular adherence; and (xiii) the keratinization of single cells or cell groups in the prickle cell layer. For each case, each pathologist recorded the grade and details of the criteria on which the decision was based. Lesions were classified as no dysplasia, mild dysplasia, moderate dysplasia, and severe dysplasia. Based on these parameters, these samples were classified into two groups: no or mild dysplasia (mild dysplasia cases, $n = 5$) and moderate or severe dysplasia (severe dysplasia cases, $n = 5$). All tissue samples were immediately snap-frozen in liquid nitrogen and stored at −80°C until use.

Table 1 Clinical and pathological data

Case	*Sex*	*Age*	*Site*	*Grading of epithelial dysplasia*
1	M	66	Tongue	Moderate
2	F	64	Upper gingiva	Moderate
3	F	54	Tongue	Moderate
4	M	76	Tongue	Moderate
5	F	76	Tongue	Severe
6	F	77	Lower gingiva	Slight
7	M	68	Lower gingiva	No
8	M	69	Tongue	Slight
9	M	37	Lower gingiva	No
10	M	71	Tongue	Slight
11	M	64	Tongue	Moderate
12	M	81	Buccal mucosa	Moderate
13	M	67	Upper gingiva	Moderate
14	F	54	Tongue	Moderate
15	M	52	Buccal mucosa	No
16	M	64	Buccal mucosa	No
17	M	66	Lower gingiva	No
18	F	54	Tongue	No
19	M	67	Tongue	Slight
20	F	76	Upper gingiva	No

Based on showing a constant expression in the internal control of the microarray analysis, we chose a Ca9-22 cell that was identified as a human squamous cell carcinoma gingival-derived cell line (15, 16).

Isolation of total RNA and microarray analysis

Total RNA was extracted from each sample by using the RNeasy mini Kit (Qiagen, Tokyo, Japan) according to the manufacture's protocol treating with DNase (Qiagen). The quality of the isolated RNA samples was routinely confirmed by examining the integrity of 28S and 18S ribosomal RNA bands using the RNA Picochip 6000 kit in a Bioanalyser (Agilent Technologies, Santa Clara, CA, USA).

Total RNA was extracted from each sample by using the RNeasy mini Kit (Qiagen) according to the manufacturer's protocol treating with DNase (Qiagen). The quality of the isolated RNA samples was routinely confirmed by examining the integrity of 28S and 18S ribosomal RNA bands using the RNA Picochip 6000 kit in a Bioanalyser (Agilent Technologies).

Total RNA from ten surgical specimens (case number 1–10) and the internal control cell line (Ca9-22) was used for oligonucleotide microarray analysis. For Two-Cycle cDNA synthesis and amplified aminoallyl antisense RNA (aRNA) synthesis, the RiboAmp™ RNA amplification kit (Arcturus, Sunnywale, CA, USA) and the amino-allyl RNA amplification kit (Sigma, Tokyo, Japan) were used. The standard protocols and reagents recommended by Sigma were used for coupling with either Cy3-UTP (the control) or Cy5-UTP (LP tissue) (Amersham Biosicences Corp, Piscataway, NJ, USA), and the labeled aRNA combining hybridization to AceGene® Human 30 K 1Chip (HitachiSoft, Hitachi, Japan). These microarray chips were scanned using GMS418 Array Scanner (BioDiscovery, El Segundo, CA, USA). The scanned Cy3 and Cy5 fluorescent signals were imported into the DNASIS Array® (HitachiSoft) and were normalized by the internal control spots including *GAPDH* and β-actin. The intensities of corresponding spots were subsequently converted into the ratios of the intensity for oral LP (Cy5) to the control (Cy3).

Semi-quantitative reverse transcriptase-polymerase chain reaction

Aliquots of total RNA from each of the seventeen samples (except in case two, in which sample a small quantity of total RNA was extracted) and the control were used in reverse transcriptase-polymerase chain reaction (RT-PCR) as the template. RT-PCR was carried out using TaKaRa Ex Taq(Takara, Shiga, Japan) and the gene-specific primers as follows: *GAPDH* sense 5′-TGCCTCCTGCACCACCAACTTGC-3′: *GAPDH* antisense 5′-AATGCCAGCCCCCAGCGTCAAAG-3′: *SLC25A11* sense 5′-TCCAAGCAGTTCTTACTGGAC-3′ and *SLC25A11* antisense the 5′-CGTAGCGGACAACTTTGAACA-3′: *TXNIP* sense 5′-TAATTGGCAGCAGATCAGGTC-3′ and *TXNIP* antisense 5′-CATTGTTGTTGAGGATGCAGG-3′: *FZR1* sense 5′-GTGCAATCTGGCCTGGTCCAA-3′ and

FZR1 antisense 5′-GGTGAAGAGGTTGAGCACA-GA-3′.

The amplification cycle for each gene fragment was in the linear range. The PCR products were then fractionated by 2% agarose gel electrophoresis followed by photography. In 18 cases, the image data processing software, imageJ, was used to digitize the intensity of each PCR product, and these values were subsequently converted into ratios of the intensity for LP tissue to the intensity for the control.

Real time reverse transcriptase – polymerase chain reaction

Aliquots of total RNA from each of the six samples and the control were used in real time reverse transcriptase-polymerase chain reaction (real time – PCR as the template. All real time – PCR reactions were performed using the Lightcycler TaqMan Master and the Universal ProbeLibrary Probes (Roche Molecular Biochemicals, Mannheim, Germany) and the gene-specific primers as follows: *GAPDH* sense 5′-AGCCACATCGCTCAGA-CAC-3′: *GAPDH* antisense 5′-GCCCAATACGACC-AAATCC-3′: *TXNIP* sense 5′-TCCCTGATACCCCA-GAAGC-3′ and *TXNIP* antisense 5′-CTTGAGAGC-CATCCATGTCA-3′: *FZR1* sense 5′-CTACCGCGTG-CTGTACCTG-3′ and *FZR1* antisense 5′-GGGTTTT-GCTAAAGACGTTCC-3′.

The comparative threshold cycle values were normalized to that of *GAPDH*, and these values were subsequently converted into ratios of the mRNA expression for LP tissue to the mRNA expression for the control.

Hierarchical clustering analysis

Following the log-transformation of the ratio (LP tissue vs. the control for each gene), we then used the clustering analysis software Expression Profiler (http://ep.ebi.ac.uk/EP/EPCLUST/), a web-based platform for microarray gene expression and other functional genomics-related data analysis, to perform hierarchical clustering analysis. The resulting expression map was visualized with Treeview using the average-linkage clustering algorithms in the same software package. Those genes that were increased in LP tissue were indicated by a red color, while those that were decreased in LP tissue were indicated by a green color. A black color indicated that those genes were not changed between LP tissue and the control.

Results

Differential gene expression profiles in leukoplakias

We identified the differential expression of the 29952 genes in 10 samples of LP analyzed using AceGene® Human 30 K 1Chip.

To identify the markers that differentiate between mild dysplasia cases and severe dysplasia cases, the candidate genes were selected on the basis of the following criteria.

If the ratios of the intensity for LP (Cy5) to the control (Cy3) were more than 2.0-fold in three or more of the five severe dysplasia cases and were < 0.5-fold in three or more of the five mild dysplasia cases, the gene was selected as a candidate. The 246 genes were selected as candidates for up-regulated in severe dysplasia. None of the down-regulated genes in severe dysplasia were selected. Then, two-group *t*-tests were used with a threshold of $P < 0.05$ and the 96 most differentially expressed genes allowing distinction of the two groups were selected. The 16 highest differentially expressed genes are extracted (Table 2). Hierarchical clustering of 96 genes resulted in a dendrogram separating mild dysplasia group from severe dysplasia group (Fig. 1a). The 16 highest differentially expressed genes are extracted (Fig. 2), and the hierarchical clustering of

Table 2 Significantly different genes between the mild dyplasia group and the severe dyplasia group

Accession number	*Name*	*Description*	*P-value*
BC003695	*KIAA1632*	Unknown (protein for image:3456134)	0.000474
NM_003562	*SLC25A11*	Solute carrier family 25 (mitochondrial carrier; oxoglutarate carrier), member 11; slc25a11	0.000539
NM_016332	*SEPX1*	Selenoprotein x, 1; sepx1	0.001503
NM_004306	*ANXA13*	Annexin a13; anxa13	0.003445
NM_000529	*MC2R*	Melanocortin 2 receptor; mc2r	0.003646
NM_004957	*FPGS*	Folylpolyglutamate synthase; fpgs	0.004753
NM_004173	*SLC7A4*	Solute carrier family 7 (cationic amino acid transporter, y+ system), member 4; slc7a4	0.005313
NM_021948	*BCAN*	Chondroitin sulfate proteoglycan behab/brevican; bcan	0.008361
AL021578	*DBNDD2*	dj453c12.4.4 (novel protein (similar to drosophila cg11753), isoform 4); dj453c12.4	0.008917
AF110465	*TCL1B*	T-cell leukemia/lymphoma 1b; tcl1b	0.009348
NM_006423	*RABAC1*	Ensembl genscan prediction AceGene oligo matches these RefSeq numbers	0.00982
D45399	*PDE6H*	cgmp phosphodiesterase gamma subunit	0.00992
BC008196	*PGAM5*	Unknown (protein for mgc:5352)	0.012351
NM_006472	*TXNIP*	Thioredoxin interacting protein; txnip	0.024796
AY007134	*CSNK1G2*	Clone cdabp0048 mrna sequence; similar to casein kinase i gamma 2 primary transcript with genbank accession number af001177.1	0.029344
NM_016263	*FZR1*	fzr1 protein; fzr1	0.035707

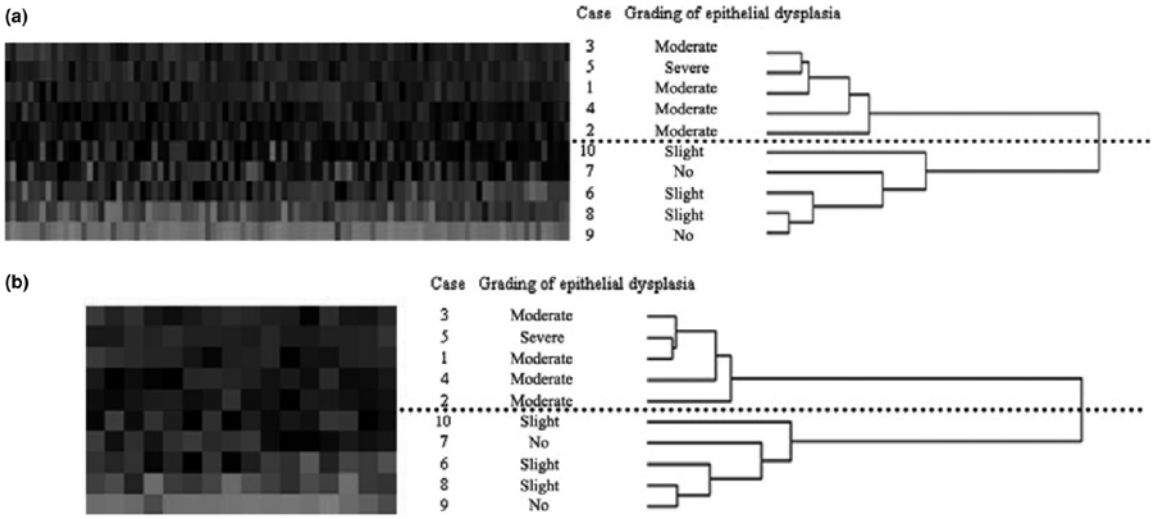

Figure 1 Hierarchical clustering based on differentially expressed genes that distinguished the mild dysplasia group from the severe dysplasis group. (a) Hierarchical clustering based on the 96 genes that distinguished the mild dysplasia group from the severe dysplasia group. (b) Hierarchical clustering based on the 16 most significantly different genes between the mild dysplasia group and the severe dyplasia group.

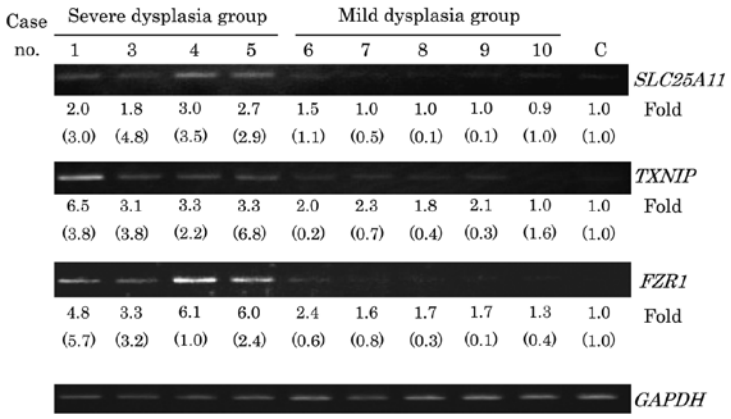

Figure 2 Validation of the expression pattern of *SLC25A11*, *TXNIP*, and *FZR1* from nine cased by semi-quantitative RT-PCR. *GAPDH* was used as a loading control. Consistent with the cDNA microarray data, the expression of *SLC25A11*, *TXNIP*, and *FZR1* genes were up-regulated in the severe dysplasia group and down-regulated in the mild dysplasia group. Arabic numerals represent fold changes of each PCR product by imageJ, and numerals in parentheses represent fold changes of microarray data by ImaGene. C, control sample with cell line (Ca9-22).

16 genes resulted in a nearly identical dendrogram (Fig. 1b).

Validation of microarray data by semi-quantitative RT-PCR and real time-PCR

To confirm these gene expression data identified by oligonucleotide microarray analysis, the three candidate genes (*SLC25A11*, *TXNIP*, and *FZR1*) were selected for RT-PCR and Real time-PCR assay. The cDNA derived from total RNA was subsequently used as a template for *GAPDH* (housekeeping gene) and the three candidate genes (*SLC25A11*, *TXNIP*, and *FZR1*). Additionally, to confirm the expression pattern of *SLC25A11*, *TXNIP*, and *FZR1*, total RNA isolated from different subset of clinical specimens (case number 11–20) was harvested for RT-PCR and real time-PCR. Consistent with case 1–10, the up and down-regulation of *SLC25A11*, *TXNIP*, and *FZR1* was also observed in different LP samples (Figs 2–4). The results of RT-PCR and real time – PCR were in accord with those of our microarray analysis, suggesting that the data obtained by our microarray gene expression analysis were valid and that these genes could potentially serve as a genetic diagnosis system.

Discussion

The ability to change our current paradigms of diagnosis and treatment of pre-malignant lesions depends in large part on the development of refined and clinically significant molecular risk markers that can assist the

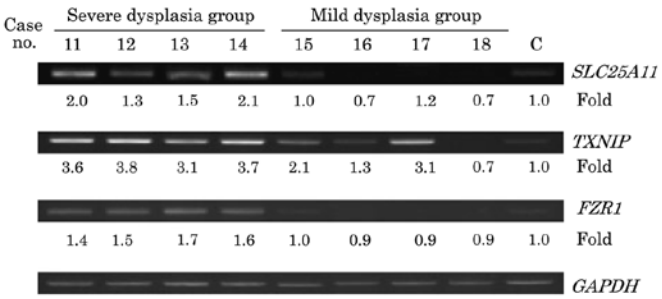

Figure 3 Validation of the expression pattern of *SLC25A11*, *TXNIP*, and *FZR1* by semi-quantitative RT-PCR. Total RNA isolated from case 11–18 was used. The expression of *SLC25A11*, *TXNIP*, and *FZR1* was consistent with case 1–10.

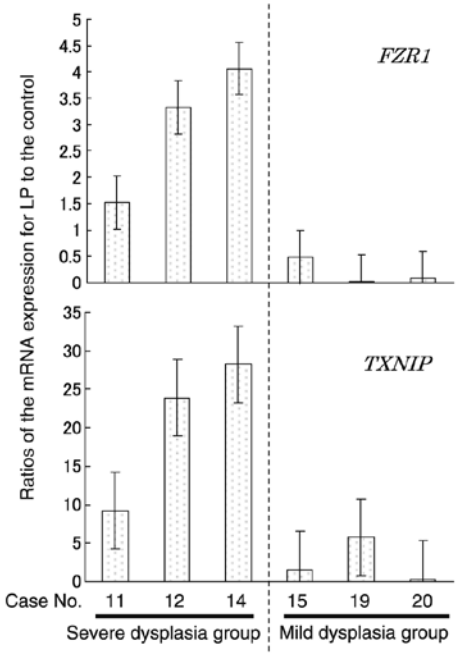

Figure 4 Validation of the expression pattern of *TXNIP*, and *FZR1* by Real time-PCR. Total RNA isolated from case 11, 12, 14, 15, 19, 20 was used. Results are the means of triplicate determinations 5 ± SD. The comparative threshold cycle values were normalized to that of *GAPDH*, and these values were subsequently converted into ratios of the mRNA expression for leukoplakias (LP) tissue to the mRNA expression for the control.

microscopic grading of oral epithelial dysplasia (17). There are a few reports that focus on oral pre-cancerous lesions by means of microarray technology.

By comparison of normal tissues with both mild and severe dysplasia, this study reveals alterations in gene expression patterns related to progression toward malignancy and include genes involved in DNA repair oxidative stress, cell adhesion/motility, cell cycle regulation and others (1). In this study, matched 'normal' epithelium may confound interpretations of gene expression changes occurring in OSCC tumorgenesis, given that histologically normal tissue samples may already harbor pre-neoplastic genetic changes that have yet to manifest phenotypically. These gene subsets might be associated with the pathogenesis and malignant transformation of oral epithelial dysplasia, but might not exactly be prediction biomarkers of cancer development.

Using cDNA microarray and RT-PCR technologies, a comprehensive gene expression profile was compared among OSCC and LP tissues (18). The *decorin* gene expression was identified using oligonucleotide microarray analysis in representive cell lines of an OSCC progression model as well as oral matched and unmatched patients (19). Through an OSCC progression model composed of cell lines, organotypic cultures, and tissue specimens, the data show that up-regulation of EMMPRIN expression occurs during the early stage of oral pre-malignancy lesions and appears to be a critical phenotypic alteration that precedes the development of OSCC (20). When the results from these studies are evaluated together, the expression of marker gene candidates may provide the role of the tumor microenvironment in oral pre-malignancy to search genetic changes.

Another study identified microarray-based transcriptional profiling as a primarily affected metabolic pathway that may be responsible for irreversible transition to progressive stages of oral cancer (21). The study also showed the protective role of these enzyme-derived metabolities in inhibiting cell proliferation using an *in vitro* oral cancer model. A molecular basis and innovative approaches for clinical intervention may prevent oral cancer progression in the future.

The ultimate goal of our study is to discover biomarkers of oral cancer progression that will provide a more accurate diagnosis. Expression profiling using oligonucleotide microarray is a useful tool in identifying tumors, in distinguishing different tumor entites, and in differentiating between progressing and non-progressing pre-malignant lesions (22). In the present study, we selected 96 differentially expressed genes of the development of oral epithelial dysplasia using the oligonucleotide microarray analysis. The expression patterns of the 96 genes could differentiate between mild dysplasia and severe dysplasia. To identify biomarker gene sets of efficacy and to quickly discriminate between the mild

dysplasia group and the severe dysplasia group, the 16 highest differentially expressed genes are extracted and we verified the expression of three genes by using RT-PCR.

In the future, on the occasion that the number of cases accumulated for the expression data using our gene sets increases and each case is observed over a long term, the data of the 10-year malignant transformation rate will be added. Additionally, to investigate into genes differentially expressed carcinogenesis using microarray, we need to designate normal tissue or OSCC tissue as samples compared with the internal control (Ca9-22).

In conclusion, our study demonstrates that the gene expression profiling that we have identified through oligonucleotide microarrays could prove to be the new genetic-diagnostic oral epithelial transformation markers and could also provide valuable information for our further understanding of the oral carcinogenesis.

References

1. Francesco C, Lorenzo LM, Adriano P, et al. Genetic portrait of mild and severe lingual dysplasia. *Oral Oncol* 2005; **41**: 365–74.
2. Holmstrup P, Vedtofte P, Reibel J, et al. Long-term treatment outcome of oral premalignant lesions. *Oral Oncol* 2006; **42**: 461–74.
3. Epstein JB, Gorsky M, Fischer D, et al. A survey of the current approaches to diagnosis and management of oral premalignant lesions. *J Am Dent Assoc* 2007; **138**: 1555–62.
4. van der Waal I, Axell T. Oral leukoplakia: a proposal for uniform reporting. *Oral Oncol* 2002; **38**: 521–6.
5. Schepman K, der Meij E, Smeele L, et al. Concomitant leukoplakia in patients with oral squamous cell carcinoma. *Oral Dis* 1999; **5**: 206–9.
6. Warnakulasuriya S. Lack of molecular markers to predict malignant potential of oral precancer. *J Pathol* 2000; **190**: 407–9.
7. Brennan M, Migliorati CA, Lockhart PB, et al. Management of oral epithelial dysplasia: a review. *Oral Surg Oral Med Oral Pathol Oral Radiol Endod* 2007; **103**(Suppl. 1): S19 e1-e12.
8. Patmore HS, Cawkwell L, Stafford ND, et al. Unraveling the chromosomal aberrations of head and neck squamous cell carcinoma: a review. *Ann Surg Oncol* 2005; **12**: 831–42.
9. Zhang L, Cheung KJ Jr, Lam WL, et al. Increased genetic damage in oral leukoplakia from high risk sites: potential impact on staging and clinical management. *Cancer* 2001; **91**: 2148–55.
10. Holmstrup P, Vedtofte P, Reibel J, et al. Oral premalignant lesions: is a biopsy reliable? *J Oral Pathol Med* 2007; **36**: 262–6.
11. Ohkura S, Kondoh N, Hada A, et al. Differential expression of the keratin-4, -13, -14, -17 and transglutaminase 3 genes during the development of oral squamous cell carcinoma from leukoplakia. *Oral Oncol* 2005; **41**: 601–13.
12. Tomioka H, Morita K, Hasegawa S, et al. Gene expression analysis by cDNA microarray in oral squamous cell carcinoma. *J Oral Pathol Med* 2006; **35**: 206–11.
13. Nguyen ST, Hasegawa S, Tsuda H, et al. Identification of a predictive gene expression signature of cervical lymph node metastasis in oral cell carcinoma. *Cancer Sci* 2007; **98**: 740–6.
14. Pindborg JJ, Reichart PA, Smith CJ, et al. Histological typing of cancer and precancer of the oral mucosa. In: Pindborg JJ, Wahl PN, eds. *World Health Organization international histological classification of tumors*, 2nd edn. Berlin Heidelberg, New York: Springer-Verlag, 1997; 551–7.
15. Yamamoto K, Konishi N, Inui T, et al. Genomic alterations in oral squamous cell carcinoma cell lines detected by two-dimensional gel analysis. *Oral Oncol* 1998; **34**: 508–12.
16. Ikuta M, Podyma KA, Maruyama K, et al. Expression of heparanase in oral cancer cell lines and oral cancer tissues. *Oral Oncol* 2001; **37**: 177–84.
17. Scott M, Lippman JS, Waun KH. Oral cancer prevention and evolution of molecular-targeted drug development. *J Clin Oncol* 2005; **23**: 346–56.
18. Kondoh N, Ohkura S, Arai M, et al. Gene expression signatures that can discriminate oral leukoplakia subtypes and squamous cell carcinoma. *Oral Oncol* 2007; **43**: 455–62.
19. Abhijit GB, Indraneel B, William ML, et al. Aberrant expression and localization of decorin in human oral dysplasia and squamous cell carcinoma. *Cancer Res* 2003; **63**: 7769–76.
20. Vigneswaran N, Beckers S, Waigel S, et al. Increased EMMPRIN expression during oral carcinogenesis. *Exp Mol Pathol* 2006; **80**: 147–59.
21. Adhijit GB, Indraneel B, Vishwanatha JK, et al. Identification of genes and molecular pathways involved in the progression of premalignant oral epithelia. *Mol Cancer Ther* 2005; **4**: 865–75.
22. Odani T, Ito D, Li MH, et al. Gene expression profiles of oral leukoplakia and carcinoma: genome-wide comparison analysis using oligonucleotide microarray technology. *Int J Oncol* 2006; **28**: 619–24.

日本経済新聞（夕刊）　2008年（平成20年）8月19日（火曜日）

夕&Eye

病を知る

口腔の健康③ 口腔がん

会話・飲食…生活への影響大きく
再建術、着実に進歩

東京医科歯科大学大学院教授
小村　健氏

口腔（こうくう）がんは、飲食や会話など日常生活にも影響が大きい。東京医科歯科大学大学院の顎（がく）口腔外科の小村健教授は治療について、「治癒率を上げるとともにQOL（生活の質）が重要」と話す。最近は失われた部分を元の状態に近づける再建手術も進歩しているという。

――口腔がんにはどんな種類がありますか。

「もっとも発生頻度が高いのは舌（ぜつ）がんで、口腔がんの約半分を占めます。次いで歯肉がんが多く、二〇％ぐらい。口腔底がんと頬（きょう）粘膜がんが各一〇―一五％で続きます。これらは狭義の口腔がんですが、広い意味では口唇がんや、唾液（だえき）をつくる組織にできる唾液腺がんもあります」

「国内患者数は推定で毎年五千―六千人。一般に中高年に多く、六十歳以上が約四〇％を占めます。最近は二十―三十歳代の若い人も増えています。男性の方が多く、女性の一・五―二倍ほどです」

――原因は何ですか。

「よく分かっていません。当たって刺激を与え続けるただ、喫煙と飲酒は大きな危険因子と考えられていま ています」

口腔がんの種類

《種　類》	《できる場所》
舌　が　ん	舌
歯肉がん	上あごと下あごの歯肉
口腔底がん	舌と歯肉の間
頬粘膜がん	ほおの内側
口　蓋　が　ん	口の中の天井部分
口　唇　が　ん	唇
唾液腺がん	口腔内にある小唾液腺、顎下（がっか）腺、舌下（ぜっか）腺など唾液をつくる組織

「がんに変化する可能性があったりする口の中の病気として白板症、紅板症、扁平（へんぺい）苔癬（たいせん）などがあります。白板症は粘膜にできる白斑で、大きさは様々。七―一〇％は十年ぐらいのうちにがん化する可能性があります。赤斑の紅板症はすでに九割方がんの状態といってもいい病変です。扁平苔癬は白いレース状で、数％ががん化する可能性があります」

――早期にはどのような症状がありますか。

「初めのうちは、しこりや腫れ、潰瘍（かいよう）がみられ、塩辛いものや刺激物がしみたり、接触痛があったりします。進行すると何もしなくても痛い自発痛があります」

「早期には自覚症状が乏しいため専門病院を訪れたときはすでに進行がんであることが多く、五年生存率は全国平均で六割ぐらいにとどまります。疑わしいものがあればすぐに専門医の診断を受けてください」

――どのような治療をしますか。

「治療法には外科手術、放射線治療、化学療法（抗がん剤）などがあり、悪性度や病期（がんの広がり）などから最適な治療法を選びます。複数を組み合わせる場合もあります。口腔がんは頸（けい）部リンパ節（首のリンパ節）にもっとも高い確率で転移を起こしますので、転移が強く疑われる場合はこれを取り除く手術もします」

「また口腔は日常生活をしていくうえで大きな働きをしており、形や外観にも関係するので、QOLと深くかかわります。治癒率を上げるとともに機能障害などを抑えることが重要です。元の状態の保存や失われた部分の再建が必要になります。例えば舌の一部を切除すると滑舌が悪くなりますので、前腕の皮膚などを移植します」

「進行がんでは広い範囲の切除が必要になることがありますが、再建術も進歩しており、遊離組織移植という手術を行っています。顕微鏡で見ながら直径数ミリメートルの血管と血管をつなぎ合わせることで、皮膚・筋肉・骨を安全、確実、またある程度自由に移植する手術です。広い範囲を切除する場合でも、従来より社会復帰しやすくなりました」

（聞き手は　編集委員　賀川雅人）

うがい後の液で早期発見可能に

口腔がんの約九〇％は口の中の粘膜から発生しており、病理組織学的には口腔扁平上皮がんと呼ぶ。小村教授らの研究グループは口をゆすいだ液で、この扁平上皮がんを早期診断する技術を開発、現在症例を増やして検証中だ。うがい液中にはがれたがん細胞に特有の遺伝子から見つけ出す手法で、早期口腔がんの九〇％以上を発見できたという。がんでない人が陽性になる例も一割ほどあるが、多人数のスクリーニングには有効とみている。

MEMO

インプラント
口腔再生医学分野

春日井 昇平

医歯学総合研究科・口腔機能再構築学系専攻
摂食機能制御学・教授

1. 研究の課題名

1) 歯科インプラントシステムの開発

(Development of dental implant system)

歯科インプラント治療は確実な治療法となっているが、治療期間が長い、侵襲性が高いという問題がある。これらの問題点を解決する目的で、骨との結合が促進されるインプラント表面の開発、骨との機械的な結合が期待できるインプラントデザイン、アバットメントとの結合部の構造について検討をおこなった。また、歯学部附属病院インプラント外来において治療を終了した患者の予後調査を継続した。

2) 骨および軟組織の再生

(Regeneration of bone and soft tissues)

骨再生に関して、骨組織に対してアナボリックに作用するsimvastatinまたはprostaglandin E1を含む骨補填材を作成し、この骨補填材が骨再生あるいはまた造成に有効に作用することが明らかになった。臨床試験においてsimvastatinを含むalpha-TCPを骨補填材として用い、その有効性を確認した。また、繊維性のhydroxyapatiteが吸収性の骨と置換する骨補填材であること、BMP-2遺伝子導入のための基材として有用であることを確認した。

2.

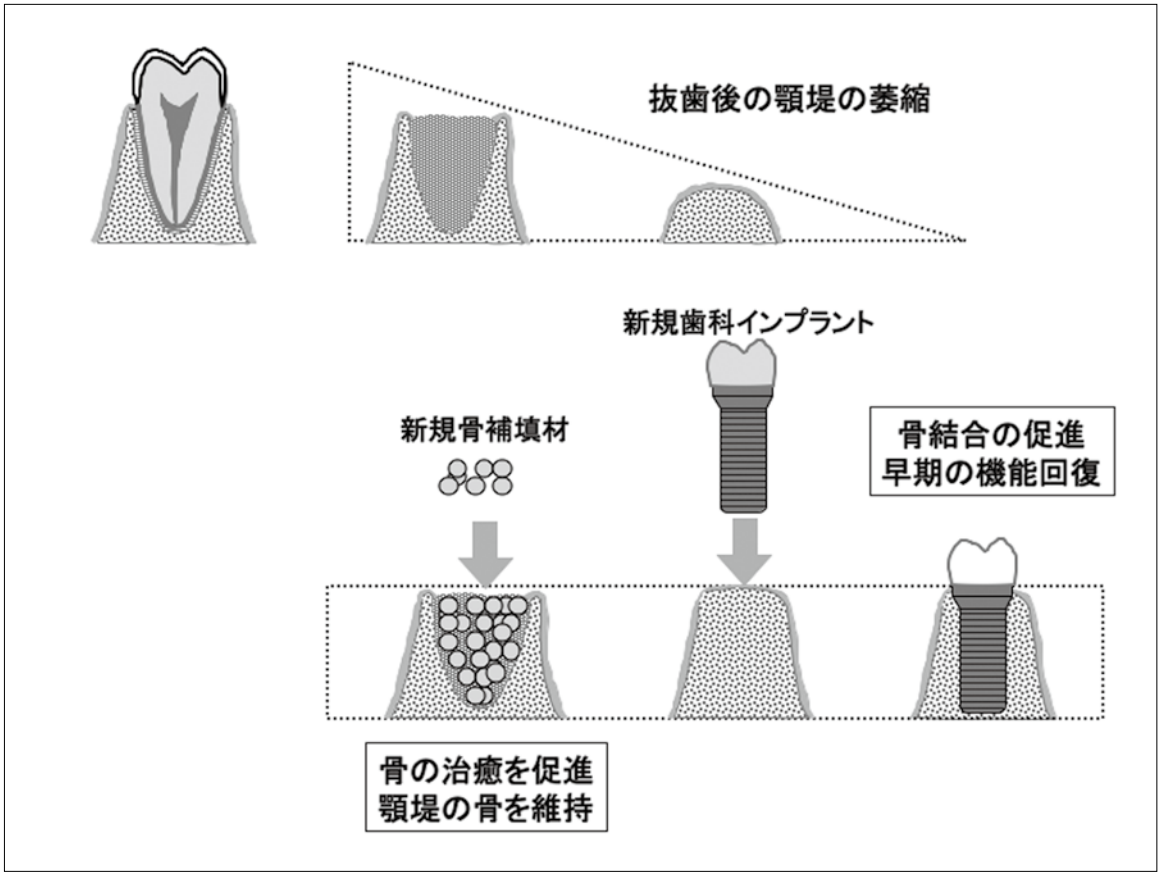

3. 2008年、2009年（平成21年3月までの）に発表した全ての研究内容についての英文要約。

Dental implant treatment is predictable and it is able to recover patients' QOL drastically; however, it requires long treatment period and invasive surgery. Furthermore, this treatment also requires bone and soft tissues for fixing an implant and esthetical outcome. To solve these problems, we conducted the following studies.

1) Development of dental implant system
We developed the surface promoting osseointegration, the design for rigid mechanical interlocking to bone and the structure for precise connection between an implant body and an abutment. We also examined the patients, who had received implant treatment in Dental Implant Clinic, Dental Hospital.

2) Regeneration of bone and soft tissues
We prepared bone substitutes containing simvastatin or prostaglandin E1, which exerts anabolic action to bone, and these bone substitutes were effective in bone regeneration and bone augmentation in animal experiments. We also proved clinically that alpha-TCP containing simvastatin was effective as bone substitute. Furthermore, we observed that fibrous hydroxyapatite material was exchangeable to bone and that it was useful as a material for BMP-2 gene transfer.

4. 本事業に関連して世界的な研究拠点形成に向けて、以下の点で改善・整備等されたこと

A（研究拠点体制）

B（研究教育環境）

C（人材確保）

D（人材育成）

E（国際化）

人材確保、人材育成、国際化:

大学院生（博士課程）あるいは専攻生を希望する海外からの学生の増加が著しい。現在、日本、韓国、台湾、中国、タイ、ミャンマー、インド、ヨルダン、エジプト、リビアの10ヶ国の異なる国籍の学生が所属しており、さらに本年4月よりドミニカ共和国とアルゼンチンからの留学生が加わる予定である。大学院を修了して母国へ帰国した2名は、タイおよび台湾の大学でAssistant Professorとして採用された。研究室のセミナーにおける発表とディスカッションは全て英語でおこなっている。

5. 英文原著論文

1 Kobayashi H, Katakura O, Morimoto N, Akiyoshi K, Kasugai S. Effects of cholesterol-bearing pullulan（CHP）-nanogels in combination with prostaglandin E1 on wound healing. Journal of Biomedical Material Research, Part B: Applied Biomaterials, in press

2 Oda M, Kuroda S, Kondo H, Kasugai S. Hydroxyapatite fiber materialwith BMP-2 gene induces ectopic bone formation. Journal of Biomedical Material Research, Part B: Applied Biomaterials, in press

3 Nyan M, Sato D, Kihara H, Machida T, Ohya K, Kasugai S. Effects of the combination with alpha-tricalcium phosphate and simvastatin on bone regeneration. Clinical Oral Implant Research, in press

4 Samee M, Kasugai S, Kondo H, Ohya K, Shimokawa H, Kuroda S. BMP-2 and VEGF transfection to human periosteal cells enhances osteoblast differentiation and bone formation. Journal of Pharmacological Sciences 108（1）:18-31, 2008

5 Iino G, Hishimura K, Omura K, Kasugai S. Effects of prostaglandin E1 application on rat incisal sockets. Int J Oral Maxillofac Implants 23（5）:835-40, 2008

6 Kaneda K, Kuroda S, Goto N, Sato D, Ohya K, Kasugai S. Is Sodium Alginate an Alternative Hemostatic Material in the Tooth Extraction Socket? Journal of Oral Tissue Engineering 5（3）:127-133, 2008

7 Ito Y, Sato D, Yoneda S, Ito D, Kondo H, Kasugai S. Relevance of resonance frequency analysis to evaluate dental implant stability: Simulation and histomorphometrical animal experiments. Clinical Oral Implant Research 19（1）:9-14, 2008

8 Yokoyama Y, Damrongrungruang T, Kuroda S, Takano Y, Ohya K, Kasugai S and Kondo H. Comparative analysis of gene expression by cDNA microarray between cementoblasts and periodontal ligament cells in the murine mandible. The Journal of Oral Bioscience 50（3）: 183-193, 2008

6. 著書

1 春日井昇平.歯科領域における再生・再構築医療のためのバイオマテリアル　骨形成を促進する化合物を含む吸収性骨補填材.バイオマテリアル 26（3）:13-18, 2008

2 春日井昇平.歯周病研究の新展開と治療戦略　スタチンを用いた歯槽骨再建.炎症と免疫16（2）:201-206, 2008

3 春日井昇平、清水勇気.文献から見たピエゾサージェリー.Quitessence Dental Implantology 15（6）:22-27, 2008

4 春日井昇平.インプラント手術をマスターするための関連機材マニュアル　診断機材からピエゾサージェリーまで （春日井昇平、古賀剛人、嶋田淳　編）、クインテッセンス出版、2009

5　春日井昇平.欠損補綴のオプション　インプラント治療.現代のパーシャルデンチャー（野首孝祠、五十嵐順正　編）、クインテッセンス出版、pp109-118, 2008
6　春日井昇平.口腔における再生医療.口と歯の事典（高戸毅、天笠光雄、葛西一貴、古郷幹彦、須佐見隆史、鈴木茂彦、谷口尚、新美成二　編）、朝倉書店、pp394-404, 2008

7. 平成21年3月までの自己評価

我国のインプラント治療とそれに関連する臨床医学は、欧米に10年以上遅れてスタートした。現在我々の治療技術は世界のトップレベルと遜色無いレベルに到達している。また、インプラントシステムの開発と、骨補填材の開発は順調に進捗している。我々の開発した骨補填材発表は、2009年2月の米国のインプラント学会でClinical Innovation Awardを受賞した。このように研究成果の臨床へのフィードバックがおこなわれている点は高く評価できる。

8. 学会発表（英文）

1　Ueno N, Sato D, Nyan M, Kondo H, Kasugai. Bone substitute of alpha-TCP containing simvastatin: Clinical study. The 24th Annual Meeting of Academy of Osseointegration 口頭2009.2.26-28 Convention Center, San Diego, USA
2　Kasugai S. IT-based safe, simple and predictable implant treatment. International Symposium 第21回日本歯科医学会総会　口頭2008.11.14-16 パシフィコ横浜　横浜
3　Kasugai S. Immediate protocol in dental implant treatment: Keys to avoid failures in this attractive protocol. Invited Lecture Annual Meeting of Thai Dental Implant Society 口頭2008.10.23-25 Landmark Bangkok Hotel, Bangkok, Thailand
4　Kasugai S. Dental implant treatment in the near future: Prosthesis or regeneration?　特別講演　第4回日中歯科医学会　口頭2008.9.27-29　西安　中華人民共和国
5　Kon K, Shiota M, Ozeki M, Kimura J, Kasugai S. Particle size effect on augmented bone volume in autologous graft. The 17th Annual Scientific Meeting of European Association of Osseointegration 示説2008.09.18-20 PKIN Convention Center, Warsaw, Poland
6　Nyan M, Kihara H, Machida T, Ueno H, Kasugai S. Combination with alpha-tricalcium phosphate and simvastatin stimulates bone regeneration. The 17th Annual Scientific Meeting of European Association of Osseointegration 示説2008.09.18-20 PKIN Convention Center, Warsaw, Poland
7　Yamaguchi Y, Tachikawa N, Kondo H, Ichinose S, Kasugai S. Analysis of fractured commercially pure titanium implants. The 17th Annual Scientific Meeting of European Association of Osseointegration 示説2008.09.18-20 PKIN Convention Center, Warsaw, Poland
8　Kasugai S. Immediate function vs. conventional protocol. Esthetic Forum Bali　口頭20085.2-4　Grand Hyatt Bali, Bali, Indonesia
9　Sato M, Fujii S, Amagasa T, Kasugai S. Hydoroxyapatite fiber material as bone substitute: Clinical study for sinus elevation. The 23rd Annual Meeting of Academy of Osseointegration 示説2008.2-28-3.1 The Hynes Convention Center, Boston, USA
10 Kasugai S, Ochi M, Shiota M, Hirose Y, Tachikawa N, Kuniyasu H, Kondo H, Matubara H, Kuroda S, Taira H, Hujimori T, Murata M, Kitajo H, Kusano K. Clinical trial of thin hydroxyapatite-coated one-piece implant. The 23rd Annual Meeting of Academy of Osseointegration 示説2008.2-28-3.1 The Hynes Convention Center, Boston, USA
11 Kasugai S. Bone substitute in dental implant treatment. 口頭2008.1.7 Khonkaen University, Thailand

9. 学会発表（和文）

1. 春日井昇平.骨形形成を促進する化合物を含む吸収性骨補填材.日本バイオマテリアル学会シンポジウム2008　2008.11.17-18　東京大学　東京
2. 藤森達也, 塩田　真, 春日井昇平, 近藤尚知, 鬼原英道, 佐藤大輔.　ITを用いたインプラント埋入外科手術の精度について.第21回日本歯科医学会総会　2008.11.14-16　パシフィコ横浜　横浜
3. 清水勇気, 春日井昇平, 立川敬子, 金井　亨.　超音波骨切削器具の組織学的研究.第21回日本歯科医学会総会　2008.11.14-16　パシフィコ横浜　横浜
4. 春日井昇平.インプラント治療のトレンドとAcademy of minimally-invasive Implantology（AMII）の研究会発足.AMII第1回Conference　2008.11.15　ランドマークホール　横浜
5. 春日井昇平.　インプラント治療の進歩と低出力超音波刺激装置（LIPUS）への期待.　LIPUSセミナー　2008.10.5　新宿NSビル　東京
6. 春日井昇平.EBMとガイドライン.インプラント治療のガイドラインのためのエビデンス　どのような考え方が提唱されてきたか　シンポジウム　第38回日本口腔インプラント学会学術大会　2008.09.12-14　東京フォーラム　東京
7. 川勝敦子、宗像源博、大庭容子、塩田真、立川敬子、春日井昇平.上顎臼歯欠損部の骨形態に関する検討.シンポジウム　第38回日本口腔インプラント学会学術大会　2008.09.12-14　東京フォーラム　東京

8. 町田哲、丸尾勝一郎、佐藤仁、春日井昇平.繊維性ハイドロキシアパタイト材料がラット抜歯窩治癒に及ぼす影響:放射線学的評価.シンポジウム　第38回日本口腔インプラント学会学術大会　2008.09.12-14　東京フォーラム　東京
9. 大藪祐子、塩田真、森川俊彦、黒田真司、近藤尚知、立川敬子、春日井昇平.糖尿病患者へのインプラント治療.シンポジウム　第38回日本口腔インプラント学会学術大会　2008.09.12-14　東京フォーラム　東京
10. 小林裕史、近藤尚知、黒田真司、立川敬子、塩田真、春日井昇平.当科におけるインプラント脱落に関する調査.シンポジウム　第38回日本口腔インプラント学会学術大会　2008.09.12-14　東京フォーラム　東京
11. 藤森達也、塩田真、春日井昇平、作山葵.超薄膜ハイドロキシアパタイトコーティングインプラント周囲における新生骨形成:ビーグル犬における早期負荷の組織観察.シンポジウム　第38回日本口腔インプラント学会学術大会　2008.09.12-14　東京フォーラム　東京
12. 春日井昇平.骨形成促進作用を示す骨補填材.シンポジウム　Periodontal Tissue Engineeringの現状と将来展望.第29回日本炎症・再生医学会　2008.7.8-10都市センターホテル　東京
13. 春日井昇平.歯科インプラント治療と再生医療の融合.第7回日本再生医療学会総会　2008.3.13-14　名古屋国際会議場
14. 塩田真、木村純一、大藪祐子、今一裕、春日井昇平.インプラント上部構造に応用した陶材の破折について　第27回日本口腔インプラント学会関東・甲信越支部学術大会　2008.2.3-4　都市センター　東京
15. 藤森達也、作山葵、塩田真、春日井昇平.血液供給不足部位へのVEGFの応用による血管ならびに骨新生に関する組織学的研究.第27回日本口腔インプラント学会関東・甲信越支部学術大会　2008.2.3-4　都市センター　東京
16. 北爪孝昌、塩田真、大庭容子、立川敬子、近藤尚知、黒田真司、春日井昇平.当科新来患者の中でインプラント治療に到った患者の内訳.第27回日本口腔インプラント学会関東・甲信越支部学術大会　2008.2.3-4　都市センター　東京
17. 長田紀子、塩田真、大庭容子、北爪孝昌、寺前智人、近藤尚智、立川敬子、春日井昇平.東京医科歯科大学歯学部附属病院インプラント外来における無歯顎患者の治療動向.　第27回日本口腔インプラント学会関東・甲信越支部学術大会　2008.2.3-4　都市センター　東京
18. 森川俊彦、近藤尚知、立川敬子、大庭容子、北爪孝昌、塩田真、春日井昇平.インプラント患者の有病率について.第27回日本口腔インプラント学会関東・甲信越支部学術大会　2008.2.3-4　都市センター　東京

10. 受賞

Clinical Innovation Award, The 24th Annual Meeting of Academy of Osseointegration, San Diego, USA 2009年2月27日“Ueno N, Sato D, Nyan M, Kondo H, Kasugai. Bone substitute of alpha-TCP containing simvastatin: Clinical study.”

11. 外部資金の獲得状況

(科学研究費補助金、受託研究費、外部財団の助成など)

科学研究費補助金 基盤B
研究題目:歯科領域における骨補填材の適正化
代表:春日井昇平
期間:平成19-21年
研究費総額:1,650万円

科学技術新興機構委託開発事業
研究題目:スタチンを用いた骨増加材
代表:春日井昇平
期間:平成17-23年（平成17-20年でであったが延長された）
研究費総額:1億2500万円

科学研究費補助金　基盤C
研究題目:生分解性ポリマーステントを利用した口腔軟組織再建
代表:立川敬子
期間:平成20-22年
研究費総額:376万円

科学研究費補助金 萌芽研究
研究題目:エンヴェロープベクターとsiRNAを応用した歯周組織再生療法
代表:近藤尚知
期間:平成18-20年
研究費総額:330万円

科学研究費補助金　萌芽研究

研究題目:粘膜・骨再生法による、新しい口蓋瘻孔閉鎖の試み
代表:黒田真司
期間:平成20-22年
研究費総額:340万円

科学研究費補助金　若手研究B
研究題目:新規骨補填剤による骨新生に関する基礎的研究
代表:鬼原英道
期間:平成19-20年
研究費総額:362万円

科学研究費補助金　若手研究B
研究題目:Msx1遺伝子の調節エレメントの解析
代表:中田秀美
期間:平成20-21年
研究費総額:399万円

科学研究費補助金　若手研究（スタートアップ）
研究題目:ソノポレーション法による骨膜への遺伝子導入
代表:金井亨
期間:平成19-20年
研究費総額:309万円

12. 特別講演、招待講演

1. 春日井昇平.歯科インプラント治療における治療期間の短縮.第22回歯科チタン学会学術講演会　特別講演　　日本大学理工学部　2009.02.14　東京
2. 春日井昇平.即時荷重、即時埋入の落とし穴.プラトンミーティング大阪　200811.30　ホテルコスモスクエア国際交流センター　大阪
3. 春日井昇平.骨形形成を促進する化合物を含む吸収性骨補填材.日本バイオマテリアル学会シンポジウム2008　2008.11.17-18　東京大学　東京
4. Kasugai S. IT-based safe, simple and predictable implant treatment. International Symposium 第21回日本歯科医学会総会　2008.11.14-16　パシフィコ横浜　横浜
5. 春日井昇平.インプラント治療のトレンドとAcademy of minimally-invasive Implantology（AMII）の研究会発足.AMII第1回Conference　2008.11.15　ランドマークホール　横浜
6. Kasugai S. Immediate protocol in dental implant treatment: Keys to avoid failures in this attractive protocol. Invited Lecture Annual Meeting of Thai Dental Implant Society 2008.10.23-25 Landmark Bangkok Hotel, Bangkok, Thailand
7. Kasugai S. Dental implant treatment in the near future: Prosthesis or regeneration?　特別講演　第4回日中歯科医学会　2008.9.27-29　西安　中華人民共和国
8. 春日井昇平.EBMとガイドライン.インプラント治療のガイドラインのためのエビデンス　どのような考え方が提唱されてきたか　シンポジウム　第38回日本口腔インプラント学会学術大会　2008.09.12-14　東京フォーラム　東京
9. 春日井昇平.　即時過重、即時埋入の落とし穴.　プラトンセミナー2008　2008.7.27　パシフィコ横浜　横浜
10. 春日井昇平.骨形成促進作用を示す骨補填材.シンポジウム　Periodontal Tissue Engineeringの現状と将来展望.第29回日本炎症・再生医学会　2008.7.8-10都市センターホテル　東京
11. Kasugai S. Immediate function vs. conventional protocol.　Esthetic Forum Bali　2008 5.2-4　Grand Hyatt Bali, Bali, Indonesia
12. 春日井昇平.歯科インプラント治療と再生医療の融合.第7回日本再生医療学会総会　2008.3.13-14　名古屋国際会議場

13. 主催学会

1. 第1回AMII
（Academy of minimally invasive Implantology、MII研究会）　2008.11.13 横浜（大会長）

14. 新聞、雑誌、TV報道

1　フジテレビ　ニュースJAPAN 「歯科インプラント治療の光と影」 2009年2月13日
2　週間朝日 「名医の最新治療　患者の希望が急増、認定専門医も500人に　インプラント（人工歯根）」 2008年11月28日
3　新聞　クイント 「歯科医療におけるピエゾサージェリーの有用性　より安全なインプラント治療を目指して」 2008年11月10日
4　新聞　クイント 「知っておきたい!　専門外来 vol.9　東京医科歯科大学附属病院インプラント外来」

2008年10月10日

15. 講座の准教授、講師、助教、特別研究員、ポスドク、指導を受けた大学院生の名前（AISSには○印）のリスト

准 教 授: 塩田真

講　　師: 立川敬子

助　　教: 近藤尚知

助　　教: 黒田真司

大学院生: 尾関　真帆、今　一裕、町田　哲、
丸尾　勝一郎、上野　憲秀、朴　浚喜、
○Myat　Nyan、
○Hudieb, Malik Ismail、木村　純一
伊達　佑生、○則武　加奈子、
Rojbani, Hisham Khalifa
○Reena Rodriguez、
Srilatha Bhargava、○郝　佳
秋野　徳雄、永山　友子、藤井　政樹、
古市　祥子、Osama Zakaria

歯髄生物学分野

須田 英明

医歯学総合研究科・口腔機能再構築学系専攻
歯髄生物学・教授

1. 研究の課題名

●歯髄組織の再生に関する研究

Tissue engineering of dental pulp

●低出力レーザーを用いた象牙芽細胞に対する分子生物学的研究

Molecular biological analysis on odontblasts by using low-level laser therapy

●神経ペプチドと根尖部免疫担当細胞の動態に関する研究

The analysis of immune-cells activated by neuropeptide VIP in peiapical lesions

●歯髄組織の再生に関する研究

血間内皮細胞の血管新生能および幹細胞の分化能に着目し、抜去歯の歯髄腔内に歯髄組織を再生させることを目的として検索を行っている。

具体的には

1) 歯および歯周組織の有する免疫防御機構に対する免疫組織化学・分子生物学的検索。
2) 抜去歯内に実験的に作製した歯髄様組織に対する幹細胞への象牙芽細胞など歯髄特有の細胞への分化を誘導する象牙質からの分子シグナルの免疫組織化学・分子生物学的検索。
3) 動物実験において、幹細胞を移植し再生した歯髄を免疫組織化学・分子生物学的に検索する。この実験に伴い幹細胞を歯髄腔内に安全に設置する方法の検索も行う（流動的足場材料の開発・インジェクションタイプの足場設置法の開発など）。

これまでの研究からin vivoにおいて、ヒト抜去歯の歯髄組織に極めて類似した組織を世界で初めて再生できることを報告した。

●低出力レーザーを用いた象牙芽細胞に対する分子生物学的研究

培養象牙芽細胞に低出力レーザーを照射し、レーザーによる創傷治癒促進効果等の生物学的効果について分子生物学的に検討を行っている。また線維芽細胞あるいは骨芽細胞の接着能についてレーザー照射の効果を形態学的に観察している。

●神経ペプチドと根尖部免疫担当細胞の動態に関する研究

神経ペプチドが根尖部免疫担当細胞の動態を制御している可能性を示唆する所見がこれまでの研究で得られている。さらにそのメカニズムの一端を明らかにする目的で、神経ペプチドの一つであるVIPがTh17活性化と関与する可能性について検討を行っている。Th17は炎症性骨吸収に関連すると報告されており、われわれはTh17関連サイトカインが根尖病変において顕著に産生されている所見をすでに得ている。今後、VIPをはじめとする神経ペプチドとTh17との関連を中心に解析を行っていく予定である。

2.

3. 2008年,2009年（平成21年3月までの）に発表した全ての研究内容についての英文要約

● Tissue engineering of dental pulp

A tissue engineering-based approach that results in new pulp tissue could potentially allow for the completion of vertical and lateral root development and, perhaps, prevent the premature loss of these teeth. In this point of view, we performed biological analysis. We have recently informed that dental pulp-like tissue in which poly-L（lactic）acid（PLLA）scaffolds were manufactured in the root canal of tooth slices sectioned from teeth. These works strongly suggests that exfoliated deciduous teeth constitute a viable source of stem cells for dental pulp tissue engineering.

● The effect of low level laser therapy on osteoblast maturation and signal transduction by evaluating integrin expression.

The aim of this study is to evaluate the effect of low level laser therapy on osteoblast cell maturation through integrin expression, playing important role in cell proliferation, migration, and cell mobility and to show how LLLT effect on healing process in cellular level. The mesenchymal stromal cells which show a strong tendency to differentiate into osteoblasts are cultivated in alpha modified MEM medium with energy density of low level laser. Cell proliferation is analyzed 24 hrs after the laser irradiation. Non-irradiated cells were served as control. Protein expression especially ß1-integrin and fibronectin expressions during successive irradiation are assessed by means of immunohistochemistry and Western blotting.

● The analysis of immune-cells activated by neuropeptide VIP in peiapical lesions

The main powers in the periapical defense system are macrophages and dendritic cells　Following the progress of pulpal inflammation, the periapical tissue became the defense line against bacterial invasion. The influx of macrophages into the periapical area at the beginning of periapical inflammation induces the production of cytokines synthesis, which would induce periapical bone destruction. Initiation of the anti inflammatory cytokine synthesis should be a sign of transition from“acute”to“chronic”. Therefore, the balance between pro-inflammatory and antiinflammatory cytokines should be the point on the progress of periapical lesions.　Our recent data suggests that the interaction between a cytokine th17 from immune cells and a neuropeptide VIP may be concerned with activation of immune cells. In this point of view, we performed molecular biological analysis.

4. 本事業に関連して世界的な研究拠点形成に向けて,以下の点で改善・整備等されたこと

A（研究拠点体制）

医局員および関係者に対する研究目的および趣旨の周知徹底を行っている。さらに、連携された研究組織の構築。趣旨に沿った研究指導とするための指導教員の選定、ユニークかつ最先端の研究テーマの選定を行い、また研究発表会の実行など研究の進展状況を把握し、きめ細かな指導を実施している。

B（研究教育環境）

研究課題ごとに 、論文抄読会、研究発表会などが随時開催され、研究の進展状況を 把握するとともに、さらなる研究成果を目指し指導が行われている。

C（人材確保）

海外との研究機関と研究協力体制を深めるとともに、諸外国からの留学生を積極的に受入れ、より優秀な若手研究者の育成を目指し、人材確保を行っている。

D（人材育成）

AISS制度を積極的に活用し、留学生を含め、研究中心に専念できる環境を構築しつつある。

E（国際化）

歯髄生物学における基礎・臨床を含めた世界一線級の成果を挙げることに務め、歯内治療学研究の向上による国際社会への貢献に関与している。これらの研究成果は、国際学術専門誌に発表されている。

5. GCOE事業を推進するに当たって力を入れた点

研究水準および研究の成果に関する目標、そして研究の実施体制等の整備を行い、先端的かつユニークな歯髄生物学分野における研究、バイオサイエンス、テクノロジー分野において国際レベルかつ最先端の研究の研究を行い、国際的発信能力を有し、国際レベルの研究拠点を形成できる研究者および先端的分野の開拓・発展を担う高度専門医療人の育成を目指し、GCOE事業の推進に務めている。

6. 英文原著論文

1. Kawamura-Hagiya Y, Yoshioka T, Suda H.
   Logistic regression equation to screen for vertical root fractures using periapical radiographs.
   Dentomaxillofacial Radiology 37（1）:28-33,2008
2. Kaneko T, Okiji T, Kaneko R, Suda H.
   Characteristics of resident dendritic cells in different regions of the rat periodontal ligament.
   Cell and Tissue Research 331（2）:413-421,2008
3. Kaneko T, Okiji T, Zhao L, Esgeurra R, Suda H.
   Heterogeneity of dendritic cells in rat apical periodontitis.
   Cell and Tissue Research 331（3）: 617-623,2008
4. Kaneko T, Okiji T, Kaneko R, Nor JE, Suda H.
   Antigen presenting cells in radicular granulomas.
   Journal of Dental Research 87（6）: 553-557,2008
5. Cordeiro M, Dong Z, Kaneko T, Zhang Z, Miyazawa M, Songtao S, Smith AJ.
   Dental pulp tissue engineering with stem cells from exfoliated deciduous. Journal of Endodontics 34（8）: 962-969,2008
6. Kabasawa Y, Nagumo K, Takeda Y, Kawashima N, Okada N, Omura K, Yamaguchi A, Katsube K.
   Amelogenin positive cells scattered in the interstitial component of odontogenic fibromas. Journal of Clinical Pathology 61: 851-855,2008
7. Sasaki H, Suzuki N, Kent R, Kawashima N, Takeda J, Stashenko P.
   T Cell response mediated by myeloid cell-derived IL-12 is responsible for porphyromonas gingivalis-Induced periodontitis in IL-10-deficient mice. Journal of Immunology 180: 6193-6198,2008
8. Leshem O, Kashino S, Goncalves R, Suzuki N, Onodera M, Fujimura A, Sasaki H, Stashenko P, Campos-Neto A.
   Th1 biased response to a novel Porphyromonas gingivalis protein aggravates bone resorption caused by this oral pathogen.
   Microbes and Infection 10: 664-672,2008

7. 著書

1）Kawashima N, Suda H: Immunopathological Aspects of Pulpal and Periapical Inflammations. Essential Endodontology - Prevention and Trearment of Apical Periodontitis: Blackwell Munksgaard, 2nd ed.; 44-80,2008.

2）和達礼子:第Ⅱ章 非ステロイド性抗炎症薬（NSAIDs）1. 非ステロイド性抗炎症薬（NSAIDs）を使用するとき.納得!歯科適応薬の相互作用-歯科治療の安全のために:ヒョウロン・パブリッシャーズ;104-109,2008.

3）須田英明,川島伸之（編集委員）:ステッドマン医学大辞典　改訂第6版:メジカルビュー社,2600ページ,2008.

4）須田英明,興地隆史,五味博之,林正規（編）:臨床歯内療法　器材・薬剤・テクニックのコンビネーション:デンタルダイヤモンド増刊号, 161ページ,2008.

5）海老原新:歯内療法におけるCT診断.臨床歯内療法　器材・薬剤・テクニックのコンビネーション:デンタルダイヤモンド増刊号;14-19,2008.

6）須田英明:根管形成を行うための前準備.臨床歯内療

法　器材・薬剤・テクニックのコンビネーション:デンタルダイヤモンド増刊号;42-45,2008.
7）和達礼子:根管洗浄の現在.臨床歯内療法　器材・薬剤・テクニックのコンビネーション:デンタルダイヤモンド増刊号;68-73,2008.
8）菊地和泉:根管貼薬の必要性.臨床歯内療法　器材・薬剤・テクニックのコンビネーション:デンタルダイヤモンド増刊号;74-79,2008.
9）石村　瞳:新しい根管充填材料-接着性根管充填シーラーについて.臨床歯内療法　器材・薬剤・テクニックのコンビネーション:デンタルダイヤモンド増刊号;104-107,2008.
10）須田英明:歯根破折への対応.臨床歯内療法　器材・薬剤・テクニックのコンビネーション:デンタルダイヤモンド増刊号;138-139,2008.
11）須田英明:瘻孔が消えない.臨床歯内療法　器材・薬剤・テクニックのコンビネーション:デンタルダイヤモンド増刊号;148-149,2008.
12）須田英明:水酸化カルシウム粉末は空気中の二酸化炭素と反応して,容易に炭酸カルシウムに変化するのか?臨床歯内療法　器材・薬剤・テクニックのコンビネーション:デンタルダイヤモンド増刊号;154-155,2008.
13）川島伸之:パラホルムアルデヒドの為害作用.臨床歯内療法　器材・薬剤・テクニックのコンビネーション:デンタルダイヤモンド増刊号;160-161,2008.
14）須田英明:歯周病を治すにはプラークコントロールが最も効果的.　暮らしと健康:保健同人社 月刊版（2008/8/2）;73,2008.
15）須田英明,恵比寿繁之,川崎孝一,中村洋,林善彦,前田勝正（編）:エンドドンティックス21　歯内療法カラーアトラス　:400ページ,永末書店,2008.
16）池田英治,須田英明:5. 偶発事故への対応,11. その他.エンドドンティック21歯内療法カラーアトラス:永末書店;70-85,186-194,2008.
17）吉岡隆知,須田英明:10. 外科的歯内療法,11. その他.エンドドンティック21歯内療法カラーアトラス:永末書店;158-171,183-185,195-199,2008.
18）海老原新,須田英明:臨床編　歯内療法領域「総論:歯内療法領域におけるレーザーの現状と可能性」:症例でみる歯科用レーザーの有効活用-CO_2レーザー,Nd:YAGレーザー,Er:YAGレーザー,半導体レーザーを網羅-:ヒョウロン・パブリッシャーズ増刊号;24-25,2008.
19）海老原新,須田英明:臨床編　歯内療法領域「レーザーの歯髄への影響と安全性:基礎研究」:症例でみる歯科用レーザーの有効活用-CO_2レーザー,Nd:YAGレーザー,Er:YAGレーザー,半導体レーザーを網羅-:ヒョウロン・パブリッシャーズ増刊号;26-27,2008.
20）竹田淳志,須田英明:臨床編　歯内療法領域「根管内異物除去　Nd:YAGレーザーを用いて」:症例でみる歯科用レーザーの有効活用-CO_2レーザー,Nd:YAGレーザー,Er:YAGレーザー,半導体レーザーを網羅-:ヒョウロン・パブリッシャーズ増刊号;40-41,2008.
21）須田英明:東京医科歯科大学.卓越する大学 2009年度版:大学通信;138-139,2008.

8. 平成21年3月までの自己評価

研究成果は、8件の海外学術専門雑誌,13件の国内雑誌に発表され、それぞれ国際的高い評価を得ている。そのうち2件は、それぞれJournal of Dental Research,Journal of Endodonticsと、歯科において最も高インパクトファクターを有する雑誌の表紙をハイライトとして飾った。

9. 和文原著論文

1）吉岡隆知,石村 瞳,萩谷洋子,須田英明,大林尚人,倉林 亨.
歯科用顕微鏡下での根管探索における歯科用CTの有用性 ―上顎第一大臼歯近心頬側根の舌側根管の探索―.
日本歯内療法学会雑誌 29（1）:9-14,2008
2）石村 瞳,福元康恵,菊地和泉,吉岡隆知,高橋英和,須田英明.
ガンマ線照射が根管治療に及ぼす影響　―根管洗浄効果および根管充填の封鎖性について―.
日本歯科保存学雑誌 51（2）:138-146,2008
3）安生智郎,渡辺 聡,三枝英敏,海老原新,須田英明.
Er:YAGレーザー照射による根管内消毒効果に関する研究.
日本レーザー歯学会誌 19（2）:58-63,2008
4）池田英治,須田英明.
歯内治療に関連する慢性痛（侵害受容性疼痛と神経因性疼痛）について.
日本歯内療法学会雑誌 29（2）:107-112,2008
5）須田英明.
歯科における臨床実習の国際比較.
日本歯科医学教育学会雑誌 24（2）:15-20,2008
6）萩谷洋子,吉岡隆知,須田英明,大林尚人.
歯科用CT画像を用いた歯根破折のスクリーニング.

日本歯科保存学雑誌 51（3）:344-351,2008
7）小林千尋,吉岡隆知,須田英明.
Obtura IIアプリケーターニードルの温度.
日本歯内療法学会雑誌 29（3）:161-164,2008
8）小林千尋,福元康恵,吉岡隆知,須田英明.
根管洗浄時に根尖孔外に生じる圧力.
日本歯内療法学会雑誌 29（3）;165-169,2008
9）小林千尋,福元康恵,吉岡隆知,須田英明.
根管内吸引洗浄法に関する基礎的研究.
日本歯内療法学会雑誌 29（3）:170-173,2008
10）小西秀和,高瀬浩造,砂川光宏,荒木孝二,加藤 熙.
歯科医師会会員の院内感染予防対策意識の現状と課題（第三報）アンケートの各回答グループ間における「スタンダードプリコーション」の理解度の比較.
日本歯科保存学雑誌 51（4）:426-434,2008
11）中野生和子,川島伸之,須田英明.
上顎第一大臼歯・近心頬側第二根管について-超音波チップと実体顕微鏡で処置した症例-.日本歯科保存学雑誌 51（4）:457-463,2008
12）金子友厚,興地隆史,金子実弘,須田英明.ラット正常歯根膜における抗原提示細胞の多様性.日本歯科保存学雑誌 51（5）:502-507,2008
13）金子友厚,興地隆史,砂川光宏,金子実弘
CHOKECHANACHAISAKUL Uraiwan,河村隼,
須田英明.
ラット臼歯に誘発した根分岐部病変の初期発症過程における免疫機能分子およびToll-like レセプターmRNA発現の亢進.
日本歯科保存学雑誌 （印刷中）,2009

10. 学会発表（英文）

1） Fukumoto Y, Yoshioka T, Suda H: Development of new aspiration needles for root canal irrigation with negative pressure. 60th American Association of Endodontists; 示説,バンクーバー・カナダ,4月12日,2008.
2） Kawashima N, Kabasawa Y, Suda H: Keratocystic odontogenic tumor: case report. 6th JEA-KAE Joint Scientific Meeting; 口頭,Gwangju・韓国,4月26日,2008.
3） Ikeda H, Suda H: Human odontoblasts communicate with each other through cell-to-cell coupling. 6th JEA-KAE Joint Scientific Meeting; 口頭,Gwangju・韓国,4月26日,2008.
4） Ikeda H, Suda H: Electrophysiological evidence of functional syncitium in the human odontoblastic layer. KADR Pulp Biology Meeting; 口頭, Daegu・韓国,4月28日,2008.
5） Ikeda H, Suda H: Recent advance of the research on microcirculation of dental pulp. KADR Pulp Biology Meeting; 口頭,Daegu・韓国,4月29日,2008.
6） Kawashima N, Takahashi S, Okuhara S, Ohi C, Sun H, Wang H, Xu J, Katsube K-I, Arany S, Nakata A, Sugiyama T, Suda H: Notch signaling in tha dental pulp. 86th General Session & Exhibition of the IADR; 示説,トロント・カナダ,7月3日,2008.
7） Takahashi S, Kawashima N, Nakata A, Kameda T, Sugiyama T, Katsube K-I, Suda H: Shh singaling is related to BMP signaling in ameloblast differentiation. 86th General Session & Exhibition of the IADR; 示説,トロント・カナダ, 7月4日,2008.
8） Wang H, Kawashima N, Xu J, Takahashi S, Okuhara S, Iwata T, Suda H: Processing of matrix extracellular phosphoglycoprotein in dental pulp cells. 86th General Session & Exhibition of the IADR; 示説,トロント･カナダ,7月4日,2008.
9） Sunakawa M, Kaneko T, Kaneko M, Suda H: p38MAPK and GFAP are upregulated by MO tooth pulp stimulation. 86th General Session & Exhibition of the IADR; 示説, トロント・カナダ,7月5日,2008.
10） Ikeda H, Suda H: Direct cell-to-cell coupling network in human odontoblasts in sectioned tooth disk. 86th General Session & Exhibition of the IADR; 口頭,トロント・カナダ,7月5日,2008.
11） Suda H: Laser in endodontics. The WFLD 2008 Hong Kong Congress; 口頭, 香港,7月26日,2008.
12） Anjo T, Watanabe S, Saegusa H, Ebihara A, Suda H: Disinfection of E.faecalis by Er:YAG laser irradiation. The WFLD 2008 Hong Kong Congress; 示説,香港,7月28日,2008.
13） Saegusa H, Watanabe S, Anjo T, Ebihara A, Suda H: The utilization of DIAGNOdent to endodontic materials. The WFLD 2008 Hong Kong Congress; 示説,香港,7月29日,2008.
14） Watanabe S, Saegusa H, Anjo T, Ebihara A, Suda H: Three dimensional dentin strain induced by Er:YAG laser irradiation. The WFLD 2008 Hong Kong Congress; 示説,香港,7月29日,2008.
15） Ebihara A, Watanabe S, Saegusa H, Anjo T, Suda H: The effects of Er:YAG irradiation on osteoblasts. The WFLD 2008 Hong Kong Congress; 示説,香港,7月29日,2008.
16） Takeda A, Katayama Y, Takahashi H, Suda H: Laser welding for the removal of broken endodontic files. The WFLD 2008 Hong Kong Congress; 示説,香港,7月29日,2008.
17） Ikeda H, Suda H: Cell-to-cell electrical communication between human odontoblasts. 12th World Congress on Pain; 口頭,エジンバラ・英国,8月9日,2008.
18） Adorno CG, Yoshioka T, Suda H: The effect of root preparation technique and working length on

the initiation of apical root cracks. Trans-Tasman Endodontic Conference; 示説,タスマニア・オーストラリア, 11月20日,2008.

19) Kawashima N, Takahashi S, Xu J, Okuhara S, Wang H, Ohi C, Suzuki N, Suda H: Role of Mef2c signaling in osteoblast differentiation. The 10th Joint Meeting between KACD & JSCD; 示説,ソウル・韓国, 11月28日,2008.

20) Ikeda H, Suda H: Drug delivery through human enamel by AC-iontophoresis measured with conductometry. The 10th Joint Meeting between KACD & JSCD; 示説, ソウル・韓国,11月28日,2008.

21) Sunakawa M, Kaneko T, Kaneko M, Kawamura J, Suda H: MNDARs, GDAP and p38MAPK mRNA up-regulations following MO tooth-pulp stimulation. The 10th Joint Meeting between KACD & JSCD; 示説, ソウル・韓国,11月28日,2008.

22) Kobayashi C: Root canal irrigation. The Annual Scientific Meeting of the ADS-ROC; 口頭,台北･台湾,12月1日,2008.

11. 学会発表（和文）

1) 小林千尋:改造Kファイルによる狭窄根管の穿通.日本歯内療法学会関東甲信越静支部大会;口頭,東京,2月17日,2008.

2) 小林千尋,吉岡隆知,須田英明:根管洗浄時に生じる圧力.第29回日本歯内療法学会;口頭,千葉,5月24日,2008.

3) 寺内吉継,吉岡隆知,須田英明:超音波振動による破折NiTiファイルの二次破折に関する基礎的検討.第29回日本歯内療法学会;口頭,千葉,5月24日,2008.

4) 吉岡隆知,花田隆周,石村 瞳,萩谷洋子,菊地和泉,小林千尋,須田英明:垂直性歯根破折.第29回日本歯内療法学会;口頭,千葉,5月25日,2008.

5) 川島伸之,高橋里美,許 婧,奥原 滋,王 捍国,大井智恵,鈴木規元,須田英明:骨芽細胞分化におけるMef2の役割.第128回日本歯科保存学会春季学術大会;口頭,新潟,6月5日,2008.

6) 池田英治,ヴァリサラ・シリマハラジ,須田英明:電気伝導度測定を用いて計測したヒトエナメル質の物質透過性.第128回日本歯科保存学会春季学術大会;口頭,新潟,6月5日,2008.

7) 小西秀和,高瀬浩造,砂川光宏,荒木孝二,加藤 熙:歯科医師会会員の院内感染予防対策意識の現状と課題（第三報）アンケートの各回答グループ間における「スタンダードプリコーション」の理解度の比較.第128回日本歯科保存学会春季学術大会;示説,新潟,6月5日,2008.

8) 鈴木規元,川島伸之,須田英明:IL-10ノックアウトマウスに誘発した根尖性歯周炎におけるIL-12の役割.第128回日本歯科保存学会春季学術大会;示説,新潟,6月6日,2008.

9) 吉岡隆知,石村 瞳,菊地和泉,須田英明,大林尚人:上顎骨唇頬側面から歯根尖が突出した症例の診断と対応.第128回日本歯科保存学会春季学術大会;口頭,新潟,6月6日,2008.

10) 和達礼子,菊地和泉,須田英明:インシデントの経験の有無が次亜塩素酸ナトリウム水溶液およびラバーダムの使用に及ぼす影響.第28回日本歯科薬物療法学会;口頭,東京,6月27日,2008.

11) 海老原新:レーザーと歯内療法の過去・現在・未来.歯科レーザー予防臨床アカデミー10周年記念学会;口頭,東京,6月29日,2008

12) 趙 永哲,南 一郎,吉岡隆知,岸川隆蔵,川島伸之,和達礼子,木下淳博,須田英明,田上順次:歯科診療室-講義室間のインターネット同時中継によるライブ講義システムの開発と評価.第27回日本歯科医学教育学会学術大会;口頭,東京,7月11日,2008.

13) 大山 篤,吉岡隆知,南 一郎,内田達郎,長澤敏行,荒木孝二,俣木志朗,木下淳博:歯学科4年生が臨床実習中の6年生に教わる臨床体験実習プログラム-6年生からのプログラム評価-.第27回日本歯科医学教育学会学術大会;口頭,東京,7月11日,2008.

14) 川島伸之,北川元生,勝部憲一:骨芽細胞分化におけるMam1の役割.第3回Notch研究会;口頭,三島,7月17日,2008.

15) 竹田淳志,須田英明:レーザー溶接による根管内破折ファイル除去に関する基礎的研究:根管内が水で満たされている状態を想定した実験.第20回日本レーザー歯学会;口頭,大阪,9月21日,2008.

16) Nuchjaree P, Watanabe S, Saegusa H, Anjo T, Ebihara A, Suda H:Characteristics of incision lines generated with different laser tips.第20回日本レーザー歯学会;口頭,大阪,9月21日,2008.

17) 小林千尋:根管洗浄とその問題点.日本歯内療法学会中部支部大会;口頭,名古屋,10月5日,2008.

18) 須田英明:歯髄生物学の立場から -垂直性歯根破折について-.第8回日本外傷歯学会総会・学術大会;口頭,沖縄,11月2日,2008.

19) 海老原新:保存治療へのレーザー応用の現状と展望.第129回日本歯科保存学会秋季学術大会・シンポジウム;口頭,富山,11月6日,2008.

20)砂川光宏,金子友厚,金子実弘,須田英明:歯髄のMustard oil刺激により誘発されたラット脳幹におけるp38MAPK及びGFAPのアップレギュレーション.第129回日本歯科保存学会秋季学術大会;示説,富山,11月6日,2008.
21)許 婧,川島伸之,鈴木規元,高橋里美,奥原 滋,衛 書盛,Subhakorn Sermsiri,小泉悠, 須田英明:VIP receptor expression in the Hertwig's epithelial root sheath.第129回日本歯科保存学会秋季学術大会;示説,富山,11月7日,2008.
22)花田隆周,吉岡隆知,岩崎直彦,高橋英和,須田英明:ファイバーポイントが垂直性歯根破折に与える影響.第129回日本歯科保存学会秋季学術大会;示説,富山,11月7日,2008.
23)八幡祥生,林 洋介,海老原 新,小林千尋,須田英明:曲率半径および荷重がニッケルチタンファイルの疲労破折に与える影響.第129回日本歯科保存学会秋季学術大会;示説,富山,11月7日,2008.
24)渡辺 聡,石澤千鶴子,Bolortuya Gombo,三枝英敏,安生智郎,海老原新,小林千尋,須田英明:Er:YAGレーザー照射による根管充填材除去時の象牙質の歪.第129回日本歯科保存学会秋季学術大会;口頭,富山,11月7日,2008.
25)石村 瞳,花田隆周,菊地和泉,吉岡隆知,小林千尋,須田英明:18ヶ月間水中保管された根管充填歯における歯根破折について.第129回日本歯科保存学会秋季学術大会;示説,富山,11月7日,2008.
26)林 洋介,八幡祥生,海老原 新,塙 隆夫,須田英明:新ニッケルチタンファイルGTXの曲げ特性.第129回日本歯科保存学会秋季学術学会;示説,富山,11月7日,2008.
27)池田英治,須田英明:ヒト象牙芽細胞層の三次元的カップリングネットワーク.第129回日本歯科保存学会秋季学術大会;口頭,富山,11月7日.
28)小林千尋,吉岡隆知,須田英明:根管洗浄の新しい評価方法.第129回日本歯科保存学会秋季学術大会;口頭,富山,11月7日,2008.
29)松本宏之,砂川光宏,須田英明:東京医科歯科大学歯学部附属病院における「針刺し事故」とその予防 -歯科臨床教育現場における報告書の分析-.第21回日本歯科医学会総会;示説,横浜,11月14日,2008.
30)砂川光宏,須田英明:歯内治療に伴う慢性痛の臨床的解析.第21回日本歯科医学会総会;口頭,横浜,11月14日,2008.
31)池田英治,須田英明:歯内治療に関与する歯の形態異常.第21回日本歯科医学会総会;示説,横浜,11月14日,2008.
32)吉岡隆知,須田英明:ビジュアライズドエンドドンティクス-セカンドジェネレーション-.第21回日本歯科医学会総会;口頭,横浜,11月15日,2008.
33)小林千尋,須田英明:歯根破折と歯内療法.第21回日本歯科医学会総会;口頭,横浜,11月15日,2008.
34)吉岡隆知:歯科用CTと歯内療法.第21回日本歯科医学会総会・シンポジウム;口頭,横浜,11月16日,2008.
35)海野雅浩,馬場一美,宮本智行,三輪全三,森崎市治郎,深山治久,鵜澤成一,和達礼子,土屋文人,嶋田昌彦:歯科における医療安全対策ガイドライン.医療の質・安全学会 第3回学術集会;示説,東京,11月23日,2008.
36)Ikeda H, Suda H: Facilitated chemical delivery through human enamel/dentin with AC-iontophoresis. 56th Annual Meeting of JADR; 示説,名古屋,11月30日,2008.
37)花田隆周,坂上 斉,吉岡隆知,岩崎直彦,高橋英和,須田英明:根管充填用接着性レジンが垂直性歯根破折に与える影響.第73回口腔病学会学術大会;口頭,東京,12月6日,2008.
38)宮本智行,海野雅浩,三輪全三,倉林 亨,島田昌彦,和達礼子,鵜澤成一,和達重郎,岡田大蔵,深山智子,三浦佳子,長川智子,鶴岡広美,多田 浩:歯科診療における医療安全対策ガイドライン.第73回口腔病学会学術大会;口頭,東京,12月6日,2008.
39)砂川光宏,松本宏之:本学歯学部における院内感染予防対策教育 -その効果と問題点―. 第73回口腔病学会学術大会;口頭,東京,12月6日,2008.

12. 受賞

・Ishimura H, Yoshioka T, Suda H.Sealing Ability of New Adhesive Root Canal Filling Materials Measured by a New Dye Penetration Method. 日本歯科理工学会論文賞,2008年4月26日,第51回日本歯科理工学会学術講演会 .
・寺内吉継,吉岡隆知,須田英明.超音波振動による破折NiTiファイルの二次破折に関する基礎的検討.ワカイ賞,2008年5月24日,第29回日本歯内療法学会.
・吉岡隆知,花田隆周,石村瞳,萩谷洋子,菊地和泉,小林千尋,須田英明.垂直性歯根破折.大会長賞,2008年5月25日,第29回日本歯内療法学会.
・吉岡隆知.Detection of the second mesiobuccal canal

in mesiobuccal roots of maxillary molar teeth ex vivo.日本歯科保存学会学術賞,2008年6月5日,第128回日本歯科保存学会春季大会.

・ Nuchjaree P.Characteristics of incision lines generated with different laser tips.日本レーザー歯学会優秀発表賞,2008年9月21日,第20回日本レーザー歯学会.

・ Ikeda H.Electrophysiological Evidence of Functional Syncitium in the Human Odontoblastic Layer.Best oral presentation award,2008年4月28日,KADR Pulp Biology Meeting.

13. 外部資金の獲得状況

(科学研究費補助金,受託研究費,外部財団の助成など)

1) 科学研究費補助金, 基盤研究 (A)
研究題目:垂直性歯根破折のメカニズムと臨床的対応.
代表:須田英明
期間:平成19年―平成22年
研究費総額:3460万円

2) 科学研究費補助金, 基盤研究 (B)
研究題目:歯髄疾患に伴う難治性の痛みに関する臨床的ならびに基礎的研究.
代表:砂川光宏
期間:平成19年―平成20年
研究費総額:1540万円

3) 科学研究費補助金, 基盤研究 (B)
研究題目:Gap-junctionを介した象牙芽細胞複合体の電気的・化学的細胞間連絡の解析.
代表:池田英治
期間:平成20年―平成24年
研究費総額:1470万円

4) 科学研究費補助金, 萌芽研究
研究題目:TRP-channelタンパクの歯髄感覚受容における機能解明.
代表:池田英治
期間:平成19年―平成20年
研究費総額:190万円

5) 科学研究費補助金, 基盤研究 (B)
研究題目:Notchシグナルの歯髄細胞分化におけるメカニズムの解明とその臨床的展開.
代表:川島伸之
期間:平成19年―平成22年
研究費総額:1460万円

6) 科学研究費補助金, 萌芽研究
研究題目:歯髄組織の分化および機能にFGF18は重要である.
代表:川島伸之
期間:平成18年―平成20年
研究費総額:230万円

7) 科学研究費補助金, 基盤研究 (C)
研究題目:根尖性歯周炎の発症・拡大におけるIL-10の機能的役割.代表:鈴木規元
期間:平成20年―平成22年
研究費総額:350万円

8) 科学研究費補助金, 若手研究 (B)
研究題目:歯髄炎と根尖性歯周炎の治癒に樹状細胞の機能を応用する分子生物学的研究.
代表:金子友厚
期間:平成18年―平成20年
研究費総額:340万円

9) 科学研究費補助金, 若手研究 (B)
研究題目:歯科用レーザーの歯内療法への応用について.
代表:安生智郎
期間:平成18年―平成20年
研究費総額:230万円

10) 科学研究費補助金, 若手研究 (B)
研究題目:口腔領域の侵襲に対する術前鎮痛剤投与効果の免疫組織化学的検討.
代表:菊地和泉
期間:平成18年―平成20年
研究費総額:320万円

11) 科学研究費補助金, 若手研究 (B)
研究題目:歯髄におけるFGF18シグナルの機能解析とその臨床的展開.
代表:大井智恵
期間:平成19年―平成21年
研究費総額:330万円

12) 科学研究費補助金, 若手研究 (ｽﾀｰﾄｱｯﾌﾟ)
研究題目:接着性根管充填用シーラーに適した根管治療システムの開発.
代表:石村　瞳
期間:平成20年―平成21年
研究費総額:217万円

13) 科学研究費補助金,若手研究 (ｽﾀｰﾄｱｯﾌﾟ)
研究題目:Shhシグナルを軸とした歯の再構築.
代表:　高橋里美
期間:平成19年―平成20年
研究費総額:267万円

14)科学研究費補助金， 若手研究（ｽﾀｰﾄｱｯﾌﾟ）
研究題目:ニッケルチタンファイルとニッケルチタン合金原線間における各種特性の変化.
代表:林　洋介
期間:平成19年―平成20年
研究費総額:267万円

15)科学研究費補助金， 基盤研究（A）(1)
研究題目:歯髄・根尖部歯周組織の創傷治癒メカニズムの解明と再生療法への応用.代表: 吉嶺嘉人（分担:川島伸之）
期間:平成18年―平成20年
研究費総額:160万円

16)科学研究費補助金， 基盤研究（B）(2)
研究題目:コンピュータによる歯科臨床シミュレーション教育システムの活用と有効性の解析
代表:木下淳博（分担:吉岡隆知）
期間:平成18年―平成20年
研究費総額:1710万円

17))科学研究費補助金， 厚生労働科学研究費（地域医療基盤開発推進研究事業）
研究題目:歯科関連職種における技術能力向上に寄与する試験のあり方の研究.
代表:石橋寛二（分担:須田英明）
期間:平成20年―平成21年
研究費総額:114万円

14. 特別講演,招待講演

1) 1 Ikeda H:Biological Approach of Dental Pain（From Molecular to System）.2008年3月6日～3月8日.ソウル大学,韓国,
2) Kawashima N:Notch signaling and the osteoblast and odontoblast differentiation.2008年4月15日～4月17日.Yonsei Univ, ソウル,韓国.
3) Ikeda H:Microcirculation of pulp.2008年4月24日～4月29日.Deague Univ,Deague,韓国,
4) 須田英明:世界レーザー歯学連合（WFLD）学術大会およびアジア部会Laser in endodontics.L'hotel Nina et Convention Center,2008年7月25日～7月28日.香港,中国.
5) 須田英明:大連医科大学にて招待講演 Microendodontics.2008年10月24日～10月29日.大連医科大学,大連,中国.
6) 須田英明.難治症例への対応とマイクロエンドドンティクス.浅草歯科医師会　学術講演会,2008年7月15日,浅草歯科医師会事務所,東京.
7) 須田英明.エンド臨床と垂直歯根破折.社団法人大津市歯科医師会　平成20年度第1回学術講演会,2008年7月24日,ピアザ淡海　滋賀県立県民交流センター,滋賀.
8) 須田英明.臨床（歯内治療学）の視点から.市民公開シンポジウム「歯科医学の将来展望」,日本学術会議講堂,東京,2008年9月2日.
9) 須田英明.歯髄生物学の立場から.日本外傷歯学会認定医セミナー,2008年10月5日,LMJ東京研修センター,東京.
10)須田英明.難治な根管治療症例への対応.中毛学術講演会,2008年10月23日,ホテル・サンラク,群馬県.
11)海老原新.保存治療へのレーザー応用の現状と展望.第129回日本歯科保存学会秋季大会,2008年11月6日,富山国際会議場,富山.
12)吉岡隆知.Endodontic Microsurgery 基礎と臨床.明海大学大学院総合セミナー,2008年11月14日,明海大学,埼玉.
13)吉岡隆知.シンポジウム「歯内療法の最前線」歯科用CTと歯内療法.第21回日本歯科医学会総会,2008年11月16日,パシフィコ横浜,神奈川.

15. 主催学会

須田英明.第28回日本歯科薬物療法学会.2008年6月26日-28日,文京シビックホール,東京.

16. 講座の准教授,講師,助教,特別研究員,ポスドク,指導を受けた大学院生の名前(AISSには○印)のリスト

准 教 授　小林千尋,
　　砂川光宏（感染対策歯科治療部兼任）
講　　師　竹田淳志,池田英治
　　COE拠点形成特任准教授　川島伸之（～3月）
助　　教　海老原新,川島伸之（4月～）,
　　松本宏之（感染対策歯科治療部兼任）
　　吉岡隆知,和達礼子,鈴木規元,
　　金子友厚（～3月）
医　　員　金子友厚（4月～）,
　　安生智郎（～3月）,菊地和泉,
　　石村 瞳,萩谷（川村）洋子（～3月）,
　　高橋里美,林 洋介,三枝英敏（4月～）
大学院生　Elham A.Benmusa Elmsallati（リビア国費留学生,3月まで）,三枝英敏（3月まで）,花田隆周,八幡祥生,渡辺聡 ,Carlos Gabriel Adorno-Quevedo（パラグアイ国費留学生）,許婧（中国私費留学生）,○河村隼（4月から）,小泉悠（4月から）,石澤千鶴子（4月から）,坂上斉（4月から）,○Bolortuya Gombo（モンゴル私費留学生　4月から）,吉岡俊彦（社会人大学院生　4月から）,Uraiwan Chokechanachaisakul（タイ国費留学生　10月から）

Journal of Dental Research
http://jdr.sagepub.com

Antigen-presenting Cells in Human Radicular Granulomas

T. Kaneko, T. Okiji, R. Kaneko, J.E. Nör and H. Suda

J DENT RES 2008; 87; 553
DOI: 10.1177/154405910808700617

The online version of this article can be found at:
http://jdr.sagepub.com/cgi/content/abstract/87/6/553

Published by:
SAGE
http://www.sagepublications.com

On behalf of:
International and American Associations for Dental Research

Additional services and information for *Journal of Dental Research* can be found at:

Email Alerts: http://jdr.sagepub.com/cgi/alerts

Subscriptions: http://jdr.sagepub.com/subscriptions

Reprints: http://www.sagepub.com/journalsReprints.nav

Permissions: http://www.sagepub.com/journalsPermissions.nav

Downloaded from http://jdr.sagepub.com at TOKYO IKASHIKA UNIVERSITY on March 17, 2009

RESEARCH REPORTS
Biological

T. Kaneko[1*,2], T. Okiji[3], R. Kaneko[1], J.E. Nör[2], and H. Suda[1]

[1]Pulp Biology and Endodontics, Graduate School, Tokyo Medical and Dental University, Yushima 1-5-45, Bunkyo-Ku, Tokyo, 113-8549, Japan; [2]Cariology, Restorative Sciences, and Endodontics, School of Dentistry, University of Michigan, Ann Arbor, MI, USA; and [3]Division of Cariology, Operative Dentistry and Endodontics, Niigata University Graduate School of Medical and Dental Sciences, Niigata, Japan; *corresponding author, tomoendo@tmd.ac.jp

J Dent Res 87(6):553-557, 2008

Antigen-presenting Cells in Human Radicular Granulomas

ABSTRACT

Substantial numbers of dendritic cells have been detected in radicular granulomas. To test the hypothesis that local antigen presentation from dendritic cells to T-cells is involved critically in immunological responses within radicular granulomas, we compared characteristics of dendritic cells and macrophages by morphological and biological analyses. Under light microscopy, HLA-DR+ and CD68+ cells showed diverse profiles, including dendritic-shaped cells. Transmission electron microscopy revealed that HLA-DR+ dendritic cells, with long cytoplasmic processes and lacking distinct phagosomes, were concentrated in the lymphocyte-rich area. HLA-DR alpha-chain, CD83, and CD86 mRNAs from HLA-DR+ dendritic cells, and CD28 mRNA from CD28+ T-cells were up-regulated in lymphocyte-rich area. Scanning electron microscopy demonstrated that the density of gold particles on dendritic cells was higher than that on HLA-DR+ macrophages. These results suggest that dendritic cells in radicular granulomas are associated with local defense reactions as stronger antigen-presenting cells, as compared with macrophages.

KEY WORDS: dendritic cell, HLA-DR, transmission electron microscopy, scanning electron microscopy, macrophage.

Received September 19, 2007; Last revision January 15, 2008; Accepted February 5, 2008

INTRODUCTION

Apical periodontitis, in the form of radicular granulomas and cysts, is caused by local defense reactions against chronic bacterial infection from the infected and necrotic root canals (Nair, 2004). These inflammatory lesions consist of granulation and fibrous tissues containing a variety of inflammatory/immunocompetent cells, such as macrophages, lymphocytes, and plasma cells (Tani *et al.*, 1992; Wallstrom *et al.*, 1993; Torabinejad, 1994; Liapatas *et al.*, 2003). Some studies have reported that T-cells outnumber B-cells (Stashenko *et al.*, 1992), suggesting that T-cell-mediated immunological reactions play a major role in the development of the lesions. Among non-lymphoid cells, involvement of macrophages in the pathogenesis of these lesions has been postulated. These cells may play some triggering role in lesion expansion by producing cytokines such as interleukin-1 (Artese *et al.*, 1991; Stashenko *et al.*, 1992) and nitric oxide (Suzuki *et al.*, 1999). Moreover, a considerable proportion of macrophages in the lesion may express major histocompatibility complex (MHC) class II molecules (Köpp *et al.*, 1989; Suzuki *et al.*, 1999), suggesting that they may contribute to lesion development through activation of T-cell-mediated immune responses, by acting as antigen-presenting cells.

Our recent studies have demonstrated the presence of dendritic cells in experimentally induced rat apical periodontitis (Kaneko *et al.*, 2001a,b, 2008). Dendritic cells express, constitutively, a high level of MHC class II molecules and act as professional antigen-presenting cells that play a pivotal role in initiating and regulating primary and secondary immune responses through the activation of T-cells (Steinman, 1991; Banchereau and Steinman, 1998). We have found that dendritic cells in rat periodontitis can be discriminated from macrophages by their ultrastructural appearances (Kaneko *et al.*, 2001b, in press). These dendritic cells are prevalent in the chronic, post-expansion stage of lesion development. As for human radicular granulomas, few studies of dendritic cells are available (Gao *et al.*, 1988; Lukić *et al.*, 2006), and the ultrastructure and precise identification of dendritic cells have not yet been reported.

In this study, we investigated several characteristics of dendritic cells in human radicular granulomas, to test the hypothesis that local antigen presentation from dendritic cells to T-cells is involved critically in immunological responses within radicular granulomas. Following HLA-DR immunostaining, we used transmission electron microscopy (TEM) to examine the morphology and distribution of dendritic cells. We also performed gene expression analysis for HLA-DR alpha-chain, CD28, CD83, CD86, and CD163, by laser capture microdissection and reverse-transcription-PCR (RT-PCR), to demonstrate that the expression levels are up-regulated within potential sites of local antigen presentation. We further conducted scanning electron microscopy (SEM) on sections colloidal-gold-immunolabeled for HLA-DR, to test if dendritic cells are efficient antigen-presenting cells in the lesions.

Downloaded from http://jdr.sagepub.com at TOKYO IKASHIKA UNIVERSITY on March 17, 2009

MATERIALS & METHODS

We examined 14 human radicular granulomas from 14 individuals who had a non-contributory medical history and were taking no medication. Periapical tissues were obtained under institutionally approved protocols and after informed consent had been obtained. All of the specimens showed radiographic signs of apical periodontitis, *i.e.*, clear radiolucency and disappearance of the periodontal ligament space, and were diagnosed as radicular granuloma according to the histological examination of hematoxylin- and eosin-stained sections. These specimens (n = 14) were cut into 2 pieces, one for immunohistochemistry, TEM, and laser capture RT-PCR, and the other for SEM.

Immunohistochemistry and TEM

The specimens were fixed with 2% paraformaldehyde containing picric acid. Frozen sections were prepared, and were incubated with one of the following monoclonal antibodies: anti-HLA-DR (DAKO, Glostrup, Denmark); CD68 (DAKO; reactive to dendritic cells and macrophages); CD3 (DAKO; a pan T-cell antibody), or CD28 (Becton Dickinson, Franklin Lakes, NJ, USA; reactive to most mature T-cells). This was followed by sequential incubations with a biotinylated anti-mouse IgG (Vector Laboratories, Burlingame, CA, USA) and avidin-biotin-peroxidase complex (Elite ABC kit; Vector). The peroxidase activity was developed with a diaminobenzidine-H_2O_2 solution (DAB substrate kit; Vector). Sections of the gingiva, processed in the same way, served as positive controls.

Using light microscopy, we counted immmnopositive cells and total numbers of nucleated cells in the whole area of each section, and then calculated the frequency of immunopositive cells.

For TEM analysis, the sections were stained with the anti-HLA-DR antibody in a manner similar to that described above. After being stained, the sections were post-fixed, dehydrated, and embedded in Epon. Ultrathin sections were cut with an ultramicrotome (Reichert Ultracut-N; Reichert-Nissei, Tokyo, Japan), and examined in a TEM (H7100; Hitachi, Tokyo, Japan).

Under TEM, all positively stained cells in the whole area of trimmed samples were classified into dendritic cells or macrophages, as described previously (Zhao *et al.*, 2006). The same analysis was also done in lymphocyte-rich areas, where more than 15 lymphocytes were seen in a grid (150 x 150 μm). The frequency of each type of cell was expressed as a percentage. Some cells showed morphology intermediate between that of macrophages and dendritic cells, such as a round profile without distinct phagosomes and cytoplasmic processes. These cells were classified as "unidentified".

Laser-capture Microdissection and RT-PCR

The frozen tissue sections were mounted on glass slides (Leica, Heidelberg, Germany). Immunostaining was performed for HLA-DR or CD28, as described previously (Kaneko *et al.*, 2007). HLA-DR+ cells in each lymphocyte-rich area and the surrounding tissues were randomly selected under a light microscope at 20x magnification. At higher magnification (63x), these were classified as: (i) type I cells, characterized by long cytoplasmic processes and lack of distinct vacuoles (mostly composed of dendritic cells according to the TEM analysis); (ii) type II cells, characterized by distinct phagosome-like vacuoles and lack of long cytoplasmic processes (mostly composed of macrophages); or (iii) unidentified cells. Type I, type II, and CD28+ cells (30 cells each) were dissected and collected separately by means of a microdissection microscope (Leica AS LMD). Total RNA was extracted, and, as we described previously (Kaneko *et al.*, 2007), cDNA synthesis and PCR amplification were done in single tubes, with simultaneous use of the primer set for the gene of interest and the glyceraldehyde-3-phosphate dehydrogenase (GAPDH) primer set, with the use of SuperScript one-step RT-PCR and a Platinum Taq kit (Invitrogen, Carlsbad, CA, USA). PCR amplification of the products was performed with the following primers: HLA-DR alpha-chain, CAAAGAAGGAGACGGTCTGG (sense) and GGCTCTCTCAGTTCCACAGG (antisense); CD28, GCTGCTCTTGGCTCTCAACT (sense) and ACCTGAAGCTGCT GGGAGTA (antisense); CD163, CGAGTTAACGCCAGTAAGG (sense) and GAACATGTCACGCCAGC (antisense); CD83, CTGGTCAACCTCCTGGACAT (sense) and CGTAAAACATCT GGGCTGGT (antisense); CD86, AGATGTCCTACGGGAACGTG (sense) and ATCCCACCTTAGAGCCAGGT (antisense); GAPDH, CATGGCCTCCAAGGAGTAAG (sense) and AGGGGTCTACA GGCAACTG (antisense).

SEM

The specimens were fixed with 1% paraformaldehyde. Sections were cut with a linear slicer (PRO7 Dosaka EM, Kyoto, Japan), and incubated with anti-HLA-DR antibody, followed by anti-mouse IgG conjugated with 30-nm colloidal gold particles. They were post-fixed, dehydrated, dried, and sputter-coated with osmium in an ion coater (IB-5, EIKO Engineering, Tokyo, Japan). Back-scattered electrons were detected with the use of an Yttrium-Aluminum-Garnet back-scattered detector (Hitachi, Tokyo, Japan). Pairs of the secondary and the back-scattered electron images were observed under a SEM (S-4500, Hitachi). Using back-scattered electron imaging, we randomly selected 10 HLA-DR+ cells from each sample. According to the results from TEM analysis, we classified HLA-DR+ cells into cells with and those without long cytoplasmic processes (referred to as dendritic cells and macrophages, respectively), under the secondary electron image of SEM. We counted the number (*per* 150 nm x 100 nm) of gold particles on the cytoplasmic membrane of HLA-DR+ cells under the back-scattered electron image.

Statistical Analysis

Statistical analysis was made by a Wilcoxon paired-sample test, or by Kruskal-Wallis non-parametric ANOVA, followed by the Mann-Whitney U test with Bonferroni correction. A difference at the 5% level was accepted as significant.

RESULTS

Light Microscopy

Numerous HLA-DR+ (Figs. 1A, 1B), CD68+ (Figs. 1C, 1D), CD3+, and CD28+ cells were distributed in all portions of the lesion. HLA-DR+ and CD68+ cells showed membrane and cytoplasmic staining, respectively, and showed diverse profiles. HLA-DR+ cells with dendritic and spindle profiles were mainly distributed in the lymphocyte-rich area (Fig. 1B). CD68+ cells were classified into 2 populations according to their staining pattern. One type was rich in immunopositive cytoplasmic structures (Fig. 1C). Most CD68+ cells belonged to this type. Another type of cells showed the immunopositive structures in restricted areas within the cytoplasm (Fig. 1D). The latter type of cells usually showed a dendritic or spindle profile (Fig. 1D). The cell count for CD3+ T-cells was highest, and the count for CD68+ cells was lowest (Fig. 1E). The counts for CD3+ and

Downloaded from http://jdr.sagepub.com at TOKYO IKASHIKA UNIVERSITY on March 17, 2009

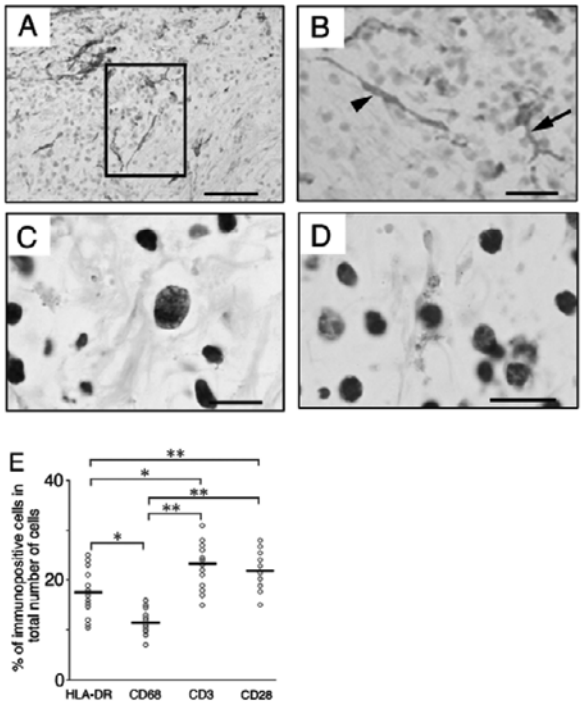

Figure 1. Immune cells in radicular granulomas. **(A)** A light micrograph of HLA-DR+ cells showing various profiles in radicular granuloma. Bar = 100 μm. **(B)** Higher magnification of the boxed area in (A). HLA-DR+ cells show dendritic (arrow) and spindle (arrowheads) profiles. These cells show cell-to-cell contacts with lymphocyte-like small round cells with a round nucleus. Bar = 50 μm. **(C)** A CD68+ cell showing an oval profile. This cell contains dense immunoreaction products in the cytoplasm. Bar = 30 μm. **(D)** A CD68+ cell showing a spindle profile with long cytoplasmic possesses. This cell contains sparse intracytoplasmic immunoreaction products. Bar = 30 μm. **(E)** Frequency of HLA-DR-, CD68-, CD3-, and CD28-positive cells in radicular granulomas. Results are expressed as mean ± SD (n=14 each). *p < 0.05 and **p < 0.01.

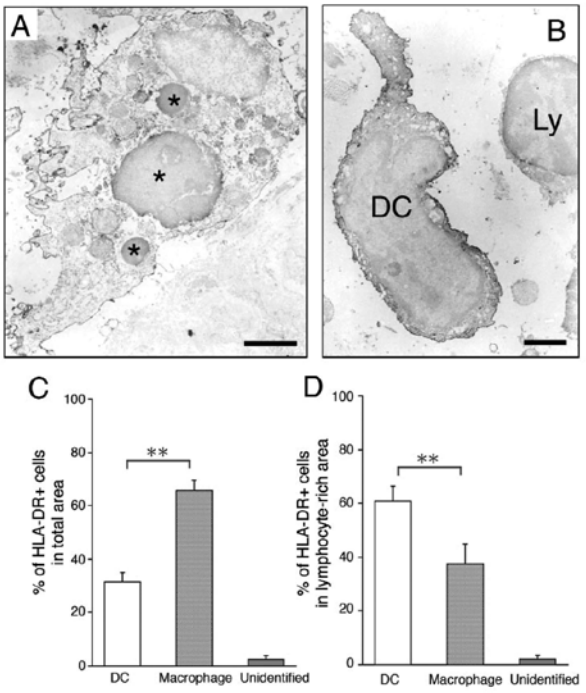

Figure 2. TEM analysis of HLA-DR+ dendritic cells and HLA-DR+ macrophages in radicular granulomas. **(A)** An HLA-DR+ macrophage. Large distinct phagosomes (*) can be seen. Bar = 3 μm. **(B)** Ultrastructure of an HLA-DR+ dendritic cell with a long cytoplasmic process in a lymphocyte (Ly)-rich area. Bar = 1.8 μm. **(C)** Frequency of HLA-DR+ dendritic cells and macrophages in the total area of the specimen (mean ± SD; n = 14). **p < 0.01. **(D)** Frequency of HLA-DR+ dendritic cells and macrophages in lymphocyte-rich areas (mean ± SD; n = 14). **p < 0.01.

CD28+ cells were not significantly different (Fig. 1E).

TEM Analysis

Under TEM, most HLA-DR+ cells were classified as either macrophages (Fig. 2A) or dendritic cells (Fig. 2B). Macrophages typically showed an oval, round, or irregular large cell body with short cytoplasmic processes, and were discriminated from dendritic cells by their distinct phagosomes within the cytoplasm (Fig. 2A). In contrast, dendritic cells normally showed a slender, spindle, or dendritic profile, possessed long cytoplasmic processes, and contained numerous tubules/vesicles, a relatively smaller quantity of lysosomes (Fig. 2B), and no distinct phagosomes. Although the percentage of HLA-DR+ macrophages in the total area was significantly higher than that of dendritic cells (Fig. 2C), dendritic cells significantly outnumbered HLA-DR+ macrophages in the lymphocyte-rich area (Fig. 2D).

RT-PCR

Gene expression levels of CD83 and CD163 were up-regulated in type I and type II cells, respectively (Fig. 3). Type I cells showed a greater up-regulation of HLA-DR alpha-chain and CD86 mRNAs as compared with type II cells. HLA-DR alpha-chain, CD83, and CD86 mRNA levels were highest in type I cells retrieved from lymphocyte-rich areas, and lowest in type II cells from the surrounding tissues. Conversely, CD163 mRNA was highest in type II cells from the surrounding tissues, and lowest in type I cells from lymphocyte-rich areas. We have also observed the up-regulation of CD28 mRNA in CD28+ T-cells in lymphocyte-rich areas.

SEM Analysis

By means of back-scattered electron imaging, immunopositive cells labeled with gold particles were identified with high contrast to the background. Using secondary electron imaging, we classified these HLA-DR+ cells into cells without long cytoplasmic processes (macrophages, Figs. 4A, 4B) and those with long cytoplasmic processes (dendritic cells, Figs. 4C, 4D). The density of gold particles on HLA-DR+ dendritic cells was significantly higher than that on HLA-DR+ macrophages ($P < 0.01$) (Fig. 4E).

DISCUSSION

In this study, identification of dendritic cells was made in human radicular granulomas. Light microscopy revealed that these cells

Downloaded from http://jdr.sagepub.com at TOKYO IKASHIKA UNIVERSITY on March 17, 2009

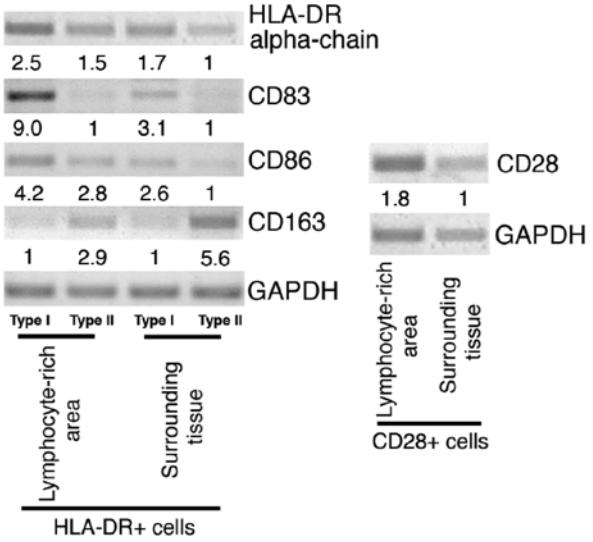

Figure 3. RT-PCR to evaluate HLA-DR alpha-chain, CD83, CD86, and CD163 mRNA expression levels in type I and type II HLA-DR+ cells, and CD28 mRNA in CD28+ cells in lymphocyte-rich areas and the surrounding tissues. The densities of the bands corresponding to HLA-DR alpha-chain, CD83, CD86, CD163, and CD28 mRNA were measured with the Image J software (Version 1.37v, NIH, Bethesda, MD, USA), normalized against the density of the bands for GAPDH, and described numerically.

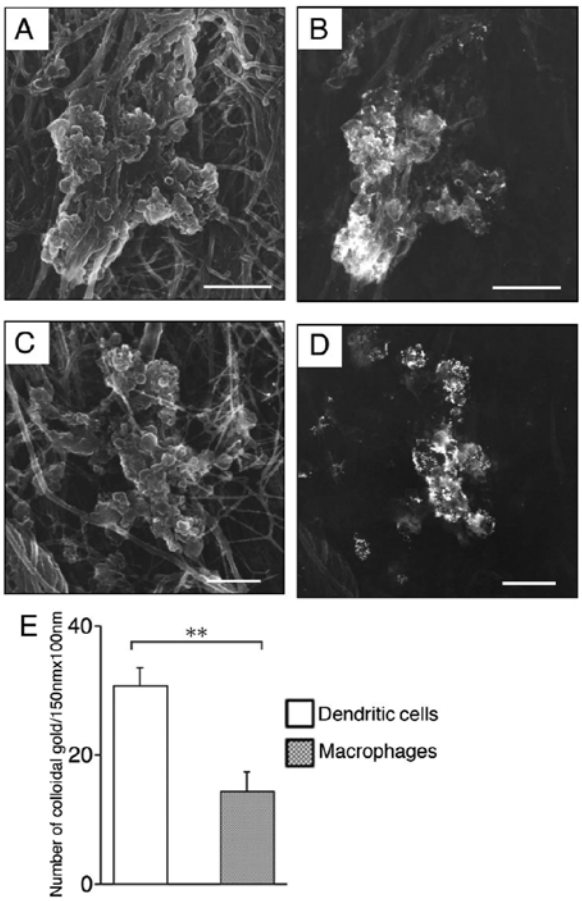

Figure 4. SEM analysis of dendritic cells and macrophages in radicular granulomas. **(A)** Secondary electron image showing an HLA-DR+ oval cell without cytoplasmic processes (macrophage). Bar = 5 μm. **(B)** Back-scattered electron image of the same cell in (A). Bar = 5 μm. **(C)** Secondary electron image showing an HLA-DR+ slender cell with long cytoplasmic processes (dendritic cell). Bar = 5 μm. **(D)** Back-scattered electron image of the same cell in (C). This cell contains more gold particles as compared with the cell shown in (B). Bar = 5 μm. **(E)** Density of colloidal gold particles on HLA-DR+ dendritic cells and macrophages *per* unit area (150 nm x 100 nm). Results are expressed as mean ± SD (n = 14). $^{**}p < 0.01$.

may express HLA-DR and/or CD68, although complete identification was not possible without the use of electron microscopy. Under TEM, dendritic cells were discriminated from macrophages, since these cells had long cytoplasmic processes, but lacked distinct phagosomes. These ultrastructural features are very similar to those we have described earlier for dendritic cells in rats (Kaneko *et al.*, 2001a,b, 2008).

The TEM analysis disclosed that dendritic cells in human radicular granulomas were mainly distributed in lymphocyte-rich areas, where their number was significantly greater than that of HLA-DR+ macrophages. This finding suggests that dendritic cells, not macrophages, primarily contribute to the local interaction with T-cells within the lesion. Such a tendency has also been seen in rat lesions at the chronic, post-expansion stage (Kaneko *et al.*, 2008).

To confirm if dendritic cells and macrophages were selectively retrieved from the samples, we performed RT-PCR for CD83 and CD163. In humans, CD83 expression is a hallmark of mature and activated dendritic cells (Zhou and Tedder, 1995; Cao *et al.*, 2005). CD163 is a marker for monocyte/macrophage lineage cells, and is highly expressed in tissue macrophages (Law *et al.*, 1993; Schaer *et al.* 2005). The expression of CD83 and CD163 in monocyte-derived dendritic cells is up-regulated and down-regulated, respectively, during differentiation and maturation (Laudanski *et al.*, 2007; Wang *et al.*, 2007). Notably, CD83 and CD163 mRNA was up-regulated in group I and group II, respectively.

The expression level of a MHC class II molecule correlates with antigen-presenting cell activity (Cella *et al.*, 1997; Villadangos *et al.*, 2001; Wilson *et al.*, 2004). In this point of view, we hypothesized that genes related to antigen-presenting cells, such as HLA-DR alpha-chain, CD83, and CD86, should be up-regulated in lymphocyte-rich areas, where dendritic cells are concentrated. CD86 is expressed on professional antigen-presenting cells to provide a critical signal for T-cell activation (Azuma *et al.*, 1993). Indeed, these genes from type I cells were up-regulated to a greater extent than those from type II cells. Furthermore, expression of these genes was higher in type I cells retrieved from lymphocyte-rich areas compared with those from surrounding tissues. Analysis of these data suggests that dendritic cells in lymphocyte-rich areas may play the most active role in antigen presentation.

CD28 interactions with CD80 and/or CD86 are essential for initiating antigen-specific T-cell responses, up-regulating cytokine expression, and promoting T-cell expansion and differentiation (Bluestone, 1995). In granulomas, co-

Downloaded from http://jdr.sagepub.com at TOKYO IKASHIKA UNIVERSITY on March 17, 2009

stimulatory signals provided by the interaction of CD28 on T-cells with CD80 and/or CD86 are essential for the activation of T helper lymphocytes and granuloma formation (King *et al.*, 1996). Our light microscopic observation revealed that the majority of T-cells may express CD28, distributed in all areas of the lesion. But, notably, CD28 mRNA from CD28+ cells was up-regulated in lymphocyte-rich areas. This result suggests that co-stimulation between antigen-presenting cells and T-cells is enhanced in the lymphocyte-rich area.

For further confirmation of whether dendritic cells play the most active role as antigen-presenting cells, SEM on colloidal-gold-immunolabeled sections was carried out. Colloidal gold has been used as an excellent marker for studies in cell biology (Manara *et al.*, 1990; Stoffel and Friess, 2002), and its high electron-density makes it useful for immunoelectron microscopy applications (Namork, 1989; Arimilli *et al.*, 2000). This study clearly showed a significantly higher density of gold particles on cells with dendritic morphology (dendritic cells), compared with cells with oval morphology (macrophages).

Taken together, these results suggested that mature and activated dendritic cells were mainly distributed and acted as antigen presentation against T-cells in lymphocyte-rich areas of radicular granulomas. Our results also support the notion that dendritic cells act as efficient antigen-presenting cells, as compared with macrophages.

ACKNOWLEDGMENTS

This study was supported by Grants-in-Aid for Scientific Research (Nos. 11470402 and 19659496 to T.O., and Nos. 15791091 and 18791393 to T.K.) from the Japan Society for the Promotion of Sciences.

REFERENCES

Arimilli S, Deshpande S, Nag B (2000). Localization of soluble major histocompatibility class II-peptide complexes on T cell surface. *Microsc Res Tech* 50:419-424.

Artese L, Piattelli A, Quaranta M, Colasante A, Musani P (1991). Immunoreactivity for interleukin 1-beta and tumor necrosis factor-alpha and ultrastructural features of monocytes/macrophages in periapical granulomas. *J Endod* 17:483-487.

Azuma M, Ito D, Yagita H, Okumura K, Phillips JH, Lanier LL, *et al.* (1993). B70 antigen is a second ligand for CTLA-4 and CD28. *Nature* 366:76-79.

Banchereau J, Steinman RM (1998). Dendritic cells and the control of immunity. *Nature* 392:245-252.

Bluestone JA (1995). New perspectives of CD28-B7-mediated T cell costimulation. *Immunity* 2:555-559.

Cao W, Lee SH, Lu J (2005). CD83 is preformed inside monocytes, macrophages and dendritic cells, but it is only stably expressed on activated dendritic cells. *Biochem J* 385(Pt 1):85-93.

Cella M, Engering A, Pinet V, Pieters J, Lanzavecchia A (1997). Inflammatory stimuli induce accumulation of MHC class II complexes on dendritic cells. *Nature* 388:782-787.

Gao Z, Mackenzie IC, Rittman BR, Korszun AK, Williams DM, Cruchley AT (1988). Immunocytochemical examination of immune cells in periapical granulomata and odontogenic cysts. *J Oral Pathol* 17:84-90.

Kaneko T, Okiji T, Kan L, Suda H, Takagi M (2001a). An immunoelectron microscopic study of class II major histocompatibility complex molecule-expressing macrophages and dendritic cells in experimental rat periapical lesions. *Arch Oral Biol* 46:713-720.

Kaneko T, Okiji T, Kan L, Takagi M, Suda H (2001b). Ultrastructural analysis of MHC class II molecule-expressing cells in experimentally-induced periapical lesions in the rat. *J Endod* 27:337-342.

Kaneko T, Zhang Z, Mantellini M, Karl E, Zeitlin B, Verhaegen M, *et al.* (2007). Bcl-2 orchestrates a crosstalk between endothelial and tumor cells that promotes tumor growth. *Cancer Res* 67:9685-9693.

Kaneko T, Okiji T, Zhao LY, Esgeurra RL, Suda H (2008). Heterogeneity of dendritic cells in rat apical periodontitis. *Cell Tissue Res* 331:617-623.

King CL, Xianli J, June CH, Abe R, Lee KP (1996). CD28-deficient mice generate an impaired Th2 response to *Schistosoma mansoni* infection. *Eur J Immunol* 26:2448-2455.

Köpp W, Schwarting R (1989). Differentiation of T lymphocyte subpupulations, macrophages and HLA-DR-restricted cells of apical granulation tissue. *J Endod* 15:72-75.

Laudanski K, De A, Miller-Graziano C (2007). Exogenous heat shock protein 27 uniquely blocks differentiation of monocytes to dendritic cells. *Eur J Immunol* 37:2812-2824.

Law SK, Micklem KJ, Shaw JM, Zhang XP, Dong Y, Willis AC, *et al.* (1993). A new macrophage differentiation antigen which is a member of the scavenger receptor superfamily. *Eur J Immunol* 23:2320-2325.

Liapatas S, Nakou M, Rontogianni D (2003). Inflammatory infiltrate of chronic periradicular lesions: an immunohistochemical study. *Int Endod J* 36:464-471.

Lukić A, Vasilijić S, Majstorović I, Vucević D, Mojsilović S, Gazivoda D, *et al.* (2006). Characterization of antigen-presenting cells in human apical periodontitis lesions by flow cytometry and immunocytochemistry. *Int Endod J* 39:626-636.

Manara GC, Soligo D, Lambertenghi-Deliliers G, Ferrari C, De Panfilis G (1990). Immunogold scanning electron microscopy applied to the study of Langerhans cells immunophenotype. *Dermatologica* 180:141-145.

Nair PN (2004). Pathogenesis of apical periodontitis and the causes of endodontic failures. *Crit Rev Oral Biol Med* 15:348-381.

Namork E, Meier HE (1989). Silver enhancement of gold probes (5-40 nm): single and double labeling of antigenic sites on cell surfaces imaged with backscattered electrons. *J Electron Microsc Tech* 11:102-108.

Schaer DJ, Schleiffenbaum B, Kurrer M, Imhof A, Bächli E, Fehr J, *et al.* (2005). Soluble hemoglobin-haptoglobin scavenger receptor CD163 as a lineage-specific marker in the reactive hemophagocytic syndrome. *Eur J Haematol* 74:6-10.

Stashenko P, Yu SM, Wang CY (1992). Kinetics of immune cell and bone resorptive responses to endodontic infections. *J Endod* 18:422-426.

Steinman RM (1991). The dendritic cell system and its role in immunogenicity. *Annu Rev Immunol* 9:271-296.

Stoffel MH, Friess AE (2002). Demonstration and cytochemical analysis of anionic sites on ejaculated boar spermatozoa: a scanning electron microscopy study using cationised colloidal gold. *Histochem Cell Biol* 117:61-67.

Suzuki N, Okiji T, Suda H (1999). Enhanced expression of activation-associated molecules on macrophages of heterogeneous populations in expanding periapical lesions in rat molars. *Arch Oral Biol* 44:67-79.

Tani N, Osada T, Watanabe Y, Umemoto T (1992). Comparative immuno-histochemical identification and relative distribution of immunocompetent cells in sections of frozen or formalin-fixed tissue from human periapical inflammatory lesions. *Endod Dent Traumatol* 8:163-169.

Torabinejad M (1994). Mediators of acute and chronic periradicular lesions. *Oral Surg Oral Med Oral Pathol* 78:511-521.

Villadangos JA, Cardoso M, Steptoe RJ, van Berkel D, Pooley J, Carbone FR, *et al.* (2001). MHC class II expression is regulated in dendritic cells independently of invariant chain degradation. *Immunity* 14:739-749.

Wallstrom JB, Torabinejad M, Kettering J, McMillan P (1993). Role of T cells in the pathogenesis of periapical lesions. A preliminary report. *Oral Surg Oral Med Oral Pathol* 76:213-218.

Wang YS, Chi KH, Liao KW, Liu CC, Cheng CL, Lin YC, *et al.* (2007). Characterization of canine monocyte-derived dendritic cells with phenotypic and functional differentiation. *Can J Vet Res* 71:165-174.

Wilson NS, El-Sukkari D, Villadangos JA (2004). Dendritic cells constitutively present self antigens in their immature state in vivo and regulate antigen presentation by controlling the rates of MHC class II synthesis and endocytosis. *Blood* 103:2187-2195.

Zhao LY, Kaneko T, Okiji T, Takagi M, Suda H (2006). Immunoelectron microscopic analysis of CD11c-positive dendritic cells in the periapical region of the periodontal ligament of rat molars. *J Endod* 32:1164-1167.

Zhou LJ, Tedder TF (1995). Human blood dendritic cells selectively express CD83, a member of the immunoglobulin superfamily. *J Immunol* 154:3821-3835.

Downloaded from http://jdr.sagepub.com at TOKYO IKASHIKA UNIVERSITY on March 17, 2009

歯周病学分野

和泉 雄一

医歯学総合研究科・生体支持組織学系専攻・教授
歯周病学／歯学博士

1. 研究の課題名

歯周炎におけるサイトカイン、プロスタグランジン、HMGB1、アナンダマイドの作用機序に関する研究

Study on functional mechanism of cytokine, prostaglandin, HMGB1 and anandamide in periodontitis.

HMGB-1（High Mobility Group Box-1）は、核内では転写因子として働き、細胞外に放出された際にはサイトカイン様活性を示すことが報告されている。この炎症のメディエーターに関して以下の事を明らかにした。HMGB-1はグラム陰性嫌気性菌のLPS刺激によって、単球、マクロファージから放出される。また、HMGB-1は、RAGE、TLR-2、TLR-4を介してNF-κBを活性化し、炎症を遷延化、拡大化する。しかしながら、HMGB-1はヒト歯根膜細胞からのIL-11産生を促し、組織再生にも関与している可能性も示唆された。内因性カンナビノイドであるanandamide（ANA）に関して以下の事を明らかにした。ANAはLPS刺激によりマクロファージから産生され、少量では炎症性サイトカインの産生促進作用、多量ではこれらの産生抑制作用があった。ANAのIL-6、IL-8、MCP-1産生抑制作用は、CB1、CB2を介したものであること。培養HGFsにおいてLPS刺激によるNF-κBの活性化は、AEAにより強く抑制されたこと。これらのことから、ヒト歯周炎患者においてAEA-CB1、CB2経路は、歯周炎の発症に対して抑制的に働いている可能性が示唆された。

2.

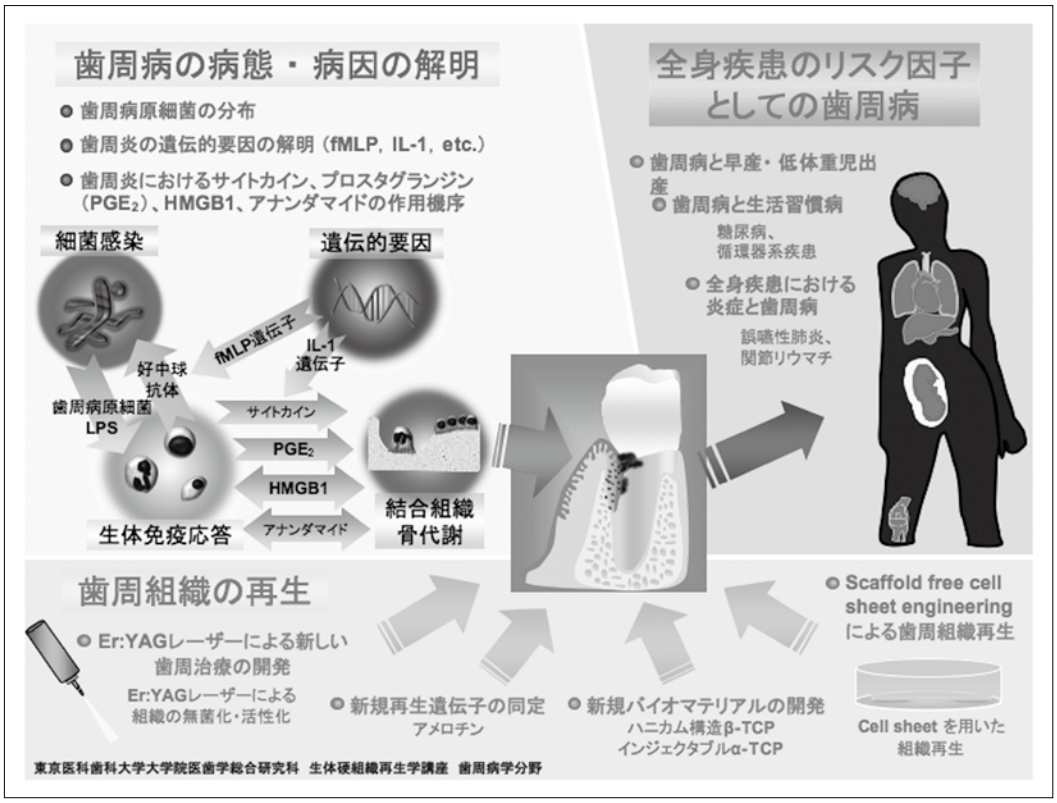

3. 研究内容の英文要約

High-mobility-group box 1（HMGB 1）is continuously released from the gingival epithelial cells modulated by TNF-α. These finding imply that HMGB1 expression and possibly p38MARK constitute important features in periodontitis. IL-6/sIL-6R enhanced ascorbic-acid-induced alkaline phosphatase activity by induction of IGF-1 production in periodontal ligament cells. This result suggests that IL-6 plays a role not only in inflammation, but also in remodeling of alveolar bone to maintain periodontal tissue by regulating osteoblastic differentiation of periodontal ligament cells. From small-case-control studies, we detected periodontitis might be associated with an increased risk of peripheral arterial disease. This association could result from the increased concentration of serum inflammatory cytokines in those with periodontitis. In comparison of different modalities, full-mouth mechanical debridement increased serum IL-6 and reduced serum-soluble thrombomodulin to a greater extent than quadrant-wise mechanical debridement, suggesting that the former technique has stronger transient effects on systemic vascular endothelial functions than the latter. To evaluate the clinical efficacy of a new, injectable calcium phosphate bone cement（CPC）in human periodontal infrabony defects, we performed a randomized clinical trial. The present study failed to demonstrate any superior clinical outcomes for CPC group compared to the open flap debridement group; however, radiographs revealed more favorable results in the CPC group showing no exposure or no loss of the CPC. The filling volume and stiffness of CPC may compromise the clinical outcomes for periodontal infrabony defects.

4. 本事業に関連しての改善・整備等

A（研究拠点体制）

米国UCSFのMark I. Ryder教授およびタイ国Khon Kaen大学のNawarat W Charoen准教授との研究協力体制を樹立した。

B（研究教育環境）

大学院講義を英語で実施し、Tufts大学のPaul Aaron Levi, Jr先生には講義と実習をお願いした。

C（人材確保）

4人のAISSを獲得した。大学院院生を新規に8名受け入れた。

D（人材育成）

新人教育に力を入れ、研究面ではNawarat先生に5名の大学院生の指導をお願いした。

E（国際化）

第9回GCOE海外研究者招聘講演会を主催した。

5. GCOE事業を推進するに当たって力を入れた点

若い研究者に出来る限り国際化の意識を植え付けるように努め、海外での研究発表を推進した。

6. 英文原著論文

1. Chen YW, Umeda M, Nagasawa T, Takeuchi Y, Huang Y, Inoue Y, Imai T, Izumi Y, Ishikawa I. Periodontitis may increase that risk of peripheral arterial disease. Eur J Vas Endovasc Surg 35:153-158, 2008.
2. Eguchi T, Koshy G, Umeda M, Iwanami T, Suga J, Nomura Y, Kawanami M, Ishikawa I. Micro changes in patients with acute periodontal abscess after treatment detected by Padotest. Oral Dis 14;180-184, 2008.
3. Ishikawa, A. Aoki, A.A. Takasaki, K. Mizutani, K.M. Sasaki, Y. Izumi, Applocation of lasers in periodontics: true innovation or myth ?, Periodontol 2000, 49: 1-37, 2009.
4. Iwasaki K, Komaki M, Mimori K, Leon E, Izumi Y, Ishikawa I. IL-6 induces osteoblastic differentiation of periodontal ligament cells. J Dent Res 87（10）:937-942, 2008.
5. Iwaya Y, Machigashira M, Kanbara K, Miyamoto M, Noguchi K, Izumi Y, Ban S. Surface properties and biocompatibility of acid-etched titanium. Dent Mater J 27:415-421, 2008
6. Kadomatsu H, Matsuyama T, Yoshimoto T, Negishi Y, Sekiya H, Yamamoto M, Izumi Y. Injectable growth/differentiation factor-5/ recombinant human collagen composite induces endochondral ossification via sox9 expression and angiogenesis in murine calvariae. J. Periodontal Res, 43: 483-489, 2008.
7. Kamiyama K, Arakawa S, Takahashi M, Chiba K, Yamami N, Yagishita K, Mano Y. Effects of nano-bubble water on periodontal disease. The Jpn J Hyperbaric and Undersea Med 43:53-60, 2008.
8. Kawakatsu N, Oda S, Kinoshita A, Kikuchi S, Tsuchioka H, Akizuki T, Hayashi C, Kokubo S, Ishikawa I, Izumi Y.: Effect of rhBMP-2 with PLGA/gelatin sponge type（PGS）carrier on alveolar ridge augmentation in dogs. Journal of Oral Rehabilitation 35: 647-655, 2008.
9. Kitamura M, Nakashima K, Kowashi Y, Fujii T, Shimauchi H, Sasano T, Furuuchi T, Fukuda M, Noguchi T, Shibutani T, Iwayama Y, Takashiba S, Kurihara H, Ninomiya M, Kido J, Nagata T, Hamachi T, Maeda K, Hara Y, Izumi Y, Hirofuji T, Imai E, Omae M, Watanuki M, Murakami S. Periodontal tissue regeneration using fibroblast growth factor -2: Randomized controlled phase II clinical trial. PLos ONE 3（7）, 2008: e2611. Doi10.1371/j.pone.0002611.
10. Kubota T, Inoue Y, Iwai T, Kurihara N, Huang Y, Umeda M. Arterial thrombosis after intravenous

infusion of oral bacterium in a rat model. Ann Vasc Surg 22:412-416, 2008.
11. Li X, Iwai T, Nakamura H, Inoue Y, Chen Y, Umeda M, Suzuki H. An ultrastructural study of Porphyromonas gingivalis-induced platelet aggregation. Thromb Res 122:810-819, 2008.
12. Maruyama H, Aoki A, Sasaki KM, Takasaki AA, Iwasaki K, Ichinose S, Oda S, Ishikawa I, Izumi Y. The effect of chemical and/or mechanical conditioning on the Er:YAG laser treated root cementum: analysis of surface morphology and periodontal ligament fibroblast attachment. Lasers Surg Med 40（3）:211-222, 2008.
13. Matsuyama, T., Tokuda, M., Izumi, Y., Significance of thrombomodulin release from gingival epithelial cells in periodontitis patients. J Periodontal Res 43: 379-385, 2008.
14. Morimoto, Y., Kawahara, K-I., Tancharoen, S., Kikuchi, K., Matsuyama, T., Hashiguchi, T., Izumi, Y., Maruyama, I., Tumor necrosisi factor-alpha stimulates gingival epithelial cells to release high mobility-group box 1., J Periodontal Res. 43: 76-83, 2008.
15. Nakamura N, Yoshida M, Umeda M, Huang Y, Kitajima S, Inoue Y, Ishikawa I, Iwai T. Extended exposure of lipopolysaccharide fraction from Porphyromonas gingivalis facilitates mononuclear cell adhesion to vascular endothelim via Toll-like receptor-2 dependent mechanism. Atherosclerosis 196:59-67, 2008.
16. Shirakata Y, Setoguchi T, Machigashira M, Matsuyama T, Furuichi Y, Hasegawa K, Nakamura T, Izumi Y. Comparison of injectable calcium phosphate bone cement grafting and open flap debridement in periodontal intrabony defects: A randomized clinical trial. J. Periodontol. 79: 25-32, 2008.
17. Soejima H, Oe Y.,Nakayama H, Matsuo K, Fukunaga T, Sugamura K, Kawano H, Sugiyama S, Shinohara M, Izumi Y, Ogawa H. Periodontal status and Prevotella intermedia antibody in acute coronary syndrome. Int J Cardiol, 2008, doi: 10,1016/j.ijcard.2008.05.057.
18. Sogabe N, Oda K, Nakamura H, Orimo H, Watanabe H, Hosoi T, Goseki-Sone M. Molecular effects of the tissue-nonspecific alkaline phosphatase gene polymorphism（787T > C）associated with bone mineral density. Biomed Res 29（4）:213-219, 2008.
19. Takeuchi, H., Setoguchi, T., Machigashira, M., Kanbara, K, Izumi, Y., Hydrogen sulfide inhibits cell proliferation and induces cell cycle arrest via an elevated p21Cip1 level in Ca9-22 cells., J Periodontal Res. 43: 90-95, 2008.
20. Tancharoen S, Matsuyama T, Abeyama K, Matsushita K, Kawahara K, Sangalungkarn V, Tokuda M, Hashiguchi T, Maruyama I, Izumi Y. The role of water channel aquaporin 3 in the mechanism of TNF-alpha-mediated proinflammatory events: Implication in periodontal inflammation. J Cell Physiol, 217: 338-349, 2008.
21. ◎Ushida Y, Koshy G, Kawashima Y, Kiji M, Umeda M, Nitta H, Nagasawa T, Ishikawa I, Izumi Y. Changes of serum IL-6, CRP, and thrombomodulin levels under periodontal ultrasonic debridement. J Clin Periodontol 35:969-975, 2008.
22. Wang D, Nagasawa T, Chen Y, Ushida Y, Kobayashi H, Takeuchi Y, Umeda M, Izumi Y. Molecular mimicry of Aggregatibacter acttinomycetemcomitans with β 2 glycoprotein 1. Oral Microbiol Immnol 23:401-405, 2008.
23. Y. Oe, H. Soejima, H. Nakayama, T. Fukunaga, K. Sugamura, H. Kawano, S. Sugiyama, K. Matsuo, M. Shinohara, Y. Izumi, H. Ogawa, Significant Association Between Score of Periodontal Disease and Coronary Artery Disease. Heart and Vessels（in press）
24. Yoshino T, Aoki A, Oda S, Takasaki AA, Mizutani K, Sasaki KM, Kinoshita A, Watanabe H, Ishikawa I, Izumi Y. Long-term histological analysis of bone tissue alteration and healing following Er:YAG laser irradiation in comparison with electrosurgery. J Periodontol（in press）
25. Miyazaki H, Kato J, Watanabe H, Harada H, Kakizaki H, Tetsumura A, Sato A, Omura K. Intralesional laser treatment of voluminous vascular lesions in the oral cavity. Oral Surg Oral Med Oral Path, Oral Rad Endodont 107（2）:164-172, 2009.
26. Miyazaki H, Kato J, Kakizaki H, Nagata T, Uetake H, Okudera H, Watanabe H, Hashimoto K, Omura K. Submucosal glycerol injection assisted laser surgical treatment of oral lesions. Lasers Med Sci 24:13-19, 2009.

7. 著書

1. Aoki A, Takasaki AA, Pourzarandian A, Mizutani K, Ruwanpura SMPM, Iwasaki K, Noguchi K, Oda S, Watanabe H, Ishikawa I, Izumi Y. Photo-bio-modulation Laser Strategies in Periodontal Therapy. Waynant R, Tata DB（Eds）, Proceedings of Light-Activated Tissue Regeneration and Therapy Conference. Springer, New York, 2008.181-190.
2. 青木 章、和泉雄一． Er:YAGレーザーを用いた歯石除去・歯周ポケット治療.日本歯科評論増刊2008-症例でみる歯科用レーザーの有効活用,ヒョウロン・パブリッシャーズ,東京.2008.68-69. 総頁: 227頁.
3. 青木 章、和泉雄一． 歯周治療領域におけるレーザーの現状と可能性.日本歯科評論増刊2008-症例でみる歯科用レーザーの有効活用,ヒョウロン・パブリッシャーズ,東京.2008.62-63. 総頁: 227頁.
4. 青木 章、丸山裕昭、和泉雄一. Er:YAGレーザーに

よるメタルタトゥーの除去.日本歯科評論増刊2008-症例でみる歯科用レーザーの有効活用,ヒョウロン・パブリッシャーズ,東京.2008.164-165. 総頁: 227頁.
5. 石川烈、矢代麗子、Mara Gomez Flores、長谷川昌輝、秋月達也.トランスレーショナルリサーチを支援する　遺伝子医学MOOK別冊 進み続ける細胞移植治療の実際　下巻 ―再生医療の実現に向けた科学・技術と周辺要素の理解―細胞移植治療の現状とその周辺環境治療を目的とした細胞移植 2.前駆細胞、幹細胞 14）歯根膜シートの歯周組織再生療法への応用　第1章　株式会社メディカルドウ 2008.98-101.
6. 和泉雄一.　歯周病と全身疾患　Floss or Die.　月刊レジデント. 医学出版社, 東京. 2008.146-149.
7. 和泉雄一.　歯周病と全身疾患　心臓・血管系疾患および糖尿病への影響.　月刊レジデント.　医学出版社, 東京. 2008.114-117.
8. 和泉雄一.　歯周病と全身疾患　早産・低体重児出産および誤嚥性肺炎への影響.　月刊レジデント.　医学出版社, 東京. 2008.142-145.
9. 和泉雄一.　歯周組織の健康と全身的リスク因子.　歯周病学の視点からみた国民の健康増進.　医歯薬出版株式会社, 東京. 2008.48-51.
10. 和泉雄一、小田　茂、秋月達也、高崎アリステオ淳志、須田智也.　GTR法の術式.　ステップアップGTR歯周組織再生誘導法.　医歯薬出版株式会社, 東京、2008.36-47.
11. 和泉雄一、荒川真一、高崎アリステオ淳志. インプラントと歯周病学.　AQBインプラントの基礎と臨床.　AQB学術研究会, 東京.2008.72-81.
12. 和泉雄一、荒川真一. 歯周基本治療（1）モチベーションとプラークコントロールの実際. YEAR BOOK 2008 現代の治療指針,欠損・審美補綴と全治療分野.　クインテッセンス出版株式会社, 東京. 2008.190-191. 総頁:257
13. 和泉雄一、小田　茂、秋月達也、高崎アリステオ敦志:GC友の会　歯周外科トレーニングDVD　マスターしよう!歯周外科　–歯周外科Basic–、2008年8月、株式会社GC、東京.
14. 小田　茂、秋月達也:歯周病と全身疾患.高戸　毅、天笠光雄、葛西一貴、古郷幹彦、須佐美隆史、鈴木茂彦、谷口　尚、新美成二編集　口と歯の辞典、朝倉書店、東京. 2008.237-240.
15. 高崎 アリステオ 淳志、青木　章、水谷　幸嗣、和泉　雄一.Er:YAGレーザーによるマイクロスコープ下での歯肉のメラニン沈着除去. 日本歯科評論増刊2008-症例でみる歯科用レーザーの有効活用,ヒョウロン・パブリッシャーズ,東京、2008.160-161. 総頁: 227頁
16. 中島京樹、青木章、津田忠政.歯科用レーザーの未来をみつめて.日本歯科評論増刊2008-症例でみる歯科用レーザーの有効活用,ヒョウロン・パブリッシャーズ,東京、2008.212-219総頁: 227頁.
17. 水谷幸嗣、青木 章、高崎アリステオ淳志、和泉雄一.歯周外科治療へのEr:YAGレーザーの応用.日本歯科評論増刊2008-症例でみる歯科用レーザーの有効活用,ヒョウロン・パブリッシャーズ,東京、2008.78-79. 総頁: 227頁
18. 渡辺　久、津久井　明.歯周形成外科におけるレーザーの応用. 現在の治療指針　歯周治療と全治療分野編　イヤーブック2008 クインテッセンス出版　東京 2008, 106-107. 総頁:257
19. 渡辺　久、和泉雄一.骨整形へのEr:YAGレーザーの応用. 平井義人、千田　彰、津田忠政編著　歯科用レーザーの有効活用　ヒョーロン・パブリッシャーズ、東京、2008.80-81. 総頁: 227頁

8. 自己評価

今年度の研究課題についてはほぼ予定通りの進行を示している。また、研究拠点体制作りでは、UCSFのMark　Raider教授やタイのKhon Kaen大学のNawarat W Charoen准教授とのコラボレーションが順調に進んでいる。

9. 和文原著論文

長谷川奈美: High Mobility Group Box 1（HMGB1）が培養ヒト歯根膜細胞に与える影響　口病誌 75 (3) :13-19, 2008.

10. 学会発表（英文）

1. Feghali K, Iwasaki K, Tanaka K, Izumi Y. Human gingival fibroblasts release HMGB1 after stimulation with LPS. 86th General session of international association of dental research. (2008.7.2-5, Toronto)
2. Morimoto Y, Kawahara K-I, Kikuchi K, Tancharosen S, Matsuyama T, Izumi Y, Maruyama I, Noguchi K. Gingival epithelial cells potently release HMGB1:Implications in periodontitis. 86th General session of international association of dental

research.（2008.7.2-5, Toronto）
3. Watanabe H, Ichinose S, Izumi Y. Bactericidal activity of Mastic against Porphyromonas gingivalis. 86th General session of international association of dental research.（2008.7.2-5, Toronto）
4. Izumi Y, Mizutani K, Takasaki AA, Ohnishi H, Suda T, Aoki A. Successful management of gingival enlargement using lasers in a patient with a serious systemic disease: a case report. 11th Meeting of the World Federation for Laser Dentistry（2008.7.28-30. Hong Kong）.
5. Maruyama H, Aoki A, Sasaki KM, Takasaki AA, Iwasaki K, Ichinose S, Oda S, Ishikawa I, Izumi Y. The effect of chemical and/or mechanical conditioning on the Er:YAG laser-treated root cementum: Analysis of surface morphology and periodontal ligament fibroblast attachment. 11th Meeting of the World Federation for Laser Dentistry（2008.7.28-30. Hong Kong）.
6. Mizutani K, Aoki A, Takasaki AA, Maruyama H, Schwarz F, Yamada T, Ichinose S, Ishikawa I , Izumi Y. Effect of high pulse rate Er:YAG laser irradiation using a chisel tip on subgingival calculus removal in vitro. 11th Meeting of the World Federation for Laser Dentistry（2008.7.28-30. Hong Kong）.
7. Takasaki AA, Aoki A, Mizutani K, Akizuki T, Kobayashi H, Oda S, Watanabe H, Umeda M, Ishikawa I, Izum Y. Clinical evaluation of high pulse rate Er:YAG laser application in periodontal flap surgery. 11th Meeting of the World Federation for Laser Dentistry（2008.7.28-30. Hong Kong）.
8. Yoshino T, Aoki A, Oda S, Takasaki AA, Mizutani K,Sasaki KM, Kinoshita A, Watanabe H, Ishikawa I, IzumiY. Long-term Histological Analysis of Bone Tissue Alteration and Healing Following Er:YAG Laser Irradiation in Comparison with Electrosurgery. 11th Meeting of the World Federation for Laser Dentistry（2008.7.28-30. Hong Kong）.
9. Yanagiuchi Y, Aoki A, Gutknecht N, Ito A, Ishikawa I, Izumi Y. The effect of the pulse duration of Er:YAG laser on bone ablation. 11th Meeting of the World Federation for Laser Dentistry（2008.7.28-30. Hong Kong）.
10. Miyazaki H, Kato J, Watanabe H, Uetake H, Hashimoto K, Omura K. Laser surgical treatment of oral lesions assisted by glycerol submucosal injection. 11th Congress of World Federation for Laser Dentistry（2008.7.28-30. Hong Kong）
11. Watanabe H, Tutsui A, Izumi Y. Clinical use of Er:YAG laser on semi-lunar coronally repositioned flap procedure. 11th Meeting of the World Federation for Laser Dentistry（2008.7.28-30. Hong Kong）.
12. Suda T, Nagasawa T, D Q Wang, Takeuchi Y, Inoue Y, Izumi Y. RANKL expression in abdominal aortic aneurysms might be associated with periodontopathic bacteria. 94th Annual Meetimg of the American Academy of Periodontology.（2008.11.6-9, Seattle）
13. Feghali K, Iwasaki K, Tanaka K, Komaki K, Izumi Y. Human gingival fibroblasts release HMGB1 through active and passive pathways. 56th Annual meeting of Japanese association of dental research.（2008.11.29-30, Nagoya）

11. 学会発表（和文）

1. 梅田　誠、三輪全三、茂木瑞穂、竹内康雄、高木裕三、和泉雄一:小児口腔内の歯周病原細菌の消長と歯周病臨床パラメータの関係について　日歯周誌50（春季特別号）pp131, 2008. 第51回春季日本歯周病学会学術大会（2008.4.25-26. 大宮）
2. 長澤敏行、王　冬青、陳イモン、牛田由佳、竹内康雄、小林宏明、須田智也、梅田　誠、和泉雄一:β-2 glycoprotein Ⅰと相同性を有する歯周病原細菌由来ペプチドに対する歯周炎患者の抗体反応　日歯周誌50（春季特別号）pp119, 2008. 第51回春季日本歯周病学会学術大会（2008.4/25-26. 大宮）
3. 佐藤郁文,秋月達也,小田　茂,岩崎剣吾,岩田隆紀,宮田　敦,高崎アリステオ淳志,石川　烈,和泉雄一.イヌ由来歯根膜細胞を使用したスキャフォールドフリー細胞シート作成.日本歯周病学会誌プログラム抄録集p.152,第51回春季日本歯周病学会学術大会（2008,4.25 大宮）
4. 和泉雄一、町頭三保、迫田賢二、吉元剛彦、門松秀司、村田道明、松山孝司、瀬戸口尚志:KCB-1D（FGF-2）歯周組織再生試験（後期第Ⅱ相）―フラップ手術施

行時にKCB-1Dを投与した慢性歯周炎患者4症例―　日歯周誌50（春季特別号）pp171, 2008. 第51回春季日本歯周病学会学術大会（2008.4.25-26. 大宮）

5. 北村正博、小田　茂、和泉雄一他29名:KCB-1D（FGF-2）歯周組織再生試験（後期第Ⅱ相）その1-有効性の評価―　日歯周誌50（春季特別号）pp169, 2008. 第51回春季日本歯周病学会学術大会（2008.4.25-26. 大宮）
6. 山田　聡、小田　茂、和泉雄一他28名:KCB-1D（FGF-2）歯周組織再生試験（後期第Ⅱ相）その2-安全性の評価―　日歯周誌50（春季特別号）pp170, 2008. 第51回春季日本歯周病学会学術大会（2008.4.25-26. 大宮）
7. 吉元剛彦、松山孝司、輿那嶺　豊、門松秀司、小薗清香、山本松男、和泉雄一:Growth/differentiation factor-5（GDF-5）による歯周組織再生の検討　日歯周誌50（春季特別号）pp147, 2008. 第51回春季日本歯周病学会学術大会（2008.4.25-26. 大宮）
8. 柳井昌之、谷村　静、中原光香、野口和行、和泉雄一:非外科的歯周治療およびMTMによって改善した重度広汎型侵襲性歯周炎の一症例　日歯周誌50（春季特別号）pp223, 2008. 第51回春季日本歯周病学会学術大会（2008.4.25-26. 大宮）
9. 和泉雄一:Papillon-Lefevre症候群患者の遺伝子解析　シンポジウム:科学研究費基盤（A）成果報告・歯周病の疾患感受性に関わる遺伝子解析　日歯周誌50（春季特別号）pp60-61, 2008. 第51回春季日本歯周病学会学術大会（2008.4.25-26. 大宮）
10. 渡辺　久:低フォスファターゼ症歯周炎患者の遺伝子解析　シンポジウム:科学研究費基盤（A）成果報告・歯周病の疾患感受性に関わる遺伝子解析　日歯周誌50（春季特別号）pp62-63, 2008. 第51回春季日本歯周病学会学術大会（2008.4.25-26. 大宮）
11. 水谷幸嗣、青木章、高崎アリステオ淳志、丸山裕昭、和泉雄一.チゼル型チップを用いた高パルスEr:YAGレーザー照射による歯石除去効果.日歯保存誌51春季特別号:p.45, 2008. 日本歯科保存学会 第128回春季学術大会（2008.6.6. 新潟）
12. 長谷川奈美、小林宏明、福井朋恵、和泉雄一;High Mobility Group Box 1（HMGB1）がヒト歯根膜に与える影響　第51回春季日本歯周病学会学術大会（2008,4/25　大宮）
13. 梅田　誠:ペリオクリンの効果的な適用と展望（シンポジウムⅡ）　抄録集pp46-47. 第28回日本歯科薬物療法学会　総会・学術大会（2008.6.26-28. 東京）
14. 長谷川奈美、小林宏明、福井朋恵、岩崎剣吾、和泉雄一;High Mobility Group Box 1は歯根膜細胞のIL-8産生を増強する　第29回日本炎症・再生医学会（2008.7.9. 都市センターホテル）
15. 堀江明子、吉田直美、須永昌代、竹内康雄、木下淳博:歯科衛生士教育における医歯学シミュレーション教材の学習システムとしての評価. 第27回日本歯科医学教育学会学術大会（2008.7.11, 東京）
16. 青木章,水谷幸嗣,高崎アリステオ淳志,石井さやか,Verica Aleksic, Chen-Ying Wang,和泉雄一.チゼルチップを用いたEr:YAGレーザーによるメラニン除去.プログラム・講演抄録集p.86,日本レーザー歯学会第20回記念大会総会・学術大会（2008.9.20. 大阪）.
17. 吉野敏明、青木章、小田茂、高崎アリステオ淳志、水谷幸嗣、木下淳博、渡辺久、石川烈、和泉雄一.骨組織に対するEr:YAGレーザー照射後の長期組織学的観察.大会プログラム・講演抄録集p.107,日本レーザー歯学会第20回記念大会総会・学術大会（2008.9.20. 大阪）
18. 和泉雄一、水谷幸嗣、高崎アリステオ淳志、青木章.薬物性歯肉増殖を伴う慢性歯周炎の治療にレーザーを併用した一症例.大会プログラム・講演抄録集p.106,日本レーザー歯学会第20回記念大会総会・学術大会（2008.9.20. 大阪）
19. 津久井　明、渡辺　久. Er:YAGレーザーによる根面被覆（半月弁切開移動術）への臨床応用. 第20回日本レーザー歯学会　（2008.9.20. 大阪）
20. 大西英知、荒川真一、中島琢磨、和泉雄一:歯周炎患者由来の歯肉溝滲出液中に存在するForsythia detaching factor:FDFに対する抗体価と歯周炎の病態との関連性の解析　プログラム抄録集P58, 第50回歯科基礎医学学術大会（2008.9.23-26,東京）
21. 竹下　晋、金澤　学、藤波由希子、水口俊介、渡辺　久. グルテンを使用した咀嚼食品の義歯付着性検討. プログラム・抄録集　pp.55, 第19回日本咀嚼学会（2008.9.27. 東京）
22. 大西英知、荒川真一、長澤敏行、小林宏明、竹内康雄、水谷幸嗣、矢代麗子、牛田由佳、甘美和、横田悟、渡辺香、北川原聡、中島啓子、関西一史、片桐さやか、梅田誠、中島琢磨、和泉雄一:歯周炎患者と健常者における歯肉溝滲出液中の抗FDF抗体価の比較　日本歯周病学会プログラム抄録集p58, 第51回秋季日本歯周病学会学術大会（2008.10.19,四日市）

23. 牛田由佳、Geena Koshy、川嶋庸子、喜地　誠、梅田　誠、新田　浩、長澤敏行、石川　烈、和泉雄一:超音波スケーラーによる full-mouth debridement 後の血清IL-6, CRP および可溶性トロンボモジュリンの変動　日本歯周病学会プログラム抄録集p151, 第51回秋季日本歯周病学会学術大会（2008.10.19,四日市）
24. 竹内康雄、渡辺 久、和泉雄一:柿ポリフェノールオリゴマーの歯周病原細菌に対する抗菌効果　日本歯科保存学会プログラムおよび講演抄録集 pp135, 2008. 第129回日本歯科保存学会秋期学術大会（2008.11.6-7. 富山）
25. 梅　田　誠、陳　イ　モ　ン、黄　怡、G. AMODINI RAJAKARUNA、ASLAM ALMEHDI、竹内康雄、長澤敏行、井上芳徳、栗原伸久、岩井武尚、和泉雄一:歯周病の血管疾患に対する関与について.第21回日本歯科医学会総会（2008.11.14-16. 横浜）
26. 青木　章,水谷幸嗣,和泉雄一.Er:YAGレーザーの歯周治療への臨床応用.（テーブルクリニック）,日本歯科医師会雑誌61（5）: 80（480）, 2008. 第21回日本歯科医学会総会（2008.11.15、横浜）.
27. 渡 辺　久,青 木　章,和 泉 雄 一.レ ー ザ ー のBiostimulation効果のメカニズムに関する研究.日本歯科医師会雑誌61（5）: 105（505）, 2008. 第21回日本歯科医学会総会（2008.11.15、横浜）.
28. 萩原さつき.　重度歯周炎を有する2型糖尿病患者に対する歯周治療の効果:血糖のコントロールと炎症のメディエーターの変化について.日本歯科医師会雑誌61（5）:125（525）, 2008. 第21回日本歯科医学会総会（2008.11.15、横浜）.
29. 秋月達也、小田茂、佐藤郁文、岩崎剣吾、田中敬子、岩田隆紀、川勝紀子、矢代麗子、大和雅之、岡野光夫、石川烈、和泉雄一. 歯根膜シートを用いた歯周組織再生療法.日本歯科医師会雑誌　Vol.61 No.5 P110, 2008. 第21回　日本歯科医学会総会.（ 2008.11.15、横浜　）
30. 渡 辺　久. Er:YAG レ ー ザ ー のbiostimulation 効果に関する分子生物学的研究. 日本レーザー医学会誌　29（3）:323, 2008, 第29回日本レーザー医学会（2008.11.16. 東京）
31. 水谷幸嗣、青木章、丸山裕昭、和泉雄一.チゼル型チップを用いた高パルスEr:YAGレーザー照射による歯石除去効果.プログラム抄録集 p.17, 口腔病学会 第73回学術大会（2008.12.6. 東京）
32. 佐藤郁文,秋月達也,小田　茂,林　千絵,水谷幸嗣,田中紀子,木下淳博,石川　烈,和泉雄一.リン酸カルシウムセメントを応用した歯槽堤増大術の組織学的評価.プログラム抄録集p.15, 口腔病学会第73回学術大会（2008.12.6. 東京）
33. 須田智也, 長澤敏行, 竹内康雄, 梅田　誠,和泉雄一.腹部大動脈瘤でのRANKL発現と歯周病原細菌の検出との関連. プログラム抄録集p.7, 口腔病学会第73回学術大会（2008.12.6. 東京）

12. 受賞

1. 吉野敏明、青木章、小田茂、高崎アリステオ淳志、水谷幸嗣、木下淳博、渡辺久、石川烈、和泉雄一. 第20回日本レーザー歯学会総会・学術大会優秀発表賞,骨組織に対するEr:YAGレーザー照射後の長期組織学的観察.（2008.9.21.大阪）.

2. 水谷幸嗣,青木　章,高崎アリステオ淳志,丸山裕昭,和泉雄一.第128回日本歯科保存学会秋季学術大会デンツプライ賞（Dentsply - Merit Award）. チゼル型チップを用いた高パルスEr:YAGレーザー照射による歯石除去効果（第128回日本歯科保存学会春季学術大会,新潟,2008.6.6発表）.（2008.11.6. 富山）

13. 外部資金獲得状況

科学研究費補助金、基盤B

研究題目:新規炎症調節物質（ANAとHMGB-1）を軸とした歯周病態形成機構の解明と制御
代表:　和泉雄一
期間:　平成18年―平成20年
研究費総額:1040万円

奨学寄附金

キャドバリー・ジャパン株式会社	390万円
野口歯科医学研究所株式会社	153万4千円
株式会社インプラント・イノベイションズ・ジャパン	85万円
株式会社松風	100万円
昭和薬品化工株式会社	50万円

14. 特別講演、招待講演

1. Izumi Y.:Periodontal tissue regeneration at present and in the near future, 21st Century COE Program for " Frontier Research Program on Molecular Destruction and Reconstruction of Tooth and Bone", The 12th Symposium（2008. 1. 20. Tokyo）

2. 和泉雄一:歯周病と全身とのかかわり、九州お茶の水会1月研修会、(2008. 1. 27. 博多)
3. 和泉雄一:歯周病と全身とのかかわりについて、平成19年度神奈川県歯科衛生士講習会、(2008. 1. 31 横浜)
4. Izumi Y.:Periodontal tissue regeneration, Advanced Course for Periodontal Surgery in Kagoshima, (2008. 2. 3. Kagoshima)
5. 和泉雄一:メタボリックシンドロームの黒幕それは歯周病?、第1回パールリボン特別企画 お口と身体の健康フェスティバル 、(2008. 2. 10. 宮崎)
6. 和泉雄一:糖尿病と歯周病のかかわり、第30回糖尿病治療研究会、(2008. 2. 23. 京都)
7. 和泉雄一:骨髄間葉系幹細胞の細胞移植や歯根膜シートによる歯周組織再生治療への取り組み、第7回日本再生医療学会総会、(2008. 3. 13,14 名古屋)
8. 和泉雄一:インプラント治療とインプラント周囲炎、インプラント実践パーフェクトセミナー、(2008. 6. 1. 東京)
9. 和泉雄一:歯周病と全身のかかわり、御茶ノ水歯学研修会、(2008. 6. 15. 東京)
10. 和泉雄一:第14回糖尿病と歯周病、たかが歯周病、されど歯周病、第14回DM京都専門家による糖尿病実践講座、(2008. 6. 22. 京都)
11. 和泉雄一:8020運動20周年を迎えて ~医科・歯科連携を中心とした歯科医療最前線~、第14回口腔保健シンポジウム、(2008. 7. 5. 東京)
12. 和泉雄一:歯周治療をめぐる最近の話題、群馬歯周治療研究会、(2008. 7. 19. 前橋)
13. 和泉雄一:インプラント周囲炎のメカニズム、OJミーティング2008、(2008. 7. 27. 東京)
14. 和泉雄一:歯周組織再生の現状と近未来、3i シンポジウム2008、(2008. 8.10. 大阪)
15. 和泉雄一:歯周病と全身疾患とのかかわり、熊本県歯科医師会8020運動事業推進者講習会、(2008. 9. 28. 熊本)
16. 和泉雄一:シンポジウムⅠ健康国家と「歯の健康」を考える、歯の健康力と全身の健康 ー歯周病と全身とのかかわりー、第57回日本口腔衛生学会・総会、(2008. 10. 3. 大宮)
17. 和泉雄一:歯周病に関する最新情報、歯科医療ビジネスにおけるセンサ開発事業の最前線、第8回産学連携フェア、(2008. 10. 8. 北九州)
18. 和泉雄一:日常臨床のための歯周組織再生療法、エムドゲイン®ゲル特別講演会、(2008. 10. 13. 東京)
19. 和泉雄一:歯周病と早産・低体重児との関連、平成20年度歯科保健関係者研修会、(2008. 10. 16. 富山)
20. 和泉雄一:歯周病と全身とのかかわり、平成20年度大和市、厚木市在宅歯科衛生士講習会、(2007. 10. 31. 大和)
21. 和泉雄一:歯周病と糖尿病との深いかかわり、歯周病と糖尿病、足利市歯科医師会市民公開講座、(2008. 11. 1. 足利)
22. 和泉雄一:ティシュエンジニアリングの基礎と応用ー歯周組織の再生を目指してー、九州インプラント研究会、(2008. 11. 22. 熊本)
23. 和泉雄一:歯周病と全身疾患とのかかわり、熊本県歯科医師会8020運動事業推進者講習会、(2008. 11. 29. 八代)
24. 和泉雄一:歯周組織の健康と全身の健康とのかかわり、日本歯科大学歯周同門会研究会、(2008. 12. 13. 東京)
25. 和泉雄一:歯周病と糖尿病との深いかかわり、8020県民公開講座　歯周病と糖尿病、(2008. 12. 14.　高松)

15. 新聞、雑誌、TV報道

1. 青木　章.テレビ出演,とくまるー現代人の持病!「歯周病」を徹底予防!,はなまる,TBS, 2008.9.10. 8:35-9:05am.
2. 和泉雄一,　岩崎剣吾,竹内康雄.　ウォーターピック®の有効性　　ウォーターピック販売パンフレット　ヨシダ　2008
3. 和泉雄一,　岩崎剣吾,竹内康雄.　ウォーターピック®の有効性　Dental Product News Dental Hygienist, ヨシダ, 東京.　p.1, vol.34, 2008.
4. 和泉雄一,　岩崎剣吾,竹内康雄.　ウォーターピック®の有効性　Dental Product News, ヨシダ, 東京.　p.1, vol.172, 2008.
5. 和泉雄一,　岩崎剣吾,竹内康雄.　ウォーターピック®の有効性　Dental Product News　矯正歯科特集号 ヨシダ, 東京, 2008.
6. 和泉雄一. あんしん診療室.　歯周病②あんしんLife. p.26-27, vol.43, 2008.
7. 和泉雄一.　健康相談　教えて!ドクター. けんぽニュース. 保健同人社, 東京.　冬号　p14, 2008.
8. 和泉雄一. インプラント治療における、現代病・歯周疾患へのアプローチ.　AQB新聞. 株式会社アドバンス, 東京.　No.22　p1-2, 2008.
9. 和泉雄一. 本気で撃退　全身の健康も寿命も左右する歯周病.　暮らしと健康. 保健同人社p.8-13, 18, 2008.
10. 和泉雄一. 知っていますか?　歯周病と生活習慣病の

深い関係． 栄養と料理. 女子栄養大学出版. P.6-11, 10月号, 2008.
11. 和泉雄一. インプラント治療における歯周病の考え方. Dialogue, Nobel Biocare. p16-17, 秋号, 2008.
12. 和泉雄一. もうはじまっている、健康長寿への新たな挑戦!歯っぴいスマイル． 日本歯科医師会, 東京. P.5-6, vol.16, 2008.
13. 和泉雄一. これからの歯周病予防 -歯の健康から全身の健康へ-． SUNSTAR NEWS. サンスター株式会社, 東京.p.2-3, vol.3, 2008.
14. 和泉雄一. 第14回口腔保健シンポジウム， 歯周病の予防 健康の入り口． 読売新聞. 読売新聞社, 東京.22-23面, 2008年7月27日
15. 小田 茂:歯周病の治療法、暮らしと健康、2009年2月号、p74、保健同人社、2009.2.1.
16. 渡辺 久:歯周病と早期低体重児出産との関連性—妊婦の羊水中に初めてP.g 菌が海外ジャーナルWatching デンタルダイヤモンド 2月号 pp. 83, 2008
17. 渡辺 久:歯周病も防いでメタボも予防 gooヘルスケア 医療と健康2008.2.26 配信 http://health.goo.ne.jp/
18. 渡辺 久:医心伝身 歯周病のプラーク除去に痛みのないレーザー治療 週刊ポスト 5月23日号, 2008 pp.118
19. 渡辺 久:歯周病で死にたいですか? 日刊ゲンダイ 2008年10月28日
20. 渡辺 久:ペリオと補綴のスペシャリストが臨床家におくる国際誌 海外ジャーナルWatching デンタルダイヤモンド 11月号 pp. 120, 2008

16. 講座の准教授、講師、助教、特別研究員、ポスドク、指導を受けた大学院生の名前（AISSには○印）のリスト

准教授 渡辺 久
講 師 小田 茂、萩原さつき
助 教 梅田 誠、長澤敏行、青木 章、荒川真一、小林宏明
外国人特別研究員
Nawarat Wara-aswapati Charoeen
大学院 長谷川奈美、佐藤郁文、須田智也、坂東由記子、○Karine Antonine
藤村麻衣子、田中敬子、大西英知、○江部典子、○Aleksic Verica
青山典生、小林知映、春田千裕、小柳達郎、鈴木允文、谷口陽一、
寺地真由、南原弘美、早雲彩絵、姫野彰子、○GAAslam AL Mehdi、
○ GA Rajakaruna 、Bharti Pariksha
（○:AISS）

Journal of Clinical Periodontology

Official Journal of The European Federation of Periodontology
Founded by the British, Dutch, French, German, Scandinavian, and Swiss Societies of Periodontology

J Clin Periodontol 2008; 35: 969–975 doi: 10.1111/j.1600-051X.2008.01316.x

Journal of Clinical Periodontology

Changes in serum interleukin-6, C-reactive protein and thrombomodulin levels under periodontal ultrasonic debridement

Yuka Ushida[1], Geena Koshy[1], Yoko Kawashima[1], Makoto Kiji[1], Makoto Umeda[1], Hiroshi Nitta[2], Toshiyuki Nagasawa[1], Isao Ishikawa[1,3] and Yuichi Izumi[1,4]

[1]Section of Periodontology, Department of Hard Tissue Engineering, Graduate School, [2]Behavioral Dentistry, Department of Comprehensive Oral Care, Tokyo Medical and Dental University, Tokyo, Japan; [3]Institute of Advanced Biomedical Engineering and Science, Tokyo Women's Medical University, Tokyo, Japan; [4]Global Center of Excellence Program, International Research Center for Molecular Science in Tooth and Bone Diseases, Tokyo Medical and Dental University, Tokyo, Japan

(Correction added on 9 October 2008, after first online publication. Affiliations 1 and 2 were amended.)

Ushida Y, Koshy G, Kawashima Y, Kiji M, Umeda M, Nitta H, Nagasawa T, Ishikawa I, Izumi Y. Changes in serum interleukin-6, C-reactive protein and thrombomodulin levels under periodontal ultrasonic debridement. J Clin Periodontol 2008; 35: 969–975. doi: 10.1111/j.1600-051X.2008.01316.x.

Abstract

Aim: This study aimed to compare the effect of single-visit full-mouth mechanical debridement (FMD) and quadrant-wise mechanical debridement (QMD) on the levels of serum interleukin (IL)-6, C-reactive protein (CRP) and soluble thrombomodulin.

Material and Methods: Thirty-six subjects with chronic periodontitis were randomly allocated to three groups: undergoing QMD, single-visit FMD with povidone iodine or with water. Serum IL-6 and soluble thrombomodulin were measured by enzyme-linked immunosorbent assay, and serum CRP was measured by the latex-enhanced nephelometric method.

Results: Serum IL-6 level increased significantly immediately after debridement in all the three groups, with this increase being greatest in the full-mouth groups. However, the increase in the full-mouth groups was not significantly higher than that of quadrant-wise group. In the quadrant-wise group, serum IL-6 level decreased significantly 1 month after debridement compared with baseline. Serum-soluble thrombomodulin decreased significantly in the full-mouth groups but not in the quadrant-wise group. Changes in CRP level were not significant at baseline or after debridement in all the three groups.

Conclusions: FMD increased serum IL-6 and reduced serum-soluble thrombomodulin to a greater extent than QMD, suggesting that the former technique has stronger transient effects on systemic vascular endothelial functions than the latter.

Key words: CRP; IL-6; periodontitis; single-visit full-mouth debridement; soluble thrombomodulin

Accepted for publication 4 August 2008

Conflict of interest and source of funding statement

There is no conflict of interests.
This study was supported in part by Grants-in-Aid for Scientific Research from the Japan Society for the Promotion of Science (nos. 18390561, 15390642 and 18592258) and the grant for the Center for Excellence Program for Frontier Research on Molecular Destruction and Reconstruction of Tooth and Bone at Tokyo Medical and Dental University.

Periodontitis is a chronic inflammatory disease caused by periodontopathic bacteria, and is the leading cause of tooth loss in the adult population. Patients with periodontitis are exposed to periodontopathic bacteria and their components including lipopolysaccharide through the periodontal pockets (Beck et al. 1996). Lipopolysaccharide, an endotoxin component of the outer membrane in gram-negative bacteria, acts as a potent stimulus to a variety of host cells, resulting in the expression of cytokines, adhesive proteins and pro-inflammatory molecules (Raetz 1990, Tapping & Tobias 1997).

Bacteremia or endotoxemia has been reported after subgingival debridement (Ide et al. 2004, Takai et al. 2005, Forner et al. 2006a). Several researchers have noted bacteremia and short term increase in serum interleukin (IL)-6 following scaling (Ide et al. 2004, Forner et al. 2006b, Tonetti et al. 2007).

© 2008 The Authors
Journal compilation © 2008 Blackwell Munksgaard

IL-6 is known to increase hepatic levels of C-reactive protein (CRP) (Steel & Whitehead 1994), and elevation of IL-6 and CRP has been associated with cardiovascular disease (Rattazzi et al. 2003).

The von Willebrand factor (vWF) and soluble thrombomodulin are circulating markers of endothelial function in cardiovascular disease (Constans & Conri 2006). Bizzarro et al. (2007) reported that more peiodontitis patients had elevated levels of vWF than periodontally healthy subjects. Soluble thrombomodulin can be released from injured endothelial cells, and is a specific marker of endothelial cell damage (Ishii et al. 1991). However, little is known about soluble thrombomodulin in periodontitis.

Full-mouth disinfection was introduced by Quirynen in 1995, based on the hypothesis that conventional quadrant scaling and root planing might cause re-infection of the treated pockets with periodontopathic bacteria from the untreated pockets (Quirynen et al. 1995). To eliminate periodontopathic bacteria and avoid re-infection, scaling and root planing of all periodontal pockets is completed in a short period of time (within 24 h) in the full-mouth disinfection approach. Various effects of this novel treatment have been recently reported (Quirynen et al. 2000, 2006, Apatzidou & Kinane 2004, Koshy et al. 2005, Wennström et al. 2005, Jervoe-Storm et al. 2006). Quirynen et al. (1999, 2000) reported that patients treated with full-mouth mechanical debridement (FMD) frequently had fever and pain, and they suggested that these symptoms were caused by transient bacteremia during subgingival instrumentation.

As soluble thrombomodulin is a specific marker for endothelial cell damage, monitoring of soluble thrombomodulin together with IL-6 and CRP might effectively indicate systemic vascular endothelial cell damage following subgingival debridement. To date, little is known about the effects of full *versus* quadrant-wise debridement on serum IL-6, CRP and soluble thrombomodulin. The purpose of this study was to compare the effects of FMD with quadrant-wise debridement on serum IL-6, CRP and soluble thrombomodulin in periodontitis patients. The effects of FMD with water on serum IL-6, CRP and soluble thrombomodulin were also compared with the effects of FMD with povidone iodine, tongue brushing and chlorhexidine (CHX) rinsing on those parameters.

Material and Methods

Selection of subjects

A total of 36 systemically healthy, non-smoking patients, aged 34–66 years (23 women and 13 men, mean 50.4 ± 8.4 years), were recruited from the Periodontics Clinic of Tokyo Medical and Dental University. All the patients exhibited moderate-to-advanced chronic periodontitis, based on clinical and radiographic findings. Each subject had at least five teeth and two pocket sites with probing depth ⩾5 mm in each quadrant, and radiographic evidence of alveolar bone loss. Subjects had not undergone antimicrobial therapy, subgingival periodontal debridement or periodontal surgery in the preceding 6 months. Patients were not included in the study if they were suffering from any chronic inflammatory or immunological conditions such as arthritis, gastrointestinal disorders, skin conditions, or bronchitis or other chronic obstructive airway disease. None of the subjects were pregnant or lactating or had known allergy to iodine. The study protocol was approved by the Ethics Committee of Tokyo Medical and Dental University, and experiments were undertaken with the informed written consent of each subject and in accordance with the principles outlined in the 2002 Declaration of Helsinki.

Treatment protocol

The demographic details, clinical study design and treatment protocol are described in our earlier report (Koshy et al. 2005). The trial design and the timing of clinical interventions and sampling are summarized in Fig. 1. Briefly, the present study compared conventional quadrant-wise mechanical debridement (QMD), FMD with water in a single visit (FMD+water) and FMD with povidone iodine in a single visit (FMD+povidone).

Mechanical debridement consisted of supra- and subgingival ultrasonic instrumentation. This was performed by two experienced and trained periodontists, mainly with an ultrasonic scaler (Piezon® Master 400, EMS, Nyon, Switzerland) equipped with a Perio Slim tip. Local anaesthesia was administered during debridement, if necessary. In both the FMD+water group and the FMD+povidone group, mechanical debridement was completed in a single visit. The irrigant was distilled water in the former group and 1% povidone iodine (Popiyodon Gargle®, Yoshida, Tokyo, Japan) in the latter. Subjects in the FMD+povidone group were advised to rinse with 15 ml of 0.05% CHX mouthwash (Concool®, Weltec, Mie, Japan) twice a day for 1 month and to practice tongue brushing in order to delay re-colonization from other intra-oral niches during the initial healing period. Subjects in the FMD+water and QMD groups were not advised to use any mouth rinse or perform tongue brushing.

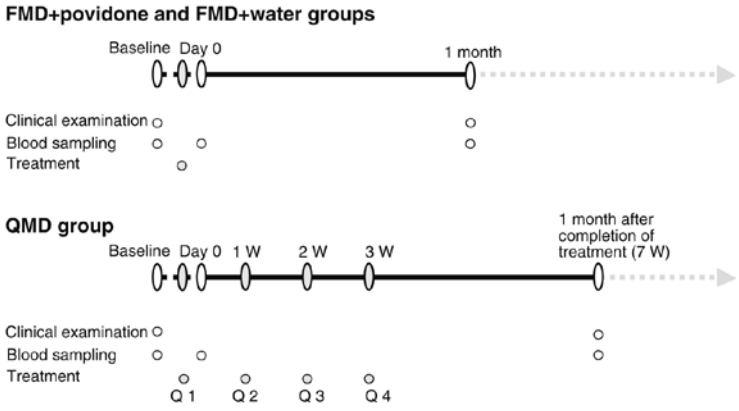

Fig. 1. Treatment schedule and blood sampling in the study groups: FMD+povidone, full-mouth mechanical debridement with povidone; FMD+water, full-mouth mechanical debridement with water; QMD, quadrant-wise mechanical debridement; TBI, toothbrushing instructions.

© 2008 The Authors
Journal compilation © 2008 Blackwell Munksgaard

Measurement of serum IL-6, CRP and soluble thrombomodulin

Blood samples were collected in endotoxin-free tubes, at baseline (before treatment), immediately after treatment (approximately 5 h after the pre-treatment blood collection), and 1 month after treatment. All analysis was performed blinded, with no knowledge of the treatment administered.

Serum was isolated from the whole blood and stored at −30°C until use. The levels of serum IL-6 were determined using an ELISA kit (Biosource International, Camarillo, CA, USA for IL-6). The detection limit of the IL-6 ELISA kit was 0.104 pg/ml. Serum soluble thrombomodulin levels were determined using an ELISA kit (Prototype-Thrombomodulin ELISA kit; Diagnostica Stago, Asnieres, France). The detection limit of the soluble thrombomodulin ELISA kit was 0.3 ng/ml. The levels of serum CRP were determined with the latex-enhanced nephelometric method (Bio-Clinical Laboratories, Tokyo, Japan). Sensitivity of the CRP measurement was 40.0 ng/ml, and if the sample CRP was below the sensitivity of the assay, the CRP level was expressed as 0 ng/ml.

Statistical analysis

Comparisons of the changes in serum IL-6, CRP and soluble thrombomodulin levels between visits within group were performed with Friedman ANOVA and Wicoxon's signed-rank test for post hoc comparison. The p-values <0.05 were considered to indicate significant differences. All the statistical analysis was carried out with the aid of statistical software (StatView® for Windows, Version 5.0, SAS Institute Inc., Cary, NC, USA).

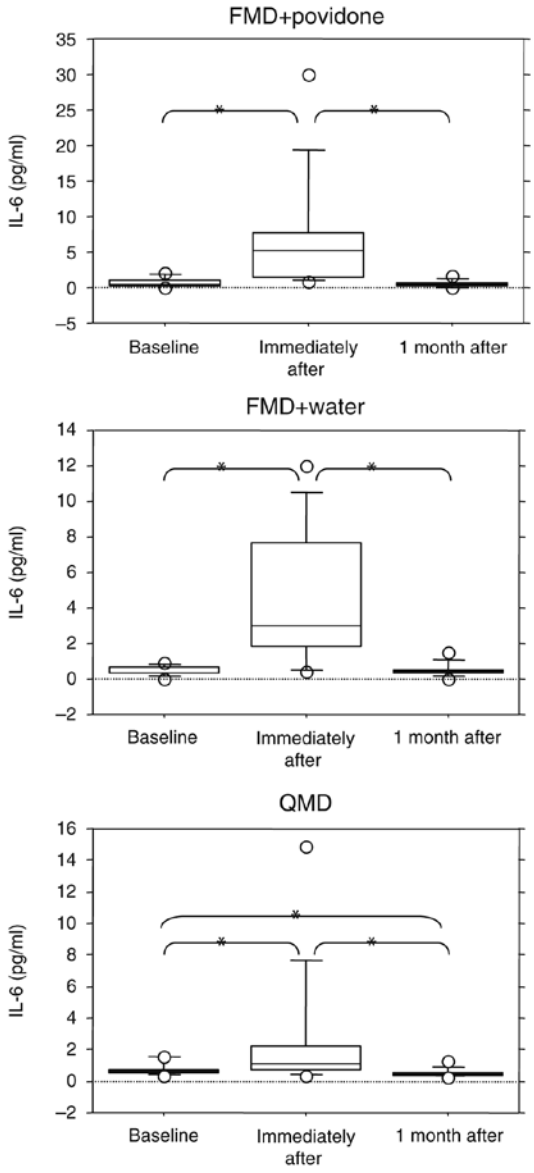

Fig. 2. Serum interleukin (IL)-6 concentration at baseline and after subgingival debridement: FMD+povidone, full-mouth mechanical debridement with povidone; FMD+water, full-mouth mechanical debridement with water; QMD, quadrant-wise mechanical debridement. Box plots show medians with 25th and 75th percentiles, whiskers represent 10th and 90th percentiles. Outlying values are shown as open circles. *$p<0.05$ (Wilcoxon's signed-rank test).

Results

Serum IL-6 levels

Serum IL-6 levels at baseline (before treatment), immediately after treatment and 1 month after FMD and QMD are shown in Fig. 2. In the FMD+povidone group, serum IL-6 was significantly elevated immediately after treatment and reduced to the baseline level at 1 month after treatment. In the FMD+water group, serum IL-6 was also significantly elevated immediately after treatment, and it reduced to the baseline level 1 month after treatment. There were no significant differences between IL-6 levels at baseline and 1 month after treatment in the FMD+povidone and FMD+water groups.

Serum IL-6 in the QMD group was also significantly increased immediately after treatment, and it was significantly decreased at 1 month after treatment compared with baseline. The increase in serum IL-6 in the FMD+water and FMD+povidone groups immediately after treatment was greater than that in the QMD group.

Serum CRP levels

Serum CRP levels at baseline, immediately after treatment and 1 month after

© 2008 The Authors
Journal compilation © 2008 Blackwell Munksgaard

FMD and QMD are shown in Fig. 3. In the FMD+povidone group, serum CRP levels did not differ significantly among the serum samples collected at baseline, immediately after treatment and at 1 month after treatment. Serum CRP levels also did not differ significantly among the three assessment points in the FMD+water and the QMD groups.

Serum soluble thrombomodulin levels

Serum soluble thrombomodulin levels at baseline, immediately after treatment and 1 month after FMD and QMD are shown in Fig. 4. In the FMD+povidone group, serum-soluble thrombomodulin levels were significantly decreased immediately after treatment, and they returned to the baseline level 1 month after treatment. In the FMD+water group, serum soluble thrombomodulin levels were significantly decreased 1 month after treatment compared with baseline. However, serum soluble thrombomodulin levels did not differ significantly among the three assessment points in the QMD group.

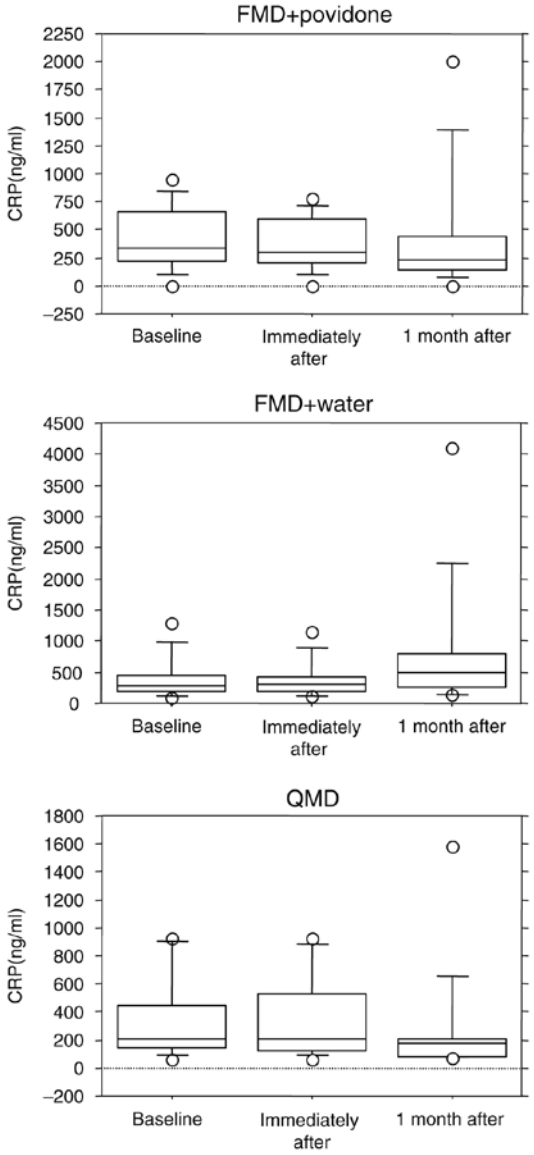

Fig. 3. Serum C-reactive protein (CRP) concentration before and after subgingival debridement: FMD+povidone, full-mouth mechanical debridement with povidone; FMD+water, full-mouth mechanical debridement with water; QMD, quadrant-wise mechanical debridement. Box plots show medians with 25th and 75th percentiles, whiskers represent 10th and 90th percentiles. Outlying values are shown as open circles.

Discussion

In the present study, serum IL-6 levels were significantly increased immediately after treatment in the FMD+povidone and FMD+water groups. The increase in serum IL-6 levels following debridement was smaller in the QMD group than in the FMD groups, but the differences were not statistically significant. Although we had collected blood samples soon after FMD, there was an interval of approximately 5 h between the initial blood sampling and the sampling after treatment (Koshy et al. 2005, Wang et al. 2006). Several investigators have found increased plasma IL-6 levels in patients with unstable angina, raising the possibility of IL-6 as a prognostic marker of cardiovascular disease outcome (Biasucci et al. 1999, Lindmark et al. 2001). Hence, elevation of serum IL-6 following FMD might increase the risk of cardiovascular events in periodontitis patients with cardiovascular disease. Alternatively, it is also possible that QMD may induce a stronger effect on systemic vascular endothelial functions than FMD, as QMD result in more frequent elevation of IL-6. In the present study, all the subjects were systemically healthy, and serum IL-6 returned to baseline levels 1 month after treatment. This transient elevation of IL-6 after periodontal treatment is consistent with the results of previous studies using healthy subjects (Ide et al. 2004, Forner et al. 2006b).

In the FMD+povidone and FMD+water groups, a significant reduction in serum soluble thrombomodulin levels was observed. In systemically healthy subjects, low levels of soluble thrombomodulin have been associated with an increased risk of coronary artery disease and brain infarction (Olivot et al. 2004). In contrast, increased soluble thrombomodulin has been associated with recurrence in coronary artery disease patients (Blann et al. 1997). Soluble thrombomodulin, which acts as a natural anticoagulant, is thought to reflect thrombomodulin

© 2008 The Authors
Journal compilation © 2008 Blackwell Munksgaard

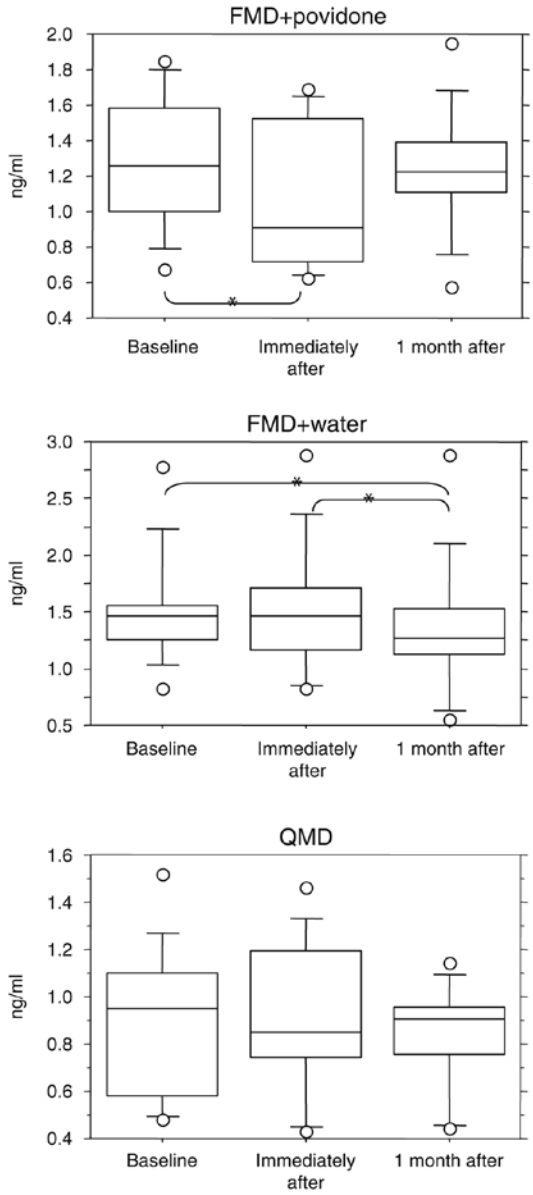

Fig. 4. Serum soluble thrombomodulin concentration before and after subgingival debridement: FMD+povidone, full-mouth mechanical debridement with povidone; FMD+water, full-mouth mechanical debridement with water; QMD, quadrant-wise mechanical debridement. Box plots show medians with 25th and 75th percentiles; whiskers represent 10th and 90th percentiles. Outlying values are shown as open circles. $^{*}p < 0.05$ (Wilcoxon's signed-rank test).

expression on the surface of endothelial cells in healthy individuals; however, it may also reflect the disease extent in patients with cardiovascular disease (Constans & Conri 2006). As the subjects in the present study were systemically healthy, decreased soluble thrombomodulin might be associated with reduced expression of thrombomodulin on endothelial cells. Endotoxin, IL-1 and TNF stimulate endothelial cells to internalize and degrade thrombomodulin expressed on their surface, and these substances also suppress transcription of the thrombomodulin gene within endothelial cells (Moore et al. 1987, 1989, Conway & Rosenberg 1988). As subgingival debridement induces transient bacteremia and release of inflammatory cytokines, the decrease in soluble thrombomodulin in the FMD+povidone and FMD+water groups might imply the internalization and degradation of thrombomodulin by endothelial cells following FMD. Tonetti et al. (2007) reported that vascular endothelial function was significantly lower in a periodontal treatment group than in a control group 24 h after treatment and that levels of CRP, IL-6, and the endothelial-activation markers soluble E-selectin and vWF were significantly higher in the periodontal treatment group. The endothelial damage following subgingival debridement in their study supports our hypothesis that the decrease in soluble thrombomodulin in the FMD groups might be caused by endothelial damage. The significant reduction in soluble thrombomodulin in the FMD groups suggests that damage to vascular endothelial cells is greater in FMD than in QMD. The patients were randomly allocated to each treatment group, and the baseline IL-6, soluble thrombomodulin and CRP were not significantly different among each groups. However, baseline IL-6, soluble thrombomodulin and CRP differed among groups, presumably due to the small sample size in this study. A further large-scale study might be necessary to exclude the possibility that significant differences between QMD and FMD groups could be attributed to differences in patients at baseline.

CRP is considered the major acute-phase reactant in humans, and IL-6 acts as the principal inducer of hepatic CRP synthesis. Elevated CRP level is a strong determinant of the risk of coronary heart disease, stroke, and peripheral arterial disease (Rattazzi et al. 2003). In the present study, serum CRP levels remained unchanged before and after debridement in both FMD groups. However, Yamazaki et al. (2005) have suggested that the distribution of serum CRP level is highly skewed toward lower levels in the Japanese population when compared with Western populations, and it might therefore be difficult to measure fluctuations of serum CRP in the Japanese population. A recent systematic review of CRP in periodontitis showed that periodontal therapy can lower the levels of CRP (Paraskevas et al. 2008). It is of note that the

© 2008 The Authors
Journal compilation © 2008 Blackwell Munksgaard

reduction in serum CRP was greater in systemic or local antibiotics with standard periodontal treatment (intensive periodontal treatment) compared with standard periodontal treatment (D'Aiuto et al. 2005, 2006). As no antibiotics have been administered in this study, decrease of CRP did not reach statistical significance.

Serum IL-6 and CRP levels did not differ significantly between the two FMD groups, suggesting that use of povidone iodine, tongue brushing and rinsing with CHX did not effectively reduce systemic effects of FMD. This finding is supported by a previous report that irrigation with a 0.12% CHX gluconate mouth rinse did not affect the incidence of bacteremia after scaling and root planing (Lofthus et al. 1991). In addition, Quirynen et al. (2000) reported fever following FMD treatment both with and without antiseptics. These findings suggest that antiseptics have a limited role in suppressing bacteremia and systemic immune responses.

The present study suggested that FMD causes a transient elevation in serum IL-6 and decrease in serum-soluble thrombomodulin, and that these changes are more pronounced after FMD than after QMD. Accordingly, FMD appears to have a greater effect on systemic vascular endothelial functions than QMD, while QMD might repeatedly induce smaller amount of serum IL-6 than FMD in periodontitis patients. Although these systemic effects of subgingival debridement are unlikely to have serious consequences in systemically healthy subjects, caution should be exercised when using FMD or QMD in periodontitis patients with cardiovascular disease. Further investigations are necessary to determine the risks and benefits of FMD in periodontitis patients who are at increased risk of cardiovascular events.

References

Apatzidou, D. A. & Kinane, D. F. (2004) Quadrant root planing versus same-day full-mouth root planing. I. Clinical findings. *Journal of Clinical Periodontology* **31**, 132–140.

Beck, J., Garcia, R., Heiss, G., Vokonas, P. S. & Offenbacher, S. (1996) Periodontal disease and cardiovascular disease. *Journal of Periodontology* **67**, 1123–1137.

Biasucci, L. M., Liuzzo, G., Fantuzzi, G., Caligiuri, G., Rebuzzi, A. G., Ginnetti, F., Dinarello, C. A. & Maseri, A. (1999) Increasing levels of interleukin (IL)-1Ra and IL-6 during the first 2 days of hospitalization in unstable angina are associated with increased risk of in-hospital coronary events. *Circulation* **99**, 2079–2084.

Bizzarro, S., van der Velden, U., ten Heggeler, J. M., Leivadaros, E., Hoek, F. J., Gerdes, V. E., Bakker, S. J., Gans, R. O., Ten Cate, H. & Loos, B. G. (2007) Periodontitis is characterized by elevated PAI-1 activity. *Journal of Clinical Periodontology* **34**, 574–580.

Blann, A. D., Amiral, J. & McCollum, C. N. (1997) Prognostic value of increased soluble thrombomodulin and increased soluble E-selectin in ischaemic heart disease. *European Journal of Haematology* **59**, 115–120.

Constans, J. & Conri, C. (2006) Circulating markers of endothelial function in cardiovascular disease. *Clinica Chimica Acta* **368**, 33–47.

Conway, E. M. & Rosenberg, R. D. (1988) Tumor necrosis factor suppresses transcription of the thrombomodulin gene in endothelial cells. *Molecular and Cellular Biology* **8**, 5588–5592.

D'Aiuto, F., Nibali, L., Parkar, M., Suvan, J. & Tonetti, M. S. (2005) Short-term effects of intensive periodontal therapy on serum inflammatory markers and cholesterol. *Journal of Dental Research* **84**, 269–273.

D'Aiuto, F., Parkar, M., Nibali, L., Suvan, J., Lessem, J. & Tonetti, M. S. (2006) Periodontal infections cause changes in traditional and novel cardiovascular risk factors: results from a randomized controlled clinical trial. *American Heart Journal* **151**, 977–984.

Forner, L., Larsen, T., Kilian, M. & Holmstrup, P. (2006a) Incidence of bacteremia after chewing, tooth brushing and scaling in individuals with periodontal inflammation. *Journal of Clinical Periodontology* **33**, 401–407.

Forner, L., Nielsen, C. H., Bendtzen, K., Larsen, T. & Holmstrup, P. (2006b) Increased plasma levels of IL-6 in bacteremic periodontis patients after scaling. *Journal of Clinical Periodontology* **33**, 724–729.

Ide, M., Jagdev, D., Coward, P. Y., Crook, M., Barclay, G. R. & Wilson, R. F. (2004) The short-term effects of treatment of chronic periodontitis on circulating levels of endotoxin, C-reactive protein, tumor necrosis factor-alpha, and interleukin-6. *Journal of Periodontology* **75**, 420–428.

Ishii, H., Uchiyama, H. & Kazama, M. (1991) Soluble thrombomodulin antigen in conditioned medium is increased by damage of endothelial cells. *Thrombosis and Haemostasis* **65**, 618–623.

Jervoe-Storm, P. M., Semaan, E., AlAhdab, H., Engel, S., Fimmers, R. & Jepsen, S. (2006) Clinical outcomes of quadrant root planing versus full-mouth root planing. *Journal of Clinical Periodontology* **33**, 209–215.

Koshy, G., Kawashima, Y., Kiji, M., Nitta, H., Umeda, M., Nagasawa, T. & Ishikawa, I. (2005) Effects of single-visit full-mouth ultrasonic debridement versus quadrant-wise ultrasonic debridement. *Journal of Clinical Periodontology* **32**, 734–743.

Lindmark, E., Diderholm, E., Wallentin, L. & Siegbahn, A. (2001) Relationship between interleukin 6 and mortality in patients with unstable coronary artery disease: effects of an early invasive or noninvasive strategy. *The Journal of the American Medical Association* **286**, 2107–2113.

Lofthus, J. E., Waki, M. Y., Jolkovsky, D. L., Otomo-Corgel, J., Newman, M. G., Flemmig, T. & Nachnani, S. (1991) Bacteremia following subgingival irrigation and scaling and root planing. *Journal of Periodontology* **67**, 602–607.

Moore, K. L., Andreoli, S. P., Esmon, N. L., Esmon, C. T. & Bang, N. U. (1987) Endotoxin enhances tissue factor and suppresses thrombomodulin expression of human vascular endothelium in vitro. *Journal of Clinical Investigation* **79**, 124–130.

Moore, K. L., Esmon, C. T. & Esmon, N. L. (1989) Tumor necrosis factor leads to the internalization and degradation of thrombomodulin from the surface of bovine aortic endothelial cells in culture. *Blood* **73**, 159–165.

Olivot, J. M., Labreuche, J., Aiach, M. & Amarenco, P. (2004) Soluble thrombomodulin and brain infarction: case–control and prospective study. *Stroke: A Journal of Cerebral Circulation* **35**, 1946–1951.

Paraskevas, S., Huizinga, J. D. & Loos, B. G. (2008) A systematic review and meta-analyses on C-reactive protein in relation to periodontitis. *Journal of Clinical Periodontology* **35**, 277–290.

Quirynen, M., Bollen, C. M., Vandekerckhove, B. N., Dekeyser, C., Papaioannou, W. & Eyssen, H. (1995) Full- vs. partial-mouth disinfection in the treatment of periodontal infections: short-term clinical and microbiological observations. *Journal of Dental Research* **74**, 1459–1467.

Quirynen, M., De Soete, M., Boschmans, G., Pauwels, M., Coucke, W., Teughels, W. & van Steenberghe, D. (2006) Benefit of ''one-stage full-mouth disinfection'' is explained by disinfection and root planing within 24 hours: a randomized controlled trial. *Journal of Clinical Periodontology* **33**, 639–647.

Quirynen, M., Gizani, S., Mongardini, C., Declerck, D., Vinckier, F. & Van Steenberghe, D. (1999) The effect of periodontal therapy on the number of cariogenic bacteria in different intra-oral niches. *Journal of Clinical Periodontology* **26**, 322–327.

Quirynen, M., Mongardini, C., de Soete, M., Pauwels, M., Coucke, W., Van Eldere, J. & Van Steenberghe, D. (2000) The role of chlorhexidine in the one-stage full-mouth disinfection treatment of patients with advanced adult periodontitis. Long-term clinical and microbiological observations. *Journal of Clinical Periodontology* **27**, 578–589.

Raetz, C. R. (1990) Biochemistry of endotoxins. *Annual Review of Biochemistry* **59**, 129–170.

Rattazzi, M., Puato, M., Faggin, E., Bertipaglia, B., Zambon, A. & Pauletto, P. (2003) C-reactive protein and interleukin-6 in vascular disease: culprits or passive bystanders? *Journal of Hypertension* **21**, 1787–1803.

© 2008 The Authors
Journal compilation © 2008 Blackwell Munksgaard

Steel, D. M. & Whitehead, A. S. (1994) The major acute phase reactants: C-reactive protein, serum amyloid P component and serum amyloid A protein. *Immunology Today* **15**, 81–88.

Takai, S., Kuriyama, T., Yanagisawa, M., Nakagawa, K. & Karasawa, T. (2005) Incidence and bacteriology of bacteremia associated with various oral and maxillofacial surgical procedures. *Oral Surgery, Oral Medicine, Oral Pathology, Oral Radiology, and Endodontics* **99**, 292–298.

Tapping, R. I. & Tobias, P. S. (1997) Cellular binding of soluble CD14 requires lipopolysaccharide (LPS) and LPS-binding protein. *The Journal of Biological Chemistry* **272**, 23157–23164.

Tonetti, M. S., D'Aiuto, F., Nibali, L., Donald, A., Storry, C., Parkar, M., Suvan, J., Hingorani, A. D., Vallance, P. & Deanfield, J. (2007) Treatment of periodontitis and endothelial function. *The New England Journal of Medicine* **356**, 911–920.

Wang, D., Koshy, G., Nagasawa, T., Kawashima, Y., Kiji, M., Nitta, H., Oda, S. & Ishikawa, I. (2006) Antibody response after single-visit full-mouth ultrasonic debridement *versus* quadrant-wise therapy. *Journal of Clinical Periodontology* **33**, 632–638.

Wennström, J. L., Tomasi, C., Bertelle, A. & Dellasega, E. (2005) Full-mouth ultrasonic debridement versus quadrant scaling and root planing as an initial approach in the treatment of chronic periodontitis. *Journal of Clinical Periodontology* **32**, 851–859.

Yamazaki, K., Honda, T., Oda, T., Ueki-Maruyama, K., Nakajima, T., Yoshie, H. & Seymour, G. J. (2005) Effect of periodontal treatment on the C-reactive protein and proinflammatory cytokine levels in Japanese periodontitis patients. *Journal of Periodontal Research* **40**, 53–58.

Address:
Yuka Ushida
Section of Periodontology
Department of Hard Tissue Engineering
Graduate School
Tokyo Medical and Dental University
Tokyo Medical and Dental University
1-5-45 Yushima
Bunkyo-ku
Tokyo 113-8549
Japan
E-mail: ushida.peri@tmd.ac.jp

Clinical Relevance

Scientific rationale for the study: With emerging evidence of association between periodontitis and cardiovascular disease, it is important to clarify the effect of various periodontal treatments on systemic inflammatory markers.

Principal findings: Both single-visit FMD and QMD caused transient elevation of IL-6. Soluble thrombomodulin decreased following FMD.

Practical implications: FMD might induce higher serum IL-6 production than QMD and reduce soluble thrombomodulin levels in periodontitis patients. QMD might repeatedly induce smaller amount of serum IL-6 in periodontitis patients.

© 2008 The Authors
Journal compilation © 2008 Blackwell Munksgaard

硬組織病態制御学

柳下 正樹

医歯学総合研究科・生体支持組織学系専攻
硬組織病態制御学・教授

1. 研究の課題名

「細胞外マトリックス分子の分子間相互作用と機能（Function and interactions of extracellular matrix molecules）」
「ヘパラン硫酸プロテオグライカンの細胞内代謝と生物学的機能（Metabolism and biological functions of heparan sulfate proteoglycans）」

細胞外マトリックスは動物の体制構築のために基本構造を与えるだけでなく、臓器、組織中で細胞に対する生存環境を与えることにより、細胞の分化、増殖、代謝、外界への反応を調節するなど多くの機能を持っている。このとき細胞外マトリックスから細胞に対してフィードバックとして送られる種々の分子シグナルは細胞機能調節にとりわけ重要である。本年度の研究の主要テーマとして、細胞表面において細胞外マトリックスと分子間相互作用を示すヘパラン硫酸プロテオグライカンの細胞表面での挙動を詳細に検討した。前年までにシンデカン-4がシグナル受容複合体として機能している膜ドメインに局在していることを証明したことに引き続きヘパラン硫酸糖鎖の存在がシンデカン-4の膜ドメインに対するターゲティング、及び膜ドメインの安定性に対する寄与を解析した。膜ドメインは、Triton X-100処理した培養細胞から界面活性剤抵抗性の細胞膜分画をショ糖密度勾配超遠心法で調製した。膜ドメインの精製は特異的タンパク（CD 38、Lynなど）の存在により確認した。副甲状腺細胞より精製した膜ドメインでは抗ヘパラン硫酸糖鎖抗体、抗シンデカン抗体を用いたウェスタンブロット分析によりシンデカン4が特異的に局在し、シンデカン1は除外されていることが示された。質量分析器を用いてさらに膜ドメイン局在分子の同定を進めている。このことから細胞外マトリックスからのヘパリン結合性リガンドのうちシンデカン4の持つヘパラン硫酸に結合特異性を示す分子が膜ドメインを介して選択的にシグナル伝達を行っていることが示唆された。このほかパラン硫酸プロテオグライカンは膜ドメイン中で他の膜タンパクと分子間相互作用を示すことにより膜ドメインの構造安定性に寄与している可能性に関する検討を加えた。ヘパラン硫酸特異的分解酵素を細胞培養に作用させた後に膜ドメインを精製、膜ドメインの形成、他の膜ドメインタンパクのターゲティングを解析した。今後は、膜ドメインにおけるヘパラン硫酸プロテオグライカンを介したシグナル伝達の分子メカニズムに関してと、膜ドメインの構造安定性に対するヘパラン硫酸プロテオグライカンの寄与に関してさらに研究を進めたい。

2.

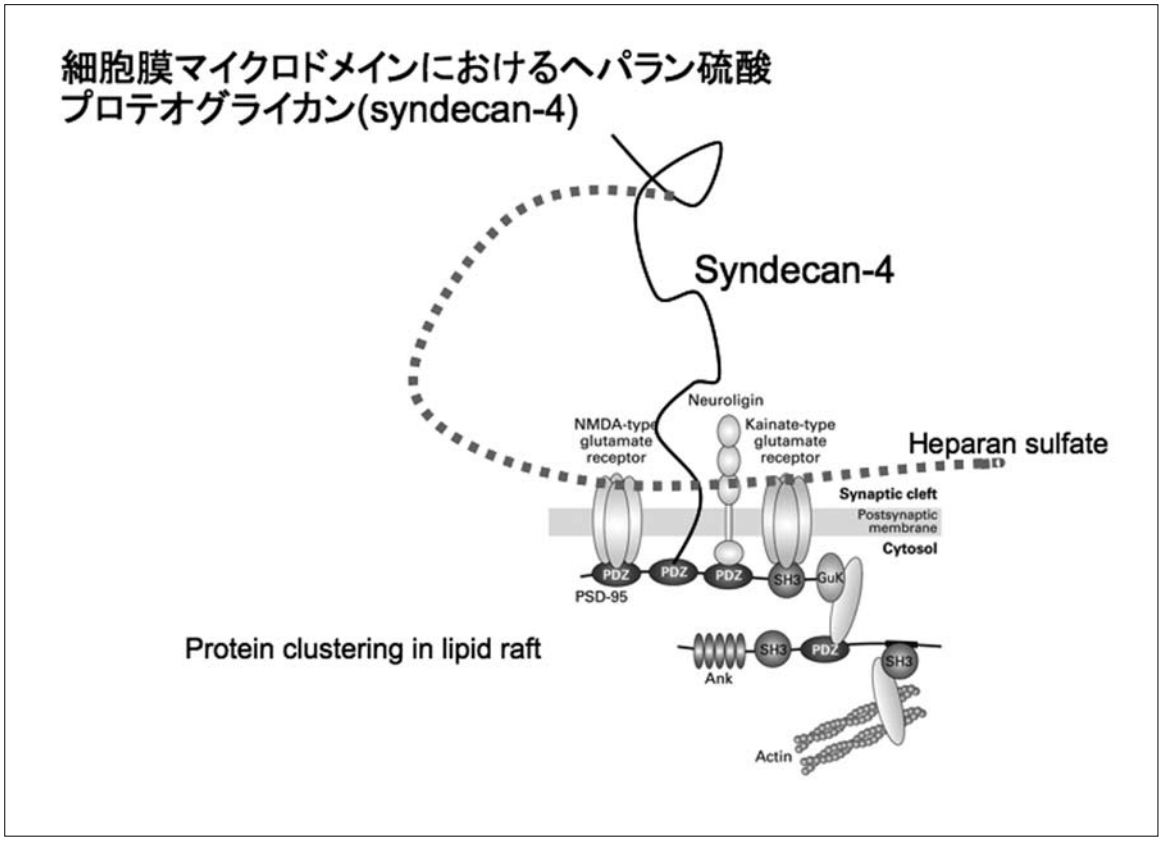

3. 2008年、2009年（平成21年3月までの）に発表した全ての研究内容についての英文要約

During the years of 2008 and 2009, we tried to focus on the demonstration of the presence of a molecular complex on the cell surface involving heparan sulfate proteoglycans, and the role of heparan sulfate chains on the integrity of membrane raft structure. Biochemical properties of heparan sulfate proteoglycans point to the presence of intimate molecular interactions in specialized domains of cell surface and their importance in the cellular signaling mechanisms. Research results, using isolation procedures of plasma membrane and identification of several membrane proteins together with heparan sulfate proteoglycans, indicated that cholesterol-rich, cell surface microdomains constitute one of specialized functional units of the plasma membrane and are associated with a species of cell surface heparan sulfate proteoglycan, syndecan-4. Biological significance of heparan sulfate proteoglycans in specialized membrane domains will be further investigated.

4. 本事業に関連して世界的な研究拠点形成に向けて、以下の点で改善・整備等されたこと

A. GCOEの発足整備に参画。
異なる分野のInnovationの確立する研究「歯周組織炎症部位における酸化ストレスの組織学的・生化学的解析」を提案。

B. 活発なシンポジウム、セミナーの開催

C. 中村博幸博士をImperial College Londonより特任講師として本GCOEに招聘。

D. 大学院生（AISS）への奨学金授与、大学院生セミナーの開催

E. 国際セミナーへの参加、発表。

5. GCOE事業を推進するに当たって力を入れた点

特任講師の招聘、大学院生への教育活動に参加することを心がけた。

6. 英文原著論文

6-1. Miki Hara-Yokoyama, Tomoko Kimura, Hiroaki Kaku, Motoaki Wakiyama, Yoko Kaitsu, Mio Inoue, Seisuke Kusano, Mikako Shirouzu, Shigeyuki Yokoyama, Toshiaki Katada, Yoshio Hirabayashi, Kiyoshi Takatsu,

Masaki Yanagishita. Alteration of enzymatic properties of cell-surface antigen CD38 by agonistic anti-CD38 antibodies that prolong B cell survival and induce activation. International Immunopharmacology 8:59-70, 2008

6-2. Masaki Yanagishita, Katarzyna Anna Podyma-Inoue and Miki Yokoyama. Extraction and separation of proteoglycans. Glycoconj. J.（2008）in press.

6-3. Miki Hara-Yokoyama, Kazue Terasawa, Akio Kihara, Jin-Wook Kim, Chan-Seo Park, Yoshio Hirabayashi, Yausyuki Hirabayashi and Masaki Yanagishita, “Sphingosine Kinase 2 Inhibitor Acceralates Fas-Medicated Cell Death Progression in A20/2J Cells”, The Open Bioactive Compounds Journal, 1, 22-27（2008）

7. 著書

7-1. Masaki Yanagishita and Katarzyna Anna Podyma-Inoue, “Degradation of Hyaluronan and Its Disorder”, In Experimental Glycoscience and Glycobiology, N. Taniguchi, A. Suzuki, H. Narimatsu, T. Kawasaki and S. Hase（eds）, Springer, Tokyo（2008）

8. 自己評価

GCOEの初年度にあたり、発足に係る人選等に参画し特任講師1名を招聘した。その他の活動内容のうちで私の参加できる主な項目としては大学院生、GCOE教官に対する評価関連の活動および、大学院生に対するセミナーシリーズでの講義であった。これらの活動はGCOE事業全体からすると微力とは思いますが、可能な限り参加させていただきました。

9. 学会発表（英文）

9-1. Sachiko Takehara, Masaki Yanagishita, Katarzyna A. Podyma-Inoue, Masayuki Ueno, Kayoko Shinada and Yoko Kawaguchi, “Comparison of glycosylated and total salivary proteins between halitosis and non-halitosis patients”, The 8th International Conference of Asian Academy of Preventive Dentistry, November 6 - 8, 2008, Jeju, Korea

9-2. Masaki Yanagishita, “Roles of nucleotide sugar transporters in the formation of extracellular matrix”, Annual Meeting for the Tumor Biology Research Group, Faculty of Medicine, University of Tromsø, September 22-24, 2008, Skibotn, Norway

10. 学会発表（和文）

10-1. 横山三紀、寺澤和恵、木原章雄、五十嵐靖之、平林義雄、柳下正樹、「スフィンゴシンキナーゼ2阻害剤によるFas依存性細胞死の亢進」、第3回スフィンゴテラピィ（STC）研究会、鳥取県、2008年7月18,19日

10-2. 平岡秀一、古市達也、柴田俊一、柳下正樹、豊田英尚、石田信宏、佐内豊、西村玄、池川志郎、古関明彦、浅原弘嗣、「糖ヌクレオチド輸送体ノックアウトマウスを利用した発生・分化における糖鎖機能の解析」、第31回日本分子生物学会年会、第81回日本生化学大会合同大会、2008年12月9-12日、神戸ポートアイランド

10-3. 竹原祥子、柳下正樹、井上カタジナアンナ、植野正之、品田佳世子、川口陽子、「口臭外来受診患者の唾液タンパク質の比較分析」、口腔衛生学会、さいたま市、2008年10月3,4日

10-4. 横山三紀、寺澤和恵、五十嵐靖之、平林義雄、柳下正樹、B細胞受容体刺激によるFas-resistanceにおけるスフィンゴシンキナーゼ2の関与、日本脂質生化学会、徳島、2008年6月5,6日

11. 外部資金の獲得状況

（受託研究）糖質科学研究所、「グリコサミノグリカンオリゴ糖の生理活性解析と医薬応用」、期間:平成17年 -平成21年、総額:840万円

12. 特別講演、招待講演

Masaki Yanagishita, “Roles of nucleotide sugar transporters in the formation of extracellular matrix”, Annual Meeting for the Tumor Biology Research Group, Faculty of Medicine, University of Tromsø, September 22-24, 2008, Skibotn, Norway

13. 主催学会

「第16回プロテオグライカンフォーラム」、2008年9月13日、東京医科歯科大学

14. 講座の准教授、講師、助教、特別研究員、ポスドク、指導を受けた大学院生の名前（AISSには○印）のリスト

（助教授）横山三紀、（講師）粂井康宏、（助教）井上-Podyma Katarzyna Anna、（大学院生、歯周病学分野より○江部典子）

22 *The Open Bioactive Compounds Journal*, 2008, *1*, 22-27

Open Access

Sphingosine Kinase 2 Inhibitor Accelerates Fas-Mediated Cell Death Progression in A20/2J Cells

Miki Hara-Yokoyama*[,1], Kazue Terasawa[1], Akio Kihara[2], Jin-Wook Kim[2,3], Chan-Seo Park[2,4], Yoshio Hirabayashi[5], Yasuyuki Igarashi[2] and Masaki Yanagishita[1]

[1]Department of Hard Tissue Engineering, Biochemistry, Division of Bio-Matrix, Graduate School, Tokyo Medical and Dental University, 1-5-45 Yushima, Bunkyo, Tokyo 113-8549, Japan, [2]Department of Biomembrane and Biofunctional Chemistry, Graduate School of Pharmaceutical Sciences, Hokkaido University, Kita 12-jo, Nishi 6-choume, Kita-ku, Sapporo 060-0812, Japan, [3]LCS biotech, 3-26, Pil-dong, Chung-gu, Seoul 100-715, Korea, (Present address) [4]Department of Chemical and Biochemical Engineering, Dongguk University, 3-26, Pil-dong, Chung-gu, Seoul 100-715, Korea (Present address) and [5]Brain Science Institute, The Institute of Physical and Chemical Research (Riken), 2-1 Hirosawa, Wako, Saitama 351-0198, Japan

Abstract: A sphingosine kinase (SPHK) type 2 inhibitor, SG-12, inhibited the SPHK2 activity in A20/2J cells and promoted Fas-dependent cell death. The effect of SG-12 on cell death was relieved by SPHK2 transfection but not by SPHK1 transfection. The results suggest a SPHK2-specific suppression of Fas-dependent cell death.

Key Words: Sphingosine-1-phosphate, Sphingosine kinase 2, Fas, Cell death, B cell.

1. INTRODUCTION

Sphingosine kinase (SPHK) catalyzes the phosphorylation of sphingosine to generate sphingosine-1-phosphate (S1P). The two mammalian isoforms of sphingosine kinase, SPHK1 [1] and SPHK2 [2], are different in their amino acid sequences, catalytic properties, intracellular localization, and tissue distribution [3]. Mice lacking SPHK1 [4], SPHK2 [5], or both [6] indicated that the functions of SPHK1 and SPHK2 are redundant in terms of their maintenance of extracellular S1P levels to support S1P-receptor mediated processes such as vascular maturation/angiogenesis [7-11], heart development [12], and lymphocyte trafficking [13]. On the other hand, it has been suggested that SPHK1 and SPHK2 have distinct roles in regulating cell survival and death [14], where S1P probably acts intracellularly [14,15]. Although SPHK1 has been shown to promote cell survival, several reports suggested that SPHK2 induces apoptosis [16] or inhibits cell growth [17]. T cells from mice lacking SPHK2 exhibit a hyperactivated phenotype with enhanced proliferation and cytokine secretion in response to IL-2 [18]. At present, the role of SPHK2 in modulating cell survival and death remains to be characterized.

Fas/CD95 is a member of the tumor necrosis factor receptor superfamily. Crosslinking Fas with its natural ligand FasL (CD178) or with agonistic antibodies induces apoptotic cell death. Fas signaling is important for elimination of self-reactive T and B lymphocytes [19, 20]. Thus, Fas deficiency in humans and mice (e.g., during autoimmune lymphoproliferative syndrome or in *lpr* mice) predisposes them to systemic autoimmunity. In B cells, susceptibility to Fas signaling is dramatically altered during activation [21].

Sphingolipid ceramide is known to regulate Fas-mediated cell death [22-25]. Ceramide activates a number of enzymes and contributes to membrane structure, by which it can lead to activation of caspase and induce cell death [26, 27]. On the other hand, the ceramide-derived metabolite S1P, counteracts the action of ceramide and suppresses Fas-mediated cell death [28, 29]. Upregulation of SPHK1 has been reported to induce Fas-resistance in B lymphoblastoid cells in case of rheumatoid arthritis [30]. However, the role of SPHK2 in Fas-mediated cell death has not been elucidated.

In the present study, we investigated the role of SPHK on Fas-mediated apoptosis. We found that the SPHK activity in A20/2J cells, a mouse B cell lymphoma cell line, is mainly due to SPHK2. Using a synthetic sphingoid analog, SG-12, previously developed as an SPHK2 inhibitor [31], we successfully demonstrated the specific involvement of SPHK2 in the suppression of Fas-dependent cell death of A20/2J cells. This effect was especially evident in the presence of BCR-crosslinking.

2. MATERIALS AND METHODS

2.1. Cell Preparation and Culture

Splenic B cells were isolated from six-week-old BALB/cAnN mice as described previously [32]. The murine B lymphoma-derived cell line A20 and A20/2J were maintained in RPMI 1640 medium (Sigma-Aldrich, St Louis, MO) supplemented with 8% fetal bovine serum (F6178, Sigma-Aldrich, St Louis, MO), 2-mercaptoethanol (50 μM), penicillin (50 U/ml), and streptomycin (50 μg/ml). Only those cells that were in exponential growth phase were used for experiments.

*Address correspondence to this author at the Department of Hard Tissue Engineering, Biochemistry, Division of Bio-Matrix, Graduate School, Tokyo Medical and Dental University, 1-5-45 Yushima, Bunkyo, Tokyo 113-8549, Japan; Tel: +81 3 5803 5567; Fax: +81 3 5803 0187;
E-mail: m.yokoyama.bch@tmd.ac.jp

1874-8473/08 2008 Bentham Open

2.2. Reagents

A compound, (2S, 3R)-2-amino-4-(4-octylphenyl)butane-1-3-diol (SG-12), was prepared as previously described [31] and dissolved in DMSO at 4 mM concentration. Anti-mouse Fas monoclonal antibody (Jo2) and FITC-annexin V were purchased from BD Pharmingen (San Diego, CA). Z-VAD-fmk was from the Peptide Institute (Osaka, Japan).

2.3. Reverse Transcription Polymerase Chain Reaction (PCR)

Total RNA was isolated from B cells, A20, and A20/2J cells using QIAzol reagent (QIAGEN) and cDNA was generated using an oligo(dT) primer and SuperScript II Reverse Transcriptase (Invitrogen). The GAPDH, SPHK1, and SPHK2 cDNAs were amplified by PCR using primers for GAPDH (5' ACCACAGTCCATGCCATCAC 3' and 5' TCCACCACCCCTGTTGCTGTA 3'), SPHK1 (5' TGCCTT CTCATTGGACTGTG 3' and 5' ACCATCAGCTCTCCA TCCAC 3') and SPHK2 (5' GGCCACCACTTATGAGGA GA 3' and 5' AGCAGTTGAGCAACAGGTCA 3'). The PCR conditions were as follows: 30 cycles; 94°C for 30 s, 60°C for 45 s, and 72°C for 60 s.

2.4. Plasmids and Transfection

The pCE-puro 3x FLAG-mSPHK1a and pCE-puro 3x FLAG-mSPHK2 plasmids are derivatives of the pCE-puro vector [33] and encode the mouse SPHK1 and SPHK2 proteins, respectively. These are both tagged with a triple FLAG (3x FLAG) epitope at their N-terminus. Transfections were performed using the Nucleofector technology (Amaxa) and puromycin-resistant cells were obtained.

2.5. SPHK Activity

In vitro SPHK assays were performed as described previously [1, 2]. The SPHK activity was measured in the presence of 0.25% Triton X-100 (inhibiting SPHK2) and 0.2 M KCl (suitable for SPHK2). To evaluate the SPHK activity within cells, A20/2J cells were incubated with [3-^{3}H]sphingosine after incubation with or without SG-12. Lipids were extracted and analyzed as described previously [1].

2.6. Flow Cytometric Analysis

A20/2J cells were stained with FITC-annexin V and propidium iodide (PI) and analyzed by flow cytometry using a FACSCalibur (BD Bioscience, Mountain View, CA). Cells were classified as live cells [Annexin V^- PI^-], apoptotic cells (Annexin V^+ PI^-), and dead cells (Annexin V^+ PI^+).

2.7. Sodium Dodecyl Sulfate-Polyacrylamide Gel Electrophresis (SDS-PAGE) and Immunoblotting

After stimulation, the A20/2J cells were lysed using 1% Triton X-100 as described previously [32] in the presence of 100 mM z-VAD-fmk. Proteins were separated by SDS-PAGE on 10-20% gradient gel (Wako Pure Chemical Industries, Japan) and were detected by immunoblotting with anti-caspase 3 (1/2000 dilution), anti-phospho-Akt (Ser473) (1/1000 dilution), and anti-Akt (1/100 dilution) antibodies from Cell Signaling (Beverly, MA) and anti-Grb2 antibody (1/1000 dilution) from Santa Cruz Biotechnology (Santa Cruz, CA) as primary antibodies. A horseradish peroxidase-conjugated antibody was used as the secondary antibody. Finally, immunoreactivity was determined by ECL (Amersham International, Buckinghamshire, England).

2.8. Statistical Analysis

Differences between mean values were assessed by a Student's t test. A p value of <0.05 or <0.01 was considered statistically significant.

3. RESULTS AND DISCUSSION

3.1. Sphingosine Kinase 2 (SPHK2) Mainly Contributed to SPHK Activity in A20/2J Cells

In B cells, the expression of both SPHK1 and SPHK2 was detected (Fig. **1A**). In case of SPHK2, two PCR products were observed using B cell cDNA as a template. Sequence analysis revealed that the slower migrating band contained an 83 bp insertion (data not shown). This finding suggested the presence of a splice variant of SPHK2 in B cells. Since a stop codon is present within the insertion, the splice variant would correspond to the N-terminal one third of SPHK2. A role of such truncated form of SPHK2 should be studied in a future work. The B cell tumor line A20/2J is a subclone of the original A20 tumor cell line derived from a BALB/cAnN mouse [34]. Since A20/2J is more susceptible to Fas-dependent cell death than A20 (data not shown), we used A20/2J for the present study. SPHK2 was clearly observed, whereas that of SPHK1 was barely detectable in A20/2J cells (Fig. **1A**) and A20 cells (data not shown).

The catalytic activity of SPHK2 is inhibited by high concentrations of Triton X-100 and activated in the presence of physiological concentrations of KCl or NaCl [2]. Thus, we measured SPHK activity in the presence of 0.25% Triton X-100 (inhibiting SPHK2) and 0.2 M KCl (suitable for SPHK2) to evaluate relative contribution of SPHK2 over that of SPHK1. As shown in Fig. (**1B**) (lanes 3 and 4), S1P was generated in B cell homogenates under both the conditions. In contrast, S1P formation in the homogenates of A20/2J cells was observed only in the presence of 0.2 M KCl (Fig. **1B**, lane 2). SPHK activity under the SPHK2 assay conditions was associated with the membrane fraction (Fig. **1C**). Thus, SPHK2 contributed more than SPHK1 to S1P formation in A20/2J cells as compared to B cells.

3.2. A Synthetic Sphingoid Analog Compound (SG-12), (2S, 3R)-2-Amino-4-(4-Octylphenyl)Butane-1-3-Diol, Inhibited SPHK2 Activity in A20/2J Cells

The sphingoid analog, SG-12, potently inhibits human SPHK2 but not SPHK1 activity *in vitro* [31]. Since SPHK2 mainly contributed to the SPHK activity in A20/2J cells, we evaluated the action of SG-12 in A20/2J cells. As shown in Fig. (**2**), SG-12 appreciably inhibited [^{3}H]S1P formation. Thus, SG-12 was shown to act as a membrane-permeable inhibitor of SPHK. To confirm the action of SG-12 on SPHK2, we transfected the A20/2J cells with either mouse SPHK1 or SPHK2. The generation of [^{3}H]S1P was not inhibited by SG-12 in SPHK1-transfected A20/2J cells, but was inhibited in SPHK2-transfected A20/2J cells (Fig. **2**). However, the effect of SG-12 in SPHK2-transfected A20/2J cells was less than that in A20/2J cells. Accordingly, the results indicated that SG-12 inhibited the SPHK2 activity in A20/2J cells.

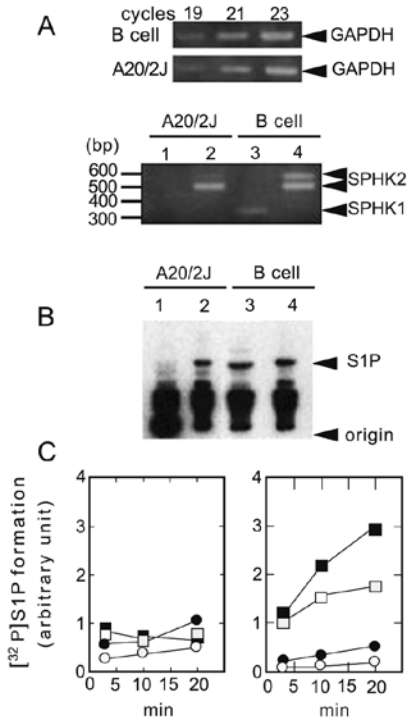

Fig. (1). SPHK2 is a major sphingosine kinase isoform in A20/2J cells. (**A**) Expression of SPHK1 and SPHK2 in A20/2J and mouse splenic B cells was detected by reverse transcription-PCR. The PCR products with cDNA from A20/2J cells (lanes 1, 2) or B cells (lanes 3, 4) using primers for SPHK1 (lanes 1, 3) or SPHK2 (2, 4) were shown. (**B**) Homogenates from A20/2J cells (lanes 1, 2) and mouse splenic B cells (lanes 3, 4) were incubated with sphingosine and [γ-^{32}P]ATP in the presence of 0.25% Triton X-100 (lanes 1, 3) and 0.2 M KCl (lanes 2, 4) as described in "Materials and Methods." Lipids were extracted and separated on TLC. (**C**) Homogenates of A20/2J cells were centrifuged at 100,000 x g for 30 min. Supernatant (open circle; 10 μg, open square; 40 μg) and pellet (closed circle 5 μg, closed square; 20 μg) fractions were incubated with sphingosine and [γ-^{32}P]ATP in the presence of 0.25% Triton X-100 (left panel) or 0.2 M KCl (right panel) as described in "Materials and Methods." Essentially the same result was obtained in another independent experiment.

3.3. Effect of SG-12 on the Progression of Fas-Mediated Cell Death from Live to Apoptotic Cells

Stimulating A20/2J cells with an anti-mouse Fas monoclonal antibody (Jo2) for 4 h resulted in increase in apoptotic cells (Fig. **3A**). Crosslinking of BCR with an anti-mouse IgG pAb reduced the apoptotic cells (Fig. **3A**) and inhibited the Fas-dependent activation of caspase-3 (Fig. **4B**), which has been known as BCR-dependent Fas-resistance [21, 35]. A proportion of the apoptotic cells was not affected by SG-12 in the absence of BCR-crosslinking, but was increased in the presence of BCR-crosslinking (Fig. **4A**). SG-12 did not produce any effects in the presence of a pan-caspase inhibitor, z-VAD-fmk (Fig. **4A**), suggesting that SG-12 promoted a caspase-dependent process. Activation of caspase-3 as revealed by the appearance of its cleaved form, was slightly increased by SG-12 either in the absence or presence of BCR-crosslinking (Fig. **4B**). Thus, it is suggested that the slight activation of caspase 3 by SG-12 does not directly result in the increase in apoptotic cells. Rather, it implied that SG-12 amplifies an additional process of apoptotic cell death subsequent to the activation of caspase 3, which is evident in the presence of BCR-crosslinking.

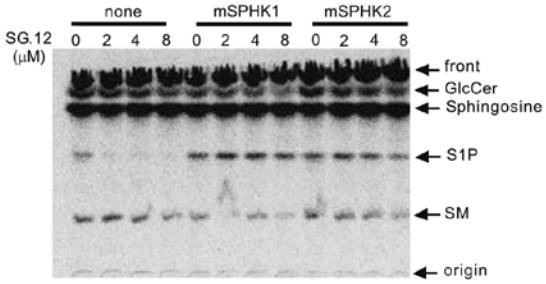

Fig. (2). The SPHK2 activity in A20/2J cells was inhibited by SG-12. A20/2J cells or A20/2J cells transfected with mouse SPHK1 or SPHK2 (2 x 10^6 cells/ml) were incubated with or without SG-12 (2, 4, 8 μM) for 5 min and then with [3-^{3}H]sphingosine for 5 min. Lipids were extracted and separated by TLC as described in "Materials and Methods." [^{3}H]Ceramide and [^{3}H]palmitic acid moved with solvent front. Essentially the same result was obtained in another independent experiment.

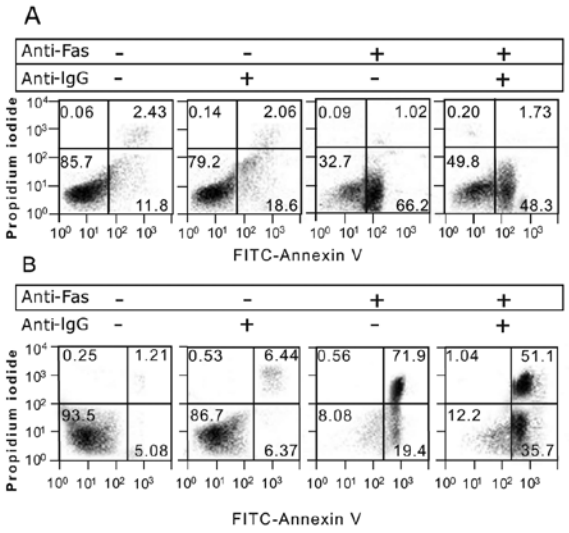

Fig. (3). Progression of Fas-mediated cell death in A20/2J cells. A20/2J cells (1 x 10^6 cells/ml) were incubated without or with 100 ng/ml anti-mouse Fas mAb or 5 μg/ml F(ab')$_2$ of anti-mouse IgG pAb for 4 h (A) or 20 h (B) and analyzed using flow cytometry as described under "Materials and methods."

The effect of SG-12 could be explained by an impairment of BCR-signaling. However, a BCR-dependent inhibition of caspase 3-activation was clearly observed in the presence of SG-12 (Fig. **3B**). In addition, an activation of PI3K as revealed by the phosphorylation of Akt, which mediates the suppressive effect of BCR-crosslinking on Fas-dependent

cell death [35], was inhibited by LY294002 but not by SG-12 (Fig. **4C**). Therefore, the effect of SG-12 in increasing in apoptotic cells may be highlighted when the increase in apoptotic cells is retarded by BCR-crosslinking.

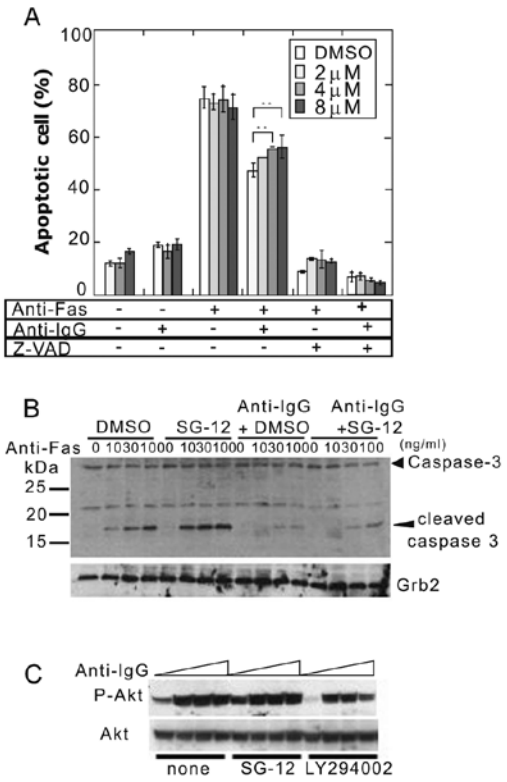

Fig. (4). SG-12 promoted the progression of early stage of Fas-mediated cell death. (**A**) A20/2J cells (1 x 10^6 cells/ml) were incubated without or with 100 ng/ml anti-mouse Fas mAb, 5 μg/ml F(ab')$_2$ of anti-mouse IgG pAb, or 50 μM z-VAD-fmk in the presence or absence of SG-12 for 4 h. Fractions of apoptotic cells (Annexin V^+PI^-) are shown. Values are means ± SD from triplicate samples. Statistically significant differences (**p< 0.01) with respect to the values without SG-12 are indicated. (**B**) A20/2J cells (1 x 10^6 cells/ml) were incubated without or with anti-mouse Fas mAb and 5 μg/ml F(ab')$_2$ of anti-mouse IgG pAb in the presence or absence of 8 μM SG-12. After 4 h, cells were lysed and proteins were detected by immunoblotting as described in "Materials and Methods." (**C**) A20/2J cells (1 x 10^8 cells/ml) were preincubated without or with 8 μM SG-12 or 4 μM LY294002 for 5 min and stimulated with an F(ab')$_2$ of an anti-mouse IgG pAb (2.5, 5, 10 μg/ml) for 5 min. Then, the cells were lysed and proteins were detected by immunoblotting as described in "Materials and Methods." Essentially the same result was obtained in another independent experiment.

3.4. Effect of SG-12 on the Progression of Fas-Mediated Cell Death from Apoptotic to Dead Cells

Next, we focused on the effect of SG-12 during the late stages of cell death, from visible apoptosis to dead cells. After Fas stimulation for 20 h, most cells became positive for Annexin V and BCR-crosslinking resulted in a decrease in dead cells and an increase in apoptotic cells (Fig. **3B**). As shown in Fig. (**5A**), the proportions of live, apoptotic, and dead cells were not affected by SG-12 in the absence of BCR-crosslinking. In contrast, the proportion of apoptotic cells was reduced and that of dead cells was increased by SG-12 in the presence of BCR-crosslinking (Fig. **5B**). It should be noted that, when the cells were stimulated with an anti-Fas antibody at concentrations higher than 10 ng/ml and in the presence of BCR-crosslinking, the levels of apoptotic and dead cells did not change (at around 35% and 50%, respectively), while the initial activation of caspase 3 was increased (Fig. **5D**). This observation suggested that BCR-crosslinking causes a pause in the progression of cells from apoptotic stage to death: addition of SG-12 relieved this pause.

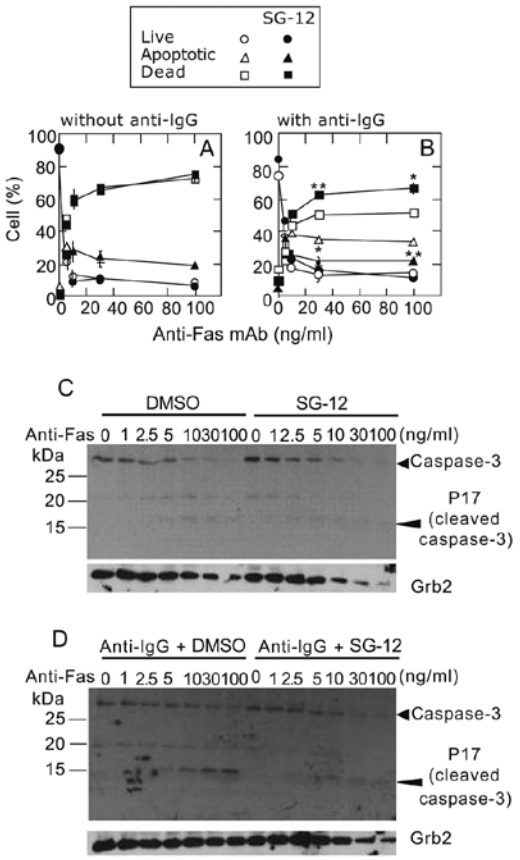

Fig. (5). SG-12 promoted the progression of late stage of Fas-mediated cell death. (**A, B**) A20/2J cells (1 x 10^6 cells/ml) were incubated without or with anti-mouse Fas mAb or 8 μM SG-12 for 20 h in the absence (**A**) or presence (**B**) of 5 μg/ml anti-mouse IgG pAb. Values are means ± SD from triplicate samples. Statistically significant differences (*p < 0.05 or **p < 0.01) with respect to the values without SG-12 are indicated. Results are representative of four independent experiments. (**C, D**) A20/2J cells (1 x 10^6 cells/ml) were incubated without or with anti-mouse Fas mAb without (**C**) or with (**D**) 5 μg/ml F(ab')$_2$ of anti-mouse IgG pAb in the presence or absence of 8 μM SG-12. After 20 h, the cells were lysed and their proteins were detected by immunoblotting as described in "Materials and Methods." Essentially the same result was obtained in another independent experiment.

An active form of caspase 3 (p17) was hardly detected in the absence of BCR-crosslinking after Fas stimulation for 20 h (Fig. **5C**). On the other hand, p17 remained in the presence of BCR-crosslinking; however, it almost disappeared following the addition of SG-12 (Fig. **5D**). Since a cytosolic protein, Grb2, was also decreased after Fas-stimulation, it is conceivable that p17 is released from dead cells due to a damage of plasma membranes. It should be noted that SG-12 promoted the decrease in Grb2 both in the absence (Fig. **5C**) and presence (Fig. **5D**) of BCR-crosslinking, whereas SG-12 did not affect the Fas-dependent decrease in uncleaved caspase 3. It implied that the addition of SG-12 promotes the progression of late stage cell death after activation of caspase 3.

Collectively, SG-12 accelerated both early and late stages of Fas-mediated cell death as shown by the exposure of phosphatidylserine (annexin V-staining) and the change of membrane permeability (PI-staining), respectively.

3.5. Effect of SG-12 on the Progression of Fas-Mediated Cell Death in A20/2J Cells Transfected with SPHK1 or SPHK2

To confirm the involvement of SPHK2 in reactions mediated by SG-12, we used SPHK1- and SPHK2-transfected A20/2J cells (Fig. **6**). SG-12 decreased the apoptotic cells and increased the dead cells after a 20 h Fas stimulation, in the presence of BCR-crosslinking in A20/2J cells (Fig. **6B**) and in SPHK1-transfected A20/2J cells (Fig. **6D**). In contrast, in SPHK2-transfected A20/2J cells (Fig. **6F**), SG-12 did not increase the dead cells. A slight SG-12 mediated decrease in apoptotic cells may reflect an increase of live cells, however, we did not investigate this point further in the present study. The results indicated that the effect of SG-12 in promoting progression of Fas-dependent cell death progression is closely related to SPHK2.

4. CONCLUSION

An SK2 inhibitor compound, SG-12, enabled us to demonstrate the involvement of SPHK2 in the suppression of Fas-dependent cell death in A20/2J cells. Interestingly, SG-12 was able to accelerate the progression of late stage cell death indicators such as a change in membrane permeability, probably due to disruption of membrane integrity. This effect was especially evident in the presence of BCR-crosslinking. Although many previous studies focused on the initiation of cell death, i.e., caspase activation, the regulation of the late stages of cell death remains largely unclear. Our results implied the potential ability of SHK2 to suppress the progression of late stage Fas-mediated cell death.

The ability of SG-12 to inhibit S1P formation in A20/2J cells was diminished by SPHK1 transfection (Fig. **2**). But SPHK1 transfection did not relieve the effect of SG-12 on the progression of cell death (Fig. **6**). Thus, the generation of S1P *per se*, may not be sufficient to suppress Fas-mediated cell death. On the other hand, it has been previously reported that the generation of ceramide is increased by SPHK2 but decreased by SPHK1 [36]. SPHK2 probably facilitates the S1P-mediated salvage pathway of ceramide synthesis in which S1P is dephosphorylated to sphingosine by S1P-phosphatase and then acylated to form ceramide in ER [37]. Corroborating previous findings, the generation of the [^{3}H] ceramide-derived metabolites, [^{3}H]GlcCer and [^{3}H]sphingomyelin, in [^{3}H]sphingosine-labeled A20/2J cells were increased by SPHK2 transfection and decreased by SG-12 (Fig. **2**). Previously, it has been reported that the generation of ceramide is involved in cell death in B cells [38, 39]. Further study is necessary to correlate such SPHK2-mediated sphingolipid metabolism and the regulation of cell death.

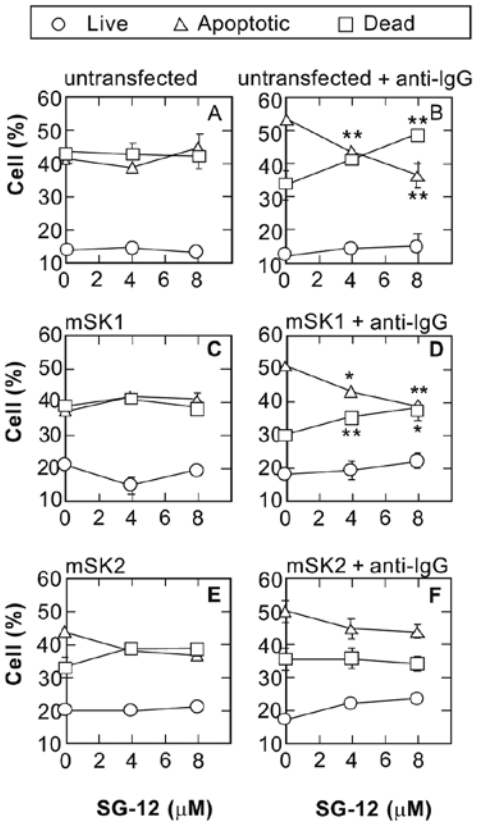

Fig. (6). Effect of SG-12 on Fas-mediated cell death was relieved by transfection of SPHK2 but not SPHK1. A20/2J cells (**A, B**) or the cells transfected with SPHK1 (C, D) or SPHK2 (**E, F**) were incubated with 100 ng/ml anti-mouse Fas mAb for 20 h without (**A, C, E**) or with (**B, D, F**) 5 μg/ml F(ab')$_2$ of anti-mouse IgG pAb in the presence of indicated concentrations of SG-12. Values are means ± SD from triplicate samples. Statistically significant differences (*$p < 0.05$ or **$p < 0.01$) with respect to the values without SG-12 are indicated. Essentially the same result was obtained in an independent experiment.

ACKNOWLEDGEMENTS

We thank Dr. Takuma Nakajima and Dr. Katarzyna A. Podyma-Inoue (Tokyo Medical and Dental University) for their valuable discussion. This work was supported by the Grants-in-Aids for 21st Century COE Program to Tokyo Medical and Dental University from the Ministry of Education, Science, Sports and Culture, Japan.

ABBREVIATIONS

SPHK	=	Sphingosine kinase
S1P	=	Sphingosine-1-phosphate
BCR	=	B cell receptor

SG-12 = (2S, 3R)-2-amino-4-(4-octylphenyl)butane-1-3-diol

PI = Propidium iodide

REFERENCES

[1] Kohama, T.; Olivera, A.; Edsall, L.; Nagiec, M.M.; Dickson, R.; Spiegel, S. *J. Biol. Chem.*, **1998**, *273*, 23722-23728.

[2] Liu, H.; Sugiura, M.; Nava, V.E.; Edsall, L.C.; Kono, K.; Poulton, S.; Milstien, S.; Kohama, T.; Spiegel, S. *J. Biol. Chem.*, **2000**, *275*, 19513-19520.

[3] Spiegel, S.; Milstien, S. *J. Biol. Chem.*, **2007**, *282*, 2125-2129.

[4] Allende, M.L.; Sasaki, T.; Kawai, H.; Olivera, A.; Mi, Y.; van Echten-Deckert, G.; Hajdu, R.; Rosenbach, M.; Keohane, C. A.; Mandala, S.; Spiegel, S.; Proia, R.L. *J. Biol. Chem.*, **2004**, *279*, 52487-52492.

[5] Kharel, Y.; Lee, S.; Snyder, A.H.; Sheasley-O'neill S.L.; Morris, M.A.; Setiady, Y.; Zhu, R.; Zigler, M.A.; Burcin, T.L.; Ley, K.; Tung, K.S.; Engelhard, V.H.; Macdonald, T.L.; Pearson-White, S.; Lynch, K.R. *J. Biol. Chem.*, **2005**, *280*, 36865-36872.

[6] Mizugishi, K.; Yamashita, T.; Olivera, A.; Miller, G.F.; Spiegel, S.; Proia, R.L. *Mol. Cell Biol.*, **2005**, *25*, 11113-11121.

[7] Wang, F.; Van Brocklyn, J.R.; Hobson, J.P.; Movafagh, S.; Zukowska-Grojec, Z.; Milstien, S.; Spiegel, S. *J. Biol. Chem.*, **1999**, *274*, 35343-35350.

[8] Lee, M.J.; Thangada, S.; Claffey, K.P.; Ancellin, N.; Liu, C.H.; Kluk, M.; Volpi, M.; Sha'afi, R.I.; Hla, T. *Cell*, **1999**, *99*, 301-312.

[9] English, D.; Welch, Z.; Kovala, A.T.; Harvey, K.; Volpert, O.V.; Brindley, D.N.; Garcia, J.G. *FASEB J.*, **2000**, *14*, 2255-2265.

[10] Liu, Y.; Wada, R.; Yamashita, T.; Mi, Y.; Deng, C.X.; Hobson, J. P.; Rosenfeldt, H.M.; Nava, V.E.; Chae, S.S.; Lee, M.J.; Liu, C.H.; Hla, T.; Spiegel, S.; Proia, R.L. *J. Clin. Invest.*, **2000**, *106*, 951-961.

[11] Okamoto, H.; Takuwa, N.; Yokomizo, T.; Sugimoto, N.; Sakurada, S.; Shigematsu, H.; Takuwa, Y. *Mol. Cell Biol.*, **2000**, *20*, 9247-9261.

[12] Kupperman, E.; An, S.; Osborne, N.; Waldron, S.; Stainier, D.Y. *Nature*, **2000**, *406*, 192-195.

[13] Graeler, M.; Shankar, G.; Goetzl, E.J. *J. Immunol.*, **2002**, *169*, 4084-4087.

[14] Hait, N.C.; Oskeritzian, C.A.; Paugh, S.W.; Milstien, S.; Spiegel, S. *Biochim. Biophys. Acta*, **2006**, *1758*, 2016-2026.

[15] Olivera, A.; Rosenfeldt, H.M.; Bektas, M.; Wang, F.; Ishii, I.; Chun, J.; Milstien, S.; Spiegel, S. *J. Biol. Chem.*, **2003**, *278*, 46452-46460.

[16] Liu, H.; Toman, R.E.; Goparaju, S.K.; Maceyka, M.; Nava, V.E.; Sankala, H.; Payne, S.G.; Bektas, M.; Ishii, I.; Chun, J.; Milstien, S.; Spiegel, S. *J. Biol. Chem.*, **2003**, *278*, 40330-40336.

[17] Igarashi, N.; Okada, T.; Hayashi, S.; Fujita, T.; Jahangeer, S.; Nakamura, S. *J. Biol. Chem.*, **2003**, *278*, 46832-46839.

[18] Samy, E.T.; Meyer, C.A.; Caplazi, P.; Langrish, C.L.; Lora, J.M.; Bluethmann, H.; Peng, S. L. *J. Immunol.*, **2007**, *179*, 5644-5648.

[19] Van Parijs, L.; Abbas, A.K. *Curr. Opin. Immunol.*, **1996**, *8*, 355-361.

[20] Siegel, R.M.; Chan, F.K.; Chun, H.J.; Lenardo, M.J. *Nat. Immunol.*, **2000**, *1*, 469-474.

[21] Mizuno, T.; Zhong, X.; Rothstein, T.L. *Apoptosis*, **2003**, *8*, 451-460.

[22] Jarvis, W.D.; Grant, S. *Curr. Opin. Oncol.*, **1998**, *10*, 552-559.

[23] Watanabe, M.; Kitano, T.; Kondo, T.; Yabu, T.; Taguchi, Y.; Tashima, M.; Umehara, H.; Domae, N.; Uchiyama, T.; Okazaki, T. *Cancer Res.*, **2004**, *64*, 1000-1007.

[24] Grassme, H.; Cremesti, A.; Kolesnick, R.; Gulbins, E. *Oncogene*, **2003**, *22*, 5457-5470.

[25] Miyaji, M.; Jin, Z.X.; Yamaoka, S.; Amakawa, R.; Fukuhara, S.; Sato, S.B.; Kobayashi, T.; Domae, N.; Mimori, T.; Bloom, E.T.; Okazaki, T.; Umehara, H. *J. Exp. Med.*, **2005**, *202*, 249-259.

[26] Hannun, Y.A. *J. Biol. Chem.*, **1994**, *269*, 3125-3128.

[27] Ruvolo, P.P. *Pharmacol. Res.*, **2003**, *47*, 383-392.

[28] Cuvillier, O.; Pirianov, G.; Kleuser, B.; Vanek, P.G.; Coso, O.A.; Gutkind, S.; Spiegel, S. *Nature*, **1996**, *381*, 800-803.

[29] Bektas, M.; Jolly, P.S.; Muller, C.; Eberle, J.; Spiegel, S.; Geilen, C. C. *Oncogene*, **2005**, *24*, 178-187.

[30] Pi, X.; Tan, S.Y.; Hayes, M.; Xiao, L.; Shayman, J.A.; Ling, S.; Holoshitz, J. *Arthritis Rheum.*, **2006**, *54*, 754-764.

[31] Kim, J.W.; Kim, Y.W.; Inagaki, Y.; Hwang, Y.A.; Mitsutake, S.; Ryu, Y.W.; Lee, W.K.; Ha, H.J.; Park, C.S.; Igarashi, Y. *Bioorg. Med. Chem.*, **2005**, *13*, 3475-3485.

[32] Hara-Yokoyama, M.; Kimura, T.; Kaku, H.; Wakiyama, M.; Kaitsu, Y.; Inoue, M.; Kusano, S.; Shirouzu, M.; Yokoyama, S.; Katada, T.; Hirabayashi, Y.; Takatsu, K.; Yanagishita, M. *Int. Immunopharmacol.*, **2008**, *8*, 59-70.

[33] Kihara, A.; Ikeda, M.; Kariya, Y.; Lee, E.Y.; Lee, Y.M.; Igarashi, Y. *J. Biol. Chem.*, **2003**, *278*, 14578-14585.

[34] McKean, D.J.; Infante, A.J.; Nilson, A.; Kimoto, M.; Fathman, C.G.; Walker, E.; Warner, N. *J. Exp. Med.*, **1981**, *154*, 1419-1431.

[35] Moriyama, H.; Yonehara, S. *Immunol. Lett.*, **2007**, *109*, 36-46.

[36] Maceyka, M.; Sankala, H.; Hait, N.C.; Le Stunff, H.; Liu, H.; Toman, R.; Collier, C.; Zhang, M.; Satin, L.S.; Merrill, A.H., Jr.; Milstien, S.; Spiegel, S. *J. Biol. Chem.*, **2005**, *280*, 37118-37129.

[37] Le Stunff, H.; Galve-Roperh, I.; Peterson, C.; Milstien, S.; Spiegel, S. *J. Cell Biol.*, **2002**, *158*, 1039-1049.

[38] Kroesen, B.J.; Pettus, B.; Luberto, C.; Busman, M.; Sietsma, H.; de Leij, L.; Hannun, Y.A. *J. Biol. Chem.*, **2001**, *276*, 13606-13614.

[39] Kroesen, B.J.; Jacobs, S.; Pettus, B.J.; Sietsma, H.; Kok, J.W.; Hannun, Y.A.; de Leij, L.F. *J. Biol. Chem.*, **2003**, *278*, 14723-14731.

Received: August 7, 2008 Revised: September 16, 2008 Accepted: September 19, 2008

© Hara-Yokoyama *et al.*; Licensee *Bentham Open*.

This is an open access article licensed under the terms of the Creative Commons Attribution Non-Commercial License (http://creativecommons.org/licenses/by-nc/3.0/) which permits unrestricted, non-commercial use, distribution and reproduction in any medium, provided the work is properly cited.

MEMO

口腔病理学分野

山口　朗

医歯学総合研究科・口腔機能再構築学系専攻
口腔病理学・教授

1. 研究課題名と研究内容

(1) 骨芽細胞分化および骨再生過程における細胞・分子間相互作用

Cellular and molecular interactions in osteoblast differentiation and bone regeneration

本研究では、骨芽細胞分化および骨再生過程における細胞・分子間の相互作用を解析し、骨再生の統合的理解を深め、優れた骨再生療法を確立するための分子基盤を構築することを目的とする。今年度は以下の研究を行った。

1) 骨芽細胞分化におけるCCN3とBMP,Notchの相互作用の解析:CCN3とBMP, Notchの分子間相互作用について詳細に解析し、CCN3はCTドメインを介して細胞外でNotchまたはBMP-2に結合し、骨芽細胞分化を抑制することを明らかにした。(Biochem Bioph Res Commun 368:808-814,2008)。現在、骨芽細胞特異的にCCN3を過剰発現するトタンスジェニックマウスおよびCCN3ノックアウトマウスにおける骨格の表現型の解析と骨再生過程の解析を行なっている。

2) 骨芽細胞分化におけるZinc finger protein 64 (Zfp64) とNotchの相互作用の解析:NotchのC末端に結合する分子としてZfp64を同定し、Zfp64がNotchシグナルと相互作用をして、骨芽細胞の分化を制御していることを明らかにした (J Cell Sci 121:1613-1623,2008)。

3) 骨芽細胞分化におけるBMP-2とosterixの相互作用の解析:我々の樹立したRunx2欠損細胞を用いて、BMP-2はMsx2を介してosterixの発現を制御していることを見出した (J Biol Chem 283:29119-29125, 2008)。

4) BMP－2とLatexinの相互作用の解析:我々の樹立したRunx2欠損細胞をBMP-2で処理するとLatexinの発現が著明に上昇することをマイクロアレイ解析で見出し、LatexinはBMP-2で制御され、軟骨分化に重要な役割を担っていることを明らかにした (Biochem Bioph Res Commun 378;600-6004,2009)。

(2) 口腔癌による顎骨破壊の分子メカニズム

Molecular mechanism of bone destruction by oral cancer

口腔癌はその解剖学的構造に依存して、容易に顎骨に直接浸潤するという特徴をもち、顎骨浸潤はその予後を規定する重要な要因の一つである。そのため、歯肉癌の顎骨浸潤の予防あるいは顎骨浸潤の進展を阻止することができれば、今後の歯肉癌治療に大きく貢献できる。この目的を達成するために、我々は口腔癌による顎骨破壊の分子メカニズムの解析を行なっている。

1) 口腔癌顎骨浸潤の外科病理学的解析:本学歯学部附属病院で下顎歯肉原発の扁平上皮癌と診断され顎骨切除術を施行された97症例の顎骨切除検体を外科病理学的に解析した。その結果、全症例の顎骨浸潤部において癌と骨組織との間には程度の差はあるものの必ず線維性間質の介在が認められることを明らかにした。さらに、免疫組織学的解析により、癌による顎骨浸潤部の破骨細胞に隣接する線維芽細胞様細胞、骨芽細胞様細胞にRANKLの発現が認められることを見出した (BONE 43:621-627,2008)。

2) 口腔癌顎骨浸潤におけるIL-6, PTHrPの役割:口腔癌による顎骨浸潤に関与する因子としてIL-6およびPTHrPに着目し、癌細胞および間質細胞との相互作用により引き起こされる破骨細胞形成におけるこれらの因子の役割を明らかにすることを目的として種々の培養細胞を用いた実験を行なった。

その結果、口腔癌の顎骨浸潤部では、癌細胞自身がIL-6及びPTHrPを産生するとともに、癌細胞が間質細胞を刺激してIL-6合成を促進させ、これらのIL-6及びPTHrPが間質細胞のRANKL発現を上昇させ、破骨細胞形成を促進していることを明らかにした（論文投稿中）。

(3) 滑膜骨軟骨腫症の病態生物学的解析

Pathobiology of synovialchondromatosis

滑膜性軟骨腫症は関節滑膜下に骨軟骨性結節で構成される遊離体を生じる疾患であるが、その病態に関与する因子は明らかでなかった。この点を明らかにするために、本研究では滑膜性軟骨腫症の病態にBone morphogenetic proteinが関与しているかを検討した。滑膜性軟骨腫症患者より採取した遊離体細胞、滑膜細胞はBMP-2, BMP-4 mRNAを発現していた。BMP-2は培養した遊離体細胞、滑膜細胞のSox9, Col2a1, Aggrecan（Agc1）mRNAの発現を促進し、滑膜細胞におけるRunx2, Col1a1, Osteocalcin（Ocn）の発現も促進した。BMP-2は培養遊離体細胞におけるアルシアンブルー陽性コロニーの形成を促進した。BMPのantagonistであるNoggin は、これらの細胞における Sox9, Col2a1, Agc1, Runx2 の発現を抑制し、滑膜細胞の Ocn の発現を抑制した。以上の結果より、BMPが滑膜性軟骨腫症の主たる病態である骨軟骨化生に関与していることが明らかとなった（Biochem Bioph Res Commun 379:914-919,2009）。

(4) 光メージングと分子生物学の融合によるオステオネットワークの解明を目指したフロンティア研究拠点

New frontier of osteonetwork research by combinational approaches of optical imaging and molecular biology

骨をさらに深く理解することを目標として、骨組織に対する光イメージングの応用と遺伝子改変マウス作製を含めた網羅的分子生物学のテクニックを有機的に結合させ、研究を推進する。これら異分野として発展しつつある2つの先端科学的なアプローチを統合し、オステオネットワーク構成分子群の同定とその機能解明にチャレンジする。今年度は骨組織のin vivoライブイメージング法の確立、発生・骨再生過程で出現する細胞群の細胞周期のライブイメージング解析、骨細胞の機能解析などを開始するための準備を行なった。

2.

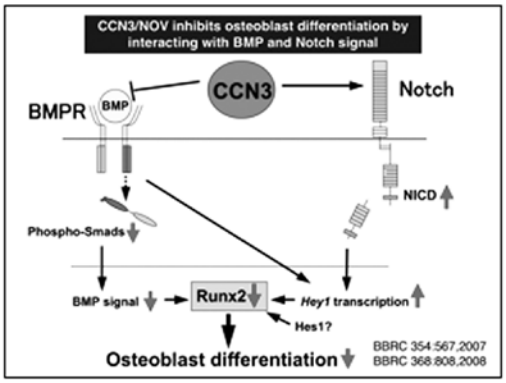

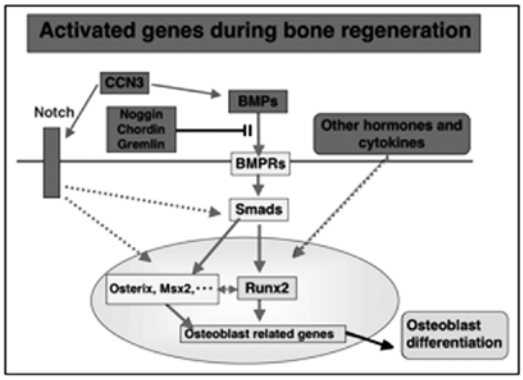

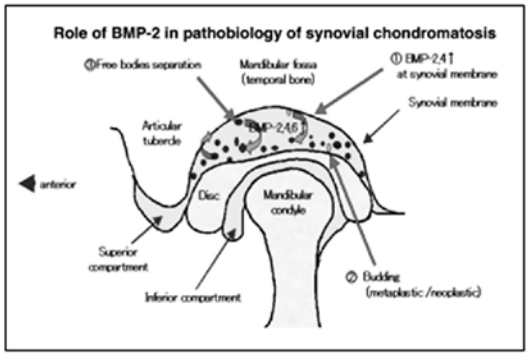

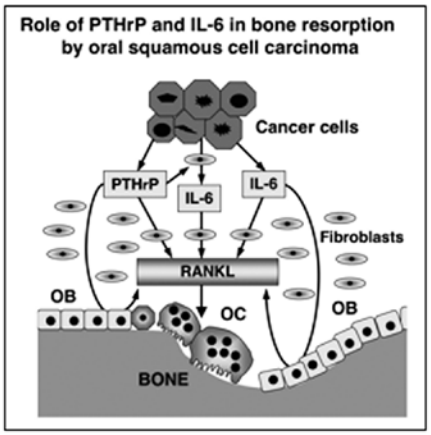

Section of Oral Pathology
Akira Yamaguchi

3. 2008年、2009年（平成21年3月までの）に発表した全ての研究内容についての英文要約

1 Katsuki Y, Sakamoto K, Minamizato T, Umezawa A, Ikeda M, Perbal B, Amagasa T, Yamaguchi A, Katsube K: Dual role of CCN3/Notch signal in mouse osteogenic mesenchymal stem cells, Kusa. Biochem Bioph Res Commun 368:808-814,2008
CCN3 transfection to Kusa-A1 inhibited osteogenic differentiation and cell proliferation, which is accompanied by upregulation of Hes/Hey, Notch downstream targets, and p21, a CDK inhibitor. Upregulation of Hes/Hey and p21 was abrogated by the deletion of CT domain. Anti-proliferative activity of CCN3 was also abrogated by CT domain deletion whereas anti-osteogenic activity was not completely abrogated. We found that CT domain-deleted CCN3 still possesses antagonistic effect on BMP-2. These results suggest that CCN3 employs Notch and BMP pathways in anti-osteogenic activity while it inhibits cell proliferation uniquely by Notch/p21 pathway.

2. Sakamoto K, Tamamura Y, Katsube K, Yamaguchi A: Zinc finger protein 64 participates in Notch signaling and regulates mesenchymal cell differentiation. J Cell Sci 121:1613-1623,2008
Notch signaling is required for multiple aspects of tissue and cell differentiation. In this study, we identified zinc finger protein 64 (Zfp64) as a novel coactivator of Notch1. Zfp64 is associated with the intracellular domain of Notch1, recruited to the promoters of the Notch target genes Hes1 and Hey1, and transactivates them. Zfp64 expression is under the control of Runx2, and is upregulated by direct transactivation of its promoter. Zfp64 suppresses the myogenic differentiation of C2C12 cells and promotes their osteoblastic differentiation. Our data demonstrate two functions of Zfp64: (1) it is a downstream target of Runx2 and, (2) its cognate protein acts as a coactivator of Notch1, which suggests that Zfp64 mediates mesenchymal cell differentiation by modulating Notch signaling.

3. Ishikuro M, Sakamoto K, Kayamori K, Izumo T, Yamaguchi A: Role of fibrous stroma in bone invasion by gingival squamous cell carcinomas. BONE 43:621-627,2008
We histopathologically investigated mandibular invasion patterns in 97 cases of primary gingival SCC and evaluated the correlations between bone invasion patterns and clinicopathological factors. Varying numbers of Howship's lacunae and osteoclasts were detected on the bone surface adjacent to the tumor cells. Tumor cells showed no direct contact with osteoclasts and the adjacent bones, and in all cases varying amounts of fibrous connective tissues intervened between the tumor cells and the bone. The number of fibroblasts was significantly greater in the infiltrative type than in the expansive type. We also found a positive correlation between the number of osteoclasts and fibroblasts at the interface of the tumor and the resorbing bone. Immunohistochemistry revealed RANKL expression in the fibroblastic cells that were adjacent to the osteoclasts in the area of bone resorption. These results indicate that the fibrous stroma plays critical roles in osteoclastic bone resorption by gingival SCC through the RANKL-dependent pathways.

4. Matsubara T, Kida K, Yamaguchi A, Hata K, Ichida F, Meguro H, Aburatani H, Nishimura R, Yoneda T:BMP2 regulates Osterix through Msx2 and Runx2 during osteoblast differentiation. J Biol Chem 283:29119-29125, 2008
We examined the role of BMP2 signaling in the regulation of Osterix using the mesenchymal cell lines C3H10T1/2 and C2C12. Osterix overexpression induced alkaline phosphatase activity and osteocalcin expression in C2C12 cells and stimulated calcification of murine primary osteoblasts. Considering that Runx2 overexpression induces Osterix, these results suggest that Osterix functions as downstream of Runx2. Surprisingly, BMP2 treatment induced Osterix expression and alkaline phosphatase activity in mesenchymal cells derived from Runx2-deficient mice. Moreover, overexpression of a homeobox gene, Msx2, which is up-regulated by BMP2 and promotes osteoblastic differentiation, induced Osterix expression in the Runx2-deficient cells. Interestingly, microarray analyses using the Runx2-deficient cells revealed that the role of Osterix was distinct from that of Runx2. These findings suggest that Osterix is regulated via both Runx2-dependent and -independent mechanisms, and that Osterix controls osteoblast differentiation, at least in part, by regulating the expression of genes not controlled by Runx2.

5. Kondo T, Kitazawa R, Yamaguchi A, Kitazawa S: Dexamethasone promotes osteoclastogenesis by inhibiting osteoprotegerin through multiple levels. J Cell Biochem 103:335-345,2008
The expression of receptor activator of nuclear factor-kappaB ligand (RANKL) is regulated by bone-seeking hormones such as PTH and 1alpha,25-dihydroxyvitamin D3 (1,25 (OH) 2D3) . Although the expression of RANKL in the steady-state was higher in RD-C6 than in ST2, 1,25 (OH) 2D3-treatment of the cells increased it 20-fold in ST2 but only 1.8-fold in RD-C6. Transient transfection studies with proximal RANKL

2kb promoter, runx2 knock-down in ST2, and forced expression of runx2 in RD-C6 all confirmed that runx2 set the steady-state expression of the RANKL gene at a low level, but exerted a positive effect on enhanced transcriptional activity in response to 1,25（OH）2D3. In the steady-state, runx2 may suppress RANKL gene by condensing the chromatin structure; however, it exerts a positive effect on 1,25（OH）2D3-induced RANKL transcription when the proximal runx2 sites are accessible. Thus, RANKL expression in stromal/osteoblastic cells is keenly regulated by 1,25（OH）2D3 which transactivates the gene at two different levels

6. Kitaura H, Yoshimatsu M, Fujimura Y, Eguchi T, Kohara H, Yamaguchi A, Yoshida N: An anti-c-Fms antibody inhibits orthodontic tooth movement. J Dent Res 87:396-400,2008
Orthodontic force induces osteoclastogenesis in vivo. It has recently been reported that administration of an antibody against the macrophage-colony-stimulating factor（M-CSF）receptor c-Fms blocks osteoclastogenesis and bone erosion induced by tumor necrosis factor-alpha（TNF-alpha）administration. This study aimed to examine the effect of an anti-c-Fms antibody on mechanical loading-induced osteoclastogenesis and osteolysis in an orthodontic tooth movement model in mice. Using TNF receptor 1- and 2-deficient mice, we showed that orthodontic tooth movement was mediated by TNF-alpha. We injected anti-c-Fms antibody daily into a local site, for 12 days, during mechanical loading. The anti-c-Fms antibody significantly inhibited orthodontic tooth movement, markedly reduced the number of osteoclasts in vivo, and inhibited TNF-alpha-induced osteoclastogenesis in vitro. These findings suggest that M-CSF plays an important role in mechanical loading-induced osteoclastogenesis and bone resorption during orthodontic tooth movement mediated by TNF-alpha.

7. Kabasawa Y, Nagumo K, Takeda Y, Kawashima N, Okada N, Omura K, Yamaguchi A, Katsube KI.: Amelogenin positive cells scattered in the interstitial component of odontogenic fibromas. J Clin Pathol 61:851-855,2008
Odontogenic tumors are often biphasic, consisting of epithelial and interstitial components, with an origin that is not well understood. Odontogenic fibromas are rich in mesenchymal component, but also have many epithelial nests. To investigate the origin of this tumour by immunohistochemistry. The expression of several odontogenic and epithelial markers, including amelogenin, was investigated by immunofluorescent studies. Immunohistochemical analysis showed that epithelial nests exhibited E-cadherin expression, but not amelogenin. Amelogenin positive cells were scattered in the fibrous tissue, which did not exhibit epithelial marker expression except for epithelial membrane antigen. In one case that had received a test biopsy before whole resection of tumour, amelogenin positive cells were distributed in the regenerating mucosal epithelium or subepithelial tissue. Results indicate that amelogenin positive cells of odontogenic fibromas have an epithelial origin and may have the potential for epithelial mesenchymal transition, which has not to date been investigated in benign tumors.

8. Matsuda N, Katsube K, Mikami S, Katsuki Y, Iseki H, Mukai M, Yamaguchi A, Takano Y, Nakajima T, Nakajima H, Kishi K: E-cadherin expression in the subepithelial nevus cells of the giant congenital nevocellular nevi（GCNN）correlates with their migration ability in vitro. J Dermatol Sci 52:21-30, 2008
Giant congenital nevocellular nevi（GCNN）are histologically characterized by the broad distribution of nevus cells in the epidermis and dermis. To characterize E-cadherin in GCNN and define its role in nevic cell migrations. Twenty-four cases were immunohistochemically examined and in five cases cells were isolated for primary culture for migration assays. The nevus cells in the superficial region showed the immunoreactivity of E-cadherin in a membranous pattern, but those in the deep part of dermis had little immunoreactivity. Ultra-structural analysis of the superficial nevus cells revealed that E-cadherin immunodeposits in the fibrillar processes around the cell body in a spotted pattern. This distribution pattern is quite different from that in the adherens junction of skin squamous epithelial cells. Boyden chamber experiments were performed using primary cultures of intradermal nevus cells. EDTA pretreatment reduced cell migration to the E-cadherin positive side when the E-cadherin positive population was relatively large in the primary cultures. These results indicate that E-cadherin in the nevus cells may affect nevus cell motility rather than intercellular attachment.

9. Kadouchi I, Sakamoto K, Liu T, Murakami T, Kobayashi E, Hoshino Y, Yamaguchi A: Latexin is involved in bone morphogenetic protein-2-induced chondrocyte differentiation. Biochem Bioph Res Commun 378;600-6004,2009
Latexin is the only known carboxypeptidase A inhibitor in mammals. We previously demonstrated that BMP-2 significantly induced latexin expression in Runx2-deficient mesenchymal cells（RD-C6 cells）, during chondrocyte and osteoblast differentiation. In

this study, we investigated latexin expression in the skeleton and its role in chondrocyte differentiation. Immunohistochemical studies revealed that proliferating and prehypertrophic chondrocytes expressed latexin during skeletogenesis and bone fracture repair. In the early phase of bone fracture, latexin mRNA expression was dramatically upregulated. BMP-2 upregulated the expression of the mRNAs of latexin, Col2a1, and the gene encoding aggrecan（Agc1）in a micromass culture of C3H10T1/2 cells. Overexpression of latexin additively stimulated the BMP-2-induced expression of the mRNAs of Col2a, Agc1, and Col10a1. BMP-2 treatment upregulated Sox9 expression, and Sox9 stimulated the promoter activity of latexin. These results indicate that latexin is involved in BMP-2-induced chondrocyte differentiation and plays an important role in skeletogenesis and skeletal regeneration.

10. Nakanishi S, Sakamoto K, Yoshitake H, Kino K, Amagasa T, Yamaguchi A: Bone morphogenetic proteins are involved in the pathobiology of synovial chondromatosis. Biochem Bioph Res Commun 379:914-919,2009
Synovial chondromatosis is characterized by the formation of osteocartilaginous nodules（free bodies）under the surface of the synovial membrane in joints. Free bodies and synovium isolated from synovial chondromatosis patients expressed high levels of BMP-2 and BMP-4 mRNAs. BMP-2 stimulated the expression of Sox9, Col2a1, and Aggrecan mRNAs in free-body and synovial cells and that of Runx2, Col1a1, and Osteocalcin mRNAs in the free-body cells only. BMP-2 increased the number of alcian blue-positive colonies in the free-body cell culture but not in the synovial cell culture. Noggin suppressed the expression of Sox9, Col2a1, Aggrecan, and Runx2 mRNAs in both the free-body and synovial cells. Further, it inhibited Osteocalcin expression in the synovial cells. These results suggest that BMPs are involved in the pathobiology of cartilaginous and osteogenic metaplasia observed in synovial chondromatosis.

11. Katsube K, Sakamoto K, Tamamura Y, Yamaguchi A: CCN, a vertebrate specific gene family and Development. Development, Growth & Differentiation 51:55067,2009
The CCN family of genes constitutes six members of small secreted cysteine rich proteins, which exists only in vertebrates. The major members of CCN are CCN1（Cyr61）, CCN2（CTGF）, and CCN3（Nov）. CCN4, CCN5, and CCN6 were formerly reported to be in the Wisp family, but they are now integrated into CCN due to the resemblance of their four principal modules: insulin like growth factor binding protein, von Willebrand factor type C, thrombospondin type 1, and carboxy-terminal domain. CCNs show a wide and highly variable expression pattern in adult and in embryonic tissues, but most studies have focused on their principal role in osteo/chondrogenesis and vasculo/angiogenesis from the aspect of migration, growth, and differentiation of mesenchymal cells. CCN proteins simultaneously integrate and modulate the signals of integrins, bone morphogenetic protein, vascular endothelial growth factor, Wnt, and Notch by direct binding. However, the priority in the use of the signals is different depending on the cell status. Even the equivalent counterparts show a difference in signal usage among species. It may be that the evolution of the CCN family continues to keep pace with vertebrate evolution itself.

4. 本事業に関連して世界的な研究拠点形成に向けて、以下の点で改善・整備等されたこと

A（研究拠点形成）

我々が従来行なってきた骨生物学的研究を基盤として、骨再生、癌による骨浸潤などの骨疾患の病態、治療法に関連する研究計画を立案し、「歯と骨の分子疾患科学の国際教育研究拠点」に相応しい研究を推進することとした。

B（研究教育環境）

多くの実験は当分野で行なうことができる環境が整っていたが、in vivo imagingの研究を効率的に推進するために、既存の共焦点顕微鏡をグレードアップした。

C（人材確保）

シャペロン教官として飯村忠浩特任准教授を採用した。また、臨床系分野からの大学院生を受入、本研究を推進している。

D（人材育成）

大学院生の研究レベルを向上させるために、各大学院生には分野内で特定の指導教官を配置し、man-to-manの指導体制をとっている。

E（国際化）

国際学会での発表を目指すよう指導し、国内における外国人の講演への積極的に参加させている。

5. GCOE事業を推進するに当たって力を入れた点

現在までに我々が行なってきた骨細胞生物学の研究を基盤として、骨疾患の病態解析、治療法の開発へ向けた研究を推進するようにしている。

6. 英文原著論文

1. Katsuki Y, Sakamoto K, Minamizato T, Umezawa A, Ikeda M, Perbal B, Amagasa T, Yamaguchi A, Katsube K: Dual role of CCN3/Notch signal in mouse osteogenic mesenchymal stem cells, Kusa. Biochem Bioph Res Commun 368:808-814,2008
2. Sakamoto K, Tamamura Y, Katsube K, Yamaguchi A: Zinc finger protein 6 4 participates in Notch signaling and regulates mesenchymal cell differentiation. J Cell Sci 121:1613-1623,2008
3. Ishikuro M, Sakamoto K, Kayamori K, Izumo T, Yamaguchi A: Role of fibrous stroma in bone invasion by gingival squamous cell carcinomas. BONE 43:621-627,2008
4. Matsubara T, Kida K, Yamaguchi A, Hata K, Ichida F, Meguro H, Aburatani H, Nishimura R, Yoneda T:BMP2 regulates Osterix through Msx2 and Runx2 during osteoblast differentiation. J Biol Chem 283:29119-29125, 2008
5. Kondo T, Kitazawa R, Yamaguchi A, Kitazawa S: Dexamethasone promotes osteoclastogenesis by inhibiting osteoprotegerin through multiple levels. J Cell Biochem 103:335-345,2008
6. Kitaura H, Yoshimatsu M, Fujimura Y, Eguchi T, Kohara H, Yamaguchi A, Yoshida N: An anti-c-Fms antibody inhibits orthodontic tooth movement. J Dent Res 87:396-400,2008
7. Kabasawa Y, Nagumo K, Takeda Y, Kawashima N, Okada N, Omura K, Yamaguchi A, Katsube KI.: Amelogenin positive cells scattered in the interstitial component of odontogenic fibromas. J Clin Pathol 61:851-855,2008
8. Matsuda N, Katsube K, Mikami S, Katsuki Y, Iseki H, Mukai M, Yamaguchi A, Takano Y, Nakajima T, Nakajima H, Kishi K: E-cadherin expression in the subepithelial nevus cells of the giant congenital nevocellular nevi（ GCNN ）correlates with their migration ability in vitro. J Dermatol Sci 5 2:2 1-3 0, 2008
9. ◎ Kadouchi I, Sakamoto K, Liu T, Murakami T, Kobayashi E, Hoshino Y, Yamaguchi A: Latexin is involved in bone morphogenetic protein-2-induced chondrocyte differentiation. Biochem Bioph Res Commun 378;600-6004,2009
10. ◎ Nakanishi S, Sakamoto K, Yoshitake H, Kino K, Amagasa T, Yamaguchi A: Bone morphogenetic proteins are involved in the pathobiology of synovial chondromatosis. Biochem Bioph Res Commun 379:914-919,2009

7. 総説

1. Yamaguchi A, Sakamoto K, Minamizato T, Katsube K, Nakanishi S: Regulation of osteoblast differentiation mediated by BMP, Notch, and CCN3/NOV. The Japanese Dental Science Review. 4 4:4 8-56,2008
2. 山口　朗:古生物から学ぶ骨細胞. 腎と骨代謝 21:227-232,2008
3. Katsube K, Sakamoto K, Tamamura Y, Yamaguchi A: CCN, a vertebrate specific gene family and development. Development, Growth & Differentiation 51:55067,2009

8. 平成21年3月までの自己評価

我々は長年、骨形成の分子メカニズムの研究を中心として骨生物学の基礎研究を推進してきた。本GCOEプログラムでは、現在までの基礎研究を継続するとともに、骨再生、癌の骨破壊、顎骨の疾患などの研究を推進し、「骨の分子疾患科学」に相応しい研究を推進した。特に、骨再生過程で発現が上昇する遺伝子の機能解析、癌により顎骨浸潤のメカニズム、顎関節に発症する滑膜軟骨軟骨腫症の病態解析に関しては論文発表を行なったので、本研究は概ね順調に推進することができたと考えている。しかし、遺伝子改変マウスの作成に時間がかかり、これらを用いた骨再生に関するin vivoの実験が予定よりやや遅れた点は反省すべき点として挙げられる。

2009年1月より、本GCOEシャペロン教官として飯村忠浩准教授を採用し、骨・歯におけるin vivo imaging研究を開始することとした。しかし、採用時期が遅かったために、in vivo imaging研究の準備をほぼ完了することができたが、具体的な研究成果を挙げるには至らなかった。

9. 和文原著論文

1. 柴原孝彦、森田章介、杉原一正、箕輪和行、山口朗、山田隆文:2005年度HO国際分類による歯原性腫瘍の発生状況に関する疫学的研究、口腔腫瘍　20;245-254,2008

10. 学会発表（英語）

1. Inoue H, Nakashima T, Iwamatsu A, suematsu A, Yamaguchi A, Takayanagi H: Novel screening system for bone matrix proteins that control bone mineralization. 30th American Society for Bone Mineral Research 29th Annual Meeting. Montreal, Canada, September 13,2008
2. Kadouchi I, Sakamoto K, Murakami T, Kobayashi E, Hoshino Y, Yamaguchi A:Latexin is a novel effector of BMP-2 signaling in modulation of chondrocyte differentiation. 30th American Society for Bone Mineral Research 29th Annual Meeting. Montreal, Canada, September 13,2008

11. 学会発表（日本語）

1. 山口　朗:骨再生におけるBMPとNotchシグナルの役割．第7回日本再生医療学会総会シンポジウム、名古屋、2008年3月14日
2. 山口　朗:骨芽細胞分化と骨再生の分子基盤（ワークショップ3:骨・関節をめぐる最近の話題）．第97回日本病理学会、金沢, 2008年5月15日
3. 河合繁夫、伊藤栄作、山口朗、江石義信、岡田憲彦:歯原性腫瘍の免疫組織学的特徴;組織発生解明と診断における有用性．第97回日本病理学会、金沢、2008年5月16日
4. 坂本啓、山口朗:口腔白板症・扁平上皮癌のバイオマーカーとなるケラチン同定の試みとその有用性の検討．第97回日本病理学会、金沢、2008年5月16日
5. 中西正一、☒武啓幸、天笠光雄、木野礼司、山口朗:顎関節における骨膜性軟骨腫瘍症におけるBMP-2の役割．第28回日本骨形態計測学会、東京、2008年7月26日
6. 栢森高、坂本啓、石黒真史、山口朗:口腔扁平上皮癌の顎骨浸潤に関与する因子の網羅的解析．第50回歯科基礎医学会、東京、2008年9月24日
7. 木田達也、佐藤瑞希、柴崎真樹、坂本啓、山口朗:口腔及び食道扁平上皮癌における腫瘍バイオマーカーとしてのケラチンの有用性．第50回歯科基礎医学会、東京、2008年9月24日
8. 門内一郎、山口朗:骨形成・骨再生におけるLxnの役割．第26回日本骨代謝学会学術集会、大阪、2008年10月29日
9. 西川恵三、竹田秀、山口朗、高柳広:加齢に伴い骨量減少の原因となる転写メカニズムの探索．第26回日本骨代謝学会学術集会、大阪、2008年10月29日
10. 寺内公一、坂本啓、玉村貞宏、尾林聡、久保田俊郎、山口朗:Interferon-gammaはWntシグナル経路を介して骨芽細胞の分化を制御する．第26回日本骨代謝学会学術集会、大阪、2008年10月30日
11. 井上宏隆、山口朗、高柳広:骨石灰化に関与する骨基質タンパク質の新規探索法．第26回日本骨代謝学会学術集会、大阪、2008年10月30日

12. 外部資金の獲得状況

（科学研究費補助金、受託研究費、外部財団の助成など）

1. 科学研究費補助金基盤研究（A）
   研究課題:骨再生過程における細胞・分子間クロストークの解析
   研究代表者:山口　朗
   期間:平成19年―平成21年3月
   研究費総額:3820万円
2. 内藤記念科学振興財団研究助成金
   研究課題:骨芽細胞分化と骨再生の分子機構
   研究代表者:山口　朗
   期間:平成20年
   研究費総額:150万円
3. 奨学寄付金
   代表者:山口　朗
   期間:平成20年
   総額:200万円

13. 特別講演、招待講演

1. Yamaguchi A: Regulation of osteoblast differentiation by BMP and Notch signaling. 2008 International Osteoporosis Expert Meeting, Incheon, Korea , February 16, 2008（invited speaker）
2. 山口　朗:骨再生研究の現状と将来．日本歯科放射線学会第49回学術大会、名古屋国際会議場（招待講演）、2008年5月18日
3. Yamaguchi A: Molecular mechanism of bone formation and regeneration. 12th International Congress on Oral Cancer in conjunction with 24th International College for Maxillo-Facial Surgery. Shanghai, China, May 23, 2008（plenary talk, invited）
4. Yamaguchi A: Role of BMP and Notch signaling in osteoblast differentiation and bone regeneration. 5th Meeting of Bone Biology Forum, Gotenba, Shizuoka, August 23, 2008（invited speaker）
5. 山口　朗:骨再生の分子メカニズムの解析とその応

用．第22回日本創外固定・骨延長学会（教育講演）、
京都、2009年3月6日

14. 講座の准教授、講師、助教、特別研究員、ポスドク、指導を受けた大学院生の名前（AISSには○印）のリスト

特任准教授　飯村（GCOEシャペロン教官）
講　　師　勝部憲一
助　　教　坂本　啓
特任助教　玉村　禎宏

指導を受けた大学院生
○ 栢森　高（4年）
○中西正一（4年）
曹　雷（3年）
○ 新垣理宣（顎顔面外科学）（3年）
梅原康佑（部分床義歯学）（2年）
木原　翼（顎顔面外科学）（2年）
市川紗如（修士2年）
寺地真由（歯周病学）（1年）
姫野彰子（歯周病学）（1年）
松本　力（顎顔面矯正学）（1年）

指導を受けた大学院特別研究学生
門内一郎（自治医科大学整形外科）（4年）

Biochemical and Biophysical Research Communications 378 (2009) 600–604

Contents lists available at ScienceDirect

Biochemical and Biophysical Research Communications

journal homepage: www.elsevier.com/locate/ybbrc

Latexin is involved in bone morphogenetic protein-2-induced chondrocyte differentiation

Ichiro Kadouchi [a,b], Kei Sakamoto [b], Liu Tangjiao [b,c], Takashi Murakami [d], Eiji Kobayashi [d], Yuichi Hoshino [a], Akira Yamaguchi [b,e,*]

[a] Department of Orthopedic Surgery, Jichi Medical University, Shimotsuke, Tochigi, Japan
[b] Section of Oral Pathology, Department of Oral Restitution, Graduate School of Tokyo Medical and Dental University, Bunkyo-ku, Tokyo 113-8549, Japan
[c] Section of Oral Pathology, College of Stomatology, Dalian Medical University, Dalian, China
[d] Division of Organ Replacement Research, Center for Molecular Medicine, Jichi Medical University, Shimotsuke, Tochigi, Japan
[e] Global Center of Excellence Program, International Research Center for Molecular Science in Tooth and Bone Diseases, Graduate School of Tokyo Medical and Dental University, Bunkyo-ku, Tokyo 113-8549, Japan

ARTICLE INFO

Article history:
Received 17 November 2008
Available online 4 December 2008

Keywords:
Latexin
BMP-2
Chondrocyte
Bone regeneration
Cartilage
Bone fracture

ABSTRACT

Latexin is the only known carboxypeptidase A inhibitor in mammals. We previously demonstrated that BMP-2 significantly induced *latexin* expression in Runx2-deficient mesenchymal cells (RD-C6 cells), during chondrocyte and osteoblast differentiation. In this study, we investigated latexin expression in the skeleton and its role in chondrocyte differentiation. Immunohistochemical studies revealed that proliferating and prehypertrophic chondrocytes expressed latexin during skeletogenesis and bone fracture repair. In the early phase of bone fracture, *latexin* mRNA expression was dramatically upregulated. BMP-2 upregulated the expression of the mRNAs of *latexin*, *Col2a1*, and the gene encoding aggrecan (*Agc1*) in a micromass culture of C3H10T1/2 cells. Overexpression of *latexin* additively stimulated the BMP-2-induced expression of the mRNAs of *Col2a*, *Agc1*, and *Col10a1*. BMP-2 treatment upregulated *Sox9* expression, and *Sox9* stimulated the promoter activity of *latexin*. These results indicate that latexin is involved in BMP-2-induced chondrocyte differentiation and plays an important role in skeletogenesis and skeletal regeneration.

© 2008 Elsevier Inc. All rights reserved.

Chondrocytes and osteoblasts originate from common progenitors called mesenchymal stem cells [1]. During the differentiation of these cells, bone morphogenetic proteins (BMPs) play a crucial role in inducing the expression of lineage-specific transcription factors such as Runx2 [1–3] and Sox9 [4,5]; Runx2 is an essential transcription factor that regulates osteoblast differentiation [1,6,7] and chondrocyte maturation [8], and Sox9 is an important transcription factor that regulates chondrocyte differentiation from mesenchymal stem cells [5,9].

We established a clonal cell line, RD-C6, from *Runx2*-deficient mouse embryos and demonstrated that this cell line could differentiate into both osteoblasts and chondrocytes in response to BMP-2 treatment via a Runx2-independent pathway [10]. By microarray analysis of this cell line with and without BMP-2 treatment, we identified latexin as a downstream factor of BMP-2 signaling [10]. This implied that latexin expression was regulated by BMP-2 signaling via a Runx2-independent pathway.

Latexin is composed of 222 amino acids and has a molecular weight of 29 kDa; further, it is the only known carboxypeptidase A inhibitor in mammals [11,12]. The latexin was discovered in the lateral neocortex of rats, and it acts as a marker of regionality and development of both the central and the peripheral nervous systems [11]. Further, *latexin* is expressed in several other tissues, including hematopoietic and lymphoid organs, and plays an important role in regulating the activity of hematopoietic stem cells [12,13]. By microarray analysis, Balint et al. [14] briefly mentioned that *latexin* was one of the upregulated genes in BMP-2-treated C2C12 cells. This suggests a possible role of latexin in osteoblast differentiation, because C2C12 cells exclusively differentiated into osteoblasts and not into chondrocytes by BMP-2 treatment [15]. In addition, we demonstrated that BMP-2 induced RD-C6 cells to differentiate into both osteoblast and chondrocyte lineage cells [10]. However, it remained unclear whether latexin is involved in osteogenic differentiation, chondrogenic differentiation, or both.

To investigate the role of latexin in skeletal cell differentiation, we first investigated latexin expression during skeletogenesis and skeletal regeneration and examined its role in chondrocyte differentiation by using a multipotent mesenchymal cell line, C3H10T1/2. Here, we describe that latexin is expressed in chondrocytes and involved in BMP-2-induced chondrocyte differentiation.

* Corresponding author. Address: Section of Oral Pathology, Department of Oral Restitution, Graduate School of Tokyo Medical and Dental University, Bunkyo-ku, Tokyo 113-8549, Japan. Fax: +81 3 5803 0188.
E-mail address: akira.mpa@tmd.ac.jp (A. Yamaguchi).

0006-291X/$ - see front matter © 2008 Elsevier Inc. All rights reserved.
doi:10.1016/j.bbrc.2008.11.111

Materials and methods

Immunohistochemistry. Immunohistochemical staining was performed on 4% paraformaldehyde-fixed, ethylenediaminetetraacetic acid (EDTA)-decalcified, and paraffin-embedded sections. Endogenous peroxidase activity was blocked with 10% hydrogen peroxidase/methanol, and nonspecific binding was blocked with 10% horse serum. The sections were incubated with goat anti-latexin (Everest Biotech, Oxfordshire, UK) or rabbit anti-Sox9 (Santa Cruz Biotechnology Inc., Santa Cruz, CA) overnight at 4 °C. After washing, they were incubated with horseradish peroxidase-conjugated secondary antibodies (Dako, Glostrup, Denmark). The antigen-bound peroxidase activity was visualized by staining the sections with 3-amino-9-ethyl-carbazole (AEC) chromogen.

Fracture model. The midshafts of the tibiae of 8-week-old mice were fractured using a bone saw and internally stabilized with an intramedullary nail by using the inner pin of a spinal needle with 22-G diameter. The mice were sacrificed and submitted for histological and real-time reverse-transcriptase polymerase chain reaction (RT-PCR) analyses on 5, 10, and 15 days after the operation. All animal studies were approved by the Animal Ethics Committee of Jichi Medical University and performed in accordance with the Jichi Medical University Guide for the Care and Use of Laboratory Animals, following the principles of laboratory animal care formulated by the National Society for Medical Research.

Cell culture. C3H10T1/2 (clone 8) cells were purchased from Cell Bank, RIKEN BioResource Center (Tsukuba, Japan). The cells were maintained in Eagle's basal medium containing 10% fetal bovine serum (FBS; Sigma, St. Louis, MO), 1-glutamine, 50 U/ml penicillin G, and 50 mg/ml streptomycin. For a micromass culture, the C3H10T1/2 cells were suspended in the medium at a concentration of 1×10^7 cells/ml, and a 10-μl drop of this cell suspension was placed in the center of a culture dish. The cells were allowed to adhere for 3 h, and a medium with or without recombinant human BMP-2 (rhBMP-2; 100 ng/ml; Astellas Pharma Inc., Tokyo, Japan) was added to the culture. The cells were stained with Alcian blue solution (pH 2.5) on days 2 and 4 *in vitro*.

Mouse cDNA containing *latexin* open reading frame was obtained by PCR and subcloned into pMSCV (Clontech, CA). Retrovirus was produced and cells were infected with the retrovirus according to the manufacturer's instructions. After infection, the cells were selected in a puromycin-containing medium for 2 weeks.

Western blot analysis. The cells were lysed with radioimmunoprecipitation assay (RIPA) buffer containing protease inhibitor cocktail (Roche Diagnostics, Basel, Switzerland). Western blot analysis was performed according to the standard procedure. SDS–polyacrylamide gel electrophoresis (PAGE) was performed using 1× sample buffer containing 5% β-mercaptoethanol. The proteins were transferred to nitrocellulose membranes, which were then incubated with the following primary antibodies for 1 h: goat anti-latexin, rabbit anti-Sox9, and anti-actin (SC-1616; Santa Cruz Biotechnology Inc.). Next, the membranes were incubated with the respective secondary antibodies for 1 h. Chemiluminescence was detected with an enhanced chemiluminescence (ECL) Plus chemiluminescence detection kit (GE Healthcare, UK).

Real-time RT-PCR. Total RNA was extracted from the cultured cells using RNA Smart Total RNA Isolation Kit (Macherey-Nagel GmbH & Co. KG, Düren, Germany). RNA aliquots of 500 ng were reverse transcribed to cDNA by using a First-Strand cDNA synthesis kit for RT-PCR (Invitrogen Corp., Carlsbad, CA) and an oligo-dT primer. mRNA expression was quantified by real-time RT-PCR, using a MiniOpticon system (Bio-Rad Laboratories, Hercules, CA) with the iQ SYBR Green supermix (Bio-Rad Laboratories). Relative amount of each mRNA was normalized to 18 S rRNA expression. The primer sequences are listed in Table 1.

Table 1
Primers used for real-time-based RT-PCR.

	Forward primer	Reverse primer
Lxn	5′- GTCGCCTGCGGTTATGTAAT	5′- GGCGGCTGTTGTGTTTTACT
Col2a1	5′-TGCACGAAACACACTGGTAAG	5′- CACCAAATTCCTGTTCAGCC
Agc1	5′- AGGAGACCCAGACAGCAGAA	5′-ACAGTGACCCTGGAACTTGG
Col10a1	5′-TGGGTAGGCCTGTATAAAGAACGG	5′-CATGGGAGCCACTAGGAATCC TGAGA
Sox9	5′- CTCGCAATACGACTACGCT	5′-CTGGTTGTTCCCAGTGCT
18S rRNA	5′-GTAACCCGTTGAACCCCATT	5′-CCATCCAATCGGTAGTAGCG

Luciferase activity assay. The proximal promoter region of human *latexin* was obtained from a bacterial artificial chromosome (BAC) clone, RP11-bA39F4, by PCR, and the product was cloned into pGL3-basic (latexin-luc; Promega, Madison, WI). The latexin-luc plasmid was transfected into C3H10T1/2 cells, using Lipofectamine 2000 (Invitrogen) according to the manufacturer's instructions. The amount of latexin-luc plasmid was 0.5 μg in every experiment. Luciferase activity was measured 48 hours after the transfection by using a luciferase assay kit (Promega) according to the manufacturer's instructions.

Statistics. Statistical analyses were performed using Student's unpaired *t*-test. Each experiment was conducted at least twice. The data presented represent means ± standard deviation (SD) of independent replicates ($n > 3$).

Results

Some chondrocytes express latexin in embryonic skeleton and regenerative bone

We first investigated latexin expression during skeletogenesis in embryonic mice and skeletal regeneration in adult mice by immunohistochemistry. Latexin expression was observed in resting to prehypertrophic chondrocytes but not in hypertrophic chondrocytes in E15.5 embryos (Fig. 1A and B). The distribution of latexin-positive cells was similar to that of Sox9-positive cells (Fig. 1C and D). Some osteoblastic cells at periosteoal region in bone collar showed weak signals for latexin expression (Fig. 1A). The peripheral nerves at perichondral membrane exhibited strong signals of latexin (Fig. 1A).

We next examined latexin expression during bone fracture healing at the tibial diaphyses by immunohistochemistry (Fig. 1E–J). In our experimental model, chondrocytes appeared at the periosteal region around the bone fracture site on day 5 after the injury (Fig. 1E). Immunohistochemical studies revealed that many of these chondrocytes were positive for latexin (Fig. 1F). Interestingly, immunoreactivity was detected in the nuclei as well as the cytoplasm of numerous chondrocytes. Numerous hypertrophic chondrocytes and newly formed trabecular bones were observed on day 10, but only proliferating or prehypertrophic chondrocytes were positive for latexin (Fig. 1G and H). Hypertrophic chondrocytes showed no apparent signals for latexin expression (Fig. 1H). On day 15, the process of new bone formation progressed by replacing the pre-existing cartilage (Fig. 1I), and osteoblasts covering newly formed bone trabeculae showed no apparent signals of latexin (Fig. 1J). The number of latexin-positive cells dramatically decreased on day 15 as compared with those on days 5 and 10. No apparent signals were found in the osteoblastic cells covering the trabecular and cortical bones away from fracture sites.

Real-time RT-PCR analysis confirmed that *latexin* expression was undetectable before the injury; however, its expression dramatically increased on day 5 after the injury and then gradually declined on days 10 and 15 (Fig. 1K).

These results indicate that latexin is expressed in chondrogenic cells during skeletogenesis in mouse embryos, and its expression is

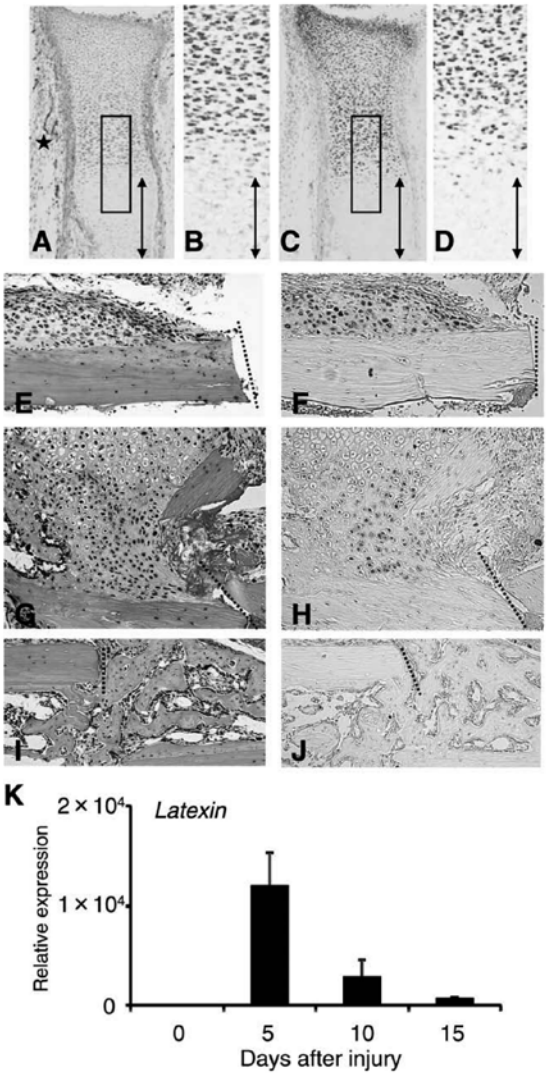

Fig. 1. Chondrocytes express latexin expression in the embryonic tibiae (A,B) and during skeletal regeneration in adult mice (F, H, and J). (A,B) Immunohistochemical staining of latexin in the tibia of an E15.5 mouse embryo. A higher magnification image of the square in A is shown in B. (C,D) Immunohistochemical staining of Sox9 in the tibia of an E15.5 mouse embryo. A higher magnification image of the square in C is shown in D. Arrows in A, B, C, and D indicate hypertrophic chondrocytes zones. An asterisk in A shows latexin-positive peripheral nerves. (E, G, and I) Hematoxylin–eosin staining images of fracture repair on days 5 (E), 10 (G) and 15 (I) after injury in tibiae of adult mice. (F, H, and J) Immunohistochemical staining of latexin during fracture repair. Note that latexin-positive chondrocytes in F and H. Hypertrophic chondrocytes in H and osteoblasts covering newly formed bone trabeculae exhibit few signals for latexin. Dotted lines in E–J indicate fracture end of cortical bones. (K) *Latexin* mRNA expression during fracture repair assessed by real-time RT-PCR as described in Materials and methods.

limited to the chondrocytes appearing during fracture repair in adult mice.

BMP-2 induces latexin expression in C3H10T1/2 cells along with chondrocyte differentiation

To investigate the role of latexin in chondrocyte differentiation, we used a micromass culture of C3H10T1/2 cells. The cultured cells produced Alcian blue-positive extracellular matrix on day 2, the amount of which increased on day 4 in the culture (Fig. 2A). BMP-2 treatment increased the production of Alcian blue-positive extracellular matrix on days 2 and 4 as compared with the respective control cultures (Fig. 2A). The treatment significantly increased the *in vitro* expression of the mRNA for *Col2a1* and *aggrecan* (*Agc1*), which encode the major components of extracellular matrices synthesized by chondrocytes, on days 2 and 4 (Fig. 2B). These results indicate that C3H10T1/2 cells maintained in a micromass culture differentiate into chondrogenic cells in response to BMP-2. We next investigated *latexin* expression in C3H10T1/2 cells cultured in this system by real-time RT-PCR and Western blot analysis. BMP-2 upregulated the latexin expression on days 2 and 4 at the mRNA and protein levels (Fig. 2C and D). These results suggest that BMP-2 induces latexin expression along with chondrocyte differentiation.

Overexpression of latexin stimulates BMP-2-induced chondrocyte differentiation

We overexpressed mouse *latexin* gene in C3H10T1/2 cells by infecting the cells with a retrovirus. The infected cells were cultured with and without rhBMP-2 for 2 days. The cells overexpressing *latexin* induced no changes in the expression of the mRNAs of *Col2a1*, *Agc1*, and *Col10a1* in the absence of BMP-2, compared with the control culture (Fig. 3). In contrast, the cells overexpressing *latexin* significantly increased the expression of the abovementioned mRNAs in the presence of BMP-2, as compared with the BMP-2-treated cells transduced with green fluorescent protein (GFP) (Fig. 3). These results suggest that latexin additively stimulates BMP-2-induced chondrocyte differentiation.

Sox9 stimulates the promoter activity of latexin

BMP-2 induced *latexin* expression in RD-C6 cells, Runx2-deficient cell line, as well as in C3H10T1/2 cells. These results prompted us to investigate whether BMP-2 directly stimulated the promoter activity of *latexin*, and we found that BMP-2 treatment induced no apparent stimulation of the promoter activity of *latexin* at concentrations of 100 and 500 ng/ml (data not shown). It has been reported that BMP-2 efficiently induces *Sox9* expression along with chondrogenic differentiation [4,5], and we also confirmed BMP-2-induced upregulation of *Sox9* mRNA expression in C3H10T1/2 cells on day 2 (Fig. 4A). Therefore, we investigated whether *Sox9* regulates the promoter activity of *latexin*. As shown in Fig. 4B, Sox9 stimulated the promoter activity of *latexin*. These findings suggest that BMP-2-induced Sox9 regulates *latexin* expression in chondrogenic differentiation.

Discussion

Latexin is expressed in various tissues, including brain tissues and hematopoietic and lymphoid organs [11–13,16,17], but its expression and function in skeletal tissues have not been reported in detail. We previously identified *latexin* as a downstream factor of BMP signaling by a microarray analysis of RD-C6 cells, a Runx2-deficient cell line, with and without BMP-2 treatment [10]. Since BMP-2 treatment induced RD-C6 cells to differentiate into both osteoblasts and chondrocytes [10], we first investigated latexin expression during skeletogenesis and skeletal regeneration to identify the skeletal cells that express latexin *in vivo* by immunohistochemistry. This study revealed that the proliferating and pre-hypertrophic chondrocytes in the embryonic tibiae and callus appearing during skeletal regeneration in adult mice expressed latexin. Real-time RT-PCR analysis also indicated the great induction

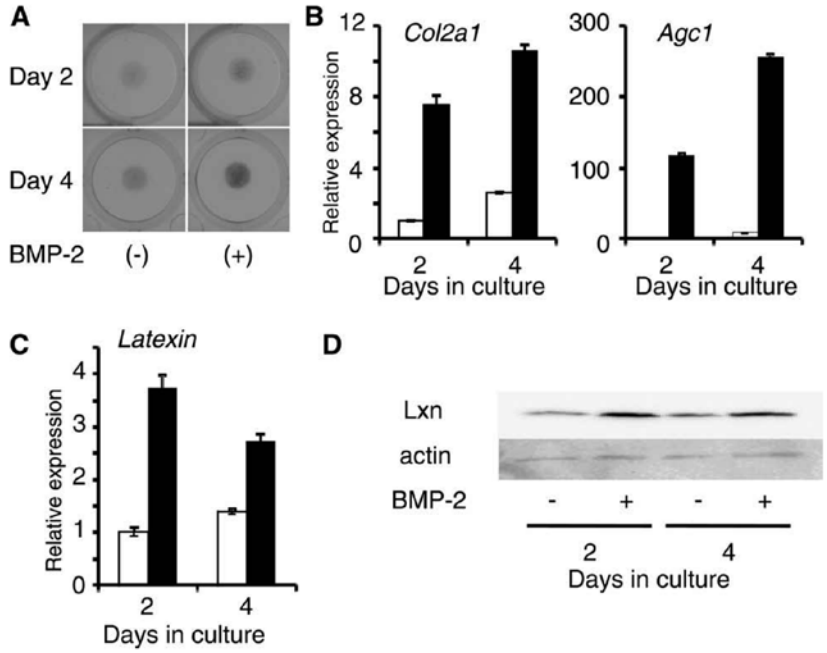

Fig. 2. BMP-2 stimulated the expression of *latexin* mRNA in a micromass culture of C3H10T1/2 cells along with chondrocyte differentiation. (A) Alcian blue staining of C3H10T1/2 cells cultured with and without BMP-2 (100 ng/ml) for 2 and 4 days. (B) Effects of BMP-2 on mRNA expression for *Col2a1* and *Agc1*. C3H10T1/2 cells were cultured for 2 and 4 days in the absence (open bars) and presence (closed bars) of BMP-2, and the expression of the abovementioned mRNAs was determined by real-time RT-PCR. (C) Effects of BMP-2 on the expression of *latexin* mRNA. C3H10T1/2 cells were cultured for 2 and 4 days in the absence (open bars) and presence (closed bars) of BMP-2. (D) Effects of BMP-2 on latexin expression. C3H10T1/2 cells were cultured for 2 and 4 days in the absence and presence of BMP-2, and latexin expression was examined by Western blot analysis as described in Materials and methods.

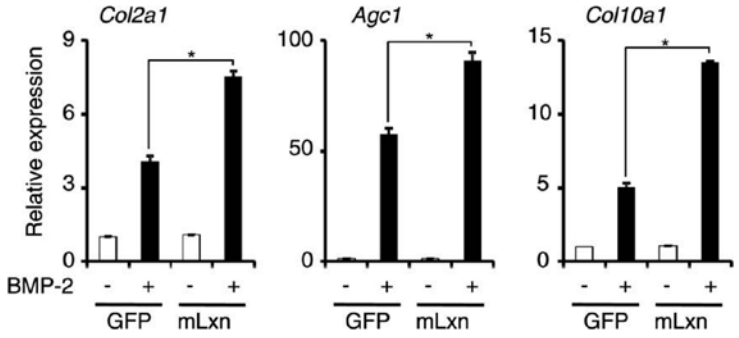

Fig. 3. Overexpression of latexin stimulated BMP-2-induced chondrocyte differentiation in a micromass culture of C3H10T1/2 cells. The cells were cultured for 2 days with and without BMP-2 (100 ng/ml). The expression of the mRNAs of *Col2a*, *Agc1*, and *Col10a1* were determined by real-time RT-PCR as described in Materials and methods). Relative amount of each mRNA was normalized to 18S rRNA expression. $^{*}P < 0.05$ versus control cells.

of *latexin* mRNA expression in the early phase of skeletal regeneration. Taken together, these results suggest that latexin plays an important role in skeletogenesis and skeletal regeneration.

These immunohistochemical findings prompted us to investigate the role of latexin in chondrocyte differentiation, for which we used a micromass culture of C3H10T1/2 cells. The culture experiments revealed that the expression of *latexin* mRNA correlated with that of other chondrocyte differentiation-related mRNAs such as those of *Col2a1* and *Agc1*. In addition, overexpression of *latexin* additively stimulated BMP-2-induced chondrocyte differentiation. Interestingly, overexpression of latexin induced no significant changes in the expression of the abovementioned mRNAs in the absence of BMP-2, suggesting a close interaction between the regulation of *latexin* expression and BMP signaling. To further investigate the underlying mechanism, we examined the effects of BMP-2 on the activation of *latexin* promoter and found that BMP-2 did not stimulate the promoter. Since it has been reported that BMP-2 induces Sox9 expression [4,5], we examined the effects of *Sox9* on the transactivation of *latexin* promoter and demonstrated that *Sox9* stimulated the promoter activity of *latexin*. These results suggest that latexin is involved in chondrocyte differentiation via Sox9, the expression of which is upregulated by BMP-2. There have been no reports about the regulatory mechanism of *latexin* expression even in neural tissues, and *Sox9* is the first candidate transcription factor that regulates *latexin* expression. However, its *latexin*-transducing activity was not observed to be

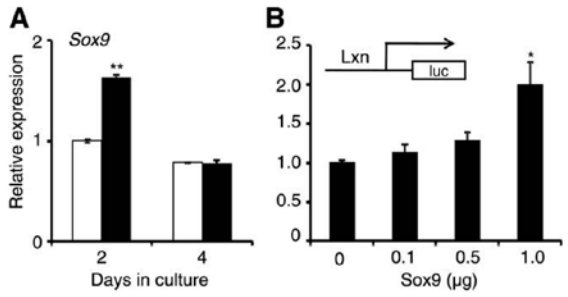

Fig. 4. BMP-2 induced the expression of *Sox9* mRNA in C3H10T1/2 cells, and Sox9 activated the promoter activity of *latexin*. (A) Effects of BMP-2 on the expression of *Sox9* mRNA in C3H10T1/2 cells on day 2, determined by real-time RT-PCR analysis. $^{**}P < 0.0001$ versus control cells. (B) Effect of Sox9 on the promoter activity of *latexin*. Data represent the fold inductions relative to the induction by mock vector transfection. $^{*}P < 0.05$ versus control cells.

strong. These findings suggest that activation of *latexin* transcription requires other transcription factors or coactivators of Sox9 such as Sox5, Sox6, and cAMP response element binding (CREB)-binding protein (CBP)/p300 [18–21].

Latexin is the only known endogenous carboxypeptidase A inhibitor in mammals [12]. It is structurally composed of two nearly identical domains that have a high conformational homology with the cystatins [22]. *Latexin* has the potential heparin/heparan sulfate-binding sites and directly interacts with a heparin component in a mast cell culture [22,16]. Heparan sulfate is an important component of the extracellular matrix of cartilage and essential for chondrocyte differentiation [23,24]. This suggests an interaction between latexin and heparan sulfate during extracellular matrix synthesis in cartilage. Our immunohistochemical study revealed the nuclear localization of latexin in chondrocytes appearing during fracture repair. It will be interesting to investigate the interaction between latexin and heparan sulfate in the nuclei, because some reports have indicated the nuclear localization of heparin sulfate [25].

In the present study, we demonstrated that latexin is expressed in chondrocytes during skeletogenesis and skeletal regeneration. *Latexin*-deficient mice, which were provided by Dr. Arimitsu [26], exhibited no growth retardation or apparent radiographic changes in the skeleton (unpublished results), suggesting the limited changes in the skeletal tissues of the mice. Since the present study revealed the dramatic upregulation of *latexin* mRNA expression in the early phase of fracture repair, it will be interesting to investigate the process of fracture repair in *latexin*-deficient mice. Such studies are currently being conducted by our group. The findings of these studies will provide important information regarding the role of latexin in skeletal growth and regeneration.

Acknowledgments

This work was supported by the Research Award to Jichii Medical University Graduate Student (I.K.) and a Grant-in-Aid for Scientific Research from the Japan Society for the Promotion of Science (A.Y.).

References

[1] A. Yamaguchi, T. Komori, T. Suda, Regulation of osteoblast differentiation mediated by bone morphogenetic proteins, hedgehogs, and Cbfa1, Endocr. Rev. 21 (2000) 393–411.
[2] K.S. Lee, H.J. Kim, Q.L. Li, X.Z. Chi, C. Ueta, T. Komori, J.M. Wozney, E.G. Kim, J.Y. Choi, H.M. Ryoo, S.C. Bae, Runx2 is a common target of transforming growth factor beta1 and bone morphogenetic protein 2, and cooperation between Runx2 and Smad5 induces osteoblast-specific gene expression in the pluripotent mesenchymal precursor cell line C2C12, Mol. Cell. Biol. 20 (2000) 8783–8792.
[3] M.H. Lee, Y.J. Kim, H.J. Kim, H.D. Park, A.R. Kang, H.M. Kyung, J.H. Sung, J.M. Wozney, H.M. Ryoo, BMP-2-induced Runx2 expression is mediated by Dlx5, and TGF-beta 1 opposes the BMP-2-induced osteoblast differentiation by suppression of Dlx5 expression, J. Biol. Chem. 278 (2003) 34387–34394.
[4] B.K. Zehentner, C. Dony, H. Burtscher, The transcription factor Sox9 is involved in BMP-2 signaling, J. Bone Miner. Res. 14 (1999) 1734–1741.
[5] M.B. Goldring, K. Tsuchimochi, K. Ijiri, The control of chondrogenesis, J. Cell Biochem. 97 (2006) 33–44.
[6] T. Komori, H. Yagi, S. Nomura, A. Yamaguchi, K. Sasaki, K. Deguchi, Y. Shimizu, R.T. Bronson, Y.H. Gao, M. Inada, M. Sato, R. Okamoto, Y. Kitamura, S. Yoshiki, T. Kishimoto, Targeted disruption of Cbfa1 results in a complete lack of bone formation owing to maturational arrest of osteoblasts, Cell 89 (1997) 755–764.
[7] P. Ducy, R. Zhang, V. Geoffroy, A.L. Ridall, G. Karsenty, Osf2/Cbfa1: a transcriptional activator of osteoblast differentiation, Cell 89 (1997) 747–754.
[8] C.A. Yoshida, T. Furuichi, T. Fujita, R. Fukuyama, N. Kanatani, S. Kobayashi, M. Satake, K. Takada, T. Komori, Core-binding factor beta interacts with Runx2 and is required for skeletal development, Nat. Genet. 32 (2002) 633–638.
[9] H. Akiyama, Control of chondrogenesis by the transcription factor Sox9, Mod. Rheumatol. 18 (2008) 213–219.
[10] T. Liu, Y. Gao, K. Sakamoto, T. Minamizato, K. Furukawa, T. Tsukazaki, Y. Shibata, K. Bessho, T. Komori, A. Yamaguchi, BMP-2 promotes differentiation of osteoblasts and chondroblasts in Runx2-deficient cell lines, J. Cell Physiol. 211 (2007) 728–735.
[11] Y. Arimatsu, Latexin: a molecular marker for regional specification in the neocortex, Neurosci. Res. 20 (1994) 131–135.
[12] Y. Liang, G. Van Zant, Aging stem cells, latexin, and longevity, Exp. Cell. Res. 314 (2008) 1962–1972.
[13] Y. Liang, M. Jansen, B. Aronow, H. Geiger, G. Van Zant, The quantitative trait gene latexin influences the size of the hematopoietic stem cell population in mice, Nat. Genet. 39 (2007) 178–188.
[14] E. Balint, D. Lapointe, H. Drissi, C. van der Meijden, D.W. Young, A.J. van Wijnen, J.L. Stein, G.S. Stein, J.B. Lian, Phenotype discovery by gene expression profiling: mapping of biological processes linked to BMP-2-mediated osteoblast differentiation, J. Cell Biochem. 89 (2003) 401–426.
[15] T. Katagiri, A. Yamaguchi, M. Komaki, E. Abe, N. Takahashi, T. Ikeda, V. Rosen, J.M. Wozney, A. Fujisawa-Sehara, T. Suda, Bone morphogenetic protein-2 converts the differentiation pathway of C2C12 myoblasts into the osteoblast lineage, J. Cell Biol. 127 (1994) 1755–1766.
[16] Y. Uratani, K. Takiguchi-Hayashi, N. Miyasaka, M. Sato, M. Jin, Y. Arimatsu, Latexin, a carboxypeptidase A inhibitor, is expressed in rat peritoneal mast cells and is associated with granular structures distinct from secretory granules and lysosomes, Biochem. J. 346 (Pt 3) (2000) 817–826.
[17] Y. Hatanaka, Y. Uratani, K. Takiguchi-Hayashi, A. Omori, K. Sato, M. Miyamoto, Y. Arimatsu, Intracortical regionality represented by specific transcription for a novel protein, latexin, Eur. J. Neurosci. 6 (1994) 973–982.
[18] H. Akiyama, M.C. Chaboissier, J.F. Martin, A. Schedl, B. de Crombrugghe, The transcription factor Sox9 has essential roles in successive steps of the chondrocyte differentiation pathway and is required for expression of Sox5 and Sox6, Genes Dev. 16 (2002) 2813–2828.
[19] T. Furumatsu, M. Tsuda, K. Yoshida, N. Taniguchi, T. Ito, M. Hashimoto, H. Asahara, Sox9 and p300 cooperatively regulate chromatin-mediated transcription, J. Biol. Chem. 280 (2005) 35203–35208.
[20] T. Ikeda, S. Kamekura, A. Mabuchi, I. Kou, S. Seki, T. Takato, K. Nakamura, H. Kawaguchi, S. Ikegawa, U.I. Chung, The combination of SOX5, SOX6, and SOX9 (the SOX trio) provides signals sufficient for induction of permanent cartilage, Arthritis. Rheum. 50 (2004) 3561–3573.
[21] Y. Han, V. Lefebvre, L-Sox5 and Sox6 drive expression of the aggrecan gene in cartilage by securing binding of Sox9 to a far-upstream enhancer, Mol. Cell. Biol. 28 (2008) 4999–5013.
[22] A. Aagaard, P. Listwan, N. Cowieson, T. Huber, T. Ravasi, C.A. Wells, J.U. Flanagan, S. Kellie, D.A. Hume, B. Kobe, J.L. Martin, An inflammatory role for the mammalian carboxypeptidase inhibitor latexin: relationship to cystatins and the tumor suppressor TIG1, Structure 13 (2005) 309–317.
[23] E. Arikawa-Hirasawa, H. Watanabe, H. Takami, J.R. Hassell, Y. Yamada, Perlecan is essential for cartilage and cephalic development, Nat. Genet. 23 (1999) 354–358.
[24] H.P. Sørensen, R.R. Vivès, C. Manetopoulos, R. Albrechtsen, M.C. Lydolph, J. Jacobsen, J.R. Couchman, U.M. Wewer, Heparan Sulfate Regulates ADAM12 through a molecular switch mechanism, J. Biol. Chem. 283 (2008) 31920–31932.
[25] M. Kobayashi, Y. Naomoto, T. Nobuhisa, T. Okawa, M. Takaoka, Y. Shirakawa, T. Yamatsuji, J. Matsuoka, T. Mizushima, H. Matsuura, M. Nakajima, H. Nakagawa, A. Rustgi, N. Tanaka, Heparanase regulates esophageal keratinocyte differentiation through nuclear translocation and heparan sulfate cleavage, Differentiation 74 (2006) 235–243.
[26] M. Jin, M. Ishida, Y. Katoh-Fukui, R. Tsuchiya, T. Higashinakagawa, S. Ikegami, Y. Arimatsu, Reduced pain sensitivity in mice lacking latexin, An inhibitor of metallocarboxypeptidases, Brain Res. 1075 (2006) 117–121.

MEMO

顎顔面矯正学分野

森山 啓司

医歯学総合研究科・顎顔面頚部機能再構築学系専攻
顎顔面矯正学・教授

1. 研究の課題名

①頭蓋早期癒合症のモデルマウスの解析と可溶型FGFR2の効果

Analysis of a model mouse of craniosynostosis and the effect of soluble FGFR2

Apert syndromeの発症の原因はFibroblast Growth Factor 2（FGFR2）の細胞外ドメインであるIg ⅡとIg Ⅲの結合領域におけるS252WおよびP253Rの変異であるとされているが、この疾患の発症の分子細胞メカニズムには不明な点が多く残されている。そこでFGFR2 IIIc S252Wを受精卵に遺伝子導入したtransgenic mouse（SW06）と、FGFR2 IIIc S252Wから細胞内ドメインを欠如する可溶型のコンストラクトを遺伝子導入したtransgenic mouse（SOL05）を作成し解析を行った。SW06の頭蓋冠由来のマウスの細胞は、アリザリンレッド染色で強染され、アルカリフォスファターゼ活性も亢進した。一方、SOL05由来の細胞は、アリザリンレッド染色にほとんど染色されずALPも低値であった。この両者を交配して得られたマウスでの頭蓋冠由来のマウスの細胞は、SW06の頭蓋冠由来のマウスの細胞と比較して、アリザリンレッド染色で淡染され、アルカリフォスファターゼ活性も低値を示した。SOL05由来の細胞を解析し、可溶型FGFR2の効果を明らかにすることは、頭蓋冠縫合部早期癒合症を主症状とする先天性疾患であるApert症候群、Crouzon症候群などに対する新しくかつ安全で非侵襲的な治療法の開発につながると期待される。

②マルファン症候群の重篤な歯周炎に関する分子機構

Molecular mechanism of severe periodontitis in Marfan syndrome

弾性線維の主要構成タンパクfibrillin-1をコードするFBN1遺伝子は、心血管（大動脈乖離や拡張）、骨格（高身長）、目（水晶体脱臼）などを主徴とする1型Marfan症候群の責任遺伝子である。この疾患ではさらに重篤な歯周疾患に罹患することが知られているが、その発症機構は不明である。そこでFbn1を遺伝子改変したhypomorphic mice（Mg Δ）に実験的に歯周疾患を誘発した。fibrillin-1の発現が58%に低下する6週齢雄Mg Δマウスヘテロ接合子（Mg Δ /+; n=6）と野生型マウス（WT; n=6）に、7日間抗生剤投与後、P.gingivalisを上顎頬側歯肉に2日毎計3回播種した。対照群では、抗生剤投与後、Mg Δ /+（n=6）とWT（n=6）の上顎頬側歯肉にPBSを塗布した。8週後、上顎臼歯のセメントエナメル境と歯槽骨縁間の距離（CEJ-ABC）と面積（AM）をμCT（Shimadzu社製 InspeXio SMX）により計測した。P.gingivalisの播種は、Mg Δ /+とWTのCEJ-ABCとAMを、各々の対照群と比較して有意に増加させた。興味深いことにWTと比較してMg Δ /+では、有意に大きなCEJ-ABCとAMの増加をみた。一方、対照群では、両者間でCEJ-ABCとAMに差はなかった。野生型fibrillin-1の正常な発現が、細菌感染に対する歯槽骨の恒常性維持に重要と考えられた。また本実験モデルは、Marfan症候群における歯周疾患重篤化のメカニズム解明や治療法開発にあたり有用な系と期待される。

③歯の再生に向けたヒト遺伝子解析

Gene analysis for human tooth regeneration

現在、歯科において歯の再生が待ち望まれている。歯の喪失や欠損が多数歯は、咀嚼、発音、摂食といった口腔機能に重大な障害を引き起こし、患者のQOLに深刻な影響を与える。 そこで本課題では、6本以上の多数歯欠損が家族性にみられ、非症候群性に発症するケースの遺伝子解析を行ってきた。そこで昨年度は、日本人とモンゴル人の家族性先天性多数歯欠損患者15名の資

料収集を行い、提供されたDNA試料から遺伝子解析を行った。これら得られた資（試）料より、PAX9遺伝子のエクソン2に変異を持つ患者1名と、エクソン4に変異を持つ患者1名を発見した。ベータベースよりいずれも報告のない新規変異であり、この変異遺伝子機能を解析中である。MSX1遺伝子のエクソン1下流に11塩基の繰り返し配列が存在する。この領域の機能と歯の発生との関連に興味が持たれ、現在遺伝子機能を解析中である。本計画では、家族性先天性多数歯欠損患の遺伝子解析をメインテーマとしている。昨年度、本課題の遂行を目的として、モンゴル Health Science University of Mongoliaに出張した際、多数の欠損歯を随伴することで知られる無汗性外胚葉異形成症のモンゴル人罹患患者を発見した。本疾患の原因遺伝子であるEDA、EDAR、EDARADDの遺伝子解析を行った結果、EDARADDのdeath domainに新規変異を同定した。現在、患者家族を含めた広範な解析を行っており、変異遺伝子機能の解析も併せて進めている。

④歯根吸収の抑制と歯根の再生

Suppression of tooth root resorption and regeneration of tooth root

エムドゲインはブタ歯胚より抽出され、歯周組織再生を目的として広く歯科臨床で使用されている。最近、エムドゲインの薬理作用として、組織再生だけでなく、歯の再植に伴う歯根の吸収抑制が報告された（Dental Traumatology, 2002）。エムドゲイン中の生理活性物質に関しては、多くの不明な点があるものの、アメロゲニンが注目されている。アメロゲニンはエナメル質の初期発生に重要な因子として知られているが、この遺伝子欠損マウスにはセメント質や歯根象牙質の顕著な吸収像がみられた（J Biol Chem, 2003）。このことは、アメロゲニンが歯根表面で歯根吸収抑制因子として働くことを示唆する。そこで我々は、アメロゲニンの破歯細胞対する作用をin vitroで検討した。(1) ヒト乳歯歯根から酵素処理により単離した細胞を1・25（OH）2Vit.D3存在下で72時間培養し、TRAP陽性破歯細胞様細胞数に対するアメロゲニンの影響を検討した。(2) 硬組織吸収系細胞への分化を検討する目的で、M-CSF存在下、PGE2、PTH、Vit.D3のいずれかの添加によりマウス培養骨髄細胞中に形成されるTRAP陽性多核細胞（TRAP（+）MNC）に対するアメロゲニンの影響を検討した。またこのcell lysateを用いてRANKLのwestern blotを行った。(3) RANKLとM-CSF存在下でマウス骨髄マクロファージより分化するTRAP（+）MNCに対するアメロゲニンの影響を検討した。(1) アメロゲニンは破歯細胞様細胞の数を有意に減少した。(2) アメロゲニンは、骨髄細胞培養系に形成されるTRAP（+）MNC数と、RANKL発現を抑制した。(3) 一方、外因性RANKLとM-CSF存在下でマウス骨髄マクロファージより形成されるTRAP（+）MNC数は、アメロゲニン添加により影響を受けなかった。アメロゲニンは、RANKL発現抑制を介し破歯細胞形成を制御することが示唆された。今後、この因子の歯根吸収抑制に対する薬理作用においに興味が持たれる。

⑤先天異常診断エキスパートシステムのためのバーチャルフェイスの合成

Evaluation of the virtual-face for diagnosis of congenital anomalies

当分野の先天異常診断エキスパートシステムを診断・矯正治療の支援、学生教育などに幅広く活用し、先天異常患者のQOLの向上につながるシステムとする目的で、本システムに個人情報保護対策を取り入れた視覚的な頭蓋顔面情報を取り入れるため、先天異常患者の顔貌の三次元画像情報から、先天異常疾患の特徴を有し、個人として特定できないバーチャルフェイスを作成し、本システムに組み込むことを本研究の目的とした。3Dデジタイザを用いて、先天異常疾患の複数患者の三次元顔データの計測を行い、所定のデータ形式に変換後、顔画像へのワイヤーフレームのフィッティングを行い、三次元先天異常バーチャルフェイスを作成した。今後はバーチャルフェイスの先天異常疾患としての妥当性の評価を行い、アンケート結果集計・解析し、バーチャルフェイスの個人としての異同評価を行い、総合判定とする。先天異常バーチャルフェイスの種類の加増の後、診断エキスパートシステムへのバーチャルフェイスの導入、E-learningへ登用する。

⑥MRI動画法を用いた構音器官運動の動的解析

Motor coordination of articulators depends on the place of articulation

/p/および/k/は両者とも破裂音と呼ばれるが、異なる構音位置（place of articulation）を有する。すなわち、前者は両口唇で発生する両唇音であり、後者は舌後方部と軟口蓋で発生する軟口蓋音である。本研究の目的は、複数の構音器官運動にplace of articulation依存性の関係があるか否かを検証することである。健常者において

MR撮像と同期して両唇音および軟口蓋音を発音させた。撮像にはgradient echoシーケンスを用いた。個々の構音器官運動および相互の時間的関係を解析する目的で基準点を設定し、線計測および角度計測を行った。これらの変数は、place of articulationに依存した変化を示した。さらに、軟口蓋運動は、両唇音においては口唇および舌前方部と、軟口蓋音においては舌後方部とそれぞれ有意な関係を示した。これらの結果から、構音器官運動はplace of articulationに依存して一つの単位として活動が調節されていることが示唆された。本研究結果は、顎顔面領域における先天異常である口唇口蓋裂におけるいわゆる口蓋裂言語と呼ばれる異常構音の解析への応用が期待される。

⑦口唇裂・口蓋裂患者に対する骨延長法の適用

Application of distraction osteogensis in patients with cleft lip and palate

近年、上顎骨の著しい劣成長を呈する口唇裂・口蓋裂患者に対して骨延長法が適用されており、良好な結果を得ている。本法の適用に際して当分野では、以下の臨床および基礎的な多角的見地より検討を行っている。1）延長効率の改善のための装置の改良:頭部に延長装置を固定する創外型骨延長に用いる口腔内装置を強固にすることにより、延長効率を改善した。2）延長に適用する牽引力の測定:延長器の牽引ワイヤーに小型張力計を組み込むことにより、上顎の牽引力を測定し力学的検討を行った結果、最大牽引力はおよそ50ニュートンとなることを明らかにした。3）CTおよび超音波画像診断による術後の骨形成評価:従来、延長術後の骨形成の評価にはCTを用いていたが、X線被曝のない超音波診断も有用であることを確認した。4）延長術前後の硬・軟組織の変化:CTおよび形態計測装置の3次元情報より、延長術による硬・軟組織の変化を明らかにした。5）骨形成促進を目的とする高気圧酸素療法の適用:高気圧酸素療法を骨延長症例に適用し、延長後の骨形成の促進をはかっている。6）18q-症候群の症例における染色体分析と骨延長術の適用:口唇口蓋裂を有する18q-症候群の歯科矯正治療に骨延長法を適用し、顔貌の改善を図った。また、本症例の核型を明らかにするとともに、染色体異常を生じたメカニズムについての仮説を立てた。

⑧歯槽骨延長部への歯の移動に高気圧酸素が与える影響

The effects of hyperbaric oxygen on tooth movement into the distracted area after distraction osteogenesis

骨延長法や、高気圧酸素療法といった新規治療法は医科歯科を問わず幅広い領域で臨床応用されるようになってきた。特に近年顎顔面領域においては口唇口蓋裂患者に適用されるケースも増加してきている。さらに骨延長部への歯の移動も行われるようになってきているが、これらに関する基礎的報告は少ない。本研究では高気圧酸素（HBO）適用下で骨延長領域に歯を移動することによってその歯根周辺の骨形成様相を観察した。10匹のビーグル犬を用い、顎裂を想定した10mmの人為的骨欠損を作成し、その骨欠損部位に向かい1mm/日の割合で10日間骨延長を行い、骨延長終了後第二前臼歯を骨延長部位に向かって牽引した。また、歯槽骨延長終了後、歯の牽引開始と同時に20日間2.5ATAで90分間HBOに曝露した群（HBO群:5匹）と、HBOに曝露しなかった群（対照群:5匹）の2群を設定した。骨切り後150日で屠殺するまでの間、経時的にレントゲン撮影を行い、グレースケールを用いた定量的解析を行った。屠殺後、末梢型コンピュータ断層骨測定装置（pQCT）を用いた骨密度解析、組織切片を用いた骨組織形態計測法による構造計測を行った。また、有意差検定はMann-Whitney U-testを行った。グレースケール解析より、骨延長部ではHBO群において有意な骨化促進を認めた。骨密度解析から新生骨内に移動された遠心根の近心側においてHBO群の骨密度が有意に高かった。また、同部位では骨形態計測からもHBO群では新生骨の骨梁間隙・骨梁数・血管数において有意に高い値を示した。これらはHBO適用下で骨延長部位への歯の移動を行うことにより、新生骨内の牽引側において血管新生が促進された結果と考えられ、移動歯の牽引側では骨形成が促進される可能性が示唆された。

⑨イヌ顎裂モデルを用いた上顎歯槽骨延長術後の歯髄血流量及び硬組織変化の観察

Observation of Pupal Blood Flow and Bone Mineralization after Alveolar Distraction Osteogenesis in a Canine Cleft Model

顎顔面領域の形態異常に対する治療として広く用いられている骨延長術は、口唇口蓋裂患者においても、顎裂閉鎖治療の選択肢の一つとして近年試みられている。しかし、骨延長後の回復には長期間を要すため、より確実で普遍性の高いプロトコールの確立が望まれているが、総骨延長量が回復速度に及ぼす影響を検討した報告はない。本研究は、上顎歯槽部骨延長量と骨延長部位の歯髄血流量及び骨組織の回復との関連を、検討することを目

的とした。ビーグル成犬6 頭を用い、上顎左側に顎裂を想定した10 ㎜の上顎歯槽骨欠損を作製した。治癒期間の後、左側上顎歯槽部に骨切りを行い、犬歯を含む移動骨片を作製し、延長装置を装着した。3日間の待機期間後、骨延長を1日1 mm の延長速度で6日間延長を行った群（3頭:6 mm延長群）、及び同様に10日間延長を行った群（3頭:10 mm延長群）とした。計測及び観察項目は、移動骨片内における犬歯歯髄血流動態の記録、peripheral Quantitative Computed Tomography（ pQCT）による骨密度解析（骨密度、骨塩量、骨面積）、及び骨形態計測法による骨面積、骨梁幅、骨梁数、骨梁間隙の構造計測であった。有意差検定はMann-Whitney U-testを用いた。血流動態において、両群とも骨切り直後は血流値の著しい低下を認めたものの、6 mm延長群では有意に早い回復を示した。pQCTによる骨密度解析では、骨密度、骨塩量、骨面積は6 ㎜延長群で有意に高く、骨形態計測からも、延長部位に新生した骨面積、骨梁幅は6 ㎜延長群で有意に高く、骨梁間隙は有意に低い値を認めた。総骨延長量が新生骨形成や骨延長部周辺組織の回復に影響することが示唆された。

2.

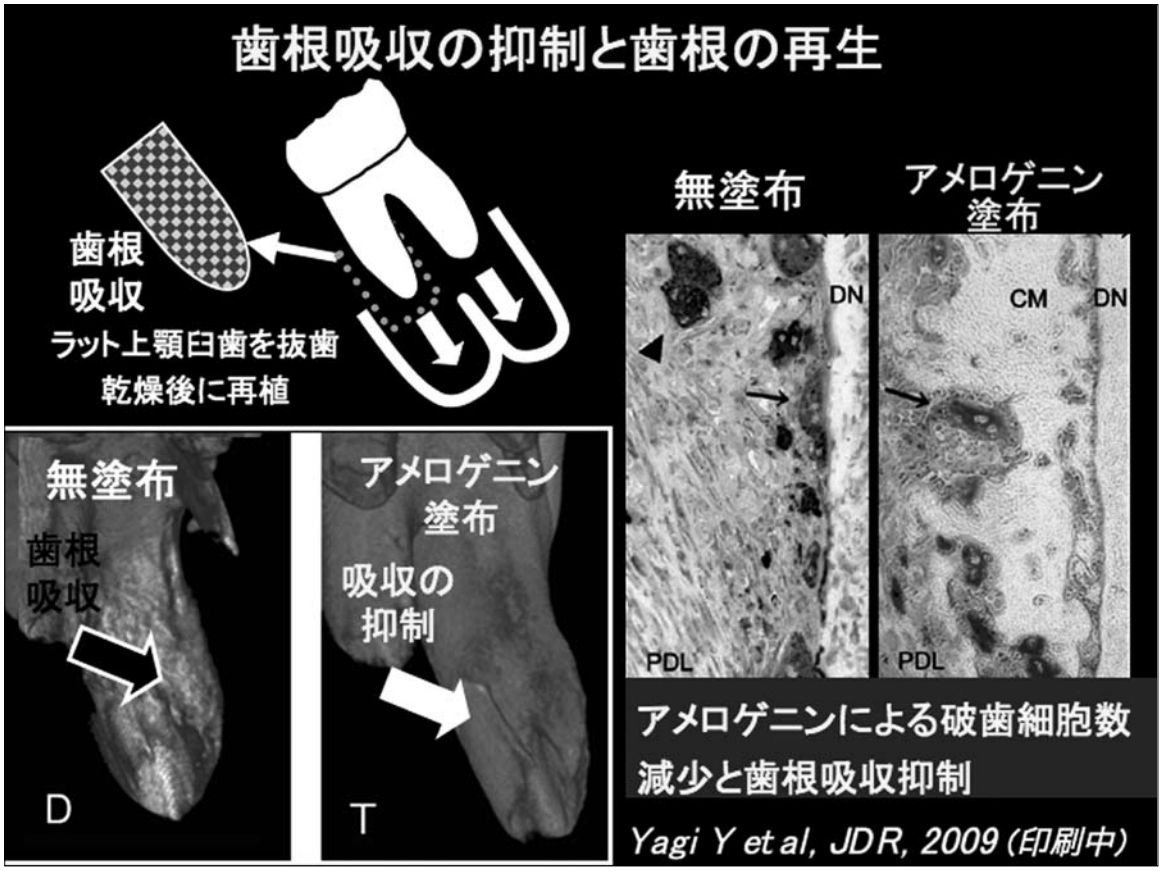

3. 研究内容についての英文要約

①Fibroblast growth factor receptor2 promotes osteogenic differentiation in mesenchymal cells via extracellular-related kinase and protein kinase c signalling.
We investigated the role of Fibroblast Growth Factor Receptor 2 (FGFR2) in osteoblast commitment and differentiation of murine mesenchymal C3H10T1/2 cells stably transfected with wild type (WT) or activated FGFR2 due to Apert S252W genetic mutation (MT). WT FGFR2 slightly whereas MT FGFR2 strongly increased FGFR2 tyrosine phosphorylation, indicating activation of the receptor. WT and MT FGFR2 increased C3H10T1/2 cell proliferation but not survival. Both WT and MT FGFR2 increased early and late osteoblast gene expression and matrix mineralization. Forced expression of WT and MT FGFR2 also increased osteoblast gene expression in MC3T3-E1 calvaria osteoblasts. In both cell types, MT FGFR2 was more effective than WT FGFR2. In contrast, WT and MT FGFR2 decreased adipocyte differentiation of C3H10T1/2 cells. WT and MT FGFR2 induced ERK1/2 but not JNK or PI3K/AKT phosphorylation. MT, but not WT, also increased protein kinase C (PKC) activity. Pharmacological inhibition of ERK1/2 prevented cell proliferation induced by WT and MT FGFR2. Using dominant-negative ERK and PKC vectors, we demonstrated that WT and MT FGFR2 promoted osteoblast gene expression through ERK1/2 and PKC signalling, respectively. This study identifies FGFR2 as a novel regulatory molecule that promotes osteogenic differentiation in murine MSCs.

②Comprehensive gene expression analysis in human periodontal ligaments of the mandibular third molars performing vertical movement and the maxillary second premolars with occlusal contact.
The periodontal ligament (PDL) is thought to be an important tissue in vertical movement during tooth eruption, but the precise molecular mechanism is not known. Thereto, comprehensive gene expression was analyzed in human PDL of mandibular third molars performing vertical movement and maxillary second premolars with occlusal contact. The expression profile of 9,243 genes in the PDL of one subject was compared between vertically moving third molars and second premolars with occlusal contact by DNA microarray. The expression of CALB1 (encoding calbindin 1), CYP26A1 (encoding cytochrome P450, family 26, subfamily A, polypeptide 1), SPOCK3 (encoding testican-3), CCK (encoding cholecystokinin) and SCRG1 (encoding scrapie responsive protein 1) was more than 30-fold higher in PDLs of the third molars than the second premolars. Interestingly, in this study, CALB1 expression showed the largest difference. In contrast, CRCT1 (encoding cysteine-rich C-terminal 1), SPRP3 (encoding small proline-rich protein 3), IL8 (encoding interleukin 8) and MMP12 (encoding matrix metalloproteinase 12) showed more than 100-fold higher expression in PDLs of the second premolars than the third molars. The present comprehensive gene expression in PDLs provides new insights into the molecular mechanism during the vertical tooth movement.

③Characteristic phenotype of immortalized periodontal cells isolated from a Marfan syndrome type I patient.
Marfan syndrome type I (MFS1, MIM #154700) is caused by mutations in FBN1 encoding fibrillin-1, which is a major microfibrillar protein of elastic system fibers. Since little is known about the biological functions of elastic system fibers in the periodontal ligaments (PDLs) and the pathogenesis of the periodontitis in MFS1, PDL cells were isolated from an MFS1 patient with a heterozygous missense mutation in a calcium-binding epidermal-growth-factor-like domain of FBN1. Isolated PDL cells were immortalized by transducing a retrovirus carrying genes for the human Polycomb group protein, Bmi-1, and human telomerase reverse transcriptase. Immortalized PDL cells from the MFS1 patient (termed M-HPL1) and those of a healthy volunteer (termed HPDL2) both expressed various PDL-related genes. The growth and attachment of M-HPL1 and HPDL2 to hydroxyapatite particles were comparable. However, when M-HPL1 were transplanted with hydroxyapatite particles into immunodeficient mice, disorganized cell alignment and irregular microfibril assembly were noted. Thus, M-HPL1 represent a powerful tool for clarifying the biological roles of elastic system fibers in PDL and the pathogenesis of periodontitis in MFS1. Our findings also suggest that FBN1 regulates cell alignment and microfibril assembly in PDLs.

④In Vivo Application of Amelogenin Suppresses Root Resorption
Prevention of pathological tooth root resorption is crucial to maintain normal oral function. Amelogenin was discovered as an enamel protein associated with enamel formation. Besides this well-known function, remarkable root resorption was seen in amelogenin-null mutant mice, raising the hypothesis that it can inhibit root dentin and cementum resorption, in vivo. This hypothesis made us to examine the application of porcine amelogenin in the experimental root resorption model, in which maxillary first molars of rats were extracted and replanted after air drying. Compared with untreated and carrier-treated tooth roots, the application dramatically reduced the odontoclast number on root surfaces and inhibited

the active root resorption. Amelogenin treatment also significantly reduced the number of cultured human odontoclastic cells. All these findings support our hypothesis that in vivo application of amelogenin suppresses odontoclastic root resorption. The present study also anticipates a novel therapeutic target for the prevention of pathological root resorption.

⑤Motor coordination of articulators depends on the place of articulation

Although the sounds /p/ and /k/ are both voiceless plosives, they have different places of articulation: bilabial and velar, respectively. The purpose of this study was to determine the relationship among articulators in plosives with reference to their place of articulation. Ten healthy subjects repeated bilabial and velar plosives in synchronization with magnetic resonance scanning. Each run was measured using a gradient echo sequence. Several linear and angular variables were defined to delineate the individual movements of articulators and to determine the temporal relationships among articulators. These variables showed distinctive changes depending on the place of articulation. In addition, movement of the velum was significantly correlated with that of the lips and the anterior part of the tongue in the bilabial plosive and with the posterior part of the tongue in the velar plosive. We conclude that unitary motor coordination of articulators depends on the place of articulation.

⑥Three-dimensional analysis of lower lip movement during articulation in subjects with mandibular prognathism

The aim of this study was to investigate lower lip movement during articulatory tasks using a three-dimensional video-based system in subjects with mandibular prognathism. Ten subjects with mandibular prognathism (mean age: 25.4 years) and 20 volunteers (mean age: 27.8 years) participated in the study. The target sounds used were five vowels (/a/, /i/, /u/, /e/ and /o/). The motion of black foam balls placed on four canthal points and four lip points was tracked using two video cameras with a three-dimensional analysis system for animated images. After three-dimensional coordinates were established using the canthal points to correct head motion, lip movement was measured with reference to the coordinates. By comparing the standardized trajectories, differences in lower lip movement between subjects and controls were examined. The results showed that (1) the trajectory of lower lip movement in subjects differed to some extent in all vowels and (2) there were significant differences in the amount of lower lip movement between subjects and controls. These results suggest that (1) lower lip movement during articulation was affected in subjects with mandibular prognathism and (2) the present method is feasible for the clinical three-dimensional analysis of lower lip movement.

⑦Soft-tissue changes in association with anterior maxillary osteotomy

The purpose of this study was to investigate and predict soft-tissue changes in the forehead, nose, lips, and chin in association with anterior maxillary osteotomy. The sample consisted of 20 adult patients (seven men and 13 women, 29.1 years of age immediately before surgery). Both hard- and soft-tissue changes were evaluated using a set of lateral cephalograms taken immediately before and at 7 months after surgery. Pearson correlation coefficients were computed to examine the relationship between hard- and soft-tissue changes. A prediction model was developed using a multiple regression equation. The findings were as follows: (1) Hard-tissue changes were only observed in the maxillary region. Soft-tissue changes included backward displacement of the subnasale and the upper and lower lips. (2) The highest correlation coefficient was obtained between hard- and soft-tissue changes in the upper lip region. (3) The horizontal soft-tissue change in the upper lip region was predicted using a multiple regression equation. These results suggest that anterior maxillary osteotomy influences hard- and soft-tissue changes in the upper lip region and that the response in the horizontal dimension in association with surgery can be predicted.

⑧Combined fMRI and MRI movie in the evaluation of articulation in subjects with and without cleft lip and palate

This study was undertaken to explore the application of functional magnetic resonance imaging (fMRI) and MRI movies in the evaluation of articulatory function in subjects with and without cleft lip and palate (CLP). The authors examined brain activation and the dynamic movement of articulators during bilabial and velar plosives using fMRI and MRI movies. Two subjects, one with unilateral cleft lip and palate (UCLP) and one with bilateral cleft lip and palate (BCLP), and 12 non-CLP volunteers. RESULTS: Activation foci were found in the precentral gyrus, thalamus, and cerebellum in non-CLP volunteers. In comparison, similar regions were activated in the UCLP subject during both plosives, whereas the regions activated in the BCLP subject were different, particularly during the velar plosive. The dynamic movement of articulators in the UCLP subject was comparable to that in a non-CLP volunteer but different from that in the BCLP subject. CONCLUSIONS: The results suggest that these two MRI modalities may be a promising evaluation methodology for articulatory

function in CLP from central and peripheral perspectives.

⑨Application of distraction osteogensis in patients with cleft lip and palate
Recently, distraction osteogenesis（DOG）has been accepted to be an effective method for the treatment of patients with cleft lip and palate showing severe maxillary deficiency. Following research have been made from clinical/basic fields: 1）Stabilization of intraoral splint of external distraction system and improvement of distraction efficiency. 2）Measurement of distraction force using micro tension gauge. 3）Diagnosis of post-distraction bone formation using CT and ultrasonographic examination. 4）Three-dimensional evaluation of hard and soft tissue in DOG. 5）Application of hyperbaric oxygen therapy for the purpose of accelerating bone formation after distraction. 6）Application of DOG and chromosomal analysis in a patient with 18q- syndrome.

⑩The effects of hyperbaric oxygen on tooth movement into the distracted area after distraction　osteogenesis
Hyperbaric oxygen（HBO）and distraction osteogenesis were applied to clinical treatment. The object of this study was to analyze the effect of HBO on newly formed bone in distracted areas surrounding the root of a moving tooth by histological and radiological analysis.10 dogs were used. After creating a 10-mm length bone defect, a bony segment was prepared and translocated toward the defect（1 mm/day for ten days）. And next, tooth movement was started and the dogs were divided into two groups. The HBO group received HBO while the control group did not receive HBO. The distracted area around the moving tooth was evaluated radiologically and histologically. Differences between groups were confirmed by Mann-Whitney rank test. Trabecular bone density and cortical and subcortical bone area in the HBO group were significantly higher than those in the control group. Histological observations revealed regenerated bone and blood vessels formation in the tension site of the moving tooth in the HBO group. The regenerated bone structure measured by bone histomorphometry was larger, more active in bone formation in the HBO group.Applying HBO to tooth movement into a distracted area appears to accelerate ossification and vascularization of regenerated bone in the distracted area.

⑪Hyperbaric Oxygen Enhances Healing of Maxillary Distraction in Dogs
A long fixation time during consolidation period is a major clinical disadvantage. Hyperbaric oxygen has been used to improve healing in ischemic wounds. We have recently started applying hyperbaric oxygen to the cleft palate patients after the maxillary distraction, but few basic evidences could be found. We hypothesized that hyperbaric oxygen would enhance the healing of distraction osteogenesis in the cleft palate model in dogs. A bony segment including a canine was transported proximally into an artificial bone defect. Three dogs were treated with hyperbaric oxygen for 20 days just after the distraction, and then sacrificed on day 100 after the corticotomy. Cortical bone mineral density and cortical bone mass were significantly higher at the distraction site in the group treated with hyperbaric oxygen compared to the untreated group（$p<0.05$）. These results suggest that hyperbaric oxygen treatment could be useful for an early removal of the fixator in distraction osteogenesis.

⑫Observation of Pupal Blood Flow and Bone Mineralization after Alveolar Distraction Osteogenesis in a Canine Cleft Model.
Distraction osteogenesis has been widely used to the craniofacial region and even applied to alveolar bones to reduce the cleft width of cleft patients. However, there have been no reports on the limitations to the total amount of lengthening that can be accomplished by distraction osteogenesis.
Therefore, we investigated how different extents of distraction osteogenesis affect the healing process using a canine cleft palate model. For six beagle dogs, a bony segment including the canine was prepared and translocated into 10-mm bone defect area, imitating a cleft, at a rate of 1 mm / day for six or ten days, resulting in two groups（6- and 10-mm groups）. Canine pulpal blood flow was monitored for 100 days with Doppler flowmetry. Then, the animals were sacrificed and the regenerated bone area was evaluated using peripheral quantitative computed tomography（pQCT）and histological process. Pulpal blood flow recovered to the original levels significantly earlier in the 6-mm group. It was showed by pQCT and histological evaluation that the amount of regenerated bone was significantly higher in the 6-mm group than in the 10-mm group. We revealed that amount of bone lengthening affects healing progress.

⑬Report of de novo Dup（18p）/Del（18q）and R（18）Mosaicism
This is a report of a 27-year-old woman with an unusual de novo chromosomal abnormality. Mosaicism was identified in peripheral blood cells examined by standard G-bands by trypsin using Giemsa（GTG）analysis and fluorescence in situ hybridization（FISH）analysis with chromosome-18 region-specific probes, 46,XX,del（18）（pter --> q21.33:）[41], 46,XX,r（18）（::p11.21 -->

q21.33::）[8], and 46,XX,der（18）（pter --> q21.33::p11.21 --> pter）[1]. On the other hand, the karyotype of periodontal ligament fibroblasts was nonmosaic, 46,XX, der（18）（pter --> q21.33::p11.21 --> pter）[50]. All cell lines appeared to be missing a portion of 18q（q21.33 --> qter）. The pattern of the dup（18p）/del（18q）in the rod configuration raises the possibility of an inversion in chromosome 18 in one of the parents. However, no chromosomal anomaly was detected in either parent. The most probable explanation is that de novo rod and ring configurations arose simultaneously from an intrachromosomal exchange. The unique phenotype of this patient, which included primary hypothyroidism and primary hypogonadism, is discussed in relation to her karyotype.

⑭ Atelocollagen-mediated local and systemic applications of myostatin-targeting siRNA increase skeletal muscle mass.
RNA interference（RNAi）offers a novel therapeutic strategy based on the highly specific and efficient silencing of a target gene. Since it relies on small interfering RNAs（siRNAs）, a major issue is the delivery of therapeutically active siRNAs into the target tissue/target cells in vivo. For safety reasons, strategies based on vector delivery may be of only limited clinical use. The more desirable approach is to directly apply active siRNAs in vivo. Here, we report the effectiveness of in vivo siRNA delivery into skeletal muscles of normal or diseased mice through nanoparticle formation of chemically unmodified siRNAs with atelocollagen（ATCOL）. ATCOL-mediated local application of siRNA targeting myostatin, a negative regulator of skeletal muscle growth, in mouse skeletal muscles or intravenously, caused a marked increase in the muscle mass within a few weeks after application. These results imply that ATCOL-mediated application of siRNAs is a powerful tool for future therapeutic use for diseases including muscular atrophy.

4. 本事業に関連して世界的な研究拠点形成に向けて、改善・整備等されたこと

A（研究拠点体制）

当分野は硬組織疾患ゲノムセンター内の未来医療展開部門においても硬組織疾患に関する研究に携わっている。そのため、GCOEの事業に携わる他の事業推進者と連携するだけでなく、ゲノムセンター内の他の分門とも連携した研究体制を整備した。

B（研究教育環境）

GCOEのテーマである歯と骨の疾患の分子病態成立のメカニズムを明らかにするには、ヒトから得られる情報を多角的に集積することが非常に大切である。当分野は、先天性疾患を有する患者の歯科矯正治療に携わっていることを特色としており、そこで本年度は、先天性疾患を有する患者より得られた医療情報のデータ化を試みた。また、疾患を有する患者の咬合機能の回復のために治療法の開発も積極的に行っており、基礎研究より得られた要素を、臨床応用に結びつける試みも行われている。教育面においては、新人教育の一環として、先天性疾患をテーマにあげ、疾患の成因から臨床的な側面を含めた幅広い内容を求めた発表を課している。

C（人材確保）

平成21年4月より、シャペロン教員として春山直人講師を任用することで、歯科臨床と基礎研究の橋渡しを担う人材を確保し、臨床研究と基礎研究を統合させうる研究体制を整備した。

D（人材育成）

GCOEプログラムでは、シャペロン制度やスーパースチューデント制度を創設して、若手研究者の人材の育成に取り組んでいるが、当分野においても、現在のところ2名の大学院生がこの制度を利用している。来年度はさらに数名の大学院生がこの制度に応募しており、当分野の特色である臨床研究と基礎研究の橋渡しが出来る幅広い視野を持った研究者の育成が期待される。

E（国際化）

積極的に海外の学会発表や学術誌に投稿し、成果を発表した。さらに、海外から外部講師を招聘し、セミナーを開催すると共に、若手研究者と英語によるディスカッションする機会を設けた。

5. GCOE事業を推進するに当たって力を入れた点

当分野は歯科矯正臨床分野において、先天性疾患を有する患者の割合が高く、その数は全国的に見ても類をみない。本年度は、先天性疾患を有する患者より得られた医療情報のデータ化を試みることに重点をおき、さらに、臨床面においては疾患を有する患者の咬合機能の回復のための治療法の開発も積極的に行った。当分野の特色を生かした基礎研究により得られた成果と臨床研究を統合させ、患者のQOLを高める研究計画を立案するに至った。

6. 英文原著論文

1. Miraoui H, Oudina K, Petite H, Tanimoto Y, Moriyama K, Marie PJ. Fibroblast growth factor receptor2 promotes osteogenic differentiation in mesenchymal cells via extracellular-related kinase and protein kinase c signalling. J Biol Chem,（in press）.
2. Suda N, Shiga M, Ganburged G, Moriyama K. Marfan syndrome and its disorder in periodontal tissues. J. Exp. Zool.（in press）.
3. ◎Yagi Y, Suda N, Yamakoshi Y, Baba O, Moriyama K. In vivo application of amelogenin suppresses root resorption. J Dent Res.（in press）.
4. Suda N, Kawafuji K, Moriyama K. Multidisciplinary management including endodontics, periodontics, orthodontics, anterior maxillary osteotomy and prosthetics in an adult case with a severe openbite. Orthod Waves.（in press）.
5. Inoue MS, Ono T, Honda E, Kurabayashi T, Moriyama K. Motor coordination of articulators depends on the place of articulation. Behav Brain Res.（in press）.
6. Gereltzul E, Baba Y, Suda N, Shiga M, Inoue M, Tsuji M, Shin I, Hirata Y, Ohyama K, Moriyama K. Case Report of de novo Dup（18p）/Del（18q）and R（18）Mosaicism. Journal of Human Genetics 53（10）:941-6, 2008
7. Putranoto P, Oba Y, Kaneko K, Shioyasono A, Moriyama K. Effects of bisphosphonates on roots resorption and cytokine expression during experimental tooth movements in rats. Orthod Waves 67（4）141-149, 2008
8. Okudaira M, Ono T, Kawamoto T, Moriyama K. Three-dimensional analysis of lower lip movement during articulation in subjects with mandibular prognathism. Orthod Waves. 67（3）93-103, 2008
9. Okudaira M, Kawamoto T, Ono T, Moriyama K. Soft-tissue changes in association with anterior maxillary osteotomy: a pilot study. Oral Maxillofac Surg. 12（3）:131-8, 2008
10. Kinouchi N, Ohsawa Y, Ishimaru N, Ohuchi H, Sunada Y, Hayashi Y, Tanimoto Y, Moriyama K, Noji S. Atelocollagen-mediated local and systemic applications of myostatin-targeting siRNA increase skeletal muscle mass. Gene Ther. 15（15）:1126-30, 2008
11. Mukai-Higashihori K, Baba Y, Tetsumura A, Tsuji M, Ishizaki T, Higashihori N, Ohbayashi N, Kurabayashi T, Suzuki S, Ohyama K. Ultrasonographic assessment of new bone formation in maxillary distraction osteogenesis. J Oral Maxillofac Surg. 66（8）:1750-3, 2008
12. Sato-Wakabayashi M, Inoue-Arai MS, Ono T, Honda E, Kurabayashi T, Moriyama K. Combined fMRI and MRI movie in the evaluation of articulation in subjects with and without cleft lip and palate. Cleft Palate Craniofac J. 45（3）:309-14, 2008
13. Hashimoto K, Otsuka R, Minato A, Sato-Wakabayashi M, Takada J, Inoue-Arai MS, Miyamoto JJ, Ono T, Ohyama K, Moriyama K. Short-term changes in temporomandibular joint function in subjects with cleft lip and palate treated with maxillary distraction osteogenesis. Orthod Craniofac Res. 11（2）:74-81, 2008
14. Murakami M, Ohkuma M, Nakamura M. Molecular mechanism of transforming growth factor-beta-mediated inhibition of growth arrest and differentiation in a myoblast cell line. Dev Growth Differ. 50（2）:121-30, 2008.
15. Yokota T, Shimokawa H, Shibata S, Itoh K, Baba Y, Ohya K, Ohyama K, Suzuki S. Insulin-like growth factor I regulates apoptosis in condylar cartilage. J Dent Res. 87（2）:159-63, 2008
16. Takada J, Ono T, Takahashi S, Honda E, Kurabayashi T. Changes in horizontal jaw position and intraoral pressure. Angle Orthod. 78（2）:254-61, 2008
17. Suda N. Comprehensive gene expression analysis in human periodontal ligaments of the mandibular third molars performing vertical movement and the maxillary second premolars with occlusal contact. Orthod Craniofac Res. 11（1）:1-7, 2008.
18. Oba Y, Yasue A, Kaneko K, Uchida R, Shioyasono A, Moriyama K. Comparison of stability of mandibular segments following the sagittal split ramus osteotomy with poly-L-lactic acid（PLLA）screws and titanium screws fixation. Orthod Waves 67（1）1-8, 2008
19. Shiga M, Saito M, Hattori M, Torii C, Kosaki K, Kiyono T, Suda N. Characteristic phenotype of immortalized periodontal cells isolated from a Marfan syndrome type I patient. Cell Tissue Res. 331（2）:461-72, 2008

7. 著書

1. 大山紀美栄, 辻美千子, 森山啓司:【外表奇形の診断と治療】顎顔面の奇形　小児科49（1）17-25, 2008.
2. 小野卓史:【セファロ分析】 睡眠学、朝倉書店、2009.

8. 平成21年3月までの自己評価

研究面において、基礎研究の成果と臨床的要素を融合した研究を遂行することが可能であった。教育面においては、海外から外部講師を招聘し、若手研究者と積極的に議論する場を設けるなど、国際的に活躍できる研究者の育成に貢献した。しかし、当分野にはGCOEプログラムで採用しているスーパースチューデント制度を利用している大学院生が2名在籍しているが、学会等の発表の数が十分でなく、今後のさらなる指導の強化を図りたい。

9. 和文原著論文

1. 片岡恵一、馬場祥行、本田綾、石崎敬、鉄村明美、大林尚人、倉林亨、鈴木聖一、森山啓司. 超音波画像を用いた片側性口唇裂・口蓋裂症例に対する上顎骨延長術後の骨形成の評価. 日顎変形誌　18（4）:251-58,2008
2. 井澤俊, 堀内信也, 辻けい子, 藤原慎視, 大庭康雄, 田中栄二, 森山啓司. 下顎枝垂直骨切り術と下顎枝矢状分割術を併用した外科的矯正治療後に下顎頭のリモデリングを認めた一症例.　日本顎関節学会雑誌20（2）134-138, 2008
3. 篠原亨太郎, 馬場祥行、横関雅彦, 森山啓司. REDシステムによりLe Fort I型骨延長術を行い反対咬合および上顎側方偏位を改善したCrouzon症候群の1例. 日顎変形誌　18（1）:39-48,2008
4. 工藤淳夫. ビーグル犬における高気圧酸素療法の骨延長術での治癒促進効果について 口病誌75（1）55-64 2008.
5. 檜山成寿、小野卓史、森山啓司. Cervical headgear使用に際しての注意点-睡眠時呼吸機能の変化に関するアンケート調査に基づく-考察-. 東矯歯誌. 18;12-18, 2008.

10. 学会発表（英文）

1. Ono T, Inoue-Arai MS, Sato-Wakabayashi M, Miyamoto JJ, Honda E, Hashimoto K, Kurabayashi T, Moriyama K. Mapping of brain activation in covert/overt articulation in subjects with/without CLP using fMRI. Poster presentation, Seoul, 2nd Joint Meeting of the Korean Association of Orthodontists and the Japanese Orthodontic Society, December 6-8, 2008.
2. Baba Y, Kataoka K, Kawafuji A, Honda A, Ishizaki T, Suzuki S, Moriyama K. Measurement of traction force using micro tension gauge in maxillary distraction osteogenesis. Poster presentation, Seoul, 2nd Joint Meeting of the Korean Association of Orthodontists and the Japanese Orthodontic Society, December 6-8, 2008.
3. Tsuji M, Baba Y, Yagishita K, Yamami N, Mano Y, Suzuki S, Moriyama K. Clinical application of hyperbaric oxygen therapy for cleft patients treated by distraction osteogenesis. Poster presentation, Seoul, 2nd Joint Meeting of the Korean Association of Orthodontists and the Japanese Orthodontic Society, December 6-8, 2008.
4. Kawafuji A, Baba Y, Shiga M, Honda A, Kataoka K, Suzuki S, Moriyama K. Midfacial soft tissue change after Le Fort I maxillary distraction osteogenesis in UCLP patients. Poster presentation, Seoul, 2nd Joint Meeting of the Korean Association of Orthodontists and the Japanese Orthodontic Society, December 6-8, 2008.
5. Kawafuji A, Suda N, Ichikawa N, Kakara S, Suzuki T, Ogawa T, Tsuji M, Moriyama K. Systemic and maxillofacial characteristics of Beckwith-Wiedemann syndrome patients without having glossectomy. Poster presentation, Seoul, 2nd Joint Meeting of the Korean Association of Orthodontists and the Japanese Orthodontic Society, December 6-8, 2008.
6. Kataoka K, Baba Y, Honda A, Ishizaki T, Tetsumura A, Ohbayashi N, Kurabayashi T, Suzuki S, Moriyama K. Ultrasonographic observation of bone formation after maxillary distraction osteogenesis. Oral presentation, Seoul, 2nd Joint Meeting of the Korean Association of Orthodontists and the Japanese Orthodontic Society, December 6-8, 2008.
7. Minato A, Ono T, Miyamoto JJ, Honda E, Kurabayashi T, Moriyama K. Preferred-chewing-side-dependent two-point discrimination and cortical activation of tactile tongue sensation. Poster presentation, Nagoya, 56th Japanese Association for Dental Research, November 29-30, 2008.
8. Yagi Y, Suda N, Yamakoshi Y, Baba O, Moriyama K. Amelogenin is a potent inhibitor of odontoclastic root resorption. Oral presentation, Nagoya, 56th Japanese Association for Dental Research, November 29-30, 2008.
9. Inoue-Arai MS, Ono T, Honda E, Kurabayashi T, Moriyama K. Non-invasive study on articulation using magnetic resonance imaging movie. Poster presentation, Canada, 87th General Session & Exhibition of the International Association for Dental Research, Toronto, July 2-5, 2008.
10. Kinouchi N, Ohsawa Y, Ishimaru N , Ohuchi H, Sunada Y, Hayashi Y, Moriyama K, Noji S.

Atelocollagen-mediated Applications of Myostatin-targeting siRNA Increase Skeletal Muscle Mass. Poster presentation, Canada, 87th General Session & Exhibition of the International Association for Dental Research, Toronto, July 2-5, 2008.

11. Inoue MS, Sato-Wakabayashi M, Ono T, Honda E, Moriyama K. Evaluation of articulation in subjects with and without CLP using functional MRI and MRI movie. Poster presentation, Lisbon, 84th Congress of the European Orthodontic Society, June 10-14, 2008.
12. Baba Y, Honda A, Ishizaki T, Suzuki S, Moriyama K. Follow-up study after maxillary distraction in growing children with cleft lip/palate. Poster presentation, Bangkok, 6th Asian Pacific Orthodontic Conference. March, 27-30, 2008
13. Tsuji M, Baba Y, Ishizaki T, Suzuki S, Moriyama K. Correction of maxillary lateral deviation using RED system with auxiliary traction wire. Poster presentation, Bangkok, 6th Asian Pacific Orthodontic Conference. March, 27-30, 2008
14. Kataoka K, Baba Y, Ishizaki Y, Suzuki S, Moriyama K. Distraction osteogenesis of dentoalveolar segment for reconstruction of Cleft Lip/Palate. Poster presentation, Bangkok, 6th Asian Pacific Orthodontic Conference. March, 27-30, 2008.

11. 学会発表（和文）

1. 湊亜紀子、小野卓史、宮本順、誉田栄一、倉林亨、森山啓司. 舌に対する2点弁別試験および触覚刺激に伴う大脳皮質一次体性感覚野の賦活パタンの解析-習慣性咀嚼側との関連-. 第73回口腔病学会学術大会、東京、2008年12月5-6日.
2. 辻 美千子、馬場祥行、本田綾、柳下和慶、山見信夫、眞野嘉洋、鈴木聖一、森山啓司.上顎骨の骨延長法に際し、高気圧酸素治療（HBO）を適用した1症例.第43回日本高気圧環境・潜水医学会学術総会、旭川、2008年10月31-11月1日.
3. 本田綾、馬場祥行、片岡恵一、辻 美千子、石﨑 敬、柳下和慶、山見信夫、眞野嘉洋、鈴木聖一、森山啓司.口唇口蓋裂症例の上顎骨延長法に対する高気圧酸素治療の適用と術後評価.第43回日本高気圧環境・潜水医学会学術総会、旭川、2008年10月31-11月1日.
4. 小川卓也、森山啓司. PAX9の変異を有する先天性多数歯欠損家系におけるMSX1の多型解析. 第26回日本骨代謝学会学術集会、大阪、2008年10月29－31日.
5. 八木優子、須田直人、山越康雄、馬場麻人、森山啓司. Amelogenin は in vivo において歯根吸収を抑制する. 第50回歯科基礎医学会学術大会、東京、2008年9月23－25日.
6. 小川卓也、シンタ　ウィラハディ　クスマ、森山啓司. 矯正治療後に長期観察を行った先天性ミオパチー患者の顎態変化. 第67回日本矯正歯科学会大会、千葉、2008年9月16－18日.
7. 高田潤一、小野卓史、宮本順、横田俊明、森山啓司. 下顎側方偏位症例における大臼歯の頬舌的位置と口腔内圧の関連. 第67回日本矯正歯科学会大会、千葉、2008年9月16－18日.
8. 八木優子、須田直人、山越康雄、馬場麻人、森山啓司． Enamel matrix derivative（EMD）の歯根吸収抑制活性はアメロゲニンが担う. 第67回日本矯正歯科学会大会、千葉、2008年9月16－18日.
9. 本田綾、馬場祥行、片岡恵一、辻美千子、石崎敬、鈴木聖一、柳下和慶、山見信夫、森山啓司． 口唇・口蓋裂症例の上顎骨延長法に対する高気圧酸素治療の適応と術後評価. 第67回日本矯正歯科学会大会、千葉、2008年9月16－18日.
10. 奥平真理子、馬場祥行、石崎敬、本田綾、片岡恵一、鈴木聖一、森山啓司. REDシステムによるLe FortI型骨延長術を適応した口唇・口蓋裂患者に対するアンケート調査. 第67回日本矯正歯科学会大会、千葉、2008年9月16－18日.
11. 井口隆人、川元龍夫、長濱浩平、青木朝里、工藤淳夫、青木和広、大谷啓一、森山啓司, 上顎歯槽部骨延長部位への歯の移動において高気圧酸素が歯周組織に及ぼす影響, 第67回日本矯正歯科学会大会、千葉、2008年9月16－18日.
12. 川藤亜樹子、馬場祥行、志賀百年、本田綾、片岡恵一、鈴木聖一、森山啓司, Le FortI型上顎骨延長術を適応した片側性口唇口蓋裂症例の中顔面の軟組織の変化. 第67回日本矯正歯科学会大会、千葉、2008年9月16－18日.
13. Ganburged Ganjargal、須田直人、森山啓司. Maran症候群にみられる重篤な歯周疾患の動物モデルの作製. 第67回日本矯正歯科学会大会、千葉、2008年9月16－18日.
14. 山田大輔、鎌田秀樹、大隈瑞恵、辻美千子、須田直人、森山啓司. 当分野を受診したhemifacial microsomia

患者の臨床症状に関する検討. 第67回日本矯正歯科学会大会、千葉、2008年9月16－18日.

15. 金谷和宏、小川卓也、辻美千子、須田直人、大林尚人、倉林亨、森山啓司. 歯科用コーンビームCT画像によるhemifacial microsomiaの顎関節周辺部の三次元的解析. 第67回日本矯正歯科学会大会、千葉、2008年9月16－18日.
16. 出井彩乃、鈴木尋之、大隈瑞恵、辻美千子、須田直人、森山啓司. 長期経過観察を行ったhemifacial microsomia1例の顎態の成長変化に関する検討, 第67回日本矯正歯科学会大会、千葉、2008年9月16－18日.
17. 佐藤麻緒、ウン・イン・ウー、小川卓也、辻美千子、須田直人、小野卓史、森山啓司. 機能的矯正装置で治療したhemifacial microsomia 5例の顎態の非対称性変化に関する検討. 第67回日本矯正歯科学会大会、千葉、2008年9月16－18日.
18. 鈴木剛史、小川卓也、佐藤麻緒、井口隆人、川元龍夫、森山啓司. 集学的歯科治療により咬合の確立を図ったoligodontiaの2症例. 第67回日本矯正歯科学会大会、千葉、2008年9月16－18日.
19. 横田俊明、下川仁彌太、馬場祥行、小野卓史、鈴木聖一、森山啓司. I型インスリン様増殖因子（IGF-I）は下顎頭軟骨のアポトーシスを制御する. 第21回日本顎関節学会学術大会、2008年7月26-27日、大阪.
20. 大隈瑞恵、大塚亮、北村良平、福岡裕樹、辻美千子、森山啓司.　歯槽部骨延長術による上顎歯列弓拡大後に上下顎移動術を施行した顔面非対称を伴う骨格性開咬症例. 第67回東京矯正歯科学会大会, 東京, 2008年7月17日.
21. 馬場祥行、須田直人、志賀百年、辻 美千子、ゲレルトゥズル エンクトゥフシン、平田 結喜緒、大山 紀美栄、森山啓司. A case report of de novo rod/ring chromosome 18 mosaicism. 第48回日本先天異常学会学術集会, 東京, 2008年6月28-30日.
22. 奥平真理子、川元龍夫、小野卓史、森山啓司. 上顎前歯部歯槽骨切り術による軟組織側貌変化について. 第18回日本顎変形症学会総会, 名古屋, 2008年6月17-18日.
23. 片岡恵一、馬場祥行、石崎敬、本田綾、鈴村明美、大林尚人、倉林亨、鈴木聖一、森山啓司.　超音波画像法を用いた上顎骨延長後の骨形成の評価. 第18回日本顎変形症学会総会, 名古屋, 2008年6月17-18日.
24. 福岡裕樹、長濱浩平、北村良平、富永直子、川元龍夫、森山啓司.　下顎枝逆L字型骨切り術と下顎枝矢状分割術を併用して治療を行った下顎非対称を伴う口唇口蓋裂の1例. 第18回日本顎変形症学会総会, 名古屋, 2008年6月17-18日.
25. 青木朝里、川元龍夫、井口隆人、工藤淳夫、長濱浩平、馬場祥行、鈴木聖一、森山啓司. ビーグル犬歯歯槽骨延長モデルにおける組織修復様相の観察―延長量が歯髄血流回復および骨新生に及ぼす影響―　第32回日本口蓋裂学会総会, 広島, 2008年5月28-29日.
26. 本田綾、馬場祥行、石崎敬、鈴木聖一、森山啓司. 思春期性成長以降にLeFortI型上顎骨延長法を適用した口唇・口蓋裂症例の術後変化. 第32回日本口蓋裂学会総会, 広島, 2008年5月28-29日.
27. 志賀百年、馬場祥行、宮本順、本田綾、片岡恵一、加々良朱摩子、金谷和宏、鈴木聖一、森山啓司. Le Fort I型上顎骨延長術を適用した口唇口蓋裂症例の中顔面軟組織の変化. 第32回日本口蓋裂学会総会, 広島, 2008年5月28-29日.
28. 若林みちる、井上マリステラ小百合、宮本順、橋本幸治、倉林亨、小野卓史、森山啓司. 機能的磁気共鳴画像法を用いた口唇口蓋裂患者における外言語・内言語生成時の脳賦活領域のマッピング. 第32回日本口蓋裂学会総会, 広島, 2008年5月28-29日.
29. 神野恵、高橋巧、大庭康雄、森山啓司. Smad3ノックアウトマウスを用いた口蓋粘膜における創傷治癒解析―第2報―　第32回日本口蓋裂学会総会, 広島, 2008年5月28-29日.
30. 辻美千子, 森山啓司. 口腔内の異常に気付いて矯正歯科を受診した鎖骨頭蓋異形成症2例について. 第32回日本遺伝カウンセリング学会学術集会, 仙台, 2008年5月23-25日.

12. 受賞

1. Ono T, Inoue-Arai MS, Sato-Wakabayashi M, Miyamoto JJ, Honda E, Hashimoto K, Kurabayashi T, Moriyama K. Mapping of brain activation in covert/overt articulation in subjects with/without CLP using fMRI.（優秀発表賞）2nd Joint Meeting of the Korean Association of Orthodontists and the Japanese Orthodontic Society, Seoul, December6-8, 2008.
2. Baba Y, Kataoka K, Kawafuji A, Honda A, Ishizaki T, Suzuki S, Moriyama K. Measurement of traction force using micro tension gauge in maxillary distraction osteogenesis.（優秀発表賞）2nd Joint Meeting of the Korean Association of Orthodontists and the Japanese Orthodontic Society, Seoul, December 6-8, 2008.

3. Tsuji M, Baba Y, Yagishita K, Yamami N, Mano Y, Suzuki S, Moriyama K. Clinical application of hyperbaric oxygen therapy for cleft patients treated by distraction osteogenesis.（優秀発表賞）2nd Joint Meeting of the Korean Association of Orthodontists and the Japanese Orthodontic Society, Seoul, December 6-8, 2008.
4. Kawafuji A, Baba Y, Shiga M, Honda A, Kataoka K, Suzuki S, Moriyama K. Midfacial soft tissue change after Le Fort I maxillary distraction osteogenesis in UCLP patients.（優秀発表賞）2nd Joint Meeting of the Korean Association of Orthodontists and the Japanese Orthodontic Society, Seoul, December 6-8, 2008.
5. Kawafuji A, Suda N, Ichikawa N, Kakara S, Suzuki T, Ogawa T, Tsuji M, Moriyama K. Systemic and maxillofacial characteristics of Beckwith-Wiedemann syndrome patients without having glossectomy.（優秀発表賞）
6. 2nd Joint Meeting of the Korean Association of Orthodontists and the Japanese Orthodontic Society, Seoul, December 6-8, 2008. Minato A, Ono T, Miyamoto JJ, Honda E, Kurabayashi T, Moriyama K. Preferred-chewing-side-dependent two-point discrimination and cortical activation of tactile tongue sensation.（学術奨励賞）56th Japanese Association for Dental Research, Nagoya, November 29-30, 2008.
7. 八木優子、須田直人、山越康雄、馬場麻人、森山啓司. Amelogenin は in vivo において歯根吸収を抑制する.（優秀ポスター発表賞）第50回歯科基礎医学会学術大会、東京、2008年9月23－25日.
8. 高田潤一、小野卓史、宮本順、横田俊明、森山啓司.下顎側方偏位症例における大臼歯の頬舌的位置と口腔内圧の関連.（優秀発表賞）第67回日本矯正歯科学会大会、2008年9月16-18日、千葉.
9. 八木優子、須田直人、山越康雄、馬場麻人、森山啓司. Enamel matrix derivative（EMD）の歯根吸収抑制活性はアメロゲニンが担う.（優秀発表賞）第67回日本矯正歯科学会大会、千葉、2008年9月16－18日.
10. 若林みちる, 井上マリステラ小百合, 宮本順, 誉田栄一, 橋本幸治, 倉林亨, 小野卓史, 森山啓司. 機能的磁気共鳴画像法を用いた口唇口蓋裂患者における外言語・内言語生成時の脳賦活領域のマッピング 第32回日本口蓋裂学会学術集会・優秀ポスター賞、2006年5月28日-29日、広島.

13. 外部資金の獲得状況

1. 科学研究費補助金 基盤A　研究題目:頭蓋顎顔面骨格先天異常に対する新規治療法開発と実用化への基礎的研究　代表:森山啓司　期間:平成18年－平成20年　研究費総額:37,700千円
2. 科学研究費補助金 萌芽　研究題目:顎顔面口腔領域の骨格筋量調節を目的とした新規医薬開発に関する研究　代表:森山啓司　期間:平成19年－平成20年　研究費総額:3,300千円
3. 独立行政法人日本学術振興会 科学研究費補助金（特別研究員奨励費）「口唇口蓋裂患者の発話時における脳活動と構音器官運動相関」:課題番号　19・07470　研究代表者 森山啓司　研究分担者 Inoue MS　期間:平成19年－平成21年　研究費総額:2,300千円
4. 科学研究費補助金 基盤B　研究題目口唇口蓋裂をモデルとした音声言語の生成、障害および可塑性のメカニズムの解明　代表:小野卓史　期間:平成20年－平成23年　研究費総額:14,700千円
5. 科学研究費補助金 萌芽　研究題目:ニューロイメージング法を用いた咬合と全身機能の脳神経生理学的解析　代表:小野卓史　期間:20年－平成22年　研究費総額:3,200千円
6. 科学研究費補助金 基盤B（海外学術）研究題目:アジアにおける先天性多数歯欠損に関する遺伝学的調査　代表:須田直人　期間:平成18年－平成21年　研究費総額:12,900千円
7. 科学研究費補助金　萌芽　研究題目:トランスレーショナルリサーチによる歯根膜弾性線維の機能解明への画期的アプローチ　代表:須田直人　期間:平成19年－平成20年　研究費総額:3,200千円
8. 科学研究費補助金　基盤C　研究題目:張力センサを用いた骨延長術時の牽引力の解析　代表:馬場祥行　期間:平成20年－平成22年　研究費総額:3,600千円
9. 科学研究費補助金　基盤C　研究題目:上顎歯槽部骨延長に伴う周辺組織再構築と高気圧酸素療法との関連　代表:川元龍夫　期間:平成19年－平成20年　研究費総額:3,500千円
10. 科学研究費補助金　若手B　研究題目:先天性多数歯欠損の家系における変異と表現系に関する研究　代表:小川卓也　期間:平成20年－平成21年　研究費総額:3,200千円
11. 独立行政法人日本学術振興会 科学研究費補助金（特別研究員奨励費）研究題目:非侵襲的脳機能画像法を用いた咀嚼運動時のヒト脳機能の解明　代表:宮本順　期間:平成20年－平成22年　研究費総額:2,400千円
12. 科学研究費補助金　若手研究スタートアップ　研究題目:超小型圧力センサを用いた顔面非対称症例の治療前後における口腔圧の変化の解析　代表:高田潤一　期間:平成20年－平成21年　研究費総額:2,420千円
13. 文部科学省科学研究費補助金　若手研究スタートアップ　研究題目:片側性臼歯部反対咬合を有する骨格性下顎前突症患者の下顎蝶番運動回転軸に関する研究

代表:横田俊明　期間:平成20年－平成21年　研究費総額:2,000千円

14. 文部科学省科学研究費補助金　若手研究スタートアップ　研究題目:ヒト吸収歯根にセメント芽細胞を移入し歯根再生を試みる基礎研究　代表:高橋優子　期間:平成20年－平成21年　研究費総額:2,540千円

14. 特別講演、招待講演

1. 辻美千子.遺伝カウンセリング.第33回遺伝カウンセリングリフレッシュセミナー「口唇裂・口蓋裂の遺伝カウンセリング」.2009年1月10-11日.大阪
2. 森山啓司. 顎顔面先天異常に対する歯科矯正学的アプローチ. 第2回硬組織疾患ゲノムセンターシンポジウム. 2008年11月25、日東京医科歯科大学.
3. 小川卓也. 先天性多数歯欠損におけるPAX9とMSX1の相互作用. 第2回硬組織疾患ゲノムセンターシンポジウム. 2008年11月25日、東京医科歯科大学.
4. 須田直人. 遺伝性疾患における歯の異常とその多様性. 岩手医科大学先端歯科医療研究センター オープンリサーチプロジェクトセミナー, 2008年年11月14日, 盛岡.
5. 須田直人. 歯の萌出路形成と副甲状腺ホルモン関連ペプチド（PTHrP）. 第1回　顎顔面の器官発生・形態形成研究会. 平成20年10月18-19日.
6. 須田直人. 結合組織疾患と歯周疾患 –弾性線維に異常をきたす遺伝性疾患を中心にして-. 日本大学松戸歯学部大学院セミナー, 2008年10月7日, 松戸.
7. 森山啓司. Craniofacial anomalies from the orthodontic point of view. 東京医科歯科大学グローバルCOE発足記念講演会. 2008年10月6日、東京.
8. 須田直人. 歯根の形態異常を伴う遺伝性疾患, 第50回歯科基礎医学会学術大会サテライトシンポジウム, 2008年9月23-25日, 東京.
9. 森山啓司. 口腔顎面領域に異常を生じる遺伝性疾患とその治療. 第18回遺伝医学セミナーカリキュラム、2008年9月5－7日、大阪.
10. 辻美千子.多因子遺伝.平成20年度遺伝カウンセリングセミナー第36回実践コース.2008年8月21-24日.東京
11. 森　山　啓　司. Fibroblast growth factor receptor（FGFR）の変異と頭蓋縫合早期癒合症. 第17回大学院医歯学総合研究科大学院セミナー、ポストゲノム時代の発生生物学展望. 2008年6月23日、東京医科歯科大学.
12. 森山啓司. 諸外国における歯科臨床シュミレーション教育システムを用いた教育改革の取り組み. 口腔病学会6月定例会. 2008年6月19日、東京医科歯科大学.
13. 須田直人.　歯根膜弾性線維のはたらきに関する一考察　–マルファン症候群の歯科的問題を出発点として-.　日本大学歯学部大学院特別講義.平成20年6月18日、日本大学.
14. Keiji Moriyama. Orthodontist as a member of the team for cleft lip and/or palate patients care. 6th Asian Pacific Orthodontic Conference. March, 27-30, 2008, Bangkok ,Thailand.

15. 講座の准教授、講師、助教、特別研究員、ポスドク、指導を受けた大学院生の名前（AISSには◯印）のリスト

准教授:鈴木聖一

講　師:小野卓史、須田直人

助　教:馬場祥行、川元龍夫、辻美千子、濱田俊（3月まで）、小川卓也（4月から）

特別研究員:

宮本順、井上マリステラ小百合（学術振興会）

大学院:

青木朝里（3月まで）、八木優子（3月まで）、若林みちる（3月まで）、井口隆人、服部架湊亜紀子、田仲眞理（3月まで）、シンタ・ウィラハディ・クスマ、ガンブルゲド・ガンジャルガル、鎌田英樹、鈴木尋之、ウン・イン・ウー、岡本奈那（4月から）、武智香織（4月から）、疋田理奈（4月から）、松本力（4月から）

RESEARCH REPORTS
Biological

Y. Yagi[1,4], N. Suda[1,4]*, Y. Yamakoshi[1,4], O. Baba[3], and K. Moriyama[1,4]

[1]Maxillofacial Orthognathics, Department of Maxillofacial Reconstruction and Function, Division of Maxillofacial/Neck Reconstruction, Graduate School, Tokyo Medical and Dental University, 1-5-45 Yushima, Bunkyo-ku, Tokyo, 113-8549, Japan; [2]Department of Biologic and Materials Sciences, University of Michigan Dental Research Laboratory, Ann Arbor, MI, USA; [3]Biostructural Science, Department of Hard Tissue Engineering, Division of Bio-Matrix, Graduate School, Tokyo Medical and Dental University, Tokyo, Japan; and [4]Global Center of Excellence (GCOE) Program, International Research Center for Molecular Science in Tooth and Bone Diseases, Tokyo, Japan; *corresponding author, n-suda.mort@tmd.ac.jp

J Dent Res X(X):000-000, 2009

In vivo Application of Amelogenin Suppresses Root Resorption

ABSTRACT

Amelogenin is recognized as an enamel protein associated with enamel formation. Besides this well-known function, remarkable root resorption has been seen in amelogenin-null mutant mice. Moreover, *in vitro* culture studies showed that amelogenin suppressed osteoclast differentiation. These studies raised the hypothesis that amelogenin can inhibit root resorption by reducing odontoclast number. To examine this hypothesis, we applied porcine amelogenins in a rat root resorption model, in which maxillary first molars were replanted after being air-dried. Compared with untreated and carrier-treated tooth roots, the application dramatically reduced the odontoclast number on root surfaces and inhibited cementum and root dentin resorption. Amelogenin significantly reduced the number of human odontoclastic cells in culture. It also inhibited RANKL expression in mouse bone marrow cell cultures. All these findings support our hypothesis that amelogenin application suppresses root resorption by inhibiting odontoclast number, and suggest that this is mediated by the regulation of RANKL expression.

KEY WORDS: amelogenin, enamel matrix derivative, odontoclast, root resorption.

DOI: 10.1177/0022034508329451

Received March 28, 2008; Last revision October 24, 2008; Accepted October 28, 2008

A supplemental appendix to this article is published electronically only at http://jdr.sagepub.com/supplemental.

INTRODUCTION

Resorption of the shedding deciduous teeth is a physiological event required for normal development of the permanent dentition (Nanci, 2007). In contrast, root resorption of permanent teeth occurs by various pathological etiologies (Fuss *et al.*, 2003), including infection, trauma, and tumor (Andreasen, 1985), dental treatments such as orthodontic treatment (Brezniak and Wasserstein, 2002), and tooth replantation/transplantation (Andreasen and Hjørting-Hansen, 1966). For tooth longevity, the maintenance of tooth functions, and successful treatment outcome, it is crucial that unfavorable resorption be prevented. As a pharmacological approach, an application of fluoride was examined in animal models, but the expected inhibitory effect was not seen (Foo *et al.*, 2007).

Amelogenin is known as a major constituent of the enamel matrix secreted by ameloblasts and plays an important role in enamel formation (Termine *et al.*, 1980). A previous study demonstrated its expression in periodontal tissues as well (Fong and Hammarström, 2000). Interestingly, significant root resorption was found in amelogenin-gene knockout mice, suggesting this protein as a negative regulator of odontoclastic root resorption (Hatakeyama *et al.*, 2003). Moreover, the application of Emdogain® (Straumann, Basel, Switzerland), which is known to contain amelogenin (Maycock *et al.*, 2002) and is widely used to promote periodontal tissue regeneration (Hammarström *et al.*, 1997), inhibited root resorption in animal (Hamamoto *et al.*, 2002) and human (Barrett *et al.*, 2005) studies. Amelogenin has also been shown to suppress cultured osteoclast formation and the expression of receptor activator of NF-κB ligand (RANKL), which is a pivotal factor for bone resorption (Hatakeyama *et al.*, 2006; Nishiguchi *et al.*, 2007). These studies raised the hypothesis that amelogenin treatment can prevent root resorption and reduce odontoclast number, *in vivo*. In this study, the effect of porcine amelogenin was examined in an experimental root resorption model, and in an odontoclastic cell culture system. Moreover, the amelogenin treatment was also examined on RANKL expression in culture.

MATERIALS & METHODS

Animals

Four- and 6-week-old male Sprague-Dawley rats were purchased from Shizuoka Laboratories Animal Center (Shizuoka, Japan). Experimental procedures were approved by the Experimental Animal Committee of Tokyo Medical and Dental University.

In vivo Model of Experimental Root Resorption

Thirty-five 6-week-old male Sprague-Dawley rats were used. Their maxillary right first molars (M1s) were extracted under anesthesia. All extracted teeth were air-dried at room temperature for 1 hr to induce root resorption. Then, the extracted M1s were replanted into the alveolar sockets, and the animals were killed 1 wk later for the following experiments. A 30-μL quantity of Emdogain® was applied to each tooth root at replantation in 7 rats. A 20- or 200-μg quantity of P173, which is an isolated porcine 25-kDa protein lacking exon 4 (Simmer *et al.*, 1994; Yamakoshi *et al.*, 1994), was mixed with 30 μL (3.0 g/L; 150 cP) of propylene glycol alginate (PGA; Wako, Osaka, Japan), which is a carrier of Emdogain®, and applied to each root at replantation (n = 7 for each group). As a control, no treatment was performed on tooth roots in 7 rats (untreated group), or 30 μL of PGA alone was applied to tooth roots in 7 rats (PGA group).

Micro-computed Tomographic (μCT) Analysis of Tooth Roots

μCT images (InspeXio SMX-90CT, Shimadzu, Kyoto, Japan) were taken before and at 1 wk after the tooth replantation. We used VG Studio MAX (Nihon Visual Science Inc., Tokyo, Japan) to visualize morphological differences on root surfaces.

Tissue Preparation and Tartrate-resistant Acid Phosphatase (TRAP) Staining

The right sides of maxillae were fixed by immersion in 4% paraformaldehyde in 0.1 M of phosphate buffer (pH 7.4), decalcified in 4.13% EDTA (pH 7.0), and dehydrated and embedded in Technovit 7100 (Kulzer, Wehrheim, Germany). Then, 3-μm-thick serial sagittal sections of M1s with surrounding tissues were prepared. TRAP staining was performed on sections as described previously (Suda *et al.*, 2001) and counterstained with methylene blue.

Histomorphometric Analysis

The following parameters were used: (1) resorbed dentin area *per* total root dentin area (%), (2) odontoclast surface *per* root surface (%), and (3) numbers of odontoclasts on root surfaces. All observations were carried out under a microscope and with the use of an image-measuring system (Finetec Co. Ltd, Tokyo, Japan).

Biolabeling of Rats by Calcein Injection

Two independent protocols were performed for the labeling of rat tooth roots: (1) M1s of 6-week-old rats were extracted and replanted after 1 hr of air-drying. Rats received a single intraperitoneal injection of calcein (15 mg/kg body weight, Wako) just after the replantation. (2) Rats received consecutive intraperitoneal injections of calcein at 4, 5, and 6 wks of age. At 6 hrs after the final injection, M1s were extracted and replanted with 30 μL of PGA, 30 μL of Emdogain®, or 200 μg of P173 mixed with 30 μL of PGA after 1 hr of air-drying.

In both protocols, rats were killed at 1 wk after replantation. The extraction and replantation of M1s were performed only on the right side, and the left side served as an unextracted control. The maxillae were dissected, fixed by immersion in 4% paraformaldehyde, and embedded in polyester resin (Rigolac 2004; Ouken, Tokyo, Japan) without decalcification. Calcein-labeled ground sections were observed under a fluorescent microscope.

Human Odontoclastic Cell Culture

The protocol for the present experiment involving human samples was approved by the Research Ethics Committee of Tokyo Medical and Dental University, and informed consent was obtained from all volunteers. Extracted shedding deciduous teeth were obtained from healthy volunteers, and periodontal/odontoclastic cells were isolated as previously described (Fukushima *et al.*, 2003). Isolated cells were cultured in α-minimum essential medium (α-MEM; Wako) with 10% fetal bovine serum (FBS; Japan Bioserum Co., Nagoya, Japan) in 12-well plates (Sumitomo Bakelite Co. Ltd, Tokyo, Japan). In some cultures, 20 μg /mL of P173 or 1.3 μg /mL of P172 (porcine recombinant amelogenin lacking first methionine from P173) was added. All cultures were maintained in a humidified, 5% CO_2 atmosphere at 37°C. After culture, cells were fixed with 4% formaldehyde for 10 min, and TRAP staining was performed as previously reported (Udagawa *et al.*, 1990). Cell nuclei were stained by incubation with 4′,6-diamidino-phenyindole (DAPI; Sigma, St. Louis, MO, USA). Immunostaining against anti-human vitronectin receptor (CD51/CD61; BD Biosciences, San Jose, CA, USA) was performed as described (Take *et al.*, 2005) with Histofine (Nichirei Corporation, Tokyo, Japan), according to the manufacturer's instructions.

Statistical Evaluations

We used Student's *t* test to examine the differences in the numbers of cultured cells. We used a one-way ANOVA and PLSD test to examine the differences in values of histomorphometric analysis. All statistical analyses were carried out with Statview (Cary, NC, USA). *P*-values less than 0.05 were considered significant.

RESULTS

The Inhibitory Effect of Amelogenin in the Experimental Root Resorption Model

μCT images showed severe root resorption in M1s of untreated (Figs. 1A-1D) and PGA-treated (Figs. 1E, 1F) M1s at 1 wk after tooth replantation. Resorption was most apparent in the distal surfaces of mesial roots (Fig. 1A). The application of Emdogain® dramatically suppressed the resorption in these areas (Figs. 1G, 1H). Application of 200 μg of P173 also had a considerable suppressive effect on resorption (Figs. 1K, 1L), and a weaker effect was seen at 20 μg (Figs. 1I, 1J).

Histological observations showed significant root resorption in untreated (Fig. 2B) and PGA-treated (Figs. 2A, 2C, 2G) M1s. The most severe resorption of the cementum and root dentin was seen on the distal surfaces of the mesial roots, by μCT (Fig. 2A). Numerous TRAP-positive odontoclasts were present on root surfaces of untreated (Fig. 2B) and PGA-treated (Figs. 2A, 2C, 2G) M1s. The cementum layer was almost totally resorbed from the root surface (Fig. 2G). The application of Emdogain® markedly inhibited cementum/root dentin resorption, and odontoclasts were rarely seen (Figs. 2D, 2H). M1s treated with 200 μg of P173 showed marked suppression of root resorption and reduced numbers of odontoclasts (Figs. 2F, 2I). A 20-μg quantity of P173 also had a moderate inhibitory effect (Fig. 2E). Quantitative analysis showed that dentin resorption was significantly suppressed in groups treated with Emdogain® and P173 compared with the PGA group (Fig. 3A). The odontoclast surfaces (%) (Fig. 3B) and the odontoclast numbers (Fig. 3C) were significantly decreased in groups treated with Emdogain® and 200 μg of P173. A 20-μg quantity of P173 also significantly reduced resorption on odontoclast surfaces (%) (Fig. 3B).

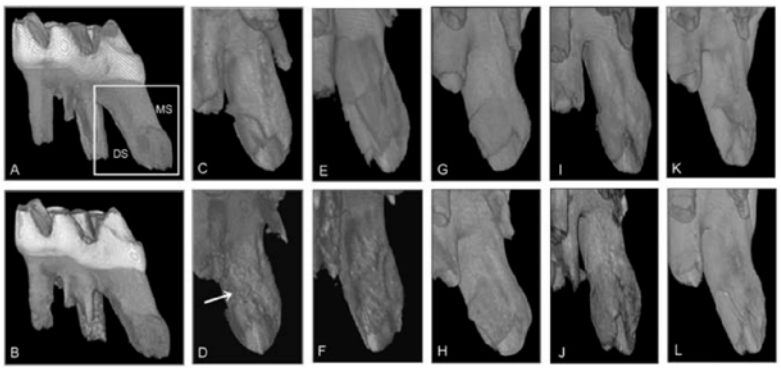

Figure 1. μCT images of the 6-week-old rat M1s before and at 1 wk after replantation. **(A,C,E,G,I,K)** Images before replantation. **(B,D,F,H,J,L)** Images at 1 wk after replantation. Distal surfaces of mesial roots (boxed area in A) are highlighted in C-L. M1s untreated (A-D), treated with the carrier, PGA (E, F), with Emdogain® (G, H), and with 20 μg (I, J) and 200 μg (K, L) of P173 mixed with PGA. Arrow in D = root resorption. DS, distal surface; MS, mesial surface.

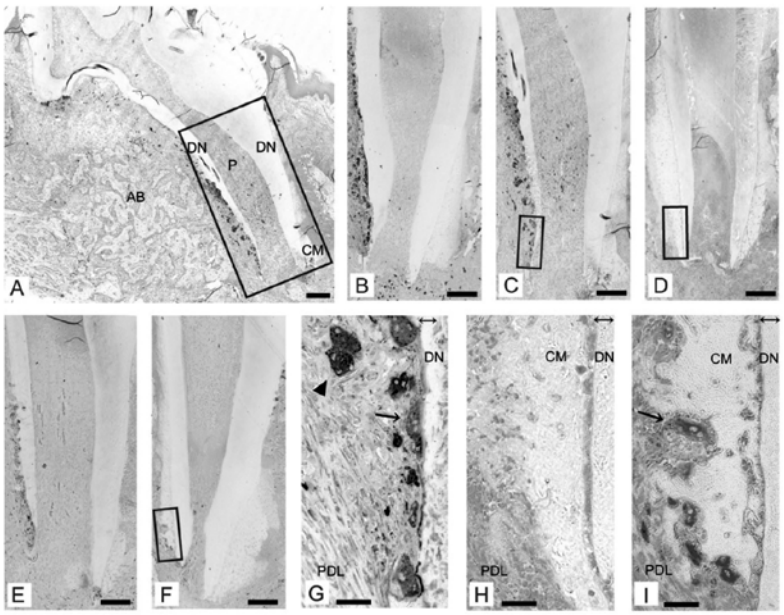

Figure 2. Histological observations of the inhibitory effects of amelogenin and Emdogain® on root resorption. **(A-I)** TRAP staining of 6-week-old rat M1s at 1 wk after replantation (left side of each panel represents the distal side). M1s untreated (B), treated with PGA (A,C), with Emdogain® (D), with 20 (E), and with 200 μg (F) of P173 mixed with PGA. Higher magnification of boxed area (mesial root) in A is shown in C. Higher magnifications of boxed areas in C, D, and F are shown in G, H, and I, respectively. Root dentin is denoted by double-ended arrows in G-I. Bars = 250 μm (A-F) and 25 μm (G-I). Arrowhead in G: TRAP-positive multinucleated cell in the periodontal ligament. Arrows in G and I: TRAP-positive multinucleated odontoclasts on the root surface. AB, alveolar bone; CM, cementum; DN, dentin; P, pulp; PDL, periodontal ligament.

De novo Cementum Formation after Replantation

The effects of extraction, 1 hr of air-drying, and replantation were examined on *de novo* cementum formation in rat teeth. First, calcein-labeling was performed in 6-week-old rats just after the extraction and replantation of M1s (Appendix Fig. 1A). One week after the injection, a calcein-labeled root surface was clearly observed on the unextracted teeth (Appendix Fig. 1B), but not on the replanted teeth (Appendix Fig. 1C), denoting that periodontal tissues had not healed enough in 1 wk for the replanted root surface to be labeled.

Next, rats received injections of calcein at 4, 5, and 6 wks of age, and M1s were extracted and replanted with PGA (Appendix Figs. 1E-1G), Emdogain® (Appendix Figs. 1H-1J), or 200 μg of P173 (Appendix Figs. 1K-1M) at 6 hrs after the final injection (Appendix Fig. 1D). Again, root resorption was apparent in the distal surfaces of mesial roots in PGA-treated teeth (Appendix Fig. 1E), and this was suppressed in both Emdogain®- (Appendix Fig. 1H) and P173-treated (Appendix Fig. 1K) teeth. After 3 injections, 3 labeled layers were seen in the apex of each tooth (Appendix Figs. 1F, 1I, 1L), representing the active cementum formation from ages 4 to 5 wks and from ages 5 to 6 wks. Since the root surface could not be labeled due to the insufficient healing of periodontal tissues in 1 wk after the replantation (Appendix Fig. 1C), *de novo* cementogenesis after replantation was expected to be seen as an unlabeled layer on the outermost calcein-labeled layer of the root surface in the merged images. In contrast to the active cementum formation from ages 4 to 5 wks and from ages 5 to 6 wks, merged images show that *de novo* cementogenesis was scarcely seen on PGA-treated (Appendix Fig. 1G), Emdogain®-treated (Appendix Fig. 1J), or P173-treated (Appendix Fig. 1M) teeth after replantation.

Effect of Amelogenin in the Human Odontoclastic Cell Culture

Large and small TRAP-positive ($TRAP^+$) odontoclastic cells were seen in the human odontoclastic cell cultures (Fig. 4A). The majority of $TRAP^+$ odontoclastic cells were mononuclear, and large cells were multinucleated (Figs. 4B, 4C). Most $TRAP^+$ mononucleated cells formed clusters in the cultures (Fig. 4A). In these cultures, many cells were immunopositive for the anti-vitronectin receptor (Fig. 4D), as has been reported for cultured human osteoclasts (Matsuzaki *et al.*, 1999). The $TRAP^+$ odontoclastic cells were evaluated for

72 hrs (Fig. 4E). The number was greatest at 24 hrs and decreased toward 72 hrs. The effect of amelogenin was examined at 24 hrs (Fig. 4F). Both P172 and P173 significantly decreased the cell numbers (Fig. 4F).

Effect of Amelogenin on RANKL Expression

To examine whether RANK-RANKL signaling was involved in the mechanism, we treated bone marrow cell culture with amelogenin. P173 treatment significantly decreased the numbers of TRAP-positive multinucleated cells and resorption pits, and it also suppressed RANKL expression (Appendix Fig. 2).

DISCUSSION

In this study, porcine amelogenin and Emdogain® inhibited odontoclastic root resorption. Previous studies reported that Emdogain® has an inhibitory effect on root resorption (Hamamoto *et al.*, 2002; Barrett *et al.*, 2005). The present observations support these studies and highlight amelogenin as a major bioactive protein fulfilling this effect in Emdogain®.

In experiments *in vivo*, extraction and replantation of rat M1s were performed. Tooth replantation and transplantation are widely used in mice and rats to evaluate periodontal (Mine *et al.*, 2005) and pulpal (Hasegawa *et al.*, 2007) healing, dental ankylosis (Lustosa-Pereira *et al.*, 2006), and root resorption (Mori *et al.*, 2006). In the present system, numerous resorption lacunae were seen at 1 wk after the replantation in M1s. Root resorption was most apparent in the distal surfaces of the mesial roots. This was probably because the mesial roots are largest and likely to receive the most serious mechanical stress during extraction and replantation.

P172 and P173 reduced the numbers of human cultured odontoclastic cells. These cells express RANK, RANKL, and calcitonin receptor, and exhibit resorbing activity (Fukushima *et al.*, 2003; Takada *et al.*, 2004), as do odontoclasts in tissues (Oshiro *et al.*, 2001; Nanci, 2007). Interestingly, the porcine leucine-rich amelogenin (LRAP) (Gibson *et al.*, 1991) and the mouse full-length amelogenin significantly decreased the cultured osteoclast numbers (Hatakeyama *et al.*, 2006; Nishiguchi *et al.*, 2007). As an underlying mechanism, amelogenin down-regulated the expression of RANKL, but not osteoprotegerin (OPG). Emdogain® treatment has been reported to suppress the expression of RANK and RANKL in rat experimental periodontitis (Fujishiro *et al.*, 2008). If these results are considered together with the down-regulation of RANKL in the bone marrow culture, it is likely that the inhibitory action of amelogenin in this study was due to suppressed RANKL expression.

At 1 wk after replantation, little *de novo* formation of cementum was seen in PGA-treated, Emdogain®-treated, or P173-treated teeth. These observations strongly suggest that the inhibition of root resorption seen in μCT images of Emdogain®- and P173-treated teeth was not reflected by *de novo* cementogenesis in the present limited experimental period.

Since P173 is the predominant amelogenin expressed by porcine ameloblasts (Hu *et al.*, 1996, 2002), this isoform lacking exon 4 was used in the experimental root resorption model. Mice (Simmer *et al.*, 1994) and rats (Li *et al.*, 1995) express

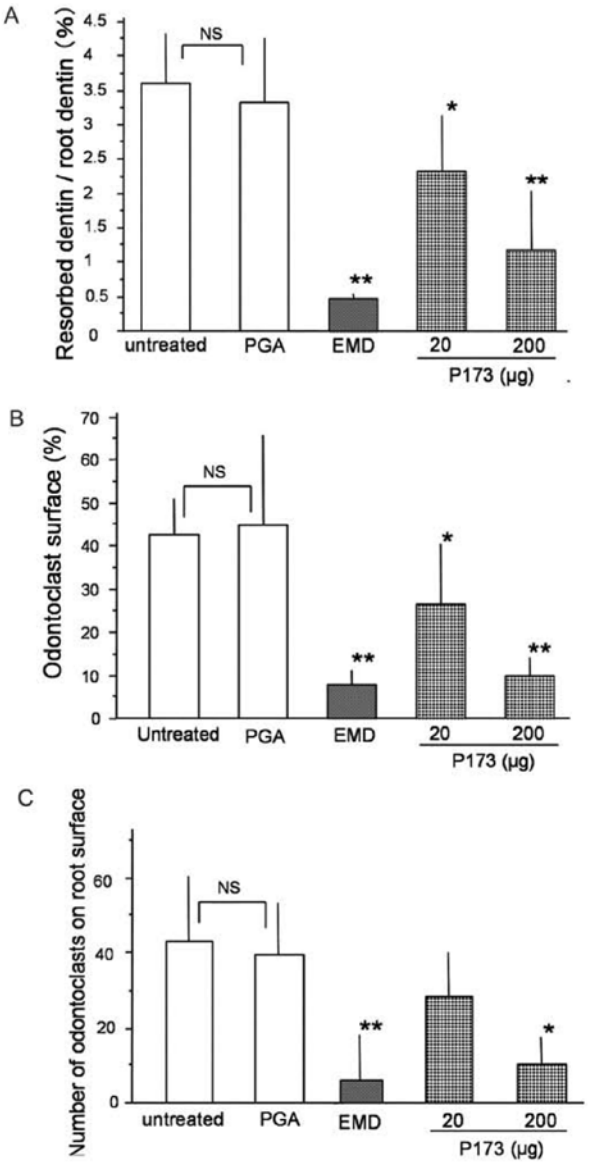

Figure 3. Quantitative analysis of replanted M1s at 1 wk after replantation, without treatment (untreated), treated with PGA, treated with Emdogain® (EMD), and treated with 20 and 200 μg of P173 mixed with PGA. **(A)** Resorbed dentin *per* total root dentin surface (%). **(B)** Odontoclast surface *per* root surface (%). **(C)** Odontoclast number. Odontoclasts were identified as TRAP-positive multinucleated cells (containing more than 2 nuclei) attached to the root surfaces. The analysis was performed from the apex to the bifurcation area of each mesial root. The data for each rat are the average value measured in 3 sections which were more than 20 μm apart from each other. Only sections in the middle part of the tooth root were used for the analysis, and those of buccal and lingual ends (within 40 μm of both ends) were excluded. All data are expressed as means ± SD (n = 7). NS: not significant compared with the PGA group. $^{**}p < 0.01$ and $^{*}p < 0.05$ compared with the PGA group.

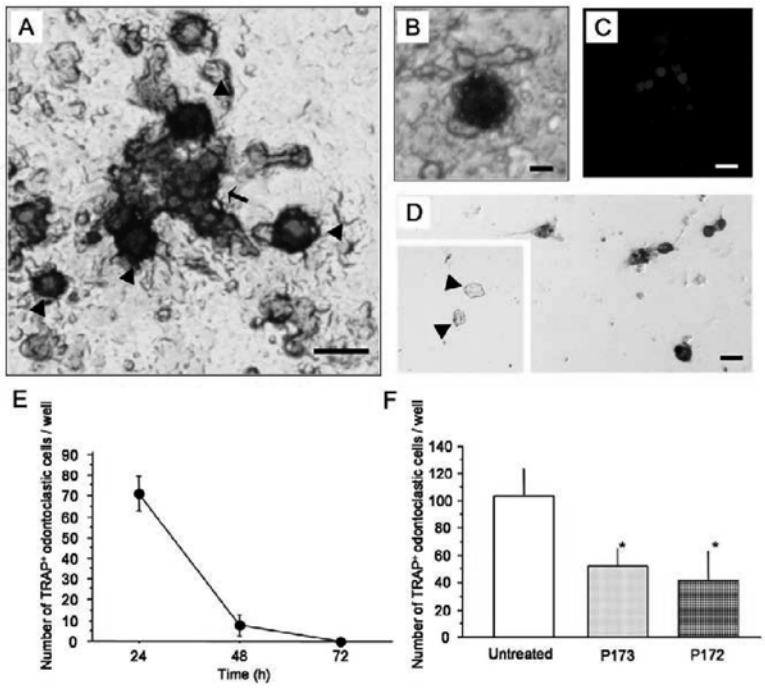

Figure 4. The effect of amelogenin on cultured human odontoclastic cells. **(A,B)** TRAP staining of cultured cells. **(C)** DAPI staining of the cultured cell shown in B. **(D)** Immunostaining with anti-human vitronectin receptor antibody ([insert] the primary antibody was replaced with phosphate buffer; arrowheads denote cells which were stained negatively). Bars = 50 μm (A,D), 20 μm (B,C). **(E)** Numbers of TRAP-positive ($TRAP^+$) odontoclastic cells cultured for 24, 48, and 72 hrs. Data are expressed as means ± SD from triplicate cultures. **(F)** Numbers of human $TRAP^+$ odontoclastic cells cultured for 24 hrs, with or without 20 μg /mL of P173 or 1.3 μg /mL of porcine recombinant amelogenin (P172). Data are expressed as means ± SD (n = 10). $^*p < 0.01$ from amelogenin-untreated cultures.

different amelogenin isoforms containing and lacking exon 4 (called [A+4] and [A-4], respectively). Mouse [A+4] and [A-4] had differential effects on cultured tooth germs, and only the former could induce the polarization of differentiated odontoblasts and ameloblasts with the induction of dentin formation (Tompkins *et al*., 2005). Furthermore, when implanted in the hind thigh muscle, rat [A+4] was reported to induce an abundant network of capillaries, whereas [A-4] was less effective (Veis *et al*., 2000). In the pig, P190 including exon 4 has also been reported, but in a much lesser amount in tooth enamel (Yamakoshi *et al*., 1994). Porcine exon 4 has a unique gene structure and lacks homology with the mouse exon 4 (Hu *et al*., 2002). It would be interesting to examine the effects of P190 and isoforms of other species in the present experimental model, to clarify the specific protein fragment essential for the inhibition of root resorption.

ACKNOWLEDGMENTS

This study was supported by Grants-in-Aid for Scientific Research (16390604, 16659570, and 18390552), a Grant for Supporting Projects for Strategic Research at Nihon University School of Dentistry at Matsudo (Team: Dental morphogenesis) from the Ministry of Education, Culture, Sports, Science, and Technology of Japan, and a grant from the Japanese Ministry of Education, Global Center of Excellence (GCOE) Program, 'International' Research Center for Molecular Science in Tooth and Bone 'Diseases.' The authors thank Dr. J.P. Simmer (Michigan University), Dr. K. Okabe (Fukuoka Dental College), Dr. S. Oida (Tsurumi University), Dr. H. Fukushima (Kyushu Dental College), Dr. M. Saito (Osaka University), and Dr. M. Shiga (Tokyo Medical and Dental University) for valuable advice. Preliminary reports were presented at the 83th General Session & Exhibition of the IADR and the 9th International Conference on Tooth Morphogenesis & Differentiation.

REFERENCES

Andreasen JO (1985). External root resorption: its implication in dental traumatology, paedodontics, periodontics, orthodontics and endodontics. *Int Endod J* 18:109-118.

Andreasen JO, Hjørting-Hansen E (1966). Replantation of teeth. II. Histological study of 22 replanted anterior teeth in humans. *Acta Odontol Scand* 24:287-306.

Barrett EJ, Kenny DJ, Tenenbaum HC, Sigal MJ, Johnston DH (2005). Replantation of permanent incisors in children using Emdogain. *Dent Traumatol* 21:269-275.

Brezniak N, Wasserstein A (2002). Orthodontically induced inflammatory root resorption. Part I: The basic science aspects. *Angle Orthod* 72:175-179.

Fong CD, Hammarström L (2000). Expression of amelin and amelogenin in epithelial root sheath remnants of fully formed rat molars. *Oral Surg Oral Med Oral Pathol Oral Radiol Endod* 90: 218-223.

Foo M, Jones A, Darendeliler MA (2007). Physical properties of root cementum: Part 9. Effect of systemic fluoride intake on root resorption in rats. *Am J Orthod Dentofacial Orthop* 131:34-43.

Fujishiro N, Anan H, Hamachi T, Maeda K (2008). The role of macrophages in the periodontal regeneration using Emdogain® gel. *J Periodontal Res* 43:143-155.

Fukushima H, Kajiya H, Takada K, Okamoto F, Okabe K (2003). Expression and role of RANKL in periodontal ligament cells during physiological root-resorption in human deciduous teeth. *Eur J Oral Sci* 111:346-352.

Fuss Z, Tsesis I, Lin S (2003). Root resorption—diagnosis, classification and treatment choices based on stimulation factors. *Dent Traumatol* 19:175-182.

Gibson CW, Golub E, Ding WD, Shimokawa H, Young M, Termine J, *et al.* (1991). Identification of the leucine-rich amelogenin peptide (LRAP) as the translation product of an alternatively spliced transcript. *Biochem Biophys Res Commun* 174:1306-1312.

Hamamoto Y, Kawasaki N, Jarnbring F, Hammarström L (2002). Effects and distribution of the enamel matrix derivative. Emdogain in the periodontal tissues of rat molars transplanted to the abdominal wall. *Dent Traumatol* 18:12-23.

Hammarström L, Heijl L, Gestrelius S (1997). Periodontal regeneration in a buccal dehiscence model in monkeys after application of enamel matrix proteins. *J Clin Periodontol* 24:669-677.

Hasegawa T, Suzuki H, Yoshie H, Ohshima H (2007). Influence of extended operation time and of occlusal force on determination of pulpal healing pattern in replanted mouse molars. *Cell Tissue Res* 329:259-272.

Hatakeyama J, Sreenath T, Hatakeyama Y, Thyagarajan T, Shum L, Gibson CW, *et al.* (2003). The receptor activator of nuclear factor-kappa B ligand-mediated osteoclastogenic pathway is elevated in amelogenin-null mice. *J Biol Chem* 278:35743-35748.

Hatakeyama J, Philp D, Hatakeyama Y, Haruyama N, Shum L, Aragon MA, *et al.* (2006). Amelogenin-mediated regulation of osteoclastogenesis, and periodontal cell proliferation and migration. *J Dent Res* 85:144-149.

Hu CC, Bartlett JD, Zhang C, Qian Q, Ryu OH, Simmer JP (1996). Cloning, cDNA sequence, and alternative splicing of porcine amelogenin mRNAs. *J Dent Res* 75:1735-1741.

Hu CC, Ryu OH, Yamakoshi Y, Zhang CH, Cao X, Qian Q, *et al.* (2002). Pig amelogenin gene expresses a unique exon 4. *Connect Tissue Res* 43:435-440.

Li R, Li W, DenBesten PK (1995). Alternative splicing of amelogenin mRNA from rat incisor ameloblasts. *J Dent Res* 74:1880-1885.

Lustosa-Pereira A, Garcia RB, de Moraes IG, Bernardineli N, Bramante CM, Bortoluzzi EA (2006). Evaluation of the topical effect of alendronate on the root surface of extracted and replanted teeth. Microscopic analysis on rats' teeth. *Dent Traumatol* 22:30-35.

Matsuzaki K, Katayama K, Takahashi Y, Nakamura I, Udagawa N, Tsurukai T, *et al.* (1999). Human osteoclast-like cells are formed from peripheral blood mononuclear cells in a coculture with SaOS-2 cells transfected with the parathyroid hormone (PTH)/PTH-related protein receptor gene. *Endocrinology* 140:925-932.

Maycock J, Wood SR, Brookes SJ, Shore RC, Robinson C, Kirkham J (2002). Characterization of a porcine amelogenin preparation, EMDOGAIN, a biological treatment for periodontal disease. *Connect Tissue Res* 43:472-476.

Mine K, Kanno Z, Muramoto T, Soma K (2005). Occlusal forces promote periodontal healing of transplanted teeth and prevent dentoalveolar ankylosis: an experimental study in rats. *Angle Orthod* 75:637-644.

Mori GG, Garcia RB, Gomes de Moraes I (2006). Morphometric and microscopic evaluation of the effect of solution of acetazolamide as an intracanal therapeutic agent in late reimplanted rat teeth. *Dent Traumatol* 22:36-40.

Nanci A, editor (2007). Physiologic tooth movement: eruption and shedding. In: Ten Cate's oral histology—development, structure, and function. 7th ed. St. Louis, MO, USA: Mosby, pp. 268-289.

Nishiguchi M, Yuasa K, Saito K, Fukumoto E, Yamada A, Hasegawa T, *et al.* (2007). Amelogenin is a negative regulator of osteoclastogenesis via downregulation of RANKL, M-CSF and fibronectin expression in osteoblasts. *Arch Oral Biol* 52:237-243.

Oshiro T, Shibasaki Y, Martin TJ, Sasaki T (2001). Immunolocalization of vacuolar-type H^+-ATPase, cathepsin K, matrix metalloproteinase-9, and receptor activator of NFkappaB ligand in odontoclasts during physiological root resorption of human deciduous teeth. *Anat Rec* 264:305-311.

Simmer JP, Hu CC, Lau EC, Sarte P, Slavkin HC, Fincham AG (1994). Alternative splicing of the mouse amelogenin primary RNA transcript. *Calcif Tissue Int* 55:302-310.

Suda N, Baba O, Udagawa N, Terashima T, Kitahara Y, Takano Y, *et al.* (2001). Parathyroid hormone-related protein is required for normal intramembranous bone development. *J Bone Miner Res* 16:2182-2191.

Takada K, Kajiya H, Fukushima H, Okamoto F, Motokawa W, Okabe K (2004). Calcitonin in human odontoclasts regulates root resorption activity via protein kinase A. *J Bone Miner Metab* 22:12-18.

Take I, Kobayashi Y, Yamamoto Y, Tsuboi H, Ochi T, Uematsu S, *et al.* (2005). Prostaglandin E_2 strongly inhibits human osteoclast formation. *Endocrinology* 146:5204-5214.

Termine JD, Belcourt AB, Christner PJ, Conn KM, Nylen MU (1980). Properties of dissociatively extracted fetal tooth matrix proteins. I. Principal molecular species in developing bovine enamel. *J Biol Chem* 255:9760-9768.

Tompkins K, Alvares K, George A, Veis A (2005). Two related low molecular mass polypeptide isoforms of amelogenin have distinct activities in mouse tooth germ differentiation in vitro. *J Bone Miner Res* 20:341-349.

Udagawa N, Takahashi N, Akatsu T, Tanaka H, Sasaki T, Nishihara T, *et al.* (1990). Origin of osteoclasts: mature monocytes and macrophages are capable of differentiating into osteoclasts under a suitable microenvironment prepared by bone marrow-derived stromal cells. *Proc Natl Acad Sci USA* 87:7260-7264.

Veis A, Tompkins K, Alvares K, Wei K, Wang L, Wang XS, *et al.* (2000). Specific amelogenin gene splice products have signaling effects on cells in culture and in implants in vivo. *J Biol Chem* 275: 41263-41272.

Yamakoshi Y, Tanabe T, Fukae M, Shimizu M (1994). Porcine amelogenins. *Calcif Tissue Int* 54:69-75.

整形外科学分野

四宮 謙一

医歯学総合研究科・先端医療開発学系専攻
脊椎・脊髄神経外科学・教授

1. 研究の課題名

(1) 多孔質ハイドロキシアパタイト・コラーゲン複合体の開発と評価

Development and evaluation of a novel artificial bone – porous hydroxyapatite / collagen composite.

新規人工骨として開発を行ってきた多孔質ハイドロキシアパタイト・コラーゲン複合体（HAp/Col）の臨床治験を7施設（東京医科歯科大学、京都大学、慶応大学、帝京大学、国立がんセンター、癌研究会附属病院、土浦協同病院）において実施中である。このHAp/Colは生体吸収性であり、またその高い骨伝導能の理由として、破骨細胞と骨芽細胞のカップリングが考えられていることから、近年急激に普及した骨粗鬆症治療薬であるビスフォスフォネートにより、移植後の骨形成、インプラントの吸収性に影響を受ける可能性が高いと考えられた。そこでウサギ大腿骨に多孔質HAp/Colを移植し、毎週ビスフォスフォネートの投与を行った。その結果、投与群ではインプラント周囲の骨形成、インプラントの吸収ともにコントロール群に比較して抑制されていることが確認された。この結果は実際に臨床でHAp/Colを使用する際にはビスフォスフォネートの投与を一時的に休止するなど、考慮する必要があることが示すものであると考えられた。また、破骨細胞と骨芽細胞のカップリングがHAp/Colの骨伝導能のメカニズムのひとつとして働いていることを示唆する結果であると考えられた。

(2) Bone Morphogenetic Proteinと骨髄間葉系細胞を使用した大型骨欠損での骨再生

Reconstruction of large bone defects using bone morphogenetic proteins and bone marrow stromal cells.

イヌやサルの巨大骨欠損モデルを用いて、骨髄由来間葉系細胞（MSC）の骨再生への応用研究を行っている。サルでは約5cmの大腿骨骨欠損を作成し、多孔質β-三リン酸カルシウム（TCP）に培養MSCを導入し移植を行い、その骨再生能および再生された骨組織の機能的評価を進めている。また、実際の臨床の骨悪性腫瘍手術で行われている温熱処理骨の再移植では、移植骨が生きた骨組織が再生される前に吸収されてしまうという問題がある。そこで、イヌの大腿骨を用いて、これを温熱処理し再び戻し移植を行う際に、培養MSCを移植し、温熱処理骨の吸収抑制ができるか検討を進めている。さらにはヒトMSCを用い、より高い骨形成能を有するMSCを獲得するため手法の開発を進めている。また、骨誘導性の増殖因子であるBone morphogenetic protein（BMP）を使用して大型の骨組織を再生すべく、BMPのキャリアとしての多孔質HAp/Colの有効性を確認したり、BMPの効果をより効率よく働かせるため多剤併用の効果などを検討している。

(3) 分化におけるRunxの意義の解明

軟骨の分化調節の分子機構を、我々が独自に樹立した変形性関節症を呈する遺伝子改変マウスモデルを用いて解明することを目的とし、それらのモデルマウスを用いて変形性関節症の発症の分子機構の解明、治療法の確立を検討するため以下の検討を行った。Runxトランスジェニックマウスの解析を組織学的に進めた。Runx2、Runx1tgマウスの椎体に明らかな異常はなく、椎間板では免疫組織学的染色によりX型コラーゲンの発現をみとめ、またサフラニン染色で軟骨染色性が低下しており、いずれも椎間板変性に合致する変化が認められた。マウス胎児の椎間板を用いてIn situ hybrydization法および免疫組織染色でRunxファミリーの発現を検討したところ、Runx2の発現が将来の椎間板部位に一致して認められたが、Runx1やRunx3の発現は認められなかった。さらに

我々はマウス尾椎をばねで圧迫させることで荷重の増大による椎間板変性モデルを作成したところ、Runx2ノックインマウスでは椎体終板特異的にRunx2の発現が上昇することを見出した。また、ヒト椎間板ヘルニア患者において対照群と比較して有意なRunx2遺伝子発現の上昇を見出した。これらの一連の検討から、Runx2の発現誘導が椎間板変性を惹起する可能性が明らかになった。

2.

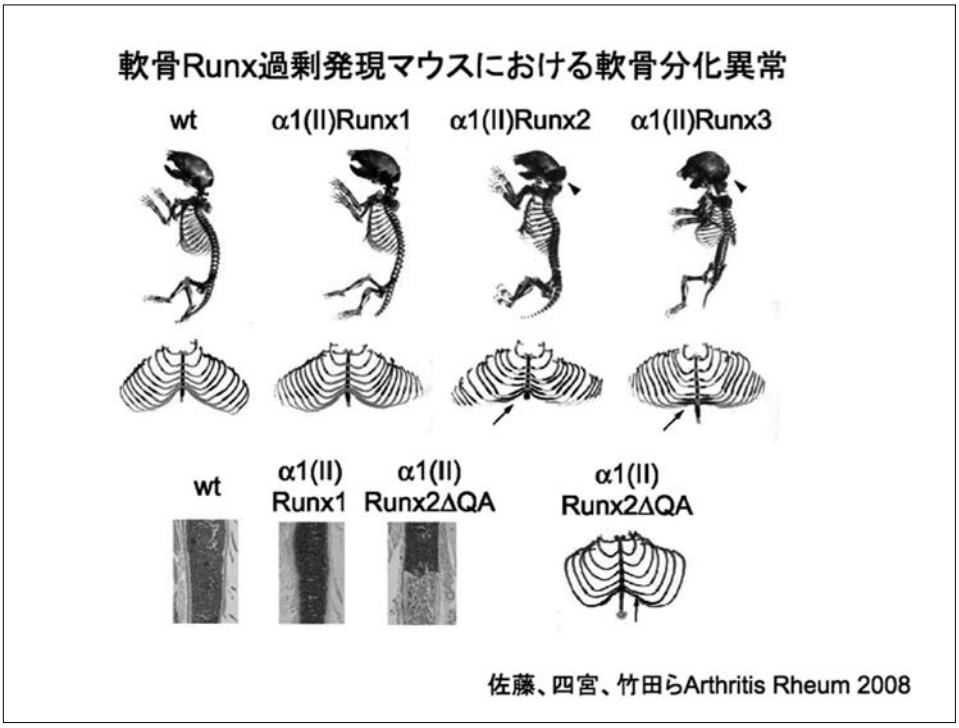

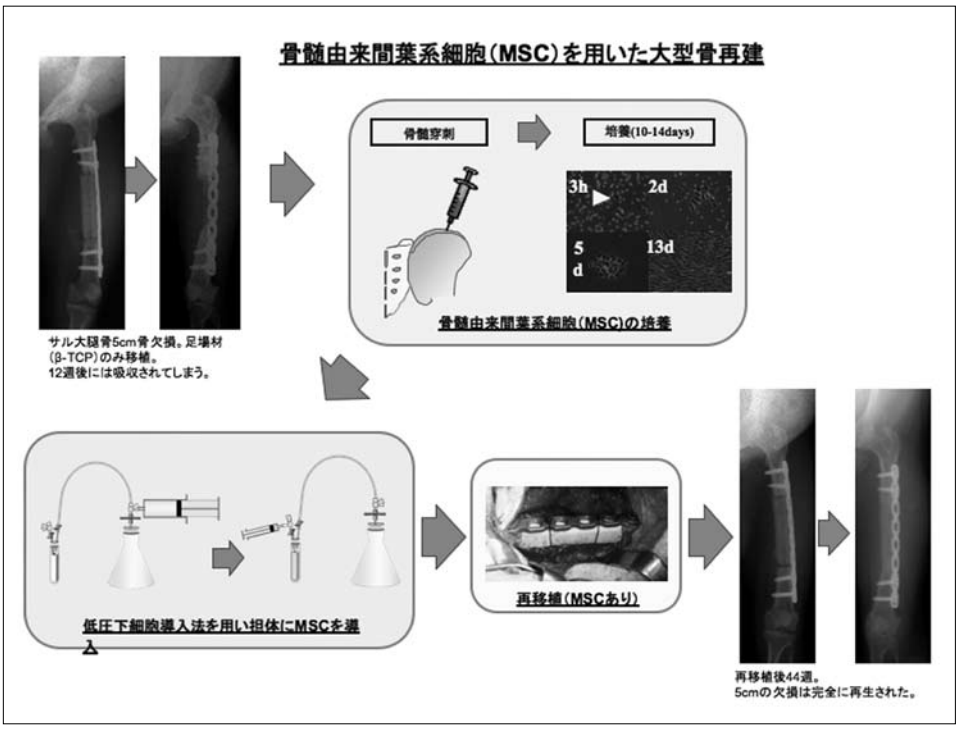

3. 2008年、2009年（平成21年3月までの）に発表した全ての研究内容についての英文要約

We tested the effects of a bisphosphonate, alendronate, on bone formation and implant absorption at a porous HAp/Col implanted site. Porous HAp/Col is a bio-absorbable bone void filler, and adsorbs bisphosphonates. Alendronate administration decreased bone formation at the implant site and retarded absorption of the HAp/Col.

We developed a bone regeneration method using bone marrow stromal cells and autologous plasma and demonstrated its efficacy using a monkey ectopic bone formation model. We have already started the evaluation of its efficacy for regeneration of large bone defects and the function of the regenerated bone.

Runx2 is a transcription factor that regulates chondrocyte differentiation. We attempted to address the role of the different Runx proteins (Runx1, Runx2 or Runx3) in chondrocyte differentiation using chondrocyte-specific Runx transgenic mice. α (1) II-Runx3 mice developed ectopic mineralization of cartilage ,like in α (1) II-Runx2 mice. In contrast, α (1) II-Runx1 mice displayed no sign of ectopic mineralization. Surprisingly, α (1) II-Runx1 and α (1) II-Runx2 mice developed scoliosis due to IVD degeneration characterized by an accumulation of extracellular matrix and ectopic chondrocyte hypertrophy. During mouse embryogenesis, Runx2, but not Runx1 or Runx3, was expressed in the IVD. Moreover, in a mouse model, as in human patients with IVD degeneration, there was significant upregulation of Runx2 expression. In conclusion, we demonstrated that Each Runx has a distinct yet overlapping role during chondrocyte differentiation. Runx2 contributes to the pathogenesis of IVD degeneration.

4. 本事業に関連して世界的な研究拠点形成に向けて、以下の点で改善・整備等されたこと

A（研究拠点体制）

・大学外との連携を図り、また研究環境（設備など）を整備することによって、研究拠点の基礎を立ち上げた（物質材料研究機構、産業技術総合研究所）。

・また、大学内連携を図り、他分野と共同で研究を行っている。（生体材料工学研究所・有機材料分野、難治研究所・分子薬理学）

・企業との連携（オリンパス、HOYA、小林メディカル、ストライカーバイオテック）により、研究設備の充実を図るとともに、基礎と臨床との橋渡し研究領域を充実させた。

B（研究教育環境）

・週に3回、論文の抄読会や研究報告会を実施することにより、分子生物学、骨・軟骨組織学、骨再生学の研究、教育体制を確立した。

・科学研究費補助金や企業との共同研究により外部資金を得ることによって、研究環境を整備（研究室の整備）し得た。

C（人材確保）

・寄付講座を開設し、研究に専念できる人材を確保した。

D（人材育成）

・10名（内留学生1名、他大大学院生1名）の大学院生および1名の専攻生（留学生）に対して、骨・軟骨に関する研究教育、指導を行った。

E（国際化）

・2名の留学生に研究教育、指導を行った。

5. GCOE事業を推進するに当たって力を入れた点

・企業を含む大学内外との連携を強化するなどして、骨・軟骨に関する基礎領域だけでなく、臨床応用を目指した研究にも重点を置いた。

・分野内で研究経過・成果に関するdiscussionを重ねるとともに、外部への研究成果の発表の機会を増やすよう努力した。

6. 英文原著論文

◎Torigoe I, Sotome S, Tsuchiya A, Yoshii T, Maehara H, Sugata Y, Ichinose S, Shinomiya K, Okawa A. Bone Regeneration with Autologous Plasma, Bone Marrow Stromal Cells, and Porous beta-Tricalcium Phosphate in Nonhuman Primates. Tissue engineering part A.（in press）2009 Feb 3. [Epub ahead of print]

Yoshii T, Sotome S, Torigoe I, Tsuchiya A, Maehara H, Ichinose S　Shinomiya K. Fresh Bone marrow introduction into porous scaffolds using a simple low-pressure loading method for effective osteogenesis　in a rabbit model. Journal of orthopaedic research. 27:1, 2009

Tokumoto S, Sotome S, Torigoe I, Omura K, Shinomiya K. Effects of cryopreservation on bone marrow derived mesenchymal cells of a nonhuman primate. Journal of medical and dental science. 55: 137, 2008

Tsuchiya A, Sotome S, Asou Y, Kikuchi M, Koyama Y, Ogawa T, Tanaka J, Shinomiya K. Effects of pore size and

implant volume of porous hydroxyapatite/collagen （HAp/Col）on bone formation in a rabbit bone defect model. Journal of medical and dental science. 55: 91, 2008

Sato S, Kimura A, Ozdemir J, Asou Y, Miyazaki M, Jinno T, Ae K, Liu X, Osaki M, Takeuchi Y, Fukumoto S, Kawaguchi H, Haro H, Shinomiya K, Karsenty G, Takeda S: The distinct role of the Runx proteins in chondrocyte differentiation and intervertebral disc degeneration: Findings in murine models and in human disease. Arthritis Rheum 58（9）: 2764-75, 2008.

Tominaga H, Maeda S, Hayashi M, Takeda S, Akira S, Komiya S, Nakamura T, Akiyama H, Imamura T: CCAAT/Enhancer-binding Protein Promotes Osteoblast Differentiation by Enhancing Runx2 Activity with ATF4. Mol. Biol. Cell 19（12）: 5373-5386, 2008.

Takeda S, Karsenty G: Molecular bases of the sympathetic regulation of bone mass. Bone 42（5）: 837-40, 2008.

Takeda S: Central control of bone remodelling. J Neuroendocrinol 20（6）: 802-7, 2008.

Takeda S: Osteoporosis: A neuroskeletal disease? Int J Biochem Cell Biol 2008.

7. 著書

Takeda , S., Ducy, P. Central control of bone remodeling（ book chapter ）/ “ Principle in bone biology”Elsevier, c2008

竹田秀:【糖尿病と内分泌機能変化】自律神経機能からみた糖尿病と骨カルシウム代謝の接点. ホルモンと臨床 56（5）: 491-496, 2008.

竹田秀:【内科医のための骨粗鬆症】中枢神経系による骨代謝の制御. Mebio 25（8）: 18-23, 2008.

竹田秀:【骨・軟骨研究の基礎と臨床】基礎編　トピックス　骨代謝を制御する中枢神経系の役割. THE BONE 22（3）: 325-329, 2008.

竹田秀:【メタボリックシンドロームと骨】肥満者の骨は異常なのか. Clinical Calcium 18（5）: 632-637, 2008.

竹田秀: 骨と食欲を調節する神経ペプチド　ニューロメジンU. 整形外科 59（2）: 148, 2008.

竹田秀:【ゲノムからみた骨・関節疾患】骨代謝と全身をむすぶ遺伝子. Clinical Calcium 18（2）: 216-221, 2008.

8. 特許取得、特許申請

「生体内薬物徐放材料の製造方法」発明者:早乙女進一、四宮謙一他、特許番号4204772、特許取得日2008年10月24日

「多孔質複合材料の製造方法」発明者:早乙女進一、四宮謙一他、特許番号3727059（国内）、特許取得日2005年10月7日、特許番号7163965（アメリカ合衆国）、特許取得日2007年1月16日

「複合生体材料」発明者:早乙女進一、四宮謙一他、特許番号3770555、特許取得日2006年2月17日　その他米国、カナダ取得

9. 平成21年3月までの自己評価

研究も概ね計画通り進めることができ、学会発表、論文発表も、質、内容的ともに十分な成果を得ることができたと考えている。

10. 学会発表（英文）

◎Sugata Y, Sotome S, Maehara H, Kawasaki Y, Yuasa M, Mochizuki N, Hirano M, Shinomiya K. The Influence of Bisphosphonate Treatment on a Hydroxyapatite-Collagen Composite. 55th Annual meeting of the orthopaedic research society. July 22-25, 2009, poster presentation, Las Vegas

Torigoe I, Sotome S, Tsuchiya A, Yoshii T, Maehara H, Sugata Y, Shinomiya K.　Bone regeneration with autologous plasma, bone marrow stromal cells, and porous beta-tricalcium phosphate in non-human primates. 54th Annual meeting of the orthopaedic research society. March 2-5, 2008, poster presentation, San Francisco

S. Takeda: Central control of bone metabolism. Annual Meeting of Korean Endocrine Society（2008.5 ソウル　韓国）

S. Takeda: A New Aspect of Central Control of Bone Remodelling: Basic Scientific Symposia: The New Era of Locomotive Science, APLAR（2008.9　横浜）

The Regulation of Osteoblast Differentiation by MicroRNA H. Inose, A. Kimura, M. Iwasaki, K. Shinomiya, S. Takeda ASBMR annual meeting示説（2008.9）

11. 学会発表（和文）

菅田裕美、早乙女進一、前原秀二、川崎雄一、湯浅将人、四宮謙一、望月直美、平野昌弘　:ビスフォスフォネートが生体吸収性骨補填材の吸収と骨形成に与える影響.第28回整形外科セラミック・インプラント研究会、横浜、2008.12.6

前原秀二, 早乙女進一, 鳥越一郎, 吉井俊貴, 川崎雄一, 菅田祐美, 平野昌弘, 望月直美, 四宮謙一　:多孔質ハイドロキシアパタイト/コラーゲン複合体（HAp/Col）とFGF-2を用いた骨軟骨欠損の修復.第23回日本整形外科基礎学術集会、京都、2008.10.23-24

早乙女進一, 前原秀二, 吉井俊貴, 鳥越一郎, 菅田祐美, 新井嘉容, 川端茂徳, 加藤剛, 大川淳, 四宮謙一　:新鮮骨髄液の多孔質β-TCPへの低圧下導入法と臨床応用.第23回日本整形外科学会基礎学術集会、京都、2008.10.23-24

早乙女進一, 土谷明男, 鳥越一郎, 吉井俊貴, 前原秀次, 望月直美, 平野昌弘, 四宮謙一　:多孔質HAp/Col大量移植時の組織学的検討および安全性の検討.第81回日本整形外科学会総会、札幌、2008.5.22-25

鳥越一郎、早乙女進一、土谷明男、吉井俊貴、前原秀二、川崎雄一、菅田裕美、四宮謙一　:骨髄間質細胞/多孔質β-TCP複合体による新生骨形成におけるフィブリンと血清の関与.第7回日本再生医療学会総会、名古屋、2008.3.13-14

猪瀬弘之, 竹田秀, 佐藤信吾, 岩崎牧子, 四宮謙一: 骨芽細胞分化におけるマイクロRNAの意義（第2報）. 日本整形外科学会2008.

冨永博之, 前田真吾, 林真琴, 竹田秀, 中村孝志, 秋山治彦, 今村健志, 小宮節郎: C/EBPβノックアウトマウスでは骨形成が遅延する. 日本整形外科学会2008.

鈴木大, 山田篤, 安原理佳, 木村文子, 妻木範行, 竹田秀, 中村雅典, 饗場篤, 上條竜太郎: 低分子量Gタンパク質Rac1は四肢形成に必須である. 補体シンポジウム2008.

猪瀬　弘之、木村　文子、四宮　謙一、竹田　秀: マイクロRNAによる骨芽細胞分化の調節,日本骨代謝学会学術集会 2008.

木村文子, 猪瀬弘之, 岩崎牧子, 矢野文子, 池田敏之, 川口浩, 鄭雄一, 四宮謙一, 竹田秀Runx1はRunx2と協調的に軟骨分化を調節する-Runx1コンディショナルノックアウトマウスを用いた検討 日本骨代謝学会学術集会2008

12. 受賞

平成20年　日本骨代謝学会奨励賞

13. 外部資金の獲得状況

（科学研究費補助金、受託研究費、外部財団の助成など）

厚生労働科学研究費補助金　（長寿科学総合研究事業）
研究題目:高齢者の腰痛症に係る効果的な診断・治療・リハビリテーション等の確立
分担:四宮　謙一
期間:平成18年-平成20年
研究費総額:\6,000,000.-　平成18年度、平成19年、平成20年度　各\2,000,000.-

厚生労働科学研究費補助金（難治性疾患克服研究事業）
研究題目:脊柱靭帯骨化症に関する調査研究
分担:四宮　謙一
期間:平成20年-平成22年
研究費総額:平成20年度\1,000,000.-

厚生労働科学研究費補助金（地域医療基盤開発推進研究事業）
研究題目:診療ガイドラインの新たな可能性と課題:患者・一般国民との情報共有と医療者の生涯学習
分担:四宮　謙一
期間:平成19年-平成21年
研究費総額:平成19年度\500,000.-　平成20年度\500,000.-

科学研究費補助金（基盤研究B）
研究題目:神経-骨のネットワークに注目した中枢性骨代謝制御機構の解析
代表:竹田　秀
期間:平成20年度
研究費総額:\7,800,000.-

科学研究費補助金（基盤研究C）
研究題目:Runx1による軟骨初期分化調節の分子機構の解明と軟骨再生医療への応用
代表:神野　哲也
期間:平成20年度
研究費総額:\1,300,000.-

科学研究費補助金（基盤研究C）
研究題目:靭帯骨化症の分子基盤-Run×3遺伝子欠損マウスを用いた検討-
代表:阿江　啓介
期間:平成20年度
研究費総額:\1,560,000.-

科学研究費補助金（基盤研究C）
研究題目:RNA干渉を用いた骨芽細胞、脂肪細胞分化調節因子の新規同定とその機能解析
代表:新井　嘉容
期間:平成18年-平成20年
研究費総額:平成18年度\1,500,000.- 平成19年度\1,300,000.- 平成20年度\1,300,000.-

科学研究費補助金（基盤研究C）
研究題目:末梢神経損傷に対する低分子Gタンパク質発現制御を標的とした遺伝子治療の確立
代表:若林　良明
期間:平成20年度
研究費総額:\1,430,000.-

科学研究費補助金（基盤研究C）
研究題目:メタボリックシンドロームに伴う関節軟骨変性の分子機構解析
代表:加藤　剛
期間:平成19年-平成20年
研究費総額:平成19年度\1,560,000.- 平成20年度\1,430,000.-

科学研究費補助金（若手研究B）
研究題目:大型骨組織再生を目指した骨髄間葉系細胞を用いた治療法の総合的研究
代表:早乙女　進一
期間:平成19年-平成20年
研究費総額:平成19年度\1,700,000.- 平成20年度\2,080,000.-

共同研究費（オリンパス株式会社）
研究題目:骨髄間葉系細胞/βTCP複合体による骨形成能の検討.民間との共同研究
代表:四宮　謙一
期間:平成平成19年-平成20
研究費総額:平成19年度\2,750,000.- 平成20年度\2,200,000.-

共同研究費（HOYA株式会社）
研究題目:アパタイト/コラーゲン多孔体（PX880）に対するビスフォスフォネート全身投与の影響
代表:早乙女　進一
期間:平成20年-平成21年
研究費総額:平成20年度\993,300.-

研究助成金（上原財団）
研究題目:神経と骨連関による骨代謝制御の解析
代表:竹田　秀
期間:平成20年度
研究費総額:\5,000,000.-

14. 特別講演、招待講演

2008/3/22
徳島県臨床整形外科医会学術講演会
阿波観光ホテル （徳島県）
「頚椎OPLLの診断と治療」

2008/4/25
第37回日本脊椎脊髄病学会
京王プラザホテル （東京都）
「Spectrum of Degenerative Disease : Molecular Basis of Disc Degeneration in Surgical Treatment」

2008/9/6
第115回愛媛整形外科集談会
愛媛医師会館 （愛媛県）
「人工骨使用の状況と将来」

2008/8/31
第19回安比夏季セミナー
ホテル安比グランド （岩手県）
「細胞を用いた人工骨による骨再生治療」

2008/9/27
鹿児島県臨床整形外科医会
城山観光ホテル （鹿児島県）
「人工骨使用の現状と将来」

2008/10/19
第106回茨城県整形外科集談会
茨城県総合福祉会館 （茨城県）
「人工骨の現状と未来」
2008/11/1
第16回日本腰痛学会ランチョンセミナー
シェーンバッハ・サボー （東京都）
「腰痛疾患のガイドラインについて」
2008/12/13
第24回整形外科カレントコンセプト
フォーシーズンホテル椿山荘東京 （東京都）
「人工骨を用いた骨再生の現状と未来」
2008/5
S. Takeda: Neuronal control of bone metabolism. Korean Bone and Mineral Society annual meeting
（韓国）

15. 主催学会

第38回日本臨床神経生理学会学術大会
2008/11/12～11/14 神戸国際会議場
第45回日本臨床神経生理学会技術講習会
2008/11/10.11 神戸国際会議場

16. 新聞、雑誌、TV報道

・新聞 日本経済新聞 「頚椎症」2008.3.25
・テレビ TBS（BS-i）「腰痛」 2008.3
・ラジオ日本 健康-知りたい話
「腰痛症について」 2009.2.16
「ぎっくり腰について」 2009.2.17
「椎間板ヘルニアについて」 2009.2.18
「腰部脊柱管狭窄症について」 2009.2.19
・雑誌 週間朝日
「新・名医の最新治療」「腰椎椎間板ヘルニア」 2009.

17. 講座の准教授、講師、助教、特別研究員、ポスドク、指導を受けた大学院生の名前（AISSには○印）のリスト

（整形外科学分野）
講 師:神野哲也、新井嘉容
助 教:麻生義則、若林良明、川端茂徳、阿江啓介、加藤剛
大学院生:古賀大介、吉井俊貴、岩崎牧子、五木田茶舞、前原秀二、小柳広高、石井宣一、友利正樹、山内裕樹、猪瀬弘之、草野和生、○木村文子、○菅田祐美、○藤田浩二、正岡智和、榊経平、平井高志、○湯浅将人

（脊椎・脊髄再生治療学講座）
寄付講座准教授:早乙女進一、 竹田秀
寄付講座講師:榎本光裕

TISSUE ENGINEERING: Part A
Volume 00, Number 00, 2009
© Mary Ann Liebert, Inc.
DOI: 10.1089/ten.tea.2008.0317

Bone Regeneration with Autologous Plasma, Bone Marrow Stromal Cells, and Porous β-Tricalcium Phosphate in Nonhuman Primates

Ichiro Torigoe, M.D., Ph.D.,[1] Shinichi Sotome, M.D., Ph.D.,[1,2] Akio Tsuchiya, M.D., Ph.D.,[1] Toshitaka Yoshii, M.D., Ph.D.,[1] Hidetsugu Maehara, M.D.,[1] Yumi Sugata, M.D.,[1,3] Shizuko Ichinose, Ph.D.,[4] Kenichi Shinomiya, M.D., Ph.D.,[1,3,5,6] and Atsushi Okawa, M.D., Ph.D.[1]

To potentiate the bone formation capability of bone marrow stromal cell (BMSC)/β-tricalcium phosphate (β-TCP) constructs, we devised an autologous plasma-based construct. We tested its effectiveness and investigated the effects of its components on a monkey ectopic bone formation model. The autologous plasma (platelet-rich plasma, PRP, or platelet-poor plasma, PPP)/BMSC/β-TCP construct (R group or P group) showed significantly more bone formation at 3 and 6 weeks after implantation than a conventional BMSC/β-TCP construct using a culture medium (M group). There was no significant difference between the P and R groups. Moreover, the P group constructs with a 10-fold lower cell concentration yielded equivalent bone formation to the M group at 5 weeks after implantation. To elucidate the effect of fibrin and serum contained in the plasma, five constructs were prepared using the following cell vehicles: autologous serum+fibrinogen (0, 1, 4, or 16 mg/mL) or phosphate-buffered saline+fibrinogen (4 mg/mL). The serum+fibrinogen (4 mg/mL, physiological concentration of monkeys) construct showed the most abundant bone formation at 3 weeks after implantation, though at 5 weeks no statistical difference existed among the groups. Autologous plasma efficiently promoted osteogenesis of BMSCs/porous β-TCP constructs, and both fibrin and serum proved to play significant roles in the mechanism.

Introduction

The supply of autologous bone grafts is insufficient to repair large bone defects. Harvesting these bone grafts has risks of infection, nerve damage, and cosmetic disability.[1,2] Despite the development of various porous ceramics with osteoconductivity,[3] including hydroxyapatite (HA) and tricalcium phosphate (TCP), by themselves, these ceramics have little osteoinductivity[4,5] and are insufficient to repair massive bone defects. To overcome these problems, bone tissue engineering methods have been developed that combine bone marrow stromal cells (BMSCs) with porous ceramic scaffolds. BMSCs are easily isolated from bone marrow and have a proliferative capability and multilineage differentiation potential, including the capacity for osteogenic differentiation.[6,7] There are many reports that demonstrate the *in vivo* bone formation capability of BMSC/porous ceramic constructs.[8–14]

Although a variety of strategies to prepare BMSC/porous ceramic constructs have been contrived, practical methods have still not been established. In well-accepted techniques, after suspended in culture medium, BMSCs were seeded into porous ceramics, and the cells were cultured on porous ceramics for a few hours,[8–10] 1 week,[12,13] or 2 weeks[11,14] to attach the cells to the scaffolds and induce osteogenic differentiation of the cells. In these constructs, it is probable that BMSCs proliferated two-dimensionally by creeping along the surface of the pores, and the nutrient was supplied from the culture medium at the early stage of implantation. Considering that the range of nutrient diffusion from surrounding tissue is limited within the surface area of cell/scaffold construct,[15–18] BMSC survival after implantation could be impaired at the center of the constructs.

To provide preferable environments to BMSCs seeded into porous ceramics, we devised a construct that utilized autologous plasma of either platelet-poor plasma (PPP) or

[1]Section of Orthopaedic and Spinal Surgery, Graduate School, Tokyo Medical and Dental University, Tokyo, Japan.
[2]Section of Regenerative Therapeutics for Spine and Spinal Cord, Graduate School, Tokyo Medical and Dental University, Tokyo, Japan.
[3]Global Center of Excellence (GCOE) Program; International Research Center for Molecular Science in Tooth and Bone Diseases, Tokyo Medical and Dental University, Tokyo, Japan.
[4]Instrumental Analysis Research Center, Tokyo Medical and Dental University, Tokyo, Japan.
[5]Hard Tissue Genome Research Center, Tokyo Medical and Dental University, Tokyo, Japan.
[6]Core to Core Program for Advanced Bone and Joint Science, Tokyo Medical and Dental University, Tokyo, Japan.

platelet-rich plasma (PRP) type. We expected the fibrin and serum in plasma to have supportive effects on BMSCs, and we tested this using a rat heterotopic bone induction model.[19] A fibrin network, which is formed by fibrinogen (fibrin conversion in a blood clotting reaction), supports migration, proliferation, and differentiation of cells,[20–22] induces angiogenesis;[22–24] and plays a crucial role in the normal wound-healing process.[22] It is also well known that serum is essential for *in vitro* expansion and differentiation of BMSCs. Further, in PRP, the promotive effects of growth factors derived from platelets, which promoted osteogenesis,[25–27] are expected. Hence, viability of seeded BMSCs and effects after implantation would be augmented by a fibrin network, serum supply, and/or growth factors from platelets. As a result, osteogenesis by seeded BMSCs would be promoted in the autologous plasma/BMSC/β-TCP construct. Our study using rats showed the promotion of bone formation by the PPP/BMSC/β-TCP construct compared with a BMSC/β-TCP construct prepared using a culture medium and a PRP/BMSCs/β-TCP construct, in spite of reports that PRP enhances bone formation by growth factors released from platelets.[25–27] Although the effect of growth factors released from platelets is still controversial, it was revealed that fibrin and/or serum in plasma promoted bone formation in rats.

Although the usefulness of the tissue-engineered constructs on bone regeneration has been revealed in many animal species, including mice,[28] rats,[8,11,13] rabbits,[29] canines,[9,30] goats,[12,13,17,31] and sheep,[10] there have been few reports examining this phenomenon in nonhuman primates.[32] It is generally known that there are large differences of bone formation capability among animal species, and monkeys are most similar to humans in this regard.[33] For clinical application, *in vivo* bone formation capability should be examined in nonhuman primates.

The purposes of this study were as follows: (1) to confirm *in vivo* bone formation capability of the autologous plasma (PPP or PRP)/BMSC/β-TCP construct compared with a BMSC/β-TCP construct using culture medium; (2) to examine the influence of cell concentration on the BMSCs/β-TCP construct using culture medium or autologous plasma; and (3) to elucidate the effect of fibrin and serum on *in vivo* bone formation by the BMSCs/β-TCP construct using a ectopic bone formation model in nonhuman primates.

Materials and Methods

Animals

All animal procedures were performed in accordance with the guidelines of Tokyo Medical and Dental University for the care and use of laboratory animals. Ten skeletally mature male cynomolgus monkeys (*Macaca fascicularis*, aged 5–6 years, weight 2.8–3.8 kg) were used for this study. After the collection of bone marrow and venous blood, the transplantation and harvest of implants were performed under general anesthesia by intramuscular injection of 10 mg/kg ketamine hydrochloride and 0.1 mg/kg medetomidine hydrochloride. No monkeys were killed during experiments.

Isolation and culture of BMSCs

Bone marrow was aspirated from both the bilateral posterior iliac crests and the bilateral greater trochanters of the femurs of each monkey using a bone marrow biopsy needle (Cardinal Health, Dublin, OH) and collected into 30 mL of Dulbecco's modified Eagle's medium (DMEM; Sigma Chemical, St. Louis, MO) containing 200 IU sodium heparin. The total volume of the bone marrow aspirated from each site was 5 mL. The bone marrow suspension was centrifuged at 1000 *g* for 5 min and resuspended in the culture medium: DMEM containing 10% fetal bovine serum (Sigma Chemical), 1% antibiotic–antimycotic (100 units/mL Penicillin G sodium, 100 μg/mL Streptomycin sulfate, and 0.25 μg/mL Amphotericine B; Invitrogen), and 100 nM dexamethasone (Sigma-Aldrich, St. Louis, MO). Aliquot of the suspension was used to count the number of nucleated cells (NCs) after hemolysis, and the bone marrow suspension was plated at 1×10^6 NCs/cm^2 into 75 cm^2 culture flasks (BD Biosciences, Franklin Lakes, NJ) and cultured at 37°C in a humidified atmosphere with 5% CO_2. The culture medium was changed twice a week thereafter. Upon subconfluence of adherent BMSCs, BMSCs were detached with 0.25% trypsin containing 1 mM EDTA (Invitrogen) and reseeded into 75 cm^2 flasks at a density of 4×10^3 BMSCs/cm^2. Four days after the subculture, the culture medium was changed to an osteogenic medium consisting of the culture medium, 50 μg/mL ascorbic acid phosphate (Wako, Osaka, Japan), and 2 mM β-glycerophosphate (Sigma-Aldrich). After 3 days' osteogenic induction, the BMSCs were used for subsequent implantation experiments.

Preparation of autologous plasma and autologous serum

For preparation of autologous plasma (PPP and PRP), whole blood was collected into a sterile tube containing citrate phosphate dextrose (CPD) solution (2.63% sodium citrate, 0.327% citric acid, 2.32% dextrose, and 0.251% sodium dihydrogen phosphate; TERUMO, Tokyo, Japan) with one-ninth volume of the collected blood as an anticoagulant. The blood was centrifuged at 800 *g* for 10 min, and the upper layer, including plasma and the buffy coat (mostly white blood cells and platelets), was transferred to another tube except for the bottom layer that included red blood cells. To spin down the buffy coat, further centrifugation of the transferred layers was performed at 1500 *g* for 10 min, the bottom layer was collected as PRP (one-tenth volume of the whole blood), and the remainder was collected as PPP (half volume of the whole blood). The number of platelets in the whole blood, PPP, and PRP was counted using Coulter Counter® (Beckman Coulter, Fullerton, CA). For preparation of autologous serum, whole blood was collected in a sterile tube and incubated at room temperature for a few hours. After the blood coagulated, the tube was centrifuged at 2380 *g* for 10 min, and the serum was collected from the upper layer. Considering the influence of the CPD solution in the plasma, serum was also mixed with the CPD solution at a 9:1 v/v ratio.

Preparation of BMSC/β-TCP constructs

Porous ceramic scaffolds. Porous β-TCP blocks (Osferion®; Olympus, Tokyo, Japan) were used in this study. The blocks were 5×5×5 mm in dimension and 75% porous, with a macropore size ranging from 200 to 400 μm and micropore size under 5 μm. The macropores were interconnected by paths with diameters of 100–200 μm.[5,34]

Experiment 1 (comparative study of BMSC/β-TCP, PPP/BMSC/β-TCP, and PRP/BMSC/β-TCP constructs). Cultured osteogenic BMSCs were suspended in the culture medium, autologous PPP, or PRP at a concentration of 2×10^6 cells/mL. The cell suspension using the culture medium was seeded into porous β-TCP cubes using the spontaneous penetration under the low-pressure method,[35] in which cell suspension is seeded into porous scaffolds under low pressure (50 mmHg) with a simple device and homogenously distributed into porous scaffolds. The procedure only requires a few minutes. Subsequently, the BMSC/β-TCP constructs using the culture medium (M group) were incubated for 3 h for cell attachment. The cell suspension prepared utilizing PPP or PRP was mixed with 2% calcium chloride at a 7:1 v/v ratio to initiate fibrin gel formation. It was immediately introduced into porous β-TCP cubes using the same technique as mentioned above. After gelation of each introduced cell suspension was completed, autologous transplantation of both PPP/BMSC/β-TCP (P group) and PRP/BMSC/β-TCP constructs (R group) was conducted with the M group and β-TCP without cells (control group) (Table 1A). Some constructs were used for analysis by scanning electron microscopy (SEM).

Experiment 2 (influence of BMSC concentration). To examine the influence of cell concentration on *in vivo* bone formation of the BMSC/β-TCP constructs, cultured osteogenic BMSCs were suspended in the culture medium or PPP at a series of concentrations: 2000×10^3 cells/mL (M2000 group or P2000 group), 200×10^3 cells/mL (M200 group or P200 group), and 20×10^3 cells/mL (M20 group or P20 group). Each construct was prepared via the same techniques as used in Experiment 1, and autologous transplantation was performed (Table 1B).

Experiment 3 (effect of fibrin and serum). The gel that formed in the implant prepared using autologous plasma is composed of fibrin networks, and serum (as basic nutrients) with low concentrations (PPP) or high concentrations (PRP) of growth factors derived from platelets. To elucidate the effects of fibrin and serum on bone formation, five groups of BMSC/β-TCP constructs were prepared and transplanted (Table 1C). Except for the 0S group, BMSCs were suspended at a concentration of 2×10^6 cells/mL in autologous serum or phosphate-buffered saline (PBS) containing the CPD solution at a 9:1 v/v ratio mixed with human fibrinogen powder (BOLHEAL®; Teijin Pharma, Tokyo, Japan) at each concentration (1, 4, or 16 mg/mL). Subsequently, the cell suspension was mixed with 7 units/mL thrombin (BOLHEAL) in 2% calcium chloride at a 7:1 v/v ratio to initiate fibrin gel formation and introduced into the scaffolds. To prepare the construct of the 0S group, BMSCs were suspended at a concentration of 2×10^6 cells/mL in autologous serum, seeded into the scaffold, and incubated for 3 h for cell attachment.

SEM examination

Extra implants from the M, P, and control groups were not implanted and were instead utilized for SEM analyses. The samples were fixed with 2.5% glutaraldehyde, divided into two halves, dehydrated through a graded series of ethanol, dried by a critical point dryer, mounted onto aluminum

Table 1. Experimental Groups

(A) Experiment 1

Groups	*Constructs*	*Cell concentration ($\times10^3$ cells/mL)*
M	BMSC/β-TCP	
P	PPP/BMSC/β-TCP	2000
R	PRP/BMSC/β-TCP	
Control	β-TCP	0

(B) Experiment 2

Groups	*Constructs*	*Cell concentration ($\times10^3$ cells/mL)*
M2000		2000
M200	BMSC/β-TCP	200
M20		20
P2000		2000
P200	PPP/BMSC/β-TCP	200
P20		20

(C) Experiment 3

Groups	*Constructs*	*Fibrinogen (mg/mL)*	*Cell concentration ($\times10^3$ cells/mL)*
4S	Fibrin/AS/BMSC/β-TCP	4	
4P	Fibrin/PBS/BMSC/β-TCP	4	
0S	AS/BMSC/β-TCP	0	2000
1S	Fibrin/AS/BMSC/β-TCP	1	
16S	Fibrin/AS/BMSC/β-TCP	16	

AS, autologous serum.

stubs, and sputter-coated with platinum. The samples were observed from the cut plane using a scanning electron microscope (S-4500; Hitachi, Tokyo, Japan).

Implantation

Three, three, and four male monkeys were used in Experiments 1, 2, and 3, respectively. Three implants were used for each group and each time point per monkey. The surgical procedures were performed under general anesthesia. After shaving and disinfecting the dorsal areas, a longitudinal skin incision was made to expose the muscle fascia. Separate fascia incisions were made, and using blunt dissection, intramuscular pockets were created that were filled with one of the constructs, according to a randomized scheme. After the constructs were implanted, the fascia and the skin were closed. After 1, 2, 3, and 6 weeks (Experiment 1), 5 weeks (Experiment 2), or 3 and 5 weeks (Experiment 3), implants were harvested under general anesthesia. The fascia and skin incision were closed, and the animals were not killed as a part of these experiments and continuously bred.

Histological and histomorphometric examination

The harvested implants were fixed in a 4% paraformaldehyde solution for 1 week, decalcified in a 4% EDTA solution, and embedded in paraffin blocks. Each block was sectioned at 5 μm thickness with five sections at equal intervals derived from one block. The sections were stained with hematoxylin and eosin (H&E) and tartrate-resistant acid phosphatase (TRAP). For immunohistochemical analysis, after deparaffinized sections were treated in turn with 0.4 mg/mL proteinase K (DakoCytomation, Glostrup, Denmark), 3% hydrogen peroxide in methanol, and 5% skim milk, they were incubated with mouse anti-human CD31 monoclonal antibody (1:100 dilution; DakoCytomation) overnight at 4°C and reacted for 10 min with biotinylated pig anti-mouse/rabbit/goat immunoglobulin G (DakoCytomation). Immunostaining was detected with peroxidase-labeled streptavidin (DakoCytomation), followed by 3,3′-diaminobenzidine tetrahydrochloride staining; counter staining was performed with methyl green. For histomorphometric examination of newly formed bone, the area of bone formation was painted black using image-editing software (Photoshop®; Adobe Systems, San Jose, CA). The black area of each section was extracted using Photoshop and measured using image analysis software (Scion Image®; Scion Corporation, Frederick, MD). Modifying the report by Dennis *et al.*,[36] the bone formation area (BFA) was defined as the ratio of newly formed bone per whole sectional area including newly formed bone, pores, and β-TCP.[35] The BFA of a single implant was an average of five sections (Fig. 1).

Statistics

Average values were expressed as the mean ± standard deviation (SD). The Tukey–Kramer test (Experiments 1 and 3) and paired *t*-test (Experiment 2) were used to assess differences. Differences were considered to be statistically significant when the *p*-value was <0.05.

Results

Experiment 1 (comparison among the M, P, and R groups)

The constructs of the M, P, and control groups just before implantation were observed by SEM. Figure 2A demonstrates the porous structure of the control group (β-TCP only) with macropores ranging from 200 to 400 μm interconnected by paths with diameters of 100–200 μm and a micropore structure below 5 μm. In the M group, BMSCs were two-dimensionally attached to the pore surface of β-TCP (Fig. 2B, D). In contrast, BMSCs in the P group were three-dimensionally retained by the fibrin network formed in the pores (Fig. 2C, E). The number of platelets in whole blood, PPP, and PRP was 26.7 ± 6.9, 5.4 ± 0.9, and 152.3 ± 23.1 × 10^4/μL, respectively. The number of platelets of PRP was approximately 30-fold that of PPP in this study.

At 3 weeks after implantation, there was a large quantity of newly formed bone in the P and R groups in the peripheral area, while the M group had less bone formation in the partial peripheral area. Moreover, six of the nine M group implants (three implants per animal) showed no bone formation (details are shown in Table 2). The invasion of many blood vessels also appeared with thicker, newly formed bone in both the P and R groups, compared to the M group, which had few blood vessels (Fig. 3A). At 6 weeks, bone formation expanded into the central area, became thicker, and was homogenously distributed throughout the whole area in the

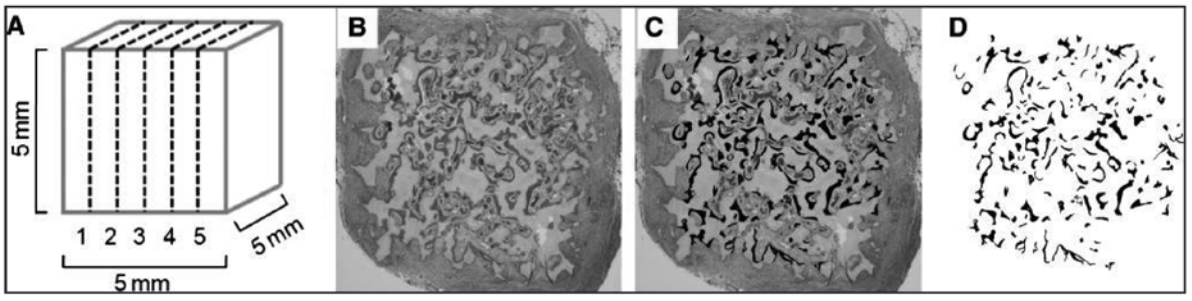

FIG. 1. Histomorphometric analysis of newly formed bone. (**A**) Five sections at equal intervals were made from one implant. (**B**) Each section was stained with H&E. (**C**) The area of bone formation was selected and painted black using Photoshop. (**D**) The area painted black in each section was extracted using Photoshop and measured using Scion Image. BFA was defined as the ratio of newly formed bone per whole sectional area including newly formed bone, pores, and β-TCP. The BFA of one implant was an average of five sections. Color image available online at www.liebertonline.com/ten.

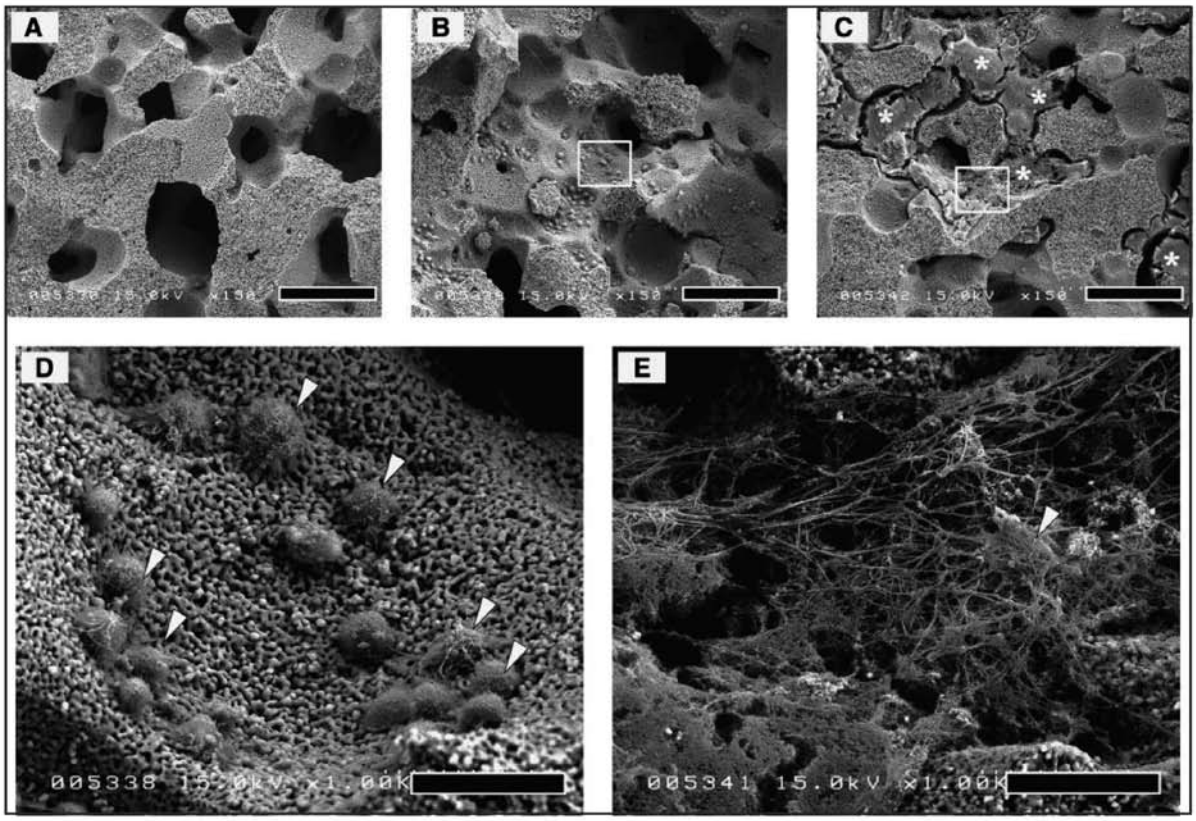

FIG. 2. SEM findings of the constructs before implantation. (**A**) Porous structure of the scaffold. The macropores and interconnecting pores are indicated. (**B, D**) The M group 3 h after seeding BMSCs. The BMSCs were attached to the pore surface. (**C, E**) The P group just after seeding BMSCs. Most of the macropores were filled with fibrin gel. The BMSCs were retained with a fibrin network formed in the pores. Arrowheads indicate seeded BMSCs; asterisks indicate fibrin gels. Scale bars: 200 μm (**A–C**) and 30 μm (**D, E**).

P and R groups; blood vessels had also developed. In the M group, there was less bone formation and invasion of blood vessels in the central area, and the distribution of newly formed bone was not uniform (Fig. 3A). In the control group, there was no bone formation at both 3 and 6 weeks (data not shown). In histomorphometric analysis of newly formed bone, the BFA in the P and R groups were significantly higher than the M group at both 3 and 6 weeks. Moreover, there was no significant difference between the P and R groups at these times (Fig. 3B). These results suggest that growth factors released from platelets had little effect on bone formation; therefore, we focused on PPP, which could be more abundantly obtained than PRP. Further, we examined the histological differences between the M and P groups in the early stages. At 1 week, in the M group invasion of more fibrous tissue into the implant was seen with few blood vessels stained with anti-CD31 antibody. On the other hand, comparatively many blood vessels appeared with less invasion of other tissues at the peripheral area in the P group (Fig. 3C). At 2 weeks, blood vessels extended and reached the central area in the P group, while invasion of blood vessels was delayed in the peripheral area in the M group (Fig. 3C). At 3 weeks, TRAP-positive cells appeared at the peripheral area in only the P group, according to the

TABLE 2. BONE FORMATION IN EXPERIMENT 1

		Case 1		*Case 2*		*Case 3*	
Groups	*Constructs*	*3 Weeks*	*6 Weeks*	*3 Weeks*	*6 Weeks*	*3 Weeks*	*6 Weeks*
M	BMSC/β-TCP	0/3	1/3	2/3	3/3	0/3	3/3
P	PPP/BMSC/β-TCP	3/3	3/3	3/3	3/3	3/3	3/3
R	PRP/BMSC/β-TCP	2/3	3/3	3/3	3/3	3/3	3/3
Control	β-TCP	0/3	0/3	0/3	0/3	0/3	0/3

Number of implants with bone formation/Total implants.

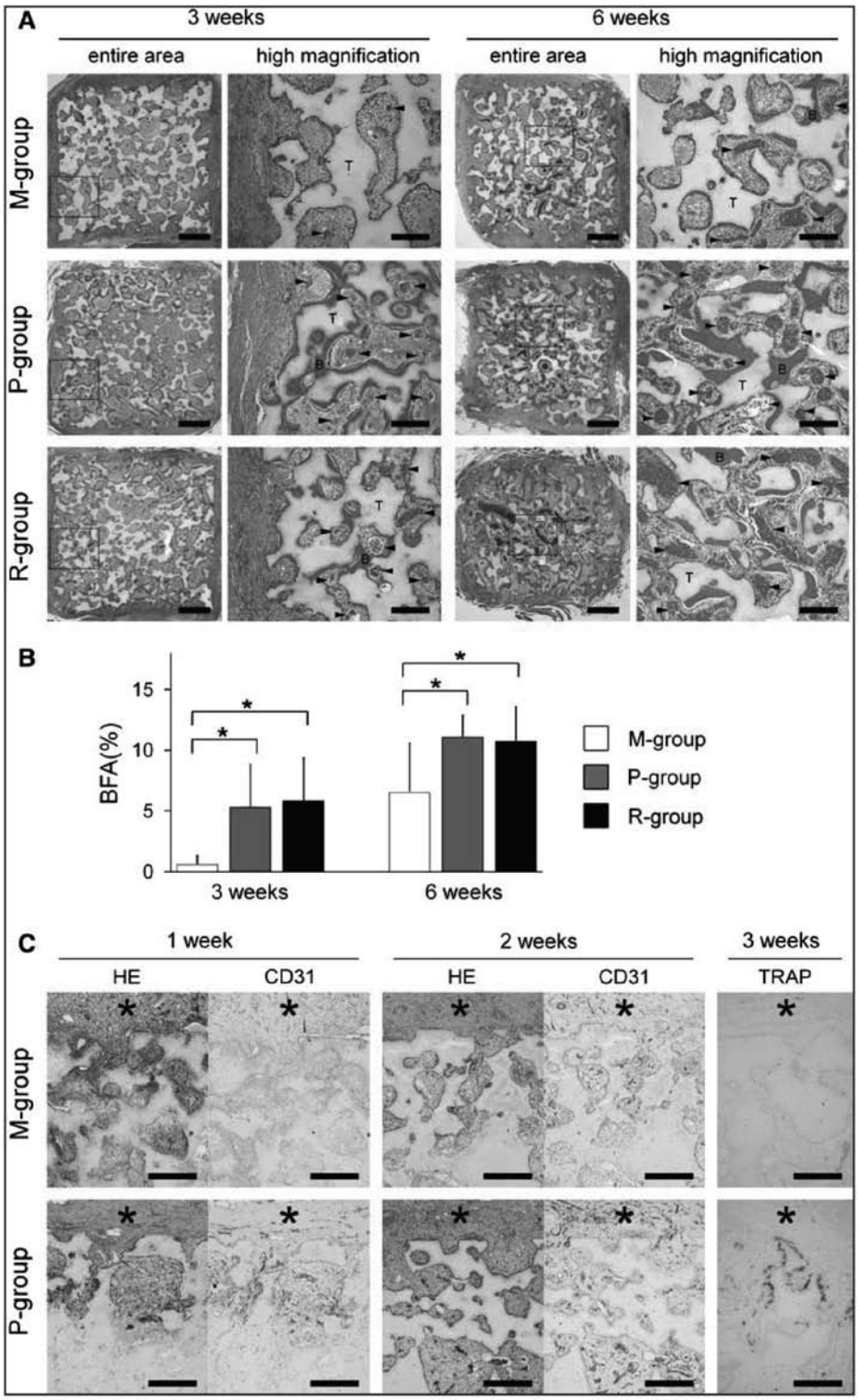
A
3 weeks
6 weeks
entire area
high magnification
entire area
high magnification
M-group
P-group
R-group
B
BFA(%)
15
10
5
0
3 weeks
6 weeks
M-group
P-group
R-group
C
1 week
2 weeks
3 weeks
HE
CD31
HE
CD31
TRAP
M-group
P-group

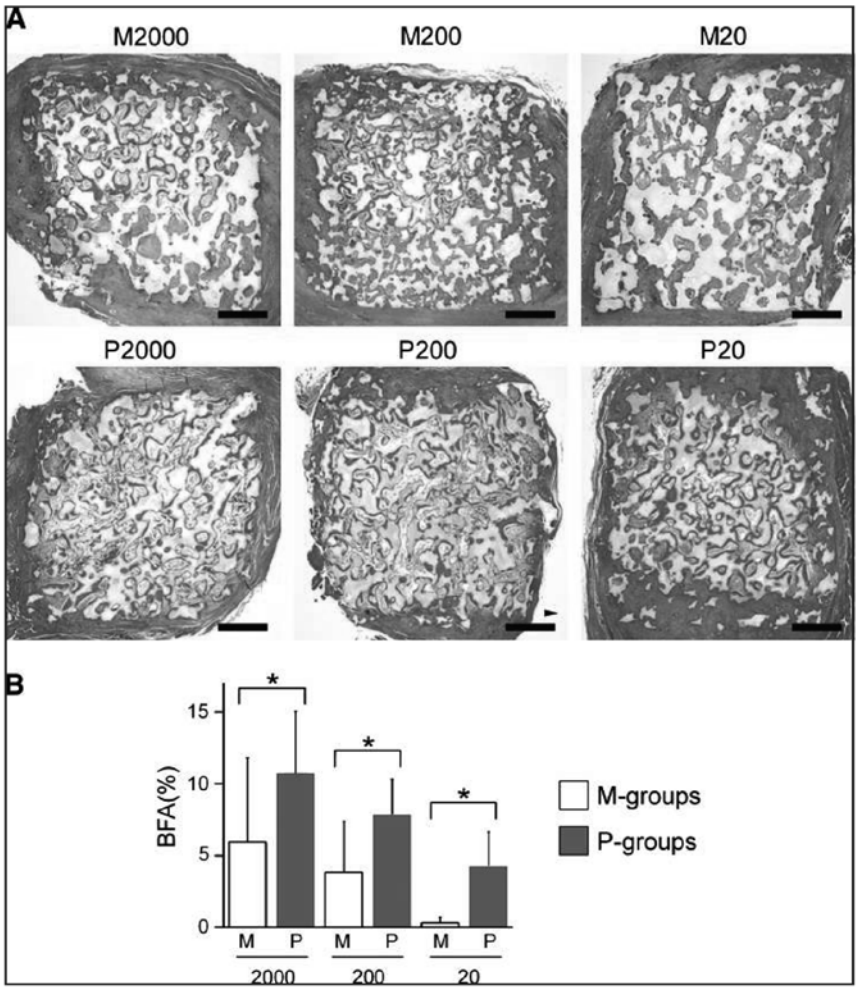

FIG. 4. Influences of BMSC concentration in the M and P groups (Experiment 2). (**A**) Representative histological sections at 5 weeks stained with H&E. Images taken from the central parts of each implant. The extent of bone formation in the M groups was reduced with a decrease in cell concentration. In contrast, the newly formed bone of both the P2000 and P200 groups distributed to the entire sectional area. Scale bar: 1 mm. (**B**) BFA at 5 weeks. BFAs of the P groups were significantly higher than those of the M groups at each concentration, especially at the concentration of 20×10^3 cells/mL. The data are expressed as mean ± SD ($^*p < 0.05$). Color image available online at www.liebertonline.com/ten.

progression of osteogenesis and angiogenesis (Fig. 3C). From these results, we confirmed that plasma enhanced osteogenesis and angiogenesis in the BMSC/β-TCP construct.

Experiment 2 (influence of BMSCs concentration in the M and P groups)

To investigate how cell concentration affects bone formation in the M and P groups, constructs were prepared with cell suspensions at three concentrations in each group. The extent of newly formed bone tended to be reduced in both groups according to the decrease in cell concentration. However, these influences were smaller in the P groups. The extent of bone formation of the P200 group was almost equal to that of the P2000 group; bone formation of the P20 group was distributed to nearly the same extent as in the M200 group. However, there was little or no bone formation in the implants of the M20 group (Fig. 4A and Table 3). The BFA of the P groups was higher than that of the M groups at each concentration. Though BFA was reduced with decreased cell concentration in both groups, the P group was less affected by the reduction of cell concentration. Further, the BFAs of

FIG. 3. Comparison among the M, P, and R groups (Experiment 1). (**A**) Representative histological sections at 3 and 6 weeks stained with H&E. Images taken from the central parts of each implant. At 3 weeks, there was much newly formed bone with many invaded blood vessels in the P and R groups in all the peripheral areas. At 6 weeks, bone formation invaded the central area, became thicker, and was homogenously distributed in the entire area in the P and R groups, differing from the M group. T, β-TCP; B, newly formed bone; arrowhead, blood vessels. Scale bars: 1 mm (whole area) and 250 μm (high magnification). (**B**) BFA at 3 and 6 weeks. The data are expressed as the mean ± SD ($^*p < 0.05$). (**C**) Representative histological sections of the peripheral area at early stages stained with H&E, TRAP, and immunohistochemistry for the anti-CD31 antibody. Blood vessels invaded and developed earlier in the P group than the M group. At 3 weeks, many TRAP-positive cells appeared only in the P group. Scale bars: 500 μm (H&E and CD31) and 200 μm (TRAP). Asterisks indicate outside area of implants. Color image available online at www.liebertonline.com/ten.

the constructs in the P groups (P200 and P20 groups) were almost equal to those of the M group constructs with, respectively, 10-fold higher cell concentrations (M2000 and M200 groups) (Fig. 4B).

Experiment 3 (effect of fibrin and serum)

Based on the results of Experiments 1 and 2, we hypothesized that the fibrin network and/or serum in plasma would be key factors promoting angiogenesis and osteogenesis. To clarify the effect of these components, we prepared and implanted constructs with five different compositions (Table 1C). To find the normal value of fibrinogen concentration in cynomolgus monkeys, the fibrinogen concentration in venous blood from monkeys was measured. The mean value of the fibrinogen concentration was 3.73 ± 1.27 mg/mL ($n = 10$). Therefore, we set 4 mg/mL as the physiological fibrinogen concentration in this experiment. At 3 and 5 weeks after implantation, constructs were extracted for histological examination; all of the extracted constructs showed bone formation. At 3 weeks, bone in the 4S and 1S groups was formed in the entire peripheral area, while there was less bone formation in the partial peripheral area in the 4P, 0S, and 16S groups (Fig. 5A). Many blood vessels were also seen in the peripheral area with newly formed bone in the 4S and 1S groups, as found in the P group (Fig. 5A). At 5 weeks, there was newly formed bone in almost the entire area of implants in all five groups. However, we observed less bone formation at the central area in the 4P, 0S, and 16S groups (Fig. 5A). In the quantitative analysis, the BFA of the 4S group was significantly higher than that of the 4P, 0S, or 16S group at 3 weeks (Fig. 5B). At 5 weeks, there was no significant difference among the five groups (Fig. 5C). These findings demonstrated that both fibrin networks from the physiological fibrinogen concentration (4 mg/mL) and serum played a crucial role for the enhancement of angiogenesis and osteogenesis, especially in the early stages.

Discussion

We showed here that the autologous plasma (PPP or PRP)/BMSC/β-TCP constructs have more potential for bone formation than the BMSC/β-TCP construct prepared using a culture medium in a monkey heterotopic bone formation model. We also showed that both fibrin networks formed from native fibrinogen concentration (4 mg/mL) and serum in plasma were essential elements for the enhancement of angiogenesis and osteogenesis in BMSC/β-TCP construct.

PRP has been widely used in the field of bone regeneration, due to the effect on bone formation of fibrin and various growth factors (transforming growth factor beta, platelet-derived growth factor, etc.) released from platelets;[25–27] therefore, we examined the bone formation capability of the PRP/BMSC/β-TCP construct using rats in previous study.[19] From this result, it was revealed that PPP, rather than PRP, had higher bone formation capability in the BMSC/β-TCP construct. This confirmed other reports that PRP had little effect on bone formation.[37,38] The function of PRP on bone formation is still controversial, and therefore, to clarify the potential effects of PPP and PRP/BMSC/β-TCP constructs, we conducted Experiment 1 using monkeys, which are most similar to humans.[33]

In contrast with our previous report using rats, there was no histological and histomorphometric difference between the P and R groups, although each of the two groups had a significantly higher BFA than the M group. The difference between our two studies suggests that PRP has diverse effects that depend on the difference in implantation sites, animal species, platelet concentration, reactivity to growth factors, and the like.[39] Considering that PPP is more easily and abundantly available than PRP and, therefore, is advantageous when applied to the repair of large bone defects, we focused on PPP and performed a detailed examination. Characteristically, enhanced angiogenesis and little other tissue invasion were found at early stages in the P group. These findings suggest that early nutrient supply by blood flow, without invasion of other tissues, could increase the potential of seeded BMSCs. Additionally, they might explain the reason why the extent of the bone formation in the P group was homogenous at 6 weeks, in contrast with the nonuniform results obtained in the M group. Based on the results of Experiment 1, we hypothesized that fibrin and serum component in plasma promoted angiogenesis and subsequent osteogenesis, even without growth factors from platelets.

In Experiment 2, the extent of bone formation and BFA were dramatically reduced in the M groups with a decrease in cell concentration, whereas these influences in the P groups were small both histologically and histomorphometrically. Additionally, it was demonstrated that the P groups required only one-tenth the number of BMSCs of the M groups. The potential of seeded BMSCs was possibly increased using PPP. Studies on bone formation that combine BMSCs and a porous scaffold generally utilize a cell suspension at concentrations of 1×10^6 to 3×10^7 cells/mL.[9–12] However, obtaining a large number of BMSCs is costly and requires long culture periods. Further, the osteogenic potential of BMSCs is known to decrease with proliferation.[40–43] Therefore, PPP, which could reduce the number of seeded BMSCs, is very beneficial in repairing massive bone defects.

Some studies reported the availability of plasma/BMSC/porous ceramic constructs.[17,19,31] However, these studies did not reveal which components in the plasma facilitated the *in vivo* bone formation capability. Therefore, we performed Experiment 3 to elucidate the mechanism of the augmentation by plasma. Because the BFAs of the P and R groups were almost equivalent in Experiment 1, we regarded effects of the growth factors released from platelets as negligible and used autologous serum from whole blood in Experiment 3. Considering that some combinations of purified fibrin/ceramic scaffolds were reported to have osteoinductivity in heterotopic sites[20] and that fibrin was known to induce angiogenesis,[22,23] the implants prepared with fibrin were predicted to obtain sufficient bone formation. Despite the prediction, the 4P and 16S groups showed statistically lower BFAs at 3 weeks, although the 0S group without fibrin showed lower BFA, as expected. In comparison with the 4S group, the result of the 4P group suggests that the fibrin network by itself is insufficient for early angiogenesis and osteogenesis; thus, serum was also necessary.

In the tissue engineering field, various porous materials have been used as scaffolds because the structure provides a large effective surface for cell expansion and tissue organization. However, the material structure was believed to have negative effects on nutrient diffusion surrounding tissues

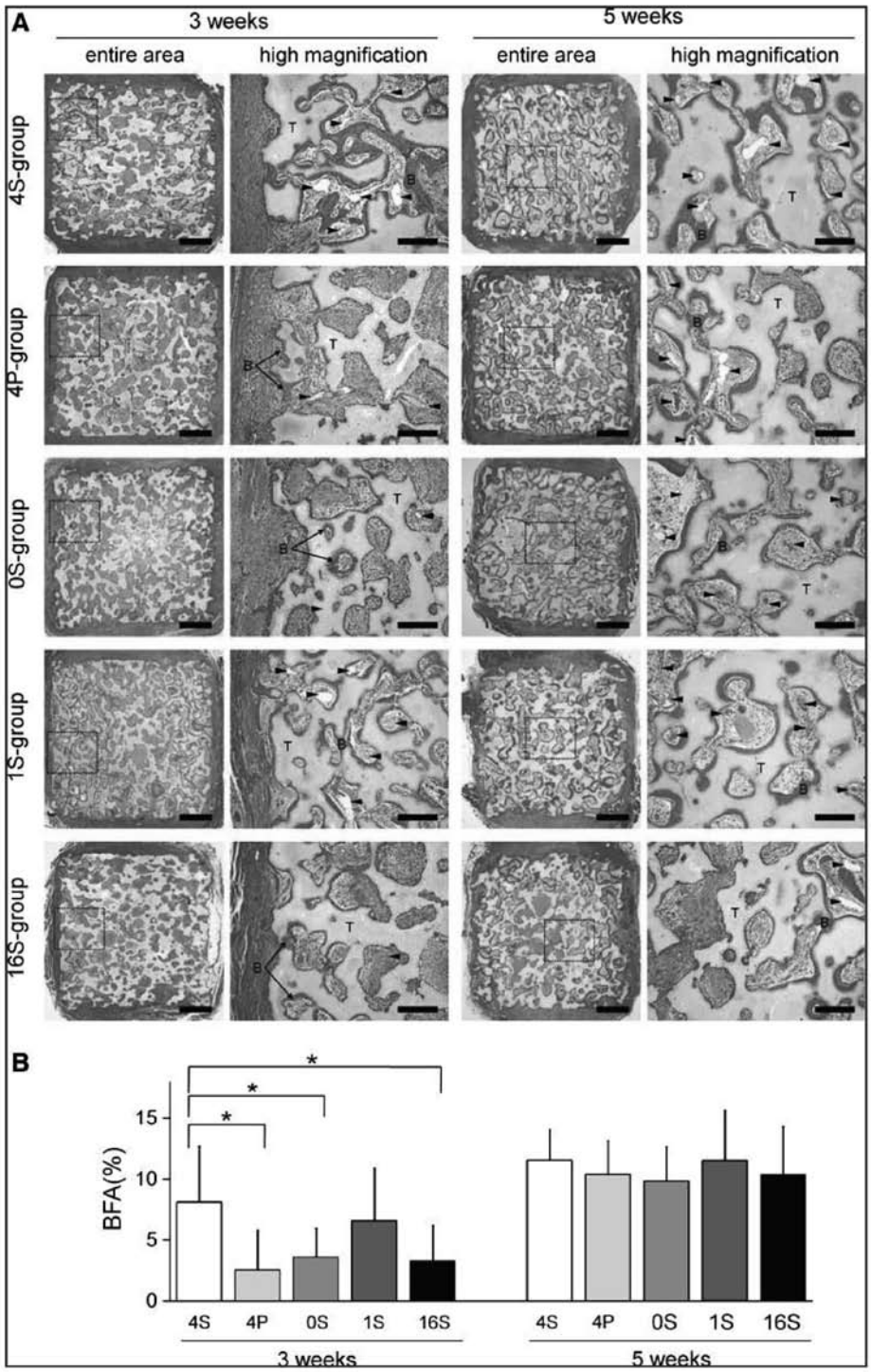

FIG. 5. Effects of fibrin and serum (Experiment 3). (**A**) Representative histological sections at 3 and 5 weeks stained with H&E. Images are from the central parts of each implant. By 3 weeks, a great quantity of bone and many blood vessels had formed in the entire peripheral area in both the 4S and 1S groups. At 5 weeks, in the 4S and 1S groups, thicker bone extended with many developed blood vessels to the central area, compared to the 4P, 0S, and 16S groups. T, β-TCP. Arrowheads indicate blood vessels. Scale bars: 1 mm (whole area) and 250 μm (high magnification). (**B**) BFA at 3 and 6 weeks. The data are expressed as mean ± SD (*$p < 0.05$). Color image available online at www.liebertonline.com/ten.

TABLE 3. BONE FORMATION IN EXPERIMENT 2

Groups	Constructs	5 Weeks		
		Case 1	Case 2	Case 3
M2000		3/3	3/3	0/3
M200	BMSC/β-TCP	3/3	3/3	0/3
M20		2/3	2/3	0/3
P2000		3/3	3/3	3/3
P200	PPP/BMSC/β-TCP	3/3	3/3	3/3
P20		3/3	3/3	3/3

Number of implants with bone formation/Total implants.

and resultant cell survival.[15–18] Therefore, as a mechanism of the augmentation of bone formation by plasma, the serum component contained in plasma was supposed to support BMSC survival after the implantation, especially in the early stages. Lower BFA in the 0S and 16S groups revealed that osteogenesis depends on fibrinogen concentration, and it is important that BMSCs are retained in the fibrin network formed from fibrinogen with the physiological concentration (the physiological fibrinogen concentration in cynomolgus monkeys is approximately 4 mg/mL). This result is consistent with the reports that fibrin from 5 mg/mL fibrinogen promoted osteogenic differentiation of BMSCs[19] and that a fibrin network formed from fibrinogen with a high concentration of inhibited cell growth and migration.[21] From these results, it was confirmed that both serum and fibrin networks that formed from the normal fibrinogen concentration, which was equal to normal plasma, are essential for enhanced angiogenesis and osteogenesis at the early stages of implantation. However, BFAs of the five groups were almost equivalent at 5 weeks, although there was a delay in bone formation in the central area in the 4P, 0S, and 16S groups. Considering the limitation of the available space for bone formation in the scaffolds, transplantation with decreased cell concentration might have revealed superior effects of the 4S group on bone formation also at 5 weeks.

This study, using nonhuman primates, indicates that utilization of the PPP/BMSCs/β-TCP construct, which can be easily prepared, will be a more advantageous strategy for clinical application of tissue-engineered bone regeneration.

Conclusion

The bone formation capability of the autologous plasma (PPP or PRP)/BMSC/β-TCP construct was enhanced in nonhuman primates compared to the BMSC/β-TCP construct prepared using a culture medium. The bone formation capability of PPP/BMSC/β-TCP construct was less influenced by the decrease in the number of BMSCs. Both fibrin networks, which formed from a native fibrinogen concentration, and serum were essential to the enhancement of angiogenesis and osteogenesis, especially in the early stages.

Acknowledgments

We thank Satoko Sunamura for excellent technical assistance, Miyoko Ojima for expert help with histological analysis, and Olympus Corporation for kindly donating the porous β-TCP blocks. This work was supported by the Japan Society for the Promotion of Science's Grant-in-Aid for Scientific Research.

Disclosure Statement

No competing financial interests exist.

References

1. Banwart, J.C., Asher, M.A., and Hassanein, R.S. Iliac crest bone graft harvest donor site morbidity. A statistical evaluation. Spine **20,** 1055–1060, 1995.
2. Arrington, E.D., Smith, W.J., Chambers, H.G., Bucknell, A.L., and Davino, N.A. Complications of iliac crest bone graft harvesting. Clin Orthop Relat Res **329,** 300–309, 1996.
3. LeGeros, R.Z. Properties of osteoconductive biomaterials: calcium phosphates. Clin Orthop Relat Res **395,** 81–98, 2002.
4. Yuan, H., van Blitterswijk, C.A., deGroot, K., and de Bruijn, J.D. Cross-species comparison of ectopic bone formation in biphasic calcium phosphate (BCP) and hydroxyapatite (HA) scaffolds. Tissue Eng **12,** 1607–1615, 2006.
5. Kondo, N., Ogose, A., Tokunaga, K., Umezu, H., Arai, K., Kudo, N., Hoshino, M., Inoue, H., Irie, H., Kuroda, K., Mera, H., and Endo, N. Osteoinduction with highly purified β-tricalcium phosphate in dog dorsal muscles and the proliferation of osteoclasts before heterotopic bone formation. Biomaterials **27,** 4419–4427, 2006.
6. Pittenger, M.F., Mackay, A.M., Beck, S.C., Jaiswal, R.K., Douglas, R., Mosca, J.D., Moorman, M.A., Simonetti, D.W., Craig, S., and Marshak, D.R. Multilineage potential of adult human mesenchymal stem cells. Science **284,** 143–147, 1999.
7. Derubeis, A.R., and Cancedda, R. Bone marrow stromal cells (BMSCs) in bone engineering: limitations and recent advances. Ann Biomed Eng **32,** 160–165, 2004.
8. Goshima, J., Goldberg, V.M., and Caplan, A.I. The osteogenic potential of cultured-expanded rat marrow mesenchymal cells assayed *in vivo* in calcium phosphate ceramic blocks. Clin Orthop **262,** 298–311, 1991.
9. Bruder, S.P., Kraus, K.H., Goldberg, V.M., and Kadiyala, S. The effect of implants loaded with autologous mesenchymal stem cells on the healing of canine segmental bone defects. J Bone Joint Surg Am **80,** 985–996, 1998.
10. Petite, H., Viateau, V., Bensaid, W., Meunier, A., de Pollak, C., Bourquiqnon, M., Oudina, K., Sedel, L., and Guillemin, G. Tissue-engineered bone regeneration. Nat Biotechnol **18,** 959–963, 2000.
11. Nishikawa, M., Myoui, A., Ohgushi, H., Ikeuchi, M., Tamai, N., and Yoshikawa, H. Bone tissue engineering using novel interconnected porous hydroxyapatite ceramics combined with marrow mesenchymal cells: quantitative and three-dimensional image analysis. Cell Transplant **13,** 367–376, 2004.
12. Kruyt, M.C., Dhert, W.J., Yuan, H., Wilson, C.E., van Blitterswijk, C.A., Verbout, A.J., and de Bruijn, J.D. Bone tissue engineering in a critical size defect compared to ectopic implantations in the goat. J Orthop Res **22,** 544–551, 2004.
13. Kruyt, M.C., Persson, C., Johansson, G., Dhert, W.J., and de Bruijn, J.D. Towards injectable cell-based tissue-engineered bone: the effect of different calcium phosphate microparticles and pre-culturing. Tissue Eng **12,** 309–317, 2006.
14. Wang, J., Asou, Y., Sekiya, I., Sotome, S., Orii, H., and Shinomiya, K. Enhancement of tissue engineered bone formation by a low pressure system improving cell seeding and medium perfusion into a porous scaffold. Biomaterials **27,** 2738–2746, 2006.
15. Ishaug-Riley, S.L., Crane, G.M., Gurlek, A., Miller, M.J., Yasko, A.W., Yaszemski, M.J., and Mikos, A.G. Ectopic bone formation by marrow stromal osteoblast transplantation using poly(DL-lactic-co-glycolic acid) foams implanted into the rat mesentery. J Biomed Mater Res **36,** 1–8, 1997.

16. Muschler, G.F., Nakamoto, C., and Griffith, L.G. Engineering principles of clinical cell-based tissue engineering. J Bone Joint Surg Am **86,** 1541–1558, 2004.
17. Kruyt, M.C., Dhert, W.J., Oner, F.C., van Blitterswijk, C.A., Verbout, A.J., and de Bruijn, J.D. Analysis of ectopic and orthotopic bone formation in cell-based tissue-engineered constructs in goats. Biomaterials **28,** 1798–1805, 2007.
18. Viateau, V., Guillemin, G., Bousson, V., Oudina, K., Hannouche, D., Sedel, L., Logeart-Avramoglou, D., and Petite, H. Long-bone critical-size defects treated with tissue-engineered grafts: a study on sheep. J Orthop Res **25,** 741–749, 2007.
19. Tajima, N., Sotome, S., Marukawa, E., Omura, K., and Shinomiya, K. A three-dimensional cell-loading system using autologous plasma loaded into a porous beta-tricalcium-phosphate block promotes bone formation at extraskeletal sites in rats. Mater Sci Eng C **27,** 625–632, 2007.
20. Abiraman, S., Varma, H.K., Umashankar, P.R., and John, A. Fibrin glue as an osteoinductive protein in a mouse model. Biomaterials **23,** 3023–3031, 2002.
21. Bensaid, W., Triffitt, J.T., Blanchat, C., Oudina, K., Sedel, L., and Petite, H. A biodegradable fibrin scaffold for mesenchymal stem cell transplantation. Biomaterials **24,** 2497–2502, 2003.
22. Eyrich, D., Gopferich, A., and Blunk, T. Fibrin in tissue engineering. Adv Exp Med Biol **585,** 379–392, 2006.
23. Mosesson, M.W. Fibrinogen and fibrin structure and functions. J Thromb Haemost **3,** 1894–1904, 2005.
24. Fan, C.L., Gao, P.J., Gu, Y.J., Tang, X.F., Liu, J.J., Wei, J., Inoue, K., and Zhu, D.L. Therapeutic angiogenesis by intramuscular injection of fibrin particles into ischaemic hindlimbs. Clin Exp Pharmacol Physiol **33,** 617–622, 2006.
25. Marx, R.E., Carlson, E.R., Eichstaedt, R.M., Schimmele, S.R., Strauss, J.E., and Georgeff, K.R. Platelet-rich plasma: growth factor enhancement for bone grafts. Oral Surg Oral Med Oral Pathol Oral Radiol Endod **85,** 638–646, 1998.
26. Wiltfang, J., Schlegel, K.A., Schultze-Mosgau, S., Nkenke, E., Zimmermann, R., and Kessler, P. Sinus floor augmentation with beta-tricalciumphosphate (beta-TCP): does platelet-rich plasma promote its osseous integration and degradation? Clin Oral Implants Res **14,** 213–218, 2003.
27. Kitoh, H., Kitakoji, T., Tsuchiya, H., Mitsuyama, H., Nakamura, H., Katoh, M., and Ishiguro, N. Transplantation of marrow-derived mesenchymal stem cells and platelet-rich plasma during distraction osteogenesis—a preliminary result of three cases. Bone **35,** 892–898, 2004.
28. Mankani, M.H., Kuznetsov, S.A., Wolfe, R.M., Marshall, G.W., and Robey, P.G. *In vivo* bone formation by human bone marrow stromal cells: reconstruction of the mouse calvarium and mandible. Stem cells **24,** 2140–2149, 2006.
29. Minamide, A., Yoshida, M., Kawakami, M., Yamasaki, S., Kojima, H., Hashizume, H., and Boden, S.D. The use of cultured bone marrow cells in type I collagen gel and porous hydroxyapatite for posterolateral lumbar spine fusion. Spine **30,** 1134–1138, 2005.
30. Yuan, J., Cui, L., Zhang, W.J., Liu, W., and Cao, Y. Repair of canine mandibular bone defects with bone marrow stromal cells and porous beta-tricalcium phosphate. Biomaterials **28,** 1005–1013, 2007.
31. Kruyt, M.C., de Bruijn, J.D., Yuan, H., van Blitterswijk, C.A., Verbout, A.J., Oner, F.C., and Dhert, W.J. Optimization of bone tissue engineering in goats: a peroperative seeding method using cryopreserved cells and localized bone formation in calcium phosphate scaffolds. Transplantation **77,** 359–365, 2004.
32. Wang, T., Dang, G., Guo, Z., and Yang, M. Evaluation of autologous bone marrow mesenchymal stem cell-calcium phosphate ceramic composite for lumbar fusion in rhesus monkey interbody fusion model. Tissue Eng **11,** 1159–1167, 2005.
33. Izadopanah, R., Joswig, T., Tsien, F., Dofour, J., Kirijan, J.C., and Bunnell, B.A. Characterization of multipotent mesenchymal stem cells from the bone marrow of rhesus macaques. Stem Cells Dev **14,** 440–451, 2005.
34. Dong, J., Uemura, T., Shirasaki, Y., and Tateishi, T. Promotion of bone formation using highly pure porous beta-TCP combined with bone marrow-derived osteoprogenitor cells. Biomaterials **23,** 4493–4502, 2002.
35. Torigoe, I., Sotome, S., Tsuchiya, A., Yoshii, T., Takahashi, M., Kawabata, S., and Shinomiya, K. Novel cell seeding system into a porous scaffold using a modified low pressure method to enhance cell seeding efficiency and bone formation. Cell Transplant **16,** 729–739, 2007.
36. Dennis, J.E., Konstantakos, E.K., Arm, D., and Caplan, A.I. *In vivo* osteogenesis assay: a rapid method for quantitative analysis. Biomaterials **19,** 1323–1328, 1998.
37. Gruber, R., Karreth, F., Kandler, B., Fuerst, G., Rot, A., Fischer, M.B., and Watzek, G. Platelet-released supernatants increase migration and proliferation, and decrease osteogenic differentiation of bone marrow-derived mesenchymal progenitor cells under *in vitro* conditions. Platelets **15,** 29–35, 2004.
38. Sarkar, M.R., Augat, P., Shefelbine, S.J., Schorlemmer, S., Huber-Lang, M., Claes, L., Kinzl, L., and Ignatius, A. Bone formation in a long bone defect model using a platelet-rich plasma-loaded collagen scaffold. Biomaterials **27,** 1817–1823, 2006.
39. Grageda, E. Platelet-rich plasma and bone graft materials: a review and a standardized research protocol. Implant Dent **13,** 301–309, 2004.
40. Bruder, S.P., Jaiswal, N., and Haynesworth, S.E. Growth kinetics, self-renewal, and the osteogenic potential of purified human mesenchymal stem cells during extensive subcultivation and following cryopreservation. J Cell Biochem **64,** 278–294, 1997.
41. Banfi, A., Muraglia, A., Dozin, B., Mastrogiacomo, M., Cancedda, R., and Quatro, R. Proliferation kinetics and differentiation potential of *ex vivo* expanded human BMSCs: implications for their use in cell therapy. Exp Hematol **28,** 707–715, 2000.
42. Simonsen, J.L., Rosada, C., Serakinci, N., Justesen, J., Stenderup, K., Rattan, S.I., Jensen, T.G., and Kassem, M. Telomerase expression extends the proliferative life-span and maintains the osteogenic potential of human bone marrow stromal cells. Nat Biotechnol **20,** 592–996, 2002.
43. Vacanti, V., Kong, E., Suzuki, G., Sato, K., Canty, J.M., and Lee, T. Phenotypic changes of adult porcine mesenchymal stem cells induced by prolonged passaging in culture. J Cell Physiol **205,** 194–201, 2005.

Address reprint requests to:
Shinichi Sotome, M.D., Ph.D.
Section of Regenerative Therapeutics
for Spine and Spinal Cord
Graduate School
Tokyo Medical and Dental University
1-5-45 Yushima, Bunkyo-ku
Tokyo 113-8519
Japan

E-mail: sotome.orth@tmd.ac.jp

Received: June 3, 2008
Accepted: October 1, 2008
Online Publication Date: January 30, 2009

日本経済新聞（夕刊） 2008年（平成20年）

夕&Eye

病を知る

痛み③ 頸椎症

手や足にまで しびれやマヒも
転倒などで悪化に注意

東京医科歯科大学教授
四宮 謙一氏

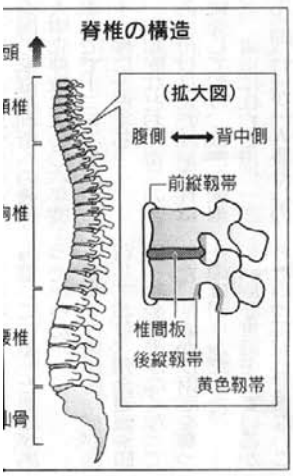

なくなった」という言葉があるように体の中でも首は最もよく動く部分のひとつだ。必然的に痛みも多い。東京医科歯科大学の四宮謙一教授（整形外科学）は「症状や生活パターンをよく見る必要があるが、手などにしびれのある場合は将来を考えると早めに手術をした方がよい」と言う。

――首の痛みにはいろいろ種類があります。多いのは頸椎（けいつい、首の骨）にかかわるものです。

「私たちの体を支えている脊柱（せきちゅう）は、頭の側から頸椎（七個の椎体骨で構成）、胸椎（十二個）、腰椎（五個）、仙骨に分けられます。椎体骨の間には椎間板（ついかんばん）があって、椎体骨同士をくっつけ、クッションの役割をしています」

「頸椎の椎間板や椎体骨は加齢とともに変性・変形し、脊柱内を通っている神経を圧迫します。頸椎は胸椎、腰椎に比べて大きく動かるスポーツや、重いものを持ち上げることも原因になります。人によって異なりますが、四十歳代以降の中高年は予備軍と見てよいでしょう。加齢のほかにラグビーなどの首に大きな力がかかりますが、この中にも脊髄されて症状を出すものがありますね。

「頸椎症性神経根症と頸椎症性脊髄症があります。頸椎症性神経根症は脊髄から出て肩や腕にいく神経が圧迫されて起き、頸椎症性脊髄症は脊髄が圧迫を受けるため起きます」

――首の痛みをもたらす変性疾患を頸椎症と呼んでいます。

「神経根が圧迫された症例では、首や肩に痛みがあるほか手の指のしびれなどをもたらします。頸椎症性脊髄症では箸（はし）がうまく使えない、うまく字が書けないなどの症状が表れます。重度になると足にも症状が表れ、歩行や排尿が困難になることもあります」

――どのような治療をしますか。

「椎間板や背骨の関節などして痛みをもたらしますから、これを和らげるのが筋弛緩（きんしかん）薬や消炎鎮痛薬を使いますし、加温や圧痛点へのレーザー治療なども行います」

「神経根が押されて手の指にしびれが出ている神経根症では、薬や首のカラーで固定で比較的短期に症状が軽減することが多いので経過を見るようにしています。しかし、手足に症状が出た脊髄症の人には私は早めの手術を勧めています。

靱帯骨化症でも痛み

首の痛みやしびれをもたらすものとしては頸椎症のほかに靱帯（じんたい）骨化症がある。靱帯は脊柱を縦走し椎体骨をつないでいる組織で、前縁（腹側）を走っている前縦靱帯と後縁（背中側）を走っている後縦靱帯、それに黄色靱帯がある。靱帯は胸椎、腰椎にもあるが、よく動かす首の靱帯が問題になることが多い。

中高年で発症し原因はいくつかの遺伝子と環境要因と考えられている。比較的多いのが後縦靱帯骨化症で全人口の二―三%で生じるといわれるが、脊髄（せきずい）を圧迫して発症しているのはその一部だ。

せんから、時がたつとともに脊髄そのものの変性が強くなっていきます。将来を考えると早めに手術をしたほうがよいでしょう。脊髄や神経根の圧迫をのぞくと痛みやしびれがなくなる人は多いようです」

「しびれや麻痺（まひ）を伴った頸椎症性脊髄症では、激しい運動や転倒で悪化することがあります。美容室で髪を洗う時に反り返って首の麻痺が強くなったという例もあります。痛いからと整体に行くことはやめた方がいいでしょう。頸椎に無理な力をかけることになりますから」

（聞き手は編集委員）

MEMO

膠原病・リウマチ内科学

宮坂 信之

医歯学総合研究科・生体環境応答学系専攻
臨床免疫学・教授

1. 研究の課題名

(1) 関節リウマチに対する細胞周期制御療法の開発

関節リウマチ（RA）動物モデルにサイクリン依存性キナーゼ阻害因子（CDKI）遺伝子を関節内導入すると、滑膜増生が抑制され関節炎が改善する。したがって、サイクリンCDK阻害薬によっても関節炎が抑制されると期待される。しかし、CDKI分子は細胞周期を抑制するのみだけでなく免疫作用も調節する。一方、近年、抗癌剤として低分子CDK阻害薬が開発されており、その臨床試験で全身投与が比較的安全であることが明らかとなってきている。そこで、臨床試験で比較的安全と判明した汎CDK阻害薬および企業から供与を受けたCDK4/6選択的阻害薬を用いて低分子化合物CDK阻害薬の動物モデル関節炎への効果を検討したところ大きな効果があった。しかも、明らかなリンパ球抑制は認められなかった。現在、治療に使うべき新たなCDK4/6選択的阻害薬のスクリーニング系を構築している。

Development of non-immunosuppressive treatments of rheumatoid arthritis: Cell cycle control for treatment of rheumatoid arthritis

Therapeutic agents of biologic nature are effective but share similar limitations in clinical response. They often induce susceptibility to serious infections. During our search for non-immunosupressive approaches, we found that intraarticular gene transfer of cyclin-dependent kinase (CDK) inhibitors to suppress synovial cell growth is effective in treating animal models of rheumatoid arthritis (RA), including collagen-induced arthritis (CIA). In the present study, small-molecule (sm) CDK inhibitors were tested. They suppressed proliferation of synovial fibroblasts in vitro and also CIA in vivo without affecting lymphocyte responses to the collagen.

(2) Triggering receptor expressed on myeloid cells (TERM) -1阻害による関節リウマチの新治療法開発

TREM-1はヒト、マウスの微生物感染に伴って発現が増強し、感染症モデルマウスにおけるTREM-1阻害は生存率および炎症反応を改善する。このことから、TREM-1阻害は微生物への抵抗性を損なうことなく炎症反応を抑制しうると考えられる。一方、これまでに我々はマウスマクロファージ上のLPS誘導TREM-1発現がCOX inhibitorで阻害され、prostaglandin E2（PGE2）がTREM-1発現を誘導することを明らかにした。この結果はTREM-1がPGE2を介して感染症以外の炎症性疾患にも関与することを示唆する。一方、関節リウマチ（RA）でCOX inhibitorは病態改善をきたさないが、ヒトにおけるPGE2によるコントロールについて不明であった。我々は、ヒト単球ではLPS誘導TREM-1発現がCOX inhibitorにより阻害されないことを示し、TREM-1の発現制御はヒトとマウスで異なることを明らかにした。そこで、RAの病態にTREM-1が関与しているか検討したところ、RA患者由来滑膜細胞のCD14+滑膜細胞においてTREM-1の発現が認められた。また、アゴニスト抗体は滑膜細胞からのTNF α 産生を促進した。RAのモデル動物であるコラーゲン誘導関節炎モデル（CIA）の滑膜細胞においても、CD11b+滑膜細胞でTREM-1の発現が強く認められたため、TREM-1阻害によるCIAの治療効果を検討した。sTREM-1-Igアデノウイルス（Ad-sTREM-1-Ig）を用いて、ウイルスを関節炎発症後のマウスに静注したところ、関節炎進展がほぼ完全に抑制された。しかし、抗原特異的T, B細胞反応は保たれていた。以上のことから、TREM-1阻害は獲得免疫系を抑制することなく関節炎を制御しうることが考えられた。従って、TREM-1は関節炎治療の有用な治療標的分子となりうる。

Triggering receptor expressed on myeloid cells-1 as a new therapeutic target of rheumatoid arthritis.

Ligation of triggering receptor expressed on myeloid cells-1（TREM-1）amplifies inflammatory responses. It was reported that TREM-1 was involved in bacterial infection-related diseases including sepsis and that its blockade ameliorated murine sepsis models, preserving host defense against bacterial infections. We report here that TREM-1 is expressed on macrophages in the RA and CIA joints. In vitro TREM-1 ligation on synovial cells promoted TNFalpha production. In vivo TREM-1 blockade with adenoviruses containing TREM-1-Ig gene and synthetic TREM-1 antagonistic peptides ameliorated CIA without affecting lymphocyte responses to the collagen. We believe that smCDK inhibitor treatment and TREM-1 blockade should be new anti-rheumatic approaches that are safer than presently available immunosuppressive treatment.

(3) レチノイドによる関節炎抑制効果

ビタミンAの活性体であるレチノイドには、Th1細胞への分化抑制、Th2細胞への分化亢進能があることが知られていた。近年、Th17細胞への分化抑制、Treg細胞への分化亢進能があることが報告され、Th1, Th17に関連する疾患に対する抑制効果が期待されている。我々は、レチノイドの一種であるAm80が筋炎モデルマウスを抑制することを見出した。そこで、Am80による関節炎への影響を解析した。マウスコラーゲン誘導関節炎（CIA）は、day 1およびday 22にコラーゲン免疫をすることにより発症するが、Am80を免疫初日（day 1）から経口投与すると、関節炎は完全に抑制された。マウス脾細胞をコラーゲン刺激しサイトカイン産生能を解析すると、IL-17産生は著明に低下したが、IFN-g産生に影響はみられなかった。また血清中の抗コラーゲン抗体産生も抑制された。しかし初回免疫2週後からのAm80投与では関節炎抑制効果はみられなかった。また、コラーゲン刺激した脾細胞からのIL-17, IFN-g産生も有意な変化を認めなかった。一方、血清中の抗コラーゲン抗体産生は抑制されていた。Am80にはIL-6産生抑制効果があることが報告されている。初回免疫時よりの投与で関節炎抑制効果があり、2週後からの投与で関節炎抑制を認めない結果は、CIAにIL-6阻害治療を行った時と同様である。今後はこのモデルにおいて、Am80のIL-6産生への影響を解析していく。

Retinoid ameliorates collagen-induced arthritis with modulating Th cell development and antibody production

Retinoids are compounds that have biological activities of vitamin A. Recent studies indicate that retinoids promote differentiation into Th2 cells and Treg cells, and suppress Th1 and Th17 cell differentiation. In this study, we examined the effects of a synthetic retinoid, Am80, on collagen-induced arthritis（CIA）, and also on Th phenpotype development and antibody production. We induced murine CIA by immunization with bovine type II collagen at days 1 and 22. When Am80 was orally administrated from day 1, clinical arthritis score was significantly lowered. Moreover, Am80 decreased IL-17 production by collagen-stimulated splenic T cells. However, IFN-g production was not changed by the treatment. Production of serum anti-collagen Abs was also decreased. When we treat the mice from day 15, arthritis score was not changed. These results by treatment with Am80 are similar to those with IL-6 blocking. Am80 may suppress IL-6 production on CIA and inhibit arthritis.

(4) 関節リウマチの病態形成におけるCXCR7の役割について

CXCL12（SDF-1）は関節リウマチ（RA）の滑膜組織で産生が亢進し,CXCR4を介して炎症細胞の滑膜への浸潤・集簇、炎症細胞の活性化、血管新生などに重要な役割を担っていると考えられている。近年CXCL12の新規レセプターとしてCXCR7が同定された。そこで、我々は滑膜組織におけるCXCR7の発現、その機能について解析した。免疫染色にて、CXCR7はRA滑膜組織の血管内皮細胞に発現していた。変形性関節症の滑膜にはほとんど発現がみられなかった。正常ヒト臍帯静脈内皮細胞（HUVECs）においてもCXCR4,CXCR7 mRNAは発現し、CXCR7 mRNA発現はIL-1b刺激により著明に亢進した。血管新生能をtube formation assayで解析すると、CXCL12はHUVECsの管腔形成を亢進したが、CXCR4阻害剤、CXCR7阻害剤いずれによってもその亢進は抑制された。マウスコラーゲン関節炎に対しCXCR7阻害剤を投与すると、関節炎の程度、骨破壊が抑制された。CXCR7はRAの病態形成において重要な役割を担っている可能性があり、特に血管新生抑制を標的としたRAの新たな治療ターゲットとなることが期待される。

Pathogenic Role of CXCR7 in Rheumatoid Arthritis

Interaction between CXCL12（SDF-1）and the receptor, CXCR4, plays an important role in the pathogenesis of rheumatoid arthritis（RA）. Recently, CXCR7 was identified as an alternative receptor for CXCL12. We analyzed CXCR7 expression in the synovium, and examined the pathogenic role in RA. CXCR7 was expressed on endothelial cells in the RA synovium. CXCR7 mRNA was detected in HUVECs, and the expression was upregulated by stimulation with IL-1b. CXCL12 promoted tube formation by HUVECs. However, the tube formation was

inhibited either by CXCR7 antagonist or CXCR4 antagonist. Treatment with CXCR7 antagonist reduced murine collagen-induced arthritis. These results indicate that CXCR7 plays an important role for angiogenesis in RA synovium. CXCR7 could be a target molecule in novel therapies for RA by blocking angiogenesis.

2.

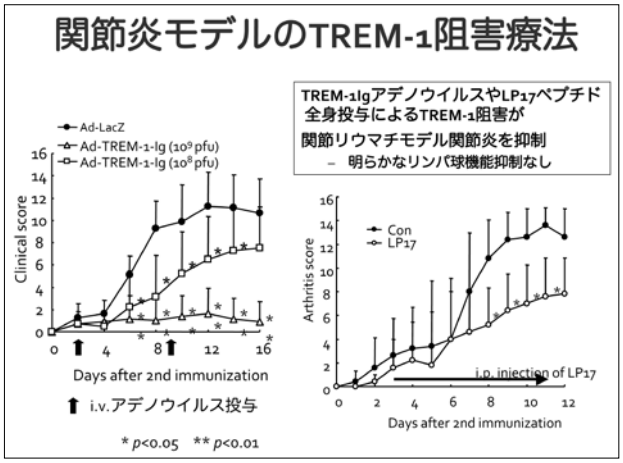

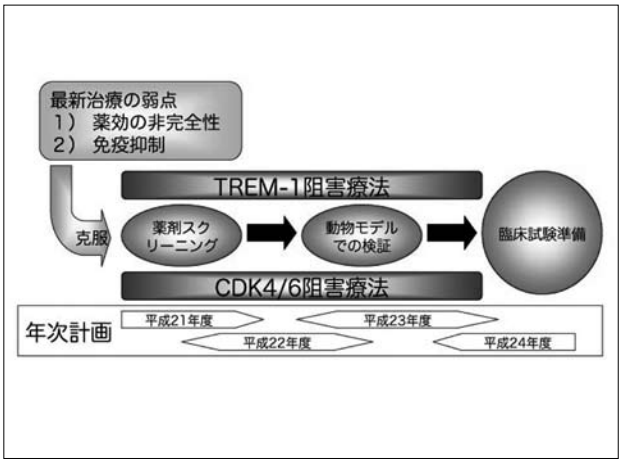

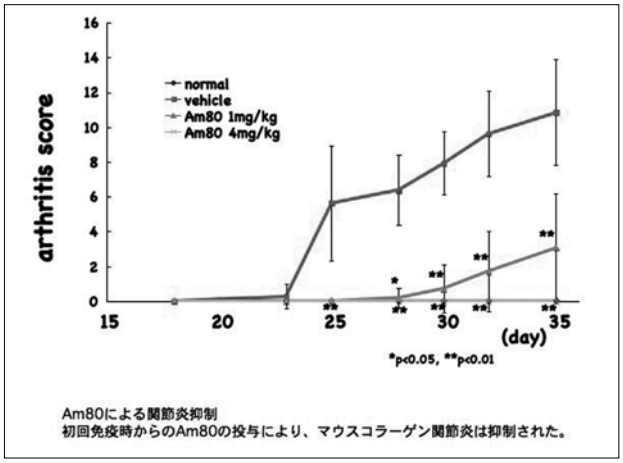

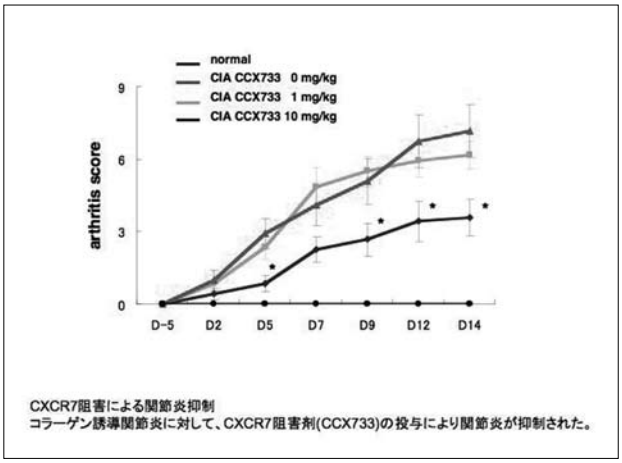

3. 2008年、2009年（平成21年3月までの）に発表した全ての研究内容についての英文要約

<Development of non-immunosuppressive treatments of rheumatoid arthritis>

We found that intraarticular gene transfer of cyclin-dependent kinase (CDK) inhibitors to suppress synovial cell growth is effective in treating animal models of rheumatoid arthritis (RA), including collagen-induced arthritis (CIA). In the present study, small-molecule (sm) CDK inhibitors were tested. They suppressed proliferation of synovial fibroblasts in vitro and also CIA in vivo without affecting lymphocyte responses to the collagen.

We also found that triggering receptor expressed on myeloid cells-1 (TREM-1) is expressed on macrophages in the RA and CIA joints. In vitro TREM-1 ligation on synovial cells promoted TNF α production. In vivo TREM-1 blockade with adenoviruses containing TREM-1-Ig gene and synthetic TREM-1 antagonistic peptides ameliorated CIA without affecting lymphocyte responses to the collagen.

We also found that CXCR7 was expressed on endothelial cells in the RA synovium. Treatment with CXCR7 antagonist reduced murine collagen-induced arthritis.

We believe that smCDK inhibitor treatment, TREM-1 blockade and XCCL12 inhibition should be new anti-rheumatic approaches that are safer than presently available immunosuppressive treatment.

4. 本事業に関連して世界的な研究拠点形成に向けて、以下の点で改善・整備等されたこと

A（研究拠点体制）

特になし

B（研究教育環境）

特になし

C（人材確保）

シャペロン教員として岩井秀之を米国スタンフォード大学より獲得した。

D（人材育成）

米国カリフォルニア大学サンディエゴ校に野々村美紀を派遣している。

E（国際化）

特になし。

5. 英文原著論文

1. Miyasaka N Clinical investigation in highly disease-affected rheumatologic arthritis patients in Japan with adalimumab applying standard and general evaluation: the CHANGE study. Mod. Rheumatol. 18（3）:252-262, 2008
2. ◎Sekine C, Sugihara T, Miyake S, Hirai H, Yoshida M, Miyasaka N, Kohsaka H Successful treatment of animal models of rheumatoid arthritis with small-molecule cyclin-dependent kinase inhibitors. J. Immunol. 180:1954-1961, 2008
3. ◎Nakamoto T, Seo S, Sakai R, Kato T, Kutsuna H, Kurokawa M, Noda M, Miyasaka N, Kitagawa S Expression and tyrosine phosphorylation of Crk associated substrate lymphocyte type（Cas-L）protein in human neutrophils. J. Cell. Biochem. 105:121-128, 2008
4. Saito E, Koike T, Hashimoto H, Miyasaka N, Ikeda Y, Hara M, Yamada H, Yoshida T, Harigai M, Ichikawa Y Efficacy of high-dose intravenous immunoglobulin therapy in Japanese patients with steroid-resistant polymyositis and dermatomyositis. Additional members of the GB-0998 Study Group Mod. Rheumatol. 18:34-44, 2008
5. ◎Mizoguchi F, Mizuno A, Hayata T, Nakashima K, Heller S, Ushida T, Sokabe M, Miyasaka N, Suzuki M, Ezura Y, Noda M Transient receptor potential vanilloid 4 deficiency suppresses unloading-induced bone loss. J. Cellular Phys. 216:47-53, 2008
6. Mizoguchi F, Nanki T, Takada K, Miyasaka N Recurrent pulmonary embolism due to intracardiac thrombi in systemic sclerosis. Clin. Exp. Rheum. 26:157, 2008
7. ◎Tazaki T, Miyazaki K, Hiyama E, Nakamoto T, Sakai R, Yamasaki T, Honda Z, Noda M, Miyasaka N, Sueda T, Honda H Functional analysis of Src homology 3-encoding exon（exon 2）of p130Cas in primary fibroblasts derived from exon 2-specific knockout mice. Genes to Cells 13:145-157, 2008
8. Harigai M, Kawamoto M, Hara M, Kubota T, Kamatani N, Miyasaka N Excessive production of IFN-γ in patients with Systemic Lupus Erythematosus and its contribution to induction of B lymphocyte stimulator / B cell-activating factor / TNF ligand superfamily-13B1. J. Immunol. 181（3）:2211-2219, 2008
9. Mizoguchi F, Nanki T, Miyasaka N Pneumatosis cystoides intestinalis following lupus enteritis and peritonitis. Intern. Med. 47（13）:1267-1271, 2008
10. Mizoguchi F, Nakamura S, Iwai H, Kubota T, Miyasaka N Varicella-Zoster virus hepatitis in polymyositis. Mod. Rheumatol. 18（3）:301-305, 2008
11. Miyasaka N Adalimumab for the treatment of rheumatoid arthritis. Expert Review of Clinical Immunology in press
12. Watanabe K, Nanki T, Sugihara T, Miyasaka N A case of polyarteritis nodosa with periurethral aseptic abscesses and testicular lesions. Clin. Exp. Rheumatol. 26:1113-1115, 2008
13. Nii T, Kubota T, Nanki T, Komano Y, Harigai M, Kohsaka H, Hirose W, Nagasaka K, Sakurai T, Miyasaka N Reevaluation of antibody titers 1 year after influenza vaccination in patients with rheumatoid arthritis receiving TNF blockers. Mod. Rheumatol. LETTER in press
14. ◎Nonomura Y, Mizoguchi F, Suzuki A, Nanki T, Kato H, Miyasaka N, Kohsaka H Hypoxia-induced abrogation of contact-dependent inhibition of rheumatoid arthritis synovial fibroblast proliferation. J. Rheumatol. in press
15. Nishimoto N, Miyasaka N, Yamamoto K, Kawai S, Takeuchi T, Azuma J, Kishimoto T Study of active controlled tocilizumab monotherapy for rheumatoid arthritis patients with an inadequate response to methotrexate（SATORI）: significant reduction in disease activity and serum vascular endothelial growth factor by IL-6 receptor inhibition therapy. Mod. Rheumatol. in press
16. Murakami Y, Akahoshi T, Aoki N, Toyomoto M, Miyasaka N, Kohsaka H Intervention of triggering receptor expressed on myeloid cells-1 signaling for modest immunosuppression to treat autoimmune arthritis. Arthritis & Rheumatism. in press
17. Okiyama N, Kohsaka H, Ueda N, Satoh T, Katayama I, Nishioka K, and Yokozeki H Seborrhic area erythema as a common skin manifestation in Japanese patients with dermatomyositis. Dermatology 217（4）:374-377, 2008
18. Matsudaira T, Tsuzuki S, Wada A, Suwa A, Kohsaka H, Tomida M, and Ito Y Automated microfluidic assay system for autoantibodies causing autoimmune diseases using a photoimmobilized autoantigen microarray. Biotechnology Progress 24（6）:1384-1392, 2008
19. Hirose W, Nishikawa K, Hirose M, Nanki T, Sugimoto H Response of early active rheumatoid arthritis to tumor necrosis factor inhibitors: evaluation by magnetic resonance imaging. Mod. Rheumatol. in press

20. Komano Y, Harigai M, Koike R, Sugiyama H, Ogawa J, Saito K, Sekiguchi N, Inoo M, Onishi I, Ohashi H, Amamoto F, Miyata M, Ohtsubo H, Hiramatsu K, Iwamoto M, Minota S, Matsuoka N, Kageyama G, Imaizumi K, Tokuda H, Okochi Y, Kudo K, Tanaka Y, Takeuchi T, Miyasaka N Pneumocystis pneumonia in patients with rheumatoid arthritis treated with infliximab: a retrospective review and case-control study of 21 patients. Arthritis Care & Res. in press
21. Kishi J, Nanki T, Watanabe K, Takamura A, Miyasaka N. A case of systemic lupus erythematosus complicated with rituximab-induced interstitial pneumonia. Rheumatology in press

6. 著書

1. 膠原病・アレルギー.宮坂信之　薬の処方ハンドブック改訂第3版　奈良信雄編　羊土社　pp.298-320,2008
2. 回帰性リウマチ.宮坂信之　今日の治療指針2009年版－私はこう治療している　山口徹、北原光夫、福井次矢編　医学書院　pp.620-621,2008
3. 抗体医薬　関節リウマチの抗体療法.宮坂信之　タンパク質研究のための抗体実験マニュアル改訂版　高津聖志,三宅健介,山元弘,瀧伸介編　羊土社　pp.241-245,2008
4. 感染症・免疫・膠原病　その他の膠原病.宮坂信之　改訂3版「老年医学テキスト」（社）日本老年医学会編　メジカルビュー社　pp.543-547,2008
5. ステロイド薬がわかる本　宮坂信之編著　法研　pp.1-196,2008
6. 改訂版　正しいステロイド剤の使い方　宮坂信之編　医薬ジャーナル社 pp.1-67,2008
7. ステロイドを使う主な病気「膠原病・リウマチ内科」.上阪　等　ステロイドがわかる本　宮坂信之編著　法研　pp.58-112, 2008年
8. 関節リウマチ　病因.上阪　等　新しい診断と治療のABC「関節リウマチ」宮坂信之編集　最新医学社　pp.59-66, 2008年
9. わが国における生物学的製剤使用ガイドライン.小池竜司　別冊・医学のあゆみ　「関節リウマチのパラダイムシフト　－生物学的製剤時代の最新治療動向－」宮坂信之編集　医歯薬出版　pp.35-42, 2008
10. 生物学的製剤使用ガイドライン.小池竜司　最新医学別冊「新しい診断と治療のABC（8）関節リウマチ」（改訂第2版）宮坂信之編集　最新医学社　pp.258-269, 2008
11. 多発性筋炎,皮膚筋炎,全身性硬化症（強皮症）.駒野有希子、宮坂信之、平松則子　「病期・病態・重症度からみた疾患別看護課程」井上智子、佐藤千史編集　医学書院　pp.993-1026, 2008

7. 特許取得、特許申請

2008年2月　日本国特許出願　膠原病の予防・治療剤　上阪等、宮坂信之（出願番号:特願2008-39292）

8. 平成21年3月までの自己評価

本年度は、関節リウマチの新規治療薬の開発研究を中心にして原著論文を多数出すことができ、それなりの成果が得られたものと考えている。今後さらに国際的レベルの研究を継続して行いたい。

9. 和文原著論文

1. 小笠原弘子,林恭子,遠井初子,萩原三千男,東田修二,宮坂信之,東條尚子　ブシラミンに起因する尿ケトン体の偽陽性について.　臨床病理　56:584-588, 2008
2. 越智小枝、窪田哲朗、杉原毅彦、小川純、駒野有希子、野々村美紀、宮坂信之　関節リウマチに伴う急速進行性間質性肺炎及び多発肺嚢胞の治療中に縦隔気腫を合併し、tacrolimusが有効であった1例.　Jpn. J. Clin. Immunol. 31（1）:62-67, 2008
3. 金子英樹、駒野有希子、渡部香織、栢森高、高田和生、南木敏宏,宮坂信之　進行性多巣性白質脳症をきたした全身性エリテマトーデスの一例. 日本臨床免疫学会誌31:465-469, 2008
4. 南木敏宏　ケモカインと膠原病.臨床リウマチ医のための基礎講座.　臨床リウマチ20:261-263, 2008
5. 鈴木文仁　レバチオ錠20mg　審査報告書2008年1月
6. 鈴木文仁　アクテムラ点滴静注用80mg、同点滴静注用200mg、同点滴静注用400mg　審査報告書2008年4月
7. 鈴木文仁　ヒュミラ皮下注40mgシリンジ0.8mL　審査報告書2008年4月

＜和文総説＞

1. 宮坂信之.膠原病における早期診断・早期治療の現況と展望.」内科　南江堂　101（4）:606-609, 2008
2. 宮坂信之.生物学的製剤のEBM-ATTRACT・ASPIRE・ERA・TEMPO・PREMIER　EBM for biologic agents to treat rheumatoid arthritis. Progress in Medicine　28（1）:15-18, 2008
3. 宮坂信之.抗TNF α抗体（キメラ、ヒト化、ヒト抗体）.

Medical Science Digest 34（5）:22-25, 2008
4. 宮坂信之.関節リウマチ　概念・定義.最新医学・別冊「新しい診断と治療のABC8」 最新医学社 pp.9-17, 2008
5. 宮坂信之.トシリズマブ（商品名:アクテムラ）、アダリムマブ（商品名:ヒュミラ）について.日本リウマチ友の会「流」261:48-51,2008
6. 宮坂信之.生涯剣道―（1）現代版養生訓.東京剣連だより 64:9-10, 2009
7. 宮坂信之.治療方針と目標のトレンド.日本内科学会会誌 97（10）11-16, 2008
8. 宮坂信之.関節リウマチの診断・治療指針―その新展開と進め方― Medical Practice 25（8）:1300-1306, 2008
9. 宮坂信之.それでも地球は回る…. Frontiers in Rheumatology & Clinical Immunology 2（4）:5 9, 2008
10. 宮坂信之.関節リウマチに対する新規生物学的製剤.関節外科 27（12）:147-149, 2008
11. 宮坂信之.日本人関節リウマチ患者におけるアダリムマブの有効性と安全性―海外臨床試験との比較― リウマチ科 39（1）:9-14, 2008
12. 宮坂信之.質問どうぞ!「関節リウマチの新しい治療薬とは?」わかさ pp.174-175, 2009
13. 中里款、野々村美紀、宮坂信之、上阪等.リウマチ滑膜に対する遺伝子導入システムの現状と展望.第35回総会ポスター賞記念論文 Jpn. J. Immunol. 31（1）:17-22, 2008
14. 竹内勤、田中良哉、宮坂信之.座談会:関節リウマチの治療の現状と展望.最新医学・別冊「新しい診断と治療のABC8」免疫1関節リウマチ 最新医学社 pp.300-309, 2008
15. 宮坂信之、駒野有希子.Window of opportunity. 日本医師会雑誌 137（6）:1228-1229, 2008
16. 上阪 等.生物学的製剤による骨破壊抑制効果 腎と骨代謝 21（1）: 69-74, 2008
17. 上阪 等.多発性筋炎・皮膚筋炎 内科 101（4）: 635-640, 2008
18. 上阪 等.内科必携画像診断 多発性筋炎・皮膚筋炎 内科 101（6）: 1414-1416, 2008
19. 大畑順子、上阪 等.Foxp3遺伝子導入細胞による自己免疫疾患の治療 炎症と免疫 16（4）: 442-447, 2008
20. 沖山奈緒子、上阪 等.多発性筋炎・皮膚筋炎の研究の発展 日本臨床免疫学会会誌 31（2）: 85-92, 2008
21. 上阪 等.関節リウマチと骨軟骨破壊 最新医学 63（11）: 39-44, 2008
22. 上阪 等.内科ガイドライン活用法 多発性筋炎・皮膚筋炎 内科 102（6）; 1355-1360, 2008
23. 南木敏宏.多発性筋炎/皮膚筋炎.膠原病診療の最近の進歩と今後の展望.Medico 39: 11-14（435-438）, 2008
24. 南木敏宏.全身性エリテマトーデス－病態解明と治療の新たな展開－ SLEの難治性病態の解明と治療の展開:SLEの難治性呼吸器病変（肺胞出血・肺高血圧症）.最新医学 63: 42-47（924-929）, 2008
25. 南木敏宏.生物学的製剤の使い方をやさしく教えます!－インフリキシマブとエタネルセプト－ 使用するにあたっての注意点は?使ってはいけない場合は? 分子リウマチ治療 1: 6-10（6-10）, 2008
26. 高田和生.Presentation Trainer:簡単な統計処理からグラフ作成まで「Frontiers in Rheumatology & Clinical Immunology」3, 2008
27. 高田和生.しっかり管理すれば怖くない˝治療に伴う副作用˝ 「EBMジャーナル」9（4）, 2008
28. 高田和生.皮膚筋炎・多発性筋炎の間質性肺炎に対するカルシニューリン阻害療法 「リウマチ科」39（5）, 2008
29. 高田和生.SLEの自己抗体産生は発症に先行する 「リウマチ科」40（3）, 2008
30. 高田和生.目でみる症例「皮膚筋炎（進行性間質性肺炎）」「内科」101（5）, 2008
31. 小池竜司.（テーマ①）生物学的製剤投与前のスクリーニング Frontiers in Rheumatology & Clinical Immunology 2（1）: 50, 2008
32. 小池竜司、窪田哲朗.Inflammasomeと疾患 Frontiers in Rheumatology & Clinical Immunology 2（4）: 217-224, 2008
33. 小池竜司、針谷正祥.関節リウマチに対するTNF阻害薬投与下におけるニューモシスチス肺炎発症の危険因子 臨床薬理の進歩29: 197-205, 2008
34. 小池竜司.第3回Biologicsケーススタディ（安全性）TNF阻害薬とニューモシスチス肺炎 分子リウマチ治療1（3）: 136-139, 2008
35. 小池竜司.再発性多発軟骨炎 内科（特集 内科必携画像診断 Imaging Revolution）101（6）: 1461-1464, 2008
36. 駒野有希子、針谷正祥.生物学的製剤と感染症

リ ス ク .Frontiers in Rheumatology & clinical Immunology 2（1）: 22-26, 2008
37. 駒野有希子、宮坂信之.米国におけるリウマチ性疾患患者数.リウマチ科 40（4）: 402-409, 2008
38. 駒野有希子、針谷正祥.PAT研究.分子リウマチ治療 1（2）: 18-21, 2008
39. 駒野有希子、針谷正祥.関節リウマチに対する生物学的製剤－その効果と安全性. 看護技術 54（13）: 19-24, 2008
40. 溝口史高、宮坂信之． 関節リウマチの診療のために: 治療ガイドライン－2008年アメリカリウマチ学会勧告を中心に－特集:一般医に必要なリウマチ診療の知識.総合臨床 57（12）: 2862-2867, 2008
41. 渡部香織、宮坂信之.New専門医を目指すCASE METHOD APROACH 膠原病・リウマチ1-11,2008
42. 渡部香織、宮坂信之.関節炎を伴う全身性リウマチ性疾患の鑑別 整形外科59: 1028-32,2008
43. 渡部香織、宮坂信之.関節リウマチでは治療開始3ヶ月後の疾患活動性が1年後の治療反応性を予知することができる リウマチ科 40（5）: 546-552,2008
44. 本根杏子、上阪 等.内科ガイドライン活用法 強皮症 内科102（6）; 1361-1365, 2008
45. 本根杏子、上阪 等.内科必携画像診断 RS3PE症候群 内科 101（6）: 1457-1459, 2008

10. 学会発表（英文）

1. Watanabe K, Nanki T, Penfold ME, Ohyanagi N, Kaneko K, Matsuda A, Matsumoto K, Miyasaka N. Pathogenic Role of CXCR7 in Rheumatoid Arthritis. American College of Rheumatology 72th National Meetings, San Francisco, CA, December, 2008
2. Yoshiya Tanaka, Kazuhiko Yamamoto, Tsutomu Takeuchi, Norihiro Nishimoto, Nobuyuki Miyasaka, T Sumida, Tetsuji Sawada, Hitoshi Kohsaka, Isao Matsumoto, K. Saito, Takao Koike. A 2 Year-Extended Follow-Up Of The Phase I/II Trial Of Rituximab For Treatment Of Refractory Systemic Lupus Erythematosus. Annual European Congress of Rheumatology EULAR Paris, France, 11-14 June 2008
3. Hitoshi Kohsaka. What we learnt from a new animal model of polymyositis International symposium on inflammatory myopathy. May 23, 2008 Seoul（招待講演）
4. Hitoshi Kohsaka, Chiyoko Sekine, Yousuke Murakami, Nobuyuki Miyasaka. New approaches to treatment of rheumatoid arthritis. 13th Congress of the Asia Pacific League of Associations for Rheumatology, September 23-27, 2008, Yokohama（招待講演）
5. Mizoguchi F, Izu Y, Hayata T, Hemmi H, Nakashima K, Nakamura T, Kohsaka H, Miyasaka N, Harfe B, Kato S, Ezura Y, Noda M. Osteoclast Specific Dicer Deficiency Suppress Osteoclast Differentiation And Increase Bone Mass. 2nd International Conference on Osteoimmunology. Rhodes, Greece June, 8-13, 2008
6. Nanki T. Chemokines in Idiopathic Inflammatory Myopthy. International Symposium for Inflammatory Myositis. Seoul, Korea, May, 2008
7. Naoko Okiyama, Takahiko Sugihara, Hiroo Yokozeki, Nobuyuki Miyasaka, Hitoshi Kohsaka. A new mouse model of polymyositis indicates IL-6 as a therapeutic target. International Society for Investigative Dermatology 2008, Kyoto May 14-17, 2008
8. Naoko Okiyama, Hitoshi Kohsaka. IL-6 as a potential therapeutic target of polymyositis International symposium on inflammatory myopathy. May 23, 2008 Seoul
9. Nanki T, Morio T, Zhao M, Kanegane H, Miyasaka N. Chemokines regulate B cell activation. Keystone symposia, Chemokines and Chemokine Receptors. Keystone, USA, January, 2008
10. Yousuke Murakami, Tohru Akahoshi, Naoko Aoki, Masayasu Toyomoto, Nobuyuki Miyasaka, Hitoshi Kohsaka. Prevention of TREM-1 suppressed the development of collagen-induced arthritis. Keystone symposia. Keystone. March. 2008

11. 学会発表（和文）

1. 上阪 等、大畑順子.関節炎抑制のために制御性T細胞に必要な抗原特異性と免疫抑制性 第52回 日本リウマチ学会総会・学術集会 札幌 2008年4月20-23日
2. 駒野有希子、針谷正祥、田中みち、小池竜司、南木敏宏、宮坂信之.日本における生物学的製剤使用関節リウマチ患者に関する疫学研究（REAL研究）による生物学的製剤の安全性の検討（中間報告） 第52回日本リウマチ学会総会・学術集会、2008年4月
3. 南木敏宏、大柳菜歩、石堂美和子、窪田哲朗、宮坂信之.実験的多発性筋炎に対するレチノイド、Am80の効果の検討.第52回日本リウマチ学会総会 札幌 2008年4月
4. 窪田哲朗、福谷泰子、南木敏宏、宮坂信之.抗リン脂質抗体症候群の向血栓傾向におけるケモカインの作用に関する検討.第52回日本リウマチ学会総会 札幌 2008年4月
5. 本根杏子、上阪 等、山本浩平、北川昌伸、宮坂信之.骨髄に多数の非大顆粒リンパ球性CD8T細胞の浸

潤を認めたFelty症候群の一例　第52回日本リウマチ学会総会・学術集会　札幌　2008年4月20-23日
6. 小池竜司、針谷正祥、宮坂信之.TNF阻害薬使用下のニューモシスチス肺炎（シンポジウム）　第52回日本リウマチ学会総会・学術集会　札幌　2008年4月
7. 小池竜司、針谷正祥、宮坂信之.膠原病患者における間質性肺疾患マーカーKL-6およびSP-D同時測定の意義の検討　第52回日本リウマチ学会総会・学術集会　札幌　2008年4月
8. 村上　洋介、赤星　透、宮坂　信之、上阪　等. 関節炎治療の新たな標的分子Triggering receptor expressed on myeloid cells-1（TREM-1）. 第52回日本リウマチ学会総会　札幌、2008年4月
9. Kaori Watanabe, Toshihiro Nanki, Mark E.T Penfold, Naho Ohyanagi, Kayoko Kaneko, Akio Matsuda, Kenj Matsumoto, Thomas J. Schall, Nobyuki Miyasaka. Pathogenic role of CXCR7 in rheumatoid arthritis.　第38回日本免疫学会総会・学術集会　京都、2008年12月
10. Yousuke Murakami, Tohru Akahoshi, Naoko Aoki, Masayasu Toyomoto, Nobuyuki Miyasaka, Hitoshi Kohsaka. Triggering receptor expressed on myeloid cells-1 as a new therapeutic target of rheumatoid arthritis. 第38回日本免疫学会総会　京都、2008年12月
11. 長谷川久紀、溝口史高、上阪　等、宮坂信之.組織球貪食性脂肪織炎とマクロファージ活性化症候群を合併した全身性エリテマトーデスの一例　第36回日本臨床免疫学会　東京　2008年10月17-18日
12. 中里　款、宮坂信之、上阪　等.リウマチ滑膜線維芽細胞におけるlet-7 microRNAの効果　第36回日本臨床免疫学会　東京　2008年10月17-18日
13. 中塩屋　大樹、宮坂　信之、松下　祥、上阪　等.マウスのコラーゲン誘発性関節炎と破骨細胞に対するドパミン受容体阻害薬の効果　第36回日本臨床免疫学会　東京　2008年10月17-18日
14. 沖山奈緒子、北嶋　隆、伊藤嘉浩、横関博雄、宮坂信之、上阪　等.コラーゲン結合ドメイン融合肝細胞成長因子による糖尿病マウスの皮膚潰瘍治癒促進効果　第36回日本臨床免疫学会　東京　2008年10月17-18日
15. 豊本雅靖、石戸　聡、宮坂信之、上阪　等.E3ユビクチンリガーゼc-MIRの抗炎症効果による関節炎治療　第36回日本臨床免疫学会　東京　2008年10月17-18日
16. 杉原毅彦、沖山奈緒子、渡部直人、鈴木美穂子、宮坂信之、上阪　等.新規多発性筋炎モデルマウスに対するIL-1阻害療法の検討　第36回日本臨床免疫学会　東京　2008年10月17-18日
17. 村上　洋介、宮坂　信之、上阪　等.関節リウマチの新しい標的分子Triggering receptor expressed on myeloid cells-1　第36回日本臨床免疫学会　東京　2008年10月17-18日
18. 高橋尚美、森尾友宏、松本健治、齋藤博久、南木敏宏、宮坂信之、水谷修紀. ICOS欠損症患者T細胞におけるTh1, Th2, Th17サイトカイン産生不全とその機構.第36回日本臨床免疫学会　東京　2008年10月
19. 溝口史高、伊豆弥生、早田匡芳、辺見弘明、中島和久、中村貴、Brian Harfe、加藤茂明、宮坂信之、江面陽一、野田政樹.　破骨細胞特異的Dicer欠損は破骨細胞分化を抑制し骨量を増加させる.　第36回臨床免疫学会　東京　2008年10月17-18日
20. 溝口史高、伊豆弥生、中村貴、早田匡芳、辺見弘一、中島和久、Brian Harfe、加藤茂明、江面陽一、宮坂信之、野田政樹.　破骨細胞におけるDicerの役割.第4回リウマチヤングアカデミー　札幌　2008年7月19日
21. 豊本雅靖、石戸　聡、宮坂信之、上阪　等.E3ユビキチンリガーゼc-MIRの抗炎症効果による関節炎治療　第29回日本炎症・再生医学会　東京　2008年7月8-10日
22. 上阪　等.Osteo-myo-immunology? －多発性筋炎と我々のモデルマウス－　第5回 Osteoimmunology Forum 2008年2月16日　東京
23. 上阪　等.多発性筋炎/皮膚筋炎 －膠原病内科医の見た目－ 第16回神経免疫フォーラム　平成20年3月22日　油谷湾温泉（山口）
24. 上阪　等.膠原病領域におけるγグロブリン療法の基礎と臨床　第18回日本小児リウマチ学会総会・学術集会　平成20年10月4-5日　札幌
25. 上阪　等.膠原病領域におけるγグロブリン療法の基礎と臨床　第30回水疱症研究会イブニングセミナー　平成20年10月25日　東京
26. 上阪　等.抗サイトカイン療法を超える次世代抗リウマチ療法の開発　技術情報協会講習会「リウマチ治療薬開発の現状と最新動向」平成20年12月16日　東京
27. 上阪　等、村上洋介、野々村美紀、宮坂信之.関節リ

ウマチ治療の新たな標的分子　第45回日本臨床分子医学会学術集会　神戸　2008年7月24-25日
28. 本根杏子、野々村美紀、上阪　等、宮坂信之.口内炎、難治性痔瘻、再生不良性貧血を合併した破壊生関節炎の症例　第49回関東リウマチ研究会　東京　2008年6月21日
29. 駒野有希子.シンポジウム「リウマチ性疾患薬物療法のリスクマネージメント」－生物学的製剤　第19回日本リウマチ学会関東支部学術集会　高崎　2008年12月
30. 細矢　匡、溝口史高、八木洋輔、長谷川久紀、南木敏宏、上阪等、宮坂信之.関節リウマチに対しetanercept投与中に半月体形成性糸球体腎炎と器質化肺炎様肺病変、MPO-ANCA陽性を認めた一例　第19回日本リウマチ学会関東支部学術集会　高崎　2008年12月6日
31. 長谷川久紀、鈴木文仁、本根杏子、上阪等、宮坂信之.多彩な中枢神経症状を呈し、MPO-ANCA陽性であったWegener肉芽腫症の1例.第555回日本内科学会関東地方会　東京　2008年7月
32. 南木敏宏.炎症性筋疾患とケモカイン.第15回自己抗体と自己免疫シンポジウム－筋炎と自己免疫myopathy & autoimmunity－　東京　2008年2月
33. 小池竜司、東條尚子.当院における過去5年間の血液培養検出菌の傾向と背景の検討　第82回日本感染症学会・学術講演会　松江　2008年4月
34. 小池竜司.医師の立場から見た医薬品の安全使用のための情報管理（シンポジウム）　第62回国立病院総合医学会　東京　2008年11月
35. 金子佳代子、小池竜司、針谷正祥.血球貪食症候群およびParadoxical Reactionを伴った粟粒結核の一例　第82回日本感染症学会　島根、2008年4月

12. 受賞

宮坂信之:日本リウマチ友の会賞（2008年）;関節リウマチ患者の全国組織から、関節リウマチ治療への貢献に対して授与された。

13. 外部資金の獲得状況

1. 宮坂信之.免疫アレルギー疾患等予防・治療研究事業「膠原病の生命予後規定因子である肺合併症の診断及び治療法の再評価と新規開発に関する研究」主任研究者:36,000,000円（うち間接経費6,000,000円）
2. 宮坂信之.難治性疾患克服研究事業「難治性疾患に関する有効な治療法選択等のための情報収集体制の構築に関する研究」（主任研究者:工藤翔二）分担研究者:1,000,000円
3. 宮坂信之.免疫アレルギー疾患等予防・治療研究事業「関節リウマチの治療法選択と治療反応性の実態把握の為の定点観測体制の構築」（主任研究者:山本一彦）分担研究者:200,000円
4. 宮坂信之.免疫アレルギー疾患等予防・治療研究事業「関節リウマチの関節破壊ゼロを目指す治療指針の確立、及び根治・修復療法の開発に関する研究」（主任研究者:田中良哉）分担研究者:2,5000,000円
5. 宮坂信之.　治験推進事業　『「多発性筋炎・皮膚筋炎に合併する間質性肺炎に対するタクロリムスの臨床試験」の調整・管理に関する研究』　主任研究者:79,937,000円
6. 宮坂信之.治験推進事業　「治験の実施に関する研究［タクロリムス水和物］」主任研究者:1,000,000円
7. 上阪　等.文部科学省科学研究費補助金　基盤研究（B）　関節リウマチ新治療戦略としてのサイクリン依存性キナーゼ4/6阻害療法　6,100千円
8. 上阪　等.厚生労働省科学研究費補助金（難治性疾患克服研究事業）新たな診断・治療法開発のための免疫学的手法の開発に関する研究　分担研究者　3,000千円
9. 上阪　等.厚生労働科学研究費補助金（免疫アレルギー疾患等予防・治療研究事業）免疫疾患の病因・病態解析とその制御戦略へのアプローチ　分担研究者　3,000千円
10. 上阪　等.共同研究（ベネシス）　多発性筋炎・皮膚筋炎などの難病に対する人免疫グロブリン療法の作用機序の解明　1,000千円
11. 上阪　等.共同研究（ファルマエイト）関節リウマチおよび糖尿病を対象とした評価・アッセイ技術および化合物の合成展開技術の融合による治療薬の開発　420千円
12. 上阪　等.共同研究（田辺三菱製薬）TREM-1の創薬可能性評価　2,000千円
13. 南木敏宏.厚生労働科学研究費補助金（免疫・アレルギー疾患予防・治療研究事業）「関節リウマチの寛解導入療法体系化に関する研究」.分担研究者.
14. 南木敏宏.科学研究費補助金（基盤研究B）.関節リウマチにおける生物学的製剤の長期安全性と副作用リスク因子に関する疫学研究.分担研究者.
15. 南木敏宏.科学研究費補助金（基盤研究C）.フラクタルカイン阻害による血管炎症候群に対する新規治

療法の開発.
16. 南木敏宏.共同研究（エーザイ（株））.ケモカイン・接着分子等の関節リウマチなどの自己免疫疾患における役割の研究.
17. 高田和生.厚生労働科学研究費補助金　難治性疾患克服研究事業「自己免疫疾患に関する調査研究班」（分担研究者）
18. 沖山奈緒子.文部科学省科学研究費補助金　特別研究員奨励費　「新しい多発性筋炎モデルマウスを用いた至適抗サイトカイン療法の開発」 1,200千円
19. 村上洋介.文部科学省科学研究費補助金　若手研究（B）　自然免疫および破骨細胞分化に及ぼすCDK4/6の新規機能の解析　総額2,210千円
20. 村上洋介.　財団法人　日本応用酵素協会　研究助成金　自然免疫および破骨細胞分化に及ぼすCDK4/6の新規機能の解析　500千円

14. 特別講演、招待講演

1. 第1回群馬県リウマチ登録医の会　2008年4月12日　群馬　「関節リウマチの最新治療」
2. リウマチTV講演会　2008年5月15日　東京　「生物学的製剤の最新の知見—TNF阻害療法施行ガイドライン改訂を中心に」
3. 日本医師会生涯教育講座　2008年6月12日　東京　「関節リウマチ—最新の治療戦略とは？—」
4. 関節リウマチメディアセミナー　2008年6月25日　東京　「関節リウマチ治療の最新知見」
5. トシリズマブ学術講演会　2008年6月28日　東京　「トシリズマブの安全性—国内外臨床試験の結果から—」
6. 第77回福岡リウマチ懇話会　2008年8月22日　東京　「RAに対する新しい生物学的製剤の使い方」
7. JCR2008全国中央教育研修会東京大会　2008年8月24日　東京　「関節リウマチに対する薬物療法—薬物選択と副作用」
8. 第17回岐阜リウマチ研究会　2008年8月30日　岐阜　「関節リウマチ治療のスタンダードとは?—治療のパラダイムシフト—」
9. 第15回BRMサイトカイン学術講演会　2008年9月2日　名古屋　「関節リウマチの抗サイトカイン療法」
10. 第3回水戸・日立リウマチフォーラム　2008年9月18日　水戸　「関節リウマチにおける生物学的製剤の使い方」
11. 御茶ノ水リウマチセミナー　2008年10月1日　東京　「抗IL-6受容体抗体療法の有効性・安全性」
12. 山形新聞市民公開講座　2008年10月5日　山形　「正しく知ろう、リウマチ治療の現在」
13. （社）日本リウマチ友の会鳥取支部総会・公開医療講演会　2008年11月2日　倉吉　「リウマチの最新薬物療法」
14. 第38回日本皮膚アレルギー・接触性皮膚炎学会総会学術大会　2008年11月8日　大阪　「膠原病の最新戦略とは?」
15. 第18回大学院医歯学総合研究科大学院セミナー「炎症と骨免疫—歯周病、関節リウマチを中心に」 2008年11月10日　東京　「関節リウマチの関節破壊防止戦略とその問題点」
16. 平成20年度リウマチ・アレルギーシンポジウム in 名古屋　2008年11月15日　名古屋　「リウマチはここまでよくなる!」
17. リウマチフロンティア市民公開講座　2008年11月16日　岡山　「関節リウマチの病態と薬物療法」
18. 平成20年度「病気を学ぶ」研修 第3回　2008年11月17日　東京　「リウマチについて」
19. 第59回神奈川リウマチ医会　2008年11月22日　横浜　「関節リウマチ治療における生物学的製剤のノウハウ—適応、選択、スイッチング、リスクマネージメント」
20. 第18回日本リウマチ学会北海道・東北支部学術集会ランチョンセミナー　2008年11月23日　福島　「アダリムマブの使い方とその注意点」
21. 鹿児島トシリズマブ適正使用研究会　2008年11月26日　鹿児島　「抗IL-6受容体抗体治療の有効性と安全性」
22. 第38回日本免疫学会総会・学術集会クリニカルセミナー　2008年12月1日　京都　「抗サイトカイン療法のもたらしたもの」
23. JCR2008全国中央教育研修会大阪大会　2008年12月7日　大阪　「関節リウマチに対する薬物療法—薬物選択と副作用」
24. 西多摩臨床整形外科医会　2009年1月22日　立川　「関節リウマチ治療—最近のトレンド—」
25. 平成20年度リウマチ・アレルギーシンポジウム in 横浜　2009年2月8日　横浜　「リウマチはここまでよくなる!」
26. バイオロジクスフォーラム第6回学術集会　2009年2月3日　東京　「生物学的製剤を用いた関節リウマチの関節破壊阻止戦略とその問題点」

15. 主催学会

宮坂信之:第36回日本臨床免疫学会総会（2008年10月17-18日、東京京王プラザホテル）

16. 講座の准教授、講師、助教、特別研究員、ポスドク、指導を受けた大学院生の名前（AISSには○印）のリスト

教　授	宮坂信之
保健衛生学研究科准教授（併任）	窪田哲朗
薬害監視学講座教授（併任）	針谷正祥
准教授	上阪　等
臨床試験管理センター長（併任）	小池竜司
薬害監視学講座准教授（併任）	南木敏宏
講　師	高田和生
助　教	鈴木文仁
	溝口史高
薬害監視学講座助教（併任）	田中みち
	駒野有希子
メディカルフェロー	中里　款
大学院生	本根杏子
	豊本雅靖
	渡部香織
	（社会人大学院生）
	高村聡人
	（社会人大学院生）
	金子佳代子
	（社会人大学院生）
留学中	西尾純子
	（Harvard大学）
	野々村美紀
	（University of California, San Diego）
	岩井秀之
	（Stanford大学）

新聞 （第3種郵便物認可）

関節リウマチに新薬

骨の破壊予防 歩行も楽に

手足の関節が腫れて痛む関節リウマチは、病状が進行すると、関節が壊れて歩けなくなることもあるなど、患者の日常活動は大きく制約される。関節の破壊を抑えるとされる新薬「生物製剤」が今年4月、2種類承認された。この種の製剤は、先に発売されている薬と合わせて計4種類となり、治療の選択肢が広がった。（坂上博）

関節リウマチは、全身の関節に炎症が起きて痛み、進行すると関節が壊れて変形する。指が動かず食事にも苦労し、歩けなくなる人もいる。患者数は約70万人とみられる。

この病気は、炎症を起こしたり、骨を破壊する細胞を活性化させたりする物質、サイトカインが病状悪化の一因となる。その働きを防ぐよう、遺伝子組み換え技術を使って作ったのが「生物製剤」だ。従来使われていた抗リウマチ薬は、ある程度、炎症を抑えることはできたが、関節破壊を防ぐ効果は低かった。

今年4月承認されたのは、「アクテムラ（一般名トシリズマブ）」と「ヒュミラ（同アダリムマブ）」。このうちアクテムラは、大阪大元学長の岸本忠三さんらの研究グループと中外製薬が開発した国産薬だ。

小学校教諭の40歳代の女性は、1990年にリウマチと診断された。既存の抗リウマチ薬を飲んだものの、関節の変形が進んだ。手の指が曲がり、ぞうきんも絞れない。ひざや股関節が痛み、教壇に立つのがつらい。

96年、大阪大でアクテムラの効果を調べる臨床試験に参加、点滴治療を受けたところ、関節の痛みが減り、歩くのも楽になった。今も体調が良い。

他の生物製剤3薬は、サイトカインの中でも「TNF（腫瘍壊死因子）－α」の働きを抑えるが、アクテムラは別のサイトカイン「IL（インターロイキン）－6」を標的とする。開発者の一人、大阪大免疫アレルギー内科客員教授の吉崎和幸さんは「薬の作用の仕方が違うので、ほかの薬が無効な場合にも効く可能性がある」と期待する。

東京医科歯科大膠原病・リウマチ内科教授の宮坂信之さんによると、これらの薬は、メトトレキサートなど既存の抗リウマチ薬が効かなくなった場合に使う。痛む関節数が半分以下に減るなどの効果が、治療開始後1年の時点で60～70％ほどの患者に表れる。

ただ、薬が高価で、患者の医療費負担は大きい。4製剤は、保険の3割負担でも、年40万～60万円ほどかかる。

副作用の問題もある。免疫を抑える薬なので、肺炎など感染症にかかりやすくなるのだ。

承認から3～5年がたつレミケードとエンブレルによる肺炎の発病率は、投与者の1～2％ほど。宮坂さんは「生物製剤の中では、効果も副作用も分かっているレミケードかエンブレ
が、現時点
う。今後、
蓄積されて
方も変わっ
言う。

肺炎の副
多量のステ
どに起きや
「リウマチ
し、肺炎球
など予防策
してほしい

マチ薬は、ある程
ることはできた
を予防する効果が

が進行して壊れた
の関節（矢印部分）▶

生物製剤が効く仕組み

TNF-αやIL-6が受容体にくっつくのを妨げ、信号を出させない

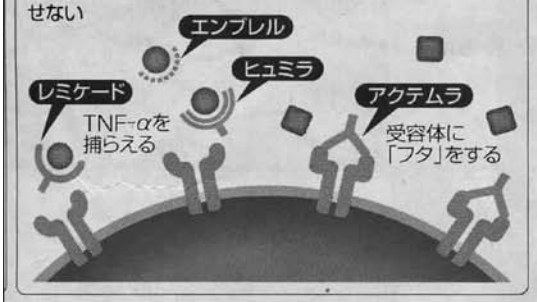

投与間隔	治療の標的とする物質	他剤との併用	日本でリウマチ治療薬として承認された時期
点滴から2週間週間後に受け、は8週間ごと	TNF-α	メトトレキサート（MTX）を必ず併用	2003年
回	TNF-α	単剤でもMTX併用でも良い	2005年
に1回	IL-6	併用しない	2008年
に1回	TNF-α	単剤でもMTX併用でも良い	2008年

日本経済新聞(夕刊) 2008年(平成20年)10月21日(火曜日)

夕&Eye

健

関節リウマチやクローン病治療

抗TNFα薬 適用広がる

体内で分泌される免疫物質「TNFα」の働きを抑える薬の適用が広がっている。関節リウマチや消化管の難病であるクローン病によく効くと注目され、四月には三つ目の薬が登場した。ただ、まれに副作用で重い肺炎などを引き起こし、長期的な安全性は不明。医師の説明をよく聞き、効果とリスクを踏まえた上で選択する必要がある。

十代のころから腹痛と下痢を繰り返し、三十一歳でクローン病と診断された仙台市のAさん(40)。これまで数年ごとに症状が悪化し、絶食や手術を繰り返してきた。二年前に抗TNFα薬インフリキシマブ(商品名レミケード)の投薬を始めて以来「まったく自覚症状がなくなった。食事も普段通り」という。

Aさんの主治医でこの分野の専門医、高木外科内科胃腸科医院(仙台市)の高木承副院長は、「炎症が落ちつき、腸から出血するリスクが下がった。経過は良好です」と話す。

手術せずに改善

TNFαは免疫細胞が分泌するたんぱく質で、細菌などに対する防御反応を担う。クローン病や関節リウマチといった自己免疫疾患はTNFαが過剰になり、炎症を引き起こす。これを抑えるのが抗TNFα薬で、インフリキシマブは日本で最初に承認された。

あらゆる消化管に炎症が起きるクローン病は、食事をすると症状が悪化するため、食事をできるだけ栄養剤に切り替える栄養療法や手術が中心だった。抗TNFα薬の登場で「クローン病の治療は劇的に変わった。手術が必要になる人は激減した」と東邦大学医療センター佐倉病院の鈴木康夫教授は言う。

日本でのデータはまだ乏しいが、海外では手術が必要になる人が三九%から二四%に減少したとの報告がある。投与率の改善でこの数字はさらに低くなることもわかった。

七十万人以上の患者がいる関節リウマチにも、抗TNFα薬はよく効く。東京医科歯科大学の宮坂信之教授は「八割以上の人に有効で、しかも即効性がある」と解説する。つえをついてやっと歩いていた患者が、投薬後に痛みがとれ、つえを忘れて帰ってしまったこともあるという。

関節リウマチにはインフリキシマブのほか、エタネルセプト(同エンブレル)、今年登場したアダリムマブ(同ヒュミラ)が承認されている。

長期間投薬を続けると、体内に薬に対する抗体ができて効果が弱まることがあるが、複数あれば、薬を切り替えて治療を継続できる。投薬の方法や間隔も違い、体の状態に合わせて選ぶことも可能だ。

長期的安全性は不明

関節リウマチの場合、以前はほかの治療が効かなくなった患者が最後に使う薬とされていた。しかし、関節の骨が壊れるのを抑える働きがあることが判明、「現在は抗リウマチ薬が三カ月間効かなかったら抗TNFα薬を追加し、骨の破壊を防いだ方がいいと考えられている」(宮坂教授)。

抗TNFα薬はベーチェット病による目のぶどう膜炎にも適用承認された。

ており、慢性の皮膚病である乾癬(かんせん)への適用も申請中。強直性脊椎(せきつい)炎、潰瘍(かいよう)性大腸炎への臨床試験(治験)も進行中で、今後、対象がさらに広がりそうだ。

感染症に注意

抗TNFα薬治療で気をつけなければならないのが、感染症対策。免疫にかかわる物質の働きを抑えるため、肺炎や結核にかかりやすくなる。

欧米で最初に承認されてから十年。長期にわたる安全性も未知数だ。悪性リンパ腫が増える可能性を指摘した報告もあり、日本リウマチ学会は今年から三千人の患者を五年間追跡、がんの発生率を調べる研究に着手した。

日本で販売・開発中の抗TNFα薬

商品名(一般名)	関節リウマチ	クローン病	ベーチェット病の網膜ぶどう膜炎	乾癬	強直性脊椎炎
レミケード(インフリキシマブ)	承認・販売	承認・販売	承認・販売	申請中	治験中
エンブレル(エタネルセプト)	承認・販売	—	—	—	—
ヒュミラ(アダリムマブ)	承認・販売	治験中	—	申請中	治験中
シムジア(セルトリズマブ・ペゴル)	治験計画中	申請準備中	—	—	—

体のシグナル わかりにくい結核

「ストレスで疲労」実は感染

Iさん(25、女性)は、事務系の派遣社員として働いている。とてもすごしやすい季節だというのに、体調がすぐれない。仕事から帰ると心身ともに疲れ果てて、くたくただ。

そもそも緊張しやすい性格で、職場でも、他の同僚のように天真爛漫(らんまん)にはふるまえない。いつもさいなことに気をまわして、疲れてしまう自分が、嫌になってしまう。

朝になっても、爽快(そうかい)な気分になれない。ある日、同僚の強い誘いで、勤務後、カラオケで遅くまで楽しんで帰ってきた。ももやや

サラリーマン新健康ワイド 日刊ゲンダイ 2008年(平成20年)9月9日(8日発行) 第3種郵便物認可 (12)

知らないと後悔する! 関節リウマチの最新情

関節リウマチは、30～60歳が発症年齢で、働き盛りに発症する人が少なくない。進行すると、軟骨や骨が破壊され、歩いたり、手を動かしたりできなくなるのだ。

「それだけではありません。これまでの治療では、健康な人に比べ、平均寿命が約10年短くなることが分かっています」(東京医科歯科大学病院膠原病・リウマチ内科の宮坂信之教授)

この関節リウマチ、今年は「医師と患者にとって画期的な年」だと、宮坂教授は言う。関節リウマチの最新情報を聞いた。

「今年4月、アクテムラとヒュミラという生物学的製剤(リウマチの治療薬)が承認されたので、03年に承認されたレミケード、05年承認のエンブレルに加えて全部で4種類になりました」

生物学的製剤とは、腫瘍壊死因子を抑え、リウマチによる関節破壊を食い止める薬のことだ。ほかに類を見ないほど、劇的に効く。それを表す例として、取材時、宮坂教授からある映像を見せてもらった。階段の手すりを持ち、一歩一歩よろよろと下りてくる関節リウマチ患者の映像だ。

「この方は、発症1年でここまで病状が進行しました。そして次にお見せする映像は、生物学的製剤の一種、レミケードをたった1回投与して2週間目のものです」

それは、階段をタタタッと駆け下りてくるもので、まるで別人!

「つえをついてきたのに、治療後帰るときにはつえを忘れていった方、

働き盛りに発症する人も多いリウマチだが……

車イス
してた
過院の
スタス
て帰ら
なども
しゃい
研究で
ミケー
例以上
(症状
った状
8割以
節破壊
を抑制する効果が
とが分かっていま
かの生物学的製剤
の効果がありま

ここまで治るようになった

関節リウマチ
は、近年まで「早
が難しく、見つか
きは重症。効き目
できる薬も十分に
という状態だった

名物コラム再開!

恐怖の自腹グルマン 友里征耶の 行っていい店わるい店 連載③

ミシュラン掲載からわずか1ヶ月で閉店を決めた1つ星フレンチ「ザ ジョージアン クラブ」。ブラッスリーなどの店舗展開が多くなり、売り上げに占めるバンケット比率が低下したからでしょうか、粗利率の高いバンケットの目玉として「ひらまつグループ」がこの大箱を引き継ぎましたが、アルザスの3つ星レストランの提携店にしたのはいかがなものか。「オーベルジュ ド リル トーキョー」の提携先は、その名の通りアルザスにある有名オーベルジュ。イギリス形式の箱が合うわけありません。

先にオープンした名古屋店ではアルザスワインが主体でありましたが、東京店では赤ワインがわずか2種しかリストに見当たりません。ブルゴーニュかボルドーしか選択肢がないのですが、そのワインの値付けがまたベラボー。NVシャンパン(ローラン ペリエ)

オーベルジュ ド リル トーキョー

バンケットに特化した

が1万6500円には開いた口がふさがりません。1万円余計ではないか。アルザスのトリンバック社の白ワイン、「ひらまつシール」を張って特別感を出していますが、1万2000円はやり過ぎです。

ワインの値付けはベラボー

反面、料理はそれほど高くはありません。1万2600円から2万1000円までの3コース。アラカルトも前菜が5000円前後、肉は1万円以内が主体で、ハーフポーションも用意されています。

その日頼んだ鶉(うずら)のフォアグラ(ハーフ4000円)はスペシャリテで有名ですが、ショッ
パイだけ。円外

リウマチを完治へ-生物学的製剤の力

70万人の患者を救う リウマチを完治へ-生物学的製剤の力

炎症を引き起こす要因のタンパク質にくっついて働きを阻害する画期的な新薬登場

発症原因が未だに不明の難病

人口の高齢化とともに、じわじわと患者が増えている関節リウマチ。腕や足などの節々が炎症で腫れて痛み、長期間経つと関節が変形して機能障害が起こる。患者の半数は10年後には寝たきりになるとされる難病だ。

がんと同じように、「欧米に比べ10年は遅れている」といわれてきた日本のリウマチ治療だが、最近日本でも画期的な新薬が相次いで発売され始めた。

日本での患者数は約70万人で、男女比は1対4と女性のほうが圧倒的に多い。40歳代で最も発症しやすい。何らか原因で、体内の免疫機構に異常が

のが特徴で、指から手首や足首、ひざ、ひじ、肩、股関節など全身に変形が広がり、日常生活に支障をきたすようになる。人工のひざ関節や股関節への置き換え手術が広まっているが、関節を人工のものに置き換えても、生活の困難さが完全に解消されるわけではない。

それゆえ、薬物による治療が基本となる。そこに、画期的な新薬が登場したわけだが、その前に従来の薬物治療の経緯を説明しておこう。

関節リウマチの診断には、米国リウマチ学会(ACR)が作成した診断基準が用いられる。診断基準は、①朝に身体が硬直したように感じるこわばり感が1時間以上続く、②3か所以上の

り、うち4項目以上該当すれば関節リウマチと診断される。

関節リウマチで最大の問題は、発症原因が未だによくわかっていないことである。このため、基本的な治療法は、痛みをとり、進行を遅らせることが主体だ。これまで関節リウマチの治療には、大きく分けて、①非ステロイド性抗炎症薬(NSAIDs)、②疾患修飾性抗リウマチ薬(DMARDs)、③副腎皮質ホルモン剤(ステロイド)の3種類の薬剤が用いられてきた。

まず、診断後3か月以内に、鎮痛薬のNSAIDsやステロイドで痛みや腫れを抑えつつ、DMARDsで治療していく。DMARDsには、免疫機

が少しずつ増えてきた。

全く新しい効果の「抗

そうしたなか、'03年に
薬が登場した。TNFα
α)をターゲットにした
剤〟と呼ばれる抗体医薬
薬は、「レミケード」(成分
シマブ)と「エンブレル」
プト)である。TNFα
き起こすサイトカイン(
一種で、関節リウマチの
は大量に産生されている
やエンブレルはこのTN
いて(働きを阻害)、炎症
でなく、TNFαを生み

破壊の進行が抑えられ、関節の変形が予防できることが分かっている。関節リウマチになると、関節炎の発症後2年以内に7割の患者で関節破壊が起こるが、レミケードやエンブレルを初期のリウマチ患者に投与しておけば、関節破壊を抑えられるのである。

海外の臨床試験で、関節リウマチの改善度を示すACRスコアで、痛みや関節の腫れなどが20%以上改善されたことを示す「ACR20」で評価すると、メトトレキサートにプラセボ(偽薬)を上乗せ投与した患者に比べ、メトトレキサートにレミケードを上乗せした患者は、およそ3倍も有効性が高かった。エンブレルもプラセボ投与患者との比較でおよそ3倍の20%の改善率だった。

さらにそこに「アクテムラ」(成分名トシリズマブ)が加わった。アクテムラは、国産第1号の抗体医薬で、インターロイキン6というサイトカインの受容体にくっついて炎症を抑制する。リンパ節の難病であるキャッスルマン病の治療薬として'05年に発売され、今年4月に関節リウマチの治療薬としても認可を受けた。埼玉医科大学総合医療センターのリウマチ・膠原病内科の竹内勤教授は、「レミケードやエンブレルで効果がなかった患者に、アクテムラは高い有効性を示しており、関節破壊の進行を止め、痛みも腫れもない〝寛解〟に導く「強力な薬剤だ」と強調する。

女性に多い難病に新薬登場

さらに、6月には「ヒュミラ」(成分名アダリブマブ)という新薬も発売された。ACR20を調べた臨床試験では、6か月間の投与で、プラセボに対しておよそ3倍も高い有効性を示した。また、2週間に1回の投与で済むことが特徴で、在宅での自己注射も可能だ。

新薬は「両刃の剣」だが効果大

ただ、リウマチの抗体医薬には強い副作用が伴う。TNFα阻害剤には、身体の免疫力が低下するという副作用がある。また、レミケードの場合、製剤を作る過程でマウスのタンパク質の一部を使うため、強いアレルギー反応が起こることがある。これを抑えるために、メトトレキサートを併用する必要がある。一方、エンブレルやヒュミラは人間のタンパク質しか用いておらず、深刻なアレルギー反応はほとんど起こらない。

しかし、米国では、新薬を審査する食品医薬品局(FDA)が今年6月、レミケードやエンブレル、ヒュミラなどTNFα阻害剤について、小児と思春期の子どものがんリスクの調査に入った。TNFαはがん細胞の破壊にも潜在的に有用とされるタンパク質であり、体内のTNFαの活動を抑えれば、がん発症リスクが高まると考えられる。当然、成人にも同じことがいえ、発売元の製薬会社から注意喚起がなされた。

小児に関しては、米国では発売から10年間に約30人の小児でがんが発生したと報告されている。年内には調査が終了する見通しだ。ちなみに、日本では、発売後の使用調査で、副作用による死亡率は許容範囲内に収まっていると、製薬各社は発表している。

東京医科歯科大学膠原病・リウマチ内科学の宮坂信之教授はこう説明する。

「『生物学的製剤』の登場によって、リウマチの治療はここ5年で劇的に変わりました。これまでは進行を遅らせることがゴールでしたが、今では関節破壊を止めることがゴー
ます。しかし、まだ治癒
ません。とはいえ、半数
気を抑えこむことができ
たのは大きな進歩です。
一般的な薬が試験管の
で合成されるのに対し、
は、遺伝子工学的手法を
とする遺伝子を生き物の
で、生き物に薬を作らせ
薬品」です。そのため、
分の薬代が年間約数十万
が高いという問題があり
滴ではなく経口の薬がで
する負担もなくなるでし
TNFなどのサイトカ
とって良い働きもしてお
えると感染症などの副作
ともあります。特に肺炎
意が必要です。生物学的
両刃の剣であることを理
大切です」
今後も、TNFα阻害
マブ」や、T細胞副刺激
1と呼ばれる新タイプの
「アバタセプト」が臨床
る。また、欧米では、T
「シムジア」(成分名セルト
ル)が販売許可を待って
本では臨床試験中)。先行
外にも、関節リウマチの
きる新薬ラッシュが続き

クスリの大図鑑 7

関節リウマチ

生物学的製剤の登場で痛みや腫れが〝半減〟

国内推定患者数	70万人？
症状	自己免疫異常で全身の関節に痛みや腫れを伴う炎症が生じる。関節破壊や手指変形に加え、発熱、貧血なども。

リウマチは「関節に起こる火事」と言われる。関節で熱を帯び、激しい炎症を起こすからだ。痛みや腫れから始まって、手足指などが変形し、最終的には関節破壊に至る。痛みや腫れは全身に広がり、治療をしなければ10年後に約半数が寝たきり状態になるとの報告もある。感染症や合併症のリスクも高まり、平均寿命は10年短くなるといわれる。30~50歳代の女性に発症率が高い。患者数70万人はあくまで〝公式見解〟で実際には人口の0・5~1%が患者だという見方さえある。

リウマチは、免疫機能の異常が原因で起こる。本来、免疫はウイルスなど体の外から入ってくる外敵(抗原)を攻撃する機能を持つ。風邪をひいた際の発熱や咳の症状は、ウイルスを排除しようとする免疫機能のよい働きである。しかしリウマチになると、自己組織を外敵と見なし攻

言いがたい。今の治療ガイドラインでは、他の免疫抑制薬を使用し、効果が見られない場合にしか使用できない。用量上限もアメリカは週あたり25ミリグラムなのに対し、日本は週あたり8ミリグラムと半分以下だ。

東京医科歯科大学の宮坂信之教授は、「臨床現場では、すでにMTX使用症例の約2~3割に8ミリグラム以上の用量が安全に使用されているという実績がある。せめて週あたり20ミリグラム程度までは使用できるよう認めてほしい」と話す。ただ、増量のための臨床試験をこれから始めるのでは時間がかかりすぎる。発売元のワイス社は、医学薬学上の実績データで

MTXを使用した患者のうち、1~2割に用量依存性(消化器・肝障害など)、非依存性(肺炎など)の副作用が発生する。

アメリカのリウマチ専門医のほとんどが内科医であるのに対し、日本のリウマチ専門医は内科医が4割で、残り6割は整形外科医だ。整形外科医にとって、専門外分野の副作用のおそれがあるMTXの使用に抵抗があることは否めない。しかし、「早期診断とリスク管理さえできれば副作用の重症化を防ぐことが可能」(宮坂教授)だ。

リウマチは発症後1年間で関節破壊が最も進む――90年代の研究で判

関節リウマチを引き起こす細胞の増殖を抑制

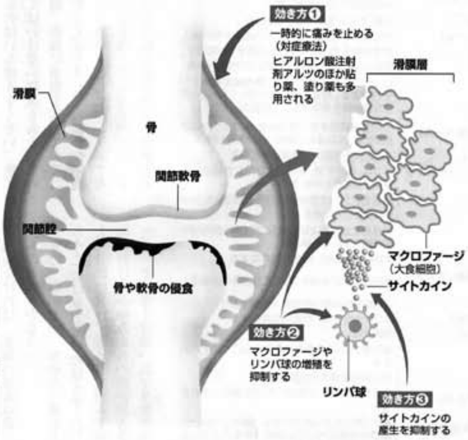

生物学的製剤のレミケードとエンブレルが急激な伸

順位	製品名(発売元)	効き方	07年度売上高(億円)	前期比(%)	発売年
1	レミケード(田辺三菱製薬)	③	28[illegible]	39.6	2002
2	エンブレル(ワイス/武田薬品)	③	18[illegible]	65.3	2005
3	リウマトレックス(MTX)(ワイス)	②	8[illegible]	8.1	1999
–	アクテムラ(中外製薬)	③	–	–	2008(効能追加)
–	ヒュミラ(エーザイ)	③	–	–	2008
(消炎鎮痛薬)	アルツ(科研製薬)	①	25[illegible]	7.9	1987

vs.ジェネリック

投与、自己負担3割ベース)

ジェネリック医薬品の薬価は2008年4月現在存在する全品目の平均値で試算

新薬の登場によって治療法が飛躍的に向上した関節リウマチだが、症状によっては手術が必要な場合がある。

群馬県在住の主婦・清水幸恵さん（仮名・58歳）は、40代になったころからおもに両ひざの関節の腫れや痛みを感じながらも、放置していた。やがて、ひざは90度近くで曲がったままの状態にまで進行。約10年前、とうとう我慢できずに地元の病院に駆け込んだ。そこで薬物治療を受けたが、治療開始が遅かったのと、当時は新薬が承認されていなかったこともあり、その後ひざは伸びないままだった。この状態での治療法は手術しか残っておらず、しかも難易度が高いため、地元の病院のすすめで実績のある日本大学板橋病院を紹介された。

手術はタイミングの見極めが重要

清水さんは家族に付き添われて寝たきりの状態で同院に運ばれてきた。診断を担当した整形外科教授の龍順之助医師は、手術、麻酔、リハビリが1回分ですみ患者の負担が少ない人工関節に、両ひざを同時に取り換える手術を実施することを決めた。

「関節リウマチの治療の主流は薬物療法です。将来的には薬のみで治る時代が来るかもしれませんが、現段階では、関節が破壊された状態の患者さんがかなりいます。また、このうち約3割は薬物療法で効果を得られていませんので、そういう人には外科的な治療が必要になります」（龍医師）

関節リウマチの外科的療法は、大きく分けて二つある。一つは、炎症部分を取り除く「**滑膜切除術**」、もう一つは関節の機能再建術で、代表的なものがひざや大腿骨の「**人工関節置換術**」である。滑膜切除術は新薬の登場でかなり少なくなってきたが、上半身の関節、とくに手指や手首、ひじ関節などで炎症を起こした滑膜を取らないと関節の変形が進んでしまう人がいるので、その際に実施される。

人工関節は、以前は10年しかもたないといわれてきたが、素材やデザインの向上、そして整形外科医の技術の向上などによって耐用年数が15～20年と飛躍的に延びた。同院と関連施設で使われているのは、龍医師が95年に開発、その後改良を加えた「日本人向け」のひざの人工関節である。

大きさは5段階あり、それまで使っていた米国製品より薄いので、手術に際しての骨の切除量が少なくてすむ。また日本人は欧米人よりひざを曲げる習慣があるので、ひざを伸ばした状態を0度とすると、当時110度までしか曲

適切な時期は、レントゲン撮影を見ればわかるそうだが、慣れていない医師が判断を誤ったり、患者自身が放置していたりすると、手術がむずか

名医のセカンドオピニオン

新薬登場で可能性拡大 副作用を恐れすぎない

東京医科歯科大学病院
膠原病・リウマチ内科教授
宮坂信之（みやさかのぶゆき）医師

「この病気の本体は関節に起こった『火事』のようなものです。その火事が今までの治療法や薬だとなかなかうまく消せませんでした。ところが、抗リウマチ薬のリウマトレックスを十分使い、さらに生物学的製剤を併用することで、従来消えなかった関節の火事を消せるようになったのです」

こう話す東京医科歯科大学病院膠原病（こうげんびょう）・リウマチ内科教授の宮坂信之医師によると、08年は、日本の関節リウマチ関係者にとって画期的な年になったという。生物学的製剤は今まで二つしかなかったが、新たにアクテムラ（トシリズマブ）と、ヒュミラ（アダリムマブ）の2製剤が承認され、強力な武器になったからだ。

新薬の一つ、アクテムラは、もともとキャッスルマン病というリンパ節の病気に使われ

マチ学会のガイドラインと、日本の規定では、リウマトレックスとレミケードの使用上限量に大きな差がある。体格の違いもあるが、日本では欧米より結核の有病率が高く、

✚東京医科歯科大学病院　東京都文京区湯島1-5-45　☎03-3813-6111

第一特集3
関節リウマチ

関節リウマチ治療のキーワードは「早期から」「積極的に」「厳密な管理」

東京医科歯科大学大学院
膠原病・リウマチ内科学教授
宮坂 信之

女性に多い難病に新薬登場

――リウマチという病名は誰でも聞いたことがありますが、改めてどんな病気かといわれるとあまり知られていないように感じます。まず、リウマチの原因や症状、またどんな人がかかりやすいのか教えてください。

宮坂 リウマチの正式な名前は「関節リウマチ」といいます。原因はまだ解明されていませんが、免疫機構の異常が原因となって発症することがわかっています。〝疫〟とは病気のこと。外から入ってくる疫を免れるために免疫機構があります。ところが何らかの原因でそこに異常が起こると、自分自身に対して免疫が反応して自分を攻撃してしまう。自爆のようなものです。その結果、関節が炎症を起し、破壊されていく病気です。

症状は、手足などの関節のこわばり、痛み、腫れ、全身のだるさなどがあります。一か所の関節だけではなく、多発性という点が痛風などとは異なります。

症状が進むと、手の関節が変形したり、寝たきりになったりすることもあります。3対7の割合で女性に多く、しかも出産後や閉経前後の30～60代の女性に多いのが特徴です。この年代の女性は家事や育児で忙しい人が多いでしょう。しかし、関節が痛むため、包丁を持ったり、洗濯物をたたんだりという日常生活に支障を来す人が患者さんの7割もいます。

地域、生活習慣を問わず世界中どこでも人口の約1㌫がかかります。日本でも70～100万人の患者がいると思われます。

――リウマチは「難病」といわれますが、治療は難しいのでしょうか。

宮坂 難病といわれたのは、進行を止める決定的な薬がなかったからです。現在でも原因はわからないので予防はできませんが、ここ数年で画期的な新薬が使えるようになり、後で説明するように、治療効果は飛躍的に向上しました。

関節破壊がどうして起こるかというと、「骨を作る細胞」と「骨を壊す細胞」を誰でも持っているのですが、そのうち「骨を壊す細胞」が元気になってしまい、バランスが崩れるからです。最初は関節内に栄養分を供給している滑膜（かつまく）の炎症から始まり、次第に軟骨、骨へと破壊が進みます。最終的には手術で人工関節を入れることもあります。

重要なのは、骨が破壊される前、つまり滑膜の炎症の段階で発見すること。最近では、早期からリウマチを診断するすべも増えてきました。また、発症後すぐの最初の1年で症状が大きく進行するので、その意味でも早期発見は大切です。

早期発見のためには、関節の腫れや朝方のこわばりが複数個所に起こったら我慢せずに受診することです。起こりやすいのは、手の指の第二関節や付け根、足の指の付け根、足首、ひじ、膝、肩です。

――最近登場した新薬で、治療方法はどのように変わったのですか。

宮坂 最近の研究で、早期に強力な薬で治療すれば、治療成績がよくなることがわかってきました。けんかと同じで、まずは強力なパンチで先制攻撃する

宮坂 信之（みやさか のぶゆき）
東京医科歯科大学医学部卒業。米国カリフォルニア大学、テキサス大学留学。東京女子医科大学リウマチ痛風センター助教授等を経て現職。主な編・著書に『ステロイド薬が分かる本』『膠原病が分かる本』がある。

8

特集1

よくなる！関節リウマチ

手や足の関節に痛みが走る関節リウマチは、高齢者に多く、全国に70万人以上の患者さんが、いらっしゃいます。かつては、不治の病とも言われていましたが、近年は治療法が進み、回復の可能性も高くなってきました。関節リウマチを専門とされている東京医科歯科大学 大学院 膠原病・リウマチ内科学教授の宮坂信之先生にお話を伺いました。

宮坂　信之先生
東京医科歯科大学 大学院
膠原病・リウマチ内科学　教授

関節の基本構造

関節リウマチとは

関節リウマチとはどのような病気なのでしょうか。宮坂先生に伺いました。

「骨と骨のつなぎ目のことを関節と言います。つなぎ目は、軟骨がクッションの役割を果たし、滑液とも呼ばれる関節液が、潤滑油の役目を担っています。そして、関節組織を滑膜という薄い膜が、くるんでいます。この滑膜に炎症が起こり、痛みが生じるのが関節リウマチです。病気が進行すると、軟骨、そして骨そのものにも炎症が生じ、やがて、関節を破壊してしまいます。

そして、30～65歳の女性に多いという特徴が関節リウマチにはあります」

解明されていない関節リウマチの原因

関節リウマチの原因はどんなことなのでしょうか。

The Journal of Immunology

Excessive Production of IFN-γ in Patients with Systemic Lupus Erythematosus and Its Contribution to Induction of B Lymphocyte Stimulator/B Cell-Activating Factor/TNF Ligand Superfamily-13B[1]

Masayoshi Harigai,[2]*†‡ Manabu Kawamoto,[¶] Masako Hara,[¶] Tetsuo Kubota,[†§] Naoyuki Kamatani,[¶] and Nobuyuki Miyasaka[†]

Expression and immunological significance of IFN-γ, a pivotal cytokine in murine lupus, have not been clearly demonstrated in human systemic lupus erythematosus (SLE). In the present study we investigated the expression of IFN-γ in peripheral blood T cells from patients with SLE and its role in the production of the soluble B lymphocyte stimulator (sBLyS). Peripheral blood T cells from patients with SLE expressed significantly larger amounts of IFN-γ in response to stimulation with anti-CD3 mAb plus anti-CD28 mAb than those from normal controls as shown by three analytical methods, including ELISA, flow cytometry, and quantitative RT-PCR. The ratio of IFN-γ-producing T cells to effector memory T cells in $CD3^+CD4^+$ and $CD3^+CD8^+$ populations in patients with SLE was significantly higher than that of normal controls. The T-box expressed in T cells (T-bet) mRNA/GATA-binding protein-3 (GATA-3) mRNA ratio was significantly higher in patients with SLE than in normal controls. T cell culture supernatants from patients with SLE contained significantly higher sBLyS-inducing activity than normal controls; this was almost completely inhibited by the addition of anti-human IFN-γ mAb. Percentages of BLyS-expressing peripheral blood monocytes in patients with SLE were significantly higher than those of normal controls. Monocytes from patients with SLE produced significantly larger amounts of sBLyS in response to IFN-γ than those from normal controls. Taken together, these data strongly indicate that the overexpression of IFN-γ in peripheral blood T cells contributes to the immunopathogenesis of SLE via the induction of sBLyS by monocytes/macrophages, which would promote B cell activation and maturation. ***The Journal of Immunology,*** **2008, 181: 2211–2219.**

Systemic lupus erythematosus (SLE)[3] is a prototypic autoimmune disease that is characterized by the production of various kinds of autoantibodies by activated B lymphocytes in vivo (1). Although the immunopathogenesis of SLE is not completely understood, the altered production of and/or response to cytokines and chemokines have been proposed to be key phenomena.

IFN-γ, consisting of 146 aa with a molecular mass of 20 kDa in humans, is classified as a type II IFN that is mainly produced by Th1-type T cells and NK cells. The IFN-γ receptor is composed of two subunits, IFN-γ receptor-1 and -2, and transduces signals through JAK and STAT. Several lines of evidence, in mice as well as humans indicate an association of IFN-γ with the immunopathogenesis of SLE. The deletion of the IFN-γ receptor gene in both (NZB × NZW)F_1 and MRL/Fas^{lpr} mice resulted in the improvement of renal disease and increased survival rate (2, 3). IFN-γ gene$^{-/-}$ MRL/Fas^{lpr} mice also showed amelioration of renal disease and a better prognosis (4). The administration of IFN-γR-Ig fusion protein to MRL/Fas^{lpr} mice significantly decreased the concentration of IFN-γ in plasma and demonstrated therapeutic benefits, including the reduction of autoantibodies and lymphadenopathy, as well as an improvement of renal disease and survival rate (5). In human SLE, associations of polymorphism (6, 7) as well as expression of IFN-γ (8, 9) with renal pathology have been demonstrated. However, controversy remains regarding the expression of IFN-γ in peripheral blood T cells in SLE. Some investigators demonstrated an increased expression of IFN-γ mRNA or protein with PHA stimulation (10) or PMA plus ionomycin stimulation (11), respectively. Others reported decreased production of IFN-γ protein with PMA plus ionomycin stimulation (12). We recently demonstrated that peripheral blood T cells from patients with SLE produced significantly larger amounts of IFN-γ protein in response to anti-CD3 mAb plus anti-inducible costimulator mAb stimulation (13). The production of cytokines and chemokines by memory T cells in response to TCR ligation is closely related to their subsets, i.e., central or effector memory T cells,

*Department of Pharmacovigilance and †Department of Medicine and Rheumatology, Tokyo Medical and Dental University Graduate School of Medicine, ‡Clinical Research Center, Tokyo Medical and Dental University, and §Department of Microbiology and Immunology, Tokyo Medical and Dental University Graduate School of Health Sciences, Tokyo, Japan; and ¶Institute of Rheumatology, Tokyo Women's Medical University, Tokyo, Japan

Received for publication April 10, 2007. Accepted for publication May 19, 2008.

The costs of publication of this article were defrayed in part by the payment of page charges. This article must therefore be hereby marked *advertisement* in accordance with 18 U.S.C. Section 1734 solely to indicate this fact.

[1] This work was supported by grant-in-aid from the Japanese Ministry of Health, Labor, and Welfare.

[2] Address correspondence and reprint requests to Dr. Masayoshi Harigai, Department of Pharmacovigilance, Tokyo Medical and Dental University Graduate School of Medicine, 1-5-45 Yushima, Bunkyo-ku, Tokyo 113-8519, Japan. E-mail address: mharigai.mpha@tmd.ac.jp

[3] Abbreviations used in this paper: SLE, systemic lupus erythematosus; BAFF, B cell-activating factor; BLyS, B lymphocyte stimulator; GATA-3, GATA-binding protein-3; PC7, PE-cyanine 7; pSS, positive Sjögren's syndrome; sBLyS, soluble BLyS; SLEDAI, SLE disease activity index; T-bet, T-box expressed in T cells; T_{CM}, central memory T cell; T_{EM}, effector memory T cell; T_{EMRA}, $CD3^+CD8^+CD45RA^-CCR7^-$ effector memory T cell.

Copyright © 2008 by The American Association of Immunologists, Inc. 0022-1767/08/$2.00

which are classified according to the expression of the CD45RA Ag found on all human B and NK cells and subsets of human T cells and CCR7. Central memory T cells (T_{CM}), $CD3^+CD45RA^-CCR7^+$ cells, home to T cell areas of secondary lymphoid organs and have only minimal cytokine-secreting capacity, whereas effector memory T cells (T_{EM}), $CD3^+CD45RA^-CCR7^-$ cells, migrate to inflamed peripheral tissues and display immediate effector functions, including the secretion of cytokines such as IFN-γ, IL-4, and IL-5 within hours following antigenic stimulation. $CD8^+$ T cells possess another effector memory subset named T_{EMRA}, which is $CD3^+CD8^+CD45RA^+CCR7^-$ (14). A deviation in memory T cell differentiation has been demonstrated in patients with SLE (15–17), but its relationship to the secretion of cytokines has not been determined in this disease.

B lymphocyte stimulator (BlyS; also known as B cell-activating factor (BAFF)/TNF ligand superfamily-13B (TNFSF-13B)), a type II transmembrane protein and a member of the TNF family, is a critical regulator of B cell proliferation, differentiation, and survival (18–23). The molecule is expressed on the surface of monocytes, dendritic cells, neutrophils, stromal cells, and activated T cells and forms homotrimers or heterotrimers with a proliferation-inducing ligand (24, 25). The extracellular domain of BLyS, which is cleaved by a furin proteinase and released into body fluids such as serum or cerebral spinal fluid, is called soluble BLyS (sBLyS) (21). BLyS transgenic mice developed a lupus-like syndrome (24, 26, 27), whereas the blockade of the BLyS signal provided a therapeutic benefit to lupus model mice (24, 28, 29). Increased levels of serum sBLyS (30–32) as well as BLyS mRNA (31) of peripheral blood leukocytes have been reported in patients with SLE. Although the expression of BLyS is enhanced by treatment with IFN-α, IFN-γ, or CD154 in dendritic cells or macrophages (33, 34), the mechanism of the overexpression of BLyS in SLE has not been completely understood.

In the present study we demonstrated the increased expression of IFN-γ, an imbalance of master transcriptional factors for production of this cytokine, the contribution of T_{EM} subsets to the increased production of IFN-γ, the involvement of IFN-γ in the induction of BLyS by monocytes, and the enhanced production of BLyS by monocytes in response to IFN-γ in patients with SLE. The present study strongly indicated the increased production of IFN-γ and its association with the immunopathogenesis of human SLE.

Materials and Methods

Patients

We enrolled 50 patients with SLE (47 females and three males) and 35 normal controls (32 females and three males) into the present study. All SLE patients fulfilled the SLE classification criteria of the American College of Rheumatology (Atlanta, GA). The disease activity of the SLE patients was evaluated using the systemic lupus erythematosus disease activity index (SLEDAI). The SLEDAI scores (mean ± SE) and the disease duration (mean ± SE) of the patients with SLE were 5.5 ± 6.9 and 7.4 ± 7.2 years, respectively. Twenty-five patients with SLE had active disease (a SLEDAI score > 4) (16). Treatments for the patients with SLE were prednisolone (n = 39, mean ± SE, 11.1 ± 11.3 mg/day) and azathioprine (n = 4). Peripheral blood samples were obtained with the written informed consent from all participating individuals. The Helsinki Declaration and the ethical guidelines for clinical research in Japan were followed throughout the study and the study protocol was approved by the ethical committee of the Tokyo Medical and Dental University Hospital (Tokyo, Japan).

Abs and other reagents

Anti-CD3 mAb and anti-CD28 mAb were purchased from Immunotech. Allophycocyanin-anti-CD3 mAb, allophycocyanin-anti-CD4 mAb, PE-cyanine 7 (PC7)-anti-CD4 mAb, PC7-anti-CD8 mAb, PE-anti-CD8 mAb, allophycocyanin-anti-CD14 mAb, FITC-anti-CD45RA mAb, FITC-anti-human IFN-γ mAb, PE-anti-human IL-4 mAb, and isotype-matched fluorochrome-conjugated control mAbs of the above mAbs were purchased from Beckman Coulter. PE-anti-CCR7 mAb, anti-CCR7 mAb, goat anti-human IFN-γ Ab, and normal goat IgG were purchased from R&D Systems. Anti-IFN-α mAbs were purchased from PBL Biomedical Laboratories. FITC-conjugated anti-human BLyS mAb and anti-human IL-10 mAb were purchased from Abcam.

Cell preparations

PBLs were separated by the centrifugation of heparinized blood over a Ficoll-Conray gradient. T cells were isolated by negative selection from PBLs using the Pan T cell isolation kit (Miltenyi Biotec) according to the manufacturer's protocol. Monocytes were further depleted from negatively selected T cells using anti-CD14 MicroBeads (Miltenyi Biotec) according to the manufacturer's protocol. The purities of T cells were >95% using flow cytometry for both normal controls and patients with SLE. In these purified T cells, monocytes were not detectable using allophycocyanin-anti-CD14 mAb and flow cytometry. In some experiments, T_{EM} were negatively selected from these T cells using anti-CCR7 mAb and anti-mouse IgG MicroBeads (Miltenyi Biotec) according to the manufacturer's protocol. Monocytes were isolated by positive selection from PBL using anti-CD14 MicroBeads.

Stimulation of T cells

Peripheral blood T cells were stimulated with immobilized anti-CD3 mAb plus anti-CD28 mAb (CD28 costimulation). Anti-CD3 mAb (0.1 μg/ml in PBS) was bound to flat-bottom, 96-well microtiter plates (Iwaki) or 24-well culture plates (Iwaki) by incubation overnight at 4°C. Anti-CD28 mAb (2 μg/ml) was added directly to medium. Preliminary experiments showed that immobilized anti-CD3 mAb alone at 0.1 μg/ml induced a modest proliferation of peripheral blood T cells, whereas immobilized anti-CD3 mAb plus anti-CD28 together provided full-activation (data not shown). T cells (2×10^5 cells/well) were cultured in flat-bottom, 96-well microtiter plates with CD28 costimulation for 72 h in RPMI 1640 (Sigma-Aldruch) supplemented with 10% FCS (Invitrogen), penicillin (100 U/ml), and streptomycin (100 μg/ml) (Invitrogen). Culture supernatants were collected to determine IFN-γ production and BLyS-inducing activity (see below). T cells (5×10^5 cells/0.5 ml/well) were also cultured in 24-well culture plates to quantify IFN-γ mRNA and intracellular IFN-γ (see below).

Stimulation of monocytes

Monocytes were cultured in 96-well, flat-bottom plates for 72 h with various concentrations of recombinant human IFN-γ (rhIFN-γ; 0, 2, 10 ng/ml) (R&D Systems) or with rhIFN-α (100 IU/ml) in RPMI 1640 supplemented with 10% FCS, penicillin (100 U/ml), and streptomycin (100 μg/ml). sBLyS in these culture supernatants from human monocytes or THP-1 cells was measured using an ELISA system (R&D Systems) according to the manufacturer's instructions. The sensitivity of the ELISA kit was 0.73 pg/ml.

Flow cytometry

Multicolor analysis was performed using the FACSCalibur flow cytometry system (BD Biosciences). Cells were washed three times in ice-cold FCM buffer (PBS, 0.1% BSA, and 0.1% sodium azide) and incubated on ice for 5 min with 10 μg of purified mouse IgG (Chemicon) to block nonspecific IgG binding. Cells were then incubated at 4°C with saturating amounts of the fluorochrome-conjugated (i.e., FITC-, PE-, PC7-, or allophycocyanin-conjugated) mAbs. For simultaneous staining of cell surface molecules and intracellular cytokines, T cells (5×10^5 cells/0.5 ml/well) were stimulated with CD28 costimulation in the presence of brefeldin A (GolgiPlug; BD Biosciences) for 6 h and stained with fluorochrome-conjugated mAbs against cell surface molecules. Then, the cells were permeabilized using the IntraPrep kit (Beckman Coulter) and stained with FITC-anti-IFN-γ mAb and/or PE-anti-IL-4 mAb. To detect expression of BLyS on the cell surface of peripheral blood monocytes, PBLs were stained with PE-conjugated anti-CD14 mAb and FITC-conjugated anti-BLyS mAb.

ELISA for IFN-γ

IFN-γ production in the culture supernatants was measured using an ELISA kit according to the manufacturer's protocol (GE Healthcare). The sensitivity of the ELISA kit was 0.63 pg/ml.

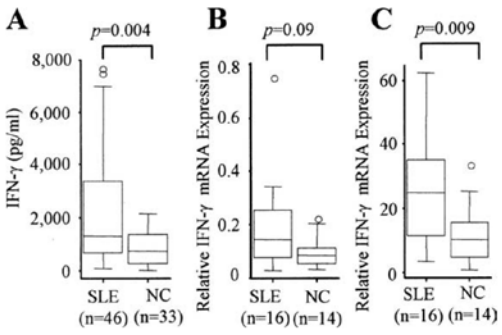

FIGURE 1. Overexpression of IFN-γ by peripheral blood T cells in SLE patients with CD28 costimulation. *A*, Peripheral blood T cells from patients with SLE ($n = 46$) and normal controls (NC) ($n = 33$) were cultured with CD28 costimulation for 72 h and IFN-γ in the culture supernatants was measured using an ELISA. *B* and *C*, Total RNA was extracted from peripheral blood T cells before (*B*) and after CD28 costimulation for 4 h (*C*) and was reverse-transcribed to cDNA. IFN-γ mRNA was quantified using the ABI PRISM 7900HT sequence detection system. Lines inside the boxes represent the median value for each group. Boxes include the 25th–75th percentiles, bars outside boxes represent the 10th and 90th percentiles, and open circles represent values beyond the 10th and 90th percentiles. *p* values were calculated using the Mann-Whitney *U* test.

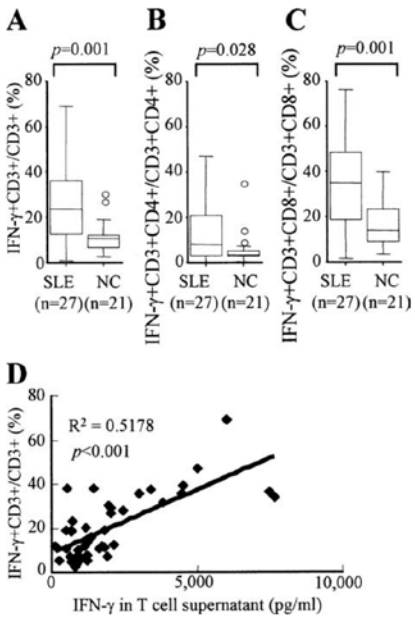

FIGURE 2. Contribution of both $CD4^+$ and $CD8^+$ T cells to the overproduction of IFN-γ in patients with SLE. *A–C*, T cells (5×10^5 cells/0.5 ml/well) from patients with SLE ($n = 27$) and normal controls (NC) ($n = 21$) were cultured with CD28 costimulation in the presence of brefeldin A for 6 h, stained with the mAbs allophycocyanin-anti-CD3, PC7-anti-CD4, PC7-anti-CD8, PE-anti-CD8, and FITC-anti-IFN-γ, and analyzed using flow cytometry. The percentages of IFN-γ-producing cells among $CD3^+$ T cells (*A*), $CD3^+CD4^+$ T cells (*B*), or $CD3^+CD8^+$ T cells (*C*) were calculated. Lines inside the boxes represent the median value for each group. The boxes include the 25th–75th percentiles, bars outside the boxes represent the 10th and 90th percentiles, and open circles represent values beyond the 10th and 90th percentiles. *p* values were calculated using Mann-Whitney *U* test in *A–C*. *D*, Correlation between the concentration of IFN-γ in the T cell culture supernatants (Fig. 1*B*) and the percentage of IFN-γ-producing cells among $CD3^+$ T cells were shown (SLE, $n = 23$; normal controls, $n = 20$; total, $n = 43$). The correlation was analyzed using the Pearson correlation coefficient.

Quantitative RT-PCR

Total RNA was extracted using TRIzol (Invitrogen) from freshly isolated T cells (1×10^6) or T cells (5×10^5 cells/0.5 ml/well) stimulated with CD28 costimulation for 4 h and reverse transcribed to cDNA using SuperScript II RNase H^- (Invitrogen). One microliter of the cDNA was used as a template for quantitative PCR, which was performed using the ABI PRISM 7900HT sequence detection system (Applied Biosystems) with the comparative threshold cycle ($\Delta\Delta C_t$) method according to the instructions of the manufacturer. Primers and probes for quantitative RT-PCR of human GAPDH and IFN-γ and the transcription factors GATA-binding protein-3 (GATA-3) and T-box expressed in T cells (T-bet), were also purchased from Applied Biosystems.

sBLyS-inducing activity

Human monocytes or cells of the human monocytic cell line THP-1 (1×10^5/200 μl/well) were cultured in 96-well, flat-bottom plates for 72 h with various concentration of rhIFN-γ (0–10 ng/ml) (R&D Systems) or T cell culture supernatants (0–30% used) in 10% FCS-RPMI 1640 containing penicillin (100 U/ml), streptomycin (100 μg/ml), and 2-ME (50 μM) (Invitrogen). In some experiments, T cell culture supernatants were incubated with goat anti-human IFN-γ IgG or control goat IgG (both used at 5.0 μg/ml), (R&D Systems) at 4°C for 30 min before being added to human monocytes or THP-1 cells. sBLyS in these culture supernatants from human monocytes or THP-1 cells was measured using an ELISA system (R&D Systems) according to the manufacturer's instructions. The sensitivity of the ELISA kit was 0.73 pg/ml.

Statistics

Differences between groups were evaluated using the Mann-Whitney *U* test. Paired samples were analyzed using the Wilcoxon rank sum test. Correlations were analyzed using the Pearson's correlation coefficient. Values of $p \leq 0.05$ were considered significant. Statistical analysis was performed using SPSS-J 15.0.

Results

Overproduction of IFN-γ by peripheral blood T cells in SLE patients with CD28 costimulation

As an initial experiment, we compared the expression of IFN-γ at the protein level in the patients with SLE and in normal controls and found a significant difference. Peripheral blood T cells were cultured with CD28 costimulation for 72 h and IFN-γ in the culture supernatants was measured using an ELISA. Peripheral blood T cells from patients with SLE ($n = 46$) produced significantly larger amounts of IFN-γ than those from normal controls ($n = 33$) with CD28 costimulation ($p = 0.004$; Mann-Whitney *U* test) (Fig. 1*A*). We also quantified the IFN-γ mRNA of peripheral blood T cells from patients with SLE ($n = 16$) and normal controls ($n = 14$) before and after CD28 costimulation, as described in *Materials and Methods*. There was no significant difference in the amounts of IFN-γ between the two groups before stimulation ($p = 0.09$) (Fig. 1*B*). Peripheral blood T cells from patients with SLE expressed significantly larger amounts of IFN-γ mRNA than those from normal controls after CD28 costimulation ($p = 0.009$; Mann-Whitney *U* test) (Fig. 1*C*). There was no correlation between SLEDAI scores and quantities of IFN-γ mRNA or protein in each group of patients with SLE (data not shown).

Both $CD4^+$ and $CD8^+$ T cells contribute to the overproduction of IFN-γ in patients with SLE

Using intracellular cytokine staining as described in *Materials and Methods*, we next determined which T cell subset, $CD4^+$ or $CD8^+$, produced IFN-γ in response to CD28 costimulation. Percentages of IFN-γ-producing $CD3^+$ T cells in patients with SLE

Table I. *Percentages of memory T cell subsets in patients with SLE*[a]

Memory T Cell Subsets	SLE (n = 27)	Normal Controls (n = 21)
$CD3^+CD4^+CD45RA^-CCR7^+/CD3^+CD4^+$	32.3 (25.1–41.1)	29.9 (25.1–37.0)
$CD3^+CD4^+CD45RA^-CCR7^-/CD3^+CD4^+$	26.1 (15.2–40.8)	22.1 (18.6–28.3)
$CD3^+CD8^+CD45RA^-CCR7^+/CD3^+CD8^+$	3.9 (3.0–7.7)	4.6 (2.0–6.2)
$CD3^+CD8^+CD45RA^-CCR7^-/CD3^+CD8^+$	24.1 (14.6–37.1)	27.3 (18.9–33.2)
$CD3^+CD8^+CD45RA^+CCR7^-/CD3^+CD8^+$	30.3 (14.9–38.1)	18.3 (10.9–23.5)
$CD3^+CD8^+CCR7^-/CD3^+CD8^+$	57.5 (34.9–77.2)	51.5 (36.4–57.4)

[a] Peripheral blood T cells were stained with the allophycocyanin-anti-CD3, PC7-anti-CD4, PC7-anti-CD8, PE-anti-CCR7, and FITC-anti-CD45RA mAbs and analyzed using flow cytometry. Data were expressed as median and 25–75 percentiles (in parentheses) for each subset. There was no statistical difference between the two groups.

(n = 27) were significantly higher than those in normal controls (n = 21) (p = 0.001; Mann-Whitney U test), which was compatible with the results of Fig. 1 (Fig. 2*A*). Percentages of IFN-γ-producing $CD4^+$ T cells as well as $CD8^+$ T cells in patients with SLE were significantly higher than those in normal controls (p = 0.028 for $CD4^+$ T cells and p = 0.001 for $CD8^+$ T cells, Mann-Whitney U test) (Fig. 2, *B* and *C*). We found a significant and strong positive correlation between the percentages of IFN-γ-producing $CD3^+$ T cells and IFN-γ in the culture supernatants of T cells (R^2 = 0.518; $p < 0.001$) (Fig. 2*D*).

Memory T cell subsets in patients with SLE

Recent studies have identified several memory T cell subsets. Among them, T_{EM} cells are considered to produce IFN-γ, IL-4,

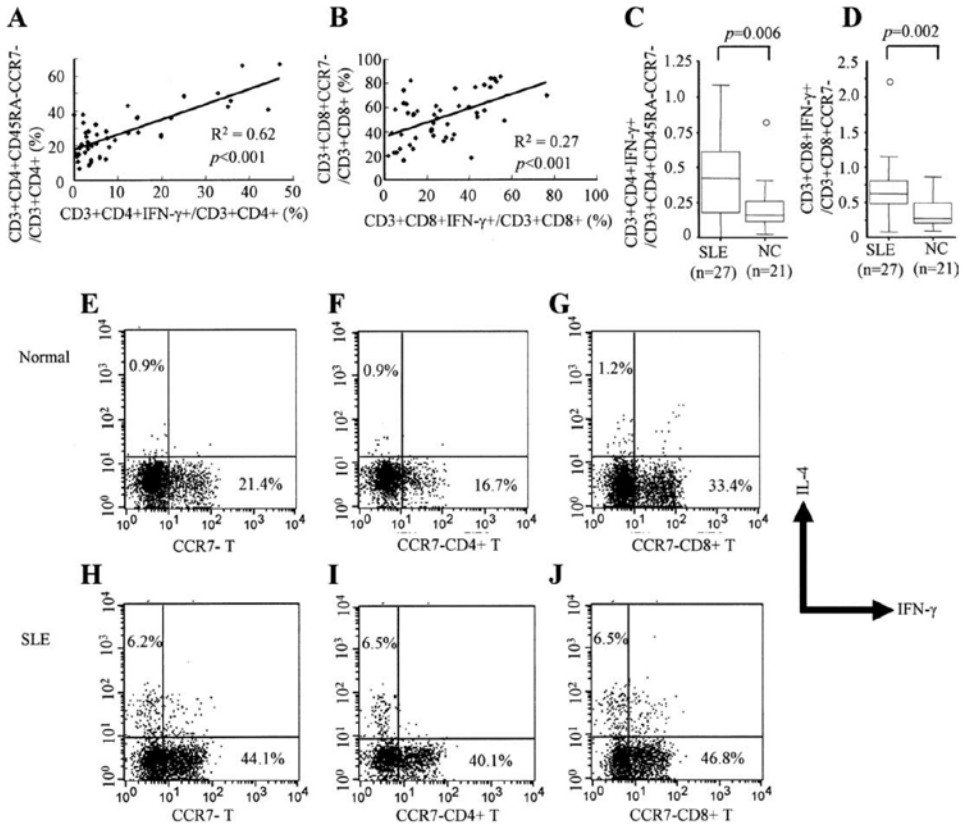

FIGURE 3. Correlation between the percentages of IFN-γ-producing T cells and the T_{EM} cells. *A* and *B*, The correlations of the percentages of IFN-γ-producing $CD3^+CD4^+$ T cells and $CD3^+CD4^+CD45RA^-CCR7^-$ T cells (T_{EM}) (*A*) and the percentages of IFN-γ-producing $CD3^+CD8^+$ T cells and $CD3^+CD8^+CCR7^-$ T cells (T_{EM} plus T_{EMRA}) (*B*) are shown. Data are from 27 patients with SLE and 21 normal controls. Correlations were analyzed using the Pearson correlation coefficient. *C* and *D*, The ratio of the percentage of IFN-γ-producing $CD3^+CD4^+$ T cells to that of $CD3^+CD4^+$ TEM cells (*C*) or the ratio of the percentage of IFN-γ-producing $CD3^+CD8^+$ T cells to that of $CD3^+CD8^+$ T_{EM} plus T_{EMRA} cells (*D*) were calculated. Data are from 27 patients with SLE and 21 normal controls (NC). p values were calculated using Mann-Whitney U test in *C* and *D*. The lines inside the boxes represent the median value for each group. Boxes include the 25th–75th percentiles, bars outside boxes represent the 10th and 90th percentiles, and open circles represent values beyond the 10th and 90th percentiles. *E–J*, Intracellular expression of IFN-γ and IL-4 in $CCR7^-$ T_{EM} cells. T_{EM} cells (5×10^5 cells/0.5 ml/well) from a normal control (*E–G*) and a SLE patient (*H–J*) were cultured with CD28 costimulation in the presence of brefeldin A for 6 hours and stained with the mAbs FITC-anti-IFN-γ mAb, PE-anti-IL-4 mAb, PC7-anti-CD8 mAb, and allophycocyanin-anti-CD4 mAb. Cytokine-producing cells in $CCR7^-$ T cells (*E* and *H*), $CCR7^-CD4^+$ T cells (*F* and *I*), or $CCR7^-CD8^+$ T cells (*G* and *J*) were analyzed. Representative data of three patients with SLE and three normal controls were shown.

and IL-5 within hours following antigenic stimulation. Because our flow cytometry analysis revealed an increased percentage of IFN-γ-producing T cells at 6 h after CD28 costimulation in patients with SLE, we postulated that there was a skewed distribution of memory T cell subsets; this was investigated in the same patients ($n = 27$) and normal controls ($n = 21$) that were used for the intracellular cytokine-staining experiments described above. As has been previously reported (15), the patients with SLE showed a significantly increased percentage of a $CD3^+CD4^+$ memory T cell population ($CD3^+CD4^+CD45RA^-/CD3^+CD4^+$) than normal controls (median (25–75 percentiles): SLE, 66.3 (52.6–75.2); normal control, 55.8 (47.3–60.3); $p = 0.014$). However, there was no significant difference between the patients with SLE and normal controls in the percentages of $CD3^+CD4^+CD45RA^-CCR7^+/CD3^+CD4^+$, $CD3^+CD4^+CD45RA^-CCR7^-/CD3^+CD4^+$, $CD3^+CD8^+CD45RA^-CCR7^+/CD3^+CD8^+$, $CD3^+CD8^+CD45RA^-CCR7^-/CD3^+CD8^+$, $CD3^+CD8^+CD45RA^+CCR7^-/CD3^+CD8^+$, and $CD3^+CD8^+CCR7^-/CD3^+CD8^+$ cells (Table I).

We next analyzed the correlation between the percentages of IFN-γ-producing T cells and T_{EM} cells. We found a significant positive correlation between the percentages of IFN-γ-producing $CD3^+CD4^+$ T cells and $CD3^+CD4^+CD45RA^-CCR7^-$ T cells (i.e., T_{EM}), as well as between those of IFN-γ-producing $CD3^+CD8^+$ T cells and $CD3^+CD8^+CCR7^-$ T cells (i.e., T_{EM} plus T_{EMRA}) ($R^2 = 0.62$, $p < 0.001$ for $CD4^+$ T cells; $R^2 = 0.27$, $p < 0.001$ for $CD8^+$ T cells) (Fig. 3, *A* and *B*); this was compatible with the strong and major contribution of memory T cells to the expression of IFN-γ immediately after stimulation. There was no significant correlation between the percentages of IFN-γ-producing $CD3^+CD4^+$ T cells and $CD3^+CD4^+CD45RA^-CCR7^+$ T cells or those of IFN-γ-producing $CD3^+CD8^+$ T cells and $CD3^+CD8^+CD45RA^-CCR7^+$ T cells (i.e., T_{CM}) (data not shown). We therefore calculated the ratio of the percentage of IFN-γ-producing T cells to that of the T_{EM} cells (i.e., T_{EM} for $CD3^+CD4^+$ T cells, T_{EM} plus T_{EMRA} for $CD3^+CD8^+$ T cells) as an indicator for the fraction of IFN-γ-producing T cells among the T_{EM} cells. The ratios in the patients with SLE were significantly higher than those of normal controls in both $CD4^+$ and $CD8^+$ T cells ($p = 0.006$ for $CD4^+$ T cells, $p = 0.002$ for $CD8^+$ T cells; Mann-Whitney *U* test) (Fig. 3, *C* and *D*). These differences remained statistically significant when we excluded the SLE patients who had a ratio >1.0 from Fig. 3, *C* and *D* (one and three patients, respectively; $p = 0.010$ and $p = 0.009$ for Fig. 3, *C* and *D*, respectively). Increased expression of IFN-γ in the T_{EM} cells was confirmed in negatively selected $CCR7^-$ T cells. $CCR7^-$ T cells were stained with allophycocyanin-anti-CD4 mAb, PC7-anti-CD8 mAb, FITC-anti-IFN-γ mAb, and PE-anti-IL-4 mAb and analyzed using flow cytometry. Representative results, which were in concordance with Fig. 3, *C* and *D*, were shown in Fig. 3, *E–J*.

Increased T-bet mRNA/GATA-3 mRNA ratio of peripheral blood T cells in patients with SLE

The differentiation of T cells into Th1 or Th2 type is under the control of the master transcriptional factors T-bet and GATA-3 (35). Because IFN-γ is a prototype of a Th1 cytokine, we quantified mRNA of these transcriptional factors in freshly isolated peripheral blood T cells and calculated the T-bet mRNA/GATA-3 mRNA ratio in each patient with SLE ($n = 17$) or in normal controls ($n = 14$). The T-bet mRNA/GATA-3 mRNA ratio was significantly higher in patients with SLE; this was compatible with the overproduction of IFN-γ in response to CD28 costimulation ($p < 0.0005$; Mann-Whitney *U* test) (Fig. 4).

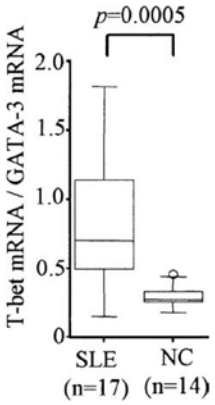

FIGURE 4. Increased T-bet mRNA/GATA-3 mRNA ratio of peripheral blood T cells in patients with SLE. Total RNA was extracted from freshly isolated peripheral blood T cells and reverse transcribed to cDNA. T-bet, GATA-3, and GAPDH mRNA were quantified using the ABI PRISM 7900HT sequence detection system. The ratios of T-bet mRNA to GATA-3 mRNA were compared between the patients with SLE ($n = 17$) and normal controls (NC) ($n = 14$). The lines inside the boxes represent the median value for each group. The boxes include 25th–75th percentiles, bars outside boxes represent the 10th and 90th percentiles, and open circles represent values beyond the 10th and 90th percentiles. *p* values were calculated using the Mann-Whitney *U* test.

Increased T cell-derived sBLyS-inducing activity in patients with SLE

To obtain insight into the pathological significance of IFN-γ in SLE, we investigated its contribution to the production of sBLyS by human monocytes or human monocytic cell line THP-1 cells. rhIFN-γ dose-dependently induced production of sBLyS in human monocytes as well as in THP-1 cells. Therefore, we used THP-1 cells in the following experiments. The sBLyS-inducing activity was significantly inhibited by preincubation of rhIFN-γ with anti-IFN-γ IgG but not with control IgG (Fig. 5*A*). T cell culture supernatants from a normal control also increased the production of sBLyS by THP-1 cells in a dose-dependent fashion. The sBLyS-inducing activity of the T cell culture supernatant was almost completely inhibited by the addition of anti-IFN-γ IgG but not by control IgG in both normal controls and patients with SLE (Fig. 5, *A* and *B*). The addition of anti-IFN-α mAb or anti-IL-10 mAb did not inhibit the sBLyS-inducing activity of the T cell culture supernatant (data not shown). Using this assay system, we measured the sBLyS-inducing activity of T cell culture supernatants from patients with SLE ($n = 22$) and normal controls ($n = 16$). T cell culture supernatants were used at 5% in this experiment. We could not perform this assay in some patients with SLE and normal controls because of the shortage of culture supernatants. T cell culture supernatants from the patients with SLE induced significantly larger amounts of sBLyS than those from normal controls ($p = 0.048$; Mann-Whitney *U* test) (Fig. 5*C*). We also measured sBLyS using an ELISA in the T cell culture supernatants diluted at 5% in medium (36), but the concentration of sBLyS was <10 pg/ml and was considered not to affect the measurement of BLyS-inducing activity in our assay system. There was a significant and strong

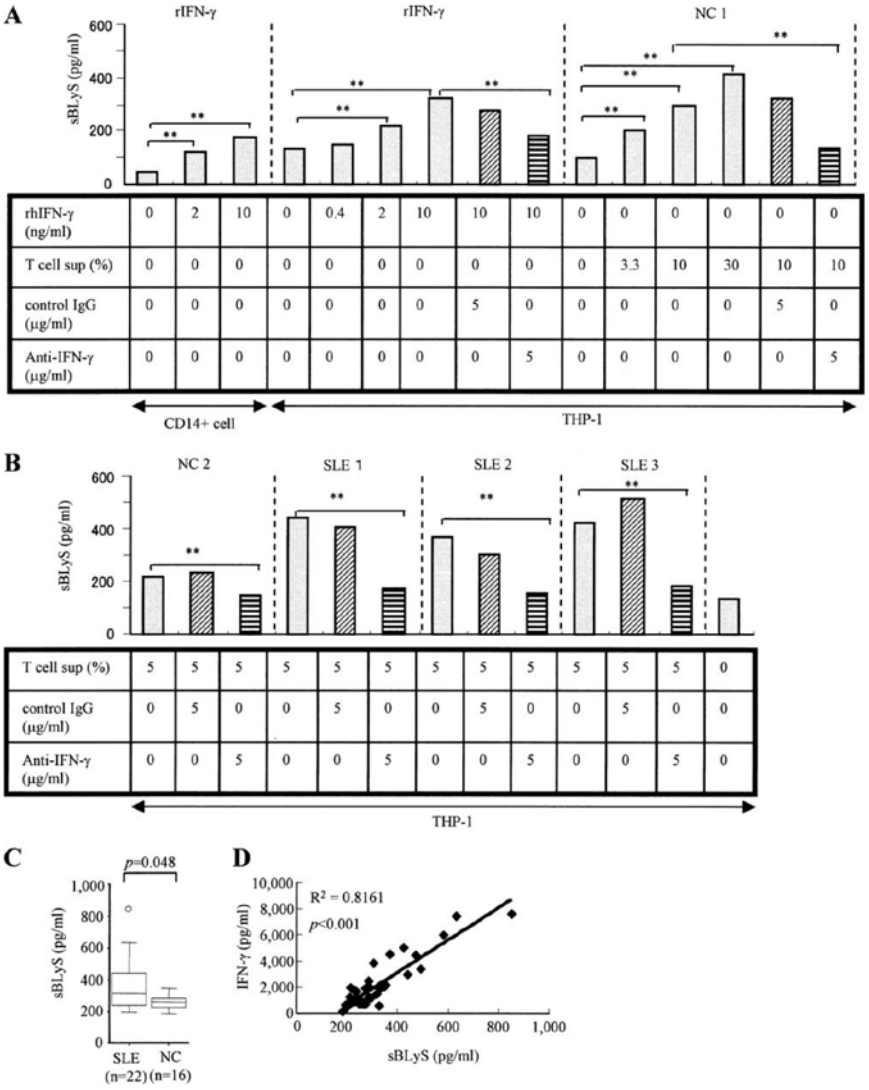

FIGURE 5. sBLyS-inducing activity in T cell culture supernatants of patients with SLE. *A* and *B*, Peripheral blood T cells were cultured with CD28 costimulation and T cell culture supernatants were collected as described in Fig. 1. Human monocytes or THP-1 cells were cultured with rhIFN-γ (0–10 ng/ml) or T cell culture supernatants (at 0–30% in *A* and 5% in *B*) for 72 h; the levels of sBLyS in the culture supernatants were measured using an ELISA. In some experiments rhIFN-γ and T cell culture supernatants were preincubated for 30 min at 4°C with anti-IFN-γ IgG (hatched column) or control IgG (diagonal column) before the addition to the cells. Assays were performed in triplicate and SD values were <10% in all columns. **, $p < 0.01$ by the Student *t* test. *C*, THP-1 cells were cultured with T cell culture supernatants from the patients with SLE ($n = 22$) and normal controls (NC) ($n = 16$) at 5% for 72 h, and levels of sBLyS in these culture supernatants were measured using an ELISA. The lines inside the boxes represent the median value for each group. The boxes include the 25th–75th percentiles, bars outside boxes represent the 10th and 90th percentiles, and the open circles represent values beyond the 10th and 90th percentiles. *p* values were calculated using the Mann-Whitney *U* test. *D*, The correlation of the concentration of sBLyS induced by the T cell culture supernatants in *C* and the concentration of IFN-γ in the T cell culture supernatants measured using ELISA (Fig. 1*B*) were plotted. The correlations were analyzed using the Pearson correlation coefficient.

correlation between the sBLyS-inducing activity and IFN-γ in the T cell culture supernatants ($R2 = 0.82$; $p < 0.001$) (Fig. 5*D*).

Increased expression of BLyS by peripheral blood monocytes in patients with SLE

To evaluate relevance of the sBLyS-inducing activity on monocytes in patients with SLE, we quantified the expression of BLyS on freshly isolated peripheral blood monocytes. Representative results of a patient with SLE and a normal control are shown in Fig. 6*A*. Percentages of $BLyS^+CD14^+/CD14^+$ were significantly higher than those of normal controls ($p = 0.034$; Mann-Whitney *U* test) (Fig. 6*B*). Mean fluorescence intensities of BLyS in patients with SLE were also significantly higher than those of normal controls (median (range): SLE, 6.8 (4.1–18.0); normal, 4.6 (1.8–10.8); $p = 0.007$; Mann-Whitney *U* test). We found no significant difference in production of sBLyS by $CD14^+$ monocytes without stimulation. rhIFN-γ as well as rhIFN-α significantly enhanced production of sBLyS by $CD14^+$ monocytes in both normal control and patients with SLE ($p < 0.0001$ for both stimuli and for both group). $CD14^+$ monocytes from patients with SLE produced

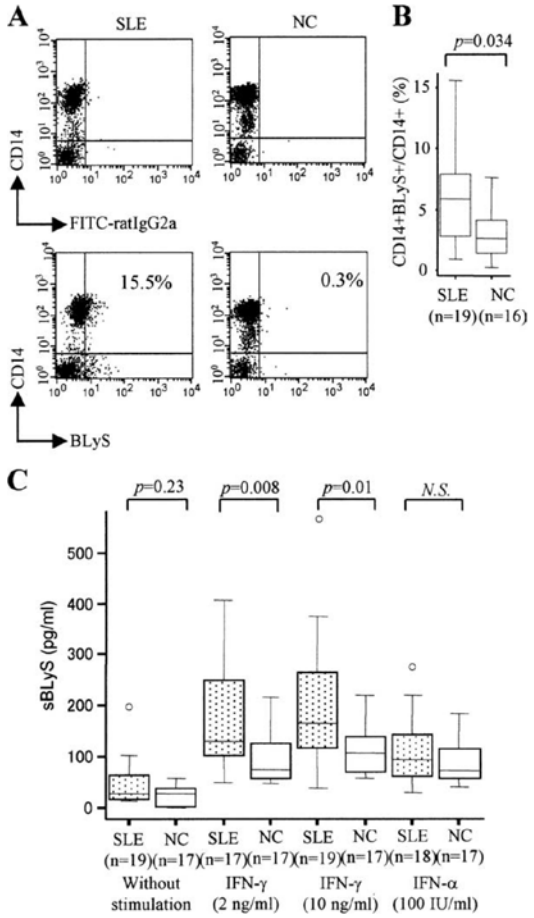

FIGURE 6. Expression of BLyS in monocytes from patients with SLE and normal controls. *A*, Freshly isolated peripheral blood monocytes were stained with allophycocyanin-anti-CD14 mAb and FITC-rat IgG2a (*upper panels*) or FITC-anti-BLyS mAb (*lower panels*) and analyzed using flow cytometry. In these experiments, BLyS on the cell surfaces of monocytes was stained. Representative flow cytometry data of a patient with SLE (*left*) and a normal control (NC) (*right*) are shown. The numbers in the upper right quadrants of each panel indicate the percentages of $CD14^+$ cells that stained for BLyS protein. Monocytes were gated using forward and side scatters and analyzed for expression of CD14 and BLyS. *B*, The percentages of BLyS-expressing cells in $CD14^+$ monocytes in patients with SLE ($n = 19$) and normal controls ($n = 16$). *C*, Freshly isolated peripheral blood monocytes from patients with SLE ($n = 17$–19) (dotted column) and normal controls ($n = 17$) (open column) were cultured with various concentration of rhIFN-γ (0, 2, 10 ng/ml) or rhIFN-α (100 IU/ml) for 48 h; the levels of sBLyS in the culture supernatants were measured using an ELISA. The lines inside the boxes represent the median value for each group. The boxes include the 25th–75th percentiles, bars outside boxes represent the 10th and 90th percentiles, and the open circles represent values beyond the 10th and 90th percentiles. *p* values were calculated using the Mann-Whitney *U* test.

significantly larger amounts of sBLyS than those from normal controls after stimulation with IFN-γ (2 and10 ng/ml), but not with IFN-α (100 IU/ml) (Fig. 6*C*).

Discussion

In the present study we demonstrated the following: 1) peripheral blood T cells from patients with SLE expressed significantly larger amounts of IFN-γ in response to CD28 costimulation than those from normal controls; 2) overexpressed IFN-γ contributed to the excessive sBLyS-inducing activity in T cell culture supernatants of patients with SLE; and 3) monocytes from patients with SLE produced significantly larger amounts of sBLyS in response to the stimulation with rhIFN-γ than those from normal controls.

Because several investigators have reported conflicting results (10–13), we addressed the expression of IFN-γ by T cells from patients with SLE with various assay methods; these included an ELISA for IFN-γ protein in T cell culture supernatants, quantitative RT-PCR for IFN-γ mRNA, and an intracellular cytokine assay for IFN-γ. The excessive expression of IFN-γ by peripheral blood T cells after CD28 costimulation was consistently demonstrated in all of these assay systems. The increased T-bet mRNA/GATA-3 mRNA ratio also supported the skewed differentiation of peripheral blood T cells into IFN-γ-producing T cells. The differing results regarding the expression of IFN-γ among several reports, including ours, could be explained to some extent by differences in the methods of stimulation. Because we used CD28 costimulation that mimics stimulation by APCs, our results would better reflect the capacity of cytokine secretion by T cells in vivo than those obtained with artificial stimulation such as that achieved by PMA plus ionomycin stimulation (12), which bypasses the TCR/CD3 complex.

We found significant positive correlations between the percentages of IFN-γ-secreting T cells and T_{EM} cells in both $CD3^+CD4^+$ and $CD3^+CD8^+$ T cells (Fig. 3, *A* and *B*); these results are compatible with the fact that T_{EM} cells, but not T_{CM} cells, have the capacity to secrete cytokines immediately after Ag stimulation. An increased percentage of $CD8^+$ T_{EM} cells (17) as well as that of $CD4^+$ T_{EM} cells (16) have been reported in patients with SLE. Although $CD3^+CD8^+CD45RA^+CCR7^+$ T cells (T_{EMRA}) showed a tendency to increase ($p = 0.07$) in our patients with SLE, we could not observe such a drastic difference in the memory T cell population between SLE and normal controls even after separating the patients into active and inactive diseases (data not shown). Nevertheless the ratio of IFN-γ-secreting T cells to T_{EM} cells in both $CD3^+CD4^+$ and $CD3^+CD8^+$ T cells was significantly increased in patients with SLE (Fig. 3, *C* and *D*), suggesting the skewed differentiation of T_{EM} cells into IFN-γ-secreting cells.

The mechanism of the preferential differentiation into IFN-γ-secreting T cells in patients with human SLE remains to be clarified. T-bet is a master transcriptional factor for the differentiation into IFN-γ-secreting T cells that cooperates with another transcriptional factor, Hlx (35, 37). The promoter analysis of the IFN-γ gene revealed several other relevant transcriptional factors, including AP-1, AP-2, NFAT1, ATF, and NF-κB (38–40). Wong et al. (41) has demonstrated a decreased NF-κB activity of T cells after CD28 costimulation in patients with SLE; therefore, transcriptional factors other than NF-κB might be more important for the overexpression of IFN-γ in SLE. In addition to the increased T-bet mRNA/GATA-3 mRNA ratio that was demonstrated in the present study, the expression of these transcriptional factors should be investigated in the future.

BLyS is a critical regulator of B cell maturation and survival. The immunopathological significance of this cytokine has been implicated by increased levels of serum sBLyS (30–32) and BLyS mRNA (31) in the peripheral blood leukocytes of patients with SLE, which are in concordance with the results of the present study. A recent study also demonstrated that BAFF-R, one of the receptors for BLyS, was occupied in patients with SLE (42), suggesting the contribution of this cytokine to disease mechanisms in SLE. Despite these intriguing findings, how BLyS is overexpressed in SLE has not been completely understood and, to our

knowledge, this is the first study that demonstrated the major contribution of IFN-γ to the sBLyS-inducing activity of T cells. The present data suggest that T cells activated by APCs (i.e., macrophages and dendritic cells) produce excessive amounts of IFN-γ in patients with SLE and stimulate sBLyS production by APCs, which in turn would activate B cells (18–23) as well as monocytes (43). The higher production of sBLyS in response to rhIFN-γ by monocytes from the patients with SLE compared with those from normal controls further support this scenario. Expression of BLyS by PBMCs in response to IFNs has been reported in patients with primary Sjögren's syndrome (pSS) (44). Expression of BLyS mRNA in PBMCs from patients with pSS after IFN-α stimulation, but not IFN-γ stimulation, was significantly higher than that from normal controls, and a similar trend was observed in peripheral blood monocytes. These data indicate that different IFNs, IFN-α and IFN-γ, are relevant to the production of BLyS in patients with pSS and SLE, respectively. It has recently been shown that BLyS activates T cells as a costimulatory molecule (45). The costimulation of T cells by BLyS indicates that T cell-induced BLyS on APCs further activates T cells and contributes to the vicious cycle in vivo. Because IFN-α, CD154, and chromatin-IgG complex are known to induce the expression of BLyS (33, 34, 46) and to be involved in the immunopathogenesis of SLE (46–48), IFN-γ additively or synergistically contributes to the overexpression of BLyS in SLE with these soluble factors or with cell surface molecules. Because CD154 as well as IFN-γ are expressed by activated T cells, these two molecules may cooperate to induce BLyS during T cell-Ag-presenting cell interaction.

In summary, the present study clearly demonstrates the increased expression of IFN-γ in patients with SLE. IFN-γ, together with other soluble factors and surface molecules, would stimulate APCs to produce BLyS. Because this immunological abnormality is a common feature of both human and mouse lupus and because targeting therapy for IFN-γ has been successfully applied to lupus mice (5), treatment with humanized anti-IFN-γ mAb or recombinant IFN-γ-Ig fusion protein would provide a novel therapeutic strategy for this intractable disease.

Acknowledgments

We thank Ryoko Yoshida for excellent technical assistance in the flow cytometric analyses. We also thank Drs. H. Kohsaka, R. Koike, T. Nanki, T. Sugihara, and J. Ogawa (Tokyo Medical and Dental University) and Dr. C. Terai (Tokyo Women's Medical University) for providing clinical samples and discussion on the present work.

Disclosures

The authors have no financial conflict of interest.

References

1. Rekvig, O. P., and J. C. Nossent. 2003. Anti-double-stranded DNA antibodies, nucleosomes, and systemic lupus erythematosus: a time for new paradigms? *Arthritis Rheum.* 48: 300–312.
2. Haas, C., B. Ryffel, and M. Le Hir. 1998. IFN-γ receptor deletion prevents autoantibody production and glomerulonephritis in lupus-prone (NZB × NZW)F_1 mice. *J. Immunol.* 160: 3713–3718.
3. Schwarting, A., T. Wada, K. Kinoshita, G. Tesch, and V. R. Kelley. 1998. IFN-γ receptor signaling is essential for the initiation, acceleration, and destruction of autoimmune kidney disease in MRL-*Fas*^{lpr} mice. *J. Immunol.* 161: 494–503.
4. Balomenos, D., R. Rumold, and A. N. Theofilopoulos. 1998. Interferon-γ is required for lupus-like disease and lymphoaccumulation in MRL-lpr mice. *J. Clin. Invest.* 101: 364–371.
5. Lawson, B. R., G. J. Prud'homme, Y. Chang, H. A. Gardner, J. Kuan, D. H. Kono, and A. N. Theofilopoulos. 2000. Treatment of murine lupus with cDNA encoding IFN-γR/Fc. *J. Clin. Invest.* 106: 207–215.
6. Miyake, K., H. Nakashima, M. Akahoshi, Y. Inoue, S. Nagano, Y. Tanaka, K. Masutani, H. Hirakata, H. Gondo, T. Otsuka, and M. Harada. 2002. Genetically determined interferon-γ production influences the histological phenotype of lupus nephritis. *Rheumatology* 41: 518–524.
7. Nakashima, H., H. Inoue, M. Akahoshi, Y. Tanaka, K. Yamaoka, E. Ogami, S. Nagano, Y. Arinobu, H. Niiro, T. Otsuka, and Y. Niho. 1999. The combination of polymorphisms within interferon-γ receptor 1 and receptor 2 associated with the risk of systemic lupus erythematosus. *FEBS Lett.* 453: 187–190.
8. Masutani, K., M. Akahoshi, K. Tsuruya, M. Tokumoto, T. Ninomiya, T. Kohsaka, K. Fukuda, H. Kanai, H. Nakashima, T. Otsuka, and H. Hirakata. 2001. Predominance of Th1 immune response in diffuse proliferative lupus nephritis. *Arthritis Rheum.* 44: 2097–2106.
9. Uhm, W. S., K. Na, G. W. Song, S. S. Jung, T. Lee, M. H. Park, and D. H. Yoo. 2003. Cytokine balance in kidney tissue from lupus nephritis patients. *Rheumatology* 42: 935–938.
10. Gerez, L., T. Shkolnik, O. Hirschmann, M. Lorber, G. Arad, and R. Kaempfer. 1997. Hyperinducible expression of the interferon-γ (IFN-γ) gene and its suppression in systemic lupus erythematosus (SLE). *Clin. Exp. Immunol.* 109: 296–303.
11. Akahoshi, M., H. Nakashima, Y. Tanaka, T. Kohsaka, S. Nagano, E. Ohgami, Y. Arinobu, K. Yamaoka, H. Niiro, M. Shinozaki, et al. 1999. Th1/Th2 balance of peripheral T helper cells in systemic lupus erythematosus. *Arthritis Rheum.* 42: 1644–1648.
12. Mishra, N., D. R. Brown, I. M. Olorenshaw, and G. M. Kammer. 2001. Trichostatin A reverses skewed expression of CD154, interleukin-10, and interferon-γ gene and protein expression in lupus T cells. *Proc. Natl. Acad. Sci. USA* 98: 2628–2633.
13. Kawamoto, M., M. Harigai, M. Hara, Y. Kawaguchi, K. Tezuka, M. Tanaka, T. Sugiura, Y. Katsumata, C. Fukasawa, H. Ichida, et al. 2006. Expression and function of inducible costimulator in patients with systemic lupus erythematosus: possible involvement in excessive interferon-γ and anti-double-stranded DNA antibody production. *Arthritis Res. Ther.* 8: R62.
14. Sallusto, F., J. Geginat, and A. Lanzavecchia. 2004. Central memory and effector memory T cell subsets: function, generation, and maintenance. *Annu. Rev. Immunol.* 22: 745–763.
15. Gordon, C., N. Matthews, B. C. Schlesinger, A. N. Akbar, P. A. Bacon, P. Emery, and M. Salmon. 1996. Active systemic lupus erythematosus is associated with the recruitment of naive/resting T cells. *Br. J. Rheumatol.* 35: 226–230.
16. Fritsch, R. D., X. Shen, G. G. Illei, C. H. Yarboro, C. Prussin, K. S. Hathcock, R. J. Hodes, and P. E. Lipsky. 2006. Abnormal differentiation of memory T cells in systemic lupus erythematosus. *Arthritis Rheum.* 54: 2184–2197.
17. Blanco, P., V. Pitard, J. F. Viallard, J. L. Taupin, J. L. Pellegrin, and J. F. Moreau. 2005. Increase in activated $CD8^+$ T lymphocytes expressing perforin and granzyme B correlates with disease activity in patients with systemic lupus erythematosus. *Arthritis Rheum.* 52: 201–211.
18. Moore, P. A., O. Belvedere, A. Orr, K. Pieri, D. W. LaFleur, P. Feng, D. Soppet, M. Charters, R. Gentz, D. Parmelee, et al. 1999. BLyS: member of the tumor necrosis factor family and B lymphocyte stimulator. *Science* 285: 260–263.
19. Shu, H. B., W. H. Hu, and H. Johnson. 1999. TALL-1 is a novel member of the TNF family that is down-regulated by mitogens. *J. Leukocyte Biol.* 65: 680–683.
20. Tribouley, C., M. Wallroth, V. Chan, X. Paliard, E. Fang, G. Lamson, D. Pot, J. Escobedo, and L. T. Williams. 1999. Characterization of a new member of the TNF family expressed on antigen presenting cells. *Biol. Chem.* 380: 1443–1447.
21. Schneider, P., F. MacKay, V. Steiner, K. Hofmann, J. L. Bodmer, N. Holler, C. Ambrose, P. Lawton, S. Bixler, H. Acha-Orbea, et al. 1999. BAFF, a novel ligand of the tumor necrosis factor family, stimulates B cell growth. *J. Exp. Med.* 189: 1747–1756.
22. Miller, J. P., J. E. Stadanlick, and M. P. Cancro. 2006. Space, selection, and surveillance: setting boundaries with BLyS. *J. Immunol.* 176: 6405–6410.
23. Kalled, S. L. 2005. The role of BAFF in immune function and implications for autoimmunity. *Immunol. Rev.* 204: 43–54.
24. Gross, J. A., J. Johnston, S. Mudri, R. Enselman, S. R. Dillon, K. Madden, W. Xu, J. Parrish-Novak, D. Foster, C. Lofton-Day, et al. 2000. TACI and BCMA are receptors for a TNF homologue implicated in B-cell autoimmune disease. *Nature* 404: 995–999.
25. Roschke, V., S. Sosnovtseva, C. D. Ward, J. S. Hong, R. Smith, V. Albert, W. Stohl, K. P. Baker, S. Ullrich, B. Nardelli, et al. 2002. BLyS and APRIL form biologically active heterotrimers that are expressed in patients with systemic immune-based rheumatic diseases. *J. Immunol.* 169: 4314–4321.
26. Mackay, F., S. A. Woodcock, P. Lawton, C. Ambrose, M. Baetscher, P. Schneider, J. Tschopp, and J. L. Browning. 1999. Mice transgenic for BAFF develop lymphocytic disorders along with autoimmune manifestations. *J. Exp. Med.* 190: 1697–1710.
27. Khare, S. D., I. Sarosi, X. Z. Xia, S. McCabe, K. Miner, I. Solovyev, N. Hawkins, M. Kelley, D. Chang, G. Van, et al. 2000. Severe B cell hyperplasia and autoimmune disease in TALL-1 transgenic mice. *Proc. Natl. Acad. Sci. USA* 97: 3370–3375.
28. Ramanujam, M., X. Wang, W. Huang, Z. Liu, L. Schiffer, H. Tao, D. Frank, J. Rice, B. Diamond, K. O. Yu, et al. 2006. Similarities and differences between selective and nonselective BAFF blockade in murine SLE. *J. Clin. Invest.* 116: 724–734.
29. Ramanujam, M., X. Wang, W. Huang, L. Schiffer, C. Grimaldi, A. Akkerman, B. Diamond, M. P. Madaio, and A. Davidson. 2004. Mechanism of action of transmembrane activator and calcium modulator ligand interactor-Ig in murine systemic lupus erythematosus. *J. Immunol.* 173: 3524–3534.
30. Zhang, J., V. Roschke, K. P. Baker, Z. Wang, G. S. Alarcon, B. J. Fessler, H. Bastian, R. P. Kimberly, and T. Zhou. 2001. Cutting edge: a role for B lymphocyte stimulator in systemic lupus erythematosus. *J. Immunol.* 166: 6–10.
31. Stohl, W., S. Metyas, S. M. Tan, G. S. Cheema, B. Oamar, D. Xu, V. Roschke, Y. Wu, K. P. Baker, and D. M. Hilbert. 2003. B lymphocyte stimulator overexpression in patients with systemic lupus erythematosus: longitudinal observations. *Arthritis Rheum.* 48: 3475–3486.

32. Pers, J. O., C. Daridon, V. Devauchelle, S. Jousse, A. Saraux, C. Jamin, and P. Youinou. 2005. BAFF overexpression is associated with autoantibody production in autoimmune diseases. *Ann. NY Acad. Sci.* 1050: 34–39.
33. Litinskiy, M. B., B. Nardelli, D. M. Hilbert, B. He, A. Schaffer, P. Casali, and A. Cerutti. 2002. DCs induce CD40-independent immunoglobulin class switching through BLyS and APRIL. *Nat. Immunol.* 3: 822–829.
34. Nardelli, B., O. Belvedere, V. Roschke, P. A. Moore, H. S. Olsen, T. S. Migone, S. Sosnovtseva, J. A. Carrell, P. Feng, J. G. Giri, and D. M. Hilbert. 2001. Synthesis and release of B-lymphocyte stimulator from myeloid cells. *Blood* 97: 198–204.
35. Mullen, A. C., F. A. High, A. S. Hutchins, H. W. Lee, A. V. Villarino, D. M. Livingston, A. L. Kung, N. Cereb, T. P. Yao, S. Y. Yang, and S. L. Reiner. 2001. Role of T-bet in commitment of TH1 cells before IL-12-dependent selection. *Science* 292: 1907–1910.
36. Yoshimoto, K., Y. Takahashi, M. Ogasawara, Y. Setoyama, K. Suzuki, K. Tsuzaka, T. Abe, and T. Takeuchi. 2006. Aberrant expression of BAFF in T cells of systemic lupus erythematosus, which is recapitulated by a human T cell line, Loucy. *Int. Immunol.* 18: 1189–1196.
37. Mullen, A. C., A. S. Hutchins, F. A. High, H. W. Lee, K. J. Sykes, L. A. Chodosh, and S. L. Reiner. 2002. Hlx is induced by and genetically interacts with T-bet to promote heritable T_H1 gene induction. *Nat. Immunol.* 3: 652–658.
38. Sica, A., L. Dorman, V. Viggiano, M. Cippitelli, P. Ghosh, N. Rice, and H. A. Young. 1997. Interaction of NF-κB and NFAT with the interferon-γ promoter. *J. Biol. Chem.* 272: 30412–30420.
39. Teixeira, L. K., B. P. Fonseca, A. Vieira-de-Abreu, B. A. Barboza, B. K. Robbs, P. T. Bozza, and J. P. Viola. 2005. IFN-γ production by $CD8^+$ T cells depends on NFAT1 transcription factor and regulates Th differentiation. *J. Immunol.* 175: 5931–5939.
40. Penix, L. A., M. T. Sweetser, W. M. Weaver, J. P. Hoeffler, T. K. Kerppola, and C. B. Wilson. 1996. The proximal regulatory element of the interferon-γ promoter mediates selective expression in T cells. *J. Biol. Chem.* 271: 31964–31972.
41. Wong, H. K., G. M. Kammer, G. Dennis, and G. C. Tsokos. 1999. Abnormal NF-κB activity in T lymphocytes from patients with systemic lupus erythematosus is associated with decreased p65-RelA protein expression. *J. Immunol.* 163: 1682–1689.
42. Carter, R. H., H. Zhao, X. Liu, M. Pelletier, W. Chatham, R. Kimberly, and T. Zhou. 2005. Expression and occupancy of BAFF-R on B cells in systemic lupus erythematosus. *Arthritis Rheum.* 52: 3943–3954.
43. Chang, S. K., B. K. Arendt, J. R. Darce, X. Wu, and D. F. Jelinek. 2006. A role for BLyS in the activation of innate immune cells. *Blood* 108: 2687–2694.
44. Lavie, F., C. Miceli-Richard, M. Ittah, J. Sellam, J. E. Gottenberg, and X. Mariette. 2008. B-cell activating factor of the tumour necrosis factor family expression in blood monocytes and T cells from patients with primary Sjogren's syndrome. *Scand. J. Immunol.* 67: 185–192.
45. Ye, Q., L. Wang, A. D. Wells, R. Tao, R. Han, A. Davidson, M. L. Scott, and W. W. Hancock. 2004. BAFF binding to T cell-expressed BAFF-R costimulates T cell proliferation and alloresponses. *Eur. J. Immunol.* 34: 2750–2759.
46. Boule, M. W., C. Broughton, F. Mackay, S. Akira, A. Marshak-Rothstein, and I. R. Rifkin. 2004. Toll-like receptor 9-dependent and -independent dendritic cell activation by chromatin-immunoglobulin G complexes. *J. Exp. Med.* 199: 1631–1640.
47. Bennett, L., A. K. Palucka, E. Arce, V. Cantrell, J. Borvak, J. Banchereau, and V. Pascual. 2003. Interferon and granulopoiesis signatures in systemic lupus erythematosus blood. *J. Exp. Med.* 197: 711–723.
48. Kirou, K. A., C. Lee, S. George, K. Louca, I. G. Papagiannis, M. G. Peterson, N. Ly, R. N. Woodward, K. E. Fry, A. Y. Lau, et al. 2004. Coordinate overexpression of interferon-α-induced genes in systemic lupus erythematosus. *Arthritis Rheum.* 50: 3958–3967.

運動器外科学分野
軟骨再生学分野

宗田　大

医歯学総合研究科・生体支持組織学系専攻
運動機能再建学・教授

1. 研究の課題名

(1) 関節組織の障害に対する組織間葉幹細胞を用いた修復・再建

Repair and reconstruction of injured joint structures using tissue-derived stem cells

教室で独自に開発した滑膜組織中の接着増殖細胞を自己血清を用いて107レベルに増殖させ、未分化のまま移植し、軟骨欠損を修復する方法を基本として研究を発展させる。軟骨欠損部を上に向け細胞浮遊液を満たして静置する“Adherent method”を用いてヒト膝関節軟骨損傷に対する臨床研究を継続する。一方細胞浮遊液の接着能を改善するためにMg++を加えることを見出した。さらに臨床使用時の適切な濃度やMg++による接着因子の変化の分析を行っている。またAdherent methodの有用性を大動物であるミニブタの膝関節を用いた検討を行い、組織学的検討に加えて、臨床を意識したMRIによるT1mappingによる軟骨基質の産生やT2 mappingによる軟骨線維構造の成熟過程を明らかにした。今後膝スポーツ外傷で手術治療を必要とすることが多い前十字靱帯損傷膝の治療時に滑膜幹細胞を補強する治療法の意義を検討する予定である。

(2) 変形性関節症における軟骨変性の分子メカニズムの解析

Molecular mechanisms of cartilage degeneration in osteoarthritis

変形性関節症（OA）の予防並びに効果的な治療法の開発に応用することを最終目標として、関節軟骨の変性の分子メカニズムの解析を行っている。まず、関節軟骨の変性に伴って軟骨や滑膜で発現量が変動する遺伝子の同定を行うために、マイクロアレイ法を用いた網羅的遺伝子発現解析を行った。その結果、ヒトOA軟骨や前十字靱帯損傷時に滑膜由来間葉系幹細胞（MSC）において発現量が増大している遺伝子の候補として、PRELP, OGN, ECRG4, YKL-39, YKL-40等を同定した。(Segawa et al., J Ortho Res, 2009 in press, Morito et al., Rheumatol, 47:1137-43, 2008、および未発表データ)。それらの中から、細胞増殖、分化や炎症反応に関与することが期待できる細胞外分泌タンパクで機能解析がいまだ行われていない三種の遺伝子、YKL-39, YKL-40, ECGR4に関して着目し、in situ hybridization法、Q-RTPCR法による発現解析を現在行っている。さらにこれら遺伝子の生理機能の解析を行うために、レンチウィルスの系を用いた発現ベクター、ノックダウンベクターの構築を行っている。

2.

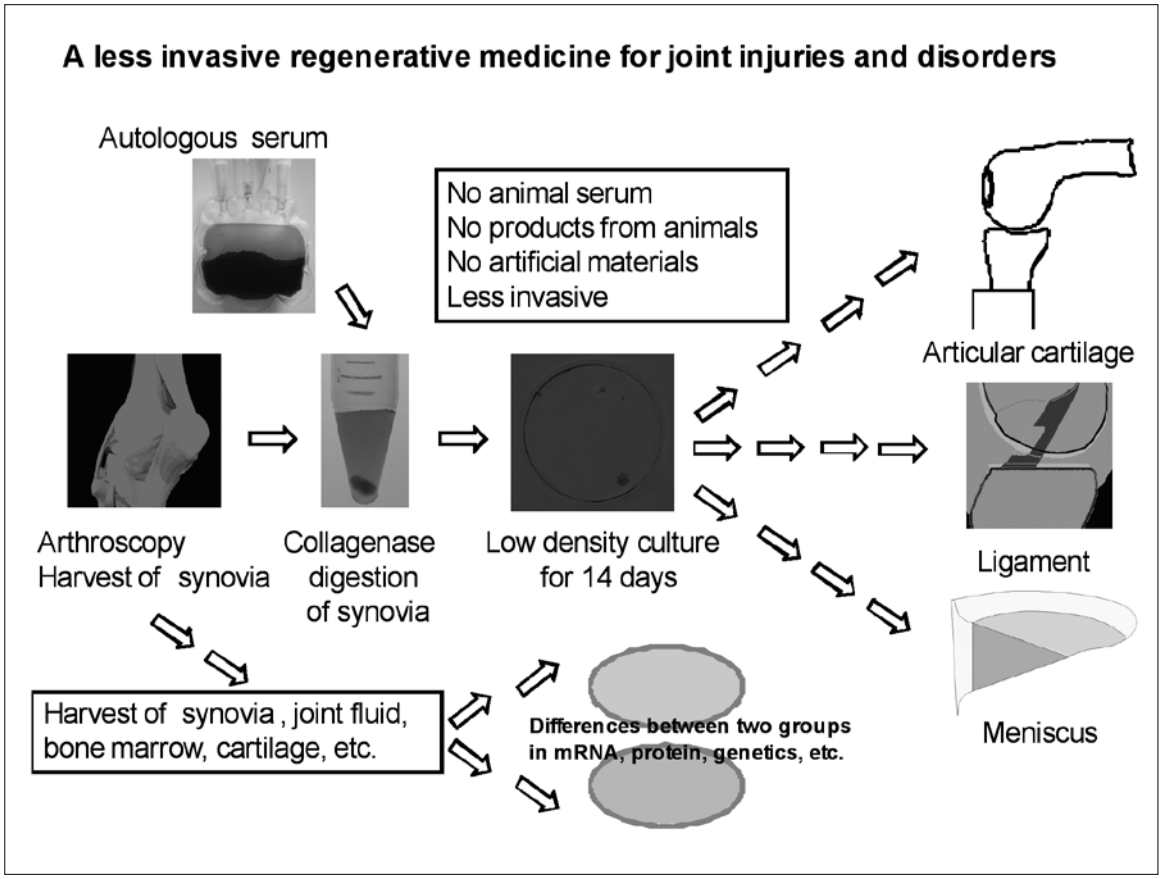

3. 2008年、2009年（平成21年3月までの）に発表した全ての研究内容についての英文要約

Asano H, Muneta T.
Stiffness of soft tissue complex in total knee arthroplasty.
Knee Surg Sports Traumatol Arthropsc 2008 Jan;16（1）:51-5.

The significance of achievement of soft tissue balancing in total knee arthroplasty is well recognized. There are few reports dealing with soft tissue tension in total knee arthroplasty. It is expected that the soft tissue tension will affect post-operative results such as postoperative ROM and stability. The purpose of this study was to evaluate tension properties of soft tissue complex of osteoarthritic knee in total knee arthroplasty. Sixty osteoarthritic knees that underwent primary total knee arthroplasty were investigated with a balancer and torque driver specially developed and adapted for this study. We gradually opened the extension and flexion space and measured the force to open it. We created a force-displacement curve in each case. Inclination of the curve indicated stiffness. We examined the stiffness average of all cases every 10 N. The stiffness was 8.9 and 8.5 N/mm（extension, flexion）in soft tissue tension of 60 N and 26.6 and 21.4 N/mm in 180 N. The stiffness became larger with an increase of soft tissue tension, and the stiffness of extension is significantly larger than that of flexion in each tension except for 60 N. Tension properties of soft tissue complex reveal that soft tissue can be easily extended in low soft tissue tension, and hardly extended in high tension.

Watanabe T, Muneta T, Ikeda H, Tateishi T, Sekiya I
Visual analog scale assessment after medial patellofemoral ligament reconstruction: with or without tibial tubercle transfer
J Orthop Sci. 2008 Jan;13（1）:32-8.

BACKGROUND: We studied the efficacy of medial patellofemoral ligament（MPFL）reconstruction, with or without tibial tubercle（TT）transfer, for recurrent dislocation of the patella, based on subjective functional assessment using the visual analog scale（VAS）.
METHODS: Forty-two consecutive knees of 40 patients who underwent MPFL reconstruction using a hamstring tendon were followed up for an average of 4.3 years. Twenty-nine knees underwent MPFL reconstruction（MPFL group）and 13 knees underwent MPFL reconstruction combined with medial transfer of TT（TT+MPFL group）. Clinical results, including the VAS score at the latest follow-up in

both groups, were assessed. RESULTS: An apparent deficit in the range of motion was observed in two cases from the TT+MPFL group. The ratio of negative apprehension test was significantly improved from 3% preoperatively to 79% postoperatively in the MPFL group and from 8% to 69% in the TT+MPFL group. The Lysholm scores were significantly improved from 70 points preoperatively to 92 points postoperatively in the MPFL group and from 72 points to 90 points in the TT+MPFL group. There was no significant difference between the two groups in the ratios of negative apprehension tests and the Lysholm scores after surgery as well as before surgery. In the VAS assessment, the MPFL group scored significantly higher than the TT+MPFL group in "Japanese full sitting" (average score 92 vs 62). The scores of the two groups were not significantly different in any of the other items, although the total average score was significantly higher in the MPFL group (91 vs 81). CONCLUSIONS: MPFL reconstruction without TT transfer achieved satisfactory results including high scores on subjective functional assessments without disadvantage caused by the TT transfer. Isolated MPFL reconstruction has been suggested to be a useful treatment method for recurrent dislocation of the patella.

Hara K, Niga S, Ikeda H, Cho S, Muneta T
Isolated anterior cruciate ligament reconstruction in patients with chronic anterior cruciate ligament insufficiency combined with grade II valgus laxity
Am J Sports Med. 2008 Feb;36 (2) :333-9.

BACKGROUND: There is no consensus about whether isolated anterior cruciate ligament reconstruction using multistrand hamstring tendon with nonoperative treatment for chronic medial collateral ligament injury is sufficient. PURPOSE: To assess clinical outcome for patients with chronic anterior cruciate ligament injury and accompanying grade II valgus laxity who received medial hamstring anterior cruciate ligament reconstruction alone. Results were compared with those of patients with isolated chronic anterior cruciate ligament injury without valgus laxity. STUDY DESIGN: Cohort study; Level of evidence, 2. METHODS: Two hundred eighty-nine patients with isolated anterior cruciate ligament injury were compared with 53 patients with accompanying valgus laxity (minimum follow-up, 24 months). The following parameters were compared between the 2 groups at the last follow-up: range of motion, KT-1000 arthrometer value, pivot-shift test result, Lysholm knee scale, knee extensor muscle strength, return to sporting activities, subjective recovery, and International Knee Documentation Committee grade. Differences in clinical outcome were evaluated between those with preoperative International Knee Documentation Committee grade B and grade C and between those with grade A and grade B or C at final evaluation. RESULTS: Postoperative KT-1000 arthrometer value averaged 1.2 mm for those with isolated anterior cruciate ligament injury and 1.6 mm for those with accompanying valgus laxity (not significant, P = .281). There was no significant difference between these 2 groups regarding the other items. In patients with preoperative valgus laxity, KT-1000 arthrometer values at final evaluation between patients with preoperative grade B and C were not significantly different. The value for subjects with grade A at final evaluation was 1.3 mm and for those with grade B or C at final evaluation was 2.7 mm (P = .065). CONCLUSION: There was no clinically significant difference regarding outcome of anterior cruciate ligament multistrand hamstring reconstruction alone for 90% of patients with grade II valgus laxity who regained medial stability with nonoperative management compared with those who underwent the same anterior cruciate ligament reconstruction for an isolated anterior cruciate ligament tear.

Nimura A, Muneta T, Koga H, Mochizuki T, Suzuki K, Makino H, Umezawa A, Sekiya I
Increased proliferation of human synovial mesenchymal stem cells with autologous human serum: comparisons with bone marrow mesenchymal stem cells and with fetal bovine serum
Arthritis Rheum. 2008 Feb;58 (2) :501-10.

OBJECTIVE: Synovial mesenchymal stem cells (MSCs) are a promising cell source for cartilage regeneration due to their high chondrogenic potential. For clinical safety, autologous human serum should be used instead of fetal bovine serum (FBS). We undertook this study to compare the 2 types of serum for their enhancement of the proliferation and chondrogenic potentials of synovial MSCs and to investigate the mechanisms of the differences. Since effectiveness of the sera might depend on the origin of the MSCs, we also examined bone marrow MSCs. METHODS: Synovium, bone marrow, and peripheral blood were obtained from 18 donors. Synovial and bone marrow MSCs were cultured with autologous human serum or FBS and analyzed. In addition, rabbit synovial MSCs cultured with autologous serum or FBS were transplanted into full-thickness cartilage defects of the knees of the same rabbits. RESULTS: Human synovial MSCs expanded more in human serum than in FBS, and the opposite results were obtained with bone marrow MSCs. Hierarchical clustering analysis showed that the cell source, rather than the type of serum, affected the gene expression profile. Human serum contained high levels of platelet-derived growth factor (PDGF), synovial MSCs expressed higher levels of PDGF receptor alpha than did bone marrow MSCs, and

neutralizing PDGF decreased the proliferation of synovial MSCs with autologous human serum. Although the in vitro chondrogenic potential of human synovial MSCs was affected by the serum source, the in vivo chondrogenic potential of rabbit synovial MSCs was similar in autologous serum and FBS groups. CONCLUSION: Autologous serum predominates in increasing the proliferation of synovial MSCs with chondrogenic potential through PDGF signaling.

Nagese T, Muneta T, Ju YJ, Hara K, Morito T, Koga H, Nimura A, Mochizuki T, Sekiya I
Analysis of the chondrogenic potential of human synovial stem cells according to harvest site and culture parameters in knees with medial compartment osteoarthritis.
Arthritis Rheum. 2008 May;58（5）:1389-98.

OBJECTIVE: Synovial mesenchymal stem cells（MSCs）are an attractive cell source for cartilage regeneration because of their high chondrogenic ability. In this study, we examined the synovium of patients with medial compartment knee osteoarthritis（OA）to determine the proportion of MSCs in relation to cellular compartmentalization, and to identify the culture parameters that could affect the chondrogenic potential of synovial MSCs. METHODS: Human synovium was collected from 4 different harvest sites in the knees of patients with medial compartment OA. Each synovial tissue sample was divided into 2 parts, one for histologic assessment and the other for analysis of the cell size, surface epitopes, and chondrogenic potential of colony-forming cells in vitro. RESULTS: The numbers of alpha-smooth muscle actin-positive vessels and CD31+ endothelial cells were higher in the medial outer region than in the other regions of OA synovial tissue. The numbers of these cells correlated with the number of colony-forming cells. In parallel with increasing duration of the preculture period, the size of the cells increased, while the chondrogenic potential decreased, and this was correlated with expression of CD90. CONCLUSION: Medial compartment knee OA demonstrates variability in the distribution of vessels, which results in a varying distribution of MSCs. The preculture period should be utilized to assess both the potential for expansion and the chondrogenic potential of MSCs.

Mochizuki T, Sugaya H, Uomizu M, Maeda K, Matsuki K, Sekiya I, Muneta T, Akita K.
Humeral insertion of the supraspinatus and infraspinatus. New anatomical findings regarding the footprint of the rotator cuff.
J Bone Joint Surg Am. 2008 May;90（5）:962-9.

BACKGROUND: It is generally believed that the supraspinatus is the most commonly involved tendon in rotator cuff tears. Clinically, however, atrophy of the infraspinatus muscle is frequently observed in patients with even small to medium-size rotator cuff tears. This fact cannot be fully explained by our current understanding of the anatomical insertions of the supraspinatus and infraspinatus. The purpose of this study was to reinvestigate the humeral insertions of these tendons. METHODS: The study included 113 shoulders from sixty-four cadavers. The humeral insertion areas of the supraspinatus and infraspinatus were investigated in ninety-seven specimens. In sixteen specimens, all muscular portions of the supraspinatus and infraspinatus were removed, leaving the tendinous portions intact, in order to define the specific characteristics of the tendinous portion of the muscles. Another twenty-six shoulders were used to obtain precise measurements of the footprints of the supraspinatus and infraspinatus. RESULTS: The supraspinatus had a long tendinous portion in the anterior half of the muscle, which always inserted into the anteriormost area of the highest impression on the greater tuberosity and which inserted into the superiormost area of the lesser tuberosity in 21% of the specimens. The footprint of the supraspinatus was triangular in shape, with an average maximum medial-to-lateral length of 6.9 mm and an average maximum anteroposterior width of 12.6 mm. The infraspinatus had a long tendinous portion in the superior half of the muscle, which curved anteriorly and extended to the anterolateral area of the highest impression of the greater tuberosity. The footprint of the infraspinatus was trapezoidal in shape, with an average maximum medial-to-lateral length of 10.2 mm and an average maximum anteroposterior width of 32.7 mm. CONCLUSIONS: The footprint of the supraspinatus on the greater tuberosity is much smaller than previously believed, and this area of the greater tuberosity is actually occupied by a substantial amount of the infraspinatus.

Toita S, Hasegawa U, Koga H, Sekiya I, Muneta T, Akiyoshi K
Protein-conjugated quantum dots effectively delivered into living cells by a cationic nanogel.
J Nanosci Nanotechnol. 2008 May;8（5）:2279-85.

Quantum dots（QDs）have attracted attention for their potential as a cell imaging regent. However, the development of effective intracellular delivery system for QDs is needed to apply various cell lines without affecting cellular function. We reported here new QDs delivery system by using cationic nanogel consisting of cholesterol-bearing pullulan modified with an amino group（CHPNH2）. The uptake of hybrid nanoparticles into HeLa cells was followed by flow cytometry, and confocal laser scanning

fluorescence microscopy. Protein-conjugated QDs were effectively internalized into cells by the nanogel compared with a cationic liposome system. The hybrid nanoparticle was used to stain rabbit mesenchymal stem cells (MSCs) so as to evaluate their effect on cell function. CHPNH2-QD hybrid nanoparticles remained detectable inside MSCs for at least 2 weeks of culture and had little effect on the in vitro chondrogenic ability of MSCs. The hybrid nanoparticles are a promising candidate as a cell tracer in tissue engineering.

Ju YJ, Muneta T, Yoshimura H, Koga H, Sekiya I
Synovial mesenchymal stem cells accelerate early remodeling of tendon-bone healing
Cell Tissue Res 2008 Jun;332 (3) :469-78.

Tendon-bone healing is important for the successful reconstruction of the anterior cruciate ligament by using the hamstring tendon. Mesenchymal stem cells (MSCs) have attracted much interest because of their self-renewing potential and multipotentiality for possible clinical use. We previously reported that MSCs derived from synovium had a higher proliferation and differentiation potential than the other MSCs that we examined. The purpose of this study was to investigate the effect and mechanism of the implantation of the synovial MSCs on tendon-bone healing in rats. Half of the Achilles' tendon grafts of rats were inserted into a bone tunnel from the tibial plateau to the tibial tuberosity with a suture-post fixation. The bone tunnel was filled with MSCs labeled with fluorescent marker DiI or without MSCs as the control. The tendon-bone interface was analyzed histologically, and collagen fibers were quantified. At 1 week, the tendon-bone interface was filled with abundant DiI-positive cells, and the proportion of collagen fiber area was significantly higher in the MSC group than in the control group. By 2 weeks, the proportion of oblique collagen fibers, which appeared to be Sharpey's fibers, was significantly higher in the MSC group than in the control group. At 4 weeks, the interface tissue disappeared, and the implanted tendon appeared to attach to the bone directly in both groups. DiI-labeled cells could no longer be observed. Implantation of synovial MSCs into bone tunnel thus accelerated early remodeling of tendon-bone healing, as shown histologically.

Morito T, Muneta T, Hara K, Ju YJ, Mochizuki T, Makino H, Umezawa A, Sekiya I
Synovial fluid-derived mesenchymal stem cells increase after intra-articular ligament injury in humans
Rheumatology (Oxford) . 2008 Aug;47 (8) :1137-43.

OBJECTIVE: The existence of mesenchymal stem cells (MSCs) in SF was previously reported. However, the behaviour and properties of MSCs derived from SF have not been fully elucidated. METHODS: Human SFs were obtained from 19 knee joints with anterior cruciate ligament injury around the time of reconstruction surgery, and from three healthy volunteers. SF was plated, cultured and examined for colony-forming number, in vitro differentiation, surface epitopes and gene profiles. Also, rabbit synovium-MSCs were injected into the knee joint in a rabbit partial anterior cruciate ligament defect model, and the injected cells were traced. RESULTS: SF-MSCs from IA ligament injury patients were 100 times more in number than those from healthy volunteers. Total colony number was positively correlated with post-injury period. No significant differences were observed among the cells derived from SF around the time of the surgery in relation to surface epitopes and differentiation potentials. Cluster analysis of gene profiles demonstrated that SF-MSCs were more similar to synovium MSCs than bone marrow MSCs. In rabbit experiments, the MSCs injected into the knee in which IA ligament was partially defective were observed more on the defected area than on the intact area of the ligament at 24 h. CONCLUSION: We demonstrated that SF-MSCs, similar to synovium MSCs, increased in number after IA ligament injury and surgery without marked alteration of the properties.

Koga H, Muneta T, Nagase T, Nimura A, Ju YJ, Mochizuki T, Sekiya I
Comparison of mesenchymal tissues-derived stem cells for in vivo chondrogenesis: suitable conditions for cell therapy of cartilage defects in rabbit.
Cell Tissue Res. 2008 Aug;333 (2) :207-15.

We previously compared mesenchymal stem cells (MSCs) from a variety of mesenchymal tissues and demonstrated that synovium-MSCs had the best expansion and chondrogenic ability in vitro in humans and rats. In this study, we compared the in vivo chondrogenic potential of rabbit MSCs. We also examined other parameters to clarify suitable conditions for in vitro and in vivo cartilage formation. MSCs were isolated from bone marrow, synovium, adipose tissue, and muscle of adult rabbits. Proliferation potential and in vitro chondrogenic potential were compared. Toxicity of the tracer DiI for in vitro chondrogenesis was also examined. MSCs from each tissue were embedded in collagen gel and transplanted into full thickness cartilage defects of rabbits. Cartilage matrix production was compared histologically. The effects of cell density and periosteal patch on the in vivo chondrogenic potential of synovium-MSCs were also examined. Synovium-

and muscle-MSCs had a higher proliferation potential than other cells. Pellets from synovium- and bone-marrow-MSCs showed abundant cartilage matrix. DiI had no significant influence on in vitro cartilage formation. After transplantation into cartilage defects, synovium- and bone-marrow-MSCs produced much more cartilage matrix than other cells. When synovium-MSCs were transplanted at a higher cell density and with a periosteal patch, more abundant cartilage matrix was observed. Thus, synovium- and bone-marrow-MSCs had greater in vivo chondrogenic potential than adipose- and muscle-MSCs, but synovium-MSCs had the advantage of a greater proliferation potential. Higher cell density and a periosteum patch were needed to obtain a high production of cartilage matrix by synovium-MSCs.

Zhang S, Muneta T, Morito T, Mochizuki T, Sekiya I
Autologous synovial fluid enhances migration of mesenchymal stem cells from synovium of osteoarthritis patients in tissue culture system
J Orthop Res. 2008 Oct;26（10）:1413-8.

Synovial fluid from osteoarthritic knee contains mesenchymal stem cells（MSCs）. One of the possible reservoirs of MSCs in synovial fluid is synovial tissue, and synovial fluid may induce mobilization of MSCs into synovial fluid in osteoarthritis patients. Here, we investigated whether synovial fluid expanded synovial MSCs in a tissue culture system. Human synovium and synovial fluid were obtained from osteoarthritis patients during total knee arthroplasties. In the tissue culture system, autologous synovial fluid expanded synovial cells statistically higher than alpha MEM + FBS, and the addition of TGF beta 3 to alpha MEM + FBS increased expansion to a similar level in all 11 donors. The addition of decorin or anti-TGFbeta neutralizing antibody to synovial fluid partially inhibited synovial cell expansion. In cell culture assay, synovial fluid proliferated synovial cells fewer than alpha MEM + FBS. The expanded synovial cells in synovial fluid retained multipotentiality and showed surface markers similar to those of MSCs. We demonstrated that autologous synovial fluid enhanced expansion of MSCs in tissue culture of synovium from osteoarthritis patients by promoting cell migration. This effect was partially affected by TGFbeta.（c）2008 Orthopaedic Research Society.

Asano H, Muneta T, Sekiya I
Knee Surg Sports Traumatol Arthrosc. 2008 Nov;16（11）:999-1003. Epub 2008 Aug 30
Soft tissue tension in extension in total knee arthroplasty affects postoperative knee extension and stability.

Knee Surg Sports Traumatol Arthrosc. 2008 Nov;16（11）:999-1003.

The purpose of this study was to assess correlation of soft tissue tension in extension with postoperative extension deficit and valgus/varus instability. Sixty-four osteoarthritic knees that underwent primary total knee arthroplasty were investigated. Soft tissue tension in extension was measured during operation with a balancer/tensor device. Extension deficit was measured, and valgus/varus laxity was assessed by stress radiographs in extension and 30 degrees -flexion 1 year after operation. The extension deficit became larger with an increase of soft tissue tension a year after operation.（$P < 0.05$）The varus laxity in extension and 30 degrees -flexion and valgus laxity in 30 degrees -flexion became smaller with an increase of soft tissue tension（$P < 0.05$）. Our results demonstrated that soft tissue tension during operation affects postoperative knee extension and stability.

Tang T, Muneta T, Ju YJ, Nimura A, Miyazaki K, Masuda H, Mochizuki T, Sekiya I
Serum keratan sulfate transiently increases in the early stage of osteoarthritis during strenuous running of rats: protective effect of intraarticular hyaluronan injection
Arthritis Res Ther. 2008;10（1）:R13.

INTRODUCTION: Osteoarthritis is influenced by genetic and environment factors, including mechanical stress; however, the relationship between running and the development of osteoarthritis remains a matter of controversy. We investigated whether osteoarthritic change could be obtained in a rat strenuous running model, whether serum keratan sulfate in rats could be detected by HPLC and was associated with onset or progression of osteoarthritis, and whether hyaluronan injection suppressed development of osteoarthritis and elevation of serum keratan sulfate. METHODS: Wistar rats were forced to run 30 km in 6 weeks on a treadmill machine. Articular cartilage of the knees was evaluated macroscopically and immunohistologically. Serum keratan sulfate was examined every week by HPLC. The effect of weekly knee injection of hyaluronan was also investigated. RESULTS: Cartilage surfaces stained with India ink became irregular, metachromasia by safranin-O staining appeared to be almost lost, and Mankin's score significantly worsened after 30 km of running. Serum keratan sulfate in rats was detected by HPLC and transiently increased（peaked at 3 to 4 weeks）along with depletion of keratan sulfate in cartilage tissue. Hyaluronan treatment suppressed morphological progression of osteoarthritis and elevation of serum keratan sulfate. CONCLUSION: Rat strenuous running induced

osteoarthritis. Serum keratan sulfate was associated with progression of osteoarthritis. Weekly intraarticular injection of hyaluronan controlled the development of osteoarthritis, and the effect was reflected by serum keratan sulfate.

Koga H, Shimaya M, Muneta T, Nimura A, Morito T, Hayashi M, Suzuki S, Ju YJ, Mochizuki T, Sekiya I
Local adherent technique for transplanting mesenchymal stem cells as a potential treatment of cartilage defect
Arthritis Res Ther. 2008;10（4）:R84.

INTRODUCTION: Current cell therapy for cartilage regeneration requires invasive procedures, periosteal coverage and scaffold use. We have developed a novel transplantation method with synovial mesenchymal stem cells（MSCs）to adhere to the cartilage defect. METHODS: For ex vivo analysis in rabbits, the cartilage defect was faced upward, filled with synovial MSC suspension, and held stationary for 2.5 to 15 minutes. The number of attached cells was examined. For in vivo analysis in rabbits, an autologous synovial MSC suspension was placed on the cartilage defect, and the position was maintained for 10 minutes to adhere the cells to the defect. For the control, either the same cell suspension was injected intra-articularly or the defects were left empty. The three groups were compared macroscopically and histologically. For ex vivo analysis in humans, in addition to the similar experiment in rabbits, the expression and effects of neutralizing antibodies for adhesion molecules were examined. RESULTS: Ex vivo analysis in rabbits demonstrated that the number of attached cells increased in a time-dependent manner, and more than 60% of cells attached within 10 minutes. The in vivo study showed that a large number of transplanted synovial MSCs attached to the defect at 1 day, and the cartilage defect improved at 24 weeks. The histological score was consistently better than the scores of the two control groups（same cell suspension injected intra-articularly or defects left empty）at 4, 12, and 24 weeks. Ex vivo analysis in humans provided similar results to those in rabbits. Intercellular adhesion molecule 1-positive cells increased between 1 minute and 10 minutes, and neutralizing antibodies for intercellular adhesion molecule 1, vascular cell adhesion molecule 1 and activated leukocyte-cell adhesion molecule inhibited the attachment. CONCLUSION: Placing MSC suspension on the cartilage defect for 10 minutes resulted in adherence of >60% of synovial MSCs to the defect, and promoted cartilage regeneration. This adherent method makes it possible to adhere MSCs with low invasion, without periosteal coverage, and without a scaffold.

Segawa Y, Muneta T, Makino H, Nimura A, Mochizuki T, Ju YJ, Ezura Y, Umezawa A, Sekiya I
Mesenchymal stem cells derived from synovium, meniscus, anterior cruciate ligament, and articular chondrocytes share similar gene expression profiles.
J Orthop Res. 2008 Oct 30. [Epub ahead of print]

Mesenchymal stem cells（MSCs）can be obtained from various tissues, and contain common features. However, an increasing number of reports have described variant properties dependent of cell sources. We examined（1）whether MSCs existed in several intraarticular tissues,（2）whether gene expression profiles in intraarticular tissue MSCs closely resembled each other, and（3）whether identified genes were specific to intraarticular tissue MSCs. Human synovium, meniscus, intraarticular ligament, muscle, adipose tissue, and bone marrow were harvested, and colony-forming cells were analyzed. All these cells showed multipotentiality and surface markers typical of MSCs. Gene profiles of intraarticular tissue MSCs and chondrocytes were closer to each other than those of extraarticular tissues MSCs. Among three characteristic genes specific for intraarticular tissue MSCs, we focused on proline arginine-rich end leucine-rich repeat protein（PRELP）. Higher expression of PRELP was confirmed in chondrocytes and intraarticular tissue MSCs among three elderly and three young donors. Synovium MSCs stably expressed PRELP, contrarily, bone marrow MSCs increased PRELP expression during in vitro chondrogenesis. In conclusion, MSCs could be isolated from various intraarticular tissues including meniscus and ligament, gene expression profiles of intraarticular tissue MSCs closely resembled each other, and the higher expression of PRELP was characteristic of intraarticular tissue MSCs.（c）2008 Orthopaedic Research Society. Published by Wiley Periodicals

Hayashi M, Muneta T, Ju YJ, Mochizuki T, Sekiya I
Weekly intra-articular injections of bone morphogenetic protein-7 inhibits osteoarthritis progression.
Arthritis Res Ther. 2008;10（5）:R118. Epub 2008 Sep 30.

INTRODUCTION: We investigated the ability of a weekly intra-articular injection of bone morphogenetic protein（BMP）-7 to prevent osteoarthritis in rabbits with anterior cruciate ligament transections. METHODS: First, 36 knee joints were randomly divided into four groups: 50, 500, 5,000 ng BMP-7, and control. Knee cartilage was evaluated at 4, 8, and 12 weeks. Then, in order to control for individual differences, 500 ng BMP-7 was injected into one knee and phosphate-buffered saline（PBS）into the other, and the two knees were compared at 4, 8, and 12 weeks（n = 5）. For pharmacokinetic analysis, cartilage was harvested at

1 hour and 1, 2, 4, and 7 days after knee injection of 500 ng BMP-7 or PBS（n = 3）. RESULTS: Histological scores in the 500 and 5,000 ng BMP-7 groups were significantly better than those in the other groups at 12 weeks. Matched pair analysis demonstrated that both macroscopic and histological scores in the 500 ng BMP-7 group were better than those in the control group. Immunohistochemical analysis revealed higher BMP-7 expression by chondrocytes in the BMP-7 injected knees. Histology of whole knee and quantitative micro computed tomography analysis showed that weekly injections of 500 ng BMP-7 did not induce synovial fibrosis, ectopic bone, or osteophyte formation. As detected by enzyme-linked immunosorbent assay, BMP-7 concentration in the cartilage tissue was still higher in the BMP-7 treated group 7 days after the injection. CONCLUSIONS: Weekly intra-articular injections of BMP-7 inhibited progression of osteoarthritis. Obvious adverse effects were not observed. BMP-7 concentration and expression in cartilage were still higher 7 days after injection.

Sekiya I, Tang T, Hayashi M, Morito T, Ju YJ, Mochizuki T, Muneta T
Periodic knee injections of BMP-7 delay cartilage degeneration induced by excessive running in rats.
J Orthop Res. 2009 Jan 23. [Epub ahead of print]

Strenuous running of rats enhances mechanical stress on the knee, thereby inducing degeneration of articular cartilage. Bone morphogenetic protein-7（BMP-7）has an inhibitory effect on cartilage degeneration, suggesting its usefulness for human osteoarthritis patients. However, its mode of administration should be investigated. We examined whether weekly knee injections of BMP-7 delayed the progression of cartilage degeneration. Wistar rats were forced to run 30 km in 6 weeks on a rodent treadmill, and BMP-7 was injected weekly into the knee. Macroscopically and histologically, this strenuous running regimen induced cartilage degeneration. Weekly injections of 250 ng BMP-7 delayed the progression of cartilage degeneration. Immunohistochemically, in the control knee, type II collagen expression decreased, while BMP-7 expression in chondrocytes slightly increased. Interestingly, weekly injection of BMP-7 increased BMP-7 expression even 9 days after the final injection. Disulfate disaccharide keratan sulfate in serum transiently increased in the control group, while it remained at a low level in the BMP-7 group. Weekly BMP-7 injection increased BMP-7 expression in chondrocytes and its effect seemed to last more than 7 days. The effect of BMP-7 could be monitored by serum keratan sulfate concentration. Periodical injections of BMP-7 delayed progression of cartilage degeneration induced by excessive running in rats.（c）2009 Orthopaedic Research Society.

Seko Y, Azuma N, Takahashi Y, Makino H, Morito T, Muneta T, Matsumoto K, Saito H, Sekiya I, Umezawa A
Human sclera maintains common characteristics with cartilage throughout evolution
PLoS ONE. 2008;3（11）:e3709. Epub 2008 Nov 12.

BACKGROUND: The sclera maintains and protects the eye ball, which receives visual　inputs.Although the sclera does not contribute significantly to visual perception, scleral diseases such as refractory scleritis, scleral perforation and pathological myopia are considered incurable or difficult to cure. The aim of this study is to identify characteristics of the human sclera as one of the connective tissues derived from the neural crest and mesoderm. METHODOLOGY/ PRINCIPAL FINDINGS: We have demonstrated microarray data of cultured human infant scleral cells. Hierarchical clustering was performed to group scleral cells and other mesenchymal cells into subcategories. Hierarchical clustering analysis showed similarity between scleral cells and auricular cartilage-derived cells. Cultured micromasses of scleral cells exposed to TGF-betas and BMP2 produced an abundant matrix. The expression of cartilage-associated genes, such as Indian hedge hog, type X collagen, and MMP13, was up-regulated within 3 weeks in vitro. These results suggest that human 'sclera'-derived cells can be considered chondrocytes when cultured ex vivo. CONCLUSIONS/SIGNIFICANCE: Our present study shows a chondrogenic potential of human sclera. Interestingly, the sclera of certain vertebrates, such as birds and fish, is composed of hyaline cartilage. Although the human sclera is not a cartilaginous tissue, the human sclera maintains chondrogenic potential throughout evolution. In addition, our findings directly explain an enigma that the sclera and the joint cartilage are common targets of inflammatory cells in rheumatic arthritis. The present global gene expression database will contribute to the clarification of the pathogenesis of developmental diseases such as high myopia

4. 本事業に関連して世界的な研究拠点形成に向けて、以下の点で改善・整備等されたこと

A（研究拠点体制）

GCOEの発足により辻邦和特任講師が運動器外科学教室の研究に加わった。このことによりHarvard Dental Schoolとの共同研究が開始され、研究の質の向上と研究課題の増加を得られると考えられる。 辻講師のBMPのConditional knockout mouseの研究の

継続により、BMP研究の研究拠点としての機能を担うことになった。 さらにヒトの関節内および周囲組織に対する解析を共同で行う体制づくりを進めている。一方滑膜間葉幹細胞を用いる軟骨欠損治療の大動物を用いた研究の実施のために3年前から自治医科大学との共同研究体制が築かれている。さらにブタを用いる研究の質の向上と供給体制の整備の目的で明治大学農学部との共同研究体制も構築中である。

B（研究教育環境）

GCOEの発足に伴い辻講師が運動器外科学に赴任し、運動器外科学の大学院生の教育の質と幅が向上した。特に遺伝子工学的技術の導入は今後の研究の厚みを増すことにつながることが期待される。研究環境としてGCOEのコモンラボを共有して使用できるようになることは、研究の質を向上させ効率を高めることに役立つ。またII期棟に49m2のコモンラボを確保でき、長期的な運営の円滑化につながると考えられる。

C（人材確保）

運動器外科学の研究推進の主体は医学部整形外科の医師である。ここ数年大学院生は平均して2,3人入学し、現在9名の大学院生が基礎研究を支えている。今後も同じようなペースで大学院生が入学することが予想される。また海外からの留学生も一定の基準のもとに積極的に受け入れている。

D（人材育成）

運動器外科学を構成する大学院生は基本的に整形外科医であり、大学院卒業後臨床の現場に戻り、臨床能力をあげつつ、大学院で養った科学的な追及心、研究実施能力、研究成果報告能力を生かしている。また大学院卒業後さらに種々の専門領域での留学も推奨している。現在ノルウェーに1名の留学生が研究に従事しており、4月からは米国に1名、6月からは米国に別の1名が留学する予定である。

E（国際化）

辻講師の留学先であったHarvard Dentalとの共同研究、さらにHarvard Medicalとの共同研究の推進が具体的に進行している。留学生の滞在するOslo大学との交流も継続中である。さらに4月から留学する米国の研究所との共同研究が進みつつある。

5. GCOE事業を推進するに当たって力を入れた点

辻特任講師が赴任し、Harvardで行っていた研究を継続発展させるために金銭的、人的支援を積極的に行い、可及的早期に辻講師の研究が軌道に乗るように配慮している。また研究設備の確保として、GCOEのコモンラボを共有することになった。さらにHarvard Dentalとの共同研究を推進するために倫理委員会に申請したうえで手術時の廃棄試料を採取することを開始している。

6. 英文原著論文

Asano H, Muneta T.
Stiffness of soft tissue complex in total knee arthroplasty.
Knee Surg Sports Traumatol Arthropsc 2008 Jan;16（1）:51-5.

Watanabe T, Muneta T, Ikeda H, Tateishi T, Sekiya I
Visual analog scale assessment after medial patellofemoral ligament reconstruction: with or without tibial tubercle transfer
J Orthop Sci. 2008 Jan;13（1）:32-8.

◎Horie M, Sekiya I, Muneta T, Murakami T, Kobayashi E.
Establishment of mesenchymal stem cells derivedfrom bone marrow and synovium of transgenic rats expressing dual reporter genes. Progress in Biomedical Optics and Imaging.
Vol.9, No27, 2008

Hara K, Niga S, Ikeda H, Cho S, Muneta T
Isolated anterior cruciate ligament reconstruction in patients with chronic anterior cruciate ligament insufficiency combined with grade II valgus laxity
Am J Sports Med. 2008 Feb;36（2）:333-9.

◎Nimura A, Muneta T, Koga H, Mochizuki T, Suzuki K, Makino H, Umezawa A, Sekiya I
Increased proliferation of human synovial mesenchymal stem cells with autologous human serum: comparisons with bone marrow mesenchymal stem cells and with fetal bovine serum
Arthritis Rheum. 2008 Feb;58（2）:501-10.

◎Nagese T, Muneta T, Ju YJ, Hara K, Morito T, Koga H, Nimura A, Mochizuki T, Sekiya I
Analysis of the chondrogenic potential of human synovial stem cells according to harvest site and culture parameters in knees with medial compartment osteoarthritis.
Arthritis Rheum. 2008 May;58（5）:1389-98.

Mochizuki T, Sugaya H, Uomizu M, Maeda K, Matsuki K, Sekiya I, Muneta T, Akita K.
Humeral insertion of the supraspinatus and infraspinatus. New anatomical findings regarding the footprint of the rotator cuff.
J Bone Joint Surg Am. 2008 May;90（5）:962-9.

◎Toita S, Hasegawa U, Koga H, Sekiya I, Muneta T,

Akiyoshi K
Protein-conjugated quantum dots effectively delivered into living cells by a cationic nanogel.
J Nanosci Nanotechnol. 2008 May;8 (5) :2279-85. （秋吉教室）

◎Ju YJ, Muneta T, Yoshimura H, Koga H, Sekiya I
Synovial mesenchymal stem cells accelerate early remodeling of tendon-bone healing
Cell Tissue Res 2008 Jun;332（3）:469-78.

◎Morito T, Muneta T, Hara K, Ju YJ, Mochizuki T, Makino H, Umezawa A, Sekiya I
Synovial fluid-derived mesenchymal stem cells increase after intra-articular ligament injury in humans
Rheumatology（Oxford）. 2008 Aug;47（8）:1137-43.

◎Koga H, Muneta T, Nagase T, Nimura A, Ju YJ, Mochizuki T, Sekiya I
Comparison of mesenchymal tissues-derived stem cells for in vivo chondrogenesis: suitable conditions for cell therapy of cartilage defects in rabbit.
Cell Tissue Res. 2008 Aug;333（2）:207-15.

◎Zhang S, Muneta T, Morito T, Mochizuki T, Sekiya I
Autologous synovial fluid enhances migration of mesenchymal stem cells from synovium of osteoarthritis patients in tissue culture system
J Orthop Res. 2008 Oct;26（10）:1413-8.

Asano H, Muneta T, Sekiya I
Knee Surg Sports Traumatol Arthrosc. 2008 Nov;16（11）:999-1003. Epub 2008 Aug 30
Soft tissue tension in extension in total knee arthroplasty affects postoperative knee extension and stability.
Knee Surg Sports Traumatol Arthrosc. 2008 Nov;16（11）:999-1003.

◎Tang T, Muneta T, Ju YJ, Nimura A, Miyazaki K, Masuda H, Mochizuki T, Sekiya I
Serum keratan sulfate transiently increases in the early stage of osteoarthritis during strenuous running of rats: protective effect of intraarticular hyaluronan injection
Arthritis Res Ther. 2008;10（1）:R13.

◎Koga H, Shimaya M, Muneta T, Nimura A, Morito T, Hayashi M, Suzuki S, Ju YJ, Mochizuki T, Sekiya I
Local adherent technique for transplanting mesenchymal stem cells as a potential treatment of cartilage defect
Arthritis Res Ther. 2008;10（4）:R84.

◎Segawa Y, Muneta T, Makino H, Nimura A, Mochizuki T, Ju YJ, Ezura Y, Umezawa A, Sekiya I
Mesenchymal stem cells derived from synovium, meniscus, anterior cruciate ligament, and articular chondrocytes share similar gene expression profiles.
J Orthop Res. 2008 Oct 30. [Epub ahead of print]

◎Hayashi M, Muneta T, Ju YJ, Mochizuki T, Sekiya I
Weekly intra-articular injections of bone morphogenetic protein-7 inhibits osteoarthritis progression.
Arthritis Res Ther. 2008;10（5）:R118. Epub 2008 Sep 30.

◎Sekiya I, Tang T, Hayashi M, Morito T, Ju YJ, Mochizuki T, Muneta T
Periodic knee injections of BMP-7 delay cartilage degeneration induced by excessive running in rats.
J Orthop Res. 2009 Jan 23. [Epub ahead of print]

Seko Y, Azuma N, Takahashi Y, Makino H, Morito T, Muneta T, Matsumoto K, Saito H, Sekiya I, Umezawa A
Human sclera maintains common characteristics with cartilage throughout evolution
PLoS ONE. 2008;3（11）:e3709. Epub 2008 Nov 12.

7. 著書

宗田　大
　変形性膝関節症の画像診断。下肢荷重関節の最新画像診断。
　関節外科27:724-732、2008

宗田　大
　症例問題トレーニング　膝・足関節・足疾患。
　整形外科59:1266-1275,2008

関矢一郎、宗田大
　関節液中の幹細胞
　関節外科　p. 240-242, vol. 28, No. 2, 2009年

関矢一郎、宗田大
　滑膜幹細胞を用いる低侵襲な軟骨再生医療の開発
　臨床雑誌　整形外科 p.1584, vol 59, No. 13, 2008年

関矢一郎、宗田大
　ヒト滑膜間葉幹細胞
　リウマチ科 p. 80-85, vol 41, No. 1, 2009年

関矢一郎
　骨折
　「病期・病態・重症度からみた疾患別看護過程＋病態関連図 」
　井上智子・佐藤千史編集（著）p.1436-1441　2008

関矢一郎、宗田大
　変形性膝関節症
　「病期・病態・重症度からみた疾患別看護過程＋病態関連図 」

井上智子・佐藤千史編集（著）p.1501-1505　2008
柳下和慶、山見信夫、外川誠一郎、宗田大、四宮謙一、眞野喜洋.
足関節捻挫に対する高気圧酸素療法の有効性.日本整形外科スポーツ医学会誌 Vol.27（4）:351-355, 2008.
張　禎浩、星野明穂、池田浩夫、岩澤大輔、古賀英之、山賀美芽、関　芳衛
Scopio NRG人工膝関節の短期成績
日本人工関節学会誌　2008, 38:442-443
望月智之,山口久美子,秋田恵一、新井隆三、菅谷啓之,吉村英哉
棘上筋と棘下筋の上腕骨停止部について-組織学的検討-.
肩関節,2008, 32:493-496
望月智之,山口久美子,秋田恵一、菅谷啓之,中川照彦、宗田　大
棘下筋腱の肉眼解剖および組織学的研究
-delaminationの発生部位の検討-.
肩関節,2008, 32:497-500
吉村英哉、望月智之、新井隆三、菅谷啓之、二村昭元、宗田　大、秋田恵一
棘上筋から棘下筋に向かう表層線維の研究
肩関節,2008, 32:501-503
二村昭元、宗田　大、望月智之、山口久美子、秋田恵一、菅谷啓之、中川照彦
棘上筋と棘下筋の上腕骨停止部について-Footprintの計測-.
肩関節,2008, 32:229-232
清水　禎則、立石　智彦、長瀬　寅、朝比奈　信太郎、長谷川　清一郎、土屋　正光
フォンダパリヌクスナトリウム投与による人工膝関節置換術後の深部静脈血栓症の発症抑制効果に関する検討
日本人工関節学会誌2008, 38: 656-7
榊　経平、渡邊　敏文、石突　正文、宗田　大
高度変形を伴う膝蓋大腿関節症の1例
日本人工関節学会誌　38:336-337,2008
三宅　論彦、渡邊　敏文、石突　正文、宗田　大
外傷性膝関節脱臼の3例
整形・災害外科　51（8）:1089-1094, 2008

8. 特許取得、特許申請

特許申請
知的財産の内容:人体模型
発明者:秋田恵一、望月智之
権利者:秋田恵一、望月智之
種類:人体模型
番号:特願　2008-283656
出願年月日:平成20年11月28日

9. 平成21年3月までの自己評価

有能な国際シャペロンを教室に迎え、シャペロンの持ち帰った技術と国際連携により今後関節傷害・障害のメカニズムや治療法に対して飛躍的な進歩が期待できる。さらに豊富な手術件数に裏打ちされた臨床材料を用いた国際共同研究が長期間にわたり発展することが見込まれる。赴任後4ヶ月の実績として十分な研究基盤を築きつつある。

10. 和文原著論文

宗田　大
変形性膝関節症の画像診断。下肢荷重関節の最新画像診断。
関節外科27:724-732、2008
宗田　大
症例問題トレーニング　膝・足関節・足疾患。
整形外科59:1266-1275,2008
関矢一郎、宗田大
滑膜幹細胞を用いる低侵襲な軟骨再生医療の開発
臨床雑誌　整形外科 p.1584, vol 59, No. 13, 2008年
関矢一郎
骨折
「病期・病態・重症度からみた疾患別看護過程＋病態関連図 」
井上智子・佐藤千史編集（著）p.1436-1441　2008
関矢一郎、宗田大
変形性膝関節症
「病期・病態・重症度からみた疾患別看護過程＋病態関連図 」
井上智子・佐藤千史編集（著）p.1501-1505　2008
柳下和慶、山見信夫、外川誠一郎、宗田大、四宮謙一、眞野喜洋.
足関節捻挫に対する高気圧酸素療法の有効性.日本整形外科スポーツ医学会誌 Vol.27（4）:351-355, 2008.
張　禎浩、星野明穂、池田浩夫、岩澤大輔、古賀英之、山賀美芽、関　芳衛
Scopio NRG人工膝関節の短期成績
日本人工関節学会誌　2008, 38:442-443
望月智之,山口久美子,秋田恵一、新井隆三、菅谷啓之,吉村英哉

棘上筋と棘下筋の上腕骨停止部について-組織学的検討-. 肩関節,2008, 32:493-496

望月智之,山口久美子,秋田恵一、菅谷啓之,中川照彦、宗田　大

棘下筋腱の肉眼解剖および組織学的研究
-delaminationの発生部位の検討-.
肩関節,2008, 32:497-500

吉村英哉、望月智之、新井隆三、菅谷啓之、二村昭元、宗田　大、秋田恵一

棘上筋から棘下筋に向かう表層線維の研究
肩関節,2008, 32:501-503

二村昭元、宗田　大、望月智之、山口久美子、秋田恵一、菅谷啓之、中川照彦

棘上筋と棘下筋の上腕骨停止部について-Footprintの計測-.
肩関節,2008, 32:229-232

清水　禎則、立石　智彦、長瀬　寅、朝比奈　信太郎、長谷川　清一郎、土屋　正光

フォンダパリヌクスナトリウム投与による人工膝関節置換術後の深部静脈血栓症の発症抑制効果に関する検討
日本人工関節学会誌2008, 38: 656-7

榊　経平、渡邊　敏文、石突　正文、宗田　大

高度変形を伴う膝蓋大腿関節症の1例
日本人工関節学会誌　38:336-337,2008

三宅　論彦、渡邊　敏文、石突　正文、宗田　大

外傷性膝関節脱臼の3例
整形・災害外科　51（8）:1089-1094, 2008

11. 学会発表（英文）

Horie M, Muneta T, Sekiya I, Kobayashi E
Establishment of mesenchymal stem cells derived from bone marrow and synovium of transgenic rats expressing dual reporter genes.
Photonics West 2008, San Jose, California, U.S.A. 2008.1.22-24

Koga H, Muneta T, Sekiya I
Comparison of Mesenchymal Stem Cells for In Vivo Chondrogenesis and Optimal Conditions of Cell Therapy for Rabbit Cartilage Defects
54th Annual Meeting Orthopaedic Research Society, San Francisco. USA. 2008.3.2-5

Koga H, Muneta T, Sekiya I
Newly-developed Implantation Procedure with Synovium-derived Mesenchymal Stem Cells for Cartilage Regeneration
54th Annual Meeting Orthopaedic Research Society, San Francisco. USA. 2008.3.2-5

Hayashi M, Sekiya I, Muneta T
Bone morphogenetic protein-7 inhibits osteoarthritis progression in a rabbit model
54th Annual Meeting Orthopaedic Research Society, San Francisco. USA. 2008.3.2-5

Ju YJ, Muneta T, Sekiya I, Yagishita K, Hara K, Yamazaki J, Shinomiya K
Serum keratan sulfate concentration in the anterior cruciate ligament injured patients.
5th World Congress of Sports Trauma & 6th Asia-Pacific Orthopaedic Society for Sports Medicine Meeting, Hong Kong. 2008.4.11-13.

Yamazaki J, Muneta T,Sekiya I, Ju YJ, Hara K
Differences in the Kinematics of Single Leg Squatting for Patients with an Injured Anterior Cruciate Ligament Evaluated Using an Electromagnetic Device
5th World Congress of Sports Trauma & 6th Asia-Pacific Orthopaedic Society for Sports Medicine Meeting, Hong Kong. 2008.4.11-13.

Watanabe T, Muneta T, Ishizuki M
A Comparison between Mini and Conventional Total Knee Arthroplasty
in the Early Stage after Surgery
13th ESSKA ,Porto, Portugal. 2008.5.21-24

Yamazaki J, Muneta T,Sekiya I, Ju YJ, Hara K
ACL injury mechanism of Anterior Cruciate Ligament Injured Patients
6th Biennial ISAKOS（ International Society of Arthroscopy, Knee Surgery and Orthopaedic Sports Medicine）Congress. Florence, Italy. 2007.5.27-31

Hayashi M, Muneta T, Sekiya I
Weekly intraarticular injections of BMP-7 inhibit osteoarthritis progression
7th International Conference on Bone Morphogenetic Proteins, Lake Tahoe, USA. 2008.7.9-13

Yagishita K, Yamami N, Togawa S, Muneta T, Shinomiya K, Mano Y. The effect of hyperbaric oxygen therapy on patients with ankle sprain. European Underwater and Baromedical Society（EUBS）Graz, Austria. 2008.9.4.

Yagishita K, Yamami N, Togawa S, Mano Y. HBO in Tokyo Medical and Dental University in 2007 and The Effects of HBO on Soft Tissue Injury in Sports Activity. Intermational

Congress on Hyperbaric Medicine（ICHM）Peking, China. 2008.10.27.

Yagishita K, Mano Y, Yamami N, Togawa S. Hyperbaric Oxygen Therapy in Tokyo Medical and Dental University Hospital. Third Conference of U.S.-Japan Panel on Aerospace-Diving Physiology & Technology, and Hyperbaric Medicine.（UJNR）Nakatsu, Japan. 2008.11.7.

12. 学会発表（和文）

柳下和慶、山見信夫、外川誠一郎、関矢一郎、朱寧進、原憲司、山崎順也、眞野喜洋、四宮謙一、宗田大.
　当院における人工関節置換術術後感染に対する高気圧酸素療法.第38回第38回日本人工関節学会　沖縄　2008.2.29.

張　禎浩、星野明穂、池田浩夫、岩澤大輔、古賀英之、山賀美芽、関　芳衛
　Scorpio NRG人工膝関節の短期成績
　第38回人工関節学会　沖縄　2008.2.29-3.1

浅野浩司
　人工膝関節置換術後の可動域に対側膝が与える影響
　第38回人工関節学会　沖縄　2008.2.29-3.1

渡邊　敏文 、宗田　大、石突正文
　人工膝関節置換術において術前の大腿骨脛骨角が骨切除量および関節gapに与える影響
　第38回人工関節学会　沖縄　2008.2.29-3.1

清水　禎則、立石　智彦、長瀬　寅、朝比奈　信太郎、長谷川　清一郎、土屋　正光
　フォンダパリヌクスナトリウム投与による人工膝関節置換術後の深部静脈血栓症の発症抑制効果に関する検討
　第38回人工関節学会　沖縄　2008.2.29-3.1

榊　経平、渡邊　敏文、石突　正文、宗田　大
　高度変形を伴う膝蓋大腿関節症の1例
　第38回人工関節学会　沖縄　2008.2.29-3.1

林将也、宗田大、関矢一郎
　BMP-7の週一回関節内投与はウサギ変形性膝関節症モデルにおける軟骨変性を抑制する
　第21回日本軟骨代謝学会　京都　2008.3.21-22.

池田　浩夫、張　禎浩、岩澤　大輔、古賀　英之、山賀　美芽、関　芳衛、長束　裕、星野　明穂、仁賀　定雄
　多重折り膝屈筋腱を用いた前十字靱帯再建術において移植腱の走行角度の変化が臨床成績に及ぼす影響について
　第81回日本整形外科学会学術総会　札幌　2008.5.22-26

柳下和慶、山見信夫、外川誠一郎、宗田大、四宮謙一、眞野喜洋.
　スポーツ軟部外傷に対する高気圧酸素療法.
　第81回日本整形外科学会学術総会　札幌　2008.5.22-26

張　禎浩、星野明穂、池田浩夫、岩澤大輔、古賀英之、山賀美芽、関　芳衛
　Interax ISA 人工膝関節の中期成績
　第81回日本整形外科学会学術総会　札幌　2008.5.22-26

山崎順也、宗田大、関矢一郎、朱寧進、原憲司、柳下和慶
　ACL損傷術前患者に対し施行した片脚スクワット動作の3次元動作解析結果
　第81回日本整形外科学会学術総会 札幌　2008 5.22-25

山崎順也、宗田大、関矢一郎、朱寧進、原憲司、柳下和慶
　女性ACL損傷患者の関節弛緩性と臼蓋形成不全
　第81回日本整形外科学会学術総会 札幌　2008 5.22-25

池田　浩夫、張　禎浩、岩澤　大輔、古賀　英之、山賀　美芽、関　芳衛、仁賀　定雄
　足関節鏡手術の適応と成績
　Combined Congress of JOSKAS 東京　2008.6.13-14

関矢一郎
　軟骨損傷に対する鏡視下滑膜幹細胞移植術
　Combined Congress of JOSKAS 東京　2008.6.13-14

柳下和慶、宗田大、関矢一郎、朱寧進、原憲司、山崎順也.
　損傷半月板に治癒能力はあるか.前十字靱帯再建膝における損傷半月板無処置例での検討.
　Combined Congress of JOSKAS 東京　2008.6.13-14

張　禎浩、星野明穂、池田浩夫、岩澤大輔、古賀英之、山賀美芽、関　芳衛
　人工膝関節置換術を施行した骨Paget病の一例
　Combined Congress of JOSKAS 東京　2008.6.13-14

浅野浩司
　FasT-fixを用いた半月板縫合術の問題点（糸のスライディングについて）
　Combined Congress of JOSKAS 東京　2008.6.13-14

渡邊　敏文、宗田　大、石突　正文
　人工膝関節置換術後の膝関節屈曲可動域と歩行能力との関係
　Combined Congress of JOSKAS 東京　2008.6.13-14

朱　寧進、関矢　一郎、柳下　和慶、原　憲司、山崎順也、四宮　謙一、宗田　大
スポーツ種目別にみた膝前十字靭帯再建術の術後成績
Combined Congress of JOSKAS 東京　2008.6.13-14
朱　寧進、関矢　一郎、柳下　和慶、原　憲司、山崎順也、四宮　謙一、宗田　大
鏡視下膝前十字靭帯再建術の長期成績
Combined Congress of JOSKAS 東京　2008.6.13-14
山崎順也、宗田大、関矢一郎、朱寧進、原憲司、柳下和慶
女性ACL損傷患者の受傷機転及び臼蓋形成不全との関連
Combined Congress of JOSKAS札幌　2007.6.14-16
八木茂典
下腿のスポーツ外傷・障害　シンスプリントの重症度評価
Combined Congress of JOSKAS 東京　2008.6.13-14
星野明穂、池田浩夫、吉村英哉、岩澤大輔、中川裕介
当院におけるTKAの実際
川口医師会学術集会 川口　2008.6.14
柳下和慶、関矢一郎、朱寧進、望月智之、原憲司、山崎順也、宗田大.
足関節捻挫に対する高気圧酸素治療.早期競技復帰に向けて.
第33回日本足の外科学会　東京　2008.6.20.
清水　禎則、立石　智彦、新井　嘉容、長瀬　寅、朝比奈　信太郎、中川　照彦、土屋　正光
大相撲力士の頚椎外傷・障害の検討
日本整形外科スポーツ医学会　東京　2008.7.4-5
朱　寧進、宗田　大、古賀　英之、関矢　一郎
滑膜由来の間葉系幹細胞はコラーゲンを産生することにより移植腱骨孔治癒を促進させる
第23回日本整形外科基礎学術集会　京都　2008.10.23
林将也、関矢一郎、望月智之、朱寧進、四宮謙一、宗田大
週1回のBMP-7関節内注射は変形性膝関節症の進行を抑制する
第23回日本整形外科基礎学術集会　京都　2008.10.23-24
瀬川裕子、関矢一郎、二村昭元、望月智之、朱寧進、四宮謙一、宗田大
関節内組織由来の間葉幹細胞は類似する遺伝子プロファイルを示す
第23回日本整形外科基礎学術集会　京都　2008.10.23-24
清水　禎則、立石　智彦、長瀬　寅、本杉　直哉、朝比奈　信太郎、中川　照彦、土屋　正光
ACL再建術における体重と手術時間との相関に関する検討
第19回日本臨床スポーツ医学会　千葉　2008.11.1-2
八木茂典
陸上競技選手における脛骨疲労骨折、シンスプリント、コンパートメント症候群の発生率と発生要因に関する前向き研究
第19回日本臨床スポーツ医学会　千葉　2008.11.1-2
山崎順也、宗田大、関矢一郎、朱寧進、原憲司、柳下和慶
ACL損傷術前患者に対し施行した片脚スクワット動作の3次元動作解析結果
第35回日本臨床バイオメカニクス学会学術集会 大阪　2008,11,14-15

13. 受賞

古賀英之　東京医科歯科大学医師会賞

14. 外部資金の獲得状況

（科学研究費補助金、受託研究費、外部財団の助成など）

科学研究費補助金　基盤研究（C）.
関節軟骨欠損に対する自己血清を用いた骨髄幹細胞移植法と滑膜幹細胞移植法の比較
代表:宗田　大
期間:平成19年―平成20年
研究費総額:350万円
科学研究費補助金　基盤研究（C）.
供給源が異なる間葉幹細胞の特性解析とその軟骨再生への応用.
代表:関矢一郎
期間:平成18年―平成19年
研究費総額:3,500　千円

15. 特別講演、招待講演

Muneta T
Revision after Double Bundle ACL Reconstruction
13th ESSKA 2008 Congress　Symposium: ACL Revision Surgery 2008.5.21 in Porto

Muneta T
Review of Double-Bundle ACL Reconstruction in ICL 10

Double-bundle ACL reconstruction May 22, ESSKA 2008 in Porto

Muneta T

MPFL reconstruction

5th WCST in Hong Kong 2008. 4.11　President　Chan KM

関矢一郎

Cartilage Regeneration by Transplantation of Synovial Mesenchymal Stem Cells with Low Invasive Technique

Seminar at Orthopaedics, Dongguk University

Seoul, Korea　2008年2月21日

関矢一郎

In Vitro and in Vivo Chondrogenesis of Synovial Mesenchymal Stem Cells

The winter meeting of the Korean Society for OA and Cartilage Research 2009

Seoul, Korea　2008年2月22日

関矢一郎

Arthroscopic Transplantation of Synovial Stem Cells into Cartilage Defect

Seminar at Orthopaedic Surgery, Stanford University

Stanford, CA、USA　2008年3月10日

関矢一郎

Synovial Fluid-derived Stem Cells Increase After Anterior Cruciate Ligament Injury in Humans Seminar at Orthopaedic Surgery, University of California-Davis

Sacramento, CA, USA　2008年3月11日

関矢一郎

Applications of Synovial Mesenchymal Stem Cells for Joint Injuries

Seminar at Orthopaedic Surgery, University of California-Irvine

Otange, CA, USA　2008年3月13日

関矢一郎

Arthroscopic Transplantation of Synovial Stem Cells into Cartilage Defect

Seminar at Orthopaedic Surgery, Oregon Health and Science University

Portland, OR, USA　2008年3月16日

関矢一郎

Applications of Synovial Mesenchymal Stem Cells for Joint Injuries

Seminar at Orthopaedic Surgery, University of New Mexico

Albuquerque, NM, USA　2008年3月19日

関矢一郎

Arthroscopic Transplantation of Synovial Stem Cells into Cartilage Defect

Seminar at Orthopaedic Surgery, Texas Tech University-Lubbock

Lubbock, TX, USA　2008年3月21日

関矢一郎

Applications of Synovial Mesenchymal Stem Cells for Joint Injuries

Seminar at Orthopaedic Surgery, University of Texas-Houston

Houston, TX, USA　2008年3月24日

関矢一郎

Arthroscopic Transplantation of Synovial Stem Cells into Cartilage Defect

International BMP Conference

Lake Tahoe, CA, USA　2008年7月11日

関矢一郎

Arthroscopic Transplantation of Synovial Stem Cells into Cartilage Defect

Seminar at Center for Gene therapy, Tulane University

New Orleans, LA, USA　2008年7月24日

関矢一郎

Cartilage Regeneration Using Synovial Stem Cells by Arthroscopic Technique

Seminar at Institute of Regenerative Medicine, Texas A&M University

Temple, TX, USA　2008年9月29日

関矢一郎

Arthroscopic transplantation of synovial stem cells into cartilage defect

Seminar at Orthopaedic Surgery, Scot & White Hospital

Temple, TX, USA　2008年9月30日

宗田　大

小児の膝疾患

第24回九州小児整形外科集談会。2008.1.19　九州大学西新プラザ。会長　津村　弘

宗田　大

シンポジウム　「軟骨の再生」 滑膜間葉幹細胞を用いた低侵襲手技による関節軟骨の修復

第7回日本再生医療学会　2008.3.13

名古屋大学　上田稔

宗田　大

「難治性軟骨性病変に対する新しい再生治療法」滑膜細胞由来間葉系幹細胞を用いた関節症に対する軟骨治療

第15回日本軟骨代謝学会　2008.3.22

京都大学　中村孝志　教授

宗田　大

診療ガイドラインからみた前十字靭帯損傷と今後の課題。

第110回中部整形災害外科学会（びわこセミナー）会長　松末吉隆

宗田　大

NHK　きょうの健康「ひざの痛み」。

2008.3.31-4.2;4.4

宗田　大

膝痛の治療。

厚木整形外科医会学術講演会2008.5.15

宗田　大

2重束ACL再建術の変遷と問題点

第5回横浜・横須賀Knee Frontier。代表世話人　齋藤知行　教授　2008.6.5

宗田　大

ACL損傷と私。

JOSKAS 2008　会長講演　2008.6.14

宗田　大

NHK　名医にQ「膝の痛み」

2008.7.19、7.26

宗田　大

変形性膝関節症の治療―EBMとその裏側―　モーラスパップ30mg発売20周年記念講演会。ホテルグランヴィア大阪　2008.7.19　座長　吉川秀樹　教授

宗田　大

「ラジオあさいちばん」「健康ライフ」コーナー出演

NHKラジオ　濱中博久さん、遠田恵子キャスター

5回シリーズ放送10.27-10.31 「膝を大切に～大事に長持ちさせる～」

宗田　大

腱・靭帯付着部症の基礎と臨床。第23回日本整形外科学会基礎学術集会

大仏セミナー　2008.10.23　奈良医科大学

宗田　大

良くある問題の現場での治療と予防。

チームドクター研修会　2008.10.31　東京ベイ幕張ホール。早稲田大学　福林　徹会長

池田　浩夫

運動と外傷―骨・関節の外傷―

日本医師会認定健康スポーツ医学講習会2008.10.19

関矢一郎

滑膜細胞による低侵襲な軟骨再生医療の開発

全国医学系大学倫理審査委員会連絡会議

東京　2008年1月26日

関矢一郎

滑膜細胞による低侵襲な軟骨再生

東京医科歯科大学整形外科シンポジウム・第13回COEシンポジウム

東京　2008年2月7日

関矢一郎

膝関節障害の知識

第268回　葛飾区整形外科集談会

東京　2008年4月8日

関矢一郎

Arthroscopic Transplantation of Synovial Stem Cells into Cartilage Defect

International BMP Conference

Lake Tahoe, CA, USA　2008年7月11日

関矢一郎

滑膜幹細胞と関節内組織修復

膝と歩む会

東京　2008年7月14日

関矢一郎

間葉幹細胞と再生医療

関節鏡セミナー

鎌倉　2008年8月22日

関矢一郎

滑膜幹細胞を用いる鏡視下軟骨再生治療

西多摩整形医学会

立川　2008年9月4日

関矢一郎

鏡視下で可能な軟骨損傷に対する滑膜幹細胞移植術

日本整形外科基礎学会

京都　2008年10月23日

関矢一郎

膝の痛みとその対処法

慈愛会健康医学講座

文京区　2008年11月29日

関矢一郎

軟骨損傷に対する鏡視下滑膜幹細胞移植術の再鏡視像

お茶の水 膝スポーツ懇話会

文京区　2008年12月4日

関矢一郎

ACL再建:移植腱治癒の促進に向けて臨床応用への試み

膝関節フォーラム

新宿区　2008年12月6日

柳下和慶

スポーツ軟部外傷に対する高気圧酸素療法について.

埼玉整形外科研究会（日本整形外科学会教育研修講演認定）さいたま　2008.7.12.

柳下和慶

高気圧酸素治療とスポーツ軟部外傷に対する適応お

よび現況.日本臨床スポーツ医学会（日本整形外科学会教育研修講演認定）幕張　2008.11.2.

張　禎浩

RA治療における生物学的製剤の役割

川口リウマチの集い 2008.6.24.

渡邊　敏文、河内　敏行、石突　正文

大腿骨頚部骨折における地域医療連携パスの試み

～第2報～

第28回御茶ノ水セミナー 東京 2008.10.18

八木茂典

肩のリハビリテーション（水泳肩を中心に）

平成19年度日本体育協会公認アスレティックトレーナー研修会　東京　2008.1.12

八木茂典

水泳のアスレティックリハビリテーション

投球障害肩へのアスレティックリハビリテーション

肩関節前方脱臼へのアスレティックリハビリテーション

肘MCL損傷へのアスレティックリハビリテーション

腰部疾患へのアスレティックリハビリテーション

扁平足障害（過回内足障害）へのアスレティックリハビリテーション

脛骨過労性骨障害へのアスレティックリハビリテーション

花田学園　東京　2008（通年）

八木茂典

トップアスリートに必要なコンディショニング

東京都スポーツ文化事業団,東京都水泳協会　東京　2008.12.23

16. 主催学会

Combined Congress of JOSKAS 東京　2008.6.13-14

17. 新聞、雑誌、TV報道

毎日新聞　2008.12.28 「ひざ半月板　再生に道」

18. 講座の准教授、講師、助教、特別研究員、ポスドク、指導を受けた大学院生の名前（AISSには○印）のリスト

准教授　関矢一郎（軟骨再生学）

講　師　辻　邦和（GCOE国際シャペロン）

助　教　朱　寧進

望月智之（軟骨再生学）

医　員　原　憲司

森戸俊行

大学院生

4年　山崎順也、平澤直之、浅野　浩司、渡邊敏文、瀬川裕子、立石智彦、林　将也

3年　島谷雅之、堀江雅史

2年　高橋　徹、中村智祐、宮本　崇、八木茂典

1年　山賀美芽、鈴木志郎

Mesenchymal Stem Cells Derived from Synovium, Meniscus, Anterior Cruciate Ligament, and Articular Chondrocytes Share Similar Gene Expression Profiles

Yuko Segawa,[1] Takeshi Muneta,[1,2] Hatsune Makino,[3] Akimoto Nimura,[1] Tomoyuki Mochizuki,[4] Young-Jin Ju,[1] Yoichi Ezura,[5] Akihiro Umezawa,[3] Ichiro Sekiya[4]

[1]Section of Orthopedic Surgery, Tokyo Medical and Dental University, 1-5-45 Yushima, Bunkyo-ku, Tokyo, 113-8519 Japan, [2]Global Center of Excellence Program, International Research Center for Molecular Science in Tooth and Bone Diseases, Tokyo Medical and Dental University, Tokyo, Japan, [3]Department of Reproductive Biology, National Institute for Child Health and Development, Tokyo, Japan, [4]Section of Cartilage Regeneration, Tokyo Medical and Dental University, Tokyo, Japan, [5]Department of Molecular Pharmacology, Medical Research Institute, Tokyo Medical and Dental University, Tokyo, Japan

Received 9 May 2008; accepted 5 September 2008
Published online ? ? ? ? in Wiley InterScience (www.interscience.wiley.com). DOI 10.1002/jor.20786

ABSTRACT: Mesenchymal stem cells (MSCs) can be obtained from various tissues, and contain common features. However, an increasing number of reports have described variant properties dependent of cell sources. We examined (1) whether MSCs existed in several intraarticular tissues, (2) whether gene expression profiles in intraarticular tissue MSCs closely resembled each other, and (3) whether identified genes were specific to intraarticular tissue MSCs. Human synovium, meniscus, intraarticular ligament, muscle, adipose tissue, and bone marrow were harvested, and colony-forming cells were analyzed. All these cells showed multipotentiality and surface markers typical of MSCs. Gene profiles of intraarticular tissue MSCs and chondrocytes were closer to each other than those of extraarticular tissues MSCs. Among three characteristic genes specific for intraarticular tissue MSCs, we focused on proline arginine-rich end leucine-rich repeat protein (PRELP). Higher expression of PRELP was confirmed in chondrocytes and intraarticular tissue MSCs among three elderly and three young donors. Synovium MSCs stably expressed PRELP, contrarily, bone marrow MSCs increased PRELP expression during in vitro chondrogenesis. In conclusion, MSCs could be isolated from various intraarticular tissues including meniscus and ligament, gene expression profiles of intraarticular tissue MSCs closely resembled each other, and the higher expression of PRELP was characteristic of intraarticular tissue MSCs. © 2008 Orthopaedic Research Society. Published by Wiley Periodicals, Inc. J Orthop Res

Keywords: mesenchymal stem cells; intraarticular tissue MSCs; synovial stem cells; gene profile; proline arginine-rich end leucine-rich repeat protein (PRELP)

Mesenchymal stem cells (MSCs) are defined as being derived from mesenchymal tissue and by their functional capacity to self-renew and to generate a number of differentiated progeny.[1] These cells participate in tissue homoeostasis, remodeling and repair by ensuring replacement of mature cells that are lost during the course of physiological turnover, senescence, injury, or disease.[2] MSCs can be obtained from both intraarticular and extraarticular tissues. MSCs derived from various mesenchymal tissues contain common features,[3] but an increasing number of reports describe distinguishing properties dependent on their origin.[4–6]

During development of joints, the noncartilaginous region, known as the interzone, occurs across the locations of the prospective joints in long bone elements. The interzone cells produce hyaluronan and an enlarged cavity consisting of articular cartilage and synovium.[7] In knee joints, meniscus and cruciate ligaments are also formed by interzone cells.[8] The common origin of the intraarticular tissues made us speculate that MSCs should reside in every kind of intraarticular tissue, and those MSCs should maintain common features distinct from MSCs residing in other tissues.

Therefore, the purposes of this study were (1) to demonstrate the existence of MSCs in several intraarticular tissues, (2) to examine whether gene expression profiles in MSCs derived from intraarticular tissues were closer to each other than those of MSCs derived from extraarticular tissues, and (3) to identify gene expressions specific to the stem cells derived from intraarticular tissues. Better understanding of MSCs in the joint would be of great importance for the progression of therapies that target stem cells to enhance reparative responses, with the end goal of reestablishing a physiological joint homoeostasis.

Correspondence to: Ichiro Sekiya (T: +81-3-5803-4675; F: +81-3-5803-0266; E-mail: sekiya.orj@tmd.ac.jp)

© 2008 Orthopaedic Research Society. Published by Wiley Periodicals, Inc.

MATERIALS AND METHODS

Isolation of Colony-Forming Cells from Various Mesenchymal Tissues

The study was approved by the Institutional review board of Tokyo Medical and Dental University, and informed consents were obtained from all study subjects. Human synovium, meniscus, intraarticular ligament (anterior cruciate ligament), muscle, adipose tissue, and bone marrow were harvested during total knee arthroplasty from three donors diagnosed with knee osteoarthritis (all females, 65, 73, and 77 years old). Bone marrow was aspirated from the tibia. Synovium, meniscus, intraarticular ligament, muscle, and adipose tissue were minced, digested with 3 mg/mL collagenase (Type 5, Sigma-Aldrich, St. Louis, MO) for 3 h for synovium, muscle, and adipose tissue, and for 5 h for meniscus and ligament. Then the tissues were filtered with a 70-μm nylon filter (Becton-Dickinson, Franklin Lakes, NJ) to remove debris, and finally resuspended nucleated cells after centrifugation. Nucleated cells from bone marrow were isolated with Ficoll density gradient (Ficoll-Paque, Pharmacia Biosystems, Uppsala, Sweden).[3,6] Nucleated cells from synovium, meniscus, and ligament were plated at 10^3, 10^4, or 10^5 cells/60-cm^2 dish (Nalge Nunc International, Rochester, NY), those from

muscle, and bone marrow at 10^4, 10^5, or 10^6 cells/60-cm^2 dish and those from adipose tissue at 10^3, or 10^4 cells/60-cm^2 dish. The cells were plated in six dishes and cultured in 10 mL complete culture medium: αMEM containing 10% fetal bovine serum (Invitrogen, Carlsbad, CA), 100 units/mL penicillin (Invitrogen), 100 μg/mL streptomycin (Invitrogen), and 250 ng/mL amphotericin B (Invitrogen) for 14 days as passage 0. Three dishes for each cell concentration were stained with 0.5% crystal violet. The optimal initial cell density was determined based on the following criteria: (1) the colony size was not affected by contact inhibition, and (2) the greatest number of colonies was obtained. We then harvested the cells plated at optimal densities from the three remaining dishes and counted them to determine the number of cells at passage 0. Passage 0 cells were replated at 50 cells/cm^2 in a 145-cm^2 dish and cultured for 14 days for the differentiation assays. Human synovium and bone marrow were also harvested from three young donors (one female and two males; 14, 26, and 23 years old, respectively) during anterior cruciate ligament reconstruction.

Isolation of Chondrocytes

Femoral heads were harvested from two donors (90-year-old male and 85-year-old female) who undertook femoral head replacement for femoral neck fracture. Cartilage was digested with 3 mg/mL collagenase for 6 h. After filtration, nucleated cells were plated at 10^4 cells/60-cm^2 dish and cultured for 14 days.

In Vitro Differentiation

For chondrogenesis, 2×10^5 cells were placed in a 15-mL polypropylene tube (Becton Dickinson) and centrifuged at $450 \times g$ for 10 min. The pellets were cultured in 400 μL chondrogenic media that contained 1000 ng/mL bone morphogenetic protein 7 (Stryker Biotech, Boston, MA), 10 ng/mL transforming growth factor-β3 (R&D Systems, Minneapolis, MN), and 100 nM dexamethasone. For microscopy, the pellets were embedded in paraffin, cut into 5-μm sections, and stained with Toluidine Blue.[9]

For adipogenesis, the cells were cultured in complete culture medium supplemented with 100 nM dexamethasone, 0.5 mM isobutylmethylxanthine (Sigma-Aldrich), and 100 μM indomethacin (Wako) for 21 days. The dishes were fixed in 10% formalin for 5 min and stained with fresh Oil red-O solution for 3 h.[10]

For calcification, the cells were cultured in complete culture medium supplemented with 1 nM dexamethasone, 50 μg/mL ascorbic acid, and 10 mM β-glycerophosphate for 21 days. The dishes were stained with 40 mM Alizarin Red.[3]

Surface Epitopes

One million cells were suspended in 200 μL PBS containing 20 μg/mL of antibody, incubated for 30 min at 4°C, and resuspended in 1 mL of PBS. Fluorescein isothiocyanate (FITC)- or phycoerythrin (PE)-coupled antibodies against CD90, CD34, and CD45 were from Becton Dickinson; CD44 was from eBioscience (San Diego, CA); CD105 and CD166 were from Ancell Corporation (Bayport, MN). For the isotype control, FITC- or PE-coupled nonspecific mouse IgG (Becton Dickinson) was substituted for the primary antibody. Cell fluorescence was evaluated by FACSCalibur instrument (Becton Dickinson), and data were analyzed using CellQuest software (Becton Dickinson).[3–6]

DNA Microarray Analysis

Total RNA was prepared from passage 0 cells using TRIzol Reagent (Invitrogen). Human Genome U133 Plus 2.0 Array (GeneChip; Affymetrix, Santa Clara, CA) containing the oligonucleotide probe set for more than 47,000 transcripts was used. The fluorescence intensity of each probe was quantified by using the GeneChip Analysis Suite 5.0 computer program (Affymetrix). Further data analysis was performed with GeneSpring GX 7.3.1 (Agilent Technologies, Santa Clara, CA). To eliminate changes within the range of background noise and to select the most differentially expressed genes, data were used only if the raw data values were less than 50 AD and gene expression was judged to be present by the Affymetrix data analysis. Gene expression data were normalized in two ways: "per chip normalization" and "per gene normalization." To analyze the data, we used agglomerative hierarchical clustering and principal component analysis (PCA) using NIA Array Analysis Tools provided by the National Institute on Aging (Bethesda, MD).[11]

Reverse Transcriptase-PCR

RNA was converted to cDNA and amplified using the Titan One Tube RT-PCR System (Roche Diagnostics, Indianapolis, IN). The products were resolved by electrophoresis on a 1.5% agarose gel and visualized with ethidium bromide.[3,9,10,12] Primers for PRELP were 5′-AGCCAGAACCACATCTCCAG-3′ (forward) and 5′-GTCATGGAACGCCACTAGGT-3′ (reverse).

Real Time-PCR

Two micrograms of total RNA were reverse transcribed into first-strand cDNA with the PrimeScript RT reagent Kit (Takara Bio, Tokyo, Japan). Quantitative PCR analysis was conducted on a Thermal Cycler Dice TP800 (Takara Bio) using a SYBR Premix Ex Taq 2 Kit (Takara Bio) for 40 cycles with denaturation at 95°C for 5 s and annealing at 60°C for 30 s. Experimental samples were matched to a standard curve generated by amplifying serially diluted products using the same PCR protocol. The amounts of mRNA were shown as relative quantities in comparison to that of GAPDH mRNA. PCR primers were as follows: *OGN* 5′-ACTTGGACCATAATGCCCTGGA-3′ (forward), 5′-GTCAT TAGCCTTGCAGAATGTGTCA-3′ (reverse); *ECRG4* 5′-CCGTTGATGAGAATAAAGCCAAAG-3′ (forward), 5′-TCGATCTCTGTTAAGCCAATAGGTG-3′ (reverse); *GAPDH* 5′-GCACCGTCAAGGCTGAGAAC-3′ (forward), 5′-TGGTGAAGACGCCAGTGGA-3′ (reverse).

RNA Collection from Cartilage Pellets

Two million undifferentiated MSCs derived from synovium and bone marrow, and 10 pellets derived from both MSCs 1, 7, and 14 days after chondrogenic induction respectively were prepared for RNA collection. Pellets incubated for 7 days or longer were digested with 3 mg/mL collagenase for 3 h. Total RNA was extracted by using an RNAqueous Kit (Ambion, Austin, TX).

RESULTS

Characterization of Colony Forming Cells as MSCs

We first analyzed the colony forming capacity of various mesenchymal tissue-derived cells. When cells were plated at the same density, the numbers of developed colonies were much fewer in cells from muscle and bone marrow than in cells from other sources (Fig. 1A). The colony number increased when an increased number of

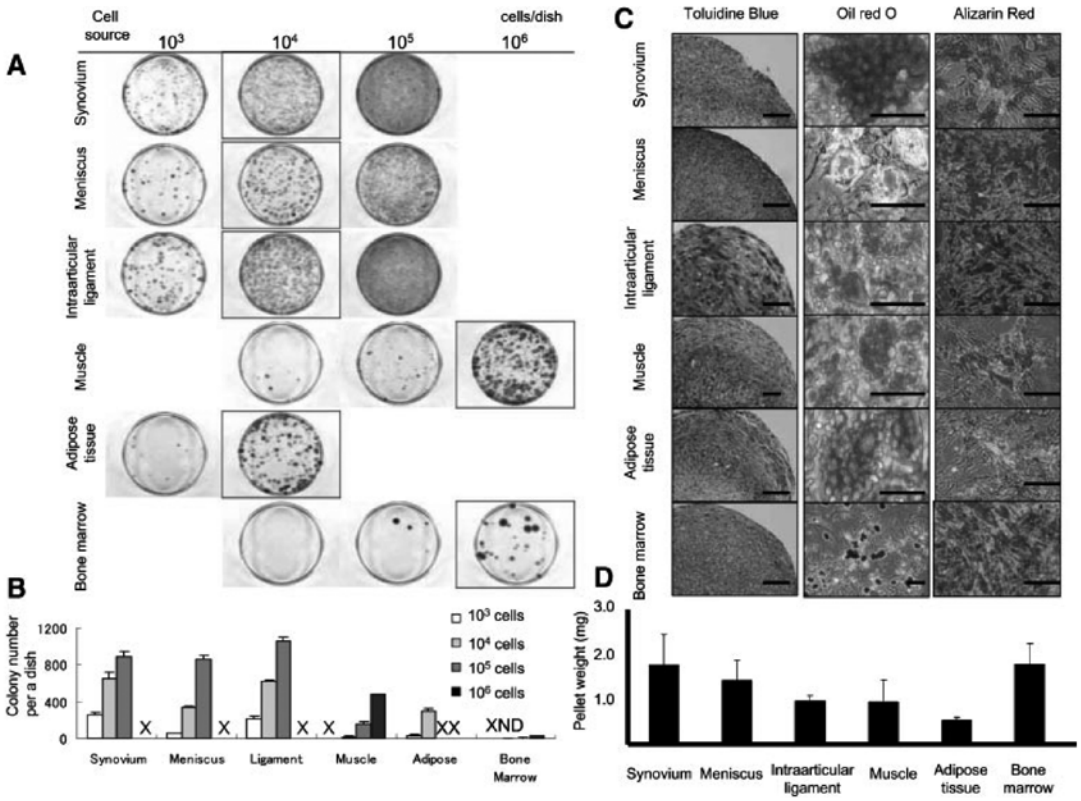

Figure 1. Properties of various mesenchymal tissue-derived cells as MSCs. (A) Colony formation of the cells at passage 0. Nucleated cells were plated at indicated cell number per 60cm^2-dish and cultured for 14 days. Culture dishes were stained with crystal violet. (B) Relation between initial nucleated cell number and colony number per dish (*ND* not detectable, *X* not examined). Values are shown as means ± SD ($n = 3$). (C) Multipotentiality of the cells. (Left) Chondrogenesis. Histological sections were stained with Toluidine Blue. Scale bar; 200 μm. (Center) Adipogenesis. The cells were stained with Oil Red-O. Scale bar; 50 μm. (Right) Osteogenesis. The cells were stained with Alizarin Red. Scale bar; 100 μm. (D) Average weight of pellets from six tissue sources. Average weight of three pellets was calculated for each source in each donor, and finally average weight of pellets from three donors was determined dependent of MSC sources. (E) Surface epitopes of the cells. Representative histograms are shown as open plot, and isotype control are shown as gray.

nucleated cells was plated (Fig. 1B). To avoid cell colony-to-cell colony contact inhibition, we determined that 10^4 cells per 60-cm^2 dish were the optimal initial cell density for synovium, meniscus, ligament, and adipose tissue, whereas 10^6 cells per 60-cm^2 dish were optimal for muscle and bone marrow. To examine whether the obtained colony forming cells had potential for multi-lineage differentiation, in vitro differentiation assays were applied to them. We confirmed that cells derived from each mesenchymal tissue differentiated into chondrocytes, adipocytes and calcified in vitro when cultured in the differentiation medium (Fig. 1C). To compare the chondrogenic potential of various mesenchymal tissue MSCs, a patient-matched quantitative analysis was performed.[6] All pellets from synovium and bone marrow were heavier than 1 mg, and pellets from adipose tissue were the lightest (Fig. 1D). We also tested whether these cells expressed surface antigen markers consistent with the assumption that these cells are the mesenchymal stem cells. Flow cytometric analysis demonstrated that each population of cells was negative for CD34, CD45, and positive for CD90, CD105, CD166, CD44 (Fig. 1E), confirming that the synovium-, meniscus-, ligament-, adipose tissue-, muscle-, and bone marrow-derived cells had characteristics of MSCs.

Profiling Gene Expression Analysis

RNAs were prepared from each population of MSCs at passage 0 derived from a common donor. RNAs were also prepared from chondrocytes derived from two other donors. Hierarchical clustering analysis revealed that synovium-, meniscus-, intraarticular ligament-derived MSCs, and chondrocytes were clustered into a group separated from the other clusters covering adipose tissue-, muscle-, and bone marrow-derived MSCs (Fig. 2A). PCA performed on the same gene sets also revealed that synovium, meniscus, intraarticular ligament MSCs, and chondrocytes could be clearly separated from the other populations of MSCs, as represented in the two-dimensional expression space (Fig. 2B). These findings indicate that synovium, meniscus, ligament MSCs, and chondrocytes, all of

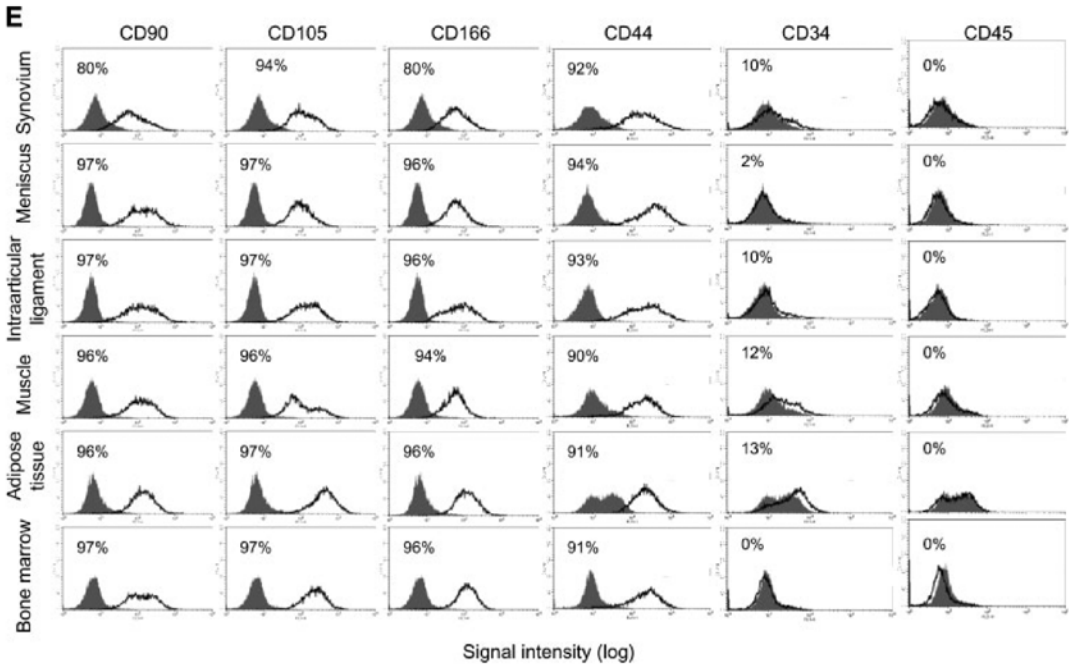

Figure 1. (*Continued*)

which are intraarticular mesenchymal tissues, represent similar gene expression profiles distinct from other mesenchymal tissue-derived cells.

Identification of Signature Genes-Specific for MSCs from Intraarticular Tissues

We selected genes whose expressions were present in all two chondrocytes, three intraarticular MSCs, and their minimum expression value was 2.5-fold higher than the maximum value in three extraarticular MSCs. As a result, we identified three genes, PRELP, OGN, and ECRG4 (Table 1). We confirmed a higher expression of PRELP in chondrocytes and intraarticular MSCs than in extraarticular MSCs from three elderly donors by reverse transcriptase-PCR (Fig. 3A). Consistent findings were confirmed in three young donors; expression of PRELP was higher in synovium MSCs than in bone marrow MSCs. Real-time-PCR confirmed that OGN and ECRG4 expressions were higher in synovium MSCs than in bone marrow MSCs (Fig. 3B). We also selected genes whose expressions were present in all three extraarticular MSCs, and their minimum expression value was 2.5-fold higher than the maximum value in two chondrocytes and three intraarticular MSCs. Based on this algorithm, we identified seven genes (Table 1).

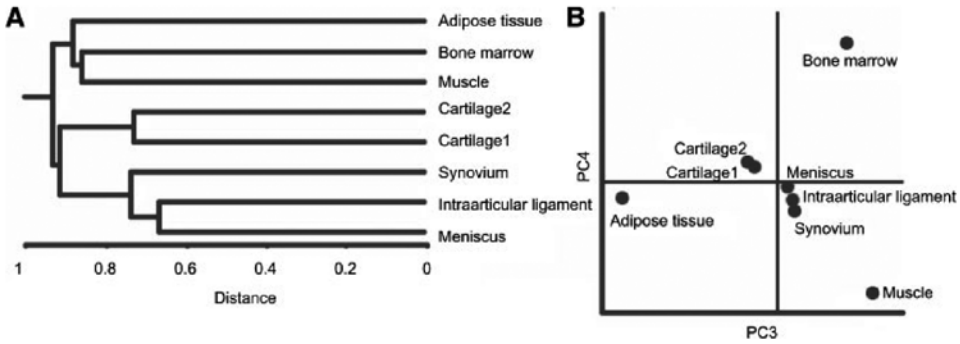

Figure 2. Gene chip analyses of various mesenchymal tissues-derived MSCs and Chondrocytes. The similarity of gene expression patterns is represented as Euclidean distance. (A) Dendrogram for clustering profile. (B) Principal component analysis. Mesenchymal tissue-derived cells of eight populations are plotted onto 2D representation, PC3 and PC4 axes.

Table 1. Genes Whose Expressions Were Distinctly Different between in Intraarticular and Extraarticular Mesenchymal Tissues-MSCs

GenBank	Gene symbol	Cartilage 1		Cartilage 2		Synovium		Meniscus		Ligament		Muscle		Adipose Tissue		Bone Marrow	
		F	Raw	F	Raw	F	Raw	F	Raw	F	Raw	F	Raw	F	Raw	F	Raw
U41344	*PRELP*	P	329	P	341	P	329	P	596	P	278	P	65	A	21	P	54
AV700059	*OGN*	P	331	P	147	P	260	P	612	P	305	A	4	P	51	A	7
AF325503	*ECRG4*	P	192	P	435	P	399	P	747	P	389	A	13	A	1	A	1
NM_004415	*DSP*	P	280	P	400	P	42	P	41	P	66	P	1642	P	1095	P	1244
NM_013957	*NRG1*	A	4	A	15	A	3	A	1	A	10	P	104	P	46	P	172
NM_002575	*SERPINB2*	P	12	A	1	A	0	A	0	A	8	P	495	P	629	P	76
AW151924	*LFNG*	A	5	A	2	A	16	A	3	A	4	P	134	P	83	P	71
AL575177	*NOG*	A	12	A	1	A	13	A	1	A	6	P	87	P	69	P	69
NM_005382	*NEF3*	A	3	A	3	A	2	A	1	A	1	P	100	P	38	P	49
AI031657	*LOC152742*	A	2	A	1	A	10	A	1	A	0	P	28	P	39	P	36

F = Flags, Flag indicates the presence or absence of gene expression determined by presence/absence call (Affymetrix), P (presence): gene is expressed. M (marginal): gene is marginally expressed. A (absence): gene is not expressed.

Sequential Expressions of PRELP during Chondrogenic Differentiation

We focused on PRELP and its expressions during chondrogenesis of synovium MSCs, and bone marrow MSCs were examined. Synovium MSCs expressed PRELP stably during the chondrogenesis, contrarily, bone marrow MSCs increased PRELP expression along with the chondrocyte differentiation (Fig. 4).

DISCUSSION

In this study, we used cells derived from synovium, meniscus, intraarticular ligament, bone marrow, muscle, and adipose tissue, all of which were patient-matched samples to rule out the variations in the properties of MSCs from different patients.[3,6,13]

We digested synovium, muscle, and adipose tissue for 3 h, and meniscus and ligament for 5 h with collagenase.

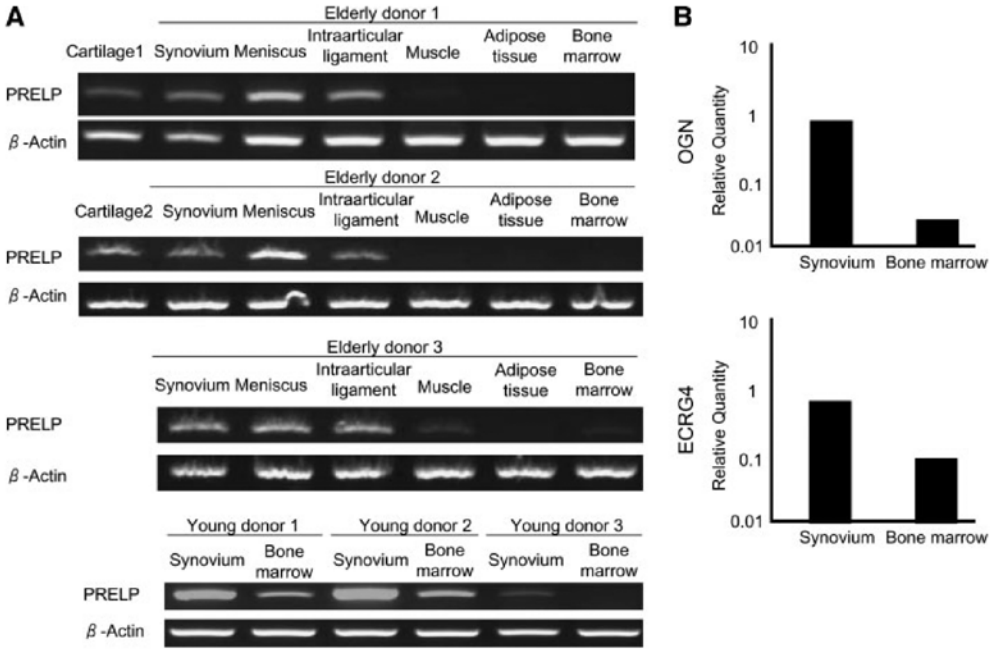

Figure 3. Expression of proline arginine-rich end leucine-rich repeat protein (PRELP), osteoglycin (OGN) and esophageal cancer related gene 4 protein (ECRG4). (A) PRELP expression by reverse transcriptase-PCR. Various mesenchymal tissues were harvested from three elderly and three young donors to isolate MSCs. Cartilage tissues were also harvested from two other donors. (B) OGN and ECRG4 expressions by real time-PCR. Synovium and bone marrow MSCs derived from elderly donor were used.

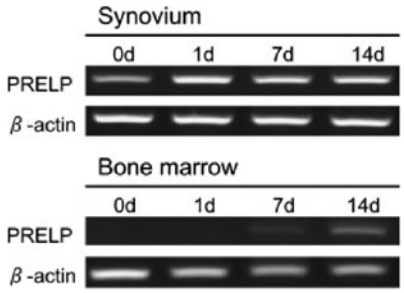

Figure 4. Sequential expressions of PRELP during chondrogenic differentiation of synovium and bone marrow MSCs by reverse transcriptase-PCR.

To increase the number of digested cells, a longer digestion period is of advantage, but this decreases cell viability because of collagenase toxicity. We adjusted the incubation period dependent on the hardness and specific gravity of each tissue.

To compare properties of MSCs derived from different sources, initial cell density should be controlled because colony-to-colony contact inhibition affects the cell size, surface epitopes, proliferation potential, and differentiation potential.[6,13–15] In this study, initial cell density was determined to avoid colony-to-colony contact inhibition.

As for chondrogenic assay, we used BMP-7 at 1000 ng/mL. We previously examined the dose effect of BMP-6 between at 0 to 500 ng/mL in bone marrow MSCs. Cartilage pellet increased its size along with the concentration of BMP-6 and a maximal effect was at 500 ng/mL.[12] Our preliminal experiments showed 1000 ng/mL BMP-6 induced larger cartilage pellets than 500 ng/mL BMP-6 in bone marrow and synovium MSCs. We obtained similar results with BMP-7 (data not shown).

For surface markers, we selected CD90, 34, 45, 44, 105, and 166. According to the statement by The International Society for Cellular Therapy, MSCs must express CD105, CD73, and CD90, and lack expression of CD45, CD34, CD14 or CD11b, CD79α, or CD19 and HLA-DR surface molecules.[16] From the list, we chose CD90 and CD105 as positive markers, and CD34 and CD45 as negative markers. Also, a large number of MSC papers have described positive expression of CD44 and CD166 in MSCs;[17] therefore, we further examined those epitopes.

There are a number of reports that have demonstrated that MSCs can be isolated from bone marrow, synovium, muscle, and adipose tissue. On the other hand, meniscus and intraarticular ligament MSCs have not been explored yet. Here, we revealed the existence of MSCs in meniscus and intraarticular ligament. Gene chip analysis of various mesenchymal tissue-derived cells demonstrated that synovium-, meniscus- and intraarticular ligament-derived cells, and chondrocytes, all of which are intraarticular tissue-derived cells, were grouped into the same subcategory. These results indicate that MSCs derived from intraarticular tissues and chondrocytes were closer to each other than those in MSCs derived from extraarticular tissues.

As signature genes that distinguish the intraarticular tissue-derived MSCs from extraarticular tissue-derived MSCs, we focused on proline arginine-rich end leucine-rich repeat protein (PRELP). PRELP is a connective tissue glycoprotein of the leucine-rich repeat family. The LRR motif is believed to participate in protein–protein interactions because this motif is found in several matrix-binding proteins.[18] Its protein sequence is 36%, which is similar to that of fibromodulin and 33%, which is similar to that of bovine lumican. Because these class-II small leucine-rich proteoglycans are demonstrated to function in regulating collagen fibril growth in various connective tissues,[19,20] PRELP may have a similar function in intraarticular connective tissues. Grover et al.[21] characterized the expression pattern and genomic structure of human PRELP. The messages of PRELP are abundant in cartilage, but are not present in cultured fibroblasts. However, at this point, there is no explanation as to why PRELP was only expressed in intraarticular MSCs but not in extraarticular MSCs. Nevertheless, PRELP may become a useful marker that can distinguish intraarticular MSCs from extraarticular MSCs. This will be greatly helpful to clarify the mechanisms of healing after intraarticular tissue injury. For example, we would be able to answer the question about the tissue origin of the MSCs, which appear in the injury site of articular cartilage defect induced by "microfracture technique."

In conclusion, we demonstrated the existence of MSCs in several intraarticular tissues. Gene expression profiles of intraarticular tissues MSCs and chondrocytes were closer to each other than those of extraarticular tissues MSCs. The higher expression of PRELP is a characteristic of stem cells derived from intraarticular tissues.

ACKNOWLEDGMENTS

We thank Kenichi Shinomiya for continuous support and Miyoko Ojima for expert help with histological analyses. The present study was supported by grants from the Japanese Ministry of Education Global Center of Excellence Program, International Research Center for Molecular Science in Tooth and Bone Diseases to T. Muneta, and from the Japan Society for the Promotion of Science (16591478) to I.S. Recombinant human BMP-7 was distributed by Stryker Biotech.

REFERENCES

1. Horwitz EM, Le Blanc K, Dominici M, et al. 2005. Clarification of the nomenclature for MSC: the international society for cellular therapy position statement. Cytotherapy 7:393–395.
2. De Bari C, Dell'ccio F. 2007. Mesenchymal stem cells in rheumatology: a regenerative approach to joint repair. Clin Sci (Lond) 113:339–348.
3. Sakaguchi Y, Sekiya I, Yagishita K, et al. 2004. Suspended cells from trabecular bone by collagenase digestion become virtually identical to mesenchymal stem cells obtained from marrow aspirates. Blood 104:2728–2735.
4. Mochizuki T, Muneta T, Sakaguchi Y, et al. 2006. Higher chondrogenic potential of fibrous synovium- and adipose

synovium-derived cells compared with subcutaneous fat-derived cells—Distinguishing properties of mesenchymal stem cells in humans. Arthritis Rheum 54:843–853.
5. Nimura A, Muneta T, Koga H, et al. 2008. Increased proliferation of human synovial mesenchymal stem cells with autologous human serum: comparisons with bone marrow mesenchymal stem cells and with fetal bovine serum. Arthritis Rheum 58:501–510.
6. Sakaguchi Y, Sekiya I, Yagishita K, et al. 2005. Comparison of human stem cells derived from various mesenchymal tissues—Superiority of synovium as a cell source. Arthritis Rheum 52:2521–2529.
7. Archer C, Dowthwaite G, Francis-West P. 2003. Development of synovial joints. Birth Defects Res C Embryo Today 69:144–155.
8. Ratajczak W. 2000. Early development of the cruciate ligaments in staged human embryos. Folia Morphol (Warsz) 59:285–290.
9. Sekiya I, Vuoristo J, Larson B, et al. 2002. In vitro cartilage formation by human adult stem cells from bone marrow stroma defines the sequence of cellular and molecular events during chondrogenesis. Proc Natl Acad Sci USA 99:4397–4402.
10. Sekiya I, Larson BL, Vuoristo JT, et al. 2004. Adipogenic differentiation of human adult stem cells from bone marrow stroma (MSCs). J Bone Miner Res 19:256–264.
11. Miyagawa Y, Okita H, Nakaijima H, et al. 2008. Inducible expression of chimeric EWS/ETS proteins confers ewing's Family tumor-like phenotypes to human mesenchymal progenitor cells. Mol Cell Biol 28:2125–2137.
12. Sekiya I, Colter DC, Prockop DJ. 2001. BMP-6 enhances chondrogenesis in a subpopulation of human marrow stromal cells. Biochem Biophys Res Commun 284:411–418.
13. Yoshimura H, Muneta T, Nimura A, et al. 2007. Comparison of rat mesenchymal stem cells derived from bone marrow, synovium, periosteum, adipose tissue, and muscle. Cell Tissue Res 327:449–462.
14. Sekiya I, Larson BL, Smith JR, et al. 2002. Expansion of human adult stem cells from bone marrow stroma: conditions that maximize the yields of early progenitors and evaluate their quality. Stem Cells 20:530–541.
15. Colter DC, Sekiya I, Prockop DJ. 2001. Identification of a subpopulation of rapidly self-renewing and multipotential adult stem cells in colonies of human marrow stromal cells. Proc Natl Acad Sci USA 98:7841–7845.
16. Dominici M, Le Blanc K, Mueller I, et al. 2006. Minimal criteria for defining multipotent mesenchymal stromal cells. The International Society for Cellular Therapy position statement. Cytotherapy 8:315–317.
17. Pittenger MF, Mackay AM, Beck SC, et al. 1999. Multilineage potential of adult human mesenchymal stem cells. Science 284:143–147.
18. Bengtsson E, Neame P, Heinegård D, et al. 1995. The primary structure of a basic leucine-rich repeat protein, PRELP, found in connective tissues. J Biol Chem 270:25639–25644.
19. Ezura Y, Chakravarti S, Oldberg A, et al. 2000. Differential expression of lumican and fibromodulin regulate collagen fibrillogenesis in developing mouse tendons. J Cell Biol 151:779–788.
20. Ameye L, Young MF. 2002. Mice deficient in small leucine-rich proteoglycans: novel in vivo models for osteoporosis, osteoarthritis, Ehlers-Danlos syndrome, muscular dystrophy, and corneal diseases. Glycobiology 12:107R–116R.
21. Grover J, Chen X, Korenberg J, et al. 1996. The gene organization, chromosome location, and expression of a 55-kDa matrix protein (PRELP) of human articular cartilage. Genomics 38:109–117.

毎日新聞
2008年（平成20年）12月28日（日）　14版　総合　2

ひざ半月板 再生に道

東京医科歯科大など

ラット実験 関節の幹細胞で

ひざの半月板損傷を、関節部分から採取した間葉系幹細胞を移植して治すことに、東京医科歯科大などの研究チームがラットで成功した。米科学誌「ステムセルズ」に発表する。

半月板はひざの内部にあり、大腿骨とすねの骨の間でクッションの役割を担う軟骨組織。けがや加齢で半月板を損傷した場合、半月板を切除する治療が一般的だが、関節症などを起こしやすい。

チームは半月板を再生させるため、骨や軟骨になる性質がある間葉系幹細胞を使った。同細胞は骨髄から取るのが一般的だが、関節の滑膜という組織から採取した。

半月板を損傷させた14匹のラットの患部に幹細胞を移植すると、約12週間で半月板と同じ性質の軟骨になった。小林英司・自治医科大教授（移植・再生医学）らが開発した、細胞を遺伝子改変によって光らせる技術で調べたところ、半月板が再生し関節を保護する様子が確認できた。

また、半月板が再生した後の間葉系幹細胞は過剰に増殖する心配がないことも分かった。人工多能性幹細胞（iPS細胞）や胚性幹細胞（ES細胞）での臨床応用を始めた的の組織ができた後も増殖が止まらず、腫瘍になったり他の臓器に移動して奇形を生む恐れがあり、課題となっている。

関矢一郎・東京医科歯科大准教授（軟骨再生学）は「滑膜からの幹細胞は採取しやすく取り扱いも簡単だ。数年以内にヒトを使う再生医療では、目い」と話す。【永山悦子】

MEMO

有機材料分野

秋吉 一成

生体材料工学研究所・素材研究部門
有機材料学・教授

1. 研究の課題名

ナノゲル基盤バイオマテリアルの創成とDDS応用

Design of Nanogel-based baiomaterials and application to DDS

我々は、新規なナノキャリアとして、ナノサイズの自己組織化ゲル微粒子（ナノゲル）を開発した。ナノ微粒子とゲルの特性を合わせ持つナノゲルは、リポソームや高分子ミセルに続く新規なDDSとして注目されている。この機能性ナノゲルを自在に設計しえる我々の独自の技術（ナノゲル工学）を駆使して、テーラーメイドのナノゲルキャリアとナノゲル基盤ヒドロゲルの開発とその利用を図っている。特に、疎水化多糖ナノゲルはタンパク質を凝集させることなく取り込み、複合体ナノ微粒子を形成し、さらに活性を保持した形でタンパク質を放出しえる、いわゆる分子シャペロン機能を有していることが他に例を見ない最大の特徴である。この特性を利用して、種々の生理活性ペプチドやタンパク質のキャリアとしての有用性を示してきた。本年度は、ナノゲルの有する疎水性薬物、タンパク質との相互作用を生かしたリザーバー型のナノゲル架橋生分解性ハイドロゲル設計を行った。特に、反応性多糖ナノゲルをポリエチレングリコール（PEG）で架橋したCHP-PEGハイドロゲルは、再生医療における徐放性担体として有用であるが明らかになった。プロスタグランジンE2（PGE2）やBMP2を取り込ませたハイドロゲルを用いることで、骨形成が顕著に促進することが明らかになった。また、TNF α とRANKLのアンタゴニストであるペプチドの徐放性キャリアとして有用であることも明らかになった。

2.

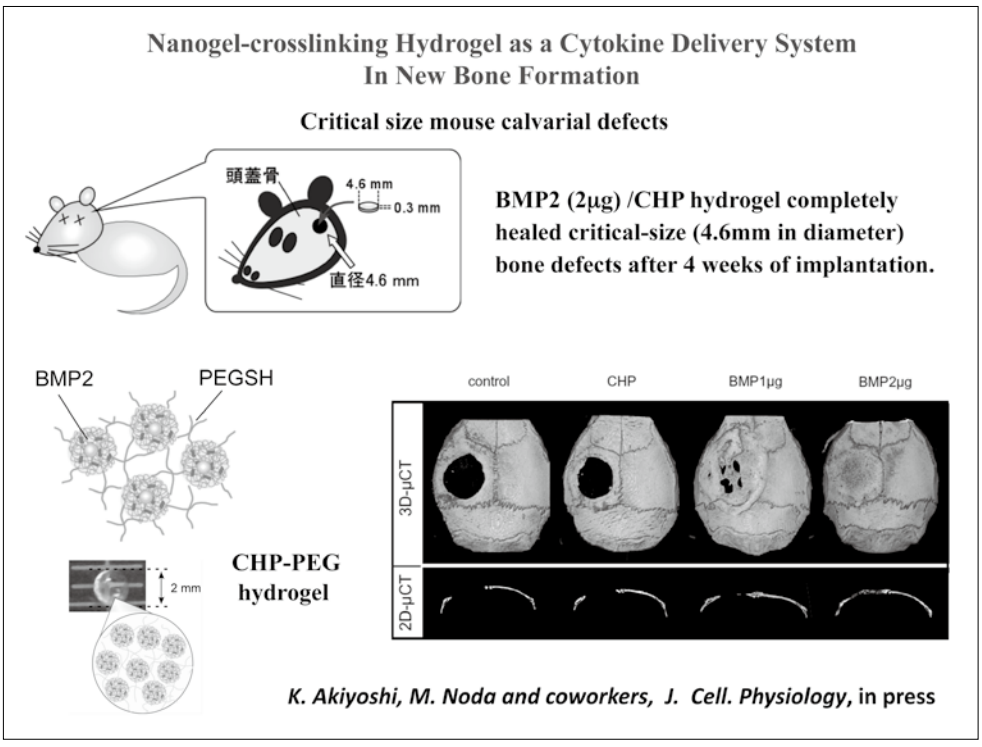

3. 2008年、2009年（平成21年3月までの）に発表した全ての研究内容についての英文要約

Tailor-made functional nanogels are developed by the self-assembly of functional associating polymers（nanogel engineering）. We reported a new method of preparation of macrogels with well-defined nanostructures by these nanogels as building blocks. We cross-linked acryloyl-group modified CHP（CHPA）nanogels with thiol-group modified poly（ethylene glycol, PEGSH）to prepare a biodegradable hydrogel（CHP-PEG gel）. Nanogel-based delivery system is expected to serve as a preferable hydrogel with the efficient drug-loading capacity for tissue engineering. The CHP-PEG hydrogel delivery system was an efficient delivery system of bone anabolic agent, PGE2. Single implantation of the hydrogel containing low amounts of BMP induced osteoblastic activation and new bone formation in vivo. The hydrogel act as an efficient and versatile scaffold for the stimulation of osteoblasts to form bone and to repair defects via delivery of BMP. CHP-nanogel also worked as a suitable carrier for the W9-peptide（TNF-α and RANKL antagonist）and it prevented aggregation and increased the stability of the W9-peptide.

4. 本事業に関連して世界的な研究拠点形成に向けて、以下の点で改善・整備等されたこと

A（研究拠点体制）

歯学部、医学部との共同研究体制を整備した。

B（研究教育環境）

共同研究関連設備の充実を図った。

C（人材確保）

歯学部との共同研究を行えるAISSとして1名参画させた。

D（人材育成）

学生とのミーンティング回数を増やして綿密な討論を行った。

E（国際化）

留学生をAISSに採用し、共同研究を遂行している。

5. GCOE事業を推進するに当たって力を入れた点

医歯工連携の共同研究をより一層展開させ、真に実りあるものにしていくための事業推進担当者との討論を綿密に行った。

6. 英文原著論文

1. Shimizu T, Kishida T, Hasegawa U, Ueda Y, Imanishi J, Yamagishi H, Akiyoshi K, Otsuji E, Mazda O. Nanogel DDS enables sustained release of a cytokine for tumor immunotherapy. Biochem Biophys Res Commun 367: 330-335, 2008.
2. Nomura SM, Kondoh S, Asayama W, Asada A, Nishikawa S, Akiyoshi K. Direct preparation of giant proteo-liposomes by in vitro membrane protein synthesis. J Biotechnol 133: 190-195, 2008.
3. Kageyama S, Kitano S, Hirayama M, Nagata Y, Imai H, Shiraishi T, Akiyoshi K, Scott A, Murphy R, Hoffman E, Old L, Katayama N, Shiku H. Humoral immune responses in patients vaccinated with 1-146 HER2 protein complexed with cholesteryl pullulan nanogel（CHP-HER2）. Cancer Sci 99: 601-607, 2008.
4. Iwata R, Iwasaki Y, Akiyoshi K. Covalent immobilization of antibody fragments on well-defined polymer brushes via site-directed method. Colloid Surf B-Biointerfaces 62: 288-298, 2008.
5. Asayama W, Sawada S, Taguchi H, Akiyoshi K. Comparison of Refolding Activities between Nanogel Artificial Chaperone and GroEL Systems. Int J Biol Macromol 42: 241-246, 2008.
6. Toita S, Hasegawa U, Koga H, Sekiya I, Muneta T, Akiyoshi K. Protein-conjugated QD effectively delivered into living cells by a cationic nanogel. J Nanosci Nanotechnol 8: 1-7, 2008.
7. Ayame H, Morimoto N, Akiyoshi K. Self-assembled cationic nanogels for intracellular protein delivery system. Bioconjugate Chem 19: 882-890, 2008.
8. Morimoto N, Ohki T, Kurita K, Akiyoshi K. Thermo-responsive hydrogels with nanodomains: rapid shrinking of nanogel-crosslinking hydrogel of poly（N-isopropyl acrylamide）Macromol Rapid Commun 29: 672-676, 2008.
9. Kudo H, Yagi T, Chu MX, Saito H, Morimoto M, Iwasaki Y, Akiyoshi K, Mitsubayashi K. Glucose sensor using phospholipid polymer-based enzyme immobilization method. Anal Bioanal Chem 391: 1269-1274, 2008.
10. Morimoto N, Qiu XP, Winnik FM, Akiyoshi K. Dual Stimuli-Responsive Nanogels by Self-Assembly of Polysaccharides Lightly Grafted with Thiol-Terminated Poly（N-isopropylacrylamide）Chains. Macromolecules 41: 5985-5987, 2008.
11. Iwasaki Y, Takami U, Sawada S, Akiyoshi K. Interfacing biomembrane mimetic polymer surfaces with living cells – Surface modification for reliable bioartificial liver. Appl Surf Sci 255: 523-528, 2008.
12. Yamane S, Sasaki Y, Akiyoshi K. Siloxane-crosslinked Polysaccharide Nanogels for Potential Biomedical Applications. Chem Lett 37: 1282-1283, 2008.
13. Morimoto N. Obeid R. Yamane S. Winnik F. M. Akiyoshi K. Composite Nanomaterials by Self-assembly and Controlled Crystallization of Poly（2-isopropyl-2-oxazoline）-Grafted Polysaccharide. Soft Matter in press.
14. Morimoto N. Ogino N. Narita T. Akiyoshi K. Enzyme-responsive artificial chaperone system with amphiphilic amylose primer. J. Biotech. in press.

15. Yamane S, Sugawara A, Watanabe A, Akiyoshi K. Hybrid nanoapatitby polysaccharide nanogel-templated mineralization, J. Bioactive and Compatible Polym, in press.
16. Yamane S, Sugawara A, Sasaki Y, Akiyoshi K. Nanogel-calcium phosphate hybrid nanoparticles with negative or positive charges for potential biomedical applications. Bull. Chem. Soc. Jpn. in press
17. ◎Alles N. Soysa N.S. Mian A. H. Tomomatsu N. Saito H. Baron R. Morimoto N. Aoki K. Akiyoshi K. Ohya K. Polysaccharide nanogel delivery of a TNF-a and RANKL antagonist peptide allows systemic prevention of bone loss. Eur. J. Pharma. Sci. in press.
18. ◎Ozawa Y. Sawada S. Morimoto N. Akiyoshi K. Self-assembeld nanogel of hydrophobized dendritic dextrin for protein delivery. Macromol. Biosci. in press.
19. Kobayashi H. Katakura O. Morimoto N. Akiyoshi K. Kasugai S. Effects of cholesterol-bearing pullulan（CHP）-nanogels in combination with prostaglandin E1 on wound healing. J. Biomed. Mater. Res. B. in press.
20. ◎Miyai K, Yoneda M , Hasegawa U , Toita S , Izu Y, Hemmi H, Hayata T, Ezura Y, Mizutani S, Miyazono K , Akiyoshi K, Yamamoto T, Noda M, ANA deficiency enhances BMP-induced ectopic bone formation via transcriptional events, J. Biological Chem. in press
21. ◎Hayashi C, Hasegawa U, Saita Y, Hemmi H, Hayata T, Nakashima K, Ezura Y, Amagasa T, Akiyoshi K, Noda M, Osteoblastic bone formation is induced by using nanogel-crosslinking hydrogel as novel scaffold for bone growth factor, J. Cell. Phys. in press

7. 著書

［著書］

1. 佐々木善浩,秋吉一成.ナノゲルキャリア.機能性DDSキャリアの製剤設計.p63-71,岡田弘晃 監修,シーエムシー出版,2008.
2. 次世代医療のための高分子材料工学.秋吉一成,岸田晶夫 監修,シーエムシー出版,2008.
3. 森本展行,秋吉一成.ナノゲル基盤ゲル材料.次世代医療のための高分子材料工学.p33-41,秋吉一成,岸田晶夫 監修,シーエムシー出版,2008.

［総説］

1. 菅原彩絵,秋吉一成.会合性高分子の自己組織化.色材における基礎科学講座（第X講）.J Jpa Soc Colour Mater 81（4）: 178-184, 2008.
2. 森本展行,秋吉一成.ナノゲルDDS研究の最前線.ファルマシア 44（8）: 764-768, 2008.
3. 佐々木善浩,秋吉一成.生体由来高分子ゲルを用いたDDS担体研究.バイオマテリアル 26（6）: 30-36, 2008.

8. 平成21年3月までの自己評価

我々の開発したDDSを利用した拠点内での協同研究を一層促進させるように努力した。

現在、野田教授、森田教授、春日井教授、大谷教授との共同研究を進めている。

野田教授との共同研究の論文が2報受理され、AISSのfirst author論文が1報受理された。

9. 学会発表（英文）

1. Akiyoshi K, Hasegawa U, Toita S, Morimoto N. Nanogel-Crosslinking Hydrogel with Chaperone-like Activity for Tissue Engineering. 8th World Biomaterials Congress, Amsterdam, Netherlands, May, 2008.
2. Toita S, Soma Y, Morimoto N, Kitamura S, Akiyoshi K. Cationic Cycloamylose for Gene Delivery. XXIV International Carbohydrate Symposium, Oslo, Norway, July, 2008.
3. Toita S, Soma Y, Morimoto N, Akiyoshi K. Functional Cycloamylose for Intracellular Delivery. JAPAN-KOREA Polymer Young Scientist Symposium, Niigata, Japan, October, 2008.
4. Setsuko Y, Yoshihiro S, Akiyoshi K. Synthesis of Nanogel-Inorganic Hybrid Nanomaterials. JAPAN-KOREA Polymer Young Scientist Symposium, Niigata, Japan, October, 2008.
5. Morimoto N, Akiyoshi K, Winnik FM. Comparative Study of Responsive Nanogels Using the Temperature Responsive Properties of Poly（N-Isopropylacrylamides）and Poly-（2-Isopropyl-2-Oxazolines）in Water. 236th ACS National Meeting, Philadelphia, PA, USA, August, 2008.
6. Akiyoshi K, Ayame H, Morimoto N. Intracellular Protein Delivery with Self-Assembled Cationic Nanogels. 236th ACS National Meeting, Philadelphia, PA, USA, August, 2008.
7. Morimoto N, Winnik FM, Akiyoshi K. Design of Dual Stimuli-Responsive Nanogels by Self-Assembly of Thiol-terminated Poly（N-Isopropylacrylamide）-graft Pullulan. 236th ACS National Meeting, Philadelphia, PA, USA, August, 2008.
8. Nochi T, Yuki Y, Mejima M, Kataoka N, Takahashi H, Sawada S, Kohda T, Kozaki S, Akiyoshi K, Kiyono H. Exploit of nanogel as a novel carrier of mucosal vaccine: Nanogel mucosal vaccine effectively induces protective immunity against botulinum toxin. 2nd vaccine global congress, Boston, MA, USA, December, 2008.

10. 学会発表（和文）

1. 山根説子,秋吉一成.ナノゲル/リン酸カルシウム複合ナノ粒子の創製.第2回バイオ・ナノテクフォーラ

ムシンポジウム,東京,2008年3月.
2. 佐々木善浩,石川雄大,橋詰峰雄,菊池純一,檜山聡,森谷優貴,須田達也.オリゴヌクレオチドによる分子カプセルの伝搬制御. 日本化学会第88春季年会,東京,2008年3月.
3. 相馬祐輝,戸井田さやか,森本展行,北村進一,秋吉一成.新規タンパク質キャリアとしてのサイクロアミロース誘導体の機能. 日本化学会第88春季年会,東京,2008年3月.
4. 高橋治子,澤田晋一,秋吉一成.疎水化グリコーゲンの合成と特性評価. 日本化学会第88春季年会,東京,2008年3月.
5. 小澤弥生,森本展行,秋吉一成.デンドリティック多糖ナノゲルの機能. 日本化学会第88春季年会,東京,2008年3月.
6. 相馬祐輝,戸井田さやか,栗田公夫,森本展行,北村進一,秋吉 一成.機能性サイクロアミロースの設計とタンパク質デリバリーへの応用.第57回高分子年次大会,横浜,2008年5月.
7. 多田陽子,澤田晋一,秋吉一成.ナノゲルシート薄膜の設計と機能.第57回高分子年次大会,横浜,2008年5月.
8. 下田麻子,長谷川麗,秋吉一成.ナノゲル架橋ハイブリッド微粒子の設計と機能評価.第57回高分子年次大会,横浜,2008年5月.
9. 高橋治子,澤田晋一,秋吉一成.疎水化グリコーゲンによるナノゲル形成と機能.第57回高分子年次大会,横浜,2008年5月.
10. 山本由香,長谷川麗,秋吉一成.ナノゲル架橋ハイドロゲルの設計と特性評価.第57回高分子年次大会,横浜,2008年5月.
11. 杉浦裕展,森谷優貴,野村慎一郎,秋吉一成.無細胞タンパク質合成系におけるリポソームシャペロン.第57回高分子年次大会,横浜,2008年5月.
12. 海老原梢,森本展行,秋吉一成.固定化人工分子シャペロンの機能評価.第57回高分子年次大会,横浜,2008年5月.
13. 室田曜史,森本展行,北村進一,秋吉一成.酵素応答性糖鎖界面活性剤の特性と機能.第57回高分子年次大会,横浜,2008年5月.
14. 澤田晋一,秋吉一成.酵素安定化剤としてのナノゲル機能.第57回高分子年次大会,横浜,2008年5月.
15. 下田麻子,長谷川麗,秋吉一成,岸田綱郎,松田修.ナノゲル架橋ナノ微粒子の設計とサイトカインデリバリー.第24回日本DDS学会,東京,2008年6月.
16. 山本由香,長谷川麗,秋吉一成.ナノゲル架橋ハイドロゲルによるタンパク質の徐放制御.第24回日本DDS学会,東京,2008年6月.
17. 相馬祐輝,戸井田さやか,菖蒲弘人,森本展行,栗田公夫,北村進一,秋吉一成.機能性サイクロアミロースの設計とタンパク質デリバリーへの応用.第24回日本DDS学会,東京,2008年6月.
18. 戸井田さやか,相馬祐輝,森本展行,北村進一,秋吉一成,岸田綱郎,松田修.機能性サイクロアミロースによる遺伝子キャリアの開発.第24回日本DDS学会,東京,2008年6月.
19. 森谷優貴,野村慎一郎,杉浦裕展,秋吉一成.無細胞タンパク質合成系による膜タンパク質組込リポソームの調製と機能.第18回バイオ・高分子シンポジウム,東京,2008年7月.
20. 戸井田さやか,相馬祐輝,森本展行,北村進一,秋吉一成.カチオン性サイクロアミロースによる遺伝子デリバリー.第57回高分子討論会,大阪,2008年9月.
21. 小澤弥生,森本展行,秋吉一成.種々の糖鎖構造を有する疎水化多糖の自己組織化と機能.第57回高分子討論会,大阪,2008年9月.
22. 山根説子,佐々木善浩,秋吉一成.ナノゲルをテンプレートとしたアパタイトナノ微粒子の合成と機能.第57回高分子討論会,大阪,2008年9月.
23. 朝山和喜子,秋吉一成.ナノゲルの人工分子シャペロン機能.第57回高分子討論会,大阪,2008年9月.
24. 秋吉一成,澤田晋一.免疫療法のためのナノゲルDDSの開発.第57回高分子討論会,大阪,2008年9月.
25. 森本展行,WINNIK Françoise M.,秋吉一成.温度応答性ポリマーグラフト化多糖による自己組織化ナノゲルの創製.第57回高分子討論会,大阪,2008年9月.
26. 下田麻子,秋吉一成.ナノゲル架橋ハイブリッド微粒子の設計とDDS応用.第57回高分子討論会,大阪,2008年9月.
27. 室田曜史,森本展行,北村進一,秋吉一成.酵素応答性糖鎖界面活性剤の機能.第57回高分子討論会,大阪,2008年9月.
28. 海老原梢,森本展行,秋吉一成.ナノゲル固定化ゲルの人工シャペロン機能.第57回高分子討論会,大阪,2008年9月.
29. 多田陽子,澤田晋一,秋吉一成.ナノゲルシートの設計と機能.第57回高分子討論会,大阪,2008年9月.
30. 山本由香,秋吉一成.ナノゲル架橋ハイドロゲルの設計と機能評価.第57回高分子討論会,大阪,2008年9月.

31. 高橋治子,澤田晋一,秋吉一成.細胞親和性ナノゲルの設計と機能.第57回高分子討論会,大阪,2008年9月.
32. 相馬祐輝,戸井田さやか,森本展行,栗田公夫,北村進一,秋吉一成.カチオン性サイクロアミロースによる細胞内タンパク質輸送.第57回高分子討論会,大阪,2008年9月.
33. 森本展行,室田曜史,秋吉一成.酵素応答型糖脂質によるミセル-ベシクル転移制御と新規膜タンパク質再構成法.第3回バイオ関連化学合同シンポジウム,横浜,2008年9月.
34. 小澤弥生,森本展行,秋吉一成.多糖ナノゲルによる新規タンパク質デリバリーシステムの開発.第3回バイオ関連化学合同シンポジウム,横浜,2008年9月.
35. 杉浦裕展,森谷優貴,朝山和喜子,野村慎一郎,秋吉一成.無細胞膜タンパク質合成系におけるシャペロン機能.第57回高分子討論会,大阪,2008年9月.
36. 林純吾,澤田晋一,栗田公夫,秋吉一成.ポリイオンコンプレックスナノゲルの設計.第57回高分子討論会,大阪,2008年9月.
37. 戸井田さやか,相馬祐輝,森本展行,北村進一,秋吉一成.機能性サイクロアミロースの遺伝子デリバリーへの応用.日本バイオマテリアル学会シンポジウム2008,東京,2008年11月.
38. 澤田晋一,秋吉一成.酵素固定化ナノゲルの機能.日本バイオマテリアル学会シンポジウム2008,東京,2008年11月.
39. 小澤弥生,森本展行,秋吉一成.タンパク質キャリアとしての多糖ナノゲルの機能評価.日本バイオマテリアル学会シンポジウム2008,東京,2008年11月.
40. 朝山和喜子,秋吉一成.無細胞タンパク質合成系におけるナノゲルの分子シャペロン機能.日本生物物理学会第46回年会,福岡,2008年12月.
41. 森谷優貴,秋吉一成.無細胞タンパク質発現系を用いて作成した膜タンパク質組込リポソームの機能評価.日本生物物理学会第46回年会,福岡,2008年12月.

11. 外部資金の獲得状況

(科学研究費補助金、受託研究費、外部財団の助成など)

科学研究費補助金　基盤研究A (2)・
課題:ナノゲルを基盤とした新規デリバリーシステムの開発」
代表:　秋吉一成
期間:平成20-24年
研究費総額: 3910万円

科学研究費補助金　特定領域研究統合がん
課題:癌免疫治療のための新規ナノキャリアの開発
代表:　秋吉一成
期間:平成20-21年
研究費総額: 2200万円

科学研究費補助金　学術創成研究費
課題:物理科学を基盤とする人工細胞の構築と機能解析
分担:秋吉一成
期間:平成18-22年
研究費総額: 5500万円

科学技術振興機構　戦略的創造研究推進事業 (CREST)
課題:分子シャペロン工学に基づく遺伝子解析
分担:秋吉一成
期間:平成17-22年
研究費総額: 3000万円

医薬基盤研究所　保健医療分野における基礎研究推進事業
課題:新規siRNAテクノロジーを用いたC型肝炎の画期的治療法の開発
分担:秋吉一成
期間:平成20-21年
研究費総額: 1200万円

12. 特別講演、招待講演

(国内)

1. 秋吉一成.ナノゲル工学による新規ゲルバイオマテリアルの創製.筑波大学学際物質科学研究センター　機能性分子シンポジウム,つくば,2008年1月.
2. 秋吉一成.癌免疫治療のための新規デリバリーシステムの開発.第3次対がん10か年総合戦略　第2回合同シンポジウム,東京,2008年2月.
3. 秋吉一成.分子シャペロン機能工学によるタンパク質の集積,機能制御.第24回日本DDS学会,東京,2008年6月.
4. 秋吉一成.創剤フォーラム第14回シンポジウム˜薬物キャリアがブレイクスルーさせるDDS˜.第2回バイオ・ナノテクフォーラムシンポジウム,東京,2008年10月.
5. 秋吉一成.癌免疫治療のためのナノゲルDDS.第67回日本癌学会学術総会,S13ナノデバイスの癌治療への応用,名古屋,2008年10月.
6. 秋吉一成.ナノゲルを用いたDDS.第19回高分子ゲル研究会講座,主題:機能性ゲルが拓く新しい医療,東

京,2008年12月.

7. 秋吉一成.人工細胞モデルリポソームとDDS.第6回東京理科大学DDS研究センターシンポジウム,主題:リポソームとDDS,東京,2008年12月.

(海外)

8. Akiyoshi K. Nanogel Engineering for Design of Drug Delivery System. 24th KAIST-TIT joint Symposium, Korea-Japan International Symposium on Polymer Nanomaterials, Daejeon, Korea, January, 2008.
9. Akiyoshi K. New method for reconstitution of membrane proteins to liposome. 11th Liposome Reserch Days Confrerence, Yokohama, Japan, July, 2008.
10. Akiyoshi K. Hydrogel biomaterials by self-assembly of hydrophobized polysaccharides. 24th International Carbohydrate Symposium, Oslo, Norway, July, 2008.
11. Akiyoshi K. Polysaccharide nanogel engineering for protein delivery, American Academy of Nanomedicine. 4th Annual Symposium, Potomac, MD, USA, September, 2008.
12. Akiyoshi K, Hsegawa U, Shimoda A, Shimizu T, Kishida T, Matsuda O. Nanogel DDS for tumor immunotherapy. The 13th World Congress on Advances in Oncology, and 11th International Symposium on Molecular Medicine, Crete, Greece, October, 2008.
13. Akiyoshi K. Self-assembled nanogels for protein delivery. The 6th China-Japan-Korea Foresight Joint Symposium on Gene Delivery and International Symposium on Biomaterials, Hainan, China, November, 2008.
14. Akiyoshi K. Protein delivery by Polysaccharide Nanogel for Cancer Immunotherapy. MRS fall meeting 2008, Symposium FF: Nanofunctional Materials, Structure, and Devices for Biomedical Applications, Boston, MA, USA, December, 2008.
15. Akiyoshi K. Nanogel protein delivery system with chaperone function. 14th International Symposium on Recent Advances in Drug Delivery Systems, Salt Lake City, Utah, USA, February, 2009

13. 講座の准教授、講師、助教、特別研究員、ポスドク、指導を受けた大学院生の名前(AISSには◯印) のリスト

佐々木善浩	准教授
森本展行	助　教
澤田晋一	助　教
朝山和喜子	研究員
小澤弥生	博士4年
◯Alles Neil	博士3年
山根説子	
戸井田さやか	博士1年
神谷厚輝	博士1年
海老原　梢	修士2年
下田麻子	修士2年
杉浦裕展	修士2年
高橋治子	修士2年
多田陽子	修士2年
室田曜史	修士2年
山本由香	修士2年
土戸優志	修士1年
安岡潤一	修士1年

Available online at www.sciencedirect.com
ScienceDirect
Journal of Biotechnology 133 (2008) 190–195
Journal of BIOTECHNOLOGY
www.elsevier.com/locate/jbiotec

Direct preparation of giant proteo-liposomes by *in vitro* membrane protein synthesis

Shin-ichiro M. Nomura [a,b], Satoshi Kondoh [a], Wakiko Asayama [a,b], Akikazu Asada [c], Shigemichi. Nishikawa [c], Kazunari Akiyoshi [a,b,*]

[a] *Institute of Biomaterials & Bioengineering, Tokyo Medical & Dental University, 2-3-10, Kanda-surugadai, Chiyoda-ku, Tokyo 101-0062, Japan*
[b] *Center of Excellence Program for Frontier Research on Molecular Destruction and Reconstruction of Tooth and Bone, Tokyo Medical and Dental University, Tokyo, Japan*
[c] *WAKENYAKU CO., LTD., Research & Development Division, 945-1, Tsujide, Shimogasa-cho, Kusatsu-shi, Shiga 525-0029, Japan*

Received 26 January 2007; received in revised form 22 July 2007; accepted 3 August 2007

Abstract

We investigated the direct constitution of membrane proteins into giant liposomes in cell-free (*in vitro*) protein synthesis. Giant liposomes were present in a translation reaction cocktail of a wheat germ cell-free protein translation system. Apo cytochrome b_5 (b5) and its fusion proteins were synthesized and directly localized in the liposomes. After the translation reaction, the proteo-liposomes were isolated by simplified discontinuous density-gradient centrifugation. Apo cytochrome b_5 conjugated dihydrofolate reductase (DHFR) was synthesized in the same procedure and the protein was directly displayed on the liposome surface. b5 acts as a "hydrophobic tag" for recruitment to the liposome surface.
© 2007 Elsevier B.V. All rights reserved.

Keywords: Giant liposome; Membrane protein; Cytochrome b5; In vitro protein synthesis; Wheat germ lysate

1. Introduction

Membrane proteins play crucial roles in diverse biological functions such as signal transduction, energy production, and cellular communication. Understanding their structures and functions has been complicated by difficulties in isolating and purifying functional membrane proteins. In living systems, the folding and function of integrated membrane proteins are assisted by the microenvironment of a lipid bilayer of biomembranes. Therefore, liposomes have been frequently used as the basis for membrane protein reconstitution (Rigaud et al., 1995; Heginbotham et al., 1998; Furukawa and Haga, 2000; Salvail et al., 2002).

We have been developing a novel method for directly obtaining pure membrane protein-containing liposomes (proteo-liposomes). This entails cell-free protein synthesis was carried out in the presence of giant liposomes, i.e., an artificial cell-model. Construction of an artificial cell-model is one of the useful approaches for understanding living cells (Yoshikawa and Nomura, 2000; Szostak et al., 2001; Noireaux et al., 2005; Luisi et al., 2006). Giant liposomes (phospholipid bilayer vesicles) with diameters of up to tens of micrometers have received considerable attention for the basis of such a cell-model because they can be visualized by optical microscopy (Hotani et al., 2003; Luisi and Lasic, 2000). Giant liposome encapsulated gene expression systems have recently been investigated (Tsumoto et al., 2001; Yu et al., 2001; Nomura et al., 2003; Noireaux and Libchaber, 2004; Ishikawa et al., 2004). *In vitro* gene expression that installed in a liposome can be regarded as a bootstrap sequence for a cell-model. In spite of the rapid advancement of *in vitro* gene expression systems, most of the research has been devoted to the synthesis of water soluble proteins (Shimizu et al., 2006; Vinarov et al., 2006; Nakano et al., 2004; Endo and Sawasaki, 2003). The synthesis of membrane proteins by a cell-free system is still limited (Klammt et al., 2006; Elbaz et al., 2004; Ishihara et al., 2005). Functional membrane protein expression with liposomes is a crucial step for constructing a more realistic cell-model and also for obtaining an understanding of the functions of membrane proteins.

* Corresponding author at: Institute of Biomaterials & Bioengineering, Tokyo Medical & Dental University, 2-3-10, Kanda-surugadai, Chiyoda-ku, Tokyo 101-0062, Japan. Tel.: +81 3 5280 8020; fax: +81 3 5280 8027.
E-mail address: akiyoshi.org@tmd.ac.jp (K. Akiyoshi).

0168-1656/$ – see front matter © 2007 Elsevier B.V. All rights reserved.
doi:10.1016/j.jbiotec.2007.08.023

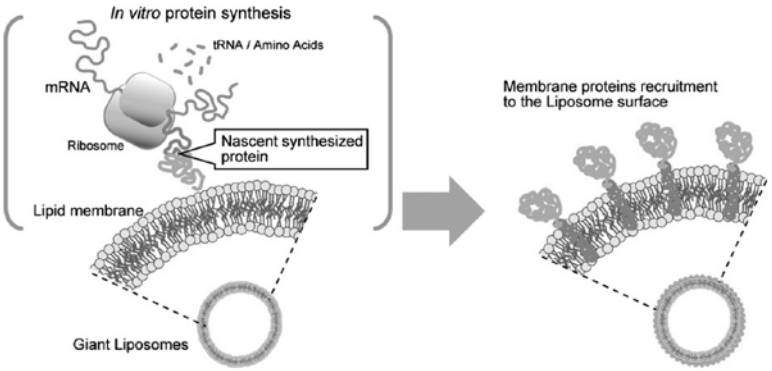

Fig. 1. Schematic illustrations of concept of the liposome displaying experiment. Synthesized nascent membrane proteins are expected to insert into the coexisting liposomal membranes.

In this study, the apo cytochrome b_5 and its fusion proteins were selected as model membrane proteins. Cytochrome b_5 is a ubiquitous electron transport hemoprotein, especially the microsomal and mitochondrial variants, which are membrane-bound proteins (Spatz and Strittmatter, 1971; Yubisui et al., 1988; Nakanishi et al., 2006). The protein has 133 amino acid residues with a polar domain and a hydrophobic membrane-binding domain that comprises approximately 40 amino acid residues. It has been extensively used as a model membrane protein (Ladokhin et al., 1993).

Apo cytochrome b_5 (b5) and EGFP-conjugated b5 (EGFP-b5) were synthesized by a wheat germ cell-free system in the presence of giant liposomes and were effectively displayed on the liposomal surface during the protein synthesis (Fig. 1). The proteo-liposome was isolated by simply centrifugation of the reaction mixture. We also report the presentation of water soluble enzymes to liposomes by conjugation of b5 as a "hydrophobic tag" for recruitment to the liposome surface. Cytochrome b_5 conjugated dihydrofolate reductase (DHFR) was synthesized and displayed on the liposome surface.

2. Materials and methods

2.1. Materials

Egg yolk phosphatidylcholine (EYPC) was obtained from Funakoshi Co., Ltd. (Tokyo, Japan). 1,2-di-Oleoyl-sn-glycero-3-phosphocholine (DOPC), 1,2-di-dimyristoyl-sn-glycero-3-phosphocholine (DMPC), cholesterol were obtained from Sigma Co., Ltd. (St. Louis, MO). PROTEIOS™, a wheat germ cell-free protein synthesis core kit, including the plasmids pEU3-NII, pEU3-DHFR, was purchased from WAKENYAKU Co., Ltd. (Shiga, Japan).

2.2. Liposome preparation and characterization

Lipids were dissolved in the organic solvent ($CHCl_3$:CH_3OH = 2:1, v/v) to 100 mM. The lipids are EYPC, DOPC and DMPC/cholesterol = 7/3 in molar ratio. One milliliter of the lipid solution was set on a round bottomed flask, and the solvent was evaporated. After vacuum drying (at least 1 h), a thin dried lipid film formed on the flask. The film was made to swell for liposome formation by adding 1 ml of 100 mM HEPES buffer solution for 30 min at 50 °C. Cell-free expression buffer mix (PROTEIOS buffer #1:buffer #2:Nuclease free water, 26.75, 31.25, 67 in volume, respectively) 270 μl and the liposome solution 30 μl were applied to an ultrafiltration membrane (Microcon YM-3, Millipore), then centrifuged at 15,000 × *g* for 15 min. The ultrafiltration process was repeated three times to exchange the liposomal exterior solution with buffer mix. The final lipid concentration was diluted to 10 mM by the buffer mix.

Size distribution of the obtained liposomes was investigated as follows. Liposomes encapsulating water soluble dye, calcein (1 mM in 100 mM HEPES buffer solution, as mentioned above) were prepared. One microliter of the liposome sample gently mixed with the 2.5 μl of 50 mM Co(II)Cl_2 solution for extra-liposomal quenching was sealed on the glass slide. The fluorescence images were obtained by the following setup: confocal laser-scanning unit (CSU10, Yokogawa) with an adapted inverted microscope (IX70, with lens objective UPlanSApo, 40×, Olympus) equipped with a cooled CCD camera (Hamamatsu). A sample was irradiated by diode laser (488 nm, 10 mW), then the signals were obtained through a band-pass filter (512–540 nm). The fluorescence images were randomly obtained for 20 focal image planes where at least three liposomes were present. The diameter of each liposome was estimated by particle-analysis software (Aquacosmos Ver.2.6, Hamamatsu).

2.3. Cell-free protein synthesis with liposomes

A cell-free cytochrome b5 synthesis in the wheat germ cell-free kit was performed according to the instruction manual and developer's report (Sawasaki et al., 2002) with slight modifications. Substrate mixture (250 μl; PROTEIOS buffer #1 26.75 μl, buffer #2 31.25 μl, the 10 mM liposome solution 125 μl and RNase free water (Promega) 67 μl) and translation mixture (50 μl; RNase free water 1.8 μl, 10 mg ml^{-1} creatine kinase (Promega) 1.7 μl, buffer #2 2.0 μl, 40 U μl^{-1} RNase inhibitor

(Wako) 1.0 μl, 1.4 μg μl^{-1} cytochrome b5 mRNA 8.5 μl, wheat germ extract (PROTEIOS) 10 μl, and the liposome solution 25 μl), were prepared. Plasmid construction and mRNA preparation are described in the supporting information. The translation mixture was carefully set into the under layer of the substrate mixture in 96 wells of the titer plate and incubated at 26 °C for 24 h. In the case of EGFP-conjugated cytochrome b5, the translation reaction time course was measured with a 96-well plate reader (Wallac 1420 ARVOsx, Perkin-Elmer. The filter set adopted was F485 and F535 for excitation and emission, respectively.)

2.4. Fluorescence microscopic observation

An 8 μl amount of the liposomal solution with the synthesized EGFP-b5 was sealed between the glass slide (24 × 60 mm, No. 1, Matsunami) and the cover slip (18 × 18, No.1, Matsunami) by nail-lacquer (Topcoat, Daiso). The sample was observed using an inverted fluorescent microscope (Olympus IX-70) equipped with a objective lens (Olympus 100 × ; UPlanApo NA. 1.35) and band-pass filter (U-MGFPHQ) for EGFP observation. The images were obtained by through a highly sensitive CCD camera system (C4742-95, HAMAMATSU).

2.5. Purification of the cytochrome b_5 with liposome

The giant liposomes were isolated from the reaction solution by simplified discontinuous density-gradient centrifugation as follows. A 50 μl amount of the solution was carefully put on a 100 μl of the 0.3 M sucrose solution. After centrifugation at 15,000 × *g* for 15 min at 4 °C, precipitation was removed. 300 μl of buffer mix was carefully put on 60 μl of the supernatant. The sample was washed three times by centrifugation at 15,000 × *g* for 15 min at 4 °C with buffer mix. After acetone treatment for removing lipids, SDS-PAGE was performed, with staining by bio-safe coomasie blue (Bio-rad).

2.6. Analysis of the synthesized DHFR-conjugated cytochrome b_5 displayed on the liposome

DHFR activity assay was performed according to Widemann et al., 1999. Assay buffer A was 0.5 mol l^{-1} Tris buffer, pH 7.5. The purified EYPC liposomal sample was desalted by ultrafiltration (Microcon YM-3, Millipore) 15,000 × *g* for 15 min by buffer A 200 μl, three times. Stock solutions of dihydrofolate (FH_2, 25 mg in 1.5 ml of 2-mercaptoethanol and 6.0 ml of buffer A), NADPH (50 mg in 10 ml of buffer A) were stored at −80 °C. The NADPH/DHFR-b5-liposome reaction solution consisted of thawed 4 μl aliquot NADPH stock solutions and the DHFR-b5 displayed-liposome solutions (30, 20, 4 μl, mixed with buffer A to 0.5, 10.5, 26.5 μl), respectively. Each reaction solution was adjusted to 34.5 μl. The FH_2 reaction solution (78 μl) was added to 1 cm square cell. The sample was gently mixed by pipetting, after which the NADPH/DHFR-b_5-liposome reaction solution (30 μl) was added. The absorbance of each sample was read in the UV/vis spectrometer V-560 (JASCO) at room temperature at wavelengths of 340 nm with a reading interval of 20 s for a duration of 20 min. The relative enzyme activity was calculated from the slopes of obtained time cause data.

3. Results and discussion

Cell-free synthesis of EGFP-conjugated apo cytochrome b5 (EGFP-b5) was carried out with the wheat germ cell-free system in the presence of liposomes. The time course of the reaction was followed by EGFP fluorescence (Fig. 2). The final yields of proteins slightly increased in the presence of liposomes, though the rate of the reaction did not change much. Fig. 3 shows the fluorescence microscopic images of the reaction mixture of EGFP-b5 synthesis in the presence of giant liposomes. The image analysis supports the expressed EGFP-b5 proteins being attached primarily in the giant liposomal membranes.

The size distribution of the liposomes used in this study was evaluated by the fluorescence quenching method. Fig. 3b shows the size distribution of the liposomes loaded into the reaction mixture. The average mean diameters are as follows: EYPC, 4.2 μm; DOPC, 3.4 μm. The estimated mode values from the histograms are 2 μm for each. From the fluorescence microscopic images, significant differences in the liposome sizes and shapes were not observed under protein synthesis.

The giant liposomes can be easily isolated from the reaction mixture by simplified discontinuous density-gradient centrifugation, although the small-sized liposomes must be separated using gel-filtration. After centrifugation of the reaction mixture of EGFP-b5 in the presence of the giant liposomes, the pellets of liposome fractions were analyzed by SDS page (Fig. 4, comasie blue staining). In the liposomal fractions (Fig. 4b, lane 3 DOPC liposome, lane 4 eggPC), the b5 band was mainly observed. By the simplified density-gradient centrifugation method, the membrane protein, b5 could be easily purified from the reaction mixtures in the case of both DOPC and egg yolk PC liposomes. Similar results were obtained in the case of apo cytchrome b_5, which is not conjugated by EGFP (Fig. 4a, lane 3 DOPC liposome, lane 4 eggPC).

There are few reports that membrane proteins are directly reconstituted into the liposomal membrane by cell-free synthesis. Noireaux and Libchaber reported that a functional membrane protein of bacterial α-hemolysin was synthesized in the presence of giant liposomes by *E. coli* extract (Noireaux and Libchaber, 2004). Recently, we succeed in expressing and displaying mam-

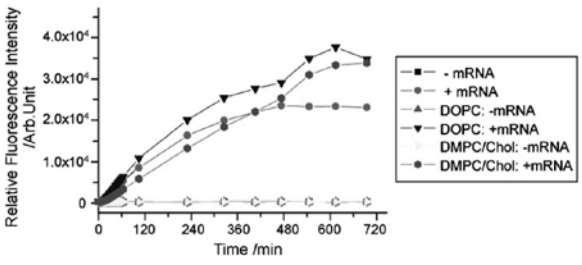

Fig. 2. Time course of the fluorescence intensity of the EGFP-conjugated apo cytochrome b5 *in vitro* translation reaction in the presence of liposomes.

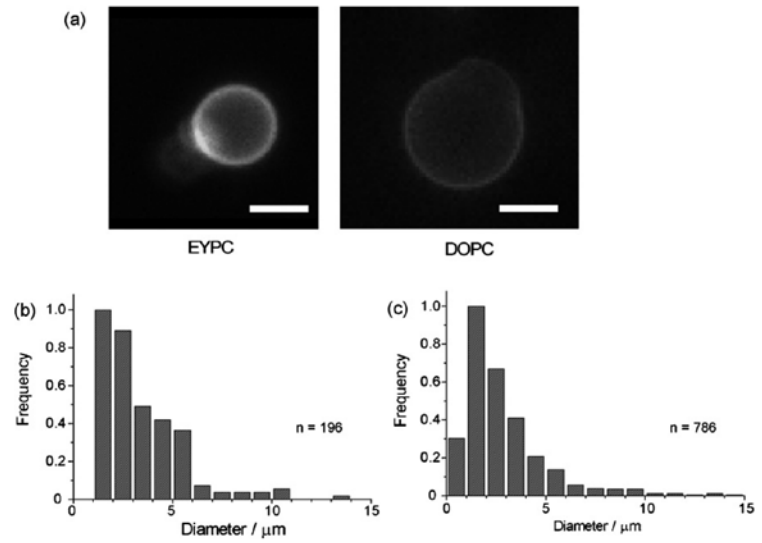

Fig. 3. (a) Fluorescence microscopic images of EGFP-b5 displaying giant liposomes. Left, EYPC; right, DOPC liposome. The high initial lipid concentration tends to make the polymorphic liposomes. Scale bar = 5 μm. (b) Size distribution of the liposomes loaded to the protein synthesis reaction solution. The frequency was normalized.

malian membrane protein connexin 43 into giant liposomes (unpublished result). In living systems, most mammalian membrane proteins are synthesized and folded at the microsomal membrane, assisting by a special complex called the "translocon" (Alder and Johnson, 2004). On the other hand, interaction between the bilayer membrane and membrane proteins has been widely discussed in the fields of molecular assembly (Owicki et al., 1978; White and von Heijne, 2005) and biosensor applications (Anrather et al., 2004; Cornell et al., 1997). Since membrane proteins are regarded as amphiphilic polymers, *in vitro* membrane proteins should directly interact with liposomes by hydrophobic interaction from the thermodynamic point of view. During the expression of b5 by the protein synthesis machinery, hydrophobic b5 may spontaneously interact with liposomes by hydrophobic interaction. Hanlon et al. (2000) reported that the membrane domain of b5 interacted to liposomes as trans-membrane type, not as hair-pinned membrane anchor type. The orientation and conformation of synthesized membrane proteins in the liposome are under investigation in our laboratory.

Presenting functional proteins on the membrane surface is of growing interest in nanobiotechnology (Kodadek, 2001; Predki, 2004; Fang et al., 2002). By using apo cytochrome b_5 as a hydrophobic tag, conjugated water soluble enzymes can be presented on the liposomal surface. To this end, cytochrome b_5 conjugated dihydrofolate reductase was synthesized by the same

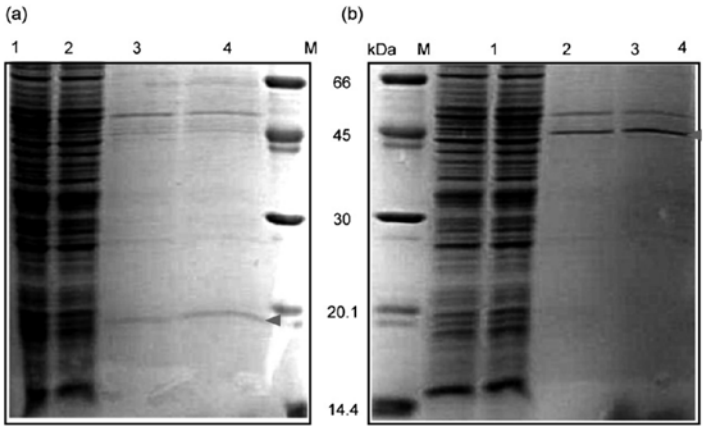

Fig. 4. SDS-PAGE analysis of *in vitro* translation of cytochrome b5 with liposomes. The gels were stained by coomassie brilliant blue. (a) Synthesized apo cytochrome b5. Lanes 1 and 3, before and after purification by simplified density-gradient centrifugation with DOPC liposomes. Lanes 2 and 4, with egg yolk PC liposomes. (b) Synthesized EGFP-conjugated apo cytochrome b5. Lanes 1 and 3, before and after purification with DOPC liposomes. Lanes 2 and 4, with egg yolk PC liposomes.

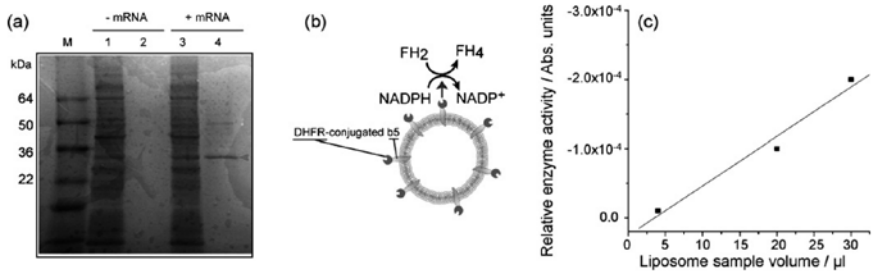

Fig. 5. DHFR-conjugated cytochromes b5 displayed on EYPC liposomes. (a) SDS-PAGE analysis. Lanes 1 and 3, before purification. Lanes 2 and 4, after the purification procedure without and with mRNA of b5. (b) Schematic illustration of the analysis of enzymatic activity of DHFR-conjugated b5 on liposomes. (c) Enzymatic activity of synthesized DHFR-conjugated apo cytochrome b_5 on liposomes. The values of relative enzyme activity were obtained from the 340 nm absorbance slopes of their time courses.

procedure. The pure proteo-liposome (made from EYPC) containing DHFR-conjugated b5 was isolated from the reaction solution by simplified discontinuous density-gradient centrifugation (Fig. 5a, lane 4). Synthesized b5 acts as a "hydrophobic tag" for recruitment to the liposome surface. Fig. 5b shows the schematic illustration for analyzing the DHFR enzyme activity assay. The assay is based on the conversion of dihydrofolate (FH_2) to tetrahydrofolate and the resulting oxidation of NADPH to $NADP^+$, which was monitored by measurement of the absorbance at 340 nm (Widemann et al., 1999). Fig. 5c shows the enzymatic activities of DHFR-conjugated cytochrome b5 at various concentrations of the reaction samples. This suggests that conjugated-DHFR is located in the native form on the liposome surface.

In conclusion, we present here a novel approach for salvaging nascent membrane proteins by cell-free synthesis with giant liposomes. The method also uses a hydrophobic tag for immobilization of the specific hydrophilic enzyme on the liposomal surface. These methods are useful for understanding the functions of membrane proteins and also for constructing realistic cell-models.

Acknowledgements

This research was supported by a grant from the Center of Excellence Program for Frontier Research on Molecular Destruction and Reconstruction of Tooth and Bone at Tokyo Medical and Dental University. This work was also supported by Grants-in-Aid for Scientific Research from the Japanese Government (Nos. 18GS0421, 18048013, 18048014). Pacific Edit reviewed the manuscript prior to submission.

Appendix A. Supplementary data

Supplementary data associated with this article can be found, in the online version, at doi:10.1016/j.jbiotec.2007.08.023.

References

Alder, N.N., Johnson, A.E., 2004. Cotranslational membrane protein biogenesis at the endoplasmic reticulum. J. Biol. Chem. 279, 22787–22790.

Anrather, D., Smetazko, M., Saba, M., Alguel, Y., Schalkhammer, T., 2004. Supported membrane nanodevices. J. Nanosci. Nanotech. 4 (1–2), 1–22.

Cornell, B.A., BraachMaksvytis, V.L.B., King, L.G., Osman, P.D.J., Raguse, B., Wieczorek, L., Pace, R.J., 1997. A biosensor that uses ion-channel switches. Nature 387 (6633), 580–583.

Elbaz, Y., Steiner-Mordoch, S., Danieli, T., Schuldiner, S., 2004. In vitro synthesis of fully functional EmrE, a multidrug transporter, and study of its oligomeric state. Proc. Natl. Acad. Sci. U.S.A. 101 (6), 1519–1524.

Endo, Y., Sawasaki, T., 2003. High-throughput, genome-scale protein production method based on the wheat germ cell-free expression system. Biotechnol. Adv. 21 (8), 695–713.

Fang, Y., Frutos, A.G., Lahiri, J., 2002. Membrane protein microarrays. J. Am. Chem. Soc. 124, 2394–2395.

Furukawa, H., Haga, T., 2000. Expression of functional M2 muscarinic acetylcholine receptor in *Escherichia coli*. J. Biochem. 127, 151–161.

Hanlon, M.R., Begum, R.R., Newbold, R.J., Whitford, D., Wallace, B.A., 2000. *In vitro* membrane-inserted conformation of the cytochrome b5 tail. Biochem. J. 352, 117–124.

Heginbotham, L., Kolmakova-Partensky, L., Miller, C., 1998. Functional reconstitution of a prokaryotic K^+ channel. J. Gen. Physiol. 111, 741–749.

Hotani, H., Inaba, T., Nomura, F., Takeda, S., Takiguchi, K., Itoh, T.J., Umeda, T., Ishijima, A., 2003. Mechanical analyses of morphological and topological transformation of liposomes. BioSystems 71, 93–100.

Ishihara, G., Goto, M., Saeki, M., Ito, K., Hori, T., Kigawa, T., Shirouzu, M., Yokoyama, S., 2005. Expression of G protein coupled receptors in a cell-free translational system using detergents and thioredoxin-fusion vectors. Protein Expr. Purif. 41 (1), 27–37.

Ishikawa, K., Sato, K., Shima, Y., Urabe, I., Yomo, T., 2004. Expression of a cascading genetic network within liposomes. FEBS Lett. 576, 387–390.

Klammt, C., Schwarz, D., Lohr, F., Schneider, B., Dotsch, V., Bernhard, F., 2006. Cell-free expression as an emerging technique for the large scale production of integral membrane protein. FEBS J. 273 (18), 4141–4153.

Kodadek, T., 2001. Protein microarrays: prospects and problems. Chem. Biol. 8 (2), 105–115.

Ladokhin, A.S., Wang, L., Steggles, A.W., Malak, H., Holloway, P.W., 1993. Fluorescence study of a temperature-induced conversion from the "Loose" to the "Tight" binding form of membrane-bound Cytochrome b5. Biochemistry 32, 6951–6956.

Luisi, P.L., Ferri, F., Stano, P., 2006. Approaches to semi-synthetic minimal cells: a review. Naturwissenschaften 93 (1), 1–13.

Luisi, P.L., Lasic, D.D., 2000. In: Luisi, P.L., Walde, P. (Eds.), Giant Vesicles, Perspectives in Supramolecular Chemistry. Wiley, Chichester, pp. 3–24.

Nakanishi, N., Takeuchi, F., Okamoto, H., Tamura, A., Hori, H., Tsubaki, M., 2006. Characterization of heme-coordinating histidyl residues of cytochrome b5 based on the reactivity with diethylpyrocarbonate: a mechanism for the opening of axial imidazole rings. J. Biochem. (Tokyo) 140, 561–571.

Nakano, H., Kawarasaki, Y., Yamane, T., 2004. Cell-free protein synthesis systems: increasing their performance and applications. Adv. Biochem. Eng. Biotechnol. 90, 135–149.

Noireaux, V., Libchaber, A., 2004. A vesicle bioreactor as a step toward an artificial cell assembly. Proc. Natl. Acad. Sci. U.S.A. 101 (51), 17669–17674.

Noireaux, V., Bar-Ziv, R., Godefroy, J., Salman, H., Libchaber, A., 2005. Toward an artificial cell based on gene expression in vesicles. Phys. Biol. 2 (3), 1–8.

Nomura, S.-i.M., Tsumoto, K., Hamada, T., Akiyoshi, K., Nakatani, Y., Yoshikawa, K., 2003. Gene expression within cell-sized lipid vesicles. ChemBioChem 4, 1172–1175.

Owicki, J.C., Springgate, M.W., McConnell, H.M., 1978. Theoretical study of protein–lipid interactions in bilayer membranes. Proc. Natl. Acad. Sci. U.S.A. 75, 1616–1619.

Predki, P.F., 2004. Functional protein microarrays: ripe for discovery. Curr. Opin. Chem. Biol. 8, 8–13.

Rigaud, J.-L., Pitard, B., Levy, D., 1995. Reconstitution of membrane proteins into liposomes: application to energy-transducing membrane proteins. Biochim. Biophys. Acta Bioenerg. 1231, 223–246.

Salvail, D., Cloutier, M., Rousseau, E., 2002. Functional reconstitution of an eicosanoid-modulated Cl-channel from bovine tracheal smooth muscle. Am. J. Physiol. Cell Physiol. 282, C567–C577.

Sawasaki, T., Hasegawa, Y., Tsuchimochi, M., Kamura, N., Ogasawara, T., Kuroita, T., Endo, Y., 2002. A bilayer cell-free protein synthesis system for high-throughput screening of gene products. FEBS Lett. 514, 102–105.

Shimizu, Y., Kuruma, Y., Ying, B.-W., Umekage, S., Ueda, T., 2006. Cell-free translation systems for protein engineering. FEBS J. 273, 4133–4140.

Spatz, L., Strittmatter, P., 1971. A form of cytochrome b5 that contains an additional hydrophobic sequence of 40 amino acid residures. Proc. Natl. Acad. Sci. U.S.A. 68, 1042–1046.

Szostak, J.W., Bartel, D.P., Luisi, P.L., 2001. Synthesizing life. Nature 409, 387–390.

Tsumoto, K., Nomura, S.-i.M., Nakatani, Y., Yoshikawa, K., 2001. Giant liposome as a biochemical reactor: transcription of DNA and transportation by laser tweezers. Langmuir 17 (23), 7225–7228.

Vinarov, D.A., Loushin Newman, C.L., Markley, J.L., 2006. Wheat germ cell-free platform for eukaryotic protein production. FEBS J. 273 (18), 4160–4169.

White, S.H., von Heijne, G., 2005. Transmembrane helices before, during, and after insertion. Curr. Opin. Struct. Biol. 15 (4), 378–386.

Widemann, B.C., Balis, F.M., Adamson, P.C., 1999. Dihydrofolate reductase enzyme inhibition assay for plasma methotrexate determination using a 96-well microplate reader. Clin. Chem. 45 (2), 223–228.

Yu, W., Sato, K., Wakabayashi, M., Nakaishi, T., Ko-mitamura, E.P., Shima, Y., Urabe, I., Yomo, T., 2001. Synthesis of functional protein in liposome. J. Biosci. Bioeng. 92, 590–593.

Yoshikawa, K., Nomura, S.-i., 2000. Toward the creation of an artificial cellular system. In: Kunitake, T., Nakahama, S., Takahashi, S., Toshima, N. (Eds.), Precision Polymers and Nano-Organized Systems. Kodansha, Tokyo, pp. 201–204.

Yubisui, T., Murakami, K., Takeshita, M., Takano, T., 1988. Purification by hydrophobic chromatography of soluble cytochrome b5 of human erythrocytes. Biochim. Biophys. Acta 936 (3), 447–451.

分子細胞遺伝学分野

稲澤 譲治

難治疾患研究所・遺伝疾患研究部門
分子細胞遺伝学・教授

1. 研究の課題名

研究課題

1. 癌のゲノム・エピゲノム解析:
2. 先天異常症、遺伝性疾患のゲノム解析
3. ゲノム情報に基づく癌と遺伝疾患の個別診断法の開発
4. ゲノムワイドDNAメチル化領域探索法の開発

邦文要約

パーソナルゲノム情報時代を迎えるにあたり、癌や生活習慣病において個々人に最適な予防、診断、治療法の開発と医療への応用において具体的な成果が強く望まれている。このような背景のもと、高密度・高精度BACアレイシステムを独自に構築した。 従来、数10キロベース（kb）~数メガベース（Mb）レベルのゲノムコピー数異常（Copy number aberration, CNA）を全染色体にわたり俯瞰的に検出するゲノム解析技術はなかった。これを克服するツールとしてヒトゲノムDNA BACクローンを搭載した高精度ゲノムアレイとその応用法を開発し、口腔領域を含む癌ならびに遺伝性疾患（主に多発奇形と精神発達遅滞の併発例:Multiple Congenital Anomalies and Mental Retardation, MCA/MR）の微細ゲノム異常を探索し、見出された特異的異常を指標に疾患関連遺伝子の同定を進めてきた。

1. Development of innovative techniques for genomics and/or epigenomics

   Standard CGH to metaphase chromosomes can provide only limited resolution: 5-10 Mb for detection of copy-number losses and gains, and 2Mb for amplifications. To circumvent this limitation, we have also constructed different types of BAC-based CGH-arrays（so-called MCG array series）as follows,（1）MCG Whole Genome Array-4500,（2）MCG Cancer Array-800,（3）MCG 1p36 Contig Array,（4）MCG X-tiling array, and（5）MCG Genome Disorder（GD）Array. In addition, we recently constructed a new type BAC-array, so called, Genome Variation（GV）array, which enables us to investigate copy number variation（CNV）at 677 loci throughout the human genome.

2. Identification of cancer-related genes within genomic aberrations detected by array-CGH

   We recently identified cancer-related genes upregulated by a gene amplification mechanism as follows, CDK6 in gastric cancer, CCND3 in liver metastatic colon cancer, and DUSP 26 in anaplastic thyroid carcinoma within the novel amplifications, that emerged via in-house BAC-array platform. Moreover, we recently detected submicroscopic homozygous deletions in many types of cancers, and within those as the landmarks for positional cloning of tumor suppressor genes（TSGs）we could identify novel candidate TSGs including LRP1B in ESCC, DBC1 and PCDH20 in non-small cell lung cancer, ADAM23 and VLDLR in gastric cancer, and RGC32 in malignant glioma. Some of those genes are also epigenetically silenced due to the promoter CpG island methylation in some GCs. In addition, recently, we successfully identified tumor suppressive microRNA by DNA hypermethylation in oral cancer.

3. Establishment of applications for array-CGH

   To accomplish genome-wide screening for methylated sites in the whole genome, we have combined array-CGH with methylated CpG-island amplification（MCA）. Our BAC array-based MCA（BAMCA）method not only allows us to explore methylated CpG sites within spotted BACs. If we apply BAMCA to a tiling-resolution CGH-array, methylated CpG sites emerge on an array platform throughout the entire genome. Recently, by

using this BAMCA method, we identified candidate tumor suppressors, NR1I2 and PTGER2 in advanced type neuroblastomas (NBs), and CEABP1 in ESCC. In addition, a combination of chromatin immunoprecipitation (ChIP) assays with hybridization to DNA arrays, the so-called "ChIP-on-chips" technique, has proven to be a powerful way to explore sites of interaction among DNA-binding proteins across the entire genome.

4. Molecular cytogenetic investigation of genomic disorders

Array CGH is also one of the most powerful tools to detect cryptic chromosome copy number aberrations (CNA) in genomic disorders including multiple congenital anomalies and mental retardation (MCA/MR). We found a causally related pathogenic CAN in 51 (10.2%) out of 499 patients with MCA/MR by MCG GD-Array. Furthermore, we performed X-tiling array analysis in 140 families with possible X-linked MR and found pathogenic CNAs in 9 (6.4%) of those patients.

2.

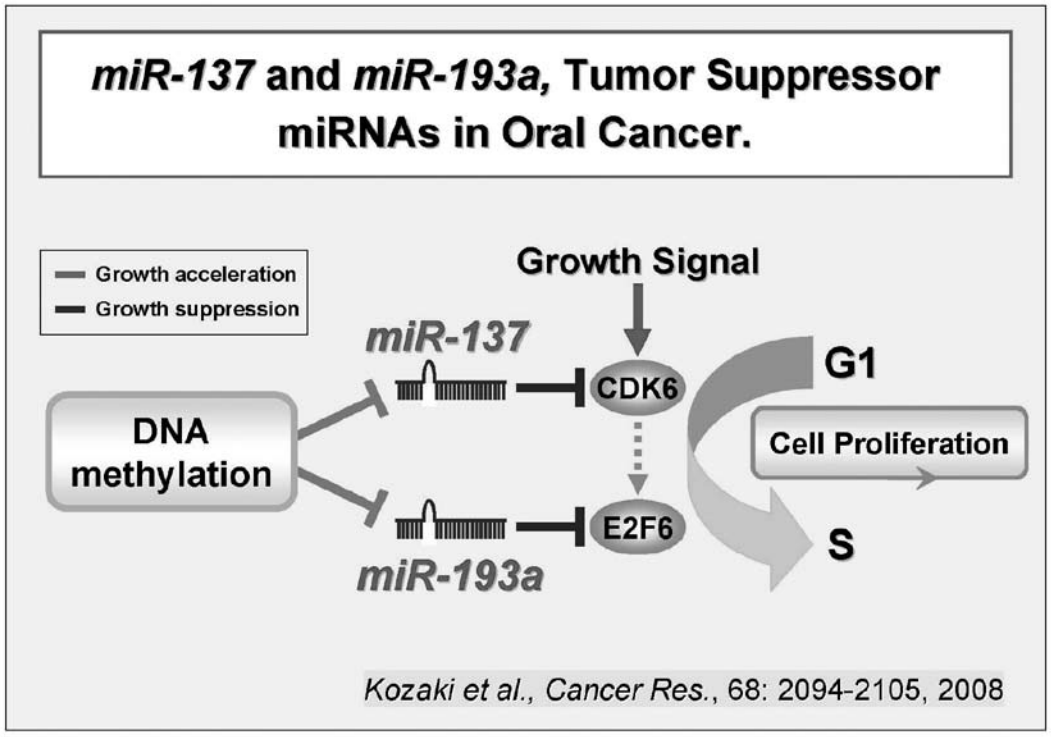

3. 2008年、2009年（平成21年3月までの）に発表した全ての研究内容についての英文要約

1. Iriyama T, Takeda K, Nakamura H, Motimoto Y, Kuroiwa T, Mizukami J, Umeda T, Noguchi T, Naguro I, Nishitoh H, Saegusa K, Tobiume K, Homma T, Shimada Y, Tsuda H, Aiko S, Imoto I, Inazawa J, Chiba K, Kamei Y, Kozuma S, Taketani Y, Matsuzawa A, Ichijo H: ASK1 amd ASK2 differentially regulate the counteracting roles of apoptosis and inflammation in tumorigenesis .EMBO J. 2009 [Epub ahead of print]

Apoptosis and inflammation generally exert opposite effects on tumorigenesis: apoptosis serves as a barrier to tumour initiation, whereas inflammation promotes tumorigenesis. Although both events are induced by various common stressors, relatively little is known about the stress-induced signalling pathways regulating these events in tumorigenesis. Here, we show that stress-activated MAP3Ks, ASK1 and ASK2, which are involved in cellular responses to various stressors such as reactive oxygen species, differentially regulate the initiation and promotion of tumorigenesis. ASK2 in cooperation with ASK1 functioned as a tumour suppressor by exerting proapoptotic activity in epithelial cells, which was consistent with the reduction in ASK2 expression in human cancer cells and tissues. In contrast, ASK1-dependent cytokine production in inflammatory cells promoted tumorigenesis. Our findings suggest that ASK1 and ASK2 are critically involved in tumorigenesis by differentially regulating apoptosis and inflammation.

2. Yamamoto S, Tsuda H, Honda K, Onozato K, Takano M, Tamai S, Imoto I, Inazawa J, Yamada T, Matsubara

O. Actinin-4 gene amplification in ovarian cancer. a candidate oncogene associated with poor patient prognosis and tumor chemoresistance. Mod Pathol. 2009 [Epub ahead of print]

Actinin-4, an isoform of non-muscular alpha-actinin, enhances cell motility by bundling the actin cytoskeleton. We previously reported a prognostic implication of high immunohistochemical expression of actinin-4 protein in ovarian cancers. Chromosomal gain or amplification of the 19q12-q13 region has been reported in ovarian cancer. We hypothesized that the actinin-4 (ACTN4) gene might be a target of the 19q12-q13 amplicon and play an essential role of ovarian cancer progression. In total, 136 advanced-stage ovarian cancers were investigated for the copy number of the ACTN4 gene on chromosome 19q13, using fluorescence in situ hybridization, and the correlation of the ACTN4 copy number with actinin-4 protein immunoreactivity and major clinicopathological factors was investigated. A higher copy number (>==4 copies) of the ACTN4 gene was detected in 29 (21%) cases and was highly associated with the intensity of actinin-4 immunoreactivity (P<0.0001), a high histological tumor grade (P=0.030), a clear-cell adenocarcinoma histology (P=0.012), resistance to first-line chemotherapies (P=0.028), and poor patient outcome (P=0.0011). Univariate analyses using the Cox regression model showed that a higher ACTN4 gene copy number was able to predict patient outcome more accurately than high actinin-4 immunoreactivity (relative risk: 2.48 vs 1.55). Multivariate analysis showed that a higher copy number of the ACTN4 gene and the degree of residual disease were independent prognostic factors for overall patient survival. The actinin-4 gene may be a target of the 19q amplicon, acting as a candidate oncogene, and serve as a predictor of poor outcome and tumor chemoresistance in patients with advanced-stage ovarian cancers.

3. Kawase T, Ohki R, Shibata T, Tsutsumi S, Kamimura N, Inazawa J, Ohta T, Ichikawa H, Aburatani H, Tashiro F, Taya Y . PH domain-only protein PHLDA3 is a p53-regulated repressor of akt. Cell 136:535-50,2009

p53 And Akt are critical players regulating tumorigenesis with opposite effects: whereas p53 transactivates target genes to exert its function as a tumor suppressor, Akt phosphorylates its substrates and transduces downstream survival signals. In addition, p53 and Akt negatively regulate each other to balance survival and death signals within a cell. We now identify PHLDA3 as a p53 target gene that encodes a PH domain-only protein. We find that PHLDA3 competes with the PH domain of Akt for binding of membrane lipids, thereby inhibiting Akt translocation to the cellular membrane and activation. Ablation of endogenous PHLDA3 results in enhanced Akt activity and decrease of p53-dependent apoptosis. We also demonstrate the suppression of anchorage-independent cell growth by PHLDA3. Loss of the PHLDA3 genomic locus was frequently observed in primary lung cancers, suggesting a role of PHLDA3 in tumor suppression. Our results reveal a new mode of coordination between the p53 and Akt pathways.

4. Arai E, Ushijima S, Fujimoto H, Hosoda F, Shibata T, Kondo T, Yokoi S, Imoto I, Inazawa J, Hirohashi S, Kanai Y. Genome-wide DNA methylation profiles in both precancerous conditions and clear cell renal cell carcinomas are correlated with malignant potential and patient outcome. Carcinoqenesis 99:1940-9, 2009.

To clarify genome-wide DNA methylation profiles during multistage renal carcinogenesis, bacterial artificial chromosome array-based methylated CpG island amplification (BAMCA) was performed. Non-cancerous renal cortex tissue obtained from patients with clear cell renal cell carcinomas (RCCs) (N) was at the precancerous stage where DNA hypomethylation and DNA hypermethylation on multiple bacterial artificial chromosome (BAC) clones were observed. By unsupervised hierarchical clustering analysis based on BAMCA data for their N, 51 patients with clear cell RCCs were clustered into two subclasses, Clusters A (N) (n = 46) and B (N) (n = 5). Clinicopathologically aggressive clear cell RCCs were accumulated in Cluster B (N), and the overall survival rate of patients in Cluster B (N) was significantly lower than that of patients in Cluster A (N). By unsupervised hierarchical clustering analysis based on BAMCA data for their RCCs, 51 patients were clustered into two subclasses, Clusters A (T) (n = 43) and B (T) (n = 8). Clinicopathologically aggressive clear cell RCCs were accumulated in Cluster B (T), and the overall survival rate of patients in Cluster B (T) was significantly lower than that of patients in Cluster A (T). Multivariate analysis revealed that belonging to Cluster B (T) was an independent predictor of recurrence. Cluster B (N) was completely included in Cluster B (T), and the majority of the BAC clones that significantly discriminated Cluster B (N) from Cluster A (N) also discriminated Cluster B (T) from Cluster A (T). In individual patients, DNA methylation status in N was basically inherited by the corresponding clear cell RCC. DNA methylation alterations in the precancerous stage

may generate more malignant clear cell RCCs and determine patient outcome.

5. Takahata M, Inoue Y, Tsuda H, Imoto I, Koinuma D, Hayashi M, Ichikura T, Yamori T, Nagasaki K, Yoshida M, Matsuoka M, Morishita K, Yuki K, Hanyu A, Miyazawa K, Inazawa J, Miyazono K, Imamura T. SKI and MEL1 cooperate to inhibit transforming growth factor-beta signal in gastric cancer cells. J Biol Chem. 284:3334-44, 2008.

   Chromosomal amplification occurs frequently in solid tumors and is associated with poor prognosis. Several reports demonstrated the cooperative effects of oncogenic factors in the same amplicon during cancer development. However, the functional correlation between the factors remains unclear. Transforming growth factor（TGF）-beta signaling plays important roles in cytostasis and normal epithelium differentiation, and alterations in TGF-beta signaling have been identified in many malignancies. Here, we demonstrated that transcriptional co-repressors of TGF-beta signaling, SKI and MDS1/EVI1-like gene 1（MEL1）, were aberrantly expressed in MKN28 gastric cancer cells by chromosomal co-amplification of 1p36.32. SKI and MEL1 knockdown synergistically restored TGF-beta responsiveness in MKN28 cells and reduced tumor growth in vivo. MEL1 interacted with SKI and inhibited TGF-beta signaling by stabilizing the inactive Smad3-SKI complex on the promoter of TGF-beta target genes. These findings reveal a novel mechanism where distinct transcriptional co-repressors are co-amplified and functionally interact, and provide molecular targets for gastric cancer treatment

6. Ishihara T, Tsuda H, Hotta A, Kozaki K, Yoshida A, Jaeduk Yoshimura Noh, Ito K, Imoto I, Inazawa J. ITCH is a putative target for a novel 20q11.22 amplification detected in anaplastic thyroid carcinoma cells by array-based comparative genomic hybridization. Cancer Sci.99:1940-49, 2008

   Anaplastic thyroid carcinoma（ATC）is one of the most virulent of all human malignancies, with a mean survival time among patients of less than 1 year after diagnosis. To date, however, cytogenetic information on this disease has been very limited. During the course of a program to screen a panel of ATC cell lines for genomic copy-number aberrations using array-based comparative genomic hybridization, we identified a high-level amplification of the ITCH gene, which is mapped to 20q11.22 and belongs to the homologous to the E6-associated protein carboxylterminus ubiquitin ligase family. The expression of ITCH was increased in 4 of 14 ATC cell lines（28.6%）, including 8305C in which there was a copy-number amplification of this gene, and six of seven primary cases（85.7%）. Among the primary thyroid tumors, a considerable number of ITCH high expressers was found in ATC（40/45, 88.9%）, papillary thyroid carcinoma（25/25, 100%）, and papillary microcarcinoma（25/25, 100%）. Furthermore, knockdown of ITCH by specific small interfering RNA significantly inhibited the growth of ITCH-overexpressing cells, whereas ectopic overexpression of ITCH promoted growth of ATC cell lines with relatively weak expression. These observations indicate ITCH to be the most likely target for 20q11.22 amplification and to play a crucial role in the progression of thyroid carcinoma.

7. Hayashi S, Okamoto N, Makita Y, Hata A, Imoto I, Inazawa J. Heterozygous Deletion at 14q22.1-q22.3 including the BMP4 gene in a patient with psychomotor retardation, congenital corneal opacity and feet polysyndactyly. Am J Med Genet A.146A:2905-10, 2008

   Here we report on a 1-year-old Japanese girl with psychomotor retardation, bilateral congenital corneal opacity and bilateral postaxial polysyndactyly of the feet. Although she had a normal female karyotype, our in-house bacterial artificial chromosome（BAC）-based array-CGH analysis successfully detected at least a 2.7-Mb heterozygous deletion at 14q22.1-q22.3 harboring 18 protein-coding genes. Among the genes, BMP4 was a candidate for the gene causing the abnormalities of both the eye and digits. It was previously reported that the BMP family was correlated with the morphogenesis of digits and ocular development, and Bmp4 heterozygous null mice revealed skeletal abnormalities including polydactyly and ocular anterior segment abnormalities. Patients with a deletion including BMP4 also hadabnormalities of the eye and digits. These previous reports support that a haplo-insufficiency of the BMP4 gene likely caused the congenital ocular and digit abnormalities. Moreover, among the other genes contained in the deletion, GMFB is a candidate for the gene responsible for the psychomotor retardation.

8. Arai E, Ushijima S, Tsuda H, Fujimoto H, Hosoda F, Shibata T, Kondo T, Imoto I, Inazawa J, Hirohashi S, Kanai Y. Genetic clustering of clear cell renal cell carcinoma based on array-comparative genomic hybridization. its association with DNA methylation alteration and patient outcome. Clin Cancer Res. 14:5531-9, 2008

PURPOSE: The aim of this study was to clarify genetic and epigenetic alterations occurring during renal carcinogenesis. EXPERIMENTAL DESIGN: Copy number alterations were examined by array-based comparative genomic hybridization analysis using an array harboring 4,361 bacterial artificial chromosome clones, and DNA methylation alterations on CpG islands of the p16, human MutL homologue 1, von Hippel-Lindau, and thrombospondin 1 genes and the methylated in tumor (MINT-1, MINT-2, MINT-12, MINT-25, and MINT-31) clones were examined in 51 clear cell renal cell carcinomas (RCC). RESULTS: By unsupervised hierarchical clustering analysis based on copy number alterations, clear cell RCCs were clustered into the two subclasses, clusters A (n=34) and B (n=17). Copy number alterations were accumulated in cluster B. Loss of chromosome 3p and gain of 5q and 7 were frequent in both clusters A and B, whereas loss of 1p, 4, 9, 13q, and 14q was frequent only in cluster B. The average number of methylated CpG islands in cluster B was significantly higher than those in cluster A. Clear cell RCCs showing higher histologic grades, vascular involvement, renal vein tumor thrombi, and higher pathologic stages were accumulated in cluster B. The recurrence-free and overall survival rates of patients in cluster B were significantly lower than those of patients in cluster A. Multivariate analysis revealed that genetic clustering was a predictor of recurrence-free survival and was independent of histologic grade and pathologic stage. CONCLUSIONS: This genetic clustering of clear cell RCC is significantly associated with regional DNA hypermethylation and may become a prognostic indicator for patients with RCC.

9. Kikuchi S, Honda K, Tsuda H, Hiraoka N, Imoto I, Kosuge T, Umaki T, Onozato K, Shitashige M, Yamaguchi U, Ono M, Tsuchida A, Aoki T, Inazawa J,Hirohashi S, Yamada T. Expression and gene amplification of actinin-4 in invasive ductal carcinoma of the pancreas. Clin Cancer Res.14:5348-56, 2008

PURPOSE: An invasive growth pattern is one of the hallmarks of pancreatic ductal carcinoma. Actinin-4 is an actin-binding protein associated with enhanced cell motility, invasive growth, and lymph node metastasis. Actinin-4 might play an important role in the development and progression of pancreatic cancer. EXPERIMENTAL DESIGN: The expression of actinin-4 was examined immunohistochemically in 173 cases of invasive pancreatic ductal carcinoma. The copy number of the actinin-4 (ACTN4) gene was calculated by fluorescence in situ hybridization. The expression of actinin-4 was stably knocked down by short hairpin RNA, and tumorigenicity was evaluated by orthotopic implantation into mice with severe combined immunodeficiency. RESULTS: The expression level of actinin-4 was increased in 109 (63.0%) of 173 cases of pancreatic cancer. Kaplan-Meier survival curves revealed that patients with increased expression of actinin-4 had a significantly poorer outcome (P=0.00001, log-rank test). Multivariate analysis by the Cox proportional hazard model showed that high expression of actinin-4 was the most significant independent negative predictor of survival (hazard ratio, 2.33; P=0.000009). Amplification (defined as more than four copies per interphase nucleus) of the ACTN4 gene was detected in 11 (37.9%) of 29 cases showing increased expression of actinin-4. Knockdown of actinin-4 expression inhibited the destructive growth of cancer cells in the pancreatic parenchyma. CONCLUSION: Recurrent amplification of chromosome 19q13.1-2 has been reported in pancreatic cancer, but the exact target gene has not been identified. Actinin-4 contributes to the invasive growth of pancreatic ductal carcinoma, and ACTN4 is one of the candidate oncogenes in this chromosome locus.

10. Katsuki Y, Nakada S, Yokoyama T, Imoto I, Inazawa J, Nagasawa M, Mizutani S. Caffeine yields aneuploidy through asymmetrical cell division caused by misalignment of chromosomes. Cancer Sci.99:1539-45, 2008

Aneuploidy has been implicated as an important step leading to various neoplasias. Although genetic factors that block aneuploidy have been the subject of intense interest, the impact of pharmacological and environmental substances on the development of aneuploidy has not been studied. Here, we show that caffeine induces aneuploidy through asymmetrical cell division. Mitotic exits of HeLa, U2OS, and primary fibroblast cells were significantly delayed by 10 mmol/L caffeine. Most caffeine-treated mitotic cells showed misalignment of chromosomes at the metaphase plates, and were arrested at prometaphase. Mitoticarrest deficient 2 (MAD2) depletion rescued the caffeine-induced delay of mitotic exit, indicating that caffeine-induced prolongation of mitosis was caused by activation of a MAD2-dependent spindle checkpoint. Enumeration of centromeres by fluorescence in situ hybridization revealed that cell division in the presence of caffeine was not symmetrical and resulted in aneuploid cell production. Most of these cells survived and underwent DNA synthesis. Our findings reveal a novel pharmacological effect of a high concentration of caffeine on genomic stability in dividing cells.

11. Hayashi S, Mizuno S, Migita O, Okuyama T, Makita Y, Hata A, Imoto I, Inazawa J. The CASK gene harbored in a deletion detected by Array-CGH as a potential candidate for a gene causative of X-linked dominant mental retardation. Am J Med Genet A.146A:2145-51, 2008

Here we report on a 5-year-old Japanese girl with developmental delay and microcephaly. Although she had a normal karyotype, a bacterial artificial chromosome-based array-comparative genome hybridization analysis detected a de novo 4.0-Mb heterozygous deletion at Xp11.3-p11.4 harboring nine genes. By comparison with a healthy carrier mother of a boy with atypical Norrie disease having a smaller deletion in the same region, we excluded four genes as candidates whose haploinsufficiency would be causative for developmental delay. Among the other five genes, CASK seems to be the most likely candidate for a causative gene, because it is strongly expressed in fetal brain and plays important roles in neural development and synaptic function. We confirmed that the expression of CASK mRNA was decreased in the patient compared with healthy controls and the patient's X-chromosomal inactivation was not skewed. These results suggested that the genetic deletion of CASK results in haploinsufficiency, which might be causative for the patient's developmental delay or mental retardation.

12. Nakajima T, Yasui K, Zen K, Inagaki Y, Fujii H, Minami M, Tanaka S, Taniwaki M, Itoh Y, Arii S, Inazawa J, Okanoue T. Activation of B-Myb by E2F1 in hepatocellular carcinoma. Hepatol Res.38:886-95, 2008

Aim: Deregulation of E2F1 transcriptional activity is observed in a variety of cancers, including hepatocellular carcinoma (HCC). The aim of the present study is to identify transcriptional target genes of E2F1 in HCC. Methods: We determined expression levels for E2F1 and ten candidate genes thought to be targets of E2F1 in primary HCCs using a real-time quantitative reverse transcription-PCR assay. Following small interfering RNA (siRNA) -mediated knockdown of E2F1 in HCC cell lines, we quantified mRNA levels of the candidate E2F1 target genes. Results: E2F1 was significantly over-expressed in 41 primary HCCs as compared to non-tumorous liver tissues. Among the candidates, MYBL2, whose product is the transcriptional factor B-Myb, which is involved in controlling cell-cycle progression and apoptosis, was significantly over-expressed in primary HCCs. Additionally, expression levels of MYBL2 correlated with those of E2F1. Knockdown of E2F1 resulted in a decrease in expression of MYBL2. A copy-number gain for MYBL2 was observed in 36 of 66 primary HCCs, suggesting that MYBL2 expression is up-regulated by amplification in addition to being regulated by E2F1. Moreover, siRNA-mediated knockdown of MYBL2 led to reduced expression of CDC2 (which encodes CDC2), cyclin A2 (CCNA2), and topoisomerase II alpha (TOP2A), implicating these genes in the cell cycle and suggesting that they may be downstream targets of B-Myb. Conclusion: MYBL2 is a probable transcriptional target of E2F1 in HCC and may therefore be a useful biomarker for diagnosis and an attractive target for molecular therapies useful to treat HCC.

13. Qi S, Mogi S, Tsuda H, Tanaka Y, Kozaki K, Imoto I, Inazawa J, Hasegawa S, Omura K. Expression of cIAP-1 correlates with nodal metastasis in squamous cell carcinoma of the tongue. Int J Oral Maxillofac Surg.37:1047-53, 2008

Cellular inhibitor-of-apoptosis protein 1 (cIAP-1) is a member of the inhibitor-of- apoptosis protein family, which predominantly regulates apoptosis. It has been suggested that expression of cIAP-1 correlates with certain clinicopathological features. The possible significance of cIAP-1 expression in cervical lymph node metastasis of tongue squamous cell carcinoma (SCC) is investigated. Seventy-five tongue SCCs were analyzed by immunohistochemistry. cIAP-1 immunoreactivity patterns were nuclear in 38 (51%), cytoplasmic in 47 (63%), and concurrent in 37 (49%) cases. Nuclear, cytoplasmic and concurrent cIAP-1 immunoreactions were significantly correlated with lymph node metastasis in tongue SCCs (P=0.0011, 0.0012, and 0.0006, respectively). The cleaved caspase-3, which is a marker of tumor apoptosis, and Ki-67 index, which is a marker of tumor proliferation, were immunohistochemically examined in 21 tongue SCCs with concurrent nuclear and cytoplasmic cIAP-1 expression and with metastasis, and in 23 tongue SCCs without concurrent nuclear and cytoplasmic cIAP-1 expression and without metastasis. Concurrent cIAP-1 expression was inversely correlated with caspase-3 (P=0.0066), but was positively correlated with Ki-67 expression (P=0.0028). The mode of invasion was associated with lymph node metastasis (P=0.014) and differentiation (P=0.013), but was not correlated with cIAP-1 expression. There was no statistically significant correlation between nuclear or cytoplasmic cIAP-1 expression and the clinicopathological factors of gender, age, clinical stage or differentiation. These results suggest that both patterns of cIAP-1 are useful markers for predicting cervical lymph node metastasis in tongue SCC.

14. Kikuchi R, Tsuda H, Kozaki K, Kanai Y, Kasamatsu T,

Sengoku K, Hirohashi S, Inazawa J, Imoto I. Frequent inactivation of a putative conditional tumor-suppressor gene, angiopoietin-like protein 2, in ovarian cancer. Cancer Res.68:5067-75, 2008

Angiopoietin-like protein 2 (ANGPTL2) is a secreted protein belonging to the angiopoietin family, the members of which are implicated in various biological processes, although its receptor remains unknown. We identified a homozygous loss of ANGPTL2 (9q33.3) in the course of screening a panel of ovarian cancer (OC) cell lines for genomic copy-number aberrations using in-house array-based comparative genomic hybridization. ANGPTL2 mRNA expression was observed in normal ovarian tissue and immortalized normal ovarian epithelial cells, but was reduced in some OC lines without its homozygous deletion (18 of 23 lines) and restored after treatment with 5-aza 2'-deoxycytidine. The methylation status of sequences around the ANGPTL2 CpG-island with clear promoter activity inversely correlated with expression. ANGPTL2 methylation was frequently observed in primary OC tissues as well. In an immunohistochemical analysis of primary OCs, ANGPTL2 expression was frequently reduced (51 of 100 cases), and inversely correlated with methylation status. Patients with OC showing reduced ANGPTL2 immunoreactivity had significantly worse survival in the earlier stages (stages I and II), but better survival in advanced stages (stages III and IV). The restoration of ANGPTL2 expression or treatment with conditioned medium containing ANGPTL2 inhibited the growth of OC cells originally lacking the expression of this gene, whereas the knockdown of endogenous ANGPTL2 accelerated the growth of OC cells with the expression of ANGPTL2. These results suggest that, at least partly, epigenetic silencing by hypermethylation of the ANGPTL2 promoter leads to a loss of ANGPTL2 function, which may be a factor in the carcinogenesis of OC in a stage-dependent manner.

15. Nakamura E, Kozaki K, Tsuda H, Suzuki, E, Pimkhaokham A, Yamamoto G, Irie T, Tachikawa T, Amagasa T, Inazawa J, Imoto I. Frequent silencing of a putative tumor suppressor gene melatonin receptor 1A (MTNR1A) in oral squamous-cell carcinoma. Cancer Sci.99:1390-400, 2008

Array-based comparative genomic hybridization (array-CGH) has good potential for the high-throughput identification of genetic aberrations in cell genomes. In the course of a program to screen a panel of 21 oral squamous-cell carcinoma (OSCC) cell lines for genome-wide copy-number aberrations by array-CGH using our in-house bacterial artificial chromosome arrays, we identified a frequent homozygous deletion at 4q35 loci with approximately 1 Mb in extent. Among the seven genes located within this region, the expression of the melatonin receptor 1 A (MTNR1A) messenger RNA (mRNA) was not detected or decreased in 35 out of the 39 (89%) OSCC cell lines, but was detected in immortalized normal oral epithelial cell line, and was restored in gene-silenced OSCC cells without its homozygous loss after treatment with 5-aza-2'-deoxycytidine. The hypermethylation of the CpG (cytosine and guanine separated by phosphate) island in the promoter region of MTNR1A was inversely correlated with its expression in OSCC lines without a homozygous deletion. Methylation of this CpG island was also observed in primary OSCC tissues. In an immunohistochemical analysis of 50 primary OSCC tumors, the absence of immunoreactive MTNR1A was significantly associated with tumor size and a shorter overall survival in patients with OSCC tumors, and seems to be an independent prognosticator in a multivariate analysis. Exogenous restoration of MTNR1A expression inhibited the growth of OSCC cells lacking its expression. Together with the known tumor-suppressive function of melatonin and MTNR1A in various tumors, our results indicate MTNR1A to be the most likely target for epigenetic silencing at 4q35 and to play a pivotal role during oral carcinogenesis.

16. Kozaki K, Imoto I, Mogi S, Omura K, Inazawa J. Exploration of tumor-suppressive microRNAs silenced by DNA hypermethylation in oral cancer. Cancer Res. 68:2094-2105, 2008

In the last few years, microRNAs (miRNA) have started a revolution in molecular biology and emerged as key players in the carcinogenesis. They have been identified in various tumor types, showing that different sets of miRNAs are usually deregulated in different cancers. To identify the miRNA signature that was specific for oral squamous cell carcinoma (OSCC), we first examined expression profiles of 148 miRNAs in a panel of 18 OSCC cell lines and the immortalized oral keratinocyte line RT7 as a control. Compared with RT7, the expression of 54 miRNAs (36.5%) was frequently down-regulated in OSCC lines (<0.5-fold expression, >or=66.7% of 18 lines). Among these 54 miRNAs, we further analyzed four of these miRNAs (i.e., miR-34b, miR-137, miR-193a, and miR-203), located around CpG islands, to identify tumor-suppressive miRNAs silenced through aberrant DNA methylation. The expression of those four genes was restored by treatment with 5-aza-2'-deoxycytidine in OSCC cells lacking their expression.

In addition, expression levels of the four miRNAs were inversely correlated with their DNA methylation status in the OSCC lines. In primary tumors of OSCC with paired normal oral mucosa, down-regulation of miRNA expression through tumor-specific hypermethylation was more frequently observed for miR-137 and miR-193a than for miR-34b and miR-203. Moreover, the ectopic transfection of miR-137 or miR-193a into OSCC lines lacking their expressions significantly reduced cell growth, with down-regulation of the translation of cyclin-dependent kinase 6 or E2F transcription factor 6, respectively. Taken together, our results clearly show that miR-137 and miR-193a are tumor suppressor miRNAs epigenetically silenced during oral carcinogenesis.

17. Suzuki A, Shibata T, Murakami Y, Horii A, Shiratori K, Hirohashi S, Inazawa J, Imoto I. Identification of SMURF1 as a possible target for 7q21.3-22.1 amplification detected in a pancreatic cancer cell line by in-house array-based comparative genomic hybridization. Cancer Sci.99:986-94, 2008

Pancreatic cancer (PC) cell lines provide a useful starting point for the discovery and functional analysis of genes driving the genesis and progression of this lethal cancer. To increase our understanding of the gene copy number changes in pancreatic carcinomas and to identify key amplification and deletion targets, we applied genome-wide array-based comparative genomic hybridization using in-house array (MCG Cancer Array-800) to 24 PC cell lines. Overall, the analyses revealed high genomic complexity, with several copy number changes detected in each line. Homozygous deletions (log (2) ratio < -2) of eight genes (clones) were seen in 14 of the 24 cell lines, whereas high-level amplifications (log (2) ratio > 2) of 10 genes (clones) were detected in seven lines. Among them, we focused on high-level amplification at 7q22.1, because target genes for this alteration remain unknown. Through precise mapping of the altered region by fluorescence in situ hybridization, determination of the expression status of genes located within those regions, and functional analysis using knockdown of the gene expression or the ectopic overexpression approach in PC cell lines, as well as immunohistochemical analyses of candidates in primary tumors of PC, we successfully identified SMURF1 as having the greatest potential as a 7q21.3-22.1 amplification target. SMURF1 may work as a growth-promoting gene in PC through overexpression and might be a good candidate as a therapeutic target. Our results suggest that array-based comparative genomic hybridization analysis combined with further genetic and functional examinations is a useful approach for identifying novel tumor-associated genes involved in the pathogenesis of this lethal disease.

18. Tanaka S, Arii S, Yasen M, Moqushi K, Su NT, Zhao C, Imoto I, Eishi Y, Inazawa J, Miki Y, Tanaka H. Aurora kinase B is a predictive factor for the aggressive recurrence of hepatocellular carcinoma after curative hepatectomy. Br J Surg.95:611-619, 2008

BACKGROUND: Patterns of cancer recurrence hold the key to prognosis after curative resection. This retrospective study aimed to identify a predictor and therapeutic candidate for aggressive recurrence of hepatocellular carcinoma (HCC). METHODS: Primary HCC tissues from 107 patients who had curative resection were analysed. Genome-wide gene expression profiles were investigated using a microarray technique, and clustering analysis was carried out based on the first diagnosis of recurrence according to the Milan criteria. Immunohistochemical expression and array-based comparative genomic hybridization (array-CGH) were also assessed. RESULTS: Microarray analysis revealed overexpression of Aurora kinase B, a chromosome passenger protein kinase, as the most significant predictor of the aggressive recurrence of HCC. Aurora kinase B protein expression was significantly associated with aggressive recurrence ($P < 0.001$) and prognosis ($P < 0.001$). Multivariable analysis identified Aurora kinase B as the only independent predictor of aggressive recurrence of HCC ($P = 0.031$). Array-CGH analysis showed that genomic instability was closely related to Aurora kinase B expression ($P = 0.011$). CONCLUSION: Aurora kinase B is an effective predictor of aggressive HCC recurrence, in relation to the genomic instability. It might be worth considering as a molecular target for the adjuvant therapy of HCC.

19. Saitoh Y, Yamamoto N, Dewan MZ, Sugimoto H, Martinez BVJ, Iwasaki Y, Matsubara K, Qi X, Saitoh T, Imoto I, Inazawa J, Utsunomiya A, Watanabe T, Masuda T, Yamamoto N, Yamaoka S. Overexpressed NF-{kappa} B inducing kinase contributes to the tumorigenesis of adult T-cell leukemia and Hodgkin Reed-Sternberg cells. Blood.111:5118-29, 2008

The nuclear factor-kappaB (NF-kappaB) transcription factors play important roles in cancer development by preventing apoptosis and facilitating the tumor cell growth. However, the precise mechanisms by which NF-kappaB is constitutively activated in specific cancer cells remain largely unknown. In our current study, we now report that NF-kappaB-inducing kinase (NIK) is

overexpressed at the pretranslational level in adult T-cell leukemia（ATL）and Hodgkin Reed-Sternberg cells（H-RS）that do not express viral regulatory proteins. The overexpression of NIK causes cell transformation in rat fibroblasts, which is abolished by a super-repressor form of IkappaBalpha. Notably, depletion of NIK in ATL cells by RNA interference reduces the DNA-binding activity of NF-kappaB and NF-kappaB-dependent transcriptional activity, and efficiently suppresses tumor growth in NOD/SCID/gammac（null）mice. These results indicate that the deregulated expression of NIK plays a critical role in constitutive NF-kappaB activation in ATL and H-RS cells, and suggest also that NIK is an attractive molecular target for cancer therapy.

20. Zhao C, Inoue J, Imoto I, Otsuki T, Iidab S, Ueda R, Inazawa J. POU2AF1, an amplification target at 11q23, promotes growth of multiple myeloma cells by directly regulating expression of a B-cell maturation factor, TNFRSF17. Oncogene.27:63-75, 2008

Multiple myeloma（MM）, a progressive hematological neoplasm, is thought to result from multiple genetic events affecting the terminal plasma cell. However, genetic aberrations related to MM are seldom reported. Using our in-house array-based comparative genomic hybridization system to locate candidate target genes with following their expression analysis, we identified POU2AF1 at 11q23.1 as a probable amplification target in MM cell lines. POU2AF1 is a B-cell-specific transcriptional co-activator, which interacts with octamer-binding transcription factors Oct-1 and Oct-2, and augments their function. Downregulation of POU2AF1 expression by specific small-interfering RNA（siRNA）inhibited MM cell growth, whereas ectopic expression of POU2AF1 promoted growth of MM cells. Among putative transcriptional targets for POU2AF1, B-cell maturation factor, TNFRSF17, enhanced its transcription by POU2AF1, and POU2AF1 directly bound to an octamer site within the 5' region of TNFRSF17. Expression level of TNFRSF17 was closely correlated with that of POU2AF1 in cell lines and primary samples of MM, and decreasing TNFRSF17 expression by means of TNFRSF17 siRNA inhibited MM cell growth. Taken together, our results suggest that POU2AF1, when activated by amplification or other mechanisms, may contribute to progression of MM by accelerating growth of MM cells through direct transactivation of one of its target genes, TNFRSF17.

21. Takano K, Nakagawa E, Inoue K, Kamada F, Kure S, Goto Y; Japanese Mental Retardation Consortium. Am J Med Genet B Neuropsychiatr Genet. 147B:479-84, 2008.

Mental retardation（MR）is a common trait, affecting approximately 2-3% of individuals in the general population. Although the etiology of MR remains largely unknown, genetics apparently play a major role. Recent molecular studies of X-linked form of MR in European and North American countries have revealed 24 nonsyndromic X-linked mental retardation（NS-XLMR）genes including FTSJ1, a human homolog of the Escherichia coli 2'-O-rRNA methyltransferase FtsJ/RrmJ gene. Here we identified a novel FTSJ1 mutation in an XLMR family through mutation screening of a cohort of 73 unrelated Japanese male probands with MR. Sequence analysis of the proband and his mother revealed a G > A substitution at the consensus for the donor splicing site in intron 8（c.571 + 1G > A）of FTSJ1. This mutation prevented the removal intron 8 from the pre-mRNA, thereby leading to a frameshift in the mutant FTSJ1 mRNA and resulting in a premature termination in exon 9. Quantitative RT-PCR showed a significant reduction of mutant FTSJ1 mRNA in the patient's lymphoblast cells, which was restored by treatment with cycloheximide, a potent inhibitor of nonsense-mediated mRNA decay（NMD）. Therefore, mRNAs carrying this mutation are likely subject to degradation by NMD. Together, loss-of-function of FTSJ1 may be a mechanism for the cognitive dysfunction observed in this family. Our study also suggested that the FTSJ1 mutation probably accounts for XLMR in Japanese at a similar frequency（1-2%）as in Europeans.

4. 本事業に関連して世界的な研究拠点形成に向けて、以下の点で改善・整備等されたこと

A（研究拠点体制）

世界トップレベルの口腔領域腫瘍、骨軟部腫瘍に関わる医学を主体とする本学の特徴である硬組織疾患のゲノム医科学に基づく先端的研究を推進し、テーラーメイド医療実践を目指した新しい疾患の診断、治療、予防法の開発を目的として、①分子医科学（野田政樹教授）、②ゲノム構造解析（稲澤譲治教授）、③ゲノム機能解析（三木義男教授）、④口腔腫瘍臨床研究（小村 健教授）、⑤硬組織腫瘍臨床研究（四宮謙一教授）、⑥顎顔面形成不全臨床研究（森山啓司教授）を主体とした硬組織疾患先端研究拠点体制を構築した。

B（研究教育環境）

口腔腫瘍、硬組織腫瘍（骨軟部組織腫瘍）、先天異常症の詳細な臨床病理学的データを付帯した疾患組織バイオリソースを構築し、集学的な疾患研究拠点の環境を整備した。また、拠点グループを主体に研究進捗状況報告、先端研究セミナーを定期開催し、

大学院学生、若手研究者の研究教育活動を支援した。

C（人材確保）

特になし

D（人材育成）

口腔癌の研究を実施している大学院生を米国癌学会に参加、発表させた。

E（国際化）

セミナー、研究進捗状況報告会を英語（一部日本語）で実施している。

5. GCOE事業を推進するに当たって力を入れた点

口腔腫瘍、硬組織腫瘍（骨軟部組織腫瘍）、先天異常症等の領域における疾患研究の先端的国際拠点を形成するよう研究教育環境を整備するとともに、拠点グループを主体に研究進捗状況報告、先端研究セミナーを定期開催し、大学院学生、若手研究者の研究教育活動の活性化等に注力した。

6. 英文原著論文

1. Iriyama T, Takeda K, Nakamura H, Motimoto Y, Kuroiwa T, Mizukami J, Umeda T, Noguchi T, Naguro I, Nishitoh H, Saegusa K, Tobiume K, Homma T, Shimada Y, Tsuda H, Aiko S, Imoto I, Inazawa J, Chiba K, Kamei Y, Kozuma S, Taketani Y, Matsuzawa A, Ichijo H: ASK1 amd ASK2 differentially regulate the counteracting roles of apoptosis and inflammation in tumorigenesis .EMBO J. 2009 [Epub ahead of print]
2. Yamamoto S, Tsuda H, Honda K, Onozato K, Takano M, Tamai S, Imoto I, Inazawa J, Yamada T, Matsubara O. Actinin-4 gene amplification in ovarian cancer. a candidate oncogene associated with poor patient prognosis and tumor chemoresistance. Mod Pathol. 2009 [Epub ahead of print]
3. Kawase T, Ohki R, Shibata T, Tsutsumi S, Kamimura N, Inazawa J, Ohta T, Ichikawa H, Aburatani H, Tashiro F, Taya Y . PH domain-only protein PHLDA3 is a p53-regulated repressor of akt. Cell 136:535-50,2009
4. Arai E, Ushijima S, Fujimoto H, Hosoda F, Shibata T, Kondo T, Yokoi S, Imoto I, Inazawa J, Hirohashi S, Kanai Y. Genome-wide DNA methylation profiles in both precancerous conditions and clear cell renal cell carcinomas are correlated with malignant potential and patient outcome. Carcinoqenesis 99:1940-9, 2009.
5. Takahata M, Inoue Y, Tsuda H, Imoto I, Koinuma D, Hayashi M, Ichikura T, Yamori T, Nagasaki K, Yoshida M, Matsuoka M, Morishita K, Yuki K, Hanyu A, Miyazawa K, Inazawa J, Miyazono K, Imamura T. SKI and MEL1 cooperate to inhibit transforming growth factor-beta signal in gastric cancer cells. J Biol Chem. 284:3334-44,2008.
6. Ishihara T, Tsuda H, Hotta A, Kozaki K, Yoshida A, Jaeduk Yoshimura Noh, Ito K, Imoto I, Inazawa J. ITCH is a putative target for a novel 20q11.22 amplification detected in anaplastic thyroid carcinoma cells by array-based comparative genomic hybridization. Cancer Sci.99:1940-49, 2008
7. Hayashi S, Okamoto N, Makita Y, Hata A, Imoto I, Inazawa J. Heterozygous Deletion at 14q22.1-q22.3 including the BMP4 gene in a patient with psychomotor retardation, congenital corneal opacity and feet polysyndactyly. Am J Med Genet A.146A:2905-10, 2008
8. Arai E, Ushijima S, Tsuda H, Fujimoto H, Hosoda F, Shibata T, Kondo T, Imoto I, Inazawa J, Hirohashi S, Kanai Y. Genetic clustering of clear cell renal cell carcinoma based on array-comparative genomic hybridization. its association with DNA methylation alteration and patient outcome. Clin Cancer Res. 14:5531-9, 2008
9. Kikuchi S, Honda K, Tsuda H, Hiraoka N, Imoto I, Kosuge T, Umaki T, Onozato K, Shitashige M, Yamaguchi U, Ono M, Tsuchida A, Aoki T, Inazawa J,Hirohashi S, Yamada T. Expression and gene amplification of actinin-4 in invasive ductal carcinoma of the pancreas. Clin Cancer Res.14:5348-56, 2008
10. Katsuki Y, Nakada S, Yokoyama T, Imoto I, Inazawa J, Nagasawa M, Mizutani S. Caffeine yields aneuploidy through asymmetrical cell division caused by misalignment of chromosomes. Cancer Sci.99:1539-45, 2008
11. Hayashi S, Mizuno S, Migita O, Okuyama T, Makita Y, Hata A, Imoto I, Inazawa J. The CASK gene harbored in a deletion detected by Array-CGH as a potential candidate for a gene causative of X-linked dominant mental retardation. Am J Med Genet A.146A:2145-51, 2008
12. Nakajima T, Yasui K, Zen K, Inagaki Y, Fujii H, Minami M, Tanaka S, Taniwaki M, Itoh Y, Arii S, Inazawa J, Okanoue T. Activation of B-Myb by E2F1 in hepatocellular carcinoma. Hepatol Res.38:886-95, 2008
13. Qi S, Mogi S, Tsuda H, Tanaka Y, Kozaki K, Imoto I, Inazawa J, Hasegawa S, Omura K. Expression of cIAP-1 correlates with nodal metastasis in squamous cell carcinoma of the tongue. Int J Oral Maxillofac Surg.37:1047-53, 2008
14. Kikuchi R, Tsuda H, Kozaki K, Kanai Y, Kasamatsu T, Sengoku K, Hirohashi S, Inazawa J, Imoto I. Frequent inactivation of a putative conditional tumor-suppressor gene, angiopoietin-like protein 2, in ovarian cancer. Cancer Res.68:5067-75, 2008
15. Nakamura E, Kozaki K, Tsuda H, Suzuki, E, Pimkhaokham A, Yamamoto G, Irie T, Tachikawa T, Amagasa T, Inazawa J, Imoto I. Frequent silencing of a

putative tumor suppressor gene melatonin receptor 1A (MTNR1A) in oral squamous-cell carcinoma. Cancer Sci.99:1390-400, 2008
16. Kozaki K, Imoto I, Mogi S, Omura K, Inazawa J. Exploration of tumor-suppressive microRNAs silenced by DNA hypermethylation in oral cancer. Cancer Res. 68:2094-2105, 2008
17. Suzuki A, Shibata T, Murakami Y, Horii A, Shiratori K, Hirohashi S, Inazawa J, Imoto I. Identification of SMURF1 as a possible target for 7q21.3-22.1 amplification detected in a pancreatic cancer cell line by in-house array-based comparative genomic hybridization. Cancer Sci.99:986-94, 2008
18. Tanaka S, Arii S, Yasen M, Moqushi K, Su NT, Zhao C, Imoto I, Eishi Y, Inazawa J, Miki Y, Tanaka H. Aurora kinase B is a predictive factor for the aggressive recurrence of hepatocellular carcinoma after curative hepatectomy. Br J Surg.95:611-619, 2008
19. Saitoh Y, Yamamoto N, Dewan MZ, Sugimoto H, Martinez BVJ, Iwasaki Y, Matsubara K, Qi X, Saitoh T, Imoto I, Inazawa J, Utsunomiya A, Watanabe T, Masuda T, Yamamoto N, Yamaoka S. Overexpressed NF-{kappa}B inducing kinase contributes to the tumorigenesis of adult T-cell leukemia and Hodgkin Reed-Sternberg cells. Blood.111:5118-29, 2008
20. Zhao C, Inoue J, Imoto I, Otsuki T, Iidab S, Ueda R, Inazawa J. POU2AF1, an amplification target at 11q23, promotes growth of multiple myeloma cells by directly regulating expression of a B-cell maturation factor, TNFRSF17. Oncogene.27:63-75, 2008
21. Takano K, Nakagawa E, Inoue K, Kamada F, Kure S, Goto Y; Japanese Mental Retardation Consortium. Am J Med Genet B Neuropsychiatr Genet. 147B:479-84, 2008.

7. 著書

著書

1. 稲澤譲治: アレイCGH診断活用ガイドブック-知っておきたい染色体微細構造異常症-（稲澤譲治、羽田明、蒔田芳男編）医薬ジャーナル社（大阪）.2008.239P
2. 稲澤譲治: がんの分子標的治療（鶴尾隆 編）.株式会社南山堂（東京）2008.441P
3. 稲澤譲治:講義録 腫瘍学.株式会社メジカルビュー社（東京）pp43-46, 2009,2,10（4P）

総説

1. 林深、井本逸勢、稲澤譲治:アレイCGHによる先天異常症の潜在的染色体異常診断と解析 医歯薬出版（株）、別冊医学のあゆみ Vol.225 No.9:845-849,2008
2. 横井左奈、稲澤譲治:遺伝子異常の全ゲノム探索 （株）日本臨牀社、日本臨牀 66巻増刊号6:45-49, 2008（2008/8/28）（4P）
3. 小崎健一、稲澤譲治:癌幹細胞とmicroRNA 医歯薬出版株式会社、医学のあゆみ Vol.227 No.1:62-66,2008（2008/10/4）（5P）
4. 林深、井本逸勢、稲澤譲治:ゲノム微細構造異常と先天異常疾患 （株）診断と治療社、小児科診療 第72巻第1号:31-37, 2009（2009/1/1）（7P）
5. 稲澤譲治:癌のゲノム構造異常とその意義 （株）日本臨牀社、日本臨牀 がん薬物療法学 67巻増刊号1（通巻950号）:167-171, 2009（2009/1/28）（5P）

8. 特許取得、特許申請

［国内］6件

1. 2008.12.25、「BACクローンを用いる肝細胞癌の発生リスク評価方法及び予後予測方法」金井弥栄・新井恵吏・稲澤譲治、財団法人ヒューマンサイエンス振興財団・国立大学法人東京医科歯科大学、特願2008-329872
2. 2008.10.27、「神経芽腫の検出方法」稲澤譲治・井本逸勢・井上純、富士フィルム株式会社・東京医科歯科大学、特願2008-275176
3. 2008.9.11、「BACクローンを用いる腎細胞癌の予後予測方法」金井弥栄・新井恵吏・廣橋説雄・稲澤譲治、財団法人ヒューマンサイエンス振興財団・国立大学法人東京医科歯科大学、特願2008-233491
4. 2008.8.8、「口腔扁平上皮癌の検出方法」稲澤譲治・井本逸勢・中村恵理奈・津田均、国立大学法人東京医科歯科大学・富士フィルム株式会社、特願2008-205138
5. 2008.8.1、「先天性異常症の染色体欠失の検出方法」、稲澤譲治・井本逸勢・林深・会津善紀、国立大学法人東京医科歯科大学・株式会社ビー・エム・エル・富士フィルム株式会社、特願2008-199541
6. 2008.7.16、「甲状腺癌の検出方法」稲澤譲治・井本逸勢・石原孝也・津田均、国立大学法人東京医科歯科大学・富士フィルム株式会社、特願2008-184982

［海外］

［US］4件

1. 「口腔扁平上皮癌の検出方法、及び抑制方法」、稲澤譲治・井本逸勢・鈴木江美奈、国立大学法人東京医科歯科大学・富士写真フィルム株式会社、2008.5.28、12/128,468、特願2007-143110
2. 「卵巣癌の検出方法、及び抑制方法」、稲澤譲治・井本逸勢・菊池良子、国立大学法人東京医科歯科大学・

富士写真フィルム株式会社、2008.5.28、12/153,967、特願2007-143111
3. 「神経芽腫の悪性度を含めた検出方法、及び抑制方法」、稲澤譲治・井本逸勢・杉野由里子、国立大学法人東京医科歯科大学・富士写真フィルム株式会社 、2008.5.23、12/126,637、特願2007-169875
4. 「癌抑制剤」、三沢あき子・井上純・井本逸勢・稲澤譲治、国立大学法人東京医科歯科大学・富士写真フィルム株式会社、2008.5.16（1）+2008.7.23（2）、12/153,342 + 12/219,508、特願2005-309921

［EP］2件
1. 「口腔扁平上皮癌の検出方法、及び抑制方法」、稲澤譲治・井本逸勢・鈴木江美奈、国立大学法人東京医科歯科大学・富士写真フィルム株式会社、2008/5/30、08009943.5、特願2007-143110
2. 「卵巣癌の検出方法、及び抑制方法」、稲澤譲治・井本逸勢・菊池良子、国立大学法人東京医科歯科大学・富士写真フィルム株式会社、2008/5/30、08009927.8、特願2007-143111

［CN］2件
1. 「口腔扁平上皮癌の検出方法、及び抑制方法」、稲澤譲治・井本逸勢・鈴木江美奈、国立大学法人東京医科歯科大学・富士写真フィルム株式会社、2008.5.30、200810108666.3、特願2007-143110
2. 「卵巣癌の検出方法、及び抑制方法」、稲澤譲治・井本逸勢・菊池良子、国立大学法人東京医科歯科大学・富士写真フィルム株式会社、2008/5/30、200810108639.6、特願2007-143111

9. 平成21年3月までの自己評価

研究・教育において充分な成果が得られた。

10. 学会発表（英文）

1. Hayashi S, Honda S, Imoto I, Inazawa J: Application of in-house array-CGH for investigation and diagnosis of congenital genome disorders. 58th Annual Meeting of the American Society of Human Genetics 2008（Philadelphia, Pennsylvania USA）11-15/November/2008
2. Honda S, Inazawa J: Exploration of genes related to X-linked mental retardation（XLMR）by in-house X-tilling array.58th Annual Meeting of the American Society of Human Genetics 2008（Philadelphia, Pennsylvania USA）11-15/November/2008
3. Kikuchi R, Imoto I, Tsuda H, Kanai Y, Kasamatsu T, Sengoku K, Hirohashi S, Inazawa J: Frequent inactivation of a putative conditional tumor-suppressor gene TSOVC1 in ovarian cancer. 99th annual meeting of American Association for Cancer Research 2008（San Diego,California USA）12-16/ April/ 2008
4. Kozaki K, Imoto I, Mogi S, Omura K, Inazawa J: Silencing of tumor-suppressive microRNAs by DNA hypermethylation in oral squamous cell carcinoma. 99th annual meeting of American Association for Cancer Research 2008（San Diego,California USA）12-16/ April/ 2008
5. Begum A, Suzuki E, Nakamura E, Imoto I, Kozaki K, Tsuda H, Amagasa T, Inazawa J: Identification of a novel amplification-target gene in oral squamous cell carcinoma（OSCC）using array-CGH-assisted strategy.99th annual meeting of American Association for Cancer Research 2008（San Diego,California USA）12-16/ April/ 2008
6. 井本逸勢、井上純、稲澤譲治:エピゲノム異常で発現抑制を受ける新規口腔、食道扁平上皮癌抑制遺伝子候補の同定.第67回日本癌学会学術総会 International Session.名古屋国際会議場.愛知.2008年10月29日

11. 学会発表（和文）

（口頭）

7. 久保田健夫、五月女雅樹、伊藤雅之、後藤雄一、稲澤譲治:レット症候群の責任蛋白質MeCP2の標的遺伝子探索-自閉症のマーカー遺伝子の同定にむけて-.第50回日本小児神経学会総会・第50回総会記念国際小児神経シンポジウム.ホテル日航東京.東京.2008年5月29日
8. 本田尚三、林深、井本逸勢、中川栄二、後藤雄一、稲澤譲治:X-tiling arrayを用いたX連鎖生精神発達遅滞（XLMR）の原因遺伝子探索.第50回日本小児神経学会総会・第50回総会記念国際小児神経シンポジウム.ホテル日航東京.2008年5月29日
9. 林深、本田尚三、井本逸勢、稲澤譲治:先天異常疾患における潜在的染色体異常を探索・診断するツールとしてのアレイCGHの有用性.第50回日本小児神経学会総会・第50回総会記念国際小児神経シンポジウム.ホテル日航東京.2008年5月29日
10. 小澤伸晃、左合治彦、高橋宏典、林聡、右田王介、小崎里華、柿島裕樹、奥山虎之、北川道弘、会津善紀、山口敏和、井本逸勢、稲澤譲治:アレイCGH法を用いた流産原因の遺伝学的解析.日本人類遺伝学会第53回大会.パシフィコ横浜.2008年9月28日
11. 横井左奈、井本逸勢、柴田龍弘、北川昌伸、廣橋説雄、稲澤譲治:アレイCGH法による肺小細胞癌の潜在的ゲノムコピー数解析と癌関連遺伝子の同定.日

本人類遺伝学会第53回大会.パシフィコ横浜.2008年9月29日

12. 牟禮岳男、小林千浩、金城薫、千代延友裕、西村陽、平井清、森本昌史、松尾雅文、稲澤譲治、戸田達史:精神発達遅滞児（者）における500K SNPチップを用いたコピー数変化領域のスクリーニングと原因遺伝子の同定. 日本人類遺伝学会第53回大会.パシフィコ横浜.2008年9月30日
13. 林深、本田尚三、井本逸勢、稲澤譲治:アレイCGHを用いた多発奇形を伴う精神遅滞症例の解析と診断.日本人類遺伝学会第53回大会.パシフィコ横浜.2008年9月30日
14. 蒔田芳男、斎藤伸治、羽田明、石井拓麿、吉橋博史、黒澤健司、小崎里華、小野正恵、沼部博直、水野誠司、古庄知己、福嶋義光、岡本伸彦、三渕浩、知念安紹、林深、井本逸勢、稲澤譲治:ゲノムアレイを用いた先天異常症の効率的診断法の確立と疾患特異的構造異常の探索. 日本人類遺伝学会第53回大会.パシフィコ横浜.2008年9月30日
15. 本田尚三、林深、井本逸勢、井ノ上逸朗、屋部登志男、徳永勝士、中川栄二、後藤雄一、稲澤譲治:X-tiling arrayを用いたX連鎖性精神発達遅滞（XLMR）の原因遺伝子探索. 日本人類遺伝学会第53回大会.パシフィコ横浜.2008年9月30日
16. 小松周平、井本逸勢、津田均、小崎健一、松井毅、嶋田裕、市川大輔、大辻英吾、稲澤譲治:食道扁平上皮癌における新規診断治療標的遺伝子OESC1の同定.第67回日本癌学会学術総会.名古屋国際会議場.愛知.2008年10月28日
17. 横井左奈、井本逸勢、柴田龍弘、北川昌伸、廣橋説雄、稲澤譲治:肺小細胞癌における1p13増幅領域の標的候補遺伝子tripartite motif33（TRIM33）の解析.第67回日本癌学会学術総会.名古屋国際会議場.愛知.2008年10月28日
18. 田中真二、茂櫛薫、藍原有弘、ヤセンマハムレット、水島洋、三木義男、稲澤譲治、田中博、有井滋樹:肝癌血管侵襲の遺伝子プロファイルに基づく新規分子標的治療への展開.第67回日本癌学会学術総会.名古屋国際会議場.愛知.2008年10月28日
19. 鶴田智彦、井本逸勢、平沢晃、小崎健一、阪埜浩司、進伸幸、青木大輔、稲澤譲治:エピジェネティック異常により発現抑制される子宮体がん関連癌抑制遺伝子のMPA療法における役割.第67回日本癌学会学術総会.名古屋国際会議場.愛知.2008年10月28日
20. 本田一文、菊池哲、津田均、平岡伸介、稲澤譲治、井本逸勢、廣橋説雄、山田哲司:浸潤生膵管がんにおけるアクチニン-4の遺伝子増幅とたんぱく質発現増加.第67回日本癌学会学術総会.名古屋国際会議場.愛知.2008年10月29日
21. 春木茂男、小松周平、井本逸勢、小崎健一、嶋田裕、河野辰幸、稲澤譲治:高密度オリゴアレイCGHを用いた新規食道扁平上皮癌関連癌抑制遺伝子の探索.第67回日本癌学会学術総会.名古屋国際会議場.愛知.2008年10月29日
22. 小崎健一、井本逸勢、茂木世紀、小村健、稲澤譲治:口腔癌において腫瘍特異的DNA過剰メチル化により発現抑制される癌抑制microRNA:miR-137とmiR-193a.第67回日本癌学会学術総会.名古屋国際会議場.愛知.2008年10月29日
23. 藍原有弘、田中真二、Mahmut Yasen、茂櫛薫、野口典夫、工藤篤、中村典明、伊東浩次、井本逸勢、稲澤譲治、三木義男、田中博、有井滋樹:肝癌に対する選択的Aurora kinase B阻害剤の前臨床研究.第67回日本癌学会学術総会.名古屋国際会議場.愛知.2008年10月29日
24. 石原孝也、津田均、堀田晶子、小崎健一、吉田明、吉村弘、伊藤公一、井本逸勢、稲澤譲治:自作BACアレイを用いた未分化甲状腺癌細胞株のコピー数異常解析により検出された新規増幅領域20q11.22の標的遺伝子候補ITCH. 第31回日本分子生物学会年会・第81回日本生化学会大会・合同大会.神戸ポートアイランド.兵庫.2008年12月11日

（ポスター）

25. 井本逸勢、稲澤譲治:PRTFDC1, a possible tumor-suppressor gene, is frequently silenced in oral squamous-cell carcinomas by aberrant promoter hypermethylation.テーラーメイド医療を目指したゲノム情報活用基盤技術 第4回公開シンポジウム.日本科学未来館みらいCANホール.東京.2008年8月1日
26. 小崎健一、稲澤譲治:Silencing of tumor-suppressive microRNAs by DNA hypermethylation in oral squamous cell carcinoma. テーラーメイド医療を目指したゲノム情報活用基盤技術 第4回公開シンポジウム.日本科学未来館みらいCANホール.東京.2008年8月1日
27. 石原孝也、稲澤譲治:ITCH is a putative target for a novel 20q11.22 amplification detected in anaplastic thyroid carcinoma cells by array-based comparative

genomic hybridization. テーラーメイド医療を目指したゲノム情報活用基盤技術 第4回公開シンポジウム.日本科学未来館みらいCANホール.東京.2008年8月1日

28. Begum Asma、稲澤譲治:Identification of a novel amplification-target gene in oral squamous cell carcinoma（OSCC）using array CGH-assisted strategy. テーラーメイド医療を目指したゲノム情報活用基盤技術 第4回公開シンポジウム.日本科学未来館みらいCANホール.東京.2008年8月1日
29. 古田繭子、小崎健一、田中真二、有井滋樹、井本逸勢、稲澤譲治:Screening of tumor suppressive microRNAs silenced by tumor-specific DNA hypermethylation in hepatocellular carcinoma. 第9回文部科学省特定領域研究「がん」5領域・若手研究者ワークショップ.アートランドホテル蓼科.長野.2008年9月4日
30. 蒔田芳男、長屋建、高橋悟、藤枝憲二、林深、井本逸勢、稲澤譲治:商用FISHプローブにてモザイクが検出されたMiller-Dieker症例群の1例.日本人類遺伝学会第53回大会.パシフィコ横浜.2008年9月28日
31. 小野正恵、林深、北爪勉、入江学、鈴木淳子、稲澤譲治:46,XY,der（9）t（6;9）（p24.1;p23）の兄弟例.日本人類遺伝学会第53回大会.パシフィコ横浜.2008年9月28日
32. 会津善紀、井本逸勢、林深、山口敏和、永田欽也、宮本力、稲澤譲治:先天異常症診断用アレイ、Genome Disorder Arrayを用いたMCA/MRのアレイCGH解析. 日本人類遺伝学会第53回大会.パシフィコ横浜.2008年9月28日
33. 白樺、井上純、井本逸勢、稲澤譲治:Inactivation of LC3A gene in human cancers. 第67回日本癌学会学術総会.名古屋国際会議場.愛知.2008年10月28日
34. 村松智輝、井本逸勢、津田均、嶋田裕、小崎健一、稲澤譲治:食道癌発生におけるYes-associated protein 1（YAP1）増幅の意義.第67回日本癌学会学術総会.名古屋国際会議場.愛知.2008年10月28日
35. 坂本宙子、横井左奈、井本逸勢、稲澤譲治:X-tilingアレイを用いたX染色体上の癌関連遺伝子群の探索.第67回日本癌学会学術総会.名古屋国際会議場.愛知.2008年10月28日
36. Asma Begum、鈴木江美奈、中村恵理奈、井本逸勢、小崎健一、津田均、天笠光雄、稲澤譲治:Identification of a novel amplification-target gene in oral squamous cell carcinoma（OSCC）using array-CGH strategy. 第67回日本癌学会学術総会.名古屋国際会議場.愛知.2008年10月28日
37. 石原孝也、津田均、小崎健一、吉田明、伊藤公一、井本逸勢、稲澤譲治:アレイCGHを用いた甲状腺未分化癌のゲノム構造解析による新規増幅領域20q11.22の標的候補遺伝子ITCHの同定.第67回日本癌学会学術総会.名古屋国際会議場.愛知.2008年10月28日
38. 細田文恵、新井康仁、安田純、中西幸浩、井本逸勢、稲澤譲治、柳原五吉、廣橋説雄、大木操、柴田龍弘:胃がんの6p21ゲノム増幅領域からの新規標的遺伝子の同定.第67回日本癌学会学術総会.名古屋国際会議場.愛知.2008年10月28日
39. 山本宗平、津田均、本田一文、高野政志、山田哲司、井本逸勢、稲澤譲治、松原修:ヒト卵巣癌におけるActinin-4遺伝子のoncogenicな性質.第67回日本癌学会学術総会.名古屋国際会議場.愛知.2008年10月28日
40. 井上純、井本逸勢、稲澤譲治:神経芽腫細胞でのLAPTM5遺伝子強制発現により誘導される細胞死の特性.第67回日本癌学会学術総会.名古屋国際会議場.愛知.2008年10月29日
41. 古田繭子、小崎健一、田中真二、有井滋樹、井本逸勢、稲澤譲治:肝細胞癌において腫瘍特異的DNA過剰メチル化により発現抑制される癌抑制microRNA.第67回日本癌学会学術総会.名古屋国際会議場.愛知.2008年10月29日
42. 古田繭子、小崎健一、田中真二、有井滋樹、井本逸勢、稲澤譲治:肝細胞癌において腫瘍特異的DNA過剰メチル化により発現抑制される癌抑制microRNA.第31回日本分子生物学会年会・第81回日本生化学会大会・合同大会.神戸ポートアイランド.兵庫.2008年12月10日
43. 石原孝也、津田均、堀田晶子、小崎健一、吉田明、吉村弘、伊藤公一、井本逸勢、稲澤譲治:自作BACアレイを用いた未分化甲状腺癌細胞株のコピー数異常解析により検出された新規増幅領域20q11.22の標的遺伝子候補ITCH. 第31回日本分子生物学会年会・第81回日本生化学会大会・合同大会.神戸ポートアイランド.兵庫.2008年12月11日
44. 小林千浩、牟禮岳男、金城薫、千代延友裕、西村陽、平井清、森本昌史、松尾雅文、稲澤譲治、戸田達史:精神発達遅滞における500K SNPチップを用いたコ

ピー数変化領域のスクリーニングと原因遺伝子の同定.第31回日本分子生物学会年会・第81回日本生化学会大会・合同大会.神戸ポートアイランド.兵庫.2008年12月11日

12. 受賞

2008年4月、稲澤譲治　平成20年度科学技術分野 文部大臣表彰科学技術賞（研究部門）受賞

13. 外部資金の獲得状況

（科学研究費補助金、受託研究費、外部財団の助成など）

科学研究費補助金、特定領域

研究題目:がんの統合的ゲノム解析と個性診断法の開発
代表:稲澤 譲治
期間:平成20年
研究費総額:33,223,250 円

受託研究費（独立行政法人新エネルギー・産業技術総合開発機構）

研究課題:個別化医療の実現のための技術融合ﾊﾞｲｵ診断技術開発/染色体解析技術開発
代表:稲澤 譲治
期間:平成20年
研究費総額:91,770,000円

文部科学省（科学技術試験研究委託事業）

研究課題:ゲノム網羅的解析情報を基盤とするオーダーメイドがん医療
代表:稲澤 譲治
期間:平成20年
研究費総額:5,000,000 円

14. 特別講演、招待講演

1. 稲澤譲治:「ゲノムの多様性からみる病気と日常」.第3回近畿血液疾患治療研究会.京都東急ホテル.京都.2008年1月19日
2. 稲澤譲治:「ゲノムアレイプラットフォームで展開する癌と遺伝疾患のゲノム・エピゲノム解析」.発生工学・疾患モデル研究会第67回定例会.東京ガーデンパレス.東京.2008年2月8日
3. 稲澤譲治:「がんのゲノム・エピゲノム異常解析と治療標的分子の探索」.京都府立医科大学研究開発センター第4回学術講演会（がんプロフェッショナル養成プラン第1回学術講演会）.京都府立医科大学第2講義室.京都.2008年2月19日
4. 稲澤譲治:「アレイプラットフォームで展開する癌と遺伝疾患のゲノム・エピゲノム解析」.第6回幹細胞シンポジウム.学術総合センター.東京.2008年5月17日
5. 稲澤譲治:「がんのゲノム・エピゲノム解析から分子診断・標的治療へ」.第18回日本サイトメトリー学会学術集会.（招請講演）.東京慈恵会医科大学1号館3階講堂.東京.2008年6月28日
6. 稲澤譲治:「がんと遺伝疾患のゲノム・エピゲノム解析:その分子診断から標的治療へ」.第7回Cell Biology Summer Meeting.鴨川グランドホテル.千葉.2008年7月5-6日
7. 稲澤譲治:「ゲノムアレイプラットフォームで展開する癌と遺伝疾患のゲノム・エピゲノム解析」.第153回環境研セミナー.（財）環境科学技術研究センター.青森.2008年9月10日
8. 稲澤譲治:「ゲノムアレイプラットフォームで展開する癌と遺伝疾患のゲノム・エピゲノム解析」.東京医科歯科大学大学院分子生物学特論.東京医科歯科大学大学院講義室.東京.2008年10月17日
9. 稲澤譲治:「消化器疾患におけるゲノム異常と臨床への展開」.日本消化器病学会四国支部第90回例会.松山市総合コミュニティセンター.愛媛.2008年11月8日
10. 稲澤譲治:「ゲノムの変化から知るがんの個性と治療法」.第3回四大学連合文化講演会.一橋記念講堂.東京.2008年11月27日

15. 主催学会

第15回癌ゲノムサイエンス研究会、
平成20年7月24日、東京ガーデンパレス
第16回癌ゲノムサイエンス研究会、
平成21年2月27日、東京ガーデンパレス

16. 新聞、雑誌、TV報道

平成20年11月27日　日経新聞朝刊

17. 講座の准教授、講師、助教、特別研究員、ポスドク、指導を受けた大学院生の名前（AISSには○印） のリスト

【講座スタッフ・協力教員】

准教授	井本逸勢
助　教	横井（石原）左奈
特任助教	井上純
特任助教	林　深
特任准教授	小崎健一
MTT特任講師	松井 毅

【大学院生】

○Begum Asma
○白樺、
本田尚三
小松周平
村松智輝
古田繭子
春木茂男
村松聡
倉沢泰浩
大前明代
坂本宙子
上杉篤史
小野宏晃
岡本奈那

平成20年11月27日　日経新聞朝刊

ゲノムの変化から知るがんの個性と治療法

高精度ゲノムアレイ実用化
先天異常症の診断にも貢献

東京医科歯科大学難治疾患研究所教授　稲澤　譲治

従来、がんや先天異常症の原因となるゲノム異常を検出する方法には直接塩基配列を決定するシーケンサーなどで一塩基から数千塩基の異常を検出するか、あるいは顕微鏡レベルで大きな異常を検出する染色体検査しかなかった。このため、がんや遺伝疾患においては、数万～数百万塩基対レベルの潜在的ゲノム異常が病態形成に大きくかかわっている可能性があると予想されながらも、これを探索する手段がないという状況が続いていた。

この技術的なギャップを埋めるために、私たちは高精度ゲノムアレイを開発して実用化した。既に肺がんや胃がんをはじめ二十五種類のがんで、延べ千七百例以上において自作アレイによるゲノム解析を行い、がんに特異的なゲノム異常を探索し、これを糸口に六十種類のがん関連遺伝子を見つけ出した。

これらの中の幾つかは、既に治療の標的分子としての、あるいはがんの悪性度を知るための診断バイオマーカーとしての取り組みが進められつつある。また全国の臨床遺伝専門医とコンソーシアムを形成し、原因の明らかでない先天異常症例を対象に疾患の原因となる潜在的ゲノム異常の有無のスクリーニングを進めてきた。

その結果、予想以上に多くの症例において病態形成と深く関与する可能性が示唆される潜在的な微細ゲノムコピー数の異常が検出されてきている。私たちが作製し標準化したゲノムアレイは、先天異常症の領域においても、従来の染色体分析を代替・補完する診断法としてその実用化が大きく期待されている。

Research Article

Exploration of Tumor-Suppressive MicroRNAs Silenced by DNA Hypermethylation in Oral Cancer

Ken-ichi Kozaki,[1,3] Issei Imoto,[1,3] Seiki Mogi,[2,4] Ken Omura,[2,4] and Johji Inazawa[1,3,5,6]

[1]Department of Genome Medicine, [2]Department of Advanced Molecular Diagnosis and Maxillofacial Surgery, Hard Tissue Genome Research Center, [3]Department of Molecular Cytogenetics, Medical Research Institute, [4]Department of Oral and Maxillofacial Surgery, Graduate School, and [5]21st Century Center of Excellence Program for Molecular Destruction and Reconstitution of Tooth and Bone, Tokyo Medical and Dental University, Tokyo, Japan and [6]Core Research for Evolutional Science and Technology of Japan Science and Technology Corp., Saitama, Japan

Abstract

In the last few years, microRNAs (miRNA) have started a revolution in molecular biology and emerged as key players in the carcinogenesis. They have been identified in various tumor types, showing that different sets of miRNAs are usually deregulated in different cancers. To identify the miRNA signature that was specific for oral squamous cell carcinoma (OSCC), we first examined expression profiles of 148 miRNAs in a panel of 18 OSCC cell lines and the immortalized oral keratinocyte line RT7 as a control. Compared with RT7, the expression of 54 miRNAs (36.5%) was frequently down-regulated in OSCC lines (<0.5-fold expression, ≥66.7% of 18 lines). Among these 54 miRNAs, we further analyzed four of these miRNAs (i.e., *miR-34b*, *miR-137*, *miR-193a*, and *miR-203*), located around CpG islands, to identify tumor-suppressive miRNAs silenced through aberrant DNA methylation. The expression of those four genes was restored by treatment with 5-aza-2′-deoxycytidine in OSCC cells lacking their expression. In addition, expression levels of the four miRNAs were inversely correlated with their DNA methylation status in the OSCC lines. In primary tumors of OSCC with paired normal oral mucosa, down-regulation of miRNA expression through tumor-specific hypermethylation was more frequently observed for *miR-137* and *miR-193a* than for *miR-34b* and *miR-203*. Moreover, the ectopic transfection of *miR-137* or *miR-193a* into OSCC lines lacking their expressions significantly reduced cell growth, with down-regulation of the translation of cyclin-dependent kinase 6 or E2F transcription factor 6, respectively. Taken together, our results clearly show that *miR-137* and *miR-193a* are tumor suppressor miRNAs epigenetically silenced during oral carcinogenesis. [Cancer Res 2008;68(7):2094–105]

Introduction

MicroRNAs (miRNA) are endogenous small non–protein-coding RNAs of ~22 nucleotides. These single-strand RNAs are considered to play crucial roles in many normal cellular processes, such as proliferation, development, differentiation, and apoptosis, by regulating target gene expression through imperfect pairing with target mRNAs of protein-coding genes, inducing direct mRNA degradation or translational inhibition (1–4). In human cancer, recent studies have shown the deregulation of miRNA expression and the contribution of miRNAs to the multistep processes of carcinogenesis either as oncogenes or tumor suppressor genes (TSG; refs. 5, 6). Tumor-specific down-regulation of subsets of miRNAs has generally been observed in various types of human cancer (7), suggesting that some of these miRNAs act as TSGs in specific tumors. Because the down-regulation of many known TSGs in human cancer has been tightly linked to the hypermethylation of CpG sites located within CpG islands with promoter activity, the same mechanism could play an important role in the silencing of tumor-suppressive miRNAs in tumors. Indeed, only a few miRNA genes were reported to be located within homozygous or hemizygous deleted regions (8–10), and several possible tumor-suppressive miRNAs, including *miR-124a* (11) and *miR-127* (12), were also reported as targets for DNA methylation for silencing in cancer cells, prompting us to screen for more tumor-suppressive miRNAs silenced through aberrant DNA methylation in a tumor-specific manner.

Oral cancer, predominantly oral squamous cell carcinoma (OSCC), is the most common head and neck neoplasm, affecting ~270,000 people worldwide in 2002 (13). In Japan, OSCC is relatively common, accounting for >5,500 deaths in 2003 (14). The carcinogenesis, including OSCC (15), is generally considered to arise through the progressive accumulation of multiple genetic abnormalities, which may impair the functions of oncogenes or TSGs that play a crucial role in the development of this disease. In addition, evidence has emerged that epigenetic mechanisms, such as altered DNA methylation patterns, play a significant role in the silencing of TSGs and contribute to malignant transformation during oral carcinogenesis (16). Recently, genome-wide screenings of DNA copy number alterations for exploring OSCC-associated oncogenes or TSGs have been reported, including by us (17–21). However, there is no report about abnormal expression of miRNA genes and their genetic or epigenetic alterations in OSCC.

We describe here the identification of tumor suppressor miRNAs, *miR-137* and *miR-193a*, frequently silenced by DNA methylation in OSCC. To explore the putative presence of DNA methylation-associated silencing of miRNAs specifically in OSCC cells, we used an approach with a series of sequential analyses. We first examined a panel of 18 OSCC cell lines and an immortalized oral keratinocyte line, RT7, for the presence of abnormal levels of expression in 148 miRNAs and then focused on four miRNAs whose down-regulated expression related to their DNA methylation status within CpG islands around them. Among four miRNAs, methylation and expression analyses using 11 primary OSCC cases with paired normal oral mucosa showed that *miR-137* and *miR-193a* show reduced expression in tumors through tumor-specific DNA methylation. Ectopic expression of *miR-137* and *miR-193a* in OSCC

Note: Supplementary data for this article are available at Cancer Research Online (http://cancerres.aacrjournals.org/).

Requests for reprints: Johji Inazawa, Department of Molecular Cytogenetics, Medical Research Institute, Tokyo Medical and Dental University, 1-5-45 Yushima, Bunkyo-ku, Tokyo 113-8510, Japan. Phone: 81-3-5803-5820; Fax: 81-3-5803-0244; E-mail: johinaz.cgen@mri.tmd.ac.jp.

©2008 American Association for Cancer Research.

doi:10.1158/0008-5472.CAN-07-5194

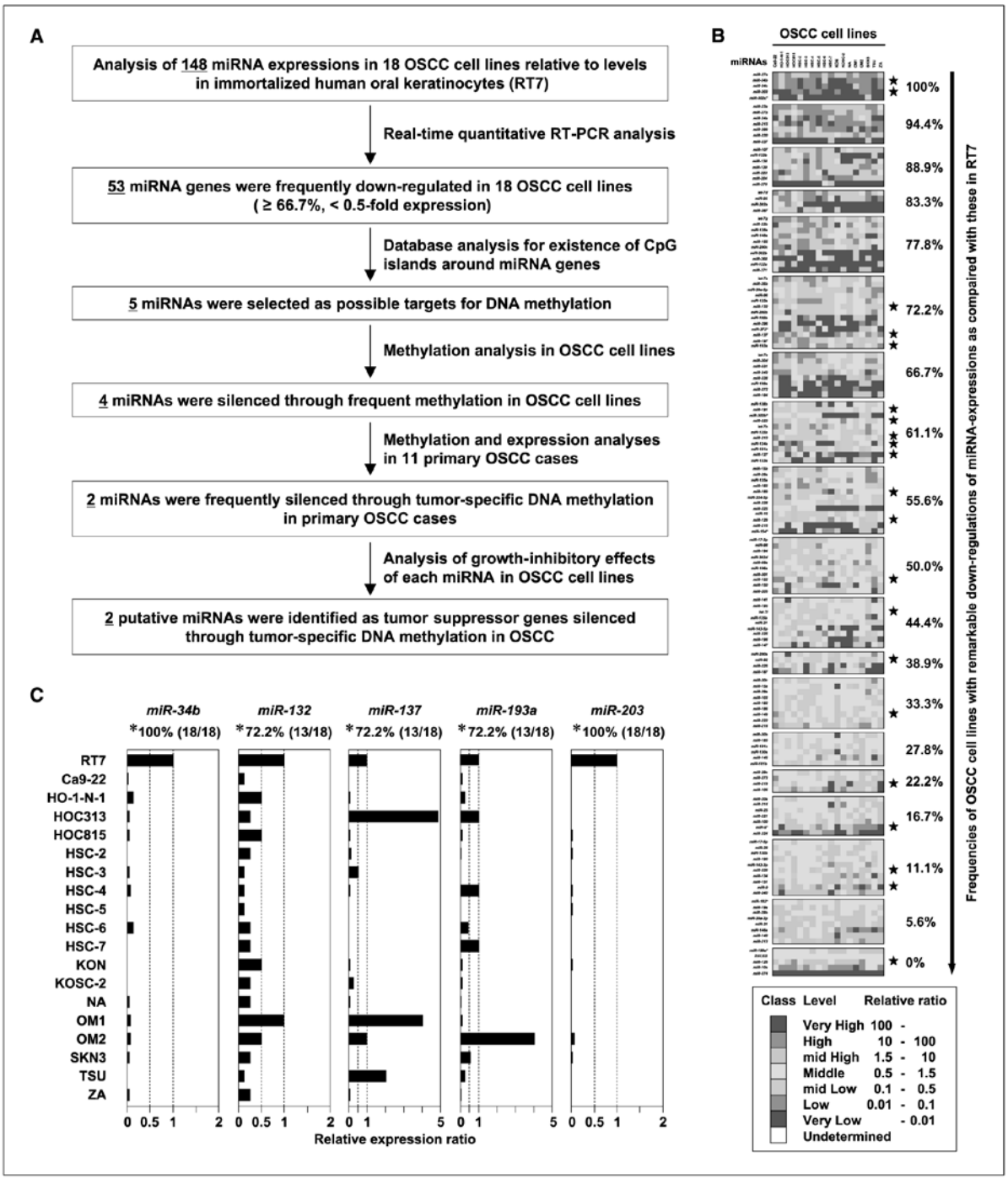

Figure 1. Strategy of this study and expression analysis for miRNAs in OSCC cell lines. *A,* schematic strategy for the identification of epigenetically silenced tumor suppressor miRNAs in OSCC. *B,* profiles of 148 miRNA expression in 18 OSCC cell lines relative to RT7 obtained with a Taqman MicroRNA Assays Human Panel Early Access kit. Expression levels of miRNA were based on the amount of target message relative to the *RNU6B* control to normalize the initial input of total RNA. *Stars,* 21 miRNAs located on/around CpG islands. RT7 cells were cultured in KGM-2 BulletKit (Cambrex) supplemented with 25% DMEM and 2.5% fetal bovine serum for 7 d. *C,* expression levels of candidate miRNAs, located on/around CpG islands, in 18 OSCC cell lines. Bar graphs in each cell line show the ratio of the expression level in each cell line to that in RT7. *, frequencies of OSCC cell lines, in which a remarkable down-regulation of candidate miRNA expression (<0.5-fold expression) was observed compared with that in RT7.

Table 1. Frequencies of OSCC cell lines with remarkable differences of miRNA expression from that in RT7 (≥66.7% of OSCC cell lines)

miRNA	Locus	Frequency (%)
miRNAs frequently up-regulated in OSCC cell lines (>1.5-fold expression)		
miR-374	Xq13.2	100.0
miR-340	5q35.3	83.3
miR-224	Xq28	83.3
miR-10a	17q21.32	77.8
miR-140	16q22.1	77.8
*miR-181a**	1q31.3	77.8
miR-146a	5q33.3	72.2
miR-126	9q34.3	66.7
miR-31	9p21.3	66.7
miR-9	*miR-9-1*, 1q22; *miR-9-2*, 5q14.3; *miR-9-3*, 15q26.1	66.7
*miR-9**	*miR-9-1*, 1q22; *miR-9-3*, 15q26.1	66.7
miRNAs frequently down-regulated in OSCC cell lines (<0.5-fold expression)		
miR-27a	19p13.12	100.0
miR-34b	11q23.1	100.0
miR-34c	11q23.1	100.0
miR-203	14q32.33	100.0
*miR-302c**	4q25	100.0
miR-23a	19p13.12	94.4
miR-27b	9q22.32	94.4
miR-34a	1p36.23	94.4
miR-215	1q41	94.4
miR-299	14q32.31	94.4
miR-330	19q13.32	94.4
miR-337	14q32.31	94.4
miR-107	10q23.31	88.9
miR-133b	6p12.2	88.9
miR-138	*miR-138-1*, 3p21.33; *miR-138-2*, 16q13	88.9
miR-139	11q13.4	88.9
miR-223	Xq12	88.9
miR-204	9q21.11	88.9
miR-370	14q32.31	88.9
let-7d	9q22.32	83.3
miR-95	4p16.1	83.3
miR-302a	4q25	83.3
miR-367	4q25	83.3
let-7g	3p21.1	77.8
miR-23b	9q22.32	77.8
miR-128a	2q21.3	77.8
miR-148a	7p15.2	77.8
miR-155	21q21.3	77.8
miR-200c	12p13.31	77.8
miR-302b	4q25	77.8
miR-368	14q32.31	77.8
miR-122a	18q21.31	77.8
miR-371	19q13.41	77.8
let-7a	*let-7a-1*, 9q22.32; *let-7a-2*, 11q24.1; *let-7a-3*, 22q13.31	72.2
miR-26b	2q35	72.2
miR-30e-5p	1p34.2	72.2
miR-96	7q32.2	72.2
miR-125a	19q13.33	72.2

Table 1. Frequencies of OSCC cell lines with remarkable differences of miRNA expression from that in RT7 (≥66.7% of OSCC cell lines) (Cont'd)

miRNA	Locus	Frequency (%)
miRNAs frequently down-regulated in OSCC cell lines (<0.5-fold expression)		
miR-132	17p13.3	72.2
miR-200b	1p36.33	72.2
miR-199b	9q34.11	72.2
miR-296	20q13.32	72.2
*miR-373**	19q13.41	72.2
miR-137	1p21.3	72.2
miR-197	1p13.3	72.2
miR-193a	17q11.2	72.2
let-7e	19q13.33	66.7
miR-30d	8q24.22	66.7
miR-331	12q22	66.7
miR-342	14q32.2	66.7
miR-338	17q25.3	66.7
miR-199a	*miR-199a-1*, 19p13.2; *miR-199a-2*, 1q24.3	66.7
miR-372	19q13.41	66.7
miR-184	15q25.1	66.7

cell lines lacking their expression inhibited cell growth through G_0-G_1 arrest and caspase-mediated apoptosis, respectively, suggesting their tumor-suppressive activity. Moreover, we identified that *cyclin-dependent kinase 6* (*CDK6*) and *E2F transcription factor 6* (*E2F6*) were potential targets of *miR-137* and *miR-193a*, respectively, in OSCC. The present study is the first to show that epigenetic silencing of *miR-137* and *miR-193a* may play a pivotal role during oral carcinogenesis.

Materials and Methods

Cell lines and primary tumor samples. Derivations and culture conditions of cell lines have been reported previously (21). To analyze the restoration of genes of interest, cells were cultured with or without 10 μmol/L of 5-aza-2′-deoxycytidine (5-aza-dCyd) for 5 d. A total of 11 frozen primary samples were obtained from OSCC patients (T1, 0 case; T2, 10 cases; T3, 0 case; and T4, 1 case) treated at Tokyo Medical and Dental University with written consent from each patient in the formal style and after approval by the local ethics committee. The tumor-node-metastasis classification of the International Union Against Cancer was used.

Real-time reverse transcription-PCR. Real-time reverse transcription-PCR (RT-PCR) was performed using an ABI Prism 7500 Fast Real-time PCR System (Applied Biosystems), Taqman Universal PCR Master Mix (Applied Biosystems), Taqman Reverse Transcription kit (Applied Biosystems), Taqman MicroRNA Assays (Applied Biosystems), and Human Panel Early Access kit (Applied Biosystems) according to the manufacturer's instructions. Expression levels of miRNA genes were based on the amount of the target message relative to that of the *RNU6B* transcript as a control to normalize the initial input of total RNA.

Methylation analysis. Genomic DNA was treated with sodium bisulfite and subjected to PCR using primer sets designed to amplify regions of interest (Supplementary Table S1). For the combined bisulfite restriction analysis (COBRA), PCR products were digested with *Bst*UI or *Taq*I, which recognizes sequences unique to methylated alleles but cannot recognize unmethylated alleles, and electrophoresed (22). For the bisulfite sequencing analysis, the PCR products were subcloned and then sequenced.

Transfection with synthetic miRNAs. Pre-miR miRNA Precursor Molecule (10 nmol/L; Ambion) mimicking *miR-137* or *miR-193a*, or control

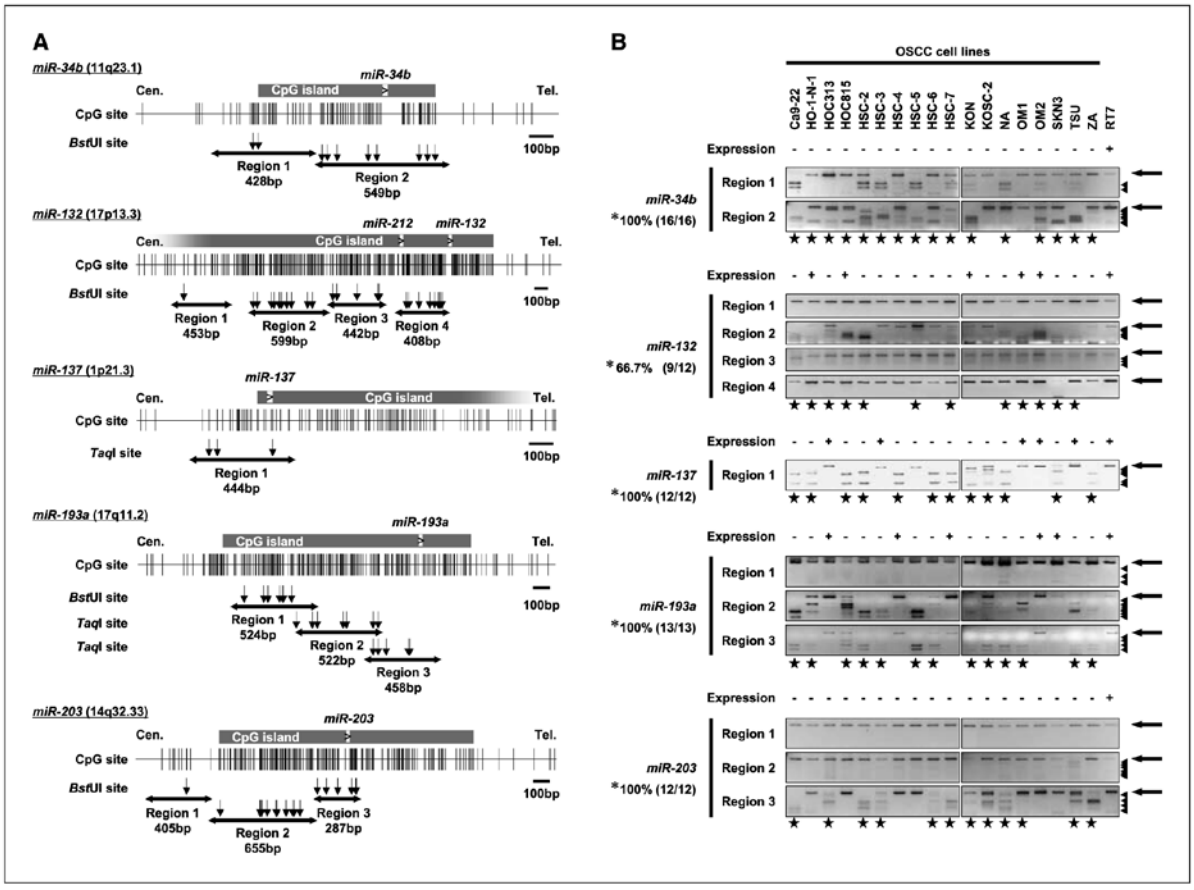

Figure 2. Analysis for the correlation between methylation status and expression of five candidate miRNA genes in OSCC cell lines. *A,* maps of miRNAs, CpG islands, CpG sites, and PCR products used for COBRA and bisulfite sequencing. *Dark gray box,* CpG islands; *light gray box,* miRNAs; *vertical tick marks,* CpG sites; *horizontal bars with arrowheads,* PCR product; *vertical arrows,* restriction enzyme sites. PCR product sizes (*horizontal arrows*) are as follows: *miR-34b* region, 1,428 bp (restricted by *Bst*UI); *miR-34b* region, 2,549 bp (restricted by *Bst*UI); *miR-132* region, 1,453 bp (restricted by *Bst*UI); *miR-132* region, 2,599 bp (restricted by *Bst*UI); *miR-132* region, 3,442 bp (restricted by *Bst*UI); *miR-132* region, 4,408 bp (restricted by *Bst*UI); *miR-137* region, 1,444 bp (restricted by *Taq*I); *miR-193a* region, 1,524 bp (restricted by *Bst*UI); *miR-193a* region, 2,522 bp (restricted by *Taq*I); *miR-193a* region, 3,458 bp (restricted by *Taq*I); *miR-203* region, 1,405 bp (restricted by *Bst*UI); *miR-203* region, 2,655 bp (restricted by *Bst*UI); and *miR-203* region, 3,287 bp (restricted by *Bst*UI). *B,* the results of COBRA in OSCC cell lines and RT7. Expression pattern of candidate miRNA genes in 18 OSCC cell lines is indicated above the results of COBRA. *Arrows,* unmethylated alleles; *arrowheads,* methylated alleles; *stars,* samples detected the restricted fragments from methylated alleles. *, frequencies of OSCC cell lines, in which DNA methylation accorded with a remarkable down-regulation of each candidate miRNA expression. Note that the denominator is the number of OSCC cell lines, in which restricted fragments from methylated alleles were detected, and the numerator is the number of OSCC cell lines, in which both DNA methylation around miRNA genes and a down-regulation of expression were detected.

nonspecific miRNA (Pre-miR Negative Control #1, Ambion) was transfected into OSCC cell lines using Lipofectamine RNAiMAX (Invitrogen) according to the manufacturer's instructions. The numbers of viable cells 24 to 72 h after transfection were assessed by the colorimetric water-soluble tetrazolium salt (WST) assay (Cell Counting Kit-8, Dojindo Laboratories). Results were normalized to the cell numbers in control cells transfected with nonspecific miRNA. Cell cycle was evaluated 48 h after transfection by fluorescence-activated cell sorting (FACS) analysis as described elsewhere (21). Apoptosis was detected 24 h after transfection by enzymatic labeling of DNA strand breaks using a terminal deoxynucleotidyl transferase–mediated dUTP nick end labeling (TUNEL) staining kit (MEBSTAIN Apoptosis Kit Direct, MBL) according to the manufacturer's directions. To evaluate the effects of caspase inhibitors on miRNA-induced growth inhibition, cells were treated with caspase-3 inhibitor zDEVD-fmk, caspase-8 inhibitor zIETD-fmk, general caspase inhibitor zVAD-fmk (R&D Systems), or vehicle 1 h before transfection, and the numbers of viable cells were assessed 48 h after transfection by WST assay.

miRNA target predictions, Western blotting, and luciferase activity assay. Predicted targets for *miR-137* or *miR-193a* and their target sites (Supplementary Table S2) were analyzed using miRanda,[7] TargetScan,[8] and PicTar.[9]

The protein expression levels of predicted targets in transiently transfected cells were analyzed 48 h after transfection by Western blotting using anti-E2F6, anti-KRAS, anti–myeloid cell leukemia 1 (MCL1), anti-NCOA2/TIF2, anti-PTK2/FAK (Abcam), anti-CDK6 (Cell Signaling Technology), anti-MYCN (Santa Cruz Biotechnology), and anti–β-actin monoclonal antibodies (Sigma) and anti–Bcl-2, anti–Bcl-X_L (Abcam), and anti-E2F1 rabbit polyclonal antibodies (Santa Cruz Biotechnology).

[7] http://microrna.sanger.ac.uk/sequences/index.shtml
[8] http://www.targetscan.org/
[9] http://pictar.bio.nyu.edu/

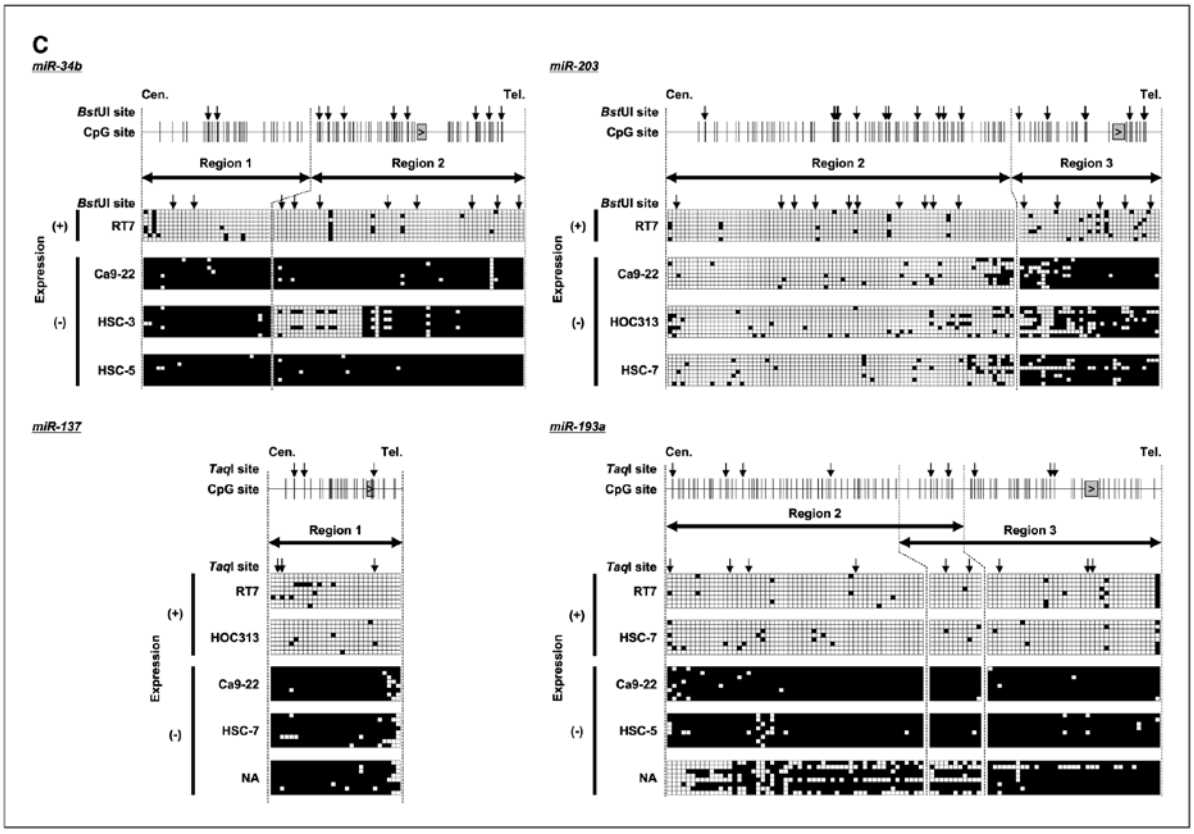

Figure 2 *Continued. C,* bisulfite sequencing of RT7 and representative OSCC cell lines with (+) or without (−) candidate miRNA expression in regions within/around candidate miRNA genes. Maps of miRNAs, CpG sites, and PCR products used for COBRA and bisulfite sequencing are indicated above the results of bisulfite sequencing. *Light gray box,* miRNAs; *vertical tick marks,* CpG sites; *horizontal bars with arrowheads,* PCR product; *vertical arrows,* restriction enzyme sites. *Open* and *filled squares* represent unmethylated and methylated CpG sites, respectively, and each *row* represents a single clone.

Luciferase constructs were made by ligating oligonucleotides containing the 3′-untranslated region (UTR) target sites of *CDK6, E2F6, MCL1, NCOA2/TIF2,* and *PTK2/FAK* (Supplementary Table S3) into downstream of the luciferase gene in pMIR-REPORT luciferase vector (Ambion). An equal amount (400 ng) of each reporter construct and 10 nmol/L of Pre-miR miRNA Precursor Molecule mimicking *miR-137* or *miR-193a*, or Pre-miR Negative Control #1 was introduced into cells with 20 ng of an internal control vector (pRL-hTK, Promega) using Lipofectamine 2000 (Invitrogen). Firefly luciferase and *Renilla* luciferase activities were each measured 48 h after transfection using the Dual-Luciferase Reporter Assay System (Promega); relative luciferase activities were calculated and normalized versus *Renilla* luciferase activity. Each transfection was repeated twice in triplicate.

Statistical analysis. Differences between subgroups were tested with the Mann-Whitney *U* test.

Results

miRNA expression profiles in 18 OSCC cell lines relative to those in RT7. The present study, strategy and partial results of which are shown in Fig. 1*A*, was designed to identify tumor suppressor miRNAs silenced by tumor-specific DNA methylation in OSCC. To identify differentially expressed miRNAs in OSCC, we first performed expression profiling for 157 mature miRNAs in 18 OSCC cell lines and their normal counterpart RT7, an immortalized human oral keratinocyte line, using a highly sensitive Taqman MicroRNA Assays Human Panel Early Access kit (Fig. 1*B*). Among 157 miRNAs, *miR-124b, miR-144, miR-199-s*, and *miR-104* were excluded from analysis in this study because individual Taqman MicroRNA Assays for these miRNAs are not available. In addition, expression levels of *miR-154, miR-211, miR-220, miR-302c*, and *miR-323* in OSCC cells were unevaluated because their expression in RT7 for normalization was undetermined by real-time RT-PCR analysis. Compared with expression levels in RT7, frequent up-regulation (>1.5-fold expression, ≥66.7% of OSCC lines) was found only in 11 of 148 (7.4%) miRNAs, whereas frequent down-regulation (<0.5-fold expression, ≥66.7% of OSCC lines) was observed in 54 of 148 (36.5%) miRNAs (Table 1), suggesting that some subsets of miRNAs are generally down-regulated in OSCC lines compared with normal oral keratinocytes.

Methylation analysis of candidate miRNAs in OSCC cell lines. We next searched the human genome database (University of California Santa Cruz Genome Bioinformatics)[10] for the existence

[10] http://genome.ucsc.edu/

of CpG islands around these 157 miRNA genes and confirmed that 21 miRNAs were located on/around (within 1,000 bp) CpG islands (Supplementary Table S4). Among those 21 miRNAs, we focused on *miR-34b, miR-132, miR-137, miR-193a*, and *miR-203* due to their frequent down-regulation in a panel of 18 OSCC cell lines: the percentage of OSCC lines with a remarkable down-regulation in these five miRNA genes compared with RT7 (<0.5-fold expression) were 100% (18 of 18), 72.2% (13 of 18), 72.2% (13 of 18), 72.2% (13 of 18), and 100% (18 of 18), respectively (Fig. 1*C*). The expression of the five miRNAs was restored by demethylation with 5-aza-dCyd at a high frequency in OSCC cells lacking their expressions (Supplementary Table S5), suggesting that aberrant DNA methylation suppressed expression of these five miRNAs.

To determine the correlation between the DNA methylation status of these five miRNAs and their expression patterns in the 18 OSCC cell lines and RT7, we performed COBRA. The physical relationships between these miRNA genes, CpG islands, and the primers for COBRA are shown in Fig. 2*A*. Aberrant DNA methylation within CpG islands around *miR-34b, miR-137, miR-193a*, and *miR-203*, except *miR-132*, was detected in all of the OSCC lines having down-regulation of their expression (Fig. 2*B*). Consistent with the results of COBRA, aberrant DNA methylation was also shown by bisulfite sequencing in the OSCC lines lacking the expression of four candidate miRNAs but not in RT7 and the cell lines expressing these miRNAs (Fig. 2*C*). Therefore, we further analyzed *miR-34b, miR-137, miR-193a*, and *miR-203* as possible candidates.

Methylation and expression analysis of selected miRNAs in primary OSCC cases. To determine whether the methylation of the four miRNAs also occurs in primary OSCC tumors in a tumor-specific manner, the correlation between DNA methylation status and expression patterns of the four genes in primary OSCCs with a corresponding noncancerous oral mucosa was examined using COBRA and Taqman real-time RT-PCR analysis, respectively. In COBRA, tumor-specific DNA methylation of *miR-34b, miR-137, miR-193a*, and *miR-203* was detected in 36.4% (4 of 11), 63.6% (7 of 11), 72.7% (8 of 11), and 45.5% (5 of 11) of primary OSCC cases, respectively (Fig. 3*A*). Positive cases of *miR-137* and *miR-193a* showed conspicuous fragments from methylated alleles in a tumor-specific manner. On the other hand, most of the positive cases of *miR-34b* and *miR-203* showed a trace of fragments from methylated alleles in tumor specimens, indicating that frequencies of aberrant methylation around *miR-34b* and *miR-203* in tumor cells were very low. Although there were a few cases in which restricted fragments from methylated alleles were observed in normal tissues, we considered tumor specimens, in which large amounts of restricted fragments from methylated alleles were more clearly detected compared with paired normal tissues, to be positive cases having tumor-specific hypermethylation.

In the Taqman real-time RT-PCR analysis, expression levels of *miR-34b, miR-137, miR-193a*, and *miR-203* in tumors compared with paired normal oral mucosa were reduced in 27.2% (3 of 11), 54.5% (6 of 11), 45.5% (5 of 11), and 63.6% (7 of 11) of primary OSCC cases, respectively (Fig. 3*B*). Consequently, both tumor-specific DNA methylation and down-regulated expression of *miR-34b, miR-137, miR-193a*, and *miR-203* were observed in 25% (1 of 4), 71.4% (5 of 7), 62.5% (5 of 8), and 40% (2 of 5) of primary OSCC cases, respectively; note that the denominator is the number of primary OSCC cases, in which restricted fragments from methylated alleles were detected by COBRA, and the numerator is the

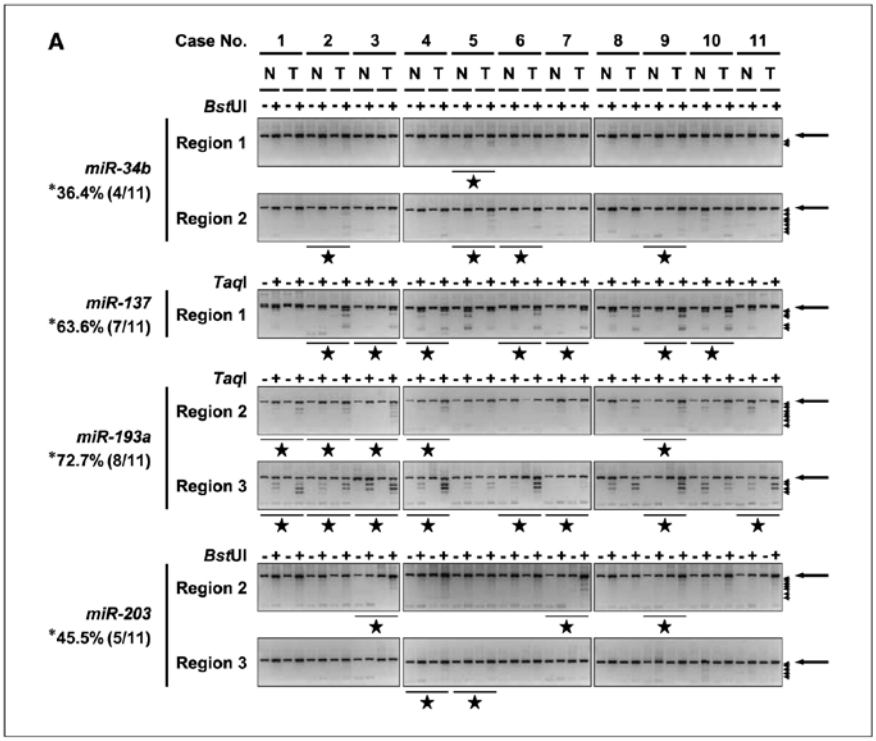

Figure 3. Methylation and expression analyses in 11 primary OSCC cases. *A*, COBRA for candidate miRNA genes in surgically resected primary OSCC tumors (*T*) and corresponding noncancerous oral mucosa (*N*). Presence of restriction enzyme processing is indicated with plus or minus above the results of COBRA. *Stars*, cases in which tumor-specific methylation was detected. *, frequencies of cases in which aberrant methylation of candidate miRNA was detected by COBRA.

number of primary OSCC cases, in which both DNA methylation around miRNA genes and down-regulation of their expressions were detected by COBRA and Taqman real-time RT-PCR analysis, respectively. Those results suggest that *miR-137* and *miR-193a* are most likely miRNAs frequently silenced through tumor-specific hypermethylation in OSCC. Bisulfite sequencing of those miRNAs in representative primary OSCC tumors clearly confirmed the results of COBRA (Fig. 3*C*). Therefore, it finally became our prime.

Tumor-suppressive effects of *miR-137* and *miR-193a* on the growth of OSCC cell lines. Because our expression and methylation analyses identified *miR-137* and *miR-193a* as candidate miRNAs silenced via tumor-specific hypermethylation in OSCC, we examined growth-inhibitory effects of *miR-137* or *miR-193a* through the transient transfection of double-strand RNA (dsRNA) mimicking either *miR-137* or *miR-193a* into OSCC cell lines lacking the expression of these two miRNAs. Restoration of *miR-137* or *miR-193a* expression significantly reduced cell growth in all of OSCC cell lines tested (Fig. 4*A*), suggesting that both *miR-137* and *miR-193a* have a tumor suppressor function in oral epithelia. In addition, we noticed that the apoptotic change was more serious in transfectants of *miR-193a* than those of *miR-137* under the phase-contrast microscope (Fig. 4*A*). At 72 h after transfection, a large number of transfectants of *miR-193a* were rounded and floating compared with the control counterpart, whereas these morphologic changes were much weaker in transfectants of *miR-137*. In FACS analysis (Fig. 4*B*), 48 h after transfection of both *miR-137* or *miR-193a* resulted in a decrease in S and G_2-M phase cells. Notably, *miR-137* mainly induced the accumulation of G_0-G_1 phase cells, whereas *miR-193a* induced the accumulation of sub-G_1 phase cells, suggesting that *miR-137* and *miR-193a* might be predominantly associated with cell cycle arrest at the G_1-S checkpoint and apoptotic change, respectively, in OSCC cells. Using the TUNEL assay, we tested whether these morphologic changes were caused by apoptosis. Twenty-four hours after the transfection of *miR-193a*, apoptotic cells were detected in both HSC-2 (Fig. 4*C*) and HO-1-N-1 (data not shown) cells but not clearly detected in transfectants of *miR-137* (data not shown). Moreover, we examined the effects of caspase inhibitors on *miR-193a*–induced reduction of cell growth in HSC-2 and HO-1-N-1 cells (Fig. 4*D*). Reduction of cell growth was partially but significantly inhibited by all three caspase inhibitors in both cells, suggesting that *miR-193a* may induce the reduction of cell growth at least in part through caspase-mediated apoptosis. In addition, effects of zDEVD-fmk or zVAD-fmk were more remarkable compared with zIETD-fmk in both cell lines, suggesting that activation of caspase-3, one of effector caspases, may be crucial in *miR-193a*–induced apoptosis in OSCC.

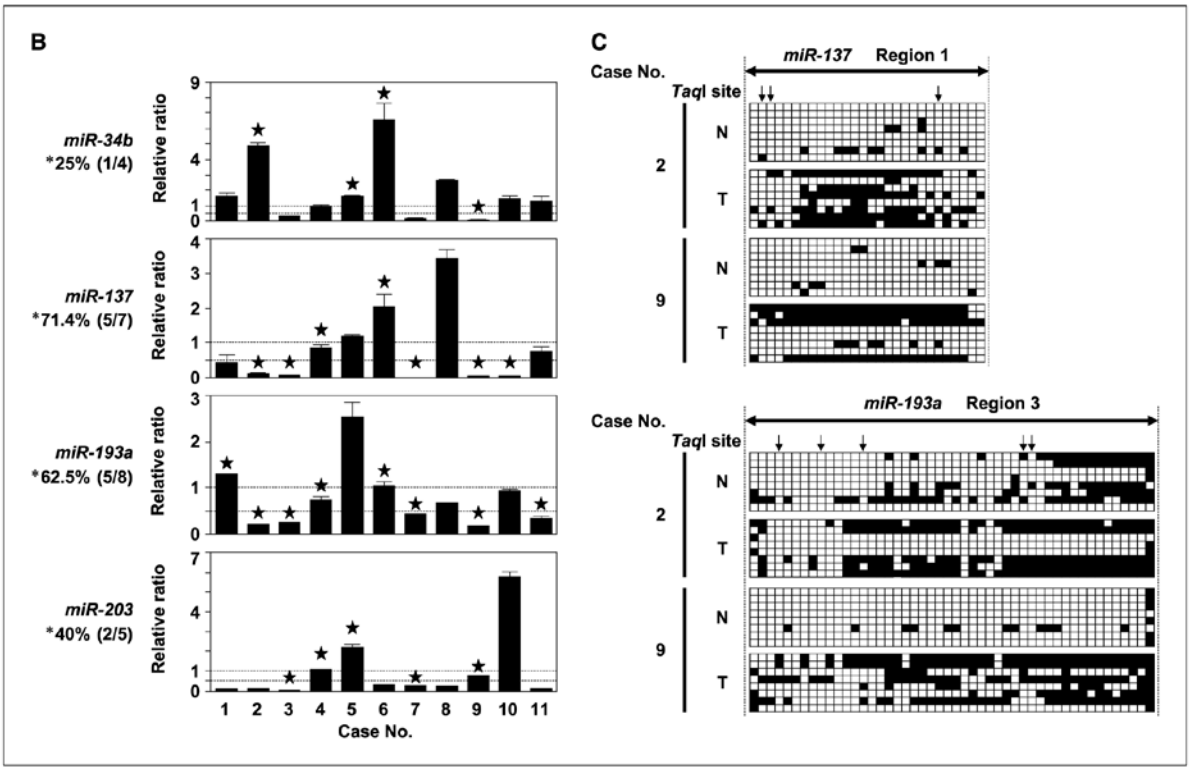

Figure 3 *Continued. B,* quantitative real-time RT-PCR analysis for expression levels of candidate miRNAs in primary OSCC tumors compared with paired normal oral mucosa. *Stars,* cases in which tumor-specific methylation was detected by COBRA. *, frequencies of cases, in which a remarkable down-regulation of candidate miRNA expression (<0.5-fold expression) was observed compared with paired normal oral mucosa, among cases found to have the tumor-specific methylation by COBRA. *C,* results of bisulfite sequencing of representative cases. *Horizontal bars with arrowheads,* PCR product; *vertical arrows,* restriction enzyme sites. *Open* and *filled squares* represent unmethylated and methylated CpG sites, respectively, and each *row* represents a single clone.

Screening of predicted targets of *miR-137* and *miR-193a*. To explore oncogenic targets of *miR-137* or *miR-193a*, we focused on CDK6, E2F6, and NCOA2/TIF2 as *miR-137* targets, and E2F1, E2F6, KRAS, MCL1, MYCN, and PTK2/FAK as *miR-193a* targets according to computational prediction[7-9] and the reported function of predicted genes. We first performed Western blot analysis of these predicted targets 48 h after transfection of dsRNA mimicking either *miR-137* or *miR-193a* into OSCC lines lacking the expression of these miRNAs (Fig. 5*A*). Protein expression levels of CDK6, E2F6, and NCOA2/TIF2 were clearly reduced in all *miR-137* transfectants compared with their control counterparts. In all *miR-193a* transfectants, protein levels of E2F6 and PTK2/FAK were remarkably decreased compared with their control counterparts. In addition, down-regulation of MCL1, an antiapoptotic

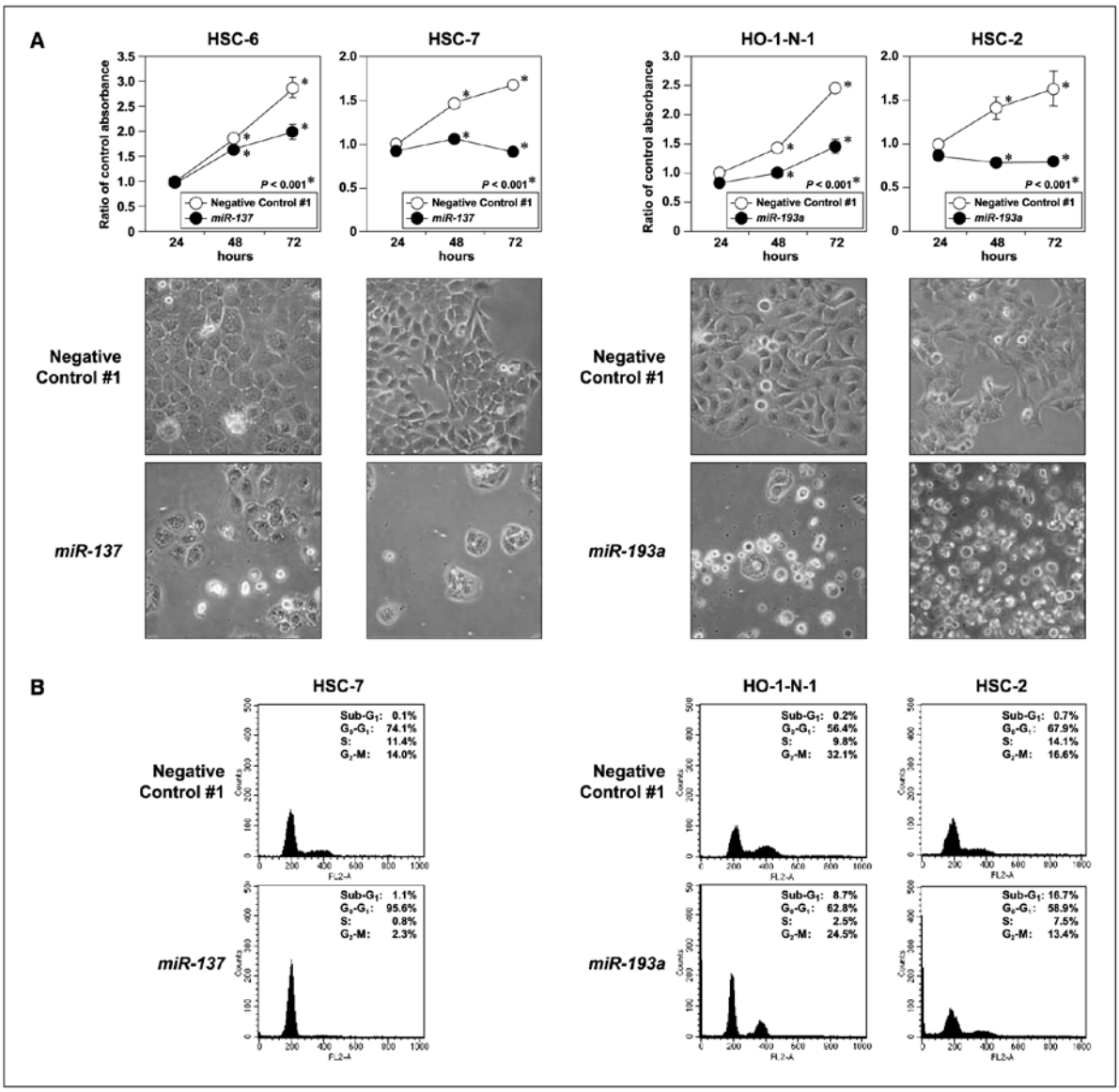

Figure 4. Tumor-suppressive effects of *miR-137* and *miR-193a* on OSCC cell lines lacking their expression. *A*, growth curves (*top*) and phase-contrast micrographs (*bottom*) of OSCC cell lines in which 10 nmol/L of Pre-miR miRNA Precursor Molecule mimicking *miR-137* or *miR-193a*, or control nonspecific dsRNA (Pre-miR Negative Control #1) was transfected using Lipofectamine RNAiMAX. The numbers of viable cells 24 to 72 h after transfection were assessed by WST assay. *Points*, mean of triplicate determinations in these experiments; *bars*, SE. Phase-contrast micrographs show the cells cultured for 72 h after transfection. *, $P < 0.05$, statistical analysis used the Mann-Whitney *U* test. *B*, representative results of the population in each phase of cell cycle assessed by FACS using cell lines 48 h after transfection of Pre-miR miRNA Precursor Molecule mimicking *miR-137* or *miR-193a*, or Pre-miR Negative Control #1. Because HSC-6 cell line contains two different populations, diploid (2n) and tetraploid (4n) clones, which show complicated pattern in cell cycle analysis by FACS, we did not include this cell line for the analysis.

Bcl-2 family member, was also detected in all OSCC cell lines transfected with *miR-193a* compared with negative control dsRNA, although we found no noticeable differences in the protein levels of Bcl-2 and Bcl-X_L between *miR-193a* and control transfectants. To further determine whether the predicted target sites against these two miRNAs in 3′-UTR of mRNAs of *CDK6, E2F6, MCL1, NCOA2/TIF2*, and *PTK2/FAK* (see Supplementary Table S3) were responsible for the translational regulation by dsRNA, we next performed luciferase assays with vectors containing these 3′-UTR target sites downstream of the *luciferase* reporter gene (Fig. 5*B*). The statistically significant reduction of luciferase activity was observed in NA cells cotransfected with *miR-137* and a reporter vector containing the *CDK6* 3′-UTR target site and those cotransfected with *miR-193a* and a vector containing the *E2F6* 3′-UTR target site compared with control transfectants. No notable alteration of luciferase activity was detected between *miR-137* or *miR-193a* transfectant and control counterpart in other genes. These data suggest that at least CDK6 and E2F6 are possible targets for *miR-137*–mediated and *miR-193a*–mediated translational down-regulation in oral epithelia, respectively, and that activation of these molecules through methylation-mediated silencing of those two miRNAs may contribute to the pathogenesis of OSCC.

Discussion

The present study clearly shows that an integrated and sequential approach using expression and methylation analyses makes it possible to efficiently identify tumor suppressor miRNAs silenced by tumor-specific DNA methylation in cancer cells. In our miRNA expression profiles of OSCC cell lines, 36.5% (54 of 148) of miRNAs were remarkably down-regulated, which is consistent with the previous reports that miRNA expression seemed globally lower in tumors than normal tissues (7, 23). These findings suggest that the global decrease in expression levels of miRNAs contributes to carcinogenesis through the activation of oncogenic pathways, which potential targets for these miRNAs might affect greatly. In addition, recent studies also showed that *miR-127* was decreased by aberrant alterations in

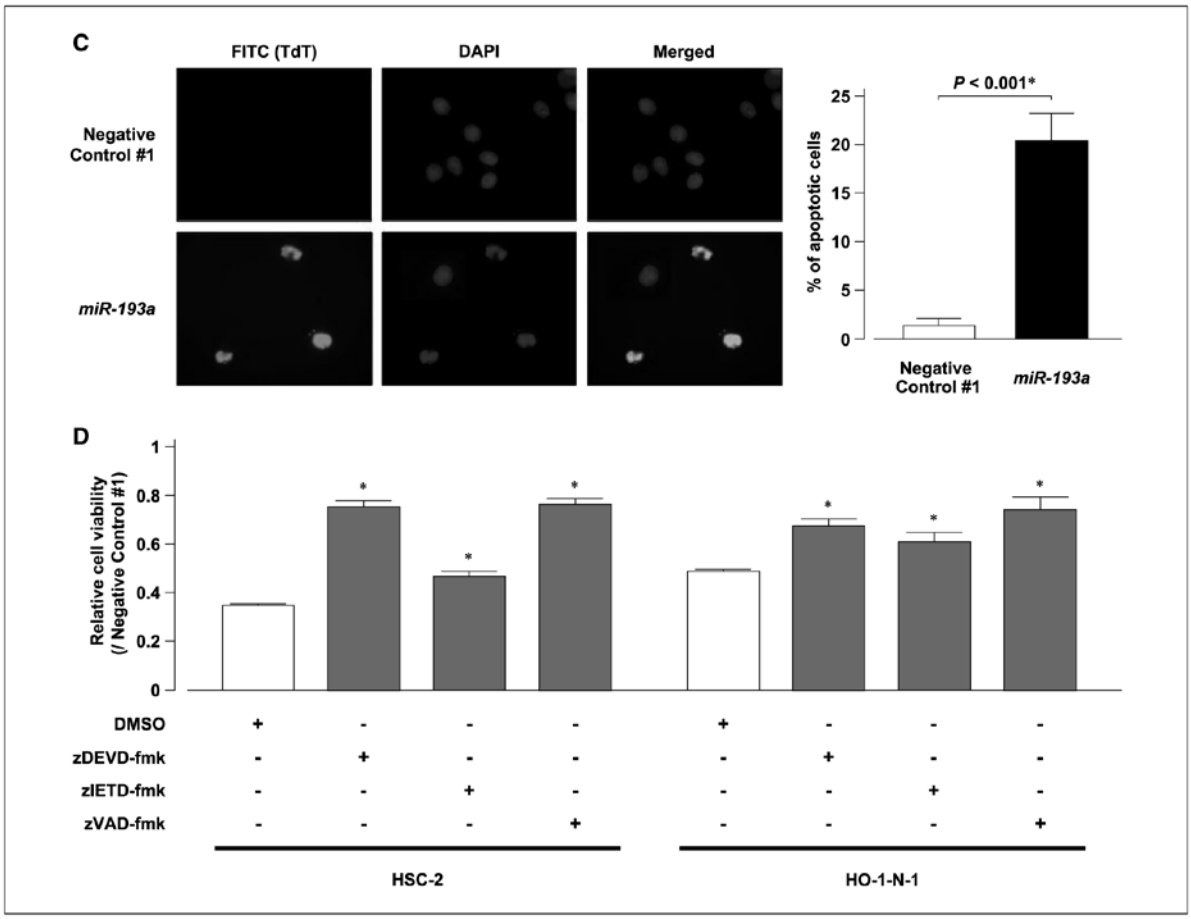

Figure 4 *Continued. C, left,* representative images of TUNEL staining in HSC-2 cells at 24 h after transfection of Pre-miR miRNA Precursor Molecule mimicking *miR-193a* or Pre-miR Negative Control #1 under the fluorescence microscope; *right,* quantitative analysis of apoptotic cells among HSC-2 cells 24 h after transfection of *miR-193a* or control nonspecific dsRNA under the fluorescence microscope. *DAPI,* 4′,6-diamidino-2-phenylindole. *D,* effects of caspase inhibitors on cell growth in HSC-2 (*left*) and HO-1-N-1 (*right*) cell lines transfected with *miR-193a*. *, $P < 0.05$ versus vehicle-treated cells, statistical analysis used the Mann-Whitney *U* test.

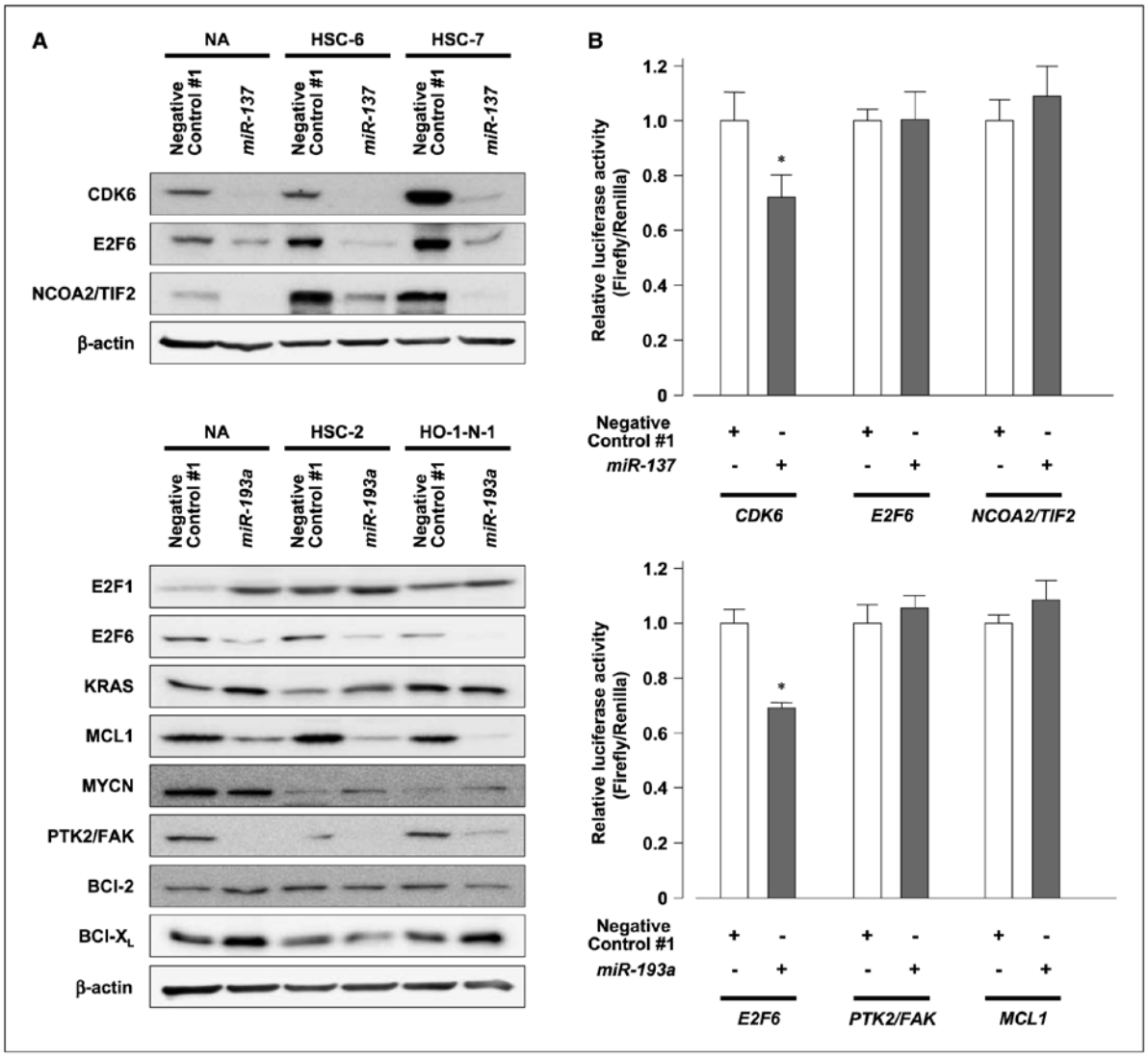

Figure 5. Screening of predicted targets of *miR-137* and *miR-193a*. *A*, representative results of Western blotting of predicted targets for *miR-137* or *miR-193a* in OSCC cell lines lacking expression of *miR-137* (NA, HSC-6, and HSC-7; *top*) or *miR-193a* (NA, HSC-2, and HO-1-N-1; *bottom*) 48 h after transfection of Pre-miR miRNA Precursor Molecule mimicking these two miRNAs, or control nonspecific dsRNA (Pre-miR Negative Control #1) using Lipofectamine RNAiMAX. *B*, luciferase assays of *miR-137*–nonexpressing and *miR-193a*–nonexpressing NA cells 48 h after cotransfection of pMIR-REPORT luciferase vectors containing 3′-UTR target sites of *CDK6*, *E2F6*, and *NCOA2/TIF2* for *miR-137* or those of *E2F6*, *PTK2/FAK*, and *MCL1* for *miR-193a* (see Supplementary Table S3), Pre-miR miRNA Precursor Molecule mimicking *miR-137* or *miR-193a*, respectively, or Pre-miR Negative Control #1, and pRL-hTK internal control vector using Lipofectamine 2000 (Invitrogen). *, $P < 0.05$ versus vehicle-treated cells, statistical analysis used the Mann-Whitney *U* test.

DNA methylation and histone modification in bladder cancer cells (12) and that *miR-124a* was inactivated by CpG island hypermethylation in several types of human cancers (11), suggesting tumor-specific DNA methylation to be an important molecular mechanism for the down-regulation of miRNA expression, similar to classic TSGs, in human cancers. Therefore, we were particular about a screening based on methylation analyses, and advanced the present study.

In the course of a program to screen a panel of 18 OSCC cell lines for tumor suppressor miRNAs silenced by aberrant DNA methylation, we selected *miR-34b*, *miR-137*, *miR-193a*, and *miR-203* as possible candidate genes. Our data showed that these miRNA expressions were frequently decreased in OSCC cell lines and that treatment with 5-aza-dCyd restored their expression levels in cells lacking their expressions. Moreover, complete consistency in the correlation between DNA methylation status around these four genes and their expression patterns was confirmed in a panel of 18 OSCC cell lines, strongly suggesting that DNA methylation around CpG islands seemed to deregulate the expression of these genes in OSCC cell lines. Recently, *miR-34* family genes, including

miR-34b, were shown to be direct transcriptional targets of p53 (24), indicating that *miR-34b* may play a pivotal role in the p53 tumor suppressor network, although marked deregulation of the expression of *miR-34b* in human cancers has not been reported. The precise functions of *miR-137*, *miR-193a*, and *miR-203* have not been characterized, but a few studies indicated their abnormal expressions in human cancers. Decreases in *miR-137* expression were described in colorectal cancer (25), central nervous system tumor cell lines (26), and neuroblastoma (27), suggesting that *miR-137* may be a TSG. Although an increase in expression levels of *miR-193a* was found in a microarray analysis for human B-cell chronic lymphocytic leukemia (28), there has been no detailed report about the aberrant expression of *miR-193a* in human cancers thus far. Down-regulation of *miR-203* expression was described in central nervous system tumor cell lines (26) and thyroid anaplastic carcinoma (29), whereas its up-regulation was also shown in breast cancer (30), lung cancer (31), and colorectal cancer (25).

In analyses using primary OSCC cases with both tumors and paired normal tissues, *miR-34b* and *miR-203* were excluded from our list of possible candidate genes for two reasons: (*a*) frequencies of aberrant methylation around *miR-34b* and *miR-203* in tumor cells were very low and (*b*) frequencies of primary cases, in which down-regulation of these genes was consistent with tumor-specific hypermethylation around these genes, were very low. Although it was unknown why these frequencies were even lower in OSCC cases than in OSCC cell lines, hypermethylation around *miR-34b* and *miR-203* might be one of the aberrant epigenetic events in a process of establishment of cell lines *in vitro*. On the other hand, frequencies of primary OSCC cases, in which down-regulation of *miR-137* and *miR-193a* expression was consistent with tumor-specific hypermethylation around these genes, were relatively high, similar to results in OSCC cell lines. *miR-137* is located in chromosomal region 1p21.3, and loss of heterozygosity (LOH) in this region has been reported in meningioma (32), pheochromocytomas (33), and paraganglioma (34). LOH at 17q11.2, where *miR-193a* is located, has also been described in Barrett's esophageal tumors (35), neurofibromatosis 1 (36), ovarian adenocarcinoma (37), cervical carcinoma (38), and breast cancer (39). These previous studies indicated that TSGs mapped to these loci and that *miR-137* and *miR-193a* might be the targets of these losses. Moreover, we found that *miR-137* and *miR-193a* might be predominantly associated with cell cycle arrest at the G_1-S checkpoint and apoptotic change, respectively, indicating that *miR-137* and *miR-193a* seem to have a tumor suppressor function in oral epithelia.

Here, we also showed that *miR-137* and *miR-193a* target *CDK6* and *E2F6*, respectively, in OSCC cell lines. CDK6 regulates major cell cycle transitions as an oncogene and has been reported the potential target of *miR-124a*, which is epigenetically silenced in human cancers (11). E2F6 is a transcriptional repressor in the E2F family (40), and its potential oncogenic capacity was also shown recently (41). Our Western blotting also showed that the protein levels of E2F6 and NCOA2/TIF2 were remarkably down-regulated in *miR-137* transfectants, and those of MCL1 and PTK2/FAK were in *miR-193a* transfectants, although the inhibition of luciferase activity through a possible 3′-UTR target sequence of each gene inserted into downstream of the *luciferase* gene within reporter vectors was not observed in those target genes, suggesting a possible indirect target effect. NCOA2/TIF2, a member of the p160 family of coactivators, and PTK2/FAK, a member of cytoplasmic nonreceptor protein tyrosine kinases, have been described to be associated with human cancer development (42, 43). MCL1 is an antiapoptotic Bcl-2 family protein, which contributes to cancer progression, resistance to chemotherapy, and poor clinical outcome (44). These results suggest that *miR-137* and *miR-193a* may induce the down-regulation of these proteins by either direct binding to their target mRNAs or their unknown indirect effects other than direct binding, resulting in cell cycle arrest at the G_1-S checkpoint and apoptosis, respectively, in oral squamous cells.

In conclusion, our study showed for the first time that (*a*) tumor-specific hypermethylation in OSCC was an important molecular mechanism causing the global down-regulation of miRNAs, in a similar manner to that shown for classic TSGs; (*b*) *miR-137* and *miR-193a* were tumor suppressor miRNAs silenced by tumor-specific hypermethylation in OSCC, suggesting that the epigenetic silencing of these miRNAs plays a pivotal role during oral carcinogenesis; and (*c*) *CDK6* and *E2F6* were potential targets for *miR-137* and *miR-193a*, respectively.

Acknowledgments

Received 9/6/2007; revised 1/23/2008; accepted 1/24/2008.

Grant support: Scientific Research and Scientific Research on Priority Areas, and a 21st Century Center of Excellence Program for Molecular Destruction and Reconstitution of Tooth and Bone from the Ministry of Education, Culture, Sports, Science, and Technology, Japan; Core Research for Evolutional Science and Technology of Japan Science and Technology Corp.; and New Energy and Industrial Technology Development Organization.

The costs of publication of this article were defrayed in part by the payment of page charges. This article must therefore be hereby marked *advertisement* in accordance with 18 U.S.C. Section 1734 solely to indicate this fact.

We thank Professor Masaki Noda (Hard Tissue Genome Research Center, Tokyo Medical and Dental University) for continuous encouragement throughout this work and Ayako Takahashi and Rumi Mori for technical assistance.

References

1. Bartel DP. MicroRNAs: genomics, biogenesis, mechanism, and function. Cell 2004;116:281–97.
2. He L, Hannon G J. MicroRNAs: small RNAs with a big role in gene regulation. Nat Rev Genet 2004;5:522–31.
3. Miska EA. How microRNAs control cell division, differentiation and death. Curr Opin Genet Dev 2005; 15:563–8.
4. Harfe BD. MicroRNAs in vertebrate development. Curr Opin Genet Dev 2005;15:410–5.
5. Esquela-Kerscher A, Slack FJ. Oncomirs—microRNAs with a role in cancer. Nat Rev Cancer 2006;6:259–69.
6. Osada H, Takahashi T. MicroRNAs in biological processes and carcinogenesis. Carcinogenesis 2007;28: 2–12.
7. Lu J, Getz G, Miska EA, Alvarez-Saavedra E, et al. MicroRNA expression profiles classify human cancers. Nature 2005;435:834–8.
8. Calin GA, Dumitru CD, Shimizu M, et al. Frequent deletions and down-regulation of micro-RNA genes miR15 and miR16 at 13q14 in chronic lymphocytic leukemia. Proc Natl Acad Sci U S A 2002;99:15524–9.
9. Calin G A, Croce CM. MicroRNAs and chromosomal abnormalities in cancer cells. Oncogene 2006;25:6202–10.
10. Garzon R, Fabbri M, Cimmino A, Calin GA, Croce CM. MicroRNA expression and function in cancer. Trends Mol Med 2006;12:580–7.
11. Lujambio A, Ropero S, Ballestar E, et al. Genetic unmasking of an epigenetically silenced microRNA in human cancer cells. Cancer Res 2007;67:1424–9.
12. Saito Y, Liang G, Egger G, et al. Specific activation of microRNA-127 with down-regulation of the proto-oncogene BCL6 by chromatin-modifying drugs in human cancer cells. Cancer Cell 2006;9:435–43.
13. Parkin DM, Bray F, Ferlay J, Pisani P. Global cancer statistics, 2002. CA Cancer J Clin 2005;55:74–108.
14. Nomura K, Sobue T, Nakatani H, et al. Number of deaths and proportional mortality rates from malignant neoplasms by site in Japan (2003). In: The Editorial Board of the Cancer Statistics in Japan. Cancer statistics in Japan 2005. Tokyo: National Cancer Center; 2005. p. 36–9.
15. Scully C, Field JK, Tanzawa H. Genetic aberrations in oral or head and neck squamous cell carcinoma (SCCHN). 1. Carcinogen metabolism, DNA repair and cell cycle control. Oral Oncol 2000;36:256–63.
16. Ha PK, Califano JA. Promoter methylation and

inactivation of tumour-suppressor genes in oral squamous-cell carcinoma. Lancet Oncol 2006;7:77–82.
17. Snijders AM, Schmidt BL, Fridlyand J, et al. Rare amplicons implicate frequent deregulation of cell fate specification pathways in oral squamous cell carcinoma. Oncogene 2005;24:4232–42.
18. Baldwin C, Garnis C, Zhang L, Rosin MP, Lam WL. Multiple microalterations detected at high frequency in oral cancer. Cancer Res 2005;65:7561–7.
19. Liu CJ, Lin SC, Chen YJ, Chang KM, Chang KW. Array-comparative genomic hybridization to detect genome-wide changes in microdissected primary and metastatic oral squamous cell carcinomas. Mol Carcinog 2006;45:721–31.
20. Nakaya K, Yamagata HD, Arita N, et al. Identification of homozygous deletions of tumor suppressor gene FAT in oral cancer using CGH-array. Oncogene 2007;26:5300–8.
21. Suzuki E, Imoto I, Pimkhaokham A, et al. PRTFDC1, a possible tumor-suppressor gene, is frequently silenced in oral squamous-cell carcinomas by aberrant promoter hypermethylation. Oncogene 2007;26:7921–32.
22. Xiong Z, Laird PW. COBRA: a sensitive and quantitative DNA methylation assay. Nucleic Acids Res 1997;25:2532–4.
23. Thomson JM, Newman M, Parker JS, Morin-Kensicki EM, Wright T, Hammond SM. Extensive post-transcriptional regulation of microRNAs and its implications for cancer. Genes Dev 2006;20:2202–7.
24. He L, He X, Lim LP, et al. A microRNA component of the p53 tumour suppressor network. Nature 2007;447:1130–4.
25. Bandres E, Cubedo E, Agirre X, et al. Identification by real-time PCR of 13 mature microRNAs differentially expressed in colorectal cancer and non-tumoral tissues. Mol Cancer 2006;5:29.
26. Gaur A, Jewell DA, Liang Y, et al. Characterization of microRNA expression levels and their biological correlates in human cancer cell lines. Cancer Res 2007;67:2456–68.
27. Chen Y, Stallings RL. Differential patterns of microRNA expression in neuroblastoma are correlated with prognosis, differentiation, and apoptosis. Cancer Res 2007;67:976–83.
28. Calin GA, Liu CG, Sevignani C, et al. MicroRNA profiling reveals distinct signatures in B cell chronic lymphocytic leukemias. Proc Natl Acad Sci U S A 2004;101:11755–60.
29. Visone R, Pallante P, Vecchione A, et al. Specific microRNAs are down-regulated in human thyroid anaplastic carcinomas. Oncogene 2007;26:7590–5.
30. Iorio MV, Ferracin M, Liu CG, et al. MicroRNA gene expression deregulation in human breast cancer. Cancer Res 2005;65:7065–70.
31. Yanaihara N, Caplen N, Bowman E, et al. Unique microRNA molecular profiles in lung cancer diagnosis and prognosis. Cancer Cell 2006;9:189–98.
32. Bello MJ, de Campos JM, Vaquero J, et al. High-resolution analysis of chromosome arm 1p alterations in meningioma. Cancer Genet Cytogenet 2000;120:30–6.
33. Aarts M, Dannenberg H, de Leeuw RJ, et al. Microarray-based CGH of sporadic and syndrome-related pheochromocytomas using a 0.1-0.2 Mb bacterial artificial chromosome array spanning chromosome arm 1p. Genes Chromosomes Cancer 2006;45:83–93.
34. Edstrom E, Mahlamaki E, Nord B, et al. Comparative genomic hybridization reveals frequent losses of chromosomes 1p and 3q in pheochromocytomas and abdominal paragangliomas, suggesting a common genetic etiology. Am J Pathol 2000;156:651–9.
35. Swift A, Risk JM, Kingsnorth AN, Wright TA, Myskow M, Field JK. Frequent loss of heterozygosity on chromosome 17 at 17q11.2-q12 in Barrett's adenocarcinoma. Br J Cancer 1995;71:995–8.
36. Kluwe L, Friedrich RE, Mautner VF. Allelic loss of the NF1 gene in NF1-associated plexiform neurofibromas. Cancer Genet Cytogenet 1999;113:65–9.
37. Arnold JM, Huggard PR, Cummings M, Ramm GA, Chenevix-Trench G. Reduced expression of chemokine (C-C motif) ligand-2 (CCL2) in ovarian adenocarcinoma. Br J Cancer 2005;92:2024–31.
38. Zijlmans HJ, Fleuren GJ, Baelde HJ, Eilers PH, Kenter GG, Gorter A. The absence of CCL2 expression in cervical carcinoma is associated with increased survival and loss of heterozygosity at 17q11.2. J Pathol 2006;208:507–17.
39. Pierga JY, Reis-Filho JS, Cleator SJ, et al. Microarray-based comparative genomic hybridisation of breast cancer patients receiving neoadjuvant chemotherapy. Br J Cancer 2007;96:341–51.
40. Wong CF, Barnes LM, Smith L, Popa C, Serewko-Auret MM, Saunders NA. E2F6: a member of the E2F family that does not modulate squamous differentiation. Biochem Biophys Res Commun 2004;324:497–503.
41. Chen C, Wells AD. Comparative analysis of E2F family member oncogenic activity. PLoS ONE 2007;2:e912.
42. Agoulnik IU, Vaid A, Nakka M, et al. Androgens modulate expression of transcription intermediary factor 2, an androgen receptor coactivator whose expression level correlates with early biochemical recurrence in prostate cancer. Cancer Res 2006;66:10594–602.
43. Mitra SK, Hanson DA, Schlaepfer DD. Focal adhesion kinase: in command and control of cell motility. Nat Rev Mol Cell Biol 2005;6:56–68.
44. Youle RJ, Strasser A. The BCL-2 protein family: opposing activities that mediate cell death. Nat Rev Mol Cell Biol 2008;9:47–59.

分子遺伝分野

三木 義男
難治疾患研究所・遺伝疾患研究部門
遺伝子応用医学・教授

1. 研究課題名

Ⅰ. 骨軟部腫瘍のゲノム応用学

(Medical genomics of bone and soft tissue tumors)

ゲノムからフェノーム（個体の表現形質）に至る生命活動の各階層を包含するオミックス情報の構築を目的に、本研究室では骨軟部腫瘍を対象に先進的なトランスクリプトーム解析によるオーダーメイド医療の実現を目指す。具体的には、トランスクリプトーム情報とDNAのコピー数情報を解析し、それらの情報を基盤に各フェノームとの関連を解明する。

脂肪細胞の腫瘍は良性病変である脂肪腫と悪性病変である脂肪肉腫とに大別され、治療法は両者で大きく異なる。病理学的には、良性病変である脂肪腫は、通常細胞密度が低く核の異型度も低いのが特徴で、一方高分化型脂肪肉腫も細胞密度や核の異型度が低い低悪性の症例が存在する。しかしこれらの場合、病理学的変化は良悪性を決定的に区別できるものではない。腫瘍の染色体核型解析において、主に12番染色体の増幅を含むリング染色体が認められれば悪性の脂肪肉腫と診断されるが、リング染色体を含まず病理学的に高分化型脂肪肉腫と診断される症例があり、これらのボーダーラインのWDLPSと脂肪腫の真の悪性度鑑別に有用な遺伝子の同定、および「ボーダーライン」のWDLPSの発現パターンとコピー数の変化を解析した。その結果、高分化型脂肪肉腫の鑑別診断として分子生物学的手法は有用で、リング陰性のWDLPSの存在を認識し検討を重ねることで腫瘍の良・悪性とは何かという本質に迫ることが可能と考えられた。

Ⅱ. 骨軟部腫瘍のアポトーシス誘導機構

(Induction of apoptosis in bone and soft tissue tumors)

細胞は、DNA損傷や酸化ストレスによってアポトーシスが誘導され、その制御機構の破綻は、癌をはじめとする広範な疾患の原因となる。そこで骨軟部腫瘍を対象に、アポトーシスを制御するいくつかのキナーゼに焦点を当て、アポトーシス誘導機構の解明を目指す。DNA損傷によって惹起される細胞死（アポトーシス）では、がん抑制遺伝子であるp53がその中心的な働きを担っている。p53はリン酸化を中心とした多彩な修飾を受けてその機能を使い分けていることから、アポトーシス誘導に関わるp53のリン酸化によって特異的に誘導される遺伝子を網羅的に探索し、p53依存性アポトーシス機構の詳細な解析を行った。具体的には、アポトーシス誘導に関わる新規遺伝子の網羅的探索を目的として、shRNA発現ベクターライブラリーを用いたスクリーニング系を構築した。同定された転写因子TAF1の発現を抑制するshRNAは、再現性良くアポトーシスを抑制した。またTAF1によってp27kip1の発現が制御されていることが分かり、DNA損傷刺激に応答して起こるアポトーシスの誘導にはこれらの分子が関与していることが示唆された。そこで、本研究では、骨肉腫細胞株のうちp53の機能が正常なU2OS細胞とp53が発現していないSaos-2細胞それぞれでTAF1をRNAiによりノックダウンし、p53の下流分子の発現変化をマイクロアレイ解析によって比較することにより、TAF1依存的なp53の発現低下に伴って発現の変化する遺伝子の同定を行った。また、TAF1の持つ多様な機能のうちp53の発現変化に影響を与える機能を同定し、p53発現制御メカニズムの解明を目指し解析を行った。

2.

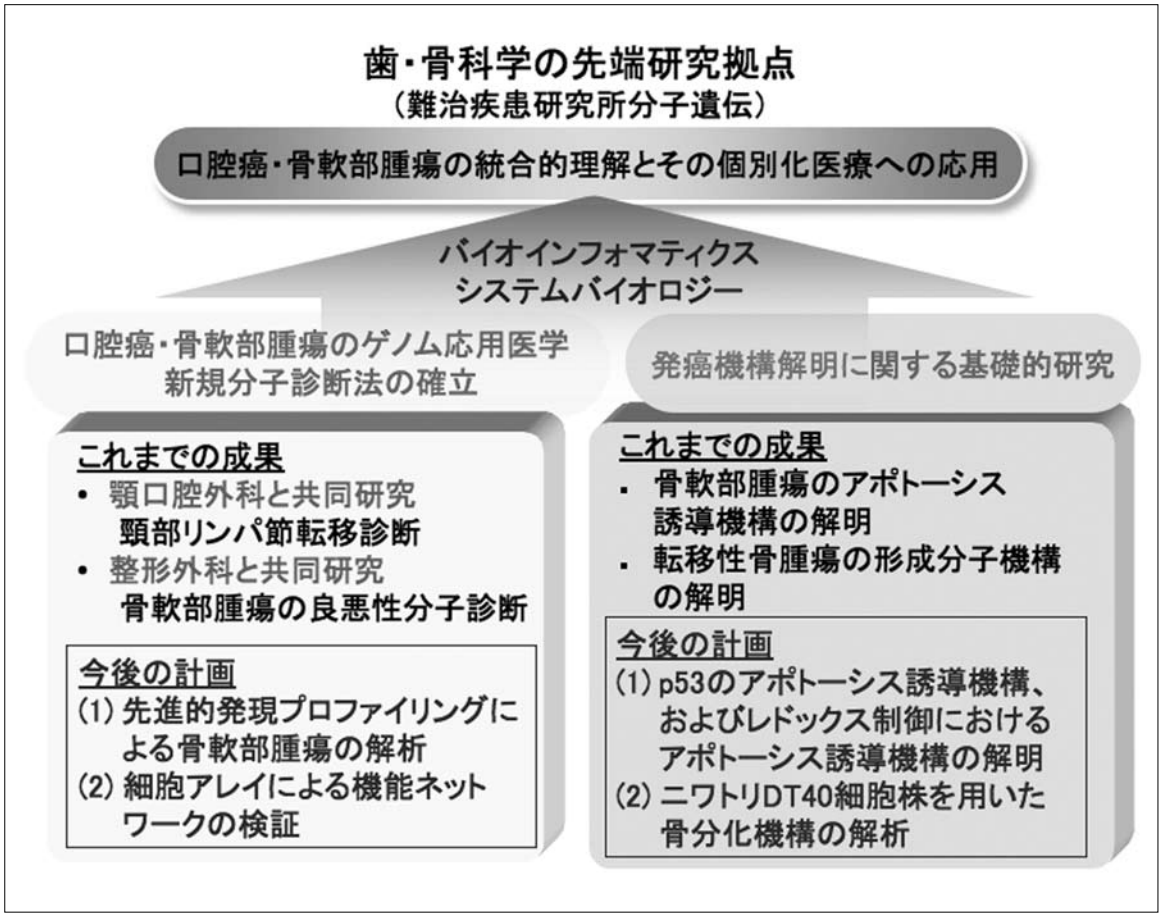

3. 英文要約

(1) Introduction and characterization of a polymerase-dead point mutation into the POLK gene in vertebrates.
The chicken DT40 cell line is widely used for gene knock-outs. We attempted to introduce a polymerase-dead point mutation into Polkappa, a polymerase for translesion DNA synthesis, taking advantage of the highly efficient targeted integration in DT40 cells. The resulting cells (REV3 (-/-) POLK (/) (pol-dead)) proliferated with the same kinetics as the parental REV3 (-/-) cells. Though the mock-treated REV3 (-/-) POLK (/) (mock) cells showed the same sensitivity as the parental REV3 (-/-) cells to methyl methanesulfonate, the REV3 (-/-) POLK (/) (pol-dead) cells demonstrated the same sensitivity as the REV3 (-/-) POLK (/-) double knock-out cells. This implies that the presence of the polymerase-dead Polkappa does not interfere with other polymerases repairing monoalkylation damage.

(2) A CRM1-mediated nuclear export signal governs cytoplasmic localization of BRCA2 and is essential for centrosomal localization of BRCA2.
Germ-line mutations of the BRCA2 gene cause inherited susceptibility to breast and ovarian cancers. BRCA2 contains two nuclear localization signals, predominantly localizes in the nucleus and plays significant roles in DNA double-strand break repair. Recently, we reported that BRCA2 localizes to the centrosomes during the S and early M phases of the cell cycle. In this study, for the first time, we identified a functional nuclear export sequence (NES1; (1383) DLSDLTFLEVA (1393)) in BRCA2. The green fluorescent protein (GFP) -NES1 fusion protein was localized in the cytoplasm and could be blocked by the chromosomal region maintenance 1-specific export inhibitor leptomycin B. Mutation of a leucine residue in the NES1 motif to alanine (L1384A) resulted in both cytoplasmic and nuclear localization of the GFP-NES1 fusion protein and a nuclear accumulation of ectopic full-length BRCA2-FLAG. Moreover, treatment of cells with leptomycin B decreased centrosomal localization of BRCA2. Finally, by microinjection of an anti-BRCA2 antibody into the cytoplasm of HeLa S3 cells, we found that depletion of normal BRCA2 proteins in the cytoplasm leads to centrosome amplification and binucleated cells. Our results suggest that disruption of the NES function by genetic changes results in deregulation of BRCA2

export, which ultimately leads to centrosome disorder.

(3) Molecular epidemiological and mutational analysis of DNA mismatch repair (MMR) genes in endometrial cancer patients with HNPCC-associated familial predisposition to cancer.
Recently, a high rate of endometrial cancer has been reported in women with hereditary non-polyposis colorectal cancer (HNPCC), suggesting a relationship between familial endometrial cancers and HNPCC. Familial endometrial cancers constitute only about 0.5% of all endometrial carcinomas and it is essential to examine family histories in detail. A mutational analysis of three DNA mismatch repair (MMR) genes (hMLH1, hMSH2 and hMSH6) in patients with endometrial cancer who meet our criteria for familial predisposition to HNPCC-associated endometrial cancers was performed. Mutations were detected in 18 of the 120 patients (15.0%). Most HNPCC-related endometrial cancers do not meet the New Amsterdam Criteria for HNPCC. These clinical criteria may identify only some HNPCC-associated endometrial cancers. Establishing the correct family history for endometrial cancer patients is important for diagnosing familial endometrial carcinomas. An analysis of MMR genes may be useful for patients with endometrial cancer showing familial aggregation. In addition, gynecologists must be accurately informed, and it is important to perform large-scale, multicenter studies both nationwide and internationally.

(4) IL12RB2 and ABCA1 genes are associated with susceptibility to radiation dermatitis.
PURPOSE: Severe acute radiation dermatitis is observed in approximately 5% to 10% of patients who receive whole-breast radiotherapy. Several factors, including treatment-related and patient-oriented factors, are involved in susceptibility to severe dermatitis. Genetic factors are also thought to be related to a patient's susceptibility to severe dermatitis. To elucidate genetic polymorphisms associated with a susceptibility to radiation-induced dermatitis, a large-scale single-nucleotide polymorphism (SNP) analysis using DNA samples from 156 patients with breast cancer was conducted. EXPERIMENTAL DESIGN: Patients were selected from more than 3,000 female patients with early breast cancer who received radiotherapy after undergoing breast-conserving surgery. The dermatitis group was defined as patients who developed dermatitis at a National Cancer Institute Common Toxicity Criteria grade of > or =2. For the SNP analysis, DNA samples from each patient were subjected to the genotyping of 3,144 SNPs covering 494 genes. RESULTS: SNPs that mapped to two genes, ABCA1 and IL12RB2, were associated with radiation-induced dermatitis. In the ABCA1 gene, one of these SNPs was a nonsynonymous coding SNP causing R219K (P = 0.0065). As for the IL12RB2 gene, the strongest association was observed at SNP-K (rs3790568; P = 0.0013). Using polymorphisms of both genes, the probability of severe dermatitis was estimated for each combination of genotypes. These analyses showed that individuals carrying a combination of genotypes accounting for 14.7% of the Japanese population have the highest probability of developing radiation-induced dermatitis. CONCLUSION: Our results shed light on the mechanisms responsible for radiation-induced dermatitis. These results may also contribute to the individualization of radiotherapy.

(5) A Japanese patient with Li-Fraumeni syndrome who had nine primary malignancies associated with a germline mutation of the p53 tumor-suppressor gene.
We describe a patient who had nine primary malignant tumors and a germline mutation in the p53 tumor-suppressor gene, characteristically found in the Li-Fraumeni syndrome (LFS). A 15-year-old girl with no family history of cancer was referred to our hospital because of pain and swelling of the right knee. Osteosarcoma was diagnosed. The patient received chemotherapy followed by surgery and had a remission. After the age of 28 years, nine primary malignant tumors developed successively, including right breast cancer, colon cancer, malignant fibrous histiocytoma (MFH) of the abdominal wall, right lung double cancers, bilateral breast cancers, and MFH of the left thigh. This is the second highest number of types of primary malignant tumors to be reported in LFS. All tumors were treated by a multidisciplinary approach, including surgery. Genetic analysis revealed a germline missense mutation in the p53 gene (c.659 A > G), resulting in Y220C, which has been reported in three families with LFS. The patient died of lung metastasis from MFH at the age of 37 years. Despite the multiple tumors, repeated induction of remissions resulted in long survival. Our findings suggest that a multidisciplinary approach to treatment, including surgery, is beneficial in patients with LFS.

(6) A functional genome-wide RNAi screen identifies TAF1 as a regulator for apoptosis in response to genotoxic stress.Kimura J, Nguyen ST, Liu H, Taira N, Miki Y, Yoshida K.
Evasion from apoptotic cell death is a characteristic of cancer; genes that modulate this process may be optimal for therapeutic attack. Identifying key regulators of apoptosis is thus a central goal in cancer therapy. Here,

we describe a loss-of-function screen that uses RNA interference libraries to identify genes required for induction of apoptosis. We used a short-hairpin RNA expressing vector with high gene-expression silencing activity that contained fetal brain cDNAs. Survived cells from genotoxic stress were isolated to determine knock-down of molecules that are crucial for induction of apoptosis. We identified TBP-associated factor 1 (TAF1), a gene previously implicated as an essential component of transcription machinery. Depletion of TAF1 was associated with substantial attenuation of apoptosis induced by oxidative as well as genotoxic stress. Microarray analysis further demonstrated that a number of genes were transcriptionally declined in cells silenced for TAF1. Surprisingly, knocking down TAF1 exhibited a marked decrease in p27 (Kip1) expression, allowing cells resistant from oxidative stress-induced apoptosis. These results suggest that TAF1 regulates apoptosis by controlling p27 (Kip1) expression. Our system provides a novel approach to identifying candidate genes that modulate apoptosis.

(7) Identification of novel deletion polymorphisms in breast cancer.
Breast cancer is the most frequent cancer in females worldwide and it has long been known that multiple genetic rearrangements correlate with complex biology and clinical behavior. In addition, copy number variations (CNVs) of DNA sequences account for a significant proportion of normal phenotypic variation and may have an important role in human pathological variation. In this study, we carried out a high-density oligonucleotide array comparative genomic hybridization (CGH) analyses in a series of breast cancer cell lines to identify novel homozygous deletion loci. The results were confirmed by quantitative PCR (Q-PCR) and 4 genes, the REV1L, ZNF14, NPAS1 and APOBEC3B genes, were selected. Analyses of 30 microdissected human breast tumors and paired normal mammary tissue samples indicated that these homozygous deletions are small-scale deletion polymorphisms. The variation in copy number at the loci of the 4 genes in blood-derived DNA demonstrated the frequency of deletions including homozygous deletions and single copy variants to be higher in breast cancer patients than healthy females. Notably, the homozygous deletion of APOBEC3B involved part of exon 5 and seemed to be cancer-specific in some patients, indicating that this is a functionally important structural variant. These copy number changes may play an important role in breast cancer and array-CGH analyses can thus be expected to provide new insight into the genetic background of breast cancer.

(8) TTK/Mps1 controls nuclear targeting of c-Abl by 14-3-3-coupled phosphorylation in response to oxidative stress.
Upon exposure to genotoxic stress, the c-Abl tyrosine kinase is released from cytoplasmic 14-3-3 proteins and then is targeted to the nucleus. Phosphorylation of Thr735 in c-Abl is critical for binding to 14-3-3; however, kinases responsible for this phosphorylation are unknown. Here, we identify CLK1, CLK4, MST1, MST2 and TTK (also known as Mps1) as novel Thr735 kinases in vitro by expression cloning strategy using phosphospecific antibody. We also demonstrate that ectopic expression of these kinases is capable for phosphorylation of Thr735 in cells. Importantly, upon exposure to oxidative stress, phosphorylation of Thr735 is transiently upregulated, and the status of this phosphorylation remains unchanged in cells silenced for CLK1, CLK4, MST1 or MST2. By contrast, knockdown of TTK attenuates phosphorylation of Thr735, suggesting that TTK is a physiological kinase that phosphorylates Thr735. In concert with these results, we show that, in cells silenced for TTK, c-Abl is accumulated in the nucleus even in unstressed condition and no further targeting into the nucleus occurs after oxidative stress. Moreover, nuclear entrapment of c-Abl by knocking down TTK enhances oxidative stress-induced apoptosis. These findings provide evidence that TTK phosphorylates c-Abl at Thr735 and that this phosphorylation is of importance to the cytoplasmic sequestration of c-Abl.

(9) Identification of the molecular mechanisms for dedifferentiation at the invasion front of colorectal cancer by a gene expression analysis.
PURPOSE: The aim of this study is to identify gene expression signatures that accompany dedifferentiation at the cancer invasion front in colorectal cancer. EXPERIMENTAL DESIGN: Two types of colorectal cancer were selected. Both types were well-differentiated adenocarcinomas at the superficial lesion. One type showed a dedifferentiated phenotype at the invasion front (type A, 13 samples); the other showed almost no dedifferentiated cancer cells at the invasion front (type B, 12 samples). Laser microdissection was combined with a cDNA microarray analysis to investigate the superficial lesions and the invasion front in colorectal cancers. RESULTS: Eighty-three genes were differentially expressed between types A and B in the superficial lesions, and the samples of superficial lesions were divided correctly into two clusters by these genes. Interestingly, the samples of the invasion front were also divided into the two same clusters

by these genes. The text mining method selected 10 genes involved in potential mechanisms causing dedifferentiation of cancer cells at the invasion front. The potential mechanisms include the networks of transforming growth factor-beta, Wnt, and Hedgehog signals. The expression levels of 10 genes were calculated by quantitative reverse transcription-PCR and 8 genes were confirmed to be significantly differentially expressed between two types（P < 0.05）. The gene expression profiles of 8 genes divided 12 test cases into two clusters with one misclassification. CONCLUSIONS: The molecular mechanisms constructed with 8 genes from three networks of transforming growth factor-beta, Wnt, and Hedgehog signals were found to correlate with dedifferentiation at the invasion front of colorectal cancer.

（10）BRCA1-mediated ubiquitination inhibits topoisomerase II alpha activity in response to oxidative stress.
Topoisomerase IIalpha is known to be critically involved in both cell proliferation and cell death. The mechanisms responsible for stress-dependent topoisomerase IIalpha alterations, however, remain unclear. This study focused on the behavior of topoisomerase IIalpha in response to oxidative stress induced by hydrogen peroxide（H（2）O（2））. The catalytic activity of topoisomerase IIalpha in MOLT-4 cells treated with H（2）O（2）decreased in parallel with the alteration of topoisomerase IIalpha expression. The ubiquitination of topoisomerase IIalpha was dependent on oxidative stress. BRCA1, a tumor-suppressor gene, appeared to be involved in these alterations in topoisomerase IIalpha. Furthermore, the retinoblastoma protein（pRb）was required for the ubiquitination of topoisomerase IIalpha by BRCA1. We conclude that the functions of topoisomerase IIalpha are regulated by ubiquitination on exposure to oxidative stress.

（11）Cross-sectional analysis of germline BRCA1 and BRCA2 mutations in Japanese patients suspected to have hereditary breast/ovarian cancer.
The prevalence of BRCA1/2 germline mutations in Japanese patients suspected to have hereditary breast/ovarian cancer was examined by a multi-institutional study, aiming at the clinical application of total sequencing analysis and validation of assay sensitivity in Japanese people using a cross-sectional approach based on genetic factors estimated from personal and family histories. One hundred and thirty-five subjects were referred to the genetic counseling clinics and enrolled in the study. Full sequencing analysis of the BRCA1/2 gene showed 28 types of deleterious mutations in 36 subjects（26.7%）, including 13 types of BRCA1 mutations in 17 subjects（12.6%）and 15 types of BRCA2 mutations in 19 subjects（14.1%）. Subjects were classified into five groups and 22 subgroups according to their personal and family history of breast and/or ovarian cancer, and the prevalence of deleterious mutations was compared with previously reported data in non-Ashkenazi individuals. Statistical analysis using the Mantel-Haenszel test for groups I through IV revealed that the prevalence of Japanese subjects was significantly higher than that of non-Ashkenazi individuals（P = 0.005, odds ratio 1.87, 95% confidence interval 1.22-2.88）. Family history of the probands suffering from breast cancer indicated risk factors for the presence of deleterious mutations of BRCA1/2 as follows:（1）families with breast cancer before age 40 within second degree relatives（P = 0.0265, odds ratio 2.833, 95% confidence interval 1.165-7.136）and（2）families with bilateral breast cancer and/or ovarian cancer within second degree relatives（P = 0.0151, odds ratio 2.88, 95% confidence interval 1.25-6.64）.

（12）Aurora kinase B is a predictive factor for the aggressive recurrence of hepatocellular carcinoma after curative hepatectomy.
BACKGROUND: Patterns of cancer recurrence hold the key to prognosis after curative resection. This retrospective study aimed to identify a predictor and therapeutic candidate for aggressive recurrence of hepatocellular carcinoma（HCC）. METHODS: Primary HCC tissues from 107 patients who had curative resection were analysed. Genome-wide gene expression profiles were investigated using a microarray technique, and clustering analysis was carried out based on the first diagnosis of recurrence according to the Milan criteria. Immunohistochemical expression and array-based comparative genomic hybridization（array-CGH）were also assessed. RESULTS: Microarray analysis revealed overexpression of Aurora kinase B, a chromosome passenger protein kinase, as the most significant predictor of the aggressive recurrence of HCC. Aurora kinase B protein expression was significantly associated with aggressive recurrence（P < 0.001）and prognosis（P < 0.001）. Multivariable analysis identified Aurora kinase B as the only independent predictor of aggressive recurrence of HCC（P = 0.031）. Array-CGH analysis showed that genomic instability was closely related to Aurora kinase B expression（P = 0.011）. CONCLUSION: Aurora kinase B is an effective predictor of aggressive HCC recurrence, in relation to the genomic instability. It might be worth considering as a molecular target for the adjuvant therapy of HCC.

（13）Novel BRCA2-interacting protein BJ-HCC-20A inhibits

the induction of apoptosis in response to DNA damage. The major hereditary breast cancer susceptibility gene BRCA2 is associated with familial breast and ovarian cancer. BRCA2 plays a role in DNA repair, transcription, cell cycle regulation, maintenance of genomic stability in response to DNA damage, centrosome regulation, and cytokinesis. To further understand the function of BRCA2, we used a yeast two-hybrid method and identified a novel BRCA2-interacting protein, BJ-HCC-20A, which is reported to be a potential cancer-testis antigen. We confirmed the interaction between endogenous BJ-HCC-20A and BRCA2 in mammalian cells, and showed that BJ-HCC-20A interacts with a portion of the highly conserved region of BRCA2 in various mammals, and M phase-specific phosphorylation of the binding region of BRCA2 modulates BJ-HCC-20A binding. Overexpression of BJ-HCC-20A increases cell growth, and downregulation of endogenous BJ-HCC-20A expression using small interfering RNA suppresses cell growth and leads to the induction of apoptosis. Importantly, the BJ-HCC-20A mRNA level is downregulated by adriamycin（ADR）-induced DNA damage and depletion of BJ-HCC-20A expression by small interfering RNA promotes the reduction of BRCA2 expression and enhances cell apoptosis in response to DNA damage. Additionally, the recovery of BJ-HCC-20A expression in ADR-induced DNA damage inhibits ADR-induced apoptosis. The data suggest that BJ-HCC-20A promotes cell growth and may regulate the induction of cell apoptosis in response to DNA damage in cooperation with BRCA2 in an M phase-dependent manner. Therefore, we speculate that targeting BJ-HCC-20A may aid in the treatment of breast tumors.

4. 本事業に関連して世界的な研究拠点形成に向けて、以下の点で改善・整備等されたこと

A（研究拠点体制）

研究室におけるスペースの確保、機器の整備および補充、研究推進のためのスケジュール等を作成し研究室内部の体制を整備するとともに、整形外科、口腔外科等の臨床グループとの共同研究計画を立案し総合的に研究拠点体制の整備を進めた。

B（研究教育環境）

ジャーナルクラブ、研究進捗ミーティング、GCOEセミナー等研究教育環境の整備を進めた。

C（人材確保）

大学院生3人がGCOE研究を遂行している。

D（人材育成）

新たに入学する大学院生を含め上記体制で人材育成に努めている。

E（国際化）

GCOEプログラムの中で国際セミナーへの参加、海外招聘研究者との議論等を通して国際化を図っている。

5. GCOE事業を推進するに当たって力を入れた点

GCOE推進研究者間で共同研究計画案を立案し、特に臨床グループとの共同研究で患者臨床検体を用いたゲノム研究推進体制の構築に努力した。

6. 英文原著論文

1. Takenaka, K. and Miki, Y. Introduction and characterization of a polymerase-dead point mutation into the POLK gene in vertebrates. FEBS Letters 583: 661–664. 2009
2. Han, X., Saito, H., Miki, Y.,* and Nakanishi, A. A CRM1-mediated nuclear export signal governs cytoplasmic localization of BRCA2 and is essential for centrosomal localization of BRCA2. Oncogene, 27: 2969-77, 2008. *Corresponding author
3. Hirai, Y., Banno, K., Suzuki, M., Ichikawa, Y., Udagawa, Y., Sugano, K., and Miki, Y. Molecular epidemiological and mutational analysis of DNA mismatch repair（MMR）genes in endometrial cancer patients with HNPCC-associated familial predisposition to cancer. Cancer Sci, 99: 1715-9, 2008.
4. Isomura, M., Oya, N., Tachiiri, S., Kaneyasu, Y., Nishimura, Y., Akimoto, T., Hareyama, M., Sugita, T., Mitsuhashi, N., Yamashita, T., Aoki, M., Sai, H., Hirokawa, Y., Sakata, K., Karasawa, K., Tomida, A., Tsuruo, T., Miki, Y.,* Noda, T., and Hiraoka, M. IL12RB2 and ABCA1 genes are associated with susceptibility to radiation dermatitis. Clin Cancer Res, 14: 6683-9, 2008. *Corresponding author
5. Izawa, N., Matsumoto, S., Manabe, J., Tanizawa, T., Hoshi, M., Shigemitsu, T., Machinami, R., Kanda, H., Takeuchi, K., Miki, Y., Arai, M., Shirahama, S., and Kawaguchi, N. A Japanese patient with Li-Fraumeni syndrome who had nine primary malignancies associated with a germline mutation of the p53 tumor-suppressor gene. Int J Clin Oncol, 13: 78-82, 2008.
6. Kimura, J., Nguyen, S. T., Liu, H., Taira, N., Miki, Y.,* and Yoshida, K. A functional genome-wide RNAi screen identifies TAF1 as a regulator for apoptosis in response to genotoxic stress. Nucleic Acids Res, 36: 5250-9, 2008. *Corresponding author
7. Komatsu, A., Nagasaki, K., Fujimori, M., Amano, J., and Miki, Y. Identification of novel deletion polymorphisms in breast cancer. Int J Oncol, 33: 261-70, 2008.
8. Nihira, K., Taira, N., Miki, Y.,* and Yoshida, K. TTK/Mps1 controls nuclear targeting of c-Abl by

14-3-3-coupled phosphorylation in response to oxidative stress. Oncogene, 27: 7285-95, 2008. *Corresponding author
9. Oku, Y., Shimoji, T., Takifuji, K., Hotta, T., Yokoyama, S., Matsuda, K., Higashiguchi, T., Tominaga, T., Nasu, T., Tamura, K., Matsuura, M., Miyata, S., Kato, Y., Yamaue, H., and Miki, Y. Identification of the molecular mechanisms for dedifferentiation at the invasion front of colorectal cancer by a gene expression analysis. Clin Cancer Res, 14: 7215-22, 2008.
10. Shinagawa, H., Miki, Y.,* and Yoshida, K. BRCA1-mediated ubiquitination inhibits topoisomerase II alpha activity in response to oxidative stress. Antioxid Redox Signal, 10: 939-49, 2008. *Corresponding author
11. Sugano, K., Nakamura, S., Ando, J., Takayama, S., Kamata, H., Sekiguchi, I., Ubukata, M., Kodama, T., Arai, M., Kasumi, F., Hirai, Y., Ikeda, T., Jinno, H., Kitajima, M., Aoki, D., Hirasawa, A., Takeda, Y., Yazaki, K., Fukutomi, T., Kinoshita, T., Tsunematsu, R., Yoshida, T., Izumi, M., Umezawa, S., Yagata, H., Komatsu, H., Arimori, N., Matoba, N., Gondo, N., Yokoyama, S., and Miki, Y. Cross-sectional analysis of germline BRCA1 and BRCA2 mutations in Japanese patients suspected to have hereditary breast/ovarian cancer. Cancer Sci, 99: 1967-76, 2008.
12. Tanaka, S., Arii, S., Yasen, M., Mogushi, K., Su, N. T., Zhao, C., Imoto, I., Eishi, Y., Inazawa, J., Miki, Y., and Tanaka, H. Aurora kinase B is a predictive factor for the aggressive recurrence of hepatocellular carcinoma after curative hepatectomy. Br J Surg, 95: 611-9, 2008.
13. Tomiyoshi, G., Nakanishi, A., Takenaka, K., Yoshida, K., and Miki, Y. Novel BRCA2-interacting protein BJ-HCC-20A inhibits the induction of apoptosis in response to DNA damage. Cancer Sci, 99: 747-54, 2008.

7. 著書

1. Nagasaki, K., and Miki, Y. Molecular prediction of the therapeutic response to neoadjuvant chemotherapy in breast cancer. Breast Cancer, 15: 117-20, 2008.
2. 磯村　実, 三木　義男：遺伝子多型解析、鶴尾　隆　編【がんの分子標的】、南光堂　62-66,2008
3. 野田弘志, 三木義男, 小西文雄【大腸IIc　未来に向けて】大腸IIcの特徴　遺伝子学的特徴　早期大腸癌の発育形態とRas-signaling pathway異常の関係. 早期大腸癌, 12, 579-583, 2008

8. 自己評価

GCOEプログラムに参加し、骨軟部腫瘍（骨肉腫、軟骨肉腫、歯肉癌など）を中心に、ゲノム科学を応用した研究を進めてきた。一方、骨肉腫におけるアポトーシス誘導メカニズムについても、生化学的に解明を進めその一部を解明することに成功した。今度は、臨床系グループとの共同研究体制を構築し臨床検体収拾システムを作製、順次癌組織の収集を促進し遺伝子発現プロファイル解析を進める。教育等には大きく貢献できたと判断している。

9. 学会発表（英文）

1. Miki Y. Molecular prediction of therapeutic response and adverse effect of chemotherapy in breast cancer. The First International Symposium of Nagasaki University Global COE Program “Global Strategic Center for Radiation Health Risk Control”. Nagasaki, February 2008
2. Miki Y. Molecular diagnosis of response and adverse events to chemotherapy in breast cancer Second JCA-AACR Special Joint Conference - The Latest Advances in Breast Cancer Research -, Hyogo, Japan, July, 2008
3. Taira N, Nihira K, Yamaguchi T, Miki Y, Yoshida K. DYRK2 induces apoptosis via p53 phosphorylation at Ser46 in response to DNA damage.Apoptosis World 2008, Luxembourg, Luxembourg, January, 2008
4. Nagasaki K, Shimoji T, Matsuura M, Noda T, Miki Y, Molecular prediction of the therapeutic response to preoperative chemotherapy with paclitaxel in breast cancer. 2nd World Conference on Magic Bullets（Ehrlich II）Nurnberg, Germany October, 2008
5. Kimura J, Nguyen ST, Liu H, Taira N, Miki Y, Yoshida K. A functional genome-wide RNAi screen identifies TAF1 as a regulator for apoptosis in response to genotoxic stress. Second JCA-AACR Special Joint Conference, Hyogo, Japan, July, 2008
6. Tomiyoshi G, Nakanishi A, Takenaka K, Yoshida K, Miki Y. A novel BRCA2-interacting protein BJ-HCC-20A inhibits the induction of apoptosis in response to DNA damage. Second JCA-AACR Special Joint Conference, Hyogo, Japan, July, 2008

10. 学会発表（和文）

1. 田中真二, 藍原有弘, YasenMahmet, 茂櫛薫, 野口典男, 工藤篤, 中村典明, 伊東浩次, 三木義男, 稲澤譲治, 田中博, 有井滋樹. 分子標的治療の最前線　基礎研究　肝細胞癌基準外再発のオミックス解析に基づく新規分子標的治療の開発. 第46回日本癌治療学会学術集会, 名古屋,2008年10月
2. 大石陽子, 松永浩子, 川村徹, 佐藤康, 中嶋昭, 三木義男, 三浦妙太. 鎖骨上リンパ節転移陽性乳がんの機能ネットワーク解析. 第108回日本外科学会定期学術集

会,長崎, 2008年5月.

3. 大石陽子, 松永浩子, 川村徹, 佐藤康, 中嶋昭, 三木義男, 三浦妙太. Stathmin 1染色を用いた予後予測と抗がん剤感受性予測の検討. 第16回日本乳癌学会学術総会,大阪,2008年9月
4. 小松哲, 長崎光一, 藤森実, 天野純, 三木義男. 乳癌における新規欠失遺伝子多型の同定. 第108回日本外科学会定期学術集会,長崎, 2008年5月.
5. 三木義男, 丹羽隆善, 斉藤弘子, 中西啓. 乳がん　基礎・病理・1次予防 BRCA2-Plectin複合体は中心体の固定に関与する. 第14回日本家族性腫瘍学会学術集会,東京, 2008年6月
6. 奥喜全, 瀧藤克也, 堀田司, 横山省三, 松田健司, 冨永敏治, 那須亨, 田村耕一, 家田淳司, 下地尚, 加藤洋, 三木義男, 山上裕機. 大腸癌先進部脱分化に関与する機能ネットワークの構築. 第63回日本大腸肛門病学会学術集会,東京,2008年10月.
7. 奥喜全, 瀧藤克也, 堀田司, 横山省三, 松田健司, 冨永敏治, 那須亨, 家田淳司, 加藤洋, 三木義男, 山上裕機. 網羅的遺伝子発現解析による大腸癌先進部脱分化規定因子の同定. 第46回日本癌治療学会学術集会,名古屋,2008年10月
8. 平直江, 三木義男, 吉田清嗣. ATMによるDYRK2のリン酸化はキナーゼ活性を制御するとともに、MDM2による分解からの回避を引き起こす（ATM phosphorylation of DYRK2 regulates its kinase activity and MDM2-mediated degradation）. 第67回日本癌学会学術総会,名古屋,2008年10月
9. 平井康夫, 滝沢憲, 阪埜浩司, 鈴木光明, 市川喜仁, 宇田川康博, 菅野康吉, 三木義男. 遺伝性子宮体癌の臨床的検討（Molecular Epidemiological and Mutational Analysis of DNA Mismatch Repair Genes In Endometrial Cancer Patients With HNPCC）. 第67回日本癌学会学術総会,名古屋,2008年10月
10. 冨吉郷, 中西啓, 竹中克也, 吉田清嗣, 三木義男. 新規BRCA2結合タンパク質BJ-HCC-20AはDNA損傷に応答したアポトーシス誘導を抑制する（Novel BRCA2-interacting protein BJ-HCC-20A inhibits the induction of apoptosis in response to DNA damage）. 第67回日本癌学会学術総会,名古屋,2008年10月
11. 長崎光一, 星川裕, 下地尚, 牛嶋大, 松浦正明, 野田哲生, 三木義男. トランスフェクションアレイを用いた薬剤感受性遺伝子機能ネットワーク解析システムの構　築（Development of high-throughput functional screening system for chemo-sensitivity related genes using transfection array）. 第67回日本癌学会学術総会,名古屋,2008年10月
12. 中西啓, 斉藤広子, 大海忍, 三木義男. BRCA2は14-3-3γと結合して中心体の凝集に関与する（BRCA2 binds 1 4-3-3　γ and functions in centrosome cohesion）. 第67回日本癌学会学術総会,名古屋,2008年10月
13. 丹羽隆善, 中西啓, 大海忍, 上西紀夫, 瀬戸泰之, 三木義男. BRCA2とPlectinは中心体のポジショニングに影響を及ぼす（BRCA2 complexed with plectin is required for centrosome positioning）. 第67回日本癌学会学術総会,名古屋,2008年10月
14. 須貝幸子, 佐藤之俊, 小松美樹, 奥村栄, 中川健, 石川雄一, 三木義男. 原発性非小細胞肺癌切除時の胸腔内洗浄液におけるTRCによるCEA mRNAの迅速的検出の検討（Rapid intraoperative detection of CEA mRNA in the pleural lavage of non-small cell lung cancers by TRC method）. 第67回日本癌学会学術総会,名古屋,2008年10月
14. 小松哲, 長崎光一, 藤森実, 伊藤研一, 三木義男. 乳癌における新規欠失遺伝子多型の同定（Identification of novel deletion copy number variations in Breast cancer）. 第67回日本癌学会学術総会,名古屋,2008年10月
16. 磯村実, 松浦正明, 野田哲生, 三木義男. パクリタキセルの細胞毒性に関連する遺伝子多型のゲノムワイド探索（Genome-wide survey of genetic polymorphisms associated with cytotoxicity of paclitaxel using HapMap cell lines）. 第67回日本癌学会学術総会,名古屋,2008年10月
17. 木村純子、グェンティエンスー、平直江、三木義男、吉田清嗣　アポトーシス誘導関連遺伝子の網羅的探索によるTAF1の同定と機能解析　BMB2008、神戸;2008年12月
18. 呂正光、劉寒梢、山口智子、三木義男、吉田清嗣　Protein kinase C delta activates RelA/p65 and NF-kappaB signalling in response to TNFalpha　BMB2008、神戸、2008年12月
19. 仁平啓史、安藤雄祐、山口智子、三木義男、吉田清嗣　Pim-1はRelA/p65のリン酸化を介してNF-kBの活性化を制御する　BMB2008、神戸、2008年12月

20. 平直江、山本宙亨、山口智子、三木義男、吉田清嗣　ATMはDYRK2のリン酸化はキナーゼ活性を制御するとともに、MDM2を介したプロテアソーム系による分解からの回避を引き起こす　BMB2008、神戸、2008年12月

11. 外部資金の獲得状況

・科学研究費補助金、特定領域（C）(2)
　研究題目: 乳腺発がんにおけるBRCA1、BRCA2の役割
　代表: 三木　義男
　期間: 平成20年―21年
　研究費総額: 2,140万円
・科学研究費補助金、基盤研究（B）
　研究題目: 乳癌におけるストレス応答性アポトーシス誘導機能破綻の分子機構
　代表: 三木　義男
　期間: 平成19-20年
　研究費総額: 1,700万円

12. 特別講演、招待講演

1. 三木義男, 長崎光一, 牛嶋大, 松浦正明. 乳癌診療標準化から個別化へ 乳癌の化学療法感受性予測の試み. . 第16回日本乳癌学会学術総会,大阪,2008年9月
2. 三木義男. 乳がん術前化学療法の効果予測システム開発の試み（Molecular prediction of the therapeutic response to neoadjuvant chemotherapy in breast cancer）. 第108回日本外科学会定期学術集会,長崎,2008年5月.
3. 菅野康吉, 中村清吾, 安藤二郎, 神野浩光, 池田正, 青木大輔, 福富隆志, 吉田輝彦, 新井正美, 平井康夫, 霞富士雄, 福井崇史, 三木義男, and Brca1/2多施設共同研究グループ. 遺伝性の癌　その研究と臨床の最前線 遺伝性乳癌卵巣癌が疑われる日本人を対象とするBRCA1/2遺伝子変異の横断的研究（Forefront of Basic and Clinical Researches in Hereditary Cancer Cross-sectional study of BRCA1 and BRCA2 mutations in Japanese patients suspected of hereditary breast/ovarian carcinoma）. 第67回日本癌学会学術総会,名古屋,2008年10月

13. 学会主催

Second JCA-AACR Special Joint Conference - The Latest Advances in Breast Cancer Research
July 14 -16, 2008, Hyogo, Japan
Chairpersons:
　Yoshio Miki, Tokyo Medical and Dental University and the Cancer Institute of JFCR, Tokyo, Japan
　Carlos L. Arteaga, Vanderbilt-Ingram Cancer Center, Nashville, TN

14. 講座の准教授、講師、助教、特別研究員、ポスドク、指導を受けた大学院生の名前（AISSには○印）のリスト

	准教授	吉田　清嗣
	助　教	竹中　克也
	D4	Yun　Xia
		云　霞
○	D3	Lu　Zheng Guang
		呂　正光
○	D3	Wang　Hui Feng
		王　慧峰
○	D2	木村　純子
	D2	平　直江
	D2	Hew　Hoi Chin
		侯 韋君
	D2	高岡 美帆
	D1	仁平　啓史
	D1	Wali Nadila
		瓦力 娜迪拉
	M2	Mariku　Sadiya
		真利久 サディヤ
	M1	工藤 卓也

Novel BRCA2-interacting protein BJ-HCC-20A inhibits the induction of apoptosis in response to DNA damage

Go Tomiyoshi,[1,2] Akira Nakanishi,[3] Katsuya Takenaka,[1] Kiyotsugu Yoshida[1] and Yoshio Miki[1,2,3,4]

[1]Department of Molecular Genetics, Medical Research Institute, and [2]21st Century Center of Excellence Program for Molecular Destruction and Reconstitution of Tooth and Bone, Tokyo Medical and Dental University, 1-5-45 Yushima, Bunkyo-ku, Tokyo 113-8510; [3]Department of Genetic Diagnosis, The Cancer Institute, Japanese Foundation for Cancer Research, 3-10-6 Ariake, Koto-ku, Tokyo 135-8550, Japan

(Received October 10, 2007/Revised December 1, 2007/Accepted December 3, 2007/Online publication February 27, 2008)

The major hereditary breast cancer susceptibility gene *BRCA2* is associated with familial breast and ovarian cancer. BRCA2 plays a role in DNA repair, transcription, cell cycle regulation, maintenance of genomic stability in response to DNA damage, centrosome regulation, and cytokinesis. To further understand the function of BRCA2, we used a yeast two-hybrid method and identified a novel BRCA2-interacting protein, BJ-HCC-20A, which is reported to be a potential cancer–testis antigen. We confirmed the interaction between endogenous BJ-HCC-20A and BRCA2 in mammalian cells, and showed that BJ-HCC-20A interacts with a portion of the highly conserved region of BRCA2 in various mammals, and M phase-specific phosphorylation of the binding region of BRCA2 modulates BJ-HCC-20A binding. Overexpression of BJ-HCC-20A increases cell growth, and downregulation of endogenous BJ-HCC-20A expression using small interfering RNA suppresses cell growth and leads to the induction of apoptosis. Importantly, the BJ-HCC-20A mRNA level is downregulated by adriamycin (ADR)-induced DNA damage and depletion of BJ-HCC-20A expression by small interfering RNA promotes the reduction of BRCA2 expression and enhances cell apoptosis in response to DNA damage. Additionally, the recovery of BJ-HCC-20A expression in ADR-induced DNA damage inhibits ADR-induced apoptosis. The data suggest that BJ-HCC-20A promotes cell growth and may regulate the induction of cell apoptosis in response to DNA damage in cooperation with BRCA2 in an M phase-dependent manner. Therefore, we speculate that targeting BJ-HCC-20A may aid in the treatment of breast tumors. (*Cancer Sci* 2008; 99: 747–754)

Genetic factors contribute to an ill-defined proportion of breast cancer incidence, estimated to be approximately 5% of all breast cancer cases.[1] The two major hereditary breast cancer susceptibility genes, *BRCA1* and *BRCA2*, are associated with familial breast and ovarian cancer. Germline mutations in the *BRCA1* gene increase the risk of development of early onset breast cancer and ovarian cancer.[2] Alterations in the *BRCA2* gene result in an increased risk of development of breast cancer in both women and men,[3,4] and a moderately increased risk of a variety of other cancers, including carcinomas of the ovary, pancreas, prostate, and colon.[5] Because inactivation of both alleles of either *BRCA1* or *BRCA2* is a key feature in neoplastic development in hereditary cancers, these genes are believed to act as tumor-suppressor genes required for cell growth. BRCA2 plays an important role in DNA repair in response to DNA damage.[6–10] In addition, BRCA2 is also involved in the regulation of transcription,[11–13] cell cycle checkpoints,[14–16] inhibition of cell growth,[17,18] maintenance of genomic stability,[19–22] centrosome regulation,[23] and cytokenesis.[24] BRCA2 is specifically phosphorylated in M phase.[10,25,26] Phosphorylation of BRCA2 by the cyclin-dependent kinase cdk1 in M phase blocks C-terminal interaction between BRCA2 and RAD51, and reduces the efficiency of recombinational repair.[10]

BRCA2 has several regions that are highly conserved in various mammals. Several proteins interact with these conserved regions of BRCA2 and are reported to play important roles, especially in DNA damage repair.[10,13,15,27] Therefore, functional analysis of the conserved regions has important significance in understanding the roles of BRCA2 in breast carcinogenesis. To further understand the function of BRCA2, we used the yeast two-hybrid system to identify novel proteins that interact with the conserved regions of BRCA2. We identified BJ-HCC-20A as a novel BRCA2-interacting protein. Human BJ-HCC-20 is reported to be a potential CT antigen.[28] Because the function of BJ-HCC-20 is largely unknown whereas a number of CT antigens are involved in cell growth,[18,29] we investigated the effects of BJ-HCC-20A overexpression on cell growth and apoptosis, and the effects of knocking down BJ-HCC-20 expression using siRNA. We further determined the role of BJ-HCC-20A in response to DNA damage because it forms *in vivo* complexes with BRCA2. The data suggest that BJ-HCC-20A may serve as an effecter or regulator of cell growth in cooperation with BRCA2 in the DNA damage/cell apoptosis pathway.

Materials and Methods

Yeast two-hybrid screening. A yeast two-hybrid screening assay using the ProQuest two-hybrid system (Invitrogen, Carlsbad, CA, USA) was carried out according to the manufacturer's instructions. In brief, the cDNA coding for the conserved region (amino acids 121–465) of *BRCA2* was subcloned into pDBLeu. This was used as the bait in the yeast two-hybrid screening of the mouse embryo (10.5-day) cDNA library and the human fetal brain cDNA library.

Cell cultures, synchronization, and transfection. MCF-7 and HeLa cells were grown in Dulbecco's modified Eagle's medium supplemented with 10% fetal bovine serum, penicillin, and streptomycin. U2OS cells were grown in RPMI-1640 medium supplemented with 10% fetal bovine serum, penicillin, streptomycin and L-glutamine. Cells were treated with 30 ng/mL nocodazole (Sigma-Aldrich, St Louis, MO, USA) for 24 h or 0.5 μg/mL ADR (Sigma-Aldrich) for 24 h. Cells were transfected with expression plasmids using FuGENE 6 (Roche

[4]To whom correspondence should be addressed. E-mail: miki.mgen@mri.tmd.ac.jp
Abbreviations: ADR, adriamycin; *BRCA*, breast-cancer susceptibility gene; BrdU, 5-bromo-2′-deoxy-uridine; CT antigen, cancer–testis antigen; DAPI, 4′,6-diamidino-2-phenylindole; G418, geneticin; GFP, green fluorescent protein; GST, glutathione S-transferase; HA, hemaglutinin; IB, immunoblot; IP, immunopracipitation; Plk, Polo-like kinase; RT-PCR, reverse transcription–polymerase chain reaction; SDS-PAGE, sodium dodecyl sulfate–polyacrlamide gel electrophoresis; siRNA, small interfering RNA; TUNEL, terminal deoxynucleotidyltransferase-mediated dUTP-biotin nick-end labeling.

doi: 10.1111/j.1349-7006.2008.00733.x
© 2008 Japanese Cancer Association

Diagnostics, Tokyo, Japan) and Lipofectamine 2000 (Invitrogen) according to the manufacturer's instructions.

Plasmids. BJ-HCC-20A cDNA was isolated by RT-PCR from human testis total RNA (BD Clontech, Palo Alto, CA, USA) and cloned into pcDNA3.1HA and pEGFP-C1 (BD Clontech). Flag-tagged BRCA2 was prepared as described previously.[23] GST-tagged BJ-HCC-20A, BJ-HCC-20A mutants, and BRCA2 mutants were cloned into pGEX4T1 (Amersham Biosciences, Piscataway, NJ, USA).

Antibodies. Rabbit anti-BJ-HCC-20 antibody was raised against the synthetic peptide BJ-HCC-20 (amino acids 97–112), and affinity-purified by MBL, (Nagoya, Japan). Anti-BRCA2 (Ab1; Calbiochem, San Diego, CA, USA), anti-Flag (Sigma-Aldrich), anti-HA (3F10; Roche Diagnostics), anti-GFP (Nacalai Tesque, Kyoto, Japan), anti-GST (Nacalai Tesque), and anti-α-tubulin (Sigma-Aldrich) antibodies were used.

Immunoprecipitation and immunoblot analysis. Cells were suspended in 1% Nonidet P-40 lysis buffer (50 mM Tris-HCl pH 7.6, 150 mM NaCl, 1% Nonidet P-40, 10 mM NaF, 1 mM Na_3VO_3, 1 mM dithiothreitol, 1 mM phenylmethylsulfonyl fluoride, 10 μg/mL leupeptin, and 10 μg/mL pepstatin), and then incubated on ice for 30 min. After centrifugation, cell lysates were immunoprecipitated with anti-BJ-HCC-20 or anti-BRCA2 antibodies, protein A (Amersham Biosciences) or G (Zymed Laboratories, South San Francisco, CA, USA) sepharose, or anti-HA affinity matrix (Roche Diagnostics). The immunoprecipitates were washed three times with 0.1% Nonidet P-40 lysis buffer and immunoblot analysis was carried out. Cell lysates or immunoprecipitated proteins were separated by SDS-PAGE and transferred to nitrocellulose filters (Bio-Rad, Tokyo, Japan) or polyvinylidene difluoride membranes (Millipore, Bedford, MA, USA). The membranes were then incubated with anti-BJ-HCC-20, anti-BRCA2, anti-HA, anti-GFP, or anti-α-tubulin antibodies. Immunoreactive protein bands were visualized using chemiluminescence (PerkinElmer, Wellesley, MA, USA).

***In vitro* binding assays.** GST fusion proteins were expressed in *Escherichia coli* and purified on glutathione sepharose (Amersham Biosciences). Cell lysates were incubated with purified GST fusion proteins. The adsorbates were resolved by SDS-PAGE and analyzed by immunoblotting with anti-Flag or anti-HA antibodies.

Small interfering RNA transfection. Cells were transfected with siRNA using Lipofectamine RNAiMAX (Invitrogen) according to the manufacturer's instructions. The siRNA duplex for BJ-HCC-20 was synthesized and purified by Invitrogen (Stealth RNAi). The Stealth RNAi sequence was 5′-UGGAUGUUGUGCCUCGCCAUCUUUA-3′ for BJ-HCC-20 siRNA1 and 5′-CCAUAGCCAUUGUUUCUGAAGAUUU-3′ for BJ-HCC-20 siRNA2. Scrambled siRNA was used as a negative control (Invitrogen).

Reverse transcription–polymerase chain reaction analysis. Total cellular RNA was extracted using the RNeasy kit (Qiagen, Valencia, CA, USA). The relative mRNA expression was analyzed by RT-PCR using the SuperScript III One-Step RT-PCR System according to the manufacturer's instructions (Invitrogen). The primer sequences were as follows: BJ-HCC-20 forward, 5′-ATGCTCAGGCTTCTGAGACTTGC-3′; BJ-HCC-20 reverse, 5′-TTAAATGCTTTGGCTCCGACGTTC-3′; BRCA2 forward, 5′-GCACATTTACAGAGTAGTGTAGTTG-3′; BRCA2 reverse, 5′-GTCATTTTTCAACAGGCCAGCAAA-3′; and β-actin using the β-actin RT-PCR Primer Set (Toyobo, Osaka, Japan).

Colony-formation assay. HeLa cells transfected with GFP vector or GFP-BJ-HCC-20A were cultured with an appropriate concentration of G418 for 15 days. The cells were fixed with 70% ethanol and stained using Giemsa solution (Wako, Osaka, Japan).

Cell-proliferation assay. Cell proliferation was detected using BrdU incorporation by immunofluorescence. After transfection, the cells were incubated with BrdU for 1 h and stained with anti-BrdU antibody according to the manufacturer's instructions (Roche Diagnostics).

Apoptosis assay. To visualize the apoptotic nuclear changes, the cells were fixed and stained with DAPI. The percentage of cells with a condensed or fragmented nucleus was determined by counting at least 800 cells (nuclei stained with DAPI). Apoptotic cells were detected using the TUNEL assay with the DeadEnd colorimetric TUNEL system (Promega, Madison, WI, USA).

Results

Identification of BJ-HCC-20A as a BRCA2-interacting protein and confirmation of the interaction *in vivo*. To identify novel proteins that interact with BRCA2, we used the yeast two-hybrid system. After screening the mouse embryo cDNA library using a portion of the highly conserved region of BRCA2 (amino acids 121–465) as bait, several candidate clones were obtained and characterized using DNA sequence analysis. Of the candidate clones identified, five independent clones coded for 4930502E18Rik were located on the mouse chromosome X. Using a BLAST analysis, we determined that the human homolog of 4930502E18Rik was BJ-HCC-20, located on human chromosome X. There is 42.5% identity in amino acids between the mouse clone and human BJ-HCC-20. Human BJ-HCC-20 is reported to be a potential CT antigen that has two splicing isoforms, BJ-HCC-20A and BJ-HCC-20B, differing at the C-terminal region (Fig. 1a).

An interaction between BJ-HCC-20 and BRCA2 was confirmed in mammalian cells. HA-tagged BJ-HCC-20A was overexpressed in HeLa cells, and coimmunoprecipitation and immunoblot analysis were carried out. As shown in Figure 1b, BJ-HCC-20A interacts with BRCA2 in the overexpression system. To further characterize the binding region of BJ-HCC-20A and BRCA2, groups of GST-fusion proteins of BRCA2 and BJ-HCC-20A fragments were purified. Using GST pull-down assays, BRCA2 (amino acids 121–235) interacted with BJ-HCC-20A, and BJ-HCC-20A (amino acids 1–105) interacted with BRCA2 (Fig. 1c). Importantly, the binding region of BRCA2 (amino acids 121–235) with BJ-HCC-20A identified here includes several M phase-specific phosphorylation sites by Plk1 (Ser193, Thr203, Ser205, Ser206, and Thr207).[25] To determine the interaction between endogenous BJ-HCC-20 and BRCA2, we generated rabbit polyclonal anti-BJ-HCC-20 antibody against the synthetic peptide corresponding to BJ-HCC-20 amino acids 97–112. As shown in Figure 2a, this antibody detected endogenous BJ-HCC-20A as a 29-kDa protein in MCF-7 cells. However, this antibody did not detect endogenous BJ-HCC-20B as the 27-kDa protein, indicating that the BJ-HCC-20B protein may be expressed at an extremely low level. A similar result was obtained with HeLa and U2OS cells (data not shown). As shown in Figure 2b, coimmunoprecipitation and immunoblot analysis using anti-BJ-HCC-20 and anti-BRCA2 antibodies showed an interaction between endogenous BJ-HCC-20A and BRCA2 in MCF-7 cells. For this reason, we focused on BJ-HCC-20A in the present study.

Phosphorylation by Plk1 modulates BJ-HCC-20A binding. It has been shown that BRCA2 is phosphorylated (an alteration in electrophoretic mobility of the BRCA2 protein) in M phase by Plk1,[25,26] and the region of BRCA2 (amino acids 121–235) binding with BJ-HCC-20A identified in the present study has several M phase-specific Plk1 phosphorylation sites. To investigate the interaction between BJ-HCC-20A and BRCA2 during M phase, HeLa cells were synchronized in M phase by nocodazole treatment. As shown in Figure 3, an alteration in electrophoretic mobility of the BRCA2 protein was detected after treating the cells with nocodazole (Fig. 3, lanes 2, 4, and 6); however, BJ-HCC-20A didn't interact with the M phase-specific

doi: 10.1111/j.1349-7006.2008.00733.x
© 2008 Japanese Cancer Association

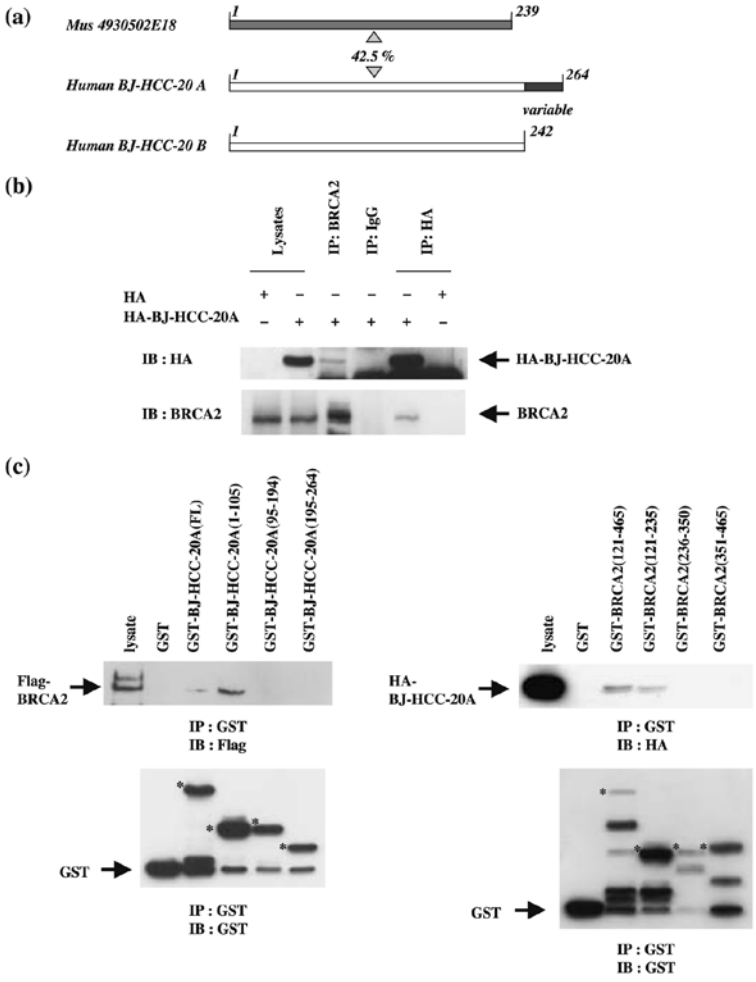

Fig. 1. Interaction of BJ-HCC-20A and BRCA2. (a) Schematic representation of mouse 4930502E18 and human BJ-HCC-20 showing the structures of BJ-HCC20A and BJ-HCC-20B. The blue box indicates the variable region of BJ-HCC-20A and BJ-HCC-20B. (b) Coimmunoprecipitation of endogenous BRCA2 and hemaglutinin (HA)-BJ-HCC-20A. HA-BJ-HCC-20A was expressed in HeLa cells. Cell lysates were immunoprecipitated with anti-HA, normal mouse IgG, or anti-BRCA2 followed by immunoblotting with anti-HA (upper panel) or anti-BRCA2 (lower panel). Cell lysates were also analyzed by immunoblotting with anti-HA (upper panel) or anti-BRCA2 (lower panel). (c) Glutathione S-transferase (GST) pull-down assays of BRCA2 and BJ-HCC-20A. Cell lysates expressing Flag-tagged BRCA2 or HA-tagged BJ-HCC-20A were incubated with each GST fragment as indicated above the panels. The adsorbates were analyzed by immunoblotting with anti-Flag, anti-HA, or anti-GST. Each band specific for the GST-BJ-HCC-20A and BRCA2 fragments is indicated by an asterisk. IB, immunoblot; IP, immunoprecipitation.

phosphorylated BRCA2 with nocodazole treatment (Fig. 3, lane 10). This suggests that the interaction between BJ-HCC-20A and BRCA2 is at least in part regulated by phosphorylation in an M phase-dependent manner.

Expression of BJ-HCC-20A promotes cell growth. A number of CT antigens are involved in cell growth.[18,30] To determine the effect of BJ-HCC-20A on cell growth, BJ-HCC-20A was overexpressed, or endogenous BJ-HCC-20A was downregulated in cells. As shown in Figure 4a, BJ-HCC-20A overexpression significantly increased cell-growth activity compared to the control in HeLa cells using the colony-formation assay. To further confirm whether BJ-HCC-20A is involved in cell growth, expression of endogenous BJ-HCC-20 was knocked down by transfection using BJ-HCC-20 siRNA. In Figure 4b, immunoblot analysis shows that cells transfected with BJ-HCC-20 siRNA1 reduced the level of endogenous BJ-HCC-20 expression. The BrdU-incorporation assay showed that downregulation of endogenous BJ-HCC-20 expression results in the suppression of cell growth compared to the controls (untransfected and transfected with scrambled siRNA) in U2OS and HeLa cells (Fig. 4c). A similar result was obtained with MCF-7 cells. These data suggest that BJ-HCC-20A may be involved in the promotion of cell growth.

Downregulation of BJ-HCC-20A causes the induction of apoptosis. In the execution phase of apoptosis, characteristic morphological changes of cells are induced, including dynamic membrane blebbing and nuclear changes. In the previous BrdU-incorporation assay, endogenous BJ-HCC-20 expression was downregulated in U2OS cells using siRNA. In order to visualize the apoptotic nuclear changes (condensation and fragmentation), these cells were fixed and stained with DAPI. As shown in Figure 5a, some U2OS cells exhibited apoptotic nuclear changes, and downregulation of BJ-HCC-20 increased the number of cells with apoptotic nuclear changes compared to the control (transfected with scrambled siRNA) ($8.4 \pm 0.4\%$ vs $0.9 \pm 0.3\%$, $P < 0.0005$). A similar result was obtained with HeLa cells (data not shown). Importantly, these results indicate that downregulation of BJ-HCC-20A expression using siRNA suppresses cell growth and induces apoptotic nuclear changes simultaneously. To confirm that the cellular morphological changes induced by downregulation of BJ-HCC-20A are caused by the induction of apoptosis, the TUNEL assay was carried out. As shown in Figure 5b, downregulation of endogenous BJ-HCC-20A increased the induction of apoptosis compared to the controls (untransfected and transfected with scrambled siRNA) in U2OS cells. A similar result was obtained with HeLa cells

© 2008 Japanese Cancer Association

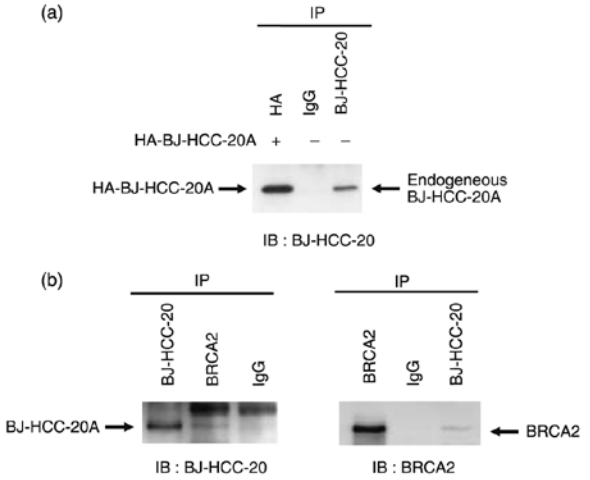

Fig. 2. Interaction of endogenous BJ-HCC-20A and BRCA2. (a) Characterization of the anti-BJ-HCC-20 antibody. Cell lysates from MCF-7 cells were immunoprecipitated and immunoblotted with affinity-purified anti-BJ-HCC-20 polyclonal antibody. Cell lysates from MCF-7 cells transfected with hemaglutinin (HA)-BJ-HCC-20A were used as a control. (b) Cell lysates from MCF-7 cells were immunoprecipitated with anti-BJ-HCC-20 or anti-BRCA2 antibodies followed by immunoblotting with anti-BJ-HCC-20 (left panel) or anti-BRCA2 (right panel) antibodies. Normal rabbit or mouse IgG were used as negative controls for immunoprecipitation. IB, immunoblot; IP, immunoprecipitation.

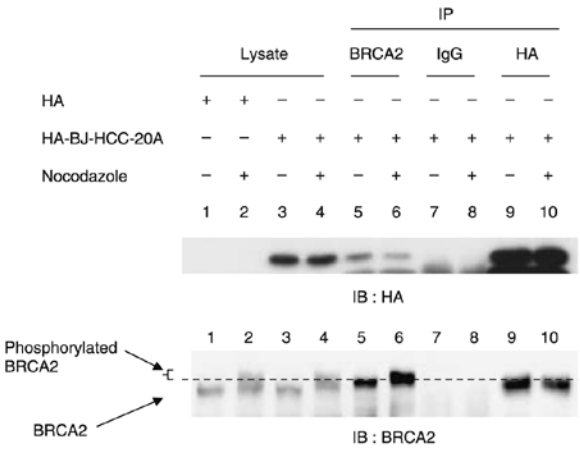

Fig. 3. Modulation of BJ-HCC-20A binding with an M phase-specific phosphorylated BRCA2. HeLa cells were transfected with hemaglutinin (HA) vector or HA-BJ-HCC-20A. At 24 h post-transfection, the cells were treated with dimethyl sulfoxide or 30 ng/mL nocodazole for 24 h. Cell lysates were immunoprecipitated with anti-HA or anti-BRCA2 antibodies followed by immunoblotting with anti-HA or anti-BRCA2 antibodies. IB, immunoblot; IP, immunoprecipitation.

(data not shown). These suggest that BJ-HCC-20A may regulate the induction of apoptosis.

BJ-HCC-20A is involved in the inhibition of apoptosis in response to DNA damage. Reports show that BRCA2 is involved in DNA damage-induced apoptosis.[6,22,31] Several DNA-damaging agents are shown to downregulate BRCA2 expression in cancer cells.[30,32–35] To determine the effect of BJ-HCC-20A in response to DNA damage, U2OS cells were treated with the DNA-damaging agent ADR. As shown in Figure 6a, ADR caused decreased expression of BJ-HCC-20A mRNA. Similar results were obtained with HeLa and MCF-7 cells (data not shown). This suggests that BJ-HCC-20A may be involved in response to DNA damage. Next, U2OS cells were transfected with HA-BJ-HCC-20A, and then treated with ADR for 24 h. As shown in Figure 6b, expression of BJ-HCC-20A inhibited ADR-induced apoptosis significantly. To further investigate the involvement of BJ-HCC-20A in response to DNA damage, U2OS cells were transfected with BJ-HCC-20 siRNA, and then treated with ADR for 24 h. As shown in Figure 6c, the combination of downregulation of BJ-HCC-20 expression and DNA damage increased ADR-induced apoptosis compared to a combination of scrambled siRNA and DNA damage, or downregulation of BJ-HCC-20A expression alone. This suggests that downregulation of BJ-HCC-20A expression enhanced the sensitivity of cells to DNA damage-induced apoptosis. Because BRCA2 is involved in DNA repair and forms a complex with BJ-HCC-20A, we determined whether downregulation of BJ-HCC-20A affects BRCA2 expression in response to DNA damage. U2OS cells were transfected with BJ-HCC-20 siRNA, and then treated with ADR for 24 h. As shown in Figure 6d, downregulation of BJ-HCC-20A promoted the reduction of BRCA2 expression in response to DNA damage compared to the controls (untransfected and transfected with scrambled siRNA). This suggests that BJ-HCC-20A expression may be involved in the inhibition of apoptosis in response to DNA damage through the interaction with BRCA2.

Discussion

Here, we identified that the protein BJ-HCC-20A interacts with a portion of a highly conserved region of BRCA2 using a yeast two-hybrid system, and showed an interaction between endogenous BJ-HCC-20A and BRCA2 *in vivo*. Human BJ-HCC-20 is reported to be a potential CT antigen. Because CT antigens are expressed in a variety of cancers and in the normal testis, some of the CT antigens are being studied as potential therapeutic cancer vaccines. In addition, a number of CT antigens are reported to be involved in cell growth and contribute to some features of neoplastic phenotypes including immortality, invasiveness, and metastatic capacity.[36,37] Here, we show that overexpressed BJ-HCC-20A results in the promotion of cell growth, and downregulation of endogenous BJ-HCC-20 expression using siRNA results in the suppression of cell growth. This suggests that BJ-HCC-20A may have an oncogenic role. Downregulation of endogenous BJ-HCC-20 expression by siRNA leads to the induction of apoptosis, suggesting that BJ-HCC-20 has an antiapoptotic role. Taken together, BJ-HCC-20 may promote cell growth by inhibiting the induction of apoptosis.

DNA damage disrupts the balance between DNA repair/cell survival and DNA damage/cell apoptosis signaling pathways in cells. Other studies have shown BRCC (BRCA1/2-containing complex) is involved in the imbalance between the DNA damage/cell apoptosis and DNA repair/cell survival signaling pathways.[38] Severe damage using high-dose ADR, as in the present study, may lead cells to DNA damage and cell apoptosis. BRCA2 is involved in DNA damage repair and apoptosis,[6–8,22,31] and several DNA-damaging agents, including ADR, camptothecin, and ultraviolet, have been shown to down-regulate BRCA2 expression in cancer cells.[30,32–35] Here, we show that similar to BRCA2, the BJ-HCC-20 mRNA level is also decreased by ADR-induced DNA damage, and the depletion of BJ-HCC-20 expression by siRNA enhances cell apoptosis and promotes the reduction of BRCA2 expression in response to DNA damage. In addition, the recovery of BJ-HCC-20A expression

doi: 10.1111/j.1349-7006.2008.00733.x
© 2008 Japanese Cancer Association

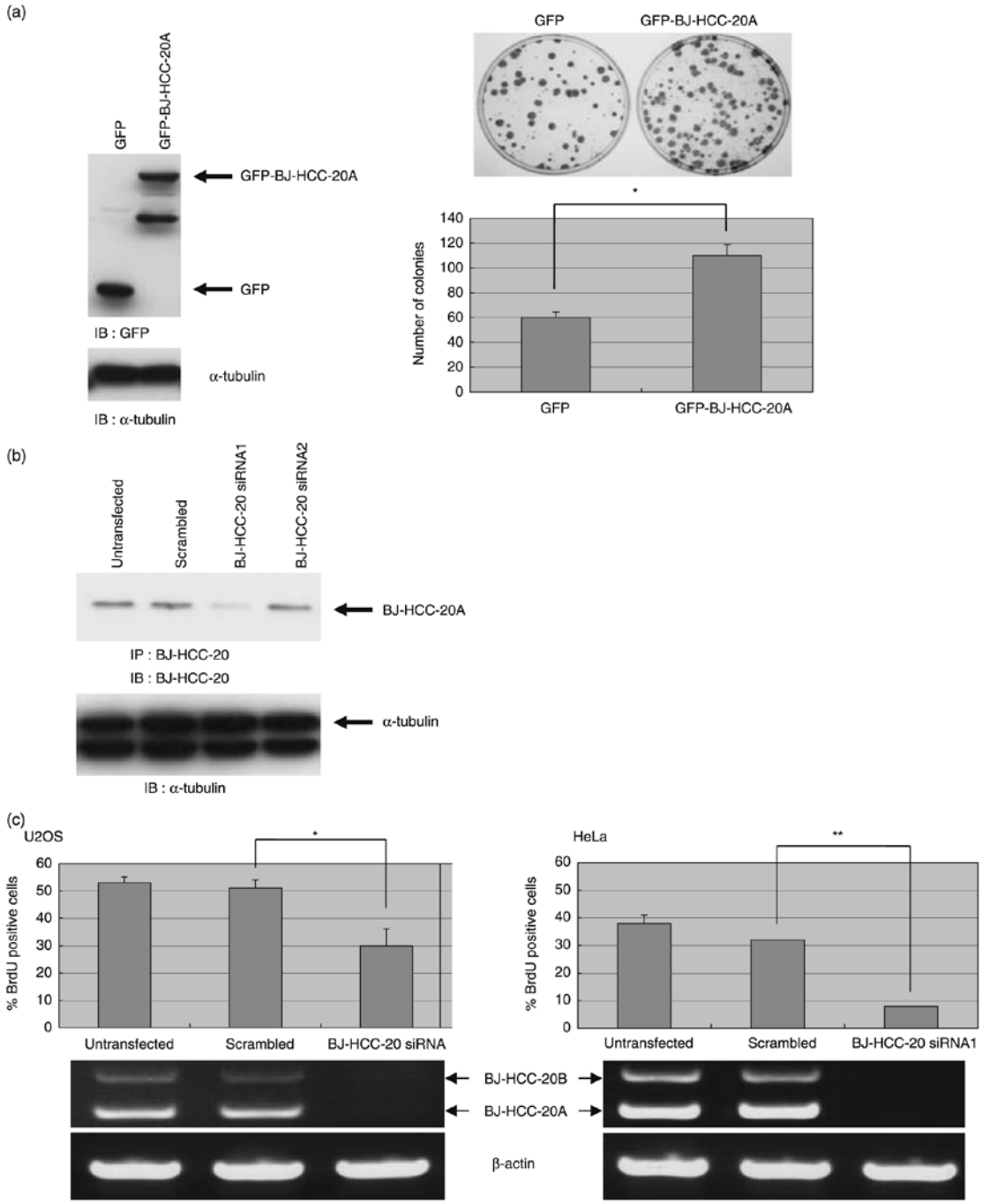

Fig. 4. Expression of BJ-HCC-20A promotes cell growth. (a) Expression of green fluorescent protein (GFP) vector or GFP-BJ-HCC-20A in HeLa cells was analyzed by immunoblotting with anti-GFP (left panels). The colony-formation assays showed that BJ-HCC-20A promotes cell growth in HeLa cells (right panels) (carried out in triplicate). Statistical analysis was carried out using Student's *t*-test. $*P < 0.005$. (b) Reduction of endogenous BJ-HCC-20A expression by BJ-HCC-20 small interfering RNA (siRNA). MCF-7 cells were transfected with the indicated siRNA for 48 h. BJ-HCC-20A expression was determined by immunoprecipitation and immunoblotting with anti-BJ-HCC-20 (upper panel). Immunoblot of cell lysates with anti-α-tubulin was used as a control (lower panel). (c) Suppression of cell growth by BJ-HCC-20 siRNA. U2OS and HeLa cells were transfected with the indicated siRNA for 48 h, and the effects on cell growth were determined using 5-bromo-2'-deoxy-uridine (BrdU)-incorporation assays. At least 700 cells (4',6-diamidino-2-phenylindole) from five fields were counted and the percentage of BrdU-positive cells was calculated. The results are shown as the mean ± SD of three independent experiments (upper panel). The lower panel shows the knockdown effects of BJ-HCC-20 mRNA expression by BJ-HCC-20 siRNA in U2OS and HeLa cells. Statistical analysis was carried out using Student's *t*-test. $*P < 0.05$, $**P < 0.005$. IB, immunoblot; IP, immunoprecipitation.

© 2008 Japanese Cancer Association

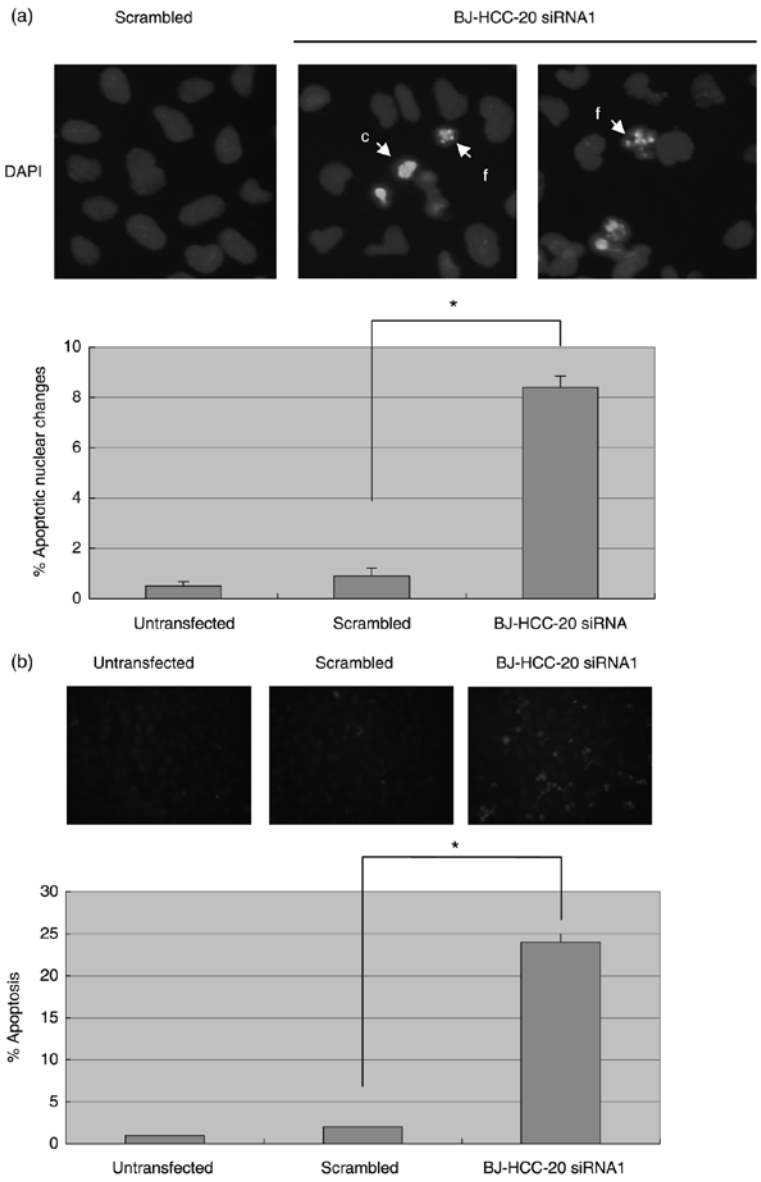

Fig. 5. Downregulation of BJ-HCC-20 causes the induction of apoptosis. (a) Cell morphological changes in the nucleus caused by BJ-HCC-20 small interfering RNA (siRNA). U2OS cells that were transfected with the indicated siRNA for 48 h in the BrdU-incorporation assays were stained with 4′,6-diamidino-2-phenylindole (DAPI). Arrowheads indicate the apoptotic nuclear changes (c, condensation; f, fragmentation). At least 800 cells (nuclei stained with DAPI) from five fields were observed and the percentage of cells exhibiting apoptotic nuclear changes was calculated. The results are shown as the mean ± SD of three independent experiments. Statistical analysis was carried out using Student's *t*-test. $*P < 0.0005$. (b) Induction of cell apoptosis by BJ-HCC-20 siRNA. U2OS cells were transfected with the indicated siRNA for 72 h, and the effects on apoptosis were determined using the terminal deoxynucleotidyltransferase-mediated dUTP-biotin nick-end labeling (TUNEL) assay. At least 600 cells (DAPI) from five fields were counted and the percentage of TUNEL-positive cells was calculated. The results are shown as the mean ± SD of three independent experiments. Statistical analysis was carried out using Student's *t*-test. $*P < 0.005$.

in ADR-induced DNA damage inhibits DNA damage-induced apoptosis. Based on these findings, we propose that in the DNA damage/cell apoptosis signaling pathway, downregulation of BJ-HCC-20 promotes the induction of apoptosis and simultaneously interferes with DNA repair by promoting the downregulation of BRCA2, resulting in the acceleration of cell apoptosis. Considering that the enhancement of ADR-induced apoptosis occurs by depletion of BJ-HCC-20 expression using siRNA, in addition to the fact that BJ-HCC-20A is a potential CT antigen, BJ-HCC-20A may serve as a potential target for the treatment of human tumors using DNA-damaging agents coupled with small molecules inhibiting BJ-HCC-20A or siRNA drugs to induce tumor death.

The mechanism by which BJ-HCC-20 may prevent the reduction of BRCA2 expression following DNA damage is not clear. p53 may be involved in the induction of apoptosis and sensitivity to the reduction of BRCA2 expression in response to DNA damage by downregulation of BJ-HCC-20 expression. Interestingly, previous studies have shown that p53 interacts with BRCA2,[12] and is involved in downregulation of BRCA2 mRNA and protein levels in response to DNA damage.[35] This hypothesis requires further investigation.

The binding domain of BRCA2 with BJ-HCC-20A includes five M phase-specific phosphorylation sites by Plk1, and M phase-specific phosphorylation of this domain is shown to modulate the interaction between BJ-HCC-20A and BRCA2. This suggests that the interaction is at least in part regulated by phosphorylation in an M phase-dependent manner, and may provide new insights into the involvement of BRCA2 in the DNA damage/cell apoptosis pathway. Importantly, the phosphorylation status of the binding domain by Plk1 may be crucial in regulating

doi: 10.1111/j.1349-7006.2008.00733.x
© 2008 Japanese Cancer Association

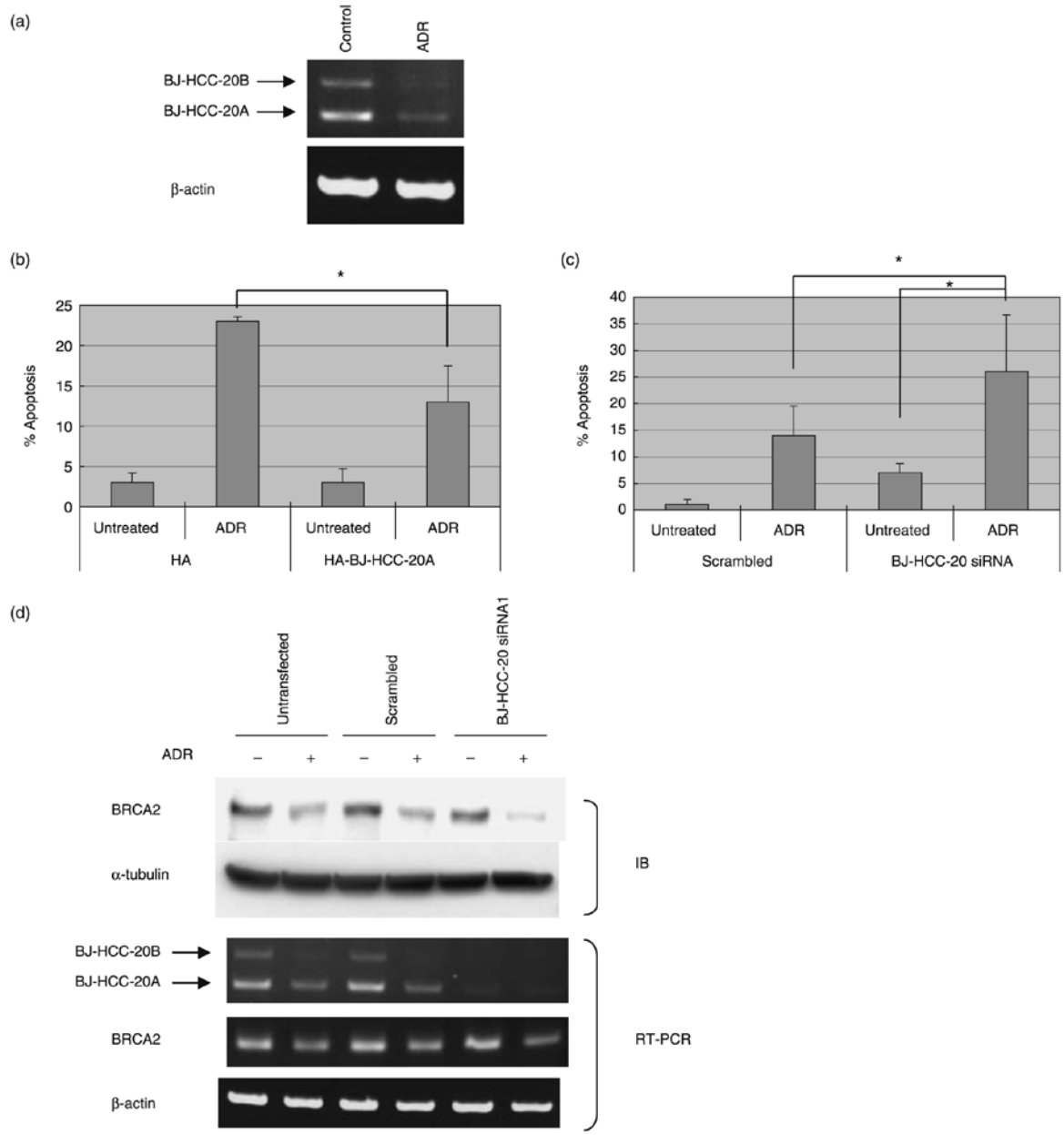

Fig. 6. Involvement of BJ-HCC-20 in apoptosis in response to DNA damage. (a) BJ-HCC-20 expression in response to DNA damage. U2OS cells were untreated or treated with 0.5 μg/mL adriamycin (ADR) for 24 h. A reverse transcription–polymerase chain reaction (RT-PCR) assay of the total RNA was carried out using primer sets for BJ-HCC-20 or β-actin. (b) U2OS cells were transfected with the indicated plasmids for 24 h and then untreated or treated with 0.5 μg/mL ADR for 24 h. Cell apoptosis was then determined using the terminal deoxynucleotidyltransferase-mediated dUTP-biotin nick-end labeling (TUNEL) assay. At least 300 cells (4′,6-diamidino-2-phenylindole) from three fields were counted and the percentage of TUNEL-positive cells was calculated. The results are shown as the mean ± SD of three independent experiments. Statistical analysis was carried out using Student's *t*-test. $^*P < 0.05$. (d) U2OS cells were transfected with the indicated small interfering RNA (siRNA) for 24 h and then untreated or treated with 0.5 μg/mL ADR for 24 h. Cell lysates were analyzed by immunoblotting with anti-BRCA2 or anti-α-tubulin antibodies. A RT-PCR assay of the total RNA was carried out using primer sets for BJ-HCC-20, BRCA2 or β-actin. IB, immunoblot.

© 2008 Japanese Cancer Association

the interaction of BJ-HCC-20A with the binding region of BRCA2. We found that ADR treatment resulted in reduced expression of BRCA2 and BJ-HCC-20A, which induced cell apoptosis in response to DNA damage. The complex of BRCA2 and BJ-HCC-20A may regulate the induction of cell apoptosis after DNA-damaging treatment in S phase. None or low levels of phosphorylation in S phase are likely to be important for regulating cell apoptosis by this complex. Conversely, phosphorylation of the binding domain during mitosis may be responsible for inactivation of the DNA damage/cell apoptosis pathway.

In conclusion, we found that the BJ-HCC-20A protein promotes cell growth and is involved in the inhibition of apoptosis induced by DNA damage, and may regulate the induction of cell apoptosis in response to DNA damage in cooperation with BRCA2 in an M phase-dependent manner. Therefore, we speculate that targeting BJ-HCC-20A may aid in the treatment of breast tumors.

Acknowledgments

This work was supported by a 21st Century Center of Excellence Program for Frontier Research on Molecular Destruction and Reconstruction of Tooth and Bone, Grants-in-Aid for scientific research from the Ministry of Education, Science, Sports and Culture of Japan.

References

1 Stratton MR, Wooster R. Hereditary predisposition to breast cancer. *Curr Opin Genet Dev* 1996; **6**: 93–7.
2 Miki Y, Swensen J, Shattuck-Eidens D *et al*. A strong candidate for the breast and ovarian cancer susceptibility gene *BRCA1*. *Science* 1994; **266**: 66–71.
3 Wooster R, Bignell G, Lancaster J *et al*. Identification of the breast cancer susceptibility gene *BRCA2*. *Nature* 1995; **378**: 789–92.
4 Tavtigian SV, Simard J, Rommens J *et al*. The complete *BRCA2* gene and mutations in chromosome 13q-linked kindreds. *Nat Genet* 1996; **12**: 333–7.
5 Gudmundsson J, Johannesdottir G, Bergthorsson JT *et al*. Different tumor types from BRCA2 carriers show wild-type chromosome deletions on 13q12-q13. *Cancer Res* 1995; **55**: 4830–2.
6 Sharan SK, Morimatsu M, Albrecht U *et al*. Embryonic lethality and radiation hypersensitivity mediated by Rad51 in mice lacking Brca2. *Nature* 1997; **386**: 804–10.
7 Patel KJ, Yu VP, Lee H *et al*. Involvement of Brca2 in DNA repair. *Mol Cell* 1998; **1**: 347–57.
8 Tutt A, Bertwistle D, Valentine J *et al*. Mutation in Brca2 stimulates error-prone homology-directed repair of DNA double-strand breaks occurring between repeated sequences. *EMBO J* 2001; **20**: 4704–16.
9 Yuan SS, Lee SY, Chen G, Song M, Tomlinson GE, Lee EY. BRCA2 is required for ionizing radiation-induced assembly of Rad51 complex *in vivo*. *Cancer Res* 1999; **59**: 3547–51.
10 Esashi F, Christ N, Gannon J *et al*. CDK-dependent phosphorylation of BRCA2 as a regulatory mechanism for recombinational repair. *Nature* 2005; **434**: 598–604.
11 Milner J, Ponder B, Hughes-Davies L, Seltmann M, Kouzarides T. Transcriptional activation functions in BRCA2. *Nature* 1997; **386**: 761–3.
12 Marmorstein LY, Ouchi T, Aaronson SA. The *BRCA2* gene product functionally interacts with p53 and RAD51. *Proc Natl Acad Sci USA* 1998; **95**: 13 869–74.
13 Hughes-Davies L, Huntsman D, Ruas M *et al*. EMSY links the BRCA2 pathway to sporadic breast and ovarian cancer. *Cell* 2003; **115**: 523–35.
14 Vaughn JP, Cirisano FD, Huper G *et al*. Cell cycle control of BRCA2. *Cancer Res* 1996; **56**: 4590–4.
15 Chen CF, Chen PL, Zhong Q, Sharp ZD, Lee WH. Expression of BRC repeats in breast cancer cells disrupts the BRCA2–Rad51 complex and leads to radiation hypersensitivity and loss of G_2/M checkpoint control. *J Biol Chem* 1999; **274**: 32 931–5.
16 Marmorstein LY, Kinev AV, Chan GK *et al*. A human BRCA2 complex containing a structural DNA binding component influences cell cycle progression. *Cell* 2001; **104**: 247–57.
17 Wang SC, Shao R, Pao AY, Zhang S, Hung MC, Su LK. Inhibition of cancer cell growth by BRCA2. *Cancer Res* 2002; **62**: 1311–14.
18 Tian XX, Rai D, Li J *et al*. BRCA2 suppresses cell proliferation via stabilizing MAGE-D1. *Cancer Res* 2005; **65**: 4747–53.
19 Gretarsdottir S, Thorlacius S, Valgardsdottir R *et al*. BRCA2 and p53 mutations in primary breast cancer in relation to genetic instability. *Cancer Res* 1998; **58**: 859–62.
20 Tutt A, Gabriel A, Bertwistle D *et al*. Absence of Brca2 causes genome instability by chromosome breakage and loss associated with centrosome amplification. *Curr Biol* 1999; **9**: 1107–10.
21 Gudmundsdottir K, Ashworth A. The roles of BRCA1 and BRCA2 and associated proteins in the maintenance of genomic stability. *Oncogene* 2006; **25**: 5864–74.
22 Cheung AM, Hande MP, Jalali F *et al*. Loss of Brca2 and p53 synergistically promotes genomic instability and deregulation of T-cell apoptosis. *Cancer Res* 2002; **62**: 6194–204.
23 Nakanishi A, Han X, Saito H *et al*. Interference with BRCA2, which localizes to the centrosome during S and early M phase, leads to abnormal nuclear division. *Biochem Biophys Res Commun* 2007; **355**: 34–40.
24 Daniels MJ, Wang Y, Lee M, Venkitaraman AR. Abnormal cytokinesis in cells deficient in the breast cancer susceptibility protein BRCA2. *Science* 2004; **306**: 876–9.
25 Lin HR, Ting NS, Qin J, Lee WH. M phase-specific phosphorylation of BRCA2 by Polo-like kinase 1 correlates with the dissociation of the BRCA2-P/CAF complex. *J Biol Chem* 2003; **278**: 35 979–87.
26 Lee M, Daniels MJ, Venkitaraman AR. Phosphorylation of BRCA2 by the Polo-like kinase Plk1 is regulated by DNA damage and mitotic progression. *Oncogene* 2004; **23**: 865–72.
27 Lu H, Guo X, Meng X *et al*. The BRCA2-interacting protein BCCIP functions in RAD51 and BRCA2 focus formation and homologous recombinational repair. *Mol Cell Biol* 2005; **25**: 1949–57.
28 Dong XY, Li YY, Yang XA, Chen WF. BJ-HCC-20, a potential novel cancer–testis antigen. *Biochem Cell Biol* 2004; **82**: 577–82.
29 Park JH, Lin ML, Nishidate T, Nakamura Y, Katagiri T. PDZ-binding kinase/T-LAK cell-originated protein kinase, a putative cancer/testis antigen with an oncogenic activity in breast cancer. *Cancer Res* 2006; **66**: 9186–95.
30 Andres JL, Fan S, Turkel GJ *et al*. Regulation of BRCA1 and BRCA2 expression in human breast cancer cells by DNA-damaging agents. *Oncogene* 1998; **16**: 2229–41.
31 Hay T, Patrick T, Winton D, Sansom OJ, Clarke AR. Brca2 deficiency in the murine small intestine sensitizes to p53-dependent apoptosis and leads to the spontaneous deletion of stem cells. *Oncogene* 2005; **24**: 3842–6.
32 Fan S, Twu NF, Wang JA *et al*. Down-regulation of BRCA1 and BRCA2 in human ovarian cancer cells exposed to adriamycin and ultraviolet radiation. *Int J Cancer* 1998; **77**: 600–9.
33 Yuan R, Fan S, Wang JA *et al*. Coordinate alterations in the expression of BRCA1, BRCA2, p300, and Rad51 in response to genotoxic and other stresses in human prostate cancer cells. *Prostate* 1999; **40**: 37–49.
34 Su J, Ciftci K. Changes in BRCA1 and BRCA2 expression produced by chemotherapeutic agents in human breast cancer cells. *Int J Biochem Cell Biol* 2002; **34**: 950–7.
35 Wu K, Jiang SW, Couch FJ. p53 mediates repression of the BRCA2 promoter and down-regulation of BRCA2 mRNA and protein levels in response to DNA damage. *J Biol Chem* 2003; **278**: 15 652–60.
36 Simpson AJ, Caballero OL, Jungbluth A, Chen YT, Old LJ. Cancer/testis antigens, gametogenesis and cancer. *Nat Rev Cancer* 2005; **5**: 615–25.
37 Mischo A, Kubuschok B, Ertan K *et al*. Prospective study on the expression of cancer testis genes and antibody responses in 100 consecutive patients with primary breast cancer. *Int J Cancer* 2006; **118**: 696–703.
38 Chen X, Arciero CA, Wang C, Broccoli D, Godwin AK. BRCC36 is essential for ionizing radiation-induced BRCA1 phosphorylation and nuclear foci formation. *Cancer Res* 2006; **66**: 5039–46.

doi: 10.1111/j.1349-7006.2008.00733.x
© 2008 Japanese Cancer Association

MEMO

分子生物学分野

石野 史敏

難治疾患研究所・ゲノム応用医学研究部門
分子生物学・教授

1. 研究課題名

Non-coding antiPeg11転写産物はどのように肋骨形成制御に関わるのか?—antiPeg11からの組織特異的なmiRNA生成機構の解明—

How does non-coding antiPeg11 transcript regulate rib development? —mechanism of tissue-specific miRNA production from antiPeg11 transcript—

ヒト新生児の肋骨形成に、父親性発現インプリント遺伝子PEG11/RTL1が重要な働きをしていることを発見した（Sekta et al. Nat Genet 2008, Kagami and Sekita et al. Nat Genet 2008）。PEG11/RTL1 mRNA量は、母親性発現のアンチセンスRNAであるantiPEG11/RTL1にコードされる複数のmicroRNAによって制御されている。これらの遺伝子が存在する染色体14番の父親性2倍体では、2倍体の父親性染色体からのPEG11/RTL1の発現量の増加にantiPEG11/RTL1の欠失が加わるため、実際には4－6倍の発現量の増加がみられ、肋骨形成異常を伴う新生児致死、生後の発育不良、高度の精神遅滞等の重篤な疾患が現れる。antiPEG11/RTL1は自然のアンチセンスRNAであるため、antiPEG11/RTL1にふくまれるmicroRNAの投与がこれらの疾患の症状改善に役立つ可能性が高い。生体内におけるmicroRNA投与の効果を評価するモデル系の開発を行ない、将来の治療につなげたい。

2. インプリント遺伝子の発現異常による肋骨形成異常

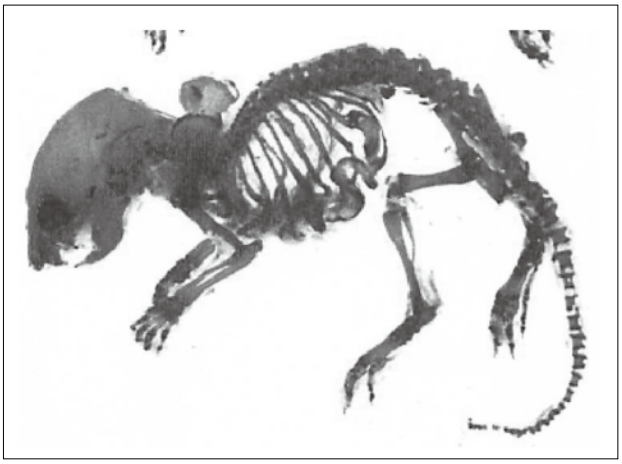

3. 2008年、2009年（平成21年3月までの）に発表した全ての研究内容についての英文要約

1. Human chromosome 14q32.2 carries a cluster of imprinted genes including paternally expressed genes（PEGs）such as DLK1 and PEG11/RTL1 and maternally expressed genes（MEGs）such as GTL2, PEG11//RTL1as（antiPEG11/RTL1 antisense）, and MEG8, together with the intergenic differentially methylated region（IG-DMR）and the GTL2-DMR. Consistent with this, paternal and maternal uniparental disomy for chromosome 14（upd（14）pat and upd（14）mat）cause distinct phenotypes. We studied eight cases with a upd（14）pat-like phenotype and three cases with a upd（14）mat-like phenotype in the absence of upd（14）, and identified various deletions and epimutations affecting the imprinted region. The results, together with recent mouse data imply an important cis-acting regulatory function for the IG-DMR on the maternally inherited chromosome, and the major relevance of excessive PEG11/RTL1 expression and decreased DLK1 and PEG11/RTL1 expression to upd（14）pat-like and

upd（14）mat-like phenotypes, respectively.

2. Eutherian placenta is an organ which emerged in the course of mammalian evolution and provides essential architecture, the so-called feto-maternal interface, for fetal development by exchanging nutrition, gas and waste between fetal and maternal blood. Functional defects of the placenta cause several developmental disorders, such as intrauterine growth retardation in humans and mice. A series of new inventions and/or adaptations must have been necessary to form and maintain eutherian chorioallantoic placenta, which consists of capillary endothelial cells and a surrounding trophoblast cell layer（s）[1]. Although many placental genes are identified[2], it remains unknown how the feto-maternal interface is formed and maintained during development, and how this novel design evolved. Here we demonstrate that retrotransposon-derived Rtl1（retrotransposon-like 1）, also known as Peg11（paternally expressed 11）, is essential for maintenance of the fetal capillaries, and that both its loss and overproduction cause late-fetal and/or neonatal lethality in mice.

3. We assessed the possibility of Meg1/Grb10 transgenic mice（Meg1 mice）as a non-obese type 2 diabetes（2DM）animal model. Meg1 mice were born normal, but their weight did not increase as much as normal after weaning and showed about 85% of normal size at 20 weeks of age. Body mass index of Meg1 mice was also smaller than that of control mice. The glucose tolerance test and insulin tolerance test showed that Meg1 mice had reduced ability to normalize the blood glucose level. Blood urea nitrogen（BUN）in Meg1 mice（19.6 ± 1.2 mg/dl）was significantly lower than in controls（22.0 ± 0.8 mg/dl）, while plasma triglyceride, insulin, adiponectin and resistin levels were significantly higher（202.0 ± 23.4 mg/dl vs. 146.3 ± 23.4 mg/dl, 152.4 ± 16.3 pg/ml vs. 88.1 ± 16.9 pg/ml, 74.4 ± 10.9 mg/ml vs. 48.3 ± 7.0 mg/ml, and 4.0 ± 0.2 ng/ml vs. 3.6 ± 0.2 ng/ml, respectively）. Body, visceral fat weight and liver weights were significantly lower（19.6 ± 0.4 g vs. 24.3 ± 0.3 g, 376.7 ± 29.6 mg to 507.5 ± 23.0 mg and 906.0 ± 41.8 mg to 1001.0 ± 15.1 mg, respectively）. Thus, hyperinsulinemia observed in Meg1 mice indicates that their insulin signaling pathway is somehow inhibited. With high fat diet, the diabetes onset rate of Meg1 mice increased up to 60%. These results suggest that Meg1 mice resemble human 2DM.

4. Therapeutic cloning has been demonstrated successfully using nuclear transfer（NT）from blastocysts to enucleated oocytes to generate embryonic stem cells（NT-ES cells）. Such cells are transcriptionally and functionally indistinguishable from normal fertilization-derived ES cells. Mice can be cloned from adult somatic cells or ES cells by NT and such cloned embryos can be used to establish new NT-ES cell lines. However, ES cells derived from parthenogenetic embryos（pES cells）show epigenetic disorders and low potential for normal differentiation unless used to produce subsequent generations of NT-ES lines. Thus, enucleated oocytes can initialize epigenetic modification, but the extent and efficacy of this remains unclear. In this study we aimed to clarify why the contribution rate of pES cells appears to improve after NT. We compared gene expression profiles between pES and NT-pES cell lines using DNA microarray analysis, quantitative real-time polymerase chain reaction amplification and allele-specific DNA methylation analysis. Although changes in expression level were observed for 4% of 34,967 genes, only 81（0.2%）showed common changes across multiple cell lines. In particular, the expression level of a paternally expressed gene, U2af1-rs1, was increased significantly in all NT-pES cell lines investigated. The methylation status at the upstream differentially methylated region（DMR）of U2af1-rs1 was also changed significantly after NT. This was observed in NT-pES cells, but also in conventionally produced NT-ES cells, which has never been reported previously. These results suggest that NT affects the epigenetic status of a few gene regions in common and that a change in the methylation status U2af1-rs1 could be used as a genetic marker to investigate the effects of NT.

5. Hyperplastic placentas in mice have been reported in several experimental models including somatic cell nuclear transfer, inter（sub）species hybridization, and somatic cytoplasm-introduced intracytoplasmic sperm injection. Of great interest about these placental phenotypes are the common gross and histological features such as enlargement of the spongiotrophoblast layers, despite their quite different etiologies. To obtain morphological clues for the pathways leading to these similar placental phenotypes, ultrastructural analysis of the three different hyperplastic placentas was performed. The majority of cells affected were the trophoblast-origin and their subcellular ultrastructural lesions were common among the groups; e.g., heavy accumulation of cytoplasmic vacuoles in the trophoblastic cells composing the labyrinthine wall and an increased volume of spongiotrophoblastic cells with extraordinarily dilated rough endoplasmic reticulum. Although the number of trophoblastic glycogen cells greatly increased, they maintained their normal ultrastructural morphology. Fetal endothelium and small

vessels are nearly intact. Our ultrastructural study suggest that these three types of placental hyperplasias with different etiologies may have common pathological pathways, which probably affect exclusively the development of the trophoblastic lineage cells during mouse placentation.

6. Mammalian androgenetic embryos can be produced by pronuclear exchange of fertilized oocytes or by dispermic in vitro fertilization of enucleated oocytes. Here we report a new technique for producing mouse androgenetic embryos by injection of two round spermatid nuclei into oocytes, followed by female chromosome removal. We found that injection of round spermatids resulted in high rates of oocyte survival (88%). Androgenetic embryos thus produced developed into mid-gestation fetuses at various rates, depending on the mouse strain used. All the fetuses examined maintained paternally specific genomic imprinting memories. This technique also enabled us to produce complete heterozygous F1 embryos by injecting two spermatids from different strains. The best rate of fetal survival (12% per embryos transferred) was obtained with C57BL/6 × DBA/2 androgenetic embryos. We also generated embryonic stem cell lines efficiently with the genotype of Mus musculus domesticus × M. m. molossinus. Thus, injection of two round spermatid nuclei followed by maternal enucleation is an effective alternative method of producing androgenetic embryos that consistently develop into blastocysts and mid-gestation fetuses.

7. Mice with maternal duplication of proximal Chromosome 11 (MatDp (prox11)), where Meg1/Grb10 is located, exhibit pre- and postnatal growth retardation. To elucidate the responsible imprinted gene for the growth abnormality, we examined the precise structure and regulatory mechanism of this imprinted region and generated novel model mice mimicking the pattern of imprinted gene expression observed in the MatDp (prox11) by deleting differentially methylated region of Meg1/Grb10 (Meg1-DMR). It was found that Cobl and Ddc, the neighboring genes of Meg1/Grb10, also comprise the imprinted region. We also found that the mouse-specific repeat consisting of several CTCF-binding motifs in the Meg1-DMR functions as a silencer, suggesting that the Meg1/Grb10 imprinted region adopted a different regulatory mechanism from the H19/Igf2 region. Paternal deletion of the Meg1-DMR (+/ΔDMR) caused both upregulation of the maternally expressed Meg1/Grb10 Type I in the whole body and Cobl in the yolk sac and loss of paternally expressed Meg1/Grb10 Type II and Ddc in the neonatal brain and heart, respectively, demonstrating maternalization of the entire Meg1/Grb10 imprinted region. We confirmed that the +/ΔDMR mice exhibited the same growth abnormalities as the MatDp (prox11) mice. Fetal and neonatal growth was very sensitive to the expression level of Meg1/Grb10 Type I, indicating that the two-fold increment of the Meg1/Grb10 Type I is one of the major causes of the growth retardation observed in the MatDp (prox11) and +/ΔDMR mice. This suggests that the corresponding human GRB10 Type I plays an important role in the etiology of Silver-Russell syndrome (SRS) caused by partial trisomy of 7p11-p13.

4. 本事業に関連して世界的な研究拠点形成に向けて、以下の点で改善・整備等されたこと

A（研究拠点体制）

難治疾患研究所形質発現分野（萩原正敏教授）とanitPeg11/Rtl1　の解析に関する共同研究体制を整えた。

B（研究教育環境）

新棟に研究室を移し、その施設・環境整備を行った。

C（人材確保）

PIシャペロン教官として京都大学から李知英さんを採用した。

D（人材育成）

AISSとして岩舩浩孝の研究指導を行なっている。

E（国際化）

PIシャペロン教官として採用した李知英さんは韓国出身の研究者である。

5. GCOE事業を推進するに当たって力を入れた点

ゲノムインプリンティングという哺乳類特異的な遺伝子発現機構と歯と骨の研究の接点における研究を進めている。

6. 英文原著論文

1. Kagami, M.*, Sekita, Y.*, Nishimura, G., Irie, M., Kato, F., Okada, M., Yamamori, S., Kishimoto, H., Nakayama, M., Tanaka, Y., Matsuoka, K., Takahashi, T., Noguchi, M., Tanaka, Y., Masumoto, K., Utsunomiya, T., Kouzan, H., Komatsu, Y., Ohashi, H., Kurosawa, K., Kosak, K., Ferguson-Smith, A. C., Ishino F. and Ogata, T. Deletions and epimutations affecting the human chromosome 14q32.2 imprinted region in individuals with paternal and maternal upd (14)-like phenotypes. Nat. Genet. 40 (2), 237-242 (2008).
2. Sekita, Y., Wagatsuma, H., Nakamura, K., Ono, R., Kagami, M., Wakisaka-Saito, N., Hino, T., Suzuki-

Migishima, R., Kohda, T., Ogura, A., Ogata, T. Yokoyama, M., Kaneko-Ishino T. and Ishino, F. Role of retrotransposon-derived imprinted gene, Rtl1, in the feto-maternal interface of mouse placenta. Nat. Genet. 40（2）, 243-248（2008）.
3. Hikichi, T., Kohda, T., Wakayama, S., Ishino, F. and Wakayama, T. Nuclear transfer alters the DNA methylation status of specific genes in fertilized and parthenogenetically activated mouse embryonic stem cells. Stem Cells. 26（3）,783-788（2008）.
4. Yamamoto, Y., Ishino, F., Kaneko-Ishino, T., Shiura H., Uchio-Yamada, K., Matsuda, J., Suzuki, O. and Sato, K. Type 2 diabetes mellitus in a non-obese mouse model induced by Meg1/Grb10 overexpression. Exp. Animals 57（4）, 385-395（2008）. July
5. Wakisaka, N., Ogonuki, N., Miki, Y., Sekita, Y., Hanaki, K., Aikatsuka, A., Kaneko-Ishino, T., Ishino F., and Ogura, A. Ultrastructure of placental hyperplasia in mice: Comparison of placental phenotypes with three different etiologies. Placenta 29（8）, 753-759（2008）.
6. ◎Shiura, H., Nakamura, K., Hikichi, T,. Hino, T., Oda, K., Suzuki-Migishima, R., Kohda, T., Kaneko-Ishino, T., Ishino, F. Paternal deletion of Meg1/Grb10 DMR causes maternalization of the Meg1/Grb10 cluster in mouse proximal Chromosome 11 leading to severe pre- and postnatal growth retardation. Hum. Mol. Genet.（in press）.

7. 著書

1. 関田洋一、金児-石野知子、石野史敏　レトロトランスポゾンに由来する胎児成長に重要な遺伝子の機能と哺乳類の進化　メディカルバイオ 5（2）, 18-19（2008）.3月号
2. 関田洋一、金児-石野知子、石野史敏　レトロトランスポゾン由来の印譜リンティング遺伝子Peg11/Rtl1は胎盤の母子間相互作用部位で必須機能を果たしている　細胞工学 27（3）, 256-257（2008）.
3. 金児-石野知子、石野史敏 ゲノムインプリンティングと進化　蛋白質・核酸・酵素　53（7）, 836-843（2008）.
4. 小野竜一, 成瀬美衣, 金児-石野知子, 石野史敏, “Peg10 KO マウス（胎盤形成不全）”, 分子細胞治療, 7（4）, 62-65, 2008.
5. 石野史敏 エピジェネティクス　ベーシックマスター発生生物学　（東中川徹・八杉貞雄・西駕秀俊　共編）12章　オーム社　pp.273-289（2008）.
6. 石野史敏 哺乳類の個体発生とゲノムインプリンティング　生体の科学　59（5）, 409-409（2008）.
7. 石野史敏、金児-石野知子　個体発生・成長とエピジェネティクス　特集消化器疾患とエピジェネティクス　分子消化器病　5（4）,330-336（2008）.
8. 関田洋一、金児-石野知子、石野史敏　染色体14番の父親性2倍体症候群の治療を目指したmicroRNA投与法の開発　Chemical Biology 2（1）12-13（2009）.
9. 金児-石野知子、石野史敏　哺乳類の原点? カモノハシ ―哺乳類のゲノム機能の進化を探る―　蛋白質・核酸・酵素　54（1）, 58-64（2009）.

8. 自己評価

ゲノムインプリンティングと歯と骨の接点を考えて、新しい実験系を立ち上げた。microRNAを使った治療という新しい領域なので、充分な検討を重ねて考えたテーマであるので、このGCOE期間中に仕事がまとまることを楽しみにしている。

9. 学会発表（英文）

1）Fumitoshi Ishino, Ryuichi Ono, Sunsuke Suzuki Takashi Kohda and Tomoko Kaneko-Ishino. Evolution of genomic imprinting and placentation in mammals by retrotransposons. 6th NIBB-EMBL Joint Meeting “Evolution of Epigenetic Regulaton” March 17-19 2008（EMBL Heidelberg, Germany）.
2）Shunsuke Suzuki,Ryuichi Ono, Taka Narita, Takashi Kohda, Yuji Kohara, Fumitoshi Ishiono, Marilyn Renfree and Tomoko Kaneko-Ishino. Retrotransposon Silencing by DNA methylation can drive mammalian genomic imprinting. 6th NIBB-EMBL Joint Meeting “Evolution of Epigenetic Regulaton” March 17-19 2008（Heidelberg, Germany）.
3）Yocihi Sekita, Masayo Kagami, Daisuke Endo, Ryuichi Ono, Takashi Kohda, Tsutomo Ogata, Tomoko Kaneko-Ishino and Fumitoshi Ishino. Roles of Peg11/Rtl1, in neo- and postnatal growth. EMBO Workshop on Genomic Imprinting September 21-24 2008（TEMASEK LifeScience Laboratory, Singapore）.
4）Tomoko Kaneko-Ishino, Shunsuke Suzuki, Andrew Pask, Geoffrey Shaw, Takashi Kohda, Jennifer Graves, Marilyn Renfree and Fumitoshi Ishino. Origins of retrotransposon-derived PEG10 and imprinted regulation by DNA methylation. EMBO Workshop on Genomic Imprinting September 21-24 2008（TEMASEK LifeScience Laboratory, Singapore）.
5）Hirosuke Shiura, Takafusa Hikichi, Kenji Nakamura, Toshiaki Hino, Kanako Oda, Rika Suzuki-Migishima, Takashi Kohda, Tomoko Kaneko-Ishino and Fumitoshi Ishino. Disruption of imprinted regulation in Meg1/Grb10 cluster results in pre- and postnatal growth

retardation. EMBO Workshop on Genomic Imprinting, September 21-24 2008（TEMASEK LifeScience Laboratory, Singapore）.

6) Fumitoshi Ishino, Genomic imprinting diseases:Patients with paternal UPD14 and maternal deletion of imprinting control region in 14q32.2 characterized by bell-shaped thorax. Global COE Kickoff Symposium, November 6 2009（Tokyo Garden Parace, Tokyo）.

7) Fumitoshi Ishino, Ryuichi Ono, Sunsuke Suzuki, Yoichi Sekita, Mie Naruse, Takashi Kohda and Tomoko Kaneko-Ishino. Evolution of placentation in eutherian mammals contributed by exaptation of PEG10 and PEG11/RTL1 from retrotransposons. 8th NIBB-EMBL Joint Meeting“Evolution:Genomces, Cell Types and Shapes”, November 21-23 2008（Okazaki Conference Center, Okazaki）.

8) Fumitoshi Ishino, Ryuichi Ono, Shunsuke Suzuki, Yoichi Sekita, Mie Naruse, Takashi Kohda and Tomoko Kaneko-Ishino. Contribution of Retrotransposons to the Evolution of Genomic Imprinting and Placentation in Mammals International Symposium on Decoding Epigenetic Code, December 15-16（Tokyo University, Tokyo）.

10. 学会発表（和文）

1) 石野史敏　ゲノムインプリンティングからみた哺乳類の進化　―生物進化におけるレトロトランスポゾンの役割―　かずさDNA研究所所長セミナー―　平成20年5月14日（かずさDNA研究所、千葉）。

2) 石野史敏　哺乳類の胎生はどのように獲得されたのか?　第17回大学院医歯学総合研究科セミナー　“ポストゲノム時代の発生生物学展望”　平成20年6月23日（東京医科歯科大学、東京）。

3) 石野史敏　“生殖細胞研究・発生研究”から“生殖医療・再生医療へ”―鍵をにぎるエピジェネティック制御―　特定胚及びヒトES細胞等研究専門委員会 平成20年8月26日　（文部科学省、東京）。

4) 石野史敏、小野竜一、関田洋一、鈴木俊介、成瀬美衣、入江将仁、幸田尚、横山峯介、中村健司、金児－石野知子　哺乳類特異的なレトロトランスポゾンによる哺乳類の胎生進化　シンポジウム“哺乳類成立の為の分子基盤”　BMB2008　平成20年12月9日－12日（神戸ポートアイランド、神戸）。

5) 金児－石野知子、関田洋一、遠藤大輔、鏡雅代、小野竜一、幸田尚、緒方勤、石野史敏　個体発生に必須な機能をはたすアンチセンスRNA: RNAi機構を介したアンチセンスRNAによるPeg11/Rtl1遺伝子の発現制御　BMB2008　平成20年12月9日－12日（神戸ポートアイランド、神戸）。

6) 成瀬美衣、小野竜一、関田洋一、石井雅之、中村健司、日野敏昭、鈴木―右島理可、幸田尚、横山峯介、金児－石野知子、石野史敏　レトロトランスポゾン由来の遺伝子Sirh-familyの解析　BMB2008　平成20年12月9日－12日（神戸ポートアイランド、神戸）。

7) 小野竜一、成瀬美衣、中村健司、日野敏昭、鈴木―右島理可、高部美穂、宇佐美貴子、幸田尚、小倉淳郎、横山峯介、金児－石野知子、石野史敏　　レトロトランスポゾン由来の遺伝子Peg10の胎盤での機能　BMB2008　平成20年12月9日－12日（神戸ポートアイランド、神戸）。

8) 小林慎、藤原祥高、三瀬名丹、かせ田一弘、阿部訓也、石野史敏、岡部勝　着床前に雌特異的発現を示すFat45ファミリー遺伝子の解析　BMB2008　平成20年12月9日－12日（神戸ポートアイランド、神戸）。

9) 志浦寛相、引地貴亮、中村健司、日野敏昭、小田佳奈子、鈴木―右島理可、幸田尚、金児－石野知子、石野史敏　マウスMeg1/Grb10領域のインプリンティング発現制御と個体成長への影響　BMB2008　平成20年12月9日－12日（神戸ポートアイランド、神戸）。

10) 幸田尚、井上貴美子、引地貴亮、岩崎佐和、越後貫成美、三木洋美、若山照彦、小倉淳郎、金児－石野知子、石野史敏　　顕微授精によるエピジェネティックシフトの誘導　BMB2008　平成20年12月9日－12日（神戸ポートアイランド、神戸）。

11. 外部資金の獲得状況

科学研究費補助金、 学術創成研究

研究題目:　ゲノム刷込みに関連する哺乳類特異的遺伝子群の個体発生・系統発生にお ける役割

代表:　石野史敏

期間:　平成18年―平成22年

研究費総額:415,090,000

12. 新聞、雑誌、TV報道

・2008年1月7日　朝日新聞　　朝刊
・2008年1月7日　読売新聞　　朝刊
・2008年1月13日　毎日新聞　　日曜版
・2008年1月7日　東奥日報　　朝刊　（共同通信配信）
・2008年1月7日　京都新聞　　朝刊　（共同通信配信）
・2008年1月7日　西日本新聞　朝刊　（共同通信配信）
・2008年1月7日　山形新聞　　朝刊　（共同通信配信）
・2008年1月7日　茨城新聞　　朝刊　（共同通信配信）

・2008年1月7日　神戸新聞　　朝刊　（共同通信配信）
・2008年1月7日　河北新報　　朝刊　（共同通信配信）

13. 講座の准教授、講師、助教、特別研究員、ポスドク、指導を受けた大学院生の名前（AISSには○印）のリスト

准教授	幸田 尚
助　教	小野竜一
特任講師	李知英（GCOE）、小林慎（MTT）
特任助教	鈴木俊介、関田洋一、志浦寛相、遠藤大輔
大学院生	松本和也、入江将仁、成瀬美衣、○岩舩浩孝、王長山、石井雅之、岩崎佐和、山口祐季、夏希佳

LETTERS

nature genetics

© 2008 Nature Publishing Group http://www.nature.com/naturegenetics

Role of retrotransposon-derived imprinted gene, *Rtl1*, in the feto-maternal interface of mouse placenta

Yoichi Sekita[1], Hirotaka Wagatsuma[2], Kenji Nakamura[3], Ryuichi Ono[1], Masayo Kagami[4], Noriko Wakisaka[1,5], Toshiaki Hino[3], Rika Suzuki-Migishima[3], Takashi Kohda[1], Atsuo Ogura[6], Tsutomu Ogata[4], Minesuke Yokoyama[3,7], Tomoko Kaneko-Ishino[5] & Fumitoshi Ishino[1]

Eutherian placenta, an organ that emerged in the course of mammalian evolution, provides essential architecture, the so-called feto-maternal interface, for fetal development by exchanging nutrition, gas and waste between fetal and maternal blood. Functional defects of the placenta cause several developmental disorders, such as intrauterine growth retardation in humans and mice. A series of new inventions and/or adaptations must have been necessary to form and maintain eutherian chorioallantoic placenta, which consists of capillary endothelial cells and a surrounding trophoblast cell layer(s)[1]. Although many placental genes have been identified[2], it remains unknown how the feto-maternal interface is formed and maintained during development, and how this novel design evolved. Here we demonstrate that retrotransposon-derived *Rtl1* (retrotransposon-like 1), also known as *Peg11* (paternally expressed 11), is essential for maintenance of the fetal capillaries, and that both its loss and its overproduction cause late-fetal and/or neonatal lethality in mice.

To elucidate *Rtl1* function, we produced knockout (KO) mice (**Supplementary Fig. 1a,b** online). *Rtl1* is a paternally expressed imprinted gene highly expressed at the late-fetal stage in both the fetus and placenta (**Supplementary Fig. 1c**), and it is located in a large imprinted region on distal chromosome 12 (ref. 3; see **Supplementary Table 1** online for imprinting phenotypes[4–6]). Paternally expressed *Rtl1* has an overlapping maternally expressed antisense transcript, *Rtl1* antisense (*Rtl1as*, also known as *antiPeg11*), which contains several microRNAs (miRNAs) targeting the *Rtl1* transcript through an RNAi mechanism[3,7] (**Supplementary Fig. 1a**). We removed the entire Gag- and Pol-like domains of *Rtl1* with approximately 30% homology to the sushi-ichi retrotransposons, together with six of seven miRNAs in *Rtl1as*. Then, we produced two different types of mice: mice with no *Rtl1* expression upon paternal transmission of the KO allele (Pat-KO) and those with 2.5–3.0 times overexpression of the *Rtl1* as a result of deficiency of *Rtl1as* upon maternal transmission (Mat-KO; **Fig. 1a**). We confirmed that the imprinting regulation of distal chromosome 12 was not affected by the KO construct[8,9] (**Supplementary Fig. 1d,e**).

In the course of producing mice with the C57BL/6 (B6) background, we observed that the Pat-KO mice showed pre- and postnatal growth retardation in the F_1 and F_2 generations (**Supplementary Fig. 2a** online), and after the F_3 generation, most showed late-fetal or neonatal lethality (**Fig. 1b,c** and **Supplementary Fig. 3** online). When F_2 males mated with normal B6 females, all the pups, including the wild-type (WT) pups, were born dead as a result of a 3- to 4-d delay of the birth date (**Fig. 1c**; I and II in F_3 generation). When removed by caesarean sections at 19.0 days post coitus (d.p.c.) of the F_3 generation (**Fig. 1c**; III in F_3 generation), the WT pups grew normally, but half of the Pat-KO pups were already resorbing, and the other half were born small (about 80% the weight of the controls) and died by the next day (**Fig. 1c**; III in F_3 generation and **Table 1**). Pat-KO fetuses showed no abnormal phenotypes until 14.5 d.p.c., but half of them died from 15.5 to 19.0 d.p.c. (**Table 1**), and growth retardation of both the fetuses and placentas was observed even in the living half after 15.5 d.p.c. (**Fig. 1d–f**).

In Mat-KO mice, pups, at least after F_2, showed an approximately 15% retardation in growth after weaning (**Supplementary Fig. 2b,c**). Their birth rate gradually diminished after the F_4 generation, and neonatal lethality was predominant in the F_6 generation (**Fig. 1c**, F4–F6; **Supplementary Fig. 3b**, F_4–F_6 and **Supplementary Table 2** online). All the Mat-KO pups reached term normally, with normal weight, but they showed 150% placentomegaly compared to the normal size, and most died within a day (**Fig. 1g,h**). Although the genetic background affected both the Pat-KO and Mat-KO phenotypes to a large degree (**Supplementary Tables 2** and **3** online), these results demonstrate that both the loss and the overproduction

[1]Department of Epigenetics, Medical Research Institute, Tokyo Medical and Dental University, 2-3-10 Kandasurugadai, Chiyoda-ku, Tokyo 101-0062, Japan. [2]Graduate School of Bioscience and Biotechnology, Tokyo Institute of Technology, 4259 Nagatsuta-cho, Midori-ku, Yokohama 226-8501, Japan. [3]Mitsubishi Kagaku Institute of Life Sciences, 11 Minamiooya, Machida, Tokyo 194-8511, Japan. [4]Department of Endocrinology and Metabolism, National Research Institute for Child Health and Development, 2-10-1 Okura, Setagaya-ku, Tokyo 157-8535, Japan. [5]School of Health Sciences, Tokai University, Bohseidai, Isehara, Kanagawa 259-1193, Japan. [6]BioResource Center, RIKEN, 3-1-1 Koyadai, Tsukuba, Ibaraki 305-0074, Japan. [7]Present address: Brain Research Institute, Niigata University, 1-757 Asahimachi-dori, Niigata 951-8585, Japan. Correspondence should be addressed to T.K.-I. (tkanekoi@is.icc.u-tokai.ac.jp) or F.I. (fishino.epgn@mri.tmd.ac.jp).

Received 21 May 2007; accepted 16 October 2007; published online 6 January 2008; doi:10.1038/ng.2007.51

LETTERS

of *Rtl1* interfered with normal fetal development, providing direct evidence for the importance of both retrotransposon-derived *Rtl1* and microRNAs in *Rtl1as*.

Histological analyses demonstrated that severe abnormalities occur in the same place in both the Pat-KO and Mat-KO placentas (that is, the fetal capillaries where the feto-maternal interaction occurs), but the consequences of these abnormalities were different (**Fig. 2**). The mouse placenta consists of three major zones: the decidua basalis, the junctional zone and the labyrinth zone. In the Pat-KO placenta at 15.5 d.p.c., we found abnormal, dark-stained regions in the labyrinth zone upon hematoxylin and eosin (HE) staining (**Fig. 2a**, WT; **b**,**c**, Pat-KO). Using truidin blue staining and electron microscopy, we confirmed several morphological abnormalities throughout the labyrinth zone, such as splitting of the basement membrane (**Fig. 2d**,**h**, WT; **e**,**i**, Pat-KO), the emergence of a number of lysosomes in layer III trophoblast cells (**Fig. 2f**,**j**) and clogging in the fetal capillaries (**Fig. 2g**,**k**). When we did immunohistochemical (IHC) staining with CD31, an endothelial cell–specific marker, we observed that its

© 2008 Nature Publishing Group http://www.nature.com/naturegenetics

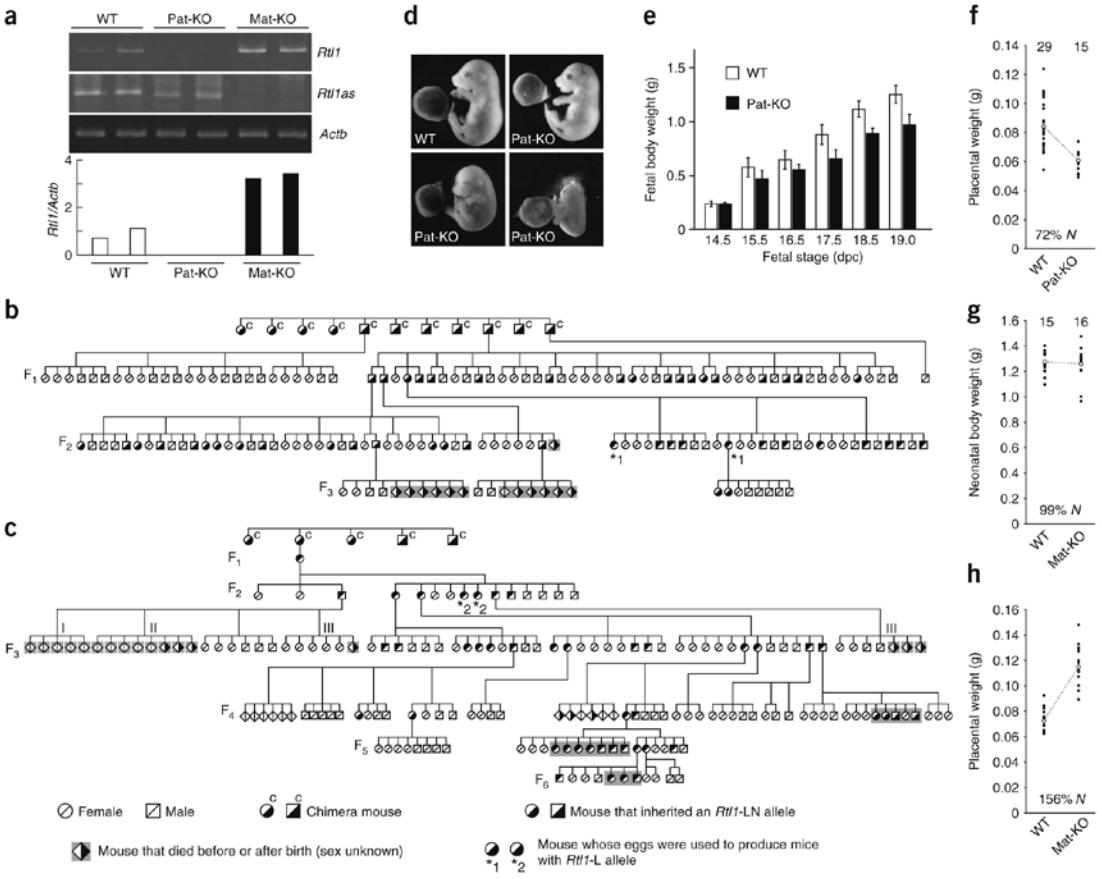

Figure 1 Pedigree of *Rtl1* KO mice. (**a**) Expression of *Rtl1* and *Rtl1as* in WT, Pat-KO and Mat-KO fetuses (*Rtl1*-LN) as determined by RT-PCR. β-actin (encoded by *Actb*) used as a control. The band intensities, measured using ImageJ software are shown below. (**b**) A pedigree from a male chimera. (**c**) A pedigree from a female chimera. A 4-d delay of natural delivery (I) and a caesarean section after a 3-d delay from the expected delivery date (II). All pups were dead in both cases. Caesarean sections were carried out at 19.0 d.p.c. when paternal transmission was analyzed (III). From the F_1 males and females, we obtained many Pat-KO and Mat-KO mice, although the number of Pat-KO mice was slightly smaller than expected from the mendelian ratio (WT/Pat-KO = 24:19, **Supplementary Table 1**) and they grew to adulthood with a reduced body weight (**Supplementary Fig. 2**). Thus, it is clear that the F_1 males and females with the C57BL/6 × 129/Sv F1 (B6/129) genetic background from chimera mice can produce some viable Pat-KO and Mat-KO pups. (**d**) Fetuses at 16.5 d.p.c, including a WT fetus (upper left) and Pat-KO fetuses: small normal-looking (alive) fetus (upper right), pale dead fetus (lower left), and resorbing fetus (lower right). Scale bar, 10 mm. (**e**) Late-fetal growth retardation in Pat-KO fetuses. Open bars, WT fetal body weight; solid bars, Pat-KO fetal body weight. (**f–h**) Growth phenotype of Pat-KO placentas at 18.5 d.p.c. (**f**) and Mat-KO neonates (**g**) and Mat-KO placentas (**h**) at birth (caesarean section). The data in **g** and **h** are from the same litters. Each filled circle represents a single placenta and neonate, respectively. The number at the top represents the total number of weighted samples. Open circles represent average weight. The degree of growth deficiency or promotion of mutant mice is shown as the percentage of WT weight (*N*). Placental and neonatal body weights (mean ± s.d.) are as follows: **f**; WT, 0.085 ± 0.015 ($n = 29$); Pat-KO, 0.061 ± 0.008 ($n = 15$); $P = 1.805 \times 10^{-65}$ (*t*-test), **g**; WT, 1.279 ± 0.087 ($n = 15$); Mat-KO, 1.262 ± 0.126 ($n = 16$), **h**; WT, 0.073 ± 0.009 ($n = 15$); Mat-KO, 0.116 ± 0.016 ($n = 16$); $P = 9.721 \times 10^{-105}$ (*t*-test).

© 2008 Nature Publishing Group http://www.nature.com/naturegenetics

Table 1 Lethality of *Rtl1*-LN (Pat-KO) fetuses and neonates at F_3

Dissection stage (d.p.c.)	WT total	Pat-KO total (dead)	Percentage death in Pat-KO
12.5	5	4 (0)	0
14.5	5	5 (0)	0
15.5	9	7 (1)	14.3
16.5	9	11 (5)	45.5
17.5	10	11 (6)	54.5
18.5	21	24 (13)	54.2
Neonate	35	13 (13)	100

signal diffused to the area of the trophoblast cells (**Fig. 2l**, WT; **m**,**n**, Pat-KO). These results indicate that a phagocytic reaction to the endothelial cells was induced in the surrounding layer III trophoblast cells. Thus, the resulting placental infarction seems to cause placental malfunction, such as incomplete material transport between the maternal and the fetal blood, presumably leading to the late-fetal growth retardation and lethality in the Pat-KO fetuses.

We confirmed functional deficiency of the Pat-KO placenta by nutrition transfer assay[10,11]. We examined both active and passive transport at 15.5 d.p.c. using two radiolabeled substrates, [^{14}C]methylaminoisobutyric acid (Me-AIB) and [^{14}C]inulin, respectively. We did not find any significant difference between WT and Pat-KO placentas in materno-fetal transfer of [^{14}C]Me-AIB, a non-metabolizable amino acid analog, through the System A amino acid transport system ($P = 0.158$; **Fig. 3a**). However, the passive permeability of inulin was significantly lower in Pat-KO placenta (48% compared with WT, $P = 0.000123$; **Fig. 3b**), indicating that Rtl1 deficiency had damaged the placental physical barrier but had not affected the active transport system[12]. In the case of Mat-KO, placentomegaly was associated with expansion of the inner spaces of the fetal capillaries (**Fig. 1h** and **Fig. 2o**, WT; **p**, Mat-KO, and **q**). The most severe abnormalities were found in the surrounding layer III trophoblast cells, which showed a large number of vacuoles, indicating that these cells were starving (**Fig. 2r**, WT; **s**,**t**, Mat-KO).

IHC staining with antibody to Rtl1 showed that Rtl1 protein localized exclusively in the labyrinth zone at 18.5 d.p.c.; no signals in the other layers of the placenta were observed (**Fig. 4a–d**). Co-immunostaining with CD31 showed that Rtl1 localized around the nuclei of the capillary endothelial cells, where anomalies in both Pat-KO and Mat-KO were observed (**Fig. 4e**). We did not observe any signals in the Pat-KO placentas, but we observed strong signals in the

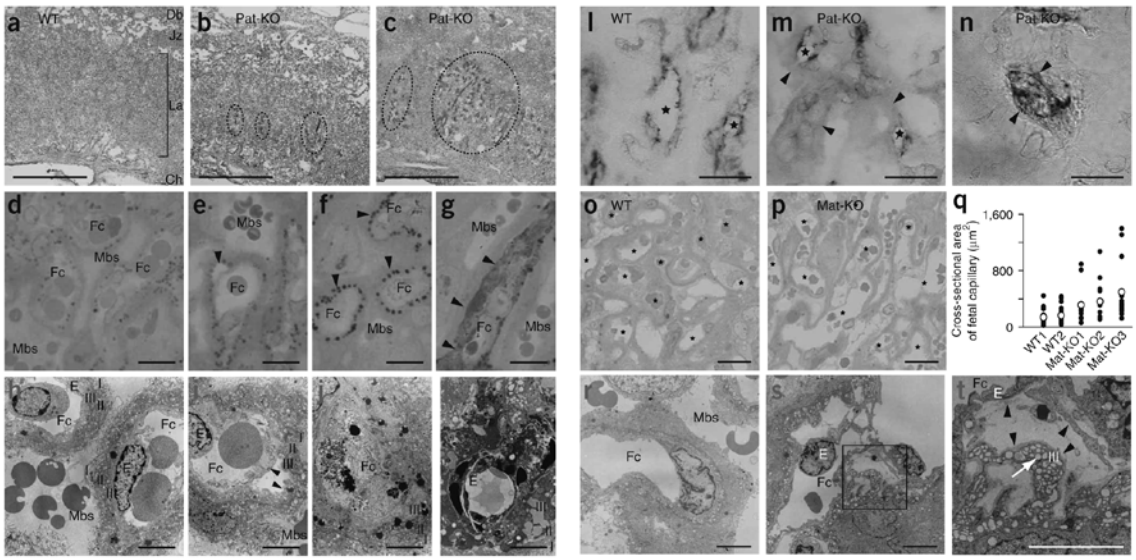

Figure 2 Histological abnormalities observed in day 15.5 Pat-KO placentas and in day 18.5 Mat-KO placentas. Most abnormalities were observed near the endothelial cells and the surrounding layer III trophoblast of the fetal capillaries in the labyrinth zone. (**a**–**n**) The labyrinth zone of WT placentas at 15.5 d.p.c. is shown in **a**, **d**, **h** and **l** and that of Pat-KO placentas at the same stage is shown in **b**, **c**, **e**–**g**, **i**–**k**, **m** and **n**. (**o**–**s**) The labyrinth zone of WT placenta at 18.5 d.p.c. is shown in **o** and **r**, and that of the Mat-KO placenta at the same stage is shown in **p** and **s**. H&E staining in **a**–**c**; scale bar, 0.5 mm. Truidin blue staining in **d**–**g**,**o** and **p**; scale bar, 10 μm for **d**–**g**, 20 μm for **o** and **p**. The arrowheads indicate an abnormal space between the endothelial cell and the layer III trophoblast in **e**, abnormally appearing lysosomes in **f** and a clogged fetal capillary in **g**. Clogging, as seen in **g** and **k**, was found mainly in the dark-stained regions, as shown in the dotted circles in **b** and **c**. Electron microscopy images in **h**–**k**,**r** and **s**; scale bar, 5 μm. The arrowheads indicate an abnormal space between the endothelial cell and the layer III trophoblast in **i**. (**t**) Magnified figure of the square area in **s**; scale bar, 5 μm. The black arrowheads indicate an abnormal space between the endothelial cell and the layer III trophoblast, and the white arrow indicates vacuoles in the layer III trophoblast. IHC staining in **l**–**n** with antibody to CD31; scale bar, 20 μm. The arrowheads indicate an abnormally diffused signal of endothelial cell marker in **m** and a disrupted fetal capillary in **n**. The same result was obtained with an antibody to CD34, another endothelial specific marker (data not shown). **q** shows a cross-sectional area of fetal capillary that was measured using ImageJ. The Pat-KO fetus associated with placenta **c** and **n** was already dead at 15.5 d.p.c. At present, it remains unclear whether the neonatal lethal phenotypes in both Pat-KO and Mat-KO are primarily due to direct or indirect effects of the severe placental anomalies, although both are likely to be involved. Further investigation will be necessary to reveal whether there is a specific cause for neonatal lethality. Db, decidua basalis; Jz, junctional zone; Lz, labyrinth zone; Ch, chorionic plate; Mbs, maternal blood sinus; Fc, fetal capillary; E, endothelial cell; I/II/III, layer I/II/III trophoblast. The asterisks in **l**–**p** indicate fetal capillaries.

© 2008 Nature Publishing Group http://www.nature.com/naturegenetics

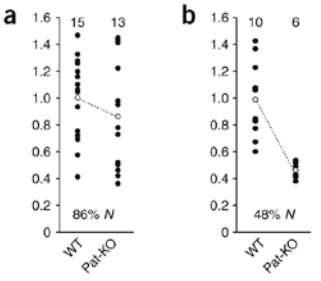

Figure 3 Placental transfer assay. (**a**) Placental transfer of [^{14}C]Me-AIB at 15.5 d.p.c. (**b**) Placental transfer of [^{14}C]inulin at 15.5 d.p.c. Each substrate was injected from the jugular vein of pregnant females at 15.5 d.p.c., and the amount of the labeled substances that entered the fetus through the placenta was determined 3–4 min after injection[10,11]. The fetal accumulation of radioisotope per milligram of placenta was calculated and compared between WT and Pat-KO. The average of WT in every littermate was defined as 1. No significant difference in the active transfer of Me-AIB between WT and Pat-KO placenta was found (86%, $P = 0.158$). However, the passive permeability of inulin in Pat-KO was decreased to about 50% of that in WT (48%, $P = 0.000123$).

Mat-KO placentas, as expected (**Fig. 4f,g**; see also **Supplementary Fig. 4** online). No Rtl1 protein was detected in the endothelial cells of the umbilical cord, although they are connected to the fetal capillaries and are of the same origin as placental endothelial cells (**Fig. 4a,d**). Therefore, we concluded that Rtl1 functions exclusively in the placental endothelial cells for the maintenance of the feto-maternal interface during late-fetal development. To create the novel feto-maternal interface in the course of evolution, the endothelial cells may need a unique protein to regulate the trophoblast cells that have intrinsically invasive and phagocytotic features.

These experiments demonstrate that among several candidate imprinted genes, *Rtl1* is one of the major genes responsible for maternal and paternal duplication of distal chromosome 12 (PatDp (dist12) and MatDp(dist12)) as well as for the corresponding uniparental disomies (MatDi(12) and PatDi(12))[4–6] (**Supplementary Table 1**). The MatDp(dist12) phenotypes of late-fetal and neonatal lethality associated with intrauterine growth retardation are consistent with those of *Rtl1* Pat-KO. *Dlk1* Pat-KO and *Dio3* null mice also showed reduced neonatal size and viability to a certain degree, but this did not account for the severe lethality of MatDp(dist12) and MatDi(12)[13,14]. Therefore, we conclude that the loss of *Rtl1* expression has an important role in such late-fetal viability and that *Dlk1, Rtl1* and possibly *Dio3* can independently contribute to late-fetal growth and neonatal lethality. *Rtl1* Mat-KO mice show notable overgrowth and morphological abnormalities of the placenta consistent with the PatDi(12) mice phenotypes[15]. The Mat-KO mice show only a 2.5- to 3.0-fold increment of *Rtl1* from a single normal paternal allele as a result of the lack of *Rtl1as* from the maternal allele. Therefore, an approximately 4.5-fold overexpression of *Rtl1* from the two paternal alleles that would be expected in PatDi(12) and PatDp(dist12) mice[9] may explain their late-fetal lethality, rather than the neonatal lethality in the Mat-KO.

Rtl1 is one of 11 retrotransposon-derived genes related to the sushi-ichi retrotransposon that are specifically conserved in eutherian mammals[16–20]. Eutherian orthologs of *Rtl1* have a high degree of amino acid conservation and low synonymous-to-nonsynonymous substitution rates (dN/dS), supporting the claim that *Rtl1* has a common and crucially important function in the placenta among eutherians, including human beings[17,21] (**Supplementary Fig. 5** online). This work provides evidence for exaptation, the acquisition

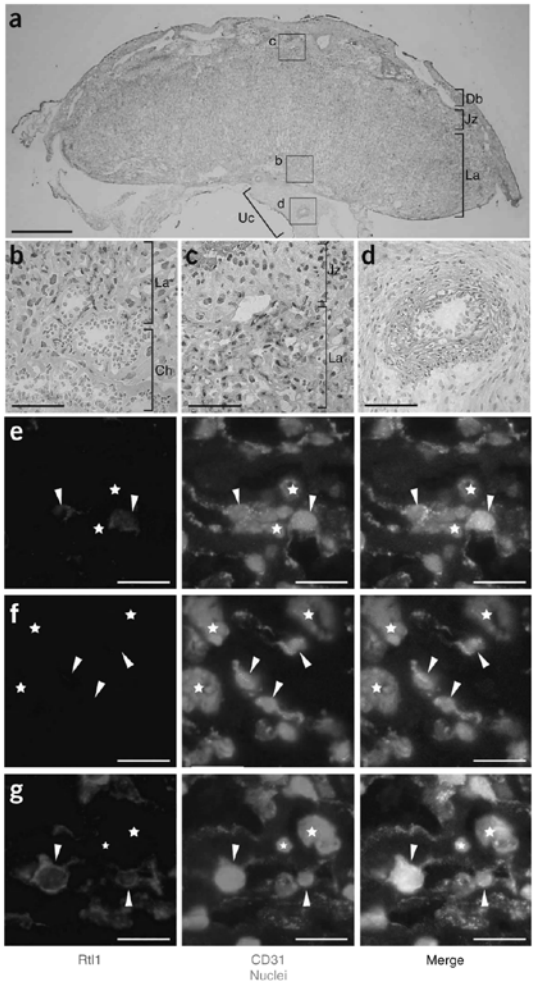

Figure 4 Rtl1 protein localization in the placentas at 18.5 d.p.c. by immunohistochemistry. (**a–c**) Whole placenta image (**a**) and its magnified images (indicated as each small square) of the boundary regions of the placental zones between the labyrinth zone (La) and chorionic plate (Ch) (**b**) and between La and the junctional zone (Jz) (**c**). (**d**) Umbilical cord (Uc) connecting to the fetal capillaries. The signals of Rtl1 (brown by DAB staining) are seen exclusively in La but not in Ch, Jz, decidual basalis (Db) or Uc. Scale bar, 1 mm for **a** and 100 μm for **b–d**. (**e–g**) Co-immunostaining of Rtl1 (red, left), CD31 and nuclei (green and blue, respectively, middle) and their merged image (right). The labyrinth zones of WT (**e**), Pat-KO (**f**) and Mat-KO (**g**) are shown. The arrowheads and stars indicate nuclei of endothelial cells and trophoblast cells, respectively. Scale bar, 20 μm. Only the perinuclear region in the endothelial cells were stained by antibody to Rtl1 in WT (**e**) and Mat-KO (**g**). Note that the inner areas of the endothelial cells were also stained when Rtl1 was overproduced in Mat-KO (**g**; left and right).

© 2008 Nature Publishing Group http://www.nature.com/naturegenetics

of new genomic function from transposons[22–29]. We have recently shown that *Peg10* is also essential for placenta formation[18]. Although both *Rtl1* and *Peg10* are derived from the sushi-ichi–related retrotransposon, they have divergent roles, as expected from their amino acid sequences and as shown by the results of knockout experiments. *Peg10* has a DNA/RNA binding motif and an aspartyl protease motif, and it functions in placenta formation, especially in the trophoblast lineage, at an early embryonic stage. *Rtl1*, however, has only an aspartyl protease motif and functions in the maintenance of the feto-maternal interface at the late-fetal stage[16]. The important implication of these findings is that two independent exaptation events of the sushi-ichi–related retrotransposons have contributed to two different steps of placental development in the mouse.

In this work, we demonstrate that the retrotransposon-derived gene *Rtl1* is a key gene in placental development and evolution and is one of the primary genes responsible for phenotypic development in mouse PatDp(dist12)/MatDp(dist12) as well as PatDi(12)/MatDi(12). Because the remaining nine retrotransposon-derived genes also possess putative proteins, and at least some of them show expression in the placenta[16–20], identification of their origins and functions may provide important insight into placental evolution.

METHODS

Deletion of the *Rtl1* gene. Experimental procedures in this work were approved by the Animal Ethics Committees of Tokyo Medical and Dental University. We obtained 1.8-kb (nucleotides 67,582,103–67,580,338) and 7.3-kb (nucleotides 67,586,373–67,593,715) genomic DNA fragments from a mouse BAC (mRG158M19) clone containing the *Rtl1* ORF (nucleotides 67,581,614–67,586,845) and used them as the right- and left-arm sequences of a construct in which the *Rtl1* ORF was replaced with the neomycin-resistance gene. The nucleotide numbers refer to the sequence with accession number NT_039551.6. After a 2-week incubation under G418 selection, followed by electroporation of the linearized DNA into embryonic stem cells (CCE) of 129/SvEv mouse origin, we obtained 120 colonies. The genomic DNA was checked using DNA blot analysis with DNA fragments of nucleotides 67,580,998–67,581,906 and 67,607,241–67,608,065 as the 5′ and 3′ probes, respectively.

Using the *Rtl1*-targeted embryonic stem cells resulting from the homologous recombination of the construct, we made chimeric mice by blastocyst injection. Germline transmission of the knockout allele was confirmed in one male and one female chimera (*Rtl1*-LN). We carried out *in vitro* fertilization using normal C57BL/6 sperm and eggs from two *Rtl1*-LN females (indicated by the asterisks 1 and 2 in **Figure 1b** and **c**, respectively) and injected the *Cre* recombinase expression vector (pCAGGS-Cre) into the resulting fertilized eggs to produce mice that had *Rtl1*-L alleles.

All of the *Rtl1* KO lines were maintained by continuous crossing with WT B6 males and females to the F_8 generation, unless otherwise indicated.

Expression analyses of imprinted genes. Genomic DNA and total RNA were prepared from day 14.5 fetuses using ISOGEN (Nippon Gene). The methods for the quantitative RT-PCR for *Dlk1*, *Dio3*, *Meg3/Gtl2*, *Meg8/Rian* and 3′-RACE for *Rtl1* and *Rtl1as* followed by cDNA synthesis have been described previously[30]. The band intensity of *Rtl1* was measured using ImageJ software (see URLs section below).

DNA methylation analyses of IG-DMR and *Gtl2*-DMR. Purified genomic DNA was treated with sodium bisulfite solution, and the resulting DNA was amplified by the primers described previously[30]. We used the combined bisulfite restriction analysis (COBRA) method with the restriction enzyme *Aci*I for IG-DMR and *Taq*I for *Gtl2*-DMR.

Placenta functional assay. We examined the efficiencies of nutrition transfer through the placenta at 15.5 d.p.c. in every fetus and placenta of the two to three litters using two radiolabeled substrates, [^{14}C]Me-AIB and [^{14}C]inulin, to measure the active and passive transport, respectively[10,11]. These substrates were dissolved in PBS and injected into the jugular vein of pregnant females. Three to four minutes after injection, the females were dissected and fetuses and placentas were sampled, because it is reported that there is minimal backflux of the radioisotopes from fetus to mother for up to 5 min[11]. The amount of the labeled substance in the fetuses and placentas was determined by a liquid scintillation counter. The counts of fetuses per milligram of placentas were calculated as the placental transfer efficiency, and the average of WT fetuses in each litter was set as 1. We compared WT and Pat-KO. Materno-fetal transfer of Me-AIB, a non-metabolizable amino acid analog usually transported across the placenta, reflects the activity of the System A amino acid transport system, whereas that of inulin reflects the passive permeability that is usually affected by the exchange barrier surface area, thickness and fetal blood flow. Using this assay, we detected only background levels of radioisotopes in the dead fetuses, whereas we found that the levels in their placentas were almost the same as that of WT and living Pat-KO placentas, providing evidence that the maternal blood flow in the placentas was still normal, even in the dead fetuses.

Histological analyses. The placentas for hematoxylin and eosin staining and IHC staining were collected and embedded in OCT compound immediately. Then, 5-μm sections were made. For hematoxylin and eosin staining, we fixed the sections in 4% paraformaldehyde (PFA) before performing the standard staining procedure. The sections were fixed in acetone for the immunostaining of CD31 and CD34, or 4% PFA for the immunostaining of Rtl1. Antibody to CD31 and antibody to CD34 (BD Pharmingen) were each used as the primary antibody, and then horseradish peroxidase (HRP)-labeled anti-rat IgG (Jackson ImmunoResearch Laboratories) was added as the secondary antibody. The antibody to Rtl1 that was produced from rabbit serum by immunizing with the synthetic Rtl1 peptide (NH_2-CGDQEAVTFRPRN-COOH) was used as the primary antibody, and then HRP-labeled anti-rabbit IgG (GE Healthcare Bio-Sciences) was added as the secondary antibody. HRP activities were visualized by diaminobenzidine (DAB) staining, and the nuclei were stained using 2% methyl green. For co-immunostaining of Rtl1 and CD31, the sections were fixed in 4% PFA. The primary antibody mixture including the antibody to CD31 and the antibody to Rtl1, and the secondary antibody mixture including the Alexa 488-conjugated anti-rat IgG (Invitrogen), Cy3-conjugated anti-rabbit IgG (Jackson ImmunoResearch Laboratories) and Hoechst 33342, were used. Images were captured and overlaid by a VB-7000 Digital Camera System (Keyence). For truidin blue staining and transmission electron microscopy, we fixed the placentas in 2.5% glutaraldehyde in 0.05 M PBS and 1% osmium tetroxide before following the standard staining methodology.

URLs. ImageJ software, http://rsb.info.nih.gov/ij/.

GenBank accession codes. The nucleotide numbers refer to the sequence of mouse chromosome 12 with accession number NT_039551.6.

Note: Supplementary information is available on the Nature Genetics website.

ACKNOWLEDGMENTS

We thank S. Aizawa of Center for Developmental Biology, RIKEN for providing the DT-A vector that was used for making *Rtl1* KO construct, E. Robertson of University of Oxford for the CCE ES cells, M. Constancia of University of Cambridge for placenta functional assay protocol, Y. Nakahara and M. Takabe of the Mitsubishi Kagaku Institute of Life Sciences for animal breeding and H. Hasegawa, N. Kawabe and A. Akatsuka of the Tokai University and S. Ichinose of the Tokyo Medical and Dental University for their assistance in immunohistochemistry and electron microscopy along with helpful discussion. This work was supported by grants from Creative Science Research, the research program of Japan Society for the Promotion of Science (JSPS), the Uehara Memorial Science Foundation, the Mitsubishi Foundation and the Ministry of Health, Labour and Welfare for Child Health and Development (17C-2) and a Grant-in-Aid for Scientific Research on Priority Areas form the Ministry of Education, Culture, Sports, Science and Technology of Japan (1508023) to F.I., the grant for young investigators from Medical Research Institute to Y.S., and the Asahi Glass Foundation and JSPS, Grants-in Aid for Scientific Research to T.K.-I. Pacific Edit reviewed the manuscript before submission.

AUTHOR CONTRIBUTIONS

Most analyses in this work were performed by Y.S. with collaboration of H.W., R.O., N.W., T.K. and M.K. in molecular and histological experiments.

LETTERS

Construction of *Rtl1* targeting vector was done by H.W. under supervision of K.N. and M.Y., and KO mice were produced by T.H., R.S.-M., K.N. and M.Y. The study was designed and coordinated by T.K.-I. and F.I., and the results were discussed by A.O., T.O., T.K.-I. and F.I. The paper was written by Y.S. and F.I.

Published online at http://www.nature.com/naturegenetics
Reprints and permissions information is available online at http://npg.nature.com/reprintsandpermissions

1. Rossant, J. & Cross, J.C. Placental development: lessons from mouse mutants. *Nat. Rev. Genet.* **2**, 538–548 (2001).
2. Watson, E.D. & Cross, J.C. Development of structures and transport functions in the mouse placenta. *Physiology (Bethesda)* **20**, 180–193 (2005).
3. Seitz, H. *et al.* Imprinted microRNA genes transcribed antisense to a reciprocally imprinted retrotransposon-like gene. *Nat. Genet.* **34**, 261–262 (2003).
4. Cattanach, B.M. & Rasverry, C.V. Evidence of imprinting involving the distal region of Chr 12. *Mouse Genome* **91**, 858 (1993).
5. Georgiades, P., Watkins, M., Surani, M.A. & Ferguson-Smith, A.C. Parental origin-specific developmental defects in mice with uniparental disomy for chromosome 12. *Development* **127**, 4719–4728 (2000).
6. Tevendale, M., Watkins, M., Rasberry, C., Cattanach, B. & Ferguson-Smith, A.C. Analysis of mouse conceptuses with uniparental duplication/deficiency for distal chromosome 12: comparison with chromosome 12 uniparental disomy and implications for genomic imprinting. *Cytogenet. Genome Res.* **113**, 215–222 (2006).
7. Davis, E. *et al.* RNAi-mediated allelic trans-interaction at the imprinted *Rtl1/Peg11* locus. *Curr. Biol.* **15**, 743–749 (2005).
8. Takada, S. *et al.* Epigenetic analysis of the *Dlk1-Gtl2* imprinted domain on mouse chromosome 12: implications for imprinting control from comparison with *Igf2-H19*. *Hum. Mol. Genet.* **11**, 77–86 (2002).
9. Lin, S.P. *et al.* Asymmetric regulation of imprinting on the maternal and paternal chromosomes at the *Dlk1-Gtl2* imprinted cluster on mouse chromosome 12. *Nat. Genet.* **35**, 97–102 (2003).
10. Constância, M. *et al.* Placental-specific IGF-II is a major modulator of placental and fetal growth. *Nature* **417**, 945–948 (2002).
11. Sibley, C.P. *et al.* Placental-specific insulin-like growth factor 2 (*Igf2*) regulates the diffusional exchange characteristics of the mouse placenta. *Proc. Natl. Acad. Sci. USA* **101**, 8204–8208 (2004).
12. Angiolini, E. *et al.* Regulation of placental efficiency for nutrient transport by imprinted genes. *Placenta* **27** (Suppl. A), S98–S102 (2006).
13. Moon, Y.S. *et al.* Mice lacking paternally expressed Pref-1/Dlk1 display growth retardation and accelerated adiposity. *Mol. Cell. Biol.* **22**, 5585–5592 (2002).
14. Hernandez, A., Martinez, M.E., Fiering, S., Galton, V.A. & St Germain, D. Type 3 deiodinase is critical for the maturation and function of the thyroid axis. *J. Clin. Invest.* **116**, 476–484 (2006).
15. Georgiades, P., Watkins, M., Burton, G.J. & Ferguson-Smith, A.C. Roles for genomic imprinting and the zygotic genome in placental development. *Proc. Natl. Acad. Sci. USA* **98**, 4522–4527 (2001).
16. Butler, M., Goodwin, T., Simpson, M., Singh, M. & Poulter, R. Vertebrate LTR retrotransposons of the Tf1/sushi group. *J. Mol. Evol.* **52**, 260–274 (2001).
17. Lynch, C. & Tristem, M. A co-opted gypsy-type LTR-retrotransposon is conserved in the genomes of humans, sheep, mice, and rats. *Curr. Biol.* **13**, 1518–1523 (2003).
18. Ono, R. *et al.* Deletion of *Peg10*, an imprinted gene acquired from a retrotransposon, causes early embryonic lethality. *Nat. Genet.* **38**, 101–106 (2006).
19. Brandt, J. *et al.* Transposable elements as a source of genetic innovation: expression and evolution of a family of retrotransposon-derived neogenes in mammals. *Gene* **345**, 101–111 (2005).
20. Youngson, N.A., Kocialkowski, S., Peel, N. & Ferguson-Smith, A.C. A small family of sushi-class retrotransposon-derived genes in mammals and their relation to genomic imprinting. *J. Mol. Evol.* **61**, 481–490 (2005).
21. Kagami, M. *et al.* Deletions and epimutations affecting the human 14q32.2 imprinted region in individuals with paternal and maternal upd(14)-like phenotypes. *Nat. Genet.* advance online publication, doi:10.1038/ng.2007.56 (6 January 2008).
22. Gould, S. & Vrba, S. Exaptation—a missing term in the science of form. *Paleobiology* **8**, 4–15 (1982).
23. Brosius, J. & Gould, S.J. On "genomenclature": a comprehensive (and respectful) taxonomy for pseudogenes and other "junk DNA". *Proc. Natl. Acad. Sci. USA* **89**, 10706–10710 (1992).
24. Smit, A.F. Interspersed repeats and other mementos of transposable elements in mammalian genomes. *Curr. Opin. Genet. Dev.* **9**, 657–663 (1999).
25. Mi, S. *et al.* Syncytin is a captive retroviral envelope protein involved in human placental morphogenesis. *Nature* **403**, 785–789 (2000).
26. Kazazian, H.H., Jr. Mobile elements: drivers of genome evolution. *Science* **303**, 1626–1632 (2004).
27. Dupressoir, A. *et al.* Syncytin-A and syncytin-B, two fusogenic placenta-specific murine envelope genes of retroviral origin conserved in Muridae. *Proc. Natl. Acad. Sci. USA* **102**, 725–730 (2005).
28. Bejerano, G. *et al.* A distal enhancer and an ultraconserved exon are derived from a novel retroposon. *Nature* **441**, 87–90 (2006).
29. Biémont, C. & Vieira, C. Genetics: junk DNA as an evolutionary force. *Nature* **443**, 521–524 (2006).
30. Sekita, Y. *et al.* Aberrant regulation of imprinted gene expression in *Gtl2*^{lacZ} mice. *Cytogenet. Genome Res.* **113**, 223–229 (2006).

© 2008 Nature Publishing Group http://www.nature.com/naturegenetics

2008年1月7日
朝日新聞　朝刊

フグから発見DNA
「スシイチ」胎児成長に大事

フグで見つかり、すしにちなみ「スシイチ」と名付けられたDNA断片が、進化の過程で変化し、哺乳類では胎児が育つ際に重要な役割を担う遺伝子として定着していることを東京医科歯科大や東海大などのグループが突き止めた。

東京医歯大などが解明

6日付の米専門誌ネイチャージェネティクス電子版に発表する。

グループは、この遺伝子を働かなくしたマウスでは、胎児と母親を結ぶ胎盤の毛細血管が異常になり、誕生前後に死ぬことを見つけた。

また、人の胎児でこの遺伝子が過剰に働くと胸郭の発達が異常になるなどの症状が出ることも、国立成育医療センター研究所との共同研究で明らかにした。原因不明とされた成長障害の診断につながる可能性があるという。

2008年1月13日　毎日新聞　日曜版

胎児毛細血管維持に必要な遺伝子発見
哺乳類の進化解明に貢献

母体から胎児に栄養や酸素を供給している胎盤の「胎児毛細血管」の維持に必須の遺伝子を、東京医科歯科大と東海大などの研究チームがマウスで発見した。哺乳類のみに存在する外部から癒得された遺伝子で、研究チームは「哺乳類の進化解明に貢献する成果」としている。

石野史敏・東京医科歯科大教授（分子生物学）らは、マウスの12番染色体で遺伝子の働く仕組みに異常が起きると、胎児の成長不良や死につながることを発見。この原因遺伝子も見つけた。

さらに、この遺伝子をなくすなどしたマウスを作成したところ、半数が胎児後期で、残りは生後1日以内に死んだ。いずれも、胎児毛細血管がつぶれるなどの異常で、胎児への栄養補給が低下していた。

この遺伝子は、進化の途中で外部からウイルスのように感染して入り込んだ「レトロトランスポゾン」に由来する。同研究チームは06年にも、レトロトランスポゾン由来の別の遺伝子が、胎盤形成の初期段階に不可欠であることを発見している。哺乳類が胎盤という新しい臓器を獲得する際に、複数のレトロトランスポゾンが重要な役割を果たしたとみられる。

一方、この遺伝子は、ヒトでは14番染色体に存在する。ここに異常が起きると、妊娠中の羊水過多や新生児の胸骨形態異常による呼吸困難などが生じる。石野教授と国立成育医療センター研究所の緒方勤部長らの研究チームは、患者や家族のゲノム解析により、ヒトでもこの遺伝子が症状を起こす主要原因遺伝子であることを突き止めた。

これらの成果は関連論文として、米科学誌「ネイチャー・ジェネティクス」電子版で6日、発表した。【倉田桃子】

2008年1月7日
読売新聞　朝刊

胎盤働かす遺伝子 発見
哺乳類の進化解明へ一歩

母体と胎児との間で栄養などのやり取りを行う胎盤がうまく働くために重要な遺伝子を、東京医科歯科大や国立成育医療センター研究所のチームが発見した。この遺伝子は、細胞に感染するウイルスのように外来の遺伝子が起源であることがわかっており、哺乳類の進化の過程を明らかにする一歩になるという。研究成果は6日付の科学誌ネイチャー・ジェネティクス電子版に掲載される。

研究チームが発見した遺伝子はPegl1/Rtl1。マウスの実験で、この遺伝子を失わせると、胎児が母体から栄養や酸素を得る胎盤の毛細血管の形が異常になり、胎児は出産前後に死んでしまったという。また、この遺伝子の働きが弱くなったり弱くなったりしている人では、胎児期や生後に発育障害などを起こしていることも確認した。

2008年1月7日　東奥日報　朝刊　（共同通信配信）

胎盤遺伝子はウイルス由来
東京医科歯科大 東海大チーム発見
哺乳類の進化解明へ

哺乳（ほにゅう）類の特徴である胎盤の働きに欠かせない遺伝子が、哺乳類の祖先が感染したウイルスに由来する可能性が高いことを、東京医科歯科大や東海大などのチームが発見し、六日、米科学誌ネイチャージェネティクス電子版に発表した。卵で生まれていた原始的な哺乳類が、胎盤を獲得して体内で子を育てる「胎生」に進化した過程の解明に役立つという。

胎盤では毛細血管を通じて母体と子どもの間で栄養や酸素をやりとりする。研究チームは、マウスや人間にある「Pegl1」という遺伝子が、感染したウイルスからDNAに組み込まれた特徴を残していることに着目。

マウスでPegl1をなくしたり過剰に働かせたりしたところ、胎盤の毛細血管の構造が異常になり、栄養などの交換機能が低下。胎児が成長不良で生まれないか、生後すぐに死に、この結果から、Pegl1が胎盤の毛細血管の形成に欠かせないことが明らかになった。

2008年1月7日　京都新聞　朝刊　（共同通信配信）

胎盤遺伝子はウイルス由来
東海大など発見

哺乳（ほにゅう）類の特徴である胎盤の働きに欠かせない遺伝子が、哺乳類の祖先が感染したウイルスに由来する可能性が高いことを、東京医科歯科大や東海大などのチームが発見し、六日、米科学誌ネイチャージェネティクス電子版に発表した。

卵で生まれていた原始的な哺乳類が、胎盤を獲得して体内で子を育てる「胎生」に進化した過程の解明に役立つという。

胎盤では毛細血管を通じて母体と子どもの間で栄養や酸素をやりとりする。研究チームは、マウスや人間にある「Pegl1」という遺伝子が、感染したウイルスからDNAに組み込まれた特徴を残していることに着目。

マウスでPegl1をなくしたり過剰に働かせたりしたところ、胎盤の毛細血管の構造が異常になり、栄養などの交換機能が低下。胎児が成長不良で生まれないか、生後すぐに死に、「この結果から、Pegl1が胎盤の毛細血管の形成に欠かせないことが明らかになった。チームはこれまでに胎盤そのものの形成に必須の「Pegl10」という別のウイルス由来の遺伝子があることも突き止めている。

東海大など発見

哺乳類進化 解明の鍵に

胎盤遺伝子はウイルス由来

哺乳類の特徴である胎盤の働きに欠かせない遺伝子が、哺乳類の祖先が感染したウイルスに由来する可能性が高いことを、東京医科歯科大や東海大などのチームが発見し、六日、米科学誌ネイチャージェネティクス電子版に発表した。

卵で生まれていた原始的な哺乳類が、胎盤を獲得して体内で子を育てる「胎生」に進化した過程の解明に役立つという。

胎盤では毛細血管を通じて母体と子どもの間で栄養や酸素をやりとりする。研究チームは、マウスや人間にある「Peg11」という遺伝子が、感染したウイルスからDNAに組み込まれた特徴を残していることに着目。

マウスでPeg11をなくしたり過剰に働かせたりしたところ、胎盤の毛細血管の構造が異常になり、栄養などの交換機能が低下。胎児が成長不良で生まれないか、生後すぐに死に、この結果から、Peg11が胎盤の毛細血管の形成に欠かせないことが明らかになった。

チームはこれまでに、胎盤そのものの形成に必須の「Peg10」という別のウイルス由来の遺伝子があることも突き止めている。

チームの石野史敏東京医科歯科大教授は「胎盤を作るだけでなく、毛細血管という重要な機能でも外来遺伝子を活用したことが明らかになった」と話している。

2008年1月7日　西日本新聞　朝刊　（共同通信配信）

胎盤遺伝子

ウイルスに由来か

哺乳類の進化過程解明へ

哺乳（ほにゅう）類の特徴である胎盤の働きに欠かせない遺伝子が、哺乳類の祖先が感染したウイルスに由来する可能性が高いことを、東京医科歯科大や東海大などのチームが発見し、六日、米科学誌ネイチャージェネティクス電子版に発表した。

卵で生まれていた原始的な哺乳類が、胎盤を獲得して体内で子を育てる「胎生」に進化した過程の解明に役立つという。

胎盤では毛細血管を通じて母体と子どもの間で栄養や酸素をやりとりする。研究チームは、マウスや人間にある「Peg11」という遺伝子が、感染したウイルスからDNAに組み込まれた特徴を残していることに着目。

マウスでPeg11をなくしたり過剰に働かせたりしたところ、胎盤の毛細血管の構造が異常になり、栄養などの交換機能が低下。胎児が成長不良で生まれないか、生後すぐに死に、この結果から、Peg11が胎盤の毛細血管の形成に欠かせないことが明らかになった。

チームはこれまでに、胎盤そのものの形成に必須の「Peg10」という別のウイルス由来の遺伝子があることも突き止めている。

ゆかりの地に 篤姫館が開館

鹿児島

江戸時代、鹿児島から徳川将軍家に嫁いだ女性を描く今年のNHK大河ドラマにちなんだ「篤姫（あつひめ）館」が、放送開始と同じ六日、鹿児島市本港新町の商業施設の一角にオープンした。初日のセレモニーには関係者や観覧者ら約五十人が集まり、篤姫役の女優宮崎あおいさん（22）が「ドラマをみなさんお願

2008年1月7日　山形新聞　朝刊　（共同通信配信）

胎盤の重要遺伝子発見

東京医科歯科大など 進化解明のカギに

哺乳類の特徴である胎盤の働きに欠かせない遺伝子が、哺乳類の祖先が感染したウイルスに由来する可能性が高いことを、東京医科歯科大や東海大などのチームが発見し、六日、米科学誌ネイチャージェネティクス電子版に発表した。卵で生まれていた原始的な哺乳類が、胎盤を獲得して体内で子を育てる「胎生」に進化した過程の解明に役立つという。

胎盤では毛細血管を通じて母体と子どもの間で栄養や酸素をやりとりする。研究チームは、マウスや人間にある「Peg11」という遺伝子が、感染したウイルスからDNAに組み込まれた特徴を残していることに着目。

マウスでPeg11をなくしたり過剰に働かせたりしたところ、胎盤の毛細血管の構造が異常になり、栄養などの交換機能が低下。胎児が成長不良で生まれないか、生後すぐに死に、この結果から、Peg11が胎盤の毛細血管の形成に欠かせないことが明らかになった。

チームはこれまでに、胎盤そのものの形成に必須の「Peg10」という別のウイルス由来の遺伝子があることも突き止めている。

チームの石野史敏東京医科歯科大教授は「胎盤を作るだけでなく、毛細血管という重要な機能でも外来遺伝子を活用したことが明らかになった」と話している。

◆羽田―香港に定期便

全日本空輸が4月に羽田―香港の国際定期チャーター便を就航させると

2008年1月7日
神戸新聞　朝刊
（共同通信配信）

胎盤遺伝子はウイルス由来

東京医科歯科大 東海大のチーム 哺乳類の進化解明へ

哺乳（ほにゅう）類の特徴である胎盤の働きに欠かせない遺伝子が、哺乳類の祖先が感染したウイルスに由来する可能性が高いことを、東京医科歯科大や東海大などのチームが発見し、六日、米科学誌ネイチャージェネティクス電子版に発表した。

卵で生まれていた原始的な哺乳類が、胎盤を獲得して体内で子を育てる「胎生」に進化した過程の解明に役立つという。

胎盤では毛細血管を通じて母体と子どもの間で栄養や酸素をやりとりする。研究チームは、マウスや人間にある「Peg11」という遺伝子が、感染したウイルスからDNAに組み込まれた特徴を残していることに着目。

マウスでPeg11をなくしたり過剰に働かせたりしたところ、胎盤の毛細血管の構造が異常になり、栄養などの交換機能が低下。胎児が成長不良で生まれないか、生後すぐに死に、この結果から、Peg11が胎盤の毛細血管の形成に欠かせないことが明らかになった。

チームはこれまでに、胎盤そのものの形成に必須の「Peg10」という別のウイルス由来の遺伝子があることも突き止めている。

チームの石野史敏東京医科歯科大教授は「胎盤を作るだけでなく、毛細血管という重要な機能でも外来遺伝子を活用したことが明らかになった」と話している。

2008年1月7日　茨城新聞　朝刊　（共同通信配信）

管子 血伝 細遺 毛の 盤成 胎形

感染ウイルスに由来

「胎生」への進化解明期待

哺乳（ほにゅう）類の特徴である胎盤の働きに欠かせない遺伝子が、哺乳類の祖先が感染したウイルスに由来する可能性が高いことを、東京医科歯科大や東海大などのチームが発見し、六日、米科学誌ネイチャージェネティクス電子版に発表した。

卵で生まれていた原始的な哺乳類が、胎盤を獲得して体内で子を育てる「胎生」に進化した過程の解明に役立つという。

胎盤では毛細血管を通じて母体と子どもの間で栄養や酸素をやりとりする。研究チームは、マウスや人間にある「Peg11」という遺伝子が、感染したウイルスからDNAに組み込まれた特徴を

残していることに着目。

マウスでPeg11をなくしたり過剰に働かせたりしたところ、胎盤の毛細血管の構造が異常になり、栄養などの交換機能が低下。胎児が成長不良で生まれないか、生後すぐに死に、この結果から、

芥川賞 直木賞 中国人作家ら

第百三十八回芥川、直木賞（日本文学振興会主

逸さん（四三）が日本語で書いた作品が芥川賞候補に

2008年1月7日　河北新報　朝刊　（共同通信配信）

分子細胞生物学分野

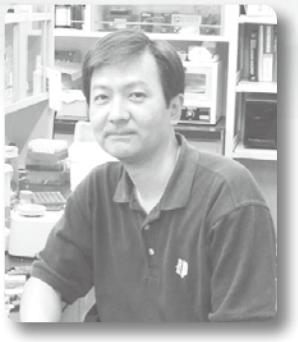

澁谷 浩司

医歯学総合研究科・器官システム制御学系専攻
細胞機能調節学・教授

1. 研究の課題名

偽性低アルドステロン症Ⅱ型原因遺伝子WNKの機能解析

セリン/スレオニンキナーゼWNK（with no lysine（K））ファミリーは、線虫・ショウジョウバエから哺乳類にいたるまで保存されており、哺乳類には四つのWNKファミリー分子が存在する。そのうちWNK1及びWNK4は偽性低アルドステロン症Ⅱ型（PHA Ⅱ）と呼ばれる常染色体優性遺伝性の高血圧症の原因遺伝子として同定されている。このファミリー分子の機能を明らかにするために、酵母two-hybridスクリーニング法あるいはエピトープタグと質量分析を用いた方法により、複数のWNK1結合タンパク質を同定した。その中の一つであるプロテインキナーゼSPAK/OSR1は、WNKファミリー分子により直接リン酸化され、SPAK/OSR1はさらに腎臓遠位尿細管に存在するNa+-Cl-共輸送体（NCC）や腎臓ヘンレループに存在するNKCC2のN末端側細胞内領域をin vitroで直接リン酸化することを明らかにした。さらに遺伝子改変マウスを用いた実験により、腎臓におけるWNK→SPAK/OSR1→共輸送体の制御異常が病気の発症の一因であることを示した。また、WNK1を欠損したマウス・線虫・ショウジョウバエは発生過程で致死になることを見出し、WNKファミリー分子が腎臓での機能のみならず種を超えて発生・器官形成に重要な役割をはたしていることを明らかにした。

2.

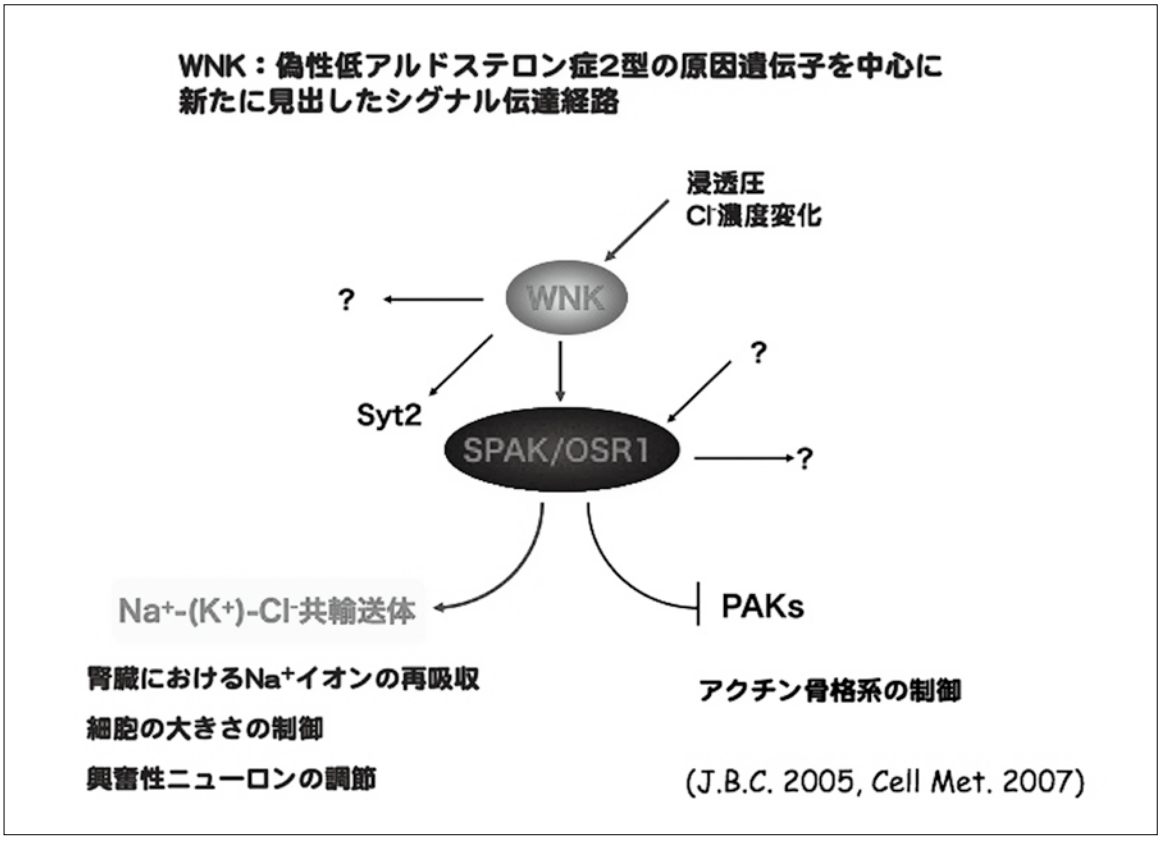

3. 本事業に関連して世界的な研究拠点形成に向けて、以下の点で改善・整備等されたこと
C（人材確保）

PIシャペロン教員を採用した。

4. GCOE事業を推進するに当たって力を入れた点
PIシャペロン教員の採用

5. 自己評価
様々な理由から昨年来、論文を出せなかったことは評価に値しない。この事実は甚だ遺憾ではあるが、現在、投稿中の論文も含め、進行中の研究内容は優れたものであると自負しており、今後巻き返していきたい。

6. 学会発表（英文）
Mi-sun Kim, Shigeaki Kato, Hiroshi Shibuya「DNA demethylation for hormone-induced transcriptional derepression」The 21th NAITO CONFERENCE, Nuclear Dynamics and RNA[I], Japan, June, 2008

Shigeaki Kato, Mi-sun Kim, Hiroshi Shibuya「Hormonal control of DNA demethylation for gene activation」Advanced Bone and Joint Science（ABJS）Symposium-Workshop "Molecular Regulation of Bone and Cartilage", December, 2008

7. 学会発表（和文）
澁谷浩司 「NLKと結合因子による頭部形成制御」 文部科学省科学研究費助成金「特定領域研究」2領域合同公開シンポジウム、2008年1月8日、東京。

小川　靖、吉田　実代、大西　英理子、平松　俊行、小野木　博、澁谷　浩司、細谷　孝充、萩原正敏　ダウン症治療薬の創成　第119回日本薬理学会関東部会、2008年10月4日、東京。

澁谷浩司　p38-NLKによる頭部形成制御　第1回XCIJ首都圏支部会（XCIJ-MA）研究集会　2008年10月18日、東京。

佐藤　淳、Andrew Tomlinson、澁谷　浩司　CRDタンパク質Corinの機能解析　第31回日本分子生物学会年会・第81回日本生化学会大会　合同大会、2008年12月9日、神戸。

金 美善, 近藤剛史, 延みんよん, 高田伊知郎,　武山 健一, 大竹史明, 澁谷浩司, 加藤 茂明　DNA脱メチル化はビタミンD一位水酸化酵素遺伝子の活性型ビタミンD依存的な転写抑制解除を制御する　第31回日本分子生物学会年会・第81回日本生化学会大会　合同大会、2008年12月10日、神戸。

Strahil Ivanov Pastuhov、花房洋、家村俊一郎、夏目徹、澁谷浩司、稲垣昌樹、松本邦弘　パーキンソン病原因因子LRRK2によるvimentin cage形成　第31回日本分子生物学会年会・第81回日本生化学会大会　合同大会、2008年12月10日、神戸。

伊東進、渡邊幸秀、大西英理子、佐藤清敏、澁谷浩司、加藤光保　TMEPAIによるTGF-β/アクチビンシグナル抑制機構　第31回日本分子生物学会年会・第81回日本生化学会大会　合同大会、2008年12月11日、神戸。

福島沖之、ストラヒルパストゥホフ、花房洋、家村俊一郎、夏目徹、澁谷浩司、松本邦弘、久本直毅　線虫C.elegansをモデル系としたBAG-2-Hsc70-CHIP複合体によるROCOファミリーキナーゼLRRKの制御機構　第31回日本分子生物学会年会・第81回日本生化学会大会　合同大会、2008年12月11日、神戸。

花房洋、石川光紀、澁谷浩司、駒田雅之、松本邦弘　LRRK1はESCRT-0複合体と相互作用することでEGFR細胞内トラフィックを制御している　第31回日本分子生物学会年会・第81回日本生化学会大会　合同大会、2008年12月12日、神戸。

大西淳之、大西英理子、家村俊一郎、丸山剛、西頭英起、石谷太、夏目徹、澁谷浩司　p38 MAPK-NLK経路によるXenopus前頭部形成の制御機構　第31回日本分子生物学会年会・第81回日本生化学会大会　合同大会、2008年12月12日、神戸。

慶田城迅、花房洋、家村俊一郎、夏目徹、澁谷浩司、松本邦弘　Dynein モータータンパク質結合因子 Nud C は EGFR の細胞内トラフィックを制御している　第31回日本分子生物学会年会・第81回日本生化学会大会　合同大会、2008年12月12日、神戸。

石川光紀、花房洋、澁谷浩司、松本邦弘　LRRK1キナーゼ活性依存的なEGFRの細胞内トラフィッキング制御　第31回日本分子生物学会年会・第81回日本生化学会大会　合同大会、2008年12月12日、神戸。

小川　靖、吉田　実代、大西　英理子、平松　俊行、小野木　博、澁谷　浩司、細谷　孝充、萩原正敏　リン酸化阻害剤によるダウン症治療薬開発アプローチ　第82回日本薬理学会年会、 2009年3月16-18日、横浜。

8. 外部資金の獲得状況

（科学研究費補助金、受託研究費、外部財団の助成など）

科学研究費補助金、特定領域研究

「発生分化を制御するDECODE回路の解明」

代表:澁谷浩司

期間:平成17-21年度

研究費総額:9000万円

9. 講座の准教授、講師、助教、特別研究員、ポスドク、指導を受けた大学院生の名前（AISSには○印）のリスト

助　　教　　金　美善

PIシャペロン教員　　後藤利保

MEMO

分子代謝学分野

小川 佳宏

医歯学総合研究科・器官システム制御学系専攻
内分泌学・教授

1. 研究の課題名

1）多価不飽和脂肪酸（n-3 PUFA）による単球の血管内皮接着抑制作用の分子機構に関する研究

In vivo and in vitro inhibition of monocyte adhesion to endothelial cells and endothelial adhesion molecules by eicosapentaenoic acid.

2）肥満の脂肪組織に対するマクロファージ浸潤における骨髄細胞CCR2の機能的意義に関する研究

Role of C-C chemokine receptor 2 in bone marrow cells in the recruitment of macrophages into obese adipose tissue

1）飽和遊離脂肪酸は、自然免疫反応に関与するTLR4を介して炎症性変化をもたらすが、肥満者ではしばしば飽和遊離脂肪酸濃度が上昇しており、飽和遊離脂肪酸による炎症性変化が動脈硬化病変形成に関与する可能性がある。一方、代表的なn-3多価不飽和脂肪酸（n-3 PUFA）であるEPAが炎症性変化に対して拮抗することが知られている。本研究では、動脈硬化の初期病変と考えられる単球の血管壁の接着現象に着目し、個体レベルと細胞レベルにおいて単球の血管内皮細胞接着におけるEPAの抑制作用を検討した。NEMOes法と共焦点顕微鏡により、EPA投与マウスでは非投与群と比較して、LPSにより誘導される単球の血管内皮接着、血管内皮細胞における接着分子の発現とNF-κB p65の核内移行が有意に抑制されることが明らかになった。フローアッセイ法により、EPA処理したHUVECでは非処理群と比較して、単球接着と接着分子の発現、NF-κBp65のリン酸化が有意に抑制されることが明らかになった。EPA投与群では非投与群と比較してメタボリックシンドローム患者においてsICAM-1とsVCAM-1の血中濃度は有意に抑制された。多変量解析では、sICAM-1とsVCAM-1の変化は血中EPA濃度の変化と有意に相関したが、他の代謝パラメータの変化と明らかな相関関係はなかった。以上より、臨床的に証明されているn-3 PUFAの抗動脈硬化作用の少なくとも一部は血管内皮における単球接着抑制作用によることが示唆された（Arterioscler. Thromb. Vasc. Biol. 28: 2173-2179, 2008）。

2）肥満の脂肪組織に対するマクロファージ浸潤にはMCP-1/CCR2系が重要であると考えられているが、単球遊走の分子機構には不明な点が多い。本研究では、細胞遊走を遊走速度と方向性に分けて解析することが可能なリアルタイム細胞動体測定装置TAXIScanを用いて、脂肪組織由来液性因子に対する細胞遊走能を検討した。マウス骨髄単核球細胞は、脂肪組織の培養上清に対して著しい走化性を示したが、CCR2拮抗剤プロパゲルマニウムの添加により抑制された。CCR2を強制発現させたヒトTリンパ球系Jurkat細胞も同様に脂肪組織培養上清に対して強い走化性を示したが、プロパゲルマニウムの添加により抑制された。このとき、プロパゲルマニウムは、細胞遊走速度には影響を及ぼさず、方向性のみを阻害した。高脂肪食を負荷したKKA^{y}マウスあるいはob/obマウスにプロパゲルマニウムを経口投与したところ、いずれのマウスにおいても非投与群と比較して脂肪組織へのマクロファージ浸潤が有意に抑制された。骨髄移植法により作製した骨髄細胞特異的CCR2欠損ob/obマウスは、対照ob/obマウスと比較して脂肪組織へのマクロファージ浸潤が有意に抑制された。本研究により、骨髄細胞のCCR2が、脂肪組織由来液性因子に対する細胞遊走の方向決定において重要であることが明らかになり、肥満の脂肪組

織に対するマクロファージ浸潤において骨髄細胞のCCR2を介した細胞遊走の質的変化が関与する可能性が示唆された。細胞遊走の質的な評価により、肥満の病態形成における走化性因子の新たな役割が明らかになる可能性が期待される（J. Biol. Chem. 283: 35715-35723, 2008）。

2.

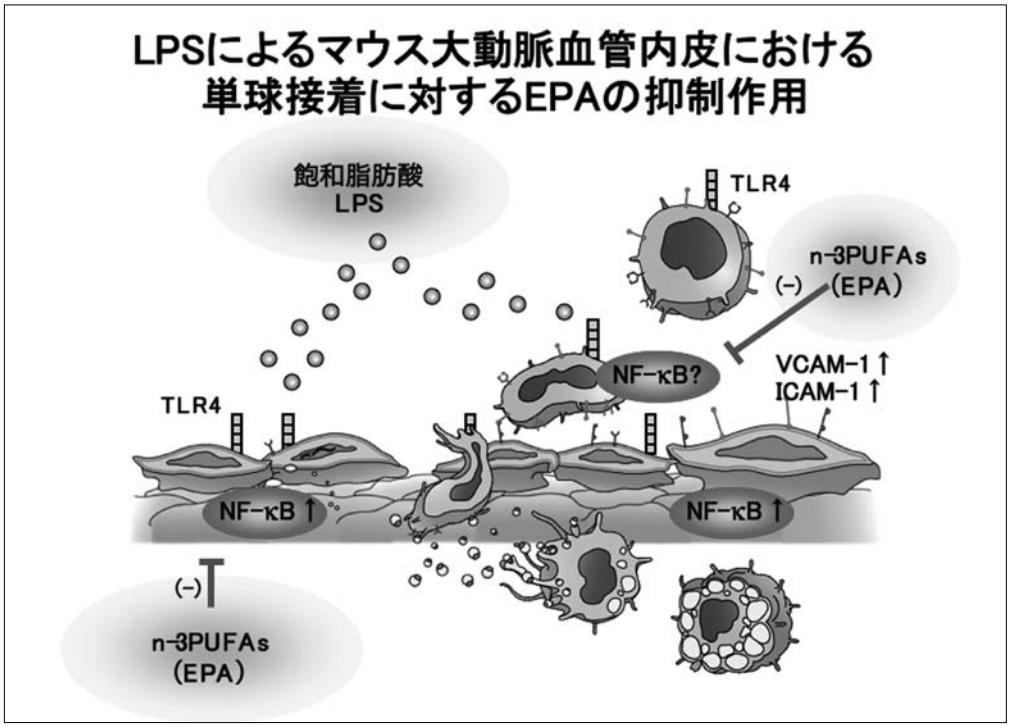

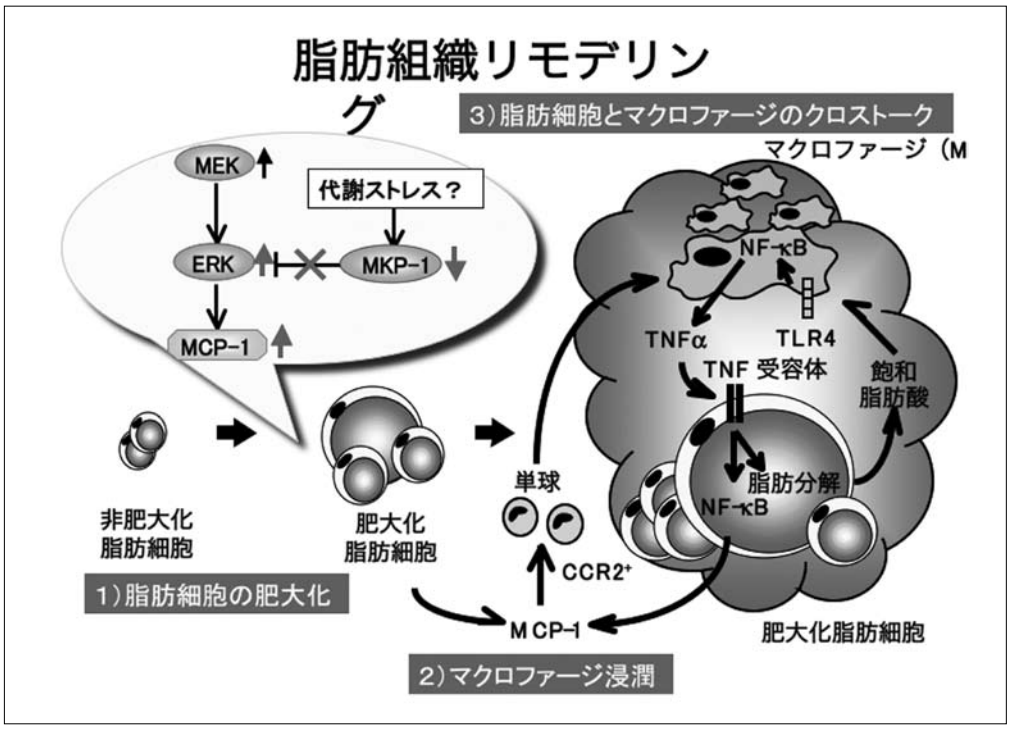

3. 2008年、2009年（平成21年3月までの）に発表した全ての研究内容についての英文要約

1） A large-scale, prospective, randomized clinical trial has recently revealed that the addition of highly purified eicosapentaenoic acid（EPA）to low-dose statin therapy significantly reduces the incidence of major coronary events. Here we investigated in vivo and in vitro effect of EPA on monocyte adhesion to endothelial cells and adhesion molecules. A new en face immunohistochemistry of endothelial surface in combination with confocal microscopy revealed marked reduction of LPS-induced monocyte adhesion to the aortic endothelium in parallel with the suppression of VCAM-1 and nuclear translocation of NF-κB p65 in EPA-treated mice relative to vehicle-treated groups. In an in vitro adhesion assay system under physiological flow conditions, EPA inhibited LPS-induced monocyte adhesion and endothelial adhesion molecules. We found significant decrease in plasma concentrations of sICAM-1 and sVCAM-1 in patients with the metabolic syndrome after a 3-month administration of highly purified EPA（1.8g daily）. Multivariate regression analysis revealed that EPA administration is the only independent determinant of sICAM-1 and sVCAM-1. This study provides evidence that EPA inhibits monocyte adhesion to endothelial cells in parallel with the suppression of endothelial adhesion molecules in vivo and in vitro.

2） Here we investigated the role of CCR2 in the recruitment of bone marrow-derived macrophages into obese adipose tissue in vitro and in vivo. Using the TAXIScan device which can measure quantitatively the directionality and velocity of cell migration at time-lapse intervals in vitro, we demonstrated that bone marrow cells（BMCs）from wildtype mice migrate directly toward MCP-1 or serum-free medium conditioned by adipose tissue explants of genetically obese ob/ob mice, which are efficiently suppressed by pharmacological blockade of CCR2 signaling. The number of F4/80-positive macrophages was reduced in the adipose tissue from high-fat diet-fed obese KKA^{y} or ob/ob mice treated with a CCR2 antagonist propagermanium relative to vehicle-treated groups. We also found that the number of macrophages is reduced in the adipose tissue from ob/ob mice reconstituted with $CCR2^{-/-}$ BMCs（ob/ob + $CCR2^{-/-}$ BMCs）relative to those with $CCR2^{+/+}$ BMCs（ob/ob + $CCR2^{+/+}$ BMCs）. Expression of mRNAs for CD11c, TLR4, and surface markers of pro-inflammatory M1 macrophages, was also decreased in the adipose tissue from ob/ob + $CCR2^{-/-}$ BMCs relative to ob/ob + $CCR2^{+/+}$ BMCs. This study provides evidence that CCR2 in bone marrow cells plays an important role in the recruitment of macrophages into obese adipose tissue.

4. 本事業に関連して世界的な研究拠点形成に向けて、以下の点で改善・整備等されたこと

D（人材育成）

学会・論文を通じて若手に研究成果の発表の機会を与えた。分野内で海外研究者のセミナーを随時開催し、若手研究者に交流の機会を作るようにした。

5. GCOE事業を推進するに当たって力を入れた点

若手研究者の育成

6. 英文原著論文

S. Yura*, H. Itoh*, N. Sagawa, H. Yamamoto, H. Masuzaki, K. Nakao, M. Kawamura, H. Mogami, Y. Ogawa, and S. Fujii（*These authors contributed equally to this work）. Neonatal exposure to leptin augments diet-induced obesity in leptin-deficient ob/ob mice. Obesity 16:1289-1295, 2008.

T. Toyoda, Y. Kamei, H. Kato, S. Sugita, M. Takeya, T. Suganami, and Y. Ogawa. Anti-inflammatory effect of peroxisome proliferator activated receptor α ligands in the interaction between adipocytes and macrophages in obese adipose tissue. Obesity 16:1199-1207, 2008.

Y. Kamei, S. Miura, T. Suganami, F. Akaike, S. Kanai, S. Sugita, A. Katsumata, H. Aburatani, T. G. Unterman, O. Ezaki, and Y. Ogawa. Regulation of SREBP1c gene expression in skeletal muscle: role of retinoid X receptor/liver X receptor and forkhead-O1 transcription factor. Endocrinology 149:2293-2305, 2008.

N. Satoh, A. Shimatsu, Y. Kato, R. Araki, K. Koyama, T. Okajima, M. Tanabe, M. Ooishi, K. Kotani, and Y. Ogawa for the Japan Obesity and Metabolic Syndrome Study（JOMS）Group. Evaluation of the cardio-ankle vascular index, a new indicator of arterial stiffness independent of blood pressure, in obesity and metabolic syndrome. Hypertens. Res. 31:1921-1930, 2008.

◎H. Yamada, M. Yoshida, Y. Nakano, T. Suganami, N. Satoh, T. Mita, K. Azuma, M. Itoh, Y. Yamamoto, Y. Kamei, M. Horie, H. Watada, and Y. Ogawa. In vivo and in vitro inhibition of monocyte adhesion to endothelial cells and endothelial adhesion molecules by eicosapentaenoic acid. Arterioscler. Thromb. Vasc. Biol. 28:2173-2179, 2008.

◎A. Ito, T. Suganami, A. Yamauchi, M. Degawa-Yamauchi, M. Tanaka, R. Kouyama, Y. Kobayashi, N. Nitta, K. Yasuda, Y. Hirata, W. A. Kuziel, M. Takeya, S. Kanegasaki, Y. Kamei, and Y. Ogawa. Role of C-C chemokine receptor 2 in bone marrow cells in the recruitment of macrophages into obese adipose tissue. J. Biol. Chem. 283:35715-35723, 2008.

7. 著書

1. 小川佳宏、菅波孝祥、伊藤綾香、田中都、伊藤美智子、亀井康富:「脂肪組織理モデリングの分子機構と医学応用」:肥満と脂肪エネルギー代謝-メタボリックシンドロームへの戦略-,203-215, 2008
2. 山崎芳浩、菅波孝祥、亀井康富、小川佳宏:「TLRシグナルとメタボリックシンドローム」:Diabetes Frontier VOL.19, NO.2, 237-242,2008
3. 亀井康富、小川佳宏:「エピジェネティクスと生活習慣病」:医学のあゆみ Vol225, No.7,585-587,2008
4. 伊藤美智子、伊藤綾香、菅波孝祥、小川佳宏:「アディポネクチンと炎症」:アディポネクチンとその受容体抗生活習慣病ホルモンの全貌,148-153,2008
5. 亀井康富、小川佳宏:「骨格筋とリポトキシシティ」:The Lipid Vol.19, No.3,38-42,2008
6. 亀井康富、小川佳宏:「脂肪細胞分化における核内受容体の役割」:分子心血管病 6 Vol.9, No.3,38-41,2008
7. 伊藤綾香、菅波孝祥、亀井康富、小川佳宏:「脂肪組織肥大化におけるMCP-1発現誘導とMKP-1の役割」:肥満研究 Vol.14,NO.2,2008
8. 亀井康富、河内浩行、柴田昌宏、小川佳宏:「骨格筋形質決定の分子機序　食肉の品質改良への可能性」:化学と生物　Vol.46,No.10,697-701,2008
9. 小川佳宏:「脂肪組織リモデリングの分子機構」:糖尿病学の進歩,41-44,2008
10. 小川佳宏:「レプチン（1）レプチンとレプチン受容体」:臨床栄養 Vol.113,No.5,594-595,2008
11. 豊田拓矢、小川佳宏:「脂肪組織と炎症」:最新医学10,52-59,2008
12. 伊藤美智子、菅波孝祥、小川佳宏:「ω3多価不飽和脂肪酸と肥満・糖尿病」:The Lipid Vol.19,No.4,48-53,2008
13. 小川佳宏:「レプチン（2）レプチンと肥満の関係」:臨床栄養 Vol.113,No.6,712-713,2008
14. 小川佳宏:「レプチン」:臨床検査 Vol.52, No.11, 1304-1307,2008
15. 小川佳宏:「総論:炎症・面積とメタボリックシンドローム」:Medical Science Digest Vol.34,474-475,2008
16. 小川佳宏:「レプチン（3）臨床応用と今後の展望」:臨床栄養 Vol.113,No.7,824-822,2008
17. 亀井康富、小川佳宏:「骨格筋機能とFOXOタンパク質」:生化学 Vol.80,No.11,1026-1029,2008
18. 山田英人、田中都、菅波孝祥、中野恭幸、小川佳宏:「肥満遺伝子産物レプチンの炎症誘起作用」:THE LUNG Vol.17,No.1,67-71,2009
19. 伊藤綾香、菅波孝祥、小川佳宏:「肥満の脂肪組織における炎症性変化」:日本臨床 第67巻,第2号,270-276,2009
20. 佐藤哲子、小川佳宏:「肥満遺伝子」:最新医学別冊 肥満症 代謝5,46-57,2009

8. 自己評価

脂肪組織リモデリングの分子機構に関する研究や飽和脂肪酸あるいはω3多価不飽和脂肪酸の病態生理的意義に関して一定の研究成果を挙げることはできた。今後、得られた研究成果をより高いレベルの論文に発表したい。

9. 学会発表（英文）

◎A. Ito, T. Suganami, A. Yamauchi, M. Degawa-Yamauchi, R. Kouyama, M. Tanaka, Y. Hirata, S. Kanegasaki, Y. Kamei, Y. Ogawa. Molecular mechanism of macrophage infiltration into obese adipose tissue-Analysis with TAXIScan, a real-time horizontal chemotaxis assay system-: Keystone Symposia Obesity: Novel Aspect of the Regulation of Body Weight:示説:Banff, Canada:2009年1月22日

◎M. Tanaka, T. Suganami, Y. Ogawa. Role of central leptin signaling in renal macrophage infiltration: Keystone Symposia: Complications of Diabetes and Obesity:示説:Vancouver, Canada:2009年2月27日

10. 学会発表（和文）

1. 田中都、菅波孝祥、杉田聡、竹屋元裕、笠原正登、亀井康富、小川佳宏:中枢神経系を介するレプチンの炎症調節作用:マウス腎尿細管間質障害モデルを用いて:第29回日本肥満学会,大分,2008.10.17-18
2. 伊藤綾香、菅波孝祥、田中都、神山隆治、平田結喜緒、亀井康富、小川佳宏:脂肪細胞組織へのマクロファージ浸潤と単球遊走能:リアルタイム細胞動態測定装置を用いた解析:第29回日本肥満学会,大分,2008.10.17-18
3. 赤池史子、亀井康富、菅波孝祥、金井紗綾香、岡淳一郎、三浦進司、江崎治、小川佳宏:骨格筋で核内受容体RXRγを過剰発現させた遺伝子改変マウスは食餌性肥満に抵抗性を示す:第29回日本肥満学会,大分,2008.10.17-18
4. 亀井康富、三浦進司、菅波孝祥、赤池史子、金井紗綾香、杉田聡、勝又阿貴、江崎治、小川佳宏:骨格筋におけるSREBP1c遺伝子の発現調節:LXR/RXR/FOXO1の役割:第29回日本肥満学会,大分,2008.10.17-18

5. 山本貴信、菅波孝祥、木曽美奈子、亀井康富、磯部光章、東山繁樹、小川佳宏:脂肪細胞におけるHB-EGF sheddingの分子機構の検討:第29回日本肥満学会,大分,2008.10.17-18

11. 外部資金の獲得状況

(科学研究費補助金、受託研究費、外部財団の助成など)

科学研究費補助金、基盤B
研究題目:「脂肪組織リモデリングと脂肪毒性の分子機構の解明」
代表:小川佳宏
期間:平成20―平成22年
研究費総額:610万円

科学研究費補助金、萌芽研究
研究題目:「肥満に関連するDNAメチル化標的遺伝子の同定と機能解析」
代表:小川佳宏
期間:平成20-平成21年
研究費総額:180万円

厚生労働省科学研究費補助金、難治性疾患克服事業
研究題目:中性性摂食異常症に関する調査研究
代表:小川佳宏
期間:平成20-平成22年
研究費総額:5100万円

循環器疾患等生活習慣病対策総合研究事業(18公-7)
研究題目:メタボリックシンドロームの発症予防に資する胎児期・乳幼児期の関連要因の解明に関する研究
代表:宮本恵宏
期間:平成18-平成20年
研究費総額:300万円

大和證券ヘルス財団研究助成
研究題目:n-3多価不飽和脂肪酸の単球・血管内皮細胞接着抑制作用に関する分子医学的研究
代表:小川佳宏
期間:平成20年
研究費総額:100万円

12. 特別講演、招待講演

1. Yoshihiro Ogawa. Crosstalk between adipocytes and Macrophages in adipose tissue remodeling. Seoul Symposium on Obesity and Diabetes, 2008.4.12, Seoul
2. Yoshihiro Ogawa. Adipose tissue inflammation in the metabolic syndrome. The 5th International Forum on Progressive Endocrinology I' FOPE 2008,2008.5.24,Tokyo
3. 小川佳宏 肥満の脂肪組織で一体何が起こっているのか? 第30回日本臨床栄養学会総会/第29回日本臨床栄養協会総会:第6回大連合大会イブニングセミナー3,2008.10.10,東京
4. 小川佳宏:Adipose tissue remodeling. CBI 2008, 2008.10.22-24, Tokyo
5. Yoshihiro Ogawa: Role of epigenetics in the metabolic syndrome. Northeastern Asian Symposium on Cancer Epigenetics, 2008. 11. 6-7, Jeju
6. 小川佳宏　脂肪組織リモデリング 第13回静岡 健康・長寿学術フォーラム 2008.11.8,静岡
7. 小川佳宏　肥満の脂肪組織で一体何が起こっているのか? 第45回日本臨床生理学会イブニングセミナー 2008.11.21,東京
8. 小川佳宏　脂肪組織の多面性とメタボリックシンドローム 栄養科学シンポジウム 2008.11.28,東京

13. 新聞、雑誌、TV報道

産経新聞　2008年9月30日
東京新聞　2008年10月26日

14. サマリー

肥満の脂肪組織では、脂肪細胞の肥大とともに血管新生やマクロファージの浸潤の増加、脂肪細胞とマクロファージの炎症性変化がもたらされ、「脂肪組織リモデリング」とも言うべきダイナミックな変化をきたしている。脂肪組織リモデリングと脂肪組織を起点とする全身の炎症性変化の分子機構を解き明かすことにより、全身臓器の機能障害を特徴とするメタボリックシンドロームの成因の解明と治療戦略の確立が期待される。

15. 講座の准教授、講師、助教、特別研究員、ポスドク、指導を受けた大学院生の名前（AISSには　○印）のリスト

（准教授）　亀井康富

（助教）　菅波孝祥

（特任助教）　伊藤綾香

（大学院生）　伊藤美智子、蜂屋瑠見、杉田 聡、
○田中　都、○山崎芳浩、山田英人、
山本貴信、山城健二、市岡誠之、
南部宏英、赤池史子

（受託研究員）　江原達弥、津田直人

Supplemental Material can be found at:
http://www.jbc.org/cgi/content/full/M804220200/DC1

THE JOURNAL OF BIOLOGICAL CHEMISTRY VOL. 283, NO. 51, pp. 35715–35723, December 19, 2008
© 2008 by The American Society for Biochemistry and Molecular Biology, Inc. Printed in the U.S.A.

Role of CC Chemokine Receptor 2 in Bone Marrow Cells in the Recruitment of Macrophages into Obese Adipose Tissue*[S]

Received for publication, June 2, 2008, and in revised form, October 8, 2008 Published, JBC Papers in Press, October 30, 2008, DOI 10.1074/jbc.M804220200

Ayaka Ito[‡1], Takayoshi Suganami[‡], Akira Yamauchi[§], Mikako Degawa-Yamauchi[§], Miyako Tanaka[‡¶2], Ryuji Kouyama[‡‖], Yuko Kobayashi[§], Nao Nitta[§], Kazuki Yasuda[**], Yukio Hirata[‖], William A. Kuziel[‡‡], Motohiro Takeya[§§], Shiro Kanegasaki[§], Yasutomi Kamei[‡], and Yoshihiro Ogawa[‡¶3]

From the [‡]Department of Molecular Medicine and Metabolism, Medical Research Institute, [‖]Department of Clinical and Molecular Endocrinology, [¶]Global Center of Excellence Program International Research Center for Molecular Science in Tooth and Bone Diseases, Tokyo Medical and Dental University, 1-5-45 Yushima, Bunkyo-ku, Tokyo 113-8510, Japan, [§]Central Laboratory, ECI, Inc., 4-7-7, Aobadai, Meguro-ku, Tokyo 153-0042, Japan, the [**]Department of Metabolic Disorder, Research Institute, International Medical Center of Japan, 1-21-1 Toyama, Shinjuku-ku, Tokyo 162-8655, Japan, the [‡‡]Department of Autoimmune and Inflammatory Diseases, Protein Design Laboratories, Inc., Fremont, California 94555, and the [§§]Department of Cell Pathology, Graduate School of Medical Sciences, Kumamoto University, 1-1-1 Honjo, Kumamoto 860-8556, Japan

The MCP-1 (monocyte chemoattractant protein-1)/CCR2 (CC motif chemokine receptor-2) pathway may play a role in macrophage infiltration into obese adipose tissue. Here we investigated the role of CCR2 in the recruitment of bone marrow-derived macrophages into obese adipose tissue *in vitro* and *in vivo*. Using the TAXIScan device, which can measure quantitatively the directionality and velocity of cell migration at time lapse intervals *in vitro*, we demonstrated that bone marrow cells (BMCs) from wild type mice migrate directly toward MCP-1 or culture medium conditioned by adipose tissue explants of genetically obese *ob/ob* mice, which are efficiently suppressed by pharmacological blockade of CCR2 signaling. The number of F4/80-positive macrophages was reduced in the adipose tissue from high fat diet-fed obese KKA^{y} or *ob/ob* mice treated with a CCR2 antagonist propagermanium relative to vehicle-treated groups. We also found that the number of macrophages is reduced in the adipose tissue from *ob/ob* mice reconstituted with *CCR2*$^{-/-}$ BMCs (*ob/ob* + *CCR2*$^{-/-}$ BMCs) relative to those with *CCR2*$^{+/+}$ BMCs (*ob/ob* + *CCR2*$^{+/+}$ BMCs). Expression of mRNAs for CD11c and TLR4 (Toll-like receptor 4) markers of proinflammatory M1 macrophages was also decreased in the adipose tissue from *ob/ob* + *CCR2*$^{-/-}$ BMCs relative to *ob/ob* + *CCR2*$^{+/+}$ BMCs, whereas mannose receptor and CD163, markers of anti-inflammatory M2 macrophages, were unchanged. This study provides *in vivo* and *in vitro* evidence that CCR2 in bone marrow cells plays an important role in the recruitment of macrophages into obese adipose tissue.

Obesity is a state of chronic, low grade inflammation; it is characterized by increased infiltration of macrophages, suggesting that macrophages are an important source of inflammation in obese adipose tissue (1–3). Using an *in vitro* co-culture system composed of adipocytes and macrophages, we have demonstrated that a paracrine loop involving saturated fatty acids and tumor necrosis factor-α derived from adipocytes and macrophages, respectively, establishes a vicious cycle that augments the inflammatory changes (*i.e.* marked up-regulation of proinflammatory adipocytokines, such as MCP-1 (monocyte chemoattractant protein-1) and tumor necrosis factor-α, and down-regulation of adiponectin) (4, 5). These findings have led us to speculate that macrophages, when infiltrated, may participate in the inflammatory pathways that are activated in obese adipose tissue.

CCR2 (CC motif chemokine receptor-2) is a major receptor that recognizes MCP-1 and some other chemokines, which control the recruitment of macrophages to the site of inflammation (6, 7). There is considerable evidence for the pathophysiologic role of the MCP-1/CCR2 pathway in macrophage infiltration into obese adipose tissue. For instance, Weisberg *et al.* (8) reported the attenuation of macrophage accumulation and inflammatory changes in the adipose tissue from mice lacking CCR-2 (*CCR2*$^{-/-}$ mice) during a high fat diet. Moreover, two previous studies with transgenic mice overexpressing MCP-1 in the adipose tissue and/or MCP-1-deficient mice (*MCP-1*$^{-/-}$ mice) showed that MCP-1 plays a role in the recruitment of macrophages into obese adipose tissue (9, 10). Recent studies demonstrated the heterogeneity of macrophages in obese adipose tissue; they follow two different polarization states: M1 or "classically activated" (proinflammatory) macrophages and M2 or "alternatively activated" (anti-inflammatory) macrophages (11, 12). Evidence has accumulated indicating an increase in M1 macrophages and decrease in M2 macrophages in obese adipose tissue (11–13). Interestingly, such a phenotypic switch was not observed in *CCR2*$^{-/-}$ mice (11), suggesting that the MCP-

* This work was supported in part by a Grant-in-Aid for Scientific Research from the Ministry of Education, Culture, Sports, Science, and Technology of Japan and the Ministry of Health, Labour, and Welfare of Japan and research grants from the Takeda Science Foundation and Smoking Research Foundation. The costs of publication of this article were defrayed in part by the payment of page charges. This article must therefore be hereby marked "*advertisement*" in accordance with 18 U.S.C. Section 1734 solely to indicate this fact.

[S] The on-line version of this article (available at http://www.jbc.org) contains supplemental Figs. S1–S7, Table 1, and Movies 1–8.

[1] Supported by the Tokyo Biochemical Research Foundation.

[2] Supported by the Mishima Kaiun Memorial Foundation.

[3] To whom correspondence should be addressed: Dept. of Molecular Medicine and Metabolism, Medical Research Institute, Tokyo Medical and Dental University, 1-5-45 Yushima, Bunkyo-ku, Tokyo 113-8510, Japan. Tel./Fax: 81-3-5803-4931; E-mail: ogawa.mmm@mri.tmd.ac.jp.

Downloaded from www.jbc.org at Tokyo Ikashika Daigaku on December 29, 2008

1/CCR2 pathway contributes to macrophage polarization in the adipose tissue. Although macrophages infiltrated into obese adipose tissue have been reported to be mostly derived from the bone marrow (1), there is no direct evidence for the contribution of CCR2 to the recruitment of bone marrow-derived macrophages into obese adipose tissue.

In this study, we examined the role of CCR2 in the recruitment of bone marrow-derived macrophages into obese adipose tissue through a combination of an optically accessible, horizontal chemotaxis apparatus with which to measure cell migration at time lapse intervals *in vitro* and bone marrow transplantation techniques *in vivo*. The data from this study provide evidence that CCR2 in bone marrow cells (BMCs)[4] is involved in the recruitment of macrophages into obese adipose tissue.

EXPERIMENTAL PROCEDURES

Materials—Recombinant mouse MCP-1 and human stromal-derived factor-1 (SDF-1) were purchased from PeproTech (Rocky Hill, NJ). Propagermanium, a CCR2 antagonist, was a gift from Sanwa Kagaku Kenkyusho (14). RS504393, a CCR2 antagonist, was purchased from TOCRIS Cookson (Bristol, UK). All other reagents were purchased from Sigma or Nacalai Tesque (Kyoto, Japan).

Animal Studies—Generation of male $CCR2^{-/-}$ mice on the C57BL/6J background was reported previously (15). Four-week-old female C57BL/6J mice and *ob/ob* mice were purchased from Charles River Japan (Tsukuba, Japan). Four-week-old male KK mice and KKA^{y} mice were purchased from Nippon CLEA (Shizuoka, Japan). The green fluorescence protein (GFP) transgenic mice were kindly provided by Dr. M. Okabe (Osaka University, Suita, Japan) (16). The animals were housed in individual cages in a temperature-, humidity-, and light-controlled room (12-h light and 12-h dark cycle) and allowed free access to water and standard chow (Oriental MF; 362 kcal/100 g, 5.4% energy as fat; Oriental Yeast) except when otherwise noted. At the end of the experiments, mice were sacrificed after a 1-h fast under intraperitoneal pentobarbital anesthesia (30 mg/kg). All animal experiments were conducted according to the guidelines of the Tokyo Medical and Dental University Committee on Animal Research (No. 0050140).

High Fat Diet Experiment—Twelve-week-old $CCR^{+/+}$ and $CCR2^{-/-}$ mice were given free access to water and high fat diet (D12492, 524 kcal/100g, 60% energy as fat; Research Diets, New Brunswick, NJ) for 20 weeks.

Administration of Propagermanium—Five-week-old male KKA^{y} mice fed high fat diet were given a CCR2 antagonist propagermanium (8 mg/kg/day) (14) in drinking water for 4 weeks. Five-week-old female *ob/ob* mice were fed standard chow supplemented with propagermanium (3 or 8 mg/kg/day) for 5 weeks.

Bone Marrow Transplantation—BMCs were collected from the femur and tibia of female $CCR2^{+/+}$ and $CCR2^{-/-}$ donor mice. Red blood cells were depleted by ACK lysing buffer (0.15 M NH_4Cl, 1 mM $KHCO_3$, 0.1 mM EDTA), and the remaining cells were washed with PBS and resuspended at a density of 10^7 cells/ml in PBS containing 3% fetal bovine serum (Sanko Junyaku). BMCs (3×10^6 cells) obtained from $CCR2^{+/+}$ or $CCR2^{-/-}$ donor mice were washed three times with cold PBS, and injected intravenously into 7 gray irradiated 7-week-old female wild type or *ob/ob* recipient mice. Each recipient mouse received $CCR2^{+/+}$ or $CCR2^{-/-}$ BMCs. The efficiency of bone marrow transplantation was determined by counting GFP-positive cells in peripheral blood of wild type or *ob/ob* mice reconstituted with BMCs obtained from GFP transgenic donor mice (16). In this study, more than 90% of peripheral blood cells were substituted by GFP-positive cells (data not shown). Eleven weeks after the bone marrow transplantation, the perigonadal adipose tissue was harvested and analyzed.

Histological Analysis—The perigonadal adipose tissue was fixed with neutral buffered formalin and embedded in paraffin. An immunohistochemical study was carried out using 5-μm-thick paraffin-embedded sections for the macrophage marker F4/80 as previously described (5, 17, 18). The number of F4/80-positive cells was counted in a blinded fashion through the microscope with a ×400 objective and an eyepiece grid indicating a 0.0625-mm^2 field of view. More than 100 serial fields were examined, and the data were expressed as the mean number/mm^2.

Blood Parameter Analysis—Blood was sampled from the tail vein of mice. Blood glucose was measured as previously described (19).

Preparation of Conditioned Medium—The perigonadal adipose tissue was harvested aseptically from 14-week-old female C57BL/6J wild type mice and *ob/ob* mice as previously described (20, 21). Half of the adipose tissue was minced and then cultured for 24 h in Dulbecco's modified Eagle's medium containing 1% bovine serum albumin. The supernatants thus obtained were used for chemotaxis assay. The culture medium was used as a control.

Cell Culture—The CCR2 expression vector was constructed by ligating the full-length mouse CCR2 cDNA into the XhoI-NotI site of BCMGSNeo vector and transfected into Jurkat cells using FuGENE-HD transfection reagent (Roche Applied Science) according to the manufacturer's instructions. The Jurkat cells stably expressing CCR2 (CCR2-Jurkat) were obtained by selecting with 1 mg/ml G418 (Invitrogen). CCR2-Jurkat was maintained in RPMI (Nacalai Tesque) containing 10% fetal bovine serum (Biowest, Nuaille, France) and antibiotics and incubated at 37 °C in a humidified 5% CO_2, 95% air atmosphere. BMCs were collected from the femur and tibia, suspended to 10^6 cells/ml in RPMI 1640 medium supplemented with 20 mM HEPES buffer, pH 7.2, and kept at 37 °C before use.

Real Time Horizontal Chemotaxis Assay Using TAXIScan—Chemotaxis of CCR2-Jurkat and BMCs was examined using the TAXIScan device (ECI, Inc., Tokyo, Japan) (22, 23). CCR2-Jurkat was injected into one of two compartments through a hole connected to the compartment. To adjust the position of the cells, the medium was drawn out from the other hole provided for the other compartment. Drawing was stopped when cells were aligned in the channel close to the edge. One microliter of chemoattractant solution was injected into the other compartment to initiate chemotaxis and monitoring. Cell migration at 37 °C was recorded every 1 min for 30 min, and the migration

[4] The abbreviations used are: BMCs, bone marrow cells; GFP, green fluorescence protein; PBS, phosphate-buffered saline.

The Journal of Biological Chemistry ASBMB jbc

Downloaded from www.jbc.org at Tokyo Ikashika Daigaku on December 29, 2008

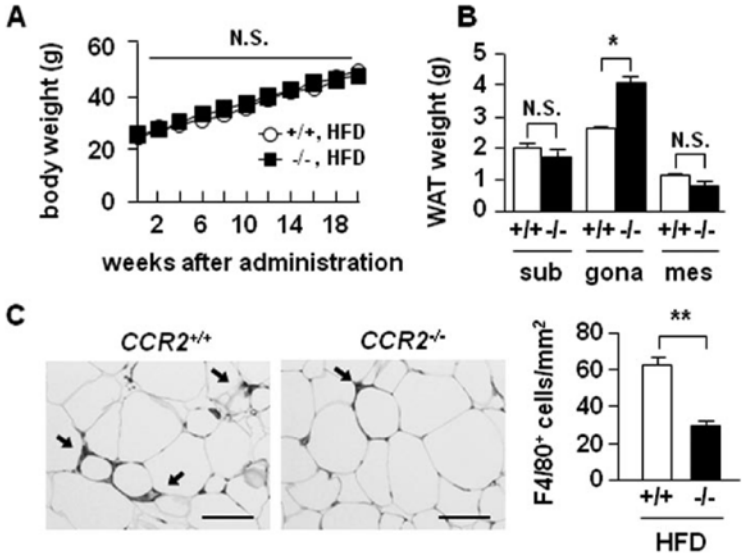

FIGURE 1. **Macrophage infiltration in $CCR2^{+/+}$ and $CCR2^{-/-}$ mice with high fat diet-induced obesity.** *A*, growth curve of $CCR2^{+/+}$ and $CCR2^{-/-}$ mice fed high fat diet (*HFD*) for 20 weeks. *Open circle*, $CCR2^{+/+}$ mice fed high fat diet; *closed square*, $CCR2^{-/-}$ mice fed high fat diet. *B*, weight of the subcutaneous (*sub*), perigonadal (*gona*), and mesenteric (*mes*) adipose tissue (*WAT*). *C*, F4/80 immunostaining (*left*) and the number of F4/80-positive cells (*right*) in the perigonadal adipose tissue. Original magnification, ×200. *Scale bars*, 100 μm. *, $p < 0.05$; **, $p < 0.01$; *N.S.*, not significant. $n = 4–5$.

pathway was recorded by clicking each cell on a display. The directionality of migration is expressed as the angle (radian) toward the concentration gradient (*i.e.* $\pi/2$ indicates that the cell is migrating toward the concentration gradient, whereas radian $-\pi/2$ indicates that the cell is migrating against the gradient). The velocity of cell migration is expressed as μm/s. The average directionality and velocity of migration were calculated by the values obtained every 1 min (Fig. S1) (23, 24). In this study, we confirmed that CCR2-Jurkat migrate dose-dependently toward recombinant mouse MCP-1; 100 nM was most effective to induce chemotaxis (Fig. S2), which is consistent with a previous report (25). Thus, 100 nM recombinant MCP-1 was used for further analysis.

Quantitative Real Time PCR—Quantitative real time PCR was performed with an ABI Prism 7000 Sequence Detection System using TAQMAN® or SYBR® Green PCR Master Mix reagent kit (Applied Biosystems, Foster City, CA). Primers used were described in supplemental Table 1. Levels of mRNA were normalized to those of housekeeping gene 36B4 mRNA.

Enzyme-linked Immunosorbent Assay—The MCP-1 concentrations in culture medium conditioned by adipose tissue explants were determined by the commercially available enzyme-linked immunosorbent assay kits (R&D Systems, Minneapolis, NM).

Fluorescence-activated Cell Sorting Analysis—BMCs were harvested from the femur and tibia of $CCR2^{+/+}$ or $CCR2^{-/-}$ mice, and mononuclear cells were separated by HISTOPAQUE (Sigma). Cells were incubated with Fc receptor-blocking reagent (Miltenyi Biotec, Bergisch Gladbach, Germany). Cells were then stained in staining buffer (PBS containing 0.1% bovine serum albumin and 5 mM EDTA) using fluorochrome-conjugated combinations of the following antibodies: fluorescein isothiocyanate-conjugated anti-mouse CD11b and phycoerythrin-conjugated anti-mouse CD11c (BD Biosciences). After washing twice with the staining buffer, flow cytometry was performed on EPICS ALTRA (Beckman Coulter, Fullerton, CA).

Statistical Analysis—Data were expressed as the mean ± S.E. Statistical analysis was performed using analysis of variance followed by Scheffe's test. $p < 0.05$ was considered to be statistically significant.

RESULTS

Macrophage Infiltration in $CCR2^{+/+}$ and $CCR2^{-/-}$ Mice with High Fat Diet-induced Obesity—To investigate the role of CCR2 in macrophage infiltration into obese adipose tissue, we examined the response of $CCR2^{+/+}$ and $CCR2^{-/-}$ mice to a high fat diet. Although there was no significant change in body weight between the genotypes, the weight of perigonadal adipose tissue was even increased in $CCR2^{-/-}$ mice relative to $CCR2^{+/+}$ mice (Fig. 1, *A* and *B*). Histological examination revealed that the number of F4/80-positive cells in the adipose tissue is markedly reduced in $CCR2^{-/-}$ mice relative to $CCR2^{+/+}$ mice (Fig. 1*C*; $p < 0.01$). We found that $CCR2^{-/-}$ mice have significantly lower blood glucose levels than $CCR2^{+/+}$ mice 20 weeks after the high fat diet feeding (280.25 ± 29.09 mg/dl *versus* 193.33 ± 15.62 mg/dl; $p < 0.05$). These observations are consistent with the previous report on reduced macrophage infiltration in $CCR2^{-/-}$ mice fed a high fat diet during the course of obesity (8).

Chemotaxis of BMCs toward MCP-1 and Obese Adipose Tissue-conditioned Medium—It has been reported that macrophages in obese adipose tissue are mostly derived from the bone marrow (1), but there is no direct evidence for the involvement of CCR2 expressed in BMCs. To explore the role of CCR2 in the recruitment of bone marrow-derived macrophages into obese adipose tissue, using the TAXIScan device, we examined the real time horizontal chemotactic response of mouse BMCs toward MCP-1 and adipose tissue-conditioned medium *in vitro*. The BMCs derived from wild type mice randomly migrated with the vehicle or PBS containing 3% bovine serum albumin. By contrast, BMCs migrated directly toward 10^{-7} M recombinant MCP-1, the dose of which was most effective to induce chemotaxis (Fig. S2). The directionality of migration was abrogated by pharmacological blockade of CCR2 signaling with a CCR2 antagonist, propagermanium (Fig. 2*A*). We also examined the chemotactic response of BMCs toward the culture medium conditioned by adipose tissue explants from

Downloaded from www.jbc.org at Tokyo Ikashika Daigaku on December 29, 2008

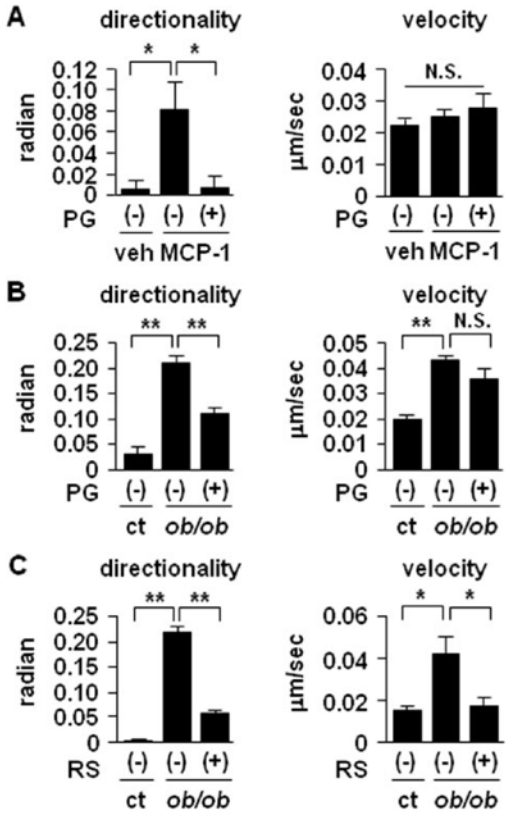

FIGURE 2. **Chemotaxis of BMCs toward MCP-1 and obese adipose tissue-conditioned medium.** *A*, effect of propagermanium on chemotaxis of $CCR2^{+/+}$ BMCs toward recombinant mouse MCP-1. The directionality (*left*) and velocity (*right*) of migration were determined from digital time lapse movies. *B*, effect of propagermanium on chemotaxis of $CCR2^{+/+}$ BMCs toward *ob/ob*-conditioned medium. The directionality (*left*) and velocity (*right*) of migration were determined from digital time lapse movies. The $CCR2^{+/+}$ BMCs were incubated with 5 μg/ml propagermanium 30 min before and during the assay. *C*, effect of RS504393 on chemotaxis of $CCR2^{+/+}$ BMCs toward *ob/ob*-conditioned medium. The directionality (*left*) and velocity (*right*) of migration were determined from digital time lapse movies. $CCR2^{+/+}$ BMCs were incubated with 5 μg/ml RS504393 30 min before assay and during the assay. *veh*, vehicle; *ct*, control; *PG*, propagermanium; *RS*, RS504393. *, $p < 0.05$; **, $p < 0.01$; *N.S.*, not significant. $n = 4$.

ob/ob mice (*ob/ob*-conditioned medium). The BMCs randomly migrated with the control culture medium. By contrast, BMCs migrated toward *ob/ob*-conditioned medium directly and quickly. Furthermore, the directionality of migration was significantly abrogated by preincubation with propagermanium (Fig. 2*B*; $p < 0.01$). We also obtained essentially the same results with another CCR2 antagonist, RS504393 (Fig. 2*C*). These observations, taken together, suggest that BMCs migrate toward MCP-1 or *ob/ob*-conditioned medium via CCR2. The MCP-1 concentrations in *ob/ob*-conditioned medium were ~150 ng/ml (*i.e.* 20 nM), which are roughly comparable with the dose of recombinant MCP-1 used *in vitro* (100 nM) (data not shown). In this study, we found that the migration of BMCs is direct toward *ob/ob*-conditioned medium relative to wild type-conditioned medium, whereas the velocity of migration is not different between the conditioned media used (Fig. S3). In addition, MCP-1 concentrations in *ob/ob*-conditioned medium were increased relative to wild type-conditioned medium (93.96 ± 8.71 ng/ml *versus* 150.75 ± 5.02 ng/ml, $p < 0.01$, $n = 5$). These observations are consistent with the concept that increased production of MCP-1 is involved in macrophage infiltration into obese adipose tissue (8–10).

Chemotaxis of CCR2-Jurkat toward MCP-1 and Obese Adipose Tissue-conditioned Medium—Because of the heterogeneity of BMCs, we next generated Jurkat cells stably expressing CCR2 (CCR2-Jurkat) to confirm that CCR2 is involved in cell migration toward MCP-1 or *ob/ob*-conditioned medium. In this study, CCR2 mRNA levels in CCR2-Jurkat were roughly comparable with those in BMCs from wild type mice (Fig. S4). The CCR2-Jurkat migrated directly toward recombinant MCP-1 at a dose of 10^{-7} M, whereas they moved randomly with the vehicle alone. By contrast, the directionality of migration was abrogated by preincubation with propagermanium (Fig. 3*A* and supplemental Movies 1–3, $p < 0.05$). The CCR2-Jurkat also migrated toward *ob/ob*-conditioned medium with the directionality of migration being significantly inhibited by propagermanium (Fig. 3*B* and supplemental Movies 6–8). The parent Jurkat, a human T lymphocyte cell line, expresses CXCR4 (*CXC* motif chemokine receptor 4) and binds SDF-1 with high affinity (26). We previously reported that the parent Jurkat migrates toward recombinant human SDF-1 through CXCR4 (22). However, it was unable to migrate toward recombinant mouse MCP-1 (data not shown). We also confirmed that the directionality and velocity of CCR2-Jurkat migration toward recombinant human SDF-1 are unaffected by preincubation with propagermanium (Fig. S5 and supplemental Movies 4 and 5), which suggests the specificity of propagermanium as a CCR2 antagonist in the chemotaxis assay. In this study, chemotaxis of CCR2-Jurkat toward *ob/ob*-conditioned medium was also significantly inhibited by another CCR2 antagonist, RS504393 ($p < 0.05$) (Fig. 3*C*). These observations indicate that migration of CCR2-Jurkat in response to recombinant MCP-1 or *ob/ob*-conditioned medium is CCR2-dependent.

Chemotaxis of BMCs toward Culture Medium Conditioned by Adipose Tissue Explants from Pioglitazone-treated ob/ob Mice—Previous reports showed that peroxisome proliferator-activated receptor γ activation suppresses adipose tissue expression of MCP-1 and thus improves insulin sensitivity (27, 28). We also examined the chemotaxis of BMCs toward culture medium conditioned by adipose tissue explants from pioglitazone- and vehicle-treated *ob/ob* mice (*ob/ob* + pio- and *ob/ob* + veh-conditioned medium, respectively). In this study, we confirmed that MCP-1 and tumor necrosis factor-α mRNA expression is decreased and adiponectin mRNA expression is increased in the adipose tissue by pioglitazone treatment, which is consistent with previous reports (27, 28) (Fig. S6). The BMCs migrated directly toward *ob/ob*-conditioned medium, and the directionality of migration of BMCs was markedly abrogated with *ob/ob* + pio-conditioned medium (Fig. S6). On the other hand, there was no significant change in the velocity of migration between the conditioned medium used. These

Downloaded from www.jbc.org at Tokyo Ikashika Daigaku on December 29, 2008

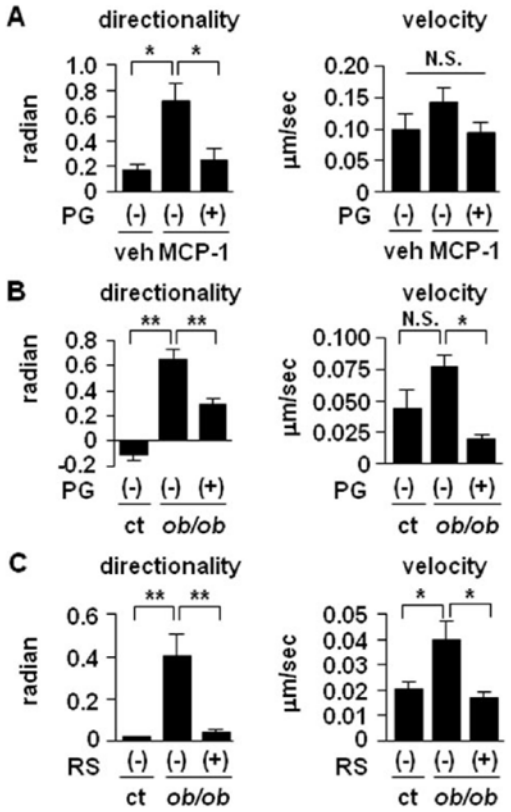

FIGURE 3. **Chemotaxis of CCR2-Jurkat toward MCP-1 and obese adipose tissue-conditioned medium.** *A*, effect of propagermanium on chemotaxis of CCR2-Jurkat toward recombinant mouse MCP-1. The directionality (*left*) and velocity (*right*) were determined from digital time lapse movies (supplemental Movies 1–3). *B*, effect of propagermainum on chemotaxis of CCR2-Jurkat toward the culture medium conditioned by adipose tissue explants from *ob/ob* mice (*ob/ob*). The directionality (*left*) and velocity (*right*) were determined from digital time lapse movies (supplemental Movies 6–8). The $CCR2^{+/+}$ BMCs were incubated with 5 μg/ml propagermanium 30 min before and during the assay. *C*, effect of RS504393 on chemotaxis of $CCR2^{+/+}$ BMCs toward *ob/ob*-conditioned medium. The directionality (*left*) and velocity (*right*) of migration were determined from digital time lapse movies. $CCR2^{+/+}$ BMCs were incubated with 5 μg/ml RS504393 30 min before and during the assay. *veh*, vehicle; *ct*, control; *PG*, propagermanium; *RS*, RS504393. *, $p < 0.05$; **, $p < 0.01$; *N.S.*, not significant. $n = 4$.

observations support the concept that treatment with a peroxisome proliferator-activated receptor γ agonist, pioglitazone, reduces the potential to induce macrophage infiltration into obese adipose tissue (11, 12).

Effect of Propagermanium on Macrophage Infiltration into Obese Adipose Tissue—To explore the involvement of CCR2 in macrophage infiltration into obese adipose tissue *in vivo*, we examined the effect of propagermanium (8 mg/kg/day) in KKA^y mice fed a high fat diet. Although there was no significant difference in body weight and adipose tissue weight between the propagermanium- and the vehicle-treated groups, the number of F4/80-positive cells was significantly decreased in the propagermanium-treated KKA^y mice relative to the vehicle-treated group (Fig. 4, *A–C*, $p < 0.01$). In this study, we also found that the number of F4/80-positive cells is significantly reduced in *ob/ob* mice treated with propagermanium (3 mg/kg/day or 8 mg/kg/day) relative to the vehicle-treated group ($p < 0.05$), although body weight and adipose tissue weight are unchanged (Fig. 5, *A–C*). These observations, taken together, indicate that pharmacological blockade of CCR2 effectively reduces macrophage infiltration into obese adipose tissue.

Role of CCR2 in the Recruitment of Bone Marrow-derived Macrophages into Obese Adipose Tissue—Using the bone marrow transplantation technique, we examined whether bone marrow-derived macrophages are infiltrated into obese adipose tissue through CCR2 *in vivo*. There was no significant difference in body weight and adipose tissue weight between *ob/ob* mice reconstituted with $CCR2^{-/-}$ BMCs (*ob/ob* + $CCR2^{-/-}$ BMCs) and those reconstituted with $CCR2^{+/+}$ BMCs (*ob/ob* + $CCR2^{+/+}$ BMCs) (Fig. 6, *A* and *B*). Histological analysis revealed that the number of F4/80-positive cells is significantly reduced in the adipose tissue from *ob/ob* + $CCR2^{-/-}$ BMCs relative to *ob/ob* + $CCR2^{+/+}$ BMCs (Fig. 6*C*, $p < 0.01$). Moreover, expression of CD11c and TLR4 (Toll-like receptor-4), markers of M1 macrophages, was significantly decreased in *ob/ob* + $CCR2^{-/-}$ BMCs relative to *ob/ob* + $CCR2^{+/+}$ BMCs (Fig. 7; $p < 0.01$). In this study, there was no significant difference in expression of mannose receptor and CD163, markers of M2 macrophages, between the genotypes of BMCs (Fig. 7). We also observed no significant difference in the population of $CD11b^+CD11c^+$ cells in BMCs between the genotypes (Fig. S7), suggesting that CCR2 is not involved in $CD11b^+CD11c^+$ cell differentiation in the bone marrow. These observations, taken together, suggest that CCR2 expressed in BMCs, especially in M1 macrophages, plays an important role in the recruitment of bone marrow-derived macrophages into obese adipose tissue.

DISCUSSION

There is considerable evidence that CCR2 and its major ligand MCP-1 are important for macrophage accumulation in obese adipose tissue (8–10, 29). Weisberg *et al.* (1) previously reported that macrophages in obese adipose tissue are mostly derived from the bone marrow. However, whether CCR2 expressed in BMCs contributes to the recruitment of macrophages into obese adipose tissue has not been addressed. Furthermore, there has been no quantitative analysis of CCR2-mediated migration of BMCs in response to soluble factor(s) released from the adipose tissue *in vitro* even with conventional methods such as Boyden's chamber (30) and under-agarose technique (31–33), which have only enabled end point analysis of cell migration with limited information. This study was designed to elucidate the role of CCR2 in the recruitment of bone marrow-derived macrophages into obese adipose tissue both *in vivo* and *in vitro*.

Using the TAXIScan device, an optically accessible, horizontal chemotaxis apparatus, we demonstrated that BMCs from wild type mice migrate toward recombinant MCP-1 or *ob/ob*-conditioned medium. The data were also confirmed using the CCR2-Jurkat. Moreover, the chemotactic responses are all blunted by treatment with propagermanium, which targets gly-

Downloaded from www.jbc.org at Tokyo Ikashika Daigaku on December 29, 2008

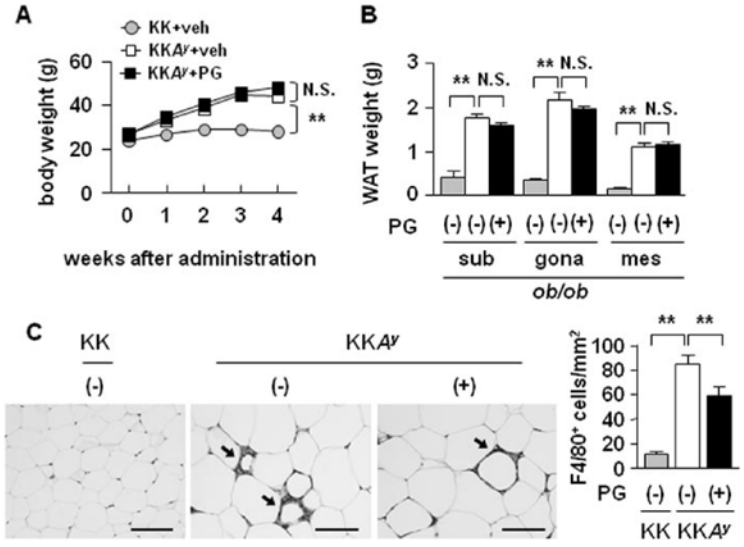

FIGURE 4. **Effect of propagermanium on adipose tissue macrophage infiltration in KKA^y mice.** *A*, growth curve of high fat diet-fed KK and KKA^y mice treated with propagermanium for 4 weeks. *Gray circle*, KK mice treated with vehicle; *open square*, KKA^y mice treated with vehicle; *closed square*, KKA^y mice treated with propagermanium (8 mg/kg/day). *B*, weight of the subcutaneous (*sub*), perigonadal (*gona*), and mesenteric (*mes*) adipose tissue. *C*, F4/80 immunostaining (*left*) and the number of F4/80-positive cells (*right*) in the perigonadal WAT from KKA^y mice. Original magnification was ×200. *Scale bars*, 100 μm. *veh*, vehicle; *PG*, propagermanium. *, $p < 0.05$; **, $p < 0.01$. *N.S.*, not significant. $n = 6$.

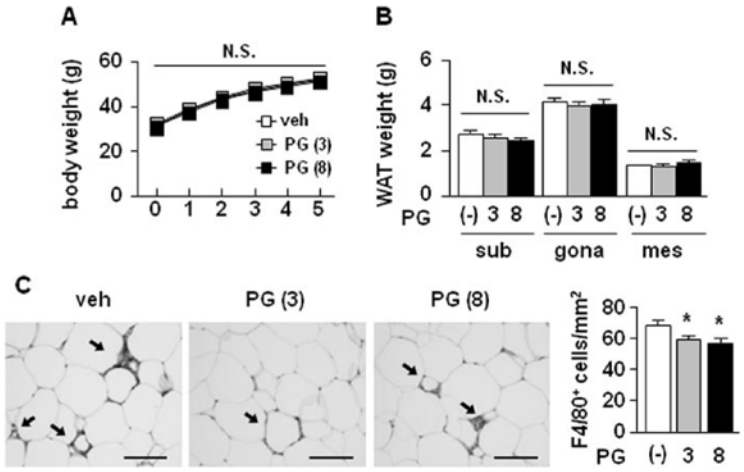

FIGURE 5. **Effect of propagermanium on adipose tissue macrophage infiltration in *ob/ob* mice.** *A*, growth curve of *ob/ob* mice treated with propagermanium for 5 weeks. *Open square*, vehicle; *gray square*, propagermanium (3 mg/kg/day); *closed square*, propagermanium (8 mg/kg/day). *B*, weight of the subcutaneous (*sub*), perigonadal (*gona*), and mesenteric (*mes*) adipose tissue. *C*, F4/80 immunostaining (*left*) and the number of F4/80-positive cells (*right*) in the perigonadal adipose tissue. Original magnification was ×200. *Scale bars*, 100 μm. *veh*, vehicle; *PG*, propagermanium. *, $p < 0.05$; **, $p < 0.01$; *N.S.*, not significant. $n = 6–7$.

cosylphosphatidylinositol-anchored proteins closely associated with CCR2 and thus inhibits the MCP-1-induced chemotactic migration of monocytes (14). These observations suggest the chemotactic response is CCR2-dependent. In this study, we demonstrated that pharmacologic blockade of CCR2 by propagermanium for 4 weeks effectively reduces macrophage accumulation in the adipose tissue from both high fat diet-fed KKA^y mice and *ob/ob* mice, which is consistent with the previous report with INCB3344, another CCR2-specific antagonist (8). These observations, taken together, suggest that obese adipose tissue is capable of releasing a large amount of chemokine(s) involved in the migration of BMCs via CCR2, and one such factor might be MCP-1. We also found that BMCs migrate directly toward *ob/ob*-conditioned medium relative to wild type-conditioned medium and that MCP-1 concentrations in *ob/ob*-conditioned medium were increased relative to wild type-conditioned medium. Furthermore, the directionality of migration of BMCs is markedly abrogated with *ob/ob* + pio-conditioned medium relative to *ob/ob* + veh-conditioned medium, suggesting that treatment with peroxisome proliferator-activated receptor γ agonist reduces the potential to induce macrophage infiltration into obese adipose tissue (11, 12). Therefore, TAXIScan provides a unique *in vitro* experimental system with which to assess quantitatively the chemotactic activity of chemokines responsible for cell migration *in vivo*.

The *in vitro* chemotaxis assay system applied herein enables us to quantify the directionality and velocity of cell migration, which cannot be assessed by conventional methods. The *in vivo* implication of the directionality and velocity observed *in vitro* has not been fully elucidated; however, Terashima *et al.* (25) recently reported that a cytoplasmic protein FROUNT, which is implicated in the directionality of CCR2-mediated monocyte chemotaxis *in vitro*, is indispensable to macrophage infiltration in a murine peritonitis model *in vivo*. Given that the role of macrophages in obese adipose tissue has recently attracted the interest of many researchers of metabolic diseases, this study has introduced a new approach toward the understanding of the molecular mechanism underlying macrophage infiltration into obese adipose tissue.

In this study, we demonstrated that macrophage infiltration is reduced in adipose tissue from *ob/ob* + *CCR2*$^{-/-}$ BMCs relative to *ob/ob* + *CCR2*$^{+/+}$ BMCs. The data of this study suggest

Downloaded from www.jbc.org at Tokyo Ikashika Daigaku on December 29, 2008

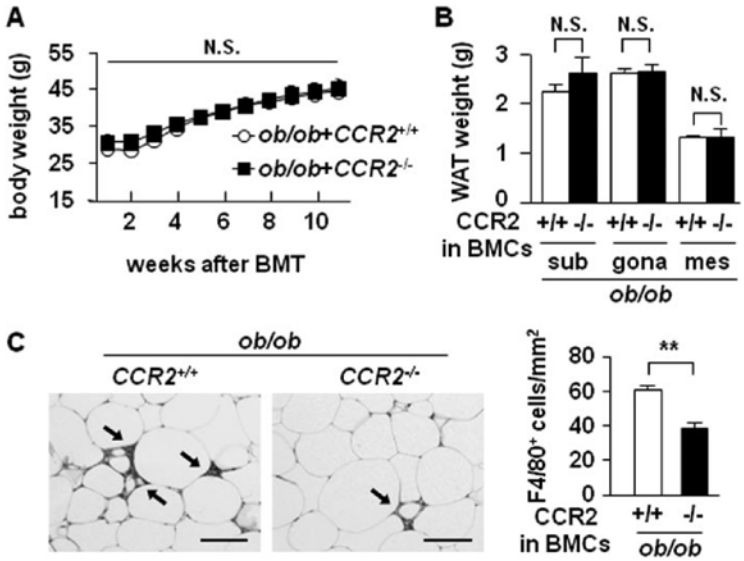

FIGURE 6. **Phenotypic characterization of *ob/ob* mice reconstituted with $CCR2^{+/+}$ or $CCR2^{-/-}$ BMCs.** *A*, growth curve of *ob/ob* mice reconstituted with $CCR2^{+/+}$ BMCs (*ob/ob* + $CCR2^{+/+}$ BMCs) and *ob/ob* mice reconstituted with $CCR2^{-/-}$ BMCs (*ob/ob* + $CCR2^{-/-}$ BMCs) after bone marrow transplantation. *Open circle*, *ob/ob* + $CCR2^{+/+}$ BMCs; *closed square*, *ob/ob* + $CCR2^{-/-}$ BMCs. *B*, weight of the subcutaneous (*sub*), perigonadal (*gona*), and mesenteric (*mes*) adipose tissue. *C*, F4/80 immunostaining (*left*) and the number of F4/80-positive cells (*right*) in the perigonadal adipose tissue. Original magnification was ×200. *Scale bars*, 100 μm. *, $p < 0.05$; **, $p < 0.01$; *N.S.*, not significant. $n = 4–6$.

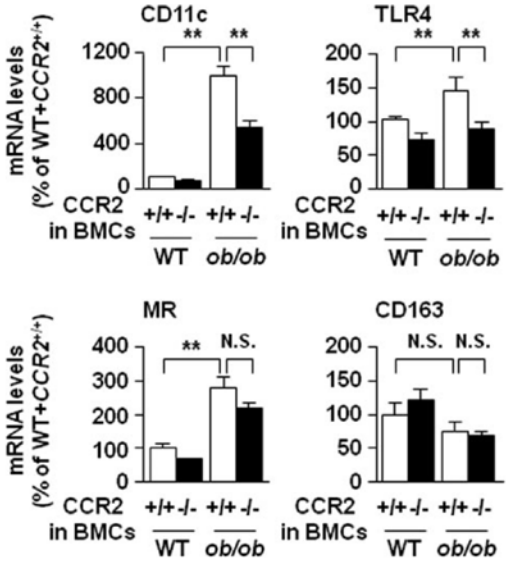

FIGURE 7. **Characterization of adipose tissue macrophages from *ob/ob* mice.** Shown is expression of mRNAs for CD11c and TLR4 (M1 macrophage markers) and that for mannose receptor (*MR*) and CD163 (M2 macrophage markers) in the perigonadal adipose tissue from WT + $CCR2^{+/+}$ BMCs, WT + $CCR2^{-/-}$ BMCs, *ob/ob* + $CCR2^{+/+}$ BMCs, and *ob/ob* + $CCR2^{-/-}$ BMCs. *, $p < 0.05$; **, $p < 0.01$; *N.S.*, not significant. $n = 4–6$.

that CCR2 expressed in BMCs is involved in the recruitment of bone marrow-derived macrophages into obese adipose tissue *in vivo*. In this regard, Tsou *et al.* (34) recently demonstrated by intravenous infusion of *ex vivo*-labeled $CCR2^{-/-}$ BMCs into WT recipient mice with thioglycollate-induced peritonitis that CCR2 and its ligands MCP-1 and MCP-3 are necessary for efficient monocyte recruitment from the systemic circulation to the site of acute inflammation. On the other hand, there are a couple of reports that CCR2 also plays a role in monocyte recruitment from the bone marrow to the systemic circulation (34, 35). In this regard, it would be interesting to know how CCR2 expressed in bone marrow-derived monocytes contributes to the recruitment of monocytes from the bone marrow to the systemic circulation and that from the systemic circulation to obese adipose tissue.

Recent studies have pointed to the heterogeneity of macrophages infiltrated into obese adipose tissue (*i.e.* macrophages in obese adipose tissue have at least two different activation states, M1 or "classically activated" (proinflammatory) and M2 or "alternatively activated" (anti-inflammatory) macrophages) (11, 36). In this study, we demonstrated that mRNA expression of markers for M1-polarized macrophages, CD11c and TLR4, is decreased in *ob/ob* + $CCR2^{-/-}$ BMCs relative to *ob/ob* + $CCR2^{+/+}$ BMCs. On the other hand, there was no significant difference in expression of markers for M2-polarized macrophages, mannose receptor and CD163, between the genotypes of BMCs. Importantly, there was no appreciable difference in the population of $CD11b^{+}CD11c^{+}$ cells in BMCs between the genotypes, suggesting that CCR2 is not involved in $CD11b^{+}CD11c^{+}$ cell differentiation in the bone marrow. Given that CCR2 expression is enriched in proinflammatory M1 macrophages (37), the data of this study support the concept that CCR2 expressed in BMCs plays an important role in the recruitment of bone marrow-derived M1 macrophages into obese adipose tissue (11, 29). Determination of whether CCR2 is sufficient to the recruitment of M1 macrophages into obese adipose tissue must await further investigation.

In this study, we observed that the number of macrophages is significantly reduced in $CCR2^{-/-}$ mice relative to $CCR2^{+/+}$ mice during a high fat diet. This is consistent with a previous report using $CCR2^{-/-}$ mice on the C57BL/6 background, which is identical to ours (8). However, Chen *et al.* (38) did not observe such a difference in macrophage infiltration into obese adipose tissue using $CCR2^{-/-}$ mice on the DBA background. On the other hand, there are several reports supporting the concept that MCP-1 does not contribute to the recruitment of macrophages into obese adipose tissue (39, 40). Given the mildly reduced macrophage infiltration by genetic as well as pharmacologic blockade of

Downloaded from www.jbc.org at Tokyo Ikashika Daigaku on December 29, 2008

CCR2 *in vivo*, there might be other soluble factors that compensate, when CCR2 is disrupted, for the recruitment of macrophages into obese adipose tissue. For instance, recent studies have suggested that osteopontin and CXCL14 (CXC motif chemokine ligand-14) play a role in obesity-induced macrophage infiltration into adipose tissue (41, 42). Indeed, we found that the chemotactic response of CCR2-Jurkat and BMCs is suppressed significantly but not completely by propagermanium, which may be explained by other soluble factor(s) or chemokine(s) secreted from obese adipose tissue. In this study, we also found that concentrations of osteopontin as well as MCP-1 are increased in *ob/ob*-conditioned medium relative to wild type-conditioned medium.[5] Furthermore, we have recently observed that mRNA expression of osteopontin, CCL5 (CC motif chemokine ligand-5), and macrophage colony-stimulating factor, which are all known to recruit macrophages to the site of inflammation, is markedly up-regulated in the adipose tissue from $CCR2^{-/-}$ mice relative to $CCR2^{+/+}$ mice during the course of obesity.[6] It is also important to note that CCR2 is able to recognize other monocyte chemoattractants, such as MCP-2, MCP-3, MCP-4, and MCP-5 (6). In this regard, our *in vitro* assay system herein may help identify novel adipocyte-derived chemokine(s) or even therapeutic agents that target macrophage infiltration into obese adipose tissue.

In conclusion, this study highlights the role of CCR2 expressed in BMCs in the recruitment of bone marrow-derived macrophages into obese adipose tissue, thereby facilitating the better understanding of the pathophysiologic role of CCR2 in obesity-related metabolic syndrome.

Acknowledgments—We thank Dr. M Sata for advice on bone marrow transplantation, Dr. T. Tamatani for discussion, and Dr. G. Quinn for reading the manuscript. We are also grateful to the members of the Ogawa laboratory for discussions.

REFERENCES

1. Weisberg, S. P., McCann, D., Desai, M., Rosenbaum, M., Leibel, R. L., and Ferrante, A. W., Jr. (2003) *J. Clin. Invest.* **112,** 1796–1808
2. Xu, H., Barnes, G. T., Yang, Q., Tan, G., Yang, D., Chou, C. J., Sole, J., Nichols, A., Ross, J. S., Tartaglia, L. A., and Chen, H. (2003) *J. Clin. Invest.* **112,** 1821–1830
3. Berg, A. H., and Scherer, P. E. (2005) *Circ. Res.* **96,** 939–949
4. Suganami, T., Nishida, J., and Ogawa, Y. (2005) *Arterioscler. Thromb. Vasc. Biol.* **25,** 2062–2068
5. Suganami, T., Mieda, T., Itoh, M., Shimoda, Y., Kamei, Y., and Ogawa, Y. (2007) *Biochem. Biophys. Res. Commun.* **354,** 45–49
6. D'Ambrosio, D., Panina-Bordignon, P., and Sinigaglia, F. (2003) *J. Immunol. Methods* **273,** 3–13
7. Charo, I. F., and Taubman, M. B. (2004) *Circ. Res.* **95,** 858–866
8. Weisberg, S. P., Hunter, D., Huber, R., Lemieux, J., Slaymaker, S., Vaddi, K., Charo, I., Leibel, R. L., and Ferrante, A. W., Jr. (2006) *J. Clin. Invest.* **116,** 115–124
9. Kamei, N., Tobe, K., Suzuki, R., Ohsugi, M., Watanabe, T., Kubota, N., Ohtsuka-Kowatari, N., Kumagai, K., Sakamoto, K., Kobayashi, M., Yamauchi, T., Ueki, K., Oishi, Y., Nishimura, S., Manabe, I., Hashimoto, H., Ohnishi, Y., Ogata, H., Tokuyama, K., Tsunoda, M., Ide, T., Murakami, K., Nagai, R., and Kadowaki, T. (2006) *J. Biol. Chem.* **281,** 26602–26614
10. Kanda, H., Tateya, S., Tamori, Y., Kotani, K., Hiasa, K., Kitazawa, R., Kitazawa, S., Miyachi, H., Maeda, S., Egashira, K., and Kasuga, M. (2006) *J. Clin. Invest.* **116,** 1494–1505
11. Lumeng, C. N., Bodzin, J. L., and Saltiel, A. R. (2007) *J. Clin. Invest.* **117,** 175–184
12. Odegaard, J. I., Ricardo-Gonzalez, R. R., Goforth, M. H., Morel, C. R., Subramanian, V., Mukundan, L., Eagle, A. R., Vats, D., Brombacher, F., Ferrante, A. W., and Chawla, A. (2007) *Nature* **447,** 1116–1120
13. Hevener, A. L., Olefsky, J. M., Reichart, D., Nguyen, M. T., Bandyopadyhay, G., Leung, H. Y., Watt, M. J., Benner, C., Febbraio, M. A., Nguyen, A. K., Folian, B., Subramaniam, S., Gonzalez, F. J., Glass, C. K., and Ricote, M. (2007) *J. Clin. Invest.* **117,** 1658–1669
14. Yokochi, S., Hashimoto, H., Ishiwata, Y., Shimokawa, H., Haino, M., Terashima, Y., and Matsushima, K. (2001) *J. Interferon Cytokine Res.* **21,** 389–398
15. Kuziel, W. A., Morgan, S. J., Dawson, T. C., Griffin, S., Smithies, O., Ley, K., and Maeda, N. (1997) *Proc. Natl. Acad. Sci. U. S. A.* **94,** 12053–12058
16. Okabe, M., Ikawa, M., Kominami, K., Nakanishi, T., and Nishimune, Y. (1997) *FEBS Lett.* **407,** 313–319
17. Ito, A., Suganami, T., Miyamoto, Y., Yoshimasa, Y., Takeya, M., Kamei, Y., and Ogawa, Y. (2007) *J. Biol. Chem.* **282,** 25445–25452
18. Itoh, M., Suganami, T., Satoh, N., Tanimoto-Koyama, K., Yuan, X., Tanaka, M., Kawano, H., Yano, T., Aoe, S., Takeya, M., Shimatsu, A., Kuzuya, H., Kamei, Y., and Ogawa, Y. (2007) *Arterioscler. Thromb. Vasc. Biol.* **27,** 1918–1925
19. Kouyama, R., Suganami, T., Nishida, J., Tanaka, M., Toyoda, T., Kiso, M., Chiwata, T., Miyamoto, Y., Yoshimasa, Y., Fukamizu, A., Horiuchi, M., Hirata, Y., and Ogawa, Y. (2005) *Endocrinology* **146,** 3481–3489
20. Flachs, P., Mohamed-Ali, V., Horakova, O., Rossmeisl, M., Hosseinzadeh-Attar, M. J., Hensler, M., Ruzickova, J., and Kopecky, J. (2006) *Diabetologia* **49,** 394–397
21. Toyoda, T., Kamei, Y., Kato, H., Sugita, S., Takeya, M., Suganami, T., and Ogawa, Y. (2008) *Obesity* (*Silver Spring*) **16,** 1199–1207
22. Kanegasaki, S., Nomura, Y., Nitta, N., Akiyama, S., Tamatani, T., Goshoh, Y., Yoshida, T., Sato, T., and Kikuchi, Y. (2003) *J. Immunol. Methods* **282,** 1–11
23. Nitta, N., Tsuchiya, T., Yamauchi, A., Tamatani, T., and Kanegasaki, S. (2007) *J. Immunol. Methods* **320,** 155–163
24. Nishio, M., Watanabe, K., Sasaki, J., Taya, C., Takasuga, S., Iizuka, R., Balla, T., Yamazaki, M., Watanabe, H., Itoh, R., Kuroda, S., Horie, Y., Forster, I., Mak, T. W., Yonekawa, H., Penninger, J. M., Kanaho, Y., Suzuki, A., and Sasaki, T. (2007) *Nat. Cell Biol.* **9,** 36–44
25. Terashima, Y., Onai, N., Murai, M., Enomoto, M., Poonpiriya, V., Hamada, T., Motomura, K., Suwa, M., Ezaki, T., Haga, T., Kanegasaki, S., and Matsushima, K. (2005) *Nat. Immunol.* **6,** 827–835
26. Maki, W., Morales, R. E., Carroll, V. A., Telford, W. G., Knibbs, R. N., Stoolman, L. M., and Hwang, S. T. (2002) *J. Immunol.* **169,** 2346–2353
27. Maeda, N., Takahashi, M., Funahashi, T., Kihara, S., Nishizawa, H., Kishida, K., Nagaretani, H., Matsuda, M., Komuro, R., Ouchi, N., Kuriyama, H., Hotta, K., Nakamura, T., Shimomura, I., and Matsuzawa, Y. (2001) *Diabetes* **50,** 2094–2099
28. Tsuchida, A., Yamauchi, T., Takekawa, S., Hada, Y., Ito, Y., Maki, T., and Kadowaki, T. (2005) *Diabetes* **54,** 3358–3370
29. Lumeng, C. N., Deyoung, S. M., Bodzin, J. L., and Saltiel, A. R. (2007) *Diabetes* **56,** 16–23
30. Boyden, S. (1962) *J. Exp. Med.* **115,** 453–466
31. Cutler, J. E., and Munoz, J. J. (1974) *Proc. Soc. Exp. Biol. Med.* **147,** 471–474
32. John, T. J., and Sieber, O. F., Jr. (1976) *Life Sci.* **18,** 177–181
33. Nelson, R. D., Quie, P. G., and Simmons, R. L. (1975) *J. Immunol.* **115,** 1650–1656
34. Tsou, C. L., Peters, W., Si, Y., Slaymaker, S., Aslanian, A. M., Weisberg, S. P., Mack, M., and Charo, I. F. (2007) *J. Clin. Invest.* **117,** 902–909
35. Serbina, N. V., and Pamer, E. G. (2006) *Nat. Immunol.* **7,** 311–317
36. Zeyda, M., Farmer, D., Todoric, J., Aszmann, O., Speiser, M., Gyori, G.,

[5] A. Ito, T. Suganami, A. Yamauchi, M. Degawa-Yamauchi, M. Tanaka, R. Kouyama, Y. Kobayashi, N. Nitta, K. Yasuda, Y. Hirata, W. A. Kuziel, M. Takeya, S. Kanegasaki, Y. Kamei, and Y. Ogawa, unpublished data.

[6] M. Tanaka, T. Suganami, Y. Ogawa, unpublished data.

Downloaded from www.jbc.org at Tokyo Ikashika Daigaku on December 29, 2008

Zlabinger, G. J., and Stulnig, T. M. (2007) *Int. J. Obes.* (*Lond.*) **31,** 1420–1428
37. Tacke, F., and Randolph, G. J. (2006) *Immunobiology* **211,** 609–618
38. Chen, A., Mumick, S., Zhang, C., Lamb, J., Dai, H., Weingarth, D., Mudgett, J., Chen, H., MacNeil, D. J., Reitman, M. L., and Qian, S. (2005) *Obes. Res.* **13,** 1311–1320
39. Chow, F. Y., Nikolic-Paterson, D. J., Ma, F. Y., Ozols, E., Rollins, B. J., and Tesch, G. H. (2007) *Diabetologia* **50,** 471–480
40. Inouye, K. E., Shi, H., Howard, J. K., Daly, C. H., Lord, G. M., Rollins, B. J., and Flier, J. S. (2007) *Diabetes* **56,** 2242–2250
41. Nara, N., Nakayama, Y., Okamoto, S., Tamura, H., Kiyono, M., Muraoka, M., Tanaka, K., Taya, C., Shitara, H., Ishii, R., Yonekawa, H., Minokoshi, Y., and Hara, T. (2007) *J. Biol. Chem.* **282,** 30794–30803
42. Nomiyama, T., Perez-Tilve, D., Ogawa, D., Gizard, F., Zhao, Y., Heywood, E. B., Jones, K. L., Kawamori, R., Cassis, L. A., Tschop, M. H., and Bruemmer, D. (2007) *J. Clin. Invest.* **117,** 2877–2888

The Journal of Biological Chemistry ASBMB jbc

Downloaded from www.jbc.org at Tokyo Ikashika Daigaku on December 29, 2008

MEMO

形質発現分野

萩原 正敏

疾患生命科学研究部・高次生命制御研究部門
形質発現制御学・教授

1. 研究の題目

スプライシング暗号の解明

Deciphering of splicing codes

2. 研究内容

ヒトのタンパク質をコードする遺伝子数が約2万数千個程度と、当初予想された数よりはるかに少なく、一方で、75%以上の遺伝子に複数の型の成熟mRNAが存在しており、多細胞生物の複雑な形態や巧妙な機能を支えるタンパク質の多様性には、mRNA前駆体の選択的スプライシングが大きく寄与している。しかし、生体内で選択的スプライシングを組織特異的、発生段階依存的に制御する分子機構、すなわち「スプライシング暗号」の解明はあまり進んでいない。形質発現制御学研究室では、生体における選択的スプライシング制御機構を明らかにするために、複数の蛍光タンパク質をレポーターとして、細胞ごとの選択的スプライシング・パターンを色として可視化するトランスジェニック動物の作製法を開発してきた。本研究は、モデル生物として線虫（C. elegans）を用い、発生段階依存的に制御される遺伝子の選択的スプライシング制御機構を解明したものである。

線虫のコラーゲンの遺伝子let-2は、線虫の成長に伴って、生成される成熟mRNAが胚型から成虫型へと選択的スプライシングによって切り替わる。そこで、胚型なら緑色の蛍光タンパク質GFPが、成虫型なら赤色の蛍光タンパク質RFPが造られるようにレポーター・ミニ遺伝子を作製し、トランスジェニック線虫を作製した。その結果、成長に伴うlet-2の選択的スプライシング・パターンの変化を、緑色から赤色への蛍光の変化として、生きたまま観察することに成功した。そして、成虫になっても緑色のままである変異体を単離することによって、胚型から成虫型へ切り替わるのに必要な制御因子を同定し、ASD-2と命名した。さらに、このasd-2変異体で見られるスプライシングの途中段階の生成物を解析することによって、let-2遺伝子の選択的スプライシングの制御には、イントロン除去の順序が重要であることを明らかにした。

3.

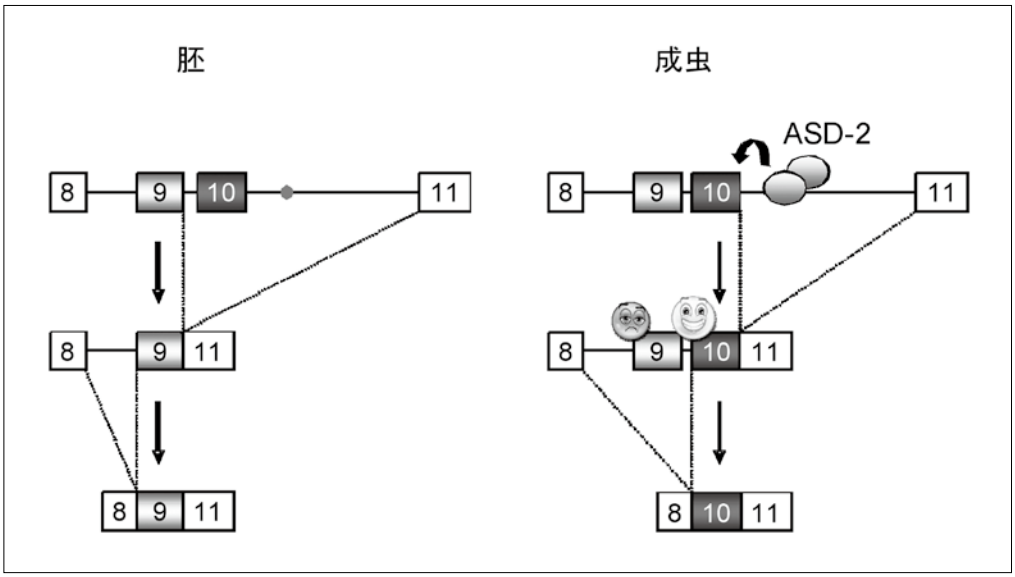

4. 研究内容（英文）

Spatiotemporal patterns of gene expression in metazoans are defined through transcription1 and alternative splicing of pre-mRNA. However, the mechanisms and importance of developmentally regulated alternative splicing are poorly understood in comparison with the transcriptional regulation. As let-2 gene encoding α 2（IV）collagen in Caenorhabditis elegans shows dramatic switching of its mutually exclusive exons 9 and 10 during larval development, we tried to identify the splicing regulator, using originally developed splicing reporter system in living worms. Here we isolated alternative splicing defective-2（asd-2）gene, encoding a novel member of evolutionarily conserved GSG/STAR family of RNA binding proteins, as a regulator of the selection of let-2 alternative exons. We found that removal of either of their downstream introns is the first and determinant step of the let-2 mutually exclusive exons. We further show that the biased removal of the intron between exons 10 and 11 in larval stages depends on asd-2 and specific sequence of the let-2 pre-mRNA. Our results demonstrate how modulated use of the mutually exclusive exons of let-2 is defined. The splicing mechanism of let-2 described here is the first case to reveal the sequence of processing steps of developmentally regulated mutually exclusive splicing in vivo.

5. 本事業に関連して世界的な研究拠点形成に向けて、以下の点で改善・整備等されたこと

A（研究拠点体制）

海外との共同研究を新たに3件開始した。

C（人材確保）

瀋陽（中国）およびハノイ（ベトナム）で大学院説明会を開催した。

D（人材育成）

博士課程前期学生1名が優秀賞の表彰を受け修了した。

E（国際化）

カナダのケベック大学より、留学生を受け入れた。

6. GCOE事業を推進するに当たって力を入れた点

質の高いサイエンスを自ら切り開く優秀な大学院生の育成に注力している。

7. 英文原著論文

1. Jiang K, Patel NA, Watson JE, Apostolatos H, Kleiman E, Hanson O, Hagiwara M, Cooper DR.（2009）Akt2 regulation of Cdc2-like kinases（Clk/Sty）, serine/arginine-rich（SR）protein phosphorylation, and insulin-induced alternative splicing of PKCssII mRNA. Endocrinology in press.
2. Yomoda, J., Muraki, M., Kataoka, N., Hosoya, T., Suzuki, M., Hagiwara, M. and Kimura, H.（2008）Combination of Clk family kinase and SRp75 modulates alternative splicing of Adenovirus E1A. Genes Cells, 13, 233-244.
3. Ohno, G., Hagiwara, M. and Kuroyanagi, H.（2008）STAR family RNA-binding protein ASD-2 regulates developmental switching of mutually exclusive alternative splicing in vivo. Genes & Dev., 22,360-374.

8. 著書

萩原正敏（2008）

ケミカルバイオロジー概論　日薬理誌 132, 4-6.

萩原正敏（2008）

リン酸化酵素阻害薬によるケミカルバイオロジー研究の展開　日薬理誌 132, 22-25.

9. 特許権

1）発明の名称:発光タンパク質を用いたリン酸化酵素阻害物質のスクリーニング方法

①発明者:萩原正敏、野村奈美子、木村広、野崎直仁

②出願日:2008年3月4日（特願 2008-053502）

③出願人:国立大学法人東京医科歯科大学

④発明の内容の概略:発光タンパク質エクオリンを用いて、non-RIで高感度かつ簡便にリン酸化酵素阻害物質をスクリーニングする技術に関する特許。

2）発明の名称:抗ウイルス作用を有するアニリン誘導体

①発明者:萩原正敏、小野木博、鈴木正昭

②出願日:2008年3月25日（特願 2008-078728）

③出願人:株式会社　キノファーマ

④発明の内容の概略: RNAウイルスに対して抗ウイルス作用を有するアニリン誘導体に関する特許。

10. 自己評価

大学院生1名がGenes & Devの表紙を飾る論文を、筆頭著者として書き上げ採択されたことは、質の高いサイエンスを自ら切り開く優秀な大学院生の育成に成功しつつあると自負している。Gordonや国際生化学・分子生物学会に招待されるなど、本研究室自体も世界的な研究拠点として高い評価を受けはじめている。

11. 外部資金の獲得状況

（科学研究費補助金、受託研究費、外部財団の助成など）

保健医療分野における基礎研究推進事業

SR蛋白リン酸化酵素阻害剤の抗ウイルス活性に関するinvivo及びinvitroでの検討

代表:萩原　正敏
期間:H16-H20
研究費総額:220,000,000

キーテクノロジー研究開発の推進
(社会のニーズを踏まえたライフサイエンスの研究開発)
難治感染症に対する新規治療薬開発のためのイメージング研究
代表:萩原　正敏
期間:H19-H21
研究費総額:60,700,000

一般共同
リン酸化阻害剤による難治疾患治療に関する研究
代表:萩原　正敏
期間:H17-H20
研究費総額:5,439,000

科学研究費補助金、特定
ヘルペスウイルスRNAの核外輸送制御機構の解明
代表:萩原　正敏
期間:H19-H20
研究費総額:7,600,000

科学研究費補助金、基盤B
イントロンレスRNAの核外輸送の分子メカニズム
代表:萩原　正敏
期間:H19-H20
研究費総額:18,980,000

12. 特別講演、招待講演

萩原正敏:
POST-TRANSCRIPTIONAL　GENE REGULATION,THE　BIOLOGY　OF、アメリカ、2008年7月

萩原正敏:
中国医科大学国際シンポジウム、中国、2008年11月

萩原正敏:
Visualization and manipulation of alternative splicing
BMB2008、神戸、2008年12月

萩原正敏:
The Expanding World of Post-transcriptional Regulation on Gene Expression 病態発現機構国際シンポジウム、東京、2008年12月

13. 主催学会　(学会名、日時、場所)

1.BMB2008、神戸、2008年12月

2.The Expanding World of Post-transcriptional Regulation on Gene Expression 病態発現機構国際シンポジウム　東京、2008年12月

14. 新聞、雑誌、TV報道

2001年1月30日
毎日新聞

たんぱく作り分け
遺伝子の暗号特定
東京医科歯科大が手法開発

生物の体内で、一つの遺伝子から多種のたんぱく質を作り分ける「選択的スプライシング」が起きる際、作り分けを指示する遺伝子内の"暗号"を特定する手法を、東京医科歯科大の研究グループが開発した。スプライシングは、限られた遺伝子で複雑な生体を作るのに不可欠だが、作り分けを指示する暗号を特定する手段はなかった。スプライシングの異常で起こる遺伝病の解明にもつながる成果で、28日付の米国の専門誌に発表した。

ヒトの遺伝子の数はショウジョウバエの約2倍の二万数千しかないが、約20万種類のたんぱく質を作る。スプライシングは、一つの遺伝子から必要な部分だけを抜き出して組み合わせ、たんぱく質を作るもとの伝令RNA(mRNA)を作り出す仕組み。組み合わせによって異なる色で光るスプライシングが分かる。遺伝子の一部に傷をつけて光らせる実験によって、作り分けを指示する暗号となるmRNAの変化を、生きたまま観察することに成功した。色の変化によって、正常なスプライシングが分かるようにした遺伝子を線虫に導入して成長させ、スプライシングによるmRNAの変化を、生きたまま観察することに成功した。色の変化によって、正常なスプライシングが分かるようにした遺伝子を線虫に導入して成長させ、スプライシングによるmRNAの変化を、生きたまま観察することに成功した。色の変化によって、正常なスプライシングが分かる。遺伝子の一部に傷をつけて光らせる実験によって、作り分けを指示する暗号となるmRNAの変化を、生きたまま観察することに成功した。色の変化によって、正常なスプライシングが分かる。遺伝子の一部に傷をつけて光らせる実験によって、作り分けを指示する暗号となるmRNAの変化を、生きたまま観察することに成功した。色の変化によって、正常なスプライシングが分かる。遺伝子の一部に傷をつけて光らせる実験によって、作り分けを指示する暗号となるmRNAの変化を、生きたまま観察することに成功した。色の変化によって、正常なスプライシングが分かる。遺伝子の一部に傷をつけて光らせる実験によって、作り分けを指示する暗号となるmRNAの変化を、生きたまま観察することに成功した。色の変化によって、正常なスプライシングが分かる。遺伝子の一部に傷をつけて光らせる実験によって、作り分けを指示する暗号となる部分を見つけることができた。【須田桃子】

2008年4月7日
日本経済新聞

C型肝炎やインフルエンザ
多種ウイルス 増殖抑制
新薬候補を発見
科学
13万年前の大気分析
細胞実験で効果確認
日米欧など 南極と比較も

2008年5月29日
日経産業新聞

データ構築、新薬の源に

15. サマリー

ヒトの蛋白質をコードする遺伝子数が約2万3千個程度と、当初予想された数よりはるかに少なく、蛋白質の多様性には、選択的スプライシングが大きく寄与すると推測される。実際に、ヒトでは全遺伝子の実に3分の2が複数のmRNAフォームを持つとされ、多くの遺伝子が組織特異的あるいは細胞種特異的な選択的スプライシングを示すことが確かめられつつあり、遺伝病の多くはスプライシングへの影響に起因するとの推測もなされている。しかしながら、生体内で選択的スプライシングのパターンを決定する制御機構、すなわち”スプライシング暗号（splicing code）”の解明は進んでいない。そこで我々は、以下に述べる様々なアプローチで、スプライシング暗号の解明に挑戦している。

16. 講座の准教授、講師、助教、特別研究員、ポスドク、指導を受けた大学院生の名前（AISSには○印）のリスト

教　授	萩原　正敏
准教授	黒柳　秀人
准教授（客員）	廣瀬　哲朗
助　教	武内　章英
特任助教	小川　靖、野島　孝之、 二宮　賢介（4月～）
技術補佐員	井手上　社子、土橋　泉（～8月）、 堀内　真千子（4月～） 遠藤　澄恵（～3月）
大学院生	川村　豪伸、山本　誠、 大野　源太, 野中　洋介（4月～）、 仲野谷　宗図（～3月）、 細川　元靖、 都甲　麻理奈（4月～）、 ジュネィドゥ　パラヤン（9月～）、

Downloaded from genesdev.cshlp.org on March 17, 2009 - Published by Cold Spring Harbor Laboratory Press

Genes & Development

STAR family RNA-binding protein ASD-2 regulates developmental switching of mutually exclusive alternative splicing in vivo

Genta Ohno, Masatoshi Hagiwara and Hidehito Kuroyanagi

Genes Dev. 2008 22: 360-374 originally published online January 29, 2008
Access the most recent version at doi:10.1101/gad.1620608

Supplemental Material http://genesdev.cshlp.org/content/suppl/2008/01/16/gad.1620608.DC1.html

References This article cites 78 articles, 43 of which can be accessed free at:
http://genesdev.cshlp.org/content/22/3/360.full.html#ref-list-1

Article cited in:
http://genesdev.cshlp.org/content/22/3/360.full.html#related-urls

Email alerting service Receive free email alerts when new articles cite this article - sign up in the box at the top right corner of the article or **click here**

To subscribe to *Genes & Development* go to:
http://genesdev.cshlp.org/subscriptions

Copyright © 2008, Cold Spring Harbor Laboratory Press

STAR family RNA-binding protein ASD-2 regulates developmental switching of mutually exclusive alternative splicing in vivo

Genta Ohno,[1] Masatoshi Hagiwara,[1,2,4] and Hidehito Kuroyanagi[1,2,3]

[1]Laboratory of Gene Expression, School of Biomedical Science, Tokyo Medical and Dental University, Tokyo 113-8510, Japan; [2]Department of Functional Genomics, Medical Research Institute, Tokyo Medical and Dental University, Tokyo 113-8510, Japan

Alternative splicing of pre-mRNAs greatly contributes to the spatiotemporal diversity of gene expression in metazoans. However, the molecular basis of developmental regulation and the precise sequence of alternative pre-mRNA processing in vivo are poorly understood. In the present study, we focus on the developmental switching of the mutually exclusive alternative splicing of the *let-2* gene of *Caenorhabditis elegans* from the exon 9 form in embryos to the exon 10 form in adults. By visualizing the usage of the *let-2* mutually exclusive exons through differential expression of green fluorescent protein (GFP) and red fluorescent protein (RFP), we isolated several switching-defective mutants and identified the *alternative splicing defective-2* (*asd-2*) gene, encoding a novel member of the evolutionarily conserved STAR (signal transduction activators of RNA) family of RNA-binding proteins. Comparison of the amounts of partially spliced *let-2* RNAs in synchronized wild-type and *asd-2* mutant worms suggested that either of the introns downstream from the *let-2* mutually exclusive exons is removed prior to the removal of the upstream ones, and that *asd-2* promotes biased excision of intron 10 in the late larval stages. We propose that the developmental switching between alternative sequences of intron removal determines the ratio between the mature *let-2* mRNA isoforms.

[*Keywords*: Alternative splicing; *C. elegans*; reporter; development; GSG/STAR; processing intermediate]

Supplemental material is available at http://www.genesdev.org.

Received September 27, 2007; revised version accepted December 4, 2007.

Alternative pre-mRNA splicing is a crucial step of gene expression and provides proteome diversity from a limited number of genes in metazoan. Recent global studies have demonstrated that as many as two thirds of human genes have multiple alternative isoforms of mature mRNAs (Modrek and Lee 2002; Johnson et al. 2003; Blencowe 2006), and that deregulation of alternative splicing may cause hereditary diseases and cancer (Faustino and Cooper 2003; Venables 2004; Licatalosi and Darnell 2006). Many alternative splicing events are controlled in tissue- and cell-type-dependent manners (Black 2003; Matlin et al. 2005), and a variety of auxiliary *trans*-acting factors and *cis*-acting elements involved in the regulation of alternative splicing have been identified through biochemical, genetic, and bioinformatic analyses.

Mutually exclusive alternative splicing is a strictly regulated form of alternative splicing; only one out of two or more candidate exons are used in the mature mRNA isoform (Smith 2005). This type of alternative splicing raises two main questions; what ensures selection of only one out of multiple exons at one time, and how the selection of the exons is switched. The most extreme example of the mutually exclusive alternative splicing is in the *Dscam* gene of *Drosophila*. It has multiple clusters of variable exons and potentially produces >38,000 different mRNA and protein isoforms (Schmucker et al. 2000). Graveley raised a model that interaction between the only one docking site and one of multiple selector sequences that reside in the introns upstream of the variable exons allows only one variable exon out of 48 alternative exons in the exon 6 cluster to be selected (Graveley 2005). It has been demonstrated that mutually exclusive selection of two exons of the α-tropomyosin and the α-actinin genes in vertebrates is enforced by the absolute incompatibility of the two adjacent exons due to the close proximity of the branchpoint(s) for the downstream exon to the donor site of the upstream exon (Smith and Nadal-Ginard 1989; Southby

Corresponding authors.
[3]E-MAIL kuroyana.end@tmd.ac.jp; FAX 81-3-5803-5853.
[4]E-MAIL m.hagiwara.end@mri.tmd.ac.jp; FAX 81-3-5803-5836.
Article published online ahead of print. Article and publication date are online at http://www.genesdev.org/cgi/doi/10.1101/gad.1620608.

et al. 1999). The mutually exclusive selection of duplicated exons in the human *JNK1* gene is considered to be ensured by the incompatibility between the U2-type major intron and the U12-type minor intron (Letunic et al. 2002). Mutually exclusive exons may not necessarily be strictly regulated, but nonsense-mediated mRNA decay (NMD) may contribute to the apparent fidelity of the mutually exclusive selection when neither of the exons is a multiple of three nucleotides (Jones et al. 2001b).

Mutually exclusive alternative splicing is often regulated in a tissue-specific manner. Several *trans*-acting factors and multiple *cis*-elements have been demonstrated to regulate the mutually exclusive exons of the FGFR2, α-actinin, and α- and β-tropomyosin genes in the cultured cells (Chen et al. 1999; Jones et al. 2001a; Muh et al. 2002; Baraniak et al. 2003, 2006; Gromak et al. 2003a,b; Expert-Bezancon et al. 2004; Lin and Tarn 2005; Wagner et al. 2005; Crawford and Patton 2006). However, the mechanisms of the tissue-specific mutually exclusive alternative splicing are to be evaluated in vivo.

To pave the way to identify regulators of alternative splicing in living organisms, we recently developed a transgenic reporter worm system that visualizes the tissue-specific expression profiles of each of the mutually exclusive exons through differential expression of green fluorescent protein (GFP) and red fluorescent protein (RFP) (Kuroyanagi et al. 2006). With this system, we demonstrated that the evolutionarily conserved Fox-1 subfamily of RNA-binding proteins ASD-1 (for Alternative Splicing Defective-1) and FOX-1 regulate tissue-specific alternative splicing of the fibroblast growth factor (FGF) receptor gene in *Caenorhabditis elegans* (Kuroyanagi et al. 2006). This work provided an example of tissue-specific regulation of mutually exclusive exons in vivo, and provided evidence that the Fox-1-mediated regulation of alternative splicing (Jin et al. 2003) is conserved between vertebrates and nematodes.

The *let-2* gene, encoding α2 (IV) collagen of *C. elegans*, has a unique property in that selection of its mutually exclusive exon 9 and exon 10 in body wall muscles undergoes dramatic switching along with the larval development (see Fig. 1A); in embryos, an mRNA isoform with exon 9 is exclusively expressed, while in late larval and adult stages, an mRNA isoform with exon 10 predominates (Sibley et al. 1993; Graham et al. 1997). This developmental regulation of *let-2* alternative splicing is evolutionarily conserved in two distantly separated nematodes, *C. elegans* and *Ascaris* (Sibley et al. 1993; Pettitt and Kingston 1994), and it is speculated that switching of exon 9 and exon 10 alters the characteristics of basement membranes during nematode development. In the present study, we applied the transgenic alternative splicing reporter system to analyze the developmentally regulated switching mechanism of the mutually exclusive exons of the *let-2* gene, and identified a novel member of the highly conserved STAR (signal transduction activators of RNA) family RNA-binding proteins, ASD-2 (for Alternative Splicing Defective-2), as a regulator of the *let-2* alternative splicing.

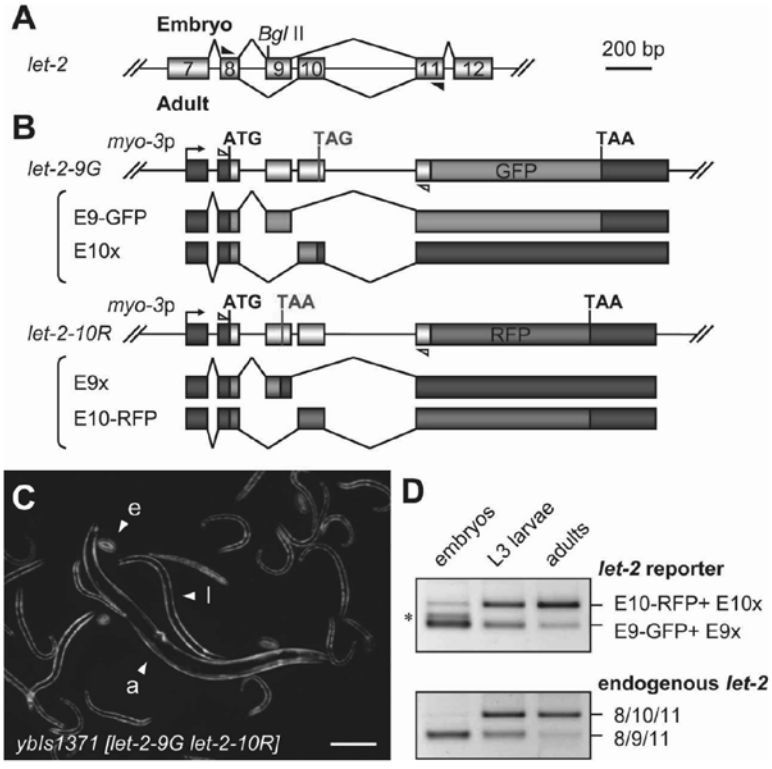

Figure 1. Visualization of the developmentally regulated mutually exclusive alternative splicing patterns of the *let-2* gene. (*A*) Schematic view of the alternatively spliced regions of the endogenous *let-2* gene. Boxes indicate exons. Closed triangles indicate positions and directions of the PCR primers used to amplify the cDNA fragments from the endogenous *let-2* mRNAs in *D* and Figure 2B. (*B*) Structure of a pair of the *let-2* reporter minigenes, *let-2*-9G and *let-2*-10R, and mRNAs derived from the minigenes. Predicted ORFs are colored in green (E9-GFP), red (E10-GFP), or gray (E10x and E9x). Open triangles indicate positions and directions of the PCR primers used to amplify the cDNAs derived from the *let-2* reporter mRNAs in *D* and Figure 2B. (*C*) A microphotograph of worms with a transgenic allele *ybIs1371 [myo-3::let-2-9G myo-3::let-2-10R]*, expressing the *let-2* reporters under the *myo-3* promoter. Arrowheads indicate an embryo (e), an L3 larva (l), and a young adult (a). Bar, 100 µm. (*D*) RT–PCR analysis of the *let-2* reporter (*top*) and the endogenous *let-2* (*bottom*). Note that BglII digested the PCR products containing exon 9 into halves. An asterisk denotes a nonspecific band.

Results

Transgenic reporter system visualizes the developmentally regulated mutually exclusive alternative splicing of the let-2 *gene in vivo*

In order to monitor the selection of the *let-2* mutually exclusive exons (Fig. 1A) in vivo, we constructed a pair of reporter minigenes, *let-2-9G* and *let-2-10R* (Fig. 1B). The minigenes carry the same *let-2* genomic DNA fragment spanning from exon 8 to exon 11 connected in-frame to cDNAs for fluorescent proteins, and termination codons are artificially introduced into exon 10 of *let-2-9G* and exon 9 of *let-2-10R* (Fig. 1B). We expected that, from the *let-2-9G* minigene, selection of exon 9 would lead to expression of an mRNA encoding a GFP fusion protein (E9-GFP), while selection of exon 10 would result in a nonproductive mRNA (E10x) due to the termination codon (Fig. 1B). In the same way, selection of exon 10 would lead to expression of an mRNA encoding an RFP fusion protein (E10-RFP) and selection of exon 9 would result in a nonproductive mRNA (E9x) from the *let-2-10R* minigene (Fig. 1B).

The *let-2* reporter successfully visualized the alternative exon usage. We drove expression of the *let-2* reporter minigenes under the body wall muscle-specific *myo-3* promoter, since the endogenous *let-2* is primarily expressed in the body wall muscles (Graham et al. 1997). As expected, expression of the *let-2* reporter in the body wall muscles gradually and almost completely switched from GFP to RFP along with the development; embryos exclusively express E9-GFP and elder worms express E10-RFP (Fig. 1C). RT–PCR analyses of mRNA isoforms derived from the minigenes confirmed that the alternative exons are selected mutually exclusively to produce the E9-GFP and E10x mRNA isoforms from the *let-2-9G* minigene, and the E9x and E10-RFP isoforms from the *let-2-10R* minigene (data not shown). Consistent with the color switch of the *let-2* reporter worms, the composition of the reporter mRNAs gradually switched from the exon 9 forms to the exon 10 forms in parallel with that of the endogenous *let-2* mRNAs along with the developmental stage (Fig. 1D). These results indicate that the *let-2* reporter visualizes the developmental switching of the *let-2* mutually exclusive exons in vivo.

asd-2 *mutants are defective in the developmental switching of alternative splicing of both the* let-2 *reporter and the endogenous* let-2 *gene*

To identify factors regulating the *let-2* alternative splicing in vivo, we screened for mutants defective in the developmental switching of the *let-2* alternative splicing reporter expression in the body wall muscles. We mutagenized the transgenic reporter allele *ybIs1371* (Fig. 1C) and screened ~5×10^4 genomes for F2 progeny that remain green until adulthood or that turn red as younger larvae. We isolated several independent mutant alleles, all of which remain green during larval development but eventually turn red in the senile stage (Fig. 2A; data not shown). RT–PCR analysis of the *let-2* reporter confirmed that the mutants are defective in the switching to the exon 10 forms in the late larval stage (Fig. 2B, top panel) in parallel with the defect in the color switch. Furthermore, the mutants are also defective in the exon switching of the endogenous *let-2* mRNAs (Fig. 2B, bottom panel), indicating that the *let-2* reporter reflected the expression of the endogenous *let-2* gene and allowed the isolation of alternative splicing defective mutants.

Single nucleotide polymorphism (SNP)-based chromosome mapping and genomic DNA sequencing suggested that the mutants are alleles of a single uncharacterized gene, T21G5.5 (see below). RNAi of the gene reproduced the color phenotype (Fig. 2C), confirming that the defect in the switching of the *let-2* reporter expression resulted from loss or reduction of function of the gene. We therefore named it *alternative splicing defective-2* (*asd-2*). Figure 2D represents a schematic structure of the *asd-2* gene and summarizes the mutations identified in the *asd-2* mutant alleles. Expressed sequence tag (EST) analysis has predicted that the *asd-2* gene produces two protein isoforms, ASD-2a and ASD-2b, that differ in the N terminus sequence due to alternative use of the first exons (Fig. 2D), and we confirmed expression of both of the isoforms by cloning RT–PCR products (deposited to GenBank under accession nos. EF630625 and EF630626).

ASD-2 is a novel member of the evolutionarily conserved STAR family

ASD-2 belongs to the evolutionarily conserved STAR family of RNA-binding proteins (Vernet and Artzt 1997). The family members share a highly conserved tripartite GSG (for GRP33, Sam68, GLD-1)/STAR domain (Jones and Schedl 1995; Vernet and Artzt 1997) composed of a single KH-type RNA-binding domain and two flanking domains called QUA1 and QUA2 (Fig. 3A). QUA1 is required and sufficient for homodimer formation of *C. elegans* GLD-1 and mouse QKI (Chen and Richard 1998; Ryder et al. 2004). QUA2 is involved in the RNA binding together with the KH domain for GLD-1 and human SF1 (Liu et al. 2001; Ryder et al. 2004; Lehmann-Blount and Williamson 2005). Figure 3B shows the phylogenetic tree of the GSG/STAR domains of the STAR family proteins from *C. elegans* and mammals and *Drosophila* Held Out Wings (HOW). ASD-2 GSG/STAR domain has 68%, 66%, and 74% identity with those of GLD-1, QKI, and HOW, respectively, while the ASD-2 KH-QUA2 domains have only 37% identity to those of human SF1. These sequence analyses indicated that ASD-2 belongs to the GLD-1 subfamily that includes QKI and HOW.

Mutations identified in the *asd-2* mutants affect conserved residues in the GSG/STAR domain or the entire structure of the ASD-2b protein. Five missense mutations were assigned to the conserved residues within the GSG/STAR domain (Fig. 3A). *yb1422* causes G125E substitution within the QUA1 domain. *yb1415*, *yb1470*, and *yb1419* cause R154C, H193Y, and L202F substitutions within the KH RNA-binding domain, respectively. *yb1423* causes E244K substitution within the QUA2 do-

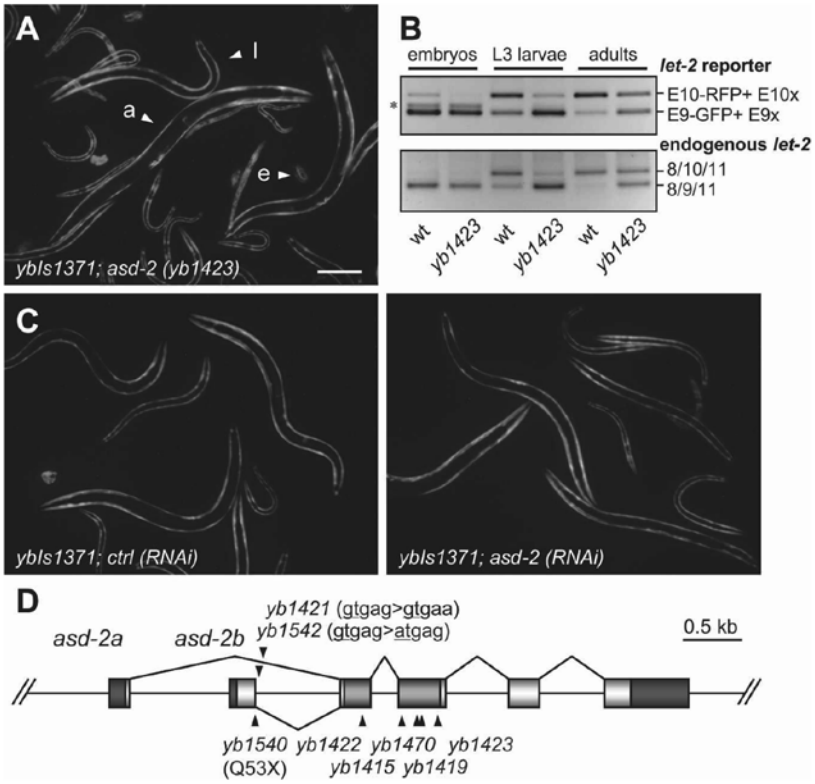

Figure 2. The *asd-2* mutants defective in the developmental switching of the *let-2* alternative splicing. (*A*) A microphotograph of a mutant allele, *ybIs1371; asd-2 (yb1423)*. Arrowheads indicate an embryo (e), an L3 larva (l), and a young adult (a). (*B*) RT–PCR analysis of the *let-2* reporter (*top*) and the endogenous *let-2* (*bottom*). The genotypic backgrounds and the stages of the worms are indicated. An asterisk denotes a nonspecific band. (wt) Wild type. (*C*) RNAi of the *asd-2* gene. Microphotographs of the F1 progeny of the *ybIs1371* reporter worms treated with buffer alone (*left* panel) or with *asd-2* dsRNA (*right* panel). Bar in *A*, 100 µm. (*D*) Schematic representation of the *asd-2* gene. Boxes indicate exons. The ORFs are in white. The GSG/STAR domain is in light gray. UTRs are in dark gray. Mutations identified in the mutant alleles are indicated.

main. Putative *asd-2b*-specific null mutations were identified in the other three alleles. *yb1540* causes nonsense mutation in the first exon of the *asd-2b* isoform (Fig. 2D). *yb1421* and *yb1542* have base substitutions at the splice donor site in the first intron of the *asd-2b* isoform (Fig. 2D). These results suggested that the RNA-binding property of the ASD-2b isoform is responsible for the developmental switching of the *let-2* mutually exclusive exons in the body wall muscles.

ASD-2b regulates the switching of the let-2 reporter in the body wall muscles

We then analyzed the expression profiles of the *asd-2a* and *asd-2b* isoforms. We constructed transcriptional fusion minigenes, *asd-2a*::*GFP* and *asd-2b*::*RFP* (Fig. 4A). These reporters showed differential tissue-specific expression profiles throughout development (Fig. 4B). Expression of *asd-2a*::*GFP* was detected in hypodermis and pharyngeal muscles. On the other hand, expression of *asd-2b*::*RFP* was observed in the body wall muscles and the pharyngeal muscles, consistent with the idea that *asd-2b* is responsible for the regulation of the *let-2* alternative splicing in the body wall muscles.

Next, we asked whether expression of ASD-2b in the body wall muscle rescues the color phenotype of the *asd-2* mutant. Overexpression of ASD-2b under the body wall muscle-specific *myo-3* promoter overrescued the *asd-2 (yb1423)* mutant, and enforced E10-RFP expression even in early developmental stages (Fig. 4C). Figure 4D summarizes the effects of the *asd-2* expression on the *let-2* reporter. We concluded that the ASD-2b isoform regulates the *let-2* alternative splicing reporter in the body wall muscles.

ASD-2b regulates the switching of the let-2 alternative exons via a short element in intron 10

Then, we searched for a *cis*-acting element for the ASD-2b function in the *let-2* pre-mRNA processing. Kabat et al. (2006) have recently reported that evolutionarily conserved intronic stretches are likely to be involved in the

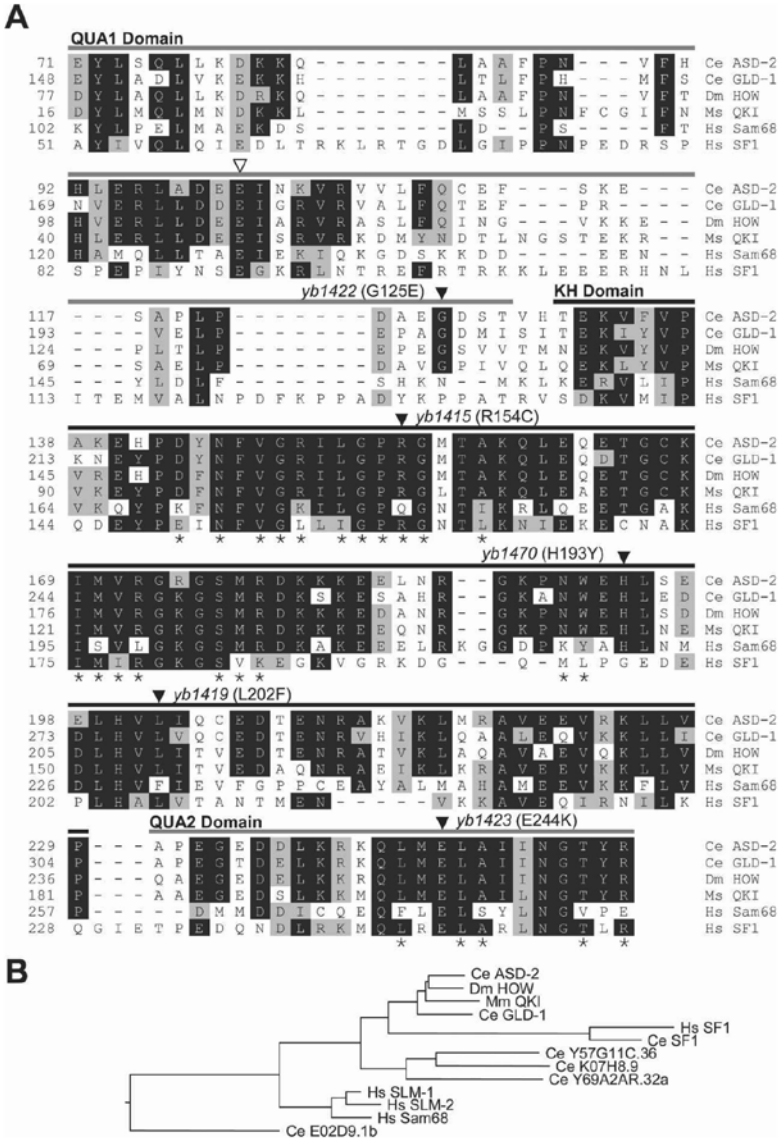

Figure 3. GSG/STAR domain of ASD-2 and other STAR family proteins. (*A*) Amino acid sequence alignment of the GSG/STAR domains. Identical amino acid residues are shaded in black. Amino acid residues with similar properties are shaded in gray. The GSG/STAR domain and the QUA1 and QUA2 domains are indicated with black and gray lines, respectively, *above* the sequence alignment. Closed triangles indicate the positions of the missense mutations identified in *asd-2* mutant alleles. An open triangle indicates the position of the E48 residue of mouse QKI essential for dimerization (Chen and Richard 1998). Asterisks under the sequences indicate the human SF1 amino acid residues contacting the branchpoint RNA 5′-AUACUAACAA-3′ (Liu et al. 2001). (Ce GLD-1) *C. elegans* GLD-1 (Francis et al. 1995); (Dm HOW) *Drosophila* HOW (Zaffran et al. 1997); (Ms QKI) mouse QKI (Ebersole et al. 1996); (Hs Sam68) human Sam68 (Matter et al. 2002); (Hs SF1) human SF1 (Kramer and Utans 1991). (*B*) Phylogenetic tree of the GSG/STAR domains from the STAR family proteins. (Ce) *C. elegans*; (Dm) *Drosophila*; (Ms) mouse; (Hs) human.

regulation of alternative pre-mRNA splicing in nematodes. Furthermore, they demonstrated that deletion of short stretches within *let-2* intron 10 affected the alternative splicing regulation (Kabat et al. 2006). We therefore constructed a pair of modified *let-2* reporter minigenes (M1) with a deletion of a short sequence in intron 10 (Fig. 5A), and observed that the M1 mutant reporter continued expressing E9-GFP in the late larval stages (Fig. 5B). Since the sequence deleted in the M1 minigenes contained a half-site of the QKI response element (QRE, NACUAAY-N_{1-20}-UAAY), a consensus sequence of mouse QKI (Galarneau and Richard 2005), we modified two residues in the short stretch, CUAACUCUAAC, in another pair of modified *let-2* reporter minigenes (M2) (Fig. 5A), and found that disruption of the stretch also phenocopied the *asd-2* mutants (Fig. 5C). Furthermore, the M2 mutant reporter no longer responded to the overexpression of the ASD-2b cDNA (Fig. 5D). We also constructed a pair of minigenes (M3) in which a conserved UGCAUG element is disrupted (Fig. 5A), and found that the M3 mutant reporter responded to ASD-2b overexpression (Fig. 5E) as did the wild-type (WT) reporter (Fig. 4C). These results indicated that the QRE-like stretch is essential for ASD-2b to enforce expression of E10-RFP.

To examine whether ASD-2 directly binds to the QRE-like stretch in vitro, we performed an electrophoretic mobility shift assay (EMSA) with RNA probes harboring the intact stretch or the mutation as in the M2 mutant reporter (Fig. 5F). The recombinant protein of the ASD-2 GSG/STAR domain (ASD-2 STAR) shifted the mobility

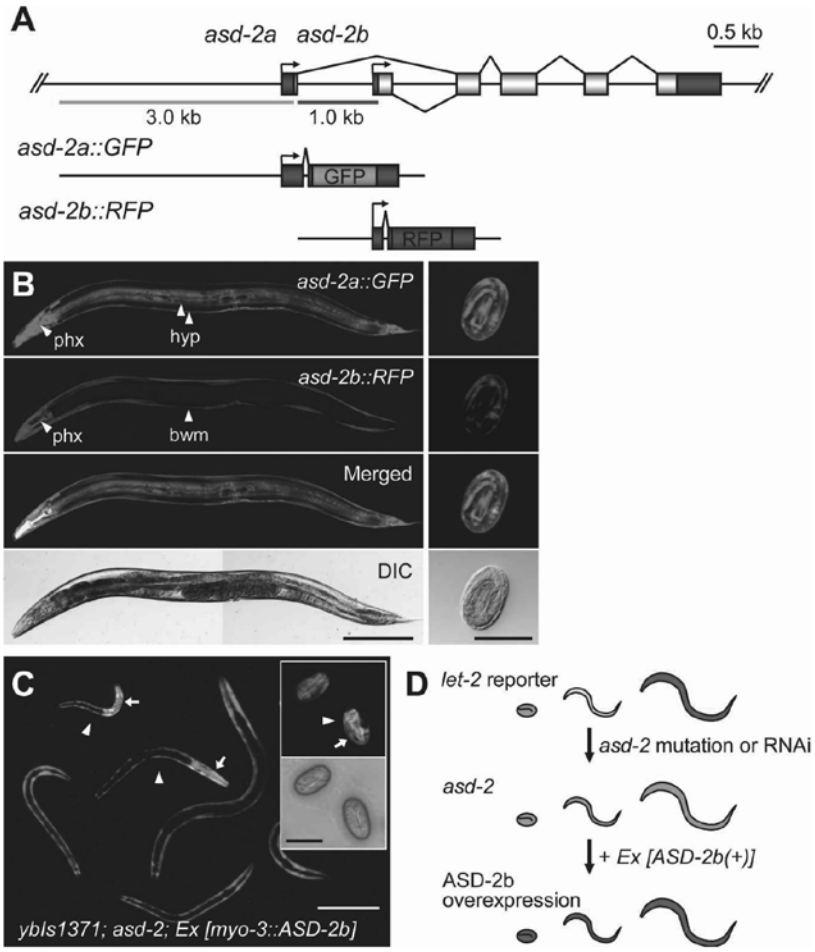

Figure 4. Expression and function of *asd-2b* in the body wall muscles. (*A*) Schematic representation of the *asd-2* transcriptional fusion minigenes *asd-2a*::*GFP* and *asd-2b*::*RFP*. Green and magenta lines indicate the *asd-2a* promoter and the *asd-2b* promoter regions, respectively, used in the constructs. (*B*) Confocal images of the expression patterns of the *asd-2* transcriptional fusions in an adult (*left* column) and a late embryo (*right* column). Expression of *asd-2a*::*GFP* (green) is detected in hypodermis (hyp) and pharyngeal muscles (phx). Expression of *asd-2b*::*RFP* (magenta) is detected in the body wall muscles (bwm) and the pharyngeal muscles (phx). (*Bottom*) A DIC image of the same field. Bars: *left* column, 100 µm; *right* column, 50 µm. (*C*) Microphotograph of the *let-2* reporter allele *ybIs1371* in the *asd-2 (yb1423)* mutant background carrying an extrachromosomal array for ASD-2b expression under the *myo-3* promoter. Arrowheads indicate young larvae and an embryo (shown in *inset*) carrying the array. Arrows indicate the pharynges of transgenic worms expressing GFP from *myo-2*::*GFP*, a coinjected marker of transformation. Bars: 100 µm; *inset*, 50 µm. (*D*) Summary of the effects of *asd-2* expression on the *let-2* reporter.

of the wild-type RNA probe (WT) in a dose-dependent manner (Fig. 5F, lanes 2–6), but not of the M2 mutant probe (Fig. 5F, lanes 8–11), demonstrating the direct and specific binding of ASD-2 to the QRE-like stretch in vitro.

asd-2 *promotes removal of* let-2 *intron 10 in the late larval stages*

Next, we examined the processing steps of the endogenous *let-2* pre-mRNA. When we look at exon 8 to exon 11 of the *let-2* pre-mRNA, mutually exclusive inclusion of exon 9 or exon 10 requires sequential removal of two flanking introns. As intron 9 (30 nucleotides) is too short to be excised due to steric interference between the donor and the possible branch site (Smith et al. 1993; Southby et al. 1999), we can expect four introns to be removed in the first splicing, and the subsequent second splicing to produce either of the two mature *let-2* mRNAs (Fig. 6A). To gain insight into the processing course of the endogenous *let-2* pre-mRNA, we tried to detect and compare the amounts of the four possible processing intermediates or partially spliced RNAs (Fig. 6A) in the synchronized wild-type and *asd-2* mutant worms.

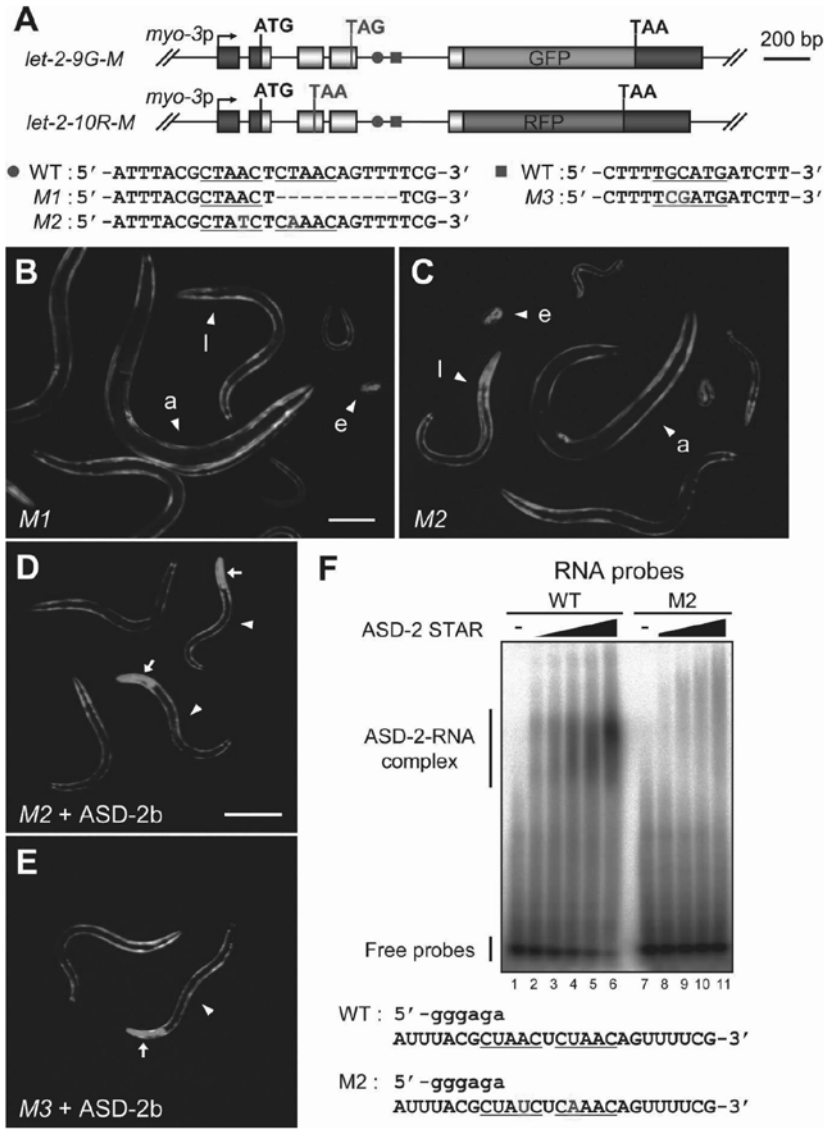

Figure 5. A regulatory element essential for the developmental switching of the *let-2* alternative splicing by ASD-2b. (*A*) Schematic representation (*top*) and sequences (*bottom*) of the modified *let-2* reporter minigenes *M1*, *M2*, and *M3*. A red circle and a red square indicate the positions of the mutation sites for *M1*/*M2* and *M3*, respectively. Sequences fitting the consensus of QRE and a UGCAUG element are underlined. Mutated sequences are indicated in red. Dashed line indicates deletion. (*B*,*C*) Transgenic worms expressing a pair of the *let-2-M1* minigenes (*B*) and a pair of the *let-2-M2* minigenes (*C*). Arrowheads indicate an embryo (e), an L3 larva (l), and a young adult (a). Bar in *B*, 100 µm. (*D*,*E*) Transgenic worms overexpressing ASD-2b in body wall muscles, and carrying a pair of either the *let-2-M2* minigenes (*D*) or the *let-2-M3* minigenes (*E*). Arrowheads indicate young larvae carrying the extrachromosomal array for ASD-2b expression with a pharyngeal GFP marker (arrows). Bar in *D*, 100 µm. (*F*) EMSA. Twofold dilution series of the recombinant ASD-2 STAR protein is used. Sequences of the wild-type and M2 probes are indicated at the *bottom*. The QRE-like sequences are underlined. Mutation sites are indicated in red.

To quantify the amounts of the *let-2* processing intermediates, we prepared two pairs of PCR primers to amplify the complementary DNA fragments for the *let-2* RNAs retaining intron(s). One primer set was designed on exon 8 and intron 10 to amplify partially spliced RNAs in which either of the upstream flanking introns was removed (Fig. 6B, left panel). The primer set amplified the unspliced pre-mRNA (8–9–10–11) and partially spliced RNAs in which intron 8 was excised (8/9–10–11) or the intron between exon 8 and exon 10 was excised (8/10–11). The other primer set was designed on intron 8 and exon 11 to amplify partially spliced RNAs in which

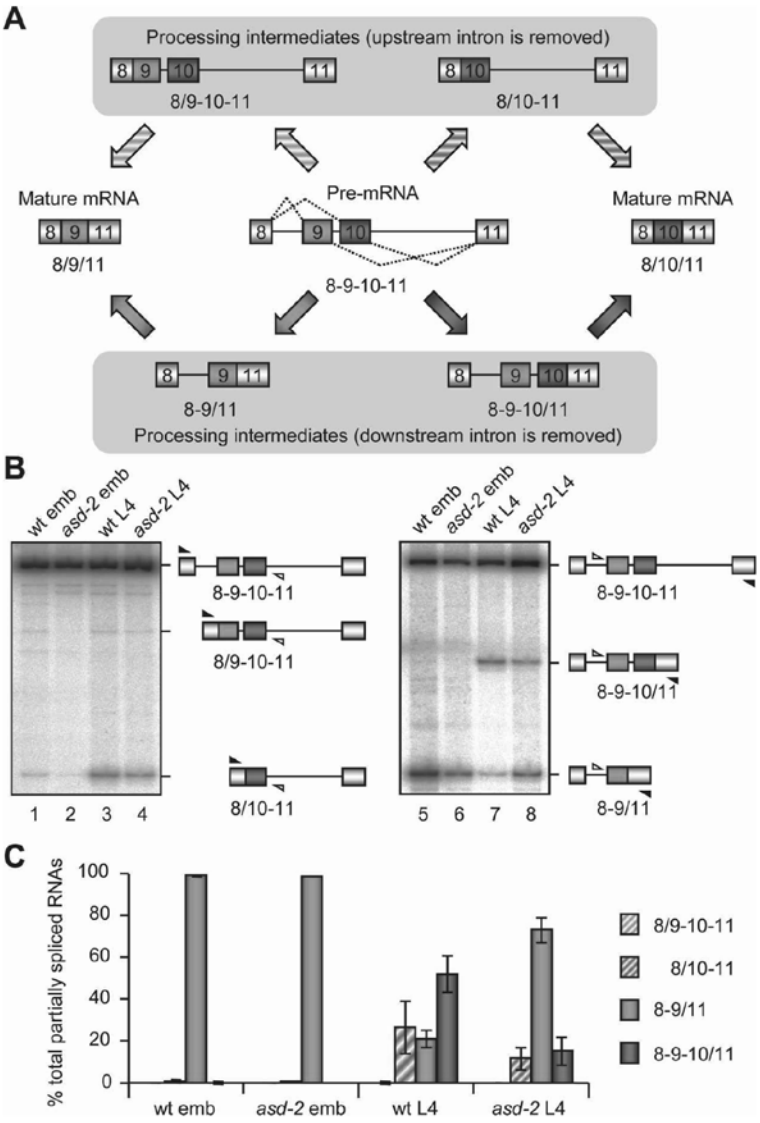

Figure 6. Analysis of partially spliced *let-2* RNAs as the intermediates of the alternative pre-mRNA processing. (*A*) A model of two-step pre-mRNA processing ensuring the *let-2* mutually exclusive alternative splicing. Four possible courses leading to the production of the two mature mRNAs are indicated. One of four introns (dotted lines) flanking the mutually exclusive exons is removed in the first splicing to generate one of the four possible processing intermediates (shaded in gray), and the remaining intron is removed in the second splicing. We assumed that intron 9 is too short to be excised. (*B*) Radioactive RT–PCR detection of the partially spliced *let-2* RNAs in the synchronized embryos (emb) and L4 larvae (L4) of the wild-type (wt) and the *asd-2 (yb1423)* mutant worms. Two pairs of the PCR primers were used to detect the *let-2* RNAs in which either of the upstream introns was removed (*left* panel), and either of the downstream introns was removed (*right* panel). The structure of each PCR product was analyzed by cloning and sequencing, and is schematically indicated. Closed and open triangles indicate the positions of the exonic and the intronic primers, respectively. (*C*) The relative amount of each of the partially spliced RNAs. The amount of each of the RNA species was calculated by normalization to the amount of the unspliced pre-mRNA. $n = 1$ for *asd-2* embryos; $n = 3$ for others. Error bars indicate standard error of mean (SEM).

either of the downstream flanking introns was removed (Fig. 6B, right panel). The primer set amplified the pre-mRNA (8–9–10–11) as well as partially spliced RNAs in which intron 10 was removed (8–9–10/11), or the intron between exon 9 and exon 11 was removed (8–9/11).

The normalized amounts of the four partially spliced RNAs are shown in Figure 6C. In both the wild-type and the *asd-2* mutant embryos, the 8–9/11 form, which is committed to the exon 9 mRNA isoform, was almost exclusively detected (Fig. 6B [lanes 1,2,5,6], C), consistent with the exclusive expression of the exon 9 mRNA in the embryos. In parallel with the developmental switching to the exon 10 mRNA isoform in the wild-type L4 larvae, we observed switching in the major form of the partially spliced RNAs from the 8–9/11 form to the 8–9–10/11 form, one of two possible intermediates leading to the exon 10 mRNA (Fig. 6B [lane 7], C). On the other hand, the amount of the 8–9/11 form still predominated over that of the 8–9–10/11 form in the L4 larvae of the *asd-2* mutant (Fig. 6B [lane 8], C), consistent with its switching-defective phenotype. These results indicated that *asd-2* is required for selective removal of intron 10 in this stage. We also observed substantial increase in the amount of the 8/10–11 form in the L4 larvae independent of the *asd-2* functions (Fig. 6B [lanes 3,4], C), which may contribute to the fraction of the exon 10 mRNA in the adult stage (Fig. 2B) and the color change of the *let-2* reporter in the *asd-2* senile adults.

The 8–9/11 form, the only intermediate detected in the embryos, will further be processed exclusively into

the exon 9 mRNA (Fig. 6A). However, the 8–9–10/11 form, the major intermediate in the wild-type L4 larvae, has two remaining splice acceptors, for exon 9 and exon 10, and may not necessarily be processed into the exon 10 mRNA. We therefore analyzed the fate of a pre-mRNA from a modified *let-2* reporter minigene that carried only exon 8 to exon 10, and observed a selective use of the exon 10 splice acceptor (Fig. 7A [top panel], B [lane 1]). We reasoned that the selective use of the exon 10 acceptor (TTTTTAG) was due to the relative weakness of the exon 9 splice acceptor (ATTCTAG), since the exon 9 acceptor became predominantly selected (Fig. 7A [bottom panel], B [lane 2]) when the reporter was further modified, so that the exon 9 acceptor matched the consensus of U2AF65 binding for *C. elegans* (TTTTCAG) (Hollins et al. 2005). These results are schematically summarized in Figure 7C.

Discussion

In the present study, we isolated *asd-2* mutants defective in the switching of the developmentally regulated mutually exclusive alternative exons in the *let-2* mRNAs, and compared the amounts of the intermediates of the post-transcriptional *let-2* pre-mRNA processing between the wild-type and the *asd-2* mutant.

Course of mutually exclusive alternative splicing of let-2 *pre-mRNA and the switching mechanism by ASD-2*

The unique property of the developmental switching and the isolation of the mutants of the *let-2* alternative splicing allowed us to analyze the relative amounts of the partially spliced RNAs (Fig. 6). In the case of Nova-2-regulated cassette exons in mice, Ule et al. (2006) ob-

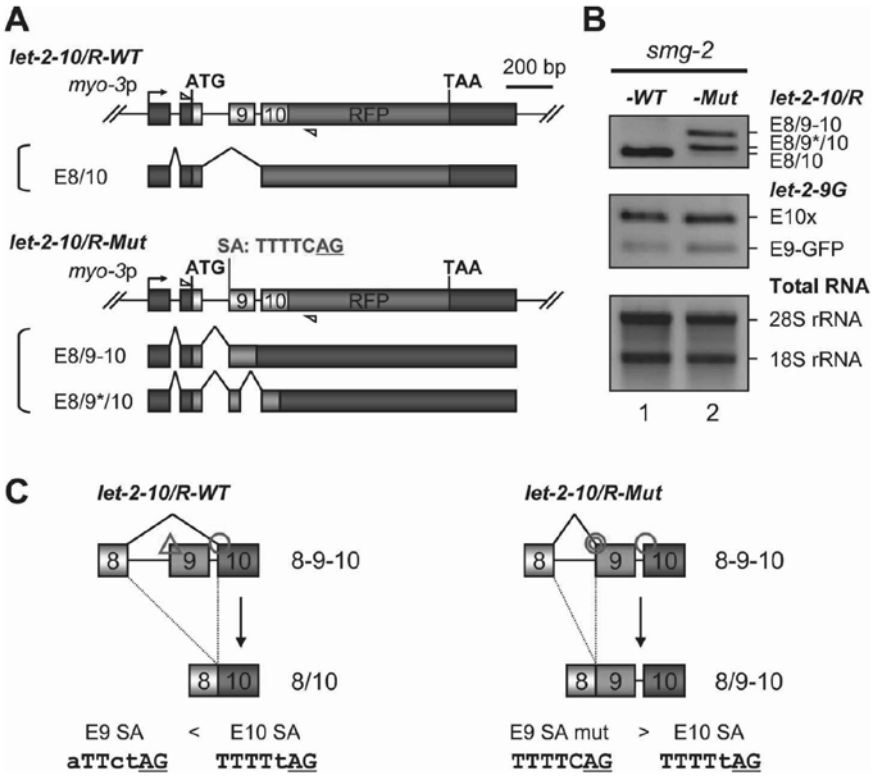

Figure 7. Biased selection between the splice acceptors for exon 9 and exon 10. (*A*) Structure of the *let-2* reporter minigenes *let-2-10/R-WT* (*top*) and *let-2-10/R-Mut* (*bottom*), and mRNAs derived from the minigenes. The *let-2* genomic DNA fragment spanning from exon 8 to exon 10 is connected in-frame to RFP cDNA. The splice acceptor (SA) for exon 9 (aTTctAG) is mutagenized to TTTTCAG in *let-2-10/R-Mut*. Structure of the mRNAs was confirmed by cloning and sequencing the RT–PCR products. Predicted ORFs are colored in red (E8/10-RFP) or gray (E8/9–10 and E8/9*/10). A cryptic donor site within exon 9 is used in the E8/9*/10 form. Open triangles indicate positions and directions of the PCR primers used to amplify the cDNAs in *B*. (*B*) RT–PCR analysis of the mRNAs derived from the *let-2-10/R* minigenes (*top*) and coinjected *let-2-9G* (*middle*). (*Bottom*) Total RNAs prepared from mixed-stage population. (Lane *1*) *let-2-10/R-WT*. (Lane *2*) *let-2-10/R-Mut*. Either of the *let-2-10/R* minigenes was coinjected with *let-2-9G* (Fig. 1B) into the *smg-2 (yb979)* mutant (Kuroyanagi et al. 2007), defective in NMD, to avoid degradation of the nonproductive mRNAs. Note that the E8/10-RFP form was exclusively produced from *let-2-10/R-WT*, while the E8/9–10 and E8/9*/10 forms were preferentially produced from *let-2-10/R-Mut*. (*C*) Schematic models of the biased selection of the exon 10 acceptor in *let-2-10/R-WT* pre-mRNA (*left* panel) and the exon 9 acceptor in *let-2-10/R-Mut* pre-mRNA (*right* panel). Note that the relatively stronger acceptor is selected in each case.

served biased accumulation of a partially spliced RNA in which either of the upstream or the downstream flanking introns was removed in the exon-including condition, either in the wild-type or the Nova-2 knock-out brain. In general, the steady-state amount of the processing intermediate is determined by the rate of production (removal of an intron in the first splicing) and the rate of degradation (mainly the subsequent splicing), and therefore it does not necessarily reflect the rate of production of the mature mRNA isoform produced from the intermediate. Nevertheless, we found a dramatic switching in the major species of the partially spliced *let-2* RNAs during larval development in parallel with the switching from the exon 9 to the exon 10 isoforms of the mature *let-2* mRNA (Fig. 6C), suggesting that the major species of the partially spliced RNAs is the processing intermediate of the major course of the pre-mRNA processing. Furthermore, we observed a defect in the switching in the major species of the partially spliced *let-2* RNAs in L4 larvae of the *asd-2* mutant (Fig. 6C), consistent with the defect of the *asd-2* mutant to produce the exon 10 mRNA. Assuming that *asd-2* mutation does not affect the rate of the second splicing, the result indicates that *asd-2* is required for the production of the major 8–9–10/11 form in the wild-type L4 larvae, and strongly suggests that the 8–9–10/11 form is the intermediate in the course of the *let-2* pre-mRNA processing by which most of the exon 10 mRNA is produced in the later stages.

Figure 8 illustrates a model of the processing courses of the *let-2* pre-mRNA and the mode of switching regulation by ASD-2 raised by the present study. The unique feature of the *let-2* alternative splicing is that either of the two introns downstream from the mutually exclusive exons is removed in the first splicing out of four possible flanking introns (Fig. 6A). In the embryonic stage, or when *asd-2* is inactive (Fig. 8, left panel), the splice donor of exon 9 (Fig. 8, green circle, GTACTG) is preferentially selected to produce the 8–9/11 intermediate, since the splice donor of exon 10 (Fig. 8, green triangle, GCAAGA) is noncanonical and weaker (Farrer et al. 2002; Kabat et al. 2006), leading to the production of the exon 9 mRNA. On the other hand, when *asd-2* is active in the late larval stages (Fig. 8, right panel), ASD-2 binds to the QRE-like *cis*-acting element in intron 10 to promote the selection of the weak exon 10 splice donor, leading to the production of the 8–9–10/11 intermediate. Thereafter, the splice acceptor of exon 10 (Fig. 8, red circle, TTTTTAG) is preferentially selected, as that of exon 9 (Fig. 8, red triangle, ATTCTAG) is weaker.

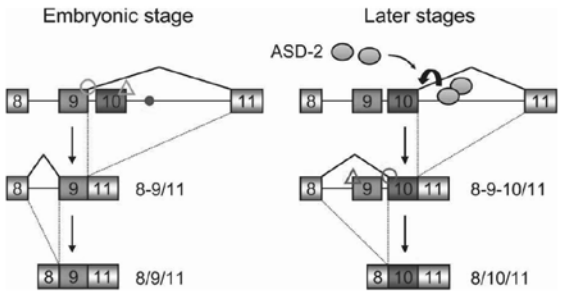

Figure 8. Models of the sequences of the *let-2* alternative splicing and the mechanism of exon switching by ASD-2. (*Left* panel) A model of exon 9 selection in the embryonic stage or when *asd-2* is inactive. (*Right* panel) A model of exon 10 selection when *asd-2* is active in the late larval stages. Red dot indicates the ASD-2-binding site. See the text for detail.

The model described above indicates that the fate of the pre-mRNA, whether to be the exon 9 or exon 10 mRNA, is primarily determined by the removal of a flanking intron in the first splicing. The model also indicates that the mutually exclusive nature of the *let-2* alternative exons is ensured by the ordered removal of the flanking introns and the asymmetric strength of the splice donors and the acceptors of the two alternative exons, as well as by the steric interference of the two exons. In the present study, we observed that endogenous *asd-2b* was expressed in embryos (Fig. 4B) and that the *let-2* exon 10 mRNA isoform was eventually produced in the adult stage, even in the *asd-2* mutant background. These observations suggest a possibility that besides ASD-2, other regulators, such as modulators of the ASD-2 function and/or other *trans*-factors, are involved in the *let-2* alternative splicing. Regulation of the order of the intron removal may also be involved in the developmental switching as implicated by the substantial increase in the 8/10–11 intermediate in the L4 stage (Fig. 6C). It would be an interesting challenge to elucidate all of the factors involved in the precise control of developmental switching of the *let-2* mutually exclusive alternative splicing in vivo.

STAR family RNA-binding protein ASD-2b regulates alternative splicing in C. elegans

STAR family proteins are known as key regulators of the various aspects of biological processes through multiple functions in the RNA metabolism. In the STAR family, the GLD-1 subfamily has been shown to play multiple roles through direct binding to the target RNAs. The *Quaking* gene generates three isoforms of proteins by alternative splicing. The nuclear isoform QKI-5 regulates alternative splicing of the myelin-associated glycoprotein (MAG) gene (Wu et al. 2002), while the balance of the nuclear and cytoplasmic isoforms QKI-6 and QKI-7 regulates the nuclear export of the myelin basic protein (MBP) mRNA (Larocque et al. 2002). *Drosophila how* encodes two alternative isoforms and the balance between the opposing activities of the two isoforms regulates tendon cell differentiation through the level of the transcription factor Stripe (Nabel-Rosen et al. 1999, 2002). Unlike vertebrates and insects, *C. elegans* has two members of the GLD-1 subfamily of genes. The cytoplasmic protein GLD-1 (Jones et al. 1996) regulates the germ cell development and sexual identity by regulating mRNA translation and stability (Jan et al. 1999; Lee and Schedl 2001, 2004; Schumacher et al. 2005). Our genetic studies demonstrate that ASD-2b regulates alternative splicing in the body wall muscles. Although the molecu-

lar function of the ASD-2a isoform should be characterized further, ASD-2a may play essential roles in the nematode development, since the *asd-2* deletion allele *ok483*, in which common exon 3 and exon 4 are deleted, is lethal (WormBase, http://www.wormbase.org), while the *asd-2b*-specific mutants look otherwise normal and only show the color phenotype. The multiple nuclear and cytoplasmic isoforms produced by alternative splicing and/or gene duplication may have conferred the multiple functions in mRNA metabolisms to the subfamily.

Sam68 and its paralogs, SLM1 and SLM2 of mammals constitute of the Sam68/SLM subfamily in the STAR family (Fig. 3B; Di Fruscio et al. 1999). The subfamily has been shown to mediate the signal transduction to RNA metabolism by modulating the RNA-binding properties upon phosphorylation (Stoss et al. 2001; Matter et al. 2002; Haegebarth et al. 2004; Paronetto et al. 2007). Although signals regulating the GLD-1 subfamily are to be elucidated, regulation of the RNA-binding property may be involved in the regulation of the *let-2* alternative splicing by ASD-2b in vivo.

RNA-binding specificity of ASD-2

We identified the essential QRE-like *cis*-element for ASD-2b to regulate *let-2* alternative splicing. Several studies have identified the direct binding sites of the GLD-1 subfamily and addressed the consensus of the binding sequences. Ryder et al. (2004) demonstrated that GLD-1 preforms a dimer, and specifically binds to the UACU(C/A)A stretch(es) in the target mRNAs. They also showed that QKI recognizes the consensus NA(A>C)UAA by extensive mutagenesis of the GLD-1 consensus sequence (Ryder and Williamson 2004). Enrichment of the high-affinity RNA ligands using systematic evolution of ligands by exponential enrichment (SELEX) defined the QRE as a bipartite consensus sequence NACUAAY-N_{1-20}-UAAY, consisting of a core site (NACUAAY) and a tetra-nucleotide half site (UAAY) (Galarneau and Richard 2005). Recently, the primary sequence and the secondary structure requirement for *Drosophila* HOW response element (HRE) has been determined as the ACUAA stretch in the loop (Israeli et al. 2007). The results from these studies indicate that the GSG/STAR domains of the GLD-1 subfamily share not only the high amino acid sequence identity, but also the consensus binding sequence determined as QRE, although the sequence that binds with the highest affinity may differ among the GLD-1 subfamily members (Saccomanno et al. 1999; Ryder and Williamson 2004).

The *cis*-element we identified in this study consists of direct repeats of the penta-nucleotide stretch, CUAAC, which matches five out of six nucleotides of the QRE core site. The tetra-nucleotide QRE half site, which can be either upstream of or downstream from the core site, has been shown to be required for the high-affinity binding (Galarneau and Richard 2005) and the requirement of the half site in the proximity has also been suggested for GLD-1 (Ryder et al. 2004). It is likely that the direct repeats of the penta-nucleotide compensated the requirement of the complete core site for *let-2* regulation by ASD-2 as in the case of QRE-1 in the 3′-untranslated region (UTR) of MBP mRNA, where multiple clusters of the half site constitute QRE (Galarneau and Richard 2005). QKI and GLD-1 form homodimers via the QUA1 domain (Chen and Richard 1998; Ryder et al. 2004) and the E48 residue of QKI, conserved among the GLD-1 subfamily proteins (Fig. 3A), is essential for the dimer formation and the function of the *Quaking* gene (Chen and Richard 1998). We identified a substitution of a conserved residue in the QUA1 domain in the *asd-2 (yb1422)* mutant (Fig. 3A), suggesting the functional importance of the QUA1 domain for the ASD-2 function. ASD-2 may also form a homodimer via the conserved QUA1 domain, and each subunit may contact one CUAAC stretch in binding to the *let-2* pre-mRNA. Comparison of the dimer formation activities and the RNA-binding properties of the GSG/STAR domains derived from the various *asd-2* mutants isolated in this study would lead to further understanding of the RNA-recognition by the STAR family proteins.

Recent global and comparative analyses of the alternatively spliced exons have demonstrated that the (A)CTAAC stretch, which resembles the QRE, is enriched in the introns flanking the alternative exons in both mammals and nematodes, suggesting that the stretch is an intronic alternative splicing regulator (Kabat et al. 2006; Sugnet et al. 2006; Das et al. 2007; Yeo et al. 2007). The GLD-1 subfamily may be involved in the regulation of these genes, although the requirement of the (A)CTAAC stretch and the function of the GLD-1 subfamily are to be experimentally addressed.

Visualization of the alternative splicing patterns in vivo

In the present study, we utilized a pair of symmetric minigenes, both of which contain four exons and three intervening introns for visualizing the expression profiles of the *let-2* mutually exclusive alternative exons (Fig. 1B). In contrast, for visualizing the tissue-specific expression profiles of the *egl-15* mutually exclusive exons, we utilized a single unified minigene, in which GFP and RFP cDNAs were introduced into the alternative exons (Kuroyanagi et al. 2006). With the unified reporter minigene, we demonstrated that mutually exclusive selection of the *egl-15* alternative exons is regulated by the upstream-most intron, and that the downstream-most intron is dispensable for the regulation (Kuroyanagi et al. 2006). In general, the downstream flanking intron and the downstream constitutive exon should be included in the alternative splicing reporter minigenes, since the *cis*-element(s) in the intron downstream from the alternative exon(s) could be essential for the regulation, as demonstrated in this study. As the *let-2* reporter minigenes are symmetric and contain the intact genomic sequence, except for a modification in one exon in each of the reporter minigenes, we can assume that expression of the reporter reflects the regulation of the endogenous gene, and that the simultaneous modification of the *cis*-ele-

ment(s) in both of the minigene pairs should cause the same effect on the pre-mRNAs derived from these minigenes, as demonstrated in this study. We therefore conclude that a symmetric pair of minigenes is feasible for the visualization of the alternative splicing patterns and for the elucidation of the regulation mechanisms in *C. elegans*.

The utilization of dichromatic alternative splicing reporters has recently been described in other organisms. Carstens and colleagues (Newman et al. 2006) utilized a pair of reporter minigenes for the *FGFR2* mutually exclusive exons IIIb and IIIc with a similar structure to the *let-2* reporter. They demonstrated that the reporter and a fluorescence-activated cell sorter (FACS) facilitated the analysis of the function of various *trans*-factors in the selection of the mutually exclusive exons. Cooper and colleagues (Orengo et al. 2006) utilized another type of a single dichromatic reporter minigene, in which GFP and RFP cDNAs were fused in the different frame so that mutually exclusive expression of GFP and RFP from the single minigene reflected the expression of the alternative isoforms. Garcia-Blanco and colleagues (Bonano et al. 2006) generated knock-in mice that visualized the repression of the *FGFR2* exon IIIb in vivo. The mice carry an RFP-minigene to monitor efficiency of constitutive splicing and a GFP-minigene to monitor repression of *FGFR2* exon IIIb at a single-cell resolution in vivo. The advantage of these dichromatic fluorescent alternative splicing reporters, including those in our study, is that relative abundance of the two alternative isoforms in each cell can be reliably analyzed with a minimal effect of other aspects of gene expression such as a transcription level. Application of these alternative splicing reporters will facilitate expression profiling and experimental identification of *trans*-factors and *cis*-elements of various alternative splicing events.

In conclusion, visualization of the expression profiles of the alternative exons enabled us to isolate the splicing mutants and identify *trans*-acting factors and *cis*-acting elements. Isolation of the splicing mutants enabled us to detect and analyze the partially spliced pre-mRNAs or processing intermediates. These experimental data led to a model of how only one out of two exons is exclusively included in each mRNA and how the factor and elements regulate the fate of the exons. Experimental approaches of visualization of the splicing patterns, genetic analyses of splicing mutants, and detection of the processing intermediates in vivo, together with the comprehensive bioinformatic approaches, would open the way to further elucidate the spatiotemporally regulated fate of pre-mRNAs, or deciphering the splicing codes in metazoans.

Materials and methods

Plasmid construction

We constructed the reporter minigenes essentially as described in the text. To construct the reporter cassettes for *let-2-9G*, *let-2-10R*, and *let-2-10/R-WT*, we amplified the *let-2* genomic DNA fragments spanning from exon 8 to either exon 11 or exon 10 and cloned them into Gateway Entry vectors (Invitrogen) carrying either EGFP (Clontech) or mRFP1 (Campbell et al. 2002) cDNAs using the In-Fusion system (BD Biosciences). We introduced termination codons by using QuickChange (Stratagene). To construct the ASD-2b Entry vector, we amplified the ASD-2b cDNA fragment and cloned it in pENTR-D/TOPO (Invitrogen). We constructed the Expression vectors by homologous recombination between the reporter cassettes and the *myo-3* promoter vector pDEST-myo-3p (Kuroyanagi et al. 2006) by utilizing the Gateway system (Invitrogen). We generated *M1*, *M2*, and *M3* mutant minigenes from *myo-3*::*let-2-9G* and *myo-3*::*let-2-10R*, and *myo-3*::*let-2-10/R-Mut* from *myo-3*::*let-2-10/R-WT* by mutagenesis utilizing QuickChange (Stratagene). We amplified the genomic fragments of the *asd-2a* and *asd-2b* promoter regions and cloned them into promoterless Expression vectors to construct *asd-2a*::*GFP* and *asd-2b*::*RFP*. We confirmed all of the constructs by sequence analysis. Sequences of the primers used in the construction are available in the Supplemental Material.

Worm culture and microscopy

We cultured worms following standard methods (Brenner 1974). We prepared the transgenic lines essentially as described (Mello et al. 1991) using *lin-15 (n765)* as a host. We generated integrant lines by ultraviolet light irradiation (Mitani 1995). We treated *ybIs1371 [myo-3*::*let-2-9G myo-3*::*let-2-10R lin-15(+)]* animals with 47 mM ethyl methanesulfonate (EMS) for 4 h at room temperature, and we screened the F2 progeny for mutants with altered expression profiles of the GFP and RFP under a fluorescence stereoscope (MZ16FA; Leica) equipped with a dual-band-pass filter set. We captured the images of the *let-2* reporter worms with CCD cameras (E300 and DP71; Olympus). We used a confocal microscope (Fluoview FV500; Olympus) for image scanning and processed the acquired images with Metamorph (Molecular Devices). We identified the *asd-2* gene by SNP-based mapping essentially as described (Wicks et al. 2001). Briefly, we crossed the mutants with the Hawaiian wild-type strain, CB4856, which has many SNPs compared with the standard wild-type strain N2, and the SNPs of each F2 progeny with the green phenotype were analyzed by either restriction fragment length polymorphisms or direct sequencing of the PCR-amplified genomic fragments. Of ~75 predicted genes within the defined 391-kb region, we amplified and sequenced 13 RNA-related genes. We performed RNAi by soaking L4 hermaphrodites as described previously (Kuroyanagi et al. 2000; Maeda et al. 2001) by using dsRNAs corresponding to nucleotides 164–841 of the ASD-2b ORF.

RT–PCR

We prepared total RNAs and performed RT–PCR analysis essentially as described previously (Kuroyanagi et al. 2006). We digested the RT–PCR products for the *let-2* reporter and the endogenous *let-2* mRNAs with BglII before electrophoresis separation. Sequences of the primers used in the RT–PCR assays are available in the Supplemental Material.

EMSA

We prepared the recombinant protein for the GSG/STAR domain of ASD-2 (ASD-2 STAR), corresponding to amino acids 55–280 of ASD-2b, as a His-tagged protein. We introduced the ASD-2 STAR cDNA fragment into the modified bacterial cold-induction vector (Kuroyanagi et al. 2007) and induced the pro-

tein production following the standard cold-induction procedure (Takara). We purified the His-ASD-2 STAR protein with Ni-NTA agarose (Qiagen). We prepared the ^{32}P-labeled wild-type and M2 RNA probes by in vitro transcription with [α^{32}P]UTP and T7 RNA polymerase (Takara). We incubated the gel-purified RNA probes alone or with increasing concentrations of His-ASD-2 STAR in 25 µL of RNA-binding buffer (20 mM HEPES-KOH at pH 7.9, 320 mM KCl, 5% glycerol, 1% Triton X-100, 1 mM DTT, 0.1 mM PMSF) supplemented with 130 ng/µL *Escherichia coli* tRNA and 50 ng/µL BSA for 30 min at 20°C. Each sample was separated on a nondenaturing polyacrylamide gel and visualized with a phosphorimage analyzer (FLA-3000G; Fuji Film).

Analysis of partially spliced let-2 *RNAs*

We performed RT with random hexamers. We performed PCR following standard protocols supplemented with [α^{32}P]dCTP, and separated the PCR products on 5% nondenaturing polyacrylamide gels and quantified the signal intensity of each band with a phosphorimage analyzer (FLA-3000G; Fuji Film). We calculated the amount of each processing intermediate by normalization to that of the pre-mRNA in the same reaction, taking their G + C contents into account. We confirmed the identity of each band by cloning and sequence analysis. We performed control PCRs using RT products without reverse transcriptase (shown in Supplemental Fig. 1) to calculate the contamination of genomic DNAs in the total RNA fraction. Sequences of the primers used in the PCRs are available in the Supplemental Material.

Database information

The gene assignment *asd-2* has been approved by the CGC Genetic Map and Nomenclature Curator. The nucleotide sequences of the *asd-2* cDNAs have been deposited in the GenBank/EMBL/DDBJ databases with the accession numbers EF630625 and EF630626.

Acknowledgments

We thank S. Mitani at Tokyo Women's Medical University for assistance in the mutant screening. We thank T. Nojima, A. Takeuchi, Y. Ogawa, and N. Kataoka at TMDU for discussions and comments on the manuscript. We thank R.Y. Tsien at University of California at San Diego and the *Caenorhabditis* Genetics Center for materials. We thank Y. Kikuchi, Y. Usami, and M. Hagiwara for technical assistance. This work was supported by a Grant-in-Aid for Scientific Research on Priority Areas from the Ministry of Education, Culture, Sports, Science, and Technology of Japan (to H.K. and M.H.). G.O. contributed to overall experiments. M.H. and H.K. organized this work. We all discussed the results and wrote the manuscript.

Reference

Baraniak, A.P., Lasda, E.L., Wagner, E.J., and Garcia-Blanco, M.A. 2003. A stem structure in fibroblast growth factor receptor 2 transcripts mediates cell-type-specific splicing by approximating intronic control elements. *Mol. Cell. Biol.* **23:** 9327–9337.

Baraniak, A.P., Chen, J.R., and Garcia-Blanco, M.A. 2006. Fox-2 mediates epithelial cell-specific fibroblast growth factor receptor 2 exon choice. *Mol. Cell. Biol.* **26:** 1209–1222.

Black, D.L. 2003. Mechanisms of alternative pre-messenger RNA splicing. *Annu. Rev. Biochem.* **72:** 291–336.

Blencowe, B.J. 2006. Alternative splicing: New insights from global analyses. *Cell* **126:** 37–47.

Bonano, V.I., Oltean, S., Brazas, R.M., and Garcia-Blanco, M.A. 2006. Imaging the alternative silencing of *FGFR2* exon IIIb *in vivo*. *RNA* **12:** 2073–2079.

Brenner, S. 1974. The genetics of *Caenorhabditis elegans*. *Genetics* **77:** 71–94.

Campbell, R.E., Tour, O., Palmer, A.E., Steinbach, P.A., Baird, G.S., Zacharias, D.A., and Tsien, R.Y. 2002. A monomeric red fluorescent protein. *Proc. Natl. Acad. Sci.* **99:** 7877–7882.

Chen, T. and Richard, S. 1998. Structure-function analysis of Qk1: A lethal point mutation in mouse quaking prevents homodimerization. *Mol. Cell. Biol.* **18:** 4863–4871.

Chen, C.D., Kobayashi, R., and Helfman, D.M. 1999. Binding of hnRNP H to an exonic splicing silencer is involved in the regulation of alternative splicing of the rat β-tropomyosin gene. *Genes & Dev.* **13:** 593–606.

Crawford, J.B. and Patton, J.G. 2006. Activation of α-tropomyosin exon 2 is regulated by the SR protein 9G8 and heterogeneous nuclear ribonucleoproteins H and F. *Mol. Cell. Biol.* **26:** 8791–8802.

Das, D., Clark, T.A., Schweitzer, A., Yamamoto, M., Marr, H., Arribere, J., Minovitsky, S., Poliakov, A., Dubchak, I., Blume, J.E., et al. 2007. A correlation with exon expression approach to identify *cis*-regulatory elements for tissue-specific alternative splicing. *Nucleic Acids Res.* **35:** 4845–4857.

Di Fruscio, M., Chen, T., and Richard, S. 1999. Characterization of Sam68-like mammalian proteins SLM-1 and SLM-2: SLM-1 is a Src substrate during mitosis. *Proc. Natl. Acad. Sci.* **96:** 2710–2715.

Ebersole, T.A., Chen, Q., Justice, M.J., and Artzt, K. 1996. The quaking gene product necessary in embryogenesis and myelination combines features of RNA binding and signal transduction proteins. *Nat. Genet.* **12:** 260–265.

Expert-Bezancon, A., Sureau, A., Durosay, P., Salesse, R., Groeneveld, H., Lecaer, J.P., and Marie, J. 2004. hnRNP A1 and the SR proteins ASF/SF2 and SC35 have antagonistic functions in splicing of β-tropomyosin exon 6B. *J. Biol. Chem.* **279:** 38249–38259.

Farrer, T., Roller, A.B., Kent, W.J., and Zahler, A.M. 2002. Analysis of the role of *Caenorhabditis elegans* GC-AG introns in regulated splicing. *Nucleic Acids Res.* **30:** 3360–3367.

Faustino, N.A. and Cooper, T.A. 2003. Pre-mRNA splicing and human disease. *Genes & Dev.* **17:** 419–437.

Francis, R., Barton, M.K., Kimble, J., and Schedl, T. 1995. *gld-1*, a tumor suppressor gene required for oocyte development in *Caenorhabditis elegans*. *Genetics* **139:** 579–606.

Galarneau, A. and Richard, S. 2005. Target RNA motif and target mRNAs of the Quaking STAR protein. *Nat. Struct. Mol. Biol.* **12:** 691–698.

Graham, P.L., Johnson, J.J., Wang, S., Sibley, M.H., Gupta, M.C., and Kramer, J.M. 1997. Type IV collagen is detectable in most, but not all, basement membranes of *Caenorhabditis elegans* and assembles on tissues that do not express it. *J. Cell Biol.* **137:** 1171–1183.

Graveley, B.R. 2005. Mutually exclusive splicing of the insect *Dscam* pre-mRNA directed by competing intronic RNA secondary structures. *Cell* **123:** 65–73.

Gromak, N., Matlin, A.J., Cooper, T.A., and Smith, C.W. 2003a. Antagonistic regulation of α-actinin alternative splicing by CELF proteins and polypyrimidine tract binding protein. *RNA* **9:** 443–456.

Gromak, N., Rideau, A., Southby, J., Scadden, A.D., Gooding, C., Huttelmaier, S., Singer, R.H., and Smith, C.W. 2003b.

The PTB interacting protein raver1 regulates α-tropomyosin alternative splicing. *EMBO J.* **22:** 6356–6364.

Haegebarth, A., Heap, D., Bie, W., Derry, J.J., Richard, S., and Tyner, A.L. 2004. The nuclear tyrosine kinase BRK/Sik phosphorylates and inhibits the RNA-binding activities of the Sam68-like mammalian proteins SLM-1 and SLM-2. *J. Biol. Chem.* **279:** 54398–54404.

Hollins, C., Zorio, D.A., MacMorris, M., and Blumenthal, T. 2005. U2AF binding selects for the high conservation of the *C. elegans* 3′ splice site. *RNA* **11:** 248–253.

Israeli, D., Nir, R., and Volk, T. 2007. Dissection of the target specificity of the RNA-binding protein HOW reveals *dpp* mRNA as a novel HOW target. *Development* **134:** 2107–2114.

Jan, E., Motzny, C.K., Graves, L.E., and Goodwin, E.B. 1999. The STAR protein, GLD-1, is a translational regulator of sexual identity in *Caenorhabditis elegans*. *EMBO J.* **18:** 258–269.

Jin, Y., Suzuki, H., Maegawa, S., Endo, H., Sugano, S., Hashimoto, K., Yasuda, K., and Inoue, K. 2003. A vertebrate RNA-binding protein Fox-1 regulates tissue-specific splicing via the pentanucleotide GCAUG. *EMBO J.* **22:** 905–912.

Johnson, J.M., Castle, J., Garrett-Engele, P., Kan, Z., Loerch, P.M., Armour, C.D., Santos, R., Schadt, E.E., Stoughton, R., and Shoemaker, D.D. 2003. Genome-wide survey of human alternative pre-mRNA splicing with exon junction microarrays. *Science* **302:** 2141–2144.

Jones, A.R. and Schedl, T. 1995. Mutations in *gld-1*, a female germ cell-specific tumor suppressor gene in *Caenorhabditis elegans*, affect a conserved domain also found in Src-associated protein Sam68. *Genes & Dev.* **9:** 1491–1504.

Jones, A.R., Francis, R., and Schedl, T. 1996. GLD-1, a cytoplasmic protein essential for oocyte differentiation, shows stage- and sex-specific expression during *Caenorhabditis elegans* germline development. *Dev. Biol.* **180:** 165–183.

Jones, R.B., Carstens, R.P., Luo, Y., and McKeehan, W.L. 2001a. 5′- and 3′-terminal nucleotides in the FGFR2 ISAR splicing element core have overlapping roles in exon IIIb activation and exon IIIc repression. *Nucleic Acids Res.* **29:** 3557–3565.

Jones, R.B., Wang, F., Luo, Y., Yu, C., Jin, C., Suzuki, T., Kan, M., and McKeehan, W.L. 2001b. The nonsense-mediated decay pathway and mutually exclusive expression of alternatively spliced FGFR2IIIb and -IIIc mRNAs. *J. Biol. Chem.* **276:** 4158–4167.

Kabat, J.L., Barberan-Soler, S., McKenna, P., Clawson, H., Farrer, T., and Zahler, A.M. 2006. Intronic alternative splicing regulators identified by comparative genomics in nematodes. *PLoS Comput. Biol.* **2:** e86. doi: 10.1371/journal.pcbi.0020086.

Kramer, A. and Utans, U. 1991. Three protein factors (SF1, SF3 and U2AF) function in pre-splicing complex formation in addition to snRNPs. *EMBO J.* **10:** 1503–1509.

Kuroyanagi, H., Kimura, T., Wada, K., Hisamoto, N., Matsumoto, K., and Hagiwara, M. 2000. SPK-1, a *C. elegans* SR protein kinase homologue, is essential for embryogenesis and required for germline development. *Mech. Dev.* **99:** 51–64.

Kuroyanagi, H., Kobayashi, T., Mitani, S., and Hagiwara, M. 2006. Transgenic alternative-splicing reporters reveal tissue-specific expression profiles and regulation mechanisms in vivo. *Nat. Methods* **3:** 909–915.

Kuroyanagi, H., Ohno, G., Mitani, S., and Hagiwara, M. 2007. Fox-1 family and SUP-12 coordinately regulate tissue-specific alternative splicing *in vivo*. *Mol. Cell. Biol.* **27:** 8612–8621.

Larocque, D., Pilotte, J., Chen, T., Cloutier, F., Massie, B., Pedraza, L., Couture, R., Lasko, P., Almazan, G., and Richard, S. 2002. Nuclear retention of MBP mRNAs in the quaking viable mice. *Neuron* **36:** 815–829.

Lee, M.H. and Schedl, T. 2001. Identification of in vivo mRNA targets of GLD-1, a maxi-KH motif containing protein required for *C. elegans* germ cell development. *Genes & Dev.* **15:** 2408–2420.

Lee, M.H. and Schedl, T. 2004. Translation repression by GLD-1 protects its mRNA targets from nonsense-mediated mRNA decay in *C. elegans*. *Genes & Dev.* **18:** 1047–1059.

Lehmann-Blount, K.A. and Williamson, J.R. 2005. Shape-specific nucleotide binding of single-stranded RNA by the GLD-1 STAR domain. *J. Mol. Biol.* **346:** 91–104.

Letunic, I., Copley, R.R., and Bork, P. 2002. Common exon duplication in animals and its role in alternative splicing. *Hum. Mol. Genet.* **11:** 1561–1567.

Licatalosi, D.D. and Darnell, R.B. 2006. Splicing regulation in neurologic disease. *Neuron* **52:** 93–101.

Lin, J.C. and Tarn, W.Y. 2005. Exon selection in α-tropomyosin mRNA is regulated by the antagonistic action of RBM4 and PTB. *Mol. Cell. Biol.* **25:** 10111–10121.

Liu, Z., Luyten, I., Bottomley, M.J., Messias, A.C., Houngninou-Molango, S., Sprangers, R., Zanier, K., Kramer, A., and Sattler, M. 2001. Structural basis for recognition of the intron branch site RNA by splicing factor 1. *Science* **294:** 1098–1102.

Maeda, I., Kohara, Y., Yamamoto, M., and Sugimoto, A. 2001. Large-scale analysis of gene function in *Caenorhabditis elegans* by high-throughput RNAi. *Curr. Biol.* **11:** 171–176.

Matlin, A.J., Clark, F., and Smith, C.W. 2005. Understanding alternative splicing: Towards a cellular code. *Nat. Rev. Mol. Cell Biol.* **6:** 386–398.

Matter, N., Herrlich, P., and Konig, H. 2002. Signal-dependent regulation of splicing via phosphorylation of Sam68. *Nature* **420:** 691–695.

Mello, C.C., Kramer, J.M., Stinchcomb, D., and Ambros, V. 1991. Efficient gene transfer in *C.elegans*: Extrachromosomal maintenance and integration of transforming sequences. *EMBO J.* **10:** 3959–3970.

Mitani, S. 1995. Genetic regulation of *mec-3* gene expression implicated in the specification of the mechanosensory neuron cell types in *Caenorhabditis elegans*. *Dev. Growth Differ.* **37:** 551–557.

Modrek, B. and Lee, C. 2002. A genomic view of alternative splicing. *Nat. Genet.* **30:** 13–19.

Muh, S.J., Hovhannisyan, R.H., and Carstens, R.P. 2002. A Non-sequence-specific double-stranded RNA structural element regulates splicing of two mutually exclusive exons of fibroblast growth factor receptor 2 (FGFR2). *J. Biol. Chem.* **277:** 50143–50154.

Nabel-Rosen, H., Dorevitch, N., Reuveny, A., and Volk, T. 1999. The balance between two isoforms of the *Drosophila* RNA-binding protein how controls tendon cell differentiation. *Mol. Cell* **4:** 573–584.

Nabel-Rosen, H., Volohonsky, G., Reuveny, A., Zaidel-Bar, R., and Volk, T. 2002. Two isoforms of the *Drosophila* RNA binding protein, how, act in opposing directions to regulate tendon cell differentiation. *Dev. Cell* **2:** 183–193.

Newman, E.A., Muh, S.J., Hovhannisyan, R.H., Warzecha, C.C., Jones, R.B., McKeehan, W.L., and Carstens, R.P. 2006. Identification of RNA-binding proteins that regulate FGFR2 splicing through the use of sensitive and specific dual color fluorescence minigene assays. *RNA* **12:** 1129–1141.

Orengo, J.P., Bundman, D., and Cooper, T.A. 2006. A bichromatic fluorescent reporter for cell-based screens of alternative splicing. *Nucleic Acids Res.* **34:** e148.

Paronetto, M.P., Achsel, T., Massiello, A., Chalfant, C.E., and

Sette, C. 2007. The RNA-binding protein Sam68 modulates the alternative splicing of Bcl-x. *J. Cell Biol.* **176:** 929–939.
Pettitt, J. and Kingston, I.B. 1994. Developmentally regulated alternative splicing of a nematode type IV collagen gene. *Dev. Biol.* **161:** 22–29.
Ryder, S.P. and Williamson, J.R. 2004. Specificity of the STAR/GSG domain protein Qk1: Implications for the regulation of myelination. *RNA* **10:** 1449–1458.
Ryder, S.P., Frater, L.A., Abramovitz, D.L., Goodwin, E.B., and Williamson, J.R. 2004. RNA target specificity of the STAR/GSG domain post-transcriptional regulatory protein GLD-1. *Nat. Struct. Mol. Biol.* **11:** 20–28.
Saccomanno, L., Loushin, C., Jan, E., Punkay, E., Artzt, K., and Goodwin, E.B. 1999. The STAR protein QKI-6 is a translational repressor. *Proc. Natl. Acad. Sci.* **96:** 12605–12610.
Schmucker, D., Clemens, J.C., Shu, H., Worby, C.A., Xiao, J., Muda, M., Dixon, J.E., and Zipursky, S.L. 2000. *Drosophila* Dscam is an axon guidance receptor exhibiting extraordinary molecular diversity. *Cell* **101:** 671–684.
Schumacher, B., Hanazawa, M., Lee, M.H., Nayak, S., Volkmann, K., Hofmann, E.R., Hengartner, M., Schedl, T., and Gartner, A. 2005. Translational repression of *C. elegans* p53 by GLD-1 regulates DNA damage-induced apoptosis. *Cell* **120:** 357–368.
Sibley, M.H., Johnson, J.J., Mello, C.C., and Kramer, J.M. 1993. Genetic identification, sequence, and alternative splicing of the *Caenorhabditis elegans* α 2(IV) collagen gene. *J. Cell Biol.* **123:** 255–264.
Smith, C.W. 2005. Alternative splicing—When two's a crowd. *Cell* **123:** 1–3.
Smith, C.W. and Nadal-Ginard, B. 1989. Mutually exclusive splicing of α-tropomyosin exons enforced by an unusual lariat branch point location: Implications for constitutive splicing. *Cell* **56:** 749–758.
Smith, C.W., Chu, T.T., and Nadal-Ginard, B. 1993. Scanning and competition between AGs are involved in 3′ splice site selection in mammalian introns. *Mol. Cell. Biol.* **13:** 4939–4952.
Southby, J., Gooding, C., and Smith, C.W. 1999. Polypyrimidine tract binding protein functions as a repressor to regulate alternative splicing of α-actinin mutually exclusive exons. *Mol. Cell. Biol.* **19:** 2699–2711.
Stoss, O., Olbrich, M., Hartmann, A.M., Konig, H., Memmott, J., Andreadis, A., and Stamm, S. 2001. The STAR/GSG family protein rSLM-2 regulates the selection of alternative splice sites. *J. Biol. Chem.* **276:** 8665–8673.
Sugnet, C.W., Srinivasan, K., Clark, T.A., O'Brien, G., Cline, M.S., Wang, H., Williams, A., Kulp, D., Blume, J.E., Haussler, D., et al. 2006. Unusual intron conservation near tissue-regulated exons found by splicing microarrays. *PLoS Comput. Biol.* **2:** e4.
Ule, J., Stefani, G., Mele, A., Ruggiu, M., Wang, X., Taneri, B., Gaasterland, T., Blencowe, B.J., and Darnell, R.B. 2006. An RNA map predicting Nova-dependent splicing regulation. *Nature* **444:** 580–586.
Venables, J.P. 2004. Aberrant and alternative splicing in cancer. *Cancer Res.* **64:** 7647–7654.
Vernet, C. and Artzt, K. 1997. STAR, a gene family involved in signal transduction and activation of RNA. *Trends Genet.* **13:** 479–484.
Wagner, E.J., Baraniak, A.P., Sessions, O.M., Mauger, D., Moskowitz, E., and Garcia-Blanco, M.A. 2005. Characterization of the intronic splicing silencers flanking FGFR2 exon IIIb. *J. Biol. Chem.* **280:** 14017–14027.
Wicks, S.R., Yeh, R.T., Gish, W.R., Waterston, R.H., and Plasterk, R.H. 2001. Rapid gene mapping in *Caenorhabditis elegans* using a high density polymorphism map. *Nat. Genet.* **28:** 160–164.
Wu, J.I., Reed, R.B., Grabowski, P.J., and Artzt, K. 2002. Function of *quaking* in myelination: Regulation of alternative splicing. *Proc. Natl. Acad. Sci.* **99:** 4233–4238.
Yeo, G.W., Nostrand, E.L., and Liang, T.Y. 2007. Discovery and analysis of evolutionarily conserved intronic splicing regulatory elements. *PLoS Genet.* **3:** e85. doi: 10.1371/journal.pgen.0030085.
Zaffran, S., Astier, M., Gratecos, D., and Semeriva, M. 1997. The *held out wings (how) Drosophila* gene encodes a putative RNA-binding protein involved in the control of muscular and cardiac activity. *Development* **124:** 2087–2098.

東京医科歯科大学

歯と骨の分子疾患科学 国際教育研究拠点

～デント・メドミクスのインテリジェンスハブ～

平成20年度 実績報告書